ETHYLENE: A KEY REGULATORY MOLECULE IN PLANTS

EDITED BY: Nafees A. Khan, M. Iqbal R. Khan, Antonio Ferrante and Péter Poór
PUBLISHED IN: Frontiers in Plant Science and Frontiers in Physiology

frontiers Research Topics

ISSN 1664-8714
ISBN 978-2-88945-341-2
DOI 10.3389/978-2-88945-341-2

About Frontiers

Frontiers is more than just an open-access publisher of scholarly articles: it is a pioneering approach to the world of academia, radically improving the way scholarly research is managed. The grand vision of Frontiers is a world where all people have an equal opportunity to seek, share and generate knowledge. Frontiers provides immediate and permanent online open access to all its publications, but this alone is not enough to realize our grand goals.

Frontiers Journal Series

The Frontiers Journal Series is a multi-tier and interdisciplinary set of open-access, online journals, promising a paradigm shift from the current review, selection and dissemination processes in academic publishing. All Frontiers journals are driven by researchers for researchers; therefore, they constitute a service to the scholarly community. At the same time, the Frontiers Journal Series operates on a revolutionary invention, the tiered publishing system, initially addressing specific communities of scholars, and gradually climbing up to broader public understanding, thus serving the interests of the lay society, too.

Dedication to Quality

Each Frontiers article is a landmark of the highest quality, thanks to genuinely collaborative interactions between authors and review editors, who include some of the world's best academicians. Research must be certified by peers before entering a stream of knowledge that may eventually reach the public - and shape society; therefore, Frontiers only applies the most rigorous and unbiased reviews.
Frontiers revolutionizes research publishing by freely delivering the most outstanding research, evaluated with no bias from both the academic and social point of view.
By applying the most advanced information technologies, Frontiers is catapulting scholarly publishing into a new generation.

What are Frontiers Research Topics?

Frontiers Research Topics are very popular trademarks of the Frontiers Journals Series: they are collections of at least ten articles, all centered on a particular subject. With their unique mix of varied contributions from Original Research to Review Articles, Frontiers Research Topics unify the most influential researchers, the latest key findings and historical advances in a hot research area! Find out more on how to host your own Frontiers Research Topic or contribute to one as an author by contacting the Frontiers Editorial Office: **researchtopics@frontiersin.org**

ETHYLENE: A KEY REGULATORY MOLECULE IN PLANTS

Topic Editors:
Nafees A. Khan, Aligarh Muslim University, India
M. Iqbal R. Khan, International Rice Research Institute, Philippines
Antonio Ferrante, Università degli Studi di Milano, Italy
Péter Poór, University of Szeged, Hungary

Image: 24Novembers/Shutterstock.com

Ethylene is a simple gaseous phytohormone with multiple roles in regulation of metabolism at cellular, molecular, and whole plant level. It influences performance of plants under optimal and stressful environments by interacting with other signaling molecules. Understanding the ethylene biosynthesis and action through the plant's life can contribute to improve the knowledge of plant functionality and use of this plant hormone may drive adaptation and defense of plants from the adverse environmental conditions. The action of ethylene depends on its concentration in cell and the sensitivity of plants to the hormone. In recent years, research on ethylene has been focused, due to its dual action, on the regulation of plant processes at physiological and molecular level. The involvement of ethylene in the regulation of transcription needs to be widely explored involving the interaction with other key molecular regulators. The aim of the current research topic was to explore and update our understanding on its regulatory role in plant developmental mechanisms at cellular or whole plant level under optimal and changing environmental conditions. The present edited volume includes original research papers and review articles describing ethylene's regulatory role in plant development during plant ontogeny and also explains how it interacts with biotic and abiotic stress factors. This comprehensive collection of researches provide evidence that ethylene is essential in different physiological processes and does not always work alone, but in coordinated manner with other plant hormones. This research topic is also a source of tips for further works that should be addressed for the biology and molecular effects on plants.

Citation: Khan, N. A., Khan, M. I. R., Ferrante, A., Poór, P., eds. (2017). Ethylene: A Key Regulatory Molecule in Plants. Lausanne: Frontiers Media. doi: 10.3389/978-2-88945-341-2

Table of Contents

frontiers in Plant Science

EDITORIAL
published: 16 October 2017
doi: 10.3389/fpls.2017.01782

Editorial: Ethylene: A Key Regulatory Molecule in Plants

Nafees A. Khan[1], M. I. R. Khan[2], Antonio Ferrante[3] and Peter Poor[4]*

[1] Department of Botany, Aligarh Muslim University, Aligarh, India, [2] Crop and Environmental Sciences Division, International Rice Research Institute, Metro Manila, Philippines, [3] Department of Agricultural and Environmental Sciences, Università degli Studi di Milano, Milan, Italy, [4] Department of Plant Biology, University of Szeged, Szeged, Hungary

Keywords: ethylene, physiology, metaboilsm, phytohormones, signaling molecules

Editorial on the Research Topic

Ethylene: A Key Regulatory Molecule in Plants

Ethylene is a simple gaseous phytohormone with multiple roles in regulation of metabolism at cellular, molecular, and whole plant level (Pierik et al., 2006; Lin et al., 2009; Schaller, 2012; Khan N. A. and Khan M. I. R., 2014). It influences performance of plants under optimal and stressful environments by interacting with other signaling molecules (Müller and Munné-Bosch, 2015; Thao et al., 2015). The action of ethylene depends on its concentration in cell and the sensitivity of plants to the hormone (Pierik et al., 2006; Habben et al., 2014; Arraes et al., 2015; Sun et al., 2016). In recent years, research on ethylene has been focused due to its dual action on the regulation of plant processes at physiological and molecular level. The aim of the current research topic was to explore and update our understanding on its regulatory role of ethylene in plant developmental mechanisms at cellular or whole plant level under optimal and changing environmental conditions. The present edited volume includes original research papers and reviews articles describing ethylene's regulatory role in plant development during plant ontogeny and how it interacts with biotic and abiotic stress factors. For better understanding of the articles included in this volume, papers have been grouped into three categories.

OPEN ACCESS

Edited by:
Hong Qiao,
University of Texas at Austin,
United States

Reviewed by:
Jin-Song Zhang,
Institute of Genetics and Developmental Biology (CAS), China

****Correspondence:***
Nafees A. Khan
naf9@lycos.com

Specialty section:
This article was submitted to Plant Physiology, a section of the journal Frontiers in Plant Science

Received: *16 August 2017*
Accepted: *02 October 2017*
Published: *16 October 2017*

Citation:
Khan NA, Khan MIR, Ferrante A and Poor P (2017) Editorial: Ethylene: A Key Regulatory Molecule in Plants. Front. Plant Sci. 8:1782. doi: 10.3389/fpls.2017.01782

ROLE OF ETHYLENE IN DEVELOPMENTAL PROCESS

Flower Development and Fruit Ripening

The development of plants is well regulated by several processes working co-ordinately. This involves hormonal regulation in synchronization with other processes. Phytohormones influence plant development more precisely acting as a signaling molecule. The review article by Iqbal et al. emphasized the ethylene's roles in growth, development and senescence of leaves, flowers, and fruits. The ethylene controls longevity of plants that depends on ethylene level, its perception, and the hormonal crosstalk. It has been found that exogenously applied ethylene up-regulated *PhEIL2* gene and down-regulated *PhEIL3* gene, the genes responsible for flower senescence. Functional analysis of these two genes using VIGS system demonstrated that by silencing both *PhEIL2* and *PhEIL3* genes the flower life was significantly extended. In a study on silenced petunia lines, it was found that the expression of *PhERF3* and *PhCP2* genes was associated with ethylene production (Liu et al.). The EIN3 is an important transcription factor that regulates primary plant response to ethylene. The EIN3 regulates the gene expression by different DNA-binding sequences in the gene promoters. Results of the study on *EIN3/EIL1* binding sites and chromatin states in *Arabidopsis thaliana* showed that the chromatin state 4 was particularly important in regulation of plant response to ethylene. The homolog of *EIN3* of *Arabidopsis* in *Petunia* is the *EIL* gene and its role has been studied in flower senescence. The data confirms that EIN3 is the most important transcriptional regulator in the ethylene signaling pathway (Zemlyanskaya et al.).

Ethylene Response Factors (ERFs) have been reported to be involved in ethylene signaling and/or ethylene response, but little is known about their roles in fruit ripening. Fan et al. reported that ethylene plays an essential role in fruit ripening via modulation of ethylene signaling pathway by identifying DREB transcription factor with EAR motif, designated as *MaDEAR1*. They found that *MaDEAR1* binds to the DRE/CRT motifs in promoters of several cell wall-modifying genes, which repressed their activities and negatively involved in ethylene-mediated ripening of banana fruit. The study of Tranbarger et al. revealed that during fruit ripening of monocotyledonous plants and in particular in *Elaeis guineensis*, the ethylene induced cell wall and middle lamella expansion and degradation. This transition was regulated by different transcription factors some of them under ethylene regulation. The most important in the fruit ripening of this monocot has been found to be NAC domain transcription factors. Ethylene exposure studies revealed that the most inducible were *EgNAC6* and *EgNAC7* (Tranbarger et al.). The comparison of expression data of these genes with other eudicots could provide useful information on fruit ripening species evolution.

Growth and Nodulation

In this research topic, the interaction of ethylene and light on hypocotyl growth of *A. thaliana* has been reviewed (Yu and Huang). They showed that role of ethylene on hypocotyls growth under light or dark conditions could be ascertained through over-expression of ethylene production or inhibition of ethylene biosynthesis using *Arabidopsis* mutants. In light condition, ethylene induces the expression of *PHYTOCHROME INTERACTING FACTOR 3* (PIF3) and degradation of *ELONGATED HYPOCOTYL 5* (HY5), resulting in hypocotyl growth. In dark, instead, the suppression of hypocotyl development occurs by inducing the *ETHYLENE RESPONSE FACTOR 1* (ERF1) and *WAVE-DAMPENED 5* (WDL5) through the EIN3. This gene is additionally regulated by *CONSTITUTIVE PHOTOMORPHOGENIC 1* (COP1) and phytochrome B (phyB). Plant floral organ abscission is also one of the important developmental processes, which is mediated by ethylene. Wang et al. found that ethylene accelerated the organ abscission in *Arabidopsis* by regulating the expression of *AtDOF4.7* transcription factor and the peptide ligand *INFLORESCENCE DEFICIENT IN ABSCISSION* (*IDA*), which repressed expression of *AtDOF4.7*. MAPK cascades are involved in downstream of *IDA*-mediated abscission pathway. Wang et al. found *in vivo* interaction between MPK3/6 and AtDOF4.7 suggesting that AtDOF4.7 protein levels were regulated by this phosphorylation. Choong et al. showed that temperate crops cannot grow well in the tropics without root zone cooling. They reported that lower ethylene concentrations in root zone corresponded to higher shoot growth at cooler root zone temperatures; the cultivars that were less sensitive could be selected for agricultural purposes. Ma et al. observed that ethylene significantly inhibited postharvest peel browning in pear plants. In this study it was shown that protection of "Huangguan" pear from skin browning was possible through exogenous ethylene application. Genome wide identification and gene expression profiling during legume plant nodulation reveal that ethylene signaling pathway regulates nodulation in soybean (Wang et al.). They identified 11 ethylene receptor family genes in soybean through homology searches. The analysis of their expression patterns showed that these ethylene receptor genes are differentially expressed in various soybean tissues and organs, during rhizobia–host cell interactions and nodulation.

Interaction of Ethylene with Other Hormones

Liu et al. found an interaction of ethylene with methyl jasmonate (MeJA). They analyzed the phenolic compounds in *Catharanthus roseus* using a non-targeted metabolomics method. There were 34 phenolics, which belonged to 3 categories: 7 C6C1-, 11 C6C3-, and 16 C6C3C6-compounds, in addition to seven other metabolites. Among these compounds, vanillyl alcohol in leaves was elevated 50 times in the presence of ethylene and MeJA. However, in case of C6C3C6- type compounds, ethylene and MeJA presence exhibited an inhibitory effect. Explaining the interaction of ethylene and auxin, Abts et al. observed that the early root growth of sugar beet showed a biphasic ethylene response. The exogenously applied auxin (indole-3-acetic acid; IAA) induced root elongation in sugar beet by stimulating ethylene biosynthesis by redirecting the pool of available ACC toward ethylene instead of malonyl-ACC (MACC). In addition, IAA induced the expression of several *ACS* and *ACO* genes during seedling development suggesting that the general ethylene-auxin cross talk model was different in this plant. Ethylene in coordination with nitric oxide (NO) is also known to influence the cell cycle. Novikova et al. reported that ethylene and NO signaling interacts and plays important role in regulating cell cycle in *Arabidopsis*. They found that cell cycle progression was dependent on NO presence in the cells and on EIN2 (for ethylene production) in *Arabidopsis*.

ETHYLENE REGULATES RESPONSES OF PLANTS TO ABIOTIC STRESS CONDITIONS

Ethylene is regarded as a stress-responsive hormone besides its roles in regulation of plant growth and development (Khan M. I. R. and Khan N. A., 2014). In the current topic, Zapata et al. found that salt shock caused rapid increase in the production of ethylene, ACC and polyamine concentrations both in shoots and roots of the four investigated plant species, which were related in the sensitivity to salt stress. In salt tolerant plants, ethylene production was lower, which was found still higher in the most sensitive one. Moreover, they did not observe any competition between polyamines and ethylene biosynthesis for their common precursor, S-adenosylmethionine (SAM). In tomato, it has been demonstrated that ethylene biosynthesis is influenced by the vigor of rootstock in grafted plants and potassium availability. In particular, results showed that low ACC content was able to improve K^+ uptake in grafted tomato plants. The effect of ethylene was the outcome of the interaction with other plant hormones. It is considered a negative ethylene regulation since

high biosynthesis has been found associated with low tolerance of plants to K^+ deficiency (Martínez-Andújar et al.). Pan et al. found the role of ethylene in antagonizing salt induced growth retardation and cell death process by transcription controlling of ethylene-BAG and senescence associated genes in *Arabidopsis*. Ethylene and salinity antagonistically controlled BAG family, ethylene, and senescence related genes to alleviate the salt induced cell death. Abozeid et al. reported that ethylene played a role in modulating root morphogenesis under cadmium stress in *A. thaliana* by increase in the activity of SOD isoenzymes. It was noted that ethylene-insensitive mutants (*ein2-5* and *ein3-1eil1-1*) have decreased root growth compared to wild type Col-0 along with increased superoxide concentration in roots of *ein2-5* and *ein3-1*, *eil1-1*. However, application of exogenous ACC (precursor of ethylene biosynthesis) decreased superoxide accumulation in Col-0 root tips and increased the activity of SOD isoenzymes under Cd stress. Khan et al. found that exogenous application of ethylene with sufficient sulfur level counteracted the cadmium-induced photosynthetic and growth inhibition in mustard plants. They reported that the combined application of ethephon and sulfur synergistically improved photosynthetic performance under the stress condition by reducing oxidative stress, ethylene and glucose sensitivity. On the other hand, the better performance of plants was correlated with increase in cysteine and methionine content and reduced glutathione (GSH) contents. Valluru et al. selected two wheat genotypes as drought-tolerant and drought-sensitive and observed the effect on endogenous ethylene and abscisic acid (ABA). Both the drought tolerant and drought sensitive groups increased endogenous ethylene and ABA concentrations under mild drought condition. Further, they observed that shoot dry weight of the drought tolerant and drought sensitive groups distinctly regulated by specific ABA: ethylene ratio. Application of exogenous ABA and ethylene increased relative growth rate in both groups compared to control with increased carbohydrate content. A review by Li and Lan showed that Fe deficiency developed hindrance in various physiological, morphological, metabolic, and gene expression changes with cellular Fe homeostasis in strategy I plants, and ethylene was involved in Fe deficiency responses of plants. Additionally, the review highlighted a way to find out how ethylene participates in the Fe deficiency response via integration of important genes and proteins, regulated both by Fe deficiency, and ethylene into a systemic network by gene co-expression analysis.

ETHYLENE REGULATES RESPONSES OF PLANTS TO BIOTIC STRESS CONDITIONS

The role of ethylene in plants exposed to biotic stress has been studied in different crops and different diseases. In this research topic, Wang et al. have shown that ethylene plays a pivotal role in the sensitivity to *Alternaria alternata* in sand pear (*Pyrus pyrifolia*). The two cultivars used in the study were Cuiguan (tolerant cultivar) and Sucui1 (sensitive cultivar). High ethylene production induced fungus development, while low ethylene evolution was associated to plant resistance (Wang et al.). In both the cultivars a correlation was found between ethylene biosynthesis and detoxifying enzyme activities. In particular, a close relationship was found between ethylene and catalase (CAT) activity. In sensitive cultivar, it was found that high ethylene biosynthesis associated with high level of hydrogen peroxidase and low CAT activity were the favorable conditions for *A. alternata* development and programmed cell death (PCD) induction. Analogously, it has been shown that ethylene has a primary role in endophytic fungi growth as observed in *Atractylodes lancea*. The endophytic fungus *Gilmaniella* sp. AL12 induced ethylene in *A. lancea* and subsequently the accumulation of sesquiterpenoids. The ethylene seems to play an upstream regulation of sesquiterpenes biosynthesis, interacting with other plant hormones such as jasmonic acid and salicylic acid (Yuan et al.).

Wang et al. showed that ethylene was involved in the susceptibility of maize to *Aspergillus flavus*. Interestingly, both colonization and conidiation of *A. flavus* were reduced in kernels treated with ethylene biosynthesis inhibitor. Surprisingly, kernels of *acs2* and *acs6*, in case of the two ethylene biosynthetic mutants, displayed enhanced seed colonization and conidiation, but without increasing the levels of aflatoxin after the infection. These results suggested that ethylene emitted by infected seeds facilitated colonization by *A. flavus* but without any aflatoxin production. Boex-Fontvieille et al. reported that exogenous application of ethylene precursor ACC and wounding strongly up-regulated the HEC1-dependent Kunitz-protease inhibitor 1 (Kunitz-PI;1) gene expression in apical hook of etiolated *Arabidopsis* seedlings. They summarized that the ethylene-triggered expression of *Kunitz-PI;1* contributed to the protection of seedlings against herbivorous arthropods such as *Porcellioscaber* (woodlouse) and *Armadillidium vulgare* (pillbug), because it can play role in the herbivore deterrence by inhibiting the digestive proteases.

Frontiers research topic provides an excellent platform and opportunity to publish perspective papers in ethylene biology research. Contributed authors significantly attempted a solution for abiotic and biotic stresses tolerance via ethylene manipulation. Additionally, authors also gave a depth insight into the understanding the role of ethylene in growth and development of plants. Altogether, the research topic as presented here documents recent advances in ethylene biology research. In the present volume, numbers of problems from basics to applied scientific knowledge-based questions were addressed and drive plant scientists for a common future goal through this research topic.

AUTHOR CONTRIBUTIONS

All authors listed have made a substantial, direct and intellectual contribution to the work, and approved it for publication.

REFERENCES

Arraes, F. B. M., Beneventi, M. A., de Sa, M. E. L., Paixao, J. F. R., Albuquerque, E. V. S., Marin, S. R. R., et al. (2015). Implications of ethylene biosynthesis and signaling in soybean drought stress tolerance. *BMC Plant Biol.*15:213. doi: 10.1186/s12870-015-0597-z

Habben, J. E., Bao, X., Bate, N. J., DeBruin, J. L., Dolan, D., Hasegawa, D., et al. (2014). Transgenic alteration of ethylene biosynthesis increases grain yield in maize under field drought-stress conditions. *Plant Biotech. J.* 12, 685–693. doi: 10.1111/pbi.12172

Khan, M. I. R., and Khan, N. A. (2014). Ethylene reverses photosynthetic inhibition by nickel and zinc in mustard through changes in PS II activity, photosynthetic nitrogen use efficiency, and antioxidant metabolism. *Protoplasma* 251, 1007–1019. doi: 10.1007/s00709-014-0610-7

Khan, N. A., and Khan, M. I. R. (2014). The Ethylene: from senescence hormone to key player in plant metabolism. *J. Plant Biochem. Physiol.* 2:e124. doi: 10.4172/2329-9029.1000e124

Lin, Z., Zhong, S., and Grierson, D. (2009). Recent advances in ethylene research. *J. Exp. Bot.* 60, 3311–3336. doi: 10.1093/jxb/erp204

Müller, M., and Munné-Bosch, S. (2015). Ethylene response factors: a key regulatory hub in hormone and stress signaling. *Plant Physiol.* 169, 32–41. doi: 10.1104/pp.15.00677

Pierik, R., Tholen, D., Poorter, H., Visser, E. J., and Voesenek, L. A. (2006). The Janus face of ethylene: growth inhibition and stimulation. *Trends Plant Sci.* 11, 176–183. doi: 10.1016/j.tplants.2006.02.006

Schaller, G. E. (2012). Ethylene and the regulation of plant development. *BMC Biol.* 10:9. doi: 10.1186/1741-7007-10-9

Sun, X., Zhao, T., Gan, S., Ren, X., Fang, L., Karungo, S. K., et al. (2016). Ethylene positively regulates cold tolerance in grapevine by modulating the expression of ETHYLENE RESPONSE FACTOR 057. *Sci. Rep.* 6:24066. doi: 10.1038/srep24066

Thao, N. P., Khan, M. I. R., Thu, N. B. A., Hoang, X. L. T., Asgher, M., Khan, N. A., et al. (2015). Role of ethylene and its cross talk with other signaling molecules in plant responses to heavy metal stress. *Plant Physiol.* 169, 73–84. doi: 10.1104/pp.15.00663

Conflict of Interest Statement: The authors declare that the research was conducted in the absence of any commercial or financial relationships that could be construed as a potential conflict of interest.

frontiers in Plant Science

REVIEW
published: 04 April 2017
doi: 10.3389/fpls.2017.00475

Ethylene Role in Plant Growth, Development and Senescence: Interaction with Other Phytohormones

Noushina Iqbal[1], Nafees A. Khan[2], Antonio Ferrante[3], Alice Trivellini[4], Alessandra Francini[4] and M. I. R. Khan[5]**

[1] Department of Botany, Jamia Hamdard, New Delhi, India, [2] Plant Physiology and Biochemistry Laboratory, Department of Botany, Aligarh Muslim University, Aligarh, India, [3] Department of Agricultural and Environmental Sciences, Università degli Studi di Milano, Milano, Italy, [4] Institute of Life Sciences, Scuola Superiore Sant'Anna, Pisa, Italy, [5] Crop and Environmental Sciences Division, International Rice Research Institute, Manila, Philippines

The complex juvenile/maturity transition during a plant's life cycle includes growth, reproduction, and senescence of its fundamental organs: leaves, flowers, and fruits. Growth and senescence of leaves, flowers, and fruits involve several genetic networks where the phytohormone ethylene plays a key role, together with other hormones, integrating different signals and allowing the onset of conditions favorable for stage progression, reproductive success and organ longevity. Changes in ethylene level, its perception, and the hormonal crosstalk directly or indirectly regulate the lifespan of plants. The present review focused on ethylene's role in the development and senescence processes in leaves, flowers and fruits, paying special attention to the complex networks of ethylene crosstalk with other hormones. Moreover, aspects with limited information have been highlighted for future research, extending our understanding on the importance of ethylene during growth and senescence and boosting future research with the aim to improve the qualitative and quantitative traits of crops.

Keywords: ethylene, flower senescence, fruit ripening, leaf senescence, phytohormones, VOCs

OPEN ACCESS

Edited by:
Wim Van den Ende, KU Leuven, Belgium

Reviewed by:
Bram Van De Poel, KU Leuven, Belgium
Ravi Valluru, Cornell University, USA

****Correspondence:***
Antonio Ferrante
antonio.ferrante@unimi.it
M. I. R. Khan
amu.iqbal@gmail.com

Specialty section:
This article was submitted to Plant Physiology, a section of the journal Frontiers in Plant Science

Received: *10 October 2016*
Accepted: *17 March 2017*
Published: *04 April 2017*

Citation:
Iqbal N, Khan NA, Ferrante A, Trivellini A, Francini A and Khan MIR (2017) Ethylene Role in Plant Growth, Development and Senescence: Interaction with Other Phytohormones. Front. Plant Sci. 8:475. doi: 10.3389/fpls.2017.00475

INTRODUCTION

The growth and development of plants under varied environmental conditions determine agricultural production. The growth, development, and senescence of plant's organs can influence crop production by modulating photosynthesis, nutrient remobilization efficiency, and harvest index (Paltridge et al., 1984; Jing et al., 2005; Iqbal et al., 2012). Phytohormones have been shown to increase growth and yield of plants. The phytohormone ethylene controls growth and senescence of plants (Reid, 1995; Lutts et al., 1996; Thompson et al., 1998; Pierik et al., 2006; Masood et al., 2012; Nazar et al., 2014). Ethylene is regarded as a multifunctional phytohormone that regulates both growth, and senescence. It promotes or inhibits growth and senescence processes depending on its concentration, timing of application, and the plant species. The application of ethephon, an ethylene releasing compound enhanced ethylene evolution and increased leaf area of mustard at a lower concentration, while inhibited at higher concentration (Khan, 2005; Khan et al., 2008).

Ethylene governs the development of leaves, flowers, and fruits. It may also promote, inhibit or induce senescence depending upon the optimal or sub-optimal ethylene levels (Konings and Jackson, 1979; Khan, 2005; Pierik et al., 2006). It appears quite interesting to examine how the same hormone influences the two contradictory processes of growth and senescence. This review covers the discussion on the role of ethylene in the growth and development and explores its interaction with other hormones in regulating these processes.

LEAF GROWTH AND DEVELOPMENT

Ethylene

Leaf growth and development are affected by various environmental factors and endogenous hormonal signals (**Table 1**). These processes are regulated by phytohormones, transcriptional regulators and mechanical properties of the tissue (Bar and Ori, 2014). The role of ethylene in the leaf growth and development has been confirmed physiologically using ethylene inhibitors, and genetically using ethylene-insensitive mutants or transgenic plants lacking the key enzymes of ethylene biosynthesis (Oh et al., 1997; Bleecker et al., 1998). It has been observed that ETHYLENE RESPONSE FACTOR5 (ERF5) and ERF6, in *Arabidopsis,* improve leaf growth to environmental challenges (Dubois et al., 2015). The response of leaf growth and development to ethylene depends on concentration and species involved in the study (Fiorani et al., 2002; Kawa-Miszczak et al., 2003; Khan, 2005). In support of this, Fiorani et al. (2002) showed that the slower growing species of *Poa* (*Poa alpina* and *Poa compressa*) were more responsive to ethylene, with greater inhibition in leaf elongation than the fast growing species. However, a promoting effect on leaf elongation rate at a low ethylene concentration was observed in the slower growing species, while at the same concentration, leaf elongation rate was only slightly inhibited in the two fast-growing species. This response was reversed at higher concentrations, showing an inhibition effect. The study of Khan (2005) on mustard suggested that there exists a correlation between ethylene and growth of plants following the defoliation of mature leaves. Furthermore, ethylene-insensitive genotypes of *Arabidopsis* (*Arabidopsis thaliana*), tobacco (*Nicotiana tabacum*) and petunia (*Petunia x hybrid*) showed no increase in the total leaf area when compared to normal ethylene-sensitive control plants (Tholen et al., 2004). Treatment with ethephon, a compound that releases ethylene, resulted in an increase in both ethylene biosynthesis and leaf area expansion (Khan, 2005; Khan et al., 2008). In contrast, Voisin et al. (2006) determined that the rate of ethylene evolution had no relation to the leaf elongation rate variability in maize (*Zea mays*). Ethylene-induced reductions in leaf growth have been reported in pea (*Pisum sativum*) plants, around which rhizobacteria with enhanced ACC deaminase activity were added to soil (Belimov et al., 2009). Interestingly, the lower leaf area was observed in lettuce (*Lactuca sativa*) grown in closed environments, where ethylene produced from the plants reached stressful levels. The plants showed lower relative leaf growth rates compared to those grown in containers from which the ethylene had been scrubbed (He et al., 2009). This reduced leaf area was an indirect effect of ethylene on the leaf epinasty with reduced light capture, and/or on a reduced CO_2 assimilation, which was found to be more sensitive to the ethylene increase than the reduction in growth. Both reactive oxygen species (ROS) and nitric oxide (NO), which could be potentially up-regulated by ethylene, have also been involved in leaf expansion (Wilkinson and Davies, 2010).

The ethylene effect on leaf growth and development may be independent or dependent on its interaction with other hormones. Multiple receptors of one phytohormone might be involved in non-redundant responses, either in different tissues, at different developmental stages, or upon different environmental cues.

Interaction between Ethylene and Other Hormones during Leaf Growth and Development

The following section highlights the interaction of ethylene with other hormones and plant responses during leaf growth and development.

Ethylene and Auxin

The action of ethylene on leaf growth may be auxin-dependent or auxin-independent. Hormonal coordination is an important aspect, which regulates leaf growth processes. Auxin induces ethylene production, and many effects of exogenous auxins are, in fact, ethylene responses (Abeles et al., 1992). Auxin plays an important role in leaf development and it is potentially able to increase shoot apical meristem at the time of leaf initiation, through increased auxin biosynthesis (Cheng et al., 2007; Pinon et al., 2013). Auxin regulates the initiation of the new leaves in tomato (*Solanum lycopersicum*) (Reinhardt et al., 2000), leaf vascular development (Mattsson et al., 2003), and cell division phase during leaf expansion (Ljung et al., 2001) in *Arabidopsis*. In *Arabidopsis*'s shoot, the radial position and the size of the leaf during organ formation were mediated by indole-3-acetic acid (IAA) (Reinhardt et al., 2000).

Studies have shown that leaf epinasty could be attributed to auxin-stimulated ethylene or an activity of auxin alone (Abeles et al., 1992; Sterling and Hall, 1997; Grossmann, 1998; Hansen and Grossmann, 2000). The inhibition of leaf growth induced by auxin was found to be independent of ethylene in common bean (*Phaseolus vulgaris*) plants (Keller et al., 2004). The inhibition of ethylene by applying 1 mM ethylene synthesis inhibitor aminooxyacetic acid (AOA) with 1 mM IAA did not affect auxin-induced inhibition of leaf growth. The daily application of 1 mM AOA alone did not affect leaf growth, but over a 24-h period, a 1 mM AOA treatment was effective as an inhibitor of ethylene biosynthesis in detached common bean leaves.

Ethylene and Cytokinin

The reports on the interaction between ethylene and cytokinin are scanty. However, cytokinin may play an important role in leaf initiation through the maintenance of S-adenosyl-methionine (SAM); an immediate metabolite for biosynthesis of ethylene (Kurakawa et al., 2007; Gordon et al., 2009). Cytokinins regulate a wide range of growth and developmental processes throughout

the life cycle of a plant, including seed germination, leaf expansion, induction of flowering, as well as flowering and seed development (Sun and Gubler, 2004; Yamaguchi, 2008). In Zea mays, the response regulator (RR) protein ABPHYL1 (ABPH1), together with PIN1, was also expressed at the site of future leaf initiation, and both are induced by the cytokinins (Lee et al., 2009). ABPH1 positively regulates organ initiation, perhaps by inhibiting the cytokinins response. Carabelli et al. (2007) showed that CKX6, a cytokinin oxidase/hydrolase, was induced in the simulated shade and promoted cytokinin depletion specifically in pre-procambial cells of developing leaf primordial, substantiating the role of cytokinin breakdown in the inhibition of leaf development during shade avoidance. The CKX6 induction has been reported to be an auxin response and was mediated by the auxin receptor TIR1. Thus, auxins and cytokinins act synergistically in leaf development. However, more efforts should be done to gain a better understanding on the crosstalk of ethylene with cytokinins in the whole context especially on the link between SAM and cytokinins regulation.

Ethylene and Gibberellins

Gibberellins (GA) play a role in the leaf expansion. Spraying dilute aqueous GA solutions to leaves and stems of potato caused lesser internode growth with larger leaf growth and mature leaves (Humphries, 1958). The response of GA on the leaf development showed photoperiodic regulation of the leaf elongation in bluegrass (*Poa pratensis*), and indicated a photoperiodic control of oxidation of GA_{53} to GA_{44} and GA_{19} to GA_{20}, and also of 3 β-hydroxylation of GA_{20} to GA_1 (Junttila et al., 1997). Limited water sources can also cause reductions in leaf size (Sack et al., 2003; Royer et al., 2005). In *Arabidopsis*, these responses were at least in part executed by ethylene response factors and GA catabolism (Dubois et al., 2013).

The crosstalk between ethylene and GA was revealed from the study of Achard et al. (2006), who found that the destabilization of DELLA proteins induced by GA was modulated by environmental signals and the plant hormone signaling (such as auxin and ethylene). De Grauwe et al. (2008) reported that a functional GA response pathway was required for the increased ethylene biosynthesis in eto2-1 (ethylene overproducing mutant) since the gai eto2-1 (GA-insensitive; ethylene overproduction) double mutant did not overproduce ethylene, suggesting that the stability of the ACS5 protein was dependent on GA. The GA-signaling cascade appeared to be regulated by ethylene in GIBBERELLIN INSENSITIVE DWARF1 (GID1c) (more than twofold induction after ethylene treatment) (Zimmermann et al., 2004; Dugardeyn et al., 2008). The relationship between ethylene signaling and the GA–GID1–DELLA mechanism has shown that ethylene inhibited the seedling growth DELLA-deficient mutant Arabidopsis less than wild type. However, ethylene inhibited the GA-induced disappearance of GFP-RGA via CTR1-dependent signaling (Achard et al., 2003), indicating an antagonistic relation between ethylene and GA. Dubois et al. (2013) reported that under osmotic stress in actively growing leaves, the expression of ERF5 and ERF6 gene was induced. The expression of ERF6 gene inhibited the cell proliferation and growth of leaves and the inhibition was dependent on gibberellin and DELLA signaling. ERF6 provides a link between 1- aminocyclopropane 1 carboxylic acid (ACC), the ethylene forming enzyme and DELLA signaling in the cell cycle pause-and-stop model, improving our understanding of growth inhibition in the proliferating leaf primordia of plants subjected to water limitation.

Ethylene and Abscisic Acid

Abscisic acid (ABA) may limit ethylene production to enhance leaf growth (Hussain et al., 2000). Normal levels of endogenous ABA maintains leaf expansion in *Arabidopsis*, partly through limiting ethylene biosynthesis and partly by another mechanism that is independent of ethylene. To analyze how ABA functions by ethylene suppression, LeNoble et al. (2004) studied ABA-deficient (*aba2-1*) and ethylene-insensitive (*etr1-1*) single and double mutants of *Arabidopsis*. Shoot growth was found to be inhibited in ABA-deficient *Arabidopsis*. Exogenous treatment with ABA resulted in the complete recovery of shoot growth in *aba2-1* relative to wild type, and also significantly increases growth of *aba2-1 etr1-1*. The total leaf area and shoot fresh weight were not significantly lower than in *etr1-1*. ABA from avocado (*Persea americana*) induced formation of "floating-type"

TABLE 1 | Some representative studies in relation to the effect of ethylene on leaf growth, development and senescence.

Plant Species	Ethylene treatments	Effect on plants	Reference
Cotton (*Gossypium hirsutum*)	12 $\mu L\ L^{-1}$ of ethylene at 18 l min^{-1}	Leaf abscission in plants 5 weeks olds	Beyer, 1976
Rice (*Oryza sativa*)	Submergence condition (7 days) with 1 $\mu L\ L^{-1}$ in the internods	Stimulate the internodes growth 3–5 fold	Métraux and Kende, 1983
Celery-leaved buttercup *(Ranunculus sceleratus)*	10–50 nL mL^{-1} ethylene	Increased 4–5 times petiole growth	Musgrave and Walters, 1973
Maize (*Zea mays*)	0.1–5.0 $\mu L\ L^{-1}$ ethylene	Inhibited leaf extension	Jackson et al., 1981
Arabidopsis (*Arabidopsis thaliana*)	Col-0 plants exposed to 1–5 $\mu L\ L^{-1}$ ethylene	Strong hyponastic response of leaf	Millenaar et al., 2005
Oat (*Avena sativa*)	0.2 Mm ACC	Leaf chlorophyll loss followed by leaf senescence.	Gepstein and Thimman, 1987
Potato (*Solanum tuberosum*)	5 nL L^{-1}	Severe leaf senescence symptoms such as yellowing, epinasty and lack of growth	Özgen et al., 2005
Rocket salad (*Eruca sativa*)	1 $\mu L\ L^{-1}$	Leaf chlorophyll loss	Koukounaras et al., 2006

leaves in American pondweed (*Potamogetgon nodosus*) at low concentration (5×10^{-7} M) (Anderson, 1982). The influence of the ABA on the leaf growth could be through increased conductance to water transfer in plants as a result of an increased tissue hydraulic conductivity (Tardieu et al., 2010).

LEAF SENESCENCE

Ethylene

Ethylene has an important role in the regulation of leaf senescence. Ethylene is one of the most important hormones in the leaf senescence regulation (**Table 1**). Ethylene can trigger the senescence process, especially in the sensitive species. The ethylene biosynthesis is higher during the first stage of leaf formation and declines until it reaches maturity when the leaf is completely expanded, then it increases again during the early step of the senescence initiation. The ACC content only increases in senescing leaves and shows the same pattern of ethylene production (Hunter et al., 1999). At the molecular level, it has been shown that different genes of the same family encode for the enzymes of ethylene biosynthesis that are activated during leaf development and their expression is timely regulated (Hunter et al., 1999). The biosynthesis occurs in any part of the plant and at any stage of leaf development. Consequently, the biological responses depend on the tissue sensitivity. The exposure of plant sensitive to ethylene induces premature senescence symptoms such as leaf yellowing, abscission, or desiccation/necrosis. The plant responses to ethylene vary considerably between and within species and are modulated by differential hormonal sensitivity. The visual symptoms of leaf senescence are represented by chlorophyll degradation and the leaf abscission (Lewington et al., 1967; Gepstein and Thimman, 1987). At the molecular level, ethylene has been shown to be involved in the organized cell dismantling and the activation of nutrients recycling from senescing leaves to the other organs. Leaf cells undergo a sequential and organized dismantling process which includes nucleic acid reduction, protein degradation, and turnover reduction, (Lutts et al., 1996), membrane disruption, lipid degradation, peroxidation (Buchanan-Wollaston, 1997; Thompson et al., 1998; Buchanan-Wollaston et al., 2003), and leaf pigment breakdown (Matile et al., 1996).

Leaf senescence is activated at the mature stage of leaf development when leaves are fully expanded. During leaf senescence, three different stages can be identified: initiation, organization of degradation, and death processes.

The most common visible symptom of leaf senescence is the yellowing caused by the chlorophyll degradation and its impaired biosynthesis. The initial step of chlorophyll breakdown is catalyzed by chlorophyllase that convert chlorophyll *a* and *b* to chlorophyllide and phytol (Matile et al., 1996). Chlorophyll loss increases after ethylene exposure in different cut flowers such as stock (*Matthiola incana*) and chrysanthemum (*Dendranthema grandiflora*; Reyes-Arribas et al., 2001) and many other flowers (Ferrante et al., 2004, 2005, 2009). Özgen et al. (2005) have reported that the signs of senescence induced by ethylene include malformed, thickened leaves, lack of growth and epinasty. Tobacco leaves treated for 24 h showed higher chlorophyll degradation but did not anticipate the increase in ethylene biosynthesis and respiration, typically of the climacteric trend (Aharoni and Lieberman, 1979). The effect of ethylene was found tightly associated with leaf age as demonstrated in old *Arabidopsis* mutants and also depended on the length of the treatment (Jing et al., 2005). The chlorophyll reduction has also been observed in rocket salad (*Eruca sativa*) leaves exposed to 1 μL L^{-1} during storage, a condition that shortens the shelf life by approximately 2 days (Koukounaras et al., 2006). Another effect induced by ethylene on leaf senescence is the abscission or induction of necrosis. Leaf abscission is a coordinated process, which involves several structural changes in the cells located in the abscission zone. It is a seasonal process that normally occurs in deciduous plants (Taylor and Whitelaw, 2001), where ethylene and auxins also have a crucial role.

Interaction between Ethylene and Other Hormones during Leaf Senescence

Plant hormones can repress or enhance leaf senescence in plants or after harvest. This section gives an insight into the interaction of ethylene with other hormones and provides responses during leaf senescence.

Ethylene and Auxin

Leaf senescence is affected by auxin content and ethylene biosynthesis (Ferrante and Francini, 2006). In particular, leaf abscission is under the control of auxin and ethylene. Burg (1968) suggested that ethylene caused leaf abscission *in vivo* by inhibiting auxin synthesis and transport or enhancing auxin degradation, thus, lowering diffusible auxin level. In the abscission zone, ethylene and auxin act antagonistically and auxin concentrations were associated with tissue sensitivity to ethylene. The equilibrium between ethylene and auxin is crucial for the regulation of leaf abscission. During leaf senescence, the auxin concentration declined and tissue sensitivity to ethylene increased as well as ethylene biosynthesis (Brown, 1997). Using a transcriptome approach, 1,088 transcription factors (TFs) were found to be differentially regulated in the soybean leaf abscission. Among these, 188 TFs were differentially expressed in the abscission zone (Kim et al., 2016). Ethylene and auxin were strongly regulated by these transcription factors. However, the exogenous applications of these hormones also regulated the expression of these genes delaying or anticipating the leaf senescence and abscission. Riov and Goren (1979) suggested that ethylene inhibited auxin transport in the veinal tissues and reduced the amount of auxin transported from the leaf blade to the abscission zone in orange (*Citrus sinensis*), necklace poplar (*Populus deltoids*), and eucalyptus (*Eucalyptus camaldulensis*). La Rue (1936) showed that the removal of leaf blade induced abscission, but the application of auxin to the site of removal resulted in the inhibition of abscission. Ethylene has been shown to play an antagonistic role to auxins in the abscission of various organs. Abscission was delayed in the ethylene-insensitive *Arabidopsis* mutants *ein2* and *etr1-1* (Patterson and Bleecker, 2004), while ethylene application hastened abscission in various organs and species. Ethylene induced the expression of a

polygalacturonase which is required for cell separation in tomato petioles (Hong et al., 2000; Jiang et al., 2008) and interestingly this polygalacturonase was inhibited by the exogenous auxin. This suggested the antagonistic effects of auxin and ethylene in the abscission.

Ethylene and Cytokinins

Cytokinins can suppress leaf senescence leading to greater retention of chlorophyll known as Richmond and Lang (1957) demonstrated. The effect of cytokinins on leaf senescence was demonstrated by the autoregulation of cytokinins biosynthesis during senescence using an isophentenyl transferase (*IPT*) gene under the regulation of senescence-associated gene 12 (*SAG12*) promoter (Gan and Amasino, 1995). This promoter has been widely used to activate genes expression during senescence. The SAG12 gene encodes for a cysteine protease that was activated during senescence independently from the trigger events. Therefore, the *SAG12* promoter can have great application in the agricultural science and the postharvest sector. Deletion studies on the *SAG12* promoter demonstrated that young and mature leaves contained factors that exhibited differential binding to the senescence responsive promoter element (Noh and Amasino, 1999). The construct *SAG12::IPT* gene has been studied in different species and all showed delayed senescence. This strategy was effective in delaying leaf senescence in several crops such as alfalfa (*Medicago sativa*; Calderini et al., 2007), broccoli (*Brassica oleracea*; Chen et al., 2001), cassava (*Manihot esculenta*; Zhang et al., 2010), creeping bentgrass (*Agrostis stolonifera*; Xu et al., 2009), lettuce (McCabe et al., 2001), petunia (Chang et al., 2003), rose (*Rosa hybrid*; Zakizadeh et al., 2013), tobacco (Jordi et al., 2000), and wheat (*Triticum aestivum*; Sýkorová, 2008). The senescence delay reduced ethylene biosynthesis in the transformed plants. The exogenous application of cytokinins in potted and cut flowers delayed the leaf yellowing and decreased ethylene biosynthesis. The 6-benzyladenine (BA) applied as pulse treatments successfully delayed leaf yellowing in cut goldenrod (*Solidago canadensis*; Philosoph-Hadas et al., 1996), potted lilies (*Lilium longiflorum*; Han, 1997), and cut Peruvian lily (*Alstreomeria*) flowers (Mutui et al., 2003). The effect of BA treatment on the ethylene is due to the inhibition of leaf senescence that leads to lower ethylene biosynthesis.

Ethylene and Gibberellins

Gibberellins are considered as leaf senescence inhibitors and are able to avoid or delay leaf yellowing. Gibberellins are commonly used as postharvest treatments in several cut flowers to prevent the leaf yellowing (Ferrante et al., 2009). The reduction of functional gibberellins content or the conjugation of them with glucose (inactivation) induced leaf yellowing in several sensitive species. The exogenous applications are able to delay senescence and reduce ethylene biosynthesis. In cut stock flowers, the gibberellin 3 (GA_3) applications did not enhance the ethylene biosynthesis, but strongly increased ethylene production, combining with thidiazuron (TDZ) (Ferrante et al., 2009). However, leaf yellowing was not affected by the ethylene production. This showed that the tissues were insensitive to ethylene because the leaves probably were not ready to senesce. However, further research should be taken into consideration to reveal the exact role of both the hormones in leaf senescence.

Ethylene and Abscisic Acid

Abscisic acid is considered a leaf senescence inducer and its exogenous applications lead to leaf senescence in mature leaves of different crops. The ABA content increased during leaf senescence and the exogenous treatment with ABA accelerate the leaf senescence (Oh et al., 1997; Yang et al., 2003). The *saul1* mutant (Senescence-Associated E3 Ubiquitin Ligase 1) naturally exhibited an accelerated leaf senescence phenotype with an increase of the ABA level, providing genetic evidence of the ABA signaling role during leaf senescence (Raab et al., 2009). The use of *ore* mutants which showed a delayed leaf senescence phenotypes in the following treatments with ABA and ACC suggested that ORE1, ORE3, and ORE9 were required for the proper progression of leaf senescence mediated by both ABA and ethylene (Kim et al., 2011).

FLOWER DEVELOPMENT

Ethylene

The floral transition is a major progress in the plant's life cycle that signals the onset of conditions favorable for reproductive success (Simpson and Dean, 2002). The exact timing of flowering can be controlled by the plant-environment interaction and endogenous developmental competence of plants to flower, which allows the transition from the vegetative phase to a reproductive phase (Lin et al., 2009). Changes in the levels of ethylene influence the genetic circuits that integrate different signals for the regulation of flowering timing. In *Arabidopsis*, through the growth comparison of ethylene-related mutants, *eto1*, *etr1*, *ein2-1* and *ein3-1*, with the wild-type (WT), the regulatory role of ethylene in the transition from vegetative to reproductive growth in *Arabidopsis* was discovered (Ogawara et al., 2003). The ethylene-overproducing mutant *eto1*, produces an excessive amount of ethylene (Guzman and Ecker, 1990) by affecting the post-transcriptional regulation of a key enzyme of ethylene biosynthesis, the 1-aminocyclopropane-1-carboxylic acid synthase (ACS) (Woeste et al., 1999), whereas the *ein2-1*, *ein3-1* and *etr1* mutants are insensitive or had a reduced sensitivity to ethylene (Bleecker et al., 1988; Guzman and Ecker, 1990). These perturbations in the ethylene signaling may flow large or less amount of ethylene signal respectively, into the hormonal pathway leading to an early- or late-flowering phenotype compared to WT (Ogawara et al., 2003). However, the effects of ethylene in the regulation of flower transition appear complex. In fact, the mutation of Ser/Thr kinases *CTR1* (At*ctr1*), which is the key negative regulator of ethylene signaling and the ACC-treated WT showed delayed flowering, indicating that ethylene inhibited flowering in *Arabidopsis* (Achard et al., 2007). In addition, contrasting roles of ethylene have been noticed in rice (*Oryza sativa*). Ethylene promotes a reproductive transition in rice through the activity of its receptor protein *OsETR2* (Wuriyanghan et al., 2009). In this study, the overexpression of *OsETR2* reduced ethylene sensitivity and delayed flower

development, whereas the knockdown mutations of *OsETR2*, *OsETR3*, and *OsERS2* exhibited enhanced ethylene sensitivity and early flowering. Conversely, flowering time was delayed in *Osctr2* loss-of-function and *35S:OsCTR2* transgenic lines, indicating that ethylene represses the floral transition in rice (Wang Q. et al., 2013). These evidences suggest that ethylene signaling delays flowering in both rice and *Arabidopsis*. On the other hand, exogenous ethylene, or ethephon, has been widely used to induce flowering of Bromeliads, such as *Ananas comosus* and *Aechmea fasciata*, as well as early sprouting, early flowering and formation of more flowers per inflorescence in dormant corms of common triteleia (*Triteleia laxa*; Han et al., 1989). Furthermore, an inhibitor of ethylene biosynthesis, amino vinylglycine (AVG), can delay the natural flowering of pineapple (Kuan et al., 2005). Trusov and Botella (2006) proposed that the pineapple flowering is triggered by a small burst of ethylene production in the meristem in response to environmental cues through the induction of ACC synthase gene *AcACS2*. Moreover, the silencing of this gene *AcACS2* has been shown to delay flowering in pineapple. Overall, these results are consistent with ethylene having a fundamental role in flower development and may be related to different endogenous and external cues, which affected the ethylene signaling components.

Flower development occurs through a series of sequential steps required for the cell proliferation proper regulation, expansion, and the reproductive tissue development. The expression of ethylene biosynthesis genes seems to be linked to the formation of particular flower tissues. In tobacco, ACC oxidase (*ACO*) gene was expressed in early developing stigma, style, and ovary (De Martinis and Mariani, 1999). In tomato, *LeACO1*,*2*,*3*, and *4* and *LeACS1A* transcripts were detected in pistils (Llop-Tous et al., 2000). In the China rose (*Hibiscus rosa-sinensis*), *ACS* and *ACO* were found to be specifically expressed in developing style–stigma plus stamen and ovary tissues (Trivellini et al., 2011a). Similar evidence has been reported in carnation (*Dianthus caryophyllus*) and petunia (Tang et al., 1994; Jones, 2002), and may indicate that ethylene plays a role in the reproductive process during the development of flowers. Ethylene receptors are involved in reproductive organ development. In China rose *HrsETR* and *HrsERS* transcript levels were differentially expressed in the bud flower stage in style-stigma plus stamen, petals and ovary with different temporal patterns suggesting a possible tissue-specific role (Trivellini et al., 2011a). In pineapple, the expression of the ethylene receptors *AcERS1a*, *AcERS1b*, *AcETR2a*, and *AcETR2b* was higher in bract primordia and flower primordia ethephon-treated (Li et al., 2016), suggesting an important role during inflorescence development because ethylene induces pineapple flowering. In *Arabidopsis*, *ETR2* receptor was developmentally regulated in the inflorescence, floral meristems, and developing petals and ovules (Sakai et al., 1998).

Flower development occurs with the specification of floral identity in shoot meristem and then floral organ primordial initiates and rises to the formation of sepal, petal, stamen, carpel, and ovule. The development of floral organ is controlled by homeotic genes during reproductive phase. Each of these steps involves elaborate networks of factors that regulate floral morphogenesis. A potential genetic network involving ethylene as a regulator of flower development and homeotic genes has been emerging. Flower locus protein T (FT) is the major component of the mobile flower-promoting signal florigen and promotes the transition from vegetative growth to flowering in plants, ensuring the regulation of floral meristem identity genes such as APETALA (*AP*) and *LEAFY* (Krizek and Fletcher, 2005). In silver vase (*A. asciata*) using a comparative global transcriptome profile between adult and juvenile plants under ethylene, treatment was reported of the downregulation of TARGET OF EAT 1 (*TOE1*) and *TOE3*, belonging to *AP2*-like transcription factors, in adult plants (Li et al., 2015). These results suggest that the *AP2* family genes, such as *TOE1* and *TOE3* acting as repressors of *FT*, may participate in the induction of flowering by ethylene. In tomato, the ectopic expression of *LeHB-1* was reported to disrupt flower development, suggesting a critical role in floral organogenesis (Lin et al., 2008). *LeHB-1* encodes a class-I HD-Zip protein that binds to the promoter of *LeACO1*, involved in the regulation of tomato floral organogenesis, carpel development and ripening (Lin et al., 2008). A novel tomato mutant altered in the formation of floral organs, called unfinished flower development (*ufd*), showed higher hormone contents, particularly the ethylene precursor ACC compared to wild type (Poyatos-Pertíñez et al., 2016). Moreover, the global transcriptome profile showed that several MADS-box genes regulating floral identity as well as genes related to ethylene response were affected in *ufd* mutant inflorescences. These results suggest that ethylene signaling may interact with the development of flower primordia and *UFD* may have a key function as a positive regulator of floral organ identity and growth genes, together with hormonal signaling pathways.

Interaction between Ethylene and Other Hormones during Flower Development

The present section gives an insight into the interaction of ethylene with other hormones during flower development.

Ethylene and Auxin

Auxins may influence flowering in plants by affecting ethylene evolution. In a classical study, Burg and Burg (1966) reported that auxin-induced flowering in pineapple by stimulating ethylene formation. Treatment of pineapple plants with naphthalene acetic acid (NAA) enhanced ethylene levels. However, this is an exceptional case, and ethylene generally inhibits flowering in many plant species, including *Arabidopsis* and pharbitis (*Ipomoea nil*, synonym *Pharbitis nil*) (Achard et al., 2007; Kęsy et al., 2008, 2010). Achard et al. (2007) showed that in *Arabidopsis* grown under short-day (SD) conditions, ethylene delayed flowering in a DELLA-dependent manner and the inhibitory effect of auxins on flowering in pharbitis was caused by the induction of ethylene production (Kęsy et al., 2008). Both the induction and inhibition of flowering have been reported by IAA, inhibition in SD plants cultivated under an inductive photoperiod, whereas stimulation in long-day (LD) plants under non-inductive conditions (Kulikowska-Gulewska et al., 1995; Wijayanti et al., 1997).

Ethylene and Abscisic Acid

Ethylene acts as a strong inhibitor of flowering in SD plants but only when it is applied in the second half of the inductive night (Kęsy et al., 2008; Wilmowicz et al., 2008). ABA plays an important role in the photoperiodic induction of flowering in pharbitis seedlings, and the inhibitory effect of ethylene on pharbitis flowering inhibition may depend on its influence on the ABA level. The inhibition of flowering was observed when ABA was applied just before or at the beginning of a 16-h-long dark period (Wilmowicz et al., 2014). Moreover, the application of AVG partially reversed the inhibitory effect of ABA on flowering, suggesting that ABA influenced ethylene production which directly inhibited flowering. Thus, ABA could affect flowering indirectly by modifying other hormones. In Arabidopsis, ABA-deficient mutants *aba2-1* and *aba1-6* have a late flowering phenotype (Riboni et al., 2013) and the level of floral suppressing hormone ethylene have been shown to increase in *aba* mutant (LeNoble et al., 2004), and this condition may contribute to their late flowering phenotype.

Ethylene and Gibberellins

Various GAs, such as GA_{32} and 2,2-dimethyl G_4, are especially florigenic when applied to non-induced Darnel ryegrass (*Lolium temulentum*) plants (Pharis et al., 1987). The treatment of GA to the foliar bud of japtropha (*Jatropha curcas*) increased the number of female flowers and fastened the flower development due to an increased endogenous level of GA and auxin. In contrast, ethrel (ethylene source) treatment decreased flower development due to the decreased endogenous level of auxin, while GA treatment significantly increased it (Makwana and Robin, 2013). Lee et al. (1998) suggested that the rhythm of bioactive GA production might play a role in the initiation of flowering. The pulses of GAs (especially GA_1) may have different effects on floral initiation according to the time of day that they occur. The diurnal rhythm might be one way by which the absence of phytochrome B causes early flowering in 58M (phytochrome B null mutant) under most photoperiods. The expression of key oxidase genes in the biosynthesis of gibberellin, gibberellin 20 oxidase 2 (*GA20OX2*) is high in flowers and siliques, as is the expression *of GA20OX3* (Phillips et al., 1995; Dugardeyn et al., 2008). However, Mitchum et al. (2006) reported lower levels of *GA3OX2* during the later stages of development (in stems, flowers, and siliques). The GA-deficient mutant, *gal-3*, which is severely defective in ent-kaurene production (Zeevaart and Talon, 1992) flowers later than the Thale cress (*Landsberg erecta*) wild type in a long day but is totally unable to flower in SD unless treated with exogenous GA_3 (Wilson et al., 1992). Although it is quite apparent that GA governs flowering in plants, however, its independence of ethylene is also an important question to be addressed.

The growth of plants in the presence of an ethylene precursor (ACC) or in an ethylene-enriched atmosphere delayed WT flowering (Achard et al., 2006). These findings were the basis for the current model for integration of the ethylene and GA–DELLA signaling pathways in the regulation of the floral transition (Achard et al., 2007). Previous analyses have shown that *CTR1* is the major negative regulator of ethylene signaling (Kieber et al., 1993). A study of Achard et al. (2007) found that the *ctr1–1* loss-of-function mutation confers late flowering under any photoperiod. Moreover, the ethylene-mediated inhibition of *CTR1* activity resulted in a reduction in bioactive GA levels, causing increased accumulation of DELLAs, a family of nuclear growth repressor proteins (Achard et al., 2007). DELLAs repress plant growth, whereas GA promotes growth via the mitigation of DELLA-mediated growth inhibition (King et al., 2001). Accumulation of DELLAs, in turn, delayed the initiation of the floral transition by repressing the up-regulation of the floral meristem identity genes *LEAFY (LFY)* and *SUPPRESSOR OF OVEREXPRESSION OF CONSTANS1 (SOC1)* (Achard et al., 2007). These results indicate that ethylene affects the GA biosynthesis and its interaction with GA governs the stability of DELLA proteins and hence flowering.

Transcript meta-analysis suggests that applying exogenous ethylene to plants represses the expression of GA metabolism genes. Conversely, upon treatment with GAs, the expression of some ethylene synthesis genes is up-regulated. At reduced ethylene levels, the growth of *gai-t6 rga-24* double loss-of-function mutants is more resistant to the effects of ACC than the wild type. Furthermore, in WT seedlings, GA treatment can substantially overcome the ACC-induced inhibition of root growth (Achard et al., 2003). Ethylene up-and down-regulates different GA biosynthesis and catabolism genes in *Arabidopsis* seedlings (Vandenbussche et al., 2007).

FLOWER SENESCENCE

The life of flowers is genetically determined due to their role in sexual reproduction and fertilization, and the maintenance of floral structure has a considerable cost in terms of respiratory energy, nutrients, and water loss (Stead, 1992; Jones et al., 2009). The flowers are therefore programmed to senesce after pollination or when the stigma is no longer receptive. In fact, young and mature petals are sinks, and only after pollination, when fertilization and fruit set are accomplished, a controlled senescence program allows important nutrients to be salvaged from dying tissue, from the petal to the developing ovary or transported to other sink tissues (i.e., young leaves), before flower death occurs (Rogers, 2013; Rogers and Munné-Bosch, 2016).

Flower senescence involves an ordered set of events coordinated at tissue and cellular level that can be regulated by endogenous signals, such as plant hormones, and by environmental factors, such as temperature, nutrients, light, and pathogen attack. All major plant hormones have been reported to affect flower senescence, with ethylene, jasmonic acid, salicylic acid (SA), ABA, and brassinosteroids as inducers and with cytokinins, GA, and auxin as inhibitors (Reid and Chen, 2008).

Ethylene is known to be a key player of plant aging, including fruit ripening, and flower and leaf senescence (Abeles et al., 1992). Ethylene in flower petals is involved in the inhibition of cell expansion through the regulation of water channel proteins (aquaporin) that facilitate the passage of water through biological membranes (Ma et al., 2008). The crucial role of aquaporins in flower development suggests that cellular collapse during the

flower aging process might be regulated by transcellular and the transmembrane water transport which are important for motor cell dynamics. This condition might be supported by the massive transcriptional regulation of over 300 genes encoding for aquaporins among different flower developmental stages, from anthesis to senescence, in China rose (Trivellini et al., 2016).

A large number of flowers are affected by ethylene, but sensitivity to ethylene varies according to species and cultivars (Van Doorn, 2001). In many ethylene sensitive species, pollination triggers senescence leading to a climacteric rise in ethylene production, which becomes autocatalytic and coordinates cellular events among and within the different floral tissues, leading to wilt, fade, and abscise (Woltering and Van Doorn, 1988). The use of pharmacological treatments affect at different levels the ethylene signaling pathway, [i.e., AVG and AOA which affect the ACS enzyme, or, silver thio sulfate (STS) and 1-MCP which prevent ethylene to bind to its receptor, thus modulating the tissue sensitivity to the hormone], reveals collectively an intricate network of interactions as exemplified by numerous studies of senescence in flowers reviewed in Ferrante et al. (2015). For example, the exogenous application of ethylene or its biosynthetic precursor such as ACC accelerates corolla senescence in China rose flowers (Trivellini et al., 2011a). On the other hand, senescence can significantly delayed the treatment of flowers with inhibitors of ethylene biosynthesis, such as AOA (Trivellini et al., 2011b), or action, such as 1-MCP (Trivellini et al., 2011a).

Acid synthase catalyzes the synthesis of ACC, which is directly converted into ethylene by the ACO (Wang et al., 2002). Expression of *ACS* and *ACO* genes increased and are often coordinately regulated during flower senescence (Trivellini et al., 2011a; Ichimura and Niki, 2014; Tanase et al., 2015). Their suppression by antisense technology has been successful in prolonging floral display life. The down-regulation of the *ACS* and *ACO* genes in carnation reduced ethylene production and was effective in delaying floral senescence (Savin et al., 1995; Kiss et al., 2000). The antisense transformations of ethylene biosynthetic genes have been successfully attempted in other ornamental species including petunia (Huang et al., 2007), torenia (Torenia fournieri; Aida et al., 1998), and Christmas begonia (*Begonia x cheimantha*; Hvoslef-Eide et al., 1995). ACS is the rate-limiting enzyme of ethylene biosynthesis in plants (Wang et al., 2002), and its activity regulation may involve post-transcriptional regulation through its degradation (Wang et al., 2004). In *Arabidopsis* the *ETHYLENE-OVERPRODUCER1*-like (*EOL1*), negatively regulates ethylene biosynthesis (Wang et al., 2004) and in petunia the VIGS-mediated suppression of *PhEOL1* accelerated the senescence of flowers and increased ethylene production in corollas (Liu et al., 2016).

A positive feedback regulation, in senescing the China rose flowers through an increase in ethylene production among the different flower organs (Trivellini et al., 2011a,b) with the activation of *ACS* and/or *ACO* (Trivellini et al., 2016) is shown in **Figure 1**. Recently, the global transcriptome profiling of China rose reveals that the senescence is caused by the enhancement of signals that would naturally occur via transcriptional upregulation of the ethylene biosynthetic pathway during aging (Trivellini et al., 2016). In addition to the transcripts associated with biosynthetic genes (*ACO* and *ACS*), also the ethylene response factors (*ERFs*) were differentially regulated among flower tissues during senescence (**Figure 1**).

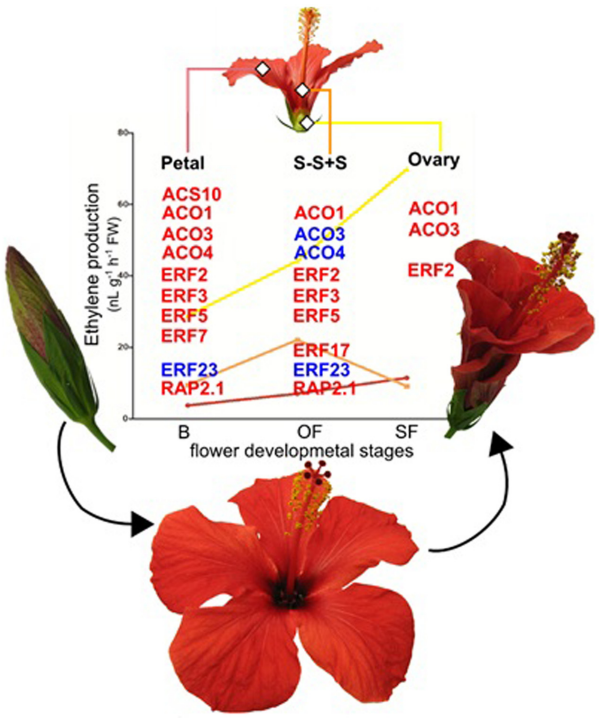

FIGURE 1 | Schematic representation of flower senescence in *H. rosa-sinesis* L.. Representative flowers in bud (B), open (OF) and senescent (SF) flower stages. Ethylene changes in different flower organs, petal (pink line bar), style-stigma plus stamens (S-S+S; orange line bar) and ovary (yellow line bar). Data from Trivellini et al. (2011b). Ethylene biosynthetic (ACS and ACOs) and ethylene response factor genes (ERFs) differentially expressed in senescence flower organs. Red and blue indicate up-regulation and down-regulation, respectively. Data from Trivellini et al. (2016).

Ethylene perception mechanism and its signaling pathway are based on the presence of its receptors, which are essential to carry on the aging process (Kieber et al., 1993; Yoo et al., 2009; An et al., 2010; Ju et al., 2012; Ju et al., 2015). The alteration of ethylene signaling by transformations of several ornamental species (such as campanula, dianthus and kalanchoe) with the *ETR1* mutated gene under control of the flower-specific promoters resulted in plants with considerably higher ethylene tolerance and a better flower longevity (Gubrium et al., 2000; Sriskandarajah et al., 2007; Sanikhani et al., 2008). Moreover, transgenic petunia plants with reduced *PhEIN2* expression exhibited significant delays in flower senescence (Shibuya et al., 2004). And in *Arabidopsis*, a mutation in the *CTR1* gene causes a constitutive ethylene response and early senescence and abscission of the flowers (Huang et al., 2003) suggesting again a central role of ethylene in the promotion of flower senescence.

The role of ethylene receptors in the regulation of ethylene signaling is subject to modification from various proteins such

as RESPONSIVE TO ANTAGONIST1 (RAN1; Binder et al., 2010), REVERSION TO ETHYLENE SENSITIVITY1 (RTE1; Dong et al., 2010; Qiu et al., 2012) and RTE1-HOMOLOG (RTH; Stepanova and Alonso, 2009). In petunia, no interaction was detected between *cEYFP–PhGRL2,* (homolog to *Arabidopsis RTE1* and the tomato GREEN RIPE, *SlGR*) and *nEYFP–PhETR1-3a* (closest homolog to the *Arabidopsis ETR1*) (Tan et al., 2014). By co-immunoprecipitation analysis, these authors demonstrated that *PhGRL2* interacts with *PhACO1*. Moreover, the suppression of *PhGRL2* by VIGS system conferred an accelerated flower senescence phenotype with enhanced ethylene production, and when *PhGRL2* was transiently overexpressed in petunia buds, the ethylene production was reduced and the longevity of flowers treated with *35Spro:PhGRL2* was significantly prolonged. These results raised the possibility that *PhGRL2* directly negatively regulates ACO activity.

EIN3-regulated genes trigger a diverse array of ethylene responses (Solano et al., 1998; Fujimoto et al., 2000; Potuschak et al., 2003; Yoo et al., 2008). In the petunia flowers, expression profiles of the *ETHYLENE RESPONSE FACTOR* (*ERF*) transcription factor family genes were studied in detail (Liu et al., 2011) and these transcription factors appear to be associated with corolla senescence. Recently, silencing an *ERF* petunia transcription factor homeodomain-leucine zipper protein (*PhHD-Zip*) dramatically reduced ethylene production and the abundance of transcripts of genes involved in ethylene (*ACS*, *ACO*) and led to an increase in flower longevity (Chang et al., 2014).

The dynamic activation of transcription factors during flower senescence is a key mechanism that controls the age-dependent expression of several senescence-related genes. These transcription factors, in turn, regulate the expression levels of various genes that may influence the ethylene pathway indirectly (Olsen et al., 2015). The MADS box genes are transcription factors that contain the conserved MADS domain that is responsible for DNA binding (Immink et al., 2002). A delay in senescence and flower abscission has been observed in *35S:AGL15* and *35S:AGL18 Arabidopsis* overexpressing plants (Fernandez et al., 2000; Adamczyk et al., 2007). The ectopic expression of a MADS box gene *FOREVER YOUNG FLOWER* (*FYF*) caused a significant delay of senescence and a deficiency of abscission in flowers of transgenic *Arabidopsis* plants by the down-regulation of *ETHYLENE RESPONSE DNA-BINDING FACTOR 1* (*EDF1*) and *EDF2*, downstream genes in the ethylene response (Chen et al., 2011) and by activating an *ERF* gene (Chen et al., 2015) suggesting a role for *FYF* in regulating senescence/abscission by suppressing the ethylene response.

Interaction between Ethylene and Other Hormones during Flower Senescence

In addition to studies which describe the influence of the individual ethylene hormone on flower senescence, there are also reports that describe the importance of hormonal interactions.

Ethylene and Cytokinins

Previous studies have shown that either exogenous application (Taverner et al., 1999) or increased exogenous production of cytokinins in transgenic lines overexpressing a senescence-associated gene (*SAG12*)-specific promoter for driving the expression of the isopentenyl transferase gene (*SAG12-IPT*) delays senescence (Xu et al., 2010). The overproduction of cytokinins in petunia flowers transformed with *P-SAG12- IPT* has been reported to delay corolla senescence and decrease sensitivity to ethylene (Chang et al., 2003). The *PSAG12-IPT* gene was also transferred to a miniature rose, as the first woody species to be transformed with *SAG12-IPT* system, resulting in increased ethylene tolerance due to specific up-regulation of the *IPT* gene under senescence promoting conditions (Zakizadeh et al., 2013). An increase in ethylene, in petunia flowers exogenously treated with cytokinin, was found during senescence, and the lack of a negative effect can be explained considering the expression of the ethylene receptors was down-regulated by treatment with BA (Trivellini et al., 2015). Similarly, the application of thidiazuron, a cytokinin-like compound, enhanced ethylene production but simultaneously extended vase life by inhibiting leaf yellowing in cut stock flowers (Ferrante et al., 2012). These results suggest that despite the enhanced ethylene production, flowers that accumulated cytokinins showed an increased flower longevity. In Iris (*Iris germanica*), the flower senescence is apparently not regulated by endogenous ethylene, auxins, GA or SA (Van Doorn et al., 2013). In contrast, exogenous cytokinins delayed senescence, suggesting they might play a role in the regulation of the time of senescence (Van Doorn et al., 2013).

Ethylene and Gibberellins

The *HD–Zip I* transcription factors are unique to plants and have been reported to be involved in various plant development responses, including flower senescence (Xu et al., 2007). In rose, ABA or ethylene treatment clearly accelerated petal senescence, while the application of the gibberellin GA_3 delayed the process and silencing of *RhHB1* delayed the ABA- or ethylene-mediated senescence in the rose petals (Lü et al., 2014). Moreover, the silencing of the key regulatory enzyme in the GA biosynthetic pathway, *RhGA20ox1* accelerated the senescence in rose petals. Thus, *RhHB1* mediates the antagonistic effect of GAs on ABA and ethylene during rose petal senescence, and the induction of petal senescence by ABA or ethylene operates through a *RhHB1-RhGA20ox1* regulatory checkpoint. Another recent study suggests that a reduction in the bioactive GA content enhances the ethylene-mediated flower senescence (Yin et al., 2015). In this study, the overexpression of a basic helix-loop-helix (*bHLH*) transcription factor, *PhFBH4*, increased the abundance of transcripts of ethylene biosynthesis genes and also increased ethylene production. Moreover, the increased expression of the GA metabolic gene *GA2ox3* in *PhFBH4-OX* transgenic plants would raise bioactive GAs content, while silencing *PhFBH4* would reduce their levels (Yin et al., 2015). Another study reported that the transcriptome changes associated with delayed flower senescence on transgenic petunia by inducing the expression of *etr1-1*, down-regulated genes involved in gibberellin biosynthesis, response to gibberellins stimulus, and

ethylene biosynthesis, at different time points (Wang H. et al., 2013).

Ethylene and Abscisic Acid

Similarly to the ethylene, ABA accumulation accelerates the senescence of cut flowers and flowering potted plants (Ferrante et al., 2015). In rose, ABA was reported to increase the sensitivity of flowers to ethylene, as the gene expression of some ethylene receptors increased after exogenous ABA treatment (Muller et al., 2000). On the other hand, ABA negatively affected the ethylene biosynthetic pathway and in hibiscus (*Hibiscus rosa-sinensis*) tissue sensitivity in all flower tissues, reducing the transcript abundance of *HrsACS*, *HrsACO*, *HrsETR*, and *HrsERS* when exogenously applied (Trivellini et al., 2011a). The over-expression of *PhHD-Zip* accelerated petunia flower senescence and this condition is another example highlighting the interaction of different hormones (Chang et al., 2014). In fact, *PhHD-Zip* transcript abundance in petunia flowers was increased by the application of hormones (ethylene, ABA) and the transcript abundance of 9-*cis*-epoxycarotenoid dioxygenase (*NCED*), a key enzyme in the ABA biosynthesis pathway, was in contrast in *PhHD-Zip* silenced flowers. These results suggest that *PhHD-Zip* plays an important role in regulating petunia flower senescence. Moreover, a transcriptome study reported that several genes involved in ABA biosynthesis, catabolism, and signaling pathways were induced by exogenous cytokinins (BA) treatment (Trivellini et al., 2015). In the experiment reported by Chang et al. (2003), transgenic lines of petunia overexpressing *IPT* gene, displayed a lower endogenous ABA level compared to the wild type, and this condition was confirmed by BA treatment which delayed senescence by lowering the ABA content with a higher ethylene production (Trivellini et al., 2015). These results suggest that in addition to the ethylene pathway, the cytokinins seem to be strongly involved in the regulation of ABA biosynthesis and its degradation in flower tissues, thus ABA plays a primary role in petunia flower senescence.

FRUIT RIPENING

Ethylene

The fruit is the development of the ovary after the fertilization and protects the seeds until complete maturation. The seeds represent the germ plasm of the plants and are responsible for the dissemination of the species. From an ecological point of view, fruits during the unripe stage represent an organ that must be protected from insects or frugivores. A fruit must be unattractive and its green color allows the camouflage itself with leaves. The ripening of fruits is a unique coordination of various biochemical and developmental pathways regulated by ethylene, which affects color, texture, nutritional quality and aroma of fruits (Barry and Giovannoni, 2007).

During ripening in climacteric fruits, the ethylene regulates firmness and color changes involving chlorophyll reduction, increase in carotenoids or anthocyanins, sugars, and biosynthesis of volatile organic compounds (VOCs).

Ethylene is tightly correlated with the VOCs biosynthesis, which increases in ripe fruit and enhances the attraction of frugivores. The inhibition of ethylene biosynthesis reduces production of VOCs and reduces the aroma of fruits (**Figure 2**). It has been found that transgenic apples expressing antisense genes for ACS or ACO produced lower VOCs and in particular, the strongest reduction was observed in the esters, which were 3–4 fold lower compared with WT (Dandekar et al., 2004). The same behavior has been observed in ACO antisense melon (*Cucumis melo*) fruits, the esters were inhibited and were 60–85% less than the control plants (Bauchot et al., 1998; Flores et al., 2002). The exogenous application of ethylene reconverted the VOCs evolution. This result indicates that ethylene inhibits the key steps of volatile biosynthesis. The study with the application of 1-MCP or AVG demonstrated that ethylene regulates VOCs biosynthesis directly through the pathway of volatile biosynthesis and indirectly through the ethylene perception. In fact, apricots (*Prunus armeniaca*) treated with ethylene biosynthesis inhibitor, such as AVG, strongly reduced the VOCs biosynthesis, while the 1-MCP, an ethylene action inhibitor, enhanced the evolution of aldehydes (Valdes et al., 2009).

The relationship between fruit ripening and ethylene/respiration pattern allows the classification of fruits as climacteric or non-climacteric. In climacteric fruits, ethylene biosynthesis increases and shows a peak corresponding to respiration pattern, while in non-climacteric fruits the ethylene declines with fruit ripening and senescence.

The tomato has been used as a model plant for studying the role of ethylene in fruit ripening. The transition from unripe to ripe fruit induces several biochemical changes that involve ethylene biosynthesis and perception. Unripe fruits produce a low amount of ethylene and are insensitive to exogenous ethylene. Hence, ethylene treatments do not induce the fruit ripening (system 1). At the beginning of ripening, ethylene production increases and induces an increase of autocatalytic biosynthesis. These fruits, in this development stage, if exposed to exogenous ethylene show a burst of ethylene production and ripen faster (system 2). These two systems are proposed to explain the auto-inhibitory effect of the ethylene during vegetative growth and the auto-stimulatory effect of the ethylene during ripening (Lelièvre et al., 1998). Fruits are classified in system 1 when they produce a low amount of ethylene and tissues are insensitive to exogenous ethylene (Alexander and Grierson, 2002). At this stage, ethylene biosynthesis is regulated by *ACS6* and *ACS1* genes. The delay of ethylene increase is the most common strategy used in post-harvest for prolonging the storage and increasing the shelf life. The inhibition of ethylene biosynthesis or action usually leads to an extension of shelf life of the climacteric fruits.

Ethylene regulates fruit ripening by affecting the *ACS* and *ACO* genes and the fruit specific polygalacturonase, involved in the depolymerization of cell wall pectin during ripening (Smith et al., 1988). It affects pectin methylesterase (PME), which provides accessibility to pectin by polygalacturonase and phytoene synthase responsible for the pigmentation of many fruits and flowers (Koch and Nevins, 1989; Fray and Grierson, 1993).

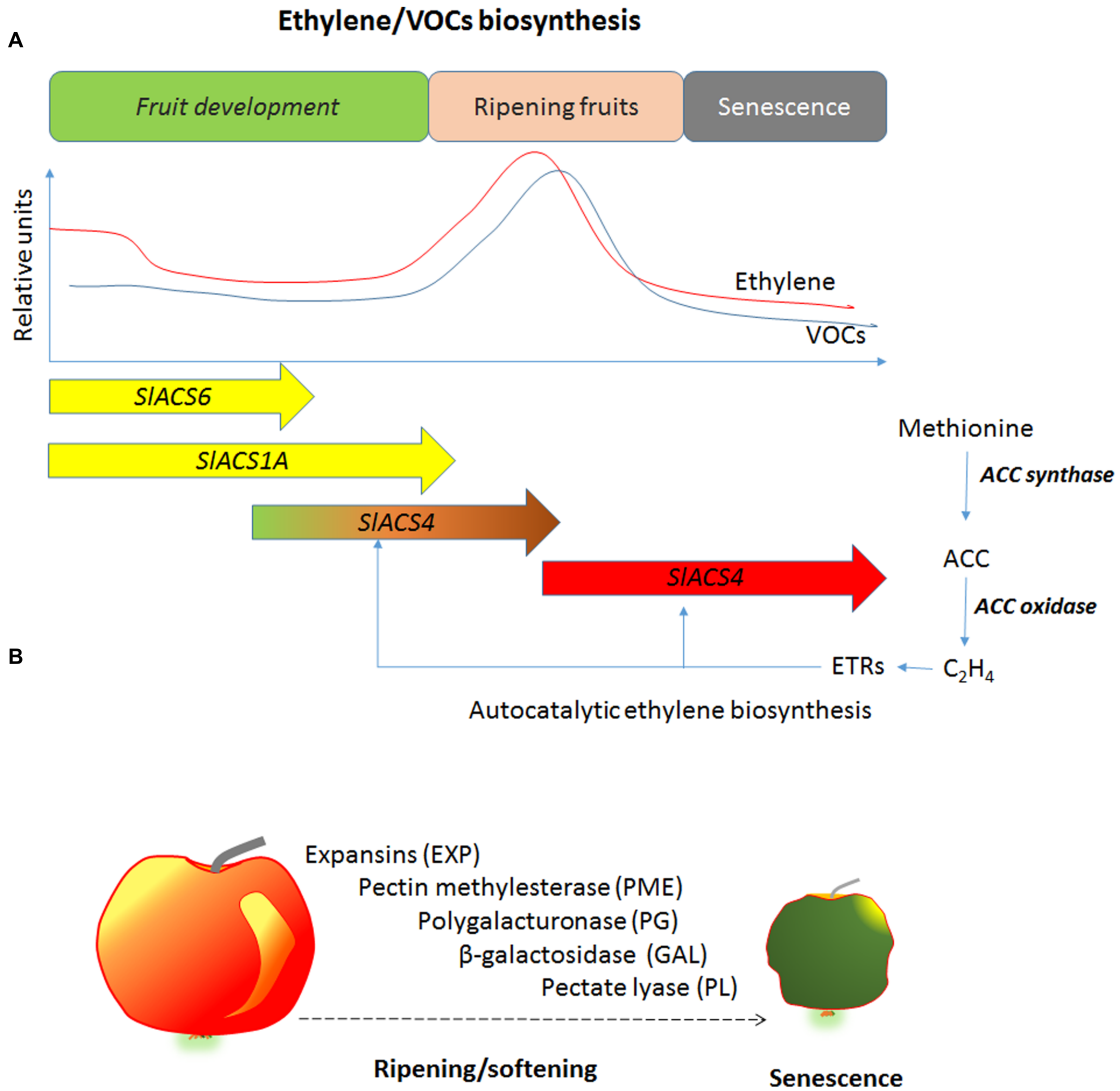

FIGURE 2 | (A) Schematic and simplified ethylene and VOCs biosynthesis during fruit development. *SlACS* (*Solanum lycopersicum* ACC synthase) families are differentially expressed during fruit development. VOCs biosynthesis derive from different pathways such as phenylpropanoids, fatty acid, and carotenoids degradation. **(B)** The main enzymes involved in cell wall degradation during fruit ripening and senescence. The action of these enzymes induces loss of firmness and softening.

Cloned mRNAs that accumulate in the unripe tomato fruits exposed to exogenous ethylene were investigated through blot hybridization experiment. The expression of cloned genes was developmentally regulated by the ethylene during fruit ripening, with more mRNAs produced by these genes in ripe fruits than in unripe fruits and the increase in mRNA was repressed by norbornadiene, an ethylene action inhibitor (Lincoln et al., 1987).

Tomato ethylene receptor, *LeETR4* or *LeETR6,* played an important role in flowering and reduction in its expression level (Tieman et al., 2000; Kevany et al., 2007). Gene expression analysis of Never-ripe (*Nr*) and additional tomato receptor homologs indicated that *Nr* and *LeETR4* transcripts were most abundant in the ripen fruit tissues (Zhou et al., 1996; Lashbrook et al., 1998).

Alba et al. (2005) identified 869 genes, differentially expressed in developing tomato pericarp. A 37% of these differentially expressed genes showed altered expression patterns in the *Nr* mutant background. The mutation of the ethylene receptor *Nr*, which reduces ethylene sensitivity and inhibits ripening, also influenced fruit morphology, seed number, ascorbate accumulation, carotenoid biosynthesis, ethylene evolution, and the expression of many genes during fruit maturation, indicating that ethylene governed multiple aspects of development both prior and during fruit ripening in tomato (Alba et al., 2005). In tomato, the E8 gene plays a role in the negative regulation of ethylene biosynthesis through repression of ethylene signal transduction. The expression of the gene increased during ripening and its antisense repression resulted in an increased

ethylene evolution but delayed ripening (Penarrubia et al., 1992).

Interaction between Ethylene and Other Hormones during Fruit Ripening and Senescence

Ethylene and Auxin

The relationship between ethylene and auxin in the fruit development has been studied. Auxins are involved in fruit development and inhibit ripening (Brady, 1987). The exogenous application of auxins in different fruits delayed the senescence such as observed in Bartlett pears (*Pyrus communis*; Frenkel and Dyck, 1973), banana (*Musa acuminate*; Purgatto et al., 2001), peaches (Trainotti et al., 2007) and strawberry (*Fragaria ananassa*; Harpster et al., 1998). The application of auxin lowered the ethylene production in sliced apples (*Malus domestica*), if applied at pre-climacteric phase, while enhancing its biosynthesis at the climacteric stage (Lieberman et al., 1977). The transcription factor *AUXIN RESPONSE FACTOR 2A (ARF2A)* has been recognized as an auxin signaling component and was able to control ripening (Breitel et al., 2016). There exists a crosstalk between auxin and ethylene; and Bleecker and Kende (2000) pointed out that auxins can stimulate the biosynthesis of more climacteric ethylene through its inductive action on the expression of the key enzyme ACS (Abel and Theologis, 1996).

Ethylene and auxins are tightly related during fruit senescence. The free auxin increases during senescence and stimulates ethylene biosynthesis. Further studies are required to understand the ethylene sensitivity changes after 1-MCP treatment. The CTG134, a calcineurin B-like protein similar to GOLVEN (GLV) peptides, seems to shut down genes that are commonly repressed during ripening by ethylene and auxin treatments (Tadiello et al., 2016). The nature and transcriptional response of CTG134 led to discovering a rise in free auxin in the 1-MCP treated fruits.

Ethylene and Cytokinin

The exogenous application of cytokinins or compounds with cytokinins-like activity increased the sugar content of fruits and induced earlier ripening. Spray application on kiwi (*Actinidia deliciosa*) using *N*-(2-chloro-4-pyridyl)-*N*'-phenylurea (CPPU), a diphenylurea derivative cytokinin, increased the starch content and induced faster fruit development. Recent studies have shown that CPPU delayed the ethylene increase during fruit ripening and also delayed central placenta softening (Ainalidou et al., 2016). In avocado, the application of isopentenyl adenosine increased the ethylene and fruit ripening (Bower and Cutting, 1988). The studies regarding the role of cytokinins in the plant senescence are available in the literature, but the relationship between cytokinins and ethylene during fruit ripening and senescence has not yet completely been elucidated and needs further investigations.

Ethylene and Abscisic Acid

In tomato fruit, ABA biosynthesis occurs via carotenoids degradation pathways and the key enzyme is the 9-*cis*-epoxycarotenoid dioxygenase (NCED). The ABA content increases following the biosynthesis of carotenoids during ripening. These changes are associated with ripening and also with ethylene production. During fruit ripening, NCED gene expression occurs earlier than ACS or ACO which are also involved in the ethylene biosynthesis. The exogenous application of ABA increases ethylene biosynthesis (Mou et al., 2016). These results suggest that ABA can be a trigger for ethylene production and influence fruit ripening (Zhang et al., 2009). In banana fruit, ABA stimulates ripening independently from the ethylene. ABA application increases all hydrolases, which can enhance the softening, with exception to the polygalacturonase activity (Lohani et al., 2004). Recently, it has been reported that an ABA Stress Ripening (ASR) transcription factor acts as a downstream component of a common transduction pathway for ABA and sucrose signals during fruit ripening (Jia et al., 2016). Interestingly, these authors provide new insights into the regulatory mechanism underlying tomato fruit development and ripening with the ethylene involved in the downstream signal transduction of ABA and sucrose, as a negative regulator of ASR gene expression, which influenced the expression of several cell wall and ripening-related genes leading to fruit softening.

The relationship of other phytohormones such as ABA and GA with ethylene during fruit senescence needs to be elucidated.

FRUIT SENESCENCE

Ethylene and Enzymes Involved in Fruit Senescence

The loss of firmness or softening of fruits is a very important quality parameter. The softening is due to cell wall degradation induced from several enzymes that are synergistically activated. These enzymes are pectine methyl esterases, polygalacturonase, cellulase, galactosidases, pectate lyase (PL), xyloglucan transglucosylase/hydrolases, and expansins. Almost all these enzymes are encoded by multi-genes family, which regulates the spatial-temporal activation of these enzymes. Ethylene plays a crucial role in regulating these genes and enzymes during ripening and senescence. The cell wall degradation is facilitated by expansins that are proteins, which are involved in the enlargement of cell matrix. This phenomenon occurs during cell wall growth and disruption. The action of these enzymes has been found to be tightly associated with the fruit ripening and senescence (Civello et al., 1999). The expansins are tightly dependent on pH. The transcription of these enzymes is carried out by gene families, which have been isolated and characterized in several plant species. Different isoforms can provide the expansins action during plant growth and fruit senescence, linking the development stage with the activation of specific isoforms. During tomato ripening, *EXP1* was induced by ethylene exposure to concentrations higher than 1 μL L^{-1}. The inhibition of ethylene biosynthesis also reduced and inhibited the *EXP1* gene expression (Rose et al., 1997). The activation of the expansin *EXP1* has also been shown in other climacteric fruits such as banana (Trivedi and Nath, 2004).

Pectin methylesterase is an enzyme activated before fruit ripening and catalyzes the de-esterification of pectin, by removing the methyl group C-6 of galacturonic acid and

allows the polygalacturonase action. The PME has an important role during fruit senescence and cell wall degradation with loss of firmness. This enzyme is stimulated by ethylene and inhibited by ethylene inhibitors such as 1-MCP (El-Sharkawy et al., 2016). Exo- and endopolygalacturonase are involved in depolymerization of galacturonic acid, hydrolysis of bonds 1, 4 of homopolymers of α-D-galacturonic acid. This enzyme is activated after the action of PME and is also induced by ethylene. In antisense ACC synthase tomato, the exposure to ethylene rapidly increased transcript accumulation of the PG. The gene expression of PG was directly correlated with ethylene concentrations used (Sitrit and Bennett, 1998).

The β-galactosidase breaks bonds between β-(1,4)-galactans in the cell wall. This enzyme is involved in fruit softening by degrading the β-(1,4)-galactans pericarp cell wall (Eda et al., 2016). Transgenic tomato for antisense of β-galactosidase showed higher firmness at the red ripening stage (Smith et al., 2002). The inhibition of ethylene action in avocado using 1-MCP reduced β-galactosidase activity (Jeong and Huber, 2004). The exogenous ethylene application increased β-galactosidase activity in watermelon and the higher activities of these enzymes were observed in immature fruits (Karakurt and Huber, 2002). PL catalyzes the breakdown of 1-4 of α-D-galacturonic acid (Uluisik et al., 2016). Bananas treated with ethylene increased the activity of this enzyme, while the use of 1-MCP reduced its activity (Lohani et al., 2004). Analogous results were observed in mango treated with ethylene for inducing ripening or treated with 1-MCP for delaying ripening (Chourasia et al., 2006). The cell wall degrading enzymes is sequentially activated during ripening and senescence. Ethylene is one key regulator of these enzymes at transcriptional and post-transcriptional level (**Figures 2A,B**).

CONCLUSION AND FUTURE PROSPECTS

It may be summarized that ethylene plays a key role in plant growth and development. The action of ethylene in the growth and development may not be isolated. It triggers the network of signaling pathways and influences through the interaction with other phytohormones regulation of several processes. The understanding of the crosstalk between ethylene and other phytohormones in regulating growth and senescence could provide a promising strategy to manipulate the content of these hormones through molecular techniques in order to get specific plant responses.

During plant life, the transition from vegetative to reproductive stages and senescence is largely influenced by ethylene and its interplay with other plant hormones. This networking not only influences the ethylene concentration but also tissues sensitivity. There are few studies focusing on the molecular changes in plant tissues after the combined treatments of ethylene with other plant hormones. These studies should be extended to different organs and development stages to deeply understand the intricate network affecting relevant agronomic traits such as yield, longevity, and appearance (morphology). The discovery of new synergistic or antagonist relationships among ethylene and other hormones can have great potential to support cell division and differentiation processes during plant development, to enhance crop yield by delaying aging and prolong shelf-life of flowers and maintain the quality of climacteric fruits.

Moreover, the equilibrium between the ethylene biosynthesis and its perception influences the crop adaptability and performance under different stress conditions. It has been shown that other plant hormones can positively or negatively influence this equilibrium. The interplay of ethylene and plant hormones on plant performance should also be investigated at the post-translation level.

AUTHOR CONTRIBUTIONS

NI and MK wrote on the role of ethylene in leaf, flower and fruit growth and development and its interaction with other hormones in the process, together with the introduction. NK suggested the concept of the manuscript, wrote the abstract and looked over the whole manuscript order and language and contributed to the overall look of the manuscript. AFe, AT, and AFr wrote on the role of ethylene in leaf, flower and fruit senescence and its interaction with other hormones in the process.

REFERENCES

Abel, S., and Theologis, A. (1996). Early genes and auxin action. *Plant Physiol.* 111, 9. doi: 10.1104/pp.111.1.9

Abeles, F. B., Morgan, P. W., and Saltveit, M. E. Jr. (1992). *Ethylene in Plant Biology*, 2nd Edn. San Diego, CA: Academic Press.

Achard, P., Baghour, M., Chapple, A., Hedden, P., Van Der Straeten, D., Genschik, P., et al. (2007). The plant stress hormone ethylene controls floral transition via DELLA-dependent regulation of floral meristem-identity genes. *Proc. Natl. Acad. Sci. U.S.A.* 104, 6484–6489. doi: 10.1073/pnas.0610717104

Achard, P., Cheng, H., De Grauwe, L., Decat, J., Schoutteten, H., Moritz, T., et al. (2006). Integration of plant responses to environmentally activated phytohormonal signals. *Science* 311, 91–94. doi: 10.1126/science.1118642

Achard, P., Vriezen, W. H., Van Der Straeten, D., and Harberd, N. P. (2003). Ethylene regulates Arabidopsis development via the modulation of DELLA protein growth repressor function. *Plant Cell* 15, 2816. doi: 10.1105/tpc.015685

Adamczyk, B. J., Lehti-Shiu, M. D., and Fernandez, D. E. (2007). The MADS domain factors AGL15 and AGL18 act redundantly as repressors of the floral transition in Arabidopsis. *Plant J.* 50, 1007–1019. doi: 10.1111/j.1365-313X.2007.03105.x

Aharoni, N., and Lieberman, M. (1979). Ethylene as a regulator of senescence in tobacco leaf discs. *Plant Physiol.* 64, 801–804. doi: 10.1104/pp.64.5.801

Aida, R., Yoshida, T., Ichimura, K., Goto, R., and Shibata, M. (1998). Extension of flower longevity in transgenic torenia plants incorporating ACC oxidase transgene. *Plant Sci.* 138, 91–101. doi: 10.1016/S0168-9452(98)00139-3

Ainalidou, A., Tanou, G., Belghazi, M., Samiotaki, M., Diamantidis, G., Molassiotis, A., et al. (2016). Integrated analysis of metabolites and proteins reveal aspects of the tissue-specific function of synthetic cytokinin in kiwifruit development and ripening. *J. Proteom.* 143, 318–333. doi: 10.1016/j.jprot.2016.02.013

Alba, R., Payton, P., Fei, Z., McQuinnb, R., Debbiea, P., Martin, G. B., et al. (2005). Transcriptome and selected metabolite analyses reveal multiple points

of ethylene control during tomato fruit development. *Plant Cell* 17, 2954–2965. doi: 10.1105/tpc.105.036053

Alexander, L., and Grierson, D. (2002). Ethylene biosynthesis and action in tomato: a model for climacteric fruit ripening. *J. Exp. Bot.* 53, 2039–2055. doi: 10.1093/jxb/erf072

An, F., Zhao, Q., Ji, Y., Li, W., Jiang, Z., Yu, X., et al. (2010). Ethylene-induced stabilization of ETHYLENE INSENSITIVE3 and EIN3-LIKE1 is mediated by proteasomal degradation of EIN3 binding F-box 1 and 2 that requires EIN2 in Arabidopsis. *Plant Cell* 22, 2384–2401. doi: 10.1105/tpc.110.076588

Anderson, L. W. J. (1982). Effects of abscisic acid on growth and leaf development in american pondweed (*Potamogeton nodosus* POIR.). *Aquat. Bot.* 13, 29–44. doi: 10.1016/0304-3770(82)90038-9

Bar, M., and Ori, N. (2014). Leaf development and morphogenesis. *Development* 141, 4219–4230. doi: 10.1242/dev.106195

Barry, C. S., and Giovannoni, J. J. (2007). Ethylene and fruit ripening. *J. Plant Growth Regul.* 26, 143. doi: 10.1007/s00344-007-9002-y

Bauchot, A. D., Mottram, D. S., Dodson, A. T., and John, P. (1998). Effect of aminocyclopropane-1-carboxylic acid oxidase antisense gene on the formation of volatile esters in Cantaloupe *Charentais melon* (cv. Védrantais). *J. Agric. Food Chem.* 46, 4787–4792. doi: 10.1021/jf980692z

Belimov, A. A., Dodd, I. C., Hontzeas, N., Theobald, J. C., Safronova, V. I., and Davies, W. J. (2009). Rhizosphere bacteria containing 1-aminocyclopropane-1-carboxylate deaminase increase yield of plants grown in drying soil via both local and systemic hormone signalling. *New Phytol.* 181, 413–423. doi: 10.1111/j.1469-8137.2008.02657.x

Beyer, E. M. (1976). A potent inhibitor of ethylene action in plants. *Plant Physiol.* 58, 268–271. doi: 10.1104/pp.58.3.268

Binder, B. M., Rodríguez, F. I., and Bleecker, A. B. (2010). The copper transporter RAN1 is essential for biogenesis of ethylene receptors in *Arabidopsis*. *J. Biol. Chem.* 285, 37263–37270. doi: 10.1074/jbc.M110.170027

Bleecker, A. B., Esch, J. J., Hall, A. E., Rodriguez, F. I., and Binder, B. M. (1998). The ethylene-receptor family from Arabidopsis: structure and function. *Philos. Trans. R. Soc. Lond. B* 353, 1405–1412.

Bleecker, A. B., Estelle, M. A., Somerville, C., and Kende, H. (1988). Insensitivity to ethylene conferred by a dominant mutation in *Arabidopsis thaliana*. *Science* 241, 1086–1089. doi: 10.1098/rstb.1998.0295

Bleecker, A. B., and Kende, H. (2000). Ethylene: a gaseous signal molecule in plants. *Ann. Rev. Cell Dev. Biol.* 16, 1–18. doi: 10.1126/science.241.4869.1086

Bower, J. P., and Cutting, J. G. (1988). Avocado fruit development and ripening physiology. *Hort. Rev.* 10, 229–271. doi: 10.1146/annurev.cellbio.16.1.1

Brady, C. J. (1987). Fruit ripening. *Ann. Rev. Plant Physiol.* 38, 155–178. doi: 10.1002/9781118060834.ch7

Breitel, D. A., Chappell-Maor, L., Meir, S., Panizel, I., Puig, C. P., Hao, Y., et al. (2016). AUXIN RESPONSE FACTOR 2 intersects hormonal signals in the regulation of tomato fruit ripening. *PLoS Genet.* 12:e1005903. doi: 10.1371/journal.pgen.1005903

Brown, K. M. (1997). Ethylene and abscission. *Physiol. Plant.* 100, 567–576. doi: 10.1371/journal.pgen.1005903

Buchanan-Wollaston, V. (1997). The molecular biology of leaf senescence. *J. Exp. Bot.* 48, 181–199. doi: 10.1111/j.1399-3054.1997.tb03062.x

Buchanan-Wollaston, V., Earl, S., Harrison, E., Mathas, E., Navabpour, S., Page, T., et al. (2003). The molecular analysis of leaf senescence - a genomics approach. *Plant Biotechnol. J.* 1, 3–22. doi: 10.1046/j.1467-7652.2003.00004.x

Burg, S. P. (1968). Ethylene, plant senescence and abscission. *Plant Physiol.* 43, 1503. doi: 10.1093/jxb/48.2.181

Burg, S. P., and Burg, E. A. (1966). Auxin-induced ethylene formation: its relation to flowering in the pineapple. *Science* 152, 1269. doi: 10.1126/science.152.3726.1269

Calderini, O., Bovone, T., Scotti, C., Pupilli, F., Piano, E., and Arcioni, S. (2007). Delay of leaf senescence in *Medicago sativa* transformed with the ipt gene controlled by the senescence-specific promoter SAG12. *Plant Cell Rep.* 26, 611–615. doi: 10.1007/s00299-006-0262-y

Carabelli, M., Possenti, M., Sessa, G., Ciolfi, A., Sassi, M., Morelli, G., et al. (2007). Canopy shade causes a rapid and transient arrest in leaf development through auxin-induced cytokinin oxidase activity. *Genes Dev.* 21, 1863–1868. doi: 10.1101/gad.432607

Chang, H., Jones, M. L., Banowetz, G. M., and Clark, D. G. (2003). Overproduction of cytokinins in petunia flowers transformed with P-SAG12- IPT delays corolla senescence and decreases sensitivity to ethylene. *Plant Physiol.* 132, 2174–2183. doi: 10.1104/pp.103.023945

Chang, X., Donnelly, L., Sun, D., Rao, J., Reid, M. S., and Jiang, C.-Z. (2014). A petunia homeodomain-leucine zipper protein, PhHD-Zip, Plays an important role in flower senescence. *PLoS ONE* 9:e88320. doi: 10.1371/journal.pone.0088320

Chen, L. F. O., Hwang, J. Y., Charng, Y. Y., Sun, C. W., and Yang, S. F. (2001). Transformation of broccoli (*Brassica oleracea* var. italica) with isopentenyltransferase gene via *Agrobacterium tumefaciens* for post-harvest yellowing retardation. *Mol. Breed.* 7, 243–257. doi: 10.1023/A:1011357320259

Chen, M. K., Hsu, W. H., Lee, P. F., Thiruvengadam, M., Chen, H. I., and Yang, C. H. (2011). The MADS box gene, FOREVER YOUNG FLOWER, acts as a repressor controlling floral organ senescence and abscission in Arabidopsis. *Plant J.* 68, 168–185. doi: 10.1111/j.1365-313X.2011.04677.x

Chen, W. H., Li, P. F., Chen, M. K., Lee, Y. I., and Yang, C. H. (2015). FOREVER YOUNG FLOWER negatively regulates ethylene response DNA-binding factors by activating an ethylene-responsive factor to control *Arabidopsis* floral organ senescence and abscission. *Plant Physiol.* 168, 1666–1683. doi: 10.1104/pp.15.00433

Cheng, Y., Dai, X., and Zhao, Y. (2007). Auxin synthesized by the YUCCA flavin monooxygenases is essential for embryogenesis and leaf formation in *Arabidopsis*. *Plant Cell* 19, 2430–2439. doi: 10.1105/tpc.107.053009

Chourasia, A., Sane, V. A., and Nath, P. (2006). Differential expression of pectate lyase during ethylene-induced postharvest softening of mango (*Mangifera indica* var. Dashehari). *Physiol. Plant.* 128, 546–555. doi: 10.1111/j.1399-3054.2006.00752.x

Civello, P. M., Powell, A. L., Sabehat, A., and Bennett, A. B. (1999). An expansin gene expressed in ripening strawberry fruit. *Plant Physiol.* 121, 1273–1279. doi: 10.1104/pp.121.4.1273

Dandekar, A. M., Teo, G., Defilippi, B. G., Uratsu, S. L., Passey, A. J., Kader, A. A., et al. (2004). Effect of down-regulation of ethylene biosynthesis on fruit flavor complex in apple fruit. *Trans. Res.* 13, 373–384. doi: 10.1023/B:TRAG.0000040037.90435.45

De Grauwe, L., Dugardeyn, J., and Van Der Straeten, D. (2008). Novel mechanisms of ethylene-gibberellin crosstalk revealed by the gai eto2-1 double mutant. *Plant Signal. Behav.* 3, 1113–1115. doi: 10.4161/psb.3.12.7037

De Martinis, D., and Mariani, C. (1999). Silencing gene expression of the ethylene-forming enzyme results in a reversible inhibition of ovule development in transgenic tobacco plants. *Plant Cell* 11, 1061–1072. doi: 10.1105/tpc.11.6.1061

Dong, C. H., Jang, M., Scharein, B., Malach, A., Rivarola, M., Liesch, J., et al. (2010). Molecular association of the Arabidopsis ETR1 ethylene receptor and a regulator of ethylene signaling, RTE1. *J. Biol. Chem.* 285, 40706–40713. doi: 10.1074/jbc.M110.146605

Dubois, M., Skirycz, A., Claeys, H., Maleux, K., Dhondt, S., De Bodt, S., et al. (2013). ETHYLENE RESPONSE FACTOR6 acts as a central regulator of leaf growth under water-limiting conditions in *Arabidopsis*. *Plant Physiol.* 162, 319–332. doi: 10.1104/pp.113.216341

Dubois, M., Van den Broeck, L., Claeys, H., Van Vlierberghe, K., Matsui, M., and Inzé, D. (2015). The ETHYLENE RESPONSE FACTORs ERF6 and ERF11 antagonistically regulate mannitol-induced growth inhibition in Arabidopsis. *Plant Physiol.* 169, 166–179. doi: 10.1104/pp.15.00335

Dugardeyn, J., Vandenbussche, F., and Van Der Straeten, D. (2008). To grow or not to grow: what can we learn on ethylene-gibberellin cross-talk by in silico gene expression analysis? *J. Exp. Bot.* 59, 1–16. doi: 10.1093/jxb/erm349

Eda, M., Matsumoto, T., Ishimaru, M., and Tada, T. (2016). Structural and functional analysis of tomato β-galactosidase 4: insight into the substrate specificity of the fruit softening-related enzyme. *Plant J.* 86, 300–307. doi: 10.1111/tpj.13160

El-Sharkawy, I., Sherif, S., Qubbaj, T., Sullivan, A. J., and Jayasankar, S. (2016). Stimulated auxin levels enhance plum fruit ripening, but limit shelf-life characteristics. *Posthar. Biol. Technol.* 112, 215–223. doi: 10.1016/j.postharvbio.2015.09.012

Fernandez, D. E., Heck, G. R., Perry, S. E., Patterson, S. E., Bleecker, A. B., and Fang, S.-C. (2000). The embryo MADS domain factor AGL15 acts postembryonically: inhibition of perianth senescence and abscission via constitutive expression. *Plant Cell* 12, 183–197. doi: 10.1105/tpc.12.2.183

Ferrante, A., and Francini, A. (2006). "Ethylene and leaf senescence," in *Ethylene Action in Plants*, ed. N. A. Khan (Berlin: Springer), 51–67. doi: 10.1007/978-3-540-32846-9_3

Ferrante, A., Mensuali-Sodi, A., and Serra, G. (2009). Effect of thidiazuron and gibberellic acid on leaf yellowing of cut stock flowers. *Central Eur. J. Biol.* 4, 461–468. doi: 10.2478/s11535-009-0039-8

Ferrante, A., Mensuali-Sodi, A., Tognoni, F., and Serra, G. (2005). Postharvest studies on leaf yellowing of chrysanthemum cut flowers. *Adv. Hortic. Sci.* 19, 81–85.

Ferrante, A., Trivellini, A., and Mensuali-Sodi, A. (2012). Interaction of 1-methylcyclopropene and thidiazuron on cut stock flowers vase life. *Open Hortic. J.* 5, 1–5. doi: 10.2174/1874840601205010001

Ferrante, A., Trivellini, A., Scuderi, D., Romano, D., and Vernieri, P. (2015). Post-production physiology and handling of ornamental potted plants. *Posthar. Biol. Technol.* 100, 99–108. doi: 10.1016/j.postharvbio.2014.09.005

Ferrante, A., Vernieri, P., Serra, G., and Tognoni, F. (2004). Changes in abscisic acid during leaf yellowing of cut stock flowers. *Plant Growth Regul.* 43, 127–134. doi: 10.1023/B:GROW.0000040119.27627.b2

Fiorani, F., Bogemann, G. M., Visser, E. J. W., Lambers, H., and Voesenekm, L. A. C. J. (2002). Ethylene emission and responsiveness to applied ethylene vary among Poa species that inherently differ in leaf elongation rates. *Plant Physiol.* 129, 1382–1390. doi: 10.1104/pp.001198

Flores, F., El Yahyaoui, F., De Billerbeck, G., Romojaro, F., Latché, A., Bouzayen, M., et al. (2002). Role of ethylene in the biosynthetic pathway of aliphatic ester aroma volatiles in Charentais *Cantaloupe melons*. *J. Exp. Bot.* 53, 201–206. doi: 10.1093/jexbot/53.367.201

Fray, R. G., and Grierson, D. (1993). Molecular genetics of tomato fruit ripening. *Trend Genet.* 9, 438–443. doi: 10.1016/0168-9525(93)90108-T

Frenkel, C., and Dyck, R. (1973). Auxin inhibition of ripening in Bartlett pears. *Plant Physiol.* 51, 6–9. doi: 10.1104/pp.51.1.6

Fujimoto, S. Y., Ohta, M., Usui, A., Shinshi, H., and Ohme-Takagi, M. (2000). Arabidopsis ethylene-responsive element binding factors act as transcriptional activators or repressors of GCC box-mediated gene expression. *Plant Cell* 12, 393–404. doi: 10.1105/tpc.12.3.393

Gan, S., and Amasino, R. M. (1995). Inhibition of leaf senescence by autoregulated production of cytokinin. *Science* 270, 1986. doi: 10.1126/science.270.5244.1986

Gepstein, S., and Thimman, K. V. (1987). The role of ethylene in the senescence of oat leaves. *Plant Physiol.* 68, 349–354. doi: 10.1104/pp.68.2.349

Gordon, S. P., Chickarmane, V. S., Ohno, C., and Meyerowitz, E. M. (2009). Multiple feedback loops through cytokinin signaling control stem cell number within the *Arabidopsis* shoot meristem. *Proc. Natl Acad. Sci. U.S.A.* 106, 16529–16534. doi: 10.1073/pnas.0908122106

Grossmann, K. (1998). Quinclorac belongs to a new class of highly selective auxin herbicides. *Weed Sci.* 46, 707–716. doi: 10.1016/j.saa.2009.08.018

Gubrium, E. K., Clevenger, D. J., Clark, D. G., Barrett, J. E., and Nell, T. A. (2000). Reproduction and horticultural performance of transgenic ethylene-insensitive petunias. *J. Am. Soc. Hortic.* 125, 277–281.

Guzman, P., and Ecker, J. R. (1990). Exploiting the triple response of *Arabidopsis* to identify ethylene-related mutants. *Plant Cell* 2, 513–524. doi: 10.1105/tpc.2.6.513

Han, S., Halevy, A. H., Sachs, R. M., and Reid, M. S. (1989). Effect of ethylene on growth and flowering of *Triteleia laxa*. *Acta Hortic.* 261, 209–214. doi: 10.17660/ActaHortic.1989.261.26

Han, S. S. (1997). Preventing postproduction leaf yellowing in *Easter lily*. *J. Am. Soc. Hort. Sci.* 122, 869–872.

Hansen, H., and Grossmann, K. (2000). Auxin-induced ethylene triggers abscisic acid biosynthesis and growth inhibition. *Plant Physiol.* 124, 1437–1448. doi: 10.1104/pp.124.3.1437

Harpster, M. H., Brummell, D. A., and Dunsmuir, P. (1998). Expression analysis of a ripening-specific, auxin-repressed endo-1, 4-β-glucanase gene in strawberry. *Plant Physiol.* 118, 1307–1316. doi: 10.1104/pp.118.4.1307

He, C., Davies, F. R. Jr., and Lacey, R. E. (2009). Ethylene reduces gas exchange and growth of lettuce plants under hypobaric and normal atmospheric conditions. *Physiol. Plant.* 135, 258–271. doi: 10.1111/j.1399-3054.2008.01190.x

Hong, S. B., Sexton, R., and Tucker, M. L. (2000). Analysis of gene promoters for two tomato polygalacturonases expressed in abscission zones and the stigma. *Plant Physiol.* 123, 869–881. doi: 10.1104/pp.123.3.869

Huang, L. C., Lai, U. L., Yang, S. F., Chu, M. J., Kuo, C. I, Tsai, M. F., et al. (2007). Delayed flower senescence of *Petunia hybrida* plants transformed with antisense broccoli ACC synthase and ACC oxidase genes. *Posthar. Biol. Technol.* 46, 47–53. doi: 10.1016/j.postharvbio.2007.03.015

Huang, Y., Li, H., Hutchison, C. E., Laskey, J., and Kieber, J. J. (2003). Biochemical and functional analysis of CTR1, a protein kinase that negatively regulates ethylene signaling in *Arabidopsis*. *Plant J.* 33, 221–233. doi: 10.1046/j.1365-313X.2003.01620.x

Humphries, E. C. (1958). Effect of gibberellic acid and kinetin on growth of the primary leaf of dwarf bean (*Phaseolus vulgaris*). *Nature* 181, 1081–1082. doi: 10.1038/1811081a0

Hunter, D. A., Yoo, S. D., Butcher, S. M., and McManus, M. T. (1999). Expression of 1-aminocyclopropane-1-carboxylate oxidase during leaf ontogeny in white clover. *Plant Physiol.* 120, 131–142. doi: 10.1104/pp.120.1.131

Hussain, A., Black, C. R., Taylor, I. B., and Roberts, J. A. (2000). Does an antagonistic relationship between ABA and ethylene mediate shoot growth when tomato (*Lycopersicon esculentum* Mill.) plants encounter compacted soil?. *Plant Cell Environ.* 23, 1217–1226. doi: 10.1046/j.1365-3040.2000.00639.x

Hvoslef-Eide, A. K., Fjeld, T., and Einset, J. W. (1995). Breeding Christmas begonia Begonia 3 cheimantha Everett for increased keeping quality by traditional and biotechnological methods. *Acta Hortic.* 1995, 197–204. doi: 10.17660/ActaHortic.1995.405.25

Ichimura, K., and Niki, T. (2014). Ethylene production associated with petal senescence in carnation flowers is induced irrespective of the gynoecium. *J. Plant Physiol.* 171, 1679–1684. doi: 10.1016/j.jplph.2014.08.006

Immink, R. G., Gadella, T. W. Jr., Ferrario, S., Busscher, M., and Angenent, G. C. (2002). Analysis of MADS box protein-protein interactions in living plant cells. *Proc. Natl Acad. Sci. U.S.A.* 99, 2416–2421. doi: 10.1073/pnas.042677699

Iqbal, N., Khan, N. A., Nazar, R., and Teixeira da Silva, J. A. (2012). Ethylene-stimulated photosynthesis results from increased nitrogen and sulfur. *Environ. Exp. Bot.* 78, 84–90. doi: 10.1016/j.envexpbot.2011.12.025

Jackson, M. B., Drew, M. C., and Giffard, S. C. (1981). Effects of applying etnylene to the root system of *Zea mays* on growth and nutrient concentration in relation to flooding tolerance. *Physiol. Plant* 52, 23–28. doi: 10.1111/j.1399-3054.1981.tb06028.x

Jeong, J., and Huber, D. J. (2004). Suppression of avocado (*Persea americana* Mill.) fruit softening and changes in cell wall matrix polysaccharides and enzyme activities: differential responses to 1-MCP and delayed ethylene application. *J. Am. Soc. Hortic. Sci.* 129, 752–759.

Jia, H., Jiu, S., Zhang, C., Wang, C., Tariq, P., Liu, Z., et al. (2016). Abscisic acid and sucrose regulate tomato and strawberry fruit ripening through the abscisic acid-stress-ripening transcription factor. *Plant Biotechnol. J.* 4, 2045–2065. doi: 10.1111/pbi.12563

Jiang, C. Z., Lu, F., Imsabai, W., Meir, S., and Reid, M. S. (2008). Silencing polygalacturonase expression inhibits tomato petiole abscission. *J. Exp. Bot.* 59, 973–979. doi: 10.1093/jxb/ern023

Jing, H. C., Schippers, J. H., Hille, J., and Dijkwel, P. P. (2005). Ethylene-induced leaf senescence depends on age-related changes and OLD genes in Arabidopsis. *J. Exp. Bot.* 56, 2915–2923. doi: 10.1093/jxb/eri287

Jones, M. L. (2002). Ethylene responsiveness in carnation styles is associated with stigma receptivity. *Sex. Plant Reprod.* 15, 107–112. doi: 10.1007/s00497-002-0146-4

Jones, M. L., Stead, A. D., and Clark, D. G. (2009). "Petunia flower senescence," in *Petunia: A Model System for Comparative Research*, eds T. Gerats and J. Strommer (New York, NY: Springer), 301–324.

Jordi, W., Schapendonk, A. H. C. M., Davelaar, E., Stoopen, G. M., Pot, C. S., De Visser, R., et al. (2000). Increased cytokinin levels in transgenic PSAG12–IPT tobacco plants have large direct and indirect effects on leaf senescence, photosynthesis and N partitioning. *Plant Cell Environ.* 23, 279–289. doi: 10.1046/j.1365-3040.2000.00544.x

Ju, C., Van de Poel, B., Cooper, E. D., Thierer, J. H., Gibbons, T. R., Delwiche, C. F., et al. (2015). Conservation of ethylene as a plant hormone over 450 million years of evolution. *Nat. Plants* 1, 14004. doi: 10.1038/nplants.2014.4

Ju, C., Yoon, G. M., Shemansky, J. M., Lin, D. Y., Ying, Z. I., Chang, J., et al. (2012). CTR1 phosphorylates the central regulator EIN2 to control ethylene hormone signaling from the ER membrane to the nucleus in Arabidopsis. *Proc. Natl. Acad. Sci. U.S.A.* 109, 19486–19491. doi: 10.1073/pnas.1214848109

Junttila, O., Heide, O. M., Lindgard, B., and Ernstsen, A. (1997). Gibberellins and the photoperiodic control of leaf growth in *Poa pratensis*. *Physiol. Plant.* 101, 599–605. doi: 10.1111/j.1399-3054.1997.tb01043.x

Karakurt, Y., and Huber, D. J. (2002). Cell wall-degrading enzymes and pectin solubility and depolymerization in immature and ripe watermelon (*Citrullus lanatus*) fruit in response to exogenous ethylene. *Physiol. Plant.* 116, 398–405. doi: 10.1034/j.1399-3054.2002.1160316.x

Kawa-Miszczak, L., Wêgrzynowicz-Lesiak, E., Miszczak, A., and Saniewski, M. (2003). Effect of methyl jasmonate and ethylene on leaf growth, anthocyanin accumulation and CO2 evolution in tulip bulbs. *J. Fruit Orna. Plant Res.* 11, 59–68.

Keller, C. P., Stahlberg, R., Barkawi, L. S., and Cohen, J. D. (2004). Long-term inhibition by auxin of leaf blade expansion in Bean and Arabidopsis. *Plant Physiol.* 134, 1217–1226. doi: 10.1104/pp.103.032300

Kęsy, J., Frankowski, K., Wilmowicz, E., Glaziñska, P., Wojciechowski, W., and Kopcewicz, J. (2010). The possible role of PnACS2 in IAA-mediated flower inhibition in *Pharbitis nil*. *Plant Growth Regul.* 61, 1–10. doi: 10.1016/j.jplph.2008.02.013

Kęsy, J., Maciejewska, B., Sowa, M., Szumilak, M., Kawałowski, K., Borzuchowska, M., et al. (2008). Ethylene and IAA interactions in the inhibition of photoperiodic flower induction of *Pharbitis nil*. *Plant Growth Regul.* 55, 43–50. doi: 10.1007/s10725-008-9256-9

Kevany, B. M., Tieman, D. M., Taylor, M. G., Cin, V. D., and Klee, H. J. (2007). Ethylene receptor degradation controls the timing of ripening in tomato fruit. *Plant J.* 51, 458–467. doi: 10.1111/j.1365-313X.2007.03170.x

Khan, N. A. (2005). The influence of exogenous ethylene on growth and photosynthesis of mustard (*Brassica juncea*) following defoliation. *Sci. Hortic.* 105, 499–505. doi: 10.1016/j.scienta.2005.02.004

Khan, N. A., Mir, M. R., Nazar, R., and Singh, S. (2008). The application of ethephon (an ethylene releaser) increases growth, photosynthesis and nitrogen accumulation in mustard (*Brassica juncea* L.) under high nitrogen levels. *Plant Biol.* 10, 534–538. doi: 10.1111/j.1438-8677.2008.00054.x

Kieber, J. J., Rothenberg, M., Roman, G., Feldmann, K. A., and Ecker, J. R. (1993). CTR1, a negative regulator of the ethylene response pathway in Arabidopsis, encodes a member of the raf family of protein kinases. *Cell* 72, 427–441. doi: 10.1016/0092-8674(93)90119-B

Kim, J., Yang, J., Yang, R., Sicher, R. C., Chang, C., and Tucker, M. L. (2016). Transcriptome analysis of soybean leaf abscission identifies transcriptional regulators of organ polarity and cell fate. *Front. Plant Sci.* 7:125. doi: 10.3389/fpls.2016.00125

Kim, J. H., Chung, K. M., and Woo, H. R. (2011). Three positive regulators of leaf senescence in Arabidopsis, ORE1, ORE3 and ORE9, play roles in crosstalk among multiple hormone-mediated senescence pathways. *Genes Genomics* 33, 373–381. doi: 10.1007/s13258-011-0044-y

King, K. E., Moritz, T., and Harberd, N. P. (2001). Gibberellins are not required for normal stem growth in *Arabidopsis thaliana* in the absence of GAI and RGA. *Genetics* 159, 767–776.

Kiss, E., Veres, A., Galli, Z., Nagy, N., Tóth, E., Varga, A., et al. (2000). Production of transgenic carnation with antisense ACS (1-aminocyclopropane-1-carboxylate synthase) gene. *Int. J. Hortic. Sci.* 6, 103–107.

Koch, J. L., and Nevins, D. J. (1989). Tomato fruit cell wall. I. Use of purified tomato polygalacturonase and pectinmethylesterase to identify developmental changes in pectins. *Plant Physiol.* 91, 816–822. doi: 10.1104/pp.91.3.816

Konings, H., and Jackson, M. B. (1979). A relationship between rates of ethylene production by roots and the promoting or inhibiting effects of exogenous ethylene and water on root elongation. *Z. Pflanzenphysiol.* 92, 385–397. doi: 10.1016/S0044-328X(79)80184-1

Koukounaras, A., Siomos, A. S., and Sfakiotakis, E. (2006). 1-Methylcyclopropene prevents ethylene induced yellowing of rocket leaves. *Posthar. Biol. Technol.* 41, 109–111. doi: 10.1016/j.postharvbio.2006.01.018

Krizek, B. A., and Fletcher, J. C. (2005). Molecular mechanisms of flower development: an armchair guide. *Nat. Rev. Genet.* 6, 688–698. doi: 10.1038/nrg1675

Kuan, C. S., Yu, C. W., Lin, M. L., and Hsu, H. T. (2005). Foliar application of aviglycine reduces natural flowering in pineapple. *HortScience* 40, 123–126.

Kulikowska-Gulewska, H., Cymerski, M., Czaplewska, J., and Kopcewicz, J. (1995). IAA in the control of photoperiodic flower induction of *Pharbitis nil* Chois. *Acta Soc. Bot. Pol.* 64, 45–50. doi: 10.5586/asbp.1995.008

Kurakawa, T., Ueda, N., Maekawa, M., Kobayashi, K., Kojima, M., Nagato, Y., et al. (2007). Direct control of shoot meristem activity by a cytokinin-activating enzyme. *Nature* 445, 652–655. doi: 10.1038/nature05504

La Rue, C. D. (1936). The effect of auxin on the abscission of petioles. *Proc. Natl. Acad. Sci. U.S.A.* 22, 254–259. doi: 10.1073/pnas.22.5.254

Lashbrook, C., Giovannoni, J., Hall, B., Fischer, R., and Bennett, A. (1998). Transgenic analysis of tomato endo-beta-1,4-glucanase gene function: role of *CEL1* in floral abscission. *Plant J.* 13, 303–310. doi: 10.1046/j.1365-313X.1998.00025.x

Lee, B. H., Yu, S. I., and Jackson, D. (2009). Control of plant architecture: the role of phyllotaxy and plastochron. *J. Plant Biol.* 52, 277–282. doi: 10.1007/s12374-009-9034-x

Lee, I. J., Foster, K. R., and Morgan, P. W. (1998). Photoperiod control of gibberellin levels and flowering in sorghum. *Plant Physiol.* 116, 1003–1011. doi: 10.1104/pp.116.3.1003

Lelièvre, J. M., Latché, A., Jones, B., Bouzayen, M., and Pech, J. C. (1998). Ethylene and fruit ripening. *Physiol. Plant.* 101, 727–739. doi: 10.1111/j.1399-3054.1997.tb01057.x

LeNoble, M. E., Spollen, W. G., and Sharp, R. E. (2004). Maintenance of shoot growth by endogenous ABA: genetic assessment of the involvement of ethylene suppression. *J. Exp. Bot.* 55, 237–245. doi: 10.1093/jxb/erh031

Lewington, R. J., Tablot, M., and Simon, E. W. (1967). The yellowing of attached and detached cucumber cotyledons. *J. Exp. Bot.* 18, 526–531. doi: 10.1093/jxb/18.3.526

Li, Y., Wu, Q. S., Huang, X., Liu, S. H., Zhang, H. N., Zhang, Z., et al. (2016). Molecular cloning and characterization of four genes encoding ethylene receptors associated with pineapple (*Ananas comosus* L.) Flowering. *Front. Plant Sci.* 7:710. doi: 10.3389/fpls.2016.00710

Li, Z., Wang, J., Zhang, X., Lei, M., Fu, Y., Zhang, J., et al. (2015). Transcriptome sequencing determined flowering pathway genes in *Aechmea fasciata* treated with ethylene. *J. Plant Growth Regul.* 35, 316–329. doi: 10.1007/s00344-015-9535-4

Lieberman, M., Baker, J. E., and Sloger, M. (1977). Influence of plant hormones on ethylene production in apple, tomato, and avocado slices during maturation and senescence. *Plant Physiol.* 60, 214–217. doi: 10.1104/pp.60.2.214

Lin, Z., Hong, Y., Yin, M., Li, C., Zhang, K., and Grierson, D. (2008). A tomato HB-zip homeobox protein, LeHB-1, plays an important role in floral organogenesis and ripening. *Plant J.* 55, 301–310. doi: 10.1111/j.1365-313X.2008.03505.x

Lin, Z., Zhong, S., and Grierson, D. (2009). Recent advances in ethylene research. *J. Exp. Bot.* 60, 3311–3336. doi: 10.1093/jxb/erp204

Lincoln, J. E., Cordes, S., Read, E., and Fischer, R. L. (1987). Regulation of gene expression by ethylene during *Lycopersicon esculentum* (tomato) fruit development. *Proc. Natl. Acad. Sci. U.S.A.* 84, 2793–2797. doi: 10.1073/pnas.84.9.2793

Liu, J., Zhao, J., Xiao, Z., Chang, X., Chen, G., and Yu, Y. (2016). Expression and functional analysis of PhEOL1 and PhEOL2 during flower senescence in petunia. *Funct. Plant Biol.* 43, 413–422. doi: 10.1071/fp15311

Liu, J. X., Li, J. Y., Wang, H. N., Fu, Z. D., Liu, J. A., and Yu, Y. (2011). Identification and expression analysis of ERF transcription factor genes in petunia during flower senescence and in response to hormone treatments. *J. Exp. Bot.* 62, 825–840. doi: 10.1093/jxb/erq324

Ljung, K., Bhalerao, R. P., and Sandberg, G. (2001). Sites and homeostatic control of auxin biosynthesis in Arabidopsis during vegetative growth. *Plant J.* 28, 465–474. doi: 10.1046/j.1365-313X.2001.01173.x

Llop-Tous, I. I., Barry, C. S., and Grierson, D. (2000). Regulation of ethylene biosynthesis in response to pollination in tomato flowers. *Plant Physiol.* 123, 971–978. doi: 10.1104/pp.123.3.971

Lohani, S., Trivedi, P. K., and Nath, P. (2004). Changes in activities of cell wall hydrolases during ethylene-induced ripening in banana: effect of 1-MCP, ABA and IAA. *Postharvest Biol. Technol.* 31, 119–126. doi: 10.1016/j.postharvbio.2003.08.001

Lü, P., Zhang, C., Liu, J., Liu, X., Jiang, G., Jiang, X., et al. (2014). RhHB1 mediates the antagonism of gibberellins to ABA and ethylene during rose (*Rosa hybrida*) petal senescence. *Plant J.* 78, 578–590. doi: 10.1111/tpj.12494

Lutts, S., Kinet, J. M., and Bouharmont, J. (1996). NaCl-induced senescence in leaves of rice (*Oryza sativa* L.) cultivars differing in salinity resistance. *Ann. Bot.* 78, 389–398. doi: 10.1006/anbo.1996.0134

Ma, N., Xue, J. Q., Li, Y. H., Liu, X. J., Dai, F. W., Jia, W. S., et al. (2008). RhPIP2;1, a rose aquaporin gene, is involved in ethylene-regulated petal expansion. *Plant Physiol.* 148, 894–907. doi: 10.1104/pp.108.120154

Makwana, V., and Robin, P. (2013). Interaction between GA and ethrel in inducing female flowers in *Jatropha curcas*. *Int. J. Biotechnol. Bioeng. Res.* 4, 465–472.

Masood, A., Iqbal, N., and Khan, N. A. (2012). Role of ethylene in alleviation of cadmium-induced photosynthetic capacity inhibition by sulphur in mustard. *Plant Cell Environ.* 35, 524–533. doi: 10.1111/j.1365-3040.2011.02432.x

Matile, P., Hörtensteiner, S., Thomas, H., and Kräutler, B. (1996). Chlorophyll breakdown in senescent leaves. *Plant Physiol.* 112, 1403–1409. doi: 10.1104/pp.112.4.1403

Mattsson, J., Ckurshumova, W., and Berleth, T. (2003). Auxin signaling in *Arabidopsis* leaf vascular development. *Plant Physiol.* 131, 1327–1339. doi: 10.1104/pp.013623

McCabe, M. S., Garratt, L. C., Schepers, F., Jordi, W. J. R. M., Stoopen, G. M., Davelaar, E., et al. (2001). Effects of PSAG12–*IPT* gene expression on development and senescence in transgenic lettuce. *Plant Physiol.* 127, 505–516. doi: 10.1104/pp.010244

Métraux, J. P., and Kende, H. (1983). The role of ethylene in the growth response of submerged deep water rice. *Plant Physiol.* 72, 441–446. doi: 10.1104/pp.72.2.441

Millenaar, F. F., Cox, M. C., van Berkel, Y. E. D. J., Welschen, R. A., Pierik, R., Voesenek, L. A., et al. (2005). Ethylene-induced differential growth of petioles in Arabidopsis. Analyzing natural variation, response kinetics, and regulation. *Plant Physiol.* 137, 998–1008. doi: 10.1104/pp.104.053967

Mitchum, M. G., Yamaguchi, S., Hanada, A., Kuwahara, A., Yoshioka, Y., Kato, T., et al. (2006). Distinct and overlapping roles of two gibberellin 3-oxidases in *Arabidopsis* development. *Plant J.* 45, 804–818. doi: 10.1111/j.1365-313X.2005.02642.x

Mou, W., Li, D., Bu, J., Jiang, Y., Khan, Z. U., Luo, Z., et al. (2016). Comprehensive analysis of ABA effects on ethylene biosynthesis and signaling during tomato fruit ripening. *PLoS ONE* 11:e0154072. doi: 10.1371/journal.pone.0154072

Muller, R., Stummann, B. M., and Serek, M. (2000). Characterization of an ethylene receptor family with differential expression in rose (*Rosa hybrida* L.) flowers. *Plant Cell Rep.* 19, 1232–1239. doi: 10.1007/s002990000251

Musgrave, A., and Walters, J. (1973). Ethylene-stimulated growth and auxin ansport in ranunculus sceleratus petioles. *New Phytol.* 72, 783–789. doi: 10.1111/j.1469-8137.1973.tb02053.x

Mutui, T. M., Emongor, V. N., and Hutchinson, M. J. (2003). Effect of benzyladenine on the vase life and keeping quality of *Alstoemeria* cut flowers. *J. Agric. Sci. Technol.* 5, 91–105.

Nazar, R., Khan, M. I. R., Iqbal, N., Masood, A., and Khan, N. A. (2014). Involvement of ethylene in reversal of salt-inhibited photosynthesis by sulfur in mustard. *Physiol. Plant.* 152, 331–344. doi: 10.1111/ppl.12173

Noh, Y. S., and Amasino, R. M. (1999). Identification of a promoter region responsible for the senescence-specific expression of SAG12. *Plant Mol. Biol.* 41, 181–194. doi: 10.1023/A:1006342412688

Ogawara, T., Higashi, K., Kamada, H., and Ezura, H. (2003). Ethylene advances the transition from vegetative growth to flowering in *Arabidopsis thaliana*. *J. Plant Physiol.* 160, 1335–1340. doi: 10.1078/0176-1617-01129

Oh, S. A., Park, J. H., Lee, G. L., Pack, K. H., Park, S. K., and Nam, H. G. (1997). Identification of three genetic loci controlling leaf senescence in *Arabidopsis thaliana*. *Plant J.* 12, 527–535. doi: 10.1046/j.1365-313X.1997.00527.x

Olsen, A., Lutken, H., Hegelund, J. N., and Muller, R. (2015). Ethylene resistance in flowering ornamental plants–improvements and future perspectives. *Hortic. Res.* 2:15038. doi: 10.1038/hortres.2015.38

Özgen, M., Park, S., and Palta, J. P. (2005). Mitigation of ethylene-promoted leaf senescence by a natural lipid, lysophosphatidylethanolamine. *HortScience* 40, 1166–1167.

Paltridge, G. W., Denholm, J. V., and Connor, D. J. (1984). Determinism, senescence and the yield of plants. *J. Theor. Biol.* 110, 383–398. doi: 10.1016/S0022-5193(84)80181-2

Patterson, S. E., and Bleecker, A. B. (2004). Ethylene-dependent and–independent processes associated with floral organ abscission in *Arabidopsis*. *Plant Physiol.* 134, 194–203. doi: 10.1104/pp.103.028027

Penarrubia, L., Aguilar, M., Margossian, L., and Fischer, R. (1992). An antisense gene stimulates ethylene hormone production during tomato fruit ripening. *Plant Cell* 4, 681–687. doi: 10.1105/tpc.4.6.681

Pharis, R. P., Evans, L. T., Klng, R. W., and Mander, L. M. (1987). Gibberellins, endogenous and applied, in relation to flower induction in the long-day plant *Lolium temulentum*. *Plant Physiol.* 84, 1132–1138. doi: 10.1104/pp.84.4.1132

Phillips, A. L., Ward, D. A., Uknes, S., Appleford, N. E. J., Lange, T., and Huttly, A. K. (1995). Isolation and expression of 3 Gibberellin 20-Oxidase CDNA clones from *Arabidopsis*. *Plant Physiol.* 108, 1049–1057. doi: 10.1104/pp.108.3.1049

Philosoph-Hadas, S., Michaeli, R., Reuveni, Y., and Meir, S. (1996). Benzyladenine pulsing retards leaf yellowing and improves quality of goldenrod (*Solidago canadensis*) cut flowers. *Postharvest Biol. Technol.* 9, 65–73. doi: 10.1016/0925-5214(96)00023-3

Pierik, R., Tholen, D., Poorter, H., Visser, E. J., and Voesenek, L. A. C. J. (2006). The Janus face of ethylene: growth inhibition and stimulation. *Trends Plant Sci.* 11, 176–183. doi: 10.1016/j.tplants.2006.02.006

Pinon, V., Prasad, K., Grigg, S. P., Sanchez-Perez, G. F., and Scheres, B. (2013). Local auxin biosynthesis regulation by PLETHORA transcription factors controls phyllotaxis in *Arabidopsis*. *Proc. Natl. Acad. Sci. U.S.A.* 110, 1107–1112. doi: 10.1073/pnas.1213497110

Potuschak, T., Lechner, E., Parmentier, Y., Yanagisawa, S., Grava, S., Koncz, C., et al. (2003). EIN3-dependent regulation of plant ethylene hormone signaling by two Arabidopsis F box proteins: EBF1 and EBF2. *Cell* 115, 679–689. doi: 10.1016/S0092-8674(03)00968-1

Poyatos-Pertíñez, S., Quinet, M., Ortíz-Atienza, A., Yuste-Lisbona, F. J., Pons, C., Giménez, E., et al. (2016). A factor linking floral organ identity and growth revealed by characterization of the tomato mutant unfinished flower development (ufd). *Front. Plant Sci.* 7:1648. doi: 10.3389/fpls.2016.01648

Purgatto, E., Lajolo, F. M., do Nascimento, J. R. O., and Cordenunsi, B. R. (2001). Inhibition of β-amylase activity, starch degradation and sucrose formation by indole-3-acetic acid during banana ripening. *Planta* 212, 823–828. doi: 10.1007/s004250000441

Qiu, L., Xie, F., Yu, J., and Wen, C. K. (2012). Arabidopsis RTE1 is essential to ethylene receptor ETR1 amino-terminal signaling independent of CTR1. *Plant Physiol.* 159, 1263–1276. doi: 10.1104/pp.112.193979

Raab, S., Drechsel, G., Zarepour, M., Hartung, W., Koshiba, T., Bittner, F., et al. (2009). Identification of a novel E3 ubiquitin ligase that is required for suppression of premature senescence in *Arabidopsis*. *Plant J.* 59, 39–51. doi: 10.1111/j.1365-313X.2009.03846.x

Reid, M., and Chen, J. C. (2008). "Flower senescence," in *Senescence Process in Plant. Annual Plant Reviews*, Vol. 26, ed. S. Gan (Ithaca NY: Blackwell Publishing), 256–277.

Reid, M. S. (1995). "Ethylene in plant growth, development, and senescence," in *Plant Hormones*, ed. P. J. Davis (Dordrecht: Springer). doi: 10.1007/978-94-011-0473-9_23

Reinhardt, D., Mandel, T., and Kuhlemeier, C. (2000). Auxin regulates the initiation and radial position of plant lateral organs. *Plant Cell* 12, 507–518. doi: 10.1105/tpc.12.4.507

Reyes-Arribas, T., Barrett, J. E., Huber, D. J., Nell, T. A., and Clark, D. G. (2001). Leaf senescence in a non-yellowing cultivar of chrysanthemum (*Dendranthema grandiflora*). *Physiol. Plant.* 111, 540–544. doi: 10.1034/j.1399-3054.2001.1110415.x

Riboni, M., Galbiati, M., Tonelli, C., and Conti, L. (2013). GIGANTEA enables drought escape response via abscisic acid-dependent activation of the florigens and SUPPRESSOR OF OVEREXPRESSION OF CONSTANS. *Plant Physiol.* 162, 1706–1719. doi: 10.1104/pp.113.217729

Richmond, A. E., and Lang, A. (1957). Effect of kinetin on protein content and survival of detached xanthium leaves. *Science* 125, 650–651. doi: 10.1126/science.125.3249.650-a

Riov, J., and Goren, R. (1979). Effect of ethylene on auxin transport and metabolism in midrib sections in relation to leaf abscission of woody plants. *Plant Cell Environ.* 2, 83–89. doi: 10.1111/j.1365-3040.1979.tb00778.x

Rogers, H., and Munné-Bosch, S. (2016). Production and scavenging of reactive oxygen species and redox signaling during leaf and flower senescence: similar but different. *Plant Physiol.* 171, 1560–1568. doi: 10.1104/pp.16.00163

Rogers, H. J. (2013). From models to ornamentals: how is flower senescence regulated? *Plant Mol. Biol.* 82, 563–574. doi: 10.1007/s11103-012-9968-0

Rose, J. K., Lee, H. H., and Bennett, A. B. (1997). Expression of a divergent expansin gene is fruit-specific and ripening-regulated. *Proc. Natl. Acad. Sci. U.S.A.* 94, 5955–5960. doi: 10.1073/pnas.94.11.5955

Royer, D. L., Wilf, P., Janesko, D. A., Kowalski, E. A., and Dilcher, D. L. (2005). Correlations of climate and plant ecology to leaf size and shape: potential proxies for the fossil record. *Am. J. Bot.* 92, 1141–1151. doi: 10.3732/ajb.92.7.1141

Sack, L., Cowan, P. D., Jaikumar, N., and Holbrook, N. M. (2003). The 'hydrology' of leaves: co-ordination of structure and function in temperate woody species. *Plant Cell Environ.* 26, 1343–1356. doi: 10.1046/j.0016-8025.2003.01058.x

Sakai, H., Hua, J., Chen, Q. G., Chang, C., Medrano, L. J., Bleecker, A. B., et al. (1998). ETR2 is an ETR1-like gene involved in ethylene signaling in Arabidopsis. *Proc. Natl. Acad. Sci. U.S.A.* 95, 5812–5817. doi: 10.1073/pnas.95.10.5812

Sanikhani, M., Mibus, H., Stummann, B. M., and Serek, M. (2008). Kalanchoe blossfeldiana plants expressing the Arabidopsis *etr1-1* allele show reduced ethylene sensitivity. *Plant Cell Rep.* 27, 729–737. doi: 10.1007/s00299-007-0493-6

Savin, K. W., Baudinette, S. C., Graham, M. W., Michael, M. Z., Nugent, G. D., Lu, C. Y., et al. (1995). Antisense ACC oxidase RNA delays carnation petal senescence. *Hortic. Sci.* 30, 970–972.

Shibuya, K., Barry, K. G., Ciardi, J. A., Loucas, H. M., Underwood, B. A., Nourizadeh, S., et al. (2004). The central role of PhEIN2 in ethylene responses throughout plant development in petunia. *Plant Physiol.* 136, 2900–2912. doi: 10.1104/pp.104.046979

Simpson, G. G., and Dean, C. (2002). Arabidopsis, the Rosetta Stone of flowering time? *Science* 296, 285–289.

Sitrit, Y., and Bennett, A. B. (1998). Regulation of tomato fruit polygalacturonase mRNA accumulation by ethylene: a re-examination. *Plant Physiol.* 116, 1145–1150. doi: 10.1104/pp.116.3.1145

Smith, C. J. S., Watson, C. F., Ray, J., Bird, C. R., Morris, P. C., Schuch, W., et al. (1988). Antisense RNA inhibition of polygalacturonase gene expression in transgenic tomatoes. *Nature* 334, 724–726. doi: 10.1038/334724a0

Smith, D. L., Abbott, J. A., and Gross, K. C. (2002). Down-regulation of tomato β-galactosidase 4 results in decreased fruit softening. *Plant Physiol.* 129, 1755–1762. doi: 10.1104/pp.011025

Solano, R., Stepanova, A., Chao, Q. M., and Ecker, J. R. (1998). Nuclear events in ethylene signaling: a transcriptional cascade mediated by ETHYLENE-INSENSITIVE3 and ETHYLENE-RESPONSE-FACTOR1. *Genes Dev.* 12, 3703–3714. doi: 10.1101/gad.12.23.3703

Sriskandarajah, S., Mibus, H., and Serek, M. (2007). Transgenic *Campanula carpatica* plants with reduced ethylene sensitivity. *Plant Cell Rep.* 26, 805–813. doi: 10.1007/s00299-006-0291-6

Stead, A. D. (1992). Pollination-induced flower senescence: a review. *Plant Growth Regul.* 11, 13–20. doi: 10.1007/BF00024427

Stepanova, A. N., and Alonso, J. M. (2009). Ethylene signaling and response: where different regulatory modules meet. *Curr. Opin. Plant Biol.* 12, 548–555. doi: 10.1016/j.pbi.2009.07.009

Sterling, T. M., and Hall, J. C. (1997). "Mechanism of action of natural auxins and the auxinic herbicides," in *Herbicide Activity: Toxicology, Biochemistry and Molecular Biology*, eds R. M. Roe, J. D. Burton, and R. J. Kuhr (Amsterdam: IOS Press).

Sun, T. P., and Gubler, F. (2004). Molecular mechanism of gibberellin signaling in plants. *Ann. Rev. Plant Biol.* 55, 197–223. doi: 10.1146/annurev.arplant.55.031903.141753

Sýkorová, B., Kurešová, G., Daskalova, S., Trèková, M., Hoyerová, K., Raimanová, I., et al. (2008). Senescence-induced ectopic expression of the A. tumefaciens ipt gene in wheat delays leaf senescence, increases cytokinin content, nitrate influx, and nitrate reductase activity, but does not affect grain yield. *J. Exp. Bot.* 59, 377–387. doi: 10.1093/jxb/erm319

Tadiello, A., Ziosi, V., Negri, A. S., Noferini, M., Fiori, G., Busatto, N., et al. (2016). On the role of ethylene, auxin and a GOLVEN-like peptide hormone in the regulation of peach ripening. *BMC Plant Biol.* 16:1. doi: 10.1186/s12870-016-0730-7

Tan, Y., Liu, J., Huang, F., Guan, J., Zhong, S., Tang, N., et al. (2014). PhGRL2 protein, interacting with PhACO1, is involved in flower senescence in the petunia. *Mol. Plant* 7, 1384–1387. doi: 10.1093/mp/ssu024

Tanase, K., Otsu, S., Satoh, S., and Onozaki, T. (2015). Expression levels of ethylene biosynthetic genes andsenescence-related genes in carnation (*Dianthus caryophyllus* L.) with ultra-long-life flowers. *Sci. Hortic.* 183, 31–38. doi: 10.1016/j.scienta.2014.11.025

Tang, X., Gomes, A., Bhatia, A., and Woodson, W. R. (1994). Pistil-specific and ethylene-regulated expression of 1-aminocyclopropane-1-carboxylate oxidase genes in Petunia flowers. *Plant Cell* 6, 1227–1239. doi: 10.1105/tpc.6.9.1227

Tardieu, F., Parent, B., and Simonneau, T. (2010). Control of leaf growth by abscisic acid: hydraulic or non-hydraulic processes? *Plant Cell Environ.* 33, 636–647. doi: 10.1111/j.1365-3040.2009.02091.x

Taverner, E., Letham, D. S., Wang, J., Cornish, E., and Willcocks, D. A. (1999). Influence of ethylene on cytokinin metabolism in relation to Petunia corolla senescence. *Phytochemistry* 51, 341–347. doi: 10.1016/S0031-9422(98)00757-2

Taylor, J. E., and Whitelaw, C. A. (2001). Signals in abscission. *New Phytol.* 151, 323–340. doi: 10.1046/j.0028-646x.2001.00194.x

Tholen, D., Voesenek, L. A. C. J., and Poorter, H. (2004). Ethylene insensitivity does not increase leaf area or relative growth rate in *Arabidopsis thaliana*, *Nicotiana tabacum* and *Petunia x hybrida*. *Plant Physiol.* 134, 1803–1812. doi: 10.1104/pp.103.034389

Thompson, J. E., Froese, C. D., Madey, E., Smith, M. D., and Hong, Y. W. (1998). Lipid metabolism during plant senescence. *Prog. Lipid Res.* 37, 119–141. doi: 10.1016/S0163-7827(98)00006-X

Tieman, D. M., Taylor, M. G., Ciardi, J. A., and Klee, H. J. (2000). The tomato ethylene receptors NR and LeETR4 are negative regulators of ethylene response and exhibit functional compensation within a multigene family. *Proc. Natl. Acad. Sci. U.S.A.* 97, 5663–5668. doi: 10.1073/pnas.090550597

Trainotti, L., Tadiello, A., and Casadoro, G. (2007). The involvement of auxin in the ripening of climacteric fruits comes of age: the hormone plays a role of its own and has an intense interplay with ethylene in ripening peaches. *J. Exp. Bot.* 58, 3299–3308. doi: 10.1093/jxb/erm178

Trivedi, P. K., and Nath, P. (2004). MaExp1, an ethylene-induced expansin from ripening banana fruit. *Plant Sci.* 167, 1351–1358. doi: 10.1016/j.plantsci.2004.07.005

Trivellini, A., Cocetta, G., Hunter, D. A., Vernieri, P., and Ferrante, A. (2016). Spatial and temporal transcriptome changes occurring during flower opening and senescence of the ephemeral hibiscus flower. *J. Exp. Bot.* 67, 5919–5931. doi: 10.1093/jxb/erw295

Trivellini, A., Cocetta, G., Vernieri, P., Sodi, A. M., and Ferrante, A. (2015). Effect of cytokinins on delaying petunia flower senescence: a transcriptome study approach. *Plant Mol. Biol.* 87, 169–180. doi: 10.1007/s11103-014-0268-8

Trivellini, A., Ferrante, A., Vernieri, P., and Serra, G. (2011a). Effects of abscisic acid on ethylene biosynthesis and perception in *Hibiscus rosa-sinensis* L. flower development. *J. Exp. Bot.* 62, 5437–5452. doi: 10.1093/jxb/err218

Trivellini, A., Ferrante, A., Vernieri, P., and Serra, G. (2011b). Effects of promoters and inhibitors of ABA and ethylene on flower senescence of *Hibiscus rosa-sinensis* L. *J. Plant Growth Regul.* 30, 175–184. doi: 10.1093/jxb/err218

Trusov, Y., and Botella, J. R. (2006). Silencing of the ACC synthase gene ACACS2 causes delayed flowering in pineapple (*Ananas. comosus* (L.) Merr.). *J. Exp. Bot.* 57, 3953–3960. doi: 10.1093/jxb/erl167

Uluisik, S., Chapman, N. H., Smith, R., Poole, M., Adams, G., Gillis, R. B., et al. (2016). Genetic improvement of tomato by targeted control of fruit softening. *Nat. Biotechnol.* 34, 1072. doi: 10.1038/nbt.3602

Valdes, H. H., Pizarro, M. M., Campos-Vargas, R. R., Infante, R. R., and Defilippi, B. (2009). Effect of ethylene inhibitors on quality attributes of apricot cv. Modesto and Patterson during storage. *Chilean J. Agric. Res.* 69, 134–144. doi: 10.4067/S0718-58392009000200002

Van Doorn, W. G. (2001). Categories of petal senescence and abscission: a re-evaluation. *Ann. Bot.* 87, 447–456. doi: 10.1006/anbo.2000.1357

Van Doorn, W. G., Fisun, G. C., Pak, C., and Harkema, H. (2013). Delay of Iris flower senescence by cytokinins and jasmonates. *Physiol. Plant.* 148, 105–120. doi: 10.1111/j.1399-3054.2012.01690.x

Vandenbussche, F., Vancompernolle, B., Rieu, I., Ahmad, M., Phillips, A., Moritz, T., et al. (2007). Ethylene induced Arabidopsis hypocotyl elongation is dependent on but not mediated by gibberellins. *J. Exp. Bot.* 58, 4269–4281. doi: 10.1093/jxb/erm288

Voisin, A. S., Reidy, B., Parent, B., Rolland, G., Redondo, E., Gerentes, D., et al. (2006). Are ABA, ethylene or their interaction involved in the response of leaf growth to soil water deficit? An analysis using naturally occurring variation or genetic transformation of ABA production in maize. *Plant Cell Environ.* 29, 1829–1840. doi: 10.1111/j.1365-3040.2006.01560.x

Wang, H., Stier, G., Lin, J., Liu, G., Zhang, Z., Chang, Y., et al. (2013). Transcriptome changes associated with delayed flower senescence on transgenic Petunia by inducing expression of etr1-1, a mutant ethylene receptor. *PLoS ONE* 8:e65800. doi: 10.1371/journal.pone.0065800

Wang, K. L., Li, H., and Ecker, J. R. (2002). Ethylene biosynthesis and signaling networks. *Plant Cell* 14, 131–151.

Wang, K. L., Yoshida, H., Lurin, C., and Ecker, J. R. (2004). Regulation of ethylene gas biosynthesis by the *Arabidopsis* ETO1 protein. *Nature* 428, 945–950. doi: 10.1038/nature02516

Wang, Q., Zhang, W., Yin, Z., and Wen, C. K. (2013). Rice CONSTITUTIVE TRIPLE-RESPONSE2 is involved in the ethylene-receptor signaling and regulation of various aspects of rice growth and development. *J. Exp. Bot.* 264, 4863–4875. doi: 10.1093/jxb/ert272

Wijayanti, L., Fujioka, S., Kobayashi, M., and Sakurai, A. (1997). Involvement of abscisic acid and indole-3-acetic acid in the flowering of *Pharbitis nil*. *J. Plant Growth Regul.* 16, 115–119. doi: 10.1007/PL00006977

Wilkinson, S., and Davies, W. J. (2010). Drought, ozone, ABA and ethylene: new insights from cell to plant to community. *Plant Cell Environ.* 33, 510–525. doi: 10.1111/j.1365-3040.2009.02052.x

Wilmowicz, E., Frankowski, K., Kućko, A., Kęsy, J., and Kopcewicz, J. (2014). Involvement of the iaa-regulated acc oxidase gene PNACO3 in *Pharbitis nil* flower inhibition. *Acta Biol. Crac. Ser. Bot.* 56, 90–96. doi: 10.2478/abcsb-2014-0013

Wilmowicz, E., Kęsy, J., and Kopcewicz, J. (2008). Ethylene and ABA interactions in the regulation of flower induction in *Pharbitis nil*. *J. Plant Physiol.* 165, 1917–1928. doi: 10.1016/j.jplph.2008.04.009

Wilson, R. N., Heckman, J. W., and Somerville, C. R. (1992). Gibberellin is required for flowering in *Arabidopsis thaliana* under short days. *Plant Physiol.* 100, 403–408. doi: 10.1104/pp.100.1.403

Woeste, K. E., Ye, C., and Kieber, J. J. (1999). Two Arabidopsis mutants that overproduce ethylene are affected in the posttranscriptional regulation of 1-aminocyclopropane-1-carboxylic acid synthase. *Plant Physiol.* 119, 521–530. doi: 10.1104/pp.119.2.521

Woltering, E. J., and Van Doorn, W. (1988). Role of ethylene in senescence of petals-morphological and taxonomical relationships. *J. Exp. Bot.* 39, 1605–1616. doi: 10.1093/jxb/39.11.1605

Wuriyanghan, H., Zhang, B., Cao, W. H., Ma, B., Lei, G., Liu, Y. F., et al. (2009). The ethylene receptor ETR2 delays floral transition and affects starch accumulation in rice. *Plant Cell* 21, 1473–1494. doi: 10.1105/tpc.108.065391

Xu, X., Gookin, T., Jiang, C. Z., and Reid, M. S. (2007). Genes associated with opening and senescence of *Mirabilis jalapa* flowers. *J. Exp. Bot.* 58, 2193–2201. doi: 10.1093/jxb/erm058

Xu, Y., Gianfagna, T., and Huang, B. R. (2010). Proteomic changes associated with expression of a gene (ipt) controlling cytokinin synthesis for improving heat tolerance in a perennial grass species. *J. Exp. Bot.* 61, 3273–3289. doi: 10.1093/jxb/erq149

Xu, Y., Tian, J., Gianfagna, T., and Huang, B. (2009). Effects of SAG12-ipt expression on cytokinin production, growth and senescence of creeping bentgrass (*Agrostis stolonifera* L.) under heat stress. *Plant Growth Regul.* 57, 281–291. doi: 10.1007/s10725-008-9346-8

Yamaguchi, S. (2008). Gibberellin metabolism and its regulation. *Ann. Rev. Plant Biol.* 59, 225–251. doi: 10.1146/annurev.arplant.59.032607.092804

Yang, J., Zhang, J., Wang, Z., Zhu, Q., and Liu, L. (2003). Involvement of abscisic acid and cytokinins in the senescence and remobilization of carbon reserves in wheat subjected to water stress during grain filling. *Plant Cell Environ.* 26, 1621–1631. doi: 10.1046/j.1365-3040.2003.01081.x

Yin, J., Chang, X., Kasuga, T., Bui, M., Reid, M. S., and Jiang, C. Z. (2015). A basic helix-loop-helix transcription factor, PhFBH4, regulates flower senescence by modulating ethylene biosynthesis pathway in petunia. *Hortic. Res.* 2:15059. doi: 10.1038/hortres.2015.59

Yoo, S. D., Cho, Y., and Sheen, J. (2009). Emerging connections in the ethylene signaling network. *Trends Plant Sci.* 14, 270–279. doi: 10.1016/j.tplants.2009.02.007

Yoo, S. D., Cho, Y. H., Tena, G., Xiong, Y., and Sheen, J. (2008). Dual control of nuclear EIN3 by bifurcate MAPK cascades in C2H4 signalling. *Nature* 451, 789–795. doi: 10.1038/nature06543

Zakizadeh, H., Lutken, H., Sriskandarajah, S., Serek, M., and Muller, R. (2013). Transformation of miniature potted rose (*Rosa hybrida* cv. Linda) with P(SAG12)-ipt gene delays leaf senescence and enhances resistance to exogenous ethylene. *Plant Cell Rep.* 32, 195–205. doi: 10.1007/s00299-012-1354-5

Zeevaart, J. A. D., and Talon, M. (1992). "Gibberellin mutants in *Arabidopsis thaliana*," in *Progress in Plant Growth Regulation*, eds C. M. Karssen, L. C. Van Loon, and D. Vreugdenhil (Dordrecht: Kluwer), 34–42. doi: 10.1007/978-94-011-2458-4_4

Zhang, M., Yuan, B., and Leng, P. (2009). The role of ABA in triggering ethylene biosynthesis and ripening of tomato fruit. *J. Exp. Bot.* 60, 1579–1588. doi: 10.1093/jxb/erp026

Zhang, P., Wang, W. Q., Zhang, G. L., Kaminek, M., Dobrev, P., Xu, J., et al. (2010). Senescence-inducible expression of isopentenyl transferase extends leaf life, increases drought stress resistance and alters cytokinin metabolism in cassava. *J. Integr. Plant Biol.* 52, 653–669. doi: 10.1111/j.1744-7909.2010.00956.x

Zhou, D., Kalaitzis, P., Mattoo, A. K., and Tucker, M. L. (1996). The mRNA for an ETR1 homologue in tomato is constitutively expressed in vegetative and reproductive tissues. *Plant Mol. Biol.* 30, 1331–1338. doi: 10.1007/BF00019564

Zimmermann, P., Hirsch-Hoffmann, M., Hennig, L., and Gruissem, W. (2004). GENEVESTIGATOR Arabidopsis microarray database and analysis toolbox. *Plant Physiol.* 136, 2621–2632. doi: 10.1104/pp.104.046367

Conflict of Interest Statement: The authors declare that the research was conducted in the absence of any commercial or financial relationships that could be construed as a potential conflict of interest.

The reviewer BVDP and handling Editor declared their shared affiliation, and the handling Editor states that the process nevertheless met the standards of a fair and objective review.

frontiers in Plant Science

ORIGINAL RESEARCH
published: 01 November 2016
doi: 10.3389/fpls.2016.01606

Molecular Characterization and Functional Analysis of Two Petunia *PhEILs*

Feng Liu[1,2†], Li Hu[1†], Yuanping Cai[1], Hong Lin[1], Juanxu Liu[1] and Yixun Yu[1,2]**

[1] Guangdong Key Laboratory for Innovative Development and Utilization of Forest Plant Germplasm, College of Forestry and Landscape Architecture, South China Agricultural University, Guangzhou, China, [2] College of Horticulture, South China Agricultural University, Guangzhou, China

Ethylene plays an important role in flower senescence of many plants. *Arabidopsis* ETHYLENE INSENSITIVE3 (EIN3) and its homolog EIL1 are the downstream component of ethylene signaling transduction. However, the function of EILs during flower senescence remains unknown. Here, a petunia *EIL* gene, *PhEIL2*, was isolated. Phylogenetic tree showed that PhEIL1, whose coding gene is previously isolated, and PhEIL2 are the homologs of *Arabidopsis* AtEIL3 and AtEIL1, respectively. The expression of both *PhEIL1* and *PhEIL2* is the highest in corollas and increased during corolla senescence. Ethylene treatment increased the mRNA level of *PhEIL1* but reduced that of *PhEIL2*. VIGS-mediated both *PhEIL1* and *PhEIL2* silencing delayed flower senescence, and significantly reduced ethylene production and the expression of *PhERF3* and *PhCP2*, two senescence-associated genes in petunia flowers. The PhEIL2 protein activating transcription domain is identified in the 353-612-amino acids at C-terminal of PhEIL2 and yeast two-hybrid and bimolecular fluorescence complementation assays show that PhEIL2 interacts with PhEIL1, suggesting that PhEIL1 and PhEIL2 might form heterodimers to recognize their targets. These molecular characterizations of PhEIL1 and PhEIL2 in petunia are different with those of in *Vigna radiata* and *Arabidopsis*.

Keywords: petunia, VIGS, flower senescence, ethylene signaling, EIL

OPEN ACCESS

Edited by:
Antonio Ferrante, University of Milan, Italy

Reviewed by:
Clay Carter, University of Minnesota, USA
Chi-Kuang Wen, Shanghai Institutes for Biological Sciences (CAS), China

****Correspondence:***
Juanxu Liu
juanxuliu@scau.edu.cn
Yixun Yu
yuyixun@scau.edu.cn

† These authors have contributed equally to this work.

Specialty section:
This article was submitted to Plant Physiology, a section of the journal Frontiers in Plant Science

Received: *21 March 2016*
Accepted: *12 October 2016*
Published: *01 November 2016*

Citation:
Liu F, Hu L, Cai Y, Lin H, Liu J and Yu Y (2016) Molecular Characterization and Functional Analysis of Two Petunia PhEILs. Front. Plant Sci. 7:1606. doi: 10.3389/fpls.2016.01606

INTRODUCTION

Plant hormone ethylene plays an important role in plant growth and development (Abeles et al., 1992). Ethylene perception is mediated by ETR1 family (Chang et al., 1993; Hua et al., 1995, 1998; Schaller and Bleecker, 1995). CONSTITUTIVE TRIPLE RESPONSE 1 (CTR1), a Raf-like Ser/Thr protein kinase, functions in downstream of receptors and in upstream of the central regulator ETHYLENE-INSENSITIVE2 (EIN2) (Kieber et al., 1993; Alonso et al., 1999). EIN2 is phosphorylated by CTR1 to trigger its endoplasmic reticulum (ER)–to–nucleus translocation and to control ethylene signaling from the ER membrane to the nucleus (Ju et al., 2012; Qiao et al., 2012). The C-terminal end of EIN2 (CEND) is thought to participate in signaling output, as ectopic expression of this domain alone can partially activate ethylene responses (Alonso et al., 2003; Wen et al., 2012). The CEND of EIN2 can be phosphorylated by the receptors-activated CTR1 in the absence of ethylene and phosphorylation-regulated proteolytic processing of EIN2 triggers its ER-to-nucleus translocation (Ju et al., 2012; Qiao et al., 2012). Inhibition of CTR1 upon ethylene perception is a signal for cleavage and nuclear localization of the EIN2 C terminus to stabilize EIN3 protein (Wen et al., 2012; Ji and Guo, 2013).

In *Arabidopsis*, EIN3 and three related EIN3-LIKE (EIL1, EIL2, and EIL3) proteins were shown to possess amino acid sequence similarity and conserved structural features for nuclear-localized transcription factors (Chao et al., 1997). The ethylene signal is transmitted to the EIN3 family of transcription factors, which have been shown to act as a transcriptional activator and bind to the primary ethylene-response element present in the promoter of the ethylene-responsive *ERF1* gene (Chao et al., 1997; Solano et al., 1998). One found that the control of EIN3 degradation is important to regulation of ethylene signaling transduction (Yanagisawa et al., 2003). Two F-box proteins, EBF1 and EBF2 interact with EIN3 and EIL1 (Guo and Ecker, 2003; Potuschak et al., 2003), and disruption of either *EBF1* or *EBF2* leads to the increase of EIN3 protein levels and induces a hypersensitivity to ethylene. The *ebf1 ebf2* double mutant results in a large accumulation of EIN3 proteins and causes a constitutive ethylene response phenotype (Gagne et al., 2004).

Recently, another mechanism of EIN2-mediated ethylene signaling was reported in *Arabidopsis* (Li et al., 2015). The translational repression of *EBF1* and *EBF2* transcription is imposed by EIN2. The EIN2-directed translational repression is mediated by the *EBF1/2* 3′UTRs and multiple poly-uridylates (PolyU) motifs are identified as functional *cis* elements of 3′UTRs (Li et al., 2015).

Ethylene production is increased during flower senescence in many flowers, including petunia, often as the model system for studying the biological bases of flower senescence (Borochov and Woodson, 1989). However, the function of petunia EILs during flower senescence is not well known.

In petunia *EIL* family, *PhEIL1* (accession no. Y353248) has been identified and its expression in response ethylene treatment was reported (Shibuya et al., 2004). Here, another full-length cDNA of petunia *EIL* gene, *PhEIL2*, was cloned. *PhEIL1* and *PhEIL2* expression profile was established in different petunia tissues, at various stages of flower senescence and in response to ethylene. VIGS-mediated both *PhEIL1* and *PhEIL2* silencing delayed flower senescence in petunia and reduced the expression of two senescence-associated genes. Yeast two-hybrid (Y2H) and bimolecular fluorescence complementation (BiFC) assays showed that PhEIL2 interacts with PhEIL1.

MATERIALS AND METHODS

Plant Material

Petunia (*Petunia hybrida* 'Ultra') plants were grown under normal greenhouse conditions (22°C, 14-h light/10-h dark). Flowers were emasculated 1 day before flowers were fully open to prevent self-pollination. Eight to ten petunia flowers were harvested at anthesis stages and placed in distilled water for further processing. Corollas were collected from petunias at 0, 1, 2, 3, 4, 5, 6, 7, and 8 days after flower opening. Stems, leaves and roots were collected from plants at the vegetative stage when the plants were about 10 cm in height. These tissues were firstly frozen in liquid nitrogen and then stored at −80°C. All experiments were performed at least three times.

RNA Extraction and RT-PCR

RNA extraction and RT-PCR was performed according to the previous protocols (Liu et al., 2010). The RNA content was determined spectrophotometrically. One microgram of total RNA was reverse transcribed at 42°C for 1 h in a final volume of 20 μl containing reaction buffer, 20 mmol l^{-1} DTT, 0.5 mmol l^{-1} dNTP, 1 μg Oligo (dT) 15 and reverse transcriptase (AMV, Promega, USA) according to the manufacturer's instructions.

Cloning of the Petunia *PhEIL2* Gene

The partial sequence of *PhEIL2* was obtained by to the previously described approach (Yang et al., 2009). In brief, TBLASTN analysis against the Genebank EST database[1] with *AtEIN3* and *AtEIL1* identified one petunia clone, FN029455, which encodes putative protein displaying high homology with AtEIN3 and AtEIL1, respectively.

The remaining 5′ and 3′ cDNA sequences of *PhEIL2* were cloned by rapid-amplification of cDNA ends (RACE) with the forward primer 5′CTATCCTGATCGCTGCCCACCT3′ and revered primer 5′TCTCCAATGGAAATCTTCTCTG3′ (Liu et al., 2010).

Sequence Analysis

The neighbor-joining tree at amino acid level was drawn by DNAMAN software. The reliability of each branch of the tree was assessed using 1,000 bootstrap replications. Identity search for nucleotides and translated amino acids was carried out using National Center for Biotechnology Information (NCBI) BLAST network server[2].

Ethylene Measurements

Petunia flowers were treated with ethylene according to previously described protocols (Tan et al., 2014). To measure ethylene production, corollas of each individual flower were collected and placed in a 200 ml airtight container according to the method of Liu et al. (2010). Thus, to avoid the contamination of wound-induced ethylene, the containers were capped and incubated at 25°C for 1 h. Next, a 2 ml sample of head-space gas was withdrawn using a gas-tight hypodermic syringe and was injected into a gas chromatograph (GC 17A, Shimadzu, Kyoto, Japan) to measure the ethylene concentration. The gas chromatograph was equipped with a flame ionization detector and an activated alumina column. All measurements were performed in five replicates.

Quantitative Real-Time PCR Assays

Total RNA extracted from various tissues was digested with DNAase I and then reverse transcription (RT) was performed according to the kit instruction (TaKaRa, China). PCR analysis was carried out with the cDNA as a template. Specific primer design was performed using the sequences obtained for *PhEIL1*, *PhEIL2*, *PhERF3,* and *PhCP2*. The petunia *Actin* (accession no. FN014209) genes were used as the internal reference gene

[1] http://www.ncbi.nlm.nih.gov

[2] https://blast.ncbi.nlm.nih.gov/Blast.cgi

to quantify the cDNA abundance (Mallona et al., 2010). The sequences of all primers used for qPCR analysis are described in Supplementary Table S2.

Ethylene and Pollination Treatment

Petunia flowers were treated with ethylene according to the previously described protocols (Yang et al., 2015). Petunia flowers were harvested at anthesis and their stems re-cut to 5 cm, placed in flasks with distilled water, and subsequently treated with 2 $\mu l\ l^{-1}$ ethylene for 0, 2, 4, 8, 12, and 24 h. To measure the expression of *PhEIL1* and *PhEIL2* after pollination, three flowers from each of six plants (18 flowers in total per genotype) for different lines were self-pollinated on the plant on the day before anthesis (Shibuya et al., 2004). Corollas from 8 to 10 flowers were collected at each time point, immediately frozen in liquid nitrogen, and stored at −80°C for later RNA extraction.

Agroinoculation of TRV Vectors

Approximately 250 bp 3′ untranslated regions of *PhEIL1* and *PhEIL2* were cloned into the pTRV2-CHS vector to formed TRV2-CHS-PhEIL1 and TRV2-CHS-PhEIL2 vectors using their respective forward and reverse primers (Supplementary Table S3). pTRV1 and different pTRV2 derivatives vectors were transformed into *Agrobacterium tumefaciens* (strain GV3101) (Spitzer-Rimon et al., 2010). The *Agrobacterium* culture was grown overnight at 28°C in Luria-Bertani medium with 50 mg l^{-1} kanamycin and 200 mM acetosyringone. The cells were harvested and resuspended in inoculation buffer containing 10 mM MES, pH 5.5, 200 mM acetosyringone, and 10 mM $MgCl_2$ to an OD_{600} of 10. Following an additional 3 h of incubation at 28°C, the bacteria containing pTRV1 were mixed with the bacteria containing the pTRV2 derivatives in a 1:1 ratio. Next, 200 to 300 ml of this mixture was applied to the cut surface of petunia plantlets after the removal of the apical meristems.

Flower Longevity

Flower longevity was measured according to previously described methods (Tan et al., 2014). To measure flower senescence, three flowers were removed from each of 20 plants (60 flowers in total per genotype) from the wild type (purple) and VIGS-mediated gene suppression lines (white) on the day before anthesis, and the flowers were placed in vials of water. The flowers were then placed in a growth room under continuous fluorescent light at 24–26°C, and the day on which each flower completely wilted was recorded.

The data were analyzed using the ANOVA function of SAS 8.02 (Cary, NC, USA) to compare differences among genotypes. Tukey's honestly significant difference mean-separation test was used to calculate the mean separation at the 0.05% level (HSD0.05).

Deletion Mutant Construction of PhEIL2 and Analyze of Transactivation Activity

The deletion mutants of PhEIL2 were constructed by PCR. The sequences of all primers used for various PhEIL2 deletion mutants are described in Supplementary Table S4. The PCR products were fused in frame to the yeast GAL4 DNA-binding domain expression vector pGBKT7. The constructed vectors were transformed into *Saccharomyces cerevisiae* strain Y2HGold (Clontech, Palo Alto, CA, USA). The β-galactosidase assay was performed according to the kit instructions (Clontech).

Yeast Two-Hybrid Analysis

The coding sequence of PhEIL2 was cloned into the bait vector pGBKT7, and the coding sequences of *PhEIL1* were cloned into the prey vector pGADT7. The gene-specific primers of the three genes are shown in Supplementary Table S5. The mating reactions were performed between the two haploid strains containing the pGBKT7-PhEIL2 and pGADT7-PhEIL1 constructs and were plated on double dropout medium (DDO medium, SD/–Leu/–Trp) (BD Biosciences Clontech). The transformants were further streaked on quadruple dropout medium (QDO medium, SD/–Trp/–Leu/–His/–Ade) and were confirmed with a color change on β-galactosidase filter paper using a flash-freezing filter assay (Tan et al., 2014).

Bimolecular Fluorescence Complementation (BiFC) Assay

The full-length *PhEIL1* and *PhEIL2* cDNAs were inserted into pSAT-1628 (pYFC) and pSAT-1882 (pYFN) to form the pYFC-PhEIL1 and pYFN-PhEIL2 vectors, respectively. The sequences of all primers used for BiFC are described in Supplementary Table S6. pYFC-PhEIL1 and pYFN-PhEIL2, pYFC-PhEIL1 and pSAT-YFC, pSAT-YFN, and pYFN-PhEIL2 were co-transformed into petunia protoplasts with the pSAT-GFP as positive control (Tan et al., 2014).

Leaves of 5- to 6-week-old petunia plants were used for the preparation of protoplasts. The vectors were used in polyethylene glycol-mediated transformation of the petunia protoplasts (Spitzer-Rimon et al., 2010). The protoplasts were assayed for fluorescence 12–24 h after transformation. The images were produced by the confocal laser scanning system (ECLIPSE TE2000-E; Nikon, Tokyo, Japan).

Statistical Analyses

Statistical analysis was performed using one way analysis of variance (ANOVA) followed by Duncan's multiple range test (DMRT) with three replicates. *P*-values ≤ 0.05 were considered as significant.

RESULTS

Identification of a PhEIL Transcription Factor Gene in Petunia

A *PhEIL* transcription factor gene full-length cDNA was isolated in the petunia 'Ultra,' named *PhEIL2*, since *PhEIL1* had been previously submitted to GeneBank. *PhEIL2* was predicted to encode a 612 amino acid protein, with a calculated molecular weight of 69.1 kDa. The multiple sequence alignments of EIL-like proteins in petunia, tomato and *Arabidopsis* are presented in Supplementary Figure S1. PhEIL1 shares 35.1, 35.6, 29.7, 50.1, and 34.6% amino acid sequence identity with PhEIL2, AtEIL1,

AtEIL2, AtEIL3, and AtEIN3. PhEIL2 shares 62.7, 40.2, 39.3, and 61.8% amino acid sequence identity with AtEIL1, AtEIL2, AtEIL3, and AtEIN3 (Supplementary Table S1). The N-terminal half of the deduced protein of PhEIL1 and PhEIL2 had higher similarity to the corresponding regions of AtEIL3 and AtEIL1 in *Arabidopsis* than their C-terminal half to the corresponding regions of the latter two, respectively (Supplementary Figure S1). As found in other EIN3 homologs, the PhEIL1 and PhEIL2 proteins possess an amino-terminal acidic region, five small clusters of basic amino acids regions and a Pro-rich domain (158–198; 201–242, respectively) (Supplementary Figure S1). The acidic and Pro-rich regions have been proposed to be functional as transcriptional activation domains (Chao et al., 1997). Acidic and proline-rich regions have been widely described as transcriptional activation domains (Mitchell and Tjian, 1989) and may serve such a role in the EIN3/EIL proteins. PhEIL1 and PhEIL2 have a Lys residue at positions 203 and 247, respectively, which is required for the function of EIN3 (Chao et al., 1997; Solano et al., 1998; Alonso et al., 2003). In addition, phylogenetic tree showed that PhEIL1 is the homologs of AtEIL3 and PhEIL2 is the homologs of AtEIL1 and AtEIN3 (Supplementary Figure S2).

Expression of *PhEIL1* and *PhEIL2*

Quantitative real-time PCR (qPCR) analysis showed that both *PhEIL1* and *PhEIL2* mRNA levels are high in corollas and ovaries, and the expression *PhEIL1* is the lowest in stems, while that of *PhEIL2* is the lowest in leaves (**Figure 1A**). During natural flower senescence, the *PhEIL1* mRNA level did not show significant change before day 3 but increased rapidly from days 4 to 6. The expression of *PhEIL2* decreased before day 3, but then increased until day 7 (**Figure 1B**). After ethylene treatment, *PhEIL1* mRNA levels significantly increased from hours 2 to 24, whereas *PhEIL2* expression decreased from 0 to 8 h and then kept stable level until to 24 h (**Figure 1C**). In petunia, pollination induced an ethylene burst and consequently floral senescence (Shibuya et al., 2004). As shown as in **Figure 1D**, the mRNA levels of PhEIL1/PhEIL2 were significantly increased after pollination 8 h by qPCR analysis.

Silencing of Both *PhEIL1* and *PhEIL2* Delays Flower Senescence and Decrease Ethylene Production

The VIGS system with *PhCHS* as the reporter gene has been established in the petunia 'Ultra' (Violet line) by us (Tan et al.,

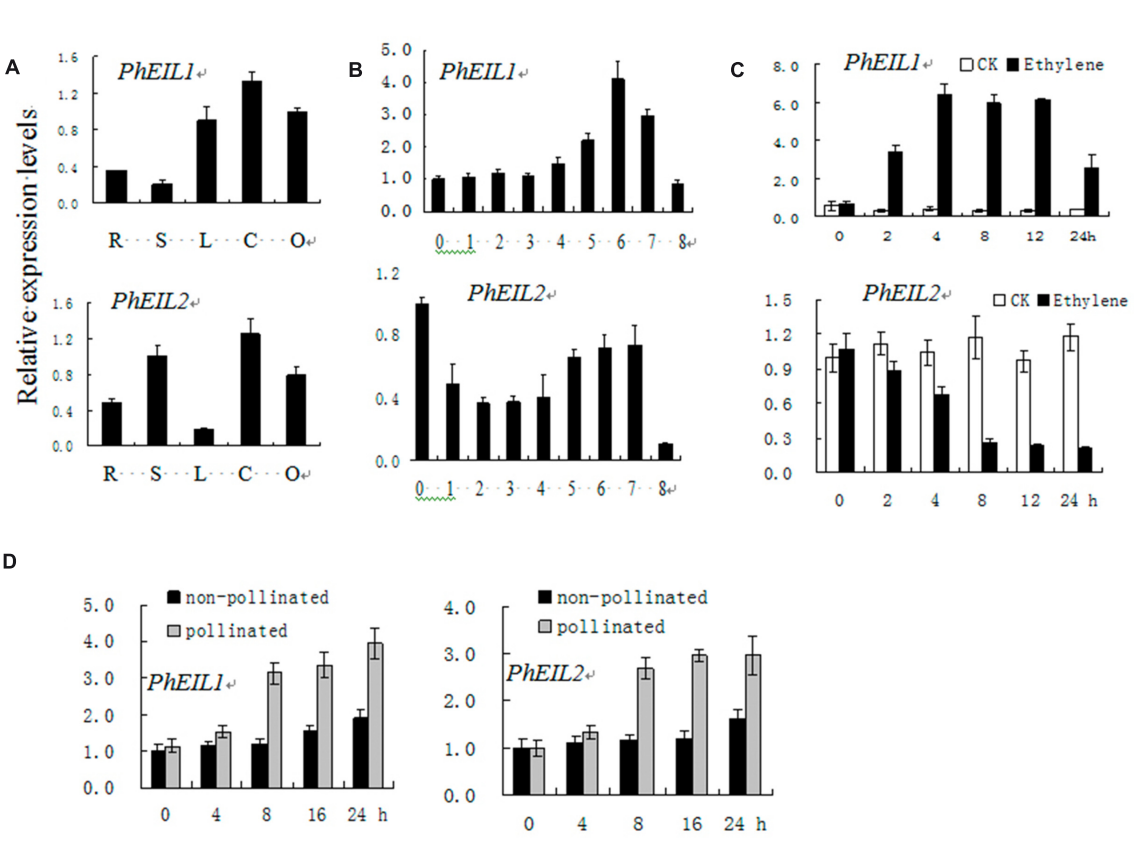

FIGURE 1 | Temporal and spatial expression analysis of *PhEIL1* and *PhEIL2* by quantitative real-time PCR. Expression analysis of *PhEIL1* and *PhEIL2* in different organs **(A)**, in corollas during natural flower senescence **(B)**, response to ethylene **(C),** and pollination **(D)**. R, roots; L, leaves; S, stems; C, corollas, O, ovaries. Relative expression levels are shown as fold change values. Data are the mean ± SD ($n = 3$). Statistical analysis was performed using one way analysis of variance (ANOVA) followed by Duncan's multiple range test (DMRT) with three replicates. P-values ≤ 0.05 were considered as significant.

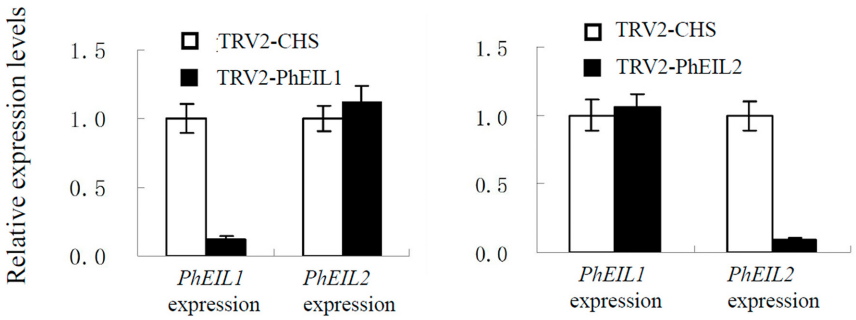

FIGURE 2 | Effects of TRV2-CHS/PhEIL1 and TRV2-CHS/PhPhEIL2 treatment on the expression of *PhEIL1* and *PhEIL2* in white flowers on day 4 after opening by quantitative real-time PCR, respectively. Relative expression levels are shown as fold change values. Data are mean ± SD ($n = 3$). Statistical analysis was performed using one way analysis of variance (ANOVA) followed by Duncan's multiple range test (DMRT) with three replicates. *P*-values ≤ 0.05 were considered as significant.

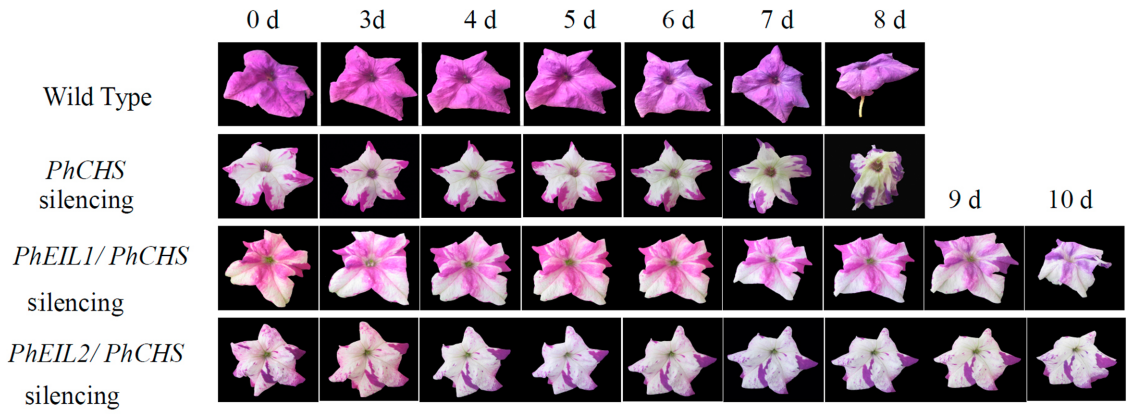

FIGURE 3 | Effects of *PhCHS* silencing, *PhCHS*/*PhEIL1* silencing, and *PhCHS*/*PhEIL2* silencing on the longevity of petunia flowers. Petunia plants were infected with TRV CHS, TRV PhCHS/PhEIL1, or TRV PhCHS/PhEIL2. Flowers showing the white silencing phenotype and purple flowers from uninfected plants were excised and photographed every day after opening.

2014). To identify the effects of *PhEIL1* and *PhEIL2* silencing on flower senescence, TRV-CHS-PhEIL1 and TRV-CHS-PhEIL2 vectors, which were inserted approximately 250 bp fragments of 3′ untranslated sequences of the petunia *PhEIL1* and *PhEIL2* cDNAs into a pTRV2-CHS vector, respectively, were constructed. The *PhEIL1* and *PhEIL2* mRNA levels in the white flowers in the TRV-CHS-PhEIL1 and TRV-CHS-EIL2 treatments, respectively, decreased to less than 20% relative to control (TRV-CHS), and *PhEIL2* and *PhEIL1* mRNA levels did not significantly changed in the flowers of *PhEIL1* and *PhEIL2* silencing, respectively (**Figure 2**).

As shown in **Figure 3** and **Table 1**, the longevity of the flowers of *PhCHS/PhEIL1* silencing and *PhCHS/PhEIL2* silencing was increased compared with that of the flowers from plants of *PhCHS* silencing and wild type plants.

The effects of *PhEIL1* and *PhEIL2* silencing on ethylene production were examined. As shown in **Figure 4**, white flowers of both *PhCHS/PhEIL1* and *PhCHS/PhEIL2* silencing produced less ethylene than those of *PhCHS* silencing (TRV-CHS treatment) in days 4 and 5 after anthesis.

Silencing of Both *PhEIL1* and *PhEIL2* Reduces the Expression of *PhERF3* and *PhCP2*

In petunia, *PhERF3* (HQ259597) and *PhCP2* (AY662988) are regard as senescence-associated genes (Jones et al., 2005; Liu et al., 2010). To further examine the involvement of PhEIL1 and PhEIL2 in flower senescence, the expression of *PhERF3* and *PhCP2* was examined by qPCR in *PhEIL1*- and *PhEIL2*-silenced flowers. Expression of *PhERF3* and *PhCP2* in white flowers with *PhCHS/PhEIL1* and *PhCHS/PhEIL2* silencing was significantly lower than that with *PhCHS* silencing after the flowers were open for 4 and 5 days (**Figure 5**).

The PhEIL2 Protein Activate Transcription in Yeast

Previous research suggested that the N-terminal acidic region (1–50 amino acids) of mung bean (*Vigna radiata*) VR-EIL2, a transcriptional activator, is the transcriptional domain (Lee and Kim, 2003). In order to determine the transcriptional domain, PhEIL2 and its several deletion mutant vectors were constructed

TABLE 1 | The effects of PhEIL1 and PhEIL2 suppression on the longevity of petunia flowers.

	Wild type	PhCHS suppression	PhEIL1 suppression	PhEIL2 suppression
longevity of flowers (day)	6.96 ± 0.82^{c}	7.0 ± 0.8^{c}	8.4 ± 0.9^{b}	10.6 ± 1.3^{a}

Data were expressed as mean ± SD. Different letters indicate significant difference among treatments at the 0.05 significance level based on Duncan's multiple-range test. Error bars indicate standard error of the mean (n = 3).

and the behavior of each construct was investigated in yeast cells. The full-length PhEIL2 protein fused to the GAL4 DNA-binding domain effectively activates the expression of the reporter gene of *lacZ* (**Figures 6A,B**), which indicates the function of PhEIL2 as a transcriptional activator in yeast. Further transcriptional activity analysis of various deletion mutants of PhEIL2 showed that the transcription-stimulating activity was still apparent when the C-terminal regions (353–470 and 471–612 amino acids) were fused to the GAL4 DNA-binding domain; both $PhEIL2_{353-470}$ and $PhEIL2_{471-612}$ mutant protein contained β-galactosidase activity while the $PhEIL2_{1-352}$ mutant protein did not (**Figure 6**). Thus, the 353–612-amino acids at C-terminal of PhEIL2 play an important role for the function of PhEIL2 as a transcriptional activator.

PhEIL2 Interacts with PhEIL1 by Y2H and BiFC Assays

Since EILs could interact with its target as dimmers (Solano et al., 1998) and both PhEIL1 and PhEIL2 are involved in flower senescence in petunia, it is necessary to test whether PhEIL1 interacts with PhEIL2 in petunia and yeast two-hybrid (Y2H) assay was performed. To avoid this activation of the reporter gene, the 5′ ORF of *PhEIL2* cDNA sequence, encoding N-terminal half of the deduced protein (amino acids 1–352), and the full length cDNA of *PhEIL1* were subcloned into the pGBKT7 and pGADT7 vectors to form pGBKT7-$PhEIL2_{1-352}$ bait vector and pGADT7-PhEIL1 prey vector, respectively. The derivative vectors of pGBKT7 and the pGADT7 were co-transformed into the yeast strain Y187. Yeast cells co-transformed with pGBKT7- $PhEIL2_{1-352}$+pGADT7-PhEIL1 grew on selective medium lacking Trp, Leu, His, and Ade in the presence of 5 mM 3-AT. On the contrary, yeast cells harboring pGBKT7+pGADT7-PhEIL1, or pGADT7-$PhEIL2_{1-352}$+pGBKT7 could not grow on the same selective medium (**Figures 7A,B**). These data showed that $PhEIL2_{1-352}$ interacts with PhEIL1 in yeast.

To further test the interaction between PhEIL2 and PhEIL1, BiFC assay was performed. Co-expression of the C-terminal half of YFP fused to PhEIL1 (cYFP-PhEIL1) and the N-terminal half of YFP fused to PhEIL2 (nYFP-PhEIL2) in petunia protoplasts led to fluorescence with GFP as positive control. No interaction was detected between nYFP-PhEIL2 and cYFP, or between nYFP and cYFP-PhEIL1, which confirms the interaction between PhEIL2 and PhEIL1 (**Figures 7C–F**). In addition, previous study showed that EOBII was located in nuclear (Spitzer-Rimon et al., 2010) and with RFP (Red Fluorescent Protein)-EOBII as the nuclear maker, the interaction between PhEIL2 and PhEIL1 was further confirmed (**Figure 7G**).

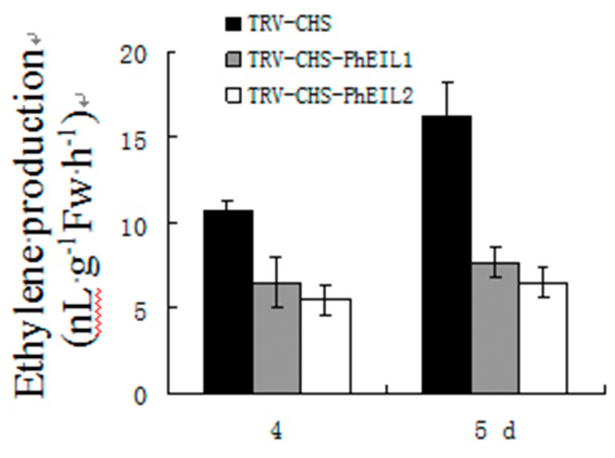

FIGURE 4 | Ethylene productions in *PhEIL1* and *PhEIL2* silencing flowers. Ethylene production was measured for flower corollas after the flowers were open for 4 and 5 days. Ethylene was collected for 2 h and subsequently measured using a gas chromatograph. Ethylene production rates were calculated based on tissue FW. Mean ± SE values were determined from five samples. Statistical analysis was performed using one way analysis of variance (ANOVA) followed by Duncan's multiple range test (DMRT) with three replicates.

DISCUSSION

Ethylene responsiveness in petunia corollas increases highly during flower senescence (Shibuya et al., 2004). In this study, a full-length cDNA of petunia *EIL* gene, *PhEIL2*, was isolated and the characters of *PhEIL2* and *PhEIL2* were identified during flower senescence.

When compared with other EILs described to date from different organisms, the N-terminal half of the deduced protein of PhEIL1 and PhEIL2 had high similarity to the corresponding regions of AtEIL3 and AtEIL1 in *Arabidopsis*, suggesting that they are indeed functional EIN3-like genes (Chao et al., 1997).

Previous research showed that other organisms *EILs* expression are regulated in tissue-specific manners (Waki et al., 2001; Lee and Kim, 2003; Iordachescu and Verlinden, 2005). Similarly, in this study, the relative expression pattern of the two different mRNAs varied in these tissues, with both *PhEIL1* and *PhEIL2* transcript being predominantly present in corollas and up-regulated during flower senescence.

The expression of most of *EILs* of other organisms, such as *Arabidopsis EIN3*, tomato *LeEILs*, and mung bean *Vr-EIL1* and *Vr-EIL2*, was not significantly changed by the treatment of exogenous ethylene in grown plants (Chao et al., 1997; Lee and Kim, 2003). However, in this study, *PhEIL1* mRNA was up-regulated by ethylene, which is in line with the result of previous report (Shibuya et al., 2004), while *PhEIL2* transcriptional level is down-regulated by ethylene. Similarly, *DC-EIL3* mRNA showed significant accumulation while *DC-EIL1* mRNA showed significant reduction upon ethylene exposure in

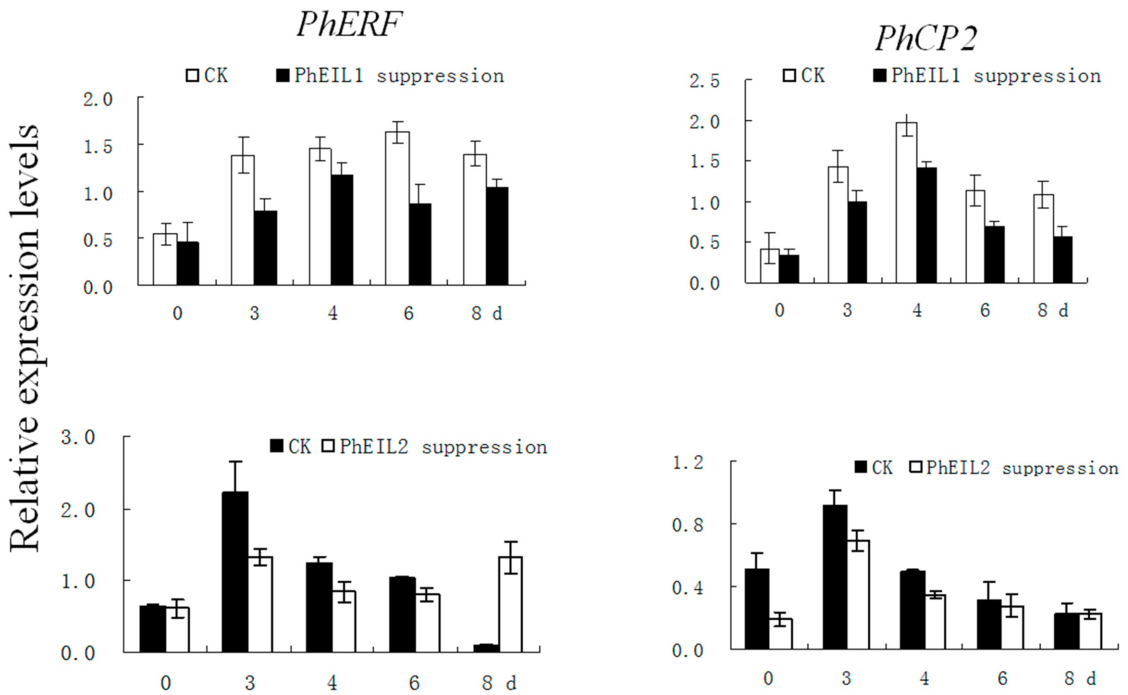

FIGURE 5 | Effects of *PhEIL1* and *PhEIL2* silencing on the expression of *PhERF3* and *PhCP2* in flowers. Flowers were detached on the day in anthesis. Total RNA was isolated from white flower tissues. *PhERF3* and *PhCP2* mRNA levels were determined by quantitative real-time PCR. Relative expression levels are shown as fold change values. Data are the mean ± SD ($n = 3$). Statistical analysis was performed using one way analysis of variance (ANOVA) followed by Duncan's multiple range test (DMRT) with three replicates. *P*-values ≤ 0.05 were considered as significant.

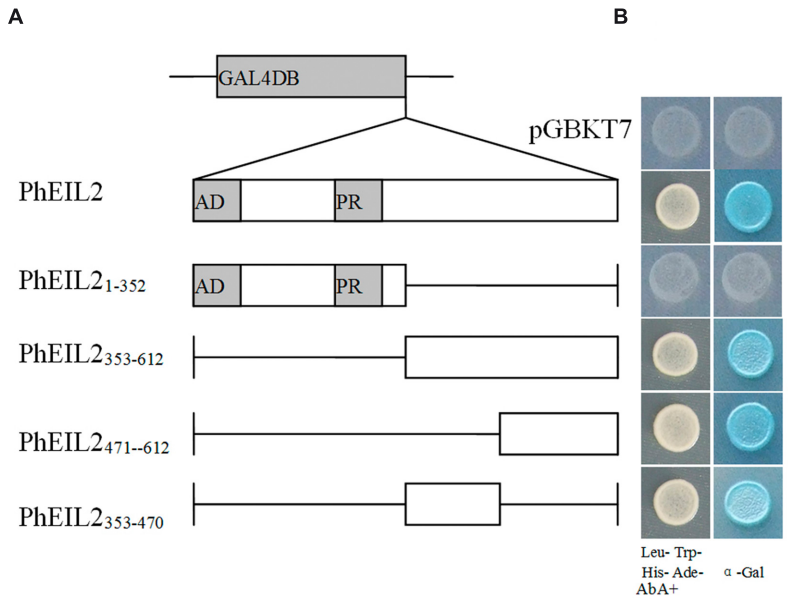

FIGURE 6 | GAL4 DB-PhEIL2 fusions and their effect on transcriptional activation of the *lacZ* reporter gene in yeast cells. (A) Schematic overview of the fusion proteins between the GAL4 DNA-binding domain (DB) and various deletion mutants of PhEIL2 that were investigated for transcription-stimulating activity in yeast. **(B)** The *PhEIL2* and its deletion constructs fused in the GAL4 DB expression vector were transformed into yeast strain Y2HGold. The transformants were selected by growth on Trp- and Leu- medium at 30°C for 3 days. Yeast transformants were tested for growth in the absence of His, Trp, Leu, and Ade but containing 125 μM Aureobasidin A as well as turn blue in the presence of the chromagenic substrate X-β-Gal was scored as a positive interaction. The yeast strain is carrying a modified *HIS* gene whose transcription is under the control of GAL4 operator.

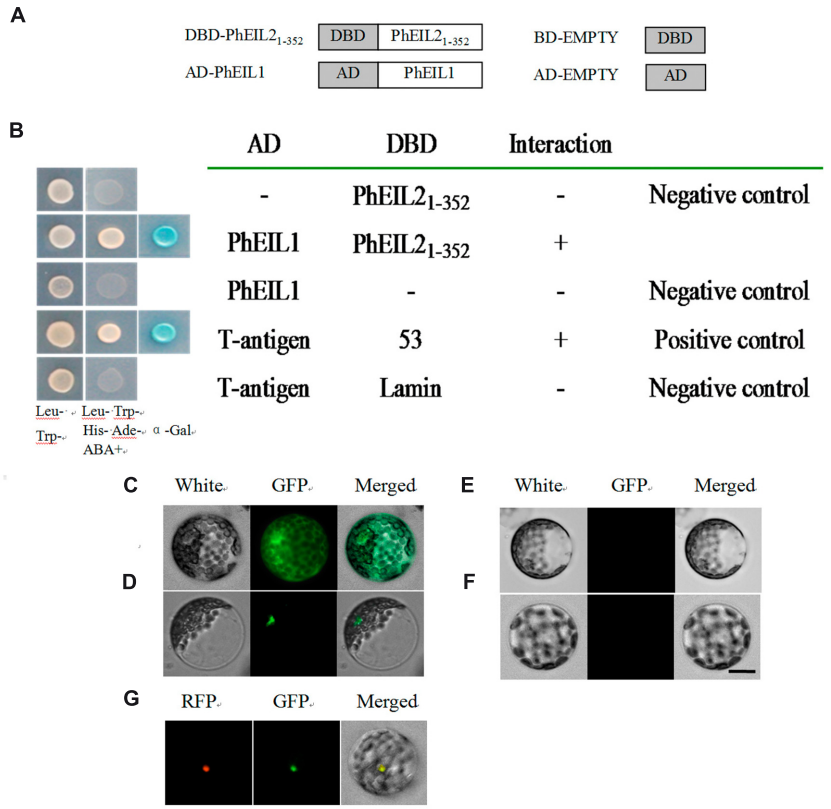

FIGURE 7 | Interaction between PhEIL2$_{1-352}$ and portions of PhEIL1. (A,B) Yeast two-hybrid assays between PhEIL2$_{1-352}$ and portions of PhEIL1. **(A)** Portions of PhEIL2 and PhEIL1 were fused to DBD and AD, respectively; **(B)** interaction between PhEIL2$_{1-352}$ and PhEIL1. Gold Y2H yeast strains were co-transformed with DBD–PhEIL2$_{1-352}$ and PhEIL1. The ability of yeast cells to grow on synthetic medium lacking tryptophan, leucine, histidine, and adenine but containing 125 μM Aureobasidin A as well as turn blue in the presence of the chromagenic substrate X-β-Gal was scored as a positive interaction. Yeast cells transformed with pGBKT7-53+pGADT7-T, pGBKT7–PhEIL2$_{1-352}$+pGADT7-T, pGBKT7–PhEIL2$_{1-352}$+pGADT7-PhEIL1, pGBKT7+pGADT7-PhEIL1, or pGBKT7-Lamin+pGADT7-T were included as positive or negative controls. C-F, BiFC assays between PhEIL2 and PhEIL1. Translational fusion constructs of the coding region of PhEIL2 to pSAT-YFC and the coding region of PhEIL1 to pSAT-YFN were transferred into petunia protoplasts and tested for fluorescence complementation. **(C)** pSAT-GFP; **(D)** YFC-PhEIL2 and YFN-PhEIL1; **(E)** YFC-PhEIL2 and pSAT-YFN; **(F)** pSAT-YFC and YFN-PhEIL1. **(G)** YFC-PhEIL2, YFN-PhEIL1, and RFP-EOBII. Three biological replicates do these results represent in **(G)**. Images of **(C–F)** were captured with a confocal laser scanning system. Scale bars: 5 μm.

carnation (*Dianthus caryophyllus*) (Waki et al., 2001; Iordachescu and Verlinden, 2005). It is possible that the activities of EILs are controlled by a posttranslational mechanism (Chao et al., 1997; Kosugi and Ohashi, 2000; Tieman et al., 2001; Lee and Kim, 2003). Moreover, EIN3 and EIL1 proteins are degraded by EBF1/2 in ethylene signaling (Potuschak et al., 2003).

In petunia, pollination induced an ethylene burst and consequently floral senescence (Shibuya et al., 2004). The mRNA levels of both *PhEIL1* and *PhEIL2* were significantly increased after pollination 8 h by qPCR analysis, although *PhEIL2* expression showed down-regulated by exogenous ethylene treatment, suggesting that *PhEIL2* expression is regulated by multi-factors after pollination.

The etiolated T2 generation seedlings of *Arabidopsis* plants overexpressing the *EIN3* and *EIL1* genes and *TEIL* cDNA, showed a phenotype of constitutive triple response under the condition of lack of exogenous ethylene (Chao et al., 1997; Kosugi and Ohashi, 2000). Consistent with these results, VIGS-mediated both *PhEIL1* and *PhEIL2* silencing delayed flower senescence in petunia in this study. Furthermore, the expression of two senescence-associated genes, *PhERF3* and *PhCP2,* decreased in flowers in which VIGS-mediated silencing of *PhEIL1* and *PhEIL2* occurred. In addition, both *PhCHS/PhEIL1* and *PhCHS/PhEIL2* silencing led less ethylene production than *PhCHS* suppression in white flowers in days 4 and 5 after anthesis, which may suggest it exerts feedback control over ethylene production and the reduced ethylene evolution could be due to the partial block of ethylene autocatalysis. These results showed that both PhEIL1 and PhEIL2 are involved in flower senescence. On the other hand, in tomato, antisense plants with reduced transcription of a single *LeEIL* did not result in notable changes in ethylene response, but reduced the mRNA levels of multiple *LeEIL* reduced significantly ethylene response, showing functional redundancy of *LeEILs* in tomato (Tieman et al., 2001).

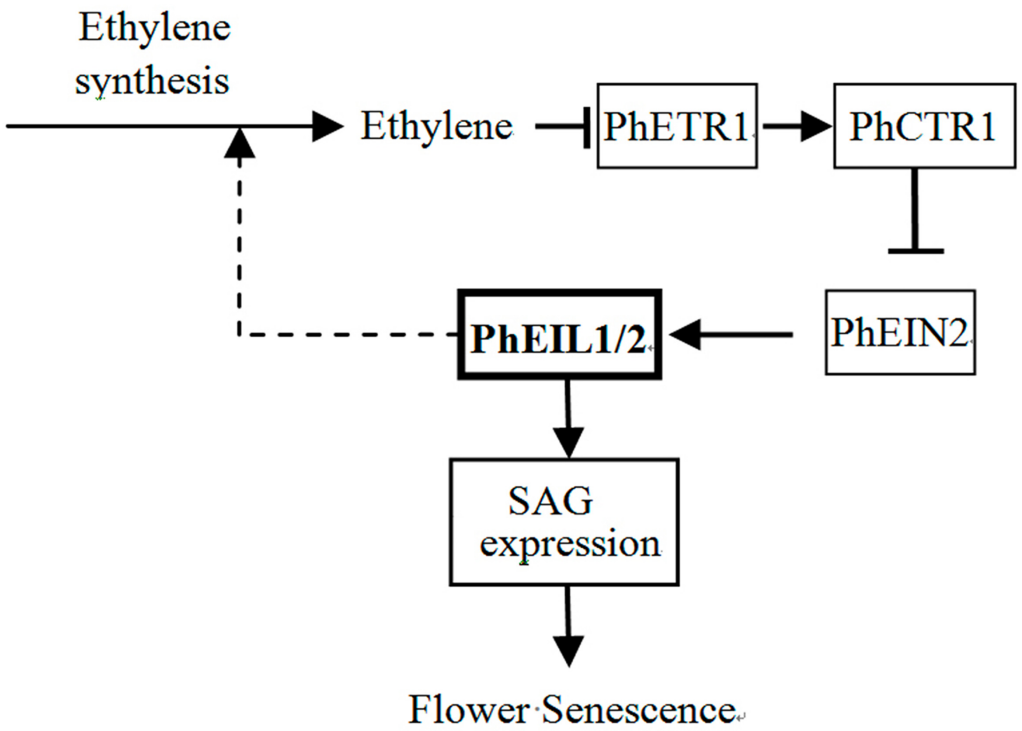

FIGURE 8 | Proposed models for the involvement of PhEIL1 and PhEIL2 in flower senescence in petunia.

To uncover the transcriptional activation domain of PhEIL2, yeast one-hybrid assay was performed using several PhEIL2 deletion mutants. The results showed that the C-terminal 353-612 amino acid region that consists of 260 amino acid residues is the essential domain for transcription-stimulating activity. In contrast, the essential domain for transcription-stimulating activity in mung bean VR-EIL2 was laid in the acidic region that comprises 50 amino acid residues in N-terminal. In our experimental conditions, the $PhEIL2_{1-353}$ mutant protein has only the background level of activity in yeast, suggesting that it is not essential domain for transcriptional activation. Further analysis showed that acid domain of PhEIL2 shares only 58.3% identity with that of Vr-EIL2. These results showed that essential domain for transcription-stimulating activity is not conserved in different EILs or in different species and requires further study.

Previous study suggested that homodimers of both EIN3 and EIL1 proteins are able to bind the promoters of *ERF1*, while EIN3 and EILs are not capable of forming heterodimers in *Arabidopsis* (Solano et al., 1998). In contrast, in this study, PhEIL2 interacts with PhEIL1 by Y2H and BiFC assays. In addition, both PhEIL1 and PhEIL2 are involved senescence. So, it is possible that heterodimers of PhEIL1 and PhEIL2 recognize their targets *in vivo*.

Based on the experimental data presented here and the model of ethylene signaling in *Arabidopsis* (Ji and Guo, 2013), we proposed a model to explain the involvement of the PhEIL1 and PhEIL2 in senescence in petunia flowers (**Figure 8**). In the present of ethylene, ethylene binds the receptor PhETR1 and ethylene signaling is transmitted to PhEIL1 and PhEIL2 heterodimers through PhCTR1 and PhEIN2 in petunia flowers (Shibuya et al., 2004). The heterodimers then activate the expression of senescence-related genes and accelerate senescence of flowers. In contrast, PhEIL1 or PhEIL2 suppression leads to the reduction of the heterodimers and the expression of senescence-related genes, and delays senescence of flowers. At the same time, ethylene production is reduced in petunia corollas, suggesting that PhEIL1 and PhEIL2 heterodimers could be involved in the regulation of the biosynthesis of ethylene in petunia flowers.

AUTHOR CONTRIBUTIONS

YY and JL designed research. FL, LH, YC, HL, and JL performed research. YY and FL, wrote paper.

FUNDING

This work was supported by National Natural Science Foundation of China (31270736, 31170653, and 31470700).

SUPPLEMENTARY MATERIAL

The Supplementary Material for this article can be found online at: http://journal.frontiersin.org/article/10.3389/fpls.2016.01606/full#supplementary-material

REFERENCES

Abeles, F. B., Morgan, P. W., Saltveit, M. E. Jr., Abeles, F. B., Morgan, P. W., and Saltveit, M. E. Jr. (1992). Regulation of ethylene production by internal, environmental and stress factors. *Ethylene Plant Biol.* 2, 56–119. doi: 10.1016/B978-0-08-091628-6.50010-2

Alonso, J. M., Hirayama, T., Roman, G., Nourizadeh, S., and Ecker, J. R. (1999). EIN2, a bifunctional transducer of ethylene and stress responses in *Arabidopsis*. *Science* 284, 2148–2152. doi: 10.1126/science.284.5423.2148

Alonso, J. M., Stepanova, A. N., Leisse, T. J., Kim, C. J., Chen, H., Shinn, P., et al. (2003). Genome-wide insertional mutagenesis of *Arabidopsis thaliana*. *Science* 301, 653–657. doi: 10.1126/science.1086391

Borochov, A., and Woodson, W. R. (1989). Physiology and biochemistry of flower petal senescence. *Hortic. Rev.* 11, 15–43. doi: 10.1002/9781118060841.ch2

Chang, C., Kwok, S. F., Bleecker, A. B., and Meyerowitz, E. M. (1993). *Arabidopsis* ethylene-response gene ETR1: similarity of product to two-component regulators. *Science* 262, 539–544. doi: 10.1126/science.8211181

Chao, Q., Rothenberg, M., Solano, R., Roman, G., Terzaghi, W., and Ecker, J. R. (1997). Activation of the ethylene gas response pathway in *Arabidopsis* by the nuclear protein ETHYLENE-INSENSITIVE3 and related proteins. *Cell* 89, 1133–1144. doi: 10.1016/S0092-8674(00)80300-1

Gagne, J. M., Smalle, J., Gingerich, D. J., Walker, J. M., Yoo, S., Yanagisawa, S., et al. (2004). *Arabidopsis* EIN3-binding F-box 1 and 2 form ubiquitin-protein ligases that repress ethylene action and promote growth by directing EIN3 degradation. *Proc. Natl. Acad. Sci. U.S.A.* 101, 6803–6808. doi: 10.1073/pnas.0401698101

Guo, H., and Ecker, J. R. (2003). Plant responses to ethylene gas are mediated by SCF EBF1/EBF2-dependent proteolysis of EIN3 transcription factor. *Cell* 115, 667–677. doi: 10.1016/S0092-8674(03)00969-3

Hua, J., Chang, C., Sun, Q., and Meyerowitz, E. M. (1995). Ethylene insensitivity conferred by *Arabidopsis* ERS gene. *Science* 269, 1712–1714. doi: 10.1126/science.7569898

Hua, J., Sakai, H., Nourizadeh, S., Chen, Q. G., Bleecker, A. B., Ecker, J. R., et al. (1998). EIN4 and ERS2 are members of the putative ethylene receptor gene family in *Arabidopsis*. *Plant Cell* 10, 1321–1332. doi: 10.1105/tpc.10.8.1321

Iordachescu, M., and Verlinden, S. (2005). Transcriptional regulation of three EIN3-like genes of carnation (*Dianthus caryophyllus* L. cv. Improved White Sim) during flower development and upon wounding, pollination, and ethylene exposure. *J. Exp. Bot.* 56, 2011–2018. doi: 10.1093/jxb/eri199

Ji, Y., and Guo, H. (2013). From endoplasmic reticulum (ER) to nucleus: EIN2 bridges the gap in ethylene signaling. *Mol. Plant* 6, 11–14. doi: 10.1093/mp/sss150

Jones, M. L., Chaffin, G. S., Eason, J. R., and Clark, D. G. (2005). Ethylene-sensitivity regulates proteolytic activity and cysteine protease gene expression in petunia corollas. *J. Exp. Bot.* 56, 2733–2744. doi: 10.1093/jxb/eri266

Ju, C., Yoon, G. M., Shemansky, J. M., Lin, D. Y., Ying, Z. I., Chang, J., et al. (2012). CTR1 phosphorylates the central regulator EIN2 to control ethylene hormone signaling from the ER membrane to the nucleus in *Arabidopsis*. *Proc. Natl. Acad. Sci. U.S.A.* 109, 19486–19491. doi: 10.1073/pnas.1214848109

Kieber, J. J., Rothenberg, M., Roman, G., Feldmann, K. A., and Ecker, J. R. (1993). CTR1, a negative regulator of the ethylene response pathway in *Arabidopsis*, encodes a member of the raf family of protein kinases. *Cell* 72, 427–441. doi: 10.1016/0092-8674(93)90119-B

Kosugi, S., and Ohashi, Y. (2000). Cloning and DNA-binding properties of a tobacco Ethylene-Insensitive3 (EIN3) homolog. *Nucleic Acids Res.* 28, 960–967. doi: 10.1093/nar/28.4.960

Lee, J., and Kim, W. T. (2003). Molecular and biochemical characterization of VR-EILs encoding mung bean ETHYLENE INSENSITIVE3-LIKE proteins. *Plant Physiol.* 132, 1475–1488. doi: 10.1104/pp.103.022574

Li, W., Ma, M., Feng, Y., Li, H., Wang, Y., Ma, Y., et al. (2015). EIN2-directed translational regulation of ethylene signaling in *Arabidopsis*. *Cell* 163, 670–683. doi: 10.1016/j.cell.2015.09.037

Liu, J., Li, J., Wang, H., Fu, Z., Liu, J., and Yu, Y. (2010). Identification and expression analysis of ERF transcription factor genes in petunia during flower senescence and in response to hormone treatments. *J. Exp. Bot.* 62, 825–40. doi: 10.1093/jxb/erq324

Mallona, I., Lischewski, S., Weiss, J., Hause, B., and Egea-Cortines, M. (2010). Validation of reference genes for quantitative real-time PCR during leaf and flower development in *Petunia hybrida*. *BMC Plant Biol.* 10:4. doi: 10.1186/1471-2229-10-4

Mitchell, P. J., and Tjian, R. (1989). Transcriptional regulation in mammalian cells by sequence-specific DNA binding proteins. *Science* 245, 371–378. doi: 10.1126/science.2667136

Potuschak, T., Lechner, E., Parmentier, Y., Yanagisawa, S., Grava, S., Koncz, C., et al. (2003). EIN3-dependent regulation of plant ethylene hormone signaling by two *Arabidopsis* F box proteins: EBF1 and EBF2. *Cell* 115, 679–689. doi: 10.1016/S0092-8674(03)00968-1

Qiao, H., Shen, Z., Huang, S. C., Schmitz, R. J., Urich, M. A., Briggs, S. P., et al. (2012). Processing and subcellular trafficking of ER-tethered EIN2 control response to ethylene gas. *Science* 338, 390–393. doi: 10.1126/science.1225974

Schaller, G. E., and Bleecker, A. B. (1995). Ethylene-binding sites generated in yeast expressing the *Arabidopsis* ETR1 gene. *Science* 270, 1809–1811. doi: 10.1126/science.270.5243.1809

Shibuya, K., Barry, K. G., Ciardi, J. A., Loucas, H. M., Underwood, B. A., Nourizadeh, S., et al. (2004). The central role of PhEIN2 in ethylene responses throughout plant development in petunia. *Plant Physiol.* 136, 2900–2912. doi: 10.1104/pp.104.046979

Solano, R., Stepanova, A., Chao, Q., and Ecker, J. R. (1998). Nuclear events in ethylene signaling: a transcriptional cascade mediated by ETHYLENE-INSENSITIVE3 and ETHYLENE-RESPONSE-FACTOR1. *Genes Dev.* 12, 3703–3714. doi: 10.1101/gad.12.23.3703

Spitzer-Rimon, B., Marhevka, E., Barkai, O., Marton, I., Edelbaum, O., Masci, T., et al. (2010). EOBII, a gene encoding a flower-specific regulator of phenylpropanoid volatiles' biosynthesis in petunia. *Plant Cell* 22, 1961–1976. doi: 10.1105/tpc.109.067280

Tan, Y., Liu, J., Huang, F., Zhong, S., and Yu, Y. (2014). PhGRL2 protein, interacting with PhACO1, is involved in flower senescence in the petunia. *Mol. Plant* 7, 1384–1387. doi: 10.1093/mp/ssu024

Tieman, D. M., Ciardi, J. A., Taylor, M. G., and Klee, H. J. (2001). Members of the tomato LeEIL (EIN3-like) gene family are functionally redundant and regulate ethylene responses throughout plant development. *Plant J.* 26, 47–58. doi: 10.1046/j.1365-313x.2001.01006.x

Waki, K., Shibuya, K., Yoshioka, T., Hashiba, T., and Satoh, S. (2001). Cloning of a cDNA encoding EIN3-like protein (DC-EIL1) and decrease in its mRNA level during senescence in carnation flower tissues. *J. Exp. Bot.* 52, 377–379. doi: 10.1093/jexbot/52.355.377

Wen, X., Zhang, C., Ji, Y., Zhao, Q., He, W., An, F., et al. (2012). Activation of ethylene signaling is mediated by nuclear translocation of the cleaved EIN2 carboxyl terminus. *Cell Res.* 22, 1613. doi: 10.1038/cr.2012.145

Yanagisawa, S., Yoo, S., and Sheen, J. (2003). Differential regulation of EIN3 stability by glucose and ethylene signalling in plants. *Nature* 425, 521–525. doi: 10.1038/nature01984

Yang, W., Liu, J., Tan, Y., Zhong, S., Tang, N., Chen, G., et al. (2015). Functional characterization of PhGR and PhGRL1 during flower senescence in the petunia. *Plant Cell Rep.* 34, 1561–1568. doi: 10.1007/s00299-015-1808-7

Yang, Y., Wu, Y., Pirrello, J., Regad, F., Bouzayen, M., Deng, W., et al. (2009). Silencing Sl-EBF1 and Sl-EBF2 expression causes constitutive ethylene response phenotype, accelerated plant senescence, and fruit ripening in tomato. *J. Exp. Bot.* 61, 697–708. doi: 10.1093/jxb/erp332

Conflict of Interest Statement: The authors declare that the research was conducted in the absence of any commercial or financial relationships that could be construed as a potential conflict of interest.

frontiers in Plant Science

ORIGINAL RESEARCH
published: 11 July 2016
doi: 10.3389/fpls.2016.01021

The Banana Transcriptional Repressor MaDEAR1 Negatively Regulates Cell Wall-Modifying Genes Involved in Fruit Ripening

*Zhong-qi Fan[1], Jian-fei Kuang[1], Chang-chun Fu[1], Wei Shan[1], Yan-chao Han[1], Yun-yi Xiao[1], Yu-jie Ye[1], Wang-jin Lu[1], Prakash Lakshmanan[2], Xue-wu Duan[3] and Jian-ye Chen[1]**

[1] State Key Laboratory for Conservation and Utilization of Subtropical Agro-bioresources/Guangdong Key Laboratory for Postharvest Science, College of Horticultural Science, South China Agricultural University, Guangzhou, China, [2] Sugar Research Australia, Brisbane, QLD, Australia, [3] Key Laboratory of Plant Resources Conservation and Sustainable Utilization, South China Botanical Garden, Chinese Academy of Sciences, Guangzhou, China

OPEN ACCESS

Edited by:
M. Iqbal R. Khan, International Rice Research Institute, Philippines

Reviewed by:
Athanassios Molassiotis, Aristotle University of Thessaloniki, Greece
Ioannis S. Minas, Colorado State University, USA
Tomotsugu Koyama, Suntory Foundation for Life Sciences, Japan

***Correspondence:**
Jian-Ye Chen
chenjianye@scau.edu.cn

Specialty section:
This article was submitted to Crop Science and Horticulture, a section of the journal Frontiers in Plant Science

Received: *23 March 2016*
Accepted: *28 June 2016*
Published: *11 July 2016*

Citation:
Fan Z-q, Kuang J-f, Fu C-c, Shan W, Han Y-c, Xiao Y-y, Ye Y-j, Lu W-j, Lakshmanan P, Duan X-w and Chen J-y (2016) The Banana Transcriptional Repressor MaDEAR1 Negatively Regulates Cell Wall-Modifying Genes Involved in Fruit Ripening. Front. Plant Sci. 7:1021. doi: 10.3389/fpls.2016.01021

Ethylene plays an essential role in many biological processes including fruit ripening via modulation of ethylene signaling pathway. Ethylene Response Factors (ERFs) are key transcription factors (TFs) involved in ethylene perception and are divided into AP2, RAV, ERF, and DREB sub-families. Although a number of studies have implicated the involvement of DREB sub-family genes in stress responses, little is known about their roles in fruit ripening. In this study, we identified a DREB TF with a EAR motif, designated as MaDEAR1, which is a nucleus-localized transcriptional repressor. Expression analysis indicated that *MaDEAR1* expression was repressed by ethylene, with reduced levels of histone H3 and H4 acetylation at its regulatory regions during fruit ripening. In addition, *MaDEAR1* promoter activity was also suppressed in response to ethylene treatment. More importantly, MaDEAR1 directly binds to the DRE/CRT motifs in promoters of several cell wall-modifying genes including *MaEXP1/3*, *MaPG1*, *MaXTH10*, *MaPL3,* and *MaPME3* associated with fruit softening during ripening and represses their activities. These data suggest that MaDEAR1 acts as a transcriptional repressor of cell wall-modifying genes, and may be negatively involved in ethylene-mediated ripening of banana fruit. Our findings provide new insights into the involvement of DREB TFs in the regulation of fruit ripening.

Keywords: banana (*Musa acuminata*), cell wall modification, DREB, fruit ripening, transcriptional repression

INTRODUCTION

The phytohormone ethylene plays an essential role in many biological processes of plant growth and development, including germination, organ senescence, stress response, and fruit ripening (Salehin and Estelle, 2015). The ethylene signaling pathway is well studied in *Arabidopsis*, which reveals a linear transduction pathway with the transduction of ethylene signal from receptors to dedicated transcription factors (TFs) (Pirrello et al., 2012). The last components of the ethylene signaling pathway are the Ethylene Response Factor (ERF) TFs which possess a highly conserved DNA-binding domain called the APETALA2/ethylene-responsive element binding (AP2/ERF) domain (Ohme-Takagi and Shinshi, 1995).

The AP2/ERF proteins are divided into four major sub-families, namely the AP2, related to ABI3/VP1 (RAV), ERF and dehydration-responsive element-binding protein (DREB), according to the number and similarity of the AP2/ERF domains (Sakuma et al., 2002). DREB TFs, as a sub-family of the AP2/ERF proteins, were first isolated using an 6-bp conserved sequence (A/GCCGAC), named the dehydration responsive element (DRE), in yeast one-hybrid screening in *Arabidopsis* cDNA (Stockinger et al., 1997; Liu et al., 1998). Extensive studies have established important regulatory roles for DREB TFs in response to environmental stimuli. For example, in *Arabidopsis*, *DREB1A* was induced by cold, while *DREB2* like genes (*DREB2A* and *DREB2B*) were induced by drought, salt and heat (Nakashima et al., 2000). By contrast, other *DREB1*-related genes such as *DREB1D* regulate high osmotic stress-induced gene expression (Haake et al., 2002), whereas *DREB1E* and *DREB1F* are responsive to high salinity (Mizoi et al., 2012). Except for these transcriptional activators, several members of DREB TFs with ERF-associated amphiphilic repression (EAR) motif at C-terminus act as transcriptional repressors of stress responses (Ohta et al., 2001; Kagale and Rozwadowski, 2010). These EAR motif-containing DREB repressors negatively modulate the responses of plants to cold and dehydration, as are the cases of DEAR1 (Tsutsui et al., 2009), RAP2.1 (Dong and Liu, 2010), and GhDREB (Gao et al., 2009). Despite these findings, less is known about the functions of these proteins in agricultural crops, especially in relation to natural processes like fruit ripening where ethylene plays a major role.

Banana is one of the most important fruit species in tropical and sub-tropical countries, ranking as the world's second largest fruit crop and listing among the world's ten most important food commodities (Sreedharan et al., 2012). Banana is a typical climacteric fruit, characterized by a burst in respiration and a typical increase in ethylene biosynthesis that initiates ripening-associated processes. This, from an economic perspective, limits fruit shelf-life with rapid deterioration of peel color and pulp firmness (Ba et al., 2016). For example, ripened bananas become unmarketable within 1–3 days at ambient temperature (Ahmed and Palta, 2016). Although numerous post-harvest practices such as low temperature storage, thermal processing, chemical, and biological treatments coupled with other preservation techniques are applied on fresh produces to maintain or extend the shelf-life, severe post-harvest losses still occur (Kuan et al., 2015). Therefore, a better understanding of the regulators involved in banana fruit ripening will help develop more effective post-harvest storage technologies. Since bananas are climacteric fruits, considerable effort has been directed to study genes involved in ethylene biosynthesis and signaling pathways including 1-aminocyclopropane-1-carboxylic acid (ACC) synthase (ACS), ACC oxidase (ACO), ethylene receptor, CTR1 ortholog, ethylene insensitive3 (EIN3)/EIN3-like (EIL), EIN3 binding F-box (EBF) and ERF genes (Liu et al., 1999; Mbéguié-A-Mbéguié et al., 2008; Kuang et al., 2013; Xiao et al., 2013; Jourda et al., 2014). Interestingly, opposing functions have been reported for banana ERF genes. For instance, among the fifteen ERF TFs that have been isolated from banana fruit, MaERF11 binds to *MaACS1* and *MaACO1* promoters to suppress their activities whereas MaERF9 activates *MaACO1* promoter activity (Xiao et al., 2013). Whilst DREB and ERF TFs belong to the AP2/ERF families, little is known about DREBs role in fruit ripening, especially those with EAR motif.

In this study, we identified a DREB TF with EAR motif, designated as MaDEAR1, which is a nucleus-localized transcriptional repressor. MaDEAR1 was ethylene- and ripening-inhibited, with reduced levels of histone H3 and H4 acetylation at its regulatory regions during fruit ripening. More importantly, MaDEAR1 binds to and represses promoters of several cell wall-modifying genes associated with fruit softening, including expansins (*MaEXP1/3*), polygalacturonase (*MaPG1*), xyloglucan endotransglycosylase/hydrolase (*MaXTH10*), pectate lyase (*MaPL3*), and pectin methylesterase (*MaPME3*). Our results suggest that MaDEAR1 may be acting as a negative regulator of cell wall-modifying genes, unraveling new information on EAR motif-containing DREB TFs in relation to fruit ripening.

MATERIALS AND METHODS

Plant Materials and Treatments

Pre-climacteric banana (*Musa acuminata*, AAA group, cv. Cavendish) fruit at the 70–80% plump stage were obtained from a local commercial plantation near Guangzhou, southern China. Harvested fruit were separated into fingers, and fruit of uniform weight, shape, and maturity with no visual defects were selected, rinsed in tap water, and then air-dried before treatments were applied. The post-harvest treatments include a control (natural ripening), ethylene-induced ripening (100 μL L^{-1} ethylene, 18 h), and 1-methylcyclopropene (1-MCP)-delayed ripening (0.5 μL L^{-1} 1-MCP, 18 h), as described previously by Shan et al. (2012). All assessments were conducted using three biological replicates and fruit pulp of all samples were frozen in liquid nitrogen immediately after sampling, and stored at −80°C for further use.

Tobacco bright yellow 2 (BY-2) suspension cells were cultured and prepared as described by Kumagai-Sano et al. (2006). Tobacco (*Nicotiana benthamiana*) plants were grown under a 16-h light (25°C) and 8-h dark (22°C) photoperiod. Four- to six-week-old tobacco plants were used for transient assays.

RNA Extraction, Gene Isolation, and Sequence Analysis

Frozen banana fruit pulp were ground in liquid nitrogen using a mortar and pestle. Total RNA was extracted using the hot borate method described by Wan and Wilkins (1994). Total RNA (∼1 μg) from each sample was treated with DNAse I digestion using an RNAse-free kit (Promega Madison, Fitchburg, WI, USA). The above DNA-free total RNA was then used as template for RT-PCR. The first-strand cDNA of the product was subjected to PCR amplification. According to gene annotation, bioinformatics and RNA sequencing analyses (D'Hont et al., 2012), one full-length *DREB* gene containing an EAR motif, with complete start and stop codons, termed *MaDEAR1* (GSMUA_Achr3T13190_001 in Banana Genome Hub, XP_009392127 in NCBI), was identified and selected from

banana whole-genome sequence. This segment was cloned and sequenced. Alignments were carried out on ClustalX (version 1.83) and GeneDoc software, and a phylogenetic tree was constructed using the Neighbor–Joining method in the MEGA5 program.

Quantitative Real-Time PCR (qRT-PCR) Analysis

All qRT-PCR analysis and synthesis of first-strand cDNA were performed as described previously (Chen et al., 2011; Shan et al., 2012). The sequences of all primers used for qRT-PCR analysis are listed in Supplementary Table S1. qRT-PCR was carried out on a Bio-Rad CFX96 Real-Time PCR System using the SYBR®Green PCR Supermix Kit (Bio-Rad Laboratories) following the manufacturer's instructions. *MaRPS2* (ribosomal protein 2) was selected as a reference gene according to our previous study on the selection of reliable reference genes under different experimental conditions (Chen et al., 2011). All qRT-PCR reactions were normalized using Ct value corresponding to the reference gene. The relative expression levels of target gene were calculated with the formula $2^{-\Delta\Delta CT}$. Three independent biological replicates were used in the analysis.

Sub-cellular Localization of MaDEAR1 Protein

The coding sequences of *MaDEAR1* were amplified and cloned into the pEAQ-GFP vectors (kindly gifted by Dr. George P. Lomonossoff), then the fusion construct and positive control GFP vector were electroporated into the *Agrobacterium tumefaciens* strain GV3101 using Gene PulserXcell™ Electroporation Systems (Bio-Rad, Hercules, CA, USA). The primers for construct development are listed in Supplementary Table S1. The *Agrobacterium* harboring MaDEAR1-GFP or the positive control was inoculated for 16 h at 28°C. Cells were pelleted, resuspended at OD600 = 0.1 in infiltration buffer [10 mM MgCl2, 10 mM MES (pH 5.6), 100 μM acetosyringone], incubated for 4 h at room temperature, then was infiltrated into the abaxial side of 4- to 6-week-old tobacco leaves using a 1-mL needleless syringe as described previously by Sainsbury et al. (2009). Two days after infiltration, GFP fluorescence signals were observed by a fluorescence microscope (Zeiss Axioskop 2 Plus) with a beam splitter for excitation at 500 nm. All assays were repeated at least three times.

Promoter Isolation and Analysis

Genomic DNA was extracted from banana leaves using the DNeasy Plant Mini Kit (Qiagen). The promoters of *MaDEAR1*, and genes including *MaEXP1/3*, *MaPG1*, *MaXTH10*, *MaPL3,* and *MaPME3* involved in cell wall loosening of banana fruit associated with softening (Pua et al., 2001; Asif and Nath, 2005; Asha et al., 2007; Mbéguié-A-Mbéguié et al., 2009; Asif et al., 2014), were isolated using a Genome Walker Kit (Clontech) with nested PCR according to the manufacturer's instructions (specific primers are listed in Supplementary Table S1). After sequencing, conserved *cis*-element motifs of promoters were predicted using Plant-CARE[1] databases.

Promoter Activity Assay

The MaDEAR1 promoter region was amplified by PCR using the specific primers listed in Supplementary Table S1. The PCR product was inserted into the pGreenII 0800-LUC double reporter vector (Hellens et al., 2005) at the *Kpn*I *and Nco*I sites to fuse it with the Firefly luciferase (LUC) reporter gene (MaDEAR1 pro-LUC). A Renilla luciferase (REN) under the control of the 35S promoter at the same vector was used as an internal control. The construct CaMV35S-REN/*MaDEAR1* pro-LUC (∼20 μg) was transformed into tobacco BY-2 protoplasts (∼2 × 10^4) by polyethylene glycol (PEG) methods as described previously (Abel and Theologis, 1994).

The promoter activity was assayed according to Ba et al. (2014a). The transformed protoplasts were subjected to 0 mM (control) or 0.8 mM of ethrel (ethylene releaser) treatment and then incubated at 23°C for 14 h, and LUC and REN activities were assayed using the dual luciferase assay kits (Promega), and the promoter activity is indicated by the ratio of LUC to REN. The analysis was carried out using the Luminoskan Ascent Microplate Luminometer (Thermo) according to the manufacturer's instructions, with a 5-s delay and 15-s integrated measurements. At least six assay measurements were included for each.

Chromatin Immunoprecipitation (ChIP) and Quantitative PCR Analysis

Chromatin immunoprecipitation (ChIP) was performed as described earlier (Gendrel et al., 2005; Benhamed et al., 2006). Unripe and ripe banana fruit pulp were collected and crosslinked in 1% formaldehyde for 15 min in a vacuum and then neutralized by 0.125 M glycine. After washing with sterilized water, 5 g of banana fruit pulp were ground in liquid nitrogen, and suspended in a buffer containing 0.25 M sucrose, 10 mM Tris-HCl (pH 8.0), 10 mM $MgCl_2$, 1% Triton X-100, 5 mM β-mercaptoethanol, 0.1 mM PMSF, and protease inhibitors (one minitablet per milliliter; Roche). The suspensions were transferred to microfuge tubes and centrifuged at 12,000 *g* for 10 min. The pellets were suspended in 1.7 M sucrose, 10 mM Tris-HCl (pH 8.0), 2 mM $MgCl_2$, 0.15% Triton X-100, 5 mM β-mercaptoethanol, 0.1 mM PMSF, and protease inhibitors and centrifuged through a layer of the same buffer in microfuge tubes. The chromatin extracts were lysed in a buffer containing 50 mM Tris-HCl, pH 8, 10 mM EDTA, 1% SDS, and protease inhibitors, and were sheared to an average length of 500 bp by sonication at 4°C using the Sonics VCX800 apparatus followed by centrifugation. The supernatants were diluted 10-fold with 1% Triton X-100, 1.2 mM EDTA, 16.7 mM Tris-HCl (pH 8.0), and 167 mM NaCl. A 1 mL aliquot of the dilution was immunoprecipitated with specific antibodies of anti-acetyl-histone H3 (anti-H3ac) and anti-acetyl-histone H4 (anti-H4ac) (Millipore), while immunoglobulin G (IgG)

[1]http://bioinformatics.psb.ugent.be/webtools/plantcare/html/

was used as a negative control. ChIP assays were repeated with three biological replicates. The DNA cross-linked to immunoprecipitated proteins and input DNA were detected by qRT-PCR. *MaACT2* (GSMUA_Achr9G03170_001) was used as internal control since its histone acetylation level is stable during ripening (Han et al., 2016). The percentage of IP/Input was calculated by determining $2^{-\Delta Ct}$ ($=2^{-[Ct(IP)-Ct(Input)]}$). The primers used for ChIP-qPCR analysis are listed in Supplementary Table S1.

Protein Expression and Electrophoretic Mobility Shift Assay (EMSA)

MaDEAR1 was cloned into pGEX-4T-1 (Amersham Biosciences) to fuse in frame with GST and expressed in BM Rosetta (DE3) by induction with 1 mM of isopropyl-β-D-thiogalactopyramoside (IPTG) for 6 h at 30°C. The recombinant protein was purified with Glutathione Sepharose 4B (GE Healthcare). The EMSA was performed using the EMSA kit (Thermo) according to the manufacturer's instructions. The probes containing the DRE/CRT (core sequence for A/GCCGAC) element (2×10^{-6} μmol) derived from *MaEXP1/3*, *MaPG1*, *MaXTH10*, *MaPL3,* and *MaPME3* promoters were labeled with biotin using DNA 3′ End Biotinylation Kit (Thermo). The same unlabeled DNA fragment with 2×10^{-5} μmol, 2×10^{-4} μmol, or 2×10^{-3} μmol, respectively, was used as a competitor. After cross-linking, the membrane was detected by the chemiluminescence method according to the manufacturer's protocol on a ChemiDoc^{TM} MP Imaging System (Bio-Rad). The primers used in protein expression and EMSA assays are listed in Supplementary Table S1.

Transient Assay in Tobacco Leaves

A dual-luciferase reporter system was used in the transient assay, and all primers used for the following constructs are listed in Supplementary Table S1. For transcriptional activity analysis of MaDEAR1, the coding sequence of *MaDEAR1* was inserted into the constructed pBD vector driven by the 35S promoter as the effector, and the double reporter vector includes a native GAL4-LUC, and an internal control REN driven by 35S promoter, which was modified based on pGreenII 0800-LUC reporter vector (Hellens et al., 2005). GAL4-LUC contains five copies of GAL4 binding element and 35S promoter, and these sequences are located upstream of the LUC. For the assay of MaDEAR1 repressing the *MaEXP1/3*, *MaPG1*, *MaXTH10*, *MaPL3,* and *MaPME3* promoters, *MaDEAR1* were inserted into the pEAQ vector as effector, while the promoters were cloned into pGreenII 0800-LUC double-reporter vector as reporter.

The constructed effector and reporter plasmids were co-transformed into tobacco leaves by *Agrobacterium tumefaciens* strain GV3101. LUC and REN luciferase activities were measured as described above. The transcriptional activity of MaDEAR1 and the binding activity of MaDEAR1 to the promoter are indicated by the ratio of LUC to REN. At least six biological replicates were assayed for each combination.

Statistical Analysis

Experiments were conducted using a completely randomized design. Each sample time point for each treatment comprised three independent biological replicates. Data were plotted as means ± standard errors (SE) in figures. Least significant difference (LSD) at the 5% level was estimated using DPS software (version 3.01; Zhejiang University, Hangzhou, China).

RESULTS

MaDEAR1 Is an A-5 Sub-group Member of the DREB Family

Based on gene annotation, bioinformatics and RNA sequencing analyses (D'Hont et al., 2012), one full-length *DREB* gene containing an EAR motif, designated as *MaDEAR1* (*M. acuminata* DREB and EAR motif protein 1) (GSMUA_Achr3T13190_001 in Banana Genome Hub, XP_009392127 in NCBI), which was found down-regulated during fruit ripening, did attract our attention. MaDEAR1 encodes a protein of 184 amino acids, with calculated molecular weight of 20.24 kDa and *p*I value of 10.10. Analysis of deduced amino acid sequence of MaDEAR1 revealed a typical AP2/ERF domain of 58 amino acids with the conserved valine (V) and glutamic acid (E) at the 14th and 19th positions, respectively (**Figure 1A**), which are considered to be essential sites for the binding of DREBs to the DRE *cis*-elements (Sakuma et al., 2002). In addition, a repressor domain, the ERF-associated amphiphilic repression (EAR) motif was observed at the C-terminus of the protein (**Figure 1A**), suggesting that the MaDEAR1 might function as a transcriptional repressor. Phylogenetic analyses showed that DREB proteins can be classified into six sub-groups (A1–A6), in which MaDEAR1 together with AtRAP2.1, GmDREB2, GhDBP1, and MsDREB5 belong to A-5 sub-group (**Figure 1B**). Collectively, these data suggest that MaDEAR1 is an A-5 sub-group member of the DREB family.

MaDEAR1 Is a Nucleus-Localized Transcriptional Repressor

To examine the sub-cellular localization of MaDEAR1 *in vivo*, we fused the *MaDEAR1* coding region in-frame with the N-terminal side of green fluorescent protein (GFP) under the control of CaMV 35S promoter. The MaDEAR1-GFP and GFP control plasmids were transiently expressed in tobacco leaves by *Agrobacterium* infiltration. While control GFP accumulated in both nucleus and cytoplasm, the MaDEAR1-GFP fusion protein was clearly localized in the nucleus (**Figure 2A**). This suggests that MaDEAR1, like other reported DREB proteins, is a nuclear protein which is a typical feature of TFs.

To investigate whether MaDEAR1 possesses transcriptional repression activity *in vivo*, a dual luciferase assay was performed. The dual-luciferase reporter harbors five copies of the GAL4 DNA-binding element and CaMV 35S fused to the firefly luciferase (LUC) reporter, whereas a renilla luciferase (REN) reporter under the control of the 35S promoter was used as an internal control. Full-length *MaDEAR1* was fused with

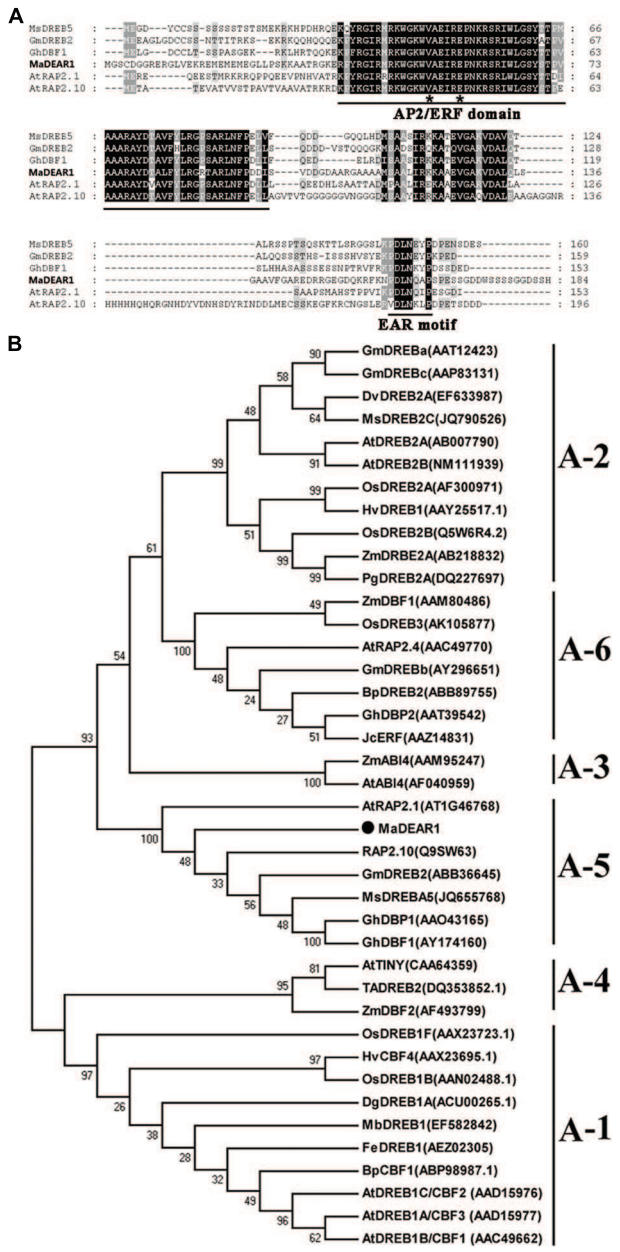

FIGURE 1 | Sequence analysis of MaDEAR1. (A) Alignment of the deduced amino acid sequences of the banana MaDEAR1 and its respective homologs MsDREBA5 (JQ655768), GmDREB2 (DQ208968), AtRAP2.1 (AT1G46768), and AtRAP2.10 (AT4G36900). Identical and similar amino acids were presented by black and gray shading, respectively. The AP2/ERF domain and the EAR-motif (DLNXXP) were underlined. The 14th and 19th amino acids were indicated by asterisks. **(B)** Phylogenetic analysis of plant DREB family proteins. The multiple alignment was made using ClustalW, and the phylogenetic tree was constructed with MEGA 5.0 using a bootstrap test of phylogeny with minimum evolution test and default parameters. Numbers indicate bootstrap values.

GAL4 DNA-binding domain (GAL4-BD) as the effector, and the empty GAL4-BD (pBD-empty) was used as a negative control (**Figure 2B**). As shown in **Figure 2C**, compared with the pBD-empty control, pBD-MaDEAR1 significantly repressed the expression of the LUC reporter, with approximately fivefold less LUC/REN value than the control. To further confirm whether the conserved EAR motif (DLNQAP) was important for the MaDEAR1-mediated repression, site-specific mutations were made to convert two conserved amino acids (DL) to NV (**Figure 2B**). As expected, the transcriptional repression ability of MaDEAR1 was abolished when the EAR-motif was mutated (**Figure 2C**). These results confirm that MaDEAR1 may act as a transcriptional repressor, and the EAR motif is important for its repression activity.

MaDEAR1 Is Inhibited by Ethylene and Ripening

Our previous study showed that fruits in natural ripening group start ethylene production after storage at 22°C and 90% relative humidity for 15 days, which peaks around day-21, and declines thereafter. Ethylene-treated fruit ripened rapidly, with an ethylene peak appearing at day 3 following treatment. In contrast, 1-MCP treatment delayed ripening, with ethylene peaking at day 30 (Shan et al., 2012). To investigate the expression of *MaDEAR1* during banana fruit ripening, we performed quantitative RT-PCR analysis using banana fruit in three different ripening behaviors caused by natural, ethylene-induced, and 1-MCP-delayed ripening treatments. As shown in **Figure 3A**, *MaDEAR1* expression was repressed by ethylene, and its transcript level in natural, ethylene-induced or 1-MCP-delayed ripening was decreased following ethylene production appearance, revealing that *MaDEAR1* expression was suppressed by ethylene and ripening.

To better understand the mechanism(s) of *MaDEAR1* expression modulation, a 976 bp upstream sequence from the start codon of *MaDEAR1* was isolated from the genome of *M. acuminata* using a genome-walking PCR method. Analysis of the promoter using the PLACE and Plant-CARE databases revealed a site for the ethylene-responsive element (ERE), ATTTCAAA, with one nucleotide change found in the promoter at −507 to −515 bp from the initiation codon (Supplementary Data Sheet S1), indicating that *MaDEAR1* promoter might respond to ethylene. We then fused the *MaDEAR1* promoter in front of LUC in the dual luciferase reporter vector, while the REN driven by the CaMV 35S promoter at the same vector was used as an internal control (**Figure 3B**). The resultant vector was transiently expressed in tobacco BY2 protoplasts with or without ethrel treatment, and the luciferases were assayed thereafter. As shown in **Figure 3B**, after the treatment with ethrel, the promoter activity of *MaDEAR1* was dramatically decreased, as evidenced by the much lower relative LUC/REN ratio compared that of the control, indicating that *MaDEAR1* promoter activity was suppressed by ethylene.

Decrease Expression of *MaDEAR1* Is Correlated with Histone Acetylation Changes during Fruit Ripening

Histone acetylation is a type of chromatin modification facilitating the gene expression, which is closely associated with

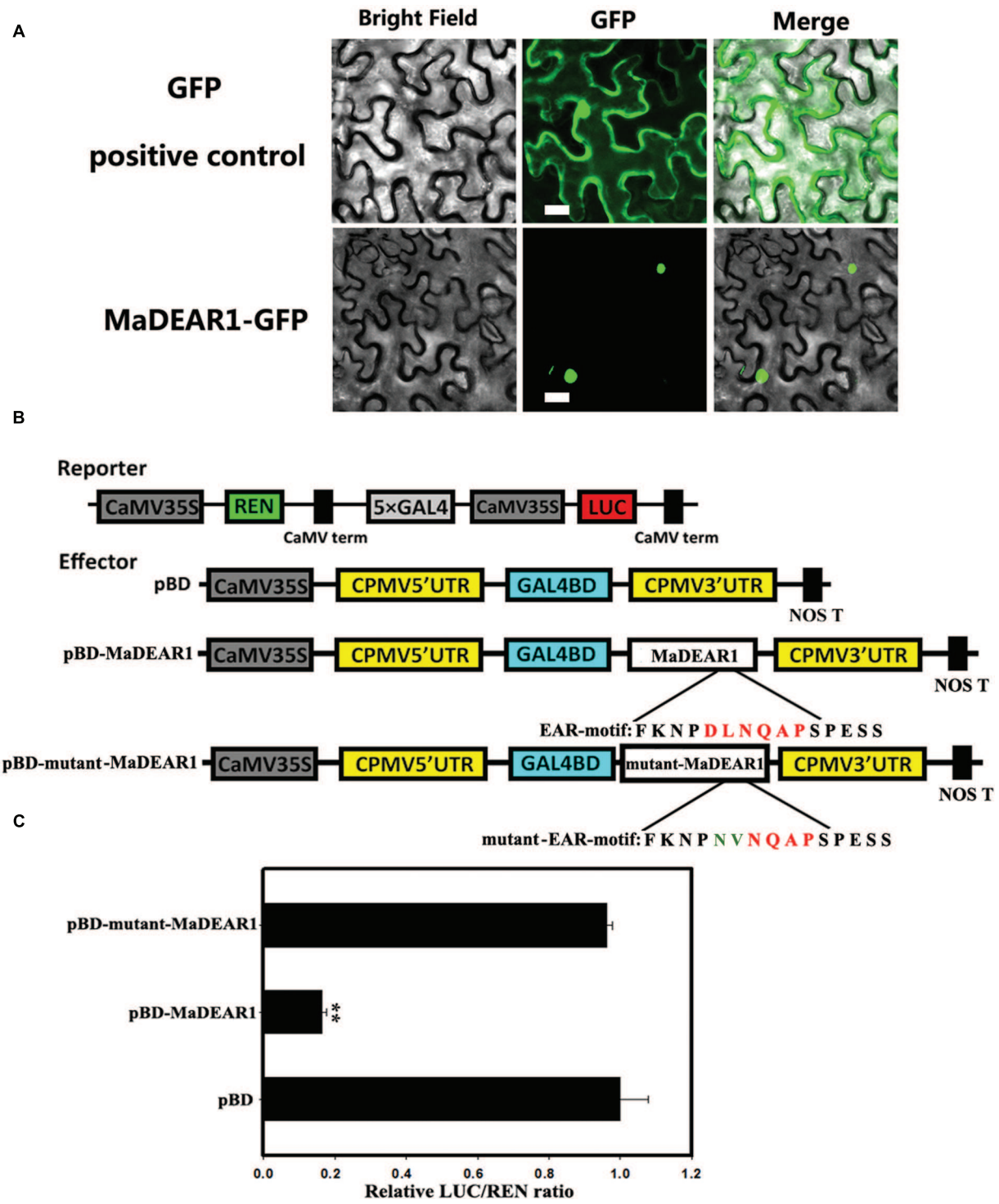

FIGURE 2 | Sub-cellular localization and transcriptional repression activity of MaDEAR1. (A) MaDEAR1 is localized in nucleus. *Agrobacterium tumefaciens* carrying MaDEAR1-GFP or GFP positive control were infiltrated into tobacco leaves. After 48 h, the fluorescence of MaDEAR1 protein was localized exclusively in the nucleus, while the fluorescence of the GFP positive control was distributed in both nucleus and cytoplasm. Bar, 20 μM. **(B)** Reporter and effector constructs. The dual luciferase reporter construct contained the LUC reporter gene fused with 5 × GAL4 and CaMV35S. The effector plasmid contained the *MaDEAR1* gene or with mutant EAR motif fused to GAL4BD driven by the CaMV35S. The two conserved amino acids (DL) of the EAR-motif without or with site-mutation (NV) are also shown. pBD was used as a negative control. **(C)** Transcriptional repression ability of MaDEAR1 *in vivo*. Compared with the pBD control, pBD-MaDREB5 significantly repressed the expression of the LUC reporter. The ratio of LUC to REN of the pBD vector was used as a calibrator (set as 1). Each value represents the means of six biological replicates, and vertical bars represent the SE Asterisks indicate a statistically significant difference compared with pBD by Student's *t*-test. $^{**}P < 0.01$.

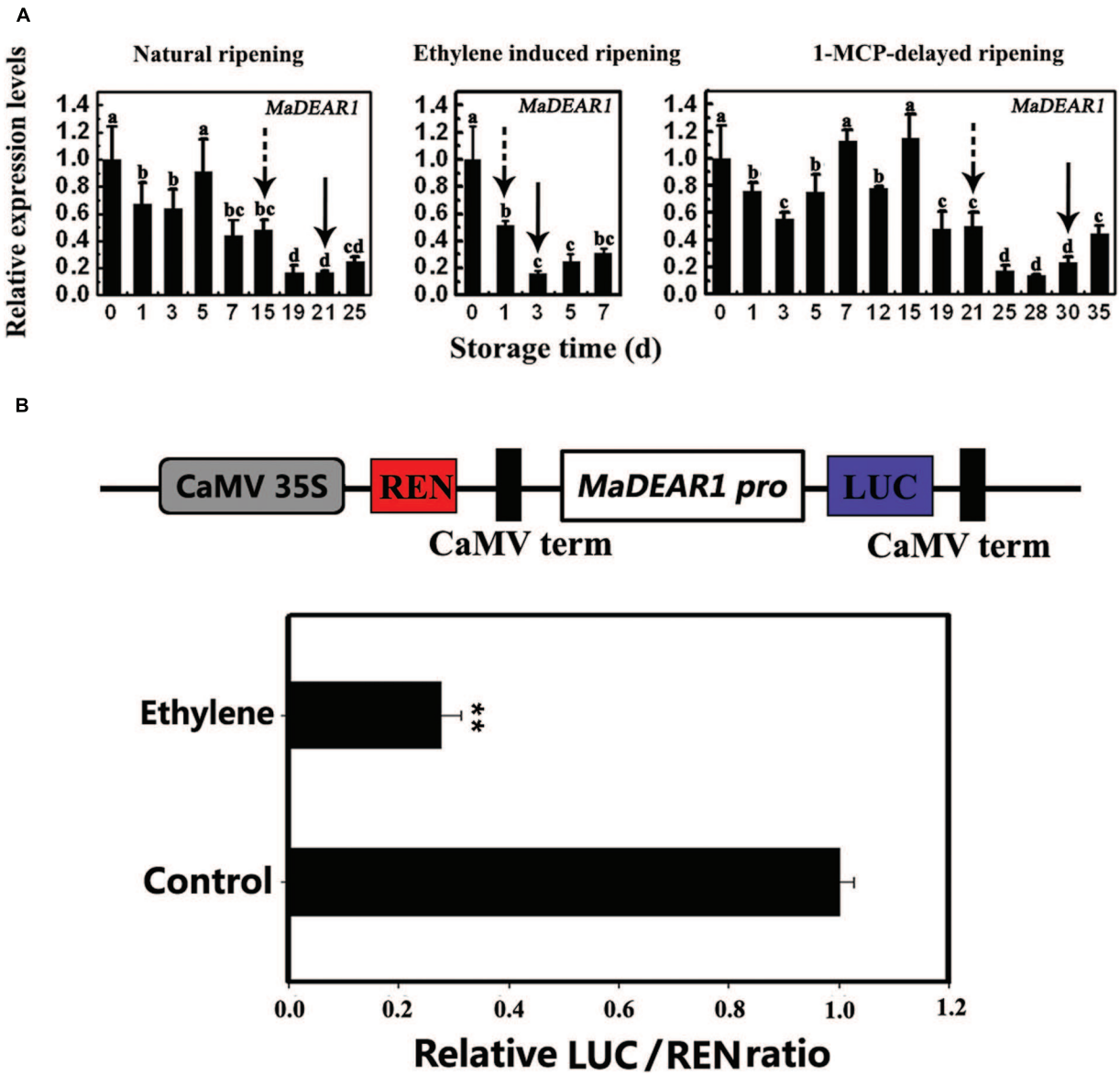

FIGURE 3 | *MaDEAR1* is inhibited by ethylene and ripening. (A) Expression of *MaDEAR1* in pulp during three ripening conditions, which include natural (control), ethylene-induced, and 1-MCP-delayed ripening. The expression levels of *MaDEAR1* are expressed as a ratio relative to the harvest time (0 days of control), which was set at 1. Each value represents the mean ± SE of three biological replicates. Different letters above bars indicate significant difference at the 5% level by Student's *t*-test. The broken arrow and full arrow indicate the time point at which ethylene production began to increase and its peak for each treatment, respectively. The physiological data such as changes in fruit firmness and ethylene production during banana fruit ripening and softening have been presented in Shan et al. (2012). **(B)** *MaDEAR1* promoter activity in response to ethylene. The dual luciferase reporter vector containing *MaDEAR1* promoter (CaMV35S–REN/*MaDEAR1* pro-LUC) was transiently transformed into tobacco BY-2 protoplasts using a modified PEG method, and the transformed protoplasts were subjected to 0 (control) or 0.8 mM ethrel (ethylene releaser) treatment. After incubation for 14 h, LUC and REN luciferase activities were assayed, and the promoter activity is indicated by the ratio of LUC to REN. Each value represents the means of six biological replicates, and vertical bars represent the SE $^{**}P < 0.01$ by Student's *t*-test.

gene activation. To assess whether the expression of *MaDEAR1* during fruit ripening is associated with histone acetylation, we examine the histone acetylation levels of *MaDEAR1* in fruit of unripe and ripe stages by ChIP-qPCR assays using antibodies such as anti-acetyl-histone H3 (H3ac) and anti-acetyl-histone H4 (H4ac). As shown in **Figure 4**, as a negative control, the enrichments of IgG in the promoter and coding region of *MaDEAR1* were low. In addition, no significant difference of histone H3 or H4 acetylation levels of *MaACT2* between unripe and ripe banana fruit was observed. On the contrary, the histone H3 acetylation (H3ac) levels of *MaDEAR1* in region B and C as well as histone H4 acetylation (H4ac) levels of *MaDEAR1* in region C were decreased in ripening bananas (**Figure 4**), which is consistent with its decreased level of expression during ripening

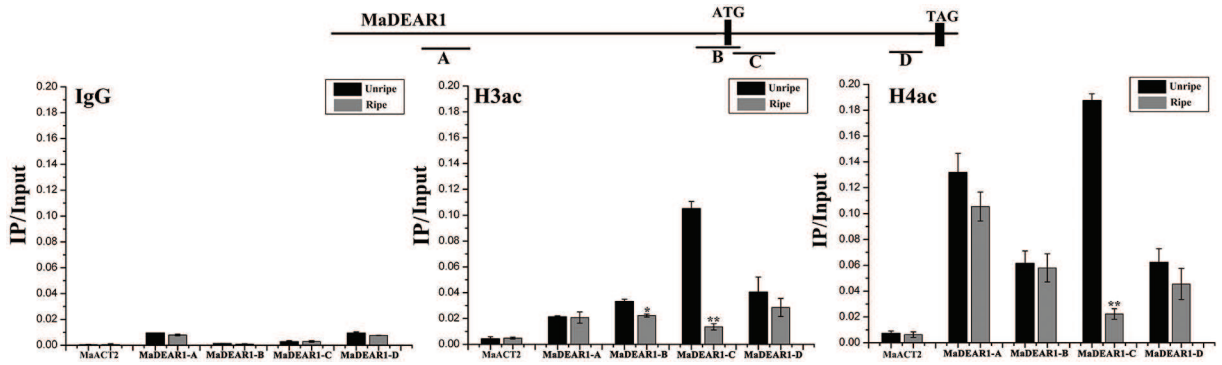

FIGURE 4 | ChIP-qPCR analysis of histone H3 (H3ac) or H4 acetylation (H4ac) levels at the regions of *MaDEAR1* in unripe and ripe banana fruit. The four regions of *MaDEAR1* (A–D) examined by ChIP-qPCR are shown in the top panel. The amounts of DNA after ChIP were quantified and normalized to *MaACT2*. IgG and *MaACT2* were used as negative controls. Data are shown as the ratio of IP to input (IP/Input). Each experiment was repeated with three biological replicates. Error bars represent SE $*P < 0.05$ and $**P < 0.01$ by Student's *t*-test, compared with unripe fruit.

(**Figure 3A**). These findings, together with the observations of its gene expression and promoter activity, suggest that *MaDEAR1* is suppressed by ethylene and ripening, and its decreased expression might be associated with reduced levels of histone H3 and H4 acetylation during ripening.

Genes Involving in Cell Wall Loosening of Banana Fruit, *MaEXP1/3*, *MaPG1*, *MaXTH10*, *MaPL3*, and *MaPME3*, Are Direct Targets of MaDEAR1

To understand the possible roles of MaDEAR1 in banana fruit ripening, we identified the potential targets of MaDEAR1 in relation to fruit ripening. Previous studies indicated that DREB proteins bind to the *cis*-acting dehydration-responsive element/C-repeat (DRE/CRT) in the promoter of their target genes, including *RD29A*, *RD17*, *COR15A*, *ERD10*, *KIN1*, and *COR6.6* (Lucas et al., 2011). Softening is an important indicator of fruit ripening, which is related to cell wall modifications, including enzymatic and non-enzymatic degradation of cell wall components (Li et al., 2010). Previously, 23 cell wall-modifying genes, including five *EXP*, nine *XET/XTH*, four *PG*, two *PE/PL* and three *PME* have been reported to be related to banana fruit softening (Pua et al., 2001; Asif and Nath, 2005; Asha et al., 2007; Mbéguié-A-Mbéguié et al., 2009; Asif et al., 2014), and we have examined the presence of the DRE/CRT core consensus sequence (A/GCCGAC) in their promoters. It was found that *MaEXP1*, *MaXTH10*, *MaPME3*, *MaPG1,* and *MaPL3* have one or two DRE/CRT elements in their promoters, while *MaEXP3* promoter contained four DRE/CRT elements (Supplementary Data Sheet S1), suggesting that these genes might be the targets of MaDEAR1.

To test whether MaDEAR1 could directly bind to these promoters, electrophoretic mobility shift assay (EMSA) was performed. DNA fragments containing the DRE/CRT element in the region of these promoters were used as probe. Recombinant glutathione S-transferase (GST)-MaDEAR1 fusion proteins were expressed in *E. coli* and purified (**Figure 5A**). As shown in **Figure 4B**, MaDEAR1 can directly bind to the DNA probes containing the DRE-motif in *MaEXP1/3*, *MaPG1*, *MaXTH10*, *MaPL3,* and *MaPME3* promoters, and the bindings were abolished by the addition of increasing amounts of unlabeled competitors with the same sequence. In addition, no parallel band shift was detected with only the GST tag (**Figure 5B**). These results show that MaDEAR1 specifically binds to the DRE motif in the promoters of *MaEXP1/3*, *MaPG1*, *MaXTH10*, *MaPL3,* and *MaPME3*, demonstrating that these genes are likely direct targets of MaDEAR1.

MaDEAR1 Represses Promoter Activities of *MaEXP1/3*, *MaPG1*, *MaXTH10*, *MaPL3,* and *MaPME3*

To further understand the regulation of *MaEXP1/3*, *MaPG1*, *MaXTH10*, *MaPL3,* and *MaPME3* by MaDEAR1, we performed transient expression assays using the dual luciferase reporter system. The dual luciferase reporter plasmid harbor *MaEXP1/3-*, *MaPG1-*, *MaXTH10-*, *MaPL3-,* or *MaPME3*-promoter fused to LUC, and the REN driven by the CaMV 35S promoter, while an effector plasmid carried MaDEAR1 expressed under the control of the CaMV 35S promoter (**Figure 6A**). As shown in **Figure 6B**, compared with the negative controls, tobacco leaves expressing MaDEAR1 showed significantly lower luciferase activity with the constructs harboring the LUC reporter gene driven by the *MaEXP1/3-*, *MaPG1-*, *MaXTH10-*, *MaPL3-*, or *MaPME3*-promoter, which is consistent with the finding that MaDEAR1 is a transcriptional repressor (**Figure 2B**).

DISCUSSION

Dehydration-responsive element-binding proteins are a class of AP2/ERF family of TFs, which are involved in plant response to drought, high salinity, low-temperature, and other environmental stresses (Agarwal et al., 2006; Lata and Prasad, 2011). The DREB proteins are divided into six small groups (A-1 to A-6) based on the sequence signature of DNA-binding domain

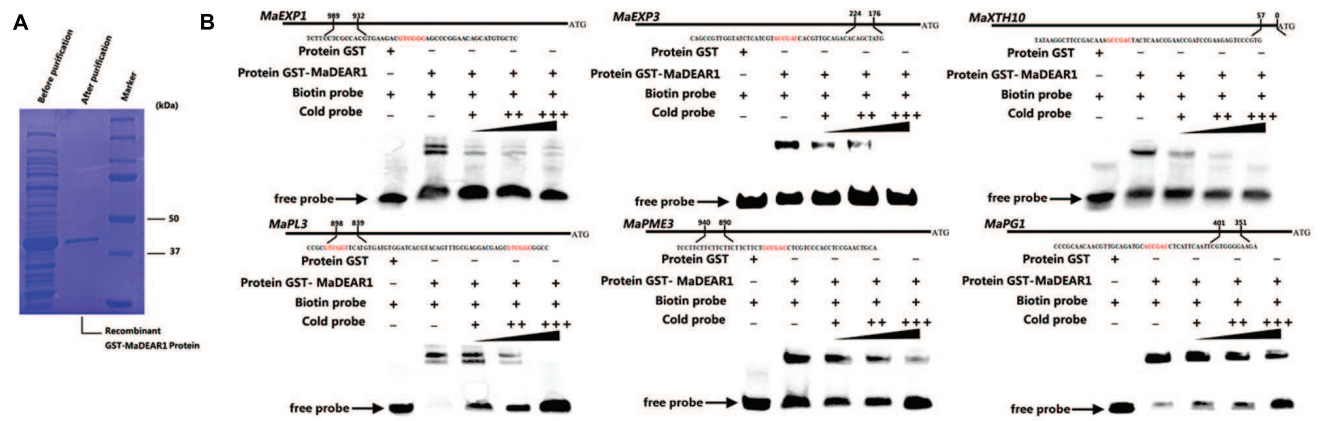

FIGURE 5 | MaDEAR1 binds to promoters of cell wall-modifying genes. (A) SDS-PAGE gel stained with Coomassie blue demonstrating affinity purification of the recombinant MaDEAR1 protein used for the electrophoretic mobility shift assay (EMSA). **(B)** EMSA showing MaDEAR1 binding to the promoter of *MaEXP1/3*, *MaPG1*, *MaXTH10*, *MaPL3*, and *MaPME3* containing DRE/CRT *cis*-acting element. Biotin-labeled DNA probe from the promoter was incubated with GST-MaDEAR1 protein, and the DNA-protein complexes were separated on 6% native polyacrylamide gels. Triangles indicate increasing amounts of unlabeled probes (2×10^{-5} μmol, 2×10^{-4} μmol, or 2×10^{-3} μmol) for competition.

and the existence of other motifs, of which A-5 group members share a conserved EAR motif at their C-terminus and act as transcriptional repressors (Ohta et al., 2001; Sakuma et al., 2002). In this study, we identified a banana *DREB* gene, *MaDEAR1*, whose predicted protein possesses an APETALA2 (AP2) domain that binds to DREs and an EAR motif that is responsible for transcriptional repression (**Figures 1A** and **2**), and thus belongs to A-5 group (**Figure 1B**). Sub-cellular localization and transcriptional activation assays indicated that MaDEAR1 is nuclear-localized and possesses transcriptional repression activity (**Figure 2**), similar to GhDBP1 in cotton (Huang and Liu, 2006) and MsDREBA5 in *Malus sieversii* Roem (Zhao et al., 2012).

To date, most reports about DREBs focus on A-1 and A-2 sub-groups, while investigation into others, such as the A-5 sub-group, is limited. Generally, the A-5 sub-group DREB proteins are transcriptional repressors of gene expression during stress. For example, transgenic *Arabidopsis* over-expressing *DEAR1* showed a cell death phenotype, resulting in reduced freezing tolerance (Tsutsui et al., 2009). Similarly, mutations in *RAP2.1*, another A-5 DREB, led to increased expression of *DREB1/CBF* and *DREB2* target genes with enhanced tolerance to drought and freezing (Dong and Liu, 2010). More recently, over-expression of *TaRAP2.1L* (a homolog of *RAP2.1* in wheat) under constitutive and stress-inducible promoters in transgenic wheat and barley caused dwarfism and decreased frost tolerance, supporting the notion that most DREB members in A-5 sub-group are negative regulators of stress tolerance (Amalraj et al., 2016). However, in addition to their role in stress responses, whether A-5 DREBs are involved in other biological processes such as fruit ripening is unknown. Here we showed that the *MaDEAR1* expression was down-regulated by ethylene and ripening. The ripening associated down-regulation is, at least in part, likely to be mediated by the repression of its promoter activity by ethylene produced during ripening (**Figure 3**). It is also important to note that the decline in *MaDEAR1* expression showed a concomitant increase in ethylene production during fruit ripening. These findings suggest that MaDEAR1 is a transcriptional repressor associated with fruit ripening, which is consistent with its transcriptional repression activity reported here (**Figure 2B**). Interestingly, we also found reduced levels of histone H3ac and H4ac in *MaDEAR1* promoter in the ripening stage of banana fruit (**Figure 4**), which closely corresponds with its decreased expression during fruit ripening (**Figure 3**). Several reports have implicated histone acetylation as an important mechanism for controlling *DREB* gene expression. For example, treatment of maize with the HDAC inhibitor trichostatin A (TSA) under cold stress conditions selectively inhibited the induction of the cold-responsive gene *ZmDREB1* through histone modification in the promoter region (Hu et al., 2011). Reports on enhanced transcript level of rice *OsDREB1b* and maize *ZmDREB2A*, as well as histone acetylation in their promoters further attest the regulation of *DREB* gene expression through histone modification (Roy et al., 2014; Zhao et al., 2014).

Fruit softening is one of the most important features that characterize the ripening process of fleshy climacteric fruits like bananas, and cell wall modification that occurs during the ripening process plays a critical role in the softening process (Li et al., 2010). The process of fruit ripening involves enzymatic and non-enzymatic factors. Expansins are non-enzymatic cell wall proteins that primarily induce cell wall extension (Cosgrove, 2000). Secondary wall-loosening factors such as XTH and PG, which enzymatically modify the structures of the cell wall, render it more responsive to wall-loosening events mediated by expansins (Cosgrove, 2000; Péret et al., 2009). XTH proteins can display two distinct enzymatic activities, including transglycosylase enzymatic (XET) activity leading to xyloglycan chain synthesis, and xyloglucan hydrolase activity (XEH) resulting in their degradation (Saladie et al., 2006). According to the previous reports, 23 cell wall-modifying genes, including five *EXP*, nine *XET/XTH*, four *PG*, two *PE/PL* and

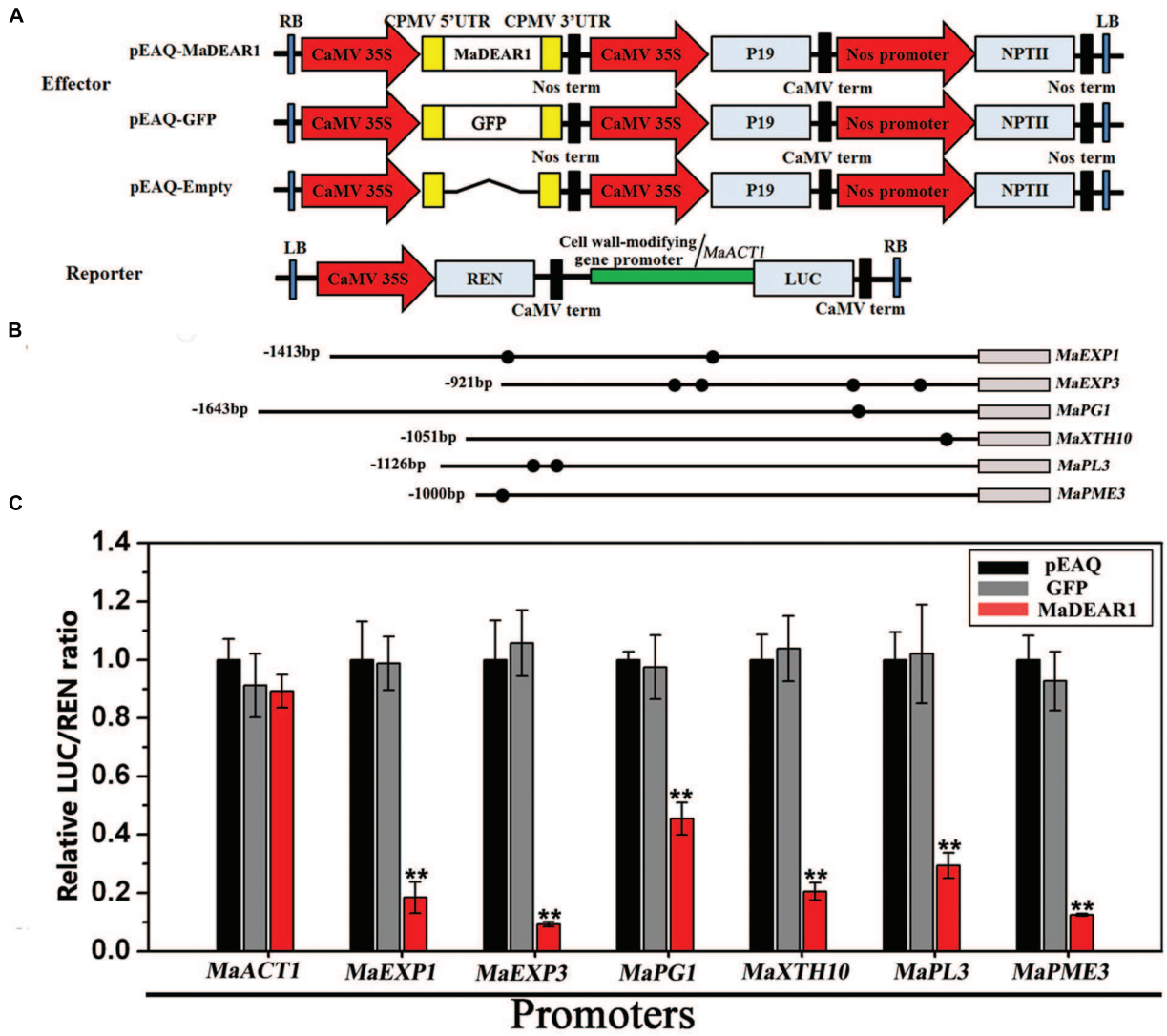

FIGURE 6 | Transient dual-luciferase reporter assays showing MaDEAR1's ability to repress the promoter activity of *MaEXP1/3*, *MaPG1*, *MaXTH10*, *MaPL3,* or *MaPME3*. (A) Constructs used in the transient assays. The reporter contained the *MaEXP1/3*, *MaPG1*, *MaXTH10*, *MaPL3,* or *MaPME3* promoters fused to LUC luciferase and REN luciferase driven by CaMV 35S as internal control. The effector contained the MaDEAR1 driven by the CaMV35S. The effector vector also contained the P19 suppressor of gene silencing, and the NPTII kanamycin resistance gene. **(B)** Schematics of the promoter of *MaEXP1/3*, *MaPG1*, *MaXTH10*, *MaPL3,* or *MaPME3*. Promoter length and DRE/CRT *cis*-acting elements are indicated with lines and black circles, respectively. **(C)** MaDEAR1 represses the promoter activity of *MaEXP1/3*, *MaPG1*, *MaXTH10*, *MaPL3,* or *MaPME3*. *Agrobacterium tumefaciens* strain GV3101 carrying the LUC reporter plasmid and different combinations of effector plasmids was infiltrated into *N. benthamiana* leaves, and the luciferase activity at the site of infiltration was measured 2 days after infiltration. The repression ability of MaDEAR1 to the promoter was shown by the ratio of LUC to REN. The ratio of LUC to REN of the empty vector (pEAQ) plus promoter was used as a calibrator (set as 1). The reporter containing the *MaACT1* promoter, and effector carrying the *GFP* gene were used as negative controls. Each value represents the means of six biological replicates, and vertical bars represent the SE $^{**}P < 0.01$ by Student's *t*-test, compared with pEAQ.

three *PME* have been isolated from banana fruit (Pua et al., 2001; Asif and Nath, 2005; Asha et al., 2007; Mbéguié-A-Mbéguié et al., 2009; Asif et al., 2014). It was found that transcripts of these genes were differentially expressed during post-harvest ripening (Mbéguié-A-Mbéguié et al., 2009; Asif et al., 2014), supporting their involvement in fruit ripening and softening. It is worth noting that transcriptional regulation of cell wall-modifying genes might be a conserved mechanism by which TFs regulate fruit ripening, as the cases of RIN in tomato (Fujisawa et al., 2013) and AdEILs and AdERFs in kiwifruit (Yin et al., 2010). Similar results were also found in bananas. For instance, MaMADS5 binds to the CArG-box sequence in the promoters of several ripening genes including *MaEXPs* (Roy Choudhury et al., 2012). Our previous studies also indicated that MaLBDs and MaBSD1 TFs are involved in fruit ripening, via transcriptional regulation of *MaEXP1/2* (Ba et al., 2014a,b). Also we found that, a transcriptional repressor MaDof23 physically interacts with a transcriptional activator MaERF9, and they act

antagonistically to regulate 10 ripening-related genes including *MaEXP1/2/3/5*, *MaXET7*, *MaPG1*, *MaPME3*, *MaPL2*, *MaCAT*, and *MaPDC* that are associated with cell wall degradation and aroma formation during banana ripening (Feng et al., 2016). In this work, we show that MaDEAR1 binds and represses the activity of six cell wall-modifying genes, such as *MaEXP1/3*, *MaPG1*, *MaXTH10*, *MaPL3,* and *MaPME3* (**Figures 5** and **6**), suggesting its regulatory role in cell wall degradation during banana fruit ripening. Nuclear localization and promoter activity of MaDEAR1 in banana protoplasts will further substantiate these results. In addition to these fruit softening-associated genes, those involved in ethylene production and aroma formation such as *MaACS1*, *MaACO1* and *MaPDC* are also associated with banana ripening (Yang et al., 2011; Xiao et al., 2013), but whether they are direct targets of MaDEAR1 remains unknown. As fruit ripening is controlled by transcriptional regulatory networks involving several TFs, it would be interesting to investigate whether MaDEAR1 interacts with other reported ripening-related TFs of banana fruit, including MaERFs (Xiao et al., 2013), MaMADSs (Roy Choudhury et al., 2012), MaNACs (Shan et al., 2012), MaLBDs and MaBSDs (Ba et al., 2014a,b), and the effects of such interactions on fruit ripening.

CONCLUSION

The data reported here represent an EAR-motif-containing DREB TF, MaDEAR1, which was found to be a nuclear-localized transcriptional repressor. Expression and promoter activity of *MaDEAR1* were repressed by ethylene and ripening, and its expression is likely to be regulated by, at least in part, by histone modification. MaDEAR1 binds to and represses several cell wall-modifying genes, including *MaEXP1/3*, *MaPG1*, *MaXTH10*, *MaPL3,* and *MaPME3*. Taken together, our results report new insights into the mechanisms underpinning ethylene-mediated banana fruit ripening, of which MaDEAR1 may be playing a role via transcriptional repression of genes involved in cell wall modification and softening of fruit.

AUTHOR CONTRIBUTIONS

JC, JK, WL, PL, and XD designed the research. ZF, WS, YH, YX, and YY performed the experiments. ZF, JK, WL, PL, and JC wrote the manuscript.

FUNDING

This work was supported in part by the National Basic Research Program of China (grant No. 2013CB127104) and the China Agriculture Research System (grant no. CARS-32-09).

ACKNOWLEDGMENTS

We thank Professor Seiichiro Hasezawa (Department of Integrated Biosciences, the University of Tokyo), Professor Shouyi Chen (Institute of Genetics and Developmental Biology, Chinese Academy of Sciences), Professor Junping Gao (Department of Ornamental Horticulture, China Agricultural University), and Professor George P. Lomonossoff (Department of Biological Chemistry, John Innes Centre, Norwich Research Park) for the generous gift of tobacco BY-2 suspension cells, the transient expression vectors, and pEAQ vectors, respectively.

SUPPLEMENTARY MATERIAL

The Supplementary Material for this article can be found online at: http://journal.frontiersin.org/article/10.3389/fpls.2016.01021

REFERENCES

Abel, S., and Theologis, A. (1994). Transient transformation of *Arabidopsis* leaf protoplasts: a versatile experimental system to study gene expression. *Plant J.* 5, 421–427. doi: 10.1111/j.1365-313X.1994.00421.x

Agarwal, P. K., Agarwal, P., Reddy, M., and Sopory, S. K. (2006). Role of DREB transcription factors in abiotic and biotic stress tolerance in plants. *Plant Cell Rep.* 25, 1263–1274. doi: 10.1007/s00299-006-0204-8

Ahmed, Z. F. R., and Palta, J. P. (2016). Postharvest dip treatment with a natural lysophospholipid plus soy lecithin extended the shelf life of banana fruit. *Postharvest Biol. Technol.* 113, 58–65. doi: 10.1016/j.postharvbio.2015.10.016

Amalraj, A., Luang, S., Kumar, M. Y., Sornaraj, P., Eini, O., Kovalchuk, N., et al. (2016). Change of function of the wheat stress-responsive transcriptional repressor TaRAP2.1L by repressor motif modification. *Plant Biotech. J.* 14, 820–832. doi: 10.1111/pbi.12432

Asha, S. V. A., Sane, A. P., and Nath, P. (2007). Multiple forms of alpha-expansin genes are expressed during banana fruit ripening and development. *Postharvest Biol. Technol.* 45, 184–192. doi: 10.1016/j.postharvbio.2007.03.003

Asif, M., and Nath, P. (2005). Expression of multiple forms of polygalacturonase gene during ripening in banana fruit. *Plant Physiol. Biochem.* 43, 177–184. doi: 10.1016/j.plaphy.2005.01.011

Asif, M. H., Lakhwani, D., Pathak, S., Gupta, P., Bag, S. K., Nath, P., et al. (2014). Transcriptome analysis of ripe and unripe fruit tissue of banana identifies major metabolic networks involved in fruit ripening process. *BMC Plant Biol.* 14:316. doi: 10.1186/s12870-014-0316-1

Ba, L., Shan, W., Kuang, J., Feng, B., Xiao, Y., Lu, W., et al. (2014a). The banana MaLBD (LATERAL ORGAN BOUNDARIES DOMAIN) transcription factors regulate EXPANSIN expression and are involved in fruit ripening. *Plant Mol. Biol. Rep.* 32, 1103–1113. doi: 10.1007/s11105-014-0720-6

Ba, L., Shan, W., Xiao, Y., Chen, J., Lu, W., and Kuang, J. (2014b). A ripening-induced transcription factor MaBSD1 interacts with promoters of MaEXP1/2 from banana fruit. *Plant Cell Rep.* 33, 1913–1920. doi: 10.1007/s00299-014-1668-6

Ba, L. J., Kuang, J. F., Chen, J. Y., and Lu, W. J. (2016). MaJAZ1 attenuates the MaLBD5-mediated transcriptional activation of jasmonate biosynthesis gene MaAOC2 in regulating cold tolerance of banana fruit. *J. Agric. Food Chem.* 64, 738–745. doi: 10.1021/acs.jafc.5b05005

Benhamed, M., Bertrand, C., Servet, C., and Zhou, D. X. (2006). *Arabidopsis* GCN5, HD1, and TAF1/HAF2 interact to regulate histone acetylation required for light-responsive gene expression. *Plant Cell* 18, 2893–2903.

Chen, L., Zhong, H. Y., Kuang, J. F., Li, J. G., Chen, J. Y., and Lu, W. J. (2011). Validation of reference genes for RT-qPCR studies of gene expression in banana fruit under different experimental conditions. *Planta* 234, 377–390. doi: 10.1007/s00425-011-1410-3

Cosgrove, D. J. (2000). Loosening of plant cell walls by expansins. *Nature* 407, 321–326. doi: 10.1038/35030000

D'Hont, A., Denoeud, F., Aury, J. M., Baurens, F. C., Carreel, F., Garsmeur, O., et al. (2012). The banana (Musa acuminata) genome and the evolution of monocotyledonous plants. *Nature* 488, 213–217. doi: 10.1038/nature11241

Dong, C. J., and Liu, J. Y. (2010). The *Arabidopsis* EAR-motif-containing protein RAP2.1 functions as an active transcriptional repressor to keep stress responses under tight control. *BMC Plant Biol.* 16:10–47. doi: 10.1186/1471-2229-10-47

Feng, B., Han, Y., Xiao, Y., Kuang, J., Fan, Z., Chen, J., et al. (2016). The banana fruit Dof transcription factor MaDof23 acts as a repressor and interacts with MaERF9 in regulating ripening-related genes. *J. Exp. Bot.* 67, 2263–2275. doi: 10.1093/jxb/erw032

Fujisawa, M., Nakano, T., Shima, Y., and Ito, Y. (2013). A large-scale identification of direct targets of the tomato MADS box transcription factor RIPENING INHIBITOR reveals the regulation of fruit ripening. *Plant Cell* 25, 371–386. doi: 10.1105/tpc.112.108118

Gao, S. Q., Chen, M., Xia, L. Q., Xiu, H. J., Xu, Z. S., Li, L. C., et al. (2009). A cotton (*Gossypium hirsutum*) DRE-binding transcription factor gene, GhDREB, confers enhanced tolerance to drought, high salt, and freezing stresses in transgenic wheat. *Plant Cell Rep.* 28, 301–311. doi: 10.1007/s00299-008-0623-9

Gendrel, A. V., Lippman, Z., Martienssen, R., and Colot, V. (2005). Profiling histone modification patterns in plants using genomic tiling microarrays. *Nat. Methods* 2, 213–218. doi: 10.1038/nmeth0305-213

Haake, V., Cook, D., Riechmann, J., Pineda, O., Thomashow, M. F., and Zhang, J. Z. (2002). Transcription factor CBF4 is a regulator of drought adaptation in *Arabidopsis*. *Plant Physiol.* 130, 639–648. doi: 10.1104/pp.006478

Han, Y. C., Kuang, J. F., Chen, J. Y., Liu, X. C., Xiao, Y. Y., Fu, C. C., et al. (2016). Banana transcription factor MaERF11 recruits histone deacetylase MaHDA1 and represses the expression of MaACO1 and expansins during fruit ripening. *Plant Physiol.* 171, 1070–1084. doi: 10.1104/pp.16.00301

Hellens, R., Allan, A., Friel, E., Bolitho, K., Grafton, K., Templeton, M., et al. (2005). Transient expression vectors for functional genomics, quantification of promoter activity and RNA silencing in plants. *Plant Methods* 1, 13. doi: 10.1186/1746-4811-1-13

Hu, Y., Zhang, L., Zhao, L., Li, J., He, S., Zhou, K., et al. (2011). Trichostatin A selectively suppresses the cold-induced transcription of the ZmDREB1 gene in maize. *PLoS ONE* 6:e22132. doi: 10.1371/journal.pone.0022132

Huang, B., and Liu, J. Y. (2006). A cotton dehydration responsive element binding protein functions as a transcriptional repressor of DRE element-mediated gene expression. *Biochem. Biophys. Res. Commun.* 343, 1023–1031. doi: 10.1016/j.bbrc.2006.03.016

Jourda, C., Cardi, C., Mbeguie-A-Mbeguie, D., Bocs, S., Garsmeur, O., D'Hont, A., et al. (2014). Expansion of banana (Musa acuminata) gene families involved in ethylene biosynthesis and signalling after lineage-specific whole-genome duplications. *New Phytol.* 202, 986–1000. doi: 10.1111/nph.12710

Kagale, S., and Rozwadowski, K. (2010). Small yet effective: the ethylene responsive element binding factor-associated amphiphilic repression (EAR) motif. *Plant Signal. Behav.* 5, 691–694. doi: 10.4161/psb.5.6.11576

Kuan, C. H., Ahmad, S. H., Son, R., Yap, E. S. P., Zamri, M. Z., Shukor, N. I. A., et al. (2015). Influence of forced-air precooling time on the changes in quality attributes and consumer acceptance of Musa AAA Berangan. *Int. Food Res. J.* 22, 1864–1869.

Kuang, J., Chen, L., Shan, W., Yang, S., Lu, W., and Chen, J. (2013). Molecular characterization of two banana ethylene signaling components MaEBFs during fruit ripening. *Postharvest Biol. Technol.* 85, 94–101. doi: 10.1016/j.postharvbio.2013.05.004

Kumagai-Sano, F., Hayashi, T., Sano, T., and Hasezawa, S. (2006). Cell cycle synchronization of tobacco BY-2 cells. *Nat. Protoc.* 1, 2621–2627. doi: 10.1038/nprot.2006.381

Lata, C., and Prasad, M. (2011). Role of DREBs in regulation of abiotic stress responses in plants. *J. Exp. Bot.* 62, 4731–4748. doi: 10.1093/jxb/err210

Li, X., Xu, C., Korban, S. S., and Chen, K. (2010). Regulatory mechanisms of textural changes in ripening fruits. *Crit. Rev. Plant Sci.* 29, 222–243. doi: 10.1080/07352689.2010.487776

Liu, Q., Kasuga, M., Sakuma, Y., Abe, H., Miura, S., Yamaguchi-Shinozak, K., et al. (1998). Two transcription factors, DREB1 and DREB2,with an EREBP/AP2 DNA binding domain separate two cellular signal transduction pathways in drought- and low-temperature responsive gene expression, respectively, in *Arabidopsis*. *Plant Cell* 10, 1391–1406. doi: 10.2307/3870648

Liu, X. J., Shiomi, S., Nakatsuka, A., Kubo, Y., Nakamura, R., and Inaba, A. (1999). Characterization of ethylene biosynthesis associated with ripening in banana fruit. *Plant Physiol.* 121, 1257–1265. doi: 10.1104/pp.121.4.1257

Lucas, S., Durmaz, E., Akpınar, B. A., and Budak, H. (2011). The drought response displayed by a DRE-binding protein from *Triticum dicoccoides*. *Plant Physiol. Biochem.* 49, 346–351. doi: 10.1016/j.plaphy.2011.01.016

Mbéguié-A-Mbéguié, D., Hubert, O., Baurens, F. C., Matsumoto, T., Chillet, M., Fils-Lycaon, B., et al. (2009). Expression patterns of cell wall-modifying genes from banana during fruit ripening and in relationship with finger drop. *J. Exp. Bot.* 60, 2021–2034. doi: 10.1093/jxb/erp079

Mbéguié-A-Mbéguié, D., Hubert, O., Fils-Lycaon, B., Chillet, M., and Baurens, F. C. (2008). EIN3-like gene expression during fruit ripening of Cavendish banana (*Musa acuminata* cv. Grande Naine). *Physiol. Plant.* 133, 435–448. doi: 10.1111/j.1399-3054.2008.01083.x

Mizoi, J., Shinozaki, K., and Yamaguchi-Shinozaki, K. (2012). AP2/ERF family transcription factors in plant abiotic stress responses. *Biochim. Biophys. Acta* 1819, 86–96. doi: 10.1016/j.bbagrm.2011.08.004

Nakashima, K., Shinwari, Z. K., Sakuma, Y., Seki, M., Miura, S., Shinozaki, K., et al. (2000). Organization and expression of two *Arabidopsis* DREB2 genes encoding DRE-binding proteins involved in dehydration- and high-salinity-responsive gene expression. *Plant Mol. Biol.* 42, 657–665. doi: 10.1023/A:1006321900483

Ohme-Takagi, M., and Shinshi, H. (1995). Ethylene-inducible DNA binding proteins that interact with an ethylene-responsive element. *Plant Cell* 7, 173–182. doi: 10.1105/tpc.7.2.173

Ohta, M., Matsui, K., Hiratsu, K., Shinshi, H., and Ohme-Takagi, M. (2001). Repression domains of class II ERF transcriptional repressors share an essential motif for active repression. *Plant Cell* 13, 1959–1968. doi: 10.1105/tpc.13.8.1959

Péret, B. D., Rybel, B., Casimiro, I., Benková, E., Swarup, R., Laplaze, L., et al. (2009). *Arabidopsis* lateral root development: an emerging story. *Trends Plant Sci.* 14, 399–408. doi: 10.1016/j.tplants.2009.05.002

Pirrello, J., Prasad, N. B. C., Zhang, W., Chen, K., Isabelle, M., Zouine, M., et al. (2012). Functional analysis and binding affinity of tomato ethylene response factors provide insight on the molecular bases of plant differential responses to ethylene. *BMC Plant Biol.* 12:190. doi: 10.1186/1471-2229-12-190

Pua, E. C., Ong, C. K., Liu, P., and Liu, J. Z. (2001). Isolation and expression of two pectate lyase genes during fruit ripening of banana (*Musa acuminata*). *Physiol. Plant.* 113, 92–99. doi: 10.1034/j.1399-3054.2001.1130113.x

Roy, D., Paul, A., Roy, A., Ghosh, R., Ganguly, P., and Chaudhuri, S. (2014). Differential acetylation of histone H3 at the regulatory region of OsDREB1b promoter facilitates chromatin remodeling and transcription activation during cold stress. *PLoS ONE* 9:e100343. doi: 10.1371/journal.pone.0100343

Roy Choudhury, S., Roy, S., Nag, A., Singh, S. K., and Sengupta, D. N. (2012). Characterization of an AGAMOUS-like MADS box protein, a probable constituent of flowering and fruit ripening regulatory system in banana. *PLoS ONE* 7:e44361. doi: 10.1371/journal.pone.0044361

Sainsbury, F., Thuenemann, E. C., and Lomonossoff, G. P. (2009). pEAQ: versatile expression vectors for easy and quick transient expression of heterologous proteins in plants. *Plant Biotechnol. J.* 7, 682–693. doi: 10.1111/j.1467-7652.2009.00434.x

Sakuma, Y., Liu, Q., Dubouzet, J. G., Abe, H., Shinozaki, K., and Yamaguchi-Shinozaki, K. (2002). DNA-binding specificity of the ERF/AP2 domain of *Arabidopsis* DREBs, transcription factors involved in dehydration- and cold-inducible gene expression. *Biochem. Biophys. Res. Commun.* 290, 998–1009. doi: 10.1006/bbrc.2001.6299

Saladie, M., Rose, J. R. C., Cosgrove, D. J., and Catala, C. (2006). Characterization of a new xyloglucan endotransglucosylase/hydrolase (XTH) from ripening tomato fruit and implications for the diverse modes of enzymicaction. *Plant J.* 47, 282–295. doi: 10.1111/j.1365-313X.2006.02784.x

Salehin, M., and Estelle, M. (2015). Ethylene prunes translation. *Cell* 163, 543–544. doi: 10.1016/j.cell.2015.10.032

Shan, W., Kuang, J. F., Chen, L., Xie, H., Peng, H. H., Xiao, Y. Y., et al. (2012). Molecular characterization of banana NAC transcription factors and their interactions with ethylene signalling component EIL during fruit ripening. *J. Exp. Bot.* 63, 5171–5187. doi: 10.1093/jxb/ers178

Sreedharan, S., Shekhawat, U. K. S., and Ganapathi, T. R. (2012). MusaSAP1, a A20/AN1zinc finger gene from banana functions as a positive regulator in

different stress responses. *Plant Mol. Biol.* 80, 503–517. doi: 10.1007/s11103-012-9964-4

Stockinger, E. J., Gilmour, S. J., and Thomashow, M. F. (1997). *Arabidopsis thaliana* CBF1 encodes an AP2 domain-containing transcriptional activator that binds to the C-repeat/DRE, a cis-acting DNA regulatory element that stimulates transcription in response to low temperature and water deficit. *Proc. Natl. Acad. Sci. U.S.A.* 94, 1035–1040. doi: 10.1073/pnas.94.3.1035

Tsutsui, T., Kato, W., Asada, Y., Sako, K., Sato, T., Sonoda, Y., et al. (2009). DEAR1, a transcriptional repressor of DREB protein that mediates plant defense and freezing stress responses in *Arabidopsis*. *J. Plant Res.* 122, 633–643. doi: 10.1007/s10265-009-0252-6

Wan, C. Y., and Wilkins, T. A. (1994). A modified hot borate method significantly enhances the yield of high-quality RNA from cotton (*Gossypium hirsutum* L.). *Anal. Biochem.* 223, 7–12. doi: 10.1006/abio.1994.1538

Xiao, Y. Y., Chen, J. Y., Kuang, J. F., Shan, W., Xie, H., Jiang, Y. M., et al. (2013). Banana ethylene response factors are involved in fruitripening through their interactions with ethylene biosynthesis genes. *J. Exp. Bot.* 64, 2499–2510. doi: 10.1093/jxb/ert108

Yang, X. T., Song, J., Fillmore, S., Pang, X. Q., and Zhang, Z. Q. (2011). Effect of high temperature on color, chlorophyll fluorescence and volatile biosynthesis in green-ripe banana fruit. *Postharvest Biol. Technol.* 62, 246–257. doi: 10.1016/j.postharvbio.2011.06.011

Yin, X. R., Allan, A. C., Chen, K. S., and Ferguson, I. B. (2010). Kiwifruit EIL and ERF genes involved in regulating fruit ripening. *Plant Physiol.* 153, 1280–1292. doi: 10.1104/pp.110.157081

Zhao, L., Wang, P., Yan, S., Gao, F., Li, H., Hou, H., et al. (2014). Promoter-associated histone acetylation is involved in the osmotic stress-induced transcriptional regulation of the maize ZmDREB2A gene. *Physiol. Plant.* 151, 459–467. doi: 10.1111/ppl.12136

Zhao, X. J., Lei, H. J., Zhao, K., Yuan, H. Z., and Li, T. H. (2012). Isolation and characterization of a dehydration responsive element binding factor MsDREBA5 in *Malus sieversii* Roem. *Sci. Hort.* 142, 212–220. doi: 10.1016/j.scienta.2012.05.020

Conflict of Interest Statement: The authors declare that the research was conducted in the absence of any commercial or financial relationships that could be construed as a potential conflict of interest.

frontiers in Plant Science

ORIGINAL RESEARCH
published: 09 January 2017
doi: 10.3389/fpls.2016.02044

The Interplay of Chromatin Landscape and DNA-Binding Context Suggests Distinct Modes of EIN3 Regulation in *Arabidopsis thaliana*

Elena V. Zemlyanskaya[1,2†], Victor G. Levitsky[1,2†], Dmitry Y. Oshchepkov[1], Ivo Grosse[2,3,4] and Victoria V. Mironova[1,2]*

[1] Institute of Cytology and Genetics, Siberian Branch of the Russian Academy of Sciences (SB RAS), Novosibirsk, Russia, [2] Department of Natural Sciences, Novosibirsk State University, Novosibirsk, Russia, [3] Institute of Computer Science, Martin Luther University Halle-Wittenberg, Halle(Saale), Germany, [4] German Centre for Integrative Biodiversity Research (iDiv) Halle-Jena-Leipzig, Leipzig, Germany

The plant hormone ethylene regulates numerous developmental processes and stress responses. Ethylene signaling proceeds via a linear pathway, which activates transcription factor (TF) EIN3, a primary transcriptional regulator of ethylene response. EIN3 influences gene expression upon binding to a specific sequence in gene promoters. This interaction, however, might be considerably affected by additional co-factors. In this work, we perform whole genome bioinformatics study to identify the impact of epigenetic factors in EIN3 functioning. The analysis of publicly available ChIP-Seq data on EIN3 binding in *Arabidopsis thaliana* showed bimodality of distribution of EIN3 binding regions (EBRs) in gene promoters. Besides a sharp peak in close proximity to transcription start site, which is a common binding region for a wide variety of TFs, we found an additional extended peak in the distal promoter region. We characterized all EBRs with respect to the epigenetic status appealing to previously published genome-wide map of nine chromatin states in *A. thaliana*. We found that the implicit distal peak was associated with a specific chromatin state (referred to as chromatin state 4 in the primary source), which was just poorly represented in the pronounced proximal peak. Intriguingly, EBRs corresponding to this chromatin state 4 were significantly associated with ethylene response, unlike the others representing the overwhelming majority of EBRs related to the explicit proximal peak. Moreover, we found that specific EIN3 binding sequences predicted with previously described model were enriched in the EBRs mapped to the chromatin state 4, but not to the rest ones. These results allow us to conclude that the interplay of genetic and epigenetic factors might cause the distinct modes of EIN3 regulation.

Keywords: bioinformatics, transcriptional regulation, TEIL, ETHYLENE-INSENSITIVE3, ChIP-Seq, EIN3 binding site (EBS), position weight matrix, Gene Ontology

Abbreviations: EBR, EIN3 binding region; EBS, EIN3 binding site; EIL, ETHYLENE-INSENSITIVE3-LIKE; EIN3, ETHYLENE-INSENSITIVE3; GO, Gene Ontology; TEIL, TOBACCO EIN3-LIKE; TF, transcription factor; TSS, transcription start site.

OPEN ACCESS

Edited by:
Antonio Ferrante, University of Milan, Italy

Reviewed by:
Hao Peng, Washington State University, USA
Andrea Ariani, University of California, Davis, USA

****Correspondence:***
Elena V. Zemlyanskaya
ezemlyanskaya@bionet.nsc.ru

† These authors have contributed equally to this work.

Specialty section:
This article was submitted to Plant Physiology, a section of the journal Frontiers in Plant Science

Received: *20 October 2016*
Accepted: *21 December 2016*
Published: *09 January 2017*

Citation:
Zemlyanskaya EV, Levitsky VG, Oshchepkov DY, Grosse I and Mironova VV (2017) The Interplay of Chromatin Landscape and DNA-Binding Context Suggests Distinct Modes of EIN3 Regulation in Arabidopsis thaliana. Front. Plant Sci. 7:2044. doi: 10.3389/fpls.2016.02044

INTRODUCTION

The gaseous plant hormone ethylene regulates numerous plant developmental processes and stress responses, including germination, seedling growth, sex determination, fruit ripening, senescence, abscission, plant–microbe interactions and abiotic stress responses (McManus, 2012). Such a diversity is due to the fine regulation of ethylene signaling, which is under control of complex interactions with ethylene unrelated signals. Unraveling this complexity with respect to both genetic and epigenetic components is one of the major objectives in ethylene biology.

Cellular response to ethylene starts with ER-localized ethylene receptors, which transmit the signal via a linear pathway to the TFs of EIL family – the primary transcriptional regulators of ethylene response (reviewed in Merchante et al., 2013; Cho and Yoo, 2015). EILs activate transcriptional cascades, including secondary ethylene response mediated by ETHYLENE RESPONSIVE FACTOR1 (ERF1) (Solano et al., 1998). In the *Arabidopsis thaliana* genome there are six *EIL* genes (*EIN3, EIL1-5*) (Guo and Ecker, 2004), but only EIN3 and EIL1 proteins function as primary transcriptional regulators in ethylene signaling and mediate most, if not all, plant responses to ethylene (Chao et al., 1997; Solano et al., 1998; Alonso et al., 2003; An et al., 2010). EIN3 and EIL1 influence gene expression upon binding to a specific nucleotide sequence in gene promoters. The consensus binding site was described for tobacco EIN3 homolog (TEIL) as AYGWAYCT motif, where Y and W represent C/T and A/T, respectively (Kosugi and Ohashi, 2000). EBSs with a certain similarity to TEIL motif have been proven *in vivo* and *in vitro* in the upstream regions of a number of *A. thaliana* genes, e.g., *ERF1* (Solano et al., 1998), *HLS1* (An et al., 2012), *PIF3* (Zhong et al., 2012), etc. The TEIL motif was also found significantly enriched in EIN3 binding regions revealed by ChIP-Seq in *A. thaliana* (Chang et al., 2013). The majority of ChIP-Seq derived EIN3 target genes, however, did not respond to ethylene treatment, which implies the existence of more complex regulation of EIL-mediated gene expression.

In plants EIN3/EIL1 activity and DNA binding capacity are modulated by a variety of ethylene unrelated co-factors (Zhu et al., 2011; An et al., 2012; Song et al., 2014). In general, epigenetic modifications are known to play essential role in tuning activity of different TFs (Filion et al., 2010). Accordingly, epigenetic regulation was reported for EIN3/EIL1-mediated gene expression. JAZ protein, a transcriptional repressor, which participates in jasmonic acid signaling, is capable of interacting with EIN3/EIL1, recruiting an RPD3-type histone deacetylase HDA6 to the complex (Zhu et al., 2011). HDA6 introduces epigenetic chromatin modifications, thereby inactivating EIN3. However, the role of epigenetics in primary ethylene response has not been explicitly explored.

Here, we explore this possibility and study if there are associations of the occurrence of EIN3/EIL1 binding sites and different chromatin states in *A. thaliana* as published by Sequeira-Mendes et al. (2014). Based on the combinatorial co-occurrence of 16 chromatin features and the GC content Sequeira-Mendes et al. (2014) distinguish nine chromatin states. States 1, 2, and 3 contain a high amount of active chromatin marks (e.g., H3K4me3, H3K4me2, or H3K36me3), and are typically localized around the TSS, in proximal promoter regions and in genes, correspondingly. The other six chromatin states contain a low amount of active chromatin marks. Specifically, chromatin states 8 and 9 are enriched in heterochromatin marks such as H3K27me1, H3K9me2, GC methylation, and H3.1, while chromatin states 4 and 5 are enriched in the repressive chromatin mark H3K27me3. States 4 and 5 are predominantly intergenic, states 6 and 7 are intragenic.

We processed publicly available raw ChIP-Seq data on EIN3 binding (Chang et al., 2013) and investigated the whole genome distribution of obtained EIN3 binding regions (EBRs). Next, we used the genome-wide map of chromatin states in *A. thaliana* (Sequeira-Mendes et al., 2014) to characterize all EBRs with respect to the epigenetic status. Subsequently, we implied GO enrichment analysis to identify functional peculiarities of genes harboring the EBRs related to certain chromatin states in their 5′ regulatory regions. Finally, we performed motif enrichment analysis to specify interrelations between genetic and epigenetic components. Based on the results, we assumed that there is the interplay of genetic and epigenetic factors, which might cause distinct modes of EIN3 regulation.

MATERIALS AND METHODS

ChIP-Seq Data Analysis

Two publicly available raw ChIP-Seq datasets on EIN3 binding in 3-day-old *A. thaliana* etiolated seedlings (Chang et al., 2013) were taken from NCBI Sequence Read Archive (SRA)[1]. The datasets SRX216234 and SRX215430 represented data on 4-h ethylene treated plants at ethylene gas concentration of 10 μl/l and control plants with no ethylene treatment, correspondingly. Individual ChIP-Seq runs were pooled for each dataset.

The genome sequence of *A. thaliana* was retrieved from TAIR 10[2]. The ChIP-Seq reads were mapped to the reference *A. thaliana* genome with Bowtie v. 1.1.1 (Langmead et al., 2009). The Bowtie options were set to report only unique alignments with no mismatches (-n 0 -m 1 --best). Peak calling was performed with MACS v. 1.4.2. (Zhang et al., 2008). The parameters were set by default. Peak calling was performed for 4-h ethylene treated plants (dataset SRX216234) using ethylene untreated EIN3 ChIP sample (dataset SRX215430) as a control according to the procedure in the primary source (Chang et al., 2013). 2577 ChIP-Seq peaks of height at least seven were considered EBRs.

Since the standard procedure for ChIP-Seq data analysis according to the ENCODE3 standards[3] requires the presence of an input DNA control sample, we applied an alternative pipeline to confirm the robustness of the results (Supplementary Data 1).

[1] https://www.ncbi.nlm.nih.gov/sra/

[2] ftp://ftp.arabidopsis.org/home/tair/Sequences/whole_chromosomes/

[3] https://www.encodeproject.org/data-standards/chip-seq/

Analysis of the Distribution of EBRs

Genome annotation data for *A. thaliana* was retrieved from TAIR 10[4]. The GFF table was used to retrieve the chromosomal positions of transcription starts/ends and intergenic spacers.

For the analysis of EBRs distribution relative to the gene structure, we kept 35176 transcripts of protein-coding genes. The EBRs positions were classified as in (Boldyreva et al., 2016) with the following modifications: "TSS" (overlapping with at least one of the gene TSS); "GENE" (all other regions overlapping with the gene bodies); "INTERGENIC" (the regions outside of the genes). To obtain an estimate of non-randomness of EBRs distribution relative to the gene structure, Monte-Carlo permutation test was applied as described previously (Boldyreva et al., 2016). As a result, Monte-Carlo test provided a set of three *p*-values, which reflected non-randomness (enrichment or depletion) of the number of EBRs mapped to each of three location classes.

To characterize the distribution of EBRs relative to TSS we used a subset of 19434 genes with annotated 5′ untranslated region (5′UTR). The frequency of EBRs occurrence at a certain position in [−1500; +100] upstream gene region was estimated as the fraction of genes hitting EBRs.

Analysis of Chromatin States

To characterize EBRs with respect to genome functional topography we used the whole genome map of nine chromatin states in *A. thaliana* (Sequeira-Mendes et al., 2014).

To statistically evaluate the representation of EBRs in the domains of chromatin states 1/2/4 along the upstream gene regions and perform chromatin-specific motif search (see below), we intersected annotations of 2577 EBRs with those of the chromatin states and compiled three datasets of 418/734/760 continuous EBR fragments, which were strictly mapped to the corresponding chromatin domains.

Monte-Carlo Permutation Test for Genome Tracks

To estimate non-randomness of the overlap between various tracks of genome regions – EBRs, the domains of the chromatin states, EBR fragments (see above), the tracks of upstream gene regions (see below) – we used Monte-Carlo permutation test as described in (Khoroshko et al., 2016). We used the ratio of the total overlap length to the total length of the permutated track as a measure of overlap between two tracks. This ratio was referred to as the *fraction of overlap*.

The tracks of upstream gene regions representing seven 500 bp long intervals of [−3500; +1] region and entire 5′UTRs were created as follows. For the set of 31614 transcripts with distinct TSS we compiled annotations for eight regions: [3500; −3000], [−3000; −2500], etc. up to [500; +1] and [+1; AUG] relative to TSS. These datasets were referred to as the 1st, 2nd, etc. up to the 8th. We removed from the first seven datasets all sequences that had any overlap with annotation of any transcripts. We filtered out from 1st, 2nd, etc. up to the 6th dataset all sequences that have any overlap with annotation of upstream regions in the ranges [−3000; +1], [2500; +1], . . . etc. up to [−500; +1], respectively. We removed from the 8th dataset (1) all fragments of genes from the starts to the end of translation and (2) any sequences overlapping [500; +1] region. In total, the 1st, 2nd, etc. up to the 8th dataset consisted of 3430, 4152, 5179, 6620, 8856, 12645, 18768, 15238 sequences, correspondingly.

[4]ftp://ftp.arabidopsis.org/Maps/gbrowse_data/TAIR10/TAIR10_GFF3_genes.gff

Gene Ontology (GO) Enrichment Analysis

Functional annotation of genes was performed using 6.8 version of DAVID tool (Huang et al., 2009)[5] separately for two sets of genes, which were created as follows. For each EBR we defined a set of genes harboring the EBR in their [3500; +1] upstream regions and indicated if EBR overlapped with annotations of active chromatin states 1, 2, and 4. Next, we compiled two list of genes: (1) the genes with EBRs mapped to the domains of chromatin states 1 or 2, but not 4; and (2) the genes with EBRs mapped to the domains of chromatin state 4, but not 1 or 2. Finally, we removed duplications in each list and all the genes occurring simultaneously in both lists. The resulting lists of genes were referred to as 'states 1 or 2' and 'state 4.' The default whole genome background dataset of DAVID tool was used for GO enrichment analysis.

We used default annotation categories GO_TERM_BP_DIRECT, GO_TERM_MF_DIRECT, and GO_TERM_MF_DIRECT to deduce the lists of GO terms for vocabularies of *biological processes (BPs), molecular functions (MFs),* and *cellular components (CCs).* The significance of enrichment of GO terms was estimated by the EASE Score, a modified Fisher's exact *p*-value (a built-in function of DAVID tool). The following thresholds were set to distinguish the robust GO terms for each list: (1) the fraction of genes belonging to GO term $> 3\%$ and (2) false discovery rate (FDR) < 0.05 (Benjamini-Hochberg correction, a built-in function of DAVID tool). Accordingly, we compiled a set of GO terms, which were robust for either 'states 1 or 2' or 'state 4' lists.

To compare fractions of involved genes for each GO term from the compiled set between two lists we applied the exact Fisher's test of a 2 × 2 contingency table (**Table 1**), where 'Criterion 1' stands for 'The list name,' X1 and Y1 denote 'states 1 or 2' and 'state 4,' correspondingly; 'Criterion 2' stands for 'GO term,' X2 and Y2 – the numbers of genes belonging to the GO term or not, correspondingly. We applied Benjamini-Hochberg correction for multiple testing (Benjamini and Hochberg, 1995) to define robust GO terms enriched in one list in comparison with another. The false discovery rate threshold was set as FDR < 0.05.

[5]https://david.abcc.ncifcrf.gov/

TABLE 1 | The conventional 2 × 2 contingency table used in analysis.

Criterion 1	Criterion 2		Totals
	X2	Y2	
X1	*A*	*B*	*A+B*
Y1	*C*	*D*	*C+D*
Totals	*A+C*	*B+D*	*A+B+C+D*

Prediction of Putative EIN3 Binding Sites

To identify potential EBS we used the Position Weight Matrix (PWM) deduced by NLG approach of weight calculation (Levitsky et al., 2007) from the position frequency matrix for TEIL motif described in (Kosugi and Ohashi, 2000). The threshold of 0.91 for this PWM was chosen since it respected to enrichment of the potential EBS density in the control dataset in comparison with the whole genome (Supplementary Figure S1A), but still the False Positive rate was left on a permissive level (Supplementary Figure S1B). The control dataset was defined as upstream regions in the range from −1500 relative to TSS to the translation starts for 375 genes, which were earlier reported as ethylene regulated EIN3 candidate targets (list EIN3-R from Supplementary Data 1, Chang et al., 2013).

We applied the TEIL model to 16 sets of EBR fragments generated by mapping of 1152/760 EBR fragments related to chromatin states (1 or 2)/4 (see Analysis of Chromatin States) to previously described eight datasets of upstream gene regions (see Monte-Carlo Permutation Test for Genome Tracks).

To compare the occurrence of potential EBS in chromatin state 4 to the one in chromatin states 1 or 2 for eight pairs of upstream regions we applied Fisher's exact test of a 2 × 2 contingency table (**Table 1**). In this table 'Criterion 1' stands for 'Chromatin state,' X1 and Y1 – for 'states 1 or 2' and 'state 4,' correspondingly; 'Criterion 2' stands for 'Prediction of EBS,' X2 and Y2 denote the total counts of TEIL matrix scores above and below the threshold, correspondingly. Since the computations were performed for eight datasets simultaneously, we applied Bonferroni correction for the significance level threshold of p-value < 0.05/8.

RESULTS AND DISCUSSION

ChIP-Seq Derived EIN3 Binding Regions (EBRs)

To get a genome-wide view of EBRs we performed an analysis of publicly available ChIP-Seq data on EIN3 binding in 3-days-old *A. thaliana* etiolated seedlings (Chang et al., 2013). Namely, we used the data for *A. thaliana* Col-0 ecotype (1) treated by ethylene gas at 10 μl/l for 4 h and (2) without ethylene treatment. The latter dataset was used as a control. As only raw data were available, we performed mapping of raw reads and subsequent peak calling. To perform fine analysis of ChIP-Seq data, Bowtie alignment contained only uniquely mapped reads with no mismatches. Finally, we had 5285145 reads for the control dataset and 4118771 reads for the ethylene treated one. The mapping quality statistics is depicted in Supplementary Figure S2.

After peak calling with MACS (genome profile in WIG format in Supplementary Data 2) the maximal peak height value was limited by seven. As a result, 2577 peaks were mapped in chromosomes 1–5, which were considered EBRs. The majority of peaks (>95%) had the length below 500 nucleotides (Supplementary Figure S3).

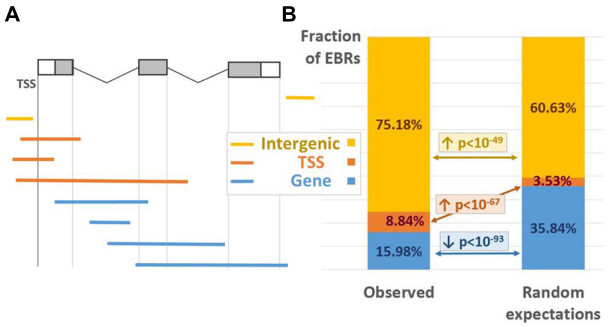

FIGURE 1 | EBRs distribution between various location classes. (A) The positioning of EBRs corresponding to three location classes relative to the gene structure. White/gray boxes denote UTRs/exons; black lines denote introns. **(B)** Observed (left) and expected (right) fractions of the EBRs referred to three location classes. The p-values were derived from Monte-Carlo permutation test (Boldyreva et al., 2016; see Analysis of the Distribution of EBRs). The arrows up/down denote significant enrichment/depletion. Yellow/red/blue colors denote INTERGENIC/TSS/GENE location classes.

Distribution of EBRs

To evaluate the distribution of ChIP-Seq derived EBRs relative to the gene structure we distinguished three EBR location classes, modified from (Boldyreva et al., 2016). The "TSS" class contained EBRs overlapping with at least one of the gene TSSs; all other EBRs overlapping the gene bodies were attributed to the "GENE" class; EBRs falling outside of any genes were classified as "INTERGENIC" (**Figure 1A**). The major fraction of EBRs (75.18%) was classified as "INTERGENIC," 15.98% were assigned to "GENE" class, 8.84% overlapped TSSs (**Figure 1B**, left). The enrichment of EBRs in three location classes relative to random expectations was statistically estimated implying permutation Monte-Carlo test (see Analysis of the Distribution of EBRs). The EBRs were distributed non-randomly relative to the gene structure (**Figure 1B**). The "TSS" and "INTERGENIC" classes were significantly enriched in EBRs (p < 1E-67 and p < 1E-49, correspondingly), whereas gene bodies showed notable underrepresentation of EBRs (p < 1E-93). In general, such a binding profile is quite common for TFs and consistent with their functions (Heyndrickx et al., 2014).

As EBRs were overrepresented in genomic regions encompassing TSS and in intergenic spacers, we performed more detailed analysis of the [−1500; +100] upstream gene regions. Namely, for each position we calculated the fraction of genes overlapping EBRs (**Figure 2**). An evidently prevalent EBS location was found immediately upstream of the TSS in agreement with previously reported observations (Chang et al., 2013). Unexpectedly, we found that the distribution of EBRs was bimodal: the additional extended peak was observed in the distal upstream region (**Figure 2**). The enrichment of EBRs in the distal region was significant according to the permutation Monte-Carlo test up to −3000 relative to TSS (**Figure 3**). The bimodal distribution was not previously reported for EBRs. Thus, we questioned if the observed bimodality is essential for EIN3-mediated transcriptional regulation.

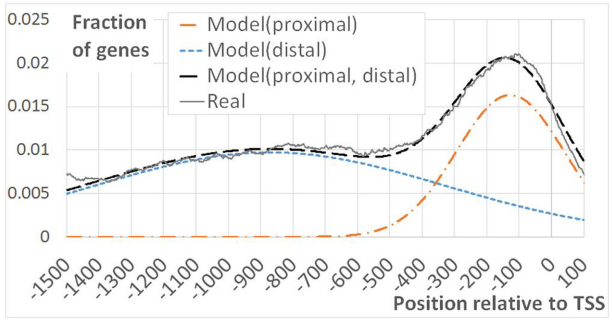

FIGURE 2 | Bimodal EBRs distribution in the upstream regions of *A. thaliana* genes. The figure shows the fraction of genes mapped to EBRs at a certain distance from TSS as a function of the distance from TSS. 19434 genes with annotated 5′UTR were considered in the analysis. Model(proximal), Model(distal) – Gaussian distribution functions. $Model_i = A_i$*Norm(x,m_i,σ_i), (i = distal/proximal), x – the distance from TSS, m, σ –mean and standard deviation of the normal distribution. Model(proximal, distal) – the joined model, defined as the linear function. Model(proximal, distal) = C + Model(proximal)+Model(distal). Here C respects to the impact of non-specific DNA-EIN3 interactions. Real – observed distribution of ChIP-Seq derived EBRs. The constants C, A_i, m_i, σ_i were chosen empirically to provide the best approximation of the real curve "Real" by the model "Model (proximal, distal)."

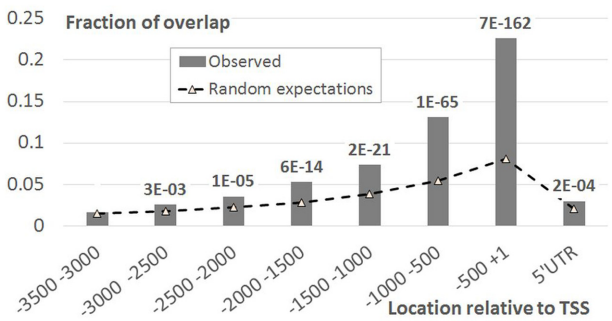

FIGURE 3 | EBRs distribution in the upstream regions of *A. thaliana* genes compared to random expectations. *X*-axis denotes the genomic intervals relative to TSS, *Y*-axis – the ratio of total length of overlap between EBRs and a certain interval to the total length of EBRs. Data labels denote *p*-values derived from Monte-Carlo permutation test (Khoroshko et al., 2016, see Monte-Carlo Permutation Test for Genome Tracks).

Distribution of EBRs in Upstream Gene Regions in Different Chromatin States

The DNA binding by TFs is often guided by the chromatin state, which is supposed to have a conserved positional order (Filion et al., 2010; Sequeira-Mendes et al., 2014). To study the consistent patterns of epigenetic impact into the formation of two distinct EIN3 binding loci we appealed to previously published genome-wide map of nine chromatin states in *A. thaliana* (Sequeira-Mendes et al., 2014). The profile of EBRs distribution in the distal and proximal regions was in good accordance with the genome distribution of chromatin states 4 and 2, correspondingly (Supplementary Figure S4). This implied that

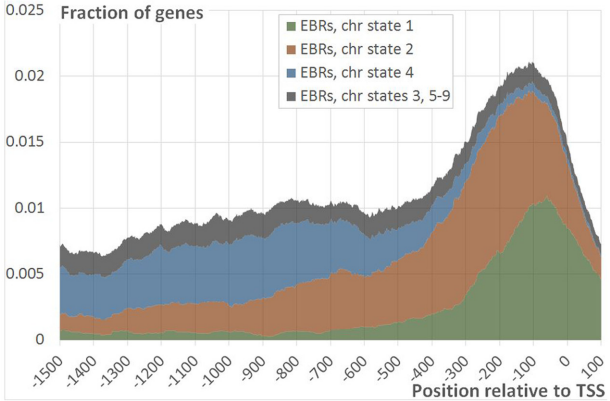

FIGURE 4 | Distribution of EBRs in different chromatin states. The figure shows the fraction of the genes mapped to EBRs within the specific chromatin state at a certain distance from TSS as a function of the position relative to TSS. Summation of fractions of genes mapped to EBRs with chromatin states 1 (green), 2 (red), 4 (blue) and all the rest states (gray) gives the total distribution of EBRs relative to TSS (data row 'Real' on **Figure 2**).

the two modes of EBRs distribution could be associated with the distinct chromatin states. To clarify the epigenetic content of two peaks (distal and proximal) we characterized all EBRs with respect to the epigenetic status and analyzed their distribution in [−1500; +100] region separately. The EBRs were significantly overrepresented not only in the domains within mentioned above active chromatin states 2 and 4, but also within active chromatin state 1 (according to permutation Monte-Carlo test p < 1E-135, p < 1E-70, p < 1E-5, correspondingly). All the rest chromatin states were significantly depleted in EBRs.

The EBRs related to two different chromatin states (states 1 and 2) formed the major fraction of the proximal peak in the EBRs distribution profile (**Figures 4** and **5A,B**; Supplementary Figure S5). The implicit distal peak predominantly consisted of EBRs mapped to the domains within chromatin state 4 (**Figure 4**), which was characterized by increased level of a repressive mark compared to the states 1 and 2 (Sequeira-Mendes et al., 2014). It is also noteworthy that non-random occurrence of the state 4 EBRs was statistically confirmed for the distal promoter region but not for the proximal one (permutation Monte-Carlo test, **Figure 5C**).

Thus, basically, the segregation of the distal peak in EBRs distribution could reflect the impact of the chromatin state 4 on EIN3 binding to DNA. In turn it might determine an alternative EIN3 regulation mode, which differs from the one implemented upon EIN3 binding to the proximal promoter region.

Association of EBRs in Chromatin State 4 and Ethylene Response

To test if the EBRs located in different epigenetic context could be related to distinct EIN3 regulation modes, we performed GO enrichment analysis. We linked all EBRs to the neighboring genes if they overlapped with their [−3500; +1] upstream regions.

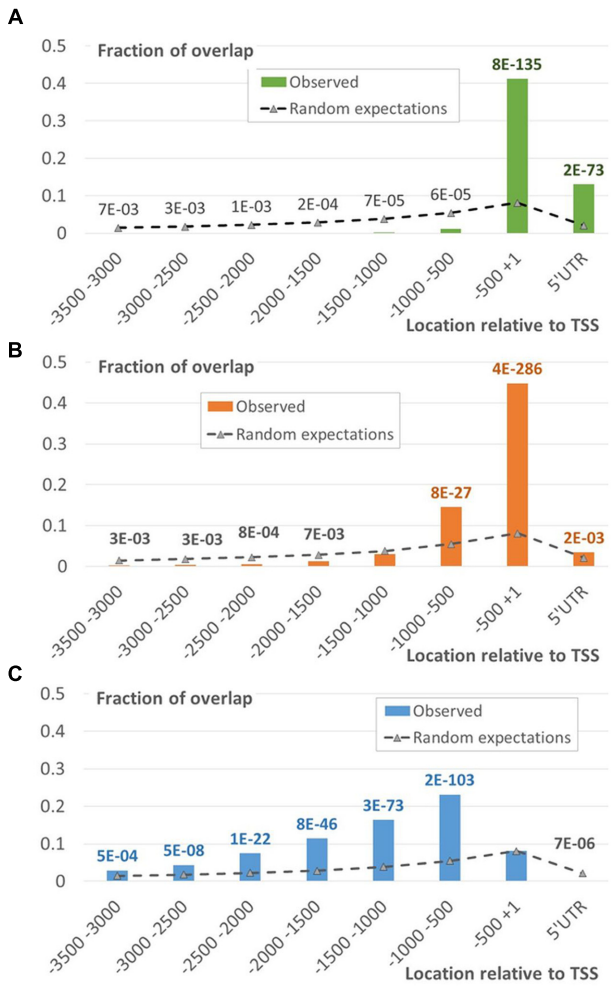

FIGURE 5 | Distribution of EBR fragments located within the chromatin states 1, 2 and 4. The distributions of EBRs located in the domains of chromatin states 1 **(A)**, 2 **(B),** or 4 **(C)** mapped to specific intervals of the upstream gene regions. *X*-axis denotes genomic intervals relative to TSS, *Y*-axis – the ratio of total length of overlap between EBR fragments and a certain interval to the total length of EBR fragments. Data labels denote *p*-values derived from the Monte-Carlo permutation test (Khoroshko et al., 2016; see Materials and Methods). Green/Blue/Red fonts of labels denote enrichment of the observed values respective to the expected ones, the gray font corresponds to depletion.

For further functional analysis, we kept only genes univocally associated with either 'state 1 or 2' or 'state 4' EBRs [see Gene Ontology (GO) Enrichment Analysis for details] since the other states of chromatin were depleted in the whole EBRs dataset (see Distribution of EBRs in Upstream Gene Regions in Different Chromatin States). As a result, we obtained two list of 1117/601 genes harboring only 'state 1 or 2'/'state 4' EBRs (Supplementary Tables S1 and S2 for respective data derived by the alternative procedure described in Supplementary Data 1). These lists of genes were analyzed separately with DAVID tool (Huang et al., 2009). Each GO term in output was estimated by a *p*-value and a fraction of involved genes. To filter the most robust GO terms, we required that the former is significant in terms of FDR < 0.05 according to Benjamini-Hochberg correction, and the latter was greater than 3%. We considered vocabularies of BP, MF, and CC and found 3/2/5 and 15/1/0 robust GO terms belonging to BP/MF/CC vocabularies enriched in the EBRs associated gene lists in 'states 1 or 2' and 'state 4,' correspondingly (Supplementary Tables S3 and S4 for respective data derived by the alternative procedure described in Supplementary Data 1).

To study if the robust GO terms specifically enriched for a certain gene list relative to the other one we performed additional Fisher's exact test [see Gene Ontology (GO) Enrichment Analysis] (Supplementary Tables S3 and S4). Thus, we distinguished (1) nine GO terms significantly overrepresented in 'state 4' list in comparison to 'states 1 or 2' list and (2) three GO terms with the reverse enrichment (**Figure 6C**). It is noteworthy, that ethylene related GO terms were significantly enriched specifically in 'state 4' over 'states 1 or 2' list (**Figure 6**, Supplementary Tables S3 and S4). Wherein, among BP GO terms, *GO:0009873~ethylene-activated signaling pathway* was most significantly enriched in 'state 4' list relative to both genome background and 'state 1 or 2' list (**Figures 6B,C**, Supplementary Tables S3 and S4). Besides, GO terms related to transcription activation were also found specifically enriched in 'state 4' over 'states 1 or 2' gene list.

Taken together, we conclude that EBRs in chromatin state 4 might play a role in general ethylene signaling. We find it noteworthy that chromatin state 4 is characterized by elevated amount of repressive mark H3K27me3 and a decreased number of active chromatin marks compared to states 1 and 2 (Sequeira-Mendes et al., 2014). Hence, an association of ethylene responsive elements with chromatin state 4 might indicate that EIN3 mediated transcription is epigenetically regulated by recruiting H3K27me3 demethylases (Gan et al., 2015). Previously, epigenetic regulation was reported for the ethylene-jasmonate crosstalk mediated by EIN3 (Zhu et al., 2011). Presumably, in other EBRs located in chromatin states 1 and 2, another mechanism of transcriptional regulation might be implemented. These findings extend our understanding of previously reported observations on EIN3 functioning. In (Chang et al., 2013) it was shown that only a minor fraction of ChIP-Seq derived EBRs (about 30%) is associated with altering gene expression upon ethylene treatment, whereas for majority of EBRs EIN3 binding is not sufficient for triggering gene expression implying that these loci function in integrating ethylene unrelated signals. Thus, we conclude that there is a spatial segregation of two mentioned types of EBRs caused (at least partially) by their epigenetic status.

Enrichment of Putative EIN3 Binding Sites in Chromatin State 4

To investigate the influence of the genetic component on functional segregation of EBRs described in the previous section, we investigated distribution of potential EBSs in EBR

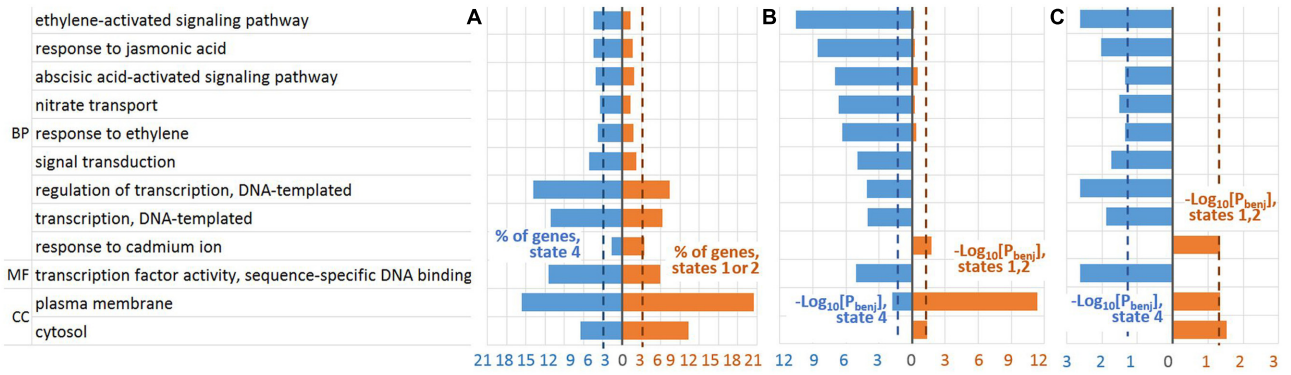

FIGURE 6 | Robust GO terms significantly enriched in the genes harboring EBRs within a specific chromatin state. EBRs of chromatin state 4 were compared against those of 'state 1 or 2'. **(A)** The fractions of involved genes. **(B)** FDR adjusted *p*-value that reflected enrichment of GO terms in the genes harboring EBRs in comparison with whole-genome expectation [see Gene Ontology (GO) Enrichment Analysis]. **(C)** FDR adjusted *p*-value that reflected the enrichment of GO terms in 'state 4' and 'states 1 or 2' gene lists [see Gene Ontology (GO) Enrichment Analysis]. BP, biological processes vocabulary; MF, molecular functions vocabulary; CC, cellular components vocabulary; P_{benj}, FDR adjusted *p*-value (Benjamini-Hochberg procedure). Blue/red color indicates the corresponding values in 'state 4'/'state 1 or 2' lists. The dotted lines denote the thresholds used to select the robust GO terms: 3% of involved genes; FDR adjusted *p*-value < 0.05.

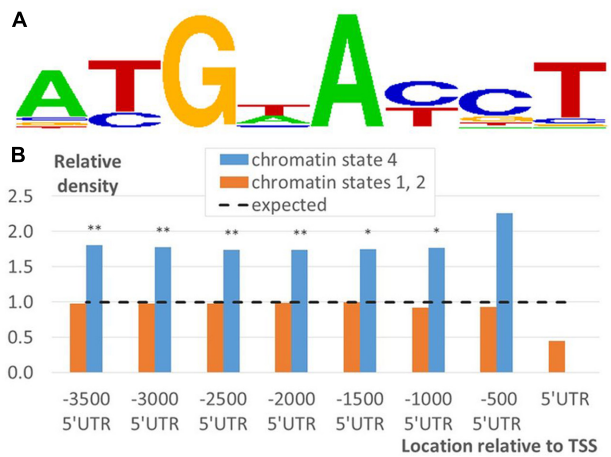

FIGURE 7 | Distribution of potential EBSs in EBRs mapped to the upstream regions of *A. thaliana* genes. (A) Logo for TEIL motif, a binding site of EIN3 homolog in tobacco (Kosugi and Ohashi, 2000), computed by STAMP tool (Mahony and Benos, 2007). **(B)** Relative density of predicted EBSs in EBRs mapped in the domains of chromatin state 4 and 1/2 over a certain distance relative to TSS. *X*-axis denotes the location of the fragments relative to TSS. *Y*-axis denotes the densities of potential sites predicted by TEIL model **(A)**. The density was normalized to the respective average density computed for the whole genome. Labels '*' and '**' denote the Bonferroni's corrected significance $p < 0.05/8$ and $0.01/8$ estimated by Fisher's exact test.

fragments corresponding to the chromatin states 1, 2, or 4 (see Prediction of Putative EIN3 Binding Sites). To evaluate the occurrence of DNA sequences specifically recognized by EIN3 we modeled potential EBS using the PWM deduced from the position frequency matrix for TEIL motif (**Figure 7A**), the binding site of EIN3 homolog in tobacco (Kosugi and Ohashi, 2000).

We find that potential EBSs were significantly enriched in 'state 4' EBR fragments relative to 'state 1 or 2' ones according to Fisher's exact test (**Figure 7B**; Supplementary Figure S6). Thus, taking into account EBRs distribution with respect to the chromatin states (**Figures 4** and **5**; Supplementary Figure S5) the implicit distal peak was significantly associated not only with ethylene response function, but also with the specific DNA context recognized by EIN3. Intriguingly, the pronounced proximal peak was not associated with neither of them. This result implies two important conclusions. First, it supports the idea of a role of epigenetic regulation in EIN3 mode of functioning, which mechanisms are to be elucidated in future studies. Second, the high density of ChIP-Seq derived binding regions does not univocally prescribe overrepresentation of the specific DNA context. Particularly, this highlights an alternative mode of functioning for the majority of proximal EBRs, which is also a subject for further investigations.

CONCLUSION

ETHYLENE-INSENSITIVE3 is the master transcriptional regulator of ethylene signaling. It acts as a hub that integrates plant signals and redistributes them triggering distinct transcriptional responses to adapt to volatile environment. We found that EBRs in upstream gene regions have a bimodal distribution with a pronounced proximal peak and a broad implicit distal peak, both significant relative to random expectations. The EBRs were significantly overrepresented only in the domains within chromatin states 1, 2, and 4. We predicted an importance of chromatin state 4 both in formation of the distal peak and in EIN3 regulation of ethylene response. The latter statement is supported by GO enrichment analysis. Moreover, we showed that the potential EBSs are associated with the chromatin state 4, but not 1 or 2. Such a profile provides the idea of interplay between genetic and epigenetic factors, which may determine at least two distinct modes of EIN3 regulation mediated by spatially separated EBRs.

AUTHOR CONTRIBUTIONS

EZ initiated, designed, and coordinated the study, interpreted the results, and wrote the manuscript. VL and DO analyzed the data. VL, DO, IG, and VM participated in the design of the study, the interpretation of the results, and the revision of the manuscript. All authors read and approved the final manuscript.

FUNDING

The study of transcriptional regulation of ethylene response was supported by Russian Foundation for Basic Research grant 15-34-20870. Development and adaptation of bioinformatics methods was supported by the Russian Science Foundation (Project no. 14 24 00123).

ACKNOWLEDGMENT

We thank Nikolay Kolchanov, Nadya Omelyanchuk, and Jian Xu for fruitful discussions.

SUPPLEMENTARY MATERIAL

The Supplementary Material for this article can be found online at: http://journal.frontiersin.org/article/10.3389/fpls.2016.02044/full#supplementary-material

REFERENCES

Alonso, J. M., Stepanova, A. N., Solano, R., Wisman, E., Ferrari, S., Ausubel, F. M., et al. (2003). Five components of the ethylene-response pathway identified in a screen for weak ethylene-insensitive mutants in *Arabidopsis*. *Proc. Natl. Acad. Sci. U.S.A.* 100, 2992–2997. doi: 10.1073/pnas.0438070100

An, F., Zhang, X., Zhu, Z., Ji, Y., He, W., Jiang, Z., et al. (2012). Coordinated regulation of apical hook development by gibberellins and ethylene in etiolated *Arabidopsis* seedlings. *Cell Res.* 22, 915–927. doi: 10.1038/cr.2012.29

An, F., Zhao, Q., Ji, Y., Li, W., Jiang, Z., Yu, X., et al. (2010). Ethylene-induced stabilization of ETHYLENE INSENSITIVE3 and EIN3-LIKE1 is mediated by proteasomal degradation of EIN3 binding F-Box 1 and 2 that requires EIN2 in *Arabidopsis*. *Plant Cell* 22, 2384–2401. doi: 10.1105/tpc.110.076588

Benjamini, Y., and Hochberg, Y. (1995). Controlling the false discovery rate: a practical and powerful approach to multiple testing. *J. R. Stat. Soc. B. Methodol.* 57, 289–300.

Boldyreva, L., Goncharov, F., Demakova, O., Zykova, T., Levitsky, V., Kolesnikov, N., et al. (2016). Protein and genetic composition of four basic chromatin types in *Drosophila melanogaster* cell lines. *Curr. Genomics* doi: 10.2174/1389202917666160512164913 [Epub ahead of print].

Chang, K. N., Zhong, S., Weirauch, M. T., Hon, G., Pelizzola, M., Li, H., et al. (2013). Temporal transcriptional response to ethylene gas drives growth hormone cross-regulation in *Arabidopsis*. *Elife* 2:e00675. doi: 10.7554/eLife.00675

Chao, Q., Rothenberg, M., Solano, R., Roman, G., Terzaghi, W., and Ecker, J. R. (1997). Activation of the ethylene gas response pathway in *Arabidopsis* by the nuclear protein ETHYLENE-INSENSITIVE3 and related proteins. *Cell* 89, 1133–1144. doi: 10.1016/S0092-8674(00)80300-1

Cho, Y. H., and Yoo, S. D. (2015). Novel connections and gaps in ethylene signaling from the ER membrane to the nucleus. *Front. Plant Sci.* 5:733. doi: 10.3389/fpls.2014.00733

Filion, G. J., van Bemmel, J. G., Braunschweig, U., Talhout, W., Kind, J., Ward, L. D., et al. (2010). Systematic protein location mapping reveals five principal chromatin types in *Drosophila* cells. *Cell* 143, 212–224. doi: 10.1016/j.cell.2010.09.009

Gan, E. S., Xu, Y., and Ito, T. (2015). Dynamics of H3K27me3 methylation and demethylation in plant development. *Plant Signal. Behav.* 10:1027851. doi: 10.1080/15592324.2015.1027851

Guo, H., and Ecker, J. R. (2004). The ethylene signaling pathway: new insights. *Curr. Opin. Plant. Biol.* 7, 40–49. doi: 10.1016/j.pbi.2003.11.011

Heyndrickx, K. S., Van de Velde, J., Wang, C., Weigel, D., and Vandepoele, K. (2014). A functional and evolutionary perspective on transcription factor binding in *Arabidopsis thaliana*. *Plant Cell* 26, 3894–3910. doi: 10.1105/tpc.114.130591

Huang, D. W., Sherman, B. T., and Lempicki, R. A. (2009). Systematic and integrative analysis of large gene lists using DAVID bioinformatics resources. *Nat. Protoc.* 4, 44–57. doi: 10.1038/nprot.2008.211

Khoroshko, V. A., Levitsky, V. G., Zykova, T. Y., Antonenko, O. V., Belyaeva, E. S., and Zhimulev, I. F. (2016). Chromatin heterogeneity and distribution of regulatory elements in the late-replicating intercalary heterochromatin domains of *Drosophila melanogaster* chromosomes. *PLoS ONE* 11:e0157147. doi: 10.1371/journal.pone.0157147

Kosugi, S., and Ohashi, Y. (2000). Cloning and DNA-binding properties of a tobacco Ethylene-Insensitive3 (EIN3) homolog. *Nucleic Acids Res.* 28, 960–967. doi: 10.1093/nar/28.4.960

Langmead, B., Trapnell, C., Pop, M., and Salzberg, S. L. (2009). Ultrafast and memory-efficient alignment of short DNA sequences to the human genome. *Genome Biol.* 10:R25. doi: 10.1186/gb-2009-10-3-r25

Levitsky, V. G., Ignatieva, E. V., Ananko, E. A., Turnaev, I. I., Merkulova, T. I., Kolchanov, N. A., et al. (2007). Effective transcription factor binding site prediction using a combination of optimization, a genetic algorithm and discriminant analysis to capture distant interactions. *BMC Bioinformatics* 8:481. doi: 10.1186/1471-2105-8-481

Mahony, S., and Benos, P. V. (2007). STAMP: a web tool for exploring DNA-binding motif similarities. *Nucleic Acids Res.* 35, W253–W258. doi: 10.1093/nar/gkm272

McManus, M. T. (2012). *The Plant Hormone Ethylene. Annual Plant Reviews*. Oxford: Wiley-Blackwell, doi: 10.1002/9781118223086

Merchante, C., Alonso, J. M., and Stepanova, A. N. (2013). Ethylene signaling: simple ligand, complex regulation. *Curr. Opin. Plant Biol.* 16, 554–560. doi: 10.1016/j.pbi.2013.08.001

Sequeira-Mendes, J., Aragüez, I., Peiró, R., Mendez-Giraldez, R., Zhang, X., Jacobsen, S. E., et al. (2014). The functional topography of the *Arabidopsis* genome is organized in a reduced number of linear motifs of chromatin states. *Plant Cell* 26, 2351–2366. doi: 10.1105/tpc.114.124578

Solano, R., Stepanova, A., Chao, Q., and Ecker, J. R. (1998). Nuclear events in ethylene signaling: a transcriptional cascade mediated by ETHYLENE-INSENSITIVE3 and ETHYLENE-RESPONSE-FACTOR1. *Genes Dev.* 12, 3703–3714. doi: 10.1101/gad.12.23.3703

Song, S., Huang, H., Gao, H., Wang, J., Wu, D., Liu, X., et al. (2014). Interaction between MYC2 and ETHYLENE INSENSITIVE3 modulates antagonism between jasmonate and ethylene signaling in *Arabidopsis*. *Plant Cell* 26, 263–279. doi: 10.1105/tpc.113.120394

Zhang, Y., Meyer, C. A., Eeckhoute, J., Johnson, D. S., Bernstein, B. E., Nusbaum, C., et al. (2008). Model-based analysis of ChIP-Seq (MACS). *Genome Biol.* 9:R137. doi: 10.1186/gb-2008-9-9-r137

Zhong, S., Shi, H., Xue, C., Wang, L., Xi, Y., Li, J., et al. (2012). A molecular framework of light-controlled phytohormone action in *Arabidopsis*. *Curr. Biol.* 22, 1530–1535. doi: 10.1016/j.cub.2012.06.039

Zhu, Z., An, F., Feng, Y., Li, P., Xue, L., Mu, A., et al. (2011). Derepression of ethylene-stabilized transcription factors (EIN3/EIL1) mediates jasmonate and ethylene signaling synergy in *Arabidopsis*. *Proc. Natl. Acad. Sci. U.S.A.* 108, 12539–12544. doi: 10.1073/pnas.110395910

Conflict of Interest Statement: The authors declare that the research was conducted in the absence of any commercial or financial relationships that could be construed as a potential conflict of interest.

frontiers in Plant Science

ORIGINAL RESEARCH
published: 25 April 2017
doi: 10.3389/fpls.2017.00603

Transcriptome Analysis of Cell Wall and NAC Domain Transcription Factor Genes during *Elaeis guineensis* Fruit Ripening: Evidence for Widespread Conservation within Monocot and Eudicot Lineages

Timothy J. Tranbarger[1], Kim Fooyontphanich[1†], Peerapat Roongsattham[1†], Maxime Pizot[1], Myriam Collin[1], Chatchawan Jantasuriyarat[2], Potjamarn Suraninpong[3], Somvong Tragoonrung[4], Stéphane Dussert[1], Jean-Luc Verdeil[5] and Fabienne Morcillo[6]*

[1] Institut de Recherche pour le Développement, IRD, UMR DIADE, Montpellier, France, [2] Department of Genetics, Kasetsart University, Bangkok, Thailand, [3] Department of Plant Science, Institute of Agricultural Technology, Walailak University, Nakhon Si Thammarat, Thailand, [4] Genome Institute, National Center for Genetic Engineering and Biotechnology, Pathumthani, Thailand, [5] Centre de Coopération Internationale en Recherche Agronomique pour le Développement, UMR AGAP, Montpellier, France, [6] Centre de Coopération Internationale en Recherche Agronomique pour le Développement, UMR DIADE, Montpellier, France

The oil palm (*Elaeis guineensis*), a monocotyledonous species in the family Arecaceae, has an extraordinarily oil rich fleshy mesocarp, and presents an original model to examine the ripening processes and regulation in this particular monocot fruit. Histochemical analysis and cell parameter measurements revealed cell wall and middle lamella expansion and degradation during ripening and in response to ethylene. Cell wall related transcript profiles suggest a transition from synthesis to degradation is under transcriptional control during ripening, in particular a switch from cellulose, hemicellulose, and pectin synthesis to hydrolysis and degradation. The data provide evidence for the transcriptional activation of expansin, polygalacturonase, mannosidase, beta-galactosidase, and xyloglucan endotransglucosylase/hydrolase proteins in the ripening oil palm mesocarp, suggesting widespread conservation of these activities during ripening for monocotyledonous and eudicotyledonous fruit types. Profiling of the most abundant oil palm polygalacturonase (*EgPG4*) and 1-aminocyclopropane-1-carboxylic acid oxidase (*ACO*) transcripts during development and in response to ethylene demonstrated both are sensitive markers of ethylene production and inducible gene expression during mesocarp ripening, and provide evidence for a conserved regulatory module between ethylene and cell wall pectin degradation. A comprehensive analysis of NAC transcription factors confirmed at least 10 transcripts from diverse NAC domain clades are expressed in the mesocarp during ripening, four of which are induced by ethylene treatment, with the two most inducible (*EgNAC6* and *EgNAC7*) phylogenetically similar to the tomato NAC-NOR master-ripening regulator. Overall, the

OPEN ACCESS

Edited by:
Antonio Ferrante, Università degli Studi di Milano, Italy

Reviewed by:
Xiaohong Kou, Tianjin University, China
Anna Mensuali, Sant'Anna School of Advanced Studies, Italy

***Correspondence:**
Timothy J. Tranbarger
timothy.tranbarger@ird.fr

†Present Address:
Peerapat Roongsattham, Department of Biology, Faculty of Science, Prince of Songkla University, Songkhla, Thailand
Kim Fooyontphanich, Kasetsart University and Winrock International, Bangkok, Thailand

Specialty section:
This article was submitted to Plant Physiology, a section of the journal Frontiers in Plant Science

Received: *09 December 2016*
Accepted: *03 April 2017*
Published: *25 April 2017*

Citation:
Tranbarger TJ, Fooyontphanich K, Roongsattham P, Pizot M, Collin M, Jantasuriyarat C, Suraninpong P, Tragoonrung S, Dussert S, Verdeil J-L and Morcillo F (2017) Transcriptome Analysis of Cell Wall and NAC Domain Transcription Factor Genes during Elaeis guineensis Fruit Ripening: Evidence for Widespread Conservation within Monocot and Eudicot Lineages. Front. Plant Sci. 8:603. doi: 10.3389/fpls.2017.00603

results provide evidence that despite the phylogenetic distance of the oil palm within the family Arecaceae from the most extensively studied monocot banana fruit, it appears ripening of divergent monocot and eudicot fruit lineages are regulated by evolutionarily conserved molecular physiological processes.

Keywords: ripening, cell wall, NAC domain, oil palm, monocotyledon, mesocarp, ethylene

INTRODUCTION

Fruit ripening is a biological character unique to flowering plants, not only of central importance to seed dispersal and the reproductive success of plants, but also essential for both human and animal diets. The color, metabolic, and textural transitions that occur in the ripening fleshy fruit tissues have economic and nutritional consequences for humans. Ethylene is known to play a central role in the ripening of climacteric fruit in which there is a shift from a basal non-catalytic (system 1) to an autocatalytic (system 2) increase in ethylene production (Lelievre et al., 1997; Klee and Giovannoni, 2011; Liu et al., 2015). Studies with the climacteric fruit model tomato indicate a central role for ethylene in the transcriptional coordination of metabolic processes that occur during ripening (Alba et al., 2005; Osorio et al., 2011). The role of ethylene is conserved across many eudicot species and is likely to play similar roles in other climacteric fleshy fruits such apple, peach, pear, mango, and banana (Prasanna et al., 2007; Bapat et al., 2010; Seymour et al., 2013a,b). Furthermore, recent studies indicate that ethylene signal transduction is also important for the transcriptional regulation or ripening process in non-climacteric fruit that lack the large climacteric increase in ethylene, such as pepper, grape, and strawberry (Trainotti et al., 2005; Chervin et al., 2008; Bapat et al., 2010; Osorio et al., 2012). While ethylene may be viewed as a common regulator for fruit ripening in general, how the ripening related regulatory networks have evolved and adapted during plant evolution is unknown. Indeed, most of the research on fruit ripening focuses on the important cultivated eudicotyledonous species, in particular tomato. However, research with the monocotyledonous banana and the basal angiosperm *Persea americana* (avocado) support the notion that the role of ethylene has been conserved through plant evolution, but given the large phylogenetic distances of these species, diversification can be expected to be discovered (Chanderbali et al., 2008, 2009; Elitzur et al., 2010, 2016; Jourda et al., 2014).

One of the most important processes regulated by ethylene during fruit ripening are the textural changes that occur due to cell wall disassembly, indeed, transgenic tomato with modified ethylene biosynthesis or perception have provided evidence that ethylene regulated cell wall metabolism is central to climacteric fruit ripening (Bennett and Labavitch, 2008). However, while extensive work has been done with the ripening tomato as a eudicot model, our understanding of how the cell wall is modified for softening to occur is still incomplete. In general, it appears that textural changes during ripening are controlled simultaneously by many genes, and may be species and/or fruit type dependent (Bennett and Labavitch, 2008; Seymour et al., 2013a).

NAC-NOR is an example of a master regulator that controls ethylene production and downstream changes in the cell wall of the ripening tomato (Giovannoni, 2004; Seymour et al., 2013a). The *non-ripening* (*nor*) tomato mutation affects a NAC domain transcription factor (TF) and results in fruit that do not ripening normally, similar to both *ripening-inhibitor* (*rin*) and *never-ripe* (*nr*) (Giovannoni, 2004; Osorio et al., 2011). All these mutants share a strong down regulation of the tomato fruit polygalacturonase (TFPG) transcript (*PG2*), indicating that the transcriptional activation of the tomato *PG2* gene is an important control point regulating the expression of *PG2* during ripening (Dellapenna et al., 1986, 1987, 1989). While PG can hydrolyze the backbone of pectin homogalacturonan polymers, the down-regulation or knockout of the TFPG transcript results in a decrease in pectin depolymerization, but no change in fruit softening, and it is generally thought that a large number of downstream cell wall related target genes are activated transcriptionally during ripening and are necessary for softening (Sheehy et al., 1988; Smith et al., 1988, 1990; Cooley and Yoder, 1998; Brummell and Harpster, 2001; Brummell, 2006; Seymour et al., 2013a). NAC domain proteins have emerged as important transcriptional regulators of tomato fruit ripening. For example, the silencing of two NAC domain TFs *SNAC4* and *SNAC9* results in decreased expression of the tomato ethylene biosynthesis genes *LeACS2*, *LeACS4* (encoding 1-amino-cyclopropane-1-carboxylic acid or ACC synthases), and *LeACO1* (tomato ACC oxidase), which consequently inhibition the ripening process (Kou et al., 2016). Indeed, the SNAC TFs bind to the promoter of these ethylene biosynthesis genes *in vitro*, while the silencing of *LeACS4*, *LeACO1,* and *LeERF2* reduced the expression of *SNAC4* and *SNAC9,* suggesting a possible feedback system between these SNAC TFs and ethylene biosynthesis gene transcription. In contrast, less is known about monocot fruit ripening. Recent studies found NAC domain transcripts were differentially expressed in the ripening oil palm mesocarp, suggesting ethylene-regulated expression, while a study with banana identified at least 6 NAC domain TFs expressed during banana ripening, two of which are induced by ethylene (Tranbarger et al., 2011; Shan et al., 2012). Together these results suggest that NAC domain TFs may have conserved central roles during ethylene induced fruit ripening of both eudicots and monocots.

The monocot–eudicot divergence occurred 130–135 million years ago (D'hont et al., 2012; Magallón et al., 2015). The best-studied monocot fruit is banana in which ethylene plays a conserved role during ripening (Elitzur et al., 2010, 2016; Jourda et al., 2014). Arecaceae (the monocot palm family) displays a very large amount of fruit diversity and is separated from its closest

monocot lineage by approximately 98 million years (Magallón et al., 2015). Ethylene appears to be involved in fruit ripening of both oil palm (*Elaeis guineensis*) and date palm (*Phoenix dactylifera* L), while oil palm has twice the number of ripening and abscission genes and more *ACO* genes than date palm (Abbas and Ibrahim, 1996; Tranbarger et al., 2011; Singh et al., 2013; Nualwijit and Lerslerwong, 2014). Recent studies by our group identified a polygalacturonase (*EgPG4*) highly induced by ethylene in oil palm fruit abscission zone cells and associated with the cell separation and fruit abscission (Roongsattham et al., 2012, 2016). Whereas, *EgPG4* is not expressed or induced in the adjacent pedicel tissue, it is also induced by ethylene and highly expressed in the mesocarp cells (Roongsattham et al., 2012). In addition, quantitative changes in the mesocarp cell walls occur during development and ripening, including thickness increases in the primary cell wall and middle lamella, while ethylene treatment of ripe fruit results in a decrease in middle lamella thickness (Roongsattham et al., 2016).

The majority of our knowledge about ethylene function during fruit ripening in higher plants comes from studies with eudicot model plants, in particular with the tomato fruit, and to a lesser extent with the monocot model fruit banana. To what extent this knowledge extends to non-model and phylogenetically distant species is not fully known. The current study focuses on the ethylene and cell wall related processes that take place during the ripening of the oil palm fruit mescarp in comparison with what is known from the main eudicot and monocot fruit models, banana, and tomato.

MATERIALS AND METHODS

Plant Material, Treatments, and RNA Extraction

Oil palm fruits for the mesocarp transcriptome were harvested at Pobè CRA-PP Station (INRAB) Benin, from a *dura* parent of Deli Dabou origin, within the same self-progeny of a single palm as described previously (Tranbarger et al., 2011). Oil palm spikelets with ripe fruit 180 days after pollination (DAP), at which time fruit are typically harvested and transported for oil extraction, were sampled from a tenera clone (clone C) at the Krabi Golden Tenera plantation, Thailand as previously described (Roongsattham et al., 2012). Spikelets were treated for 3, 6, and 9 h with 10 μl l^{-1} ethylene, a quantity of ethylene that was previously found to induce changes to the cell walls of the fruit abscission zone cells that results in 25% fruit abscission after 9 h (Roongsattham et al., 2012, 2016). For RNA extractions, mesocarp fruit tissue samples were collected and frozen immediately in liquid nitrogen. Total RNA from mesocarp was extracted as previously described (Morcillo et al., 2006). Total RNA (1 μg) was used to synthesize cDNA using the first-strand cDNA synthesis kit (ImProm-II™ Reverse Transcription System, Promega).

Quantitative Real-Time RT-PCR

qPCR was conducted as previously described (Roongsattham et al., 2012). The analysis was conducted on a LightCycler 480 (Roche) in 96-well plates in a volume of 10 μl containing 2 μl of cDNA diluted 1/100, 1.5 μl of primer forward (2 μM), 1.5 μl of reverse primer (2 μM), and 5 μl SYBR® Green Mastermix (Roche). Primers used for *EgPG4* and *ACO* amplification were previously published (Fooyontphanich et al., 2016). PCR was initiated by denaturation at 95°C for 10 min, followed by 45 cycles of 95°C for 15 s, 60°C for 15 s, and a final extension at 70°C for 1 min. All expression was normalized to the *EgEf*α1 (accession number: AY550990) mRNA from *E. guineensis*, and mRNA abundance for each experiment was calculated relative to the sample with the lowest amount of transcript present determined with the formula as described previously (Pfaffl, 2001). No change of *EgEf*α*1* transcript accumulation was found in the fruit tissues treated or not treated with ethylene. Control using RNA matrices were also conducted to validate the absence of DNA in each sample. Each time point was replicated three times from two independent biological samples, and all amplified cDNA fragments were sequenced by Beckman-Cogenics (https://www.genewiz.com) to check the specificity of the amplified products. Gene abundance is expressed as mean and standard error bars are calculated from the technical replicates of one of the biological repetitions.

Mesocarp Transcriptome Data Mining

Transcriptome data of the developing mesocarp previously clustered (clusters A, B, C, and D) was searched for transcripts with expression profiles that either increase or decrease during the burst of ethylene production observed during oil palm fruit ripening between 100 and 160 DAP (**Supplementary Table 1**; Tranbarger et al., 2011). The BLAST2GO and InterProScan web services with BLASTX using an E-value cutoff of 1e-5 were used to annotate the gene sets (Altschul et al., 1990; Zdobnov and Apweiler, 2001; Götz et al., 2008). Cell wall sequences were identified by searching the GO annotated sequences for InterPro accessions and key words related to cell wall processes, and by searching (TBLASTX) the 454 sequence database with known candidates related to cell wall biosynthesis and degradation.

RNA-Seq Data Processing

Nine RNAseq datasets generated by Orion Genomics (http://www.oriongenomics.com/index.php/en/) for selected *E. guineensis* tissues were downloaded from NCBI databases: 17 cm long leaf (SRX278048), spear leaf (SRX278049), 2.5 cm (SRX278052), and 20 cm long female inflorescence (SRX278053), pollen (SRX278051), root (SRX278062), shoot apex (SRX278055), and kernel at 10 and 15 weeks after anthesis (SRX278021 and SRX278018, respectively). Reads from these datasets in addition to RNAseq data (100-nt Illumina reads) for the *E. guineensis* ripening mesocarp (Guerin et al., 2016) and embryonic cell suspensions (kindly provided by Thierry Beulé) were then mapped on the *E. guineensis* CDS reference (NCBI website, GCF_000442705.1_EG5_rna.fna; January 2015) and the RPKM (number of reads per kilobase and million reads) for each locus were compared.

Transcription Factor Prediction

The NAC domain gene family of *E. guineensis* was retrieved from the Plant Transcription Factor Database (PlantTFDB, http://planttfdb.cbi.pku.edu.cn/prediction.php) 4.0 using the *E. guineensis* CDS reference (NCBI website, GCF_000442705.1_EG5_rna.fna; January 2015; Jin et al., 2015, 2016). From a total of 44,360 oil palm putative coding sequences (CDS), 175 NAC domain-containing sequences were identified in the oil palm reference CDS, which corresponded to a total of 124 non-redundant loci. The same result was obtained using the iTAK database (Zheng et al., 2016; http://bioinfo.bti.cornell.edu/cgi-bin/itak/online_itak.cgi).

Phylogenetic Analysis

Amino acid alignments were performed with ClustalW (Larkin et al., 2007) using default settings (http://www.ebi.ac.uk/). The amino acid sequences containing the conserved NAC subdomains (A–E) were used for the phylogenetic analysis (Ooka et al., 2003) using the default settings without the G-blocks step (Dereeper et al., 2008). Branch support values are based on the aLRT statistical test (Anisimova and Gascuel, 2006).

Histological Analysis and Cell Measurements

Mesocarp fruit samples were collected from ethylene treated fruit and fixed in 0.2 M phosphate buffer containing 2% (w/v) paraformaldehyde, 1% (w/v) caffeine, and 0.5% (v/v) glutaraldehyde or a minimum of 2 days at 4°C as previously described (Buffard-Morel et al., 1992). Serial dehydration with ethanol from 30 to 100%, then 100% butanol/100% ethanol (v/v), and finally 100% butanol was performed for each sample and followed by impregnation and embedding in Technovit 7100 resin (Heraeus Kulzer). Semi-thin sections of 3 μm were cut using a microtome. Each section was stained with toluidine blue or ruthenium red. Microphotographs were taken with a Leica camera (DFC 300 FX) on a Leica (LEITZ DMRB) light microscope (x20/0.5; x40/0.7; and x100/1.3). Cell parameter measurements were performed for cell width, cell wall width, and middle lamella as previously reported (Roongsattham et al., 2016).

RESULTS

EgACO and Polygalacturonase *EgPG4* Transcript Profiling during Mesocarp Development and in Response to Ethylene Treatment of Ripe Fruit

To provide molecular indicators of ethylene production in the mesocarp, we examined the quantitative expression profiles of the most highly abundant *ACO* previously observed in the oil palm mesocarp (CL1Contig999, *EgACO*), in addition to the most highly expressed polygalacturonase (CL1Contig5616, *EgPG4*) in the mesocarp induced by ethylene (Tranbarger et al., 2011; Roongsattham et al., 2012; Fooyontphanich et al., 2016) (**Supplementary Tables 1**, **2**). The *EgACO* nucleotide sequence aligns most significantly (E-value 0) to LOC105039092 (Chromosome 2) annotated as an *ACO3* in the oil palm genome (**Supplementary Table 2**). During mesocarp development, the *EgACO* transcript is expressed in the pollinated flower at the onset of fruit development (10 DAP) and is undetectable or barely detectable until 120 DAP, and then increases 79 and 199 fold at 140 and 160 DAP respectively (**Figure 1A**). Illumina sequencing confirmed that the *EgACO3* transcript increased between 120 and 160 DAP (**Figure 1A**, **Supplementary Table 2**). The pattern of *EgACO* expression correlates to the increase in ethylene observed between 120 and 160 DAP, which corresponds to the transition from system 1 to system 2 ethylene production (Tranbarger et al., 2011). To determine whether the *EgACO* transcript could be regulated by ethylene, the amount of *EgACO* transcript was quantified in the mesocarp of ripe fruit (150 and 180 DAP) treated with ethylene for 3–9 h (**Figure 1B**). After 3 h of ethylene treatment, in 150 DAP fruit the *EgACO* transcript increased 25 fold, while in the 180 DAP fruit, the transcript increased 9 fold. A further increase was observed at 9 h while at 6 h the *EgACO* transcript amounts remained stable (150 DAP) or decreased (180 DAP). In contrast to *EgACO*, the *EgPG4* transcript is undetectable or present at very low amounts from 10 to 140 DAP, then increases dramatically over 3,000 fold at 160 DAP, which corresponds to the autocatalytic system 2 ethylene production (**Figure 1B**). *EgPG4* is annotated at LOC105034919 (Chromosome 2, **Supplementary Table 2**). Illumina sequencing confirmed an increase of *EgPG4* transcript increased between 140 and 160 DAP (**Figure 1A**, **Supplementary Table 2**). The *EgPG4* transcript increased in both 150 and 180 DAP fruit after 3h of ethylene treatment, but the magnitude was much higher in 150 DAP (500 fold) than in the older 180 DAP fruit (10 fold). The *EgPG4* transcript continued to increase after 6 and 9 h of ethylene treatment and eventually reached over 5,000 fold by 9h in 150 DAP fruit. While both the *EgACO* and *EgPG4* transcripts increase rapidly (3 h) in response to ethylene treatment, the induction was less in 180 DAP fruit for both genes, while the magnitude of induction was consistently higher for *EgPG4*. Furthermore, *EgPG4* expression is limited to the ripest fruit in contrast to *EgACO*, which is also expressed 10 days after the flower is pollinated.

Histological Analysis of the Mesocarp in Response to Ethylene in Ripening Fruit

Histological analysis of abscission zone and mesocarp cell walls revealed changes in integrity during development and in response to ethylene treatments (Roongsattham et al., 2016). While the previous article focused on cellular changes in abscission zone cells, here we focus on changes that occur in the mesocarp cells during ripening and in response to ethylene (**Supplementary Figures 1**, **2**). To examine the cellular processes in the mesocarp, longitudinal tissue sections were analyzed from samples of mesocarp at key stages of development and ripening, and in response to ethylene. At 30 DAP, anticlinal cell divisions have taken place, cells have not fully elongated, and the formation of intercellular spaces is observed (Roongsattham et al., 2016; **Supplementary Figure 1**). By 120 DAP, cells have

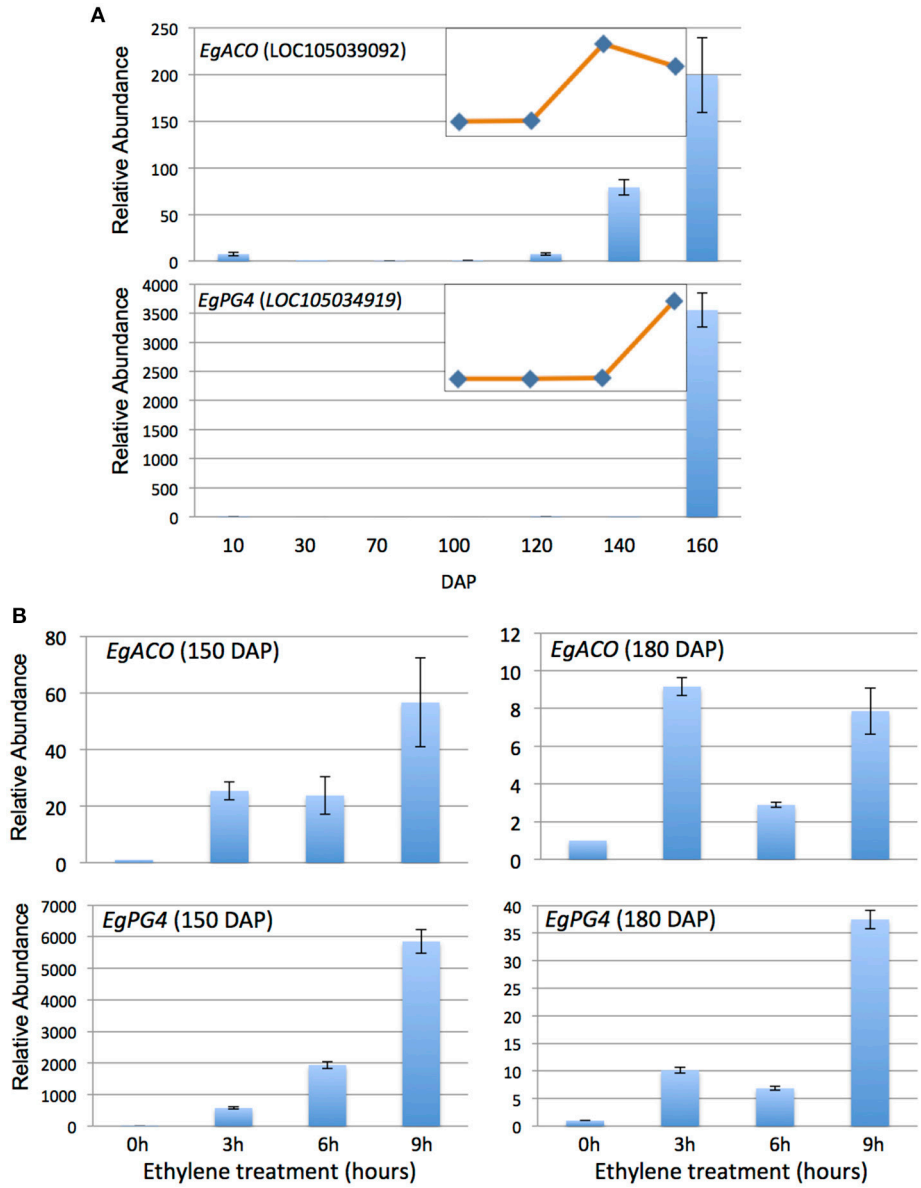

FIGURE 1 | *EgACO* and *EgPG4* expression in the oil palm mesocarp increase during fruit ripening and are induced by external ethylene treatments at two different ripening stages. qPCR analysis of *EgACO* and *EgPG4* transcript abundance in the mesocarp during development **(A)** and in response to exogenous ethylene (10 $\mu L\ l^{-1}$) treatments **(B)**. Inserts are RNA-Seq based RPKM profiles of the mesocarp at 100, 120, 140, and 160 DAP.

elongated and a significant increase in the cell wall width is observed, with the average cell wall width more than 1 μm while the middle lamella is approximately 0.6 μm wide and the presence of intercellular spaces is also observed at 120 DAP. At 180 DAP, the cell wall width increased, and cell separation between adjacent cells is apparent. By 180 DAP a 2-fold increase in cell wall width is observed, and the middle lamella width also increases significantly to ∼0.9 μm. Based on these measurements, the cell wall accounts for approximately 4, 7, and 15% of the total cell width at 30, 120, and 180 DAP respectively. After 9 h of ethylene treatment of 180 DAP fruit, the toluidine blue staining increases between adjacent cells, while ruthenium red stained sections reveal non-continuous dark strands that corresponds to an apparent breakdown of the middle lamella that is measurable after 9 h of ethylene treatment (**Figure 2**). Finally, in ethylene treated cells, intercellular material accumulates based on both toluidine blue and ruthenium red staining (**Figure 2**). Based on these data, a significant amount of cell wall and the middle lamella expansion occurs between 30 to 180 DAP, while the integrity of the middle lamella in the mesocarp cells is most affected by ethylene treatment of 180 DAP fruit (**Figure 2**).

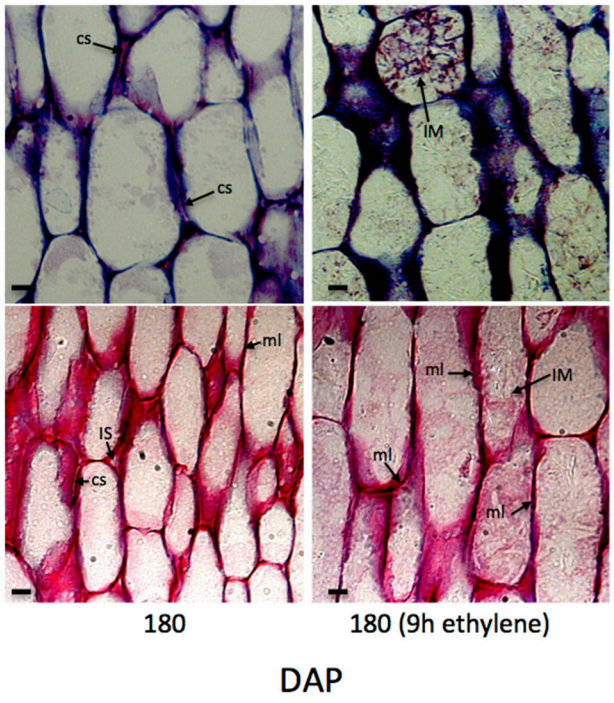

FIGURE 2 | Mesocarp cell characteristics change during development and after 9 h ethylene treatment. A longitudinal sections of mesocarp cells toward the base of the fruit stained with toluidine blue (upper panels) and ruthenium red (lower panels). cs, cell separation; dc, divided cell; IM, intercellular material; IS, intercellular space; ml, middle lamella; Scale bar, 10 μm.

Cell Wall Associated Transcriptional Activity during Mesocarp Development and Ripening

Based on the histological analysis, an increase in cell wall width occurs during mesocarp development and ripening, while exogenous ethylene treatment results in a loss of middle lamella integrity (**Figure 2**; Roongsattham et al., 2016). To provide insight into the transcriptional basis for these processes, proteins associated with cell wall assembly, metabolism, and modification were searched for within the differentially abundant transcripts previously identified in the mesocarp transcriptome at 100, 120, 140, and 160 DAP (**Supplementary Table 1**; Tranbarger et al., 2011). A total of 75 transcripts for cell wall related activities were found to be differentially expressed in the mesocarp during ripening, 63% of which have expression peaks at 140 and 160 DAP (including *EgPG4*) concomitant with the ethylene burst as measured previously (Tranbarger et al., 2011). Illumina sequencing at 100, 120, 140, and 160 DAP mesocarp validated the expression 54 of these genes annotated in the oil palm genome with roles in cell wall component biosynthesis, assembly, modification and hydrolysis during fruit ripening (**Figure 3**; **Supplementary Table 2**; Guerin et al., 2016). A global comparison of each transcript type expressed as a percentage of all cell wall transcripts gives an estimation of the transcriptional contribution of each cell wall activity during these stages of fruit ripening (**Figure 4**; **Supplementary Table 3**). Globally, the most abundant transcripts encode sequences similar to glucan endo-1,3-beta-glucosidase, with 25% of the total read counts from the 4 stages of development, and a peak of 43% at 160

Eg Name	Eg Gene (Loc)	iProfile
EgPG4	LOC105034919	
EgACO	LOC105039092	
beta-galactosidase-like	LOC105036555	
beta-glucosidase 22-like	LOC105057476	
beta-glucosidase 12-like	LOC105061257	
glucan endo-1,3-beta-glucosidase-like	LOC105033964	
glucan endo-1,3-beta-glucosidase-like	LOC105045344	
glucan endo-1,3-beta-glucosidase-like	LOC105033962	
glucan endo-1,3-beta-glucosidase-like	LOC105045348	
glucan endo-1,3-beta-glucosidase-like	LOC105045343	
lichenase-2-like	LOC105045349	
endoglucanase 19-like	LOC105040704	
endoglucanase 24-like	LOC105059603	
alpha-galactosidase	LOC105057194	
alpha-galactosidase	LOC105035858	
alpha-glucosidase	LOC105059813	
chitinase 2-like	LOC105055741	
chitinase 2-like	LOC105046567	
chitinase 2-like	LOC105053420	
chitinase 1-like	LOC105052906	
chitinase 1-like	LOC105049526	
PR-4-like	LOC105042178	
chitinase 1-like	LOC105059691	
acidic endochitinase-like	LOC105047536	
cellulose synthase A catalytic subunit 1	LOC105040177	
cellulose synthase A catalytic subunit 5	LOC105049519	
cellulose synthase-like protein E6	LOC105049957	
cellulose synthase-like protein G3	LOC105038182	
xyloglucan glycosyltransferase 5	LOC105039232	
glycosyltransferase 5	LOC105033885	
xyloglucan endotransglucosylase/hydrolase protein 32	LOC105042937	
xyloglucan endotransglucosylase/hydrolase protein 23	LOC105049189	
xyloglucan endotransglucosylase/hydrolase protein 23	LOC105049188	
xyloglucan endotransglucosylase/hydrolase protein 22-like	LOC105050826	
xyloglucan endotransglucosylase/hydrolase protein 23	LOC105037481	
xyloglucan endotransglucosylase/hydrolase protein 22-like	LOC105052932	
xyloglucan endotransglucosylase/hydrolase protein 23	LOC105039293	
mannan endo-1,4-beta-mannosidase 9	LOC105040138	
EGF domain-specific O-linked N-acetylglucosamine transferase-like	LOC105041136	
uncharacterized	LOC105041138	
expansin-A10-like	LOC105056621	
expansin-A10-like	LOC105044913	
expansin-A2-like	LOC105044813	
UDP-glucose 6-dehydrogenase 4	LOC105046638	
UDP-glucose 6-dehydrogenase 5-like	LOC105058153	
UDP-glucose 6-dehydrogenase 5-like	LOC105058063	
UDP-arabinopyranose mutase 1-like	LOC105046676	
UDP-arabinopyranose mutase 1-like	LOC105058110	
dolichyl-diphosphooligosaccharide--protein glycosyltransferase subunit 2-like	LOC105033620	
dolichyl-diphosphooligosaccharide--protein glycosyltransferase subunit 1B	LOC105055664	
dolichyl-diphosphooligosaccharide--protein glycosyltransferase subunit 1A	LOC105034534	
pectin methyltransferase QUA2	LOC105058429	
pectin methyltransferase QUA2	LOC105056805	
methyltransferase PMT2	LOC105041728	
methyltransferase PMT7	LOC105057645	
methyltransferase PMT3	LOC105033623	
pectinesterase 3	LOC105041982	

FIGURE 3 | Cell wall related transcripts with expression profiles in the mesocarp correlated to ripening stages concomitant with the increase in ethylene evolution at 140 and 160 DAP. *EgACO* and *EgPG4* are included for a comparison as known ethylene inducible transcripts. Profiles are based on RNA-Seq Illumina (iProfile) sequencing at each developmental time point and expressed as RKPM (sum of all possible transcripts, XMs, for each gene locus) A, 100 DAP; B, 120 DAP; C; 140 DAP; C, 160 DAP; Eg, *E. guineensis*. Red dot in profiles indicates maximum read peak.

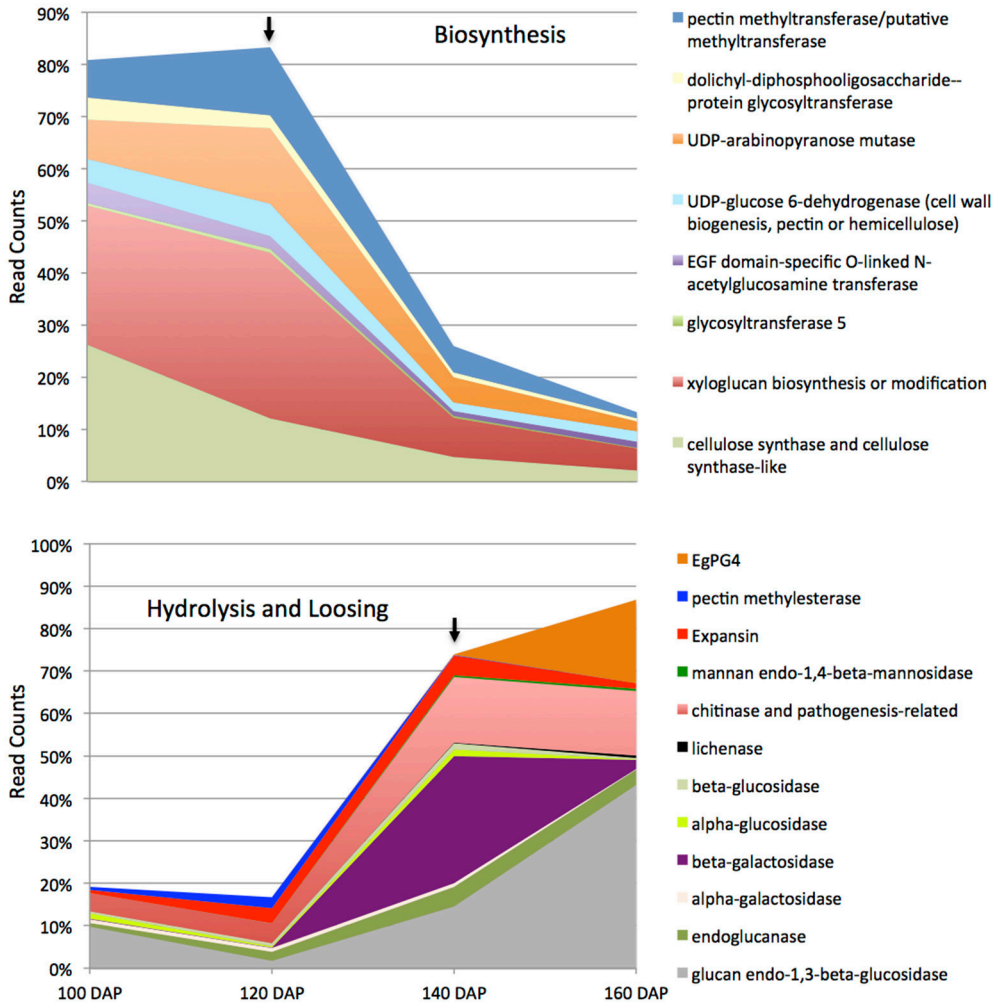

FIGURE 4 | Global cell wall related transcript abundance during mesocarp development and ripening. The transcripts and their encoded products can be grouped into two categories including biosynthesis (upper panel) and hydrolysis (lower panel) related functions. The upper black arrow indicates the stage at which the transition from ethylene system 1 to system 2 occurs while the lower arrow indicates the stage at which the ethylene burst occurs (Tranbarger et al., 2011). See **Supplementary Tables 1**, **2** for details.

DAP. Chitinase and pathogenesis-related proteins accounted for 13% of the total, with 16% and 15% at 140 DAP and 160 DAP respectively, while xyloglucan biosynthesis or modification proteins accounted for 12% of the total with 32% at 120 DAP (**Figure 4**, **Supplementary Table 3**). Xyloglucan biosynthesis or modification proteins were also highly abundant (27%) along with cellulose synthase and cellulose synthase-like transcripts (26%) at 100 DAP. Transcripts for cellulose synthase and cellulose-synthase like proteins decreased progressively during the later stages to 12% (120 DAP), 5% (140 DAP), and 2% (160 DAP). Transcripts for uridine diphosphate (UDP) glucose 6-dehydrogenase (9%), involved in both pectin and hemicellulose biogenesis, were more abundant at 120 DAP, but also present throughout the developmental stages examined (Klinghammer and Tenhaken, 2007). Pectin related transcripts included pectin methyltransferases (PMTs, 13% 120 DAP), a pectin methylesterase (PME, 3% 120 DAP) and the transcript *EgPG4*, which represents 20% of the total cell wall related transcripts at 160 DAP (**Figure 3**). Overall, there is a progressive change from cell wall biosynthesis to hydrolysis during the transition from ethylene system 1 to 2 (between 120 and 140 DAP) that includes transcripts encoding glucan endo-1,3-beta-glucosidase, endoglucanase, beta- and alpha-galactosidase, chitinase and pathogenesis-related, mannan endo-1,4-beta-mannosidase and expansin proteins. Between 140 and 160 DAP, the transcripts that increased the most were *EgPG4* (210 fold) and glucan endo-1,3-beta-glucosidase-like (LOC105033964, ~350 fold; **Supplementary Table 3**). In addition, one transcript similar to a xyloglucan endotransglucosylase/hydrolase protein 23 (LOC105039293) transcript was expressed at relatively high amounts exclusively at 160 DAP. The profile similarity of *EgPG4* with other transcripts suggest certain cell wall activities may be coordinated by ethylene during mesocarp ripening (**Figure 4**, **Supplementary Tables 2**, **3**).

Analysis of NAC Transcription Factor Transcripts Expressed in the Mesocarp and in Response to Ethylene

NAC domain containing TFs were found previously to be one of the most highly represented TFs expressed in the mesocarp (Tranbarger et al., 2011). To respond to the question whether any of these putative NAC TFs could be regulated by ethylene, first a genome wide search for NAC domain TFs was performed, then expression profiles of selected candidates were examined by qPCR in fruit treated with ethylene at two stages of ripening (**Figure 5**, **Supplementary Table 4**). A total of 124 putative NAC domain encoding genes were identified in the oil palm genome, 33 of which had total read counts higher than 50 in the ripening mesocarp (**Supplementary Table 4**). A selection was made that consisted of the top five mesocarp expressed genes in addition to five additional genes with either down regulated or up regulated expression profiles in the ripening mesocarp. Gene specific primer sets amplified 10 non-redundant NAC sequences and confirmed their expression in the mesocarp (**Supplementary Table 5**). As with the studies on *EgACO* and *EgPG4*, ripe fruit at two stages (150 and 180 DAP) were treated with ethylene and the NAC transcripts were quantified. All the transcripts examined either increased or decreased at one time point in 150 or 180 DAP fruit. Of the 10 NAC transcripts examined, 7 NAC transcripts (*EgNAC2*, *3*, *5*, *6*, *7*, *8*, and *13*) were significantly induced at one time point in either 150 or 180 DAP fruit. Notable, six of these (*EgNAC2*, *3*, *5*, *6*, *7,* and *8*) were induced after 3 h exposure to ethylene in the 180 DAP fruit, while two of those (*EgNAC5* and *6*) were also induced at 3 h in 150 DAP fruit. In addition, the *EgNAC5*, *6*, *7,* and *8* increased in abundance after 9 h of ethylene exposure in both 150 and 180 DAP fruit. *EgNAC6* and *7* were the most highly expressed transcripts expressed in response to ethylene in the mesocarp at both stages of ripening (150 and 180 DAP).

To provide insight into the diversification of NAC domain TFs, and to determine whether there is a relation between NAC domain structure and ethylene response, a phylogenetic analysis of the oil palm NAC domain sequences along with those of *Arabidopsis* and other selected NAC TFs with was performed (**Supplementary Figure 2**). Strong branch support values provided evidence for at least two major subclades of NAC domain sequences that resolve into a number of subgroups previously identified (Jensen et al., 2010). The oil palm mesocarp NAC domain sequences are distributed throughout the two major subclades, while six are found within the subgroups III-2 and III-3 (**Supplementary Figure 2**). NAC1, 2, and 3 group closely in subgroup III-3 and are also less abundant in the 150 DAP mesocarp after 3–6 h treatments with ethylene (**Figure 5**). In contrast, two of the most highly ethylene inducible NAC transcripts (*EgNAC6 and 7*) encode proteins found within subgroup III-2, along with the tomato NAC-NOR domain (**Figures 5**; **Supplementary Figure 2**). Among the other highly inducible transcripts; EgNAC5 separates in a less resolved portion of the cladogram, while EgNAC8 separates within subgroup II-3. It appears that an expansion of oil palm NAC domains occurred within the subgroups III-2 and III-3, where six sequences of the current study are found. In particular, two highly ethylene inducible genes, *EgNAC6* and EgNAC7, appear to be paralogous and encode NAC domain proteins the most homologous to the tomato NAC-NOR.

DISCUSSION

The Transition from Ethylene Production System 1 to 2 Occurs Concomitantly with a Transcriptional Activation of *EgACO*

The transition from basal auto inhibited ethylene production (system 1) to the burst of autocatalytic ethylene production (system 2) represents a central regulatory process that coordinates the expression of ripening related genes involved in pigmentation, aroma, carbohydrate, and cell wall metabolism (Seymour et al., 2013a; Liu et al., 2015). In tomato, the transition from system 1 to 2 is controlled both by developmental ethylene-independent and ethylene dependent factors and involves the transcriptional activation of specific ACS and ACO genes by the ripening related TFs Ripening-Inhibitor (RIN) and HB1 respectively (Nakatsuka et al., 1998; Barry and Giovannoni, 2007; Cara and Giovannoni, 2008; Lin et al., 2008; Yokotani et al., 2009; Klee and Giovannoni, 2011; Martel et al., 2011; Seymour et al., 2013a,b; Liu et al., 2015). The *EgACO* transcript is present in low amounts in the pollinated flowers (10 DAP), barely detectable or undetectable in at early stages of mesocarp development (30–100 DAP), and most highly expressed during the stages of fruit ripening (120–160 DAP), consistent with a role in both flower senescence and ripening similar to tomato (Blume and Grierson, 1997). However, the transcript profile differs from that observed during tomato ripening, in which the main ripening related *LeACO1* is expressed during both ethylene system 1 and system 2 stages of fruit development, with the highest expression during ripening and the autocatalytic system 2 (Holdsworth et al., 1987; Barry et al., 1996; Blume and Grierson, 1997; Nakatsuka et al., 1998; Jafari et al., 2013). Indeed, *LeACO1* is thought to participate in both system 1 and 2, and is not specific to ripening (Barry and Giovannoni, 2007; Cara and Giovannoni, 2008). Similarly in banana, the principle *MA-ACO1* transcript is also present in system 1 stage fruit, increases during the transition from system 1 to 2, and remains high at later stages of ripening (Liu et al., 1999). Our previous analysis revealed a burst of ethylene occurred in the oil palm fruit between 120 and 160 DAP, along with changes in transcript profiles related to ethylene biosynthesis and response between 100 and 160 DAP that reflect a transition from system 1 to system 2 ethylene production (Tranbarger et al., 2011). In contrast to tomato and banana, *EgACO* expression in the mesocarp is consistent with functions during the transition from system 1 to 2 (between 100 DAP and 140 DAP), and during ripening system 2 (between 140 and 160 DAP), but not during system 1 (100 DAP).

As in tomato, the increase in *EgACO* transcript during the transition from system 1 to 2 could be controlled either by ethylene independent or dependent regulation (Blume and Grierson, 1997). A comparison of *EgACO* and *EgPG4* transcript profiles during development and ripening and in response to

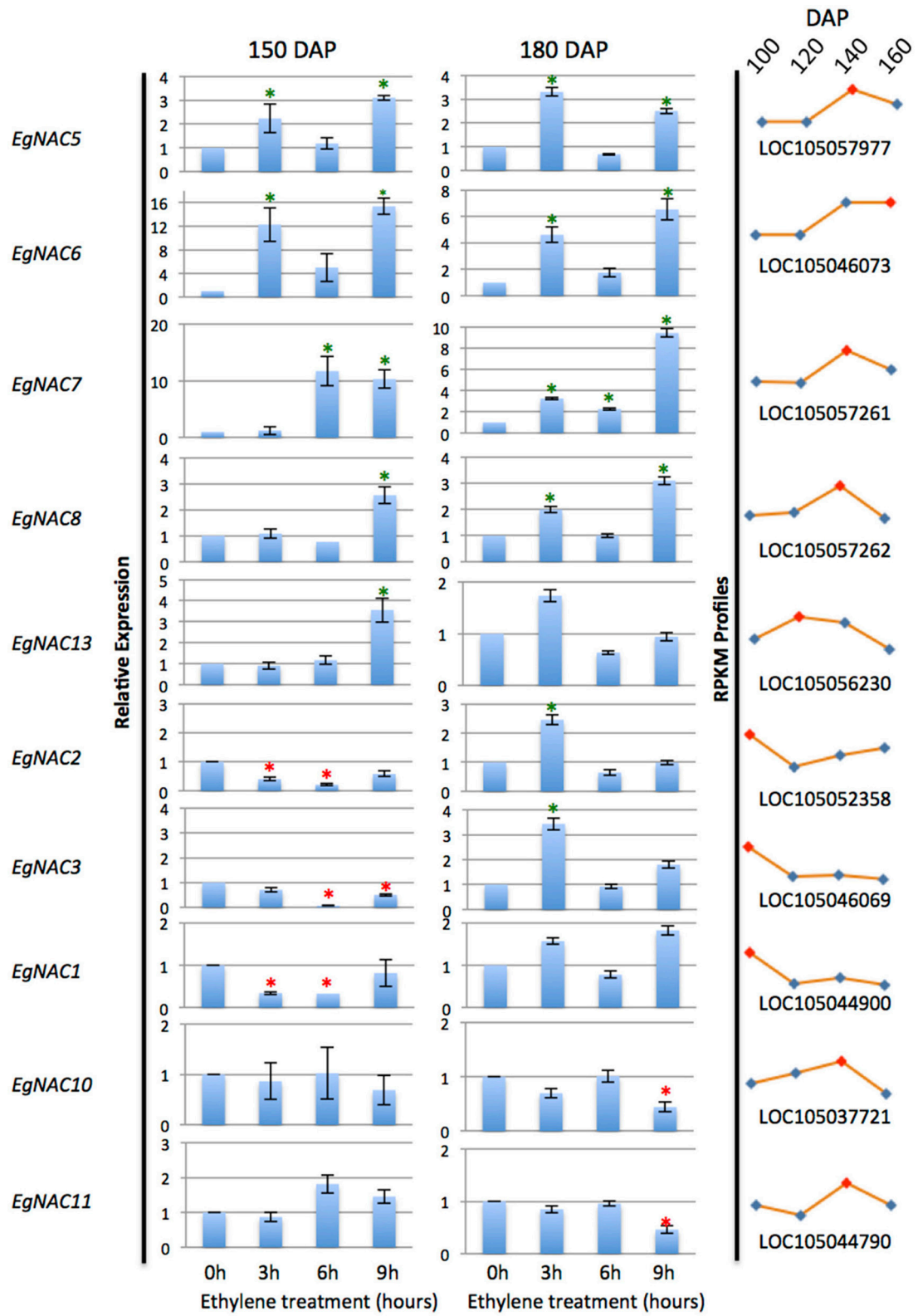

FIGURE 5 | qPCR analysis of NAC transcripts expressed in the mesocarp and induction in response to ethylene treatments. Asterisks indicate significant difference and increase or decrease in relative abundance by at least 2 fold (unpaired student's *t*-test $P > 0.05$) compared to the control at 0 h. Profile curves (right panels) are the corresponding *E. guineensis* gene locus expression during ripening at 100, 120, 140, and 160 DAP from RNA-Seq Illumina data.

ethylene suggests different modes of regulation in the mesocarp. *EgPG4* is barely detectable at the end of the transition from system 1 to system 2 ethylene production (approximated at 140 DAP), then increases dramatically at the autocatalytic ethylene stage (160 DAP), suggesting *EgPG4* expression may require a higher ethylene concentration threshold and/or does not respond to the same signals as *EgACO* during the transition from system 1 to 2. In contrast, expression of the principle tomato fruit TFPG increases more synchronistically with the increase in ethylene production (Dellapenna et al., 1986). In addition, there are at least two PGs expressed during banana ripening, one of which is the most highly expressed during ripening, and appears to be induced by ethylene (Asif and Nath, 2005; Asif et al., 2014). However, the ethylene treatments were for days and not hours as in the current study, so it is difficult to compare the results. In oil palm, the fact that *EgPG4* is consistently more highly induced by ethylene than *EgACO* at all treatment time points and stages examined suggests *EgPG4* expression is controlled differently by ethylene than *EgACO*, and argues against a higher ethylene threshold requirement for *EgPG4* regulation. The expression of *EgACO* during the transition from system 1 to 2 suggests developmental ethylene independent signals could induce *EgACO* during the transition, and not ethylene alone. One example of this in tomato is the LeHB-1 homeobox protein tomato that binds to the *LeACO1* promoter, while the inhibition of LeHB-1 mRNA results in reduced *LeACO1* mRNA (Lin et al., 2008). A search of the oil palm mesocarp transcriptome for sequences similar to LeHB-1 resulted in sequences with very low e-values (1e–26 to 1e–29) and low read counts, and therefore no evidence for a similar module was observed. Overall, while gene expression of key genes during the transition from system 1 to 2 in the oil palm mesocarp shares some similarities to that of banana and tomato, the examples of *EgACO* and *EgPG4* provided here suggest differences.

The Mesocarp Undergoes a Transcriptional Transition from Cell Wall Synthesis to Degradation during Ripening

The cell wall is an extremely complex structure made up of interlaced cellulose and hemicellulose polysaccharide polymers with structural glycoproteins embedded in a pectin matrix including HG, rhamnogalacturonan I and rhamnogalacturonan II. Unsurprisingly, many cell wall modifying proteins appear to function during ripening related cell wall disassembly and fruit softening. Attempts to silence single genes encoding only one type of modification have had little success to stop softening in the tomato fruit (Brummell, 2006; Seymour et al., 2013a). The identity of cell wall related transcripts identified in the current study that are differentially expressed during mesocarp ripening suggest a transcriptional based transition from synthesis to hydrolysis of the major cell wall polymers occurs in the mesocarp during ripening. Importantly, a single PG transcript (*EgPG4)* accounts for a large percentage of the total transcripts identified, while *EgPG4* expressed at a later stage of ripening, and is also induced by ethylene, similar to TFPG *PG2* transcript of tomato (Dellapenna et al., 1987). In addition, a number of other transcripts encoding various cell wall modifying activities were observed to have similar profiles to *EgPG4*, including glucan endo-1,3-beta-glucosidase-like, lichenase-2-like, chitinase 2-like, xyloglucan endotransglucosylase/hydrolase protein 23, UDP-glucose 6-dehydrogenase 5-like proteins were identified (**Figure 3**). In contrast, there are also a number of cell wall related transcripts with expression profiles similar to the ethylene biosynthesis transcript *EgACO*, also induced by ethylene, including, beta-galactosidase-like, alpha-glucosidase, and expansin-A10-like. Indeed, while *EgACO* and *EgPG4* are both induced by ethylene and are expressed in a ripening dependent manner, their ethylene induction and ripening expression profiles are different. That *EgACO* and *EgPG4* share similar expression profiles with various cell wall modifying protein transcripts suggests ethylene may transcriptionally regulate cell wall activities differentially as proposed previously (Ireland et al., 2014). Previous work on cell wall related gene expression during oil palm mesocarp ripening monitored only very few genes (Teh et al., 2014). In contrast, the current work includes a more comprehensive analysis of 56 differentially expressed genes from at least 20 different cell wall related gene families. The results suggest a close relation between the transcriptional activation of genes encoding expansin, polygalacturonase, mannosidases, beta-galactosidase, and xyloglucan endotransglucosylase/hydrolase proteins in the ripening oil palm mesocarp, comparable to that observed during tomato fruit ripening (Seymour et al., 2013a). While there is less available data with monocot fruit species, expansin and xyloglucan endotransglucosylase/hydrolase protein genes were also highly expressed during banana ripening (Asif et al., 2014). Overall, these observations provide evidence for the conservation of a large number of cell wall related activities that may be regulated by ethylene and other fruit ripening specific regulatory factors in diverse lineages of both eudicots and monocots.

Paralogous Members of the NAC Domain Family of Transcription Factors Are Regulated in the Mesocarp during Ripening and Induced by Ethylene

The NAC gene family is a very large group that encodes plant specific TFs involved in many processes including secondary cell wall development, stress response, and leaf senescence (Puranik et al., 2012; Kim et al., 2016; Monniaux and Hay, 2016). In addition, NAC TFs are upstream of ethylene related transcriptional regulation during both eudicot and monocot fruit ripening, and the NAC-NOR is a master regulator of tomato fruit ripening (Giovannoni, 2004; Shan et al., 2012; Seymour et al., 2013a; Kou et al., 2016). From a previous study we observed a number of NAC domain family TF genes that were differentially expressed during oil palm fruit ripening suggesting these TFs may function in response to and/or during the ethylene burst (Tranbarger et al., 2011). In the current genome wide study, we identified at least 31 NAC domain transcripts expressed in the oil palm mesocarp during the stages when ethylene production increases. Experiments with ethylene treated fruit revealed at least four have enhanced expression in the presence

of ethylene. Furthermore, two of these oil palm NAC TF genes, *EgNAC6* and *EgNAC7*, appear to encode paralogous proteins that are very similar to the tomato NAC-NOR, suggesting a conserved function in the oil palm ripening mesocarp related to ethylene. Interestingly, the ethylene induction profiles of all *EgNACs* resemble more closely the induction profiles of *EgACO* than *EgPG4*, which suggests similar modes of regulation between the *EgNACs* and *EgACO* in the mesocarp. In tomato and banana NAC domain TFs are expressed during ripening and in response to ethylene (Shan et al., 2012; Zhu et al., 2014; Kou et al., 2016). In tomato, NAC family members may regulate the transcription of *LeACS2*, *LeACS4,* and *LeACO1*, while in banana, NAC domain TFs may regulate ethylene signal transduction through interactions with the downstream component ethylene insensitive 3 (EIN3)-like protein, termed MaEIL5 and the biosynthesis of ethylene (Shan et al., 2012; Kou et al., 2016). In the oil palm mesocarp, the ripening related and ethylene induced expression of several NAC-domain family members, in particular two with the most similarity to the tomato NAC-NOR, suggest a conservation of function for NAC domain TFs during the ripening of diverse lineages of both monocot and eudicot fruit types.

AUTHOR CONTRIBUTIONS

TT and FM devised and participated in all aspects of the study. TT, CJ, and ST coordinated the logistics for fieldwork experiments. TT, FM, PR, CJ, PS, and MP performed the ethylene experiments and collected samples for RNA isolation and histological studies. PR extracted total RNA, isolated polygalacturonase cDNAs, performed cloning, designed gene specific primers, and performed preliminary RT-PCR expression studies. KF participated in the identification of the ACO and NAC domain cDNAs. MP, KF, CJ, and FM performed the qPCR analysis. TT performed the phylogenetic analysis. SD performed the statistical analysis of the transcriptome data. JV, PR, and MC prepared samples for histological analysis and performed microscopic analyses. TT, FM, SD, and JV participated in writing the article. All authors read and approved the final submitted manuscript.

FUNDING

Financial support for this project came from PHC Thailande projects 2007-2010 (codes 20621YD and 16589YK) to TT and ST, and from PalmElit SAS/IRD/CIRAD to FM and TT. PR was supported by a Fondation Agropolis RTRA doctoral grant. KF was supported by a doctoral scholarship grant from the French Embassy with cofounding from PalmElit SAS.

ACKNOWLEDGMENTS

We thank all the personnel at INRAB, CRA-PP, Pobé, Benin for their technical and logistical support during the collection of the genetic material used for the mesocarp transcriptome. We especially thank Anek Limsrivilai and the staff at GoldenTenera Oil Palm Plantation for the excellent plant material used for the ethylene experiments in Thailand. We also appreciate James W. Tregear, IRD and ST, Genome Institute, BIOTEC for their continued support of the oil palm fruit projects. Thanks to Alberto Cenci (Bioversity International) for his helpful assistance with the NAC domain phylogeny analysis. RNAseq data from embryonic cell suspension were kindly provided by Thierry Beulé (CIRAD, UMR DIADE).

SUPPLEMENTARY MATERIAL

The Supplementary Material for this article can be found online at: http://journal.frontiersin.org/article/10.3389/fpls.2017.00603/full#supplementary-material

Supplementary Figure 1 | Mesocarp cell characteristics change during development and after 9 h ethylene treatment. (A) longitudinal sections of mesocarp cells toward the base of the fruit stained with toluidine blue (upper panels) and ruthenium red (lower panels). **(B)** Cell wall, middle lamella, and cell wall width of mesocarp cells during development and after 9 h ethylene treatment. The different lower case letters represent statistical significance; the error bars represent standard error; cs, cell separation; n, number of samples measured; dc, divided cell; nd, no data; IM, intercellular material; IS, intercellular space; ml, middle lamella; Scale bar, 10 μm. Figure is reorganized from data previously.

Supplementary Figure 2 | Phylogenetic analysis of NAC domains from oil palm and other species reveals clusters of ethylene response. Green and red asterisks represent a significant increase or decrease respectively in transcript abundance in relation to ethylene treatments (for details see **Figure 5**). Branch support values are based on the aLRT statistical test (see Materials and Methods). Branches with branch values less than 50 were collapsed. ng, not grouped.

Supplementary Table 1 | Cell wall mined.

Supplementary Table 2 | Cell wall.

Supplementary Table 3 | Cell_wall_global.

Supplementary Table 4 | NAC Illumina.

Supplementary Table 5 | NAC primers.

REFERENCES

Abbas, M. F., and Ibrahim, M. A. (1996). The role of ethylene in the regulation of fruit ripening in the hillawi date palm (*Phoenix dactylifera* L). *J. Sci. Food Agric.* 72, 306–308. doi: 10.1002/(SICI)1097-0010(199611)72:3<306::AID-JSFA659>3.0.CO;2-U

Alba, R., Payton, P., Fei, Z. J., Mcquinn, R., Debbie, P., Martin, G. B., et al. (2005). Transcriptome and selected metabolite analyses reveal multiple points of ethylene control during tomato fruit development. *Plant Cell* 17, 2954–2965. doi: 10.1105/tpc.105.036053

Altschul, S. F., Gish, W., Miller, W., Myers, E. W., and Lipman, D. J. (1990). Basic local alignment search tool. *J. Mol. Biol.* 215, 403–410. doi: 10.1016/S0022-2836(05)80360-2

Anisimova, M., and Gascuel, O. (2006). Approximate likelihood-ratio test for branches: a fast, accurate, and powerful alternative. *Syst. Biol.* 55, 539–552. doi: 10.1080/10635150600755453

Asif, M. H., Lakhwani, D., Pathak, S., Gupta, P., Bag, S. K., Nath, P., et al. (2014). Transcriptome analysis of ripe and unripe fruit tissue of banana identifies major metabolic networks involved in fruit ripening process. *BMC Plant Biol.* 14:316. doi: 10.1186/s12870-014-0316-1

Asif, M. H., and Nath, P. (2005). Expression of multiple forms of polygalacturonase gene during ripening in banana fruit. *Plant Physiol. Biochem.* 43, 177–184. doi: 10.1016/j.plaphy.2005.01.011

Bapat, V. A., Trivedi, P. K., Ghosh, A., Sane, V. A., Ganapathi, T. R., and Nath, P. (2010). Ripening of fleshy fruit: molecular insight and the role of ethylene. *Biotechnol. Adv.* 28, 94–107. doi: 10.1016/j.biotechadv.2009.10.002

Barry, C. S., Blume, B., Bouzayen, M., Cooper, W., Hamilton, A. J., and Grierson, D. (1996). Differential expression of the 1-aminocyclopropane-1-carboxylate oxidase gene family of tomato. *Plant J.* 9, 525–535. doi: 10.1046/j.1365-313X.1996.09040525.x

Barry, C. S., and Giovannoni, J. J. (2007). Ethylene and fruit ripening. *J. Plant Growth Regul.* 26, 143–159. doi: 10.1007/s00344-007-9002-y

Bennett, A. B., and Labavitch, J. M. (2008). Ethylene and ripening-regulated expression and function of fruit cell wall modifying proteins. *Plant Sci.* 175, 130–136. doi: 10.1016/j.plantsci.2008.03.004

Blume, B., and Grierson, D. (1997). Expression of ACC oxidase promoter-GUS fusions in tomato and *Nicotiana plumbaginifolia* regulated by developmental and environmental stimuli. *Plant J.* 12, 731–746. doi: 10.1046/j.1365-313X.1997.12040731.x

Brummell, D. A. (2006). Cell wall disassembly in ripening fruit. *Funct. Plant Biol.* 33, 103–119. doi: 10.1071/FP05234

Brummell, D. A., and Harpster, M. H. (2001). Cell wall metabolism in fruit softening and quality and its manipulation in transgenic plants. *Plant Mol. Biol.* 47, 311–340. doi: 10.1023/A:1010656104304

Buffard-Morel, J., Verdeil, J. L., and Pannetier, C. (1992). Embryogenèse somatique du cocotier (*Cocos nucifera*-L.) à partir d'explants foliarires: étude histologique. *Can. J. Bot.* 70, 735–741. doi: 10.1139/b92-094

Cara, B., and Giovannoni, J. J. (2008). Molecular biology of ethylene during tomato fruit development and maturation. *Plant Sci.* 175, 106–113. doi: 10.1016/j.plantsci.2008.03.021

Chanderbali, A. S., Albert, V. A., Ashworth, V. E., Clegg, M. T., Litz, R. E., Soltis, D. E., et al. (2008). *Persea americana* (avocado): bringing ancient flowers to fruit in the genomics era. *Bioessays* 30, 386–396. doi: 10.1002/bies.20721

Chanderbali, A. S., Albert, V. A., Leebens-Mack, J., Altman, N. S., Soltis, D. E., and Soltis, P. S. (2009). Transcriptional signatures of ancient floral developmental genetics in avocado (*Persea americana*; Lauraceae). *Proc. Natl. Acad. Sci. U.S.A.* 106, 8929–8934. doi: 10.1073/pnas.0811476106

Chervin, C., Tira-Umphon, A., Terrier, N., Zouine, M., Severac, D., and Roustan, J. P. (2008). Stimulation of the grape berry expansion by ethylene and effects on related gene transcripts, over the ripening phase. *Physiol. Plant.* 134, 534–546. doi: 10.1111/j.1399-3054.2008.01158.x

Cooley, M. B., and Yoder, J. I. (1998). Insertional inactivation of the tomato polygalacturonase gene. *Plant Mol. Biol.* 38, 521–530. doi: 10.1023/A:1006086004262

Dellapenna, D., Alexander, D. C., and Bennett, A. B. (1986). Molecular cloning of tomato fruit polygalacturonase: analysis of polygalacturonase mRNA levels during ripening. *Proc. Natl. Acad. Sci. U.S.A.* 83, 6420–6424. doi: 10.1073/pnas.83.17.6420

Dellapenna, D., Kates, D. S., and Bennett, A. B. (1987). Polygalacturonase gene expression in rutgers, rin, nor, and Nr tomato fruits. *Plant Physiol.* 85, 502–507. doi: 10.1104/pp.85.2.502

Dellapenna, D., Lincoln, J. E., Fischer, R. L., and Bennett, A. B. (1989). Transcriptional analysis of polygalacturonase and other ripening associated genes in rutgers, rin, nor, and Nr tomato fruit. *Plant Physiol.* 90, 1372–1377. doi: 10.1104/pp.90.4.1372

Dereeper, A., Guignon, V., Blanc, G., Audic, S., Buffet, S., Chevenet, F., et al. (2008). Phylogeny.fr: robust phylogenetic analysis for the non-specialist. *Nucleic Acids Res.* 36, W465–W469. doi: 10.1093/nar/gkn180

D'hont, A., Denoeud, F., Aury, J. M., Baurens, F. C., Carreel, F., Garsmeur, O., et al. (2012). The banana (*Musa acuminata*) genome and the evolution of monocotyledonous plants. *Nature* 488, 213–217. doi: 10.1038/nature 11241

Elitzur, T., Vrebalov, J., Giovannoni, J. J., Goldschmidt, E. E., and Friedman, H. (2010). The regulation of MADS-box gene expression during ripening of banana and their regulatory interaction with ethylene. *J. Exp. Bot.* 61, 1523–1535. doi: 10.1093/jxb/erq017

Elitzur, T., Yakir, E., Quansah, L., Zhangjun, F., Vrebalov, J., Khayat, E., et al. (2016). Banana MaMADS transcription factors are necessary for fruit ripening and molecular tools to promote shelf-life and food security. *Plant Physiol.* 171, 380–391. doi: 10.1104/pp.15.01866

Fooyontphanich, K., Morcillo, F., Amblard, P., Collin, M., Jantasuriyarat, C., Tangphatsornruang, S., et al. (2016). A phenotypic test for delay of abscission and non-abscission oil palm fruit and validation by abscission marker gene expression analysis. *Acta Hortic.* 1119, 97–104. doi: 10.17660/ActaHortic.2016.1119.13

Giovannoni, J. J. (2004). Genetic regulation of fruit development and ripening. *Plant Cell* 16, S170–S180. doi: 10.1105/tpc.019158

Götz, S., Garcîa-Gómez, J. M., Terol, J., Williams, T. D., Nagaraj, S. H., Nueda, M. J., et al. (2008). High-throughput functional annotation and data mining with the Blast2GO suite. *Nucleic Acids Res.* 36, 3420–3435. doi: 10.1093/nar/gkn176

Guerin, C., Joët, T., Serret, J., Lashermes, P., Vaissayre, V., Agbessi, M. D., et al. (2016). Gene coexpression network analysis of oil biosynthesis in an interspecific backcross of oil palm. *Plant J.* 87, 423–441. doi: 10.1111/tpj.13208

Holdsworth, M. J., Bird, C. R., Ray, J., Schuch, W., and Grierson, D. (1987). Structure and expression of an ethylene-related mRNA from tomato. *Nucleic Acids Res.* 15, 731–739. doi: 10.1093/nar/15.2.731

Ireland, H. S., Gunaseelan, K., Muddumage, R., Tacken, E. J., Putterill, J., Johnston, J. W., et al. (2014). Ethylene regulates Apple (Malus x domestica) fruit softening through a dose x time-dependent mechanism and through differential sensitivities and dependencies of cell wall-modifying genes. *Plant Cell Physiol.* 55, 1005–1016. doi: 10.1093/pcp/pcu034

Jafari, Z., Haddad, R., Hosseini, R., and Garoosi, G. (2013). Cloning, identification and expression analysis of ACC oxidase gene involved in ethylene production pathway. *Mol. Biol. Rep.* 40, 1341–1350. doi: 10.1007/s11033-012-2178-7

Jensen, M. K., Kjaersgaard, T., Nielsen, M. M., Galberg, P., Petersen, K., O'shea, C., et al. (2010). The *Arabidopsis thaliana* NAC transcription factor family: structure-function relationships and determinants of ANAC019 stress signalling. *Biochem. J.* 426, 183–196. doi: 10.1042/BJ20091234

Jin, J., He, K., Tang, X., Li, Z., Lv, L., Zhao, Y., et al. (2015). An Arabidopsis transcriptional regulatory map reveals distinct functional and evolutionary features of novel transcription factors. *Mol. Biol. Evol.* 32, 1767–1773. doi: 10.1093/molbev/msv058

Jin, J., Tian, F., Yang, D. C., Meng, Y. Q., Kong, L., Luo, J. C., et al. (2016). PlantTFDB 4.0: toward a central hub for transcription factors and regulatory interactions in plants. *Mol. Biol. Evol.* 32, 1767–1773. doi: 10.1093/molbev/msv058

Jourda, C., Cardi, C., Mbéguie, A. M. D., Bocs, S., Garsmeur, O., D'hont, A., et al. (2014). Expansion of banana (*Musa acuminata*) gene families involved in ethylene biosynthesis and signalling after lineage-specific whole-genome duplications. *New Phytol.* 202, 986–1000. doi: 10.1111/nph.12710

Kim, H. J., Nam, H. G., and Lim, P. O. (2016). Regulatory network of NAC transcription factors in leaf senescence. *Curr. Opin. Plant Biol.* 33, 48–56. doi: 10.1016/j.pbi.2016.06.002

Klee, H. J., and Giovannoni, J. J. (2011). Genetics and control of tomato fruit ripening and quality attributes. *Annu. Rev. Genet.* 45, 41–59. doi: 10.1146/annurev-genet-110410-132507

Klinghammer, M., and Tenhaken, R. (2007). Genome-wide analysis of the UDP-glucose dehydrogenase gene family in Arabidopsis, a key enzyme for matrix polysaccharides in cell walls. *J. Exp. Bot.* 58, 3609–3621. doi: 10.1093/jxb/erm209

Kou, X., Liu, C., Han, L., Wang, S., and Xue, Z. (2016). NAC transcription factors play an important role in ethylene biosynthesis, reception and signaling of tomato fruit ripening. *Mol. Genet. Genomics* 291, 1205–1217. doi: 10.1007/s00438-016-1177-0

Larkin, M. A., Blackshields, G., Brown, N. P., Chenna, R., Mcgettigan, P. A., McWilliam, H., et al. (2007). Clustal W and clustal X version 2.0. *Bioinformatics* 23, 2947–2948. doi: 10.1093/bioinformatics/btm404

Lelievre, J. M., Latche, A., Jones, B., Bouzayen, M., and Pech, J. C. (1997). Ethylene and fruit ripening. *Physiol. Plant.* 101, 727–739. doi: 10.1111/j.1399-3054.1997.tb01057.x

Lin, Z. F., Hong, Y. G., Yin, M. G., Li, C. Y., Zhang, K., and Grierson, D. (2008). A tomato HD-Zip homeobox protein, LeHB-1, plays an important role in floral organogenesis and ripening. *Plant J.* 55, 301–310. doi: 10.1111/j.1365-313X.2008.03505.x

Liu, M. C., Pirrello, J., Chervin, C., Roustan, J. P., and Bouzayen, M. (2015). Ethylene control of fruit ripening: revisiting the complex

network of transcriptional regulation. *Plant Physiol.* 169, 2380–2390. doi: 10.1104/pp.15.01361

Liu, X., Shiomi, S., Nakatsuka, A., Kubo, Y., Nakamura, R., and Inaba, A. (1999). Characterization of ethylene biosynthesis associated with ripening in banana fruit. *Plant Physiol.* 121, 1257–1266. doi: 10.1104/pp.121.4.1257

Magallón, S., Gómez-Acevedo, S., Sánchez-Reyes, L. L., and Hernández-Hernández, T. (2015). A metacalibrated time-tree documents the early rise of flowering plant phylogenetic diversity. *New Phytol.* 207, 437–453. doi: 10.1111/nph.13264

Martel, C., Vrebalov, J., Tafelmeyer, P., and Giovannoni, J. J. (2011). The tomato MADS-box transcription factor RIPENING INHIBITOR interacts with promoters involved in numerous ripening processes in a COLORLESS NONRIPENING-dependent manner. *Plant Physiol.* 157, 1568–1579. doi: 10.1104/pp.111.181107

Monniaux, M., and Hay, A. (2016). Cells, walls, and endless forms. *Curr. Opin. Plant Biol.* 34, 114–121. doi: 10.1016/j.pbi.2016.10.010

Morcillo, F., Gagneur, C., Adam, H., Richaud, F., Singh, R., Cheah, S. C., et al. (2006). Somaclonal variation in micropropagated oil palm. Characterization of two novel genes with enhanced expression in epigenetically abnormal cell lines and in response to auxin. *Tree Physiol.* 26, 585–594. doi: 10.1093/treephys/26.5.585

Nakatsuka, A., Murachi, S., Okunishi, H., Shiomi, S., Nakano, R., Kubo, Y., et al. (1998). Differential expression and internal feedback regulation of 1-aminocyclopropane-1-carboxylate synthase, 1-aminocyclopropane-1-carboxylate oxidase, and ethylene receptor genes in tomato fruit during development and ripening. *Plant Physiol.* 118, 1295–1305. doi: 10.1104/pp.118.4.1295

Nualwijit, N., and Lerslerwong, L. (2014). Post harvest ripening of oil palm fruit is accelerated by application of exogenous ethylene. *Songklanakarin J. Sci. Technol.* 36, 255–259.

Ooka, H., Satoh, K., Doi, K., Nagata, T., Otomo, Y., Murakami, K., et al. (2003). Comprehensive analysis of NAC family genes in *Oryza sativa* and *Arabidopsis thaliana*. *DNA Res.* 10, 239–247. doi: 10.1093/dnares/10.6.239

Osorio, S., Alba, R., Damasceno, C. M., Lopez-Casado, G., Lohse, M., Zanor, M. I., et al. (2011). Systems biology of tomato fruit development: combined transcript, protein, and metabolite analysis of tomato transcription factor (nor, rin) and ethylene receptor (Nr) mutants reveals novel regulatory interactions. *Plant Physiol.* 157, 405–425. doi: 10.1104/pp.111.175463

Osorio, S., Alba, R., Nikoloski, Z., Kochevenko, A., Fernie, A. R., and Giovannoni, J. J. (2012). Integrative comparative analyses of transcript and metabolite profiles from pepper and tomato ripening and development stages uncovers species-specific patterns of network regulatory behaviour. *Plant Physiol.* 159, 1713–1729. doi: 10.1104/pp.112.199711

Pfaffl, M. W. (2001). A new mathematical model for relative quantification in real-time RT-PCR. *Nucleic Acids Res.* 29:e45. doi: 10.1093/nar/29.9.e45

Prasanna, V., Prabha, T. N., and Tharanathan, R. N. (2007). Fruit ripening phenomena–an overview. *Crit. Rev. Food Sci.* 47, 1–19. doi: 10.1080/10408390600976841

Puranik, S., Sahu, P. P., Srivastava, P. S., and Prasad, M. (2012). NAC proteins: regulation and role in stress tolerance. *Trends Plant Sci.* 17, 369–381. doi: 10.1016/j.tplants.2012.02.004

Roongsattham, P., Morcillo, F., Fooyontphanich, K., Jantasuriyarat, C., Tragoonrung, S., Amblard, P., et al. (2016). Cellular and pectin dynamics during abscission zone development and ripe fruit abscission of the monocot oil palm. *Front. Plant Sci.* 7:540. doi: 10.3389/fpls.2016.00540

Roongsattham, P., Morcillo, F., Jantasuriyarat, C., Pizot, M., Moussu, S., Jayaweera, D., et al. (2012). Temporal and spatial expression of polygalacturonase gene family members reveals divergent regulation during fleshy fruit ripening and abscission in the monocot species oil palm. *BMC Plant Biol.* 12:150. doi: 10.1186/1471-2229-12-150

Seymour, G. B., Chapman, N. H., Chew, B. L., and Rose, J. K. (2013a). Regulation of ripening and opportunities for control in tomato and other fruits. *Plant Biotechnol. J.* 11, 269–278. doi: 10.1111/j.1467-7652.2012.00738.x

Seymour, G. B., Ostergaard, L., Chapman, N. H., Knapp, S., and Martin, C. (2013b). Fruit development and ripening. *Annu. Rev. Plant Biol.* 64, 219–241. doi: 10.1146/annurev-arplant-050312-120057

Shan, W., Kuang, J. F., Chen, L., Xie, H., Peng, H. H., Xiao, Y. Y., et al. (2012). Molecular characterization of banana NAC transcription factors and their interactions with ethylene signalling component EIL during fruit ripening. *J. Exp. Bot.* 63, 5171–5187. doi: 10.1093/jxb/ers178

Sheehy, R. E., Kramer, M., and Hiatt, W. R. (1988). Reduction of polygalacturonase activity in tomato fruit by antisense RNA. *Proc. Natl. Acad. Sci. U.S.A.* 85, 8805–8809. doi: 10.1073/pnas.85.23.8805

Singh, R., Ong-Abdullah, M., Low, E. T., Manaf, M. A., Rosli, R., Sambanthamurthi, R., et al. (2013). Oil palm genome sequence reveals divergence of interfertile species in old and new worlds. *Nature* 500, 335–339. doi: 10.1038/nature12309

Smith, C. J. S., Watson, C. F., Ray, J., Bird, C. R., Morris, P. C., Schuch, W., et al. (1988). Antisense RNA inhibition of polygalacturonase gene-expression in transgenic tomatoes. *Nature* 334, 724–726. doi: 10.1038/334724a0

Smith, C. J., Watson, C. F., Morris, P. C., Bird, C. R., Seymour, G. B., Gray, J. E., et al. (1990). Inheritance and effect on ripening of antisense polygalacturonase genes in transgenic tomatoes. *Plant Mol. Biol.* 14, 369–379. doi: 10.1007/BF00028773

Teh, H. F., Neoh, B. K., Wong, Y. C., Kwong, Q. B., Ooi, T. E. K., Ng, T. L., et al. (2014). Hormones, polyamines, and cell wall metabolism during oil palm fruit mesocarp development and ripening. *J. Agric. Food Chem.* 62, 8143–8152. doi: 10.1021/jf500975h

Trainotti, L., Pavanello, A., and Casadoro, G. (2005). Different ethylene receptors show an increased expression during the ripening of strawberries: does such an increment imply a role for ethylene in the ripening of these non-climacteric fruits? *J. Exp. Bot.* 56, 2037–2046. doi: 10.1093/jxb/eri202

Tranbarger, T. J., Dussert, S., Joet, T., Argout, X., Summo, M., Champion, A., et al. (2011). Regulatory mechanisms underlying oil palm fruit mesocarp maturation, ripening, and functional specialization in lipid and carotenoid metabolism. *Plant Physiol.* 156, 564–584. doi: 10.1104/pp.111.175141

Yokotani, N., Nakano, R., Imanishi, S., Nagata, M., Inaba, A., and Kubo, Y. (2009). Ripening-associated ethylene biosynthesis in tomato fruit is autocatalytically and developmentally regulated. *J. Exp. Bot.* 60, 3433–3442. doi: 10.1093/jxb/erp185

Zdobnov, E. M., and Apweiler, R. (2001). InterProScan–an integration platform for the signature-recognition methods in interpro. *Bioinformatics* 17, 847–848. doi: 10.1093/bioinformatics/17.9.847

Zheng, Y., Jiao, C., Sun, H., Rosli, H. G., Pombo, M. A., Zhang, P., et al. (2016). iTAK: a program for genome-wide prediction and classification of plant transcription factors, transcriptional regulators, and protein kinases. *Mol. Plant* 9, 1667–1670. doi: 10.1016/j.molp.2016.09.014

Zhu, M., Chen, G., Zhou, S., Tu, Y., Wang, Y., Dong, T., et al. (2014). A new tomato NAC (NAM/ATAF1/2/CUC2) transcription factor, SlNAC4, functions as a positive regulator of fruit ripening and carotenoid accumulation. *Plant Cell Physiol.* 55, 119–135. doi: 10.1093/pcp/pct162

Conflict of Interest Statement: The authors declare that the research was conducted in the absence of any commercial or financial relationships that could be construed as a potential conflict of interest.

frontiers in Plant Science

MINI REVIEW
published: 24 January 2017
doi: 10.3389/fpls.2017.00057

Integration of Ethylene and Light Signaling Affects Hypocotyl Growth in *Arabidopsis*

Yanwen Yu[1] *and Rongfeng Huang*[1,2]*

[1] *Biotechnology Research Institute, Chinese Academy of Agricultural Sciences, Beijing, China,* [2] *National Key Facility of Crop Gene Resources and Genetic Improvement, Beijing, China*

As an ideal model for studying ethylene effects on cell elongation, *Arabidopsis* hypocotyl growth is widely used due to the unique characteristic that ethylene stimulates hypocotyl elongation in the light but inhibits it in the dark. Although the contrasting effect of ethylene on hypocotyl growth has long been known, the molecular basis of this effect has only gradually been identified in recent years. In the light, ethylene promotes the expression of *PHYTOCHROME INTERACTING FACTOR 3* (PIF3) and the degradation of ELONGATED HYPOCOTYL 5 (HY5) protein, thus stimulating hypocotyl growth. In the dark, *ETHYLENE RESPONSE FACTOR 1* (ERF1) and *WAVE-DAMPENED 5* (WDL5) induced by ethylene are responsible for its inhibitory effect on hypocotyl elongation. Moreover, CONSTITUTIVE PHOTOMORPHOGENIC 1 (COP1) and PHYTOCHROME B (phyB) mediate the light-suppressed ethylene response in different ways. Here, we review several pivotal advances associated with ethylene-regulated hypocotyl elongation, focusing on the integration of ethylene and light signaling during seedling emergence from the soil.

Keywords: hypocotyl elongation, ethylene signaling, light signaling, seedling emergence, transcriptional activation, protein stability

OPEN ACCESS

Edited by:
Antonio Ferrante,
University of Milan, Italy

Reviewed by:
Anil Kumar Singh,
ICAR-Indian Institute of Agricultural Biotechnology, India
Hao Peng,
Washington State University, USA
Chengwei Yang,
South China Normal University, China
Paul Dijkwel,
Massey University, New Zealand

***Correspondence:**
Rongfeng Huang
rfhuang@caas.cn

Specialty section:
This article was submitted to Plant Physiology, a section of the journal Frontiers in Plant Science

Received: *28 August 2016*
Accepted: *10 January 2017*
Published: *24 January 2017*

Citation:
Yu Y and Huang R (2017) Integration of Ethylene and Light Signaling Affects Hypocotyl Growth in Arabidopsis. Front. Plant Sci. 8:57. doi: 10.3389/fpls.2017.00057

INTRODUCTION

As cell division rarely occurs in the *Arabidopsis* hypocotyl, this system is considered an ideal model for studying cell elongation (Vandenbussche et al., 2005; Boron and Vissenberg, 2014). The hypocotyl is highly responsive to both internal and external cues, such as plant hormones, light, temperature, and gravity (Vandenbussche et al., 2005; Van de Poel et al., 2015). Among these growth regulators, ethylene is special because of its contradictory effect on hypocotyl elongation (Ecker, 1995; Smalle et al., 1997). In the light, the application of ethylene or its precursor 1-aminocyclopropane-1-carboxylic acid (ACC) stimulates hypocotyl elongation, whereas in the dark, ethylene suppresses hypocotyl growth (Zhong et al., 2012; Yu et al., 2013). Additionally, this phenotype suggests a close relationship between ethylene and light signaling in hypocotyl growth.

Ethylene signaling starts with endoplasmic reticulum (ER)-located ethylene receptors (Hua and Meyerowitz, 1998). In the absence of ethylene, ER membrane-located ethylene receptors such as ETHYLENE RESPONSE 1 (ETR1) interacts with and activates the Ser/Thr kinase CONSTITUTIVE RESPONSE 1 (CTR1), which further phosphorylates another ER membrane-located protein ETHYLENE INSENSITIVE 2 (EIN2) (Kieber et al., 1993; Alonso et al., 1999; Ju et al., 2012). The downstream transcription factors EIN3 and EIN3-LIKE 1 (EIL1) are degraded

through the F-box proteins EIN3-BINDING F BOX PROTEIN 1 (EBF1) and EBF2, leading to interruption of the ethylene-induced transcription cascade (Chao et al., 1997; Guo and Ecker, 2003; Potuschak et al., 2003). In the presence of ethylene, the interaction of ETR1 with ethylene molecules deactivates CTR1 and leads to the cleavage of unphosphorylated EIN2 (Ju et al., 2012; Qiao et al., 2012). As a result, a portion of the cleavage product, EIN2C, shuttles into the nucleus to activate the EIN3/EIL1-dependent transcription cascade, while the remaining EIN2C is retained in the cytoplasm and inhibits the translation of EBF1 and EBF2 by binding to their mRNAs (Ju et al., 2012; Qiao et al., 2012; Li et al., 2015; Merchante et al., 2015).

Light is not only an energy source but also one of the most important environmental cues for plant growth and development (Chen et al., 2004). Light signaling is perceived by various photoreceptors and leads to the modulation of downstream transcription factors such as PHYTOCHROME INTERACTING FACTORs (PIFs) and HYPOCOTYL 5 (HY5) (Lau and Deng, 2010). For example, light promotes the translocation of the red photoreceptor phyB into the nucleus to directly interact with PIFs, resulting in PIF phosphorylation and degradation (Lau and Deng, 2010; Leivar and Monte, 2014; Ni et al., 2014). In addition, light reduces the level of nuclear-localized COP1 protein and promotes the stabilization of its target protein HY5 (Osterlund et al., 2000). A recent study proposed that the binding of phyB to SPA inhibits the activity of COP1 (Sheerin et al., 2015). Finally, the protein levels of PIFs and HY5 co-determine the transcription level of genes related to seedling photomorphogenesis in the light (Lau and Deng, 2010).

Hypocotyl length changes dramatically in the early plant growth stage, especially between seed germination and seedling establishment. Recently, some studies investigating the underlying mechanisms of seedling emergence have been published and drawn great attention to this stage (Zhong et al., 2014; Shi et al., 2016a,b). Before emerging from the soil, *Arabidopsis* seedlings undergo skotomorphogenesis with closed and pale cotyledons, an apical hook and a fast-growing hypocotyl in the absence of light. Once they emerge from the soil, seedlings adopt photomorphogenesis with open and green cotyledons, especially a shortened hypocotyl (Zhong et al., 2014). Hypocotyl elongation during seedling emergence involves numerous plant hormone responses to external circumstances, which are coordinated via various pathways. Here, we present an overview of ethylene function during hypocotyl elongation, focusing on the interaction between ethylene and light signaling, especially during seedling emergence.

ETHYLENE HAS DIFFERING EFFECTS ON HYPOCOTYL GROWTH

Ethylene can promote or suppress *Arabidopsis* hypocotyl elongation depending on light conditions (Ecker, 1995; Smalle et al., 1997). In the dark or in low light intensities (<10 $\mu mol/m^2/s$), ethylene acts as a repressor of hypocotyl elongation, whereas in high light intensities or in days with more than 8 h of light, ethylene becomes an activator (Zhong et al., 2012). Furthermore, it was shown that ethylene can promote hypocotyl growth only in red light, not in far red or blue light (Shi et al., 2016b). The function of ethylene in hypocotyl growth is reflected in ethylene mutants as well. For example, ethylene overproduction mutants (*eto1/2/3*) and an ethylene constitutive-response mutant (*ctr1*) show shortened hypocotyls in the dark but elongated ones in the light, and the hypocotyls of ethylene-insensitive mutants (*etr1*, *ein2,* and *ein3 eil1*) exhibit a certain level of shortening in the light (Smalle et al., 1997; Alonso et al., 1999; Zhong et al., 2012; Yu et al., 2013; Shi et al., 2016b). In recent years, several light-signaling elements, including PhyB, PIF3, COP1, and HY5, have been identified to mediate ethylene-regulated hypocotyl elongation (Zhong et al., 2012, 2014; Yu et al., 2013; Shi et al., 2016a,b; **Figure 1**). These findings enable us to better understand how ethylene fine tunes hypocotyl growth under such complicated external environments.

The adverse effect of ethylene on hypocotyl elongation is mediated by the transcription factors PIF3 and ETHYLENE RESPONSE FACTOR 1 (ERF1), which promote hypocotyl elongation in the light and inhibit it in the dark, respectively (Zhong et al., 2012). Although both PIF3 and ERF1 are transcriptionally activated by ethylene through EIN3, their total protein level determines the differing effects of ethylene on hypocotyl growth. In the light, PIF3 protein is rapidly degraded by LIGHT-RESPONSE BRIC-A-BRACK/TRAMTRACK/BROAD (LRB) E3 ligases, whereas ERF1 protein is maintained at a high level (Zhong et al., 2012). Hence, ERF1 induced by ethylene does not function due to an excessive protein level, but PIF3 is sensitively affected by ethylene. Conversely, in the dark, PIF3 protein is saturated, and ethylene-induced ERF1 inhibits hypocotyl elongation (Zhong et al., 2012). Therefore, both ethylene-induced transcriptional control and light-regulated protein accumulation are required in this process. This result might explain why ethylene-promoted hypocotyl elongation requires a certain quantity of light. Recently, another EIN3 target gene, WAVE-DAMPENED 5 (WDL5), was reported to mediate ethylene-inhibited etiolated hypocotyl elongation (Sun et al., 2015; Ma et al., 2016). By binding to cortical microtubules, WDL5 regulates microtubule bundling and microtubule reorientation, finally affecting etiolated hypocotyl elongation (**Figure 1B**). However, the *wdl5* mutant shows a hypocotyl length similar to wild type, regardless of ACC treatment in the light, suggesting that WDL5 does not function in the ethylene-promoted hypocotyl elongation (Sun et al., 2015).

In addition, regulation at the protein level by ethylene has also been found for hypocotyl growth. It was reported that HY5 plays important roles in ethylene-promoted hypocotyl elongation in the light (Yu et al., 2013, **Figure 1A**). HY5 is a native regulator of hypocotyl growth and is controlled at the protein level by the E3 ligase COP1 (Osterlund et al., 2000). In the

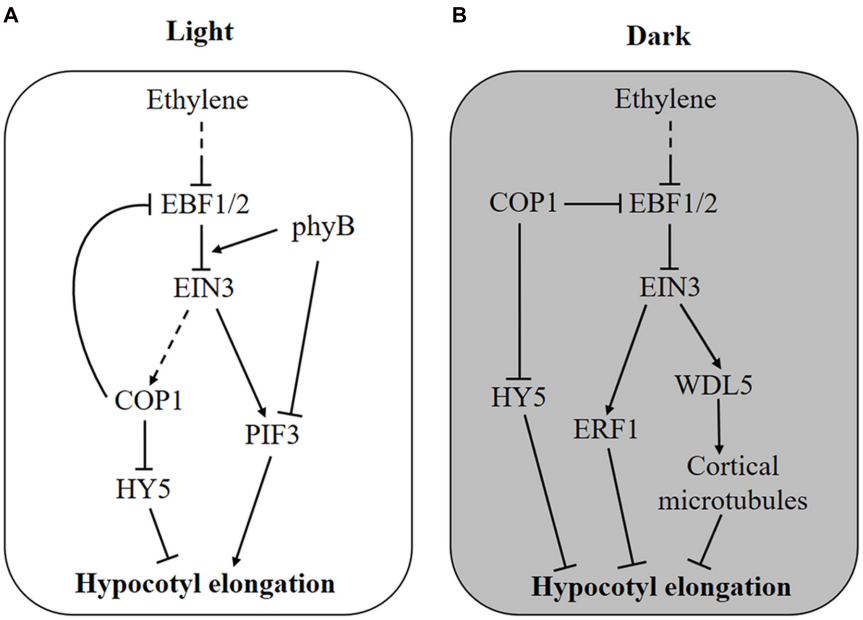

FIGURE 1 | Molecular mechanism of ethylene-regulated hypocotyl growth. (A) In the light, ethylene stimulates hypocotyl elongation via transcriptional activation of *PIF3* and degradation of HY5 protein by promoting the enrichment of nuclear COP1 protein. Feedback is probably generated as COP1 stabilizes EIN3 by degrading the F-box proteins EBF1 and EBF2. Additionally, light-activated phyB attenuates ethylene responses by promoting the interaction of EBF1/2 and EIN3. **(B)** In the dark, COP1 is enriched in the nucleus and promotes the degradation of HY5 and hypocotyl elongation, whereas ethylene counteracts this process by activating the expression of *ERF1* and *WDL5*. When seedlings grow toward the soil surface, COP1 and ethylene production are suppressed by increased light and reduced mechanical pressure, respectively, removing the inhibitory effect of EIN3 on hypocotyl elongation.

dark, COP1 is enriched in the nucleus and interacts with HY5 to promote its degradation, leading to an elongated hypocotyl, whereas in the light, COP1 is translocated out of nucleus so that HY5 protein accumulates to inhibit hypocotyl growth (von Arnim and Deng, 1994; Osterlund et al., 2000). Further experiments proved that light-triggered COP1 movement into the cytoplasm is reversed by ethylene, thus, ethylene stimulates hypocotyl elongation by promoting the nuclear localization of COP1 and HY5 degradation (Yu et al., 2013). Genetic experiments have demonstrated that ethylene-regulated COP1 localization and HY5 stabilization is dependent on EIN3 (Yu et al., 2013).

Interestingly, ethylene signaling is also suppressed by light on the protein level (Shi et al., 2016a,b, **Figure 1**). As an E3 ligase, COP1 directly interacts with EBF1/2 and promotes its degradation by the 26S proteasome, leading to the accumulation of EIN3 protein (Shi et al., 2016a). Thus, light can reduce EIN3 stabilization and ethylene signaling through the inactivation of COP1. Interestingly, once ethylene signaling is activated, nucleus-enriched COP1 is also likely to enhance ethylene signaling (**Figure 1A**). More immediately, photoactivated phyB can bind to both EIN3 and EBF1/2, resulting in enhanced interaction between them and EIN3 degradation (Shi et al., 2016b, **Figure 1A**). It is believed that EIN3 plays an important role in the balance between ethylene and light signaling in hypocotyl growth.

INTERACTIONS BETWEEN ETHYLENE AND LIGHT SIGNALING AFFECT HYPOCOTYL GROWTH DURING SEEDLING EMERGENCE

Seed plants often start life under the soil. Before reaching the light, germinated seedlings initiate signaling related to darkness and mechanical disturbance (Zhong et al., 2014). The absence of light leads to PIF3 accumulation and nucleus-enriched COP1 but HY5 degradation, both of which lead to an elongated hypocotyl so that the seedling can emerge from the soil quickly (Lau and Deng, 2010; Zhong et al., 2012, 2014). In addition, increased ethylene concentrations induced by the depth and texture of soil inhibit hypocotyl elongation (Zhong et al., 2014). In this situation, ethylene inhibits hypocotyl growth by activating EIN3-mediated ERF1 and WDL5 expression (Zhong et al., 2012; Sun et al., 2015; Ma et al., 2016). The suppression of hypocotyl growth by ethylene leads to a longer period of etiolated growth; thus, PIF3, another target of EIN3, is activated to coordinately regulate chlorophyll synthesis (Zhong et al., 2014). Moreover, the *ein3 eil1* double mutant exhibits a lower survival rate under deep and firm soil cover, further indicating that ethylene-regulated hypocotyl growth and etiolated growth are necessary for seedling emergence from soil (Zhong et al., 2014).

As seedlings grow toward the soil surface, ethylene production is reduced with decreased mechanical stress; meanwhile, the gradual increase in light penetrating through the soil will suppress COP1 activity, thus promoting EBF1/2-mediated EIN3 degradation and relieving the inhibitory effect of ethylene on hypocotyl growth (Shi et al., 2016a). Therefore, COP1 plays dual roles in hypocotyl growth during seedling emergence: Under soil cover, COP1 functions to promote hypocotyl elongation by degrading HY5 protein and enhances ethylene signaling through EBF1/2-mediated EIN3 stabilization (Osterlund et al., 2000; Shi et al., 2016a). As the seedling approaches the soil surface, increasing light relieves COP1-stabilized EIN3 protein and gradually counteracts ethylene signaling (Shi et al., 2016a). Although both ethylene and COP1 affect the stability of EIN3 through EBF1/2, they act independently, because ethylene still promotes the accumulation of EIN3 in *cop1* mutant plants (Shi et al., 2016a).

However, once the seedling breaks through the soil surface, it requires rapid changes, including hook opening and cotyledon expansion, which are counteracted by ethylene signaling (Shi et al., 2016b). At this time, photoactivated phyB functions as molecular glue to promote the interaction between EBF1/2 and EIN3, leading to the degradation of EIN3 and immediate cessation of ethylene signaling (Shi et al., 2016b). The gradual COP1-mediated and fast phyB-dependent regulation of EIN3 protein level guarantee successful seedling emergence from the soil with an appropriate hypocotyl length and accomplish de-etiolation in time.

It has been reported that ethylene production induced by flooding in rice promotes stem elongation above the water level to avoid submergence stress (Hattori et al., 2009). In addition, the positive effect of ethylene on hypocotyl elongation in the light suggests that ethylene is probably still required for hypocotyl growth after seedling emergence from the soil. In the light, ethylene promotes the translocation of COP1 into the nucleus and transcriptionally activates PIF3 expression, attenuating light signaling and thus stimulating hypocotyl elongation (Zhong et al., 2012; Yu et al., 2013). Therefore, the opposing effects of ethylene and light signaling occur throughout hypocotyl growth during seedling emergence.

CONCLUSION AND FUTURE PERSPECTIVES

Ethylene-regulated hypocotyl elongation is a good model for studying how cues from endogenous hormones and environmental factors are integrated in the control of plant growth. This mini review aimed to concisely summarize the crosstalk between ethylene and light signaling in the regulation of hypocotyl growth, focusing on detailing the function of ethylene in hypocotyl growth during seedling emergence. Some factors that were not mentioned here, such as temperature and biological rhythm, are also very important for the regulation of hypocotyl growth.

The antagonistic effect of ethylene on hypocotyl elongation occurs due to the transcription factors ERF1, PIF3, HY5, and WDL5 (**Figure 1**). In the light, ethylene promotes hypocotyl growth at both the transcriptional and the protein level: the transcriptional activation of *PIF3* and the degradation of HY5 protein (Zhong et al., 2012; Yu et al., 2013). In the dark, ethylene suppresses hypocotyl elongation by transcriptionally activating ERF1 and WDL5 via EIN3 (Zhong et al., 2012; Sun et al., 2015). In addition, light functions via COP1 and phyB to promote the degradation of EIN3, which plays important roles during seedling emergence (Shi et al., 2016a,b). Under soil cover, hypocotyl growth is promoted by darkness but inhibited by mechanical pressure-induced ethylene. As seedlings approach and break through the soil surface, the EIN3 level is reduced by increased light via COP1 and phyB, leading to the shutdown of ethylene signaling, which guarantees that seedlings transition from growing in a dark soil cover situation to the bright light soil surface (Shi et al., 2016a,b). After the seedling emerges from the soil, light-suppressed hypocotyl growth is stimulated by ethylene. This process is important for plants to resist submergence stress, because flooding-induced ethylene promotes the elongation of rice internodes to escape from submergence damage (Hattori et al., 2009). However, it is still unknown whether and how ethylene participates in normal hypocotyl growth.

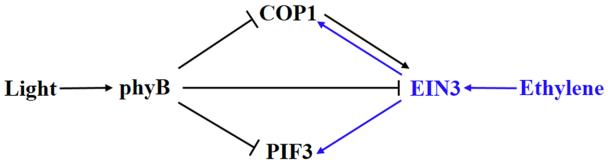

FIGURE 2 | Involvement of elements in the crosstalk between ethylene and light signaling in hypocotyl growth. COP1 and PIF3 are suppressed by light via phyB but activated by ethylene via EBF1/2-EIN3. In turn, ethylene-promoted EIN3 is inhibited by light via COP1 and phyB. Blue and dark indicates ethylene and light signaling, respectively.

In addition to ethylene, other plant hormones such as auxin, gibberellin (GA), and brassinolide (BR) participate in the regulation of hypocotyl growth. Furthermore, inhibitors of auxin transport (1-N-Naphthylphthalamic acid, NPA), auxin biosynthesis (yucasin), auxin perception (α-(phenylethyl-2-one)-indole-3-acetic acid, PEO-IAA), GA biosynthesis (paclobutrazol, PBZ) and BR biosynthesis (brassinazole, BRZ) or mutants related to these processes suppress ethylene-promoted hypocotyl elongation, suggesting that ethylene regulates hypocotyl growth partly through auxin, GA, and BR (Vandenbussche et al., 2007; Liang et al., 2012; Das et al., 2016). However, the crosstalk between ethylene and plant hormones is different in the light and the dark. For example, in the light, ethylene-promoted hypocotyl elongation can be inhibited by treatment with NPA or in auxin-insensitive mutants, whereas in the dark, ethylene still suppresses hypocotyl growth in these mutants or with NPA treatment (Liang et al., 2012; Das et al., 2016). Therefore, a more complicated regulatory network of plant hormones exists for the regulation of hypocotyl growth.

Ethylene and light converge on EIN3, COP1, and PIF3 in the regulation of hypocotyl growth (**Figure 2**). Ethylene-enhanced

EIN3 is inhibited by light through COP1 and phyB. In turn, light-suppressed COP1 and PIF3 can be activated by ethylene (Zhong et al., 2012; Yu et al., 2013; Shi et al., 2016a,b). Therefore, a competitive relationship between ethylene and light signaling is formed by the crosstalk between these elements. An organ-specific, genome-wide investigation of transcriptomic changes in ethylene-promoted and shade-promoted hypocotyl growth demonstrated that a conserved set of transcriptionally regulated genes, especially hormone-related genes, is utilized by plants to modulate hypocotyl growth in response to ethylene and shade (Das et al., 2016). Thus, there might be more elements integrating ethylene and light signaling in hypocotyl growth. Recently, our work indicated that ethylene-promoted COP1 localization in the nucleus affects seed germination under salt stress (Yu et al., 2016), indicating that the interaction between light and ethylene shown in hypocotyl growth probably plays additional roles in other pathways. In any case, the interaction between ethylene and light signaling in hypocotyl growth during seedling emergence is a good example of how plants integrate external signaling and internal hormones.

AUTHOR CONTRIBUTIONS

RH proposed the topic. RH and YY collected the literature, critically assessed the information, and wrote the manuscript together.

ACKNOWLEDGMENT

This work was supported by the National Science Foundation of China (31670280 and 91217303) and the National Basic Research Program of China (2012CB114204).

REFERENCES

Alonso, J. M., Hirayama, T., Roman, G., Nourizadeh, S., and Ecker, J. R. (1999). EIN2, a bifunctional transducer of ethylene and stress responses in *Arabidopsis*. *Science* 284, 2148–2152. doi: 10.1126/science.284.5423.2148

Boron, A. K., and Vissenberg, K. (2014). The *Arabidopsis thaliana* hypocotyl, a model to identify and study control mechanisms of cellular expansion. *Plant Cell Rep.* 33, 697–706. doi: 10.1007/s00299-014-1591-x

Chao, Q., Rothenberg, M., Solano, R., Roman, G., Terzaghi, W., and Ecker, J. R. (1997). Activation of the ethylene gas response pathway in *Arabidopsis* by the nuclear protein ETHYLENE-INSENSITIVE3 and related proteins. *Cell* 89, 1133–1144. doi: 10.1016/S0092-8674(00)80300-1

Chen, M., Chory, J., and Fankhauser, C. (2004). Light signal transduction in higher plants. *Annu. Rev. Genet.* 38, 87–117. doi: 10.1146/annurev.genet.38.072902.092259

Das, D., St Onge, K. R., Voesenek, L. A., Pierik, R., and Sasidharan, R. (2016). Ethylene-and shade-induced hypocotyl elongation share transcriptome patterns and functional regulators. *Plant Physiol.* 172, 718–733. doi: 10.1104/pp.16.00725

Ecker, J. R. (1995). The ethylene signal transduction pathway in plants. *Science* 268, 667–675. doi: 10.1126/science.7732375

Guo, H., and Ecker, J. R. (2003). Plant responses to ethylene gas are mediated by SCF EBF1/EBF2-dependent proteolysis of EIN3 transcription factor. *Cell* 115, 667–677. doi: 10.1016/S0092-8674(03)00969-3

Hattori, Y., Nagai, K., Furukawa, S., Song, X. J., Kawano, R., Sakakibara, H., et al. (2009). The ethylene response factors SNORKEL1 and SNORKEL2 allow rice to adapt to deep water. *Nature* 460, 1026–1030. doi: 10.1038/nature08258

Hua, J., and Meyerowitz, E. M. (1998). Ethylene responses are negatively regulated by a receptor gene family in *Arabidopsis thaliana*. *Cell* 94, 261–271. doi: 10.1016/S0092-8674(00)81425-7

Ju, C., Yoon, G. M., Shemansky, J. M., Lin, D. Y., Ying, Z. I., Chang, J., et al. (2012). CTR1 phosphorylates the central regulator EIN2 to control ethylene hormone signaling from the ER membrane to the nucleus in *Arabidopsis*. *Proc. Natl. Acad. Sci. U.S.A.* 109, 19486–19491. doi: 10.1073/pnas.1214848109

Kieber, J. J., Rothenberg, M., Roman, G., Feldmann, K. A., and Ecker, J. R. (1993). CTR1, a negative regulator of the ethylene response pathway in *Arabidopsis*, encodes a member of the raf family of protein kinases. *Cell* 72, 427–441. doi: 10.1016/0092-8674(93)90119-B

Lau, O. S., and Deng, X. W. (2010). Plant hormone signaling lightens up: integrators of light and hormones. *Curr. Opin. Plant Biol.* 13, 571–577. doi: 10.1016/j.pbi.2010.07.001

Leivar, P., and Monte, E. (2014). PIFs: systems integrators in plant development. *Plant Cell* 26, 56–78. doi: 10.1105/tpc.113.120857

Li, W., Ma, M., Feng, Y., Li, H., Wang, Y., Ma, Y., et al. (2015). EIN2-directed translational regulation of ethylene signaling in *Arabidopsis*. *Cell* 163, 670–683. doi: 10.1016/j.cell.2015.09.037

Liang, X., Wang, H., Mao, L., Hu, Y., Dong, T., Zhang, Y., et al. (2012). Involvement of COP1 in ethylene- and light-regulated hypocotyl elongation. *Planta* 236, 1791–1802. doi: 10.1007/s00425-012-1730-y

Ma, Q., Sun, J., and Mao, T. (2016). Microtubule bundling plays a role in ethylene-mediated cortical microtubule reorientation in etiolated hypocotyls. *J. Cell Sci.* 129, 2043–2051. doi: 10.1242/jcs.184408

Merchante, C., Brumos, J., Yun, J., Hu, Q., Spencer, K. R., Enríquez, P., et al. (2015). Gene-specific translation regulation mediated by the hormone-signaling molecule EIN2. *Cell* 163, 684–697. doi: 10.1016/j.cell.2015.09.036

Ni, W., Xu, S. L., Tepperman, J. M., Stanley, D. J., Maltby, D. A., Gross, J. D., et al. (2014). A mutually assured destruction mechanism attenuates light signaling in *Arabidopsis*. *Science* 344, 1160–1164. doi: 10.1126/science.1250778

Osterlund, M. T., Hardtke, C. S., Wei, N., and Deng, X. W. (2000). Targeted destabilization of HY5 during light-regulated development of *Arabidopsis*. *Nature* 405, 462–466. doi: 10.1038/35013076

Potuschak, T., Lechner, E., Parmentier, Y., Yanagisawa, S., Grava, S., Koncz, C., et al. (2003). EIN3-dependent regulation of plant ethylene hormone signaling by two *Arabidopsis* F box proteins: EBF1 and EBF2. *Cell* 115, 679–689. doi: 10.1016/S0092-8674(03)00968-1

Qiao, H., Shen, Z., Huang, S. S. C., Schmitz, R. J., Urich, M. A., Briggs, S. P., et al. (2012). Processing and subcellular trafficking of ER-tethered EIN2 control response to ethylene gas. *Science* 338, 390–393. doi: 10.1126/science.1225974

Sheerin, D. J., Menon, C., zur Oven-Krockhaus, S., Enderle, B., Zhu, L., Johnen, P., et al. (2015). Light-activated phytochrome A and B interact with members of the SPA family to promote photomorphogenesis in *Arabidopsis* by reorganizing the COP1/SPA complex. *Plant Cell* 27, 189–201. doi: 10.1105/tpc.114.134775

Shi, H., Liu, R., Xue, C., Shen, X., Wei, N., Deng, X. W., et al. (2016a). Seedlings transduce the depth and mechanical pressure of covering soil using COP1 and ethylene to regulate EBF1/EBF2 for soil emergence. *Curr. Biol.* 26, 139–149. doi: 10.1016/j.cub.2015.11.053

Shi, H., Shen, X., Liu, R., Xue, C., Wei, N., Deng, X. W., et al. (2016b). The red light receptor phytochrome B directly enhances substrate-E3 ligase interactions to attenuate ethylene responses. *Dev. Cell* 39, 597–610. doi: 10.1016/j.devcel.2016.10.020

Smalle, J., Haegman, M., Kurepa, J., Van Montagu, M., and Straeten, D. V. (1997). Ethylene can stimulate *Arabidopsis* hypocotyl elongation in the light. *Proc. Natl. Acad. Sci. U.S.A.* 94, 2756–2761. doi: 10.1073/pnas.94.6.2756

Sun, J., Ma, Q., and Mao, T. (2015). Ethylene regulates *Arabidopsis* microtubule-associated protein WDL5 in etiolated hypocotyl elongation. *Plant physiol.* 169, 325–337. doi: 10.1104/pp.15.00609

Van de Poel, B., Smet, D., and Van Der Straeten, D. (2015). Ethylene and hormonal cross talk in vegetative growth and development. *Plant Physiol.* 169, 61–72. doi: 10.1104/pp.15.00724

Vandenbussche, F., Vancompernolle, B., Rieu, I., Ahmad, M., Phillips, A., Moritz, T., et al. (2007). Ethylene-induced *Arabidopsis* hypocotyl elongation is dependent on but not mediated by gibberellins. *J. Exp. Bot.* 58, 4269–4281. doi: 10.1093/jxb/erm288

Vandenbussche, F., Verbelen, J. P., and Van Der Straeten, D. (2005). Of light and length: regulation of hypocotyl growth in *Arabidopsis*. *Bioessays* 27, 275–284. doi: 10.1002/bies.20199

von Arnim, A. G., and Deng, X. W. (1994). Light inactivation of *Arabidopsis* photomorphogenic repressor COP1 involves a cell-specific regulation of its nucleocytoplasmic partitioning. *Cell* 79, 1035–1045. doi: 10.1016/0092-8674(94)90034-5

Yu, Y., Wang, J., Shi, H., Gu, J., Dong, J., Deng, X. W., et al. (2016). Salt stress and ethylene antagonistically regulate nucleocytoplasmic partitioning of COP1 to control seed germination. *Plant Physiol.* 170, 2340–2350. doi: 10.1104/pp.15.01724

Yu, Y., Wang, J., Zhang, Z., Quan, R., Zhang, H., Deng, X. W., et al. (2013). Ethylene promotes hypocotyl growth and HY5 degradation by enhancing the movement of COP1 to the nucleus in the light. *PLoS Genet.* 9:e1004025. doi: 10.1371/journal.pgen.1004025

Zhong, S., Shi, H., Xue, C., Wang, L., Xi, Y., Li, J., et al. (2012). A molecular framework of light-controlled phytohormone action in *Arabidopsis*. *Curr. Biol.* 22, 1530–1535. doi: 10.1016/j.cub.2012.06.039

Zhong, S., Shi, H., Xue, C., Wei, N., Guo, H., and Deng, X. W. (2014). Ethylene-orchestrated circuitry coordinates a seedling's response to soil cover and etiolated growth. *Proc. Natl. Acad. Sci. U.S.A.* 111, 3913–3920. doi: 10.1073/pnas.1402491111

Conflict of Interest Statement: The authors declare that the research was conducted in the absence of any commercial or financial relationships that could be construed as a potential conflict of interest.

frontiers in Plant Science

ORIGINAL RESEARCH
published: 17 June 2016
doi: 10.3389/fpls.2016.00863

The Transcription Factor *AtDOF4.7* Is Involved in Ethylene- and *IDA*-Mediated Organ Abscission in *Arabidopsis*

*Gao-Qi Wang[1], Peng-Cheng Wei[2], Feng Tan[1], Man Yu[3], Xiao-Yan Zhang[1], Qi-Jun Chen[1] and Xue-Chen Wang[1]**

[1] State Key Laboratory of Plant Physiology and Biochemistry, College of Biological Sciences, China Agricultural University, Beijing, China, [2] Rice Research Institution, AnHui Academy of Agricultural Sciences, Hefei, China, [3] Department of Food and Biological Technology, College of Food Science and Nutritional Engineering, China Agricultural University, Beijing, China

Organ abscission is an important plant developmental process that occurs in response to environmental stress or pathogens. In *Arabidopsis*, ligand signals, such as ethylene or *INFLORESCENCE DEFICIENT IN ABSCISSION (IDA)*, can regulate organ abscission. Previously, we reported that overexpression of *AtDOF4.7*, a transcription factor gene, directly suppresses the expression of the abscission-related gene *ARABIDOPSIS DEHISCENCE ZONE POLYGALACTURONASE 2 (ADPG2)*, resulting in a deficiency of floral organ abscission. However, the relationship between *AtDOF4.7* and abscission pathways still needs to be investigated. In this study, we showed that ethylene regulates the expression of *AtDOF4.7*, and the peptide ligand, *IDA* negatively regulates *AtDOF4.7* at the transcriptional level. Genetic evidence indicates that *AtDOF4.7* and *IDA* are involved in a common pathway, and a MAPK cascade can phosphorylate AtDOF4.7 *in vitro*. Further *in vivo* data suggest that AtDOF4.7 protein levels may be regulated by this phosphorylation. Collectively, our results indicate that ethylene regulates *AtDOF4.7* that is involved in the *IDA*-mediated floral organ abscission pathway.

Keywords: abscission, abscission zone, DOF, ethylene, IDA, MAPK, phosphorylation

OPEN ACCESS

Edited by:
Péter Poór,
University of Szeged, Hungary

Reviewed by:
Brad M. Binder,
University of Tennessee-Knoxville, USA
Peter Ulvskov,
Copenhagen University, Denmark

****Correspondence:***
Xue-Chen Wang
xcwang@cau.edu.cn

Specialty section:
This article was submitted to Plant Physiology, a section of the journal Frontiers in Plant Science

Received: *13 January 2016*
Accepted: *01 June 2016*
Published: *17 June 2016*

Citation:
Wang G-Q, Wei P-C, Tan F, Yu M, Zhang X-Y, Chen Q-J and Wang X-C (2016) The Transcription Factor AtDOF4.7 Is Involved in Ethylene- and IDA-Mediated Organ Abscission in Arabidopsis. Front. Plant Sci. 7:863. doi: 10.3389/fpls.2016.00863

INTRODUCTION

Plant floral organ abscission is an important developmentally controlled process. *Arabidopsis thaliana* is an ideal model in which to study organ abscission (Bleecker and Patterson, 1997). In *Arabidopsis*, at the bases of the filaments, petals, and sepals in the floral organ, there are some small, high-density cell layers known as abscission zone (AZ), where the abscission process takes place (Patterson, 2001). The AZ cells perceive the abscission signal and subsequently activate cell wall-degrading proteins. Finally, the pectin-rich middle lamellae of AZ cell walls are dissolved, resulting in the detachment of unwanted organs from the main plant body (Patterson, 2001; Patterson and Bleecker, 2004; Niederhuth et al., 2013a).

Ethylene is thought to temporally regulate floral organ abscission (Jackson and Osborne, 1970; Niederhuth et al., 2013a). Historically, exogenous ethylene treatment has been shown to cause acceleration of abscission (Patterson and Bleecker, 2004; Butenko et al., 2006). Several key components of ethylene signaling, including *ETHYLENE RESPONSE 1 (ETR1) and ETHYLENE*

INSENSITIVE 2 (EIN2), have been found to participate in the regulation of floral organ abscission in *Arabidopsis* (Chang et al., 1993; Patterson and Bleecker, 2004; Butenko et al., 2006). Both the *etr1* and *ein2* ethylene-insensitive mutants exhibit significantly delayed abscission.

Several reports have indicated that abscission can be regulated in an ethylene-independent manner. It was originally found that the important plant hormone auxin could regulate the differentiation of the AZ of the leaf rachis in *Sambucus nigra* through transportation of auxin from the organ distal to the AZ (Osborne and Sargent, 1976; Morris, 1993). In *Arabidopsis*, auxin negatively regulates several polygalacturonases (*PGs*) in the dehiscence zone (DZ) to cause a delay in cell separation (Dal Degan et al., 2001; Ellis et al., 2005). Mutation of *Auxin Response Factor 2 (ARF2)* can lead to a delay in floral organ abscission. Furthermore, the effect of a delay in abscission can be enhanced by mutations in *ARF1*, *ARF2*, *NPH4/ARF7*, and *ARF19* (Ellis et al., 2005; Okushima et al., 2005), suggesting that these overlapping genes regulate auxin-mediated floral organ abscission in an ethylene-independent manner.

Other than phytohormone, signaling peptides also play important roles in the regulation of abscission. In *Arabidopsis*, a short peptide, INFLORESCENCE DEFICIENT IN ABSCISSION (IDA) has a key role in the regulation of floral organ abscission (Butenko et al., 2003; Liu et al., 2013). The *ida* single mutant fails to abscise its floral organs (Butenko et al., 2003), and constitutive expression of *IDA* in *Arabidopsis (35S:IDA)* induces premature organ abscission (Stenvik et al., 2006). Two leucine-rich repeat receptor-like protein kinases (LRR-RLKs), HAE and HSL2, are required for organ abscission. Double mutants for these two genes display organ abscission defects (Jinn et al., 2000; Cho et al., 2008; Stenvik et al., 2008; Niederhuth et al., 2013b). As previously reported, *Arabidopsis* perceives and responds to environmental signals through an interaction between extracellular peptides and plasma membrane-bound RLKs (Stenvik et al., 2008). IDA may act as a ligand binding to the HAE/HSL2 RLK, which transmits the abscission signal to downstream substrates to initiate organ abscission (Cho et al., 2008; Stenvik et al., 2008).

Mitogen-activated protein kinase (MAPK) cascades play crucial roles in regulating various plant responses. There are two MEKs (MKK4 and MKK5) that are involved in floral organ abscission in *Arabidopsis* (Cho et al., 2008). Their downstream target substrates are MPK3 and MPK6 (Ren et al., 2002; Cho et al., 2008). *MKK4* and *MKK5* RNA interference (RNAi) transgenic lines show pleiotropic effects, including organ abscission deficiency, and constitutively active mutants of $MKK4^{DD}$ (T224D/S230D) and $MKK5^{DD}$ (T215D/S221D) that strongly activate endogenous MPK3 and MPK6 can restore abscission in the *ida-2* and *hae hsl2* mutants (Ren et al., 2002; Cho et al., 2008). Although the *mpk3* and *mpk6* single mutants exhibit normal organ abscission, the *mpk3 mpk6* double mutant is lethal (Wang et al., 2007), while functionally inactive forms of *MPK6* are expressed in *mpk3* mutant plants, $mpk3/MPK6^{KR}$ (Lys, the key residue of phosphate transferring, mutated to Arg) or $mpk3/MPK6^{AF}$ (the conserved sites of phosphorylation by MKK, Thr and Tyr, mutated to Ala and Phe, respectively), survive and display loss of organ abscission (Cho et al., 2008). Furthermore, MPK6 has reduced kinase activity in *hae hsl2* and *ida-2* mutants. These results demonstrate that MPK6, but not MPK3, plays a dominant role in the regulation of floral organ abscission (Cho et al., 2008). In the ethylene-independent abscission pathway, IDA couples with HAE and HSL2, activating the downstream MAPK cascade to phosphorylate the substrates and initiate the separation of the AZ cells (Cho et al., 2008; Shi et al., 2011; Niederhuth et al., 2013a,b).

Generally, ethylene regulates the timing of floral organ abscission, while *IDA* influences the degree of abscission. The physiological process of floral organ abscission is generally divided into four stages: (1) differentiation and formation of the AZ; (2) transduction of abscission signals; (3) activation of the abscission process; and (4) post-abscission transdifferentiation (Patterson, 2001; Niederhuth et al., 2013a). The second and third stages of abscission, in which ethylene, IDA, HAE/HSL2, MAPKs and PGs play important roles, have been well-described (Niederhuth et al., 2013a). However, further investigation is needed to understand how these two stages are linked.

We previously reported that AtDOF4.7, a member of the *Arabidopsis* DNA binding with one finger (DOF) transcription factor family, functions as an abscission inhibitor to directly regulate the expression of *ADPG2*, which encodes a cell wall-hydrolyzing enzyme, to initiate cell separation (Wei et al., 2010). Nevertheless, it is still an open question whether *AtDOF4.7* is a factor that acts between the second and third stage of abscission, potentially in a cascade of abscission signals that are transmitted from the second to the third stage through *AtDOF4.7*. In the present study, we demonstrated that *AtDOF4.7* is an additional component of the *IDA*-mediated abscission pathway, and that it is regulated by ethylene and *IDA*. Our results suggest that *AtDOF4.7* is regulated by both the ethylene-dependent and ethylene-independent pathways.

MATERIALS AND METHODS

Plant Material

Arabidopsis thaliana (Columbia-0 ecotype) plants were grown at 22°C in a growth chamber under a 16 h light/8 h dark photoperiod and a light intensity of 120 μmol m^{-2} s^{-1}.

The $Promoter_{AtDOF4.7}$*::GUS* line (Wei et al., 2010) was crossed with *ein2-1*, *etr1-1*, and *ida-2* (SALK_133209), and *35S:AtDOF4.7 (S107;* Wei et al., 2010) was crossed with *35S:IDA* and $GVG\text{-}MKK5^{DD}$ (Ren et al., 2002). The sequencing primers used to verify hybrids are presented in online Supplementary Table S1. Kanamycin (50 μg ml^{-1}) was employed to select the *35S:IDA* and *ida-2* mutant plants (Butenko et al., 2003; Stenvik et al., 2006). Hygromycin B (25 μg ml^{-1}) was used to select plants overexpressing *AtDOF4.7*.

The locus codes of all genes investigated or discussed in this article are listed below: *AtDOF4.7, At4g38000; EIN2, At5g03280; ETR1, At1g66340; IDA, At1g68765; HAE, At4g28490; HSL2, AT5G65710; MKK4, At1g51660; MKK5, At3g21220; MPK3, At3g45640; MPK6, At2g43790; ACTIN2, At3g18780;* and *ADPG2, AT2G41850*.

Ethylene and DEX Treatments

Promoter$_{AtDOF4.7}$::GUS/ein2-1 seeds were germinated on 1/2 Murashige and Skoog (MS) medium containing 5 μM ACC in the dark for 3 days to select for ethylene-insensitive mutants.

To analyze the expression pattern of *AtDOF4.7* in response to ethylene, 4-weeks-old *Promoter$_{AtDOF4.7}$::GUS* plants were maintained in an air-tight growth chamber with or without ethylene at 10 ppm (10 $\mu l\, l^{-1}$) for 3 days prior to the analysis.

To observe the abscission phenotype of *S107/MKK5^{DD}*, siliques of *S107/MKK5^{DD}* plants were treated with or without 0.02 μM DEX (Sigma, USA) for 24 h to induce *MKK5^{DD}* expression. The siliques were then photographed with a Cannon G12 camera. Detached leaves from *S107/MKK5^{DD}* plants were immersed in 15 μM DEX for various times prior to western blotting. Each treatment was repeated at least three times.

β-Glucuronidase (GUS) Assay

β-Glucuronidase (GUS) gene expression was analyzed by staining different flower positions along the inflorescence as described previously (Wei et al., 2010). Histochemical GUS staining in the AZ cells of siliques was observed with an Olympus SZX16-DP72 stereo microscope system.

Quantitative Real-Time and Semi-quantitative RT-PCR

For semi-quantitative RT-PCR analysis, total RNA samples were extracted from *Arabidopsis* siliques using the RNeasy® Plant Mini Kit (Qiagen, Germany), and the RNA was reversely transcribed into cDNA with a Reverse Transcription System (Promega, USA). Semi-quantitative RT-PCR assays were run in a MJ Mini Personal Thermal Cycler (Bio-Rad, USA) with 25 thermal cycles. *ACTIN2* (*At3g18780*) was employed as an internal control.

For quantitative real-time RT-PCR (qRT-PCR) analysis, total RNA was extracted from whole flowers and siliques, and qRT-PCR assays were run using the 7500 Real-Time PCR System (ABI, USA). After normalization to an internal control (*ACTIN2*; Charrier et al., 2002), the relative levels of gene expression were calculated via the Delta-Delta Ct ($2^{-\Delta\Delta Ct}$) method (Livak and Schmittgen, 2001). All primers are given in online Supplementary Table S2. Each relative gene expression assay was repeated at least three times.

Yeast Two-Hybrid Experiment and BiFc

A yeast two-hybrid (Y2H) experiment was performed as described previously (Wei et al., 2010). Cells that had been co-transformed with the *pAD-GAL4-AtDOF4.7* (Wei et al., 2010) and *pBD-GAL4-MPK3/MPK6* constructs (Xu et al., 2008) were cultured and transferred to 5 mM 3-AT medium lacking Trp, Leu, His, and Ade, followed by incubation at 28°C for 3 days. Living yeast colonies were photographed with a Cannon G12 camera.

The bimolecular fluorescence complementation (BiFc) assay (Walter et al., 2004), co-transformation of *pUC-SPYCE-MPK3/MPK6* and *pUC-SPYNE-AtDOF4.7* (Miao et al., 2006) and examination of YFP fluorescence were all performed as described previously (Walter et al., 2004).

Preparation of Recombinant Proteins

Escherichia coli cells (strains BL21 and DE3) were transformed with the *MPK3/6*-pET30a(+)-His and *MKK5^{DD}*-pET28a(+)-FLAG constructs and then incubated as described previously (Liu and Zhang, 2004). His-tagged MPK3/6 recombinant proteins and FLAG-tagged MKK5^{DD} recombinant proteins were purified as described elsewhere (Xu et al., 2008). The *AtDOF4.7* CDS was cloned into pMal-c2x (NEB, USA) in frame with the N-terminal MBP tag, and the construct was transformed into the *E. coli* strain Rosetta (DE3). Recombinant protein expression was induced with 0.1 mM isopropylthio-β-galactoside (IPTG) for 8 h at 18°C. The MBP-tagged protein was purified using amylose resin (NEB, USA) according to the manufacturer's instructions.

Protein Extraction and Western Blotting Assay

Total protein was extracted from *Arabidopsis* silique tissues as described previously (Liu et al., 2007). The protein concentration was determined with a Bio-Rad protein assay kit (Bio-Rad, USA), using bovine serum albumin (BSA) as the standard. For western blotting assay, total protein extracts from each sample (10 μg per gel lane) were separated on 12% SDS-polyacrylamide gels. After electrophoresis, the proteins were electro-transferred to PVDF membranes (Millipore, USA). The membranes were subsequently incubated with an anti-Flag antibody (Cell Signaling, 1:10,000 dilution), washed, and then incubated with HRP-conjugated goat anti-rabbit IgG as a secondary antibody (1:10,000 dilution). The resultant protein bands were visualized by treating the membrane with the Immobilon™ Western Chemiluminescent HRP Substrate (Millipore, USA), following the manufacturer's instructions. Bands intensities in the western blots were compared using ImageJ software.

Phosphorylation of AtDOF4.7 *In Vitro*

Recombinant MPK3 (3.2 μg) and MPK6 proteins (5.7 μg) were activated by incubation with recombinant MKK5^{DD} (0.36 μg) in the presence of 50 μM ATP in 50 μl of reaction buffer (20 mM Hepes, pH 7.5, 10 mM $MgCl_2$, and 1 mM DTT) at 25°C for 1 h. The activated MPK3 and MPK6 proteins were then used to phosphorylate the AtDOF4.7 protein (1.86 μg, 1:16 enzyme:substrate ratio) in the same reaction buffer containing 25 μM ATP and [γ-^{32}P] ATP at 25°C for 30 min, according to Liu and Zhang (2014). The reaction was stopped by the addition of SDS gel-loading buffer. Using the Mini-PROTEAN® Tetra System (Bio-Rad, USA), the samples were separated via electrophoresis on a 10% SDS-polyacrylamide gel at a constant 120 V. The gel was then dried under vacuum, and the phosphorylated AtDOF4.7 was visualized through autoradiography. Primary anti-His (TIANGEN, China) and anti-Flag (Cell Signaling Technology, USA) antibodies were used to verify the presence of the corresponding proteins in the phosphorylation buffer. Pre-stained protein markers (Fermentas, USA) were employed to calculate the molecular masses of the phosphorylated proteins.

RESULTS

Ethylene Regulates the Expression of *AtDOF4.7*

A previous study indicated that overexpression of *AtDOF4.7* induces abscission defects in an ethylene-independent manner, although the flowers can perceive ethylene, suggesting that *AtDOF4.7* might not be a direct target of early ethylene-independent signal transduction (Wei et al., 2010). To investigate the role of *AtDOF4.7* downstream of the early abscission pathway, we examined the expression pattern of $Promoter_{AtDOF4.7}$*::GUS* in the mutants with ethylene-insensitive and ethylene-independent abscission deficiencies.

In the earlier report, the first flower showing visible white petals was referred as flower position 1 and then counted downward along the inflorescence in sequence (Wei et al., 2010). We initially crossed a plant carrying a single-copy of the $Promoter_{AtDOF4.7}$*::GUS* construct with *A. thaliana* Col-0 (wild-type). The *GUS* expression pattern in the $Promoter_{AtDOF4.7}$*::GUS* plant was similar to that reported previously (**Figure 1A**). *GUS* expression was observed in the AZ cells at flower position 4, while at position 20, *GUS* expression from the *AtDOF4.7* promoter could scarcely be detected in the AZ cells.

The $Promoter_{AtDOF4.7}$*::GUS* plants were then crossed with the ethylene-insensitive mutant *ein2-1*. The expression pattern of $Promoter_{AtDOF4.7}$*::GUS* in the *ein2-1* mutant was altered temporally (**Figures 1B,D** and Supplementary Figure S3B), although spatial expression was similar to that of the wild type (WT). *GUS* expression was first observed at position 8 and continued to accumulate until reaching its maximum level at position 14. At position 20, *GUS* expression was still detectable in the AZ cells (**Figure 1B**).

The expression pattern of $Promoter_{AtDOF4.7}$*::GUS* in the *etr1-1* mutant was also examined, and we found that the temporal expression pattern was altered in this mutant as well (Supplementary Figure S1). *GUS* expression was detectable at later flower positions than in $Promoter_{AtDOF4.7}$*::GUS/ein2-1* flowers and was faintly visible at position 10. Expression was clearly observed at position 20. In addition, the profile of the spatial expression of *AtDOF4.7* in the *etr1-1* mutant was similar to that in *ein2-1* (**Figure 1B** and Supplementary Figure S1).

Temporally, the expression of $Promoter_{AtDOF4.7}$*::GUS* in AZ cells in the ethylene-insensitive *ein2-1* and *etr1-1* mutants was remarkably delayed compared with that in WT. Because, flower abscission is also delayed in the inflorescences of the *ein2-1* and *etr1-1* mutants (Butenko et al., 2003; Patterson and Bleecker, 2004), we concluded that ethylene can influence *AtDOF4.7* expression. To confirm this finding, we placed transgenic plants expressing $Promoter_{AtDOF4.7}$*::GUS* in an air-tight chamber containing 10 ppm ethylene gas, which can accelerate organ abscission. Compared with the $Promoter_{AtDOF4.7}$*::GUS* plants that were exposed to air (in the absence of ethylene), *GUS* expression was detected earlier at flower position 1 in the presence of ethylene (Supplementary Figure S2). The time-course of $Promoter_{AtDOF4.7}$*::GUS* expression was shortened by ethylene treatment. These experimental results indicated that ethylene can influence the timing of *AtDOF4.7* expression, and the time-course of *AtDOF4.7* expression could be relevant to organ abscission.

AtDOF4.7 Is a Component of the *IDA*-Mediated Abscission Pathway Underlying Abscission

In the *IDA*-mediated abscission pathway in *Arabidopsis*, IDA binds as a ligand to the RLKs HAE and HSL2 (Stenvik et al., 2008). Some cytoplasmic effectors, such as MKK4, MKK5, MPK3, and MPK6, function together to control cell separation during abscission (Cho et al., 2008). As reported previously, IDA can control the intensity of organ abscission (Butenko et al., 2003; Stenvik et al., 2006). To further determine whether the expression of *AtDOF4.7* is regulated by *IDA* at the transcriptional level, we crossed a $Promoter_{AtDOF4.7}$*::GUS* transgenic plant with the *ida-2* (Col-0) mutant. The temporal expression pattern of $Promoter_{AtDOF4.7}$*::GUS* was unaltered in the AZ cells of the siliques in the *ida-2* background and was similar to that of *AtDOF4.7* in the WT background (**Figures 1A,C**). However, qRT-PCR showed that the relative expression levels of *AtDOF4.7* from flower positions 6 to 10 were significantly higher in the *ida-2* background that in WT (**Figure 1D** and Supplementary Figure S3A). These data suggested that *IDA* negatively regulates the expression of *AtDOF4.7* at the transcriptional level.

To confirm the hypothesis that *IDA* and *AtDOF4.7* are involved in a common pathway, we crossed an *AtDOF4.7*-overexpressing line (*S107*) with *35S:IDA* in the Col-0 background, which shows early abscission of the flowers at position 3 (Stenvik et al., 2006). Semi-quantitative RT-PCR demonstrated that both the *AtDOF4.7* and *IDA* genes were overexpressed in the siliques of *S107/35S:IDA* plants (**Figure 2A**). The *S107/35S:IDA* lines showed that the floral organ abscission defect phenotype was similar to that in *S107* plants (**Figures 2D,E**). Most notably, although the transcript levels of *IDA* were higher than that of *AtDOF4.7* in *S107/35S:IDA* lines, from which the floral organs could not shed (**Figures 2A,E**). This data suggested that *AtDOF4.7* might be epistatic to *IDA*. The flowers of WT plants exhibited normal abscission at position 6 (**Figure 2B**). After abscission beginning at position 6, excessive secretion of arabinogalactan protein (AGP) was observed in the AZ cells of the flowers of *35S:IDA* plants (Stenvik et al., 2006; **Figure 2C**). However, there was no AGP observed in the AZ cells of siliques of *S107/35S:IDA* plants, even after the floral parts on the fruits were removed from positions 6 to 20 (**Figure 2F**). These results support the hypothesis that *IDA* and *AtDOF4.7* act in a common pathway to regulate abscission, and *IDA* might be in the upstream abscission pathway.

Interaction of AtDOF4.7 with MPK3 and MPK6 *In Vivo* and *In Vitro*

A previous study found that the $MPK6^{KR}$*/mpk3* mutant, but not *mpk3* or *mpk6* single mutants, showed a defective floral abscission phenotype (Cho et al., 2008). Because MPK3 and MPK6 are key components of the *IDA*-mediated pathway underlying abscission, to understand how *AtDOF4.7* is regulated

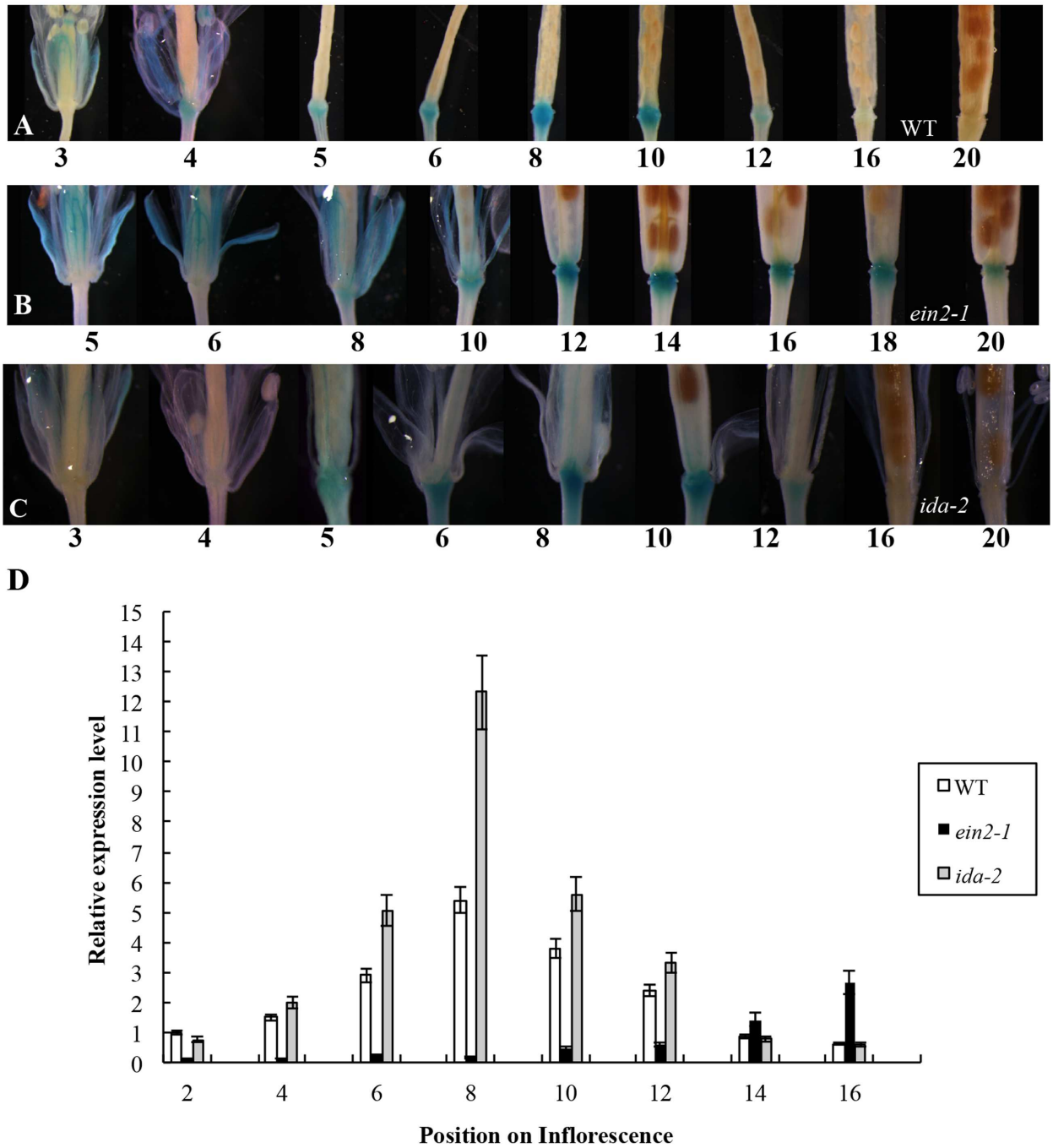

FIGURE 1 | Time-course of *Promoter*$_{AtDOF4.7}$*::GUS* expression in WT, *ein2-1*, and *ida-2* flower AZ cells. (A) *Promoter*$_{AtDOF4.7}$*::GUS* expression in *A. thaliana* Col-0 (WT). *GUS* expression was first observed at flower position 4, and reached the maximum level of expression from positions 6 to 8. After flower position 10, expression was reduced, and no expression was detected from positions 16 to 20. Four-weeks-old plants were used for *GUS* staining. **(B)** *Promoter*$_{AtDOF4.7}$*::GUS* expression in the *ein2-1* mutant. *GUS* staining was first observed at flower position 8, and accumulated to its maximum level from positions 12 to 14. After position 16, *GUS* staining declined, and little staining was observed at position 20. **(C)** *Promoter*$_{AtDOF4.7}$*::GUS* expression in the *ida-2* mutant. The expression pattern was similar to that seen in WT. **(D)** Relative expression of *AtDOF4.7* at different flower positions in WT, *ein2-1* and *ida-2* plants. Flower position 2 in WT was the control. The temporal expression pattern of *AtDOF4.7* in WT was the same as in *ida-2*. However, the relative expression of *AtDOF4.7* in *ida-2* was higher from positions 6 to 10 than in WT. At flower positions 14 and 16, the expression level of *AtDOF4.7* in the *ida-2* background was similar to WT. Compared with WT, the temporal expression pattern of *AtDOF4.7* was delayed in the *ein2-1* mutant. The relative expression level of *AtDOF4.7* in *ein2-1* from positions 2 to 12 was significantly lower than in WT. After position 12, the relative expression level of *AtDOF4.7* was elevated >2-fold in the *ein2-1* compared with WT. Relative mRNA levels were averaged over three biological replicates and are shown with the SD (error bars).

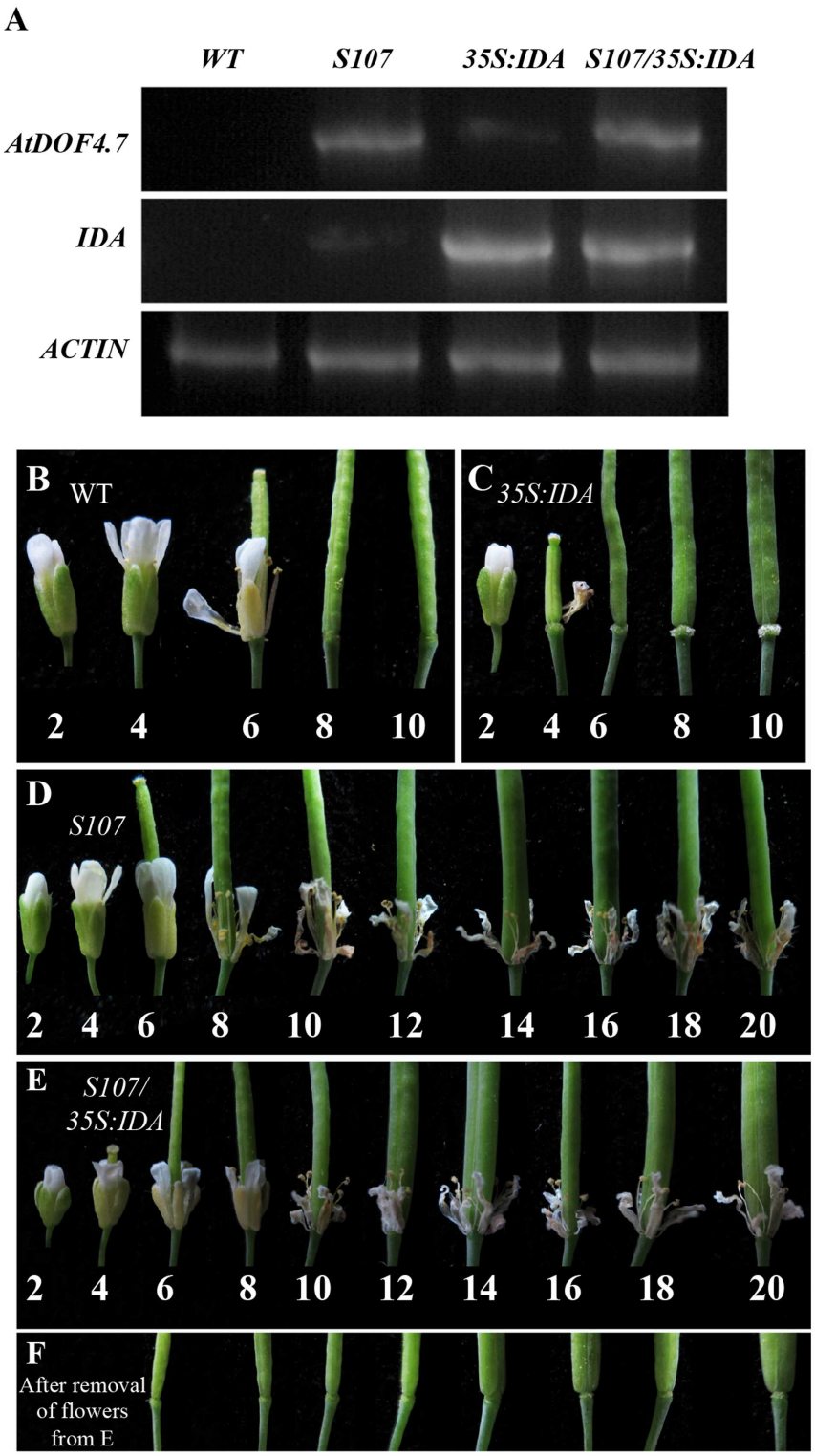

FIGURE 2 | *S107/35S:IDA* plants are deficient in floral organ abscission. (A) RT-PCR analysis of *AtDOF4.7* and *IDA* expression in *S107/35S:IDA* transgenic flowers. *ACTIN2* (*At3g18780*) was used as the internal control gene. Both *AtDOF4.7* and *IDA* were overexpressed in *S107/35S:IDA* siliques. **(B)** Normal abscission phenotype in WT. Organ abscission began at position 6 and ended at position 8. **(C)** Premature abscission at position 4 in *35S:IDA* flowers. After abscission, white substrate AGPs accumulated around AZ cells at position 6 and, apparently, at position 10. **(D)** Organ abscission defects from positions 2 to 20 in *S107* flowers. **(E)** Organ abscission defects in *S107/35S:IDA* flowers from positions 2 to 20. **(F)** After removal of the petals and filaments in **(E)** from positions 6 to 20, no AGPs were detected around the AZ cells in *S107/35S:IDA* siliques. The abscission phenotypes of 4-weeks-old plants are shown in **(B–E)**.

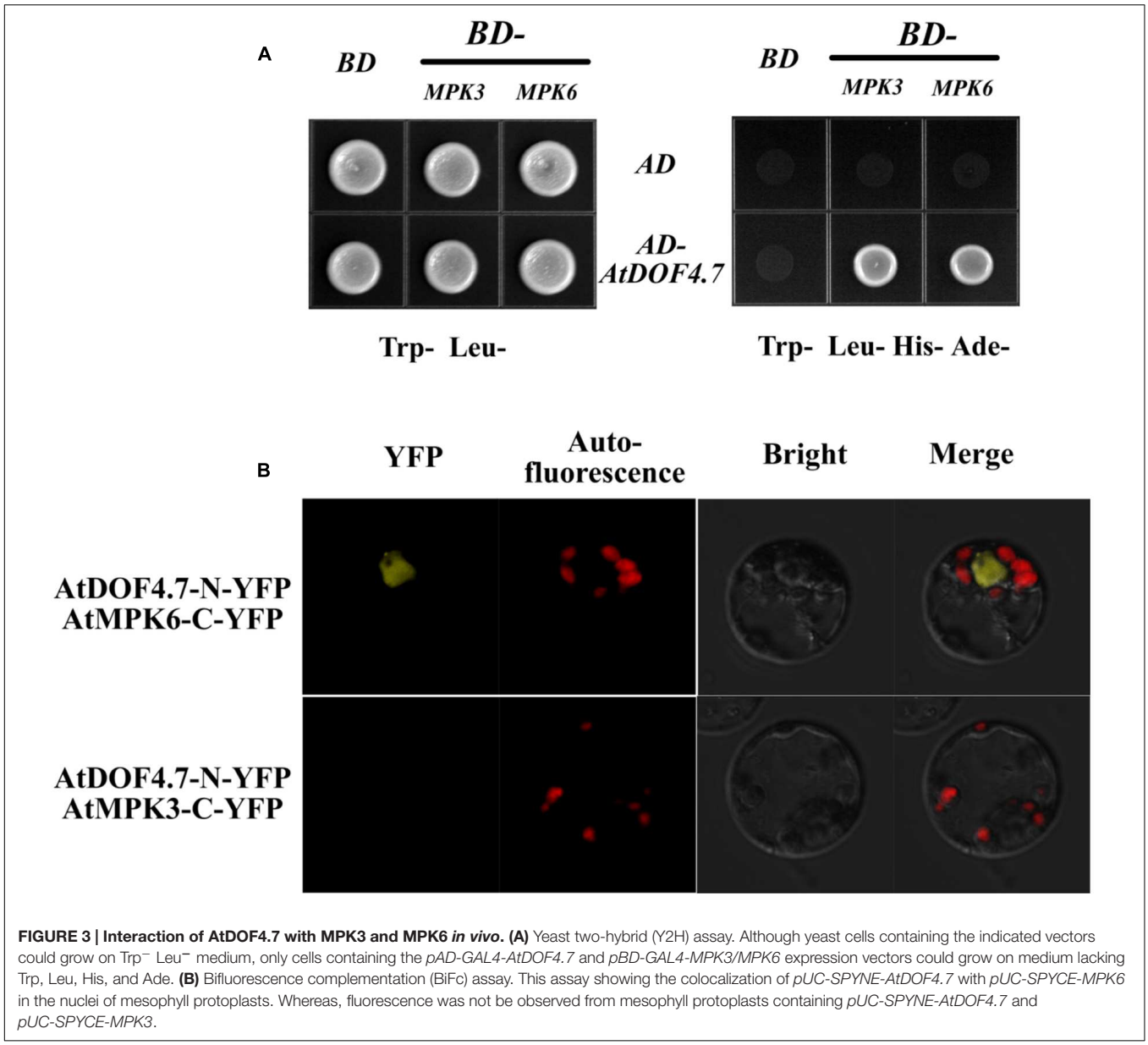

FIGURE 3 | Interaction of AtDOF4.7 with MPK3 and MPK6 *in vivo*. (A) Yeast two-hybrid (Y2H) assay. Although yeast cells containing the indicated vectors could grow on Trp$^-$ Leu$^-$ medium, only cells containing the *pAD-GAL4-AtDOF4.7* and *pBD-GAL4-MPK3/MPK6* expression vectors could grow on medium lacking Trp, Leu, His, and Ade. **(B)** Bifluorescence complementation (BiFc) assay. This assay showing the colocalization of *pUC-SPYNE-AtDOF4.7* with *pUC-SPYCE-MPK6* in the nuclei of mesophyll protoplasts. Whereas, fluorescence was not be observed from mesophyll protoplasts containing *pUC-SPYNE-AtDOF4.7* and *pUC-SPYCE-MPK3*.

by the *MAPKs*, we performed yeast two-hybrid (Y2H) and BiFC assays to determine whether AtDOF4.7 interacts with MPK3 or MPK6. The Y2H experiment showed that the transformed yeast cells were able to grow on 5 mM 3-AT medium lacking Trp, Leu, His, and Ade, suggesting an interaction between *pAD-GAL4-AtDOF4.7* and *pBD-GAL4-MPK3/MPK6 in vivo* (**Figure 3A**). To further confirm the interaction of AtDOF4.7 with MPK3 or MPK6, we constructed the BiFC vectors *pUC-SPYNE-AtDOF4.7* and pUC-SPYCE-MPK3/6, and the two constructs were co-transformed into *Arabidopsis* mesophyll protoplasts. The cells were then observed using laser fluorescence confocal microscopy; which showed that *pUC-SPYNE-AtDOF4.7* and pUC-SPYCE-MPK6 interact in the nuclei (**Figure 3B**). However, the yellow fluorescence could not be detected from the cells containing *pUC-SPYNE-AtDOF4.7* and pUC-SPYCE-MPK3. The BiFC results strongly suggested that AtDOF4.7 and MPK6 physically interact in *Arabidopsis*.

Phosphorylation of AtDOF4.7 by MPK3 and MPK6 *In Vitro*

Potential sites for MAPK phosphorylation are Ser/Thr residues followed by a Pro residue (Meng et al., 2013). There are two such sites in the *AtDOF4.7* sequence: Ser-34-Pro and Ser-104-Pro (**Figure 4A**). To determine whether MPK3/MPK6 is able to carry out phosphorylation of AtDOF4.7, we obtained the recombinant proteins MBP-tagged AtDOF4.7, His_6-tagged MPK3 and MPK6, and FLAG-tagged $MKK5^{DD}$ for phosphorylation assays. Following activation by purified FLAG-tagged recombinant $MKK5^{DD}$, either His_6-tagged MPK3 or MPK6 strongly phosphorylated AtDOF4.7 (**Figure 4B**).

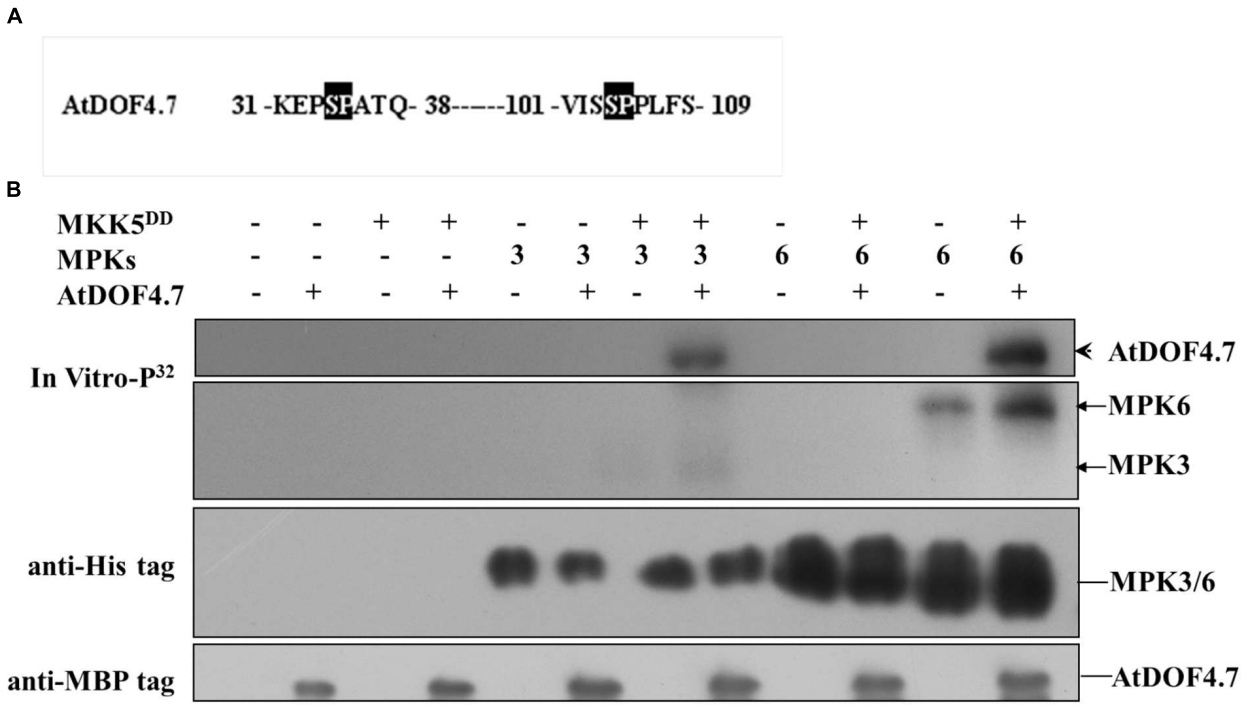

FIGURE 4 | Phosphorylation of AtDOF4.7 by activated MPK3 and MPK6 *in vitro*. (A) Partial sequences of the AtDOF4.7 protein. Black boxes indicate the conserved MAPK phosphorylation sites; **(B)** MPK3 and MPK6 phosphorylate the MBP-tagged AtDOF4.7 recombinant protein *in vitro*. The arrowhead indicates the phosphorylated AtDOF4.7 protein. Bands indicated by the arrows are MPK3 or MPK6 phosphorylated by MKK5^{DD}. Anti-His and anti-MBP tag primary antibodies were used to detect the corresponding proteins in the phosphorylation buffer.

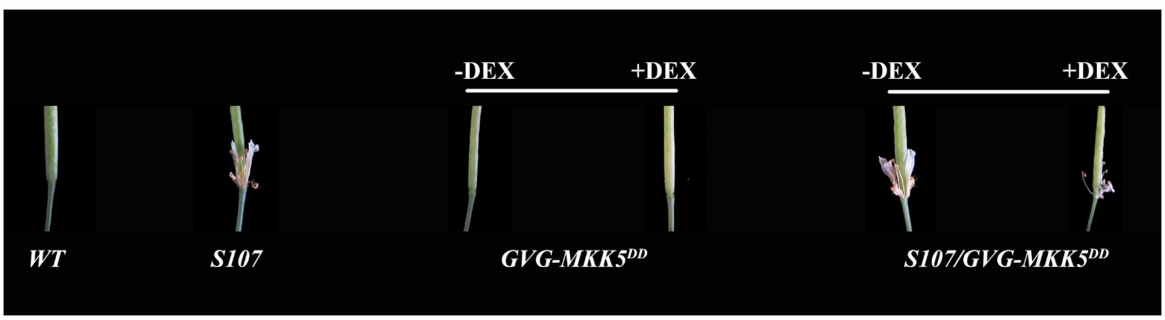

FIGURE 5 | *AtDOF4.7* is involved in abscission mediated by the *MAPK* cascade. The defective abscission defective phenotype of *S107* was partly restored in *S107/GVG-MKK5^{DD}* plants following DEX treatment. All representative siliques are from flower position 10 of WT, *S107*, *GVG-MKK5^{DD}*, and *S107/GVG-MKK5^{DD}* plants.

Constitutively Activated *MKK5* Cannot Rescue Organ Abscission in the *S107* Line

MKK4 and MKK5 are homologs found in *Arabidopsis* that act upstream of MPK3 and MPK6 in the regulation of floral abscission (Cho et al., 2008). Plants expressing the constitutively activated forms of *MKK4* or *MKK5* under the control of a steroid-inducible promoter (designated *GVG-MKK4^{DD}* or *GVG-MKK5^{DD}*) had a normal abscission phenotype (Ren et al., 2002; Cho et al., 2008). To assess the biological function of the phosphorylation of AtDOF4.7 by MAPK, we crossed the *AtDOF4.7*-overexpressing *S107* line with a *GVG-MKK5^{DD}* transgenic plant to obtain *S107/MKK5^{DD}*. We examined the siliques of *S107/MKK5^{DD}* plants at flower position 10, which is the position at which WT flowers shed completely. We observed that the organ abscission phenotype of *S107/MKK5^{DD}* was not rescued; however, small parts of the flowers were shed from the siliques of *S107/MKK5^{DD}* plants after dexamethasone (DEX) treatment (**Figure 5**). These data indicated that the two genes act in a common pathway to regulate abscission in *Arabidopsis*, and *MKK5* may negatively regulate *AtDOF4.7*.

A phosphorylation-dependent mechanism is involved in protein degradation (Willems et al., 1999; Feng et al., 2004; Yoo et al., 2008). Therefore, a western blot assay was performed to determine the changes in AtDOF4.7 protein levels in *S107/MKK5*^{DD} plants treated with DEX. The siliques of *S107/MKK5*^{DD} at flower position 10 were induced with 15 μM DEX after 10 h, resulting in greatly decreased AtDOF4.7 protein levels (**Figure 6A**). The grayscale ratio of AtDOF4.7 protein bands on the western blot were measured, and the results showed that the changes in the levels of the AtDOF4.7 protein exhibited significant differences after 10 and 12 h of DEX treatment compared with the untreated control (**Figure 6B**). ACTIN2 was used as an internal protein control, and was detected with an anti-ACTIN2 antibody. These data suggest that activated MKK5 following DEX induction could affect AtDOF4.7 at the protein level in the *S107/MKK5*^{DD} plant, providing one explanation for how organ abscission is partially recovered in *S107/MKK5*^{DD} lines.

DISCUSSION

A recent report shows that ethylene manipulates the rate of abscission, rather than directly inducing it (Niederhuth et al., 2013a). It has been indicated that several ethylene mutants of *Arabidopsis*, such as those harboring the ethylene receptor ethylene-response 1 (*etr1*) and ethylene-insensitive 2 (*ein2*) point mutations, displayed a delay of floral organ abscission (Bleecker et al., 1988; Guzman and Ecker, 1990; Patterson and Bleecker, 2004), however, the formation and differentiation of the AZ cells are not affected in these ethylene-insensitive mutants. Up to now, the genetic mechanism through which ethylene regulates abscission is still unclear. Here, we suggest that ethylene accelerates organ abscission in *Arabidopsis* by regulating the time-course of the expression of *AtDOF4.7* (**Figure 1B**, Supplementary Figures S1, S2, and S3B). To make a preliminary demonstration for this hypothesis, we analyzed the region 3000 bp upstream of the *AtDOF4.7* promoter sequence and found that the promoter sequence of *AtDOF4.7* contained

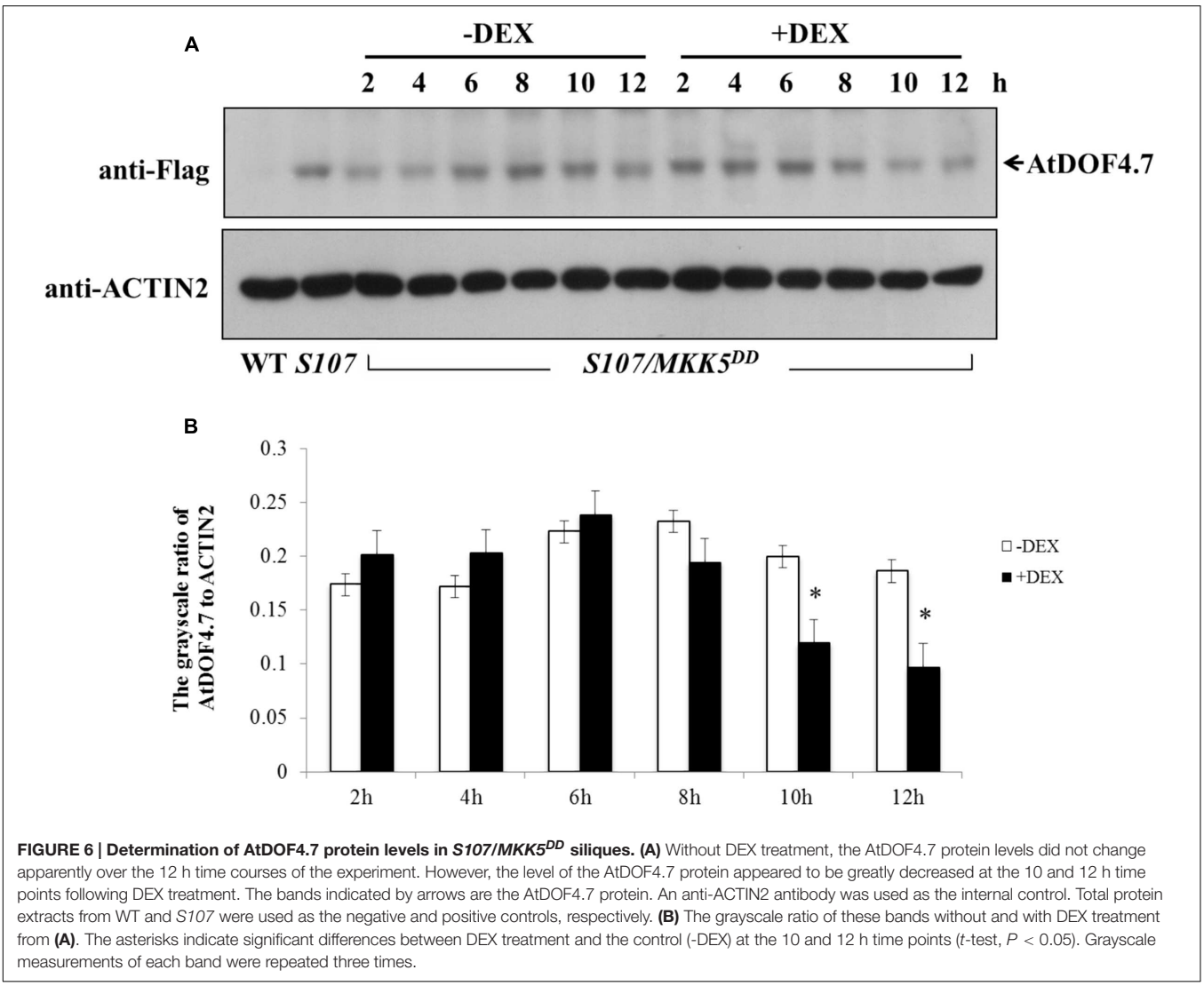

FIGURE 6 | Determination of AtDOF4.7 protein levels in *S107/MKK5*^{DD} siliques. (A) Without DEX treatment, the AtDOF4.7 protein levels did not change apparently over the 12 h time courses of the experiment. However, the level of the AtDOF4.7 protein appeared to be greatly decreased at the 10 and 12 h time points following DEX treatment. The bands indicated by arrows are the AtDOF4.7 protein. An anti-ACTIN2 antibody was used as the internal control. Total protein extracts from WT and *S107* were used as the negative and positive controls, respectively. **(B)** The grayscale ratio of these bands without and with DEX treatment from **(A)**. The asterisks indicate significant differences between DEX treatment and the control (-DEX) at the 10 and 12 h time points (*t*-test, $P < 0.05$). Grayscale measurements of each band were repeated three times.

three *cis*-acting elements in this region: a GCC box (-1702 to -1696 bp), a CRT/DRE element (-1029 to -1023 bp) and several EIN3-binding sites (EBS, ATGTA; Supplementary Figure S4). The first two elements can be recognized by Ethylene Response Factors (ERFs) in response to ethylene (GCC) and drought stress (CRT/DRE), while the last element can be recognized by EIN3. Most notably, in the ethylene signaling pathway, ERFs are critical factors responding to ethylene, which can be activated by EIN3 (Ohme-Takagi and Shinshi, 1995; Chao et al., 1997). Based on these observations, *AtDOF4.7* might be a potential target gene of ERFs or EIN3 in response to ethylene. From the data presented in this study, we hypothesize that the regulation of *AtDOF4.7* is related to ethylene, but it is unclear that how ethylene affecting the expression of *AtDOF4.7* at the transcriptional level.

Auxin, as an antagonist of ethylene, negatively regulates the cell wall-degrading enzymes, leading to a delay in cell separation via an ethylene-independent mechanism. Additionally, the AZ patterning is not affected in *arf2* mutants (Ellis et al., 2005). It has been reported that auxin may regulate *IDA* and *HAE/HSL2* to control cell separation (Kumpf et al., 2013; Niederhuth et al., 2013a). Thus, we can put forward the hypothesis that both ethylene and auxin may be involved in the regulation of *AtDOF4.7* expression.

Previous data indicated that the delay of abscission caused by *AtDOF4.7* overexpression could not be accelerated by exogenous ethylene, suggesting the potential involvement of ethylene-independent regulation. Therefore, we investigated the relationship between *IDA* and *AtDOF4.7* in this study. In the mutant of *IDA*, the expression pattern of *AtDOF4.7* promoter was not significantly altered (**Figure 1C**), while the transcript level of *AtDOF4.7* was found to be up-regulated at the same flower positions in the *ida-2* mutant (**Figure 1D**). *IDA* is involved in the regulation of *ADPG2* expression in the AZ to control cell separation during floral organ abscission (González-Carranza et al., 2002, 2007; Ogawa et al., 2009; González-Carranza et al., 2012), and its expression is suppressed by overexpression of *AtDOF4.7* in the regulation of abscission (Wei et al., 2010). Our results indicated that the overexpression of *AtDOF4.7* could inhibit the early abscission caused by *IDA* overexpressing lines (**Figure 2**). Therefore, this result provides a hint that *AtDOF4.7* might participate in the regulation of *PGs* by *IDA*. It has been well-established that MAPK cascades (mainly MKK4/MKK5-MPK3/MPK6 pathway) are involved in downstream of *IDA*-mediated abscission pathway. Thus, the relations between the *MAPK*s and *AtDOF4.7* were also investigated. First, we found two abscission-related MPKs, MPK3 and MPK6, could interact with AtDOF4.7 in yeast. The *in vitro* assay indicated that both MPK3 and MPK6 could phosphorylated AtDOF4.7, and the signal of MPK6 was apparently stronger than that of MPK3. This is consistent with the stronger *in vivo* interaction between MPK6 and AtDOF4.7, suggesting MPK6 may play more important role in the regulation of abscission. Second, our results indicated that the *AtDOF4.7*-induced abortion of abscission could be partially rescued by MKK activation (**Figure 5**), and the protein level of AtDOF4.7 is down-regulated following the MKK5 activation. Thus, it is reasonable to speculate that the AtDOF4.7 may act as a direct target of MPKs in the abscission regulation. Taken together, our results suggested that the *AtDOF4.7* should also involved in downstream of the *IDA*-*MAPK*-mediated abscission pathway.

CONCLUSION

AtDOF4.7, as a negative regulator in floral organ abscission, is regulated by the ethylene-dependent and ethylene-independent abscission pathways. It is suggested that *AtDOF4.7* might be regulated by ethylene, and also by *IDA*, which represses expression of *AtDOF4.7*. Nevertheless, the relationship between phosphorylation and ethylene signaling remains unclear. A previous study showed that phosphorylated MPK3/6 activated by MKK4/5 further phosphorylates ERF6 to regulate defense gene induction and fungal resistance ((Meng et al., 2013). Therefore, it is worthwhile to explore whether the phosphorylation of ERFs by MPK3/6 in the regulation of *AtDOF4.7* occurs in response to ethylene. Further detailed biochemical and genetic analyses will allow us to gain a better understanding of the importance of AtDOF4.7 phosphorylation and ethylene responses in plant organ abscission.

AUTHOR CONTRIBUTIONS

G-QW, P-CW, FT, MY, and X-YZ performed the research; G-QW, P-CW, FT, Q-JC, and X-CW analyzed the data; G-QW, P-CW, and X-CW designed the research, G-QW and X-CW wrote the article with contributions from G-QW, P-CW, FT, and MY.

FUNDING

This work was supported by grants from the National Basic Research Program of China [No.2012CB114204], the National Natural Science Foundation of China [No.31100216], and the Ministry of Agriculture Transgenic Major Project [No.2009ZX08009020-002].

ACKNOWLEDGMENTS

We thank Prof. Ming Yuan and Prof. Dong-Tao Ren (China Agricultural University, China) for critical reading of this manuscript. We thank Prof. Dong-Tao Ren for providing the seeds of *GVG-MKK5^{DD}* (Col), the pBD-GAL4-*MPK3/MPK6* yeast-two hybrid vectors and the MKK5^{DD} FLAG-tagged and MPK3/MPK6 His-tagged fusion proteins, Reidunn B. Aalen (University of Oslo, Norway) for providing the seeds of *ida-2* (Col) mutant and *35S:IDA* (Col), and Michael Walter (Universität Tübingen, Germany) for providing the BiFc vectors.

SUPPLEMENTARY MATERIAL

The Supplementary Material for this article can be found online at: http://journal.frontiersin.org/article/10.3389/fpls.2016.00863

REFERENCES

Bleecker, A. B., Estelle, M. A., Somerville, C., and Kende, H. (1988). Insensitivity to ethylene conferred by a dominant mutation in *Arabidopsis thaliana*. *Science* 241, 1086–1089. doi: 10.1126/science.241.2869.1086

Bleecker, A. B., and Patterson, S. E. (1997). Last exit: senescence, abscission, and meristem arrest in *Arabidopsis*. *Plant Cell* 9, 1169–1179. doi: 10.1105/tpc.9.7.1169

Butenko, M. A., Patterson, S. E., Grini, P. E., Stenvik, G. E., Amundsen, S. S., Mandal, A., et al. (2003). Inflorescence deficient in abscission controls floral organ abscission in *Arabidopsis* and identifies a novel family of putative ligands in plants. *Plant Cell* 15, 2296–2307. doi: 10.1105/tpc.014365

Butenko, M. A., Stenvik, G. E., Alm, V., Saether, B., Patterson, S. E., and Aalen, R. B. (2006). Ethylene-dependent and -independent pathways controlling floral abscission are revealed to converge using promoter::reporter gene constructs in the ida abscission mutant. *J. Exp. Bot.* 57, 3627–3637. doi: 10.1093/jxb/erl130

Chang, C., Kwok, S. F., Bleecker, A. B., and Meyerowitz, E. M. (1993). *Arabidopsis* ethylene-response gene ETR1: similarity of product to two-component regulators. *Science* 262, 539–544. doi: 10.1126/science.8211181

Chao, Q., Rothenberg, M., Solano, R., Roman, G., Terzaghi, W., and Ecker, J. R. (1997). Activation of the ethylene gas response pathway in *Arabidopsis* by the nuclear protein ETHYLENE-INSENSITIVE3 and related proteins. *Cell* 89, 1133–1144. doi: 10.1016/S0092-8674(00)80300-1

Charrier, B., Champion, A., Henry, Y., and Kreis, M. (2002). Expression profiling of the whole *Arabidopsis* shaggy-like kinase multigene family by real-time reverse transcriptase-polymerase chain reaction. *Plant Physiol.* 130, 577–590. doi: 10.1104/pp.009175

Cho, S. K., Larue, C. T., Chevalier, D., Wang, H., Jinn, T. L., Zhang, S., et al. (2008). Regulation of floral organ abscission in *Arabidopsis thaliana*. *Proc. Natl. Acad. Sci. U.S.A.* 105, 15629–15634. doi: 10.1073/pnas.0805539105

Dal Degan, F., Child, R., Svendsen, I., and Ulvskov, P. (2001). The cleavable N-terminal domain of plant endopolygalacturonases from CLADE B may be involved in a regulated secretion mechanism. *J. Biol. Chem.* 276, 35297–35304.

Ellis, C. M., Nagpal, P., Young, J. C., Hagen, G., Guilfoyle, T. J., and Reed, J. W. (2005). AUXIN RESPONSE FACTOR1 and AUXIN RESPONSE FACTOR2 regulate senescence and floral organ abscission in *Arabidopsis thaliana*. *Development* 132, 4563–4574. doi: 10.1242/dev.02012

Feng, J., Tamaskovic, R., Yang, Z., Brazi, D. P., Merlo, A., Hess, D., et al. (2004). Stabilization of MDM2 via decreased ubiquitination is mediated by protein kinase. *J. Biol. Chem.* 279, 35510–35517. doi: 10.1074/jbc.M404936200

González-Carranza, Z. H., Elliott, K. A., and Roberts, J. A. (2007). Expression of polygalacturonases and evidence to support their role during cell separation processes in *Arabidopsis thaliana*. *J. Exp. Bot.* 58, 3719–3730. doi: 10.1093/jxb/erm222

González-Carranza, Z. H., Shahid, A. A., Zhang, L., Liu, Y., Ninsuwan, U., and Roberts, J. A. (2012). A novel approach to dissect the abscission process in *Arabidopsis*. *Plant Physiol.* 160, 1342–1356. doi: 10.1104/pp.112.205955

González-Carranza, Z. H., Whitelaw, C. A., Swarup, R., and Roberts, J. A. (2002). Temporal and spatial expression of a polygalacturonase during leaf and flower abscission in oilseed rape and *Arabidopsis*. *Plant Physiol.* 128, 534–543. doi: 10.1104/pp.010610

Guzman, P., and Ecker, J. R. (1990). Exploiting the triple response of *Arabidopsis* to identify ethylene-related mutants. *Plant Cell* 2, 513–523. doi: 10.1105/tpc.2.6.513

Jackson, M. B., and Osborne, D. J. (1970). Ethylene, the natural regulator of leaf abscission. *Nature* 225, 1019–1022. doi: 10.1038/2251019a0

Jinn, T. L., Stone, J. M., and Walker, J. C. (2000). HAESA, an *Arabidopsis* leucine-rich repeat receptor kinase, controls floral organ abscission. *Genes Dev.* 14, 108–117. doi: 10.1101/gad.14.1.108

Kumpf, R. P., Shi, C. L., Larrieu, A., Sto, I. M., Butenko, M. A., Peret, B., et al. (2013). Floral organ abscission peptide IDA and its HAE/HSL2 receptors control cell separation during lateral root emergence. *Proc. Natl. Acad. Sci. U.S.A.* 110, 5235–5240. doi: 10.1073/pnas.1210835110

Liu, B., Butenko, M. A., Shi, C. L., Bolivar, J. L., Winge, P., Stenvik, G. E., et al. (2013). NEVERSHED and INFLORESCENCE DEFICIENT IN ABSCISSION are differentially required for cell expansion and cell separation during floral organ abscission in *Arabidopsis thaliana*. *J. Exp. Bot.* 64, 5345–5357. doi: 10.1093/jxb/ert232

Liu, H., Wang, Y., Xu, J., Su, T., Liu, G., and Ren, D. (2007). Ethylene signaling is required for the acceleration of cell death induced by the activation of AtMEK5 in *Arabidopsis*. *Cell Res.* 18, 422–432. doi: 10.1038/cr.2008.29

Liu, Y., and Zhang, S. (2004). Phosphorylation of 1-aminocyclopropane-1-carboxylic acid synthase by MPK6, a stress-responsive mitogen-activated protein kinase, induces ethylene biosynthesis in *Arabidopsis*. *Plant Cell* 16, 3386–3399. doi: 10.1105/tpc.104.026609

Livak, K. J., and Schmittgen, T. D. (2001). Analysis of relative gene expression data using real-time quantitative PCR and the 2(-Delta Delta C(T)) method. *Methods* 25, 402–408. doi: 10.1006/meth.2001.1262

Meng, X., Xu, J., He, Y., Yang, K. Y., Mordorski, B., Liu, Y., et al. (2013). Phosphorylation of an ERF transcription factor by *Arabidopsis* MPK3/MPK6 regulates plant defense gene induction and fungal resistance. *Plant Cell* 25, 1126–1142. doi: 10.1105/tpc.112.109074

Miao, Y., Lv, D., Wang, P., Wang, X. C., Chen, J., Miao, C., et al. (2006). An *Arabidopsis* glutathione peroxidase functions as both a redox transducer and a scavenger in abscisic acid and drought stress responses. *Plant Cell* 18, 2749–2766. doi: 10.1105/tpc.106.044230

Morris, D. A. (1993). The role of auxin in the apical regulation of leaf abscission in cotton (*Gossypium hirsutum* L.). *J. Exp. Bot.* 44, 807–814. doi: 10.1093/jxb/44.4.807

Niederhuth, C. E., Cho, S. K., Seitz, K., and Walker, J. C. (2013a). Letting go is never easy: abscission and receptor-like protein kinases. *J. Integr. Plant Biol.* 55, 1251–1263. doi: 10.1111/jipb.12116

Niederhuth, C. E., Patharkar, O. R., and Walker, J. C. (2013b). Transcriptional profiling of the *Arabidopsis* abscission mutant hae hsl2 by RNA-Seq. *BMC Genomics* 14:37. doi: 10.1186/1471-2164-14-37

Ogawa, M., Kay, P., Wilson, S., and Swain, S. M. (2009). *ARABIDOPSIS* DEHISCENCE ZONE POLYGALACTURONASE1 (ADPG1), ADPG2, and QUARTET2 are polygalacturonases required for cell separation during reproductive development in *Arabidopsis*. *Plant Cell* 21, 216–233. doi: 10.1105/tpc.108.063768

Ohme-Takagi, M., and Shinshi, H. (1995). Ethylene-inducible DNA binding proteins that interact with an ethylene-responsive element. *Plant Cell* 7, 173–182. doi: 10.1105/tpc.7.2.173

Okushima, Y., Mitina, I., Quach, H. L., and Theologis, A. (2005). AUXIN RESPONSE FACTOR 2 (ARF2): a pleiotropic developmental regulator. *Plant J.* 43, 29–46. doi: 10.1111/j.1365-313X.2005.02426.x

Osborne, D. J., and Sargent, J. A. (1976). The positional differentiation of abscission zones during the development of leaves of Sambucus nigra and the response of the cells to auxin and ethylene. *Planta* 132, 197–204. doi: 10.1007/BF00388903

Patterson, S. E. (2001). Cutting loose. Abscission and dehiscence in *Arabidopsis*. *Plant Physiol.* 126, 494–500. doi: 10.1104/pp.126.2.494

Patterson, S. E., and Bleecker, A. B. (2004). Ethylene-dependent and -independent processes associated with floral organ abscission in *Arabidopsis*. *Plant Physiol.* 134, 194–203. doi: 10.1104/pp.103.028027

Ren, D., Yang, H., and Zhang, S. (2002). Cell death mediated by MAPK is associated with hydrogen peroxide production in *Arabidopsis*. *J. Biol. Chem.* 277, 559–565. doi: 10.1074/jbc.M109495200

Shi, C. L., Stenvik, G. E., Vie, A. K., Bones, A. M., Pautot, V., Proveniers, M., et al. (2011). *Arabidopsis* class I KNOTTED-like homeobox proteins act downstream in the IDA-HAE/HSL2 floral abscission signaling pathway. *Plant Cell* 23, 2553–2567. doi: 10.1105/tpc.111.084608

Stenvik, G. E., Butenko, M. A., Urbanowicz, B. R., Rose, J. K., and Aalen, R. B. (2006). Overexpression of INFLORESCENCE DEFICIENT IN ABSCISSION activates cell separation in vestigial abscission zones in *Arabidopsis*. *Plant Cell* 18, 1467–1476. doi: 10.1105/tpc.106.042036

Stenvik, G. E., Tandstad, N. M., Guo, Y., Shi, C. L., Kristiansen, W., Holmgren, A., et al. (2008). The EPIP peptide of INFLORESCENCE DEFICIENT IN ABSCISSION is sufficient to induce abscission in *Arabidopsis* through the receptor-like kinases HAESA and HAESA-LIKE2. *Plant Cell* 20, 1805–1817. doi: 10.1105/tpc.108.059139

Walter, M., Christina, C., Katia, S., Oliver, B., Katrin, W., Christian, N., et al. (2004). Visualization of protein interactions in living plant cells using bimolecular fluorescence complementation. *Plant J.* 40, 428–438. doi: 10.1111/j.1365-313X.2004.02219.x

Wang, H., Ngwenyama, N., Liu, Y., Walker, J. C., and Zhang, S. (2007). Stomatal development and patterning are regulated by environmentally responsive

mitogen-activated protein kinases in *Arabidopsis*. *Plant Cell* 19, 63–73. doi: 10.1105/tpc.106.048298

Wei, P. C., Tan, F., Gao, X. Q., Zhang, X. Q., Wang, G. Q., Xu, H., et al. (2010). Overexpression of AtDOF4.7, an *Arabidopsis* DOF family transcription factor, induces floral organ abscission deficiency in *Arabidopsis*. *Plant Physiol.* 153, 1031–1045. doi: 10.1104/pp.110.153247

Willems, A. R., Goh, T., Taylor, L., Chernushevich, I., Shevchenko, A., and Tyers, M. (1999). SCF ubiquitin protein ligases and phosphorylation-dependent proteolysis. *Philos. Trans. R. Soc. Lond. B. Biol. Sci.* 354, 1533–1550. doi: 10.1098/rstb.1999.0497

Xu, J., Li, Y., Wang, Y., Liu, H., Lei, L., Yang, H., et al. (2008). Activation of MAPK KINASE 9 induces ethylene and camalexin biosynthesis and enhances sensitivity to salt stress in *Arabidopsis*. *J. Biol. Chem.* 283, 26996–27006. doi: 10.1074/jbc.M801392200

Yoo, S. D., Cho, Y. H., Tena, G., Xiong, Y., and Sheen, J. (2008). Dual control of nuclear EIN3 by bifurcate MAPK cascades in C2H4 signalling. *Nature* 451, 789–795. doi: 10.1038/nature06543

Conflict of Interest Statement: The authors declare that the research was conducted in the absence of any commercial or financial relationships that could be construed as a potential conflict of interest.

frontiers in Physiology

ORIGINAL RESEARCH
published: 13 September 2016
doi: 10.3389/fphys.2016.00405

Growing Different *Lactuca* Genotypes Aeroponically within a Tropical Greenhouse—Cool Rootzone Temperatures Decreased Rootzone Ethylene Concentrations and Increased Shoot Growth

Tsui-Wei Choong[1], *Jie He*[1]*, *Sing K. Lee*[1] and *Ian C. Dodd*[2]

[1] Natural Sciences and Science Education, National Institute of Education, Nanyang Technological University, Singapore, Singapore, [2] Lancaster Environment Centre, Lancaster University, Lancaster, UK

Temperate crops cannot grow well in the tropics without rootzone cooling. As cooling increased production costs, this experiment aimed to study the growth of various *Lactuca* genotypes and propose possible ways of reducing these costs, without compromising productivity. A recombinant inbred line (RIL) of lettuce and its parental lines (*L. serriola* and *L. sativa* "Salinas") were grown aeroponically in a tropical greenhouse under 24°C cool (C) or warm fluctuating 30–36°C ambient (A) rootzone temperature (RZT). Their roots were misted with Netherlands standard nutrient solution for 1 min, at intervals of either 5 min (A5, C5) or 10 min (A10, C10) in attempting to reduce electricity consumption and production costs. Lower mortality and higher productivity were observed in all genotypes when grown in C-RZT. Higher shoot fresh weight was observed under C5 than C10, for the RIL and *L. serriola*. Since "Salinas" had similar shoot fresh weight at both C-RZ treatments, this may indicate it is more sensitive to RZT than water availability. Under A-RZ treatments, higher carotenoid content, with correspondingly higher nonphotochemical quenching, was observed in A10 for the RIL and "Salinas." Further, total chlorophyll content was also highest at this RZ treatment for the RIL though photochemical quenching was contrastingly the lowest. Cumulatively, productivity was compromised at A10 as the RIL seemed to prioritize photoprotection over efficiency in photosynthesis, under conditions of higher RZT and lower water availability. Generally, higher RZ ethylene concentrations accumulated in A10 and C10 than A5 and C5, respectively—probably due to spray frequency exerting a greater effect on RZ ethylene accumulation than RZT. In the C5 RZ treatment, lowest RZ ethylene concentration corresponded with highest shoot fresh weight. As such, further research on ethylene (in)sensitivity and water use efficiency could be conducted to identify *Lactuca* cultivars that are better suited for growth in the tropics, so as to allay production costs with reduced cooling and spray intervals.

Keywords: spray intervals, SLA, chlorophyll, carotenoid, NPQ, qP, ETR

OPEN ACCESS

Edited by:
Nafees A. Khan,
Aligarh Muslim University, India

Reviewed by:
Noushina Iqbal,
Jamia Hamdard University, India
Carlos Lucena,
University of Córdoba, Spain

***Correspondence:**
Jie He
jie.he@nie.edu.sg

Specialty section:
This article was submitted to Plant Physiology, a section of the journal Frontiers in Physiology

Received: *04 July 2016*
Accepted: *29 August 2016*
Published: *13 September 2016*

Citation:
Choong T-W, He J, Lee SK and Dodd IC (2016) Growing Different Lactuca Genotypes Aeroponically within a Tropical Greenhouse—Cool Rootzone Temperatures Decreased Rootzone Ethylene Concentrations and Increased Shoot Growth. Front. Physiol. 7:405. doi: 10.3389/fphys.2016.00405

INTRODUCTION

As roots are more thermosensitive than shoots (Tachibana, 1982; Thompson et al., 1998; Sakamoto and Suzuki, 2015), temperate and subtropical crops have been successfully grown in a tropical greenhouse by cooling only their roots (Lee et al., 1994; Choong, 1998; He and Lee, 1998; He et al., 2001). Taking advantage of the innately high specific heat capacity of water, aeroponic systems use small volumes of chilled nutrient solution to lower RZTs to conditions that are ideal for the proliferation of these temperate and subtropical crops (Lee, 1993). However, this cooling inflates production costs. As such, this research ventures to better understand the growth characteristics of different *Lactuca* genotypes in attempting to lower production costs without compromising productivity.

Lactuca serriola L., the wild-type ancestor of cultivated lettuce (*Lactuca sativa* L.) (Durst, 1929; Kesseli et al., 1991; Harlan, 1992) is a drought tolerant winter annual (Werk and Ehleringer, 1985) well-adapted to Europe (Kesseli et al., 1991), nontropical parts of Eurasia and North Africa (Kirpicznikov, 1964; Jeffrey, 1975; Ferakova, 1976), North America, and South Africa (Zohary, 1991). As cultivated lettuce is a temperate plant, growing it under tropical conditions decreased head biomass and quality (He and Lee, 1998; He et al., 2001; He, J. et al., 2009; Choong et al., 2013). He and Lee (1998) obtained lettuce that was at least four times heavier when grown in C-RZT of 15–25°C than A-RZT (26–41°C), in a tropical greenhouse where aerial temperatures reached a maximum of 41°C at midday. He, J. et al. (2009) similarly reported increased total leaf number and shoot fresh mass of lettuce plants grown in 20°C-RZT when compared to plants in A-RZT. The low productivity of lettuce growing in such warm conditions has been correlated with reduced root growth (Kaspar and Bland, 1992; He and Lee, 1998; Choong et al., 2013), where the roots cannot adequately supply water and nutrients to the shoot (He et al., 2001; Dodd, 2005), thereby limiting photosynthesis (He et al., 2001). Decreased root fresh weight also correlated with root morphological traits including decreased total root length, root surface area, and number of root tips (i.e., branching) in A-RZT (Choong et al., 2013). These poorly developed root systems affect shoot growth as root-sourced signals that regulate shoot growth are transmitted via the xylem (Freundl et al., 1998; Dodd, 2005). Greater temperature tolerance of some accessions of *L. serriola* (Argyris et al., 2008) offers the possibility of minimizing shoot growth inhibition caused by A-RZT.

Salisbury and Ross (1992) reported that high air temperatures deleteriously impaired photosynthesis, while high irradiance also decreased photosynthetic rates (He et al., 2001; Barker et al., 2002; He and Lee, 2004) since excess photon energy caused photoinactivation of photosystem II (Björkman and Powles, 1984). As a result, higher nonphotochemical quenching, demonstrating greater amounts of energy being dissipated as heat (He et al., 2015), and lower electron transport rate were observed when growing lettuce in A-RZT than 20°C-RZT (He and Lee, 2004). Chronic photoinhibition in A-RZT plants was associated with a 20% reduction in chlorophyll content (He, 2009) and such reductions have been proposed to provide protection by reducing photon absorption (Verhoeven et al., 1997). Thus, plants grown at aerial temperatures of 25°C were less green and had thinner leaves than those grown at 15°C (Dale, 1965). Chlorophyll loss has further been related to environmental stress, where variations in chlorophyll/carotenoid ratios have been reported to be good indicators of plant stress (Hendry and Price, 1993). Further, Rubisco—the key photosynthetic enzyme—and other carbon metabolism enzymes were also temperature-sensitive, thereby impacting growth (Berry and Raison, 1981). As such, high RZT and light intensity compromise productivity by affecting various physiological mechanisms.

Plants synthesize ethylene, a gaseous plant hormone, and release it into the atmosphere during their normal growth and development. Regulating root growth (Ruzicka et al., 2007), low exogenous ethylene concentrations also stimulate vegetative growth (Pierik et al., 2006). However, enhanced ethylene concentrations have frequently been measured in plants exposed to environmental stresses (Abeles et al., 1992; Morgan and Drew, 1997; Lin et al., 2009), and ethylene can inhibit stem elongation (Abeles et al., 1992) and leaf expansion (Lee and Reid, 1997) without directly affecting leaf gas exchange (Pallaghy and Raschke, 1972; Woodrow et al., 1989) or photosynthesis (Abeles et al., 1992). Moreover, ethylene decreased net carbon gain indirectly by inducing leaf epinasty which decreased light interception (Woodrow and Grodzinski, 1989; He, C. J. et al., 2009). Under ambient conditions, increasing ethylene concentrations were correlated with decreased carbon dioxide assimilation and growth (He, C. J. et al., 2009). Indeed, applying ACC to aeroponically grown lettuce (*Lactuca sativa* cv. Baby Butterhead) at A-RZT in a tropical greenhouse decreased stomatal conductance, leaf relative water content, photosynthetic CO_2 assimilation, shoot and root biomass compared with plants grown at 20°C-RZT (Qin et al., 2007). Since the immediate precursor of ethylene (ACC: 1-aminocyclopropane-1-carboxylic acid) is synthesized in the roots (Dodd, 2005) and ACC synthase activity increases with temperature (Ainscough et al., 1992), it is reasonable to suggest that higher amounts of endogenous ethylene may limit root (and shoot) growth at A-RZT. This experiment examines RZ ethylene accumulation in relation to the growth and photosynthetic characteristics of lettuce, whilst varying spray intervals and RZT in the aeroponic system, as an approach toward reducing production costs.

Abbreviations: A, ambient; ACC, 1-aminocyclopropane-1-carboxylic acid; C, cool; Chl, chlorophyll; FW, fresh weight; RIL, recombinant inbred line; RZ, rootzone; RZT, rootzone temperature; SLA, specific leaf area.

MATERIALS AND METHODS

Plant Materials and Culture Methods

Seeds of maternal *L. sativa* L. "Salinas" and paternal *L. serriola* accession UC96US23 (Argyris et al., 2005), together with an F_{10} RIL were germinated on wet filter paper in a petri dish. This thermotolerant RIL was selected based upon previous research carried out (Choong et al., 2013). Five days after germination, seedlings were inserted into polyurethane cubes and left to acclimatize in ambient tropical greenhouse conditions

for 7 days before being transplanted into the aeroponic system (Lee, 1993). They were grown in either A-RZT (29–39°C) or C-RZT (21.5–28.5°C). Roots were misted for 1 min with full strength Netherlands Standard Nutrient Solution (2.2 mS, pH 6.5; Douglas, 1985), at 5 or 10 min intervals, giving rise to four experimental conditions: A5, A10, C5, and C10. Shoots were exposed to fluctuating ambient temperatures of 25–39°C and 70–95% relative humidity, under 100% prevailing solar radiation, with maximum photosynthetic photon flux density (PPFD) of 1000 μmol photon m^{-2} s^{-1}.

Measurement of RZT

RZT was tracked, at 20 min intervals, across the 28-day growing period using a temperature probe (SL52T, Signatrol) that was left in the RZ of the growing trough. Data was then downloaded using its accompanying software TempIt-Pro (Version 4.1.41, Signatrol) and plotted in Microsoft Excel (Version 14.0, 2010).

Measurements of Mortality and Growth Parameters

Some plants succumbed following transplant and the number of plants remaining was counted 28 days after transplanting, and % mortality was calculated. Three or more plants of each genotype were harvested 35 days after transplanting and their total shoot and root fresh weights (FW) per trough were measured and means calculated. Specific leaf area (SLA) was calculated by dividing the area of 10 1-cm-diameter leaf discs with their dry weights after drying for 5 days in a 65°C oven. Three or more replicates were used.

Measurements of Photosynthetic Pigments

Four 1-cm-diameter leaf discs obtained from newly expanded leaves from four different plants were soaked in 1.5 ml N,N-dimethylformamide for 48 h in the dark, at 4°C. Absorption of 4 replicates was read at 480, 647, and 664 nm, using a spectrophotometer (UV-2550, Shimadzu, Japan). Concentrations for chlorophyll (Chl) a, Chl b, and carotenoids were calculated (Wellburn, 1994).

Measurements of Photochemical Light Use Efficiency

Leaves were harvested at 0900 h for Chl fluorescence analysis, where nonphotochemical quenching (NPQ), photochemical quenching (qP) and electron transport rate (ETR) of four detached newly expanded leaves from four different plants were measured at 25°C in the laboratory, using the Imaging-PAM Chlorophyll Fluorometer (Walz, Effeltrich, Germany) (He et al., 2011).

Measurements of RZ Ethylene Accumulation

Each plant genotype for each RZ-treatment was grown within individual troughs and the ethylene gas that had accumulated in the RZ space of plants of the entire trough was extracted between spray cycles, at 1300 h on a sunny day, using a 500 ml gas syringe (Hamilton, USA). Air samples were transferred into their respective 1 L gas sampling bags (Sigma-Aldrich) in the greenhouse and brought back to the laboratory to allow air temperatures within the bags to acclimatize to room temperatures (28°C) prior to sampling. The bags were connected to the EASI-1 portable ethylene analyzer (Absoger, France), via a 15 cm long tube filled with silica gel, and left to stabilize until consistent readings (±10% variation) were obtained. At least three consecutive readings were taken per sample gas bag.

Statistical Analysis

A mixed-model nested analysis of variance (ANOVA) was performed using SPSS (Version 20, 2011) to test for significant effects of variation between genotypes and their response to the four RZ-treatments (A5, A10, C5, and C10) using *post-hoc* Tukey's pairwise tests, at a significance level of $\alpha = 0.05$.

RESULTS

RZT, Mortality, and Growth Parameters

Plants that were growing in A5 and A10 were exposed to very similar RZT ranges (**Figure 1A**), throughout the 28-day growth period. Temperature range for A5 and A10 were 29–37°C and 29–39°C, respectively. Plants in C5 and C10 were also exposed to similar RZTs (**Figure 1A**), fluctuating mostly about 23°C. Temperature range for C5 and C10 were 21.5–25.5°C and 21.5–28.5°C, respectively. RZT in C10 was much higher than C5, between 1100 and 2000 h. The temperature in C10 even exceeded 25°C for a period of 4 h from 1340 to 1740 h (**Figure 1A**).

Some mortality was observed within the seedlings that were transplanted (**Figure 1B**). Mortality was observed only in A5 and C5 RZ treatments in the RIL, and A10 and C10 RZ treatments in "Salinas." However, *L. serriola* exhibited mortality in all RZ treatments, with more than 25% mortality in A5 and A10 (**Figure 1B**). Mortality for *L. serriola* was, indeed, higher in A- than C-RZT.

In general, the RIL was the largest plant especially in C-RZT conditions, exceeding 100 g in shoot FW (**Figure 2A**), while *L. serriola* was the smallest with less than 30 g for all treatments. Shoot FW was consistently higher in C-RZT than A-RZT for all plant types (**Figure 2A**). In A-RZT, higher shoot FW was found in the RIL at A10 rather than at A5. Highest root FW for all genotypes was in C10 (**Figure 2B**). Similar to the changes in shoot FW, higher root FWs were found in C-RZT than A-RZT. For root/shoot ratios (**Figure 2C**), *L. serriola* had the highest ratios in A-RZ treatments. For RIL and *L. serriola*, SLA was higher at C5 than A5, and also at C10 than A10 (**Figure 2D**), whereas it was reversed in "Salinas" at the A-RZ treatments. The lowest SLA for *L. serriola* was in A10 while "Salinas" had its highest SLA in the same treatment (**Figure 2D**). The RIL had similar SLA values under all treatments.

Pigment Content and Photochemical Light Use Efficiency

For all genotypes and RZ treatments, Chl a/b ratio was close to 3 (**Figure 3A**). Significantly lower ratios were obtained for C5-RZ treatment ($p < 0.001$) for all genotypes. RZ treatment only affected total Chl concentrations in the RIL (**Figure 3B**) though there was significant difference between genotypes ($p < 0.05$),

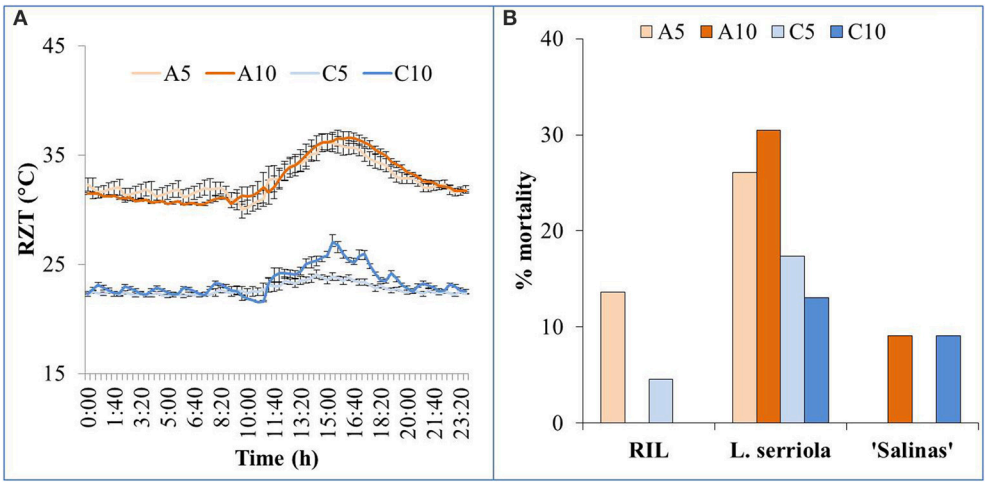

FIGURE 1 | (A) Range and variability of RZT of the four experimental conditions (A5, A10, C5, and C10) for the 3 plant types, with SE bars showing the variability across the 28-day growing period. **(B)** 22 seedlings of all plant genotypes were grown in the 4 RZ treatments and mortality was observed. Graph shows the % mortality of each genotype in each of the 4 RZ treatments, at harvest, 28 days after transplanting.

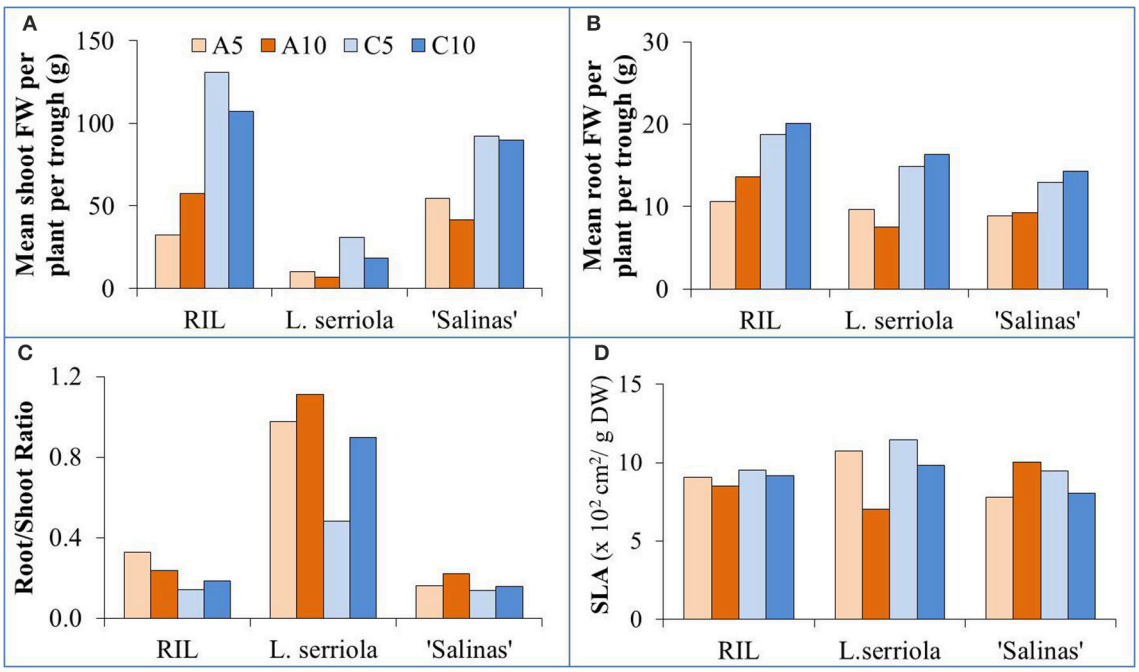

FIGURE 2 | Growth parameters of (A) mean shoot FW per plant per trough, (B) mean root FW per plant per trough, (C) root/ shoot ratio, and (D) SLA for the four experimental conditions (A5, A10, C5, and C10) for the 3 genotypes. Cumulative shoot and root FWs of all plants in each growing trough were measured and their FWs were normalized due to the different numbers of plants sampled.

with lowest total Chl in "Salinas" and highest in the RIL. A10-RZ treatment also resulted in significantly higher total Chl than C5-RZ treatments ($p < 0.005$) in the RIL. There was no significant difference in the carotenoid content of *L. serriola* across all RZ treatments (**Figure 3C**) but was significantly highest for A10 in the RIL ($p < 0.05$). The Chl/carotenoid ratio was significantly higher for C5 in all genotypes ($p < 0.005$, **Figure 3D**). Although there was no significant difference in the total Chl and carotenoid content of *L. serriola* between RZ treatments, the A10-RZ treatment had the lowest Chl/carotenoid ratio ($p < 0.05$) across the RZ treatments (**Figures 3B–D**).

All 3 genotypes exhibited slightly different NPQ behavior under the different RZ treatments (**Figure 4A**). NPQ was significantly higher for the RIL in A10 and C10 than A5 and

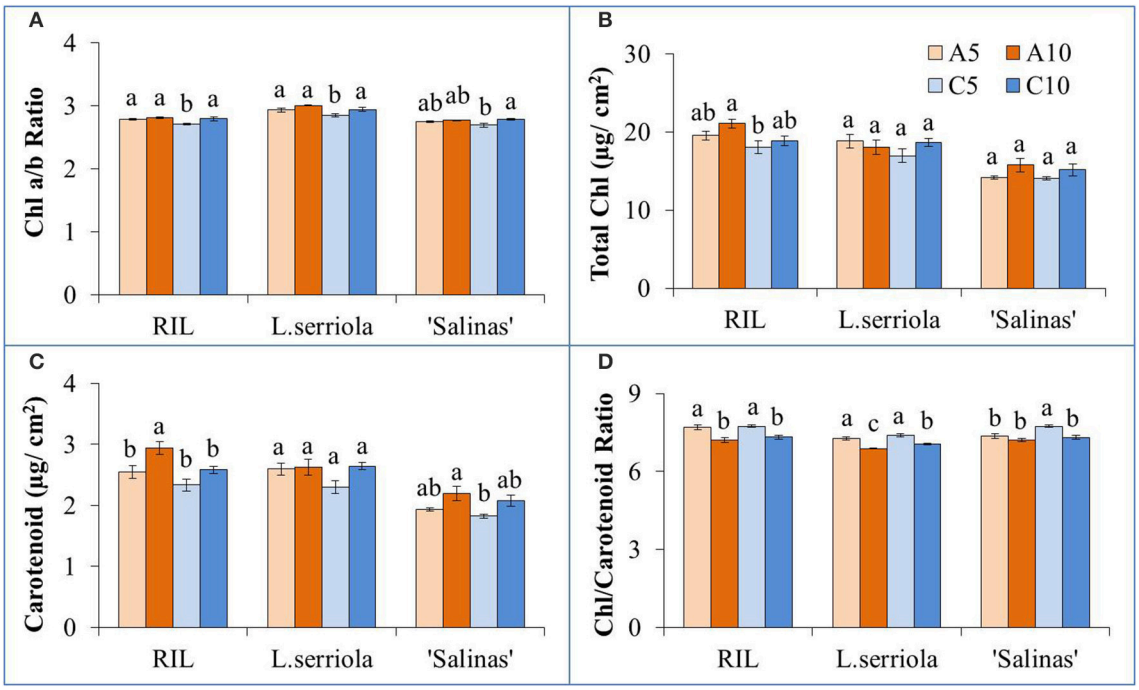

FIGURE 3 | (A) Chlorophyll a/b ratio, **(B)** total chlorophyll concentration, **(C)** carotenoid concentration, and **(D)** chlorophyll/ carotenoid ratio of *L. serriola*, "Salinas" and RIL grown in A5, A10, C5, and C10. Each bar graph is the mean of 4 measurements from at least 4 different plants ($n \geq 4$). Vertical bars represent standard errors. Different letters above the bar graphs denote statistical differences ($p < 0.05$) as determined by Tukey's multiple comparison test.

C5. However, the reverse is observed in *L. serriola* where C10 treatment resulted in even significantly lower NPQ than A10, with both lower than the A5 and C5 treatments (**Figure 4A**). Conversely, qP for the RIL in A10 and C10 was significantly lower than that of A5 and C5 (**Figure 4B**). The qP for *L. serriola* was also inverse to its NPQ behavior. However, the qP for "Salinas" behaved similarly to that of *L. serriola* in that qP at A10 and C10 are significantly higher than that for A5 and C5 (**Figure 4B**). ETR for all 3 plants are closely correlated to their qP values where the RIL had higher ETR values at A5 and C5 while *L. serriola* and "Salinas" had higher values for A10 and C10 (**Figure 4C**).

Accumulated RZ Ethylene Concentrations

In general, higher concentrations of RZ ethylene accumulated in A-RZT than C-RZT (**Figure 5**). Highest RZ ethylene per unit root FW accumulated in A10-RZ treatment for *L. serriola*, double that of the highest values of "Salinas" and the RIL. Across treatments, "Salinas" also accumulated more RZ ethylene in the A10-RZ treatment (**Figure 5**). However, the A5-RZ treatment accumulated more RZ ethylene in the RIL. The lowest RZ ethylene accumulated in C5 for the RIL and "Salinas" but in *L. serriola* there was little difference between the C-RZ treatments (**Figure 5**).

DISCUSSION

Lettuce production was possible, even at particularly high air temperatures of up to 41°C, as long as their roots were cooled (He and Lee, 1998; He et al., 2001). For this experiment, all plants were exposed to fluctuating tropical air temperatures while their RZTs were maintained within two different ranges (**Figure 1A**). The A-RZT for A5 and A10 treatments were similar (and ranged between 29–37°C and 29–39°C, respectively) but the two C-RZ treatments differed, up to almost 4°C, for 8 h (**Figure 1A**) in the latter half of the day. More frequent spraying improved growth of all genotypes at C-RZ treatments (**Figure 2A**). For all genotypes, shoot growth was greater under C-RZT than A-RZT. Under A-RZ conditions, the effects of spray frequency varied between genotypes. Shoot growth of *L. serriola* and "Salinas" fared better in A5 than A10, unlike the RIL which had better growth at A10. Higher shoot FW could be attributed to higher root FW since larger root systems improved nutrient and water uptake (He et al., 2001; Dodd, 2005), under such warm A-RZ conditions. Although the RIL had higher root/shoot ratios (**Figure 2C**) than the domesticated cultivar at all RZTs, respectively, this conferred no obvious benefits in terms of yield (i.e., shoot biomass) at A-RZT but instead only at C-RZT.

Highest mortality was observed in *L. serriola* at high A-RZT (**Figure 1B**), and high ambient day/night temperature in a tropical greenhouse, probably since it is a wild-type drought-tolerant winter annual (Werk and Ehleringer, 1985). Such mortality has been rather consistently observed across many batches of experiments (results not shown). As *L. serriola* is a wild type that is well-adapted to desert conditions of hot-day-cool-nights, its relatively higher mortality could have been due to the

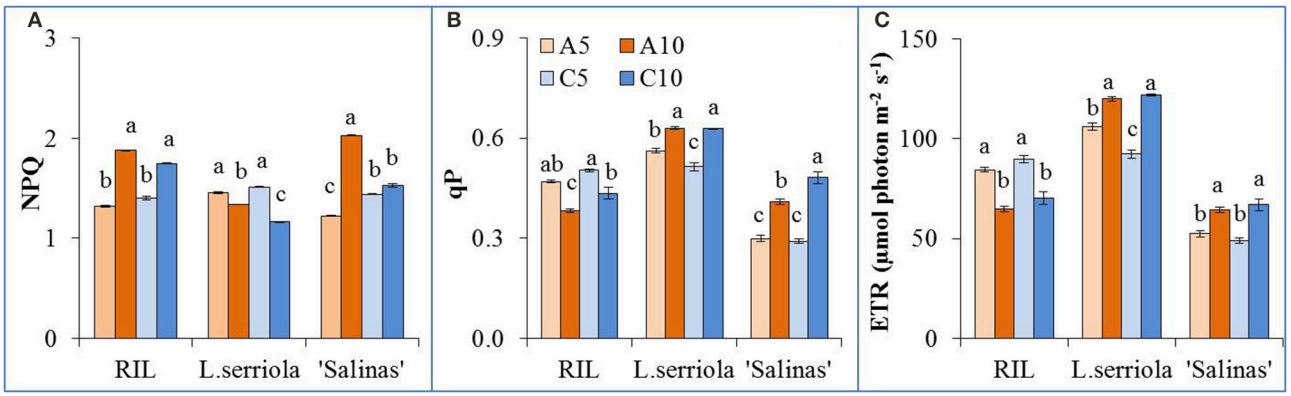

FIGURE 4 | Photochemical light use efficiency measurements of *L. serriola*, "Salinas" and RIL grown in A5, A10, C5, and C10. (A) Nonphotochemical quenching (NPQ), **(B)** photochemical quenching (qP) and **(C)** electron transport rate (ETR) at PPFD of 605 µmol photon m^{-2} s^{-1} are shown. Each bar graph is the mean of 4 measurements from 4 different plants ($n = 4$). Vertical bars represent standard errors. Different letters above the bar graphs denote statistical differences ($p < 0.05$) as determined by Tukey's multiple comparison test.

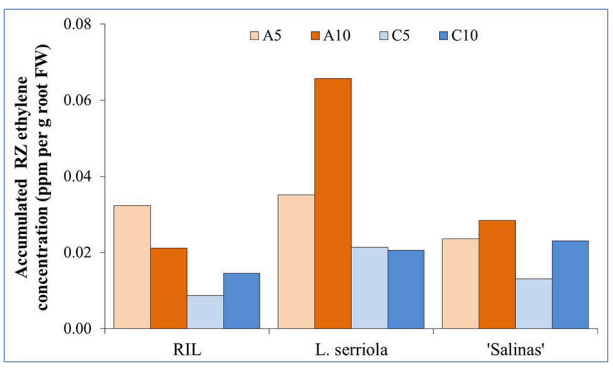

FIGURE 5 | Accumulated RZ ethylene concentration per unit root FW, measured at 1300 h on a sunny day, 28 days after transplanting into an aeroponic system. *L. serriola*, "Salinas" and the RIL were planted in four different experimental conditions of A5, A10, C5, and C10. Each bar graph is the mean of 3 consecutive measurements for each growing condition ($n = 3$).

lack of cooler "night" temperatures that aided recovery from heat stress (Xue et al., 2011), evident from the highest accumulated RZ ethylene concentrations at A10-RZ treatment (**Figure 5**).

Lower SLA, implying thicker leaves (Chatterjee and Solankey, 2015), was observed for RIL and *L. serriola* at higher tropical A-RZT than their corresponding C-RZT (**Figure 2D**)—the thickest leaves were measured under A10-RZ treatment. Conversely, "Salinas" had the thinnest leaves at this same treatment. Likewise, Dale (1965) reported thinner leaves of *Phaseolus vulgaris* at warmer growing temperatures of 25°C than at 15°C. As such, this could be a strategy adopted by "Salinas" to increase surface area for increased thermal dissipation since there was correspondingly lowest shoot growth at A10 (**Figure 2A**). On the other hand, lower SLA (i.e., thicker leaves) occurred at higher growing temperatures in tomatoes (Abdelmageed et al., 2009). For C5 and C10, the lower shoot FW and thicker leaves (**Figures 2A,D**) observed in all genotypes could be attributed to the 4 h period during which C10-RZT exceeded 25°C (**Figure 1A**). "Salinas" also had thicker leaves when grown in C10, than C5 (**Figure 2D**)—opposite to that observed under A-RZ treatments. Decreased SLA, in comparison with cooler optimal growing temperatures, may be an alternative adaptive mechanism for reducing leaf area and increasing water use efficiency (Craufurd et al., 1999; Chatterjee and Solankey, 2015), to cope with thermal stress.

Chatterjee and Solankey (2015) attributed lower SLA and thicker leaves to higher density of Chl and other proteins per unit area. However, there was no significant difference in the total Chl content between the RZ treatments of A5 and A10, and C5 and C10 (**Figure 3B**). In comparing individual quantities of Chl a and Chl b (data not shown), significantly higher amounts of Chl b was obtained for the A10-RZ treatment only for the RIL and *L. serriola*. As Chl b protects the photosystem II reaction center from photodamage (Sakuraba et al., 2010), the higher Chl b concentration indicates the plants in A10-RZ treatment were rather stressed. However, lower Chl a/b ratios (**Figure 3A**) corresponded with highest shoot FWs (**Figure 2A**), at C5-RZ treatment, for all genotypes. As such, it is worthy to note that only extremely low Chl a/b ratios demonstrate that the plants were stressed (Dinç et al., 2012). Since carotenoids are also photoprotective in function (Filella et al., 2009), the Chl/carotenoid ratio better indicates plant stress (Hendry and Price, 1993). In this experiment, the Chl/carotenoid ratios are consistently lower in the A10 and C10 RZ treatments across all genotypes. For *L. serriola*, there were no significant differences in total Chl and carotenoid content across the RZ treatments but the Chl/carotenoid ratio was still the significantly lowest at A10 (**Figure 3**). Thus, this further demonstrates that this wild-type parent plant was growing under stressed conditions (Cui et al., 2006) in A10-RZ treatment.

NPQ, which reflects energy dissipated as heat, was significantly higher for the RIL in A10 and C10, than A5 and C5 (**Figure 4A**), indicating a higher ability to dissipate excess excitation energy (He, 2009) when misted less frequently.

Comparing with the significantly lower qP and ETR values (**Figures 4B,C**) at A10 and C10 for the RIL, it demonstrates that less frequent misting has compromised photosynthetic function, and thus growth (**Figure 2A**), of these plants. In the case of *L. serriola*, NPQ was significantly lower at A10 and C10 instead (**Figure 4A**), with the C10 treatment significantly lower than A10. This drought tolerant wild-type *L. serriola* demonstrates its tolerance to high light, abundant in the tropics, despite the decreased frequency in irrigation. Though *L. serriola* had highest qP and ETR values (**Figures 4B,C**) at A10 and C10 RZ treatments, it had much lower shoot FW (**Figure 2A**) seeming to have invested its photosynthetic products into building a larger root system (**Figure 2B**) especially at C10 whilst sacrificing its shoot growth. "Salinas" most interestingly demonstrates significantly higher NPQ, qP and ETR (**Figure 4**) at A10 whilst growth is slower than at A5 and C5 RZ treatments. This could suggest that it reallocated its photosynthetic products to repair thylakoid membranes damaged by the combination of high light, typically found in a tropical greenhouse, and lowered misting frequency.

In this experiment, higher concentrations of RZ ethylene accumulated in A-RZT than C-RZT indicating greater plant stress (Abeles et al., 1992; Morgan and Drew, 1997; Lin et al., 2009) in the absence of RZ cooling. The highest RZ ethylene per unit root FW accumulated in A10-RZ treatment for *L. serriola* was doubles that of the highest values of "Salinas" and the RIL. Though it had significantly lower NPQ and higher photosynthetic performance than its counterparts in A5-RZ treatment (**Figure 4**), its shoot FW (**Figure 2A**) was also the lowest. In contrast, lowest RZ ethylene accumulated in C5-RZ treatment for the RIL (**Figure 5**) with correspondingly high photosynthetic rates (**Figures 4B,C**) which resulted in the high shoot FW (**Figure 2A**) and conversely low root/shoot ratio (**Figure 2D**). As such, these observations of higher photosynthetic rates and lower shoot FW and inversely high root/shoot ratio (**Figures 2A,D**) of *L. serriola* at A10-RZ treatment suggest that photosynthates have probably been redirected to stress recovery mechanisms.

Since shoot FW is the part of the plant with commercial value, and lower accumulated RZ ethylene concentrations corresponded with higher shoot growth at cooler RZTs, cultivars that are less RZT sensitive could be selected for agricultural purposes. As such, high electrical usage could be reduced with decreased misting frequency and/or chilling, decreasing production costs. Furthermore, root morphological analysis could be carried out to examine how the increase in RZ ethylene could affect root growth, since root systems support the shoots (He et al., 2001; Dodd, 2005) and would thus ultimately affect the commercially significant shoot FW.

AUTHOR CONTRIBUTIONS

JH and SL initiated and funded the project. JH, ID, and TC planned the experiment. TC carried out the experiment and wrote the manuscript. JH and ID contributed ideas and improved the manuscript. All authors approved the manuscript.

FUNDING

This project was funded by Singapore Millennium Foundation, Singapore.

ACKNOWLEDGMENTS

We thank the Michelmore Lab at the UC Davis Genome Centre for providing us with the RIL seeds and Antje Fiebig for instruction in the EASI-1 ethylene analyzer.

REFERENCES

Abdelmageed, A. H. A., Gruda, N., and El-Balla, M. M. A. (2009). Performance of different tomato genotypes in the arid tropics of Sudan during the summer season. I. Vegetative growth. *J. Agric. Rural De. Trop. Subtrop.* 110, 137–145.

Abeles, F. B., Morgan, P. W., and Salveit, M. E. (1992). *Ethylene in Plant Biology*. San Diego, CA: Academic Press.

Ainscough, E. W., Brodie, A. M., and Wallace, A. L. (1992). Ethylene – an unusual plant hormone. *J. Chem. Educ.* 69, 315–318. doi: 10.1021/ed069p315

Argyris, J., Dahal, P., Truco, M. J., Ochoa, O., Still, D. W., Michelmore, R. W., et al. (2008). Genetic analysis of lettuce seed thermoinhibition. *Acta Hortic.* 782, 23–34. doi: 10.17660/ActaHortic.2008.782.1

Argyris, J., Truco, M. J., Ochoa, O., Knapp, S. J., Still, D. W., Lenssen, G. M., et al. (2005). Quantitative trait loci associated with seed and seedling traits in *Lactuca*. *Theor. Appl. Genet.* 111, 1365–1376. doi: 10.1007/s00122-005-0066-4

Barker, D. H., Adams, W. W. III., Demmig-Adams, B., Logan, B. A., Verhoeven, A. S., and Smith, S. D. (2002). Nocturnally retained zeaxanthin does not remain engaged in a stage primed for energy dissipation during the summer in two Yucca species growing in the Mojave Desert. *Plant Cell Environ.* 25, 95–103. doi: 10.1046/j.0016-8025.2001.00803.x

Berry, J. A., and Raison, J. K. (1981). "Responses of macrophytes to temperature," in *Encyclopedia of Plant Physiology*, eds O. L. Lange, P. S. Nobel, C. B. Osmond, and H. Ziegler (Heidelberg: Springer-Verlag), 277–338.

Björkman, O., and Powles, S. B. (1984). Inhibition of photosynthetic reactions under water stress: interaction with light level. *Planta* 161, 490–504. doi: 10.1007/BF00407081

Chatterjee, A., and Solankey, S. S. (2015). "Functional physiology in drought tolerance of vegetable crops: an approach to mitigate climate change impact," in *Climate Dynamics in Horticultural Science,* Vol. 1: The Principles and Applications, eds M. L. Choudhary, V. B. Patel, M. W. Siddiqui, and S. S. Mahdl (Boca Raton, FL: CRC Press), 149–171.

Choong, T. W. (1998). *Effects of Rootzone Temperature and Irradiance on the Growth and Photosynthetic Characteristics of Certain Subtropical Vegetable Crops*, Honours theses, Nanyang Technological University.

Choong, T. W., He, J., Qin, L., and Dodd, I. C. (2013). Identifying heat-resistant recombinant inbred lines (RILs) of lettuce in the tropics: productivity and root phenotyping. *Acta Hortic.* 1004, 173–180. doi: 10.17660/ActaHortic.2013.1004.20

Craufurd, P. C., Wheeler, T. R., Ellis, R. H., Summerfield, R. J., and Williams, J. H. (1999). Effect of temperature and water deficit on water use efficiency, carbon isotope discrimination and specific leaf area in peanut. *Crop Sci.* 39, 136–142. doi: 10.2135/cropsci1999.0011183X003900010022x

Cui, L., Li, J., Fan, Y., Xu, S., and Zhang, Z. (2006). High temperature effects on photosynthesis, PSII functionality and antioxidant activity of two *Festuca arundinacea* cultivars with different heat susceptibility. *Bot. Stud.* 47, 61–69.

Dale, J. E. (1965). Leaf growth in Phaseolus vulgaris II. Temperature effects and the light factor. *Ann. Bot.* 29, 293–307.

Dinç, E., Ceppi, M. G., Tóth, S. Z., Bottka, S., and Schansker, G. (2012). The chl a fluorescence intensity is remarkably insensitive to changes in the chlorophyll content of the leaf as long as the chl a/b ratio remains unaffected. *Biochim. Biophys. Acta* 1817, 770–779. doi: 10.1016/j.bbabio.2012.02.003

Dodd, I. C. (2005). Root-to-shoot signalling: assessing the roles of 'up' in the up and down world of long-distance signalling *in planta*. *Plant Soil* 274, 251–270. doi: 10.1007/s11104-004-0966-0

Douglas, J. S. (1985). *Advanced Guide to Hydroponics.* London: Pelham Books.

Durst, C. E. (1929). Inheritance in lettuce. *Science* 69, 553–554. doi: 10.1126/science.69.1795.553

Ferakova, V. (1976). "*Lactuca* L," in *Flora Europaea,* Vol. 4, eds T. G. Tutin, V. H. Heywood, N. A. Burges, and D. H. Valentine (Cambridge, UK: Cambridge University Press), 328–331.

Filella, I., Porcar-Castell, A., Munne-Bosch, S., Back, J., Garbulsky, M. F., and Penuelas, J. (2009). PRI assessment of long-term changes in carotenoids/chlorophyll ratio and short-term changes in de-epoxidation state of the xanthophyll cycle. *Int. J. Remote Sens.* 30, 4443–4455. doi: 10.1080/01431160802575661

Freundl, E., Steudle, E., and Hartung, W. (1998). Water uptake by roots of maize and sunflower affects the radial transport of abscisic acid and its concentration in the xylem. *Planta* 207, 8–19. doi: 10.1007/s004250050450

Harlan, J. R. (1992). *Crops and Man*. Madison, WI: ACSESS Publications.

He, C. J., Davies, F. T. Jr, and Lacey, R. E. (2009). Ethylene reduces gas exchange and growth of lettuce plants under hypobaric and normal atmospheric conditions. *Physiol. Plant.* 135, 258–271. doi: 10.1111/j.1399-3054.2008.01190.x

He, J. (2009). "Impact of RZT on photosynthetic efficiency of aeroponically grown temperate and subtropical vegetable crops in the tropics," in *Photosynthesis*, eds T. B. Buchner and N. H. Ewingen (New York, NY: Nova Science Publishers, Inc.), 111–144.

He, J., and Lee, S. K. (1998). Growth and photosynthetic characteristics of lettuce (*Lactuca sativa* L.) under fluctuating hot ambient temperatures with the manipulation of cool rootzone temperature. *J. Plant Physiol.* 152, 387–391. doi: 10.1016/S0176-1617(98)80252-6

He, J., and Lee, S. K. (2004). Photosynthetic utilization of radiant energy by temperate lettuce grown under natural tropical condition with manipulation of root-zone temperature. *Photosynthetica* 42, 457–463. doi: 10.1023/B:PHOT.0000046166.29815.94

He, J., Lee, S. K., and Dodd, I. C. (2001). Limitations to photosynthesis of lettuce grown under tropical conditions: alleviation by rootzone cooling. *J. Exp. Bot.* 52, 1323–1330. doi: 10.1093/jexbot/52.359.1323

He, J., Qin, L., Liu, Y., and Choong, T. W. (2015). Photosynthetic capacities and productivity of indoor hydroponically grown *Brassica alboglabra* Bailey under different light sources. *Am. J. Plant Sci.* 6, 554–563. doi: 10.4236/ajps.2015.64060

He, J., Tan, B. H. G., and Qin, L. (2011). Source-to-sink relationship between green leaves and green pseudobulbs of C_3 orchid in regulation of photosynthesis. *Photosynthetica* 49, 209–218. doi: 10.1007/s11099-011-0023-1

He, J., Tan, L. P., and Lee, S. K. (2009). Rootzone temperature effects on photosynthesis, ^{14}C-photoassimilate partitioning and growth of temperate lettuce (*Lactuca sativa* cv. 'Panama') in the tropics. *Photosynthetica* 47, 95–103. doi: 10.1007/s11099-009-0015-6

Hendry, G. A. F., and Price, A. H. (1993). "Stress indicators: chlorophylls and carotenoids," in *Methods in Comparative Plant Ecology*, eds G. A. F. Hendry and J. P. Grime (London: Chapman & Hall), 148–152.

Jeffrey, C. (1975). "*Lactuca* L," in *Flora of Turkey and the east Aegean islands,* Vol. 5, eds P. H. Davis, R. R. Mill, and K. Tan (Edinburgh: Ediniburgh University Press), 776–782.

Kaspar, T. C., and Bland, W. L. (1992). Soil temperature and root growth. *Soil sci.* 154, 290–299. doi: 10.1097/00010694-199210000-00005

Kesseli, R. V., Ochoa, O., and Michelmore, R. W. (1991). Variation at RFLP loci in *Lactuca* spp. and origin of cultivated lettuce (*L. sativa*). *Genome* 34, 430–436. doi: 10.1139/g91-065

Kirpicznikov, M. E. (1964). "*Lactuca* L," in *Komarov's Flora of URSS,* Vol. 29, ed V. L. Komarov (Nuaka: Moscow-Leningrad), 274–317.

Lee, S. K. (1993). Aeroponic system as a possible alternative for crop production in Singapore. *Commonwealth Agric. Digest* 3, 1–4.

Lee, S. K., Wong, Y. W., Liu, C. Y., and Cheong, S. (1994). "Optimising aeroponic systems for urban farming in Singapore," in *Paper Presented at the International Conference on Advances in Tropical Agriculture in the Twentieth Century and Prospects for the Twenty-First Century* (Trinidad: University of the West Indies).

Lee, S., and Reid, D. (1997). The role of endogenous ethylene in the expansion of *Helianthus annuus* leaves. *Can. J. Bot.* 75, 501–508. doi: 10.1139/b97-054

Lin, Z., Zhong, S., and Grierson, D. (2009). Recent advances in ethylene research. *J. Exp. Bot.* 60, 3311–3336. doi: 10.1093/jxb/erp204

Morgan, P. W., and Drew, M. C. (1997). Ethylene and plant responses to stress. *Plant Physiol.* 100, 620–630. doi: 10.1111/j.1399-3054.1997.tb03068.x

Pallaghy, C. K., and Raschke, K. (1972). No stomatal response to ethylene. *Plant Physiol.* 49, 275–276. doi: 10.1104/pp.49.2.275

Pierik, R., Tholen, D., Poorter, H., Visser, E. J. W., and Voesenek, A. C. J. (2006). The Janus face of ethylene: growth inhibition and stimulation. *Trends Plant Sci.* 11, 176–183. doi: 10.1016/j.tplants.2006.02.006

Qin, L., He, J., Lee, S. K., and Dodd, I. C. (2007). An assessment of ethylene mediation of lettuce (*Lactuca sativa*) root growth at high temperatures. *J. Exp. Bot.* 58, 3017–3024. doi: 10.1093/jxb/erm156

Ruzicka, K., Ljung, K., Vanneste, S., Podhorska, R., Beeckman, T., Friml, J., et al. (2007). Ethylene regulates root growth through effects on auxin biosynthesis and transport-dependent auxin distribution. *Plant Cell* 19, 2197–2212. doi: 10.1105/tpc.107.052126

Sakamoto, M., and Suzuki, T. (2015). Effect of rootzone temperature on growth and quality of hydroponically grown red leaf lettuce (*Lactuca sativa* L. cv. Red Wave). *Am. J. Plant Sci.* 6, 2350–2360. doi: 10.4236/ajps.2015.614238

Sakuraba, Y., Yokono, M., Akimoto, S., Tanaka, R., and Tanaka, A. (2010). Deregulated chlorophyll b synthesis reduces the energy transfer rate between photosynthetic pigments and induces photodamage in *Arabidopsis thaliana*. *Plant Cell Physiol* 51, 1055–1065. doi: 10.1093/pcp/pcq050

Salisbury, F. B., and Ross, C. W. (1992). *Plant Physiology*. Belmont, CA: Wadsworth, Inc.

Tachibana, S. (1982). Comparison of effects of root temperature on the growth and mineral nutrition of cucumber cultivars and figleaf gourd. *J. Jpn. Soc. Hortic. Sci.* 51, 299–308. doi: 10.2503/jjshs.51.299

Thompson, H. C., Langhans, R. W., Both, A. J., and Albright, L. D. (1998). Shoot and root temperature effects on lettuce growth in a floating hydroponic system. *J. Amer. Soc. Hortic. Sci.* 123, 361–364.

Verhoeven, A. S., Demmig-Adams, B., and Adams, W. W. III. (1997). Enhanced employment of the xanthophyll cycle and thermal energy dissipation in spinach exposed to high light and N stress. *Plant Physiol.* 113, 817–824.

Wellburn, A. R. (1994). The spectral determination of chlorophylls a and b, as well as carotenoids, using various solvents with spectrophotometers of different resolution. *J. Plant Physiol.* 144, 307–313. doi: 10.1016/S0176-1617(11)81192-2

Werk, K. S., and Ehleringer, J. (1985). Photosynthetic characteristics of *Lactuca serriola* L. *Plant Cell Environ.* 8, 345–350. doi: 10.1111/j.1365-3040.1985.tb01409.x

Woodrow, L., and Grodzinski, B. (1989). An evaluation of the effects of ethylene on carbon assimilation in *Lycopersicon esculentum* Mill. *J. Exp. Bot.* 40, 361–368. doi: 10.1093/jxb/40.3.361

Woodrow, L., Jiao, J., Tsujita, L., and Grodzinski, B. (1989). Whole plant and leaf steady state gas exchange during ethylene exposure in *Xanthium strumarium*. *Plant Physiol.* 90, 85–90. doi: 10.1104/pp.90.1.85

Xue, W., Li, X. Y., Lin, L. S., Wang, Y. J., and Li, L. (2011). Effects of elevated temperature on photosynthesis in desert plant *Alhagi sparsifolia* S. *Photosynthetica* 49, 435–447. doi: 10.1007/s11099-011-0054-7

Zohary, D. (1991). The wild genetic resources of cultivated lettuce (*Lactuca sativa* L.). *Euphytica* 53, 31–35. doi: 10.1007/BF00032029

Conflict of Interest Statement: The authors declare that the research was conducted in the absence of any commercial or financial relationships that could be construed as a potential conflict of interest.

frontiers in Plant Science

ORIGINAL RESEARCH
published: 12 June 2017
doi: 10.3389/fpls.2017.00859

Genome Wide Identification and Expression Profiling of Ethylene Receptor Genes during Soybean Nodulation

*Youning Wang[1], Jinhong Yuan[1], Wei Yang[1], Lin Zhu[1], Chao Su[1], Xiaodi Wang[1], Haiyan Wu[1], Zhengxi Sun[2,3] and Xia Li[1]**

[1] State Key Laboratory of Agricultural Microbiology, College of Plant Science and Technology, Huazhong Agricultural University, Wuhan, China, [2] State Key Laboratory of Plant Cell and Chromosome Engineering, Institute of Genetics and Developmental Biology – Chinese Academy of Sciences, Beijing, China, [3] University of Chinese Academy of Sciences, Beijing, China

It has long been known that the gaseous plant hormone ethylene plays a key role in nodulation in legumes. The perception of ethylene by a family of five membrane-localized receptors is necessary to trigger the ethylene signaling pathway, which regulates various biological responses in *Arabidopsis*. However, a systematic analysis of the ethylene receptors in leguminous plants and their roles in nodule development is lacking. In this study, we performed a characterization of ethylene receptor genes based on the latest *Glycine max* genome sequence and a public microarray database. Eleven ethylene receptor family genes were identified in soybean through homology searches, and they were divided into two subgroups. Exon–intron analysis showed that the gene structures are highly conserved within each group. Further analysis of their expression patterns showed that these ethylene receptor genes are differentially expressed in various soybean tissues and organs, including functional nodules. Notably, the ethylene receptor genes showed different responses to rhizobial infection and Nod factors, suggesting a possible role for ethylene receptors and ethylene signaling in rhizobia–host cell interactions and nodulation in soybean. Together, these data indicate the functional divergence of ethylene receptor genes in soybean, and that some of these receptors mediate nodulation, including rhizobial infection, nodule development, and nodule functionality. These findings provide a foundation for further elucidation of the molecular mechanism by which the ethylene signaling pathway regulates nodulation in soybean, as well as other legumes.

Keywords: soybean, *Glycine max*, ethylene, ethylene receptors, nodulation

OPEN ACCESS

Edited by:
Péter Poór,
University of Szeged, Hungary

Reviewed by:
Katarzyna Hnatuszko-Konka,
University of Łódź, Poland
Vladimir Zhukov,
All-Russia Research Institute for Agricultural Microbiology, Russia

****Correspondence:***
Xia Li
xli@mail.hzau.edu.cn

Specialty section:
This article was submitted to Plant Physiology, a section of the journal Frontiers in Plant Science

Received: *31 August 2016*
Accepted: *09 May 2017*
Published: *12 June 2017*

Citation:
Wang Y, Yuan J, Yang W, Zhu L, Su C, Wang X, Wu H, Sun Z and Li X (2017) Genome Wide Identification and Expression Profiling of Ethylene Receptor Genes during Soybean Nodulation. Front. Plant Sci. 8:859. doi: 10.3389/fpls.2017.00859

INTRODUCTION

Symbiotic nitrogen fixation (SNF) plays critical roles in legume development and yield. SNF efficiency is determined by rhizobial infection, nodule development, and mature nodule functionality. Nodulation is initiated by flavonoids secreted from legume roots in response to nitrogen-limited conditions, which stimulate rhizobia to synthesize and secrete lipooligosaccharides called Nod factors (NFs). NFs are perceived by NF receptors, which activate

signaling cascades that promote root hair deformation, the formation and growth of infection threads, cortical and pericycle cell division, and nodule development (Stacey et al., 2006; Oldroyd and Downie, 2008; Gresshoff et al., 2009; Ferguson et al., 2013). Nodulation is thus a complex process that is precisely and dynamically regulated by both internal and external cues (reviewed in Ferguson et al., 2010).

The gaseous hormone ethylene plays multiple roles in plant development, including seed dormancy, fruit ripening, flower and leaf senescence, and plant responses to environmental cues (Abeles et al., 1992; Johnson and Ecker, 1998; Bleecker and Kende, 2000). In *Arabidopsis*, the core ethylene signal transduction pathway has been well-characterized (Kieber et al., 1993; Chen et al., 2002; Ju et al., 2012; Cho and Yoo, 2015). In *Arabidopsis*, ethylene is perceived by Ethylene Receptor 1 (ETR1)/ETR2 (Chen et al., 2002), Ethylene Response Sensor (ERS) 1/ERS2, and Ethylene Insensitive (EIN) 4. These proteins comprise a family of endoplasmic reticulum (ER) membrane-associated proteins that negatively regulate ethylene signaling (Bleecker and Kende, 2000; Chang and Stadler, 2001). Upon binding ethylene, these receptors are inactivated, allowing them to bind Ethylene Insensitive 2 (EIN2) more efficiently (Cho and Yoo, 2015) and block its phosphorylation by Constitutive Triple Response 1 (Kieber et al., 1993). The C-terminus of EIN2 is then cleaved, inducing a conformational change in the protein that enables it to move to the nucleus and enhance the transcriptional activity of the transcription factors EIN3 and EIN3-Like 1 (EIL1). EIN3 and EIL1 activate ethylene-responsive genes such as *Ethylene Response Factor 1* (*ERF1*) to switch on ethylene signaling (Ju et al., 2012). Clearly, the perception of ethylene by specific receptor proteins is essential for ethylene action (Burg and Burg, 1967). Over the past several decades, extensive effort has been made to elucidate how these receptors perceive ethylene to activate ethylene signaling. Based on a structural analysis, the receptors have been divided into two subgroups. The type I subfamily includes ETR1 and ERS1, which consist of two critical domains, an N-terminal ethylene-binding domain (the sensor domain) and a well-conserved C-terminal histidine (His) kinase domain (Guo and Ecker, 2004). The type II subfamily consists of ETR2, ERS2, and EIN4, which contain an N-terminal ethylene-binding domain and a degenerate His kinase domain lacking one or more elements necessary for kinase catalytic activity (Guo and Ecker, 2004). In addition, ETR1, ETR2, and EIN4 have a C-terminal receiver domain of unknown function (Guo and Ecker, 2004). Despite their structural differences, all of these receptors are involved in ethylene perception and redundantly regulate ethylene-mediated biological processes affecting plant development and interactions with environment (Schaller and Bleecker, 1995; Hua and Meyerowitz, 1998; Guo and Ecker, 2004).

The negative effect of ethylene on legume nodulation was documented 40 years ago in experiments using exogenously applied ethylene or an inhibitor of ethylene biosynthesis (aminoethoxyvinylglycine) (Grobbelaar et al., 1971; Goodlass and Smith, 1979; Guinel and LaRue, 1992; Lee and Larue, 1992; Penmetsa and Cook, 1997; Nukui et al., 2000; Lohar et al., 2009). In recent years, compelling experimental evidence has demonstrated the crucial role of ethylene and ethylene signaling in nodulation in legumes. Ethylene is induced by NFs, and fluctuations in ethylene levels have been detected during nodulation (Gamalero and Glick, 2015). Notably, a recent study showed that ethylene positively or negatively regulates early (i.e., 1 h after inoculation) and late (6 h after inoculation) rhizobial infection *via* NF-independent and -dependent pathways, respectively (Larrainzar et al., 2015). The authors further proposed that these regulatory pathways are responsible for the different effects of ethylene on biological processes: the former in defense, and the latter in the initiation of nodulation (Larrainzar et al., 2015). Based on these results, it appears that ethylene is a master regulator of nodulation that affects multiple hormonal signaling pathways to regulate every step of the process, including rhizobial infection, nodule organogenesis, and nodule senescence (Guinel, 2016). Despite great progress in understanding the involvement of ethylene in nodulation, genetic evidence for the role of ethylene signaling comes mainly from functional analyses of loss-of-function mutants of *Arabidopsis* EIN2 orthologs. The '*sickle*' mutant of *Medicago truncatula* which carries a loss-of-function mutation in *MtEIN2*, is insensitive to ethylene and forms 10–30 times more nodules than wild-type plants (Penmetsa and Cook, 1997; Penmetsa et al., 2008). The mutation of two *Lotus EIN2* genes was also shown to cause hypernodulation in *Lotus japonicus* (Miyata et al., 2013), highlighting the conserved role of the ethylene signaling pathway in legume nodulation. The fact that the transgenic *Lotus japonicus* harboring the mutated *Arabidopsis ETR1 or Cm-ERS1/H70A* reduced ethylene sensitivity and enhanced nodulation (Nukui et al., 2004; Lohar et al., 2009) supports the notion that canonical ethylene perception and its signaling transduction show a significant role during nodulation in legumes. However, the role of ethylene in soybean nodulation remains controversial. Several studies have shown that neither an increase in ethylene production nor treatment with aminoethoxyvinylglycine affects nodule formation (Lee and Larue, 1992; Hunter, 1993; Suganuma et al., 1995); however, one study showed increased nodule numbers in soybean plants treated with ethylene inhibitors (Caba et al., 1998). It was suggested that this controversial result might be due to the experimental methodology (Schmidt et al., 1999). However, a phenotypic analysis of an ethylene-insensitive mutant, *etr1-1*, supports the idea that ethylene is less significant in nodule development in soybean compared to other plants because the nodule number in *etr1-1* was comparable to that in wild-type (Schmidt et al., 1999). Thus, the roles of ethylene in rhizobia–soybean interactions and nodule development in soybean are unclear. Moreover, the functions of most genes related to ethylene perception and signal transduction are unknown.

The availability of a transcriptome database and the recent sequencing of the soybean genome provided us with tools to examine which genes are involved in nodulation, and they provided us with clues about whether known ethylene-related genes mediate nodulation in soybean. To gain insight into the roles of ethylene signaling in soybean, especially in nodulation, we performed a genome wide search for soybean

homologs of the *Arabidopsis* ethylene receptor genes *ETR1*, *ETR2*, *ERS1*, *ERS2*, and *EIN4*. Detailed analyses of the structures, phylogeny, conserved domains, and expression profiles of these genes were performed. In addition, the expression patterns of the genes in response to rhizobial inoculation, NFs and in functional nodules were analyzed using quantitative real-time reverse transcription-polymerase chain reaction (qRT-PCR). Through these analyses, we uncovered structural and functional divergence among soybean ethylene receptor genes and proteins. Our results provide a framework for the further functional characterization of ethylene receptor family genes in soybean.

MATERIALS AND METHODS

Phylogenetic Tree and Gene Structure Analysis

We obtained the sequences of the identified ethylene receptor genes from a published database (Phytozome[1]), including genomic DNA sequences, coding sequences, and amino acid sequences. A phylogenetic tree was constructed based on the amino acid sequences of all putative ethylene receptor genes using Clustal X 1.83 (Thompson et al., 1997) and MEGA6.0 (Tamura et al., 2011). The structures of the ethylene receptor genes were determined using the Gene Structure Display Server (GSDS) website[2].

Cis-Element Analysis

1.5 kb sequences upstream of all the ethylene receptor genes were downloaded from *Glycine max* database. The regulatory *cis*-elements were then analyzed using website PlantCARE[3].

Expression Data Collection and Heatmap Construction

Expression data for the ethylene receptor genes were collected from SoyBase[4] (Severin et al., 2010) and the eFP Browser[5] (Libault et al., 2010). Heatmaps of the ethylene receptor genes were constructed using Heatmap Illustrator v1.0 (Deng et al., 2014).

Plant Materials and Growth Conditions

Soybean (*G. max* [L.] Merrill) cv. Williams 82 plants were used in this study. To analyze gene expression in response to rhizobial inoculation, soybean plants were grown in vermiculite irrigated with a nitrogen-deficient solution in a growth room (16 h of light/8 h of dark; 25°C) (Wang et al., 2009). Ten-day-old plants were inoculated with *Bradyrhizobium japonicum* strain USDA110 (OD_{600} = 0.08; 30 mL/plant) in the same nitrogen-deficient solution, and roots were collected at specific time points after rhizobial inoculation. To examine the early root response to rhizobial infection, roots were harvested at 0, 1, 3, 6, 12, and 24 h after rhizobial inoculation. To examine the expression pattern of ethylene receptor genes in different tissues, leaves, roots, and nodules were collected at 28 days after rhizobial inoculation. The method of NF application studies was used as described by Wang et al. (2014, 2015). Root samples were collected and used to analyze the expression of ethylene receptor genes at 24 h after NF treatment.

RNA Extraction and qRT-PCR

To estimate the ethylene receptor gene expression levels, total RNA was extracted from different tissues using Trizol reagent (Tiangen Biotech [Beijing] Co. Ltd, Beijing, China). Aliquots (2 μg) of total RNA were treated with DNase I (Invitrogen, Carlsbad, CA, United States) and used to synthesize first-strand cDNA with a FastQuant RT Kit (Tiangen Biotech [Beijing] Co. Ltd). qRT-PCR was performed using SuperReal PreMix Plus (SYBR Green; Tiangen Biotech [Beijing], Co., Ltd) on an ABI 7500 Real-Time PCR System (Invitrogen). *GmELF1b* (*Eukaryotic elongation factor 1-beta*) was used as an internal control (Jian et al., 2008). The primers used in this study are listed in Supplementary Table S1.

Statistical Analysis

The expression data were analyzed by Student's *t*-test or one-way analysis of variance using SigmaPlot 10.0 or GraphPad Prism 5 software. Different letters indicate a significant difference in the relative gene expression ($P < 0.05$). Moreover, statistically significant differences were indicated as follows: $^{*}P < 0.05$; $^{**}P < 0.01$; $^{***}P < 0.001$; ns, not significant, $P > 0.05$.

RESULTS

Genome Wide Identification of Ethylene Receptor Genes in Soybean

Based on the data collected from the Phytozome website, five ethylene receptor genes, *AtETR1*, *AtERS1*, *AtETR2*, *AtEIN4*, and *AtERS2*, were used as queries against the *G. max* genome in the Plant Genome Duplication Database (Lee et al., 2012). In total, 11 homologous genes were found in the soybean genome. Except that, there has 4 homologous genes in rice and six homologous genes in *Medicago*. Basic information about homologous genes in soybean is provided in Supplementary Table S2. The deduced proteins encoded by these putative ethylene receptor genes contain 636–768 amino acid residues, and their molecular masses range from 63.6 to 76.8 kDa, similar to the ethylene receptors of *Arabidopsis*. In addition, the isoelectric points of the proteins encoded by these soybean ethylene receptor genes range from 6.19 to 8.17.

Phylogenetic and Structure Analyses of the Soybean Ethylene Receptor Genes

Further analysis showed that the 11 homologs are located on six different chromosomes three on chromosome 20, two on chromosomes 3, 10, and 19; and one on chromosomes 9 and 12 (Supplementary Table S2). To assess the phylogenetic

[1]https://phytozome.jgi.doe.gov/pz/portal.html

[2]http://gsds2.cbi.pku.edu.cn

[3]http://bioinformatics.psb.ugent.be/webtools/plantcare/html/

[4]http://soybase.org/soyseq/

[5]http://bar.utoronto.ca/efpsoybean/cgi-bin/efpWeb.cgi

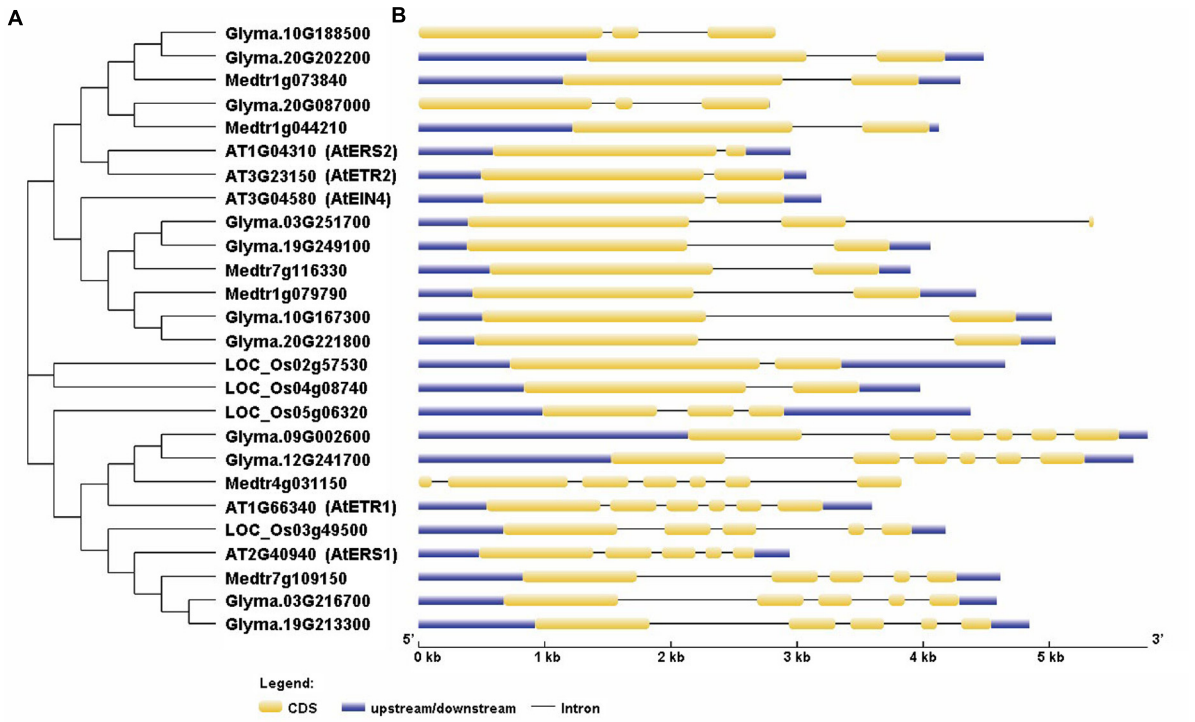

FIGURE 1 | Phylogenetic relationships of the ethylene receptor family proteins and their gene structures. The phylogenetic tree **(A)** was constructed using MEGA6.0, while the structures of the ethylene receptor genes **(B)** were created using the GSDS website.

relationships among the soybean and *Arabidopsis* receptor proteins, we constructed a phylogenetic tree with the protein sequences of the ethylene receptors by using the neighbor-joining method in MEGA6.0 (Tamura et al., 2011). To see whether other leguminous plants contain all the ethylene receptor genes, we also included the ethylene receptor proteins in *Medicago truncatula*. Our results indicate that, in soybean, four of the genes are homologs of *AtEIN4*, two are homologs of *AtETR1* and *AtERS1*, respectively, and three are homologs of *AtERS2* and *AtETR2* (**Figure 1A**). Notably, Glyma.20g08700 has been designated as *GmERS2* in PGDD. The gene names and locus IDs of these receptor genes are listed in Supplementary Table S2. In *Medicago*, totally six ethylene receptor genes were identified: one homolog for *MtETR1* and *MtERS1*, respectively; two homologs for *MtEIN4* and two potential homologs for *MtETR2* and *MtERS2*,

We next analyzed the structures of the ethylene receptor genes using GSDS 2.0[6], and the mRNA and genomic DNA sequences were downloaded from the Phytozome database. As shown in **Figure 1**, the gene structures of the homologs of *AtERS1* and *AtETR1* are highly conserved and have the same exon–intron pattern. However, the four homologs of *AtEIN4* exhibited two structural patterns. The structures of *Glyma.20g221800* (*GmEIN4a*), *Glyma.10g167300* (*GmEIN4b*), and *Glyma.19g249100* (*GmEIN4c*) were similar, whereas the structure of *Glyma.03g251700* (*GmEIN4d*) was different, with three exons and two introns (**Figure 1B**). In terms of the *AtETR2* and *AtERS2* homologs, *Glyma.10g188500* (*GmETR2b*) and *Glyma.20g087000* (*GmERS2*) each have three exons and two introns, in contrast to *AtETR2* and *AtERS2*, which contain one intron and two exons each. A duplication analysis conducted using EnsemblPlants[7] identified five pairs of duplicates. As shown in **Figure 2**, the duplicated pairs are *GmETR1a-GmETR1b*, *GmERS1a-GmERS1b*, *GmETR2a-GmETR2b*, *GmEIN4a-GmEIN4b*, and *GmEIN4c-GmEIN4d*.

Protein Structure Analysis of the Ethylene Receptors in Soybean

It has been proposed that ethylene receptor family proteins are highly conserved in plants, and that they are typical ER membrane-associated proteins sharing similarity with bacterial two-component regulators (Chang and Stadler, 2001; Guo and Ecker, 2004). To obtain detailed information about the structures of these ethylene receptor proteins in soybean, the deduced amino acid sequences collected from the Phytozome database were aligned, and the proteins structures were analyzed using PFAM[8]. As shown in **Figure 3**, the soybean ethylene receptor proteins all contain one GAF domain (green box), just like in *Arabidopsis*; by contrast, the protein domains [e.g., His kinase A (phospho-acceptor) domain (red box), His kinase domain (blue box), and response regulator receiver domain]

[6]http://gsds.cbi.pku.edu.cn/

[7]http://plants.ensembl.org/index.html

[8]http://pfam.xfam.org/search

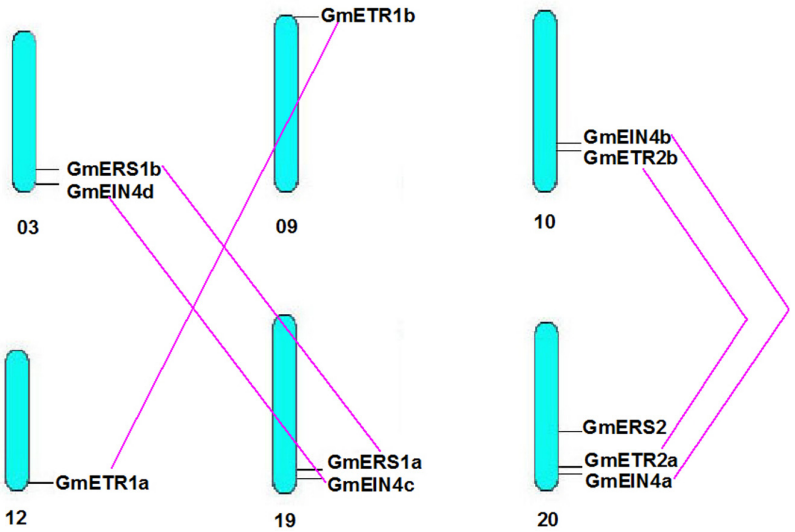

FIGURE 2 | Chromosomal distribution of the identified ethylene receptor genes. Based on soybean genome annotation v1.1, the chromosomal locations of the homologous ethylene receptor genes in soybean were analyzed and marked on the corresponding chromosomes from top to bottom. Duplicated genes are marked with a purple line.

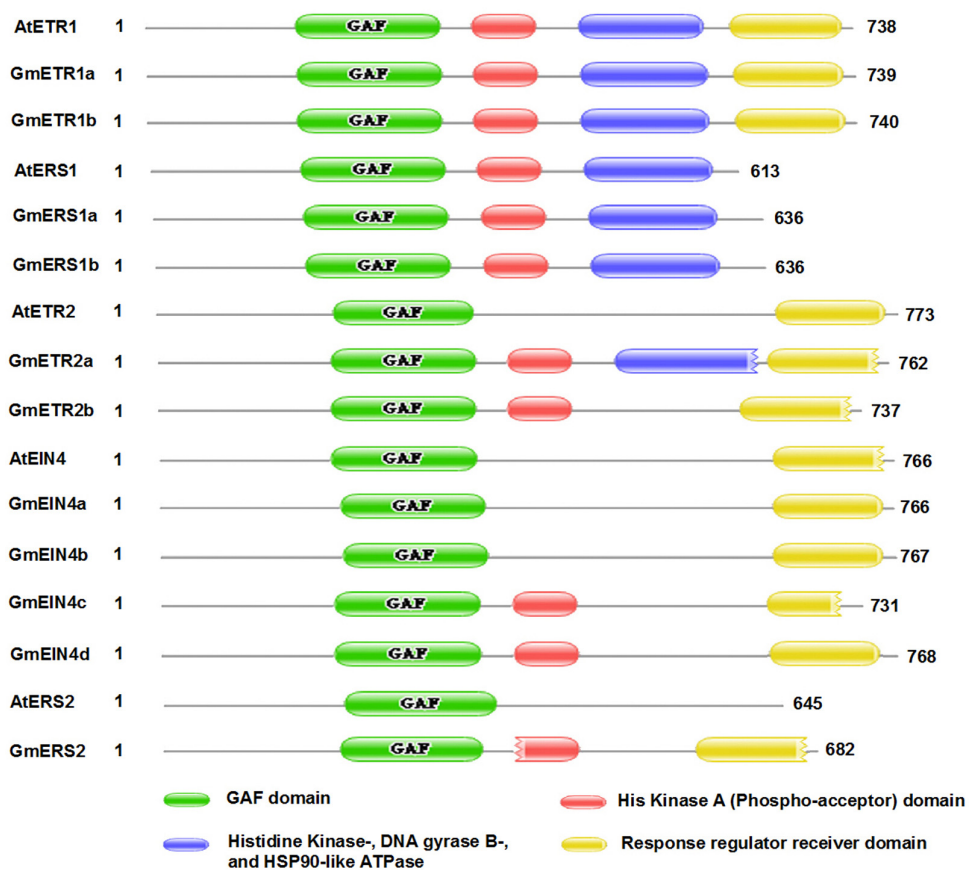

FIGURE 3 | The conserved domains of the homologous ethylene receptor proteins in soybean. The conserved domains of the homologous proteins were analyzed using the PFAM website (http://pfam.xfam.org/).

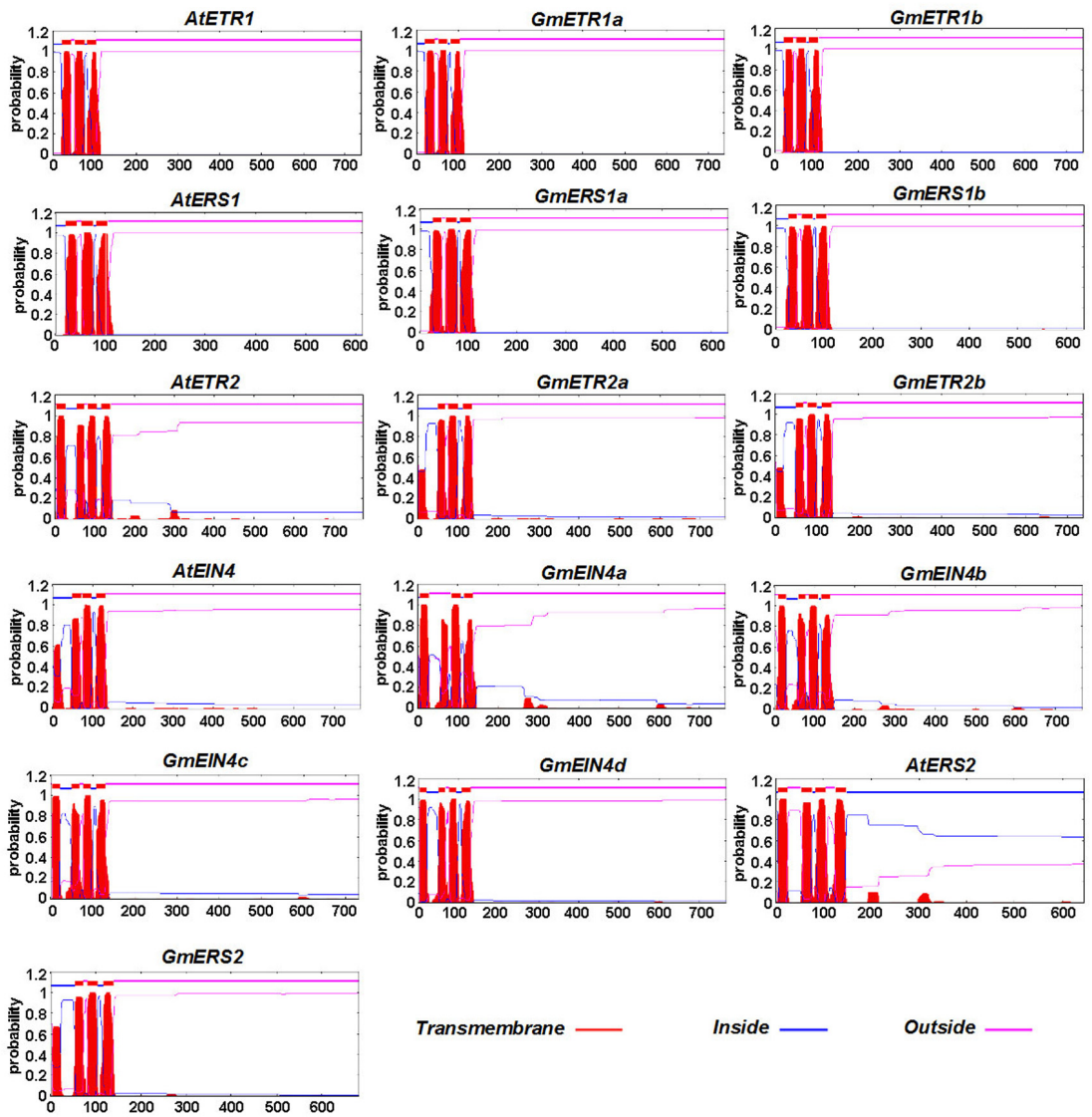

FIGURE 4 | The predicted protein profiles of the soybean ethylene receptors. The transmembrane helices of the ethylene receptor proteins were predicted using TMHMM2 (http://www.cbs.dtu.dk/services/TMHMM-2.0/). The transmembrane domains of the predicted proteins are shown by red peaks.

in the soybean receptors are variable. Notably, the protein structures of GmETR1 and GmERS1 are identical to those of AtETR1 and AtERS1. However, the predicted proteins GmETR2, GmEIN4, and GmERS2 show some variation compared with their *Arabidopsis* homologs. For example, GmETR2, GmEIN4c/d, and GmERS2 contain a His kinase A domain, which does not appear in AtETR2, AtEIN4, and AtERS2 (**Figure 3**). In addition, GmETR2a contains a His kinase domain. It was also found that the receiver domain at the C-terminus shows divergence among most subfamily members, except for ETR1 (**Figure 3**). AtETR2 has a complete receiver domain (yellow box), while GmETR2a and GmETR2b appear to have a degenerate domain lacking one or more elements (**Figure 3** and Supplementary Figure S1). As for the structures of the AtEIN4 homologs, only GmEIN4c was found to have a degenerate domain similar to that of AtEIN4; in contrast, the other three proteins have a complete receiver domain (**Figure 3**). The conservation of these receptors between *Arabidopsis* and soybean indicates that these proteins likely have conserved functions, while the differences in domains between these species suggest that the proteins have divergent functions in soybean.

The transmembrane architecture of the ethylene receptor proteins was also predicted using TMHHM 2.0[9]. As shown in **Figure 4**, these ethylene receptors contain several transmembrane domains, although the number of transmembrane domains varies by receptor. Like AtETR1 and AtERS1, GmETR1a/b and GmERS1a/b have three conserved transmembrane domains at their N-terminus. However, the

[9]http://www.cbs.dtu.dk/services/TMHMM-2.0/

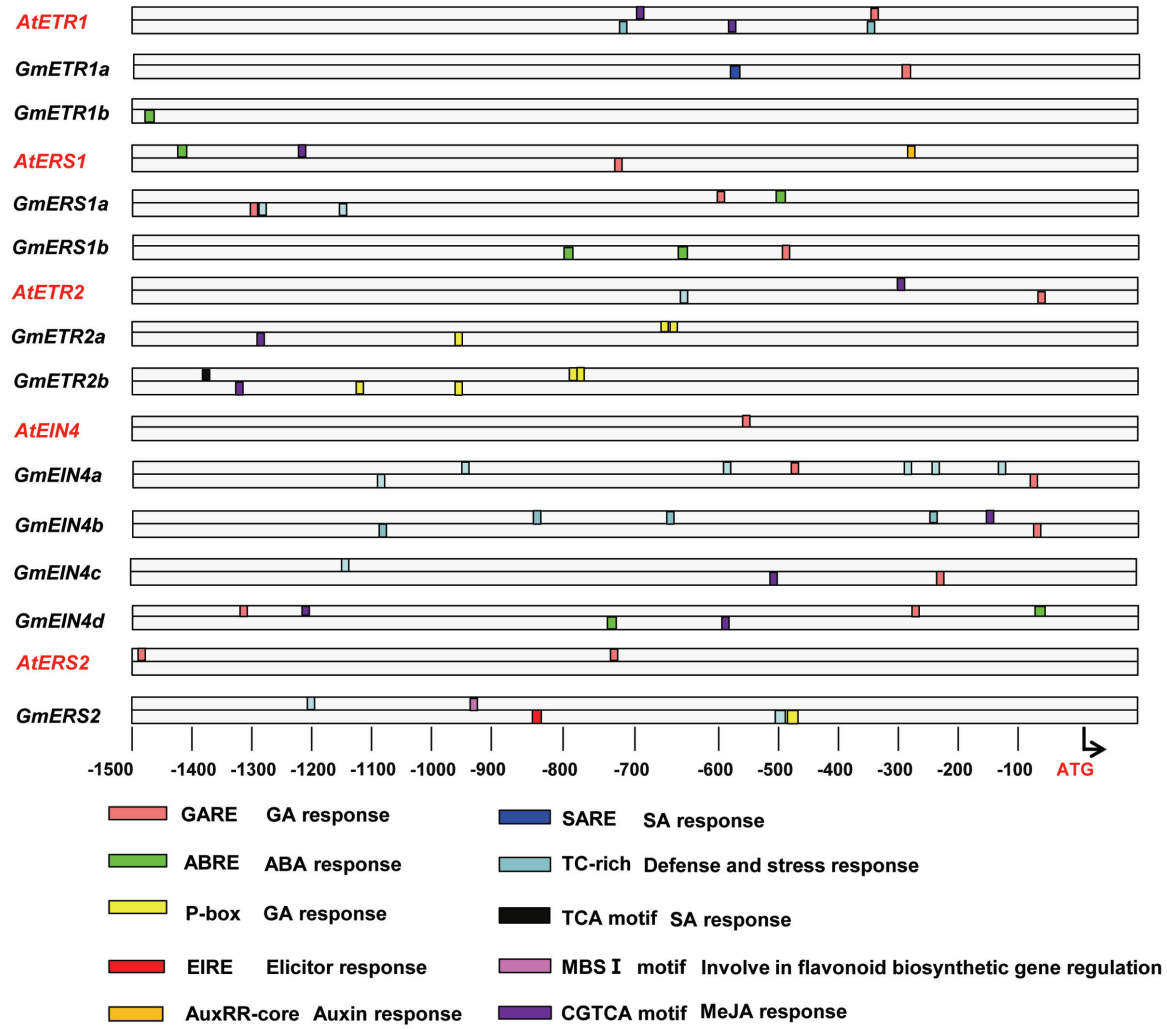

FIGURE 5 | Promoter analysis of the homologous ethylene receptor genes. The promoters of the genes (1,500 bp) were analyzed online (http://bioinformatics.psb.ugent.be/webtools/plantcare/html/) to detect *cis*-elements using PLACE software (http://www.dna.affrc.go.jp/PLACE/).

number of typical transmembrane domains in GmETR2 and GmERS2 is reduced compared with AtETR2 and AtERS2, while the number of transmembrane domains in GmEIN4b, GmEIN4c, and GmEIN4d appears to be increased compared with their homologs (**Figure 4**).

Cis-Elements in the Promoters of the Ethylene Receptor Genes in Soybean

In order to aid in understanding the putative functions of these ethylene receptor genes in soybean, we further performed the promoter analysis to identify the regulatory *cis*-elements that are involved in various biological processes, in particular plant hormonal response, defense response and nodulation. As shown in **Figure 5**, when compared with the conserved *cis*-elements identified from the promoters of *Arabidopsis* ethylene receptor genes and its' homologous genes in soybean, we found that they share some *cis*-elements, such as CGTCA motif, which might related with MeJA response; but interestingly, some *cis*-elements (i.e., P-box, TCA motif) only appeared in the promoters of the homolog genes in soybean. For example, the P-box, which was also predicted to be involved in GA response, was only observed in the promoters of *GmETR2a*, *GmETR2b,* and *GmERS2*. Another regulatory *cis*-element unique to soybean ethylene receptors is TC-rich repeat element, which is involved in defense and stress response. TC-rich repeat element occurs in the promoters of ethylene receptors *GmERS1a, GmEIN4a/b/c* and *GmERS2*, although the numbers of the *cis*-element are different; in sharp contrast, only single element was found in the promoters of *Arabidopsis* ethylene receptors *AtETR1* and *AtETR2*. The ABRE elements, which is related to ABA response, were found only in the promoter regions of *GmETR1b, GmERS1a/1b,* and *GmEIN4d* (**Figure 5**). Interestingly, both EIRE element and MBS I element, which were related to Elicitor response and flavonoid biosynthetic gene regulation, respectively, were only observed in the promoter of *GmERS2*. These observations

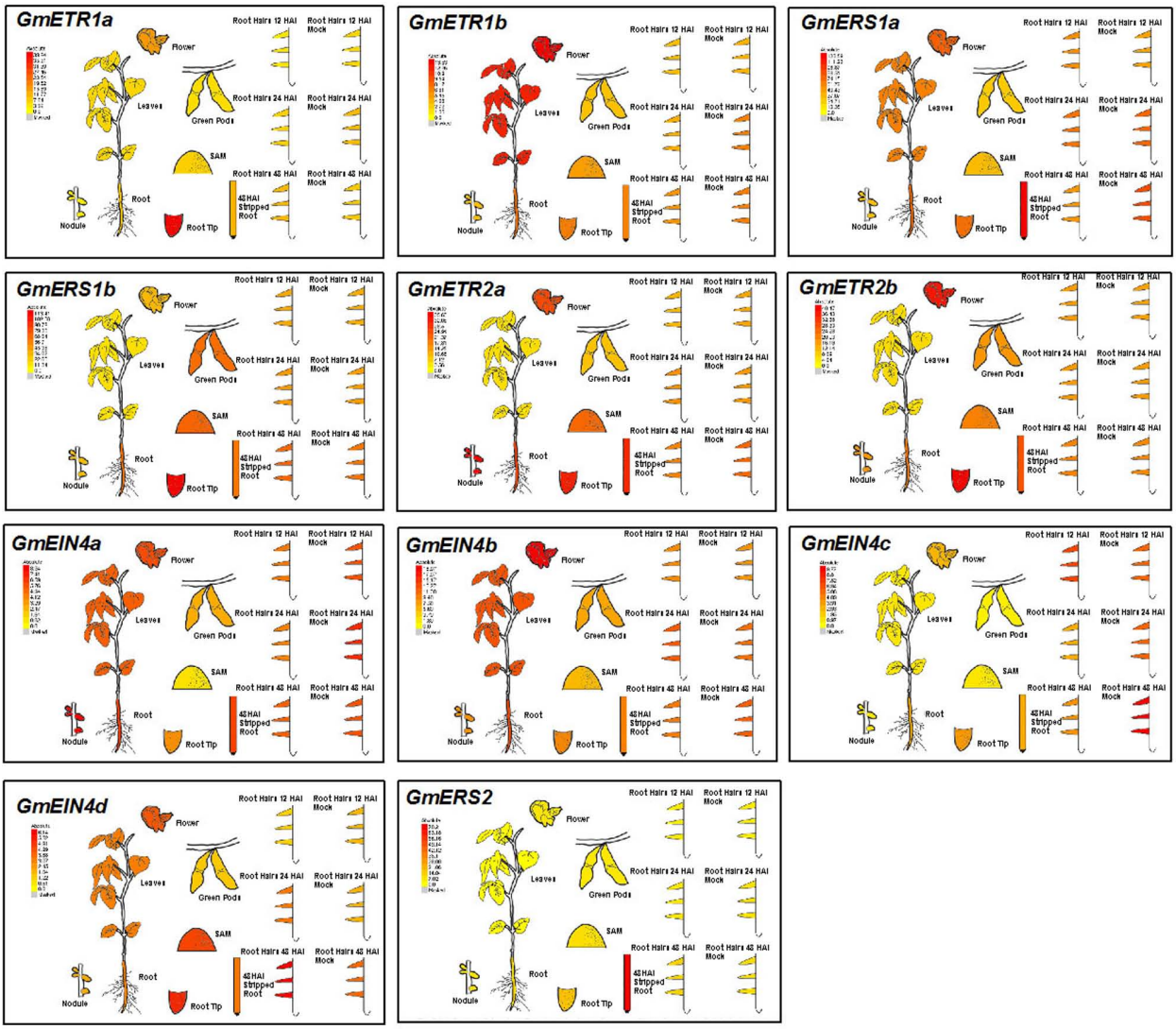

FIGURE 6 | Expression patterns of the ethylene receptor genes based on Hiseq data. Based on information from the eFP Browser (http://bar.utoronto.ca/efpsoybean/cgi-bin/efpWeb.cgi), the tissue-specific expression patterns of the ethylene receptor genes and the expression patterns in response to rhizobial inoculation were analyzed.

indicate that regulations of the ethylene receptor genes are divergent in soybean and *Arabidopsis* and that the ethylene receptors may modulate different biological processes during plant development and responses to environmental stimuli in soybean and *Arabidopsis*.

Expression Patterns of Soybean Ethylene Receptor Genes Based on HiSeq Data

To investigate the possible roles of the ethylene receptor genes in soybean, we first analyzed the expression patterns of these genes in different tissues and organs including leaves, roots and mature nodules by collecting the HiSeq data from the eFP website (Libault et al., 2010)[10]. As shown in **Figure 6**, these ethylene receptor genes exhibited distinct tissue/organ expression patterns. For example, *GmETR1b*, *GmERS1a*, *GmEIN4a*, *GmEIN4b,* and *GmEIN4d* had relative high expression levels in soybean leaves; *GmETR1b*, *GmERS1a/b*, *GmEIN4a*, *GmEIN4b* were expressed at higher levels in roots. In addition, *GmETR1a* was specifically expressed in root tips, while *GmEIN4c* and *GmERS2* were expressed at relative low levels in all tissues and organs. This observation indicates that the ethylene receptor genes are differentially expressed during soybean growth and development.

Interestingly, *GmETR2a* and *GmEIN4a* were highly expressed in mature nodules (**Figure 6**). Furthermore, several ethylene receptor genes were differentially regulated by rhizobial infection. Among them, the expression of *GmEIN4c* was downregulated by rhizobial inoculation at 24 and 48 h after

[10]http://bar.utoronto.ca/efpsoybean/cgi-bin/efpWeb.cgi

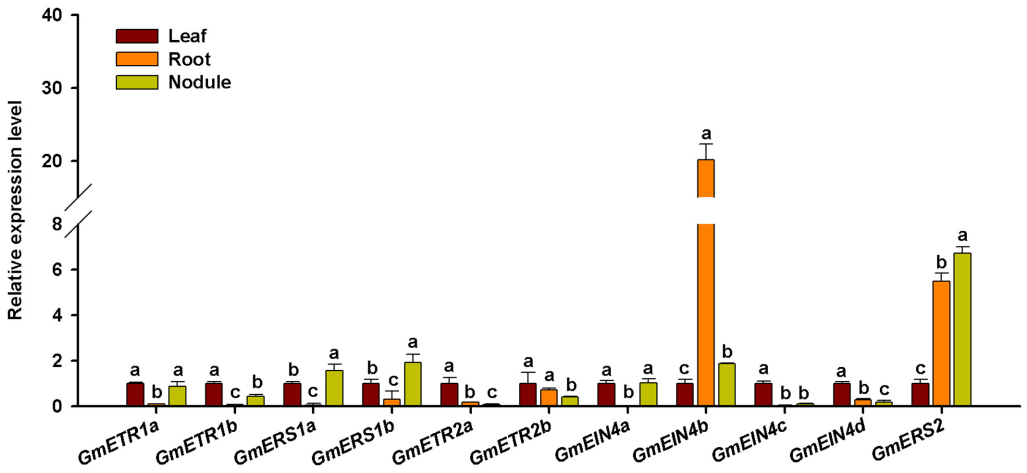

FIGURE 7 | Expression analysis of the ethylene receptor genes in different tissues of soybean. The expression patterns of the ethylene receptor genes in leaf, root, and mature nodule of soybean plants at 28 days after rhizobia inoculation were analyzed by qRT-PCR. Expression levels were normalized against the geometric mean of the reference gene *GmELF1b*. Three independent biological repeats were done; the results shown are the averages ± standard deviation. Different letters indicate significant differences in relative gene expression by the Student-Newman-Keuls test ($P < 0.05$).

infection, while *GmERS1a* expression was decreased at 48 h after rhizobial inoculation (**Figure 6**). By contrast, only *GmEIN4d* was induced by rhizobia at 24 h after infection (**Figure 6**). Together, these results suggest that ethylene receptor genes might be involved in rhizobia–soybean interactions and have different functions during nodule development.

Experimental Validation of Tissue Expression of Soybean Receptor Genes

To validate the tissue specific expression patterns of the ethylene receptor genes, RT-qPCR was used to analyze the expression pattern of those ethylene receptor genes in different tissues of soybean plants at 28 days after rhizobia inoculation. As shown in **Figure 7**, all the ethylene receptor genes were differentially expressed in leaf, root, and nodule. Majority of them were showed higher levels of expression in leaf than in root and nodule. Interestingly, the duplicates of the ethylene receptor genes *GmETR1*, *GmETR2,* and *GmEIN4* except *GmERS1* exhibited different patterns in the tissues examined. Among 11 ethylene receptor genes, only *GmETR1a* and *GmEIN4a* displayed the same expression pattern. Intriguingly, among the ethylene receptor genes, *GmEIN4b* showed highest expression in root, followed by *GmERS2* in nodule and root.

In addition, association between promoter and gene expression pattern was analyzed based on the digital expression data. The expression data of each gene in eight different tissues of soybean[10] and 47 tissues of *Arabidopsis* ethylene receptor genes collected from the website[11] were used to be analyzed (Tamura et al., 2004) (Supplementary Tables S3, S4). As shown in Supplementary Figure S2, the relative correlation coefficient (R^2) in soybean and *Arabidopsis* were 0.12 and 0.35, respectively. These data indicates that the promoter sequence similarity and expressional pattern of ethylene receptor genes might show positive association. In order to make a further understanding about the ethylene receptor genes, a molecular evolution analysis has been done for pairs of duplicated genes. The coding sequences collected from the Phytozome database were aligned with MEGA6 and parameters between paired genes were estimated with SNAP[12]. dn/ds indicates the ratio of non-synonymous to synonymous substitutions. As shown in Supplementary Table S5, the dn/ds ratio of all paired genes showed lower than one, which suggested that the molecular evolution of these ethylene receptor genes was conservative.

Expression Validation of Soybean Receptor Genes in Response to Rhizobial Infection and Nod Factor

Because we were interested in the roles of ethylene receptor genes in soybean nodulation, we performed qRT-PCR assays to analyze the expression patterns of soybean ethylene receptor genes in response to rhizobial infection and during early process of nodulation. Soybean seedlings were inoculated with rhizobial strain *B. japonicum* USDA110, and root samples were collected at specific time points. The qPCR analysis results detected variable expression of the ethylene receptor genes in response to rhizobia infection (**Figure 8**). Among them, *GmERS1a, GmERS1b,* and *GmEIN4c* were highly induced within 24 h (**Figures 8C,D,I**), while the expression of *GmETR1b, GmETR2a, GmETR2b, GmEIN4a,* and *GmEIN4b* were significantly repressed within 24 h (**Figures 8B,E–H**). The rest of the ethylene receptor genes *GmETR1a*, *GmEIN4d,* and *GmERS2* were slightly upregulated and then downregulated during the experimental period of time

[11]http://www.arabidopsis.org/

[12]https://www.hiv.lanl.gov/content/sequence/SNAP/SNAP.html

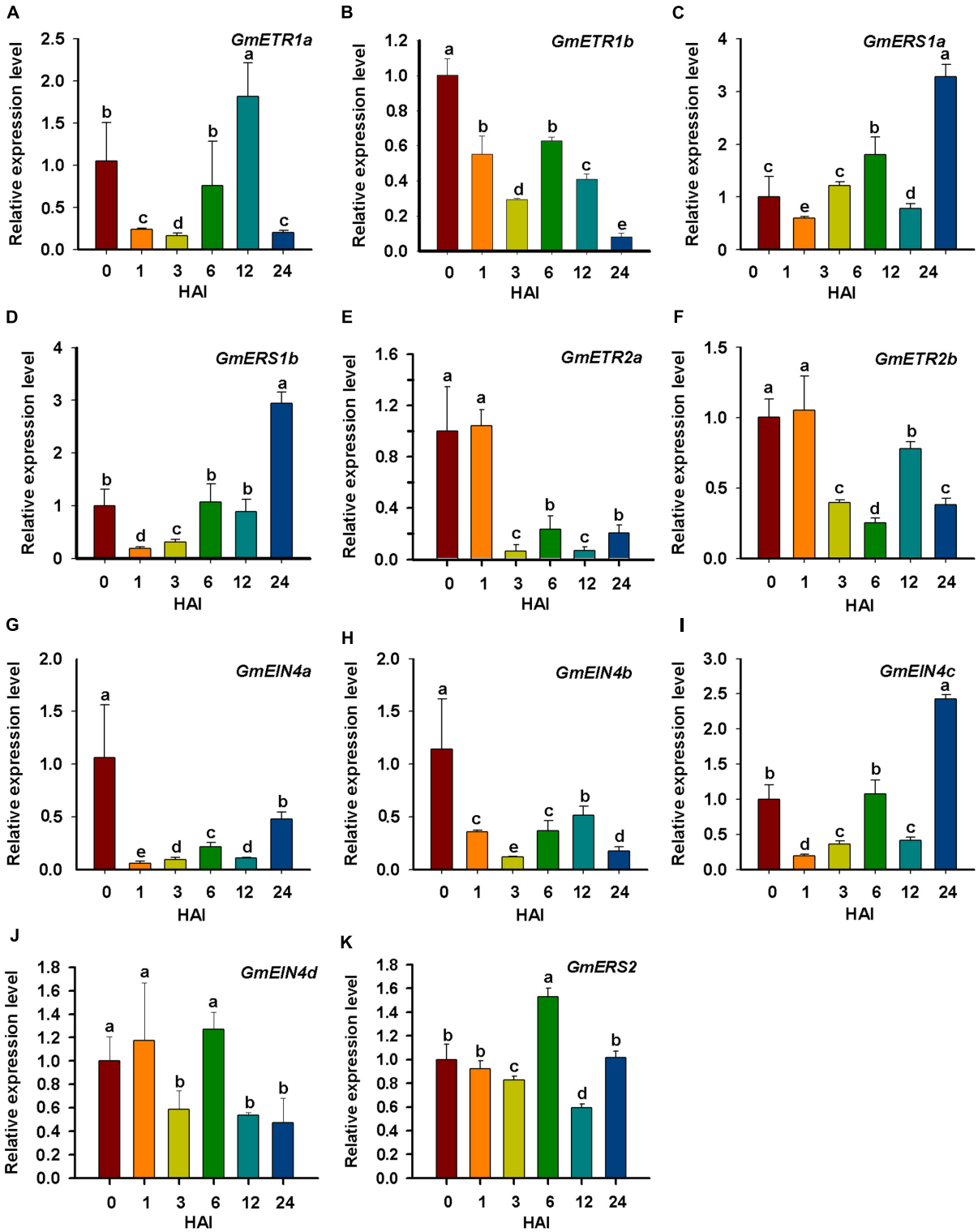

FIGURE 8 | Expression analysis of the ethylene receptor genes to outline the early response to rhizobial inoculation. (A–K) The relative expression level of ethylene receptor genes *GmETR1a*, *GmETR1b*, *GmERS1a*, *GmERS1b*, *GmETR2a*, *GmETR2b*, *GmEIN4a*, *GmEIN4b*, *GmEIN4c*, *GmEIN4d*, and *GmERS2* in response to rhizobial inoculation at different time points (0, 1, 3, 6, 12, and 24 h). The short-term expression patterns of the ethylene receptor genes in response to rhizobial inoculation was analyzed by qRT-qPCR. The expression level of each gene was normalized against the geometric mean of the soybean reference gene *GmELF1b*. Three independent biological repeats were done; the results shown are the averages ± standard deviation. Different letters indicate significant differences by the Student-Newman-Keuls test ($P < 0.05$).

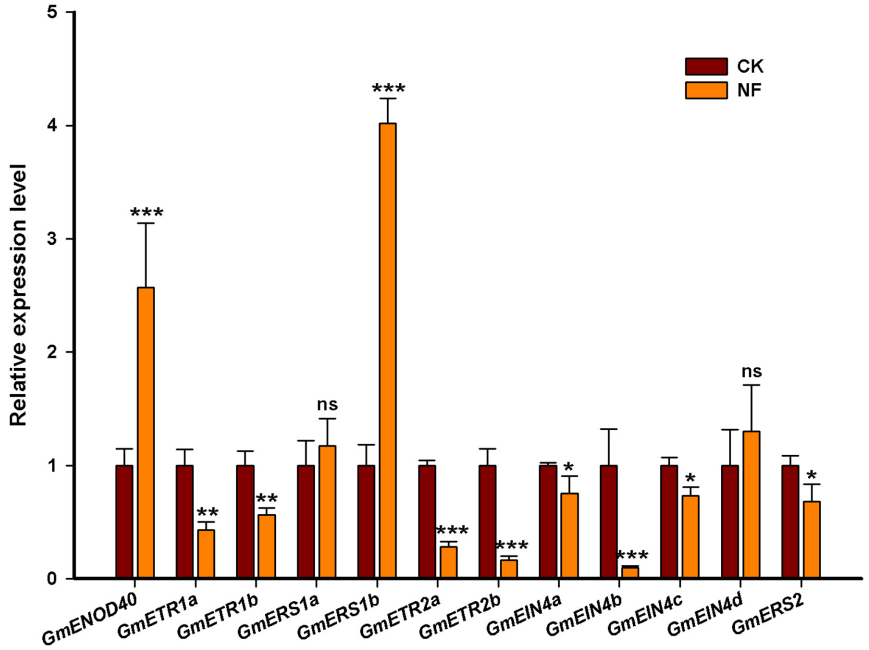

FIGURE 9 | Expression analysis of the ethylene receptor genes in response to Nod factor (NF). The expression pattern of the ethylene receptor genes was analyzed by qRT-qPCR in response to NF (10^{-8} M) treatment, where *GmENOD40* was chosen to be a positive control. The expression was normalized against the geometric mean of the reference gene *GmELF1b*. The experiments were done for three independent times. Error bars indicate SD. Statistically significant difference (Student's *t*-test) are indicated as follows: ns, no significance $P > 0.05$; *$P < 0.05$; **$P < 0.01$; ***$P < 0.001$.

(**Figures 8A,J,K**). These results confirm that majority of soybean ethylene receptor genes are responsive to rhizobial infection.

To further confirm the responsiveness of the ethylene receptor genes, we also tested whether these genes could be affected by NF. Four-day-old soybean seedlings were treated with NF for 24 h, and root samples were collected for qRT-PCR. As shown in **Figure 9**, compared with the induction of early nodulin gene *GmENOD40*, the transcript levels of *GmETR1a/b, GmETR2a/b, GmEIN4a/b*, *GmEIN4c,* and *GmERS2* were repressed significantly in response to NF application in soybean roots. However, the expression of *GmERS1a* and *GmEIN4d* were not significantly changed in response to NF treatment compared with the untreated control. Notably, the expression of *GmERS1b* was highly induced by NF and the expression level of *GmERS1b* was increased about fourfold (**Figure 9**). These results suggest that ethylene receptor genes may mediate rhizobia–plant cell interaction and early nodule development in soybean.

DISCUSSION

Ethylene receptors are central regulators that turn the downstream ethylene signaling transduction pathway on/off. Since ethylene controls various biological processes in different tissues/organs and at different developmental stages, plants have evolved multiple ethylene receptors with divergent gene structures, protein structures, kinase activities, and patterns of transcriptional regulation to precisely and dynamically modulate plant responses to ethylene. Compelling evidence suggests that ethylene receptors regulate plant development and plant responses to environmental stimuli in a complex manner. In this study, we performed a systematic analysis of the ethylene receptors in soybean, including their gene structures, conserved domains, and gene expression patterns in response to rhizobial infection. Our results provide an overview of the main characteristics of these receptors and their potential functions in soybean.

Previous studies have shown that the numbers of ethylene receptors vary in different plant species (Cao et al., 2003; Gallie, 2015b). For example, *Arabidopsis* and rice both have five ethylene receptors, although the types are different (Cao et al., 2003). The number of ethylene receptors in a species represents the level of functional complexity in terms of ethylene perception and cellular responses. Soybean is an allotetraploid plant, and most of its genes have several duplicates (Shoemaker et al., 2006; Schlueter et al., 2007). By searching the soybean genome and gathering data from PGDD, we found 11 ethylene receptors instead of 8 (GmETR1b, GmETR2a, and GmERS2 were missing) used in the previous study (Gallie, 2015a). A phylogenetic analysis showed that soybean has homologs of all of the ethylene receptors in *Arabidopsis*, but that these receptors were not equally duplicated during evolution. Among them, *GmETR1*, *GmERS1*, and *GmETR2* have two duplicates and *GmEIN4* has four duplicates, whereas *GmERS2* exists as a single copy, like in *Arabidopsis*. It is clear that these ethylene receptors are not equally duplicated in soybean. Thus far, we do not know why these receptors have different numbers of duplicates.

It is conceivable that the members of the first receptor family subgroup (ETR1 and ERS1) are more conservative because they play a more important role in ethylene signaling and plant responses to ethylene (Qu et al., 2007; Rivarola et al., 2009). Although we do not know why the members of the second subgroup (GmETR2, GmEIN4, and GmERS2) show such big differences in duplicate number, it is likely that alterations in the numbers of these receptors can increase the regulatory flexibility and complexity of plant responses to ethylene. Notably, our finding support the notion that soybean and *Medicago* also contain all types of ethylene receptors including ERS2, which is apparently not in agreement with the conclusion drawn by Gallie (2015a) that ERS2 homologs exist only in the *Brassicaceae*. The different conclusions about ERS2 are due to the incomplete data used in the previous study. Therefore, the conclusion drawn in the previous study need to be further analyzed using more completed data from various plant species. But our analysis results favor the hypothesis that ERS2 is the most newly evolved ethylene receptor because there is only a single copy of *ERS2*, which may arise after genome duplication (Gallie, 2015a). Interestingly, we found that *Medicago* contains a single copy of ETR1, ETR2, ERS1 and ERS2, but two copies of EIN4. It remains unknown whether extra copy (copies) of EIN4 in *Medicago* and soybean mediate the biological processes unique to legumes.

Interestingly, our domain analysis showed that all 11 receptors contain a GAF domain at their N-terminus, though some receptors have extra domains compared with their *Arabidopsis* homologs. Notably, the protein structures of ETR1 and ERS1 are highly conserved in *Arabidopsis* and soybean. Specifically, they share exactly the same domains [a GAF, a His kinase A (phospho-acceptor) domain, a His kinase domain, and a receiver domain], supporting the key role of ETR1 and ERS1 in ethylene perception and responses. It is worth noting that in GmETR2 and GmEIN4 half of the protein is similar to its *Arabidopsis* homolog, whereas the other half contains an extra His kinase A domain. Since the His kinase domain is responsible for dimerization with the phospho-acceptor domain, the evolution of the His kinase A domain suggests that these ethylene receptors have additional functions in mediating ethylene perception and the activation of downstream ethylene signaling events. However, the underlying molecular mechanism of these new ethylene receptor members is unknown. Further characterization of these proteins with an extra domain will help us understand how these receptors mediate ethylene perception and regulate plant responses to ethylene.

In *Arabidopsis*, five ethylene receptors also show tissue/organ or developmental stage specificity, although they are functionally redundant (Schaller and Bleecker, 1995; Hua and Meyerowitz, 1998; Guo and Ecker, 2004). In soybean, we found that the 11 ethylene receptors exhibit tissue/organ specificity. Some receptor genes have a similar expression pattern to their duplicates (e.g., *GmERS1a* and *GmERS1b*), which consistent with a low dn/ds ratio suggested the evolutionary conservation of these ethylene receptor genes. However, the duplicates of some receptor genes display a different expression pattern. For example, *GmEIN4a* was found to be highly expressed in leaf and nodule, whereas *GmEIN4b* showed its highest expression level in root. Notably, among these receptor genes, only *GmEIN4b* showed highest expression in root, whereas *GmERS2* showed the highest expression level in nodules. Furthermore, majority of the soybean receptor genes were found to be responsive to rhizobial infection. It worthy to note that eight of these ethylene receptor genes were downregulated by NF, indicating that these genes and the ethylene signaling pathway might play a role in the early process of nodulation in soybean. Interestingly, *GmERS1b* was highly induced by NF, suggesting a different role of this gene during rhizobia infection. Furthermore, we do not exclude the possibility that these ethylene receptor genes may also exhibit different expression patterns during nodule formation and organogenesis to mediate late development process of nodulation in soybean. These expression analysis results suggest that in addition to their differences in protein structure, these receptor genes are regulated at the transcriptional level. These multiple levels of regulation may enable the receptors to precisely and collaboratively modulate various biological processes in soybean. It is possible that apart from the general functions of ethylene receptors in higher plants, some members may be evolved to specifically regulate nodulation and SNF in soybean. Functional analysis of individual ethylene receptor genes will uncover the roles of these genes in plant development and symbiotic nodulation in soybean.

AUTHOR CONTRIBUTIONS

YW and XL conceived the study. YW and XL designed the experiments. WY, XW, CS, HW did the bioinformatics analysis. YW, JY, LZ, and ZS performed the experiments. YW and XL wrote the article.

ACKNOWLEDGMENTS

This study was funded by the National Natural Science Foundation of China (Grants 31230050 and 30971797), the Ministry of Agriculture of the People's Republic of China (Grants 2014ZX0800929B and 2009ZX08009-132B), the Huazhong Agricultural University Scientific & Technological Self-innovation Foundation (Program No. 2015RC014), and the Youth Innovation Promotion Association of the Chinese Academy of Sciences.

SUPPLEMENTARY MATERIAL

The Supplementary Material for this article can be found online at: http://journal.frontiersin.org/article/10.3389/fpls.2017.00859/full#supplementary-material

REFERENCES

Abeles, F. B., Morgan, P. W., and Saltveit, M. E. Jr. (1992). *Ethylene in Plant Biology*, 2nd Edn. New York, NY: Academic Press.

Bleecker, A. B., and Kende, H. (2000). Ethylene: a gaseous signal molecule in plants. *Annu. Rev. Cell Dev. Biol.* 16, 1–18. doi: 10.1146/annurev.cellbio.16.1.1

Burg, S. P., and Burg, E. A. (1967). Molecular requirement for the biological activity of ethylene. *Plant Physiol.* 42, 144–152. doi: 10.1104/pp.42.1.144

Caba, J. M., Recalde, L., and Ligero, F. (1998). Nitrate-induced ethylene biosynthesis and the control of nodulation in alfalfa. *Plant Cell Environ.* 21, 87–93. doi: 10.1046/j.1365-3040.1998.00242.x

Cao, W. H., Dong, Y., Zhang, J. S., and Chen, S. Y. (2003). Characterization of an ethylene receptor homolog gene from rice. *Sci. China C Life Sci.* 46, 370–378. doi: 10.1007/BF03192580

Chang, C., and Stadler, R. (2001). Ethylene hormone receptor action in *Arabidopsis*. *Bioessays* 23, 619–627. doi: 10.1002/bies.1087

Chen, Y. F., Randlett, M. D., Findell, J. L., and Schaller, G. E. (2002). Localization of the ethylene receptor ETR1 to the endoplasmic reticulum of *Arabidopsis*. *J. Biol. Chem.* 277, 19861–19866. doi: 10.1074/jbc.M201286200

Cho, Y.-H., and Yoo, S.-D. (2015). Novel connections and gaps in ethylene signaling from the ER membrane to the nucleus. *Front. Plant Sci.* 5:733. doi: 10.3389/fpls.2014.00733

Deng, W., Wang, Y., Liu, Z., Cheng, Z. L., and Xue, C. Y. (2014). HemI: a toolkit for illustrating heatmaps. *PLoS ONE* 9:e111988. doi: 10.1371/journal.pone.0111988

Ferguson, B., Lin, M.-H., and Gresshoff, P. M. (2013). Regulation of legume nodulation by acidic growth conditions. *Plant Signal. Behav.* 8:e23426. doi: 10.4161/psb.23426

Ferguson, B. J., Indrasumunar, A., Hayashi, S., Lin, M.-H., Lin, Y.-H., Reid, D. E., et al. (2010). Molecular analysis of legume nodule development and autoregulation. *J. Integr. Plant Biol.* 52, 61–76. doi: 10.1111/j.1744-7909.2010.00899.x

Gallie, D. R. (2015a). Appearance and elaboration of the ethylene receptor family during land plant evolution. *Plant Mol. Biol.* 87, 521–539. doi: 10.1007/s11103-015-0296-z

Gallie, D. R. (2015b). Ethylene receptors in plants - why so much complexity? *F1000Prime Rep.* 7, 39. doi: 10.12703/P7-39

Gamalero, E., and Glick, B. R. (2015). Bacterial modulation of plant ethylene levels. *Plant Physiol.* 169, 13–22. doi: 10.1104/pp.15.00284

Goodlass, G., and Smith, K. A. (1979). Effects of ethylene on root extension and nodulation of pea (*Pisum sativum* L.) and white clover (*Trifolium repens* L.). *Plant Soil* 51, 387–395. doi: 10.1007/BF02197785

Gresshoff, P. M., Lohar, D., Chan, P.-K., Biswas, B., Jiang, Q., Reid, D., et al. (2009). Genetic analysis of ethylene regulation of legume nodulation. *Plant Signal. Behav.* 4, 818–823. doi: 10.4161/psb.4.9.9395

Grobbelaar, N., Clarke, B., and Hough, M. C. (1971). The nodulation and nitrogen fixation of isolated roots of *Phaseolus vulgaris* L.III. The effect of carbon dioxide and ethylene. *Plant Soil* 35, 215–223. doi: 10.1016/j.syapm.2012.04.003

Guinel, F. C. (2016). Ethylene, a hormone at the center-stage of nodulation. *Front. Plant Sci.* 6:1121. doi: 10.3389/fpls.2015.01121

Guinel, F. C., and LaRue, T. A. (1992). Ethylene inhibitors partly restore nodulation to pea mutant E 107 (*brz*). *Plant Physiol.* 99, 515–518. doi: 10.1104/pp.99.2.515

Guo, H., and Ecker, J. R. (2004). The ethylene signaling pathway: new insights. *Curr. Opin. Plant Biol.* 7, 40–49. doi: 10.1016/j.pbi.2003.11.011

Hua, J., and Meyerowitz, E. M. (1998). Ethylene responses are negatively regulated by a receptor gene family in *Arabidopsis thaliana*. *Cell* 94, 261–271. doi: 10.1016/S0092-8674(00)81425-7

Hunter, W. J. (1993). Ethylene production by root nodules and effect of ethylene on nodulation in *Glycine max*. *Appl. Environ. Microbiol.* 59, 1947–1950.

Jian, B., Liu, B., Bi, Y., Hou, W., Wu, C., and Han, T. (2008). Validation of internal control for gene expression study in soybean by quantitative real-time PCR. *BMC Mol. Biol.* 9:59. doi: 10.1186/1471-2199-9-59

Johnson, P. R., and Ecker, J. R. (1998). The ethylene gas signal transduction pathway: a molecular perspective. *Annu. Rev. Genet.* 32, 227–254. doi: 10.1146/annurev.genet.32.1.227

Ju, C., Yoon, G. M., Shemansky, J. M., Lin, D. Y., Ying, Z. I., Chang, J., et al. (2012). CTR1 phosphorylates the central regulator EIN2 to control ethylene hormone signaling from the ER membrane to the nucleus in *Arabidopsis*. *Proc. Natl. Acad. Sci. U.S.A.* 109, 19486–19491. doi: 10.1073/pnas.1214848109

Kieber, J. J., Rothenberg, M., Roman, G., Feldmann, K. A., and Ecker, J. R. (1993). CTR1, a negative regulator of the ethylene response pathway in *Arabidopsis*, encodes a member of the raf family of protein kinases. *Cell* 72, 427–441. doi: 10.1016/0092-8674(93)90119-B

Larrainzar, E., Riely, B. K., Kim, S. C., Carrasquilla-Garcia, N., Yu, H. J., Hwang, H. J., et al. (2015). Deep sequencing of the *Medicago truncatula* root transcriptome reveals a massive and early interaction between nod factor and ethylene signals. *Plant Physiol.* 169, 233–265. doi: 10.1104/pp.15.00350

Lee, K. H., and Larue, T. A. (1992). Exogenous ethylene inhibits nodulation of *Pisum sativum* L. cv Sparkle. *Plant Physiol.* 100, 1759–1763. doi: 10.1104/pp.100.4.1759

Lee, T. H., Tang, H., Wang, X., and Paterson, A. H. (2012). PGDD: a database of gene and genome duplication in plants. *Nucleic Acids Res.* 41, D1152–D1158. doi: 10.1093/nar/gks1104

Libault, M., Farmer, A., Joshi, T., Takahashi, K., Langley, R. J., Franklin, L. D., et al. (2010). An integrated transcriptome atlas of the crop model *Glycine max*, and its use in comparative analyses in plants. *Plant J.* 63, 86–99. doi: 10.1111/j.1365-313X.2010.04222.x

Lohar, D., Stiller, J., Kam, J., Stacey, G., and Gresshoff, P. M. (2009). Ethylene insensitivity conferred by a mutated *Arabidopsis* ethylene receptor gene alters nodulation in transgenic *Lotus japonicus*. *Ann. Bot.* 104, 277–285. doi: 10.1093/aob/mcp132

Miyata, K., Kawaguchi, M., and Nakagawa, T. (2013). Two distinct EIN2 genes cooperatively regulate ethylene signaling in *Lotus japonicus*. *Plant Cell Physiol.* 54, 1469–1477. doi: 10.1093/pcp/pct095

Nukui, N., Ezura, H., and Minamisawa, K. (2004). Transgenic *Lotus japonicus* with an ethylene receptor gene *Cm-ERS1/H70A* enhances formation of infection threads and nodule primordia. *Plant Cell Physiol.* 45, 427–435. doi: 10.1093/pcp/pch046

Nukui, N., Ezura, H., Yuhash, K. I., Yasuta, T., and Minamisawa, K. (2000). Effects of ethylene precursor and inhibitors for ethylene biosynthesis and perception on nodulation in *Lotus japonicus* and *Macroptilium atropurpureum*. *Plant Cell Physiol.* 41, 893–897. doi: 10.1093/pcp/pcd011

Oldroyd, G. E., and Downie, J. A. (2008). Coordinating nodule morphogenesis with rhizobial infection in legumes. *Annu. Rev. Plant Biol.* 59, 519–546. doi: 10.1146/annurev.arplant.59.032607.092839

Penmetsa, R. V., and Cook, D. R. (1997). A legume ethylene-insensitive mutant hyper infected by its rhizobial symbiont. *Science* 275, 527–530. doi: 10.1126/science.275.5299.527

Penmetsa, R. V., Uribe, P., Anderson, J., Lichtenzveig, J., Gish, J.-C., Nam, Y.-W., et al. (2008). The *Medicago truncatula* of the *Arabidopsis EIN2* gene, sickle, is a negative regulator of symbiotic and pathogenic microbial interactions. *Plant J.* 55, 580–595. doi: 10.1111/j.1365-313X.2008.03531.x

Qu, X., Hall, B. P., Gao, Z., and Schaller, G. E. (2007). A strong constitutive ethylene-response phenotype conferred on *Arabidopsis* plants containing null mutations in the ethylene receptors ETR1 and ERS1. *BMC Plant Biol.* 7:3. doi: 10.1186/1471-2229-7-3

Rivarola, M., McClellan, C. A., Resnick, J. S., and Chang, C. (2009). ETR1-specific mutations distinguish ETR1 from other *Arabidopsis* ethylene receptors as revealed by genetic interaction with RTE1. *Plant Physiol.* 150, 547–551. doi: 10.1104/pp.109.138461

Schaller, G. E., and Bleecker, A. B. (1995). Ethylene-binding sites generated in yeast expressing the *Arabidopsis* ETR1 gene. *Science* 270, 1809–1811. doi: 10.1126/science.270.5243.1809

Schlueter, J. A., Lin, J. Y., Schlueter, S. D., Vasylenko-Sanders, I. F., Deshpande, S., Yi, J., et al. (2007). Gene duplication and paleopolyploidy in soybean and the implications for whole genome sequencing. *BMC Genomics* 8:330. doi: 10.1186/1471-2164-8-330

Schmidt, J. S., Harper, J. E., Hoffman, T. K., and Bent, A. F. (1999). Regulation of soybean nodulation independent of ethylene signaling. *Plant Physiol.* 119, 951–959. doi: 10.1104/pp.119.3.951

Severin, A. J., Woody, J. L., Bolon, Y.-T., Joseph, B., Diers, B. W., Farmer, A. D., et al. (2010). RNA-seq atlas of *Glycine max*: a guide to the soybean transcriptome. *BMC Plant Biol.* 10:160. doi: 10.1186/1471-2229-10-160

Shoemaker, R. C., Schlueter, J., and Doyle, J. J. (2006). Paleopolyploidy and gene duplication in soybean and other legumes. *Curr. Opin. Plant Biol.* 9, 104–109. doi: 10.1016/j.pbi.2006.01.007

Stacey, G., Libault, M., Brechenmacher, L., Wan, J., and May, G. D. (2006). Genetics and functional genomics of legume nodulation. *Curr. Opin. Plant Biol.* 9, 110–121. doi: 10.1016/j.pbi.2006.01.005

Suganuma, N., Yamauchi, H., and Yamamoto, K. (1995). Enhanced production of ethylene by soybean roots after inoculation with *Bradyrhizobium japonicum*. *Plant Sci.* 111, 163–168. doi: 10.1016/0168-9452(95)04239-Q

Tamura, K., Nei, M., and Kumar, S. (2004). Prospects for inferring very large phylogenies by using the neighbor-joining method. *Proc. Natl. Acad. Sci. U.S.A.* 101, 11030–11035. doi: 10.1073/pnas.0404206101

Tamura, K., Peterson, D., Peterson, N., Stecher, G., Nei, M., and Kumar, S. (2011). MEGA5: molecular evolutionary genetics analysis using maximum likelihood, evolutionary distance, and maximum parsimony methods. *Mol. Biol. Evol.* 28, 2731–2739. doi: 10.1093/molbev/msr121

Thompson, J. D., Gibson, T. J., Plewniak, F., Jeanmougin, F., and Higgins, D. G. (1997). The CLUSTAL_X windows interface: flexible strategies for multiple sequence alignment aided by quality analysis tools. *Nucleic Acids Res.* 25, 4876–4882. doi: 10.1093/nar/25.24.4876

Wang, Y., Li, P., Cao, X., Wang, X., Zhang, A. and Li, X. (2009). Identification and expression analysis of miRNAs from nitrogen-fixing soybean nodules. *Biochem. Biophys. Res. Commun.* 378, 799–803. doi: 10.1016/j.bbrc.2008.11.140

Wang, Y. N., Li, K. X., Chen, L., Zou, Y. M., Liu, H. P., Li, D. X., et al. (2015). MicroRNA167-directed regulation of the auxin response factors, GmARF8a and GmARF8b, is required for soybean (*Glycine max* L.) nodulation and lateral root development. *Plant Physiol.* 168, 101–116. doi: 10.1104/pp.15.00265

Wang, Y. N., Wang, L. X., Zou, Y. M., Chen, L., Cai, Z. M., Zhang, S. L., et al. (2014). Soybean miR172c targets the repressive AP2 transcription factor NNC1 to activate *ENOD40* expression and regulate nodule initiation. *Plant Cell* 26, 4782–4801. doi: 10.1105/tpc.114.131607

Conflict of Interest Statement: The authors declare that the research was conducted in the absence of any commercial or financial relationships that could be construed as a potential conflict of interest.

frontiers in Physiology

ORIGINAL RESEARCH
published: 07 June 2016
doi: 10.3389/fphys.2016.00217

The Combined Effects of Ethylene and MeJA on Metabolic Profiling of Phenolic Compounds in *Catharanthus roseus* Revealed by Metabolomics Analysis

Jia Liu[1], *Yang Liu*[1], *Yu Wang*[1], *Zhong-Hua Zhang*[1], *Yuan-Gang Zu*[1], *Thomas Efferth*[2]* *and Zhong-Hua Tang*[1]*

[1] The Key Laboratory of Plant Ecology, Northeast Forestry University, Harbin, China, [2] Department of Pharmaceutical Biology, Institute of Pharmacy and Biochemistry, Johannes Gutenberg University, Mainz, Germany

Phenolic compounds belong to a class of secondary metabolites and are implicated in a wide range of responsive mechanisms in plants triggered by both biotic and abiotic elicitors. In this study, we approached the combinational effects of ethylene and MeJA (methyl jasmonate) on phenolic compounds profiles and gene expressions in the medicinal plant *Catharanthus roseus*. In virtue of a widely non-targeted metabolomics method, we identified a total of 34 kinds of phenolic compounds in the leaves, composed by 7 C6C1-, 11 C6C3-, and 16 C6C3C6 compounds. In addition, 7 kinds of intermediates critical for the biosynthesis of phenolic compounds and alkaloids were identified and discussed with phenolic metabolism. The combinational actions of ethylene and MeJA effectively promoted the total phenolic compounds, especially the C6C1 compounds (such as salicylic acid, benzoic acid) and C6C3 ones (such as cinnamic acid, sinapic acid). In contrast, the C6C3C6 compounds displayed a notably inhibitory trend in this case. Subsequently, the gene-to-metabolite networks were drawn up by searching for correlations between the expression profiles of 5 gene tags and the accumulation profiles of 41 metabolite peaks. Generally, we provide an insight into the controlling mode of ethylene-MeJA combination on phenolic metabolism in *C. roseus* leaves.

Keywords: ***Catharanthus roseus,*** **phenolic compounds, ethylene, methy jasmonate, non-targeted metabolomics**

OPEN ACCESS

Edited by:
M. Iqbal R. Khan,
International Rice Research Institute, Philippines

Reviewed by:
Akira Oikawa,
Yamagata University, Japan
Péter Poór,
University of Szeged, Hungary

***Correspondence:**
Thomas Efferth
efferth@uni-mainz.de;
Zhong-Hua Tang
tangzh@nefu.edu.cn

Specialty section:
This article was submitted to Plant Physiology, a section of the journal Frontiers in Physiology

Received: *02 December 2015*
Accepted: *24 May 2016*
Published: *07 June 2016*

Citation:
Liu J, Liu Y, Wang Y, Zhang Z-H, Zu Y-G, Efferth T and Tang Z-H (2016) The Combined Effects of Ethylene and MeJA on Metabolic Profiling of Phenolic Compounds in Catharanthus roseus Revealed by Metabolomics Analysis. Front. Physiol. 7:217. doi: 10.3389/fphys.2016.00217

INTRODUCTION

Catharanthus roseus (Madagascar periwinkle) is a medicinal plant producing about more than 150 different terpenoid indole alkaloids (TIAs). Among the many pharmaceutically important TIAs are vinblastine and vincristine, the well-known anticancer agents that have been long in clinical use (van Der Heijden et al., 2004). Nevertheless, report has also suggested that *C. roseus* contains a wide

Abbreviations: TIAs, terpenoid indole alkaloids; ABA, abscisic acid; ET, ethylene; MeJA, methyl jasmonate; PAL, phenylalanine ammonia lyase; CM, chorismate mutase; ICS, isochorismate synthase; AS, anthranilate synthase; C4H, cytochrome P450 hydroxylation; 5.6-D-7,8,2,3,4-PF, 5,6′-dihydroxy-7,8,2′,3′,4′-Pentamethoxyflavone; Pro acid-*O*-hexoside, Protocatechuic acid-*O*-hexoside; Q-3-*O*-rhamnoside, Quercetin-3-*O*-rhamnoside; LC-MS/MS, liquid chromatography tandem mass spectrometry; ESI, electrospray ionization.

spectrum of phenolic compounds besides TIAs (Filippini et al., 2003; Mustafa and Verpoorte, 2007; Ferreres et al., 2008), such as flovonoids, caffeic acid, benzoic acid, and cinnamic acid derivatives. These natural products are often involved in signaling pathways triggered as a defense mechanism against biotic and abiotic stresses (Demkura et al., 2010). Furthermore, they contribute to human health by exerting various biological activities including antioxidant, antibacterial and anticancer (Valentao et al., 2001; Sousa et al., 2008).

Phenolics are the most widely distributed metabolites that are involved in the interactions between biology and environments (Garcia-Calderon et al., 2015). In plants, phenolic compounds are synthesized via the phenylpropanoid pathway that begins with the conversion of phenylalanine to cinnamic acid by phenylalanine ammonia lyase (*PAL*) and hence also compete with the indole alkaloid biosynthesis for common precursor chorismate (Ferreres et al., 2008). Based on the so far gathered knowledge on spatial and temporal complexities associated with phenolic pathway in *C. roseus*, the involvement of at least 20 coordinately regulated enzymatic steps occurring in different tissues types has been implicated, such as *CM* (chorismate mutase), *ICS* (isochorismate synthase), *PAL* (phenylalanine ammonia-lyase), and *C4H* (*trans*-cinnamate 4-monooxygenase) (Mustafa and Verpoorte, 2005; Ferreres et al., 2011). Phenolic compounds are referred to as cyclic compounds with exchangeable hydroxyl groups and are classified based on the number and binding position of convertible hydroxyl groups on the aromatic chain into three major groups: simple phenolic compounds (mass compounds have a C6C1 carbon skeleton, usually with a carboxyl group attached to the aromatic ring, such as benzoic acid), phenolic acid derivatives (derived from phenylalanine, having a C6C3 carbon skeleton, such as caffeic acid), and flavonoids (compounds having C6C3C6 carbon skeleton such as flavonoids and isoflavonoids; Dixon, 2001; Mustafa and Verpoorte, 2007). So far, around 5000 phenolic compounds have been identified and their contents fluctuate depending on environmental conditions and plant species (Mustafa and Verpoorte, 2007; Simirgiotis et al., 2015; Vos et al., 2015). The accumulation of phenolics may also affect other secondary metabolite pathways including alkaloid pathways, since plant defense is a complex system (Mustafa and Verpoorte, 2007; Ferreres et al., 2008; **Figure 1**).

Identification and structural characterization of phenolic compounds has been well developed and achieved using LC-MS/MS in different plant species (Ferreres et al., 2004; Lin and Harnly, 2007; Dong et al., 2014). The metabolic profiling analysis of phenolic compounds in some plant extracts showed that the *C. roseus* extracts contained the highest amount of a C6C3 hydroxytyrosol and a C6C1 gallic acid when compared to 26 other plant extracts analyzed. Other phenolics detected in this plant were ferulic acid and vanillic acid. No flavonoids were detected in this study (Proestos et al., 2005). Filippini et al. developed a stable callus of *C. roseus* producing anthocyanins by continuous cell-aggregate selection (Filippini et al., 2003). Similar anthocyanins were identified by LC-MS/MS metabolic profiling. They were also identified as 3-*O*-glucosides and 3-*O*-(6-*O*-*p*-coumaroyl) glucosides of petunidin, malvidin, and hirsutidin. Moreover, three caffeoylquinic acids and fifteen flavonol glycosides were identified by the same level of technology (Ferreres et al., 2008). As mentioned above, the potential of developing a platform for qualitative analysis of phenolic compounds has been highlighted in several studies. Therefore, we approached the comprehensively analysis of phenolic compounds located in *C. roseus* leaves using this method.

The phytohormones ET and methyl jasmonate (MeJA) were reported to elicit secondary metabolites such as alkaloids and phenolic compounds regulating plant growth and adaptation (Demkura et al., 2010; Vanstraelen and Benkova, 2012; Wasternack and Hause, 2013; Cocetta et al., 2015; Pozo et al., 2015). ET acts as an intermediate signaling molecule in elicitor-induced terpenoid indole alkaloids accumulation (Papon et al., 2005; Pan et al., 2015). ET is also able to induce flavonol accumulation alone or interact with auxin (Lewis et al., 2011; Watkins et al., 2014). The addition of MeJA to *C. roseus* hairy root cultures increased the yields of ajmalicine, serpentine, lochnericine, and hörhammericine (Rijhwani and Shanks, 1998). MeJA also tightly modulated phenolic metabolism and gene expression in blueberry (Cocetta et al., 2015), under solar ultraviolet B radiation (Demkura et al., 2010), or in broccoli sprouts (Carvacho et al., 2014). In some cases, concomitant activation of JA and ET response pathways is required for induction of plant defensive gene, such as PDF1.2 (Penninckx et al., 1998). These reports provided critical insight into the roles of ET or MeJA in the modulation of alkaloids and phenolic compounds, however, their combined effects on phenolic profiles remain into investigation. Here, we mainly focused on the combinational effects of ET and MeJA on phenolic compound profiles and gene expressions in *C. roseus* leaves in virtue of metabolomics approach.

RESULTS

The Combined Effects of ET and MeJA on the Metabolic Profiles of Total Phenolic Compounds

Using LC-QTOF-MS/MS, we developed a novel widely non-targeted metabolomics method for the comprehensive profiling analysis of phenolic compounds in *C. roseus*. According to the identity check based on raw data and the features of peaks, the target masses of candidate metabolites identified in the profiling process were searched over a narrow + 5 ppm mass window in HMDB, METLIN, and KEGG databases. A total of 34 phenolics that belong to three categories (7 C6C1-, 11 C6C3-, and 16 C6C3C6 compounds; **Table 1**), and seven other metabolites were identified in our study (Table S2). The relatively level of total phenolic compounds significantly increased ($p < 0.01$) in plants treated with ET and MeJA compared with those under conditions of control or plus ET only (**Figure 2A**).

Subsequently, the visualization of the phenolic compounds profiles was performed by hierarchical cluster analysis (HCA; **Figure 2B**). The results showed that accumulation of phenolic metabolites displayed a clear variation in terms of their

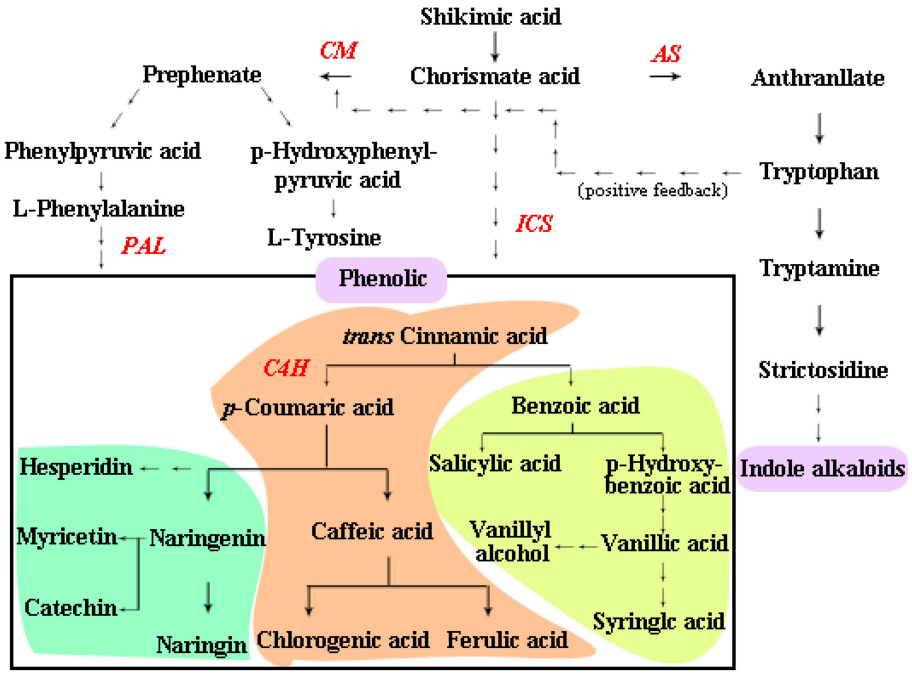

FIGURE 1 | The biosynthetic pathway of phenolic compounds. *Green region* indicates C6C3C6-compounds; *Orange region* indicates C6C3-compounds; *Yellow region* indicates C6C1-compounds; *Purple region* indicates a class of metabolites. *Red* indicates the key enzymes, the following abbreviations are used for different pathway enzymes: *CM* (chorismate mutase), *ICS* (isochorismate synthase), *PAL* (phenylalanine ammonia-lyase), *C4H* (*trans*-cinnamate 4-monooxygenase), and *AS* (amyrin synthase). The solid-line arrow represents one-step reaction, and dashed-line arrow means multi-steps reactions.

abundance upon different treatment. Co-treatment of both hormones contained the highest levels of most phenolics, followed by treatment with ET alone. Based on their responses to different treatment, phenolic profiles could be clearly grouped into three main clusters with six subclusters. Phenolics in cluster I were mainly represented by C6C3C6 compounds with lower levels detected in ET and MeJA, such as hesperidin, petunidin, quercetin, mauritianin, nicotiflorin, malvidin, 5,6-D-7,8,2,3,4-PF, myricetin, naringin, hirsutidin, catechin, isoscutellarein, and naringenin. Major C6C3-(chlorogenic acid, coumaric acid-hexose, sinapic acid, caffeic acid, and cinnamic acid) and C6C1-(vanillic acid and pro acid-O-hexoside) compounds were tightly grouped in subcluster 2. These phenolic displayed higher levels upon the combined action of ET and MeJA compared to the controls. In addition, those in subcluster 3 were mainly represented by compound C6C1-(benzoic acid and vanillyl alcohol) and C6C3C6-(Q-3-O-rhamnoside and kaempferol), also displaying highest levels under the combined condition. Three C6C3-(*p*-coumaric acid, ferulic acid, and *trans*-cinnamic acid) and one C6C1-(salicylic acid) in subcluster 6 showed ET-specific accumulation pattern. However, *o*-coumarica acid, quercetin 3-sulfate, and sinapic acid hexose in subcluster 4 and 5, respectively, showed little sensitivity to ET or/and MeJA, which subcluster 4, 5, and 6 belonging to the last cluster III. The results showed that ET and MeJA combination could mainly promote C6C1- and C6C3-metabolites accumulation, except for C6C3C6 compounds.

The Combined Effects of ET and MeJA on C6C1-, C6C3-, and C6C3C6-Type Compounds

Plant phenolic compounds are synthesized via the chorismate and can be majorly divided into three types, including C6C1, C6C3, and C6C3C6. Their specific responses were further clarified. For most of the C6C1- and C6C3-type compounds, there was a significant promotion by the combinational action of ET and MeJA compared with the treatments with control solution and plus ET alone (**Figures 3A,B**). Among these compounds, vanillyl alcohol in the leaves was found to be elevated 50 times in the presence of ET and MeJA compared with the control case. In contrast, the C6C3C6-type compounds displayed an inhibited accumulation upon ET plus MeJA compared with the cases upon ET alone or control solution (**Figure 3C**). Furthermore, parts of the intermediates in the phenolic or TIA biosynthetic pathway were identified here, including chorismic acid, phenylpyruvic acid, isochorismic acid, L-tyrosine, L-phenylalaine, tryptophan, and *p*-hydroxyphenylpyruvic acid. The actions of ET plus MeJA obviously promoted the first three compounds and inhibited the remaining four ones, respectively (**Figure 3D**). The further analysis of other major C6C3- and C6C3C6 compounds identified in our research showed that cinnamic acid (C6C3) was largely promoted and most of the C6C3C6 compounds were decreased by the combination of ET and MeJA (Figure S1).

TABLE 1 | Structure of identified phenolic compounds.

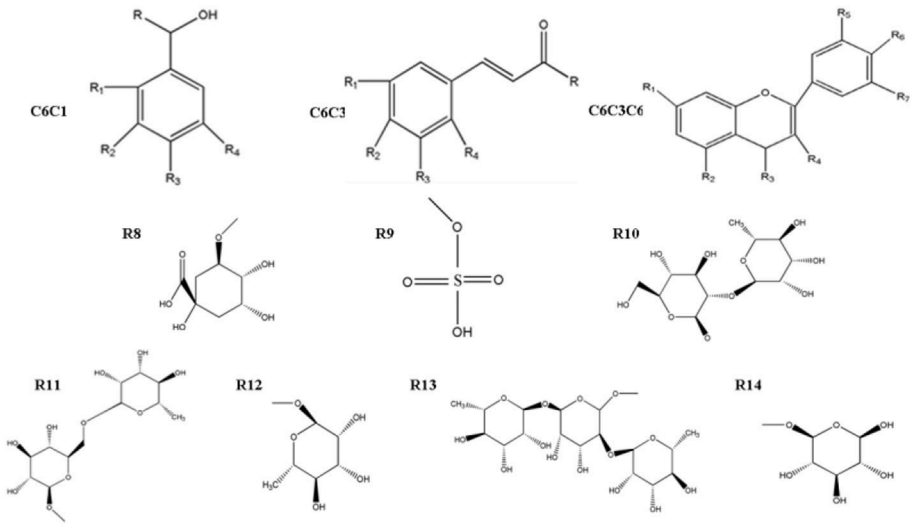

Structure	Derivates	R	R_1	R_2	R_3	R_4	R_5	R_6	R_7
C6C1	Salicylic acid	=O	−OH						
	Vanillic acid	=O		$-OCH_3$	−OH				
	Vanillyl alcohol			$-OCH_3$	−OH				
	Syringic acid	=O		OCH_3	−OH	$-OCH_3$			
	Gallic acid	=O		−OH	−OH	−OH			
	Benzoic acid	=O							
C6C3	*Trans*-cinnamric acid	−OH							
	Cinnamic acid	−OH							
	p-Coumanic acid	−OH		−OH					
	o-Cumamic acid	−OH				−OH			
	Caffeic acid	−OH	−OH	−OH					
	Ferulic acid	−OH	$-OCH_3$	−OH	$-OCH_3$				
	Sinapic acid		−OH	−OH					
	Chlorogenic acid	R_8	−OH	−OH					
C6C3C6	Catechin	−OH	−OH	−OH		−OH	−OH		
	Naringenin		−OH	−OH	−O			−OH	
	Hirsutidin		$-OCH_3$	O^-		−OH	$-OCH_3$	−OH	$-OCH_3$
	Myricetin		−OH	−OH	O	−OH	−OH	−OH	−OH
	Kaempferol	−OH	−OH	−OH	=O			−OH	
	Isoscutellarein	−OH	−OH	−OH	=O			−OH	
	Quercetin		−OH	−OH	=O	−OH	−OH	−OH	
	Quercetin-3-sulfate		−OH	−OH	=O	R_9	−OH	−OH	
	Malvidin		O^-	−OH	–	OH	$-OCH_3$	−OH	$-OCH_3$
	Naringin		R_{10}	−OH	=O			−OH	
	Hesperidin		R_{11}	−OH	=O		−OH	$-OCH_3$	
	Nicotiflorin		−OH	−OH	=O	R_{11}		−OH	
	Petunidin		R_{13}	−OH	=O	R_{11}	−OH	−OH	
	Quercetin-3-*o*-rhamnoside		−OH	−OH	=O	R_{12}		−OH	−OH
	Mauritianin		−OH	−OH	=O	R_{14}		−OH	

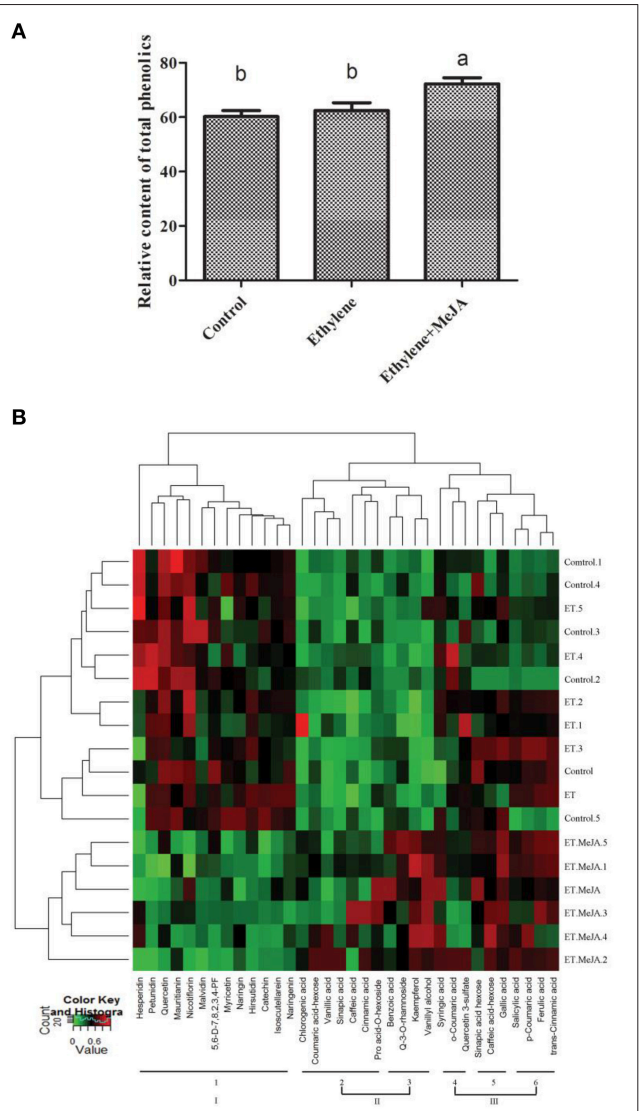

FIGURE 2 | The combined effects of ET and MeJA on the metabolic profiles of total phenolic compounds. (A) Ethlyene and/or jasmonate enhance the total phenolic production in *C. roseus* leaves. CK: control, ET: ET, MeJA: jasmonate. **(B)** Heat map visualization of relative differences of phenolics in different treatment. Data of the relative content value of each phenolic were normalized to complete linkage hierarchical clustering. Each phenolic is visualized in a single column and each hormone type is represented by a single row, including six repeat. Abbreviations: 5.6-D-7,8,2,3,4-PF (5,6′-dihydroxy-7,8,2′,3′,4′-Pentamethoxyflavone), Pro acid-*O*-hexoside (Protocatechuic acid-*O*-hexoside), and Q-3-*O*-rhamnoside (Quercetin-3-*O*-rhamnoside). *Red* indicates high abundance, whereas low relative phenolics are green. Each bar represents the mean ± S. E. M., $n = 6$.

The Combined Effects of ET and MeJA on the Gene Expression Responsible for Phenolic or Alkaloid Biosynthesis

Other than the metabolic analysis, the gene expressions responsible for phenolic biosynthesis (CM: chorismate mutase; ICS: isochorismate synthase; PAL: phenylalanine ammonia lyase; C4H: cytochrome P450 hydroxylation) were compared with that for indole alkaloid pathway (AS: anthranilate synthase). The treatment with ET precursor ACC alone enhanced the expression levels of *ICS*, *AS*, *PAL*, and *C4H* genes than the control treatment. The inclusion of MeJA plus ET further significantly improved the expression levels of *PAL* and *C4H* genes when compared with the treatment with ET alone (**Figure 4**). In this case, the *CM, ICS, and AS* gene expressions were not obviously changed.

Integrated Response Analysis of Genes—Metabolites Network

To facilitate access to the total metabolic profiles, the metabolites, genes and corresponding pathways were imported into Cytoscape for visualization of the network models. The intersection of the networks was done using the advanced network merge function in Cytoscape. Altered metabolites with KEGG from the merged data set were mapped to KEGG reference pathways, and interaction networks were generated in Cytoscape. As seen in **Figure 5**, the association network of differentially expressed metabolites using Cytoscape was constructed. Modes of action are shown in different colors and shapes. Networks are represented as graphs, where the green diamond, red polygon, and blue square nodes represent metabolites, genes, and related pathways detected, respectively. These closely connected and differentially expressed metabolites are regarded as the target signatures. The significantly overrepresented categories indicated that this emergent new and advanced network was composed by metabolites, genes, and related pathways. Fortunately, for the greater part of the identified metabolites and genes could be included in a network together through indirect interaction or only one intermediate partner. However, a small portion of phenolic derivatives were not found their compound identifiers (IDs) from KEGG, so these could not be included, such as protocatechuic acid-*O*-hexoside, coumaric acid-hexose, sinapic acid-hexose, quercetin-3-*O*-rhamnoside, and caffeic acid-hexose. The regulatory patterns of phenolic compounds presented here provide evidence that metabolites are actively involved in multifunctional pathways, and these insights help us to better understand the mechanisms underlying their responses to ET plus MeJA.

DISCUSSIONS

In this study, we utilized the widely non-targeted metabolomics method for the direct chemical screening of phenolic compounds in the medicinal plants *C. roseus*. We identified a total of 34 phenolic compounds, mainly including C6C1-, C6C3-, and C6C3C6-type compounds. The result is consistent with previous reports that *C. roseus* contains the C6C1-, C6C3-, and C6C3C6 compounds (Dixon, 2001; Choi et al., 2004; Mustafa and Verpoorte, 2005, 2007). Our further analysis showed that there were 7, 11, and 16 kinds of compounds, respectively, belonging to C6C1-, C6C3-, and C6C3C6-type. MBRole performs enrichment analysis of a number of annotations of diverse nature coming from KEGG, which are annotated with their associated pathways, enzymes and chemical groups, as well as other interactions (Chagoyen and Pazos, 2011). However, a number of phenolic

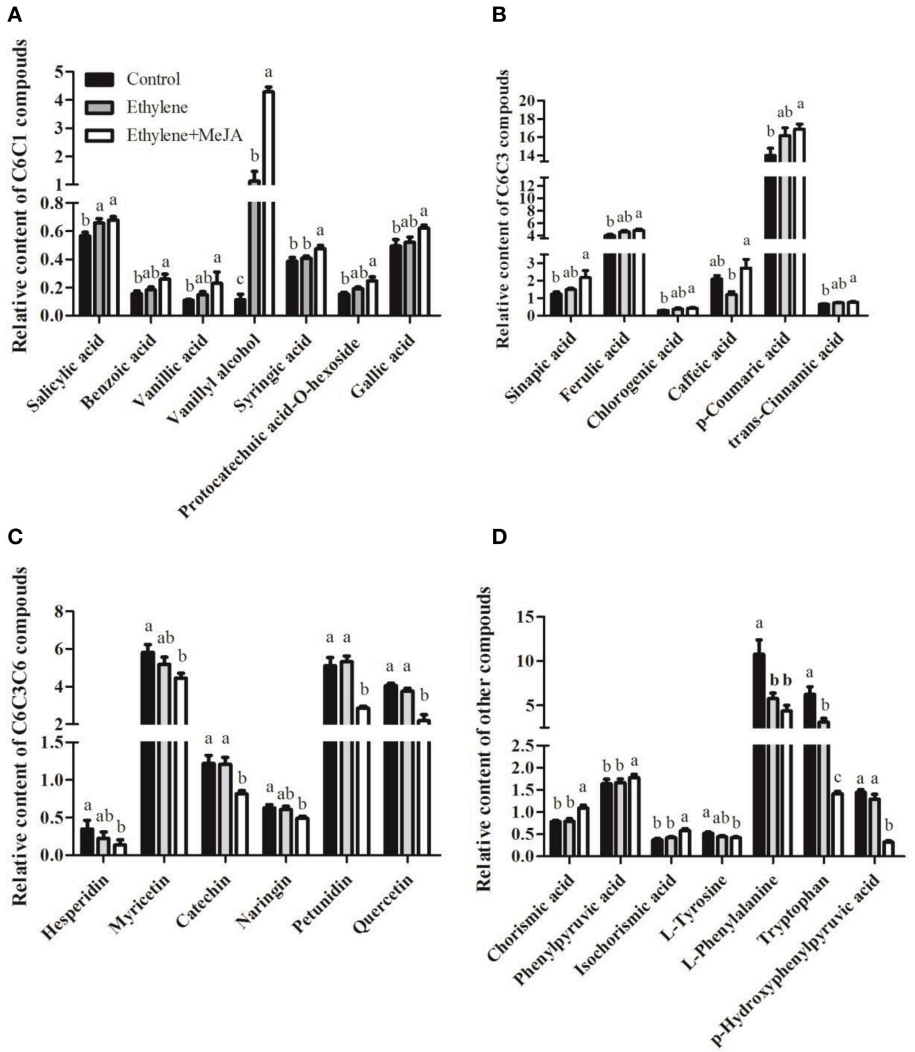

FIGURE 3 | The combined effects of ET and MeJA on C6C1-, C6C3-, and C6C3C6-type compounds. (A) The relative content of the structure formula C6C1. **(B)** Six major C6C3-phenolic relative contents. **(C)** Six major C6C3C6-phenolic relative contents. **(D)** Other metabolites relative contents. Other C6C3- and C6C3C6-compounds are given in Figure S1. Each bar represents the mean ± S. E. M., $n = 6$.

derivatives did not find these corresponding IDs, such as protocatechuic acid-*O*-hexoside, coumaric acid-hexose, sinapic acid-hexose, quercetin-3-*O*-rhamnoside, and caffeic acid-hexose. In addition, the results (Table S3) contain the list of annotations over-represented in the input set with respect to the background set and their associated $P < 0.005$ (Zhang et al., 2013). Every pathway listed in the MBRole data set with at least on metabolite identified by the MS associated with that pathway was noted, and the MS-identified metabolites were crossly listed with the pathway. Each metabolite could belong to multiple pathways (**Figure 5**).

The phenolic compounds play diverse and important functions in plant development and defense as reactive oxygen species scavengers, disease resistance inducer (Moreno et al., 1994; Murphy et al., 2000; Mustafa and Verpoorte, 2007; Watkins et al., 2014). In our study, C6C1-, C6C3-, and C6C3C6-compounds comprised 3.58, 51.81, and 44.60% of total phenolic compounds, respectively. It suggested that C6C3C6 compounds are mainly involved in plant flavonoid biosynthesis, functioning as filters against ultraviolet irradiation (Trantas et al., 2015). In contrast, the C6C1 compounds might mainly play an important role as signaling molecules, such as the BA (benzoic acid)-derivatives SA (salicylic acid; Cheynier et al., 2013). Because, the biosynthesis of C6C1 compounds are reported to be most strictly induced by biotic elicitors (Mustafa and Verpoorte, 2007) and these low-molecular weight phenolics occur universally in higher plants (Cheynier et al., 2013). We found that the elevated compounds in the leaves after the co-treatment mainly belonged to either the C6C1 or C6C3-compounds. Evidence is accumulating that components from SA-, JA-, and ET-dependent defense pathways can affect each other's signaling (van Wees et al., 2000). The synergistic

cross-talk between JA and ET is known to occur preferentially for the response to necrotrophic pathogens (Wasternack and Hause, 2013) and activate JA-dependent plant defenses against herbivores via alkaloid biosynthesis (Onkokesung et al., 2010). However, SA and its functional analogs suppress JA-dependent defense gene expression, possibly through the inhibition of JA synthesis and action (van Wees et al., 2000; Vos et al., 2015). Conversely, other reports showed that ET and MeJA were shown to stimulate SA action (van Wees et al., 2000). We found that the exogenous ET plus MeJA slightly promoted accumulations of salicylic acid (SA) and its derivatives benzoic acid, isochorismic acid, whereas largely enhanced levels of vanillic acid, vanillyl alcohol, and syringic acid than did ET alone (**Figures 3A,B**). The compound syringic acid and its precursors (vanillic acid and vanillyl alcohol) compete with SA for benzoic acid as substrate (Mustafa and Verpoorte, 2007), thus, we proposed that ET-JA crosstalk mainly antagonized SA *in vivo* synthesis and bring carbon flux to vanillic acid accumulation. However, our further clustering analysis found that SA was induced in an ET-specific way, suggesting that SA interplays synergistically with ET.

Our clustering results showed the C6C3 branch pathway metabolites, namely *p*-coumaric acid, ferulic acid, and *trans*-cinnamic acid, were grouped together with SA. These phenylpropanoids are derived from phenylalanine catalyzed by PAL enzyme (Mustafa and Verpoorte, 2007; Cheynier et al., 2013). Besides the precursors of C6C1 compounds, the above phenylpropanoids are also precursors of other phenolics, which in many plants act as phytoalexiins or phytoanticipins, such as

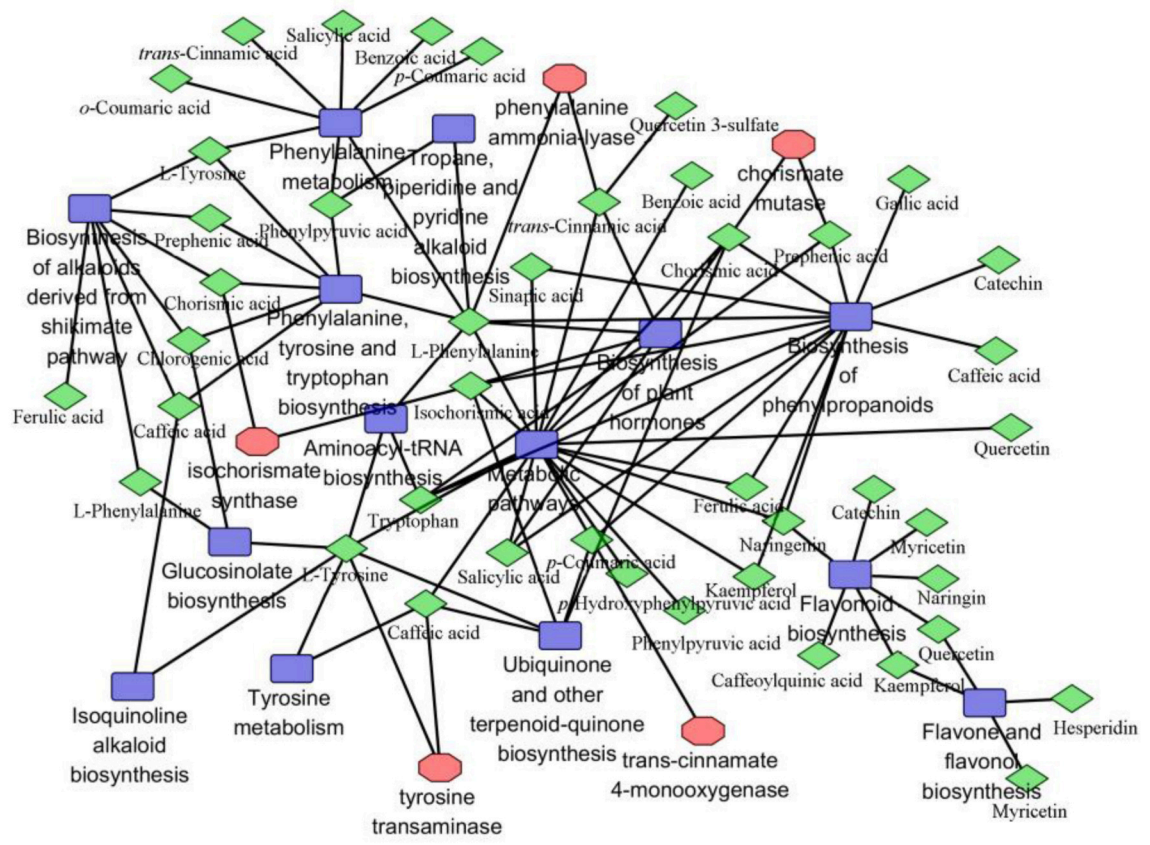

FIGURE 4 | Differential expression of genes in leaves treated with either ET alone or ET plus MeJA. Each treatment is compared with CK: if greater than 1, it means promotion; if lower than 1, it means suppression.

FIGURE 5 | Gene and metabolite network analysis in elicited *C. roseus* leaves. Metabolites are represented by green-diamond, genes by red-rolygon, and related pathway by blue-square. Correlation network is composed of 34 phenolic compounds combine with five genes and other relevant metabolites. Metabolites with KEGG from the merged data set were mapped to KEGG and MBRole reference pathway, and interaction networks were generated in Cytoscape, $p > 0.005$.

flavonoids, isoflavonoids (Dixon, 2001) or as physical barrier against pathogen attack, such as lignin (Mustafa and Verpoorte, 2007). Activation of PAL is often considered as a hallmark for elicitation of SAR (systemic acquired resistance) in plants and SA is a necessary and sufficient signal for SAR (Clarke et al., 2000; van Wees et al., 2000). We found that ET alone or plus MeJA increased *PAL* transcripts and effectively decreased L-phenylalanine level, suggesting SA-dependent SAR process was induced. ET and MeJA are also implicated in induced systemic resistance (ISR; van Wees et al., 2000). ISR pathway may result in induction of different pathways leading to the production of phenolic compounds and/or other secondary metabolites (Glazebrook et al., 2003; Mustafa and Verpoorte, 2007). In contrast to C6C1 and C6C3 compounds, almost all the C6C3C6-metabolites displayed inhibitory accumulation after treatment with ET plus MeJA (**Figure 3C** and Figure S1B). The biosynthetic pathway of C6C3C6 compounds lead to productions of flavonoids (flavonols) and isoflavonoids (Mustafa and Verpoorte, 2007; Mouradov and Spangenberg, 2014). In vegetative tissues, anthocyanins and other flavonoids usually accumulate transiently, as a plastic response to biotic or abiotic stressors (Del Valle et al., 2015). For example, IAA and ET were able to regulate flavonol biosynthesis through distinct signaling networks and quercetin is revealed to be the flavonol that modulates basipetal auxin transport (Lewis et al., 2011). Our result is consistent with this report, because the reduced quercetin was caused by ET plus MeJA, whilst not by ET alone.

Other than phenolic compounds, a serial of intermediates in the biosynthetic pathway of phenolic and alkaloids were identified in this study (**Figure 3D**). Among them, the chorismate is a critical substrate for multiple enzymes, such as CM, ICS, and AS, resulting in different secondary metabolic pathway and carbon flux (Mustafa and Verpoorte, 2007; Van Lanen et al., 2008). The restrained expression of *CM* gene in our transcriptional analysis paralleled with the decreased levels of L-phenylalanine and L-tyrosine. In contrast, the *ICS* and *AS* expressions were slightly activated in this case. This evidence suggests that ET and MeJA prefer to elicit benzoic acid-derived phenolic compounds (C6C1), for example, vanillyl alcohol (50-fold increase) in our study. Our subsequent correlation analysis showed that the C6C1 compounds correlated positively with their precursors including chorismate acid and isochorismic acid, but showed a negative correlation with the tryptophan (Figure S2). Tryptophan is a pivotal precursor for indole alkaloids in relation with AS enzyme function and found to be reduced in our research. It was interesting that *AS* expression, however, was activated in this case. We interpret this result that the combined action of ET and MeJA simultaneously promotes the indole alkaloid and phenolic pathways, whilst tryptophan was rapidly consumed for indole alkaloid synthesis (Choi et al., 2004; Chung et al., 2007). Phenylpyruvic acid and *p*-hydroxyphenylpyruvic acid are precursors of L-phenylalanine and L-tyrosine, respectively, essential for C6C3 and C6C3C6 biosynthesis (Mustafa and Verpoorte, 2007). The *p*-hydroxyphenylpyruvic acid largely decreased in our research under the combined action of ET and MeJA, interpreting globally inhibited levels of C6C3C6 compounds. The gene expression level of *PAL* was both elevated obviously in this study, leading to the conversion of phenylalanine into cinnamic acid, which is a precursor for several phenolic compounds such as cinnamic acid, p-coumaric acid, caffeic acid, naringenin, and syringlc acid. The expression of C4H responsible for the hydroxylation at the C-4 position of cinnamic acid to form *p*-coumaric acid significantly increased, thereby contributing to the C6C3 compounds synthesis (Hotze et al., 1995).

CONCLUSIONS

In conclusion, we report a comprehensive profiling analysis of phenolic compounds in response to the combinational action of ET and MeJA. Application of a widely non-targeted metabolomics method facilitated the identification of a total of 34 phenolic compounds and 7 intermediates for biosynthesis of phenolic compounds and indole terpenoid alkaloids (TIAs) using LC-MS/MS. Gene-to-metabolite networks were drawn up by searching for correlations between the expression profiles of 5 gene tags and the accumulation profiles of 41 metabolite peaks. The network revealed that the different branches of phenolic compounds biosynthesis and various other metabolic pathways are tightly regulated by ET-MeJA combination. Especially, the ET-MeJA cross-talk mainly promote C6C1- and C6C3-type, whilst inhibit C6C3C6-type phenolic compounds. Thus, this study provides an insight into the controlling mode of ET-MeJA combination on phenolic metabolism in *C. roseus* leaves. However, the underlying mechanisms in this induction process remain to be unraveled.

MATERIALS AND METHODS

Chemicals

All chemicals were of analytical reagent grade. Gradient grades of methanol, acetonitrile and acetic acid were purchased from Merck Company, German (http://www.merck-chemicals.com). Water was doubly deionized with a Milli-Q water purification system (Milford, MA, USA). Ethephon used to release ET and methyl jasmonate (MeJA) were both obtained from Sigma-Aldric (St. Louis, MO, USA).

Plant Material, Growth Conditions, and Sample Preparation

C. roseus seeds were planted in pots containing perlite and kept moistened until the seeds had germinated, and then irrigated with 1/2 strength Hoagland's solution (Pan et al., 2015). On the basis of process conditions screened, the concentrations of ethephon and MeJA used for treatment were 30 μM and 150 μM, respectively. Seedlings were used for treatments 30 d after cultivation with roots subjected to the 1/2 strength Hoagland's solution (control, T1), or plus 30 μM ethephon alone (T2) or 30 μM ethephon + 150 μM MeJA (T3). The total 30 individual plants were randomly selected and equally subjected into the conditions of T1, T2, and T3. The experiments were biologically repeated three times. The leaves of plants were harvested, 3 d after treatment for analysis of

phenolic compounds and 4 h after treatment for analysis of gene expressions.

LC-ESI-QTOF/MS Analysis of Phenolic Compounds

For phenolic compound analysis, leaves were pulverized by grinding instrument (MM 400, Retsch, GmbH, Haan, Germany), and 50 mg tissue aliquots were extracted with 1.0 mL 70% aqueous methanol containing 0.1 mg/L lidocaine for water-soluble metabolites at 4°C overnight with three times vortexing. The extracts were clarified by centrifugation, combined, evaporated, and then filtered through 0.22 μm nylon membranes (SCAA 104; ANPEL http://www.anpel.com.cn/) before LC-MS analysis. Samples were analyzed using a liquid chromatography (LC) system coupled to a (QTOF) tandem mass spectrometer via electrospray ionization (ESI) interface (Agilent 6520) (Agilent Technologies, Santa Clara, CA, USA). Sample extracts were separated through a reversed phase on a Shim-pack LC column (VP-ODS C_{18} pore size 5.0 μm, 2*150 mm). The mobile phase consisted of solvent A and B. Solvent A contained 0.04% acetic acid in water, and solvent B 0.04% acetic acid in acetonitrile. The following gradient was used with a flow rate of 0.5 mL/min: 0–20 min, 5%B–95%B; 20–22.1 min: 95%B–5%B; 22.1–28 min: 5%B–5%B. Blank measurement with the initial solvent was carried out after each HPLC run. Injection volume and column temperature were set to 5 μL and 40°C, respectively. The optimized parameters for positive ion electrospray were as follows: capillary temperature of 350°C; curtain gas pressure of 40 psi; capillary voltage of 3500 V, fragmentation voltage of 135 V. The instrument was tuned prior to each batch run. A full-scan ranging between 50–1000 m/z was conducted with a scan time of 1 s and an interscan delay of 0.1 s in centered mode. The peak detection and matching were performed by Mass Hunter Qualitative (MHQ version B.03.01) and Mass Profiler Professional (MPP, version B.02.01) (Both from Agilent Technologies, Santa Clara, CA, USA). Metabolic features with mass, retention time, and abundance were obtained.

RNA Isolation and Quantitative Real Time PCR Analysis

For gene expression analysis, the total leaf RNA was extracted by TRIZOL reagent (Invitrogen). DNA contamination was removed using Dnase I following the instructions provided by the manufacturer (TaKaRa, Japan). DNA and RNA purity were observed using 1% agarose gel electrophoresis and RNA concentration was determined using a Nanodrap spectrophotometer (Thermo). cDNA was synthesized from total RNA (2 μg) using ReverTra Ace QPCR RT Kit (TOYOBO, Japan) according to the manufacturer's instructions, using oligo (dT) as the primer. qRT- PCR analysis using cDNA as template and gene-specific primers was performed using a SYBR Premix Ex Taq (TaKaRa, Japan) with an initial denaturation at 95°C for 30 s, followed by 35 cycles at 94°C for 30 s, 56°C for 30 s and 72°C for 30 s. Amplification, detection, and data analysis were carried out on a Rotor-Gene 6000 real-time rotary analyzer (Corbett Life Science, Sydney, Australia). The primers used were 5′-GCG AAC ATT TGC AGA TCC AT-3′ and 5′-GGC CGA TTT GTT ATT GTT CC-3′ for *AS*; 5′-GGC CAC CAA GAT GAT CGA-3′ and 5′-CAA TGG CCA ATC TTG CAT TG-3′ for *PAL*; 5′-GCC GAT TCT CTG TAT CAC TAT C -3′ and 5′-ATG ATT AAA ATG ATC TTG GCT TT-3′ for *C4H*; 5′-CGA TTT GTT GAA ATT GCA GAC G-3′ and 5′-ATT GCA GAC GAT CGT TTA ACT C-3′ for *CM*; 5′-ATT GCA GAC GAT CGT TTA ACT C-3′ and 5′-TTC CTC GGT CAA ACA TTT CG-3′ for *ICS*; (from ExPlant Technologies B.V.) (Table S1). These were repeated three times for each sample to ensure the reproducibility of results. Ribosomal protein subunit 9 (*Rsp9*) 5′-GAG GGC CAA AAC AAA CTT GA-3′ and 5′-CCC TTA TGT GCC TTT GCC TA-3′ was used as an internal control to evaluate all *C. roseus* plants.

Statistical Analysis

Metabolic pathways were performed in the Metaboanalyst web portal (http://www.metaboanalyst.ca) and MBRole (http://csbg.cnb.csic.es/mbrole). The pathways of metabolites were carried out on database sources including the KEGG (http://www.genome.jp/kegg/) to identify the top affected metabolic pathways and facilitate further metabolites interpretation. The metabolites and corresponding pathways were imported into Cytoscape software (v. 3.1.0) for visualization of the network models. The intersection of the networks was done using the advanced network merge function in Cytoscape. Pearson's correlation coefficients were calculated between metabolites and genes by SPSS 17.0. The Student's *t*-test and Tukey's test were used for mean value comparison. A total of 34 phenolic compounds were used for hierarchical clustering analysis by R (http://www.r-project.org/) to analyze phenolic profiles in response hormones.

AUTHOR CONTRIBUTIONS

Conceived and designed the experiments: ZT; Performed the experiments: YL and YW; Analyzed the data: ZZ and JL; Wrote the paper: TE and JL.

ACKNOWLEDGMENTS

We sincerely thank Prof. Yu Fang for his constructive and critical comments on this manuscript. This study was financially supported by National Natural Science Foundation of China (31570520).

SUPPLEMENTARY MATERIAL

The Supplementary Material for this article can be found online at: http://journal.frontiersin.org/article/10.3389/fphys.2016.00217

REFERENCES

Carvacho, H. B., Perez, C., Zuniga, G., and Mahn, A. (2014). Effect of methyl jasmonate, sodium selenate and chitosan as exogenous elicitors on the phenolic compounds profile of broccoli sprouts. *J. Sci. Food Agric.* 94, 2555–2561. doi: 10.1002/jsfa.6596

Chagoyen, M., and Pazos, F. (2011). MBRole: enrichment analysis of metabolomic data. *Bioinformatics* 27, 730–731. doi: 10.1093/bioinformatics/btr001

Cheynier, V., Comte, G., Davies, K. M., Lattanzio, V., and Martens, S. (2013). Plant phenolics: recent advances on their biosynthesis, genetics, and ecophysiology. *Plant Physiol. Biochem.* 72, 1–20. doi: 10.1016/j.plaphy.2013.05.009

Choi, Y. H., Tapias, E. C., Kim, H. K., Lefeber, A. W., Erkelens, C., Verhoeven, J. T., et al. (2004). Metabolic discrimination of *Catharanthus roseus* leaves infected by phytoplasma using 1H-NMR spectroscopy and multivariate data analysis. *Plant Physiol.* 135, 2398–2410. doi: 10.1104/pp.104.041012

Chung, I. M., Hong, S. B., Peebles, C. A., Kim, J. A., and San, K. Y. (2007). Effect of the engineered indole pathway on accumulation of phenolic compounds in *Catharanthus roseus* hairy roots. *Biotechnol. Prog.* 23, 327–332. doi: 10.1021/bp060258e

Clarke, J. D., Volko, S. M., Ledford, H., Ausubel, F. M., and Dong, X. (2000). Roles of salicylic acid, jasmonic acid, and ethylene in cpr-induced resistance in arabidopsis. *Plant Cell* 12, 2175–2190. doi: 10.1105/tpc.12.11.2175

Cocetta, G., Rossoni, M., Gardana, C., Mignani, I., Ferrante, A., and Spinardi, A. (2015). Methyl jasmonate affects phenolic metabolism and gene expression in blueberry (*Vaccinium corymbosum*). *Physiol. Plant* 153, 269–283. doi: 10.1111/ppl.12243

Del Valle, J. C., Buide, M. L., Casimiro-Soriguer, I., Whittall, J. B., and Narbona, E. (2015). On flavonoid accumulation in different plant parts: Variation patterns among individuals and populations in the shore campion (*Silene littorea*). *Front. Plant Sci.* 6:939. doi: 10.3389/fpls.2015.00939

Demkura, P. V., Abdala, G., Baldwin, I. T., and Ballare, C. L. (2010). Jasmonate-dependent and -independent pathways mediate specific effects of solar ultraviolet B radiation on leaf phenolics and antiherbivore defense. *Plant Physiol.* 152, 1084–1095. doi: 10.1104/pp.109.148999

Dixon, R. A. (2001). Natural products and plant disease resistance. *Nature* 411, 843–847. doi: 10.1038/35081178

Dong, X., Chen, W., Wang, W., Zhang, H., Liu, X., and Luo, J. (2014). Comprehensive profiling and natural variation of flavonoids in rice. *J. Integr. Plant Biol.* 56, 876–886. doi: 10.1111/jipb.12204

Ferreres, F., Figueiredo, R., Bettencourt, S., Carqueijeiro, I., Oliveira, J., Gil-Izquierdo, A., et al. (2011). Identification of phenolic compounds in isolated vacuoles of the medicinal plant *Catharanthus roseus* and their interaction with vacuolar class III peroxidase: an H(2)O(2) affair? *J. Exp. Bot.* 62, 2841–2854. doi: 10.1093/jxb/erq458

Ferreres, F., Llorach, R., and Gil-Izquierdo, A. (2004). Characterization of the interglycosidic linkage in di-, tri-, tetra- and pentaglycosylated flavonoids and differentiation of positional isomers by liquid chromatography/electrospray ionization tandem mass spectrometry. *J. Mass Spectrom.* 39, 312–321. doi: 10.1002/jms.586

Ferreres, F., Pereira, D. M., Valentao, P., Andrade, P. B., Seabra, R. M., and Sottomayor, M. (2008). New phenolic compounds and antioxidant potential of *Catharanthus roseus*. *J. Agric. Food Chem.* 56, 9967–9974. doi: 10.1021/jf8022723

Filippini, R., Caniato, R., Piovan, A., and Cappelletti, E. M. (2003). Production of anthocyanins by *Catharanthus roseus*. *Fitoterapia* 74, 62–67. doi: 10.1016/S0367-326X(02)00296-4

Garcia-Calderon, M., Pons-Ferrer, T., Mrazova, A., Pal'ove-Balang, P., Vilkova, M., Perez-Delgado, C. M., et al. (2015). Modulation of phenolic metabolism under stress conditions in a *Lotus japonicus* mutant lacking plastidic glutamine synthetase. *Front. Plant Sci.* 6:760. doi: 10.3389/fpls.2015.00760

Glazebrook, J., Chen, W., Estes, B., Chang, H. S., Nawrath, C., Metraux, J. P., et al. (2003). Topology of the network integrating salicylate and jasmonate signal transduction derived from global expression phenotyping. *Plant J.* 34, 217–228. doi: 10.1046/j.1365-313X.2003.01717.x

Hotze, M., Schroder, G., and Schroder, J. (1995). Cinnamate 4-hydroxylase from *Catharanthus roseus*, and a strategy for the functional expression of plant cytochrome P450 proteins as translational fusions with P450 reductase in *Escherichia coli*. *FEBS Lett.* 374, 345–350. doi: 10.1016/0014-5793(95)01141-Z

Lewis, D. R., Ramirez, M. V., Miller, N. D., Vallabhaneni, P., Ray, W. K., Helm, R. F., et al. (2011). Auxin and ethylene induce flavonol accumulation through distinct transcriptional networks. *Plant Physiol.* 156, 144–164. doi: 10.1104/pp.111.172502

Lin, L. Z., and Harnly, J. M. (2007). A screening method for the identification of glycosylated flavonoids and other phenolic compounds using a standard analytical approach for all plant materials. *J. Agric. Food Chem.* 55, 1084–1096. doi: 10.1021/jf062431s

Moreno, P. R., van der Heijden, R., and Verpoorte, R. (1994). Elicitor-mediated induction of isochorismate synthase and accumulation of 2,3-dihydroxy benzoic acid in *Catharanthus roseus* cell suspension and shoot cultures. *Plant Cell Rep.* 14, 188–191. doi: 10.1007/BF00233788

Mouradov, A., and Spangenberg, G. (2014). Flavonoids: a metabolic network mediating plants adaptation to their real estate. *Front. Plant Sci.* 5:620. doi: 10.3389/fpls.2014.00620

Murphy, A., Peer, W. A., and Taiz, L. (2000). Regulation of auxin transport by aminopeptidases and endogenous flavonoids. *Planta* 211, 315–324. doi: 10.1007/s004250000300

Mustafa, N. R., and Verpoorte, R. (2005). Chorismate derived C6C1 compounds in plants. *Planta* 222, 1–5. doi: 10.1007/s00425-005-1554-0

Mustafa, N., and Verpoorte, R. (2007). Phenolic compounds in *Catharanthus roseus*. *Phytochem. Rev.* 6, 243–258. doi: 10.1007/s11101-006-9039-8

Onkokesung, N., Baldwin, I. T., and Galis, I. (2010). The role of jasmonic acid and ethylene crosstalk in direct defense of Nicotiana attenuata plants against chewing herbivores. *Plant Signal. Behav.* 5, 1305–1307. doi: 10.4161/psb.5.10.13124

Pan, Y. J., Liu, J., Guo, X. R., Zu, Y. G., and Tang, Z. H. (2015). Gene transcript profiles of the TIA biosynthetic pathway in response to ethylene and copper reveal their interactive role in modulating TIA biosynthesis in *Catharanthus roseus*. *Protoplasma* 252, 813–824. doi: 10.1007/s00709-014-0718-9

Papon, N., Bremer, J., Vansiri, A., Andreu, F., Rideau, M., and Creche, J. (2005). Cytokinin and ethylene control indole alkaloid production at the level of the MEP/terpenoid pathway in *Catharanthus roseus* suspension cells. *Planta Med.* 71, 572–574. doi: 10.1055/s-2005-864163

Penninckx, I. A., Thomma, B. P., Buchala, A., Métraux, J. P., and Broekaert, W. F. (1998). Concomitant activation of jasmonate and ethylene response pathways is required for induction of a plant defensin gene in Arabidopsis. *Plant Cell* 10, 2103–2113. doi: 10.1105/tpc.10.12.2103

Pozo, M. J., López-Ráez, J. A., Azcón-Aguilar, C., and García-Garrido, J. M. (2015). Phytohormones as integrators of environmental signals in the regulation of mycorrhizal symbioses. *New Phytol.* 205, 1431–1436. doi: 10.1111/nph.13252

Proestos, C., Chorianopoulos, N., Nychas, G. J., and Komaitis, M. (2005). RP-HPLC analysis of the phenolic compounds of plant extracts. investigation of their antioxidant capacity and antimicrobial activity. *J. Agric. Food Chem.* 53, 1190–1195. doi: 10.1021/jf040083t

Rijhwani, S. K., and Shanks, J. V. (1998). Effect of elicitor dosage and exposure time on biosynthesis of indole alkaloids by *Catharanthus roseus* hairy root cultures. *Biotechnol. Prog.* 14, 442–449. doi: 10.1021/bp980029v

Simirgiotis, M. J., Benites, J., Areche, C., and Sepulveda, B. (2015). Antioxidant capacities and analysis of phenolic compounds in three endemic nolana species by HPLC-PDA-ESI-MS. *Molecules* 20, 11490–11507. doi: 10.3390/molecules200611490

Sousa, C., Valentao, P., Ferreres, F., Seabra, R. M., and Andrade, P. B. (2008). Tronchuda cabbage (*Brassica oleracea* L. var. costata DC): scavenger of reactive nitrogen species. *J. Agric. Food Chem.* 56, 4205–4211. doi: 10.1021/jf072740y

Trantas, E. A., Koffas, M., Xu, P., and Ververidis, F. (2015). When plants produce not enough or at all: metabolic engineering of flavonoids in microbial hosts. *Front. Plant Sci.* 6:7. doi: 10.3389/fpls.2015.00007

Valentao, P., Fernandes, E., Carvalho, F., Andrade, P. B., Seabra, R. M., and Bastos, M. L. (2001). Antioxidant activity of *Centaurium erythraea* infusion evidenced by its superoxide radical scavenging and xanthine oxidase inhibitory activity. *J. Agric. Food Chem.* 49, 3476–3479. doi: 10.1021/jf001145s

van Der Heijden, R., Jacobs, D. I., Snoeijer, W., Hallard, D., and Verpoorte, R. (2004). The Catharanthus alkaloids: pharmacognosy and biotechnology. *Curr. Med. Chem.* 11, 607–628. doi: 10.2174/0929867043455846

Van Lanen, S. G., Lin, S., and Shen, B. (2008). Biosynthesis of the enediyne antitumor antibiotic C-1027 involves a new branching point in

chorismate metabolism. *Proc. Natl. Acad. Sci. U.S.A.* 105, 494–499. doi: 10.1073/pnas.0708750105

Vanstraelen, M., and Benkova, E. (2012). Hormonal interactions in the regulation of plant development. *Annu. Rev. Cell Dev. Biol.* 28, 463–487. doi: 10.1146/annurev-cellbio-101011-155741

van Wees, S. C., de Swart, E. A., van Pelt, J. A., van Loon, L. C., and Pieterse, C. M. (2000). Enhancement of induced disease resistance by simultaneous activation of salicylate- and jasmonate-dependent defense pathways in *Arabidopsis thaliana*. *Proc. Natl. Acad. Sci. U.S.A.* 97, 8711–8716. doi: 10.1073/pnas.130425197

Vos, I. A., Moritz, L., Pieterse, C. M., and Van Wees, S. C. M. (2015). Impact of hormonal crosstalk on plant resistance and fitness under multi-attacker conditions. *Front. Plant Sci.* 6:639. doi: 10.3389/fpls.2015.00639

Wasternack, C., and Hause, B. (2013). Jasmonates: biosynthesis, perception, signal transduction and action in plant stress response, growth and development. An update to the 2007 review in Annals of Botany. *Ann. Bot.* 111, 1021–1058. doi: 10.1093/aob/mct067

Watkins, J. M., Hechler, P. J., and Muday, G. K. (2014). Ethylene-induced flavonol accumulation in guard cells suppresses reactive oxygen species and moderates stomatal aperture. *Plant Physiol.* 164, 1707–1717. doi: 10.1104/pp.113.233528

Zhang, A. H., Wang, P., Sun, H., Yan, G. L., Han, Y., and Wang, X. J. (2013). High-throughput ultra-performance liquid chromatography-mass spectrometry characterization of metabolites guided by a bioinformatics program. *Mol. Biosyst.* 9, 2259–2265. doi: 10.1039/c3mb70171a

Conflict of Interest Statement: The authors declare that the research was conducted in the absence of any commercial or financial relationships that could be construed as a potential conflict of interest.

frontiers in Plant Science

ORIGINAL RESEARCH
published: 30 March 2017
doi: 10.3389/fpls.2017.00444

The Role of Auxin-Ethylene Crosstalk in Orchestrating Primary Root Elongation in Sugar Beet

Willem Abts[1†], Bert Vandenbussche[2], Maurice P. De Proft[1] and Bram Van de Poel[1]*

[1] Division of Crop Biotechnics, Department of Biosystems, University of Leuven, Leuven, Belgium, [2] SESVanderHave N.V., Tienen, Belgium

It is well-established in *Arabidopsis* and other species that ethylene inhibits root elongation through the action of auxin. In sugar beet (*Beta vulgaris* L.) ethylene promotes root elongation in a concentration dependent manner. However, the crosstalk between ethylene and auxin remains unknown during sugar beet seedling development. Our experiments have shown that exogenously applied auxin (indole-3-acetic acid; IAA) also stimulates root elongation. We also show that auxin promotes ethylene biosynthesis leading to longer roots. We have further demonstrated that the auxin treatment stimulates ethylene production by redirecting the pool of available 1-aminocyclopropane-1-carboxylic acid (ACC) toward ethylene instead of malonyl-ACC (MACC) resulting in a prolonged period of high rates of ethylene production and subsequently a longer root. On the other hand we have also shown that endogenous IAA levels were not affected by an ACC treatment during germination. All together our findings suggest that the general model for auxin-ethylene crosstalk during early root development, where ethylene controls auxin biosynthesis and transport, does not occur in sugar beet. On the contrary, we have shown that the opposite, where auxin stimulates ethylene biosynthesis, is true for sugar beet root development.

Keywords: auxin, ethylene, sugar beet, root elongation, crosstalk

OPEN ACCESS

Edited by:
Péter Poór,
University of Szeged, Hungary

Reviewed by:
Helene S. Robert,
CEITEC Masaryk University, Czechia
Stephan Pollmann,
Centre for Plant Biotechnology and Genomics, Spain

****Correspondence:***
Bram Van de Poel
bram.vandepoel@kuleuven.be

†Present Address:
Willem Abts,
Bayer Crop Science, Diegem, Belgium

Specialty section:
This article was submitted to Plant Physiology, a section of the journal Frontiers in Plant Science

Received: *12 November 2016*
Accepted: *14 March 2017*
Published: *30 March 2017*

Citation:
Abts W, Vandenbussche B, De Proft MP and Van de Poel B (2017) The Role of Auxin-Ethylene Crosstalk in Orchestrating Primary Root Elongation in Sugar Beet. Front. Plant Sci. 8:444. doi: 10.3389/fpls.2017.00444

INTRODUCTION

Sugar beet (*Beta vulgaris* L.) is a root crop which is primarily cultivated for extracting sugars from its tap root. The initial root development phase immediately after germination is a crucial process that primes the seedling for a steady development and is important for the further outgrowth of the tap root which ultimately determine sugar yield. Currently, little is known about the hormonal regulation of sugar beet root development.

In *Arabidopsis thaliana* multiple studies have shown that root elongation during early root development is inhibited by the gaseous plant growth regulator ethylene (Ruzicka et al., 2007; Stepanova et al., 2007; Swarup et al., 2007; Markakis et al., 2012). However, Pierik et al. (2006) have proposed a biphasic ethylene response model where ethylene has both an inhibitory and stimulatory effect on root elongation depending on the ethylene concentration and the species. Recently we have shown that the early root growth in sugar beet also shows a biphasic ethylene response (Abts et al., 2014). Application of low concentrations of the ethylene precursor 1-aminocyclopropane-1-carboxylic acid (ACC) stimulates root growth while high concentrations inhibit root growth (Abts et al., 2014). It is also known that auxin can inhibit root elongation in

many species (e.g., *Arabidopsis*, *Brassica*, maize, pea...; Eliasson et al., 1989; Rahman et al., 2007; Ruzicka et al., 2007; Stepanova et al., 2007; Swarup et al., 2007; Alarcón et al., 2012; Polit et al., 2014). In contradiction, it was also previously shown in *Arabidopsis* that low auxin levels could stimulate root elongation (Evans et al., 1994) which might suggest that auxins can also exert a biphasic response in root growth. However, the auxin response during early root growth of sugar beet remains elusive.

The regulation of root elongation is often the result of a complex interaction between ethylene and auxin (reviewed by Benková and Hejátko, 2009; Muday et al., 2012; Van de Poel et al., 2015; Hu et al., 2017). Studies in *Arabidopsis* have shown that ethylene stimulates auxin biosynthesis and upregulates the transcription of several auxin transporters (e.g., *PIN1*, *PIN2*, *AUX1*; Ruzicka et al., 2007; Stepanova et al., 2007; Swarup et al., 2007). The ethylene-induced auxin production is localized in the root tip (Swarup et al., 2007) and the auxin signal is subsequently redistributed by polar auxin transport toward the elongation zone. This results in an auxin accumulation in the elongation zone and leads to an inhibited cell elongation (Ruzicka et al., 2007). Inhibition of auxin transport using auxin transport mutants (e.g., *pin2* and *aux1*) results in an ethylene insensitive root growth due to the lack of crosstalk possibilities (Ruzicka et al., 2007). Another possible point of auxin-ethylene crosstalk is the enzyme VAS1 which regulates both auxin and ethylene production (Zheng et al., 2013; Pieck et al., 2015).

The reciprocal regulation in which auxin controls ethylene biosynthesis during root development is also well-described (reviewed by Benková and Hejátko, 2009; Muday et al., 2012). Application of the auxin indole-3-acetic acid (IAA) induces the expression and enzyme activity of both ACC-synthase (ACS) and ACC-oxidase (ACO) in roots of both pea and *Arabidopisis* (Peck and Kende, 1995, 1998; Tsuchisaka and Theologis, 2004; Stepanova et al., 2007). The complex crosstalk between ethylene and auxin also occurs during the regulation of root gravitropism (Lee et al., 1990), root hair initiation and elongation (Tanimoto et al., 1995; Pitts et al., 1998; Rahman et al., 2002), hypocotyl growth (Collett et al., 2000) and apical hook formation (Lehman et al., 1996). The formation of malonyl-ACC (MACC) by ACC-N-malonyltransferase (Martin and Saftner, 1995), as a mechanism to control the pool of ACC and subsequently ethylene production levels, is often neglected in ethylene and hormonal crosstalk studies (Van de Poel and Van Der Straeten, 2014).

In a previous study we have shown that ethylene regulates root elongation during sugar beet germination in a dose-dependent manner (Abts et al., 2014). However, the involvement of auxin during early root growth in sugar beet seedlings remains unresolved. In order to study the relation between auxin and ethylene during early root growth of sugar beet seedlings, kinetic germination assays were set up, the ethylene biosynthesis pathway was studied and endogenous IAA levels in sugar beet fruits and seedlings were quantified during root growth. Our results show that IAA stimulates ethylene production, resulting in a prolonged period of ethylene exposure which leads to longer roots. We further show that this IAA-stimulated ethylene production is likely achieved by inhibiting the conversion of ACC to MACC. We therefore propose that the auxin-stimulated ethylene production is responsible for the promotion of root elongation in sugar beet seedlings.

MATERIALS AND METHODS

Plant Material, Morphology, and Seed Germination

Diploid monogerm sugar beet (*B. vulgaris* L.) fruits consisting of a true seed surrounded by pericarp, all originated from one seed lot (LZD-2386, SESVanderHave N.V.). The seed lot was produced in 2010 (France, Nérac) and fruits were processed to meet commercial standards. The fruits were stored at room temperature and 35% relative humidity until further use.

For germination experiments, independent triplicates of 100 fruits were incubated in darkness at 20°C in polystyrene Petri dishes (90 mm), containing one layer of moist filter paper (Whatman No 1; 3 mL deionized water). Each Petri dish contained 25 fruits. Germination was counted at specific time intervals. Radicle protrusion of both seed coats was used as criterion for germination. Where indicated indole-3-acetic acid (IAA; Acros), 1-aminocyclopropane-1-carboxylic acid (ACC; Acros), α-(p-chlorophenoxy)isobutyric acid (PCIB, Sigma-Aldrich), or silver thiosulfate (STS; Sigma-Aldrich) was added to the imbibition medium. Silver thiosulfate was prepared as described by Reid et al. (1980). PCIB was dissolved in dimethyl sulfoxide (DMSO, Sigma-Aldrich) and diluted to the appropriate concentration. The final concentration of DMSO was kept below 0.1% for all treatments.

For root length measurements, at least 40 seedlings were used. Total root length was measured using a stereo microscope (Olympus SZX9) equipped with a digital camera (Olympus, Colorview II) and a video image analysis software (Olympus, Cell B).

Ethylene and *In vivo* ACO Enzyme Activity Measurements

Ethylene production was measured using gas chromatography as described by Abts et al. (2013). Briefly, 20 seedlings were incubated in glass flasks (10 mL) at 20°C always in five replicates. After 1 h incubation 1 mL headspace was sampled and analyzed for ethylene content. The accumulated ethylene in the headspace was measured using gas chromatography (Shimadzu GC-2014) equipped with a packed column and a flame ionization detector. The injector, the column and the detector had temperatures of 150, 90, and 250°C, respectively.

In vivo ACO enzyme activity was measured as described by Abts et al. (2014). Briefly, the *in vivo* ACO enzyme activity was determined by measuring the maximal ethylene production. At specific time intervals the sugar beet seedlings were carefully removed from each Petri dish and incubated for 3 h in another Petri dish containing 3 mL of a saturating 1 mM ACC solution. Subsequently the seedlings were incubated for 30 min in a gas-tight 10 mL glass flask and ethylene content in the headspace was measured as described above.

ACC, MACC, and IAA Quantification

ACC was extracted and quantified using the Lizada and Yang (1979) method optimized by Bulens et al. (2011). Briefly, ACC and MACC was extracted from 0.5 g of frozen and crushed seedling tissue with 1 mL 5% sulfosalicylic acid (Sigma) for 30 min at 4°C. Subsequently the sample was centrifuged for 10 min at 5,000 × g at 4°C. The amount of ACC extract was quantified by converting it to ethylene using a saturated NaOH:NaOCl (5%) mixture and $HgCl_2$ (10 mM). The reaction mixture was incubated for 4 min on ice, vortexed and subsequently a 1 mL headspace sample was analyzed with the GC for ethylene content. The reaction efficiency was determined in a second analyses of the same sample, by spiking with 10 μL 10 μM ACC. MACC was converted into ACC by an acid hydrolysis according to Hoffman et al. (1982) also updated by Bulens et al. (2011). Briefly, 100 μL of the ACC extract was hydrolysed for 4 h at 100°C using 6 M HCl. The hydrolysed sample was neutralized with 6M NaOH, centrifuged for 5 min at 13,000 × g and the supernatants was collected and analyzed for total ACC content (hydrolysed ACC + free ACC) as described above.

IAA was extracted from entire sugar beet seedlings based on the extraction procedure for auxins described earlier by Prinsen et al. (2000). Homogenized plant material was extracted in 80% methanol (10 mL/g fresh weight) and extracted overnight. A stable isotope-labeled IAA ([$^{13}C_6$]-IAA, 50 pmol, CLM-1896-PK, Cambridge Isotope Laboratories Inc., Andover, Massachusetts, USA) was added as internal standard. After centrifugation (20,000 × g for 15 min at 4°C) the supernatant was passed over a C18 cartridge (500 mg) to retain pigments. The effluent was diluted to 50% methanol and concentrated on a DEAE-Sephadex anion exchange column (2 mL) for the analysis of free IAA, which was retained on the DEAE. The DEAE cartridge was eluted with 10 mL 6% formic acid and free IAA was subsequently concentrated on a C18 cartridge. This C18 cartridge was eluted with 2 × 0.5 mL diethylether. The ether was evaporated under *vacuo* and the sample was suspended in acidified methanol for methylation with diazomethane. After methylation, the samples were dried under a nitrogen stream and samples were further dissolved in 50 μL 10% MeOH (Prinsen et al., 2000).

IAA was analyzed by UPLC-MS/MS (Acquity TQD, Waters, Manchester, UK; 6 μL injection by partial loop, column temperature 30°C, solvent gradient 0–2 min: 95/5; 10% MeOH in 1 mM NH_4OAc/MeOH; 2–4 min linear gradient until 10/90 10% MeOH in 1 mM NH_4OAc/MeOH; 4–6 min, isocratic 10/90 10% MeOH in 1 mM NH_4OAc/MeOH). MS conditions were set at: polarity MS ES(+), capillary 2 kV, cone 20 V, collision energy 20 eV, source temperature 120°C, desolvation temperature 450°C, cone gas flow 50 L/h, desolvation gas flow 750 L/h, and collision gas flow 0.19 mL/h. The diagnostic ions used for quantification are 190 > 130 m/z for Me-IAA and 196 > 136 m/z for Me-[$^{13}C_6$]-IAA (dwell time 0.02 s). Methanol and water used for MS are UPLC grade.

RNA Extraction and RT-qPCR

Total RNA was extracted using the RNeasy Plus Mini Kit (Qiagen) from 0.1 g frozen crushed sugar beet seedlings. The manufacturer's protocol was used. Briefly each sample was homogenized in 600 μL of Buffer RLT Plus supplemented with 10 μL β-mercaptoethanol. A 1% agarose gel stained with ethidium bromide was used to check RNA integrity. RNA purity was determined by the 260/280 and 260/230 nm ratio. Both the RNA content as well as the RNA purity were measured with the NanoDrop 2000 (Thermo Scientific). The QuantiTect Reverse Transcription Kit (Qiagen) was used to reverse transcribe 1 μg of the total RNA into cDNA according to the manufacturer's protocol. Samples were stored at −80°C until further use.

The expression profiles of all known isoforms of *ACS* and *ACO* (Dohm et al., 2014; **Table 1**) in sugar beet were determined during early seedling growth. Quantification was obtained via real-time quantitative PCR (RT-qPCR) on a Rotor-Gene Q cycler (Qiagen) for 45 cycles. The RT-qPCR reaction consisted of a forward and reverse primer (3.75 μM), RT-template, water, and Absolute QPCR SYBR Green mix (Abgene Limited, Epsom, UK). The used primers and their properties are listed in **Table 1**. Primers were designed with Primer3 software (Rozen and Skaletsky, 2000).

Specificity of amplification was confirmed performing a melting curve analysis after each qPCR run. The melting curve was obtained by increasing the temperature in steps of 0.5°C/s

TABLE 1 | List of used primers and their properties for the quantification of mRNA abundance.

Gene code	Accession	Forward-primer (5′->3′)	Reverse-primer (5′->3′)
ACS1	Bv_27160_idme.t1	ATGAGCCAACAAAGGAAAGTG	TGACAAGATGAACCAGGAGAGA
ACS2	Bv5_094750_hwtr.t1	TCGCATAGTAATGAGTGGTGGA	CAGGATAGTAGGGTGTGGGAAC
ACS3	Bv1_004170_gcto.t1	CAGGGTGGTTTAGGGTTTGTT	TGGTCTTTCCTCCATTTTTCC
ACS4	Bv6_125280_uenw.t1	CCAACACCAACAACAACAACA	TCTCGTATTCTTCCCAACCAA
ACO1	Bv_37910_nwgk.t1	GAGCTGATGTGTGAAAACCTTG	CGCTACCTTTGTTCCTACTGCT
ACO2	Bv9_207650_gdtf.t1	TGGGGTTTCTTTGAGTTGATG	CACTTCTTGTAATGCTCCTTTGTG
ACO3	Bv4_084910_gucu.t1	TAGAGGGCAAGGATGACAAAA	CAAAAGAGCGGCAAAACTATC
ACO4	Bv3_051500_mqsu.t1	CCTCAACCTGATGCTTTTGTT	CTGCTCTGTGCCATACACTCTT
ACO5	Bv8_187920_wndh.t1	CTGTGGAAAGGATGACAAAAGA	TGATGGCGAAGGTAGAAAGTG
Actin	HQ656028	CACGAGACAACCTACAACTCCA	GCTCATACGGTCAGCAATACC
18S rRNA	FJ669720	GAAAGACGAACAACTGCGAAA	CATCGTTTATGGTTGAGACTAGGA

ranging from 55 to 95°C. Three biological replicates were used and normalized against the average expression of two reference genes (*Actin* and *18S rRNA*). Relative quantification was calculated by including a calibration curve in duplex in each run.

Statistics

For the root length measurements significant differences between the different treatments and days were calculated using SAS Enterprise Guide 6 with the linear models procedure and the Tukey means comparison test set with a 95% confidence interval. All other statistical differences were analyzed with the one-way ANOVA procedure followed by a Tukey multiple comparison test using the statistical package "R" version 2.12.2. Significance level was set at 5%.

RESULTS

Sugar Beet Root Length Is Regulated by an Interaction between Auxin and Ethylene

The role of auxin and ethylene during root growth is quite well-established in *Arabidopsis* and some other crops (Muday et al., 2012), but is still unclear in sugar beet. Furthermore, the biphasic behavior of ethylene on root growth is species dependent (Pierik et al., 2006) and might suggest a differential crosstalk with auxin. In order to investigate the role of auxin and ethylene on early root development of sugar beet we measured the root in the presence of different imbibition media. We first tested the effect of auxin on root elongation using different IAA concentrations ranging between 1 and 100 μM (**Figure 1**). Root length was significantly stimulated for IAA concentrations between 1 and 10 μM. Higher concentrations (25–100 μM IAA) did not result in a stronger elongation response (**Figure 1**). The 10 μM IAA treatment was chosen in subsequent experiments to unravel the ethylene-auxin crosstalk in sugar beet seedlings because this concentration of IAA was the lowest IAA concentration at which a maximal root elongation response was observed.

Next, we measured root elongation over a 6 day period for different IAA and ACC combinations (**Figure 2**). All treatments

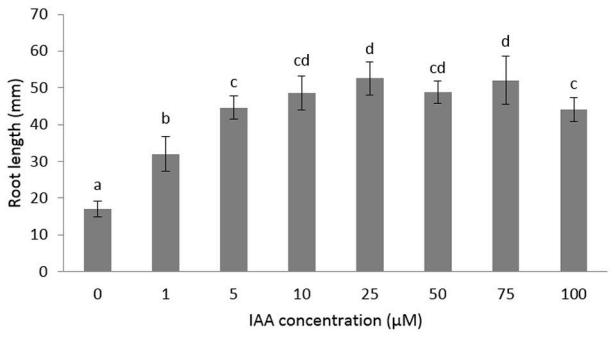

FIGURE 1 | Effects of different concentrations of indole-3-acetic acid (IAA) added to the imbibition medium on the root length of sugar beet seedlings after 6 days at 20°C in darkness. Mean values ± *SD* are presented ($n > 40$). Levels of significance ($p < 0.05$) are indicated with the letters a–d.

stimulated root growth and the largest effects were observed 6 days after imbibition. At that time point the root length of seedlings grown on 10 μM IAA were more than double in length compared to the untreated control. The addition of 10 μM ACC to the imbibition medium also stimulated root elongation similar as the 10 μM IAA treatment. Root length was even more stimulated when a combination of 10 μM IAA + 10 μM ACC was applied indicating a cooperative action of ACC and IAA. Root elongation was inhibited when seedlings were treated with a very high ACC concentration (1 mM), which was in accordance with our previous observations (Abts et al., 2014). In the presence of the high ACC concentration of 1 mM, the addition of 10 μM IAA did not reverse the inhibition of root elongation. Both ACC treatments (10 μM and 1 mM) also stimulated ethylene production of the sugar beet seedlings yet to a different extent (**Supplementary Figure 1**). A small increase in ethylene production (10 μM ACC) leads to an increase in root elongation, while a large increase in ethylene production (1 mM ACC) inhibits root elongation (**Supplementary Figure 1**).

In order to further investigate the role of auxin on root elongation in sugar beet we have performed germination experiments with the auxin response inhibitor α-(p-chlorophenoxy)isobutyric acid (PCIB; Oono et al., 2003) in combination with different concentrations of ACC (**Figure 3**). A PCIB treatment did not affect root elongation when administered in different concentrations (**Supplementary Figure 2**). The ethylene-induced root elongation response of seedlings was not influenced when administered 10 μM PCIB together with 10 μM ACC, indicating that the ethylene response is independent from the action of auxin. When 1,000 μM ACC was supplemented, the additive effect of 10 μM IAA or PCIB is abolished. The PCIB treatment did not influence ethylene production during sugar beet germination (**Supplementary Figure 3**). In order to evaluate the auxin-stimulated effect on root elongation we used the ethylene perception inhibitor silver thiosulphate (STS) in combination with 10 μM IAA. Surprisingly the 10 μM STS treatment resulted in an increased root elongation, while the 1,000 μM STS treatment did not affect root growth compared to the untreated controls. Despite this positive effect of 10 μM STS on root growth, the combined treatment with IAA (or PCIB) did not promote or inhibit root elongation (**Figure 3**). The increase in root length observed for the 10 μM STS treatment might be explained by the subtle but significant increase in ethylene production of the STS treatment (**Supplementary Figure 4**). Previous work with STS as an ethylene response inhibitor also reported a drastic increase in ethylene production in tomato fruit (Atta-Aly et al., 1987). At the end, one can question the functionality of STS to inhibit ethylene responses. Perhaps the STS treatment causes phytotoxicity or abiotic stress (silver as a heavy metal), which might trigger ethylene production.

IAA Does Not Affect Germination Rate of Sugar Beet

In this study we aim to unravel the effect of IAA and ethylene (via ACC supplementation) on root elongation. However, a possible delay or promotion of germination might mask a root elongation

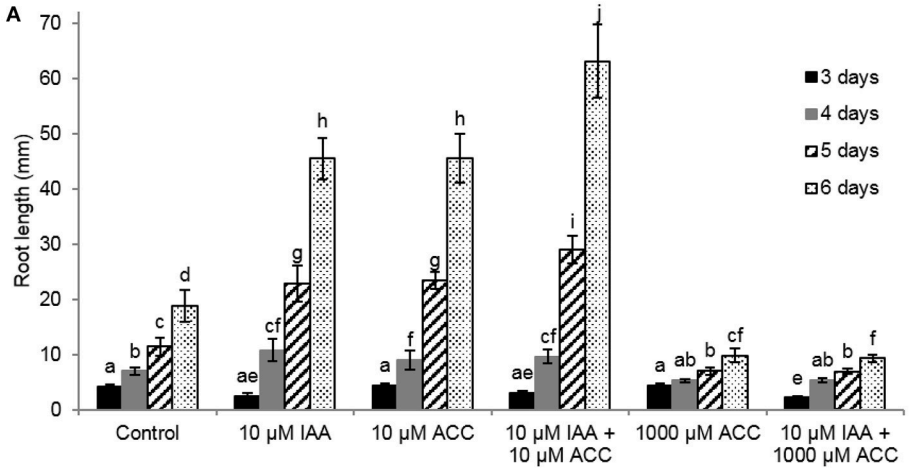

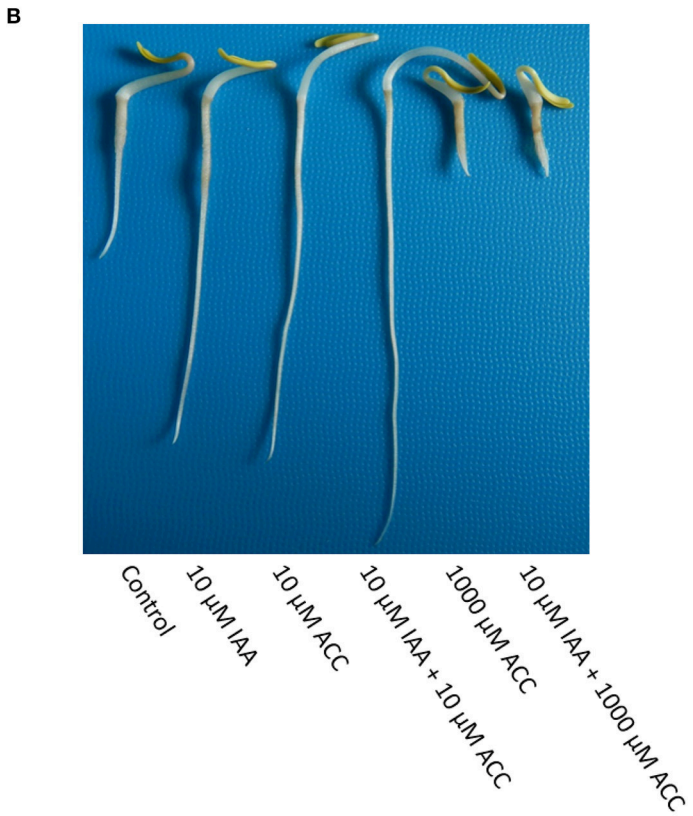

FIGURE 2 | Effect of indole-3-acetic acid (IAA) and 1-aminocyclopropane-1-carboxylic acid (ACC) added to the imbibition medium on (A) root length (mm) of sugar beet seedlings after 3, 4, 5, and 6 days at 20°C in darkness. Mean values ± *SD* are presented ($n > 40$). A linear models procedure and the Tukey means comparison test was used to check statistical differences between the treatments and days. Levels of significance ($p < 0.05$) are indicated with the letters a–j. **(B)** Representative examples of 6 day old sugar beet seedlings incubated at 20°C in darkness in the presence of different 1-aminocyclopropane-1-carboxylic acid (ACC) and/or indole-3-acetic acid (IAA) concentrations.

response, complicating the interpretation of the effect of IAA and ACC. Consequently, it is possible that differences in root length are (partially) caused by an altered germination rate. It was shown previously that ACC had no effect on the germination rate of sugar beet fruits (Abts et al., 2013). Interestingly, IAA delayed germination for just a few hours (**Figure 4**). The time to reach 50% germination (t_{50}) was 46 h for the control, compared to 52 h for the IAA treatment. The time to reach 90% germination (t_{90}) was not influenced by IAA. This result suggests that IAA only moderately affects the germination rate of sugar beet and that the differences in root length between the control and the ACC and IAA treatments, observed in **Figures 1**–**3**, are

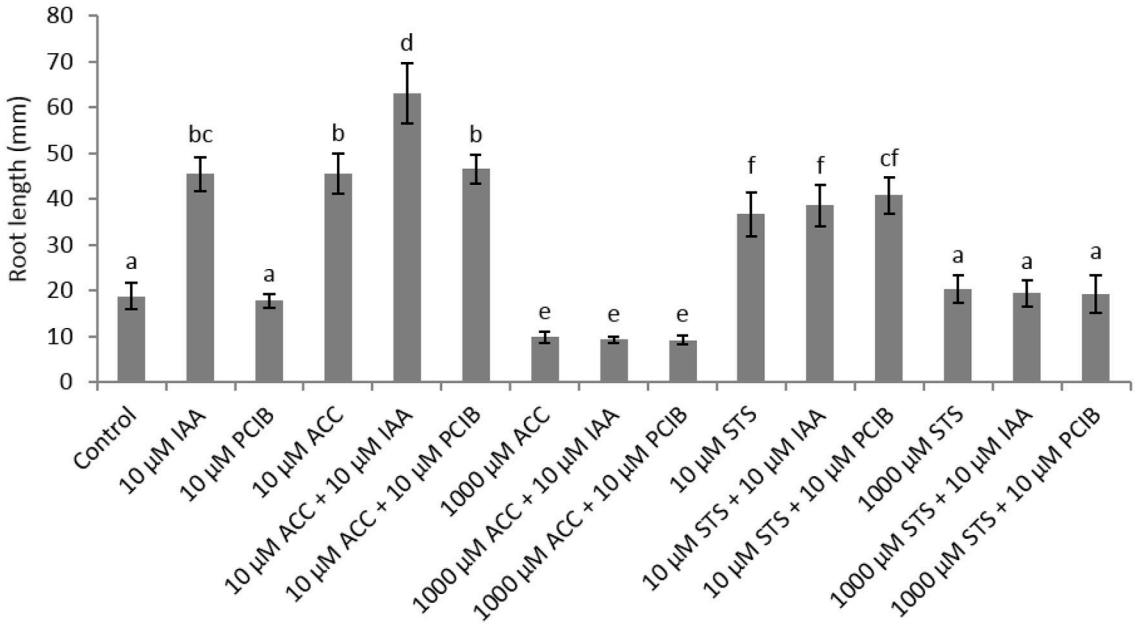

FIGURE 3 | Effect of indole-3-acetic acid (IAA), 1-aminocyclopropane-1-carboxylic acid (ACC), p-chlorophenoxyisobutyric acid (PCIB), silver thiosulphate (STS), and the combinations of these plant growth regulators on the root length (mm) of sugar beet seedlings after 6 days at 20°C in darkness. Mean values ± *SD* are presented ($n > 40$). Levels of significance ($p < 0.05$) are indicated with the letters a–f.

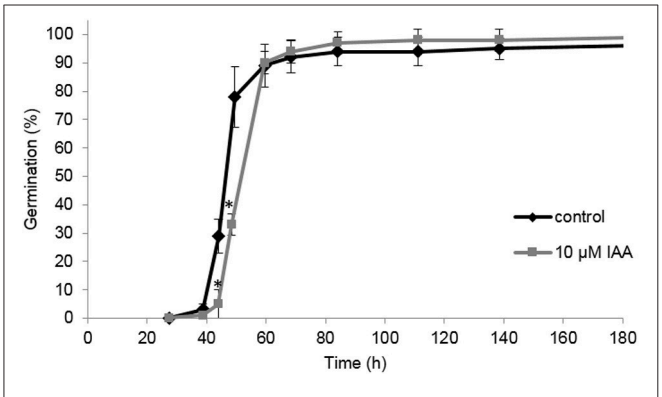

FIGURE 4 | Effect of indole-3-acetic acid (IAA) on the germination percentage of sugar beet incubated at 20°C in darkness. Each point represents the mean of three independent replicates of 100 fruits. Mean values ± *SD* are presented. The asterisk indicates that the IAA treatment differs significantly from the corresponding controls ($p < 0.05$).

predominantly caused by the hormonal regulation of root growth after germination.

Ethylene Biosynthesis Is Regulated by Auxin during Sugar Beet Seedling Growth

In order to investigate the crosstalk between ethylene and auxin during sugar beet root development, we analyzed the ethylene biosynthesis pathway in sugar beet seedlings treated with IAA. We also measured the content of the ethylene precursor ACC and its derivative MACC, and *ACS* and *ACO* gene expression levels during sugar beet germination and early seedling growth. Our results showed that the onset of ethylene production (48 h after imbibition) was not affected by the IAA treatment (**Figure 5**). On the other hand, IAA treated seedlings showed higher ethylene production levels compared to the control seedlings at 60 and 72 h after imbibition. The control seedlings reached their maximal ethylene production rate at 84 h after imbibition which subsequently declined again until 108 h after imbibition. Both the IAA treated and control seedlings reached the same maximal ethylene production level, respectively at 72 and 84 h after imbibition. However, the decline in ethylene production for the IAA treated seedlings was slower compared to the control seedlings (between 108 and 132 h after imbibition) resulting in a higher ethylene production rate for the IAA treated seedlings during this period. After 144 h, the ethylene production levels of the control and IAA treatment were the same. This prolonged ethylene production of the IAA treated seedlings might explain the longer root phenotype observed in **Figures 1**, **2**.

At the metabolic level, the ACC content of the seedlings rapidly decreased during the first 12 h after imbibition (**Figure 6A**) which is most probably a consequence of water uptake and ACC leaching into the imbibition medium (Hermann et al., 2007; Abts et al., 2014). ACC levels were not significantly affected by IAA during the first 72 h after imbibition. At 84 h after imbibition, ACC levels peaked and the IAA treatment showed a significant higher ACC content compared to the control. The time-point of the ACC peak (84 h) corresponded to the moment when the ethylene production rate was highest (**Figure 5**).

Similar as ACC, MACC levels were not significantly affected by IAA during the first 72 h after imbibition (**Figure 6B**).

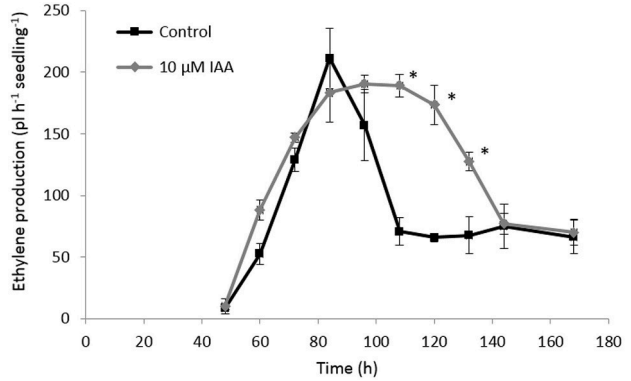

FIGURE 5 | Effect of indole-3-acetic acid (IAA) on the ethylene production (pL.h^{-1}.seedling^{-1}) during seedling growth of sugar beet at 20°C in darkness. Mean values ± *SD* are presented ($n = 5$). The asterisk indicates that the IAA treatment differs significantly from the corresponding controls ($p < 0.05$).

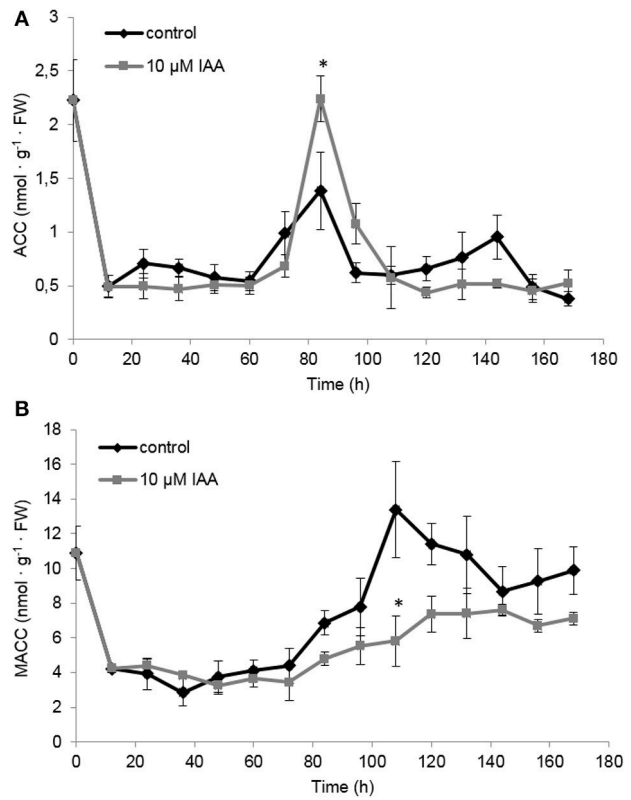

FIGURE 6 | Effect of indole-3-acetic acid (IAA) on the (A) 1-aminocyclopropane-1-carboxylic acid (ACC) and **(B)** malonyl-ACC (MACC) profile during seedling growth of sugar beet at 20°C in darkness. Mean values ± *SD* are presented ($n = 5$). The asterisk indicates that the IAA treatment differs significantly from the corresponding controls ($p < 0.05$).

Interestingly, around 84 h MACC levels started to increase and this rise was much more pronounced for the control seedlings compared to the IAA treated seedlings. Untreated seedlings showed a maximal MACC level around 108 h after imbibition followed by a gradual decline. The IAA treatment resulted in a maximal MACC level around 120 h after imbibition after which the levels remained constant. IAA treated seedlings never reach the high MACC levels of untreated seedlings indicating that the formation of MACC is inhibited by the IAA treatment.

Subsequently we investigated the effect of IAA on the expression of ethylene biosynthesis genes. Therefore, we quantified gene expression levels of all *ACS* and *ACO* isoforms. For *ACS1*, the control treatment showed two time points with peaking transcript levels: the first after 84 h and the second after 120 h (**Figure 7A**). IAA delayed the first increase with 12 h, while the IAA treatment did not induce a second increase in expression. Similar as *ACS1*, the expression of *ACS2* showed an upregulation after 84 and 120 h in the control treatment (**Figure 7B**). The IAA treatment resulted in a temporal increase of *ACS2* expression at 84 h. IAA delayed the second increase in transcript levels with ∼12 h. Transcript levels of *ACS3* and *ACS4* were not detected at any time point.

The *ACO1* expression profile showed a strong upregulation after 48 h until 96 h (**Figure 7C**) corresponding with the increase in ethylene production levels during this period (**Figure 5**). Expression levels quickly dropped and subsequently increased again resulting in a second peak of *ACO1* transcripts around 120 h. IAA delayed the strong upregulation of *ACO1* with 12 h and did not result in a second upregulation of *ACO1* expression. For *ACO2* expression, the IAA treatment resulted in an upregulation after 36 h which was ∼12 h earlier compared to the control treatment (**Figure 7D**). Between 48 and 132 h no differences in *ACO2* transcript levels were observed between the control and the IAA treatment. Thereafter, the IAA treatment showed higher expression levels of *ACO2* compared to the control. The expression profile of *ACO3* was not influenced by IAA until 120 h after the start of imbibition (**Figure 7E**). Thereafter, IAA showed significantly higher expression levels compared to the control. In general, the expression profile of *ACO4* was not influenced by IAA except from the time point 60 h (**Figure 7F**). At that time point, the control showed a peak in expression, whereas this increase was lacking in the IAA treatment. Comparable to *ACO3*, transcript levels of *ACO5* were not much changed by IAA until 120 h (**Figure 7G**). Between 132 and 168 h, the IAA treatment resulted in an increased *ACO5* expression compared to the control which was also observed in the expression pattern of *ACO2* and *ACO3*.

IAA Does Not Affect ACO Activity during Sugar Beet Seedling Growth

The differences in *ACO* gene expression observed for the IAA treated seedlings (**Figures 7C–G**) made us wonder if this could explain the sustained ethylene production levels observed in **Figure 6**. Therefore, we also measured the maximal *in vitro* ACO enzyme activity. We observed that the ACO enzyme activity was not influenced by the IAA treatment, except for a single time point 84 h (**Figure 8A**). Interestingly, the ACO *in vivo* activity profiles for both the control and the IAA treatment were similar to the ethylene production profile of the IAA treated seedlings

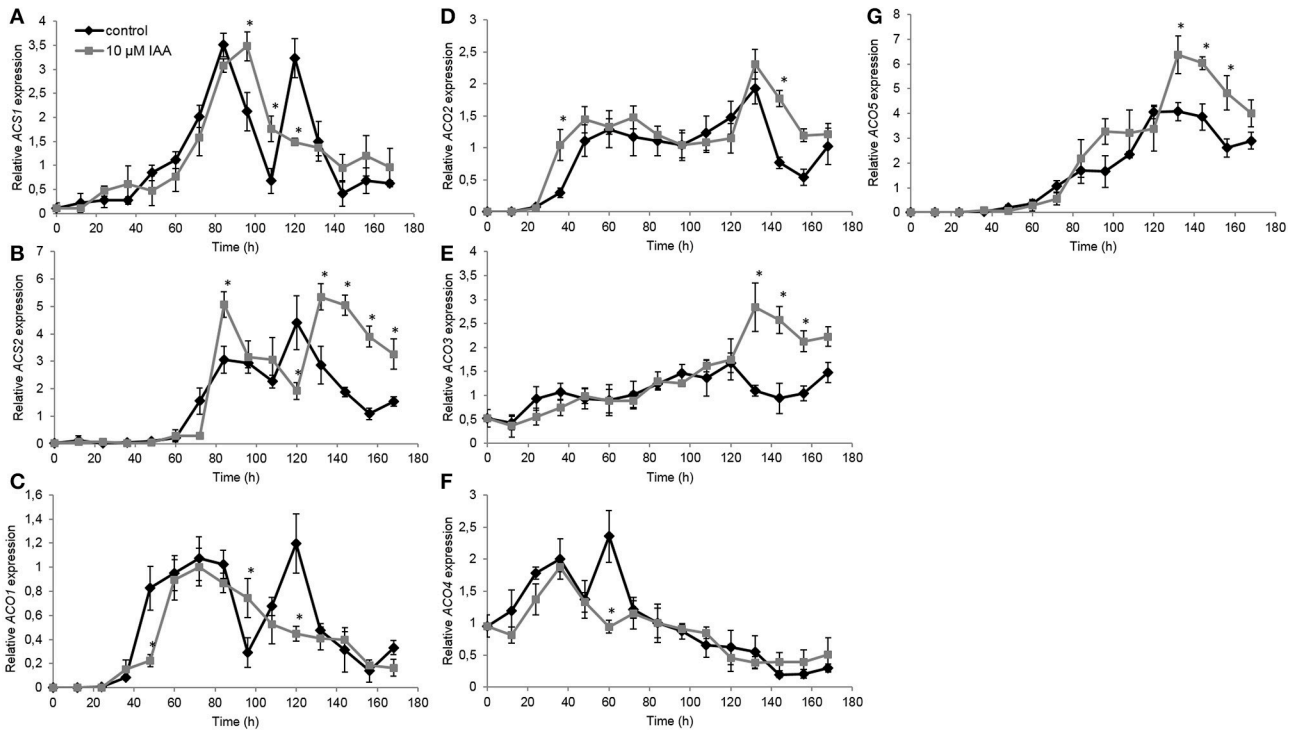

FIGURE 7 | Effect of indole-3-acetic acid (IAA) on the relative gene expression of *ACS1* (A), *ACS2* **(B)**, *ACO1* **(C)**, *ACO2* **(D)**, *ACO3* **(E)**, *ACO4* **(F)**, and *ACO5* **(G)** during seedling growth of sugar beet at 20°C in darkness. Mean values ± *SD* are presented ($n = 3$). The asterisk indicates that the IAA treatment differs significantly from the corresponding controls ($p < 0.05$).

(**Figure 5**). This result indicates that the differences in ethylene production between the control and IAA treatment (**Figure 5**) are most likely not attributed to a difference in ACO activity (**Figure 8A**), but rather to a difference in ACC availability.

Ethylene Does Not Affect IAA Levels during Sugar Beet Seedling Growth

Because it is well-documented that auxin biosynthesis is also regulated by ethylene during root growth (Ruzicka et al., 2007; Stepanova et al., 2007; Swarup et al., 2007), we investigated the possible effect of ACC on free IAA levels in sugar beet seedlings. In **Figure 1** we showed that 10 µM ACC stimulates root elongation while 1 mM ACC inhibits root elongation. However, none of these ACC concentrations influenced the IAA levels compared to the control (**Figure 8B**). Note that our IAA analyses were conducted on entire seedlings, and that tissue-specific differences in IAA content could be masked. Nonetheless, our results suggest that free IAA levels are not affected by ethylene during seedling development of sugar beet. **Figure 8B** also shows that endogenous IAA levels drastically drop after imbibition and gradually further decline during seedling development.

DISCUSSION

Our previous study (Abts et al., 2014) showed that ACC regulates early seedling development of sugar beet in a concentration dependent manner, with low concentrations stimulating root growth and high concentrations inhibiting root growth. However, the regulation of root elongation is often the result of a complex interaction between ethylene and auxin (reviewed by Benková and Hejátko, 2009; Muday et al., 2012). Hence we evaluated the effect of auxin during early root growth of sugar beet and checked for a possible interaction with the ethylene biosynthesis pathway.

Auxin Stimulates Root Growth in Sugar Beet by Interacting with Ethylene

Although auxin is mostly described to inhibit root elongation (Rahman et al., 2007; Ruzicka et al., 2007; Stepanova et al., 2007; Swarup et al., 2007; Alarcón et al., 2012), our results showed that auxin can stimulate root elongation during seedling growth of sugar beet. Evans et al. (1994) also found that low concentrations of auxin can stimulate root elongation in *Arabidopsis*. In a previous study (Abts et al., 2014) we showed that physiological relevant ACC levels also stimulated root elongation in sugar beet in contradiction to many other species where ACC inhibits root elongation. Based on these observations we can conclude that both auxin and ethylene have a stimulating effect on early root growth in sugar beet seedlings.

In this study we also showed that the combined application of auxin and ACC resulted in a cooperative effect with an even longer root. The use of an ethylene and auxin inhibitor (STS and PCIB, respectively) indicated that IAA was not able to

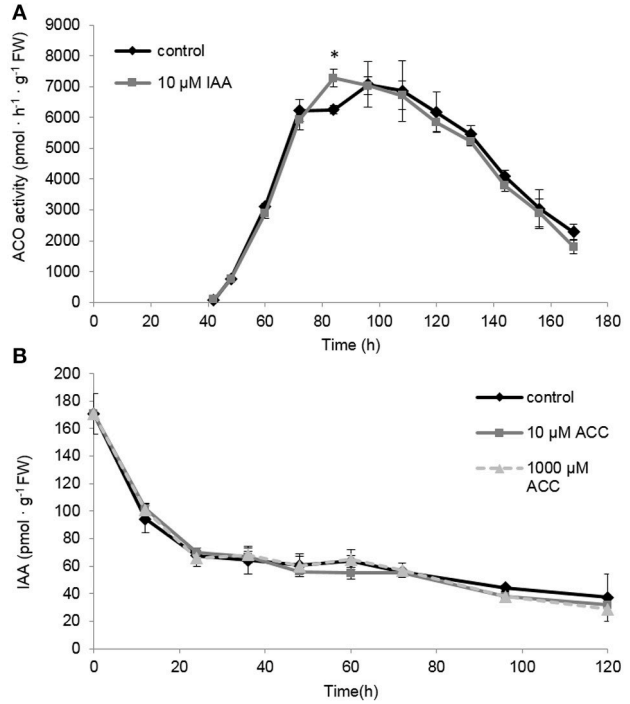

FIGURE 8 | (A) The effect of indole-3-acetic acid (IAA) on the *in vivo* ACO enzyme activity during seedling growth of sugar beet at 20°C in darkness. **(B)** Effect of 1-aminocyclopropane-1-carboxylic acid (10 µM ACC, gray solid line; 1,000 µM ACC, gray dotted line) on the indole-3-acetic acid profile (IAA) during seedling growth of sugar beet at 20°C in darkness. Mean values ± *SD* are presented ($n = 5$). The asterisk indicates that the IAA treatment differs significantly from the corresponding controls ($p < 0.05$).

overrule the STS effect on root elongation and that PCIB did not affect the stimulating effect of ACC on root elongation. These results suggest that root elongation is primarily regulated by the action of ethylene and not auxin. Additional experiments with other inhibitors of ethylene [e.g., 1-methylcyclopropene (1-MCP), aminooxyacetic acid (AOA), or aminoisobutyric acid (AIB)] and/or auxin [e.g., L-kynurenine, 5-(4-chlorophenyl)-4H-1,2,4-triazole-3-thiol (yucasin), 4-biphenylboronic acid (BBo), 4-phenoxyphenylboronic acid (PPBo)] could be done to further unravel the auxin-ethylene crosstalk in sugar beet root development (Hu et al., 2017). Our results also showed that free IAA levels in the seedling were not affected by the ACC treatment, suggesting that auxin biosynthesis is not stimulated by ethylene in sugar beet in contradiction to previous observations in *Arabidopsis* where an ACC treatment induces IAA production (Ruzicka et al., 2007; Swarup et al., 2007). It should be noted that despite unchanged levels of free IAA, the balance of IAA derivatives and conjugates can regulate the cellular IAA homeostasis and should be assessed in future studies. Altogether, these results indicate that the actual signal resulting in root elongation is likely to originate from ethylene and not from auxin, but it is possible that auxin can still exert an ethylene-independent effect on root elongation in sugar beet.

Auxin-Induced Root Elongation Is Achieved by Redirecting ACC toward Ethylene Production Instead of MACC, Prolonging the Total Ethylene Exposure Period

In our previous work we have shown that ethylene production starts just after the radicle emergence of the root during sugar beet germination (Abts et al., 2013). Maximal ethylene levels were observed around completion of germination and subsequently declined during further root growth (Abts et al., 2013). The present study reveals that auxin promotes ethylene production during early stages of root elongation and especially delays the decline in ethylene production ensuring a persisted high rate of ethylene production. This longer exposure period of the seedling toward ethylene might explain why the IAA treatment results in longer roots. These observations also suggest that auxin promotes ethylene biosynthesis during sugar beet seedling development. By dissecting the ethylene biosynthesis pathway we found that the maximal *in vivo* ACO capacity is the same for IAA treated and control seedlings, indicating that the regulation of ethylene biosynthesis is achieved at the level of ACS or ACC itself. It has been stated numerously that ACS is the rate limiting step of ethylene biosynthesis (Yang and Hoffman, 1984). One explanation could be that auxin induces *ACS* expression. It was previously shown in *Arabidopsis* that IAA can specifically and very rapidly induce the expression of *ACS4* in dark grown seedlings (Abel et al., 1995). Although, we did not capture the vary rapid *ACS* responses (within 1 h), our results showed that *ACS* gene expression was not drastically affected by the auxin treatment on the long-term, except during the very late stages of seedling development (later than 132 h after imbibition). The sugar beet *ACS* expression profiles might suggest that the supply of ACC by ACS was more or less similar between IAA treated and untreated seedlings. Nonetheless, we observed a higher ACC level at 84 h after imbibition for the IAA treated seedlings (**Figure 6A**). Our biochemical analysis of MACC content have revealed that MACC levels in IAA treated seedlings were lower compared to the control seedlings for the entire time frame of the experiment (**Figure 6B**). This discrepancy in MACC content might suggest that the auxin-induced surplus in ethylene production is likely to be caused by an inhibited conversion of ACC to MACC, leading to a shift in the pool of available ACC toward ethylene. Far too often, the formation of MACC is neglected in ethylene-related crosstalk studies undermining the importance of this ACC derivative, as reflected by our observations in sugar beet.

Ethylene Does Not Affect the Pool of IAA during Seedling Development of Sugar Beet

Although, it is generally assumed that ethylene modulates auxin biosynthesis during early root growth (Ruzicka et al., 2007; Stepanova et al., 2007; Swarup et al., 2007; Muday et al., 2012) our study shows that free IAA levels (in the entire seedling) are not affected by the supplementation of ACC during sugar beet seedling development. Hermann et al. (2007) also showed

that auxin levels are not altered after an ACC treatment. All combined, this suggests that ethylene has no effect on the level of free IAA in sugar beet. Maybe it is also possible that ethylene affects the level of IAA precursors and/or conjugated forms of IAA. It can also be that ethylene has an effect on IAA signaling or IAA transport, as previously described for *Arabidopsis* (reviewed by Benková and Hejátko, 2009; Muday et al., 2012). Whether this is the case during sugar beet seedling development remains to be investigated.

CONCLUSION

Our results have shown that both auxin and ACC can stimulate root elongation in sugar beet seedlings. The combination of IAA and ACC resulted in a cooperative effect on root length but only when supplemented in a low dose. We also demonstrated that externally applied IAA stimulates ethylene production by redirecting the pool of available ACC toward ethylene instead of MACC. The IAA treatment also results in a differential regulation of both *ACS* and *ACO* gene expression during seedling development. All combined this results in a longer and higher ethylene production rate, which in turn stimulates root elongation. On the contrary we did not observe any changes in IAA content during germination when sugar beet seedlings were treated with ACC. We can conclude that auxin stimulates ethylene biosynthesis and not the other way around during sugar beet root development. This suggests that the general ethylene-auxin crosstalk model elucidated in *Arabidopsis* roots (where ethylene promotes auxin production) does not seem to exist in sugar beet.

AUTHOR CONTRIBUTIONS

WA performed the experiments. WA, BV, and MD designed the experimental work. WA, BV, MD, and BVdP analyzed the data. WA, MD, and BVdP wrote the manuscript.

FUNDING

This research and the position of WA was funded by the Department of Biosystems, University of Leuven. BVdP was partially supported by the Belgian American Educational Foundation and the Special Research Fund of the University of Leuven.

ACKNOWLEDGMENTS

We thank S. Öden (University of Antwerp) for performing the IAA measurements.

SUPPLEMENTARY MATERIAL

The Supplementary Material for this article can be found online at: http://journal.frontiersin.org/article/10.3389/fpls.2017.00444/full#supplementary-material

Supplementary Figure 1 | Effect of (A) 10 μM ACC and **(B)** 1,000 μM ACC on the ethylene production (pL.h^{-1}.seedling^{-1}) during seedling growth of sugar beet at 20°C in darkness. Mean values ± *SD* are presented ($n = 5$).

Supplementary Figure 2 | Effect of different PCIB concentrations (1–100 μM) on root length (mm) of sugar beet seedlings after 6 days at 20°C in darkness. Mean values ± *SD* are presented ($n > 10$).

Supplementary Figure 3 | Effect of different concentrations of α-(p-chlorophenoxy)isobutyric acid (PCIB) on the ethylene production (pL.h^{-1}.seedling^{-1}) during seedling growth of sugar beet at 20°C in darkness. Mean values ± *SD* are presented ($n = 5$). PCIB was dissolved in dimethyl sulfoxide (DMSO) and diluted to the appropriate concentration. The final concentration of DMSO was kept below 0.1% for all treatments.

Supplementary Figure 4 | (A) Effect of different concentrations of silver thiosulphate (STS) added to the imbibition medium on root length (mm) of sugar beet seedlings after 6 days at 20°C in darkness. Mean values ± *SD* are presented ($n > 40$). Levels of significance ($p < 0.05$) are indicated with the letters a–d. **(B)** Effect of different STS concentrations on the ethylene production (pL.h^{-1}.seedling^{-1}) during seedling growth of sugar beet at 20°C in darkness. Mean values ± *SD* are presented ($n = 5$).

REFERENCES

Abel, S., Nguyen, M. D., Chow, W., and Theologis, A. (1995). ASC4, a primary indoleacetic acid-responsive gene encoding 1-aminocyclopropane-1-carboxylate synthase in *Arabidopsis thaliana*. *J. Biol. Chem.* 270, 19093–19099. doi: 10.1074/jbc.270.32.19093

Abts, W., Van de Poel, B., Vandenbussche, B., and De Proft, M. P. (2014). Ethylene is differentially regulated during sugar beet germination and affects early root growth in a dose-dependent manner. *Planta* 240, 679–686. doi: 10.1007/s00425-014-2124-0

Abts, W., Vissers, K., Vandenbussche, B., and De Proft, M. P. (2013). Study of ethylene kinetics during and after germination of sugar beet (*Beta vulgaris* L.) seeds and fruits. *Seed Sci. Res.* 23, 205–210. doi: 10.1017/S0960258513000147

Alarcón, M. V., Lloret, P. G., Iglesias, D. J., Talón, M., and Salguero, J. (2012). Comparison of growth responses to auxin 1-naphthaleneacetic acid and the ethylene precursor 1-aminocyclopropane-1-carboxylic acid in maize seedling root. *Acta Biol. Cracov.* 54, 16–23. doi: 10.2478/v10182-012-0001-3

Atta-Aly, M. A., Saltveit, M. E., and Hobson, G. E. (1987). Effect of silver ions on ethylene biosynthesis by tomato tissue. *Plant Physiol.* 83, 44–48. doi: 10.1104/pp.83.1.44

Benková, E., and Hejátko, J. (2009). Hormone interactions at the root apical meristem. *Plant Mol. Biol.* 69, 383–396. doi: 10.1007/s11103-008-9393-6

Bulens, I., Van de Poel, B., Hertog, M., De Proft, M. P., Geeraerd, A. H., and Nicolaï, B. M. (2011). Protocol: an updated integrated methodology for analysis of metabolites and enzyme activities of ethylene biosynthesis. *Plant Methods* 7, 17–26. doi: 10.1186/1746-4811-7-17

Collett, C. E., Harberd, N. P., and Leyser, O. (2000). Hormonal interactions in the control of Arabidopsis hypocotyl elongation. *Plant Physiol.* 124, 553–562. doi: 10.1104/pp.124.2.553

Dohm, J. C., Minoche, A. E., Holtgräwe, D., Capella-Gutiérrez, S., Zakrzewski, F., Tafer, H., et al. (2014). The genome of the recently domesticated crop plant sugar beet (*Beta vulgaris*). *Nature* 505, 546–549. doi: 10.1038/nature12817

Eliasson, L., Bertell, G., and Bolander, E. (1989). Inhibitory action of auxin on root elongation not mediated by ethylene. *Plant Physiol.* 91, 310–314. doi: 10.1104/pp.91.1.310

Evans, M. L., Ishikawa, H., and Estelle, M. A. (1994). Responses of Arabidopsis roots to auxin studied with high temporal resolution: comparison of wild type and auxin-response mutants. *Planta* 194, 215–222. doi: 10.1007/BF01101680

Hermann, K., Meinhard, J., Dobrev, P., Linkies, A., Pesek, B., Hess, B., et al. (2007). 1-Aminocyclopropane-1-carboxylic acid and abscisic acid during the germination of sugar beet (*Beta vulgaris* L.): a comparative study of fruits and seeds. *J. Exp. Bot.* 58, 3047–3060. doi: 10.1093/jxb/erm162

Hoffman, N. E., Yang, S. F., and McKeon, T. (1982). Identification and metabolism of 1-(malonylamino)cyclopropane-1-carboxylic acid as a major conjugate of 1-aminocyclopropane-1-carboxylic acid, an ethylene

precursor in higher plants. *Biochem. Biophys. Res. Commun.* 104, 765–770. doi: 10.1016/0006-291X(82)90703-3

Hu, Y., Vandenbussche, F., and Van Der Straeten, D. (2017). Regulation of seedling growth by ethylene and the ethylene-auxin crosstalk. *Planta* 245, 467–489. doi: 10.1007/s00425-017-2651-6

Lee, J. S., Chang, W. K., and Evans, M. L. (1990). Effects of ethylene on the kinetics of curvature and auxin redistribution in gravistimulated roots of *Zea mays*. *Plant Physiol.* 94, 1770–1775. doi: 10.1104/pp.94.4.1770

Lehman, A., Black, R., and Ecker, J. R. (1996). HOOKLESS1, an ethylene response gene, is required for differential cell elongation in Arabidopsis hypocotyls. *Cell* 85, 183–194. doi: 10.1016/S0092-8674(00)81095-8

Lizada, M. C., and Yang, S. F. (1979). Simple and sensitive assay for 1-aminocyclopropane-1-carboxylic acid. *Anal. Biochem.* 100, 140–145. doi: 10.1016/0003-2697(79)90123-4

Markakis, M. N., De Cnodder, T., Lewandowski, M., Simon, D., Boron, A., Balcerowicz, D., et al. (2012). Identification of genes involved in the ACC-mediated control of root cell elongation in *Arabidopsis thaliana*. *BMC Plant Biol.* 12, 208–218. doi: 10.1186/1471-2229-12-208

Martin, M. N., and Saftner, R. A. (1995). Purification and characterization of 1-aminocyclopropane-1-carboxylic acid N-malonyltransferase from tomato fruit. *Plant Physiol.* 108, 1241–1249. doi: 10.1104/pp.108.3.1241

Muday, G. K., Rahman, A., and Binder, B. M. (2012). Auxin and ethylene: collaborators or competitors? *Trends Plant Sci.* 17, 181–195. doi: 10.1016/j.tplants.2012.02.001

Oono, Y., Ooura, C., Rahman, A., Aspuria, E. T., Hayashi, K., Tanaka, A., et al. (2003). p-Chlorophenoxyisobutyric acid impairs auxin response in Arabidopsis root. *Plant Physiol.* 133, 1135–1147. doi: 10.1104/pp.103.027847

Peck, S. C., and Kende, H. (1995). Sequential induction of the ethylene biosynthesis enzymes by indole-3-acetic acid in etiolated peas. *Plant Mol. Biol.* 28, 293–301. doi: 10.1007/BF00020248

Peck, S. C., and Kende, H. (1998). Differential regulation of genes encoding 1-aminocyclopropane-carboxylate (ACC) synthase in etiolated pea seedlings: effects of indole-3-acetic acid, wounding, and ethylene. *Plant Mol. Biol.* 38, 977–982. doi: 10.1023/A:1006033030081

Pieck, M., Yuan, Y., Godfrey, J., Fisher, C., Zolj, S., Vaughan, D., et al. (2015). Auxin and tryptophan homeostasis are facilitated by the ISS1/VAS1 aromatic aminotransferase in Arabidopsis. *Genetics* 201, 185–199. doi: 10.1534/genetics.115.180356

Pierik, R., Tholen, D., Poorter, H., Visser, E. J., and Voesenek, L. A. (2006). The Janus face of ethylene: growth inhibition and stimulation. *Trends Plant Sci.* 11, 176–183. doi: 10.1016/j.tplants.2006.02.006

Pitts, R. J., Cernac, A., and Estelle, M. (1998). Auxin and ethylene promote root hair elongation in Arabidopsis. *Plant J.* 16, 553–560. doi: 10.1046/j.1365-313x.1998.00321.x

Polit, J. T., Praczyk, T., Pernak, J., Sobiech, L., Jakubiak, E., and Skrzypczak, G. (2014). Inhibition of germination and early growth of rape seed (*Brassica napus* L.) by MCPA in anionic and ester form. *Acta Physiol. Plant.* 36, 699–711. doi: 10.1007/s11738-013-1448-x

Prinsen, E., van Laer, S., Öden, S., and van Onckelen, H. (2000). "Auxin analysis," in *Methods in Molecular Biology: Plant Hormone Protocols,* eds G. A. Tucker and J. A. Roberts (Totowa, NJ: Humana Press), 49–65.

Rahman, A., Bannigan, A., Sulaman, W., Pechter, P., Blancaflor, E. B., and Baskin, T. I. (2007). Auxin, actin and growth of the *Arabidopsis thaliana* primary root. *Plant J.* 50, 514–528. doi: 10.1111/j.1365-313X.2007.03068.x

Rahman, A., Hosokawa, S., Oono, Y., Amakawa, T., Goto, N., and Tsurumi, S. (2002). Auxin and ethylene response interactions during Arabidopsis root hair development dissected by auxin influx modulators. *Plant Physiol.* 130, 1908–1917. doi: 10.1104/pp.010546

Reid, M. S., Paul, J. L., Farhoomand, M. B., Kofranek, A. M., and Staby, G. L. (1980). Pulse treatments with the silver thiosulfate complex extend the vase life of cut carnations. *J. Am. Soc. Hortic. Sci.* 105, 25–27.

Rozen, S., and Skaletsky, H. (2000). "Primer3 on the WWW for general users and for biologist programmers," in *Bioinformatics Methods and Protocols: Methods in Molecular Biology,* eds S. Krawetz and S. Misener (Totowa, NJ: Humana Press), 365–386.

Ruzicka, K., Ljung, K., Vanneste, S., Podhorská, R., Beeckman, T., Friml, J., et al. (2007). Ethylene regulates root growth through effects on auxin biosynthesis and transport-dependent auxin distribution. *Plant Cell* 19, 2197–2212. doi: 10.1105/tpc.107.052126

Stepanova, A. N., Yun, J., Likhacheva, A. V., and Alonso, J. M. (2007). Multilevel interactions between ethylene and auxin in Arabidopsis roots. *Plant Cell* 19, 2169–2185. doi: 10.1105/tpc.107.052068

Swarup, R., Perry, P., Hangenbeek, D., Van Der Straeten, D., Beemster, G. T., Sandberg, G., et al. (2007). Ethylene upregulates auxin biosynthesis in Arabidopsis seedlings to enhance inhibition of root cell elongation. *Plant Cell* 19, 2186–2196. doi: 10.1105/tpc.107.052100

Tanimoto, M., Roberts, K., and Dolan, L. (1995). Ethylene is a positive regulator of root hair development in *Arabidopsis thaliana*. *Plant J.* 8, 943–948. doi: 10.1046/j.1365-313X.1995.8060943.x

Tsuchisaka, A., and Theologis, A. (2004). Unique and overlapping expression patterns among the Arabidopsis 1-aminocyclopropane-1-carboxylate synthase gene family members. *Plant Physiol.* 136, 2982–3000. doi: 10.1104/pp.104.049999

Van de Poel, B., Smet, D., and Van Der Straeten, D. (2015). Ethylene and hormonal crosstalk in vegetative growth and development. *Plant Physiol.* 169, 61–72. doi: 10.1104/pp.15.00724

Van de Poel, B., and Van Der Straeten, D. (2014). 1-Aminocyclopropane-1-carboxylic acid (ACC) in plants: more than just the precursor of ethylene! *Front. Plant Sci.* 5:640. doi: 10.3389/fpls.2014.00640

Yang, S. F., and Hoffman, N. E. (1984). Ethylene biosynthesis and its regulation higher plants. *Annu. Rev. Plant Physiol.* 35, 155–189. doi: 10.1146/annurev.pp.35.060184.001103

Zheng, Z., Guo, Y., Novak, O., Dai, Z., Zhao, Y., Ljung, K., et al. (2013). Coordination of auxin and ethylene biosynthesis by the aminotransferase VAS1. *Nat. Chem. Biol.* 9, 244–246. doi: 10.1038/nchembio.1178

Conflict of Interest Statement: The authors declare that the research was conducted in the absence of any commercial or financial relationships that could be construed as a potential conflict of interest.

frontiers in Physiology

ORIGINAL RESEARCH
published: 10 March 2017
doi: 10.3389/fphys.2017.00142

Nitric Oxide Has a Concentration-Dependent Effect on the Cell Cycle Acting *via* EIN2 in *Arabidopsis thaliana* Cultured Cells

Galina V. Novikova[1], Luis A. J. Mur[2], Alexander V. Nosov[1], Artem A. Fomenkov[1], Kirill S. Mironov[1], Anna S. Mamaeva[1], Evgeny S. Shilov[3], Victor Y. Rakitin[1] and Michael A. Hall[2]*

[1] *Laboratory of Intracellular Regulation, K.A. Timiryazev Institute of Plant Physiology, Russian Academy of Sciences, Moscow, Russia,* [2] *Molecular Plant Pathology Group, Institute of Biological, Environmental and Rural Sciences, Aberystwyth University, Aberystwyth, UK,* [3] *Department of Immunology, M.V. Lomonosov Moscow State University, Moscow, Russia*

OPEN ACCESS

Edited by:
M. Iqbal R. Khan, International Rice Research Institute, Philippines

Reviewed by:
Weibiao Liao, Gansu Agricultural University, China
Yi Wang, Institute for Horticultural Plants, College of Horticulture, China Agricultural University, China
Palakolanu Sudhakar Reddy, International Crops Research Institute for the Semi-Arid Tropics (ICRISAT), India

***Correspondence:**
Galina V. Novikova
gv.novikova@mail.ru

Specialty section:
This article was submitted to Plant Physiology, a section of the journal Frontiers in Physiology

Received: *14 November 2016*
Accepted: *23 February 2017*
Published: *10 March 2017*

Citation:
Novikova GV, Mur LAJ, Nosov AV, Fomenkov AA, Mironov KS, Mamaeva AS, Shilov ES, Rakitin VY and Hall MA (2017) Nitric Oxide Has a Concentration-Dependent Effect on the Cell Cycle Acting via EIN2 in Arabidopsis thaliana Cultured Cells. Front. Physiol. 8:142. doi: 10.3389/fphys.2017.00142

Ethylene is known to influence the cell cycle (CC) via poorly characterized roles whilst nitric oxide (NO) has well-established roles in the animal CC but analogous role(s) have not been reported for plants. As NO and ethylene signaling events often interact we examined their role in CC in cultured cells derived from *Arabidopsis thaliana* wild-type (Col-0) plants and from ethylene-insensitive mutant *ein2-1* plants. Both NO and ethylene were produced mainly during the first 5 days of the sub-cultivation period corresponding to the period of active cell division. However, in *ein2-1* cells, ethylene generation was significantly reduced while NO levels were increased. With application of a range of concentrations of the NO donor, sodium nitroprusside (SNP) (between 20 and 500 μM) ethylene production was significantly diminished in Col-0 but unchanged in *ein2-1* cells. Flow cytometry assays showed that in Col-0 cells treatments with 5 and 10 μM SNP concentrations led to an increase in S-phase cell number indicating the stimulation of G1/S transition. However, at ≥20 μM SNP CC progression was restrained at G1/S transition. In the mutant *ein2-1* strain, the index of S-phase cells was not altered at 5–10 μM SNP but decreased dramatically at higher SNP concentrations. Concomitantly, 5 μM SNP induced transcription of genes encoding *CDKA;1* and *CYCD3;1* in Col-0 cells whereas transcription of *CDK*s and *CYC*s were not significantly altered in *ein2-1* cells at any SNP concentrations examined. Hence, it is appears that EIN2 is required for full responses at each SNP concentration. In *ein2-1* cells, greater amounts of NO, reactive oxygen species, and the tyrosine-nitrating peroxynitrite radical were detected, possibly indicating NO-dependent post-translational protein modifications which could stop CC. Thus, we suggest that in *Arabidopsis* cultured cells NO affects CC progression as a concentration-dependent modulator with a dependency on EIN2 for both ethylene production and a NO/ethylene regulatory function.

Keywords: *Arabidopsis thaliana*, cell culture, cell cycle, cell proliferation, ethylene, nitric oxide

INTRODUCTION

The cell cycle (CC) is one of the most conserved processes operating in eukaryotic cells and its integrity is essential for an organism's shape and function. The CC has been extensively described in both plants (Dewitte and Murray, 2003) and animals (Norbury and Nurse, 1992) and is regulated by the sequential expression of cyclin-dependent kinases (CDK) which are activated by binding to the cyclins (CYC) (Dorée and Galas, 1994). However, newly emerging CC regulatory steps, especially in plants, require further definition. In particular, ethylene can positively or negatively affect CC progression but these steps have been poorly defined. For example, Love et al. (2009) used both the transgenic ethylene-insensitive and ethylene-overproducing hybrid aspen (*Populus tremula* × *tremuloides*) and treatment with an ethylene perception inhibitor 1-methylcyclopropene (1-MCP) to demonstrate that ethylene stimulates cell division in the cambial meristem. Similarly, Ortega-Martínez et al. (2007) suggested that ethylene production and ethylene-modulated cell division was suppressed in the quiescent center of *Arabidopsis thaliana* roots. On the other hand, CC arrest in parallel with an increase in 1-aminocyclopropane-1-carboxylate (ACC) levels and the activation of ethylene signaling in *A. thaliana* leaves was observed during osmotic stress (Skirycz et al., 2011).

Another unknown in the plant CC is the role of nitric oxide (NO). There is a considerable literature describing the biological role(s) of NO in plants such as seed dormancy, growth, and development, senescence, respiration, photosynthesis, programmed cell death, antioxidant defense system (for review, Hayat et al., 2009) with the most detailed information available for NO effects during biotic stress (for reviews, Delledonne et al., 1998; Astier and Lindermayr, 2012; Mur et al., 2013) but the potential role of NO in regulating plant CC remains to be defined. This is the case although many studies in mammalian cells have demonstrated the importance of NO to CC progression (Takagi et al., 1994; Tanner et al., 2000; Cui et al., 2005; Kumar et al., 2010).

Preliminary evidence is suggestive of a role for NO in influencing plant CC. Ötvös et al. (2005) studied NO effects on protoplasts derived from alfalfa leaves and showed that low concentrations of chemical NO-donors stimulated incorporation of 5-bromo-2′-deoxyuridine (BrdU), i.e., initiated DNA synthesis. However, higher NO-donor concentrations blocked DNA synthesis. Based on these results it was first speculated that NO at low concentrations positively affected G1/S transition. Similar, concentration-dependent effects for NO, were also suggested by Bai et al. (2012) based on an *Arabidopsis* apical root meristem model using the NO-donor, sodium nitroprusside (SNP) (2–50 μM). SNP inhibited the main root growth at concentrations higher than 20 μM and its effect was accompanied by a decrease in the size of the root apical meristem, reduced number of cells expressing mitotic cyclin B1;1 (*CYCB1;1*) and the appearance of cells with damaged DNA. No concentrations of SNP reduced the number of 2C DNA nuclei further indicating that SNP blocked G1/S transition. Considering endogenously produced NO, application of the NO scavenger 2-(4-carboxyphenyl)-4, 4, 5, 5-tetramethylimidazoline-1-oxyl-3-oxide (cPTIO) or the use of the *atnoa1* mutant (with lower NO production), resulted in reduced *CYCD3;1* expression following the application of *trans*-zeatin (Shen et al., 2013). There was also an increase in the number of nuclei with 4 and 8C DNA in *atnoa1* compared to wild-type *Arabidopsis* which lead the authors to suggest that NO inhibits endoreduplication and stimulates G1/S transition. In line with this, Zhu et al. (2016) demonstrated NO-induced accumulation of cells in the S-phase during adventitious root formation in cucumber due to up-regulation of the genes involved in G1/S transition, *CYCA*, *CYCB*, *CDKA*, and *CDKB*. Other studies suggested that NO can act at G0 phase. Addition of cPTIO blocked the derivation of tomato lateral root primordia from the pericycle while applying SNP restored this process by increasing the expression of *CYCD3;1* and reducing the expression of *KRP2*—a negative regulator of the CC (Correa-Aragunde et al., 2006).

In our previous studies on biotic stress, we have demonstrated that NO can stimulate ethylene production in tobacco and *Arabidopsis* (Mur et al., 2008, 2012). This is also the case with somatic embryogenesis where increasing NO production through suppressing the expression of NO oxidizing Glb1 (hemoglobin class 1) also increased the generation of ethylene (Mira et al., 2015). However, with fruit ripening (Manjunatha et al., 2012), abscission of plant organs (Para-Lobato and Gomez-Jimenes, 2011), and the regulation of leaf senescence (Mishina et al., 2007) NO counteracts ethylene production. Niu and Guo (2012) used both *Atnoa1* and the *ethylene insensitive 2 (ein2-1)* mutants to suggest that NO regulates dark-induced leaf senescence through EIN2. Endoplasmic reticulum (ER)-localized EIN2 (Bisson et al., 2009) is a positive regulator in ethylene signaling in *Arabidopsis* and *ein2* mutants plants are insensitive to almost all aspects of ethylene responses (Alonso et al., 1999). According to the canonical ethylene signaling pathway, in the absence of ethylene, the ethylene receptors at ER interact with CONSTITUTIVE TRIPLE RESPONSE 1 (CTR1) protein kinase, which represses EIN2 followed by ETHYLENE INSENSITIVE 3 (EIN3) and EIN-LIKE 1 (EIL1). These latter are two transcription factors that control the majority of ethylene responses (Chang et al., 2013). Without ethylene, EIN3 and EIL1 are degraded through the action of F-box proteins EIN3-BINDING F-BOX 1 (EBF1) and EBF 2 (Guo and Ecker, 2003), whereas ethylene decreases the reduction of EBF1/2 protein levels in an EIN2-dependent manner. Thus, EIN3/EIL1 are stabilized and activate ethylene responses (An et al., 2010). EIN3/EIL1 also directly regulate the expression of a diverse array of genes including *ERF1* (*ETHYLENE RESPONSE FACTOR 1*) (Chang et al., 2013).

In this current study we sought not only to define NO and ethylene-mediated effects on the plant CC but possible interactions between these signals. We chose to exploit cultured *Arabidopsis* cells as this would avoid problems associated with intact plants where CC progression may be masked by the presence of diverse intercellular interactions and complex developmental programs. Thus, we studied NO effects on the CC of cultured wild-type (Col-0) and *ein2-1 Arabidopsis* cells. Here we demonstrate that NO acts as a concentration-dependent modulator of CC progression with a dependency on EIN2

for both of ethylene production and a NO/ethylene regulatory functions.

MATERIALS AND METHODS

Derivation of Suspension Cell Cultures

Suspension cell cultures of *Arabidopsis thaliana* (L.) Heynh. wild type (Col-0) and the ethylene-insensitive mutant *ein2-1* were generated by A.V. Nosov and A.A. Fomenkov and deposited at the All-Russia Collection of Cultivated Cells of Higher Plants as NFC-0 (for Col-0) and NFCE-2 (for *ein2-1*). Both cell strains were cultured in 50 mL of Schenk and Hildebrandt medium (Schenk and Hildebrandt, 1972) supplemented with 3% sucrose, 1 mg L^{-1} 2,4-D (Sigma, St. Louis, Missouri, USA) and 0.1 mg L^{-1} kinetin (Sigma). Cells were grown under constant agitation (110 rpm) at 26°C and 70% humidity. The time of sub-culture was 10 days and inoculated volumes were 1 mL for Col-0 and 2.5 mL for *ein2-1*. To confirm that the *ein2-1* mutation is retained in the cultured cells allele-specific PCR was performed periodically as described by Stepanchenko et al. (2012).

Treatments with Sodium Nitroprusside (SNP)

Cells were treated with freshly prepared solutions of the NO-donor sodium nitroprusside (SNP, Sigma), which were added to the culture medium at concentrations ranging from 2 to 10,000 μM. Cells were incubated with the NO-donor in the light (140 μM m^{-2} s^{-1}) on an orbital shaker (110 rpm) at 26°C. The incubation time was chosen based on the kinetics of SNP decomposition in the solution (Floryszak-Wieczorek et al., 2006). In all experiments, "NO-exhausted" SNP solutions (generated by allowing NO release in the light for 48 h prior to use) were used as a control treatment. To demonstrate that SNP effects were specific to NO, cultured cells were treated with 100 μM of the NO scavenger cPTIO prior SNP application. All experiments were performed on the fourth day after inoculation of cells into fresh medium when Col-0 and *ein2-1* cells were dividing actively.

Determination of NO, $ONOO^-$, and ROS Production in Col-0 and *ein2-1* cells

NO production was assessed in 1 mL of cell suspensions with 5 μM DAF-FM DA (4-amino-5-methylamino-2′, 7′-difluorofluorescein diacetate), peroxynitrite ($ONOO^-$)—with 5 μM APF (aminophenyl fluorescein), superoxide with 10 μM DHE (dihydroethidium), intracellular ROS (ROS_{in})—with 1 μM DCFH-DA (dichlorodihydrofluorescein diacetate). All dyes were purchased from Sigma.

Cells were incubated with the corresponding fluorescent dye for 15 min in the dark and then 200 μL aliquots of cells were transferred to 96-well flat bottom plates (Greiner Bio One, Germany). Plates were scanned in Typhoon Trio$^+$ Imager (GE Healthcare, Boston, Massachusetts, USA) at λ_{ex} 480 nm and λ_{em} BP 520 nm/40 nm for DAF-FM DA, DCFH-DA, and APF, and λ_{ex} 480 nm and λ_{em} BP 580 nm/30 nm for DHE.

NO levels during the sub-cultivation period were expressed as arbitrary units (AU) per 1 g of cell dry weight (DW). Values for $ONOO^-$, superoxide and ROS_{in} production calculated as fluorescence units per 1 μg of protein measured with a BCA Protein Assay Kit (Sigma).

Dye fluorescence was also imaged using an Axio Imager Z2 microscope (Carl Zeiss, Oberkochen, Germany) with a digital camera AxioCam MR, and the appropriate filter units were used. DAF-FM DA was detected at λ_{ex} BP 475 nm/40 nm; λ_{em} BP 530 nm/50 nm. For continuous monitoring of DAF-FM DA fluorescence, module ApoTome (Carl Zeiss) was used. The images were processed using the program AxioVision 4.8 (Carl Zeiss).

All fluorescence experiments were performed with at least three independent sets of Col-0 and *ein2-1* cells. Data presented are means of three independent experiments with five replicates ± SE (standard errors).

Measurement of Ethylene and O_2 Levels in Col-0 and *ein2-1* Cells

Ethylene and O_2 levels in cultured cells were measured as described by Rakitin and Rakitin (1986). Briefly, 3–5 mL of cell suspensions in 15 mL glass vials were mounted on an orbital shaker (110 rpm) and kept at 26°C for 10 min in the dark, then vials were sealed with Suba Seals (Sigma) and kept at the same conditions for 0.5–1 h. The vials with fresh SH medium only were used as a blank reference. Prior to measurement, ethylene was concentrated in a Porapak N column (80–100 mesh, 70 × 4 mm, Supelko, purchased from Sigma) at −30°C. After desorption at 50°C, ethylene was measured with a gas chromatograph fitted with a Poropak N column (80–100 mesh, 3 m × 2 mm, Supelko). Ethylene production was calculated as nL per hour per 1 g DW. O_2 content was estimated by gas absorption chromatography.

Determination of the Viability of SNP-Treated Col-0 and *ein2-1* Cells

Cell viability was assessed after 24 h treatment of Col-0 and *ein2-1* cells with SNP at concentrations from 100 to 10,000 μM. Cells were stained with a 0.02% aqueous solution of Erythrosin B (Sigma) and counted using a Univar microscope (Reichert-Jung, Austria). Viability was calculated as percentage of the number of cells unstained with Erythrosin B from their total number.

Isolation of Protoplasts from Col-0 and *ein2-1* Cultured Cells

Protoplasts from both strains of cultured cells were isolated at 26°C on an orbital shaker (120 rpm) within 1.0–1.5 h, as described earlier (Nosov et al., 2014). Aliquots (5 mL) of Col-0 and *ein2-1* cell suspensions were mixed with equal volumes of solution with major inorganic components of SH medium containing 0.8 M sorbitol, 8 mM $CaCl_2$, 25 mM MES at pH 5.7, 2% cellulase Onozuka R10 (Kinki Yakult, Tokyo, Japan), 0.3% pectinase Macerozyme R10 (Kinki Yakult), and 0.8% hemicellulase Driselase (Fluka, Seelze, Germany). After 1.0–1.5 h incubation, the suspensions were filtered through nylon mesh (40 μm pore size) and washed twice with 2.5 mM $CaCl_2$ in 0.5 M sorbitol. For cell number counting, the protoplast suspensions in the enzyme solution were used without additional filtration and washing. For flow cytometry analysis and microscopy, 1.5 mL of

protoplast suspension was added drop-wise into 3.5 mL of cold (4°C) methanol. Protoplasts were fixed in methanol and stored at 4°C before use.

Determination of S-Phase Cells by Flow Cytometry

Cells in S-phase of the CC were determined by incorporation of 5-ethynyl-2′-deoxyuridine (EdU) into DNA. EdU (Invitrogen, Carlsbad, California, USA) was added to a final concentration of 20 μM. After 1-h incubation with EdU its incorporation into DNA was terminated by the addition of 200 μM 2′-deoxythymidine (Sigma) for 5 min then the protoplasts were isolated as described above.

Methanol-fixed protoplasts were washed twice in 0.5 M sorbitol without $CaCl_2$, once in phosphate-buffered saline (PBS, Sigma) with 0.1% Triton X-100 (Sigma), and once in PBS without Triton X-100. EdU incorporation into newly-synthesized DNA was detected by reaction with Alexa Fluor 488 using Click-iT EdU Alexa Fluor 488 HCS Kit (Invitrogen), while DNA was stained with 100 ng mL^{-1} DAPI (4′, 6-diamidino-2-phenylindol, Sigma). On average, 100,000 protoplasts were analyzed with a Gallios flow cytometer (Beckman Coulter, Brea, California, USA). Alexa Fluor 488 fluorescence was detected in channel FL1 (λ_{ex} 488 nm, λ_{em} 505–545 nm), whereas channel FL9 (λ_{ex} 405 nm, λ_{em} 430–470 nm) was adopted for reading DAPI fluorescence. Data analysis was performed using FlowJo 7.6.2 (http://www.flowjo.com). This method has been typically applied to isolated nuclei (Kotogány et al., 2010) but our earlier assessments demonstrated that isolated cell protoplasts are also suitable for two-parameter flow cytometry (Nosov et al., 2014).

RNA Isolation and Quantitative RT-PCR (qRT-PCR) Analysis

Total RNA was isolated from 100 mg of cells using a Spectrum Plant Total RNA Kit (Sigma) according to the manufacturer's manual. Synthesis of cDNA was performed using 500 ng of total RNA with $Oligo(dT)_{20}$ primer (Invitrogen) and SuperScript III First-Strand Synthesis System following manufacturer's instructions (Invitrogen).

Amplification mixture (in a total reaction volume of 25 μl) contained 5 ng template cDNA, 5 × qPCRmix-HS SYBR (5 μl) (Evrogen, Moscow, Russian Federation) and 200 nM forward and reverse primers. All the primers used for qRT-PCR are listed in the **Table 1**. Reactions were run on CFX96 Touch (Bio-Rad, Hercules, California, USA) under the following cycling conditions: 95°C for 3 min, 45 cycles at 95°C for 10 s and 63°C for 30 s followed by melting curve analysis.

The Cq value was calculated from three independent biological experiments, each with four PCR replicates. At*ACT2* (At3g18780.2) and At*UBQ10* (At4g05320.2) were used as reference genes for data normalization as described by Pfaffl (2001) and Vandesompele et al. (2002).

TABLE 1 | Sequences of oligonucleotide primers used for qRT-PCR analysis.

Gene name	Gene ID	Forward or reverse primer (5′–3′) (F or R)	Fragment size, bp
AtCDKA;1	At3g48750.1	(F) ACTGACACTACATCCGATCG	140
		(R) GTGCCTTATAAACCACACCG	
AtCDKB2;1	At1g76540.1	(F) CTGGCAAGAACATTCCAACC	142
		(R) AGCCTCATTGTCTTGGGATC	
AtCYCA2;3	At1g15570.1	(F) AAGAGCCACTGGACCCAAC	136
		(R) ACTCGCCAATCCATGACCG	
AtCYCB1;1	At4g37490.1	(F) CCCAAAGAACAACGAACCGG	138
		(R) CCAGCCACTTTCTTCGGCT	
AtCYCD3;1	At4g34160.1	(F) CCTCCCATCAGTAGTTGCC	164
		(R) TGCGGTCCACTGGTAGTTG	
AtACT2	At3g18780.2	(F) CTCCTTGTACGCCAGTGGTC	111
		(R) CGGAGGATGGCATGAGGAAG	
AtUBQ10	At4g05320.2	(F) CCGTGATCAAGATGCAGATC	120
		(R) GAATGCCCTCCTTATCCTGG	

Statistical Analyses

Data were subjected to analysis of variance using Minitab v.14 (Minitab Ltd, Coventry, UK), after which residual plots were inspected to confirm that data conformed to normality. Comparisons of data points from different treatments with controls were performed using Tukey multiple pairwise comparison test. Differences with $P < 0.05$ were considered significant.

RESULTS

Ethylene and NO Production during the Cell Suspension Sub-Cultivation Cycle

Using actively growing *Arabidopsis* Col-0 and *ein2-1* suspension cells (**Figure S1**), we studied the roles of ethylene and NO in CC progression. Initial experiments focused on observing the patterns of ethylene and NO generation over the sub-cultivation period. Measurements of ethylene using gas chromatography indicated that maximum ethylene production occurred over the first 5 days following sub-cultivation in both Col-0 (**Figure 1A**) and *ein2-1* (**Figure 1B**) cell lines although in the latter case levels were very low. To ensure that the observed patterns of ethylene production did not reflect hypoxic culture conditions, which would affect ACC oxidase (ACO) enzyme activity, O_2 content was measured. Gas absorption chromatography of Col-0 and *ein2-1* cells in Suba Seal closed vials indicated that O_2 levels did not drop lower than 20% which would allow ACO function and ethylene production.

NO production was evaluated within the same sub-cultivation cycle by measuring fluorescence from the NO-specific DAF-FM DA dye. Fluorescence was localized mainly in the cytoplasm and was most pronounced around the nuclei [**Figure S2 (video)**]. In Col-0 cells, maximum NO production occurred over the first 2–4 days following sub-cultivation (**Figure 1A**), while in *ein2-1* cell suspensions NO production was much higher compared to Col-0 over the same period (**Figure 1B**).

In Col-0 and *ein2-1* cells, ethylene and NO production over the cell sub-cultivation period were compared with cell division. Although both genotypes exhibited similarly shaped

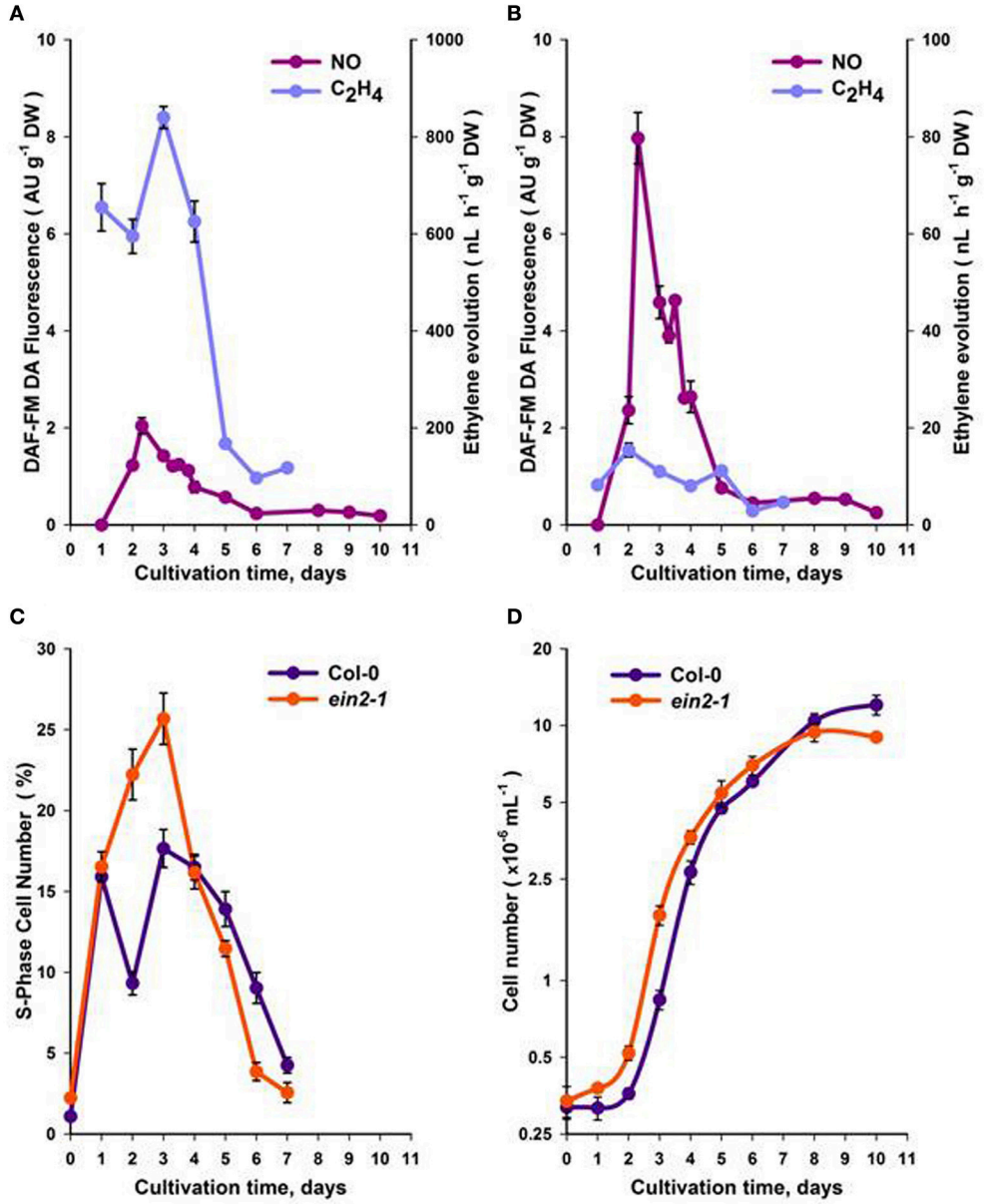

FIGURE 1 | Production of NO and ethylene within a sub-cultivation period of Col-0 (A) and *ein2-1* **(B)** cultures. The portion of S-phase cells **(C)** and the total cell number **(D)**. On **(D)**, the ordinate axis is represented in a log scale. All values (means ± SE) are the averages of three independent biological experiments with five analytical replicates.

curves (**Figures 1C,D**), within 3–4 days of culturing Col-0 cells displayed fewer S-phase cells compared to *ein2-1* but after the 5th day rather more S-phase cells were observed (**Figure 1C**). This correlated with initially reduced levels of Col-0 cells (to 6 days) but with more cells at 10 days in comparison to *ein2-1* cells (**Figure 1D**).

Assessing the Effects of NO on Suspension Cell Cultures

To assess the effects of NO, cells were treated with the NO-donor, SNP at the day 4 following sub-cultivation, which corresponded to some deceleration of the logarithmic growth phase (**Figure 1D**) when both Col-0 and *ein2-1* cultures retained similar numbers of S-phase cells (**Figure 1C**).

Addition of increasing concentrations of SNP to Col-0 and *ein2-1* cells resulted in corresponding increases in NO production as reported by DAF-FM DA fluorescence (**Figure 2A**). The specificity of the fluorescence signal was established by its reduction when SNP was co-applied with 100 μM of the NO scavenger, cPTIO (**Figure 2A**). NO has also been linked to the initiation of cell death (Mur et al., 2008) but neither culture exhibited any significant loss in

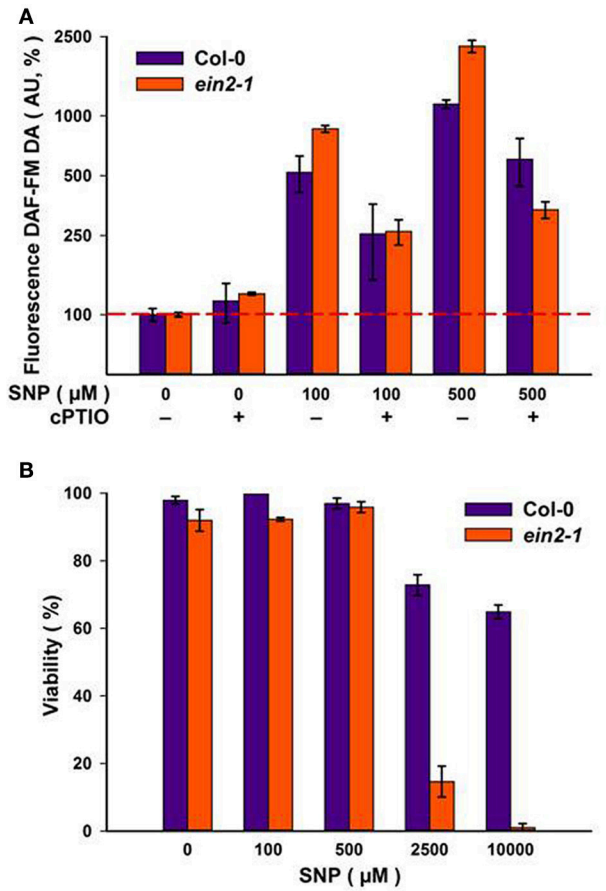

FIGURE 2 | Levels of NO as detected by DAF-FM DA fluorescence at the day four of sub-cultivation of Col-0 and *ein2-1* cells after 3-h treatment with sodium nitroprusside (SNP). The specificity of the fluorescent signal is demonstrated by parallel treatments with 100 μM of the NO scavenger cPTIO **(A)**. Cell viability was detected using Erythrosin B **(B)**. On **(A)**, the ordinate axis is represented on a log scale. Values are expressed as mean ± SE of biological triplicates with five analytical replicates.

viability at SNP concentrations up to 500 μM (**Figure 2B**). Col-0 cells retained 60–70% viability at even higher SNP concentrations, whereas *ein2-1* cells exhibited considerable levels of cell death (**Figure 2B**). These results defined the range of SNP concentrations used in the further experiments.

To assess the impact of SNP on S-phase cells, flow cytometry after incorporation of the thymidine analog, EdU into DNA was used. Both suspension cultures were treated with either exhausted SNP or freshly prepared SNP solutions at concentrations of 5, 10, 20, 100, and 500 μM for 6 h at day 4 of sub-cultivation. EdU was added 1 h before the end of incubation with SNP and detected in the Click-iT reaction with the azide of Alexa Fluor 488.

In Col-0 cultures, a 6-h treatment with SNP at 5 and 10 μM led to an increase in the number of S-phase cells from 13.6% in untreated cells to 16.6 and 21.5% in SNP-treated cells, respectively (**Figures 3A,B**). When the concentration of the SNP was increased to 20, 100, and 500 μM, the proportion of S-phase cells decreased significantly to 10.1, 9.1, and 7.6, respectively. This decrease was not linked to any effect on cell viability (**Figure 2B**).

In *ein2-1* cells, low SNP concentrations (5 and 10 μM) did not seriously affect the number of S-phase cells as compared to untreated cells (**Figures 3C,D**), however, when *ein2-1* cells were treated with higher concentrations of SNP (20, 100, and 500 μM), a dramatic fall in the number of S-phase cells was observed (**Figures 3C,D**).

The assessment of SNP effects on ethylene production in cultured cells of both genotypes revealed that it was repressed in Col-0 cells at all concentrations tested but was mostly unchanged in *ein2-1* cells (**Table 2**). Additionally, the *ein2-1* cultured cells showed a higher production of reactive oxygen and nitrogen species compared to Col-0 cells (**Table 3**).

NO and EIN2 Effects on the Expression of Cyclin-Dependent Kinases and Cyclins

To define the molecular events underlying the impact of NO on the transition of CC checkpoints, we examined the effect of SNP on the expression of genes for some *CDK*s and C*YC*s (**Figure 4**). Addition of 5 μM SNP to Col-0 cultures induce significant increases ($P < 0.001$) with *CDKA;1* (**Figure 4A**) and *CYCD3;1* (**Figure 4E**) that were ≥ two fold compared to controls. With *CDKB2;1, CYCA2;3,* and *CYCB1;1* there were significant increases with 5 μM SNP but were < two fold compared to untreated controls (**Figures 4B,C,D**). In the Col-0 cultures, addition of SNP at 100 and 500 μM SNP reduced the proportion of S-phase cells (**Figures 3A,B**) and this was accompanied by the significant ($P < 0.01$) reduction in the expression of *CYCA2;3*, *CYCD3;1, CDKA;1, CDKB2;1* (**Figure 4**), whereas the transcription of mitotic cyclin *CYCB1;1* was significantly reduced only at 500 μM SNP (**Figure 4D**). There were no significant changes in *CDKs* and *CYC*s gene expression compared to untreated controls with *ein2-1* at any SNP concentration with exception in *CYCD3;1* at 500 μM SNP (**Figure 4E**). **Figure 4** also compares the response of Col-0 and *ein2-1* to SNP and highlight (with the exception of *CYCD3;1*) the abolition of a significant change in analyzed genes expression in *ein2-1* at > 10 μM SNP.

DISCUSSION

In animal cells, the role of NO in perturbing G1/S transitions of CC has been extensively characterized (Cui et al., 2005; Kumar et al., 2010; Napoli et al., 2013). We here demonstrate similar effects of NO on *Arabidopsis* cultured cells in a NO concentration dependent manner. Crucially, we have used the *ein2-1* mutant to demonstrate a key interaction with ethylene in this regulatory mechanism.

NO and Ethylene Signaling Events Influence CC Progression

Any consideration of the roles of NO and ethylene in the CC must be based on measurements of when these signals are produced. To provide a focus on ethylene effects our experimental strategy was based on comparing NO effects on Col-0 and *ein2-1* suspension cultures. Thus, we observed

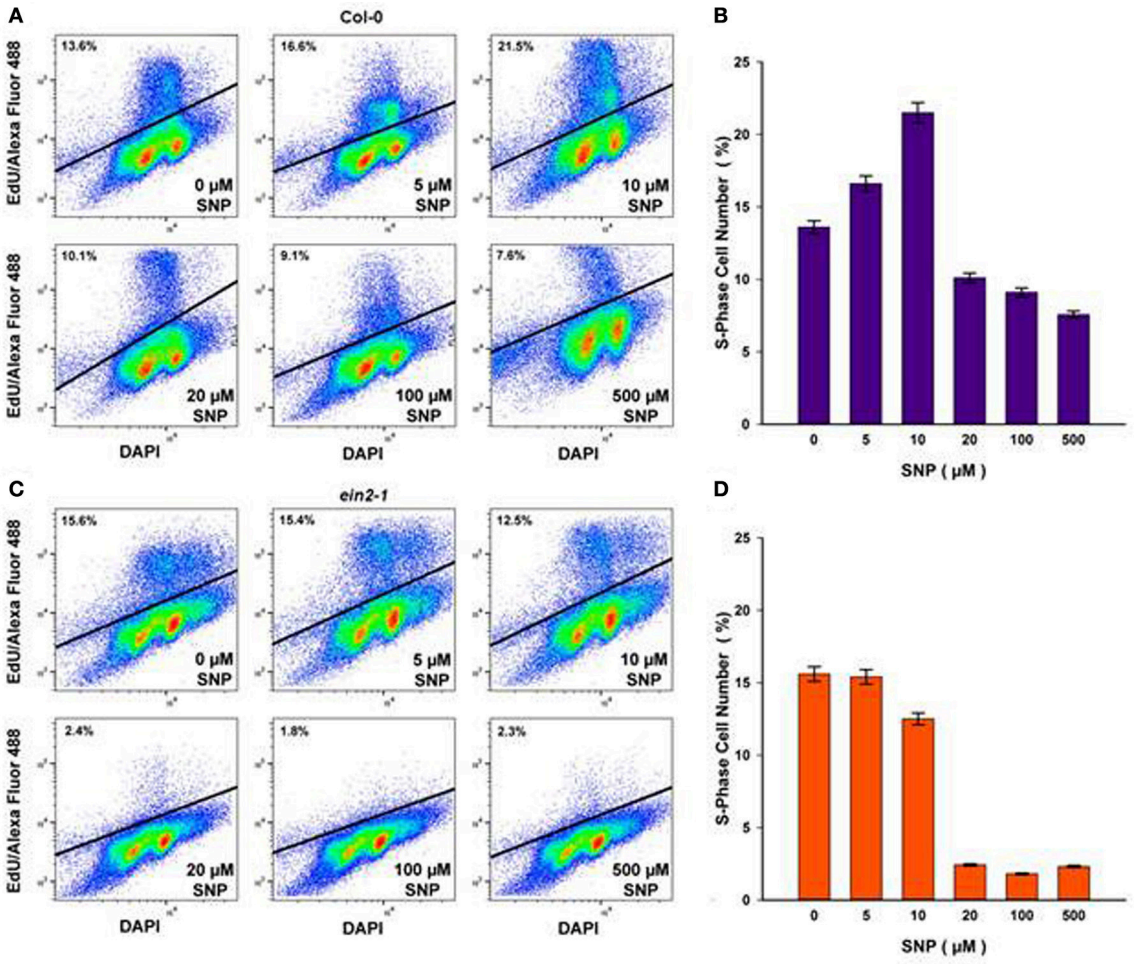

FIGURE 3 | S-phase cells (%) in Col-0 (A,B) and *ein2-1* **(C,D)** after 6-h treatment with SNP as detected by flow cytometry after incorporation of 5-ethynyl-2′-deoxyuridine (EdU) into DNA and the Click-iT reaction with azide of Alexa Fluor 488. Representative bivariate plots of DNA content (based on DAPI fluorescence) and EdU incorporation (based on Alexa fluor) are shown in **(A)** and **(C)**. Above the solid line is a cluster of protoplasts having tag EdU–Alexa Fluor 488 (S-phase cells). Values in **(B)** and **(D)** are means ± SE of three independent biological experiments.

that NO and ethylene were maximally produced during an overlapping period of sub-cultivation. Crucially, the effect of SNP on Col-0 cells suggested that NO could repress rather than initiate ethylene production in Col-0 cells (**Table 2**). This was in contrast to the hypersensitive response during plant-pathogen interactions, where NO was required for ethylene production (Mur et al., 2008). However, the effect of SNP was consistent with the observed NO-dependent post-translational modification of methionine adenosyltransferase 1 (MAT1) to lower enzyme activity thereby decreasing ethylene synthesis (Lindermayr et al., 2006). Further levels of subtlety in this interaction are revealed by examination of responses in the *ein2-1* cultures. These data suggested that when ethylene production was suppressed that of NO was augmented (**Figure 1**). This implicates EIN2 as a regulatory switch influencing the CC patterns of both NO and ethylene production. Nonetheless, even in the absence of functionally active EIN2 (the case of *ein2-1* cells) the CC appeared to operate normally (**Figures 1C,D**). This could suggest that NO and ethylene production during the CC was irrelevant to the latter's control. However, some impacts on S-phase number and total cell number (**Figures 1C,D**) were noted. Thus, the relative rates of NO and ethylene production in both Col-0 and *ein2-1* cells suggest that these may be essential for the proper progression through the CC. Further, as a recent study showed that *Arabidopsis* ERFs, including ERF1 were required for the increase in cambial cell division (Etchells et al., 2012), it is appropriate to note our data relating to *ERF1* expression (**Figure S3**). In cultured *ein2-1* cells, where the ethylene signal transduction pathway is thought to be abolished (Alonso et al., 1999), we observed a high expression level of *ERF1*, which is a specific indicator of early ethylene signaling (Lorenzo et al., 2003). Taking into account that cultured *ein2-1* cells do not demonstrate reductions in cell number (**Figure 1D**) differences in *ERF1* expression could be the result of reduced ethylene signaling. This could suggest that in the absence of functionally active EIN2 alternative ethylene signaling pathway(s), which is

likely to require a low level of ethylene, can operate (Cho and Yoo, 2015).

Ethylene and NO Act at the G1/S Checkpoint in the CC

Typically, synchronized cells are used to study CC regulation, and aphidicolin is the most common chemical employed for culture synchronization. However, aphidicolin affects DNA polymerases and thus DNA replication blocked CC at the G1/S-phase boundary. This situation can be released by washing with fresh media in order to permit cells to move into the succeeding phase of the CC, but we have also shown a sharp increase in ethylene production within an hour after inoculation of cells into the fresh medium (Fomenkov et al., 2015). Therefore, the use of aphidicolin could complicates any dissection of ethylene effects on the CC. To avoid these problems as well as to minimize the mechanical manipulations with cells prior SNP treatments we used asynchronous Col-0 and *ein2-1* cultures in order to dissect the roles of ethylene, NO and EIN2 on cell proliferation.

TABLE 2 | Sodium nitroprusside (SNP) effect on ethylene evolution by Col-0 and *ein2-1* cultured cells.

SNP, μM	Ethylene evolution, nL g^{-1} FW h^{-1}	
	Col-0	*ein2-1*
0	54.6 ± 0.3	0.65 ± 0.2
20	46.3 ± 1.6	0.65 ± 0.07
100	28.7 ± 0.3	0.84 ± 0.14
500	25.8 ± 2.1	0.85 ± 0.22

TABLE 3 | Reactive oxygen (ROS) and nitrogen species (RNS) production in *Arabidopsis* cultured cells of wild type (Col-0) and the ethylene-insensitive mutant *ein2-1*.

ROS/RNS	Col-0	*ein2-1*
Superoxide	121.0 ± 13.4	189.3 ± 16.6
Peroxynitrite	125.3 ± 8.8	295.5 ± 16.1
ROS_{in}	127.7 ± 5.7	382.5 ± 9.2

At day 3 of cultivation, Col-0 and ein2-1 cells were sampled and ROS/NOS levels were estimated by measurement of fluorescence intensity with corresponding dyes. Superoxide was detected with dihydroethidium (DHE), peroxynitrite—with aminophenyl fluorescein (APF), intracellular ROS (ROS_{in})—with dichlorodihydrofluorescein diacetate (DCFH-DA). Values calculated as fluorescence units/1 μg of protein are means of three independent experiments with five replicates ± SD (standard deviations).

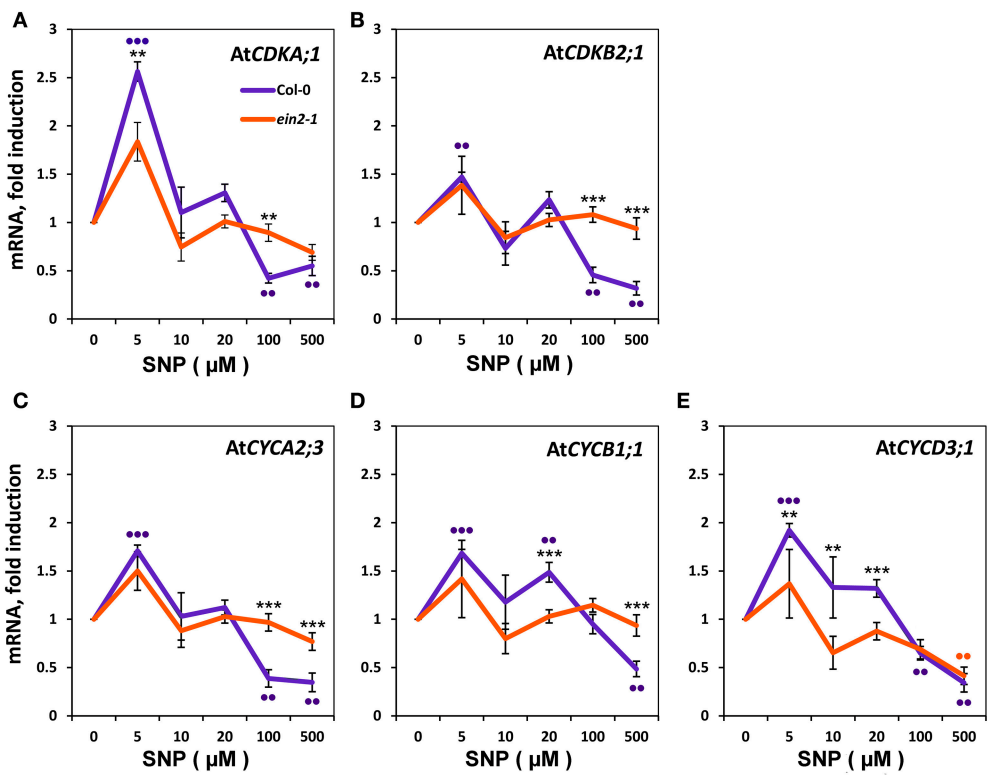

FIGURE 4 | Expression of Cyclins (*CYC*) and Cyclin-Dependent Kinases (*CDK*) in Col-0 and *ein2-1* cells after 6-h treatment with SNP. mRNA levels in cultured Col-0 and *ein2-1* cells were examined by qRT-PCR for *CDKA;1* **(A)**, *CDKB2;1* **(B)**, *CYCA2;3***(C)**, *CYCB1;1* **(D)**, and *CYCD3;1* **(E)**. For qRT-PCR analysis, At*ACT2* and At*UBQ10* were used as the reference genes. Bars indicate standard errors of four technical replicates on biological triplicates. Asterisks indicate significant changes between Col-0 and *ein2-1* at a given SNP concentration. *** $P \leq 0.001$; ** $P \leq 0.01$. Dots indicate significant changes between untreated and SNP-treated Col-0 and *ein2-1* cells. ••• $P \leq 0.001$; •• $P \leq 0.01$.

The influence of NO on S-phase cells was estimated by flow cytometry. In Col-0, rather complex NO effects on S-phase were revealed. Low (5 and 10 μM) concentrations of SNP caused S-phase progression (**Figures 3A,B**), while high concentrations (20, 100, and 500 μM) caused a decrease in the proportion of S-phase cells. This was consistent with the results obtained on animal cells, where low NO concentrations (pM-nM) seemed to favor cell proliferation (Thomas et al., 2008). This may suggest a relative insensitivity to NO in our cultured plant cells (**Figures 3A,B**) but this was in agreement with those obtained for intact plants (Ötvös et al., 2005). Moreover, it should be kept in mind that SNP does not release all of its NO instantaneously (Mur et al., 2013) and the actual dose of NO obtained by cells from the surrounding medium could be lower than the concentration of SNP which had been used for treatments.

A halt in the CC progression could be associated with cell differentiation which can be preceded by endoreduplication (De Veylder et al., 2007). However, an increase in endoreduplication was not observed in either Col-0 or *ein2-1* cells after 6-h treatment with high NO concentrations (data not shown). Currently, it is unclear how far this finding reflected an effect of exogenous NO at the highly reduced level of endogenous ethylene (**Figure 1B**). It is worth noting that there is a report that high SNP concentrations contributed to endoreduplication in the *chlorophyll a/b binding protein under-expressed* (*cue1*) mutant, which produces more NO than wild type and, moreover, is NO supersensitive (Bai et al., 2012).

Our definition of the molecular events underlying NO/ethylene effect on the CC naturally focused on the expression pattern of *CYC*s and *CDK*s. CYCs of the D-type (CYCDs) are CDKA;1 partners which control the G1/S transition (Menges et al., 2006; de Jager et al., 2009). CYCA2;3 is a marker of G2/M transition, and CYCB1;1 is a mitotic CYC. CDKB1;1 operates with CYCA2;3 and CDKB2;1/CDKB2;2—with CYCB1;1 (Menges et al., 2005; Inzé and De Veylder, 2006; Van Leene et al., 2010; Komaki and Sugimoto, 2012). Referring to the results presented, we suggest that in Col-0 cells NO application at low concentrations positively influences CC progression at G1/S transition (**Figures 3A,B**) at least due to stimulation of *CDKA;1* and *CYCD3;1* expression (**Figures 4A,E**). It should be noted, that expression of *CYCA2;3*, *CYCB1;1,* and *CDKB2;1* operating at G2/M transition and in M-phase of CC barely increased (**Figures 4C,D,B**), further suggesting that low concentrations of NO stimulated G1/S transition. At the same time, in *ein2-1* cells, low concentrations of SNP had little effect on both the S-phase index (**Figures 3C,D**) and expression of the genes associated with the CC (**Figure 4**) compared to Col-0.

Based on the above observations, it is possible to suggest a tentative model for NO/ethylene effects on the CC of *Arabidopsis* cultured cells (**Figure 5**). Under standard cultivation conditions, cells of Col-0 (with functional EIN2) and *ein2-1* (with "broken" EIN2) have opposite levels of ethylene and NO production but almost the same levels of proliferation which should be controlled by appropriate transcription/translation of CDKs and CYCs (**Figure 5A**). High levels of endogenous NO apparently inhibit ethylene production in *ein2-1* cells as exogenous NO does in Col-0 cells. Low level of endogenous ethylene in *ein2-1* cells likely provides the cell proliferation control bypassing EIN2. Treatment of Col-0 cells with low concentrations of NO (5 and 10 μM of SNP) on the background of low endogenous NO level stimulates cell transition into S-phase of CC due to increased expression of associated *CDKA;1* and *CYCD3;1* (**Figure 5B**). In *ein2-1* cells with high endogenous NO level, the low concentrations of NO supplied (5 and 10 μM of SNP) do not affect both the index of S-phase cells and expression of *CDKs* and *CYCs* tested. Under such circumstances CC progression remains unchanged (**Figure 5C**). In Col-0 cells, high levels of exogenous NO decrease the expression of *CDKA;1, CDKB2;1,* and *CYCA2;3, CYCB1;1, CYCD3;1* resulting in downregulation of CC progression (**Figure 5D**). Finally, the treatments of *ein2-1* cells with high concentrations of NO on the background of the high endogenous NO level have no significant effect on the

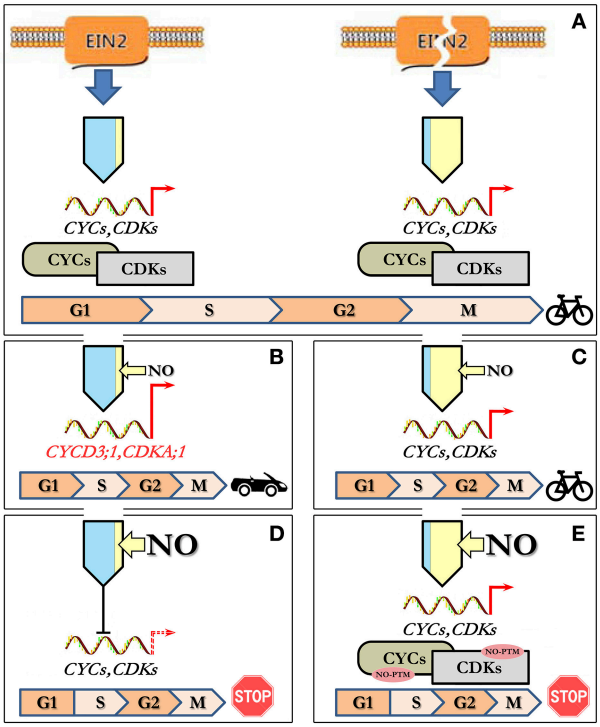

FIGURE 5 | Model describing concentration-dependent NO–ethylene interactions influencing CC progression. (A) Under standard growth conditions, cultured Col-0 and *ein2-1* cells have opposite levels of ethylene (blue) and NO (yellow) production with a similar proliferation activity controlled by appropriate regulation of CDKs and CYCs. **(B)** Treatment of Col-0 cells with low NO concentrations (narrow yellow arrow) results in stimulation of G1-to-S phase transition due to increased expression of *CDKA;1* and *CYCD3;1*. **(C)** In *ein2-1* cells with high endogenous NO, low concentrations of NO supplied do not affect either the index of S-phase cells or the expression of *CDKs* and *CYCs* leading to unchanged CC progression. **(D)** At high levels of exogenous NO (wide yellow arrow), in Col-0 cells, the expression of CC-related genes is reduced and concomitantly CC progression slows down. **(E)** Treatment of *ein2-1* cells with high NO concentrations on the background of the high endogenous NO level have no significant effect on the expression of CC-associated genes but a sharp reduce in the number of S-phase cells indicates a stop in G1/S transition most likely due to NO-dependent post-translational modifications (NO-PTM) of the CC-related proteins.

expression of the CC-associated genes but rapidly reduce the number of S-phase cells indicating that G1/S transition comes to a stop (**Figure 5E**). Thus, from the above appears that CDKA;1 is the main response to low (5 μM) SNP and EIN2 is required for full responses at each SNP concentration. Additionally or alternatively, the CC progression might be mediated by NO-dependent post-translational protein modifications including those involved in CC regulation (**Figure 5E**) since *ein2-1* cultured cells accumulate substantial amounts of both ROS and RNS (**Table 3**). Clearly, such a simple model requires further characterization but it does generate several hypotheses on which further studies can be based.

To our knowledge, this is the first report demonstrating EIN2-dependent NO-provoked CC regulation in cultured plant cells. The data presented here point to the similarity of NO effects on the CC progression in cells of whole plants and *in vitro* cultured plant cells and, moreover, show the similarity of these effects to those in animal cells. Perhaps, most importantly, the NO-dependent effects on the CC progression, which were revealed in our work, provide a possible link to the functioning of ethylene signaling pathway(s).

AUTHOR CONTRIBUTIONS

GN Designed and supervised most of the experiments and contributed to the writing of the paper; LM Contributed to the design of the experiments and the writing of the paper; AN Contributed to the design of the experiments and the writing of the paper. Contributed to the drawing up of the integrated model presented in **Figure 5**; AF provided technical support in maintaining the cell cultures and drawing up figures presented; KM undertook the qRT-PCR experiments; AM undertook all NO donor treatments and flow-cytometry based experiments; ES designed and supervised the flow-cytometry based experiments; VR undertook ethylene measurements; MH was involved in discussion on experimental design and contributed to the writing of the paper.

ACKNOWLEDGMENTS

This work is supported by grants from the Russian Science Foundation No. 14-24-00020 (for GN, KM, and AM), by a BBSRC Institute Strategic Programme Grant (BBS/E/W/10964A01A) (for LM), and the Russian Foundation for Basic Research No. 14-04-00333 (for AN), No. 16-34-00834 (for AF). The flow cytometry assays were performed with the equipment granted by Lomonosov Moscow State University Program of Development.

SUPPLEMENTARY MATERIAL

The Supplementary Material for this article can be found online at: http://journal.frontiersin.org/article/10.3389/fphys.2017.00142/full#supplementary-material

Figure S1 | Microphotographs of *Arabidopsis thaliana* cultured cells of wild type (Col-0) and ethylene-insensitive mutant *ein2-1*. Bar scales are 20 μm.

Figure S2 (video) | NO visualization within *Arabidopsis thaliana* (Col-0) cells represented as sequential series of the cell's optical sections stained with DAF-FM DA (Axio Imager Z2 with ApoTome.2 function).

Figure S3 | Expression of *ERF1* (At4g20550) in Col-0 and *ein2-1* cultured cells at day two of sub-cultivation as detected using RT-PCR. Primers used for amplification were (F) TTCAGTCCCCATTCTCCGGC, (R) GCCGTCGTCTTACGCCTCTG. The numbers under the bands indicate the expression of *ERF1* relative to At*UBQ10* expression used as the reference gene. Arrow indicates the fragment size (bp).

REFERENCES

Alonso, J. M., Hirayama, T., Roman, G., Nourizadeh, S., and Ecker, J. R. (1999). EIN2, a bifunctional transducer of ethylene and stress responses in *Arabidopsis*. *Science* 284, 2148–2152. doi: 10.1126/science.284.5423.2148

An, F., Zhao, Q., Ji, Y., Li, W., Jiang, Z., Yu, X., et al. (2010). Ethylene-induced stabilization of ETHYLENE INSENSITIVE3 and EIN3-LIKE1 is mediated by proteasomal degradation of EIN3 binding F-box 1 and 2 that requires EIN2 in *Arabidopsis*. *Plant Cell* 22, 2384–2401. doi: 10.1105/tpc.110.076588

Astier, J., and Lindermayr, C. (2012). Nitric oxide-dependent posttranslational modification in plants: an update. *Int. J. Mol. Sci.* 13, 15193–15208. doi: 10.3390/ijms131115193

Bai, S., Li, M., Yao, T., Wang, H., Zhang, Y., Xiao, L., et al. (2012). Nitric oxide restrain root growth by DNA damage induced cell cycle arrest in *Arabidopsis thaliana*. *Nitric Oxide* 26, 54–60. doi: 10.1016/j.niox.2011.12.001

Bisson, M. M., Bleckmann, A., Allekotte, S., and Groth, G. (2009). EIN2, the central regulator of ethylene signalling, is localized at the ER membrane where it interacts with the ethylene receptor ETR1. *Biochem. J.* 424, 1–6. doi: 10.1042/BJ20091102

Chang, K. N., Zhong, S., Weirauch, M. T., Hon, G., Pelizzola, M., Li, H., et al. (2013). Temporal transcriptional response to ethylene gas drives growth hormone cross-talk in *Arabidopsis*. *eLife.* 2:e00675. doi: 10.7554/eLife.00675

Cho, Y. H., and Yoo, S. D. (2015). Novel connections and gaps in ethylene signaling from the ER membrane to the nucleus. *Front. Plant Sci.* 5:773. doi: 10.3389/fpls.2014.00733

Correa-Aragunde, N., Graziano, M., Chevalier, C., and Lamattina, L. (2006). Nitric oxide modulates the expression of cell cycle regulatory genes during lateral root formation in tomato. *J. Exp. Bot.* 57, 581–588. doi: 10.1093/jxb/erj045

Cui, X., Zhang, J., Ma, P., Myers, D. E., Goldberg, I. G., Sittler, K. J., et al. (2005). cGMP-independent nitric oxide signaling and regulation of the cell cycle. *BMC Genomics.* 6:51. doi: 10.1186/1471-2164-6-151

de Jager, S. M., Scofield, S., Huntley, R. P., Robinson, A. S., den Boer, B. G., and Murray, J. A. (2009). Dissecting regulatory pathways of G1/S control in *Arabidopsis*: common and distinct targets of CYCD3; 1, E2Fa and E2Fc. *Plant Mol. Biol.* 71, 345–365. doi: 10.1007/s11103-009-9527-5

De Veylder, L., Beeckman, T., and Inzé, D. (2007). The ins and outs of the plant cell cycle. *Nat. Rev.* 8, 655–665. doi: 10.1038/nrm2227

Delledonne, M., Xia, Y., Dixon, R. A., and Lamb, C. (1998). Nitric oxide functions as a signal in plant disease resistance. *Nature* 394, 585–588. doi: 10.1038/29087

Dewitte, W., and Murray, J. A. (2003). The plant cell cycle. *Annu. Rev. Plant Biol.* 54, 235–264. doi: 10.1146/annurev.arplant.54.031902.134836

Dorée, M., and Galas, S. (1994). The cyclin-dependent protein kinases and the control of cell division. *FASEB J.* 8, 1114–1121.

Etchells, J. P., Provost, C. M., and Turner, S. R. (2012). Plant vascular cell division is maintained by an interaction between PXY and ethylene signalling. *PLoS Genet.* 8:e1002997. doi: 10.1371/journal.pgen.1002997

Floryszak-Wieczorek, J., Milczarek, G., Arasimowicz, M., and Ciszewski, A. (2006). Do nitric oxide donors mimic endogenous NO-related response in plants? *Planta* 224, 1363–1372. doi: 10.1007/s00425-006-0321-1

Fomenkov, A. A., Nosov, A. V., Rakitin, V. Y., Sukhanova, E. S., Mamaeva, A. S., Sobol'kova, G. I., et al. (2015). Ethylene in the proliferation of cultured plant

cells: regulating or just going along? *Rus. J. Plant Physiol.* 62, 815–822. doi: 10.1134/S1021443715060059

Guo, H., and Ecker, J. R. (2003). Plant responses to ethylene gas are mediated by $SCF^{EBF1/EBF2}$-dependent proteolysis of EIN3 transcription factor. *Cell* 115, 667–677. doi: 10.1016/S0092-8674(03)00969-3

Hayat, S., Hasan, S. A., Mori, M., Fariduddin, Q., and Ahmad, A. (2009). "Nitric Oxide: chemistry, biosynthesis, and physiological role," in *Nitric Oxide in Plant Physiology,* eds S. Hayat, M. Mori, J. Pichtel, and A. Ahmad (Germany: Wiley-VCH), 1–16.

Inzé, D., and De Veylder, L. (2006). Cell cycle regulation in plant development. *Annu. Rev. Genet.* 40, 77–105. doi: 10.1146/annurev.genet.40.110405.090431

Komaki, S., and Sugimoto, K. (2012). Control of the plant cell cycle by developmental and environmental cues. *Plant Cell Physiol.* 53, 953–964. doi: 10.1093/pcp/pcs070

Kotogány, E., Dudits, D., Horváth, G. V., and Ayaydin, F. (2010). A rapid and robust assay for detection of S-phase cell cycle progression in plant cells and tissues by using ethynyl deoxyuridine. *Plant Methods* 6:5. doi: 10.1186/1746-4811-6-5

Kumar, S., Barthwal, M. K., and Dikshit, M. (2010). Cdk2 nitrosylation and loss of mitochondrial potential mediate NO-dependent biphasic effect on HL-60 cell cycle. *Free Rad. Biol. Med.* 48, 851–861. doi: 10.1016/j.freeradbiomed.2010.01.004

Lindermayr, C., Saalbach, G., Bahnweg, G., and Durner, J. (2006). Differential inhibition of *Arabidopsis* methionine adenosyltransferases by protein *S*-nitrosylation. *J. Biol. Chem.* 281, 4285–4291. doi: 10.1074/jbc.M511635200

Lorenzo, O., Piqueras, R., Sánchez-Serrano, J. J., and Solano, R. (2003). ETHYLENE RESPONSE FACTOR1 integrates signals from ethylene and jasmonate pathways in plant defense. *Plant Cell* 15, 165–178. doi: 10.1105/tpc.007468

Love, J., Björklund, S., Vahala, J., Hertzberg, M., Kangasjärvi, J., and Sundberg, B. (2009). Ethylene is an endogenous stimulator of cell division in the cambial meristem of *Populus*. *Proc. Natl. Acad. Sci. U.S.A.* 106, 5984–5989. doi: 10.1073/pnas.0811660106

Manjunatha, G., Gupta, K. J., Lokesh, V., Mur, L. A. J., and Neelwarne, B. (2012). Nitric oxide counters ethylene effects on ripening fruits. *Plant Signal. Behav.* 7, 476–483. doi: 10.4161/psb.19523

Menges, M., de Jager, S. M., Gruissem, W., and Murray, J. A. H. (2005). Global analysis of the core cell cycle regulators of *Arabidopsis* identifies novel genes, reveals multiple and highly specific profiles of expression and provides a coherent model for plant cell cycle control. *Plant J.* 41, 546–566. doi: 10.1111/j.1365-313X.2004.02319.x

Menges, M., Samland, A. K., Planchais, S., and Murray, J. A. H. (2006). The D-type cyclin CYCD3;1 is limiting for the G1-to-S-phase transition in *Arabidopsis*. *Plant Cell* 18, 893–906. doi: 10.1105/tpc.105.039636

Mira, M., Adel, E.-S., and Stasolla, C. (2015). Ethylene is integrated into nitric oxide regulation of *Arabidopsis* somatic embryogenesis. *J. Genet. Eng. Biotechnol.* 13, 7–17. doi: 10.1016/j.jgeb.2015.01.001

Mishina, T. E., Lamb, C., and Zeier, J. (2007). Expression of a nitric oxide degrading enzyme induces a senescence programme in *Arabidopsis*. *Plant Cell Environ.* 30, 39–52. doi: 10.1111/j.1365-3040.2006.01604.x

Mur, L. A. J., Laarhoven, L. J. J., Harren, F. J. M., Hall, M. A., and Smith, A. R. (2008). Nitric oxide interacts with salicylate to regulate biphasic ethylene production during the hypersensitive response. *Plant Physiol.* 148, 1537–1546. doi: 10.1104/pp.108.124404

Mur, L. A. J., Mandon, J., Persijn, S., Cristescu, S. M., Moshkov, I. E., Novikova, G. V., et al. (2013). Nitric oxide in plants: an assessment of the current state of knowledge. *AoB Plants* 5:pls052. doi: 10.1093/aobpla/pls052

Mur, L. A. J., Sivakumaran, A., Mandon, J., Cristescu, S. M., Harren, F. J. M., and Hebelstrup, K. H. (2012). Haemoglobin modulates salicylate and jasmonate/ethylene-mediated resistance mechanisms against pathogens. *J. Exp. Bot.* 63, 4375–4387. doi: 10.1093/jxb/ers116

Napoli, C., Paolisso, G., Casamassimi, A., Al-Omran, M., Barbieri, M., Sommese, L., et al. (2013). Effects of nitric oxide on cell proliferation. *J. Am. Coll. Cardiol.* 62, 89–95. doi: 10.1016/j.jacc.2013.03.070

Niu, Y.-H., and Guo, F.-Q. (2012). Nitric oxide regulates dark-induced leaf senescence through EIN2 in *Arabidopsis*. *J. Integr. Plant Biol.* 54, 516–525. doi: 10.1111/j.1744-7909.2012.01140.x

Norbury, C., and Nurse, P. (1992). Animal cell cycle and their control. *Annu. Rev. Biochem.* 61, 441–470. doi: 10.1146/annurev.bi.61.070192.002301

Nosov, A. V., Fomenkov, A. A., Mamaeva, A. S., Solovchenko, A. E., and Novikova, G. V. (2014). Extra perspectives of 5-ethynyl-2'-deoxyuridine click reaction with fluorochrome azides to study cell cycle and deoxyribonucleoside metabolism. *Rus. J. Plant Physiol.* 61, 899–909. doi: 10.1134/S1021443714060144

Ortega-Martínez, O., Pernas, M., Carol, R. J., and Dolan, L. (2007). Ethylene modulates stem cell division in the *Arabidopsis thaliana* root. *Science* 317, 507–510. doi: 10.1126/science.1143409

Ötvös, K., Pasternak, T. P., Miskolczi, P., Domoki, M., Dorjgotov, D., Szücs, A., et al. (2005). Nitric oxide is required for, and promotes auxin-mediated activation of, cell division and embryogenic cell formation but does not influence cell cycle progression in alfalfa cell cultures. *Plant J.* 43, 849–860. doi: 10.1111/j.1365-313X.2005.02494.x

Para-Lobato, M. C., and Gomez-Jimenes, M. C. (2011). Polyamine-induced modulation of gene involved in ethylene biosynthesis and signaling pathways and nitric oxide production during olive mature fruit abscission. *J. Exp. Bot.* 62, 4447–4465. doi: 10.1093/jxb/err124

Pfaffl, M. W. (2001). A new mathematical model for relative quantification in real-time RT-PCR. *Nucleic Acid Res.* 29:e45. doi: 10.1093/nar/29.9.e45

Rakitin, V. Y., and Rakitin, L. Y. (1986). Determination of gas exchange and ethylene, carbon dioxide, and oxygen contents in plant tissues. *Sov. Plant Physiol.* 33, 403–413.

Schenk, R. U., and Hildebrandt, A. (1972). Medium and techniques for induction and growth of monocotyledonous and dicotyledonous plant cell cultures. *Can. J. Bot.* 50, 199–204. doi: 10.1139/b72-026

Shen, Q., Wang, Y., Tian, H., and Guo, F. (2013). Nitric oxide mediates cytokinin functions in cell proliferation and meristem maintenance in *Arabidopsis*. *Mol. Plant* 6, 1214–1225. doi: 10.1093/mp/sss148

Skirycz, A., Claeys, H., De Bodt, S., Oikawa, A., Shinoda, S., Andriankaja, M., et al. (2011). Pause-and-stop: the effects of osmotic stress on cell proliferation during early leaf development in *Arabidopsis* and a role for ethylene signaling in cell cycle arrest. *Plant Cell* 23, 1876–1888. doi: 10.1105/tpc.111.084160

Stepanchenko, N. S., Fomenkov, A. A., Moshkov, I. E., Rakitin, V. Y., Novikova, G. V., and Nosov, A. V. (2012). Phytohormone interplay controls proliferation of *in vitro* cultivated cells of *Arabidopsis thaliana* ethylene-insensitive mutants. *Doklady Biol. Sci.* 442, 46–49. doi: 10.1134/S0012496612010139

Takagi, K., Isobe, Y., Yasukawa, K., Okouchi, E., and Suketac, Y. (1994). Nitric oxide blocks the cell cycle of mouse macrophage-like cells in the early G2+M phase. *FEBS Lett.* 340, 159–162. doi: 10.1016/0014-5793(94)80128-2

Tanner, F. C., Meier, P., Greutert, H., Champion, C., Nabel, E. G., and Luscher, T. F. (2000). Nitric oxide modulates expression of cell cycle regulatory proteins: a cytostatic strategy for inhibition of human vascular smooth muscle cell proliferation. *Circulation* 101, 1982–1989. doi: 10.1161/01.CIR.101.16.1982

Thomas, D. D., Ridnour, L. A., Isenberg, J. S., Ridnour, A. L., Isenberg, J. S., Flores-Santana, W., et al. (2008). The chemical biology of nitric oxide: implications in cellular signaling. *Free Rad. Biol. Med.* 45, 18–31. doi: 10.1016/j.freeradbiomed.2008.03.020

Van Leene, J., Hollunder, J., Eeckhout, D., Persiau, G., Van De Slijke, E., Stals, H., et al. (2010). Targeted interactomics a complex core cell cycle machinery in *Arabidopsis thaliana*. *Mol. Syst. Biol.* 6, 397. doi: 10.1038/msb.2010.53

Vandesompele, J., De Preter, K., Pattyn, F., Poppe, B., Van Roy, N., De Paepe, A., et al. (2002). Accurate normalization of real-time quantitative RT-PCR data by geometric averaging of multiple internal control genes. *Genome Biol.* 3:0034.1–0034.11. doi: 10.1186/gb-2002-3-7-research0034

Zhu, Y., Liao, W., Niu, L., Wang, M., and Ma, Z. (2016). Nitric oxide is involved in hydrogen gas-induced cell cycle activation during adventitious root formation in cucumber. *BMC Plant Biol.* 16:146. doi: 10.1186/s12870-016-0834-0

Conflict of Interest Statement: The authors declare that the research was conducted in the absence of any commercial or financial relationships that could be construed as a potential conflict of interest.

frontiers in Plant Science

ORIGINAL RESEARCH
published: 23 May 2017
doi: 10.3389/fpls.2017.00855

Short Term Effect of Salt Shock on Ethylene and Polyamines Depends on Plant Salt Sensitivity

*Pedro J. Zapata[1], María Serrano[2], Manuel F. García-Legaz[3], M. T. Pretel[2] and M. A. Botella[2]**

[1] Departamento de Tecnología Agroalimentaria, Universidad Miguel Hernández, Orihuela, Spain, [2] Departamento de Biología Aplicada, Universidad Miguel Hernández, Orihuela, Spain, [3] Departamento de Agroquímica y Medioambiente, Universidad Miguel Hernández, Orihuela, Spain

In the present manuscript the short term effect (3–24 h) of a saline shock (NaCl 100 mM) on fresh weight, water content, respiration rate, ethylene production and Na^+, Cl^-, ACC and polyamine concentration was studied in four plant species with different salt sensitivity, pepper, lettuce, spinach, and beetroot. Higher reduction in fresh weight and water content as a consequence of saline shock was found in pepper and lettuce plants than in spinach and beetroot, the latter behaving as more salinity tolerant. In general, salinity led to rapid increases in respiration rate, ethylene production and ACC and polyamine (putrescine, spermidine, and spermine) concentrations in shoot and root. These increases were related to plant salinity sensitivity, since they were higher in the most sensitive species and *vice versa*. However, ethylene and respiration rates in salt stressed plants recovered similar values to controls after 24 h of treatment in salt tolerant plants, while still remaining high in the most sensitive. On the other hand, sudden increases in putrescine, spermidine, and spermine concentration were higher and occurred earlier in pepper and lettuce, the most sensitive species, than in spinach and beetroot, the less sensitive ones. These increases tended to disappear after 24 h, except in lettuce. These changes would support the conclusion that ethylene and polyamine increases could be considered as a plant response to saline shock and related to the plant species sensitivity to this stress. In addition, no competition between polyamines and ethylene biosynthesis for their common precursor was observed.

Keywords: ethylene, ACC, respiration, polyamines, salinity, salinity tolerance

OPEN ACCESS

Edited by:
Péter Poór,
University of Szeged, Hungary

Reviewed by:
Ky Young Park,
Sunchon National University, South Korea
Magda Pál,
Hungarian Academy of Sciences Centre for Agricultural Research Agricultural Institute, Hungary

****Correspondence:***
M. A. Botella
mangeles.botella@umh.es

Specialty section:
This article was submitted to Plant Physiology, a section of the journal Frontiers in Plant Science

Received: *15 November 2016*
Accepted: *08 May 2017*
Published: *23 May 2017*

Citation:
Zapata PJ, Serrano M, García-Legaz MF, Pretel MT and Botella MA (2017) Short Term Effect of Salt Shock on Ethylene and Polyamines Depends on Plant Salt Sensitivity. Front. Plant Sci. 8:855. doi: 10.3389/fpls.2017.00855

INTRODUCTION

Salinity in soils is harmful to most plants and limits crop production. Understanding the mechanisms of plant salt tolerance and adaptation is important for developing new approaches to enhance stress tolerance (Liu et al., 2015). Salt stress affects plants, leading to changes at different levels, morphological, physiological, biochemical, and molecular, and including increases in ethylene biosynthesis and in the concentration of its precursor 1-aminocyclopropane-1-carboxylic acid (ACC). Thus, in some halophyte species under high salinity, ethylene production, and ACC concentration increased in leaves and roots (Ellouzi et al., 2014). In tolerant soybean genotypes these increments were higher than in salt sensitive ones (Ma et al., 2012). In addition, the application of ethylene or ACC enhanced Arabidopsis plant tolerance to salt stress throughout

increases in the expression of genes involved in scavenging reactive oxygen species (ROS) (Peng et al., 2014), while inhibition of ethylene biosynthesis leads to increased plant sensitivity to salinity (Tao et al., 2015). These studies, as well as others related to gene mutation and transformation analysis, indicated that plant tolerance to salinity could be enhanced by the ethylene biosynthesis and signal transduction pathway (Tao et al., 2015). Accordingly, previous experiments by our group found an increase in ethylene biosynthesis induced by salinity in several cultivars of lettuce during the germination phase, although cultivars showing the most salt sensitivity (highest decrease in fresh weight) showed the lowest increase in ethylene production and *vice versa* (Zapata et al., 2003). These results suggest that the ability to increase the ethylene production under saline conditions could provide a higher tolerance to salinity during lettuce germination.

However, when comparing germination percentage and seedling growth of different plant species (lettuce, pepper, broccoli, beetroot, melon, spinach, and tomato) under saline conditions a general effect of salinity on ethylene metabolism during germination could not been found (Zapata et al., 2004). In a different approach, when saline treatment (NaCl 100 mM) was applied to plants progressively (to avoid osmotic shock) and with long term exposition to salt stress total ACC concentration increased in pepper tomato, broccoli, lettuce, melon, bean, spinach and beetroot, this increase being higher in the species most sensitive to salinity. The plant species most sensitive to saline treatment was pepper, with the highest reduction in fresh weight and the highest increase in total ACC concentration occurring. On the other hand, the least affected by salinity was beetroot which did not present changes in total ACC concentration following salt treatment (Zapata et al., 2007). These discrepancies on ethylene responses to saline treatment during germination and more developed plants could be attributed to changes on salt sensitivity during plant development. Interestingly, broccoli was found to be more saline tolerant than pepper, melon and lettuce, but it was more affected by salinity than the other plant species during the germination phase (Zapata et al., 2004).

The biosynthesis pathway of polyamines is related with that of ethylene biosynthesis. *S*-adenosylmethionine (SAM) can be used to form ACC, the precursor of ethylene and in the conversion of putrescine (Put) into spermidine (Spd) and of Spd into spermine (Spm) by two reactions catalyzed by Spd-synthase and Spm synthase respectively. Different abiotic stresses, such as low and high temperatures, drought, high salinity, and nutrient deficiency have been widely shown to produce changes in polyamine levels in a number of plant species (Liu et al., 2007; Kusano et al., 2008; Alcázar et al., 2010; Minocha et al., 2014; Tiburcio et al., 2014). In this sense, it has been proposed that polyamines have a role in plant adaptive responses to various environmental stresses since the expression of the genes involved in their biosynthesis as well as their concentration increase under stress abiotic conditions and exogenous application of Put, Spd, or Spm enhances tolerance to these stresses (Pillai and Akiyama, 2004; Duan et al., 2008; Wang B. Q. et al., 2011; Wang J. et al., 2011; Liu et al., 2015). The increase in polyamine levels under saline conditions can be considered an important adaptive mechanism as polyamines may modulate the activity of plasma membrane ion channels, reducing the uptake of Na^+ and the leakage of K^+ from mesophyll cells, therefore polyamines assist plants in their adaptation to salinity (Shabala et al., 2007). In addition, in forest trees polyamines have been considered as a possible biochemical marker for persistent environmental stress when phenotypic symptoms of stress are not yet visible (Jouve et al., 2004; Minocha et al., 2014). However, in rice salt sensitive cultivars showed higher contents of Put under control conditions, while under long term salinity Put levels decreased. These changes were correlated to salt sensitivity (Do et al., 2014).

Although polyamine accumulation is considered as a general plant response to abiotic stresses, the cause-effect relationship between PA accumulation and protection still remains unclear (Minocha et al., 2014). In fact, different results on polyamine accumulation have been obtained depending on plant species, physiological status of the examined tissues/organs, experimental conditions, short or long exposition to stress, or if the stress arises suddenly or slowly (Zapata et al., 2008; Minocha et al., 2014; Liu et al., 2015). For instance, the effect of polyamines on both K^+ and H^+ transport activities in the plasma membrane in maize and Arabidopsis roots was found to be specific to species, tissues, and growth conditions (Pandolfi et al., 2010).

The objective of this research was to study, by using the whole plant, the short term effect (hours) of a saline shock on ethylene biosynthesis and polyamine accumulation in four different plant species with different salt sensitivity, in order to find if immediate changes in ethylene or polyamines are related to plant salinity tolerance.

MATERIALS AND METHODS

Experiments were made with four plant species: pepper (*Capsicum annuum* L. cv. Pairal), lettuce (*Lactuca sativa* var. Longifolia Lam. cv. Inverna), spinach (*Spinacia oleracea* L. cv. Boeing) and beetroot [*Beta vulgaris* L. var. Crassa (Alef.) J. Helm. cv. Detroit]. The different seeds were provided by the following companies: spinach by Seminis Vegetable Seeds Iberica S.A. (Cartagena, Spain); lettuce by Battle S.A. (Madrid, Spain); pepper by Semillas Fitó (Barcelona, Spain); beetroot by Intersemillas (Valencia, Spain).

Seeds were sterilized by dipping in 5% sodium hypochlorite for 5 min. Afterward they were washed thoroughly with distilled water and germinated in vermiculite moistened with 0.5 mM Ca_2SO_4 in a germination chamber, adding distilled water when necessary. Seeds were under dark conditions in the germination chamber and at the optimum temperature for each plant species, that is 20°C for spinach, lettuce, and beetroot and 25°C for pepper. The seedlings were transferred to a growth chamber when cotyledons had fully emerged, after 3 days in lettuce and 4 days in spinach, pepper, and beetroot and were maintained in optimum conditions depending on plant species: 20/16°C for spinach, lettuce, and beetroot, and 28/22°C for pepper, a 16/8 h light/dark cycle, a relative humidity of 60% (day) and 80% (night) and with a photon flux density of 450 μmol m^{-2} s^{-1}. After

10 days the seedlings were transplanted to 13-L pots with half strength Hoagland nutrient solution. The pH was adjusted daily to 5.5–6.0 and the solutions were renewed every 3 days. Two treatments were applied, a control (NaCl 1 mM) and a saline (NaCl 100 mM), the later suddenly applied when plants were 11 days with nutrient solution, in order to induce a saline shock.

After 0, 3, 6, 12, and 24 h of saline shock application nine random plants per replicate per treatment were taken, but at 12 h of the control no plants were taken. Plants of each of the four replicates were separated into root and shoot and were used to determine fresh weight, respiration rate and ethylene production. Later, the nine plants of each replicate were divided into groups of three plants, one of them being used for water content and Na^+ and Cl^- quantifications and the remainder frozen and ground in liquid N_2, with one of these used to quantify free and total ACC concentration and the other for polyamines quantification.

Analytical Determinations

Fresh weight, dry weight, and water content were recorded in shoot and root of each individual plant from the four replicates. Results were expressed as g per plant and were the mean ± SE of four replicates for each plant species and treatment.

Ethylene production and respiration rates were determined by placing the shoots or roots of each replicate, corresponding to nine plants, in a glass jar of appropriated volume hermetically sealed with a rubber stopper. One mL of holder atmosphere was extracted after 1 h which was injected into Hewlett Packard 5890 Series II gas chromatograph, equipped with a flame ionization detector, and a 3-m stainless steel column with an inner diameter of 3.5 mm containing activated alumina of 80/100 mesh to quantify ethylene production. Column temperature was 90°C and injector and detector temperature 150°C. Ethylene was expressed in nanoliters evolved per gram of tissue per hour (nL g^{-1} h^{-1}) and results are the mean ± SE of triplicate measurements in each of the four replicates for each plant species and treatment. Another mL of the same atmosphere was used to determine respiration rate, monitoring the CO_2 concentration in a Shimadzu 14-A gas chromatograph with catarometric detector. Column temperature was 50°C. Respiration rate was expressed as μg of CO_2 evolved per gram of tissue per hour (μg g^{-1} h^{-1}) and results are the mean ± SE of triplicate measurements in each of the four replicates for each plant species and treatment.

Total ACC (free and conjugated) was extracted as previously described (Zapata et al., 2004). Shoot or root tissue from each sample was ground in a mortar with a pestle by using

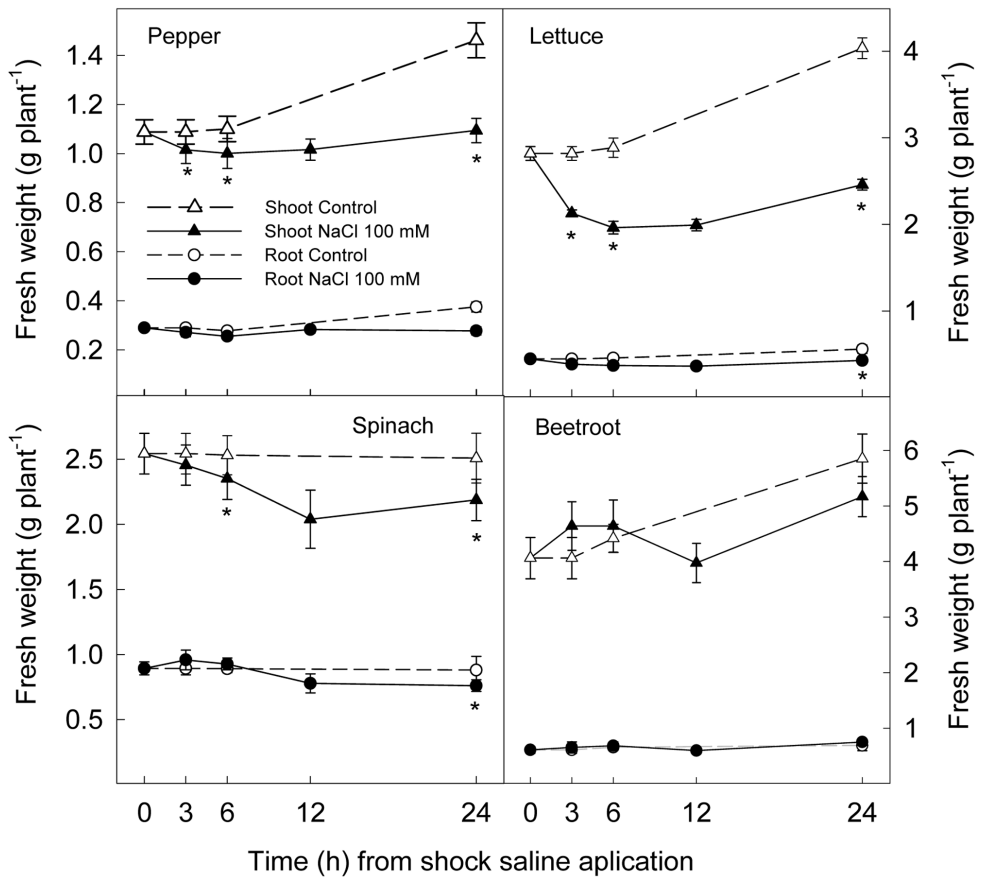

FIGURE 1 | Effect of saline shock (100 mM NaCl) on shoot and root fresh weight of different plant species. Data are the mean ± SE of four replicates of nine plants. *Shows significant differences between control and saline treatment for each sampling date.

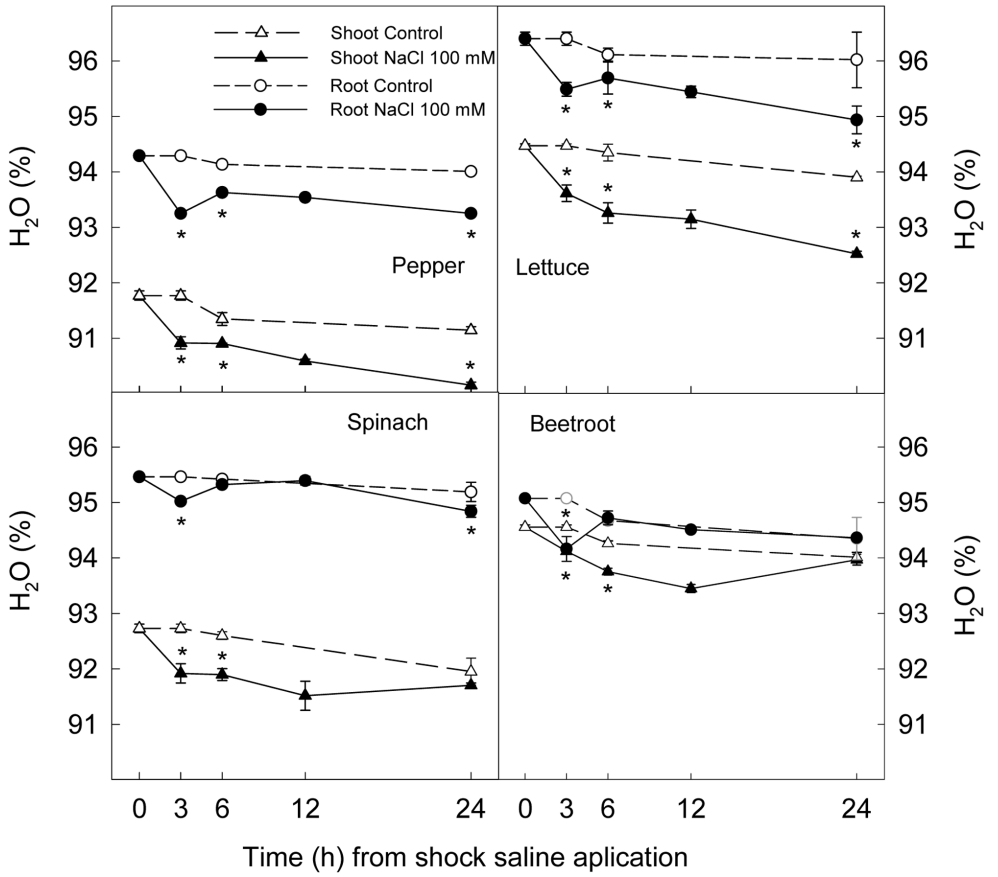

FIGURE 2 | Effect of saline shock (100 mM NaCl) on shoot and root water content of different plant species. Data are the mean ± SE of four replicates of three plants. *Shows significant differences between control and saline treatment for each sampling date.

0.2 M trichloroacetic acid (1:3 w/v) and the homogenate was centrifuged at 7000 *g* for 10 min. The supernatant was used to determine its free-ACC content by chemical conversion of ACC to ethylene in a reaction medium containing 100 μL of 10 mM $ClHg_2$, 100 μL of saturated NaOH, 0.5 mL of 5% NaOCl and 0.5 mL of extract. Five mL of the same extract were mixed with 1 mL of 2 N HCl, at 100°C for 1 h in order to hydrolyse conjugated ACC. Then total AAC was measured as described above and conjugated ACC quantified as total ACC minus free ACC. In both cases, measurements were made in triplicate and a calibration curve of ACC from Sigma (Poole, Dorset, England) was used as standard. Results were expressed as nmol per gram of fresh weight (nmol g^{-1} FW) and are the mean ± SE of triplicate measurements in each of the four replicates for each plant species and treatment.

Plant material was dried at 65°C for 4 days and dry weight determined. Dried matter from root and shoot was ground and sieved to 0.5 mm diameter and dried material was digested with HNO_3:$HClO_4$ (2:1, v:v). Na^+ was quantified by atomic absorption spectrometry by using a Perking Elmer spectrophotometer (mod. ICP-5000). Cl^- was extracted from dry material with HNO_3 0.1 N and glacial acetic acid (10%) and keeping in mechanical agitation for 2 h. Samples were quantified in duplicate by titration using an automatic titrater 702 SM Titrino model.

Free polyamines were extracted by homogenizing 1 g of shoot or root samples in 10 ml of 5% perchloric acid using a mortar and pestle. After that the homogenate was centrifuged for 30 min at 20000 *g*. Free polyamines in the supernatant were quantified after benzoilation by using a HPLC (Hewlett-Packard Company, Wilmington, DE, USA) system equipped with a reversed-phase column (LiChroCart 250–4.5 μm) and absorbance detector at 254 nm. The elution system was MeOH/H_2O (64:36) running isocratically with a flow rate of 0.8 mL min^{-1} (Zapata et al., 2003). A relative calibration procedure using 1,6-hexanediamine (100 nmol g^{-1} FW of tissue) as an internal standard, and standard curves of Put, Spd, and Spm from Sigma (Poole, Dorset, England) was used to determine the polyamines in samples. The results are expressed as nmols per gram of fresh weight (nmol g^{-1} FW) and are the mean ± SE of quantifications performed in duplicate in each of the four replicates per treatment.

Statistics

All data were statistically analyzed by ANOVA and a Student's *t*-test was performed for shoots and roots in each species to find

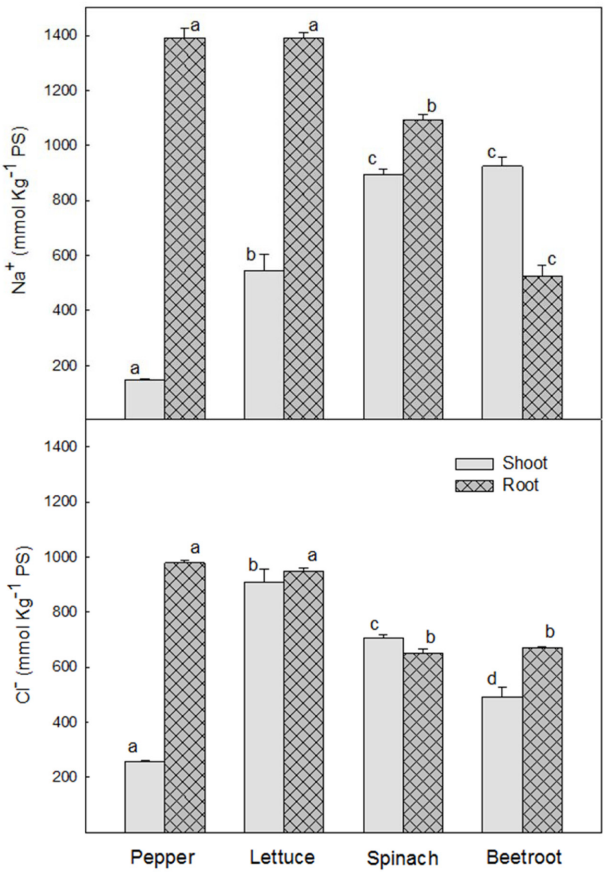

FIGURE 3 | Sodium and chloride concentration, in shoot and root of the different plant species, after 24 h of saline shock application. Data are the mean ± SE of determinations made independently in four replicates of three plants. Different letters represent significant differences among plant species at $p < 0.05$.

out significant differences between control and saline treatments at $p < 0.05$.

RESULTS

Plant Growth and Water Content

The application of a saline shock (NaCl 100 mM) decreased shoot and root fresh weight, although with significant differences among plant species. Thus, 24 h after NaCl application shoot fresh weight was reduced by 39 and 25% in lettuce and pepper respectively, while no significant reduction was found in spinach or beetroot (**Figure 1**). Root fresh weight after 24 h was reduced ≈25% in lettuce and pepper and ≈15% in spinach, while in beetroot no significant effect of saline application in root fresh weight was found (**Figure 1**). Water content was reduced by 1% in shoots and roots after 3 h of stress in all studied plant species, indicating a lower water uptake. However, after 6 h, a recovery was observed in root of beetroot and spinach, and at 24 h in the shoot of these plants. Contrarily, in pepper and lettuce plants water content was still lower in treated plants than in the control at the end of the experiments (**Figure 2**). These results show that pepper and lettuce behaved as more sensitive to saline shock, and spinach and beetroot as more tolerant.

Concentration of Na^+ and Cl^-

Levels of Na^+ and Cl^- were very low under control conditions. Thus, only data from saline treatments are presented. After 24 h of saline treatment Na^+ concentration was significantly higher in the roots of the most sensitive species, pepper and lettuce (1392 ± 35 and 1391 ± 19 mmol Kg^{-1} DW, respectively) than in the most tolerant ones, spinach and beetroot (1092 ± 19 and 526 ± 40 mmol Kg^{-1} DW, respectively), while in shoots Na^+ concentration was higher in the latter (894 ± 20 and 924 ± 35 mmol Kg^{-1} DW in spinach and beetroot, respectively), and very low in pepper (**Figure 3**).

Cl^- concentration in roots was also higher in the most sensitive species (≈950 mmol Kg^{-1} DW) than in the most tolerant (≈560 mmol Kg^{-1} DW). However, in shoots the two most sensitive species, pepper and lettuce, behaved in a different way, the highest Cl^- concentration being found in lettuce (≈1000 mmol Kg^{-1} DW), followed by spinach (≈700 mmol Kg^{-1} DW) and beetroot (≈500 mmol Kg^{-1} DW). Pepper showed the lowest (≈250 mmol Kg^{-1} DW). As can be seen, Cl^- concentration was similar in root and shoot from lettuce, spinach and beetroot, while in pepper it accumulated mainly in the root, with very little in the shoot (**Figure 3**).

Respiration Rate

Saline shock led to a significant increase in respiration rate in both shoots and roots of all plant species, although the time and intensity of this increase was dependent on species. Thus, in shoot of pepper and lettuce this increase was evident after 3 h of saline shock, decreased to values similar to controls after 6 and 12 h and increasing again thereafter. However, in spinach and beetroot shoot the increase in respiration rate as a consequence of saline shock occurred later, after 6 h, and reached similar values to control plants after 24 h. With respect to root tissues, respiration rate also increased in all plants species, although after 24 h of saline shock application these effects disappeared in pepper and beetroot. However, in lettuce and spinach the highest differences between control and treated plants were found at this time (**Figure 4**).

Ethylene Production and ACC Concentration

Ethylene production increased rapidly in shoot and root in all plant species after the saline shock application. In shoot, this increase in ethylene production tended to decrease in the least salt sensitive species, in which similar levels to those of control plants were reached after 12–24 h. Moreover, in beetroot shoot the lowest increase in ethylene production due to salinity was found. Accordingly, in root ethylene production was significantly increased by saline shock in the four plant species, this effect being evident after 3 h. Ethylene continued increasing after 24 h in the two more salt sensitive species, while in the least

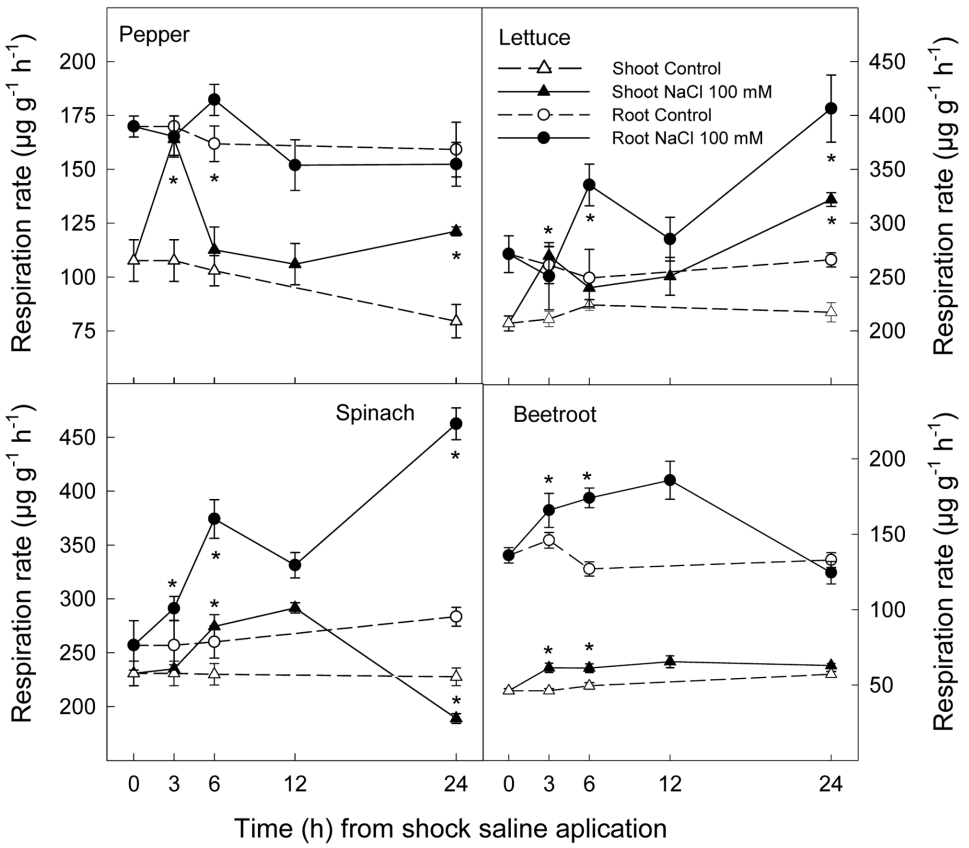

FIGURE 4 | Effect of saline shock (100 mM NaCl) on shoot and root respiration rate of different plant species. Data are the mean ± SE of four replicates of nine plants. *Shows significant differences between control and saline treatment for each sampling date.

sensitive ones a decrease occurred after 12 h. At the end of the experiment in beetroot shoot and root ethylene production was similar in both control and treated plants (**Figure 5**). The increase in ethylene production was due to a significant enhancement in ACC concentrations, that is both free ACC and total ACC, which were detected after 3 h of saline shock, except in shoot of beetroot, in which free ACC and even total ACC decreased after saline shock treatment (**Figures 6**, **7**). Ethylene production after 24 h remained higher in salinity-treated than control plants in shoot and root of pepper and lettuce, while in spinach this occurred only in root. No differences were observed in beetroot. Thus ethylene production was related to the higher free ACC concentration found in shoot and root of saline stressed plants, except in the root of beetroot, in which ethylene production was similar in control and stressed plants after 24 h in spite of the higher free ACC in the latter.

Polyamine Levels

The initial endogenous levels of Put before salinity application differed amongst the species, being the following in shoot and root for each species in nmol g^{-1} FW: 73.1 ± 7.8 and 105.3 ± 14.7 in pepper, 12.5 ± 0.9 and 41 ± 3.2 in lettuce, 18.3 ± 1.3 and 28 ± 2.4 in spinach, and 21 ± 1.7 and 58.3 ± 3.4 in beetroot. In the two most sensitive species the application of 100 mM NaCl induced a Put accumulation in shoot and root after 3 h which continued until 12 h after the treatment, when the highest concentration was reached, 120–140% increase in shoot and 70 and 122% increase in root from lettuce and pepper, respectively (**Figures 8A,B**). Put concentration then decreased, being similar to control values after 24 h, except in roots from lettuce seedlings. In the two most salinity-tolerant species, spinach and beetroot, salinity only slightly increased Put level in shoot 6 and 12 h after the NaCl application. In root Put levels slightly decreased after 3–6 h of salinity application.

Endogenous levels of Spd in shoots and roots under control conditions differed in the four studied species, with the lower levels being found in pepper and beetroot (from 10 to 45 nmol g^{-1} FW), while in lettuce and spinach the values ranged from 76 to 104 nmol g^{-1} FW. In most cases Spd changes due to salinity were higher than Put changes. Thus, Spd increased 3 h after stress in shoot and root of pepper and lettuce seedlings, reaching a maximum increase of 317% in lettuce root at 24 h, followed by pepper shoot in which Spd increased 168% at 12 h although similar levels to controls were reached after 24 h (**Figures 8C,D**). In spinach shoot and root Spd increased after 6 h of stress, but to a lesser extent than in pepper and lettuce. Contrarily, in the root from beetroot salinity had the opposite effect, decreasing Spd concentration. In the

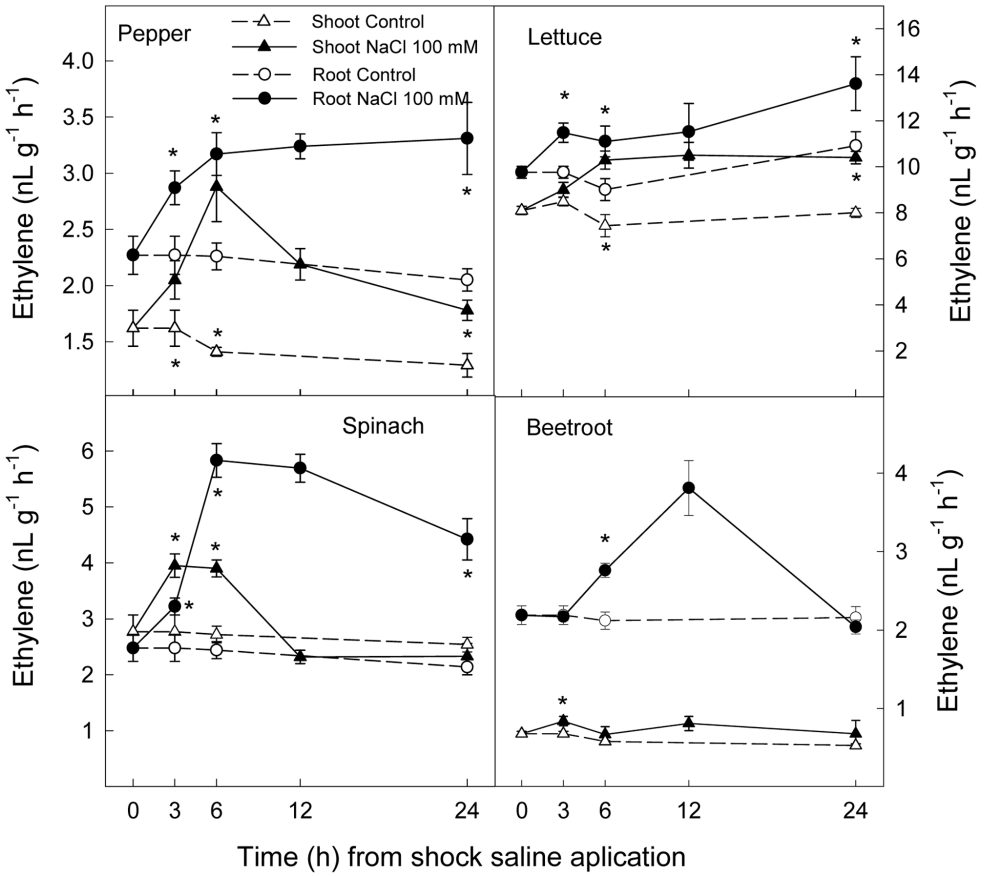

FIGURE 5 | Effect of saline shock (100 mM NaCl) on shoot and root ethylene production of different plant species. Data are the mean ± SE of four replicates of nine plants. *Shows significant differences between control and saline treatment for each sampling date.

most tolerant species, spinach and beetroot, 24 h after stress imposition levels of Spd were similar to those under control conditions.

Spermine was found at a lower concentration than Put and Spd, ca. 20 and 50 nmol g^{-1} FW in shoot and root of pepper respectively, between 9 and 15 nmol g^{-1} FW in spinach and ranged from 2 to 4 nmol g^{-1} FW in lettuce and beetroot. In shoots from pepper and lettuce Spm increased from 3 h after stress, and in spinach and beetroot from 6 to 12 h. The maximum Spm level was reached at 12 h, being an increase of 135% for pepper, 111% for lettuce, 68% for spinach, and 34% for beetroot. Salinity also increased the level of Spm in roots. However, this effect was lower than for shoots (**Figure 8E**), and even in beetroot Spm was decreased by salinity. Accumulation of Spm tended to stabilize with time, except in lettuce roots (**Figure 8F**).

Total polyamine concentration (**Figure 9**) increased markedly after saline stress imposition in shoots and roots of the two most sensitive species, pepper and lettuce. This increase started 3 h after stress imposition. In spinach total polyamine content increased to a lesser extent than for these two species in shoot and root, the increase occurring after 6–12 h. In beetroot, no effect of salinity in shoot and a decrease of total polyamine in root were found.

DISCUSSION

The effect of saline shock on reducing fresh weight is attributed to the osmotic effect of salinity reducing water uptake (Munns, 2002). Our results showed that the osmotic component of salinity provoked an osmotic shock which was related to saline sensitivity, in agreement with Lefèvre et al. (2001). In this sense, the sudden decrease in water potential of nutrient solution when saline treatment was applied led to a decrease in water content in shoot and root of the four plant species, which was observed after 3 h of treatment. However, water content in spinach and beetroot was completely recovered after 24 h of stress while lettuce and pepper shoots and roots did not totally recover the water content of control plants after 24 h. Thus the latter species behaved as more sensitive to saline shock than spinach and beetroot according to previous experiments with long term saline treatments (Zapata et al., 2007, 2008).

In general, saline shock caused a sudden increase in respiration rate in all plant species, although it tended to disappear in the most tolerant, beetroot, while remaining after 24 h in the most salt sensitive. Accordingly, during germination and early seedling development, salinity has been shown to lead to increased respiration rate in a wide range of plant species, its

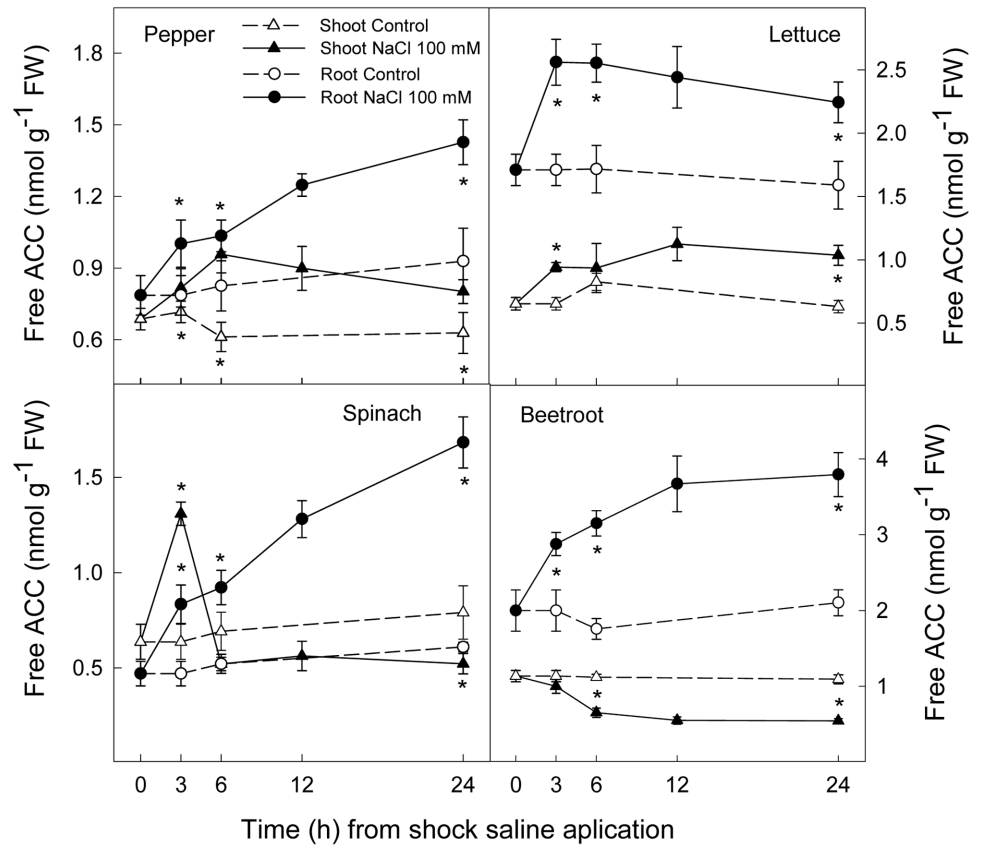

FIGURE 6 | Effect of saline shock (100 mM NaCl) on shoot and root free ACC concentration in different plant species. Data are the mean ± SE of four replicates of three plants. *Shows significant differences between control and saline treatment for each sampling date.

magnitude being related to plant saline sensitivity (Zapata et al., 2004).

Ethylene is a plant hormone having a role in plant responses to biotic and abiotic stresses including salt stress (Ryu and Cho, 2015; Tao et al., 2015). Saline stress led to a quick increase in ethylene production in all plant species, although it tended to recover to initial levels in the most tolerant and remained at higher levels after 24 h in the most sensitive species. Accordingly, free and total ACC increased as a consequence of saline shock after 3 h of treatment. Levels still remained high at the end of the experiment in all plant species, except in beetroot shoot, in which free and total ACC levels were lower in treated than in control plants. Thus, in pepper, lettuce and spinach, a sharp increase in ACS activity occurred as a consequence of saline shock, while in the most tolerant species, beetroot, ACS activity in shoot seemed to be reduced as a consequence of saline shock, since the initial total-ACC levels decreased after treatment. Similar results were found when salinity was applied in a progressive way to these plant species and analysis performed after several days. Here a continuous increase in ACC concentration was found in the most sensitive plants, while in spinach this increase was lower and in beetroot no increase occurred (Zapata et al., 2007). In addition, it is also important to note that in shoot and root of pepper and lettuce plants and in spinach and beetroot shoot the salt induced increase in total ACC was due to both free ACC and conjugated ACC, since in tissues total ACC was higher than free ACC. However, in root of spinach and beetroot, the activity of malonyl-ACC transferase (the main enzyme responsible for ACC conjugation) was very low or zero in control and saline conditions. This is recognized because similar levels of total and free ACC were found. Moreover, in root of beetroot free ACC was higher with salinity after 24 h while ethylene production was similar in control and treated plants, showing an inhibition of ACC oxidase activity in the stressed plants.

Accordingly, in wheat, corn, and soybeans cultivars it has been reported that saline treatment led to higher ethylene production in sensitive cultivars than in more tolerant ones (Lu et al., 1991; Pennazio and Roggero, 1991; El-Shintinawy, 2000). However, in lettuce cultivars saline treatment applied during germination phase increased seedling ethylene production, although its magnitude was higher in the most tolerant cultivars, suggesting that ability to increase ethylene production under saline conditions could provide a higher tolerance to salinity during germination (Zapata et al., 2003). It is not clear if ethylene is involved in the acclimatization processes that aid plants to survive or if it is just a stress response. In this sense, the role of ethylene signaling in plant tolerance to salinity should be considered. Recently, it has been claimed that the ability of plants

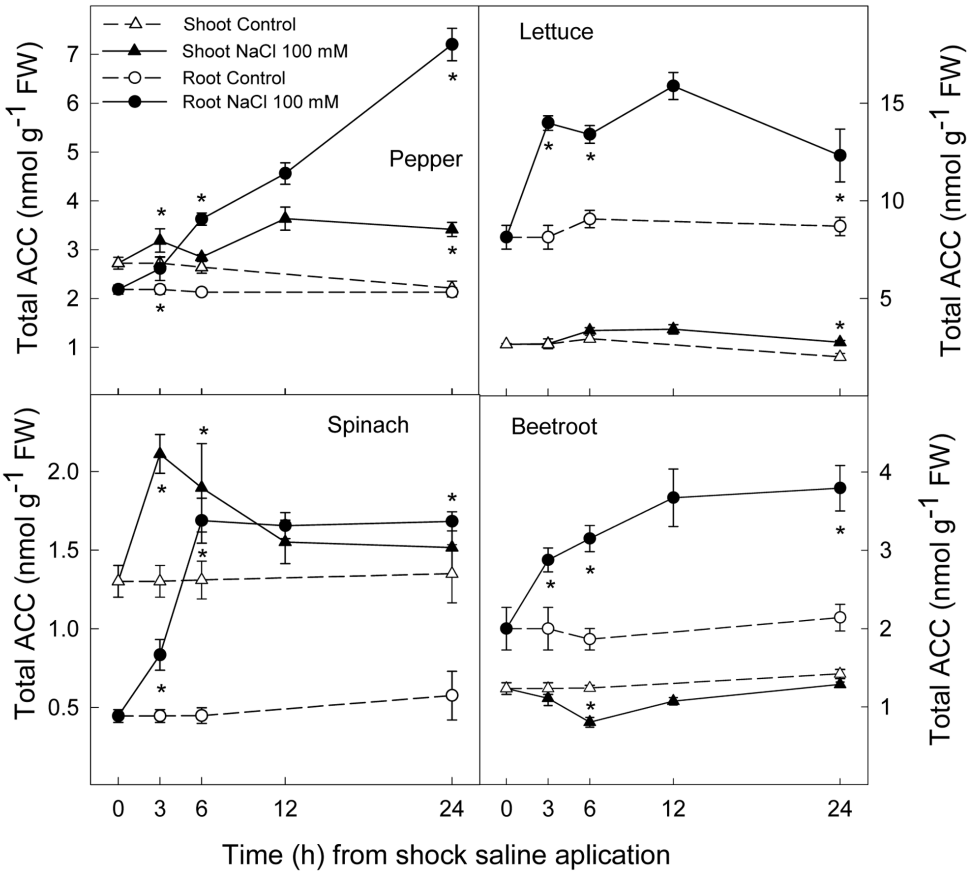

FIGURE 7 | Effect of saline shock (100 mM NaCl) on shoot and root total ACC concentration in different plant species. Data are the mean ± SE of four replicates of three plants. *Shows significant differences between control and saline treatment for each sampling date.

to retain K^+ and/or a large K^+/Na^+ ratio is more important than the efficient exclusion of Na^+ from shoots and roots or the compartmentalisation in special tissues or cells (Møller et al., 2009; Shabala et al., 2010). In fact, ethylene signaling has been found to be essential for both plant tolerance to salinity (Cao et al., 2007; Wang et al., 2007, 2009) and maintenance of high K^+ content (Jung et al., 2009). Moreover, in experiments performed with Arabidopsis it has been found that ethylene insensitive mutants were more affected by salinity than wild type plants, salt tolerance being correlated with plant ability to retain K^+ in roots and/or shoots (Yang et al., 2013).

Using whole plant systems of four plant species our results clearly show that the short-term effect of saline shock caused immediate increases in the levels of Put, Spd, and Spm in all cases in shoots, and in some cases in roots, and that those changes were related to the salinity sensitivity of the plants. In fact, in the two most sensitive species, pepper and lettuce, saline stress induced in shoot and in root a higher Put, Spd, and Spm increase than in the species considered as more tolerant, i.e., spinach and beetroot, with the latter demonstrating the smallest increase in total polyamine content. These polyamine increases were related to the highest osmotic effect (measured by water content decrease) that occurred in shoot and root from pepper and lettuce seedlings. The physiological response induced by salinity in polyamine synthesis was rapid (3 h in the most sensitive species, and 6 h in the most tolerant ones), thus polyamine may be implicated in the adaptation response to stress. However, in most cases changes in polyamines were transitory and polyamine level decreased 24 h after stress to similar levels to those of the control (except for lettuce seedlings). Similar results have been found by other authors, such as Aziz and Larher (1995) and Mutlu and Bozcuk (2005), suggesting that when salinity is applied the polyamine biosynthesis increases, but levels rapidly begin to decrease in parallel to the accumulation of ions. However, in the study from Tonon et al. (2004) with embriogenic *Fraxinus angustifolia* callus, similar results occurred in response to mannitol. Therefore, the decrease on polyamines may not be associated only with Na^+ accumulation. Similarly, Legocka and Kluk (2005) found in lupinus that prolonged (24 h) salt and osmotic stress conditions resulted in a decline in Put and Spd in root, the authors indicating that the polyamine biosynthetic pathway may be sensitive to high salinity and/or water deficit with longer exposition to both stresses, causing the change from biosynthetic processes to oxidative degradation.

Considering the idea of a reduction of polyamine levels with time related to accumulation of saline ions Na^+ and Cl^- with

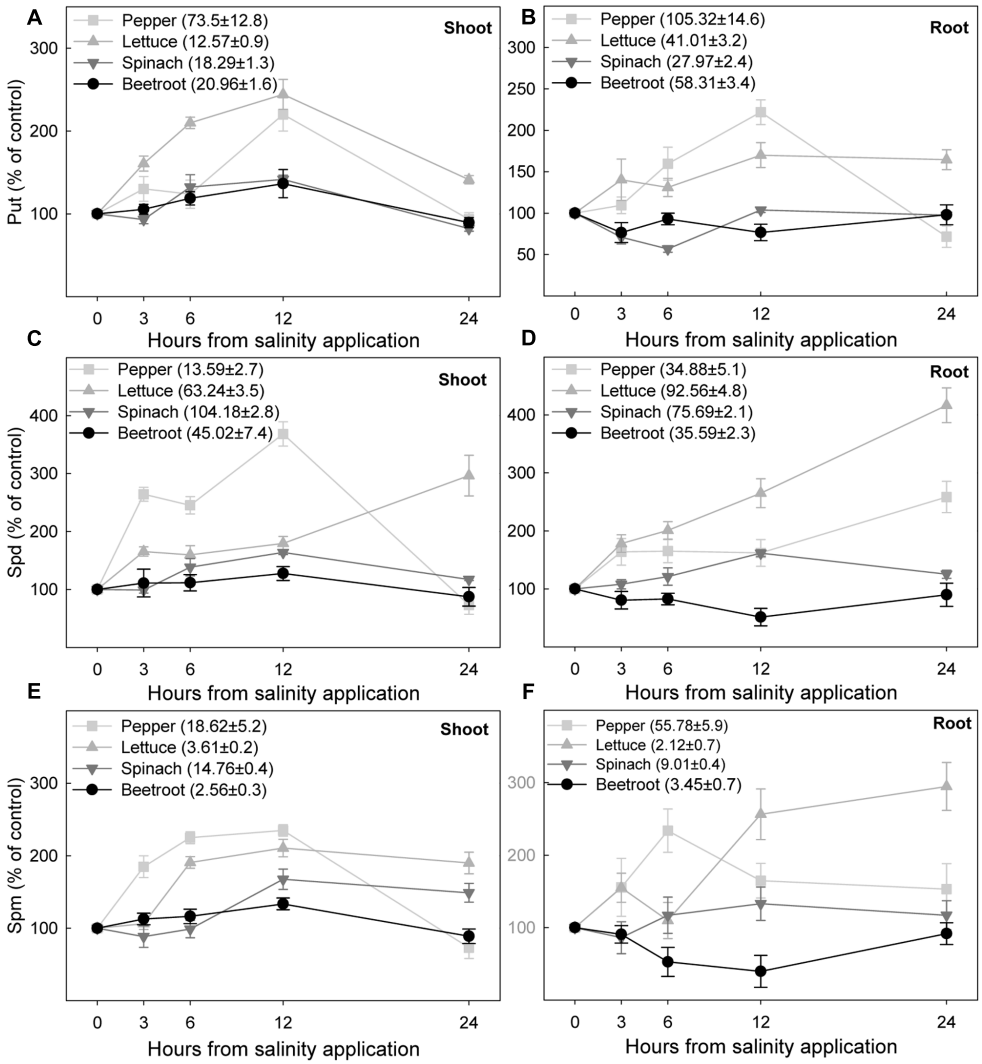

FIGURE 8 | Changes in putrescine, spermidine, and spermine under saline stress (expressed as percentage with respect to controls) in shoot (A,C,E) and root **(B,D,F)** of the different plant species, after saline shock application. Data are the mean ± SE of determinations made independently in four replicates of three plants. Data in brackets are the value of each polyamine before the application of saline shock.

time, results were different in the four considered species. In the most tolerant species, spinach and beetroot, there was an accumulation of Na^+ in shoot that was higher than in the two sensitive ones (pepper and lettuce) and as such the increase in polyamines due to salinity was lower than in the sensitive ones. Thus, those species accumulating more Na^+ and Cl^- in shoot, and more salinity tolerant, can use those ions for osmoregulation and changes in polyamines as a consequence of saline stress are lower than in the sensitive ones. These results confirm previous experimental findings (Zapata et al., 2008) about the long term effect of salinity on the same species. However, in the species considered more sensitive to salinity, pepper and lettuce, results were different. They accumulated high Na^+ concentration in root and showed a limitation for Na^+ accumulation in shoots while presenting the highest polyamine increase. The decrease in polyamines in pepper shoot after 24 h of exposition to stress cannot be explained by an accumulation of the saline ions Na^+ or Cl^- (they did not accumulate in shoot). It may be considered that the low accumulation of Na^+ and Cl^- was enough to decrease polyamine levels. In the case of lettuce, Na^+ and Cl^- accumulation was high in root, but at 24 h there was not observed a decrease in polyamine levels in that plant part. It could be argued that in lettuce a period longer than 24 h is needed in order to observe a decrease in polyamines.

When the long-term effect of salinity (days) was studied in the same plant species (Zapata et al., 2008) the changes in polyamine levels were low and even decreased, probably due to plant adaptation to that stress. Therefore, our results would agree with those from Das et al. (1995), who found in *Brassica campestris* that polyamine levels and related enzymatic activities were little affected by long-term stress, but significantly increased by short-term stress. Moreover, in tomato polyamine levels were

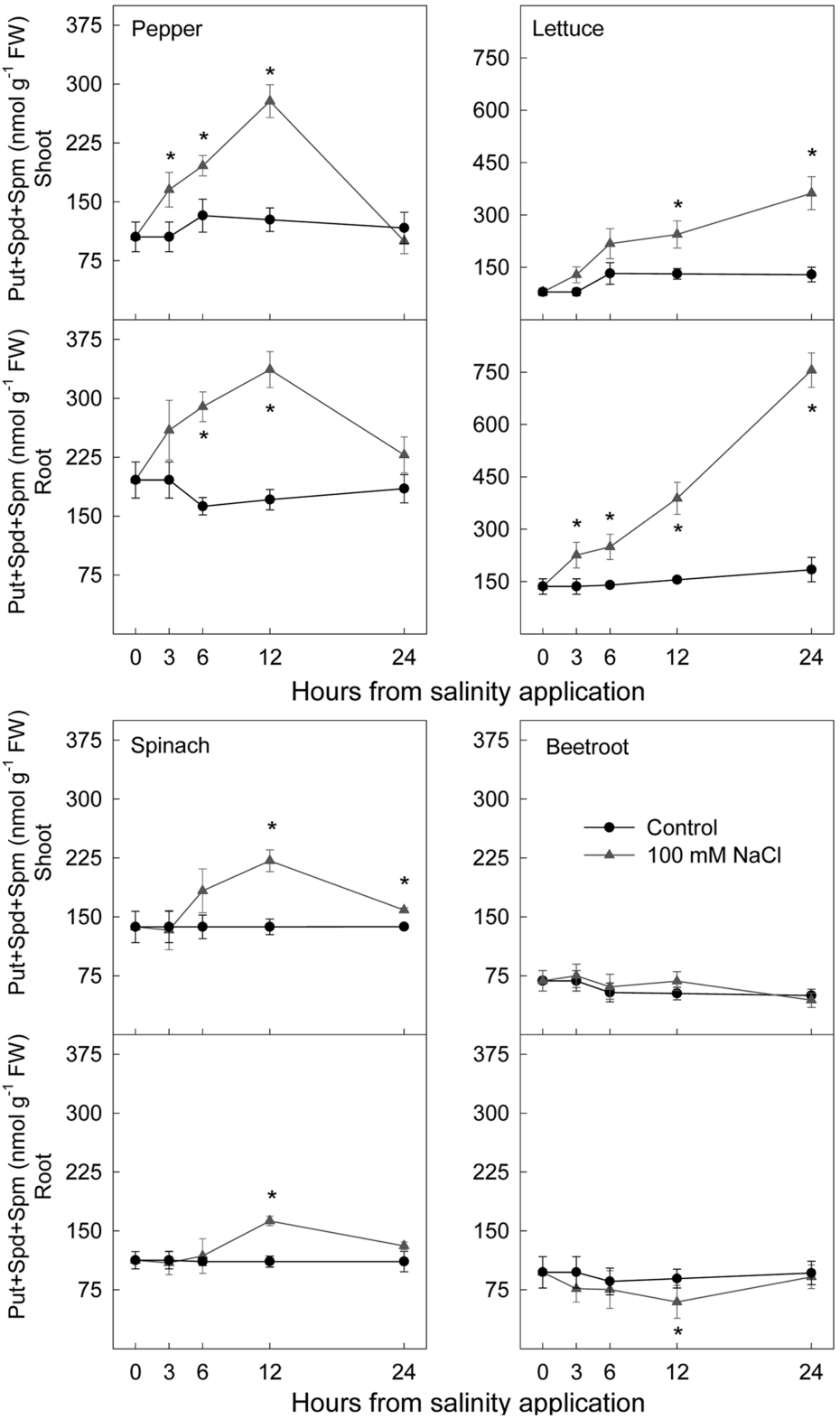

FIGURE 9 | Effect of saline shock on total polyamine concentration, in shoot and root of the different plant species. Data are the mean ± SE of determinations made independently in four replicates of three plants. *Shows significant differences between control and saline treatment for each sampling date.

affected by the length or duration of the stress (Botella et al., 2000).

In the literature there are some studies focused on comparing closely related salt sensitive and salt tolerant species or cultivars in relation to the accumulation of polyamines. Interestingly, in rice and tomato the accumulation of polyamines was greater in salt sensitive than in salt tolerant lines (Katiyar and Dubey, 1990; Aziz et al., 1999). Our results in different plant species with different tolerance to salinity clearly indicate that the increase in polyamines was higher in the two most sensitive species, pepper and lettuce, showing that a higher increase in polyamines would indicate a higher level of stress. Similarly, the study from Minocha et al. (2014) revealed that foliar Put concentration could be used as a reliable biochemical marker for early detection of stress due to soil Ca^{2+}-deficiency in natural forests before the appearance of any visual symptoms of stress damage. These results would support the idea from Jouve et al. (2004) who suggested that in order to select plants for their ability to sustain satisfactory yields under saline conditions, the characterization of several compounds of the metabolome of an organism during exposure to a stress can be a complementary approach to studies of changes in the transcriptome and proteome, which are nowadays generally used as markers.

In spite of the fact that pathways of ethylene and polyamines (Spd and Spm) biosynthesis share SAM as a common precursor, they exert opposite effects in plant development processes. Thus, reduced levels of polyamines have been correlated with increased ethylene production and senescence, while high endogenous concentrations of polyamines are associated with a delay in this process. In this sense, the balance between these two opposite growth regulators is crucial to retard or to accelerate senescence and plant responses to environmental factors and even competence for SAM has been claimed to occur (Sauter et al., 2013; Tiburcio et al., 2014; Serrano et al., 2016). However, in the four plant species studied increases in ethylene, ACC, Spd, and Spm were found as a consequence of the saline treatment, showing that no competence between them occurred and that the SAM pool is high enough to support both ethylene and polyamines biosynthesis.

We can conclude that under saline shock plants respond with increases in ethylene production and polyamine concentration, these being related to plant sensitivity to this stress. The magnitude of these increases was higher and occurred earlier in pepper and lettuce, the most salt sensitive species. Ethylene production decreased after 24 h in salt tolerant plants while still remaining high in the most sensitive. Increases in polyamines tended to disappear after 24 h, except in lettuce. Thus, ethylene and polyamines may have a role as a stress signal once increasing they might induce adaptive responses to the stress. In addition, no competition for the common precursor, SAM, was observed between ethylene and polyamines biosynthetic pathways.

AUTHOR CONTRIBUTIONS

MB has participated in the design of the experiments, the analytical determinations and the writing and discussion of the manuscript. MS has participated in the design of the experiments, the analytical determinations and the writing and discussion of the manuscript. MP has participated in the design of the experiments, the analytical determinations and the writing and discussion of the manuscript. PZ has participated in the design of the experiments and the analytical determinations. MG-L has participated in the design of the experiments and the analytical determinations. All authors revised the manuscript.

FUNDING

This work has been funded by Conselleria de Africultura, Pesca y Alimentación de la Generalitat Valenciana.

ACKNOWLEDGMENT

Authors thank Mr. Michael K. Jordan for the English correction of the manuscript.

REFERENCES

Alcázar, R., Altabella, T., Marco, F., Bortolotti, C., Reymond, M., Koncz, C., et al. (2010). Polyamines: molecules with regulatory functions in plant abiotic stress tolerance. *Planta* 231, 1237–1249. doi: 10.1007/s00425-010-1130-0

Aziz, A., and Larher, F. (1995). Changes in polyamine titers associated with the proline response and osmotic adjustment of rice leaf discs submitted to osmotic stresses. *Plant Sci.* 112, 175–186. doi: 10.1023/A:1023302012208

Aziz, A., Martin-Tanguy, J., and Larher, F. (1999). Salt stress-induced proline accumulation and changes in tyramine and polyamine levels are linked to ionic adjustment in tomato leaf discs. *Plant Sci.* 145, 83–91. doi: 10.1016/S0168-9452(99)00071-0

Botella, M. A., del Amor, F., Amorós, A., Serrano, M., Martínez, V., and Cerdá, A. (2000). Polyamine, ethylene and other physico-chemical parameters in tomato (*Lycopersicum esculentum*) fruits as affected by salinity. *Physiol. Plant.* 109, 428–434. doi: 10.1034/j.1399-3054.2000.100409.x

Cao, W. H., Liu, J., He, X. J., Mu, R. L., Zhou, H. L., Chen, S. Y., et al. (2007). Modulation of ethylene responses affects plant salt-stress responses. *Plant Physiol.* 143, 707–719. doi: 10.1104/pp.106.094292

Das, S., Bose, A., and Ghosh, B. (1995). Effect of salt stress on polyamine metabolism in *Brassica campestris*. *Phytochemistry* 39, 283–285.

Do, P. T., Drechsel, O., Heyer, A. G., Hincha, D. K., and Zuther, E. (2014). Changes in free polyamine levels, expression of polyamine biosynthesis genes, and performance of rice cultivars under salt stress: a comparison with responses to drought. *Front. Plant Sci.* 5:175. doi: 10.3389/fpls.2014.00182

Duan, J. J., Li, J., Guo, S. R., and Kang, Y. Y. (2008). Exogenous spermidine affects polyamine metabolism in salinity-stressed *Cucumis sativus* roots and enhances short-term salinity tolerance. *J. Plant Physiol.* 165, 1620–1635. doi: 10.1134/S1021443716050113

Ellouzi, H., Hamed, K. B., Hernandez, I., Cela, J., Muller, M., Magne, C., et al. (2014). A comparative study of the early osmotic, ionic, redox and hormonal signalling response in leaves and roots of two halophytes and a glycophyte to salinity. *Planta* 240, 1299–1317. doi: 10.1007/s00425-014-2154-7

El-Shintinawy, F. (2000). Photosynthesis in two wheat cultivars differing in salt susceptibility. *Photosynthetica* 38, 615–620.

Jouve, L., Hoffman, L., and Hausman, J. F. (2004). Polyamine, carbohydrate, and proline content changes during salt stress exposure of aspen

(*Populus tremula* L.): involvement of oxidant and osmoregulation metabolism. *Plant Biol.* 6, 74–80. doi: 10.1055/s-2003-44687

Jung, J. Y., Shin, R., and Schachtman, D. P. (2009). Ethylene mediates response and tolerance to potassium deprivation in *Arabidopsis*. *Plant Cell* 21, 607–621. doi: 10.1105/tpc.108.063099

Katiyar, S., and Dubey, R. S. (1990). Changes in polyamine titer in rice seedlings following NaCl salinity stress. *J. Agron. Crop Sci.* 165, 19–27. doi: 10.1111/j.1439-037X.1990.tb00830.x

Kusano, T., Berberich, T., Tateda, C., and Takahashi, Y. (2008). Polyamines: essential factors for growth and survival. *Planta* 228, 367–381. doi: 10.1007/s00425-008-0772-7

Lefèvre, I., Gratia, E., and Lutts, S. (2001). Discrimination between the ionic and osmotic components of salt stress in relation to free polyamine level in rice (*Oryza sativa*). *Plant Sci.* 161, 943–952. doi: 10.1016/S0168-9452(01)00485-X

Legocka, J., and Kluk, A. (2005). Effect of salt and osmotic stress on changes in polyamine content and arginine decarboxylase activity in *Lupinus luteus* seedlings. *J. Plant Physiol.* 162, 662–668. doi: 10.1016/j.jplph.2004.08.009

Liu, J. H., Kitashiba, H., Wang, J., Ban, Y., and Moriguchi, T. (2007). Polyamines and their ability to provide environmental stress tolerance to plants. *Plant Biotechnol.* 24, 117–126. doi: 10.5511/plantbiotechnology.24.117

Liu, J. H., Wang, W., Wu, H., Gong, X., and Moriguchi, T. (2015). Polyamines function in stress tolerance: from synthesis to regulation. *Front. Plant Sci.* 6:827. doi: 10.3389/fpls.2015.00827

Lu, W., Kirkham, M., Long, Z., and Wassom, C. (1991). Genotypic variation in ethylene production by maize grown under nutrient deficiency. *J. Plant Physiol.* 137, 483–487.

Ma, H., Song, L., Shu, Y., Wang, S., Niu, J., Wang, Z., et al. (2012). Comparative proteomic analysis of seedling leaves of different salt tolerant soybean genotypes. *J. Proteomics* 75, 1529–1546. doi: 10.1016/j.jprot.2011.11.026

Minocha, R., Majumdar, R., and Minocha, S. C. (2014). Polyamines and abiotic stress in plants: a complex relationship. *Front. Plant Sci.* 5:175. doi: 10.3389/fpls.2014.00175

Møller, I. S., Gilliham, M., Jha, D., Mayo, G. M., Roy, S. J., Coates, J. C., et al. (2009). Shoot Na^+ exclusion and increased salinity tolerance engineered by cell type-specific alteration of Na^+ transport in *Arabidopsis*. *Plant Cell* 21, 2163–2178. doi: 10.1105/tpc.108.064568

Munns, R. (2002). Comparative physiology of salt and water stress. *Plant Cell Environ.* 25, 239–250. doi: 10.1046/j.0016-8025.2001.00808.x

Mutlu, F., and Bozcuk, S. (2005). Effects of salinity on the contents of polyamines and some other compounds in sunflower plants differing in salt tolerance. *Russ. J. Plant Physiol.* 52, 29–34. doi: 10.1007/s11183-005-0005-x

Pandolfi, C., Pottosin, I., Cuin, T., Mancuso, S., and Shabala, S. (2010). Specificity of polyamine effects on NaCl-induced ion flux kinetics and salt stress amelioration in plants. *Plant Cell Physiol.* 51, 422–434. doi: 10.1093/pcp/pcq007

Peng, J., Li, Z., Wen, X., Li, W., Shi, H., Yang, L., et al. (2014). Salt-induced stabilization of EIN3/EIL1 confers salinity tolerance by deterring ROS accumulation in *Arabidopsis*. *PLoS Genet.* 10:e1004664. doi: 10.1371/journal.pgen.1004664

Pennazio, S., and Roggero, P. (1991). Effects of exogenous salicylate on basal and stress-induced ethylene formation in soybean. *Biol. Plant.* 33, 58–65.

Pillai, M. A., and Akiyama, T. (2004). Differential expression of an *S*-adenosyl-L-methionine decarboxylase gene involved in polyamine biosynthesis under low temperature stress in japonica and indica rice genotypes. *Mol. Genet. Genomics* 271, 141–149. doi: 10.1007/s00438-003-0963-7

Ryu, H., and Cho, Y.-G. (2015). Plant hormones in salt stress tolerance. *J. Plant Biol.* 58, 147–155. doi: 10.1007/s12374-015-0103-z

Sauter, M., Moffatt, B., Saechao, M. C., Hell, R., and Wirtz, M. (2013). Methionine salvage and S-adenosylmethionine: essential links between sulfur, ethylene and polyamine biosynthesis. *Biochem. J.* 451, 145–154. doi: 10.1042/BJ20121744

Serrano, M., Zapata, P. J., Martínez-Romero, D., Díaz-Mula, H. M., and Valero, D. (2016). "Polyamines as an ecofriendly postharvest tool to maintain fruit quality," in *Eco-Friendly Technology for Postharvest Produce Quality*, ed. M. W. Siddiqui (London: Academic Press-Elsevier), 219–242.

Shabala, S., Cuin, T. A., and Pottosin, I. (2007). Polyamines prevent NaCl-induced K^+ efflux from pea mesophyll by blocking non-selective cation channels. *FEBS Lett.* 581, 1993–1999. doi: 10.1016/j.febslet.2007.04.032

Shabala, S., Shabala, S., Cuin, T. A., Pang, J. Y., Percey, W., Chen, Z. H., et al. (2010). Xylem ionic relations and salinity tolerance in barley. *Plant J.* 61, 839–853. doi: 10.1111/j.1365-313X.2009.04110.x

Tao, J.-J., Chen, H.-W., Ma, B., Zhang, W.-K., Chen, S.-Y., and Zhang, J.-S. (2015). The role of ethylene in plants under salinity stress. *Front. Plant Sci.* 6:1059. doi: 10.3389/fpls.2015.01059

Tiburcio, A. F., Altabella, T., Bitrián, M., and Alcázar, R. (2014). The roles of polyamines during the lifespan of plants: from development to stress. *Planta* 240, 1–18. doi: 10.1007/s00425-014-2055-9

Tonon, G., Kevers, C., Faivre-Rampant, O., Graziani, M., and Gaspar, T. (2004). Effect of NaCl and mannitol iso-osmotic stresses on proline and free polyamine levels in embryogenic *Fraxinus angustifolia* callus. *J. Plant Physiol.* 161, 701–708. doi: 10.1078/0176-1617-01096

Wang, B. Q., Zhang, Q. F., Liu, J. H., and Li, G. H. (2011). Overexpression of PtADC confers enhanced dehydration and drought tolerance in transgenic tobacco and tomato: effect on ROS elimination. *Biochem. Biophys. Res. Commun.* 413, 10–16. doi: 10.1016/j.bbrc.2011.08.015

Wang, J., Sun, P. P., Chen, C. L., Wang, Y., Fu, X. Z., and Liu, J. H. (2011). An arginine decarboxylase gene PtADC from *Poncirus trifoliata* confers abiotic stress tolerance and promotes primary root growth in *Arabidopsis*. *J. Exp. Bot.* 62, 2899–2914. doi: 10.1093/jxb/erq463

Wang, H. H., Liang, X. L., Wan, Q., Wang, X. M., and Bi, Y. R. (2009). Ethylene and nitric oxide are involved in maintaining ion homeostasis in *Arabidopsis* callus under salt stress. *Planta* 230, 293–307. doi: 10.1007/s00425-009-0946-y

Wang, S. M., Zhang, J. L., and Flowers, T. J. (2007). Low-affinity Na^+ uptake in the halophyte *Suaeda maritima*. *Plant Physiol.* 145, 559–571. doi: 10.1104/pp.107.104315

Yang, L., Zu, Y. G., and Tang, Z. H. (2013). Ethylene improves *Arabidopsis* salt tolerance mainly via retaining K^+ in shoots and roots rather than decreasing tissue Na^+ content. *Environ. Exp. Bot.* 86, 60–69. doi: 10.1016/j.envexpbot.2010.08.006

Zapata, P. J., Botella, M. A., Pretel, M. T., and Serrano, M. (2007). Responses of ethylene biosynthesis to saline stress in seedlings of eight plant species. *Plant Growth Regul.* 53, 97–106. doi: 10.1007/s10725-007-9207-x

Zapata, P. J., Serrano, M., Pretel, M. T., Amoros, A., and Botella, A. (2003). Changes in ethylene evolution and polyamine profiles of seedlings of nine cultivars of *Lactuca sativa* L. in response to salt stress during germination. *Plant Sci.* 164, 557–563. doi: 10.1016/S0168-9452(03)00005-0

Zapata, P. J., Serrano, M., Pretel, M. T., Amorós, A., and Botella, M. A. (2004). Polyamines and ethylene changes during germination of different plant species under salinity. *Plant Sci.* 167, 781–788. doi: 10.1016/j.plantsci.2004.05.014

Zapata, P. J., Serrano, M., Pretel, M. T., and Botella, M. A. (2008). Changes in free polyamine concentration induced by salt stress in seedlings of different species. *Plant Growth Regul.* 56, 167–177. doi: 10.1007/s10725-008-9298-z

Conflict of Interest Statement: The authors declare that the research was conducted in the absence of any commercial or financial relationships that could be construed as a potential conflict of interest.

frontiers in Plant Science

ORIGINAL RESEARCH
published: 29 November 2016
doi: 10.3389/fpls.2016.01782

Root-to-Shoot Hormonal Communication in Contrasting Rootstocks Suggests an Important Role for the Ethylene Precursor Aminocyclopropane-1-carboxylic Acid in Mediating Plant Growth under Low-Potassium Nutrition in Tomato

Cristina Martínez-Andújar[1], Alfonso Albacete[1], Ascensión Martínez-Pérez[1], José Manuel Pérez-Pérez[2], María José Asins[3] and Francisco Pérez-Alfocea[1]*

[1] Centro de Edafologia y Biologia Aplicada del Segura (CSIC), Murcia, Spain, [2] Instituto de Bioingeniería, Universidad Miguel Hernández, Edificio Vinalopó, Alicante, Spain, [3] Instituto Valenciano de Investigaciones Agrarias (IVIA), Valencia, Spain

OPEN ACCESS

Edited by:
Antonio Ferrante, University of Milan, Italy

Reviewed by:
Jinpeng Gao, Washington State University, USA
Angeles Calatayud, Instituto Valenciano de Investigaciones Agrarias, Spain

***Correspondence:**
Cristina Martínez-Andújar
cmandujar@cebas.csic.es

Specialty section:
This article was submitted to Plant Physiology, a section of the journal Frontiers in Plant Science

Received: *09 September 2016*
Accepted: *11 November 2016*
Published: *29 November 2016*

Citation:
Martínez-Andújar C, Albacete A, Martínez-Pérez A, Pérez-Pérez JM, Asins MJ and Pérez-Alfocea F (2016) Root-to-Shoot Hormonal Communication in Contrasting Rootstocks Suggests an Important Role for the Ethylene Precursor Aminocyclopropane-1-carboxylic Acid in Mediating Plant Growth under Low-Potassium Nutrition in Tomato. Front. Plant Sci. 7:1782. doi: 10.3389/fpls.2016.01782

Selection and breeding of rootstocks that can tolerate low K supply may increase crop productivity in low fertility soils and reduce fertilizer application. However, the underlying physiological traits are still largely unknown. In this study, 16 contrasting recombinant inbred lines (RILs) derived from a cross between domestic and wild tomato species (*Solanum lycopersicum* × *Solanum pimpinellifolium*) have been used to analyse traits related to the rootstock-mediated induction of low (*L, low shoot fresh weight*) or high (*H, high shoot fresh weight*) vigor to a commercial F1 hybrid grown under control (6 mM, *c*) and low-K (1 mM, *k*). Based on hormonal and ionomic composition in the root xylem sap and the leaf nutritional status after long-term (7 weeks) exposure low-K supply, a model can be proposed to explain the rootstocks effects on shoot performance with the ethylene precursor aminocyclopropane-1-carboxylic acid (ACC) playing a pivotal negative role. The concentration of this hormone was higher in the low-vigor *Lc* and *Lk* rootstocks under both conditions, increased in the sensitive *HcLk* plants under low-K while it was reduced in the high-vigor *Hk* ones. Low ACC levels would promote the transport of K *vs.* Na in the vigorous *Hk* grafted plants. Along with K, Ca, and S, micronutrient uptake and transport were also activated in the tolerant *Hk* combinations under low-K. Additionally, an interconversion of *trans*-zeatin into *trans*-zeatin riboside would contribute to decrease ACC in the tolerant *LcHk* plants. The high vigor induced by the *Hk* plants can also be explained by an interaction of ACC with other hormones (cytokinins and salicylic, abscisic and jasmonic acids). Therefore, *Hk* rootstocks convert an elite tomato F1 cultivar into a (micro) nutrient-efficient phenotype, improving growth under reduced K fertilization.

Keywords: grafting, micronutrients, phytohormones, recombinant inbred lines, root-to-shoot communication, *Solanum*

INTRODUCTION

Potassium (K) is the most abundant cation in plant tissues and is required for plant development and crop yield (Wang and Wu, 2013). K deficiency is associated with lowered photosynthesis, transpiration rates, and stomatal conductance (Kanai et al., 2011), whereas photorespiration and respiration are stimulated (Singh and Blanke, 2000). However, most plants can survive under low-K conditions, largely because of the high-affinity K uptake system in the roots which is induced under K deficiency (Armengaud et al., 2004; Chérel et al., 2014; Hafsi et al., 2014).

K starvation not only triggers an upregulation of K transporters, but also involves changes in different signaling molecules including reactive oxygen species (ROS), Ca and several phytohormones such us ethylene, jasmonic acid (JA), and auxins (Armengaud et al., 2004; Shin and Schachtman, 2004; Cao et al., 2006; Hafsi et al., 2014). Ethylene signaling is a key component of the plant response to low K that stimulates the production of ROS and induces changes in root morphology, and gene expression of high affinity transporters (Jung et al., 2009). In turn, many studies suggest that ethylene acts in conjunction with other hormones and signaling molecules to regulate those responses (García et al., 2015). Although recent transcriptomic studies have revealed that many JA-related genes, including JA biosynthesis genes, are induced in response to low K stress (Ruan et al., 2015), the relationship between K deficiency and the JA pathway is still poorly characterized (Armengaud et al., 2004; Fan et al., 2014; Ruan et al., 2015). Furthermore, little is known about the roles of abscisic acid (ABA), salicylic acid (SA), gibberellins (GAs), and cytokinins (CKs) under K deficiency.

The K requirement for optimal plant growth is in the range of 2–5% of the plant dry weight of the vegetative parts and fleshy fruits (Marschner, 1995). In greenhouse tomatoes, 2 mM is the minimum K concentration required to prevent growth reduction and visible deficiency symptoms, while at least 5 mM is necessary to produce maximum fruit yield (Besford and Maw, 1975; Atherton and Rudich, 1986; Kanai et al., 2007, 2011). Although gaining insights into the regulatory mechanisms of plant responses to K deficiency in Arabidopsis may lead to improvements in K utilization efficiency (KUE), the transfer of this knowledge into crop species through conventional breeding or biotechnological approaches is still a scientific challenge that need to be addressed in order to implement a "more-with-less" agriculture. As alternative, grafting provides a tool to explore and exploit new and existing genetic variability through regulating root-shoot interactions governing a range of physiological responses, including tolerance to abiotic stresses such as drought, salinity, and nutrient deficiency (Ghanem et al., 2011; Pérez-Alfocea, 2015; Albacete et al., 2015a). Grafting can enhance nutrient uptake and/or utilization efficiency in vegetables (Rouphael et al., 2008b; Colla et al., 2010; Salehi et al., 2010; Savvas et al., 2010), thus contributing to reduce the amount of fertilizers and production costs. Enhancement of K uptake through grafting has been reported in eggplant (Leonardi and Giuffrida, 2006), melon (Qi et al., 2006), watermelon (Huang et al., 2013), mini watermelon (Rouphael et al., 2008a; Huang et al., 2013), cucumber (Zhu et al., 2008), pepper (Penella et al., 2015), and tomato (Albacete et al., 2009; Huang et al., 2013; Schwarz et al., 2013). However, the mechanisms underlying the rootstock-mediated growth improvement in response to K deprivation have not been elucidated. The availability of RIL populations derived from crosses between the cultivated tomato *Solanum lycopersicum* and wild species such as *Solanum pimpinellifolium*, provides a powerful tool to identify the physiological and genetic determinants of the rootstock-mediated improvement of crop performance (Albacete et al., 2009, 2015a; Estañ et al., 2009; Asins et al., 2010). In the present study, we selected four groups of contrasting RILs on the basis of their high (*H*) or low (*L*) induced vigor to the scion under control (*c*) and low K (*k*) conditions to gain insights into the hormonal and nutritional components involved in the rootstock-mediated adaptation to low-K supply. This knowledge could be useful for further KUE improvement in tomato and other species.

MATERIALS AND METHODS

Plant Material and Growth Conditions

This study formed part of a larger experiment in which 114 RILs derived from a cross between *S. lycopersicum* × *S. pimpinellifolium* (Monforte et al., 1997) segregating for salinity resistance (Estañ et al., 2009) were used as rootstocks of the commercial tomato hybrid cv. Boludo F1 (Seminis Vegetable Seeds Ibérica S.A., Barcelona, Spain) used as the scion to search for tolerant rootstocks under K deficiency (Albacete et al., 2015b). Grafting was performed using the splicing method at the two to three true leaf stages where the scion was attached at the first node of the rootstock (Savvas et al., 2011). One month later (25th September 2012), grafted plants were transferred to a commercial greenhouse located in the Mazarrón tomato producing area (37°33′19.96″ N, 1° 22′53.95″ W) and cultivated in a semi-hydroponic system using sand as substrate. In this study, 16 grafted RILs were phenotypically selected for the vigor induced to the scion (measured as shoot fresh weight, SFW) and classified into four groups (12 plants per group) on the basis of their growth response to each treatment: the first group comprised four rootstocks (RILs 27, 60, 267, and 240) having low vigor (low SFW) irrespective of K treatment (*LcLk*); the second group was four rootstocks (1, 62, 204, and 148) showing high vigor under *c* and low vigor under *k* conditions (*HcLk*); the third group consisted of four rootstocks (47, 132, 167, and 209) with low vigor under *c* and high vigor under *k* conditions (*LcHk*); and finally a fourth group comprising four rootstocks with high vigor regardless of treatment (*HcHk*; **Figure S1**).

Three plants per graft combination were randomly distributed and irrigated with a standard (Cadahia et al., 1995; 6 mM K, control) or modified (1 mM K, low-K) nutrient solution for a period of 7 weeks. The concentration of the other macro and micronutrients in both standard and modified nutrient solutions were: N, 12.5 mM (NO_3:NH_4, 12:0.5); P, 1.5 mM; Ca, 4 mM; Mg, 2 mM; Fe, 100 μM; B, 46 μM; Mn, 9 μM; Zn, 0.76 μM; Cu, 0.75 μM and Mo 0.02 μM.

Forty-eight days after starting the low-K treatment, the second fully expanded mature leaf of 3 plants per graft combination was

weighted and used for leaf area and physiological determinations. Leaf area was determined using an LI-3100AC Area Meter (LI-Cor, Lincoln, NE, USA). Shoot and roots were detached and immediately weighed. The plants were severed 1.5 cm above the graft union. A short length silicone tube was fitted to collect the spontaneous xylem sap exudate which was removed by means of pipette, placed in pre-weighed Eppendorf tube, and immediately frozen on liquid nitrogen and stored at −80°C until analysis. Sap volume and exudation time were recorded in order to calculate the sap flow rate (Netting et al., 2012) and nutrient and hormone delivery to the shoot (sap flow × analyte concentration in the xylem).

Chlorophyll Fluorescence

Modulated chlorophyll fluorescence was measured in dark adapted (30 min) leaves in the second fully expanded leaf leaflet in 3 plants per graft combination (12 in total per contrasting group), using a chlorophyll fluorimeter OS-30 (OptiSciences, Herts, UK) with an excitation source intensity of 3000 mmol m^{-2} s^{-1}. The minimal fluorescence intensity (*F0*) in a dark-adapted state was measured in the presence of a background far-red light. The maximal fluorescence intensity in the dark-adapted state (*Fm*) was measured by 0.8 s saturating pulses (3000 mmol m^{-2} s^{-1}). The maximum quantum yield of open photosystem II (PSII) (*Fv/Fm*) was calculated as $(Fm-F_0)/Fm$ (Maxwell and Johnson, 2000).

Ion Concentration

For ionic quantification, fresh tissue samples were oven dried for 48 h at 80°C, weighed (dry weight) and digested in a HNO_3:HClO (2:1, v/v) solution. Ion analysis was conducted in root xylem sap and leaf tissue samples with inductively coupled plasma spectrometry (ICP-OES, Thermo ICAP 6000 Series).

Hormone Analysis

Cytokinins (Z; ZR; and iP), ACC, ABA, JA, SA, and gibberellins (GA_1, GA_3, and GA_4) were analyzed according to Albacete et al. (2008) with some modifications. Briefly, xylem sap samples were filtered through 13 mm diameter Millex filters with 0.22 μm pore size nylon membrane (Millipore, Bedford, MA, USA). Ten microliters of filtrated extract were injected in a U-HPLC-MS system consisting of an Accela Series U-HPLC (ThermoFisher Scientific, Waltham, MA, USA) coupled to an Exactive mass spectrometer (ThermoFisher Scientific, Waltham, MA, USA) using a heated electrospray ionization (HESI) interface. Mass spectra were obtained using the Xcalibur software version 2.2 (ThermoFisher Scientific, Waltham, MA, USA). For quantification of the plant hormones, calibration curves were constructed for each analyzed component (1, 10, 50, and 100 μg l^{-1}).

Statistics

Analysis of variance, correlation analyses, and principal component analysis (PCA) were performed using SPSS for Windows (Version 22.0, SPSS Inc., Chicago, IL, USA). Means of different graft combinations were compared using Tukey's test at 0.05 of confidence level and the Varimax method was used for PCA.

RESULTS

Rootstock-Mediated Variation in Shoot Vigor and Chlorophyll Fluorescence

As reported previously in Albacete et al. (2015b), the whole RIL population used as rootstocks induced 2.5-fold variability in SFW in the commercial tomato hybrid cv. Boludo F1 grown under low-K supply. About 15% of rootstock genotypes significantly increased or decreased SFW of the commercial scion with respect to the self-grafted Boludo F1 plants. As shown in **Figure S1**, a weak but significant linear correlation exists in shoot biomass production between control and low-K conditions when the RIL population was used as rootstock. To carry out the present study, four contrasting groups (4 lines per group) of rootstocks were selected for their differential effect on shoot biomass under control and low-K supply (See Material and Methods): *LcLk, HcLk, LcHk,* and *HcHk*.

Shoot biomass of the non-grafted scion was reduced by 30% under low-K compared to control conditions (Albacete et al., 2015a). The *H* rootstocks produced 40–50% more SFW than the *L* ones, while low-K decreased (*HcLk*) or increased (*LcHk*) shoot biomass by 25–30%, compared to control conditions (**Figure 1A**, **Table S1**). A similar effect of the rootstock was observed for leaf area (**Figure 1B**) and leaf biomass (data not shown). In contrast, root biomass was not affected by the rootstock genotype, while only the *LcHk* plants registered a significant decrease in root biomass under low-K compared with control conditions (**Figure 1C**). The F_v/F_m after 48 days of treatment was significantly higher in the *Hk* than in the *Lk* plants under low-K, but this parameter was not affected by the low-K supply compared to the control (**Figure 1D**).

Principal Component Analysis of Rootstock-Mediated Response under Low-K

Under low-K supply, the growth parameters and F_v/F_m covaried with most of the nutrients analyzed in the xylem sap along PC1, which explained 30% of the variability, especially the micronutrients Zn, Mn, and B, as well as the K concentration in the leaves (**Figure 2**). In contrast the growth parameters were negatively associated with the leaf concentration of Mn, B, P, S, and Na. Moreover, the root biomass covaried with the shoot growth-related parameters under control conditions (data not shown) but not under low-K conditions, suggesting that root growth was not a determinant of scion vigor under the low nutrient supply in the tested conditions.

Regarding the hormone-related parameters, ZR, ZR/Z, CK/ACC, GA_1, and GA_4 covaried with shoot and leaf growth under control conditions, while total CKs, iP, ABA, SA, JA, total Gas, and the ratio ABA/ACC were associated in an opposed cluster [data not shown). However, under low-K conditions, most

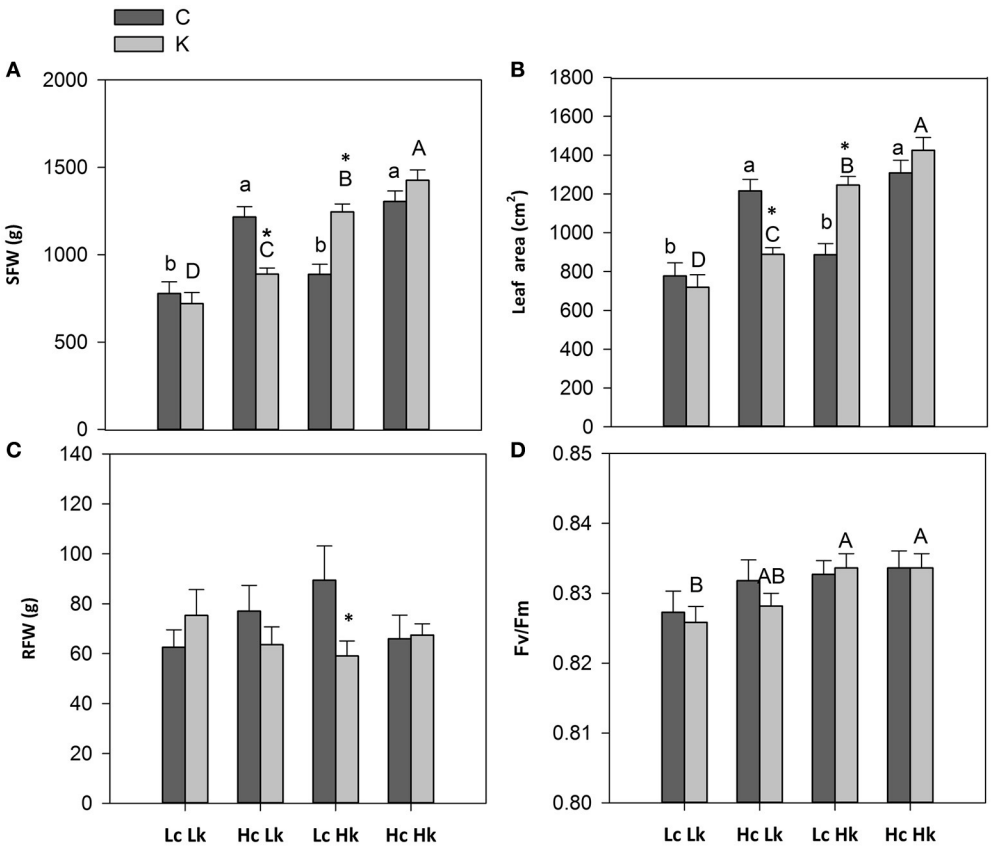

FIGURE 1 | Shoot fresh weight (SFW) (A), leaf area (LA) **(B)**, root fresh weight (RFW) **(C)**, and chlorophyll fluorescence (F_v/F_m) **(D)** of the scion (*Solanum lycopersicum* cv. Boludo F1) grafted onto a population of recombinant inbred lines (RILs) from a cross between *Solanum lycopersicum* × *Solanum pimpinellifolium* with high (*H*) or low (*L*) vigor growing under control (*c*) and low (*k*) conditions during 48 days. Different letters indicate significant differences among graft combinations ($n = 12$, $P < 0.05$) within each treatment. *indicate significant differences between control and low-K treated plants according to the Tuckey test ($P < 0.05$).

hormonal parameters (total CKs, ZR, iP, ABA, SA, JA, CK/ACC, ABA/ACC and particularly JA/ACC, and ZR/Z)] clustered with shoot vigor, while the ethylene precursor ACC clustered in opposite direction (**Figure 2**).

Root Xylem Sap Flow

No differences were observed in the xylem sap flow among graft combinations in either control or low-K conditions. Under low-K only the *LcLk* plants registered a significant 2-fold increase in sap flow compared with control K conditions (**Figure S2**).

Ionome in Root Xylem Sap and Leaf

Potassium and Potassium Use Efficiency (KUE)

K concentration in the root xylem sap was not significantly affected by the graft combination or the K treatment (**Table 1**). However, leaf K concentration was significantly affected by both factors (**Table S1**), with the vigorous *HcHk* rootstocks registering 3% higher K concentrations than the low vigor *LcLk* ones under control K nutrition (**Table 1**, **Figure 3A**). Under low-K despite no reduction in the xylem sap K levels, leaf K concentration significantly decreased 10–20% compared with control plants. Nevertheless, the *Hk* rootstocks maintained a 15% higher leaf K concentration under low-K than the *Lk* ones (**Figure 3A**). This observation suggests that high rootstock-mediated vigor under low K supply (but not under control conditions) is related to a better ability of maintain high K concentration in the leaves. *This is supported by the positive correlation between SFW and leaf K concentration under low-K conditions (**Table 2**).*

KUE, calculated as the shoot biomass generated per unit of K assimilated by a photosynthetic mature leaf, was 30–40% higher in the most vigorous *HcHk* rootstocks than in the less vigorous *LcLk* ones under both growing conditions (**Figure 3B**). Interestingly, a 35% increase in KUE was registered in the tolerant *LcHk* graft combinations under low-K.

Sodium and Na/K Ratio

Curiously, Na concentration of in root xylem sap and leaves was higher in the low-vigor *LcLk* rootstocks than in other graft combinations (**Table 1**) Moreover, Na concentrations tended to increase in the xylem sap in all graft combinations under low-K. Na concentration and Na/K ratio significantly increased in the leaves of the low-vigor *LcLk* plants under low-K (**Table 1**).

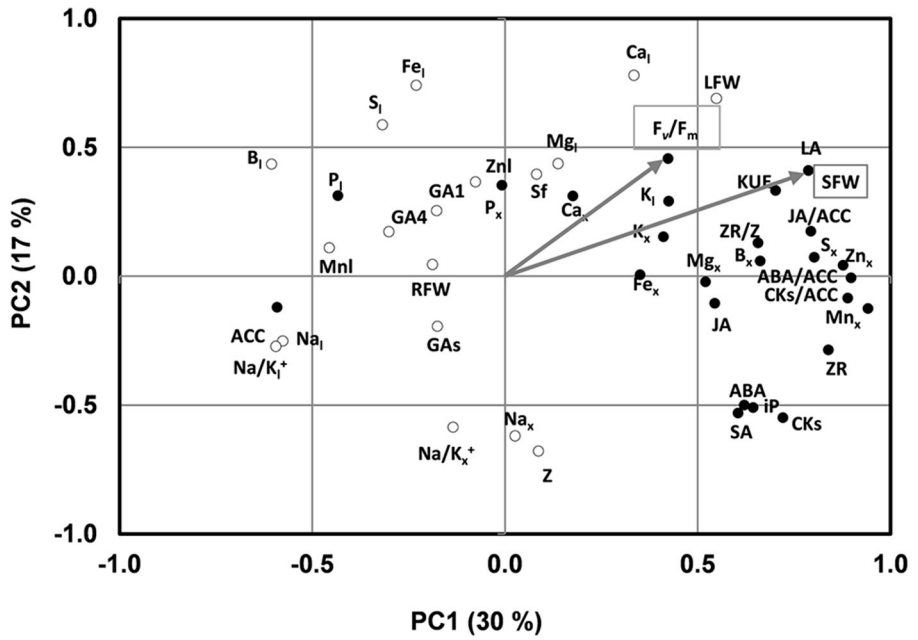

FIGURE 2 | Two axes of a principal component (PC1, PC2) analysis under low K conditions showing shoot fresh weight (SFW) and F_v/F_m trait vectors (indicated by arrow) and the position of all variables (denoted by abbreviations) studied under low K conditions. Hormonal parameters in the xylem sap: ZR, Z, iP, CKs, ACC, ABA, JA, SA, GA_1, GA_4, GAs; Hormonal ratios: ZR/Z, CKs/ACC, ABA/ACC, JA/ACC; Ionic parameters in the xylem sap: K_x, Na_x, P_x, Mg_x, S_x, Ca_x, Na_x, Zn_x, Mn_x, Fe_x, B_x, Na/K_x; ionic parameters in the leaf: K_l, Na_l, P_l, Mg_l, S_l, Zn_l, Mn_l, Fe_l, B_l, Na/K_l; biomass related parameters and others: SFW, shoot fresh weight; RFW, root fresh weight; LFW, leaf fresh weight; LA, leaf area; sf, sap flow; KUE, K use efficiency. The black and white circles indicate the variables belong to the cluster 1 and 2, respectively.

Phosphorous, Magnesium, Sulfur, and Calcium

Non-significant differences in P, Mg, and S concentrations were found in both in root xylem sap and leaves among graft combinations under both low and control K supply (**Table 1**). Curiously, the *LcHk* rootstocks registered the highest increase (but not significant) in P (only in xylem sap), Mg (in both xylem sap and leaf), and S (only in leaf) concentrations at low-K supply with respect to normal conditions (**Table 1**).

Non-significant differences were found in Ca concentration in the root xylem sap among plants grafted onto contrasting rootstocks (**Table 1**). However, leaf Ca concentration was 20–25% higher in the vigorous *HcHk* plants than in the low vigor (*Lc* and *Lk*) ones under both growing conditions. Interestingly, leaf Ca concentration was well correlated with SFW under low-K supply (**Table 2**).

Plants grafted onto the tolerant *LcHk* rootstocks registered the lowest P, S, and Ca concentrations in the root xylem sap under control K nutrition and the highest K, P, Mg, S, and Ca concentrations under low-K supply (**Table 1**), suggesting that the low vigor of those plants under normal K fertilization was due to rootstock-mediated interference with the loading of nutrients into the xylem (sap flow was similar), which was bypassed under low-K nutrition.

Micronutrients

The vigorous *HcHk* grafted plants registered 2.7–5 (Zn) and 1.5–2.2 (Mn, B) -fold higher micronutrient concentration in the root xylem sap under low-K, compared to the other rootstocks (**Table 1**). The tolerant *LcHk* plants registered intermediate values between the *LcLk* and the *HcHk* plants for those nutrients and 1.6 to 1.9-fold higher Fe concentration in the xylem sap under low-K supply. However, non-significant differences between different graft combinations were found in the leaves. Importantly, a positive correlation was found between Zn, Mn, B concentration in the rootstock xylem sap and SFW of the scion under low-K conditions (**Table 2**).

Hormone Concentrations in Root Xylem Sap

Cytokinins

The zeatin-type CKs were more abundant than the iP-type CKs in the root xylem sap (**Figure 4**). Under control K nutrition, the highest ZR concentration was observed in the high-vigor *HcHk* plants, the lowest in the low-vigor *LcLk* lines, and intermediate in the sensitive *HcLk* and tolerant *LcHk* plants (**Figure 4A**). Under low-K, the ZR concentration increased 2 to 2.5-fold in the tolerant *LcHk* and *HcHk* graft combinations, compared to control plants while they were non-significantly affected in the low-vigor and sensitive *Lk* plants (**Figure 4A**). In contrast, Z levels were higher in the low-vigor *Lc* plants (25 ng ml^{-1}), while the high-vigor *HcHk* plants registered the lowest values (15 ng ml^{-1}) under control K nutrition (**Figure 4B**). Indeed, Z concentration was negatively correlated with SFW under control conditions (**Table 2**). Low-K

TABLE 1 | Potassium (K), sodium (Na), Na/K ratio, phosphorous, (P), iron (Fe), magnesium (Mg), sulphur (S), calcium (Ca), zinc (Zn), manganese (Mn), boron (B) in root xylem sap and leaf of the scion (*Solanum lycopersicum* cv. Boludo F1) grafted onto a population of recombinant inbred lines (RILs) from a cross between *Solanum lycopersicum* × *Solanum pimpinellifolium* with high (H) or low (L) vigour growing under control (c) and low K (k) conditions during 48 days.

			Control		Low-K	
			Xylem sap (mg.l^{-1})	Leaf (mg.gDW^{-1})	Xylem sap (mg.l^{-1})	Leaf (mg.gDW^{-1})
Macronutrients	K	LcLk	426.97 ± 51.05	41.01 ± 1.32b	403.20 ± 27.24	33.43 ± 1.39b*
		HcLk	386.19 ± 40.56	44.08 ± 1.90ab	396.38 ± 18.15	35.78 ± 1.57b*
		LcHk	483.65 ± 41.12	45.08 ± 1.62ab	431.84 ± 63.89	39.98 ± 1.66a*
		HcHk	441.41 ± 31.75	47.04 ± 1.78a	384.71 ± 35.63	41.67 ± 1.19a*
	Na	LcLk	40.88 ± 4.43	4.63 ± 0.51	46.38 ± 7.15	5.73 ± 0.67a*
		HcLk	32.81 ± 5.53	4.07 ± 0.37	42.32 ± 5.38	4.12 ± 0.21b
		LcHk	36.62 ± 3.91	3.48 ± 0.29	42.35 ± 9.55	3.27 ± 0.15b
		HcHk	35.06 ± 4.42	3.65 ± 0.41	40.88 ± 5.69	3.70 ± 0.22b
	Na/K	LcLk	0.11 ± 0.02	0.12 ± 0.09	0.12 ± 0.02	0.17 ± 0.03a*
		HcLk	0.11 ± 0.03	0.09 ± 0.01	0.11 ± 0.01	0.12 ± 0.01b
		LcHk	0.08 ± 0.01	0.08 ± 0.01	0.08 ± 0.02	0.08 ± 0.02b
		HcHk	0.08 ± 0.01	0.08 ± 0.01	0.14 ± 0.05	0.09 ± 0.01b
	P	LcLk	80.70 ± 20.98	5.90 ± 0.64	75.42 ± 11.63	8.48 ± 0.25*
		HcLk	81.93 ± 9.48	6.88 ± 0.25	86.61 ± 12.33	7.59 ± 0.58
		LcHk	66.97 ± 11.37	7.04 ± 0.31	91.39 ± 13.60	7.47 ± 0.30
		HcHk	70.95 ± 7.77	7.12 ± 0.45	75.99 ± 10.75	7.49 ± 0.21
	Mg	LcLk	45.62 ± 10.32	8.76 ± 0.70	38.16 ± 4.10	8.86 ± 0.56
		HcLk	37.63 ± 4.68	7.93 ± 0.61	39.08 ± 4.64	8.27 ± 0.39
		LcHk	38.19 ± 7.34	7.95 ± 025	41.13 ± 5.60	8.99 ± 0.42
		HcHk	45.63 ± 13.76	9.13 ± 0.55	39.69 ± 3.35	8.67 ± 0.33
	S	LcLk	71.63 ± 16.69	25.28 ± 3.59	54.11 ± 5.77	29.26 ± 3.00
		HcLk	72.58 ± 11.60	25.87 ± 2.58	68.62 ± 13.13	27.06 ± 2.92
		LcHk	58.78 ± 8.75	21.43 ± 2.01	70.07 ± 9.09	33.66 ± 2.89*
		HcHk	95.39 ± 28.78	26.54 ± 2.50	73.51 ± 9.95	30.91 ± 4.64
	Ca	LcLk	190.10 ± 49.21	34.67 ± 4.27b	135.80 ± 23.92	38.17 ± 3.11b
		HcLk	203.95 ± 33.05	34.97 ± 3.09b	173.55 ± 30.75	39.19 ± 2.84b*
		LcHk	147.83 ± 26.83	35.16 ± 1.48b	177.85 ± 25.73	43.14 ± 1.47ab*
		HcHk	166.06 ± 24.07	46.22 ± 2.48a	150.44 ± 23.13	47.96 ± 2.95a
Micronutrients	Zn	LcLk	0.33 ± 0.06	0.15 ± 0.02	0.35 ± 0.06b	0.17 ± 0.14
		HcLk	0.29 ± 0.05	0.17 ± 0.02	0.25 ± 0.04b	0.16 ± 0.01
		LcHk	0.51 ± 0.12	0.18 ± 0.01	0.43 ± 0.05b	0.16 ± 0.01
		HcHk	0.37 ± 0.05	0.16 ± 0.01	1.15 ± 0.32a*	0.18 ± 0.06
	Mn		1.35 ± 0.42	0.68 ± 0.06	1.38 ± 0.32ab	0.56 ± 0.09
		HcLk	0.72 ± 0.14	0.54 ± 0.07	1.16 ± 0.20b	0.49 ± 0.09
		LcHk	1.31 ± 0.40	0.46 ± 0.08	1.74 ± 0.38ab	0.63 ± 0.07
		HcHk	1.30 ± 0.21	0.62 ± 0.06	2.54 ± 0.56a*	0.48 ± 0.08
	Fe	LcLk	0.70 ± 0.16	0.29 ± 0.06	0.32 ± 0.04b	0.25 ± 0.02
		HcLk	0.28 ± 0.04	0.23 ± 0.03	0.38 ± 0.07ab	0.29 ± 0.04
		LcHk	0.76 ± 0.27	0.27 ± 0.03	0.60 ± 0.16a	0.34 ± 0.04
		HcHk	0.44 ± 0.06	0.33 ± 0.04	0.36 ± 0.04ab	0.29 ± 0.04
	B	LcLk	0.45 ± 0.24	0.07 ± 0.07	0.37 ± 0.09b	0.11 ± 0.02*
		HcLk	0.35 ± 0.10	0.09 ± 0.01	0.36 ± 0.10b	0.09 ± 0.08
		LcHk	0.33 ± 0.11	0.08 ± 0.01	0.54 ± 0.14ab	0.11 ± 0.00*
		HcHk	0.32 ± 0.09	0.09 ± 0.03	0.80 ± 0.17a*	0.10 ± 0.00

*Different letters indicate significant differences among graft combinations ($n = 12$, $P < 0.05$) within each treatment. *indicate significant differences between control and low-K treated plants according to the Tuckey test ($P < 0.05$).*

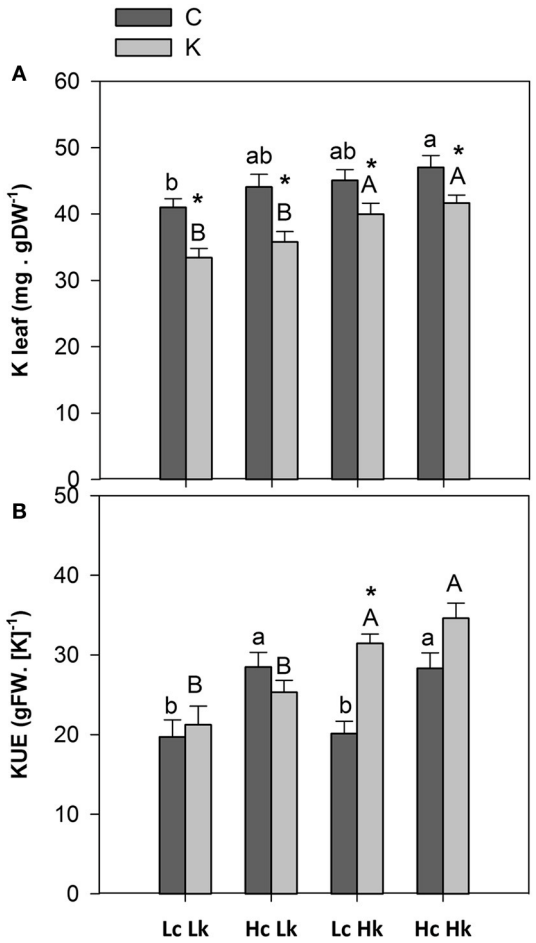

FIGURE 3 | Leaf potassium concentration (A) and potassium use efficiency (KUE, calculated as the shoot biomass generated per unit of K assimilated by a photosynthetic mature leaf) **(B)** of the scion (*Solanum lycopersicum* cv. Boludo F1) grafted onto a population of recombinant inbred lines (RILs) from a cross between *Solanum lycopersicum* × *Solanum pimpinellifolium* with high (*H*) or low (*L*) vigor growing under control (*c*) and low K (*k*) conditions during 48 days. Different letters indicate significant differences among graft combinations ($n = 12$, $P < 0.05$) within each treatment. * indicate significant differences between control and low-K treated plants according to the Tuckey test ($P < 0.05$).

supply only significantly reduced Z levels in the tolerant *LcHk* plants, but not in the high-vigor *HcHk* ones, suggesting that a conversion of Z into ZR occurred in response to low-K in the *LcHk* plants while in the *HcHk* plants, the increase in ZR and total CKs under low-K seems to be due to *de novo* CK biosynthesis.

Non-significant differences in iP or total CKs (Z+ZR+iP) concentrations in the root xylem sap were observed among graft combinations under control conditions, while low-K supply induced an increase in both iP and total CKs only in high-vigor *HcHk* plants (**Figures 4C,D**).

The greatest iP, ZR, and total CKs delivery rate was found in the plants grafted onto the vigorous *HcHk* rootstocks under low-K conditions (data not shown), with a positive correlation between the flow rate of ZR, iP, and CKs to the scion and SFW under low K fertilization (**Table 2**).

1-Aminocyclopropane-1-Carboxylic Acid

Under control K nutrition, ACC concentration was significantly higher (2 to 3-fold) in the root xylem sap of the low-vigor *Lc* rootstocks than those of the high-vigor *Hc* ones (**Figure 5A**). Low-K supply decreased ACC concentration in the *LcLk*, *LcHk,* and *HcHk* plants, but the highest and lowest concentrations were registered in the low (*Lk*) and high (*Hk*) vigor rootstocks, respectively (**Figure 5A**). Indeed, the ACC levels were negatively correlated with the SFW under both conditions and more significantly under low-K supply (**Table 2**).

Abscisic, Salicylic, and Jasmonic Acids

Similarly to ACC, ABA concentration in the root xylem sap under control conditions was higher in the low-vigor *Lc* rootstocks than in the high-vigor *Hc* ones, although the differences were only significant between *LcLk* and *HcLk* graft combinations (**Figure 5B**). Low-K supply provoked a decrease in ABA concentration in all plants except in the most vigorous *HcHk* ones, although the differences were not significant between treatments. The highest ABA levels under low-K were found in the *HcHk* graft combinations, while the lowest were registered in the sensitive *HcLk* ones (**Figure 5B**). Furthermore, the rootstock-mediated vigor under control conditions was negatively correlated with ABA concentrations in the root xylem sap (**Table 2**).

In the vigorous and tolerant *HcHk* rootstocks, SA (under control and low-K) and JA (under low-K) concentrations were twice as high as the other graft combinations (**Figures 5C,D**). The SA concentrations were positively correlated with SFW under low K (**Table 2**).

Gibberellins

GA_1, GA_3, and GA_4 concentrations in the root xylem sap were similar in all graft combinations under control K nutrition, irrespective of their related shoot vigor (**Figures S3A–D**). GA_1 and/or GA_4 concentrations decreased under low-K supply in the different graft combinations except for the tolerant *LcHk* one (**Figures S3A,C**). GA_3 was not detectable in the sensitive *HcLk* graft combination under low-K supply (**Figure S3B**). Although no significant correlation was found with SFW, the lowest GA concentrations under low-K (50% reduction compared to control K) were detected in those rootstocks inducing high-vigor under control conditions (*HcLk, HcHk*), while those inducing low-vigor were less (*LcHk*, 22% reduction) or not (*LcLk*) affected by the low-K supply (**Figure S3D**). GA_3 seems to be a particular sensitive target under low-K supply in constitutive vigorous but susceptible rootstocks to low K supply (*HcLk*).

Hormonal Ratios

The ZR/Z ratio was higher in the high-vigor *Hc* graft combinations and increased under low-K in the tolerant *Hk* ones (**Figure 6A**). Indeed, ZR/Z was positively correlated with SFW under both control and low-K conditions (**Table 2**). Similarly, the CKs/ACC ratio also increased under low-K supply in the

TABLE 2 | Linear correlation coefficients between shoot fresh weight (SFW) and ionomic and hormonal related parameters in the root xylem sap of the scion (*Solanum lycopersicum* cv. Boludo F1) grafted onto a population of recombinant inbred lines (RILs) from a cross between *Solanum lycopersicum* × *Solanum pimpinellifolium* with high (H) or low (L) vigour growing under control (c) and low K (k) conditions during 48 days.

	Ionic Parameters										
	Macronutrients							Macronutrients			
	K	Na	Na/K	P	Mg	S	Ca	Zn	Mn	Fe	B
XYLEM SAP											
C	−0.075	−0.121	−0.029	0.205	0.109	0.274	0.199	−0.058	0.036	−0.256	−0.176
K	0.097	−0.089	−0.016	0.023	0.123	0.265	0.077	**0.487****	**0.414****	0.105	**0.585****
LEAF											
C	0.045	0.001	0.005	0.260	−0.165	**0.360***	0.208	0.090	0.149	−0.136	**0.364***
K	**0.514****	**−0.458****	**−0.487****	−0.125	0.043	0.011	**0.364***	0.117	−0.052	0.172	0.364*

	Hormonal Parameters											
	ZR	Z	iP	CKs	ACC	ABA	SA	JA	ZR/Z	CKs/ACC	ABA/ACC	JA/ACC
XYLEM SAP												
C	0.250	**−0.494****	0.080	−0.349**	−0.304	**−0.471***	0.196	−0.224	**0.466****	0.139	0.027	−0.05
K	0.179	−0.145	**0.386****	0.262	**−0.557****	0.263	**0.402****	0.153	**0.318***	**0.487****	**0.679****	**0.627****

	ZR_f	iP_f	CKs_f	SA_f
C	0.171	0.108	0.027	0.099
K	**0.358***	**0.334***	**0.319***	**0.325***

$^*P < 0.05$, $^{**}P < 0.01$, $n = 48$. K, potassium; Na, sodium; Na/K ratio; P, phosphorous; Mg, magnesium; S, sulphur; Ca, calcium; Zn, zinc; Mn, manganese; Fe, iron; B, boron. ZR, zeatin riboside; Z, zeatin; iP, isopentenyladenine; CKs, total cytokinins; ACC, 1-Aminocyclopropane-1-carboxylic acid; ABA, abscisic acid; SA, salicylic acid; JA, jasmonic acid; ZR/Z ratio; CKs/ACC ratio; JA/ACC ratio; ZR_f, zeatin riboside flow rate; iP_f, Isopentenyladenine flow rate; CKs_f, total cytokinins flow rate; SA_f, salicylic acid flow rate. Bold means the correlation values are significatives.

tolerant *Hk* rootstocks, registering 4–6 times higher values than the low-vigor and sensitive *Lk* ones (**Figure 6B**).

The ABA/ACC ratio was higher in the tolerant *Hk* graft combinations compared with the *Lk* under low-K conditions (**Figure 6C**). Moreover, this ratio seems to be differentially regulated by low-K in the sensitive *HcLk* (decrease) and tolerant *LcHk* (increase) graft combinations. The JA/ACC ratio significantly increased under low-K in the xylem sap of the vigorous *HcHk* plants (**Figure 6D**). Among the hormonal parameters analyzed, CKs/ACC, ABA/ACC, and JA/ACC ratios were the parameters most positively correlated with SFW under low-K (**Table 2**), suggesting that these hormonal ratios with the ethylene precursor ACC are important in determining the rootstock-mediated shoot growth under low-K conditions.

DISCUSSION

Tomato Rootstocks Can Improve Shoot Growth and KUE under Low-K Nutrition

Although grafting offers excellent opportunities to improve water and fertilizer use efficiency by exploring and exploiting the genetic diversity existing in *Solanum* spp, little is known about the physiological and genetic determinants of the rootstock capacities to improve or maintain plant growth under low nutrient supply. The use of RILs has proven to be a useful tool for these and other purposes (Albacete et al., 2009, 2015a,b; Estañ et al., 2009; Asins et al., 2010). Using 114 RILs from a *S. lycopersicum* × *S. pimpinellifolium* cross as rootstocks of a commercial tomato cultivar generate a 2.5-fold variation in the vegetative growth of the scion growing under low-K supply (1 mM; Albacete et al., 2015b). The rootstock-mediated effect on shoot growth (and subsequently in applied KUE and nutrient use efficiency) under low-K supply is at least partially due to the constitutive plant vigor observed under control conditions, as supported by (i) the positive correlation between both conditions (**Figure S1**) and (ii) the behavior of the low-vigor *LcLk* and high-vigor *HcHk* rootstocks (**Figures 1A,B**). However, the fact that the scion variety grafted onto different RILs as rootstocks can decrease (sensitive, *HcLk*) or increase (tolerant, *LcHk*) their shoot growth under low-K supply (**Figure 1A**) indicated that specific mechanisms control the rootstock-mediated response to low K stress in order to increase both shoot growth and KUE beyond vigor. Indeed, although it is generally assumed that rootstocks have much larger and vigorous root systems allowing the grafted plants to absorb water and nutrients more efficiently as compared to non-grafted plants, this was not the case in this study since no differences in root biomass were observed and low-K tended to decrease root biomass in the tolaerant *LcHk* rootstocks (**Figure 1C**). Although changes in root system architecture under low-K cannot be excluded, other more specific traits such as changes in nutrient uptake from roots and

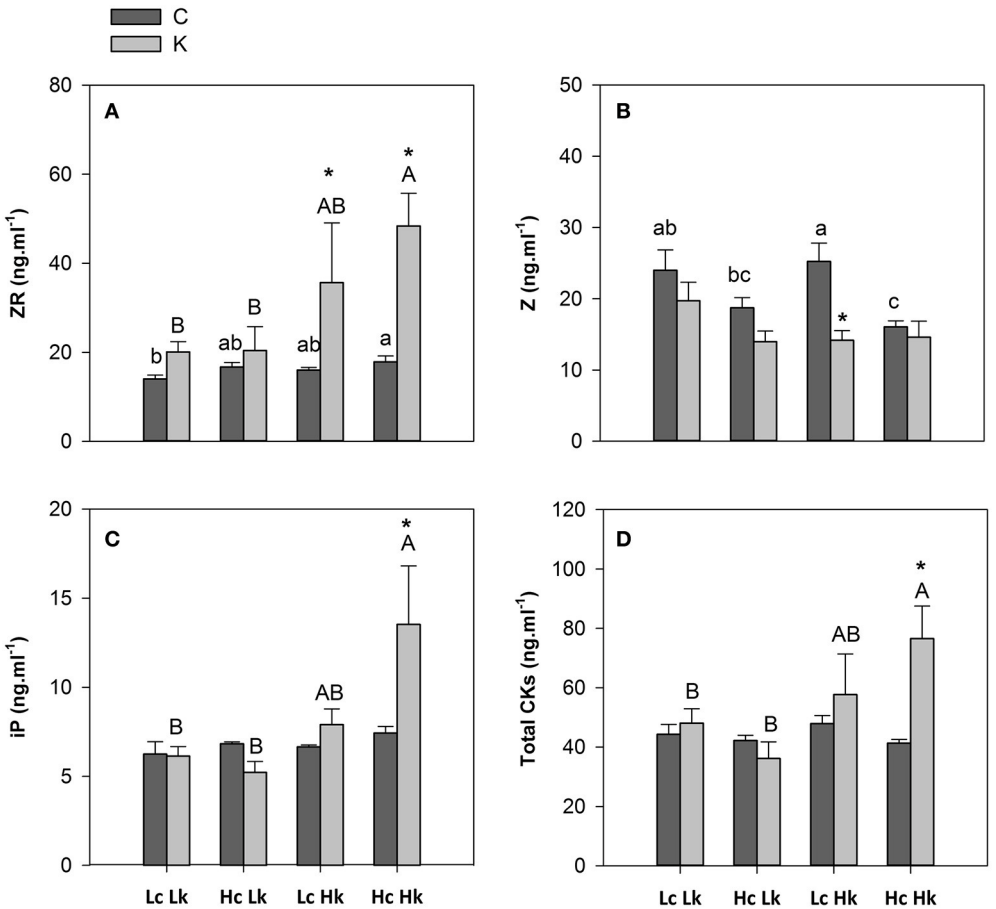

FIGURE 4 | Zeatin riboside, ZR (A), zeatin, Z **(B)**, isopentenyl adenine, iP **(C)** and total cytokinins, CKs **(D)** concentrations in root xylem sap of the scion (*Solanum lycopersicum* cv. Boludo F1) grafted onto a population of recombinant inbred lines (RILs) from a cross between *Solanum lycopersicum* × *Solanum pimpinellifolium* with high (*H*) or low (*L*) vigor growing under control (*c*) and low K (*k*) conditions during 48 days. Different letters indicate significant differences among graft combinations ($n = 12$, $P < 0.05$) within each treatment. * indicate significant differences between control and low-K treated plants according to the Tuckey test ($P < 0.05$).

root-to-shoot transport of nutrients and hormones may help to explain the rootstock influence on the growth of the scion.

K, Na, and Ca in the Leaves and Micronutrients in the Root Xylem Sap are Related to Rootstock-Mediated Changes in Shoot Growth under Low-K Supply

Leaf K and Ca concentrations were constitutively higher in the high-vigor *HcHk* grafted plants and remained more elevated under low-K also in the tolerant *LcHk* ones, with a positive correlation with shoot biomass under low-K (**Table 2**) and co-varying with leaf fresh weight and F_v/F_m in those suboptimal conditions (**Figure 2**). These results suggest that the increased Ca concentration in the leaves of those high-vigor *Hk* plants (particularly in the tolerant *LcHk* ones) could represent an important factor of the adaptive response to low-K. Indeed, Ca elevation might activate many non-selective cation channels (Amtmann and Armengaud, 2007; Demidchik and Maathuis, 2007; Wang and Wu, 2013), which could help to explain the increase in the assimilation of K and other several cations in the tolerant *Hk* rootstocks.

Since micronutrient concentrations, such as Zn, Mn, B, and Fe, were higher in the root xylem sap of high-vigor plants under low-K, specific transport mechanisms in *Hk* plants could explain these differences, rather than differences in transpiration fluxes. As foliar micronutrient concentration does not differ between graft combinations, their increased levels in root xylem sap of the *Hk* plants might stimulate growth under low-K deprivation, thus increasing the nutrient use efficiency without affecting leaf concentration (Marschner, 1995). By increasing availability in the soil or by inducing the number and/or the activity of transporters at the root membrane, micronutrient efficiency is genetically controlled and could improve crop yield under environmental stresses (Fageria et al., 2008). Importantly, QTLs controlling nutrient levels in leaves under moderate salinity were also found clustered in the RIL population from which some rootstocks were selected for this study (Asins et al., 2015). QTLs for Ca, Mn, Sr, and B levels collocated within a 10

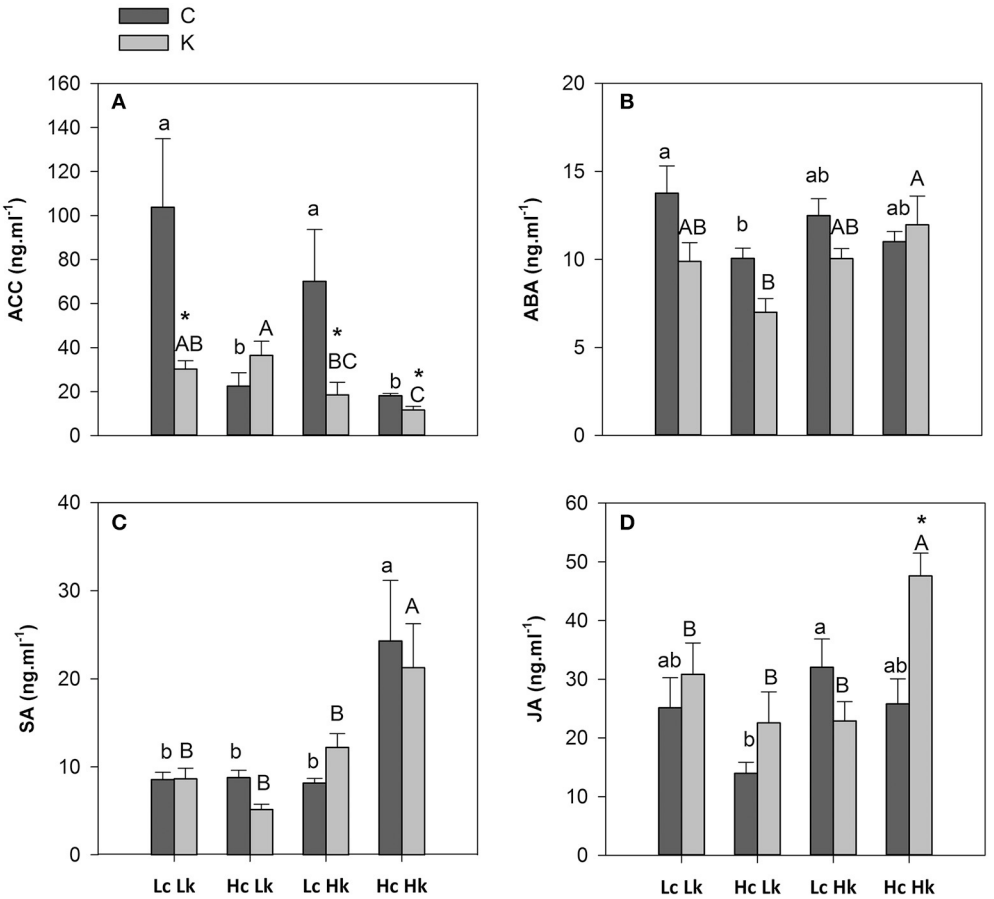

FIGURE 5 | 1-Aminocyclopropane-1-carboxylic acid, ACC (A), abscisic acid, ABA **(B)**, salicylic acid, SA **(C)**, and jasmonic acid, JA **(D)** concentrations in the root xylem sap of the scion (*Solanum lycopersicum* cv. Boludo F1) grafted onto a population of recombinant inbred lines (RILs) from a cross between *Solanum lycopersicum* × *Solanum pimpinellifolium* with high (*H*) or low (*L*) vigor growing under control (*c*) and low K (*k*) conditions during 48 days. Different letters indicate significant differences among graft combinations ($n = 12$, $P < 0.05$) within each treatment. *indicate significant differences between control and low-K treated plants according to the Tuckey test ($P < 0.05$).

cM region on chromosome 3, where several candidate genes have been previously identified (Asins et al., 2015). Favorable alleles of one or several of these QTL could be present in the tolerant *Hk* rootstocks, therefore enhancing loading of ions into the xylem from the roots (B, Mn, Zn, Fe) and nutrient assimilation in the leaves (K, Ca, S), which will increase shoot growth in low-K conditions of grafted plants. Curiously, Na in the leaves was the only element that was negatively correlated (**Table 2**) with shoot biomass under low-K, suggesting that Na/K interferences are involved in the specific rootstock-mediated responses. The underlying physiological and molecular mechanisms involved in those nutritional changes require further investigation.

Does ACC Interfere with Nutrient Uptake and Transport?

Low-K supply in Arabidopsis roots quickly (within hours) stimulates ACC and ethylene production and root hair elongation (Shin et al., 2005; Wang and Wu, 2013). In this study, ACC concentration only increased in the root xylem sap of the most low-K sensitive *HcLk* plants, while it decreased in the other graft combinations after 7 weeks growing under low-K (**Figure 5A**). Interestingly, this decrease was more significant in those plants with high constitutive ACC levels (*LcLk* and *LcHk*), and the concentrations of this hormone was negatively correlated with both shoot biomass (**Table 2**) and *Fv/Fm* under low-K supply. The effect of the rootstock-ACC on the shoot performance can be explained in terms of nutrient uptake/assimilation, leaf senescence and growth regulation in coordination with other root-to-shoot transported hormones.

Ethylene interacts with Na/K transporters in mediating salt stress responses depending on the plant species. The lack of ethylene overproducer (ETO1) function enhanced tissue K (and reduces Na) status through inducing the expression of HAK high-affinity K transporters in Arabidopsis (Jiang et al., 2013). In rice, increasing ethylene levels increases Na accumulation in the shoot and salt sensitivity by inducing *OsHKT2; 1* gene (Li et al., 2014; Yang et al., 2015). The low vigor and low K concentration of *LcLk* grafted plants (with the highest Na concentrations) suggests that the high constitutive (or induced, as occurs in

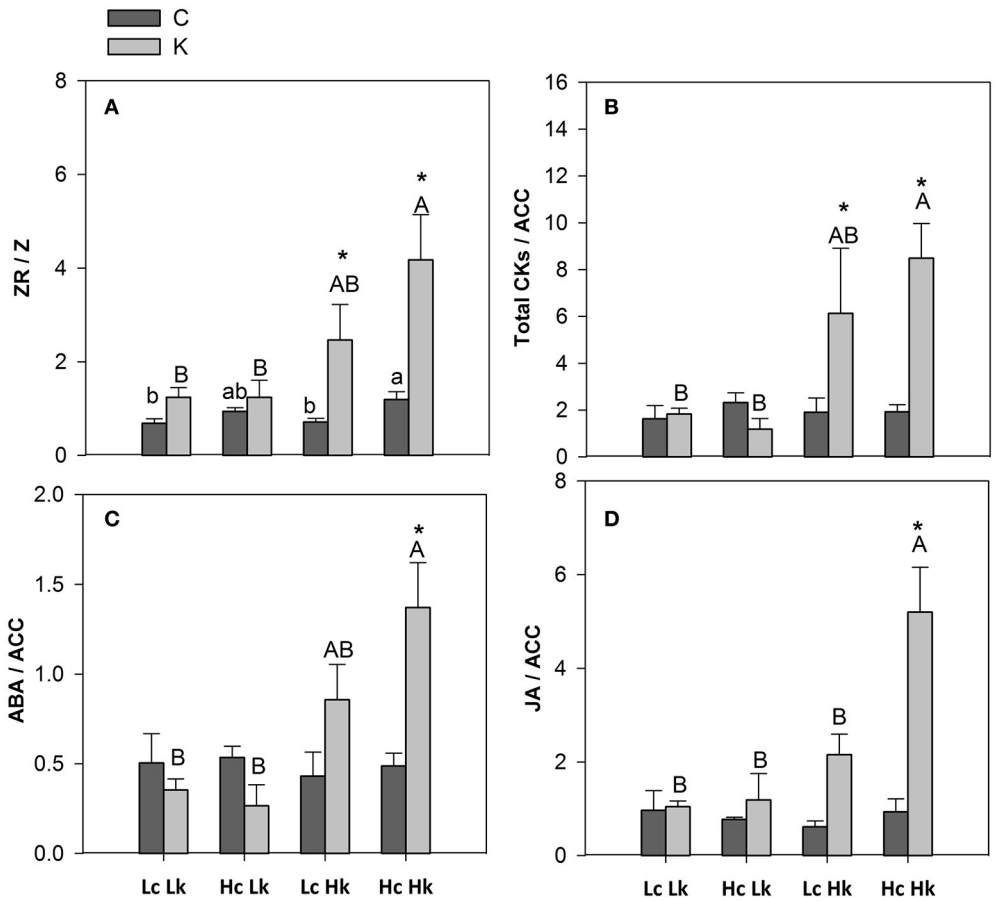

FIGURE 6 | Hormonal ZR/Z (A), total CKs/ACC **(B)**, ABA/ACC and JA/ACC **(D)** ratios in the root xylem sap of the scion (*Solanum lycopersicum* cv. Boludo F1) grafted onto a population of recombinant inbred lines (RILs) from a cross between *Solanum lycopersicum* × *Solanum pimpinellifolium* with high (*H*) or low (*L*) vigor growing under control (*c*) and low K (*k*) conditions during 48 days. Different letters indicate significant differences among graft combinations ($n = 12$, $P < 0.05$) within each treatment. *indicate significant differences between control and low-K treated plants according to the Tuckey test ($P < 0.05$).

the sensitive *HcLk*) levels of ACC in the root xylem could negatively regulate K/Na homeostasis in tomato by interacting with Na/K transporters. The *HKT1* gene apparently controls Na/K levels in this RIL population when used as rootstocks under salinity, and the Na concentrations of cv Boludo tissues grafted on rootstocks homozygous for the *S. pimpinellifolium* allele were higher than on rootstocks homozygous for the with the *S. lycopersicum* allele (Asins et al., 2015). As salinity stress resembles low-K availability due to its interaction with Na (Pottosin et al., 2014), the improved KUE and higher shoot growth under low K nutrition observed in the tolerant *LcHk* lines could result from the inherent variation on *HKT* gene expression among the rootstock population. Although Na could contribute to the osmotic adjustment when K is limiting, our results suggest that rootstock-mediated increase in leaf Na concentration is not correlated with improved shoot growth under low-K (this study) or under moderate salinity (Asins et al., 2015). This negative ACC-K interaction is supported by the fact that the sensitive *HcLk* graft combinations were the only ones registering an increase in xylem ACC (even though non-significant) under low-K (**Figure 5A**) and suffered the highest reduction in leaf K concentration (**Table 1**, **Figure 3A**). However, although ACC was the most negative hormonal factor correlated with shoot biomass under low-K (**Table 2**), ACC in the root xylem sap was not correlated with K concentrations either in the root xylem sap or in the leaves (data not shown), suggesting that other mechanisms are controlling K nutrition, such as the reallocation between old and young leaves (Amtmann and Armengaud, 2007). In addition, the correlation analysis suggests that the negative effect of ACC was mostly related to micronutrient (B, Mn, and Zn) uptake in the root xylem sap (data not shown), which was closely correlated with shoot biomass under low-K (**Table 2**). Indeed, the presence of this kind of HKT transporters in the tolerant *Hk* lines (putatively activated or upregulated by low ACC-ethylene and high Ca), that can transport a wide range of monovalent and divalent cations (Lan et al., 2010), could help to explain the higher concentration not only of K but also Zn, Mn, Fe, and B in those plants, particularly under low-K.

If ACC is a key factor regulating shoot performance under low-K in tomato by acting on nutrient transporters and/or in

other shoot growth-related processes in the shoot, it could be interesting to know how ACC levels are regulated in different rootstocks and its interaction with other hormones. According to PCA and correlation analysis, ACC was inversely correlated with CKs (mainly ZR), ABA, JA, and less significantly with SA (data not shown). Most of these hormones and their ratios with ACC were positively correlated with B, Mn, and Zn in the xylem (Data not shown) and with shoot biomass under low-K (**Table 2**).

ACC and its Interactions with Other Hormones Seem to Govern the Rootstock-Mediated Response to Low-K Supply

Long-term low-K supply decreased ACC and increased ZR (to the detriment of Z), iP, total CKs, JA (and the CK/ACC, ABA/ACC, and JA/ACC ratios) in the xylem sap of the high vigor *Hk* rootstocks, and those traits clustered with shoot growth parameters suggesting an important role for these hormones in the rootstock-mediated shoot vigor under low-K (**Figure 2**).

CKs are produced mainly in roots and translocated to the shoot through the xylem sap, playing a key role in root-to-shoot communication (Dodd et al., 2004; Albacete et al., 2008, 2009; Ghanem et al., 2011; Ko et al., 2014). Commonly, nutrient deprivation decreases CK concentration (Dodd et al., 2004; Cherkozianova et al., 2005; Rahayu et al., 2005) but the role of CKs in K signaling is poorly understood (Nam et al., 2012). Wang et al. (2012) found that K deficiency (0.03 mM treatment for 32 days) decreased CKs (ZR- and iP-type) concentration in the root xylem sap and leaves of cotton plants grafted onto sensitive rootstocks. In this study, low-K supply only decreased Z concentration in the root xylem sap of the tolerant *LcHk* plants, while iP and/or ZR increased in the *Hk* graft combinations under low-K. Indeed, a positive correlation exists in both studies between ZR, iP, and CK delivery to the shoot and plant performance measured as photosynthetic rate (Wang et al., 2012) or biomass (this study, **Table 2**), as expected from the role of CKs in delaying senescence and promoting plant growth (Gan and Amasino, 1995; Kurakawa et al., 2007).

Since the ZR/Z ratio in the root xylem sap was positively correlated with shoot biomass under control and low-K conditions (**Table 2**), and ZR levels increased in the high-vigor *Hk* plants while Z only decreased in the tolerant *LcHk* rootstocks, it can be suggested that ZR is a major form of CK transport in the root xylem while Z becomes the major form in the leaves (Albacete et al., 2008, 2009; Ghanem et al., 2011). An interconversion between Z and its storage form ZR in the root xylem could be a mechanism to adapt growth to nutrient (K) availability. This idea is supported by the reduced root biomass in the tolerant *LcHk* and by the positive correlation between ZR/Z and leaf K concentration (data not shown). This idea has been previously reported under salinity: increases in bioactive CKs (Z, iP, and their ribosides) and ZR/Z in mature leaves, root xylem sap and fruit were positively correlated with leaf biomass, chlorophyll fluorescence, shoot growth, and fruit yield in the tomato plants (i) grafted onto high and low vigor rootstocks from a RIL population derived from *S. lycopersicum* × *S. cheesmanii* cross (Albacete et al., 2009), or (ii) overproducing CKs through the heat-inducible (*HSP70::IPT*, as a whole plant) or constitutive (*35S::IPT*, as a rootstock) overexpression of the isopentenyltransferase (*IPT*) gene in the roots (Ghanem et al., 2011). In both cases, the improved salt tolerance mediated by an increased root CK production was related to improved K nutrition. However, the improved shoot growth and leaf K nutrition of the *Hk* rootstocks cannot be explained by increased K concentration in the root xylem and/or delivery (considering the xylem flow rate) to the shoot. A more specific mechanism must be operating, since the other nutrients analyzed in the leaves did not increase in the *Hk* plants, with the only exception of Ca (**Table 1**). Indeed, Ca signaling could explain not only the increased uptake of K but also an efficient re-location from older into young leaves by affecting K-transporters (Amtmann and Armengaud, 2007). In this regard, Nam et al. (2012), suggested that decreased CK levels and increases in ZR and ZR/Z ratio is a part of an ethylene mediated adaptive response to K deficiency in Arabidopsis.

CKs (negative) and ethylene (positive) seem to be antagonistic in regulating responses to low-K in Arabidopsis (Jung et al., 2009). A reduction in CK levels as a consequence of K deficiency (or in mutants affected in CK signaling or synthesis) allows fast and effective stimulation of ethylene-induced plant adaptation to low-K conditions (Nam et al., 2012). In our study, however, the CKs/ACC ratio was positively correlated with shoot biomass, suggesting that both hormones and the balance between them are important in determining the rootstock-effect on plant vigor at low-K supply, but with an inverse role in tomato compared to Arabidopsis (Albacete et al., 2009, 2015a). Consistent with these results, Albacete et al. (2009) found that the CKs/ACC ratio were closely correlated with leaf fresh weight and *Fv/Fm* in tomato plants grown under moderate salt stress. It is also possible that the CKs/ACC response is transient until optimal K status is recovered, thus reconciling short-term (Nam et al., 2012) and long-term (this study) results. Hence, different rootstock-mediated traits should be considered regarding those hormones: effect on K uptake in the roots (local) and on shoot growth (root-shoot communication).

K deficiency also induces JA biosynthetic genes such as those encoding lipoxygenase, allene oxide synthase, and allene oxide cyclase, suggesting an important role of JA in plant signaling in response to K deficiency (Armengaud et al., 2004; Wang and Wu, 2013). JA was lowest in the root xylem of sensitive *HcLk* plants under control conditions and increased significantly only in the high-vigor *HcHk* under low-K, suggesting that induced JA response can mediate plant response to low-K. Similarly, the tomato *res* (*root growth rescue under salinity*) mutant had high constitutive root JA and improved K nutrition especially under salt stress conditions compared to the WT (Garcia-Abellan et al., 2015). The JA/ethylene interaction must be investigated further since the JA/ACC ratio increased significantly in the tolerant *Hk* graft combinations and it was positively correlated not only with shoot biomass (**Table 2**) but also with Zn, Mn, and B in the root xylem sap (data not shown) under low-K supply.

SA has long been known to play a role in the induction of biotic defense mechanisms in plants; however, recent studies revealed that it also participates in abiotic stress signaling

(Jayakannan et al., 2015). SA concentration was not affected by low-K but it was 2 to 3-fold higher in the vigorous *HcHk* plants in both conditions. Moreover, SA was the only hormone positively correlated with leaf K concentration (data not shown). The fact that (i) interactions between JA, ABA, and SA have been reported in response to drought in tomato (Muñoz-Espinoza et al., 2015), (ii) SA might regulate anion and cation uptake through changes in the transmembrane electrical potential, H^+-ATPase activity and Na/K homeostasis (Jayakannan et al., 2015), and (iii) the only QTL detected in this experiment was related to the SA concentration in the rootstock-xylem sap (data not shown), guarantee further research on the role of SA in K use efficiency.

GAs were also detected in the root xylem sap and numerous studies suggest that these hormones interact with mineral nutrition (Rubio et al., 2009), as for K (Wakhloo, 1970; Chen et al., 2001), P, and Fe (Guo et al., 2015). By comparing the two contrasting graft combinations responding negatively (*HcLk*) or positively (*LcHk*) to low-K, GA_1, GA_3, and GA_4 levels decreased in the former while they were not affected in the later, contrarily to that observed for ACC, which suggest that GAs and ACC could be interacting in the rootstock-mediated response to low-K, as supported by the negative correlations found between those hormones in the root xylem sap (data not shown). Applying GA_3 enhances K uptake in rice (Chen et al. (2001), which is required for stem elongation, but also enhances micronutrient uptake, such as Fe and Mn (Guo et al., 2015), two micronutrients that are particularly high in the tolerant *LcHk* plants (**Table 1**).

The ABA/ACC ratio seems to positively regulate the growth response under low-K (as observed in *LcHk* and *HcHk* plants). In Arabidopsis, ABA negatively regulated the ethylene-responsive factors ERF1 and ERF6 (Cheng et al., 2013; Sewelam et al., 2013). ERF6 expression inhibits leaf growth by activating the transcription of the gibberellin2-oxidase-6 gene, resulting in inactivation of gibberellins, and DELLA stabilization under osmotic stress (Dubois et al., 2015). This model could help to explain the fact that levels of GAs and ACC in the root xylem sap under control conditions were positively and negatively related to plant growth under low-K, respectively (data not shown).

As shown in **Figure 7**, high ACC levels seem to favor a higher transport of Na probably in mediating cation transporters in LcLk rootstocks. The high ZR/Z ratio could contribute to reduce ACC concentrations, which may increase GA and Ca concentrations and improve micronutrients uptake in LcHk rootstocks under low-K. High constitutive SA and ABA or induced JA and CKs would help to decrease the ACC levels, thus would enhance macro and micronutrients uptake in HcHk rootstocks. Therefore, the results suggests that ACC-ethylene metabolism and signaling plays an important role by interacting with other plant hormones such as CKs, JA, SA, GAs, and ABA in the response to low-K probably by regulating ERF genes, as it seems to occur under other abiotic stresses (Müller and Munné-Bosch, 2015). These complex interactions affecting root development, nutrient uptake, root-shoot communication, and control of shoot growth and leaf senescence make it difficult to understand how the rootstock affects shoot performance but confirm grafting is a powerful tool to identify root traits for improving crops under abiotic stresses.

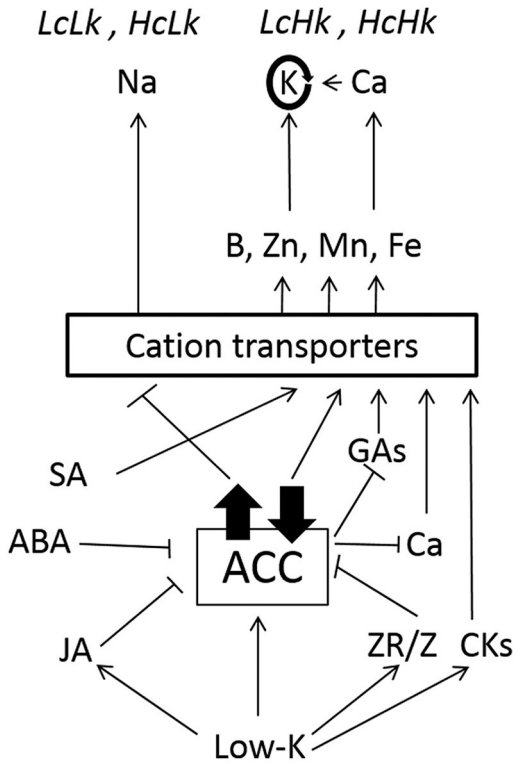

FIGURE 7 | Hormonal and nutritional interactions explaining rootstock-mediated responses to low-K supply. High constitutive or induced ACC levels would favor a higher transport of Na *vs.* K, probably in mediating HKT transporters in *LcLk*, *HcLk* plants. Reduced Z and increased ZR/Z would contribute to decrease ACC in *LcHk* plants, thus decreasing the impact on GAs and Ca levels and improving K, B, Zn, Mn, and Fe nutrition. High constitutive SA, ABA or induced JA and CKs would contribute to low ACC activity (metabolism and/or signaling) and improved macro and micronutrition in *HcHk* plants. Arrow or bar heads indicate positive and negative regulation, respectively.

AUTHOR CONTRIBUTIONS

CM-A, AA, and FP-A designed the research; CM-A, AA, and AM-P performed research; CM-A, AA, and AM-P performed data collection; CM-A and AA performed data analysis; CM-A, JP-P, and MJA performed data interpretation; JP-P and MJA performed critical revision of the article; CM-A and FP-A drafted the article; JP-P, MJA, and FP-A carried out approval of the final version.

FUNDING

This research has received funding from the Spanish MINECO-FEDER (project AGL2014-59728-R) and from the European Union's Seventh Framework Programme for research, technological development and demonstration under grant agreement no 289365 (project ROOTOPOWER).

ACKNOWLEDGMENTS

We are very grateful to Prof. Ian C. Dodd and Dr. Francisco Rubio for critical reading and constructive criticism. We also thank Mr. Aquilino Sánchez (Unigenia Bioscience) for his helpful technical assistance with grafted plants.

SUPPLEMENTARY MATERIAL

The Supplementary Material for this article can be found online at: http://journal.frontiersin.org/article/10.3389/fpls.2016.01782/full#supplementary-material

Table S1 | Two way ANOVA for the effects of the genotype and treatment on shoot fresh weight (SFW), K use efficiency (KUE) and K concentration in leaf (K leaf). The numbers in the table are F- and P-values.

Figure S1 | Shoot fresh weight (SFW) correlation between control (C) and low K condition (K) of tomato plants (*Solanum lycopersicum* cv. Boludo F1) grafted onto a population of recombinant inbred lines (RILs) from across between *Solanum lycopersicum* × *Solanum pimpinellifolium*. Lines enclosed by circles indicate the selected grafted lines within each group used in this study. *H,* high vigor; *L,* low vigor; *c,* control conditions; *k,* low K conditions. $^{**}P < 0.01$.

Figure S2 | Sap flow of the scion (*Solanum lycopersicum* cv. Boludo F1) grafted onto a population of recombinant inbred lines (RILs) from a cross between *Solanum lycopersicum* × *Solanum pimpinellifolium* with high (H) or low (L) vigor growing under standard (c) and low K (k) conditions during 48 days. Different letters indicate significant differences among graft combinations ($n = 12$, $P < 0.05$) within each treatment. *indicate significant differences between control and K-deprived plants accoding to the Tuckey test ($P < 0.05$).

Figure S3 | Giberellin A1 (GA1) (A), gibberellin A3 (GA3) **(B)** gibberellin A4 (GA4) **(C)** and total gibberellins (Total GAs) **(D)** concentrations in xylem sap of the scion (*Solanum lycopersicum* cv. Boludo F1) grafted onto a population of recombinant inbred lines (RILs) from a cross between *Solanum lycopersicum* × *Solanum pimpinellifolium* with high (H) or low (L) vigor growing under standard (c) and low K (k) conditions during 48 days. Different letters indicate significant differences among graft combinations ($n = 12$, $P < 0.05$) within each treatment. *indicate significant differences between control and K-deprived plants according to the Tuckey test ($P < 0.05$).

REFERENCES

Albacete, A., Andújar, C., Dodd, I., Giuffrida, F., Hichri, I., Lutts, S., et al. (2015a). Rootstock-mediated variation in tomato vegetative growth under drought, salinity and soil impedance stresses. *Acta Hortic.* 1086, 141–146. doi: 10.17660/actahortic.2015.1086.17

Albacete, A., Andújar, C., Pérez-Alfocea, F., Lozano, J., and Asins, M. (2015b). Rootstock-mediated variation in tomato vegetative growth under low potassium or phosphorous supplies. *Acta Hortic.* 1086, 147–152. doi: 10.17660/actahortic.2015.1086.18

Albacete, A., Ghanem, M. E., Martínez-Andújar, C., Acosta, M., Sánchez-Bravo, J., Martínez, V., et al. (2008). Hormonal changes in relation to biomass partitioning and shoot growth impairment in salinized tomato (*Solanum lycopersicum* L.) plants. *J. Exp. Bot.* 59, 4119–4131. doi: 10.1093/jxb/ern251

Albacete, A., Martínez-Andújar, C., Ghanem, M. E., Acosta, M., Sánchez-Bravo, J., Asins, M. J., et al. (2009). Rootstock-mediated changes in xylem ionic and hormonal status are correlated with delayed leaf senescence, and increased leaf area and crop productivity in salinized tomato. *Plant Cell Environ.* 32, 928–938. doi: 10.1111/j.1365-3040.2009.01973.x

Amtmann, A., and Armengaud, P. (2007). The role of calcium sensor-interacting protein kinases in plant adaptation to potassium-deficiency: new answers to old questions. *Cell Res.* 17, 483–485. doi: 10.1038/cr.2007.49

Armengaud, P., Breitling, R., and Amtmann, A. (2004). The potassium-dependent transcriptome of arabidopsis reveals a prominent role of jasmonic acid in nutrient signaling. *Plant Physiol.* 136, 2556–2576. doi: 10.1104/pp.104.046482

Asins, M. J., Bolarín, M. C., Pérez-Alfocea, F., Estañ, M. T., Martínez-Andújar, C., Albacete, A., et al. (2010). Genetic analysis of physiological components of salt tolerance conferred by Solanum rootstocks. What is the rootstock doing for the scion? *Theor. Appl. Genet.* 121, 105–115. doi: 10.1007/s00122-010-1294-9

Asins, M. J., Raga, V., Roca, D., Belver, A., and Carbonell, E. A. (2015). Genetic dissection of tomato rootstock effects on scion traits under moderate salinity. *Theor. Appl. Genet.* 128, 667–679. doi: 10.1007/s00122-015-2462-8

Atherton, J. G., and Rudich, J. (1986). *The Tomato Crop*. London: Chapman and Hall.

Besford, R. T., and Maw, G. A. (1975). Effect of potassium nutrition on tomato plant growth and fruit development. *Plant Soil* 42, 395–412. doi: 10.1007/BF00010015

Cadahia, C., Hassan, I., and Eymar, E. (1995). Incidence of the potassium/calcium plus magnesium ratio on the conifer fertigation for peat substrates. *J. Plant Nutr.* 18, 23. doi: 10.1080/01904169509364881

Cao, S., Su, L., and Fang, Y. (2006). Evidence for involvement of jasmonic acid in the induction of leaf senescence by potassium deficiency in Arabidopsis. *Can. J. Bot.* 84, 328–333. doi: 10.1139/b06-001

Chen, L., Nishizawa, T., Higashitani, A., Suge, H., Wakui, Y., Takeda, K., et al. (2001). A variety of wheat tolerant to deep-seeding conditions: elongation of the first internode depends on the response to gibberellin and potassium. *Plant Cell Environ.* 24, 469–476. doi: 10.1046/j.1365-3040.2001.00688.x

Cheng, M.-C., Liao, P.-M., Kuo, W.-W., and Lin, T.-P. (2013). The Arabidopsis ETHYLENE RESPONSE FACTOR1 regulates abiotic stress-responsive gene expression by binding to different cis-acting elements in response to different stress signals. *Plant Physiol.* 162, 1566–1582. doi: 10.1104/pp.113.221911

Chérel, I., Lefoulon, C., Boeglin, M., and Sentenac, H. (2014). Molecular mechanisms involved in plant adaptation to low K^+ availability. *J. Exp. Bot.* 65, 833–848. doi: 10.1093/jxb/ert402

Cherkozianova, A. V., Vysotskaya, L. B., Veselov, S. Y., and Kudoyarova, G. R. (2005). Hormonal control of the shoot-to-root ratio is not related to water deficiency in wheat plants under mineral deficiency. *Russ. J. Plant Physiol.* 52, 629–634. doi: 10.1007/s11183-005-0093-7

Colla, G., Suārez, C. M. C., Cardarelli, M., and Rouphael, Y. (2010). Improving nitrogen use efficiency in melon by grafting. *HortScience* 45, 559–565.

Demidchik, V., and Maathuis, F. J. M. (2007). Physiological roles of nonselective cation channels in plants: from salt stress to signalling and development. *New Phytol.* 175, 387–404. doi: 10.1111/j.1469-8137.2007.02128.x

Dodd, I. C., Ngo, C., Turnbull, C. G. N., and Beveridge, C. A. (2004). Effects of nitrogen supply on xylem cytokinin delivery, transpiration and leaf expansion of pea genotypes differing in xylem-cytokinin concentration. *Func. Plant Biol.* 31, 903–911. doi: 10.1071/FP04044

Dubois, M., Van Den Broeck, L., Claeys, H., Van Vlierberghe, K., Matsui, M., and Inzé, D. (2015). The ETHYLENE RESPONSE FACTORs ERF6 and ERF11 antagonistically regulate mannitol-induced growth inhibition in Arabidopsis. *Plant Physiol.* 169, 166–179. doi: 10.1104/pp.15.00335

Estañ, M. T., Villalta, I., Bolarín, M. C., Carbonell, E. A., and Asins, M. J. (2009). Identification of fruit yield loci controlling the salt tolerance conferred by solanum rootstocks. *Theor. Appl. Genet.* 118, 305–312. doi: 10.1007/s00122-008-0900-6

Fageria, N. K., Baligar, V. C., and Li, Y. C. (2008). The role of nutrient efficient plants in improving crop yields in the twenty first century. *J. Plant Nutr.* 31, 1121–1157. doi: 10.1080/01904160802116068

Fan, M., Huang, Y., Zhong, Y., Kong, Q., Xie, J., Niu, M., et al. (2014). Comparative transcriptome profiling of potassium starvation responsiveness in two contrasting watermelon genotypes. *Planta* 239, 397–410. doi: 10.1007/s00425-013-1976-z

Gan, S., and Amasino, R. M. (1995). Inhibition of leaf senescence by autoregulated production of cytokinin. *Science* 270, 1986–1988. doi: 10.1126/science.270.5244.1986

Garcia-Abellan, J. O., Fernandez-Garcia, N., Lopez-Berenguer, C., Egea, I., Flores, F. B., Angosto, T., et al. (2015). The tomato res mutant which accumulates

JA in roots in non-stressed conditions restores cell structure alterations under salinity. *Physiol. Plant.* 155, 296–314. doi: 10.1111/ppl.12320

García, M. J., Romera, F. J., Lucena, C., Alcántara, E., and Pérez-Vicente, R. (2015). Ethylene and the regulation of physiological and morphological responses to nutrient deficiencies. *Plant Physiol.* 169, 51–60. doi: 10.1104/pp.15.00708

Ghanem, M. E., Hichri, I., Smigocki, A. C., Albacete, A., Fauconnier, M. L., Diatloff, E., et al. (2011). Root-targeted biotechnology to mediate hormonal signalling and improve crop stress tolerance. *Plant Cell Rep.* 30, 807–823. doi: 10.1007/s00299-011-1005-2

Guo, H., Wang, Y., Liu, H., Hu, P., Jia, Y., Zhang, C., et al. (2015). Exogenous GA3 application enhances xylem development and induces the expression of secondary wall biosynthesis related genes in Betula platyphylla. *Int. J. Mol. Sci.* 16, 22960–22975. doi: 10.3390/ijms160922960

Hafsi, C., Debez, A., and Abdelly, C. (2014). Potassium deficiency in plants: effects and signaling cascades. *Acta Physiol. Plant.* 36, 1055–1070. doi: 10.1007/s11738-014-1491-2

Huang, Y., Li, J., Hua, B., Liu, Z., Fan, M., and Bie, Z. (2013). Grafting onto different rootstocks as a means to improve watermelon tolerance to low potassium stress. *Sci. Hortic.* 149, 80–85. doi: 10.1016/j.scienta.2012.02.009

Jayakannan, M., Bose, J., Babourina, O., Rengel, Z., and Shabala, S. (2015). Salicylic acid in plant salinity stress signalling and tolerance. *Plant Growth Regul.* 76, 25–40. doi: 10.1007/s10725-015-0028-z

Jiang, C., Belfield, E. J., Cao, Y., Smith, J. A., and Harberd, N. P. (2013). An Arabidopsis soil-salinity–tolerance mutation confers ethylene-mediated enhancement of sodium/potassium homeostasis. *Plant Cell* 25, 3535–3552. doi: 10.1105/tpc.113.115659

Jung, J. Y., Shin, R., and Schachtman, D. P. (2009). Ethylene mediates response and tolerance to potassium deprivation in arabidopsis. *Plant Cell* 21, 607–621. doi: 10.1105/tpc.108.063099

Kanai, S., Moghaieb, R. E., El-Shemy, H. A., Panigrahi, R., Mohapatra, P. K., Ito, J., et al. (2011). Potassium deficiency affects water status and photosynthetic rate of the vegetative sink in green house tomato prior to its effects on source activity. *Plant Sci.* 180, 368–374. doi: 10.1016/j.plantsci.2010.10.011

Kanai, S., Ohkura, K., Adu-Gyamfi, J. J., Mohapatra, P. K., Nguyen, N. T., Saneoka, H., et al. (2007). Depression of sink activity precedes the inhibition of biomass production in tomato plants subjected to potassium deficiency stress. *J. Exp. Bot.* 58, 2917–2928. doi: 10.1093/jxb/erm149

Ko, D., Kang, J., Kiba, T., Park, J., Kojima, M., Do, J., et al. (2014). Arabidopsis ABCG14 is essential for the root-to-shoot translocation of cytokinin. *Proc. Natl. Acad. Sci. U.S.A.* 111, 7150–7155. doi: 10.1073/pnas.1321519111

Kurakawa, T., Ueda, N., Maekawa, M., Kobayashi, K., Kojima, M., Nagato, Y., et al. (2007). Direct control of shoot meristem activity by a cytokinin-activating enzyme. *Nature* 445, 652–655. doi: 10.1038/nature05504

Lan, W.-Z., Wang, W., Wang, S.-M., Li, L.-G., Buchanan, B. B., Lin, H.-X., et al. (2010). A rice high-affinity potassium transporter (HKT) conceals a calcium-permeable cation channel. *Proc. Natl. Acad. Sci. U.S.A.* 107, 7089–7094. doi: 10.1073/pnas.1000698107

Leonardi, C., and Giuffrida, F. (2006). Variation of plant growth and macronutrient uptake in grafted tomatoes and eggplants on three different rootstocks. *Eur. J. Hortic. Sci.* 71, 97–101. Available online at: https://www.researchgate.net/publication/235799269

Li, J., Long, Y., Qi, G. N., Xu, Z. J., Wu, W. H., and Yi, W. (2014). The Os-AKT1 channel is critical for K+ uptake in rice roots and is modulated by the rice CBL1-CIPK23 complex. *Plant Cell* 26, 3387–3402. doi: 10.1105/tpc.114.123455

Marschner, H. (1995). "11 - relationships between mineral nutrition and plant diseases and pests," in *Mineral Nutrition of Higher Plants, 2nd Edn,* ed H. Marschner (London: A*cademic Press)*, 436–460.

Maxwell, K., and Johnson, G. N. (2000). Chlorophyll fluorescence - a practical guide. *J. Exp. Bot.* 51, 659–668. doi: 10.1093/jexbot/51.345.659

Monforte, A. J., Asíns, M. J., and Carbonell, E. A. (1997). Salt tolerance in Lycopersicon species. V. Does genetic variability at quantitative trait loci affect their analysis? *Theor. Appl. Genet.* 95, 284–293. doi: 10.1007/s001220050561

Müller, M., and Munné-Bosch, S. (2015). Ethylene response factors: a key regulatory hub in hormone and stress signaling. *Plant Physiol.* 169, 32–41. doi: 10.1104/pp.15.00677

Muñoz-Espinoza, V. A., López-Climent, M. F., Casaretto, J. A., and Gómez-Cadenas, A. (2015). Water stress responses of tomato mutants impaired in hormone biosynthesis reveal abscisic acid, jasmonic acid and salicylic acid interactions. *Front. Plant Sci.* 6:997. doi: 10.3389/fpls.2015.00997

Nam, Y.-J., Tran, L.-S. P., Kojima, M., Sakakibara, H., Nishiyama, R., and Shin, R. (2012). Regulatory roles of cytokinins and cytokinin signaling in response to potassium deficiency in Arabidopsis. *PLoS ONE* 7:e47797. doi: 10.1371/journal.pone.0047797

Netting, A. G., Theobald, J. C., and Dodd, I. C. (2012). Xylem sap collection and extraction methodologies to determine *in vivo* concentrations of ABA and its bound forms by gas chromatography-mass spectrometry (GC-MS). *Plant Methods* 8:11. doi: 10.1186/1746-4811-8-11

Penella, C., Nebauer, S. G., Quiñones, A., San Bautista, A., López-Galarza, S., and Calatayud, A. (2015). Some rootstocks improve pepper tolerance to mild salinity through ionic regulation. *Plant Sci.* 230, 12–22. doi: 10.1016/j.plantsci.2014.10.007

Pérez-Alfocea, F. (2015). Why should we Investigate vegetable grafting? *Acta Hortic.* 21–30. doi: 10.17660/ActaHortic.2015.1086.1

Pottosin, I., Velarde-Buendía, A. M., and Dobrovinskaya, O. (2014). Potassium and sodium transport channels under nacl stress. *Physiol. Mech. Adapt. Strateg Plants Chang. Environ.* 2, 325–359. doi: 10.1007/978-1-4614-8600-8_12

Qi, H.-Y., Li, T.-L., Liu, Y.-F., and Li, D. (2006). Effects of grafting on photosynthesis characteristics, yield and sugar content in melon. *J. Shenyang Agric. Univ.* 37, 155–158.

Rahayu, Y. S., Walch-Liu, P., Neumann, G., Römheld, V., Von Wirén, N., and Bangerth, F. (2005). Root-derived cytokinins as long-distance signals for NO3 –induced stimulation of leaf growth. *J. Exp. Bot.* 56, 1143–1152. doi: 10.1093/jxb/eri107

Rouphael, Y., Cardarelli, M., Colla, G., and Rea, E. (2008a). Yield, mineral composition, water relations, and water use efficiency of grafted mini-watermelon plants under deficit irrigation. *HortScience* 43, 730–736. Available online at: hortsci.ashspublications.org/content/43/3/730

Rouphael, Y., Cardarelli, M., Rea, E., and Colla, G. (2008b). Grafting of cucumber as a means to minimize copper toxicity. *Environ. Exp. Bot.* 63, 49–58. doi: 10.1016/j.envexpbot.2007.10.015

Ruan, L., Zhang, J., Xin, X., Zhang, C., Ma, D., Chen, L., et al. (2015). Comparative analysis of potassium deficiency-responsive transcriptomes in low potassium susceptible and tolerant wheat (*Triticum aestivum* L.). *Sci. Rep.* 5, 743–747. doi: 10.1038/srep10090

Rubio, V., Bustos, R., Irigoyen, M., Cardona-López, X., Rojas-Triana, M., and Paz-Ares, J. (2009). Plant hormones and nutrient signaling. *Plant Mol. Biol.* 69, 361–373. doi: 10.1007/s11103-008-9380-y

Salehi, R., Kashi, A., Lee, J. M., Babalar, M., Delshad, M., Lee, S. G., et al. (2010). Leaf gas exchanges and mineral ion composition in xylem sap of iranian melon affected by rootstocks and training methods. *HortScience* 45, 766–770. Available online at: hortsci.ashspublications.org/content/45/5/76

Savvas, D., Colla, G., Rouphael, Y., and Schwarz, D. (2010). Amelioration of heavy metal and nutrient stress in fruit vegetables by grafting. *Sci. Hortic.* 127, 156–161. doi: 10.1016/j.scienta.2010.09.011

Savvas, D., Savva, A., Ntatsi, G., Ropokis, A., Karapanos, I., Krumbein, A., et al. (2011). Effects of three commercial rootstocks on mineral nutrition, fruit yield, and quality of salinized tomato. *J. Plant Nutr. Soil Sci.* 174, 154–162. doi: 10.1002/jpln.201000099

Schwarz, D., Öztekin, G. B., Tüzel, Y., Brückner, B., and Krumbein, A. (2013). Rootstocks can enhance tomato growth and quality characteristics at low potassium supply. *Sci. Hortic.* 149, 70–79. doi: 10.1016/j.scienta.2012.06.013

Sewelam, N., Kazan, K., Thomas-Hall, S. R., Kidd, B. N., Manners, J. M., and Schenk, P. M. (2013). Ethylene response factor 6 is a regulator of reactive oxygen species signaling in Arabidopsis. *PLoS ONE* 8:e70289. doi: 10.1371/journal.pone.0070289

Shin, R., Berg, R. H., and Schachtman, D. P. (2005). Reactive oxygen species and root hairs in arabidopsis root response to nitrogen, phosphorus and potassium deficiency. *Plant Cell Physiol.* 46, 1350–1357. doi: 10.1093/pcp/pci145

Shin, R., and Schachtman, D. P. (2004). Hydrogen peroxide mediates plant root cell response to nutrient deprivation. *Proc. Natl. Acad. Sci. U.S.A.* 101, 8827–8832. doi: 10.1073/pnas.0401707101

Singh, P., and Blanke, M. (2000). Deficiency of potassium but not phosphorus enhances root respiration. *Plant Growth Regul.* 32, 77–81. doi: 10.1023/A:1006397611793

Wakhloo, J. L. (1970). Role of mineral nutrients and growth regulators in the apical dominance in *Solanum sisymbrifolium*. *Planta* 91, 190–194. doi: 10.1007/BF00385477

Wang, Y., Li, B., Du, M., Eneji, A. E., Wang, B., Duan, L., et al. (2012). Mechanism of phytohormone involvement in feedback regulation of cotton leaf senescence induced by potassium deficiency. *J. Exp. Bot.* 63, 5887–5901. doi: 10.1093/jxb/ers238

Wang, Y., and Wu, W.-H. (2013). Potassium transport and signaling in higher plants. *Annu. Rev. Plant Biol.* 64, 451–476. doi: 10.1146/annurev-arplant-050312-120153

Yang, C., Ma, B., He, S. J., Xiong, Q., Duan, K. X., Yin, C. C., et al. (2015). MAOHUZI6/ETHYLENE INSENSITIVE3-LIKE1 and ETHYLENE INSENSITIVE3-LIKE2 regulate ethylene response of roots and coleoptiles and negatively affect salt tolerance in rice. *Plant Physiol.* 169, 148–165. doi: 10.1104/pp.15.00353

Zhu, J., Bie, Z., Huang, Y., and Han, X. (2008). Effect of grafting on the growth and ion concentrations of cucumber seedlings under NaCl stress. *Soil Sci. Plant Nutr.* 54, 895–902. doi: 10.1111/j.1747-0765.2008.00306.x

Conflict of Interest Statement: The authors declare that the research was conducted in the absence of any commercial or financial relationships that could be construed as a potential conflict of interest.

The reviewer AC declared a shared affiliation, though no other collaboration, with one of the authors MJA to the handling Editor, who ensured that the process nevertheless met the standards of a fair and objective review.

frontiers in Plant Science

ORIGINAL RESEARCH
published: 19 May 2016
doi: 10.3389/fpls.2016.00696

Ethylene Antagonizes Salt-Induced Growth Retardation and Cell Death Process via Transcriptional Controlling of Ethylene-, BAG- and Senescence-Associated Genes in *Arabidopsis*

Ya-Jie Pan[1], *Ling Liu*[1], *Ying-Chao Lin*[1,2], *Yuan-Gang Zu*[1], *Lei-Peng Li*[1]* and *Zhong-Hua Tang*[1]*

[1] Key Laboratory of Plant Ecology, Northeast Forestry University, Harbin, China, [2] Guizhou Academy of Tobacco Research, Guiyang, China

OPEN ACCESS

Edited by:
Antonio Ferrante,
Università degli Studi di Milano, Italy

Reviewed by:
Alessandra Francini,
Scuola Superiore Sant'Anna, Italy
Alice Trivellini,
Scuola Superiore Sant'Anna, Italy

***Correspondence:**
Lei-Peng Li
82192098@163.com;
Zhong-Hua Tang
tangzh@nefu.edu.cn

Specialty section:
This article was submitted to Plant Physiology, a section of the journal Frontiers in Plant Science

Received: *18 December 2015*
Accepted: *06 May 2016*
Published: *19 May 2016*

Citation:
Pan Y-J, Liu L, Lin Y-C, Zu Y-G, Li L-P and Tang Z-H (2016) Ethylene Antagonizes Salt-Induced Growth Retardation and Cell Death Process via Transcriptional Controlling of Ethylene-, BAG- and Senescence-Associated Genes in Arabidopsis. Front. Plant Sci. 7:696. doi: 10.3389/fpls.2016.00696

The existing question whether ethylene is involved in the modulation of salt-induced cell death to mediate plant salt tolerance is important for understanding the salt tolerance mechanisms. Here, we employed *Arabidopsis* plants to study the possible role of ethylene in salt-induced growth inhibition and programmed cell death (PCD) profiles. The root length, DNA ladder and cell death indicated by Evan's blue detection were measured by compared to the control or salt-stressed seedlings. Secondly, the protoplasts isolated from plant leaves and dyed with Annexin V-FITC were subjected to flow cytometric (FCM) assay. Our results showed that ethylene works effectively in seedling protoplasts, antagonizing salt-included root retardation and restraining cell death both in seedlings or protoplasts. Due to salinity, the entire or partial insensitivity of ethylene signaling resulted in an elevated levels of cell death in *ein2-5* and *ein3-1* plants and the event were amended in *ctr1-1* plants after salt treatment. The subsequent experiment with exogenous ACC further corroborated that ethylene could modulate salt-induced PCD process actively. Plant Bcl-2-associated athanogene (BAG) family genes are recently identified to play an extensive role in plant PCD processes ranging from growth, development to stress responses and even cell death. Our result showed that salinity alone significantly suppressed the transcripts of BAG6, BAG7 and addition of ACC in the saline solution could obviously re-activate *BAG6* and *BAG7* expressions, which might play a key role to inhibit the salt-induced cell death. In summary, our research implies that ethylene and salinity antagonistically control BAG family-, ethylene-, and senescence-related genes to alleviate the salt-induced cell death.

Keywords: ***Arabidopsis*, ethylene, salinity, cell death, BAG family gene**

INTRODUCTION

Salinity is one of the major abiotic stresses that adversely affect plant growth and crop productivity (Zhu, 2001; Flowers, 2004; Munns and Tester, 2008). Salt stress in plant cells is primarily caused by a combination of osmotic stress and salt-specific damage resulting from high Na+ concentration in the saline solution (James et al., 2006; Yang et al., 2013; Zhu et al., 2016). To antagonize salt-induced ionic toxicity, it has been largely documented that plants evolves lines of adaptive strategies to improve salt tolerance, mainly via minimizing Na+ buildup in photosynthetic organs (James et al., 2006) or retaining defined K+ level and K+/Na+ ratio in shoot (Agarie et al., 2007; Genc et al., 2007; Shabala, 2009). Shoot Na+ homeostasis of *Arabidopsis* plants grown in saline soils is conferred by reactive oxygen species (ROS) regulation of xylem-sap Na+ concentrations (Jiang et al., 2012). Simultaneously, osmotic and ionic stresses generate a cascade of secondary effect, including oxidative stress due to enhanced reactive oxygen species (ROS; Steffens and Sauter, 2009; Jiang et al., 2012; Yang et al., 2014), nutrient deficiency (Jiang et al., 2013), impaired photosynthetic system (James et al., 2006), and, consequently, cell death and growth reduction (Achard et al., 2006; Jha and Subramanian, 2014). Among various cues, salt-induced cell death has currently emerged as one of the most crucial components in plant salt responses (Affenzeller et al., 2009; Shabala, 2009; Andronis and Roubelakis-Angelakis, 2010; Hoang et al., 2015).

Programmed cell death (PCD) is one kind of physiological cell death and genetically determined process, present in both plant and animal cells (van Doorn and Woltering, 2004; Kabbage and Dickman, 2008; Steffens and Sauter, 2009). Recent studies have established that control of programmed cell death (PCD) pathways can be an important component that controls the outcome of a given stress response in plants (Li et al., 2016). At the physiological level, several morphological and biochemical similarities between apoptosis and plant PCD have been described, including DNA laddering, caspase-like proteolytic activity and cytochrome *c* release from mitochondria (Hoeberichts and Woltering, 2003; Andronis and Roubelakis-Angelakis, 2010). The earlier indicator of PCD before DNA fragmentation is the exposure of phosphatidylserine (PS) on the outer surface of plasma membrane, which can be monitored by flow cytometry (FCM) with a fluorescent conjugate of Annexin V-FITC (O'Brien et al., 1997; Pennell and Lamb, 1997; Halweg et al., 2005). PS exposure has been proved to be an earlier and preferential hallmark for plant PCD than DNA fragmentation measured by TUNEL assay (O'Brien et al., 1997). At the level of transcription, the plant *BAG* family genes have been identified to play an important role in plant PCD processes, which ranges from development, fungal resistance to abiotic stresses (Kabbage and Dickman, 2008; Fang et al., 2013; Li et al., 2016). Currently, seven members of the *Arabidopsis thaliana BAG* family genes have been identified (*AtBAG1-7*) and they might participate in plant PCD conferring plant tolerance to stresses (Fang et al., 2013). For example, the exogenous expression of *AtBAG4* in rice significantly improved salt tolerance at the whole plant level possibly through maintaining redox states (Hoang et al., 2015). More recent report showed that the *Arabidopsis bag6* knockout lines showed a more rapidly spreading cell death and higher sensitivity upon fungal pathogen (Li et al., 2016).

Plant PCD process is strictly mediated by hormone signals, such as ethylene, ABA or SA (Asai et al., 2000; Kim et al., 2010). Meanwhile, they often act in conjunction, like ABA and GA in barley aleurone layers, or SA and ethylene in HR-induced cell death (Hoeberichts and Woltering, 2003). Ethylene has been proven to be one of the positive regulators of PCD process during development under normal condition (Yamada and Marubashi, 2003; Bouchez et al., 2007). In *Arabidopsis*, ethylene stimulates the expression of senescence-associated genes (*ANACO29, ANACO92, RPK, SAG, ATG GBF*, and *GDH*) (Kim et al., 2015) and ethylene-related genes (*ERS2, ERF1, ACS2, ETR2*, and *EIN3*) (Fang et al., 2013). On the other hand, ethylene promotes the homeostasis of Na+/K+, nutrients and ROS to enhance plant tolerance to salinity (Tao et al., 2015). The salinity-induced ethylene signal is transduced mainly through the classical receptors-CTR1-EIN2-EIN3 pathway to regulate many effectors involved in plant growth and salinity response (Jiang et al., 2013; Yang et al., 2013; Li et al., 2015; Poór et al., 2015). Although ethylene alone is not sufficient to trigger PCD in plants, the cadmium- or camptothecin-induced cell death and the associated oxidative burst can be blocked by inhibition of ethylene signaling (de et al., 2002; Hoeberichts and Woltering, 2003; Yakimova et al., 2006). This evidence predicts the critical role of ethylene in mediating salt adaptation with respect to PCD pathway.

Regarding the ethylene signaling mutation, the loss of function of CTR1 generates *Arabidopsis* mutant *ctr1-1*, which shows constitutive ethylene responses (Chen et al., 2005). Downstream of EIN2, EIN3 transcription factor stimulate the expression of ethylene response target genes and the ethylene mutants *ein2-5* and *ein3-1* show entirely or partly ethylene insensitivity (Bleecker and Kende, 2000; Guo and Ecker, 2004). Here, the mutants affected in ethylene signaling together with wild-type Col-0 were employed to dissect the role of ethylene during salt-induced PCD process. The salt-stressed seedlings of various accessions are applied into comparison of the PCD processes through the assays of DNA fragmentation and PS exposure. Secondly, the wild-type plant protoplasts were isolated and directly treated with salinity to confirm the blocked action of exogenous ethylene releaser on the salt-induced PCD hallmarks. Further, the transcript abundance of 7 *BAG* family genes were analyzed and compared with that of ethylene-associated and senescence-related genes. Our results revealed that ethylene tightly antagonized the process of salt-induced cell death to confer plant salt tolerance.

Abbreviations: ACC, 1-aminocyclopropane-1-carboxylic acid; *ACS2*, 1-aminocyclopropane 1-carboxylate (ACC) synthase 2; *BAG*, Bcl-2-associated gene; CTAB, Cetyltrimethyl ammonium bromide; *CTR*, Constitutive triple response; DPI, Diphenylene iodonium; *EBF*, *EIN3*-binding F-box; *EIN2*, Ethylene insensitive 2; *EIN3*, Ethylene insensitive 3; *ERF1*, Ethylene response factor 1; *ERS2*, Ethylene response sensor 2; *ETR2*, Ethylene receptor 2; FCM, Flow cytometry; *GBF*, G box binding factor; *GDH*, Glutamate dehydrogenase isoenzyme; PCA, Principal component analysis; PCD, Programmed cell death; PS, phosphatidylserine; *RPK*, Receptor-like protein kinase; *SAG*, Senescence associated genes.

MATERIALS AND METHODS

Plant Materials and Treatments

Arabidopsis thaliana mutants employed in this study were in the Col-0 background (WT), including *ein2-5*, *ein3-1* and *ctr1-1* mutants, kindly provided by Prof. Hong-Wei Guo from Peking University. Seeds were surface sterilized by 70% ethanol solution containing 1% Triton X-100. They were washed with ethanol and dried under sterile conditions.

Experiment 1

The sterilized seeds were then placed on agar plates including 0.8 fold MS salt, 1% sucrose, and pH 5.7, 0.6% Agar supplemented with 0, 50, 100, or 150 mM NaCl. All the plates were kept at 4°C in the dark for 4 d to synchronize germination, and then transferred to light at 23°C under a 16/8 light/dark cycle and a light intensity of approximately 220 mmol m^{-2} s^{-1} as described previously (Yang et al., 2013). After 14 d of germination, the root length and DNA ladder in NaCl-treated and control seedlings were measured (Jacyn Baker and Mock, 1994). Each treatment was replicated three times.

Experiment 2

The 7-d-old seedlings in the control medium were transferred to perlite/sand (1:1) irrigated daily with 1/2 strength Hoagland solution. After 7 d of transfer, Col-0 (WT) seedlings were collected from petri dishes after following treatments: for the measurements of PCD, Control (non-saline), 50 mM NaCl, 100 mM NaCl for 14 d; for the measurements of gene expression, Control (non-saline), 100 mM or 100 mM NaCl + 50 μM ACC NaCl for 14 d; for the measurements of protoplast PCD, Control (non-saline), 200 mM NaCl and 200 mM NaCl + 10 μM ACC, the leaves of Col-0 (WT) seedlings were bulked and used for isolation of protoplasts (Yang et al., 2014). Early PCD levels in protoplasts were measured at 10, 20, 30, 60, 90, 120, 150 min after treatments, respectively. The isolated protoplasts were simultaneously incubated in salt condition (200 mM NaCl) in the presence of 10 μM ACC, 10 μM DPI (inhibitor of NADPH oxidases, Sigma-Aldrich) or 10μM ACC + 5 mM H_2O_2. PCD profile was measured after 150 min of treatments. The DPI stock solution was prepared in 100% DMSO.

Measurement of Root Length

Seedling images were taken from the bottom of the plates using a scanner (Epson, Suwa, Japan). Root length was measured using the Neuron J plugin (Meijering et al., 2004) for Image J (Schneider et al., 2012). Three replicates were performed and every replicate used 5 plants.

DNA Extraction and Analysis

Additionally, an accepted biochemical criterion is the detection of an oligosomal DNA ladder the rungs of which are multiples of 180 bp. This ladder is due to a caspase-activated DNase that degrades DNA during apoptosis (Enari et al., 1998). *Arabidopsis* genomic DNA was extracted according to the CTAB method. Leaf tissues were ground in liquid N_2 immediately after being collected from the plants and then the frozen samples were homogenized in an extraction buffer that contained 2% CTAB, 100 mM Tris-HCl, 20 mM EDTA, pH 8.0 and 1.4 mmol NaCl, and the mix incubated at 65°C for 1 h. DNA electrophoresis was performed to assay DNA fragmentation. DNA samples of 5 μg DNA (per lane) were loaded on a 1.8% agarose gel at constant 70 V. The DNA was visualized by staining with 0.3 μg mL^{-1} ethidium bromide.

Protoplasts Preparation

Protoplasts were isolated according to the report (Halweg et al., 2005) and the protocol was modified for our specific application. The rosette leaves mentioned above were used to prepare protoplast and the leaf blade were cut into pieces of 0.5–1 cm^2 and placed upside down without midribon in a sterile petri-dish with 10 mL of protoplast solution. The protoplast solution was composed of 0.4 M mannitol, 5 mM MES and 8 mM $CaCl_2$, pH 5.6, 1% of cellulase R-10 (Yakult, Japan), 0.25% macerozyme R-10 (Yakult, Japan), and 0.03% Bovine serum albumin (Amresco, USA). Then the leaves were incubated for 4 h at 27°C in the dark. Subsequently, this mixture was passed through a sterile stainless steel mesh sieve (mesh size 100 μm). The filtered protoplast suspension was centrifuged for 5 min at low speed (600 rpm, 25°C). Intact protoplasts were collected from the interphase and transferred into a new tube. Then 10 mL protoplast washing buffer (5 mM 2-[N-morpholino] ethane-sulphonic acid, 8 mM $CaCl_2$, 0.4 M mannitol, pH 5.6) were added and mixed gently followed by a second centrifugation under the same conditions. This washing step was repeated and a small aliquot of the washed protoplasts was used for the estimation of protoplast density in a hematocytometer. Before assay of PCD, the protoplast density was adjusted to 3–5 × 10^5 mL^{-1}. Three replicates were performed and every replicate used 5 plants.

Observation and Assessment of Protoplast PCD

The protoplast PCD occurrence was observed by laser scanning confocal microscope (LSCM, Nikon C1Plus, Japan) and quantitative assessment of percentage of PCD-occurring protoplasts to the normal ones was performed with flow cytometry (FCM). Briefly, 5 × 10^5 protoplasts mL^{-1} were washed twice with protoplast washing buffer, resuspended cells in 195 μL prediluted binding buffer and added 5 μL Annexin V-FITC kit (Bender MedSystems, USA), mixed and incubated for 10 min at room temperature (Solution 1). The solution 1 was firstly observed and photographed using LSCM with 488 nm band-pass excitation and 530 nm band-pass emissions.

Protoplasts in the identical volume of the Solution 1 were re-suspended in 190 μL prediluted binding buffer, added 10 μL of the 20 μg mL^{-1} propidium iodide (PI) stock solution. After addition of another 300 μL binding buffer, the suspended protoplasts were analyzed by flow cytometer PAS (Partec GmbH, Bioflow, Martinsried, Germany) with 488 nm band-pass excitation and 530 nm band-pass emission. The events of PCD occurrence was examined according the rules (a) The $FITC^-/PI^-$ population indicate intact cells; (b) the $FITC^+/PI^-$ population indicate early PCD protoplasts; (c) the $FITC^+/PI^+$ population indicate late PCD cells. Three independent sets of experiments

were performed with 10,000 protoplasts approximately and the averages were presented. Three replicates were performed and every replicate used 5 plants.

RNA ISOLATION AND QUANTITATIVE REAL TIME RT-PCR ANALYSIS

The qPCR assay has been designed according to the Minimum Information for Publication of Quantitative Real-Time PCR Experiments (MIQE) guidelines (Table S2; Bustin, 2010; Remans et al., 2014). We treated the Col-0 (WT) seedlings to study the effects on expression of BAG family genes, ethylene-related genes and senescence-related genes in response to the treatments with salinity and ACC. Seedlings after treatments were collected and ground in liquid nitrogen. Total RNA was extracted by TRIZOL reagent (Invitrogen). DNA contamination was removed by Dnase I following the instructions provided by the manufacturer (TaKaRa, Japan). RNA purity was observed using 1% agarose gel electrophoresis and RNA concentration was determined using a Nanodrop spectrophotometer (Thermo). The cDNA was synthesized from total RNA (2 ug) using ReverTra Ace QPCR RT Kit (Toyobo, Japan) according to the manufacturer instructions, using oligo (dT20) as the primer.

In our experiment, *ACTIN2, PP2A*, and *UBC* were used as candidate reference genes to evaluate their suitability based on a single melting temperature (Tm) and a single band on a 10% polyacrylamide gel (Figures S1–S3). According to melting curves and electrophoregram, we choose *ACTIN2* gene as reference gene. All primers have been described and optimized previously in accordance with the MIQE guidelines. The qRT-PCR analysis with cDNA as template and the expression of target genes as well as reference gene was monitored by quantitative real-time PCR using appropriate transcripts and primers (Table S1) were performed using a SYBR Premix Ex Taq (TaKaRa, Japan) with an initial denaturation at 95°C for 30 s, followed by 35 cycles at 94°C for 30 s, 56°C for 30 s and 72°C for 30 s. Experiments were repeated three times for each sample as technical replicates to ensure the reproducibility of results. The relative expression value was calculated using the 2-ΔΔCt method.

Statistical Analysis

Principal component analysis (PCA), the multivariate analyze tool, is used to reduce a set of original variabilities and to extract a small number of latent factors (principal components [PCs]) for analyzing relationships among the observed variabilities. PCA was performed in order to investigate the distribution pattern of quantitative gene expression in response to ACC and NaCl in *Arabidopsis* seedlings. Statistical treatment was carried out by analysis of variance (ANOVA) and PCA using SPSS-17 statistical software package. The two-way ANOVA was performed to examine the effects of salinity and genetic mutation on root length, respectively or jointly. Results were represented as the means ± standard error (S.E.). Data were analyzed using one-way analysis of variance and Duncan multiple range tests ($P < 0.05$; Pan et al., 2015).

RESULTS

The Phenotypic Changes and Leaf DNA Fragmentation Induced by Salinity

The PCD events among various lines of plants were observed by root elongation measurement and DNA laddering after treatment of salinity. **Figure 1A** showed the leaf morphological changes of seedlings under 0 or 100 mM NaCl. The plants of *ein2-5* and *ein3-1* displayed reduction of leaf area and salt-induced senescence symptoms obviously compared to their controls. However, Col-0 or *ctr1-1* plants were not largely affected by the applied salinity as the contrast of *ein2-5* or *ein3-1*. Root elongation measurement showed that *ein2-5* mutant plants were the most hypersensitive to NaCl (**Figure 1B**). The concentration of NaCl was estimated as $I_{50,}$ which decreased the root growth rate by 50 % compared to control medium (without NaCl). The I_{50} concentrations for *ein2-5* seedlings were 100 mM, with the root of *ein2-5* and *ein3-1* entirely restrained under 150 mM NaCl condition. The root elongation of Col-0 or *ctr1-1* plants was observed to be 40–50% shorter especially upon 150 mM NaCl medium. These results showed that insensitivity of ethylene signaling exaggerated plant sensitivity to salinity in light of growth status and root elongation. DNA laddering experiment indicated that salinity induced obvious DNA fragmentation in *ein2-5* and *ein3-1* plants. However, this process did not obviously appear in salt-stressed Col-0 or *ctr1-1* plants (**Figure 1C**). The two-way ANOVA analysis showed that salinity and genetic lines significantly affected root length ($F_{\text{salinity}} = 295.75$; $F_{\text{ethylene}} = 332.46$; $F_{S*E} = 48.99$).

The *In vivo* Protoplast PCD Occurrence Induced by Salinity

The PCD events among various lines of plants were observed by FCM measurement after treatment of salinity. FCM assay of PCD occurrence showed that *ein2-5* and *ein3-1* mutant plants significantly delayed PCD occurrence under non-saline condition compared to the condition of Col-0 (**Figures 2A–C**). In contrast, salinity treatment for 14 d led to a continuous increase of PCD occurrence in Col-0, *ein2-5* and *ein3-1* plants compared to their controls (**Figures 2E–G**). The statistic results of early and late PCD occurrence among *Arabidopsis* mutants under control and saline conditions were showed in **Figure 2**. The data indicated that salt stress-induced PCD was greatly promoted in *ein2-5* and *ein3-1*. The ratios of early PCD cells to normal ones were both more than 5% with 50 mM NaCl treatment (**Figures 2F,G**), and under 100 mM NaCl, the percentage of early PCD cells increased to 11.08%, 9.16% in *ein2-5* and *ein3-1* (**Figures 2J,K**), respectively. In contrast, the early PCD cells ratio were not largely changed in Col-0 and *ctr1-1* mutant under salt stress. The percentage of early PCD cells was no more than 4% under salt stress (**Figures 2E,H**). In addition, the ratios of late PCD cells of *ein2-5* and *ein3-1* changed significantly between the concentration of 50 mM and 100 mM NaCl (**Figures 2F,G,J,K**). There was no significant difference between Col-0 and *ctr1-1* with different concentrations of NaCl treatment (**Figures 2E,H,I,L**). These results showed that ethylene insensitive mutants were

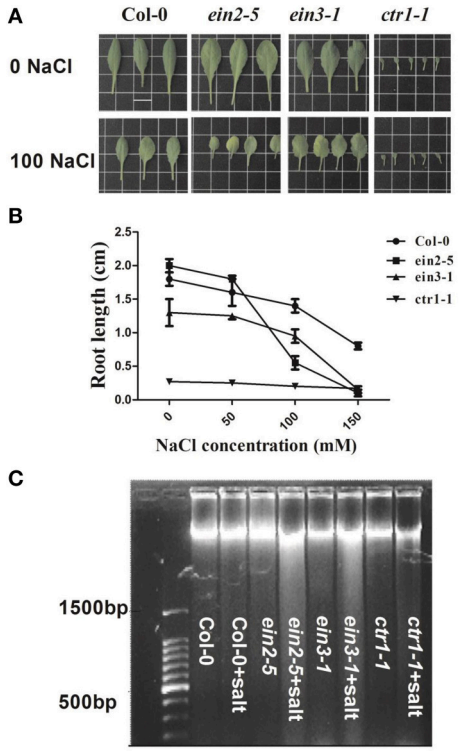

FIGURE 1 | PCD occurrence among various accessions of *Arabidopsis* plants after 14-day treatment. Seedlings of Col-0, *ein2-5, ein3-1*, and *ctr1-1* were treated with 0, 50, 100, and 150 mM NaCl contained in nutrient solution for 14 days. **(A)** Plants of above-mentioned four genotypic seedlings treated with 0 or 100 mM NaCl. Scale bars, 1 cm. **(B)** Root length reduction induced by salinity in four genotypic plants. Values are mean ± SE from 5 seedlings per replicate ($n = 5$ replicates). The different letters at the top of each bar indicate the significant difference among various treatments ($P < 0.05$). **(C)** DNA ladder when plants were treated with 0 mM or 100 mM NaCl.

more susceptibly affected by salt stress and their PCD processes were accelerated by NaCl treatment.

By summarized of Pearson' s regression coefficients (R) and *P*-value between PCD processes and increased saline concentrations for individual *Arabidopsis* accessions (**Table 1**), the results showed that the processes of early PCD in all accessions were tightly correlated with increased salt stress. Especially, the coefficients R for *ein2-5 and ein3-1* plants were 0.97 and 0.91, much higher than those in Col-0 and *ctr1-1* plants. The survey of correlations between late PCD and salt stress displayed that the significant correlation ($R = 0.809$, $P = 0.01$) was observed in *ein2-5* mutant plants only. The mutations such as ethylene insensitive mutant *ein2-5 and ein3-1* are more sensitive to salt stress than the wild type plants, and it was suggested that mutations could largely alter PCD processes in ethylene signaling pathway.

The *In vitro* Protoplasts PCD Affected by Salinity and Exogenous ACC

To testify the role of ethylene in amending salinity-PCD processes, the protoplasts were isolated from Col-0 and incubated in 0 mM NaCl, 200 mM NaCl, and 200 mM NaCl + 10 μM ACC solution (**Figure 3**). The PCD level was measured at 10, 20, 30, 60, 90, 120, 150 min, respectively (**Figure 3A**). As it shown in **Figure 3A**, the occurring rate of the protoplast PCD increased with time under such conditions. Additionally, the salinity of 200 mM NaCl applied to the protoplasts generated a rapid PCD-increasing rate compared to the events exhibited in the control solution. The application of ACC to the saline solution largely reduced the occurring rate of PCD in contrast to those without ACC.

In order to investigate the effects of redox status in the cells during PCD procedure, the isolated protoplasts were simultaneously incubated to 200 mM NaCl and 200 mM NaCl + 10 μM ACC in the presence of H_2O_2 or DPI (**Figure 3B**). After 150 min of treatment, PCD profiles were measured. The results suggested that the inhibition of salt-induced PCD by ACC was disrupted by exogenous application of H_2O_2 but retained by DPI (**Figure 3B**).

Relative Expressions of the PCD-, Ethylene-, and Senescence-Related Genes Affected by Salinity and Exogenous ACC

To reveal the molecular mechanism of ethylene controlling the salinity-induced cell death, we compared the expression levels of BAG family, ethylene-, and senescence-related genes in the wild-type plants treated with 0, 100 mM NaCl, 100 mM NaCl plus 50 μM ACC (**Figure 4**). The results showed that the treatment with salinity alone significantly suppressed the transcripts of *BAG6, BAG7, ERS2, and ACS2* (**Figures 4A,B**). However, the subsequent inclusion of ACC in the saline solution effectively reversed this inhibition of their expressions. The senescence-related genes under the above condition were then checked and the transcriptional abundance of *ANAC029* and *SAG12* was greatly triggered by salinity. Whereas, the addition of ACC in the saline solution inhibited this senescence process induced by salinity (**Figure 4C**). The above transcriptional data suggested that the PCD-, ethylene- and senescence-related genes actively participated in the salt-induced PCD process.

The Heat Map Analysis of Total Gene Profiles in the Wild-Type Plants upon Salinity Plus ACC

We then profiling the expression mode of 19 hallmark genes involved the PCD-, ethylene- and senescence-related processes in the Col-0 plants upon salinity alone or plus ACC (**Figure 5**). The hierarchical clustering of different treatments found that the control plants shared a common gene expression mode with those upon salinity plus ACC. This indicated that ACC could effectively reverse the salinity-induced transcriptional responses. In addition, the expression modes of *EIN3, ACS2, BAG6, BAG7,* and *ERS2* were in clustered common indicating their tight interaction during these treatments. On the contrast, salinity stress significantly promoted gene expression of *ANAC029* and *SAG12,* and these senescence genes were suppressed when ACC was added in the saline solution. Whereas, other investigated

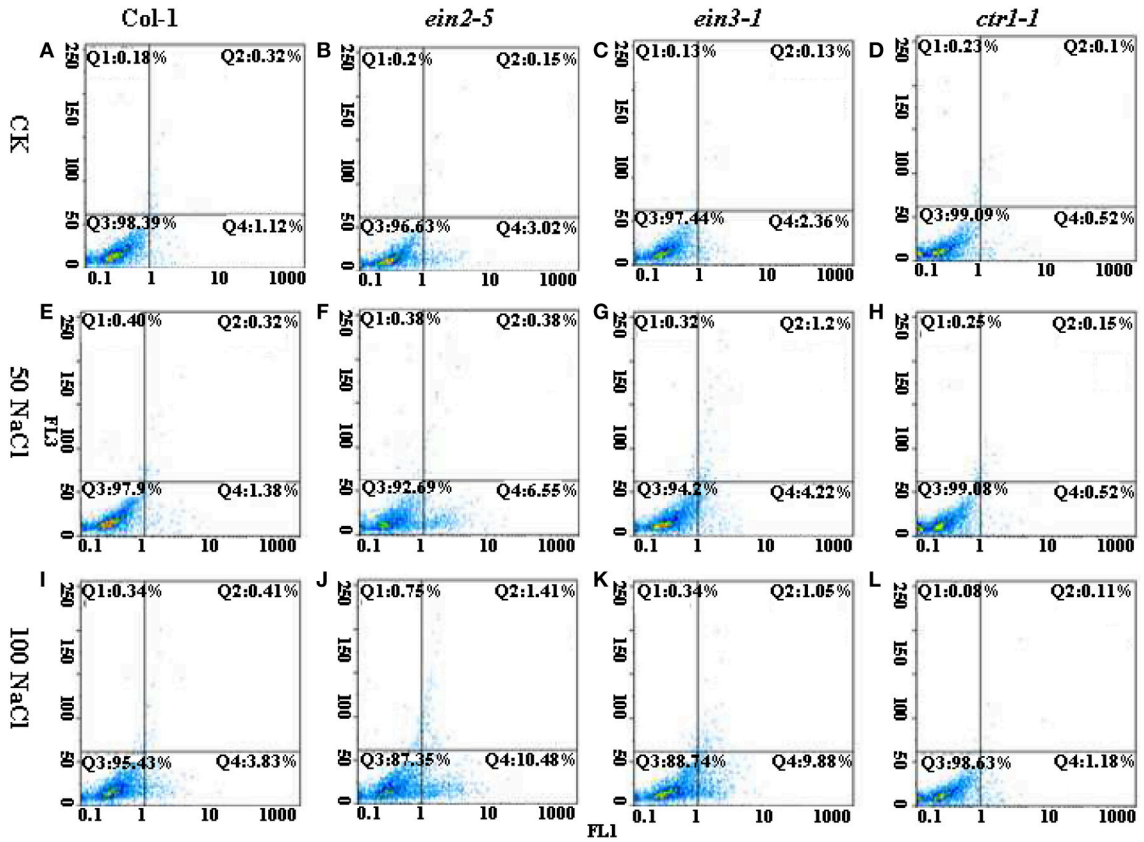

FIGURE 2 | Flow cytometric pictures of PCD occurrence among four lines of *Arabidopsis* plants under the control or saline conditions. Seedlings of Col-0, *ein2-5, ein3-1,* and *ctr1-1* were treated with 0, 50, or 100 mM NaCl. The protoplasts were stained with AnnexinV (FL1 channel) and PI (FL2 channel), and then analyzed by FCM. The Q4 Zone indicates early PCD cells; The Q2 Zone indicates late PCD cells; The Q3 Zone indicates intact cells. **(A)** The seedling of Col-0 were treated with 0 mM NaCl. **(B)** The seedling of *ein2-5* were treated with 0 mM NaCl. **(C)** The seedling of *ein3-1* were treated with 0 mM NaCl. **(D)** The seedling of *ctr1-1* were treated with 0 mM NaCl. **(E)** The seedling of Col-0 were treated with 50 mM NaCl. **(F)** The seedling of *ein2-5* were treated with 50 mM NaCl. **(G)** The seedling of *ein3-1* were treated with 50 mM NaCl. **(H)** The seedling of *ctr1-1* were treated with 50 mM NaCl. **(I)** The seedling of Col-0 were treated with 100 mM NaCl. **(J)** The seedling of *ein2-5* were treated with 100 mM NaCl. **(K)** The seedling of *ein3-1* were treated with 100 mM NaCl. **(L)** The seedling of *ctr1-1* were treated with 100 mM NaCl.

genes, such as *BAG1-BAG5*, did not displayed a consistent response as expected, displaying a diverse expression mode.

DISCUSSIONS

Ethylene has been reported to be involved in control of salt-induced ROS burst, ionic imbalance and osmotic stress to confer plant salt resistance (Jiang et al., 2013; Lin et al., 2013; Yang et al., 2013; Peng et al., 2014; Tao et al., 2015). Generally, promotion of ethylene biosynthesis and signal transduction could enhance plant tolerance to salinity, while inhibition of it leads to increased plant sensitivity to salinity (Tao et al., 2015). The salt-induced K+ deprivation and ROS burst will further activate cell death in plants (Huh et al., 2002; Affenzeller et al., 2009; Shabala, 2009). Here, we provided evidence to the critical role of ethylene controlling the salt-induced cell death process to confer salt tolerance in *Arabidopsis*.

The phenotypic changes of four lines of *Arabidopsis* were firstly compared under non-saline and saline conditions. Under control condition, the phenotipic responses of *ein2-5* and *ein3-1* resulted in an increment in leaf area and root lenght and on the other hand a constrained growth in *ctr1-1* compared to the Col-0 plants. It was proposed that smaller plants may be less vulnerable to stress because they have less surface area (Achard et al., 2006; Yang et al., 2013). The decreased leaf area pertain to a low transpiring rate, which help plants avoid excess Na+ intake, Na+ xylem loading into shoot and then Na+ over accumulation (Jiang et al., 2013; Tao et al., 2015; Zhu et al., 2016). For example, the *ctr1-1* plants were reported to display a reduced increase in shoot Na+ concentration compared with wild-type plants following salinity treatment and maintain a relatively high shoot K+ concentration in both control and salinity treatment conditions (Jiang et al., 2013). This might be a critical physiological mechanism for ethylene role in salt resistance, because gain-of-function of ethylene biosynthesis or signaling normally generates smaller plant size. Our observations confirmed that the *ctr1-1* plants displayed a slight reduction in leaf area and root elongation, while, *ein2-5*

or *ein3-1* ones showed a magnified retardation in plant growth compared to the wild-type plants under a saline condition (**Figures 1A,B**).

TABLE 1 | Regression analysis of early or late protoplast PCD occurrence of Col-0, *ein2-5, ein3-1*, and *ctr1-1* plants in response to 0, 50, and 100 mM NaCl concentration respectively.

Parameters	Mutants	Salt concentrations	
		R	*P*-value
Early PCD	Col-0	0.869**	0.00
	ein2-5	0.972**	0.00
	ein3-1	0.913**	0.00
	ctr1-1	0.766*	0.02
	Total	0.556**	0.00
Late PCD	Col-0	−0.18	0.65
	ein2-5	0.809**	0.01
	ein3-1	0.51	0.16
	ctr1-1	0.09	0.83
	Total	0.380*	0.02

*Correlation significant at the 0.05 level (2-tailed); **Correlation significant at the 0.01 level (2-tailed).

The salt-induced cell death occurrence then was compared among the four lines of plants. The salt-induced cell death acceleration in plants was generally considered as a key indicator of salt damage symptom (Dickman et al., 2001; Shabala, 2009; Jha and Subramanian, 2014; Yang et al., 2014). The recent evidence showed that exogenous expression of anti-apoptotic genes *AtBAG4* (*Arabidopsis*) significantly improves salinity tolerance in rice at the whole plant level (Hoang et al., 2015). Therefore, the ability to minimize cell death process induced by salinity is of importance for plant salt tolerance. Our DNA laddering experiment revealed that the salt-induced DNA fragmentation, one of the hallmarks of cell death, was accelerated in *ein2-5* and *ein3-1* leaves, whereas, inhibited in the Col-0 or *ctr1-1* (**Figure 1C**). In leaf protoplast, the exposure of phosphatidylserine (PS) on the outer surface of plasma membrane was detected by FCM, which is the hallmark of PCD, suggesting that loss-of-function of ethylene signaling resulted in decreased plant ability to inhibit the occurrence of salt-induced PCD (**Figure 2**). This FCM method was previously applied to quantitatively detect animal and plant cells undergoing PCD (O'Brien et al., 1997; Halweg et al., 2005).

These observations showed that ethylene signaling was helpful for plants to decrease salt-induced cell death both at the whole

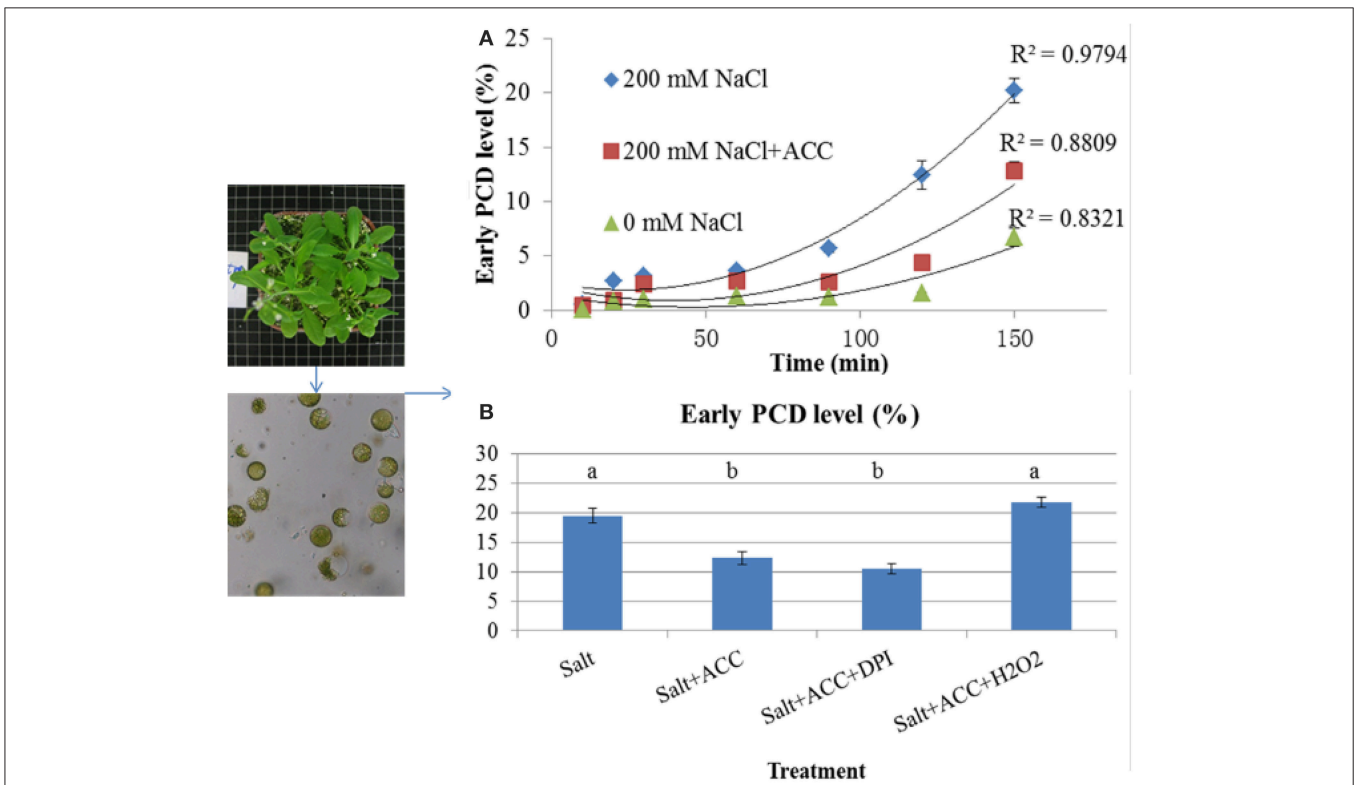

FIGURE 3 | The salt-induced PCD processes in isolated protoplasts with treatment by exogenous application of ACC and H_2O_2. (A) The isolated protoplasts from the control Col-0 seedlings were treated with 0 mM NaCl, 200 mM NaCl, or 200 mM NaCl + 10 μM ACC; **(B)** The isolated protoplasts were simultaneously incubated in salinized condition (200 mM NaCl) in the presence of 10 μM ACC, 10 μM ACC+10 μM DPI, or 10 μM ACC+5 mM H_2O_2. PCD was measured after 150 min of the treatments. The results are shown the mean ± SE of three replicates and 5 plants for each replicate. The different letters denote the significant difference among different treatments ($P < 0.05$).

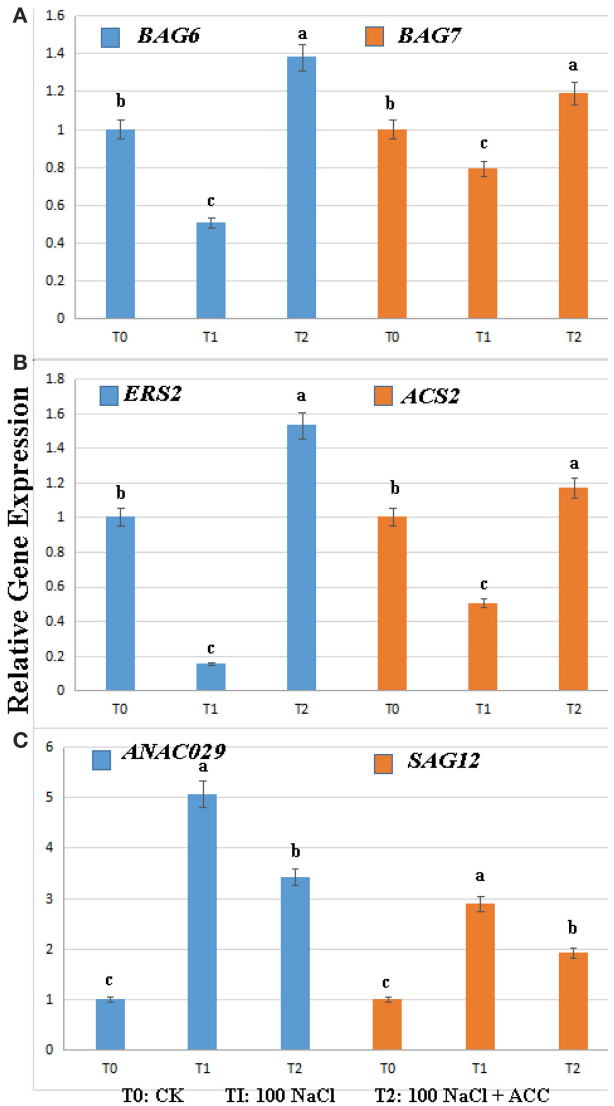

FIGURE 4 | Relative gene expression levels in the Col-0 plants upon salinity alone or plus ACC. The results were analyzed using the comparative Ct method. **(A)** The expression of *AtBAG6 and AtBAG7* genes; **(B)** The expression of *ERS2 and ACS2* genes; **(C)** The expression of *ANAO029 and SAG12* genes; Treatment with 0 mM NaCl (T0), 100 mM NaCl (T1), 100 mM NaCl + 50 μM ACC (T2). Data were analyzed using one-way analysis of variance and Duncan multiple range tests. The different letters denote the significant difference among different treatments ($P < 0.05$). Each relative gene expression represents the average of three measurements, with error bars representing Standard Errors.

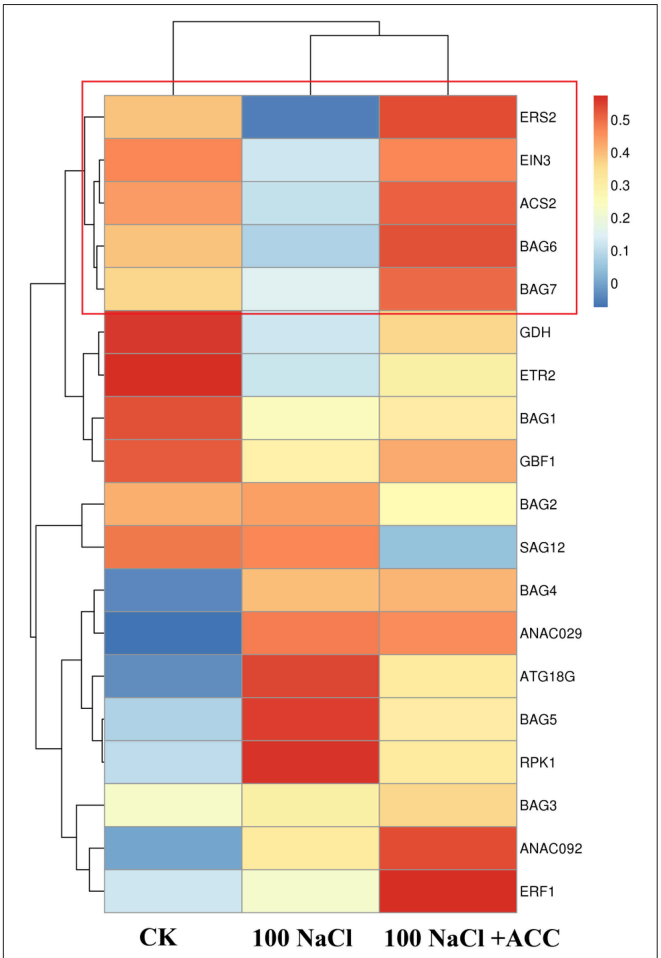

FIGURE 5 | The Heat Map analysis of gene expression mode in the Col-0 plants upon salinity alone or plus ACC. The Heat Map shows the expression of *BAG* family genes, ethylene-related genes and senescence-related genes upon induction by NaCl and ACC. Treatment with 0 mM NaCl (Col-0), 100 mM NaCl, 100 mM NaCl + 50 μM ACC. The average linkage hierarchical clustering with Pearson correlation was used. Blue and red denote relative down-regulation and up-regulation, respectively.

plant or cell levels. This action is consistent with the recent research that Silicon mitigates cell death in cultured tobacco BY-2 cells subjected to salinity relying on ethylene emission (Liang et al., 2015). Our time curve of *in vitro* protoplast PCD occurrence also confirmed that exogenous ACC effectively delayed the salt-induced PCD and this effect of ACC could be reversed by simultaneous addition of H_2O_2 (**Figure 3**). The excess accumulation of ROS is thought to be key inducers of PCD in plants under stressed conditions (Shabala, 2009; Jha and Subramanian, 2014). Our results indicated that ethylene might control the salt-induced cell death depending on redox states regulation. Large body of report illustrated that ethylene could deter the salt-induced ROS to confer plant salt tolerance (Munns and Tester, 2008; Lin et al., 2013; Peng et al., 2014; Poór et al., 2015; Tao et al., 2015).

At last, we compared the expression levels of *BAG* family, ethylene-, and senescence-related genes in the wild-type plants subjected to salinity alone or plus ACC. Interestingly, salinity alone significantly suppressed the transcripts of *BAG6, BAG7, ERS2, and ACS2* (**Figure 4**). Plant *BAG* genes are tightly involved in environmental responses and they block several biotic and abiotic cell death-mediated processes while conferring cyto-protection under sevaral adverse condition and during plant development (Dickman et al., 2001; Kabbage and Dickman, 2008; Williams et al., 2010; Li et al., 2016). For example, *BAG6* was required in resistance to fungal-induced cell death in *Arabidopsis*

(Li et al., 2016) and the deletion of BAG7 compromises heat and cold tolerance (Williams et al., 2010). Our results showed that the inclusion of ACC in the saline solution could obviously re-activate *BAG6* and *BAG7* expressions, which might play a key role to inhibit the salt-induced cell death as reported before. The Heat Map analysis of total gene profiles in our study found that *EIN3, ACS2,* and *ERS2* were in clustered common with *BAG6* and *BAG7* (**Figure 5**). In addition, SAG12, an *Arabidopsis* gene encoding a cysteine protease, which is expressed only in senescent tissues (Noh and Amasino, 1999), is specifically activated by developmentally controlled senescence pathways, in our study, as well as than the abundance of *ANAC029* was also greatly triggered by salinity and reversed by addition of ACC. These results confirmed the essential role of ethylene biosynthesis and signal transduction in plant salt tolerance (Peng et al., 2014; Tao et al., 2015).

Our results provided evidence that the salt-induced PCD process was commonly antagonized by ethylene signaling. The altered salt-induced PCD level mediated by ethylene was proposed to contribute to an improved salt sensitivity in *ein2-5* and *ein3-1* plants and increased salt tolerance in *ctr1-1*. When salinity was directly applied to *Arabidopsis* protoplasts, the external addition of ethylene precursor ACC mostly inhibited salt-induced PCD process. This phenomenon suggests that the pathway of PCD is involved in alteration of salt response which is regulated by ethylene. At the transcriptional level, we compared the expression levels of BAG family, ethylene-, and senescence-related genes in the wild-type plants subjected to salinity alone or plus ACC. Interestingly, salinity alone significantly suppressed the transcripts of *BAG6, BAG7, ERS2,* and *ACS2* and addition of ACC in the saline solution could obviously re-activate *BAG6* and *BAG7* expressions, which might play a key role to inhibit the salt-induced cell death. Based on our findings, we propose that ethylene and salinity antagonistically modulate the salt-induced cell death via controlling the transcripts of BAG family, ethylene-, and senescence-related genes in *Arabidopsis*. The complex mechanisms need to be intensively investigated in the future.

AUTHOR CONTRIBUTIONS

Conceived and designed the experiments: YP, ZT, YZ. Performed the experiments: YP, LL. Analyzed the data: YP, YL. Wrote the paper: YP, LPL.

ACKNOWLEDGMENTS

We thank Prof. Hongwei Guo from Peking University for his critical comments, Dr. Hongzheng Wang and Dr. Zhonghua Zhang for their assistance in flow cytometry assay. This work was supported by National Natural Science Foundation of China (31370007) and Special Fund for Forest Scientific Research in the Public Welfare (201104002-3).

SUPPLEMENTARY MATERIAL

The Supplementary Material for this article can be found online at: http://journal.frontiersin.org/article/10.3389/fpls.2016.00696

REFERENCES

Achard, P., Cheng, H., De Grauwe, L., Decat, J., Schoutteten, H., Moritz, T., et al. (2006). Integration of plant responses to environmentally activated phytohormonal signals. *Science* 311, 91–94. doi: 10.1126/science.1118642

Affenzeller, M. J., Darehshouri, A., Andosch, A., Lütz, C., and Lütz-Meindl, U. (2009). Salt stress-induced cell death in the unicellular green alga Micrasterias denticulata. *J. Exp. Bot.* 60, 939–954. doi: 10.1093/jxb/ern348

Agarie, S., Shimoda, T., Shimizu, Y., Baumann, K., Sunagawa, H., Kondo, A., et al. (2007). Salt tolerance, salt accumulation, and ionic homeostasis in an epidermal bladder-cell-less mutant of the common ice plant Mesembryanthemum crystallinum. *J. Exp. Bot.* 58, 1957–1967. doi: 10.1093/jxb/erm057

Andronis, E. A., and Roubelakis-Angelakis, K. A. (2010). Short-term salinity stress in tobacco plants leads to the onset of animal-like PCD hallmarks in planta in contrast to long-term stress. *Planta* 231, 437–448. doi: 10.1007/s00425-009-1060-x

Asai, T., Stone, J. M., Heard, J. E., Kovtun, Y., Yorgey, P., Sheen, J., et al. (2000). Fumonisin B1-induced cell death in arabidopsis protoplasts requires jasmonate-, ethylene-, and salicylate-dependent signaling pathways. *Plant Cell* 12, 1823–1836. doi: 10.1105/tpc.12.10.1823

Bleecker, A. B., and Kende, H. (2000). Ethylene: a gaseous signal molecule in plants. *Annu. Rev. Cell Dev. Biol.* 16, 1–18. doi: 10.1146/annurev.cellbio.16.1.1

Bouchez, O., Huard, C., Lorrain, S., Roby, D., and Balagué, C. (2007). Ethylene is one of the key elements for cell death and defense response control in the Arabidopsis lesion mimic mutant vad1. *Plant Physiol.* 145, 465–477. doi: 10.1104/pp.107.106302

Bustin, S. A. (2010). Why the need for qPCR publication guidelines?–The case for MIQE. *Methods* 50, 217–226. doi: 10.1016/j.ymeth.2009.12.006

Chen, Y. F., Etheridge, N., and Schaller, G. E. (2005). Ethylene signal transduction. *Ann. Bot.* 95, 901–915. doi: 10.1093/aob/mci100

de, J., Yakimova, E. T., Kapchina, V. M., and Woltering, E. J. (2002). A critical role for ethylene in hydrogen peroxide release during programmed cell death in tomato suspension cells. *Planta* 214, 537–545. doi: 10.1007/s004250100654

Dickman, M. B., Park, Y. K., Oltersdorf, T., Li, W., Clemente, T., and French, R. (2001). Abrogation of disease development in plants expressing animal antiapoptotic genes. *Proc. Natl. Acad. Sci. U.S.A.* 98, 6957–6962. doi: 10.1073/pnas.091108998

Enari, M., Sakahira, H., Yokoyama, H., Okawa, K., Iwamatsu, A., and Nagata, S. (1998). A caspase-activated DNase that degrades DNA during apoptosis, and its inhibitor ICAD. *Nature* 391, 43–50. doi: 10.1038/34112

Fang, S., Li, L., Cui, B., Men, S., Shen, Y., and Yang, X. (2013). Structural insight into plant programmed cell death mediated by BAG proteins in *Arabidopsis thaliana*. *Acta Crystallogr. Sect. D* 69, 934–945. doi: 10.1107/S0907444913003624

Flowers, T. J. (2004). Improving crop salt tolerance. *J. Exp. Bot.* 55, 307–319. doi: 10.1093/jxb/erh003

Genc, Y., McDonald, G. K., and Tester, M. (2007). Reassessment of tissue Na(+) concentration as a criterion for salinity tolerance in bread wheat. *Plant Cell Environ.* 30, 1486–1498. doi: 10.1111/j.1365-3040.2007.01726.x

Guo, H., and Ecker, J. R. (2004). The ethylene signaling pathway: new insights. *Curr. Opin. Plant Biol.* 7, 40–49. doi: 10.1016/j.pbi.2003.11.011

Halweg, C., Thompson, W. F., and Spiker, S. (2005). The rb7 matrix attachment region increases the likelihood and magnitude of transgene expression in tobacco cells: a flow cytometric study. *Plant Cell* 17, 418–429. doi: 10.1105/tpc.104.028100

Hoang, T. M., Moghaddam, L., Williams, B., Khanna, H., Dale, J., and Mundree, S. G. (2015). Development of salinity tolerance in rice by constitutive-overexpression of genes involved in the regulation of programmed cell death. *Front. Plant Sci.* 6:175. doi: 10.3389/fpls.2015.00175

Hoeberichts, F. A., and Woltering, E. J. (2003). Multiple mediators of plant programmed cell death: interplay of conserved cell death mechanisms and plant-specific regulators. *Bioessays* 25, 47–57. doi: 10.1002/bies.10175

Huh, G. H., Damsz, B., Matsumoto, T. K., Reddy, M. P., Rus, A. M., Ibeas, J. I., et al. (2002). Salt causes ion disequilibrium-induced programmed cell death in yeast and plants. *Plant J.* 29, 649–659. doi: 10.1046/j.0960-7412.2001.01247.x

Jacyn Baker, C., and Mock, N. M. (1994). An improved method for monitoring cell death in cell suspension and leaf disc assays using evans blue. *Plant Cell Tissue Organ. Cult.* 39, 7–12. doi: 10.1007/BF00037585

James, R. A., Munns, R., Von Caemmerer, S., Trejo, C., Miller, C., and Condon, T. (2006). Photosynthetic capacity is related to the cellular and subcellular partitioning of Na+, K+ and Cl- in salt-affected barley and durum wheat. *Plant Cell Environ.* 29, 2185–2197. doi: 10.1111/j.1365-3040.2006.01592.x

Jha, Y., and Subramanian, R. B. (2014). PGPR regulate caspase-like activity, programmed cell death, and antioxidant enzyme activity in paddy under salinity. *Physiol. Mol. Biol. Plants* 20, 201–207. doi: 10.1007/s12298-014-0224-8

Jiang, C., Belfield, E. J., Cao, Y., Smith, J. A., and Harberd, N. P. (2013). An Arabidopsis soil-salinity-tolerance mutation confers ethylene-mediated enhancement of sodium/potassium homeostasis. *Plant Cell* 25, 3535–3552. doi: 10.1105/tpc.113.115659

Jiang, C., Belfield, E. J., Mithani, A., Visscher, A., Ragoussis, J., Mott, R., et al. (2012). ROS-mediated vascular homeostatic control of root-to-shoot soil Na delivery in Arabidopsis. *EMBO J.* 31, 4359–4370. doi: 10.1038/emboj.2012.273

Kabbage, M., and Dickman, M. B. (2008). The BAG proteins: a ubiquitous family of chaperone regulators. *Cell. Mol. Life Sci.* 65, 1390–1402. doi: 10.1007/s00018-008-7535-2

Kim, H. B., Lee, H., Oh, C. J., Lee, H. Y., Eum, H. L., Kim, H. S., et al. (2010). Postembryonic seedling lethality in the sterol-deficient Arabidopsis cyp51A2 mutant is partially mediated by the composite action of ethylene and reactive oxygen species. *Plant Physiol.* 152, 192–205. doi: 10.1104/pp.109.149088

Kim, J., Chang, C., and Tucker, M. L. (2015). To grow old: regulatory role of ethylene and jasmonic acid in senescence. *Front. Plant Sci.* 6:20. doi: 10.3389/fpls.2015.00020

Li, X., Pan, Y., Chang, B., Wang, Y., and Tang, Z. (2015). NO promotes seed germination and seedling growth under high salt may depend on EIN3 protein in Arabidopsis. *Front. Plant Sci.* 6:1203. doi: 10.3389/fpls.2015.01203

Li, Y., Kabbage, M., Liu, W., and Dickman, M. B. (2016). Aspartyl protease-mediated cleavage of BAG6 is necessary for autophagy and fungal resistance in plants. *Plant Cell* 28, 233–247. doi: 10.1105/tpc.15.00626

Liang, X., Wang, H., Hu, Y., Mao, L., Sun, L., Dong, T., et al. (2015). Silicon does not mitigate cell death in cultured tobacco BY-2 cells subjected to salinity without ethylene emission. *Plant Cell Rep.* 34, 331–343. doi: 10.1007/s00299-014-1712-6

Lin, Y., Yang, L., Paul, M., Zu, Y., and Tang, Z. (2013). Ethylene promotes germination of Arabidopsis seed under salinity by decreasing reactive oxygen species: evidence for the involvement of nitric oxide simulated by sodium nitroprusside. *Plant Physiol. Biochem.* 73, 211–218. doi: 10.1016/j.plaphy.2013.10.003

Meijering, E., Jacob, M., Sarria, J. C., Steiner, P., Hirling, H., and Unser, M. (2004). Design and validation of a tool for neurite tracing and analysis in fluorescence microscopy images. *Cytometry A* 58, 167–176. doi: 10.1002/cyto.a.20022

Munns, R., and Tester, M. (2008). Mechanisms of salinity tolerance. *Annu. Rev. Plant Biol.* 59, 651–681. doi: 10.1146/annurev.arplant.59.032607.092911

Noh, Y. S., and Amasino, R. M. (1999). Identification of a promoter region responsible for the senescence-specific expression of SAG12. *Plant Mol. Biol.* 41, 181–194. doi: 10.1023/A:1006342412688

O'Brien, I. E., Reutelingsperger, C. P., and Holdaway, K. M. (1997). Annexin-V and TUNEL use in monitoring the progression of apoptosis in plants. *Cytometry* 29, 28–33.

Pan, Y. J., Liu, J., Guo, X. R., Zu, Y. G., and Tang, Z. H. (2015). Gene transcript profiles of the TIA biosynthetic pathway in response to ethylene and copper reveal their interactive role in modulating TIA biosynthesis in *Catharanthus roseus*. *Protoplasma* 252, 813–824. doi: 10.1007/s00709-014-0718-9

Peng, J., Li, Z., Wen, X., Li, W., Shi, H., Yang, L., et al. (2014). Salt-induced stabilization of EIN3/EIL1 confers salinity tolerance by deterring ROS accumulation in Arabidopsis. *PLoS Genet.* 10:e1004664. doi: 10.1371/journal.pgen.1004664

Pennell, R. I., and Lamb, C. (1997). Programmed cell death in plants. *Plant Cell* 9, 1157–1168. doi: 10.1105/tpc.9.7.1157

Poór, P., Kovács, J., Borbély, P., Takács, Z., Szepesi, Á., and Tari, I. (2015). Salt stress-induced production of reactive oxygen- and nitrogen species and cell death in the ethylene receptor mutant never ripe and wild type tomato roots. *Plant Physiol. Biochem.* 97, 313–322. doi: 10.1016/j.plaphy.2015.10.021

Remans, T., Keunen, E., Bex, G. J., Smeets, K., Vangronsveld, J., and Cuypers, A. (2014). Reliable gene expression analysis by reverse transcription-quantitative PCR: reporting and minimizing the uncertainty in data accuracy. *Plant Cell* 26, 3829–3837. doi: 10.1105/tpc.114.130641

Schneider, C. A., Rasband, W. S., and Eliceiri, K. W. (2012). NIH Image to ImageJ: 25 years of image analysis. *Nat. Methods* 9, 671–675. doi: 10.1038/nmeth.2089

Shabala, S. (2009). Salinity and programmed cell death: unravelling mechanisms for ion specific signalling. *J. Exp. Bot.* 60, 709–712. doi: 10.1093/jxb/erp013

Steffens, B., and Sauter, M. (2009). Epidermal cell death in rice is confined to cells with a distinct molecular identity and is mediated by ethylene and H2O2 through an autoamplified signal pathway. *Plant Cell* 21, 184–196. doi: 10.1105/tpc.108.061887

Tao, J. J., Chen, H. W., Ma, B., Zhang, W. K., Chen, S. Y., and Zhang, J. S. (2015). The role of ethylene in plants under salinity stress. *Front. Plant Sci.* 6:1059. doi: 10.3389/fpls.2015.01059

van Doorn, W. G., and Woltering, E. J. (2004). Senescence and programmed cell death: substance or semantics? *J. Exp. Bot.* 55, 2147–2153. doi: 10.1093/jxb/erh264

Williams, B., Kabbage, M., Britt, R., and Dickman, M. B. (2010). AtBAG7, an Arabidopsis Bcl-2-associated athanogene, resides in the endoplasmic reticulum and is involved in the unfolded protein response. *Proc. Natl. Acad. Sci. U.S.A.* 107, 6088–6093. doi: 10.1073/pnas.0912670107

Yakimova, E. T., Kapchina-Toteva, V. M., Laarhoven, L. J., Harren, F. M., and Woltering, E. J. (2006). Involvement of ethylene and lipid signalling in cadmium-induced programmed cell death in tomato suspension cells. *Plant Physiol. Biochem.* 44, 581–589. doi: 10.1016/j.plaphy.2006.09.003

Yamada, T., and Marubashi, W. (2003). Overproduced ethylene causes programmed cell death leading to temperature-sensitive lethality in hybrid seedlings from the cross *Nicotiana suaveolens* x N. *tabacum*. *Planta* 217, 690–698. doi: 10.1007/s00425-003-1035-2

Yang, L., Zhao, X., Zhu, H., Paul, M., Zu, Y., and Tang, Z. (2014). Exogenous trehalose largely alleviates ionic unbalance, ROS burst, and PCD occurrence induced by high salinity in Arabidopsis seedlings. *Front. Plant Sci.* 5:570. doi: 10.3389/fpls.2014.00570

Yang, L., Zu, Y. G., and Tang, Z. H. (2013). Ethylene improves Arabidopsis salt tolerance mainly via retaining K+ in shoots and roots rather than decreasing tissue Na+ content. *Environ. Exp. Bot.* 86, 60–69. doi: 10.1016/j.envexpbot.2010.08.006

Zhu, J. K. (2001). Plant salt tolerance. *Trends Plant Sci.* 6, 66–71. doi: 10.1016/S1360-1385(00)01838-0

Zhu, M., Zhou, M., Shabala, L., and Shabala, S. (2016). Physiological and molecular mechanisms mediating xylem Na^+ loading in barley in the context of salinity stress tolerance. *Plant Cell Environ.* doi: 10.1111/pce.12727. [Epub ahead of print].

Conflict of Interest Statement: The authors declare that the research was conducted in the absence of any commercial or financial relationships that could be construed as a potential conflict of interest.

frontiers in Plant Science

ORIGINAL RESEARCH
published: 24 February 2017
doi: 10.3389/fpls.2017.00253

Ethylene Improves Root System Development under Cadmium Stress by Modulating Superoxide Anion Concentration in *Arabidopsis thaliana*

Ann Abozeid[1,2†], Zuojia Ying[1,3†], Yingchao Lin[1,4], Jia Liu[1], Zhonghua Zhang[1] and Zhonghua Tang[1*]*

[1] Key Laboratory of Plant Ecology, Northeast Forestry University, Harbin, China, [2] Botany Department, Faculty of Science, Menoufia University, Shibin El Kom, Egypt, [3] The College of Landscape, Northeast Forestry University, Harbin, China, [4] Guizhou Academy of Tobacco Research, Guiyang, China

OPEN ACCESS

Edited by:
Nafees A. Khan,
Aligarh Muslim University, India

Reviewed by:
Naser A. Anjum,
University of Aveiro, Portugal
Mohd Asgher,
Aligarh Muslim University, India

***Correspondence:**
Zhonghua Tang
tangzh@nefu.edu.cn
Ann Abozeid
annabozeid@yahoo.com

† These authors have contributed equally to this work.

Specialty section:
This article was submitted to Plant Physiology, a section of the journal Frontiers in Plant Science

Received: 04 November 2016
Accepted: 09 February 2017
Published: 24 February 2017

Citation:
Abozeid A, Ying Z, Lin Y, Liu J, Zhang Z and Tang Z (2017) Ethylene Improves Root System Development under Cadmium Stress by Modulating Superoxide Anion Concentration in Arabidopsis thaliana. Front. Plant Sci. 8:253. doi: 10.3389/fpls.2017.00253

This work aims at identifying the effects of ethylene on the response of *Arabidopsis thaliana* root system to cadmium chloride ($CdCl_2$) stress. Two ethylene-insensitive mutants, *ein2-5* and *ein3-1eil1-1*, were subjected to (25, 50, 75, and 100 μM) $CdCl_2$ concentrations, from which 75 μM concentration decreased root growth by 40% compared with wild type Col-0 as a control. Ethylene biosynthesis increased in response to $CdCl_2$ treatment. The length of primary root and root tip in *ein2-5* and *ein3-1eil1-1* decreased compared with wild type after $CdCl_2$ treatment, suggesting that ethylene play a role in root system response to Cd stress. The superoxide concentration in roots of *ein2-5* and *ein3-1eil1-1* was greater than in wild type seedlings under Cd stress. Application of exogenous 1-aminocyclopropane-1-carboxylic acid (ACC) (a precursor of ethylene biosynthesis) in different concentrations (0.01, 0.05 and 0.5 μM) decreased superoxide accumulation in Col-0 root tips and increased the activities of superoxide dismutase (SOD) isoenzymes under Cd stress. This result was reversed with 5 μM of aminoisobutyric acid AIB (an inhibitor of ethylene biosynthesis). Moreover, it was accompanied by increase in lateral roots number and root hairs length, indicating the essential role of ethylene in modulating root system development by controlling superoxide accumulation through SOD isoenzymes activities. The suppressed Cd-induced superoxide accumulation in wild type plants decreased the occurrence of cells death while programmed cell death (PCD) was initiated in the root tip zone, altering root morphogenesis (decreased primary root length, more lateral roots and root hairs) to minimize the damage caused by Cd stress, whereas this response was absent in the *ein2-5* and *ein3-1eil1-1* seedlings. Hence, ethylene has a role in modulating root morphogenesis during $CdCl_2$ stress in *A. thaliana* by increasing the activity of SOD isoenzymes to control superoxide accumulation.

Keywords: ethylene, Cd stress, superoxide, programmed cell death, root system, *Arabidopsis thaliana*

INTRODUCTION

Heavy metal toxicity in soil was once limited to localities affected by mining, heavy industry or derived from natural mineral outcrops. Metal toxicity not only reduces crop productivity but also threatens the food chain (Poschenrieder and Barceló, 1999). Among the common heavy metal pollutants, cadmium (Cd) is perhaps one of the most aggressive and persistent and is also the most susceptible to accumulation through inappropriate agricultural practices (Choppala et al., 2014; Asgher et al., 2015; Wahid and Khaliq, 2015). The major Cd input into agricultural soils is the phosphorus fertilizers (Singh and Agrawal, 2007). Plants affected by Cd showed impaired photosynthesis (Burzynski and Klobus, 2004; Andresen et al., 2016), altered mineral nutrition and carbohydrate metabolism (Azevedo et al., 2005; Santos et al., 2010) and water imbalance (Sandalio et al., 2001). Cadmium is a non-essential element but is readily absorbed by roots and transported to the aerial parts of plants. Cadmium concentrations of 1–5 μM in the soil solution are sufficient to retard root growth: presumably such toxicity occurs because Cd can replace essential elements that play key roles at the active sites of enzymes, thus affecting many aspects of plant growth and development (Sofo et al., 2013; Vitti et al., 2013).

The plant hormone ethylene is involved in many aspects of the plant life cycle, including seed germination and root hair development (Johnson and Ecker, 1998). It is considered as a (stress hormone) for modulating a diverse array of defense responses (Montero-Palmero et al., 2014; Pan et al., 2016). Thus, ethylene is highly expected to play a role in plant response to Cd stress.

Ethylene acts as a regulator of stress-related morphological responses such as primary and secondary root growth (Parlanti et al., 2011). Interestingly, ethylene remodels the root system architecture to increase Pi uptake in responses to low phosphate (Pi) (Nagarajan and Smith, 2012). This indicates the role of ethylene in root development in relations to heavy metal stress.

Ethylene is derived from methionine, and the first committed step in this pathway is the conversion of *S*-adenosyl methionine to 1-aminocyclopropane-1-carboxylate (ACC), which is performed by the enzyme ACC synthase (ACS). ACC is then oxidized by ACC oxidase to form ethylene, CO_2 and cyanide. During these processes, ACS-catalyzed ACC synthesis is generally the rate-limiting step for ethylene production (Skottke et al., 2011). The ACS isozymes are encoded for by a large gene family, among which phosphorylation of the type 1 isozymes ACS2 and ACS6 by stress-responsive MAPKs results in increased ethylene synthesis (Han et al., 2010; Skottke et al., 2011).

In *Arabidopsis*, ethylene signaling is first perceived by a family of five receptors that are located at the Golgi and endoplasmic reticulum (ER) membranes (Dong et al., 2010). Ethylene binding is proposed to inhibit receptor function, and CONSTITUTIVE TRIPLE RESPONSE 1 (CTR1) is proposed to be activated by the unoccupied receptor via a physiological interaction (Guo and Ecker, 2003), resulting in the activation of ETHYLENE INSENSITIVE 2 (EIN2). EIN2 plays a central role in the ethylene signaling transduction pathway, and the *ein2* mutant, is completely insensitive to ethylene at the morphological, physiological and molecule levels in *Arabidopsis* (Shibuya et al., 2004). The ethylene signaling pathway then continues to the nuclear transcriptional factors EIN3 and EIN3-like (EIL). In *Arabidopsis*, there are six members in the EIN3 family, of which EIN3 and its close homolog EIL1 have been widely studied (An et al., 2010; Lingam et al., 2011; Zhu et al., 2011). Mutants in EIN3 and EIL1 have weak ethylene insensitivity (Chao et al., 1997; Binder et al., 2007). Interestingly, *ein3 eil1* double mutants display complete ethylene insensitivity in all known ethylene responses, including the triple response and pathogen resistance (Guo and Ecker, 2003). Subsequently, these primary transcription factors activate other secondary transcription factors, such as the ETHYLENE RESPONSE FACTORs (ERFs), thereby regulating the expression of genes that are involved in the response to ethylene (Guo and Ecker, 2004; Kendrick and Chang, 2008). It has been demonstrated that the expression of ERF1 can be activated rapidly by ethylene (Lorenzo et al., 2003).

The production of ethylene is tightly regulated by internal signals during development and by responses to environmental stimuli from biotic and abiotic stresses, such as wounding, ozone, chilling or freezing (Wang et al., 2002; Yoo et al., 2009). Cd induces ethylene biosynthesis in the wild-type of *Arabidopsis thaliana* (Schellingen et al., 2014). Under Cd stress, the production of ethylene increases drastically in the root tip (Arteca and Arteca, 2007), the region where superoxide is predominantly localized (Dunand et al., 2007), which led us to investigate the connections between ethylene biosynthesis and superoxide production in the root tip. Cd stress is also related to the increase of ROS (Xu et al., 2010a), the oxidative damage of ROS requires the action of antioxidative enzymes, including superoxide dismutase (SOD), which can convert superoxide radicals into hydrogen peroxide, water and oxygen. SOD activity increased by the application of exogenous ACC and ethylene decrease the concentration of hydrogen peroxide under abiotic stress (Lin et al., 2012, 2013a,b). This better support our hypothesis that ethylene regulate superoxide accumulation through SOD activity.

Programmed cell death (PCD) is a functional term used to describe cell death that eliminates harmful cells during the life cycle of multicellular organisms. Increasing evidence suggests that diverse abiotic stresses, such as salt, drought, nutrient deficiency and heavy metal toxicity, can induce PCD in plant root tips (Liu et al., 2009; Duan et al., 2010; Xu et al., 2010b; Demidchik et al., 2014). Under drought and long-term zinc exposure, the PCD program is activated in the root apical meristematic zone, so apical root dominance is removed. Thus, the root system architecture may be remodel allowing adaptation to the stressful environment (Duan et al., 2010; Xu et al., 2010b). This led us to expect that PCD might be the mechanism by which the plant responds to the damage caused by Cd stress especially because reactive oxygen species (ROS) accumulation may trigger the PCD process in stressed plants (Harding and Roberts, 1998; Chae and Lee, 2001). However, the relation between production of superoxide and the progress of PCD in root tips under Cd stress is still unknown.

So our hypothesis suggests that ethylene modulates root system by decreasing superoxide accumulations through

decreasing NADPH oxidase activity and increasing SOD enzymes activity. Ethylene-induced suppression of superoxide accumulation modulates the root development through decreasing cell death (damaging effect of superoxide accumulation) and initiating PCD.

The aim of this study is to highlight the role of ethylene in response to the damage effect caused by Cd stress through its effects on superoxide accumulation by increasing the SOD activity, and to show the relation between the progression of cell death and PCD in root tips and the mechanism by which ethylene in minimize the damage effect caused by Cd stress, to propose a schematic model elucidating this mechanism by which the plant responses to Cd stress through inducing ethylene biosynthesis to modulate the root system development.

MATERIALS AND METHODS

Plant Material and Growth Conditions

Seedlings of the following lines were used in this study: *Arabidopsis thaliana* ecotype Columbia-0 (Col-0) and the ethylene-insensitive mutants *ein2-5* (Alonso et al., 1999) and *ein3-1eil1-1* (Alonso et al., 2003) in the Col-0 background. All seeds were surface-sterilized by incubation in 70% ethanol containing 0.05% Triton X-100 (Solar Bio, Beijing, China) for 10 min, rinsed thoroughly with ethanol for 1 min and then washed with sterilized water. The sterilized seeds were sown on agar plates containing a MS basal salt mixture (Sigma–Aldrich, St. Louis, MO, USA), 1% sucrose and 0.8% agar (pH 5.7). The plates were maintained at 4°C in the dark for 48 h to enhance the germination process and then placed vertically at 23°C under a light intensity of 200 μml m^{-2} s^{-1} (16/8 h light cycle).

Treatments

To investigate the effects of Cd stress on root growth, 4-day-old seedlings cultivated in control agar plates were transferred to freshly prepared medium supplemented by various concentration of $CdCl_2$ (25, 50, 75, and 100 μM) as indicated (Cao et al., 2009; Radeva et al., 2010) for 2 and 4 days. Preliminary experiments with seedling grown with various $CdCl_2$ concentrations showed that 75 μM $CdCl_2$ decreased root growth by about 40% and so this concentration was used to compare the effects of Cd stress between the wild type and the ethylene-insensitive mutants.

To investigate the effects of exogenous ACC on the accumulation of superoxide in the root tips of the Col-0 plants under Cd stress. Four-day-old seedlings were transferred to various pretreated agar plates with 75 μM $CdCl_2$ or 75 μM $CdCl_2$ plus various concentrations of ACC (0.01, 0.05, and 0.5 μM, a precursor of ethylene biosynthesis) with or without 5 μM AIB (an inhibitor of ethylene biosynthesis), as indicated, for 4 days.

All the experiments were repeated three times with three replicates of each treatment unless otherwise noted.

Quantitative RT-PCR Analysis of Gene Expression

To investigate whether ethylene biosynthesis and signaling were involved in the plant response to Cd stress, the relative expression of genes encoding for ethylene biosynthesis, and of perception and signaling proteins were measured in seedlings that were treated with different concentrations of $CdCl_2$ for 4 days. Total RNA was isolated from 100 seedling roots using TRIzol solution (Invitrogen, Carlsbad, CA, USA). Two micrograms of total RNA was used for first-strand cDNA synthesis using RevertAid Reverse Transcriptase and Oligo d(T)primers (Takara, Dalian, China). The cDNA yield was measured according to the PCR signal generated from the internal standard, with the housekeeping gene *Actin 2* used as the internal control. The primers that were used in the quantitative RT-PCR are listed in **Table 1** (Liu et al., 2010; Lin et al., 2013b; Li et al., 2014).

Quantitative RT-PCR was performed using a RealMasterMix kit (Tiangen, Beijing, China) with 25 cycles as follows: 94°C for 30 s, 58°C for 30 s and 72°C for 30 s, followed by 72°C for 10 min gene expression quantifications was performed using the relative $2^{-\Delta\Delta Ct}$ method (Livak and Schmittgen, 2001). All experiments were performed in triplicate for each treatment.

GUS Staining

To investigate the mechanism by which $CdCl_2$ affects the synthesis and distribution of ethylene, the relative expression of the ethylene reporter construct, EBS::GUS, in which the GUS reporter gene is driven by a synthetic EIN3-responsive promoter, was tested. GUS staining was as described by He et al. (2011). Four-day-old seedlings were transferred to agar plates supplemented with 75 μM $CdCl_2$ for 4 days, then were collected and washed with staining buffer without X-Gluc and stained with GUS staining buffer (50 mM sodium phosphate buffer, pH 7.0, 10 mM Na_2EDTA, 0.5 mM $K_4[Fe(CN)_6]\cdot 3H2O$, 0.5 mM $K_3[Fe(CN)_6]$, 0.1% Triton X-100, and 1 mg/mL *X*-Gluc). Ethanol (70%) was used to terminate the staining reaction, and the seedlings were mounted on slides in 50 μL Hoyer's solution (chloral hydrate: water: glycerol; 8:3:1; w/v/v) and examined and photographed with a DM 4000B stereomicroscope (Leica, Germany).

TABLE 1 | The primers used in the quantitative RT-PCR.

Gene	Gene Bank accession no.	Primers
ACTIN2	At3g18780	F:5′- TGTGCCAATCTACGAGGGT-3′ R:5′- GCTGGTCTTTGAGGTTTCC-3′
ACS2	At1g01480	F:5′- AGGCAATTGCACATTTCATGG-3′ R:5′- CTGTCCGCCACCTCAAGTCT-3′
EIN2	At5g03280	F:5′- TGCGCATGCACTTAACCTTTT-3′ R:5′- TGACTCAGCAAGACGCCAGA-3′
EIN3	At3g20770	F:5′- AGGCAGAGACCTTTTTCTTCATCA-3′ R:5′- CAGGCTCAGCTTGTGGAACA-3′

Morphometric Analysis

To further test the involvement of ethylene signaling in regulating the plant response to Cd stress, two ethylene-insensitive mutants (*ein2-5* and *ein3-1eil1-1*) together with the wild type plant were subjected to Cd stress with or without ACC. The length of the whole primary root of the seedlings were measured either directly with a ruler or using NIS Elements software (Nikon, Japan) from digital images captured with a Nikon camera. The root tip length was also determined in the same way as the primary root. The number of the lateral roots was counted. The number of root hairs in a 2 mm section at the appropriate midpoint of the root was counted under a dissecting microscope. Root hairs from the photographs were measured with a ruler, and their length in μm was determined by comparison with an ocular micrometer photograph at the same magnification. All experiments for phenotypic analysis were performed at least three times, and the data represent one independent experiment.

Cadmium Analysis

The samples were rinsed twice with tap water then with de-ionized water before air drying is used to remove dirt and salt from root surface. High purity deionized water from a Millipore water purification system (Bedford, NY, USA) was used throughout our study. The root materials were dried at 80°C to a constant weight. The dried tissues were weighed and digested in HNO3 (100%) using the heat block (Shah et al., 2014; Olowu et al., 2015). The metal concentration was determined by inductively coupled plasma mass spectrometry (ICP-MS). Blanks (only HNO3) were analyzed for reference purposes. The cadmium standard solutions for ICP-MS (TraceCERT®, Sigma–Aldrich) were produced according to the ISO Guide 34 in the analysis of Cd concentrations. External calibration was performed using a five-point analytical curve, prepared by diluting the individual cadmium standards with 5.0% (v/v) HNO3.

Bioaccumulation factor (Bf) was calculated to measure plant uptake of Cd:

$$\mathrm{Bf} = \frac{\text{Cd concentration in tissues } (\mathrm{gkg^{-1}})}{\text{Cd concentration in solution } (\mathrm{gL^{-1}})}.$$

Measurement of Superoxide Accumulation in Root Tips by (NBT) Staining

Four-days-old wild-type seedlings cultivated on MS agar plates were transferred to agar plates supplemented with 75 μM $CdCl_2$ or 75 μM $CdCl_2$ plus various concentrations of ACC (0.01, 0.05, and 0.5 μM, a precursor of ethylene biosynthesis) with or without 5 μM AIB (an inhibitor of ethylene biosynthesis). Superoxide within the root tip was detected by nitroblue tetrazolium (NBT) staining which is used to detect O_2^- production, as well as other compounds (such as ascorbate) as described by Hernández et al. (2001). Seedlings were collected, and the roots were immersed in a 0.1% solution of NBT in 50 mM K–phosphate buffer (pH 6.4), containing 10 mM Na-azide in the absence of light. Seedlings were then transferred to distilled water to stop the reaction. The roots were observed and photographed using a DM 4000B Leica stereomicroscope equipped with a DC300F Nikon camera. The NIH ImageJ software was used to assess the mean staining intensity of the elongation and meristematic zones (0, white; 255, black) following Dunand et al. (2007). At least 20 individual roots were analyzed for each genotype and treatment, and one representative image was selected for the figure.

NADPH-Dependent $O_2^{\cdot-}$ Determination

The determination of the NADPH dependent O_2^- generating activity in isolated plasma membrane vesicles was carried out according to Quartacci et al. (2001) and Van Gestelen et al. (1997), by measuring the rate of SOD inhibitable reduction of NBT using NADPH as electron donor. The reaction mixture consisted of 50 mM TRIS HCl buffer, pH 7.5, 0.25 M sucrose, 0.1 mM NBT, and 50–100 μg proteins. After 1 min preincubation the reaction started by the addition of 0.1 mM NADPH and the absorbance changes at 530 nm were followed for 5 min. Rates of O_2^- generation were calculated using an extinction coefficient of 12.8 $\mathrm{mM^{-1}cm^{-1}}$.

Measurement of SOD and Its Three Isoenzymes Activities

To investigate whether ethylene reduced Cd stress-induced superoxide accumulation through the SOD pathway, 4-day-old seedlings were transferred to various agar plates for 4 days, and the activities of SOD and its three isoenzymes (Cu/Zn-SOD, Fe-SOD and Mn-SOD) were measured according to the method of Yu and Rengel (1999) with minor modifications. Frozen root samples (0.05 g) were weighed and homogenized on ice for 2 min in 5 ml of homogenizing solution containing 50 mm HEPES buffer and 0.1 mm Na_2EDTA (pH 7.6). The homogenate was centrifuged at 15000 *g* for 15 min at 4°C to produce the crude extract for SOD assays. SOD activity was assayed by monitoring the inhibition of the photochemical reduction of NBT. For the total SOD assay, a 5-ml reaction mixture containing 50 mM HEPES (pH 7.6), 0.1 mM EDTA, 50 mM Na_2CO_3 (pH 10.4), 13 mM methionine, 0.025% (w/v) Triton X-100, 75 μM NBT, 2 μM riboflavin and an appropriate aliquot of enzyme extract was utilized. The reaction mixtures were illuminated for 15 min at a light intensity of 350 $\mu\mathrm{mol\cdot m^{-2}\cdot s^{-1}}$. One unit of SOD activity was defined as the amount of enzyme required to cause a 50% inhibition in the reduction of NBT, as monitored at 560 nm. The activities of different SOD forms were identified by adding KCN and/or H_2O_2 to the reaction mixture (Giannopolitis and Ries, 1977). KCN inhibits Cu/Zn-SOD but does not affect Mn-SOD or Fe-SOD, whereas H_2O_2 inactivates Cu/Zn-SOD and Fe-SOD but not Mn-SOD. In addition, peroxidases might interfere with the SOD assay in the presence of exogenous H_2O_2 (Yu et al., 1998). After the extensive preliminary testing of a range of concentrations, KCN (at final concentration of 3 mM) was added to the reaction mixture before the addition of H_2O_2 (5 mM final concentration) to eliminate the interference of peroxidase and catalase enzymes (Chen and Asada, 1989). Mn-SOD activity was determined in the presence of both 3 mM KCN and 5 mM H_2O_2. Fe-SOD activity was obtained by subtracting the Mn-SOD

activity from the activity in the presence of 3 mM KCN, and Cu/Zn-SOD activity was calculated from the differences between the total activity and that of Mn-SOD and Fe-SOD. Identical reaction mixtures that had not been illuminated were used to correct for background absorbance.

Detection of Cell Death in Meristimatic and Elongation Zones under Cd Stress with Trypan Blue and Propidium Iodide (PI) Staining

To assess cell death in the root tips under Cd stress, the roots were immersed in 4 mg ml^{-1} Trypan blue solution (Sigma–Aldrich, Saint Louis, MO, USA) for 15 min at room temperature and then washed with distilled water three times. The samples were then observed by light microscopy, and pictures were taken as detailed earlier.

For PI staining, the seedlings were immersed in the PI (Sigma–Aldrich, St. Louis, MO, USA) solution (final concentration of 1 μg ml^{-1}) for 10 min at room temperature in the dark and then washed with phosphate buffer solution (PBS) (pH 7.4) three times. The samples were then examined using a DM 4000B fluorescence microscope (Leica, Germany) with an excitation wavelength of 546 nm. Both experiments were repeated three times. For each treatment and genotype, at least 20 roots were analyzed for both stains, and one representative image was selected for the figure.

Terminal Deoxynucleotidyl Transferase-Mediated dUTP Nick End Labeling (TUNEL) and 4, 6-Diamidino - 2-Phenylindole (DAPI) Assay

Cadmium-induced cell death in root tips can occur through either necrosis or PCD. To examine whether PCD is involved in the cell death at the root tips, we investigated the chromatin condensation and the internucleosomal fragmentation of the DNA by DAPI staining and the TUNEL assay, respectively. To detect cell apoptosis caused by Cd stress, an *In Situ* Cell Death Detection Kit, AP (Roche, Germany) was used. The TUNEL assay was performed according to the manufacturer's instructions with a few modifications. In brief, whole seedlings were fixed in 4% paraformaldehyde in PBS (pH 7.4) for 20 min (20°C). After washing the samples for 30 min with PBS, the samples were incubated in permeabilization solution (0.1% Triton X-100, 0.1% sodium citrate) for 2 min (4°C), followed by two washes with PBS. Fifty microliters of TUNEL reaction mixture was then added to the sample, and it was incubated for 60 min (37°C) in a humidified atmosphere in the dark. After being rinsed three times with PBS, the samples were analyzed under a DM 4000B fluorescence microscope (Leica, Germany) with a 488 nm excitation line and a 530 nm emission filter.

DAPI staining was performed by fixing roots in a solution of ethanol and acetic acid (3:1) for 1 h. The roots were then washed twice with PBS (pH 7.4) and stained in PBS containing 1 μg/ml of DAPI for 20 min at room temperature. After two PBS washes, the samples were analyzed under a DM 4000B fluorescence microscope (Leica, Germany) with a UV light filter, and the images were captured immediately. Both experiments were repeated three times. For each treatment and genotype, at least 20 roots were analyzed for each experiment, and one representative image was selected for the figure.

Statistical Analyses

For all experiments, the data were statistically analyzed using SPSS 17.0 (SPSS, Chicago, IL, USA). One-way analysis of variance with a Duncan *post hoc* test was used to test the differences at a 0.05 level for the primary root length and distance to the first root hair. The data presented here are the means with standard error (SE).

NADPH oxidase and SOD enzymes activities values were used for the calculation of abundance ratios between groups and for statistical evaluation by Student's *t*-test ($P = 0.05$).

RESULTS

Traits Indicating Involvement of Ethylene in Plant Responses to Cd Stress

To investigate whether ethylene biosynthesis and signaling were involved in the plant response to Cd stress, quantitative RT-PCR was performed using a Real Master Mix kit (Tiangen, Beijing, China) to measure the relative expression of genes encoding for ethylene biosynthesis, and of perception and signaling proteins. The relative expression of *ACS2*, *ACS6*, *ERF1,* and *EIN3* increased slightly under small concentrations of Cd but increased drastically after increasing Cd concentrations to 75 μM but decreased with further increase to 100 μM although expression still higher than the control (**Figure 1A**).

To investigate the mechanism by which CdCl2 affects the synthesis and distribution of ethylene, the relative expression of the ethylene reporter construct, EBS::GUS, in which the GUS reporter gene is driven by a synthetic EIN3-responsive promoter, was tested. Remarkably, less than 10% of root tips in unstressed seedlings exhibited GUS staining while nearly 80% of them in stressed seedlings were stained (**Figures 1B,C**). Taken these results together, suggested the involvement of ethylene signaling in plant responses to Cd stress.

Effect of Cd Stress on Root System Development

The primary root lengths of the wild-type (Col-0) and the *ein2-5* and *ein3-1eil1-1* plants were severely inhibited by 75 μM $CdCl_2$ (Supplementary Figure S1).

However, **Figure 2A** showed that the primary roots lengths of both the *ein2-5* and *ein3-1eil1-1* plants were slightly longer than those of the wild-type (Col-0) plants after 2 days of Cd stress. This phenomenon was reversed after 4 days treatment as the primary roots of the *ein2-5* and *ein3-1eil1-1* plants were significantly shorter than the wild-type plants.

The root tip length (distance to the first root hair) was also determined after 4 days of Cd treatment (**Figures 2B,C**). Similar to the results for the primary root length, the length of the

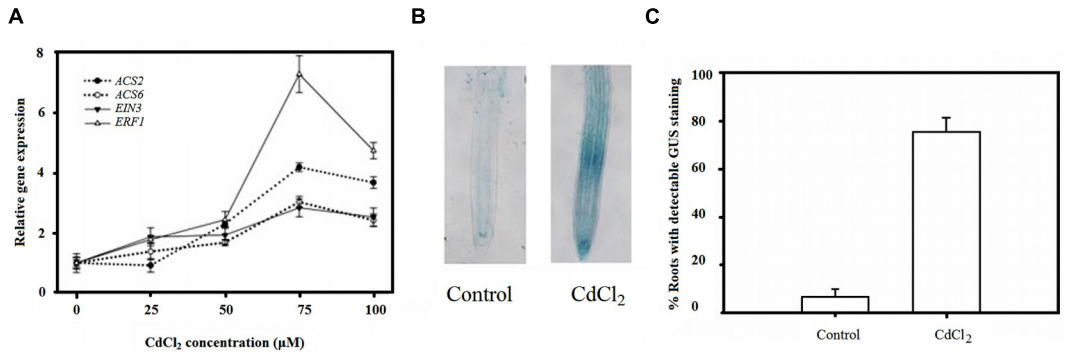

FIGURE 1 | Ethylene signaling involved in plant root response to Cd stress. (A) QRT-PCR analysis of relative gene expression of *ACS2*, *ACS6*, *EIN3* and *ERF2* in Col-0 plants under Cd stress. **(B)** Increased ethylene response after Cd treatment visualized by EBS::GUS staining. **(C)** Frequency of stained root tip as **(B)** indicated. Seeds were germinated and grown on MS agar plates for 4 days and then transferred to $CdCl_2$ (μM) pretreated plates, as indicated, for another 4 days.

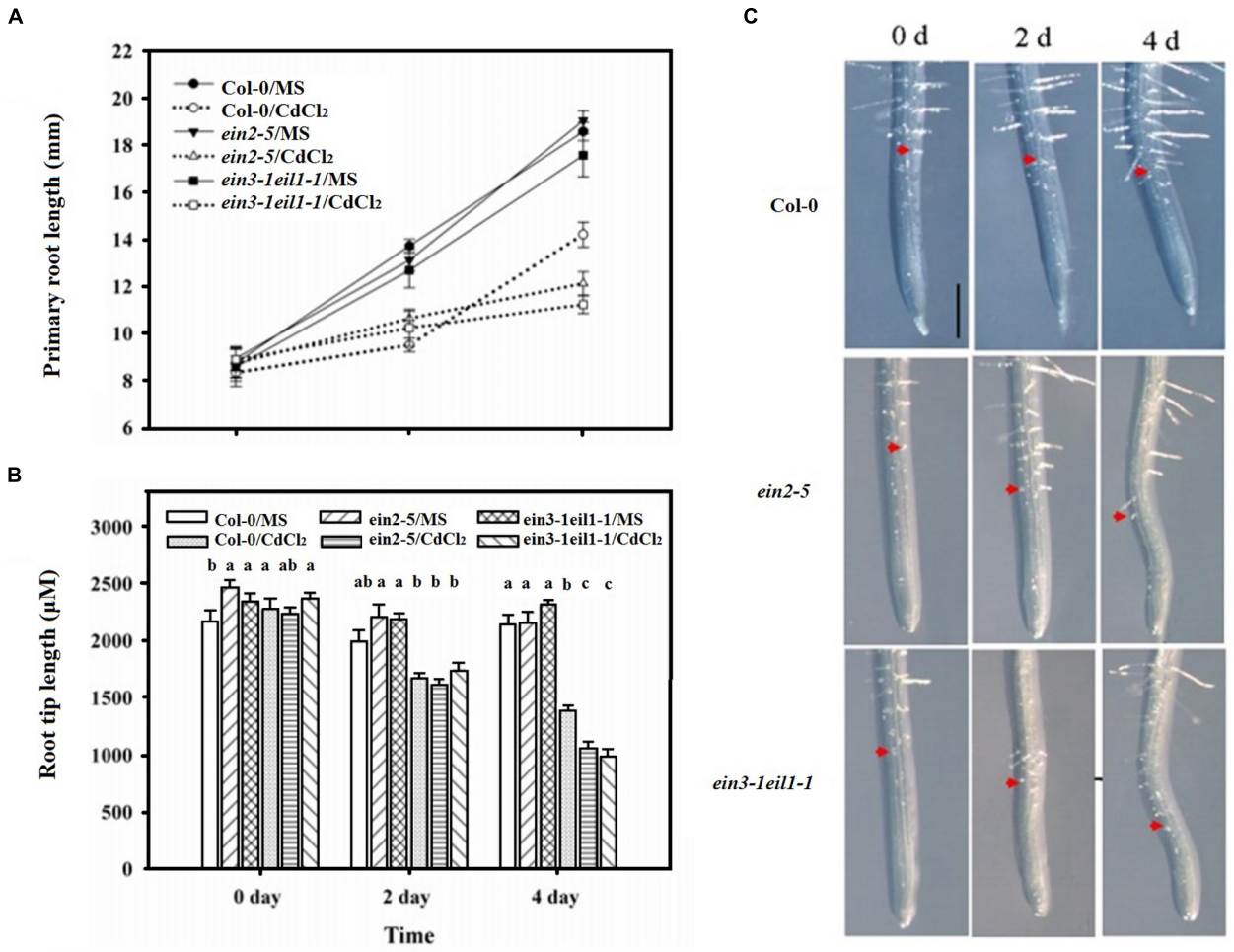

FIGURE 2 | The inhibitory effects of increased duration of exposure to Cd on the elongation of the primary roots and root tips of the Col-0, *ein2-5,* and *ein3-1eil1-1* plants. Four-day-old seedlings were transferred to $CdCl_2$ (75 μM)-treated agar plates for 2 and 4 days, as indicated. **(A)** The primary root lengths of the Col-0, *ein2-5,* and *ein3-1eil1-1* plants after being transferred to the Cd-treated agar plates for different periods, **(B)** and **(C)** the root tip length. Values represent the mean ± SE of 20 individual plants, and the letters indicate significant differences ($P < 0.05$). Scale bars = 50 μm.

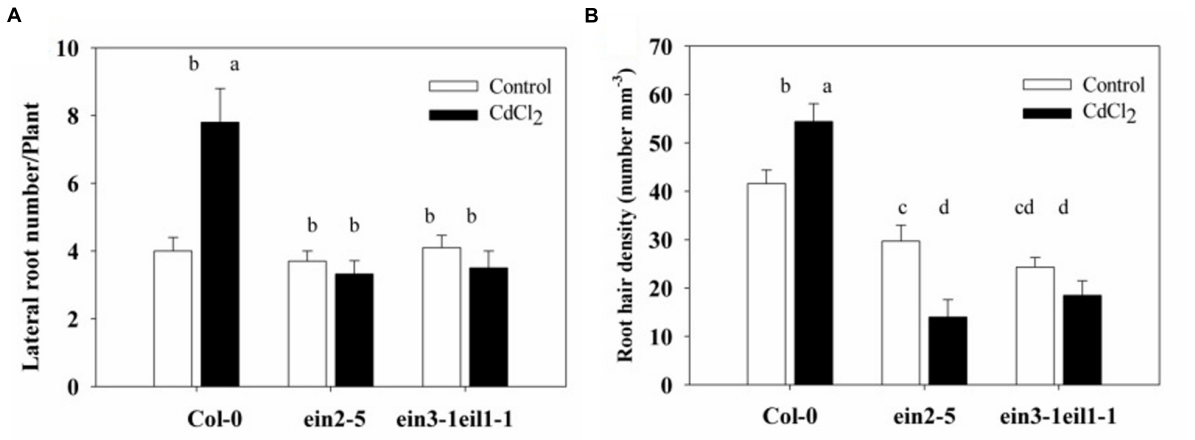

FIGURE 3 | Effects of Cd stress on the root system architecture of the Col-0, *ein2-5,* and *ein3-1eil1-1* plants. (A) Lateral root number and **(B)** Root hair density of the 4-days-old seedlings transferred to agar plates with or without $CdCl_2$ (75 μM) for 7 days. Values represent the mean ± SE of more than 20 individual seedlings, and the bars indicate the standard error. The letters indicate significant differences ($P < 0.05$).

meristematic and elongation/transition zone was less inhibited in the *ein2-5* and *ein3-1eil1-1* mutants than in the wild-type plants after 2 days of Cd treatment. The length of the zones in the wild-type plant Col-0, *ein2-5,* and *ein3-1eil1-1* plants was 1433.1, 1614.6, and 1741.7 μm, respectively. In contrast, after 4 days treatment, the root tip lengths of both the *ein2-5* (1056.6 μm) and *ein3-1eil1-1* (983.8 μm) plants were significantly shorter compared with the Col-0 (1393.1 μm) plants.

The lateral root number of the wild-type plants also significantly increased, whereas it was reduced in the *ein2-5* and *ein3-1eil1-1* mutants in response to Cd stress (**Figure 3A**). This result was expected since the primary root of wild-type plants was longer than that of the *ein2-5* and *ein3-1eil1-1* mutants under of Cd stress.

Moreover, the root hair density also significantly increased in the Col-0 plants, whereas it severely decreased in both the *ein2-5* and *ein3-1eil1-1* plants under Cd stress (**Figure 3B**). In addition, it is worth noting that very few root hairs emerged from mutants under Cd stress and also the length of these hairs decreased (Supplementary Figure S2).

These results show that the wild type plants improve their root system development under Cd stress in a better way than *ein2-5* and *ein3-1eil1-1* plants, this led us to suggest the involvement of ethylene in modulating the root system development in response to Cd stress.

Cd Contents

Three-week-old *A. thaliana* seedlings were exposed to 0, 10, 20, and 40 μM CdCl2 for 8 days. (**Figure 4**) showed that a significant accumulation of Cd content in roots treated with Cd. In the Col-0 root, the Cd content was highest-level after exposure to 20 μM CdCl2. At the 20 μM CdCl2 treatment, the Cd contents of *ein2-5* and *ein3-1eil1-1* were even higher than the Cd content of Col-0. Bioaccumulation factors (Bfs) in the Col-0 got their maximum at 20 μM CdCl2. Furthermore, the Bfs of ein2-5 and *ein3-1eil1-1* were even bigger than Col-0 under 20 μM CdCl2 treatment.

Cd content		
	Root(mg/kg)	**Root BFs**
Col-0 0	9.694976	
Col-0 10	224.2883	98.21699
Col-0 20	537.0656	117.5919
Col-0 40	526.6715	57.65803
Ein2-5 0	12.56477	
Ein2-5 20	633.3126	138.6654
Ein3-1eil1-1 0	6.539379	
Ein3-1eil1-1 20	861.8926	188.7136

FIGURE 4 | The Cd content of *Arabidopsis* seedlings roots. Three-week-old *Arabidopsis thaliana* seedlings were exposed to 0, 10, 20, and 40 μM CdCl2 for 8 days. At the 20 μM CdCl2 treatment, the Cd contents of ein2-5 and ein3-1eil1-1 were even higher than the Cd content of Col-0. Furthermore, the Bfs of ein2-5 and ein3-1eil1-1 were even bigger than Col-0 under 20 μM CdCl2 treatment.

Ein2-5 and *ein3-1eil1-1* are both ethylene insensitive mutants. Moreover, application of ACC with different concentrations of Cd (50, 60, and 75 μM) decreased the Cd content in roots compared with roots treated with Cd alone (Supplementary Figure S3).

These results showed that ethylene could play a role in plant response to Cd stress supporting the above mentioned results and led us to wonder about the mechanism by which ethylene modulates root system in response to Cd stress.

Accumulation of Superoxide in Root Tips under Cd Stress

To understand the mechanism of ethylene response to Cd stress, we determined the superoxide in the root tips of Col-0, ein2-5, and *ein3-1eil1-1* under Cd stress. As the results in

Figure 5 indicate, superoxide was predominantly localized at the meristematic and elongation zones. Treatment of the 4-days-old seedlings with 75 μM Cd for 2 days significantly increased the production of superoxide in all plants. However, the accumulation of superoxide in both the *ein2-5* and *ein3-1eil1-1* mutants was significantly greater than in the wild-type plants. Furthermore, after 4 days of Cd treatment, the concentration of superoxide in the root tips was still higher in the two ethylene-insensitive mutants than in the wild-type plants.

The altered response pattern of superoxide accumulation in *ein2-5* and *ein3-1eil1-1* suggested that ethylene signaling regulates superoxide accumulation in the Cd-stressed root tips.

Effect of ACC (an Ethylene Precursor) on Superoxide Accumulation and Root System Development under Cd Stress

To investigate whether regulating superoxide is the mechanism by which ethylene modulate root system under Cd stress, effect of exogenous ACC (a precursor of ethylene biosynthesis) on the accumulation of superoxide in the root tips of the Col-0 plants under Cd stress was determined. Generally, Cd stress-induced increases in superoxide accumulation were detected after 4 days of treatment in the Col-0 root tips as shown in **Figure 6**. Although the supplementation with ACC slightly increased superoxide accumulation, treatment with ACC together with Cd markedly reduced the production of superoxide compared with the Cd treatment alone in the root tips, especially with 0.01 μM concentration of ACC. Conversely, the ACC-induced suppression of the production of superoxide was reversed by AIB (an inhibitor of ethylene biosynthesis) application with ACC and Cd, confirming the results in **Figure 5** and supporting the involvement of ethylene in regulation of superoxide accumulation in the Cd-stressed root tips.

It was well established that PMs NADPH oxidase transfers electrons from cytoplasmic NADPH to O_2 to form O_2^- thus we subsequently determined activity of NADPH in seedlings roots. Same results were also obtained in determining NADPH oxidase activities when exogenous ACC were applied to CdCl2 stressed seedlings and also with the addition of AIB (**Figure 7**).

The effect of ACC on the root system development in Col-0 plants under Cd stress was also determined. Application of exogenous ACC significantly increased lateral roots number and the length of root hairs. The effect of ACC was reversed by AIB that decreased the root hairs density and root hairs length (Supplementary Figure S4).

Taken these results together, we suggested that ethylene modulates root system development under Cd stress by regulating superoxide concentration.

Effect of Ethylene on SOD and Its Three Isoenzymes Activities in Root under Cd Stress

To investigate whether ethylene reduces Cd stress-induced superoxide accumulation through the SOD pathway, the activities of SOD and its three isoenzymes (Cu/Zn-SOD, Fe-SOD, and Mn-SOD) were measured in Col-0, *ein2-5,* and *ein3-1eil1-1* under Cd stress.

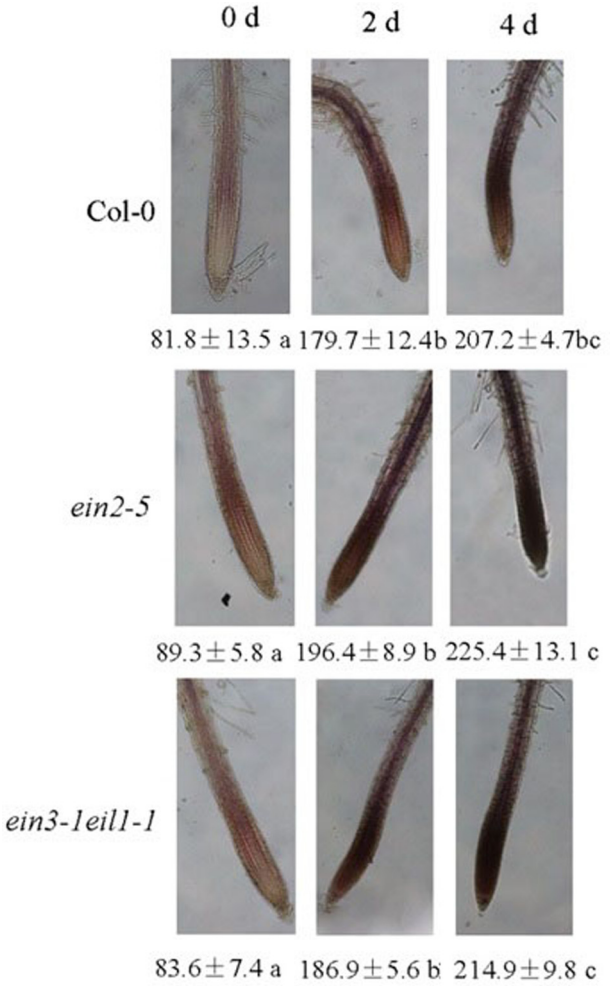

FIGURE 5 | The accumulation of superoxide in the root tips of the Col-0, *ein2-5,* and *ein3-1eil1-1* plants. Four-day-old seedlings were transferred to $CdCl_2$ (75 μM) -treated agar plates for different periods, as indicated. 2 days treatment significantly increased the production of superoxide in all plants. In addition, the accumulation of superoxide in both the *ein2-5* and *ein3-1eil1-1* mutants was significantly greater than in the wild-type plants even after 4 days of Cd treatment. Values (mean ± SE) show the staining intensity, and the letters indicate significant differences ($P < 0.05$). At least 20 individual roots were analyzed for each genotype and treatment, and one representative image was selected for the figure.

As the results in **Figure 8** illustrate, the SOD activities were increased after Cd treatment in the Col-0 but decreased in the *ein2-5* and *ein3-1eil1-1* plants. In addition, the application of exogenous ACC significantly increased these activities compared with the Cd stress in both Col-0 and the *ein3-1eil1-1* mutants. However, ACC displayed no effects on the SOD activities of the *ein2-5* plants. Furthermore, the Cu/Zn-SOD and Fe-SOD activities significantly increased while the Mn-SOD activity did not change after 5 days of Cd treatment in the Col-0. Conversely, the activities of all three isoenzymes decreased in

FIGURE 6 | Effects of exogenous ACC on the accumulation of superoxide in the root tips of the Col-0 plants under Cd stress. Four-day-old seedlings were transferred to various pretreated agar plates with $CdCl_2$ (75 μM) or $CdCl_2$ (75 μM) plus various concentrations of ACC (0.01, 0.05, and 0.5 μM, a precursor of ethylene biosynthesis) with or without 5 μM AIB (an inhibitor of ethylene biosynthesis), as indicated, for 4 days. Values (mean ± SE) show the staining intensity, and the letters indicate significant differences ($P < 0.05$). At least 20 individual roots were analyzed for each genotype and treatment, and one representative image was selected for the figure.

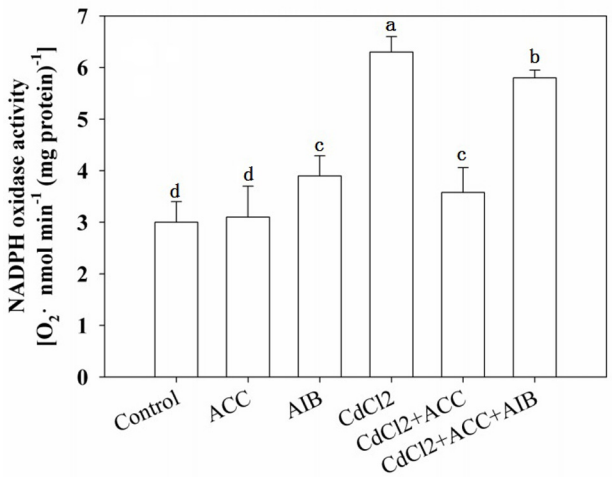

FIGURE 7 | Effects of various pretreatments (ACC, 0.01 μM; AIB, 5 μM) on the production of O_2^- in roots of *Arabidopsis* Col-0 seedlings under Cd (75 μM) stress. Four-day-old seedlings were transferred to various pretreated agar plates for 4 days. Values represent the mean ± SE, and the bars indicate the standard error.

the *ein2-5* and *ein3-1eil1-1* roots. The application of ACC to the Cd-stressed seedlings increased the activities of all three isoenzymes in both the wild-type and *ein3-1eil1-1* plants, whereas ACC only increased the activity of Fe-SOD in the *ein2-5* mutant.

The increased SOD activities in the Col-0 compared with the *ein2-5* and *ein3-1eil1-1* plants under Cd stress suggests that ethylene reduces Cd stress-induced superoxide accumulation through the SOD pathway.

Effect of Cd Stress on Cell Death in the Meristematic and Elongation Zones

High concentrations of superoxide induce oxidative stress, which ultimately leads to cell death. We evaluated the progression of cell death in the root tips using PI and Trypan blue. As the results of the PI staining show, exposing the seedlings to Cd stress generally led to significant cell death in the primary root tips after treatment, especially from the end of the meristematic zone to the elongation zone. However, the PI-positive cells staining intensity were significantly increased in the *ein2-5* and *ein3-1eil1-1* mutant root tips compared with the wild-type plants after 2 days of Cd treatment. Furthermore, after 4 days of Cd treatment, the entire meristematic and most of the elongation zone of the stressed root tips were strongly stained in the *ein2-5* and *ein3-1eil1-1* mutants, whereas only the end of the elongation zone was affected in the wild-type plants. Staining analyses using Trypan blue showed a similar progression of cell death, confirming the above mentioned results (**Figure 9**).

TUNEL and DAPI Assay

As shown in **Figure 10**, only weak DAPI (weak fluorescence and round, homogenously stained nuclei) and TUNEL signals were detected in the untreated seedling roots. However, a marked increase in DAPI fluorescence and condensed and granular

nuclear staining and TUNEL-positive signals were detected in the meristematic zone to the elongation zone from root tips after Cd treatment. However, higher intensity of DAPI fluorescence and TUNEL-positive signals were also detected in the wild-type root tips compared with the *ein2-5* and *ein3-1eil1-1* mutants.

DISCUSSION

In plants, the root system is the first part of plant to suffer from heavy metal toxicity and respond to it (Li et al., 2012; Duan et al., 2015). Thus, the root system is of significant importance and relevance when investigating the responsive and adaptive patterns of plants to environmental stress. This study is particularly to understand the mechanisms by which Cd affects the root system growth and how plants response to this kind of stress. A key feature of the effects of Cd is the increased biosynthesis of ethylene and production of superoxide in roots of *A. thaliana* seedlings. Ethylene was demonstrated to control superoxide concentrations by modulating the activities of SOD isoenzymes.

Figure 1A indicated that the expression of both *ACS2* and *ACS6*, which encode two ACS isoforms (ACS2 and ACS6) can be induced by Cd, as observed for other abiotic factors (Smith and Arteca, 2000; Wang et al., 2002; Schellingen et al., 2014). Furthermore, under Cd stress, the expression of *EIN3*, whose expression increases in the presence of ethylene, and the ethylene-responsive gene *ERF1*, which is an immediate target of EIN3 (Solano et al., 1998) were increased, indicating the presence of ethylene in the seedling roots. This confirms that ethylene signaling was involved in the plant response to Cd stress in the roots. However, expression of genes related to ethylene biosynthesis and perception reaches its maximum value at a certain dose of $CdCl_2$ (75 μM) but is decreased with a higher concentration (100 μM), indicating that at 100 μM, cells suffered from extensive damage and many cellular components are affected. This would disrupt signaling networks. Moreover, the enhanced expression of these genes might account for the observed Cd-induced stimulation of EBS::GUS activity in the root apex (**Figures 1B,C**). The present results are consistent with a previous study indicating that Cd stress induces rapid ethylene production in root tips (Arteca and Arteca, 2007), suggesting that ethylene is involved in regulating plant responses to heavy metals.

The primary root lengths of the wild-type (Col-0) and the *ein2-5* and *ein3-1eil1-1* plants were severely inhibited by 75 μM $CdCl_2$ (Supplementary Figure S1), consistent with a previous report that primary root length decreases in a Cd dose-dependent manner (Schellingen et al., 2015).

However, **Figure 2** showed that the primary roots and the root tip lengths of both the *ein2-5* and *ein3-1eil1-1* plants were slightly longer than those of the wild-type (Col-0) plants after 2 days of Cd stress. This phenomenon was reversed after 4 days treatment as *ein2-5* and *ein3-1eil1-1* plants primary roots and root tips were significantly shorter than those of the wild-type plants.

The lateral root number and the root hairs density of the wild-type plants also significantly increased, consistent with the stress-induced morphogenic response (SIMR) reported before (Bochicchio et al., 2015). Whereas they were reduced in the *ein2-5* and *ein3-1eil1-1* mutants in response to Cd stress (**Figure 3**). Several studies indicate that morphological alterations that result in increased root surface area, such as the formation of root hairs and lateral roots, could be functionally related to stress avoidance mechanisms (Sofo et al., 2013; Vitti et al., 2013).

All of these facts highlighted the essential role of ethylene in the process. It is known that ethylene upregulates auxin biosynthesis in *Arabidopsis* seedlings root tips (Swarup et al., 2007; He et al., 2011), while auxin is involved in lateral root

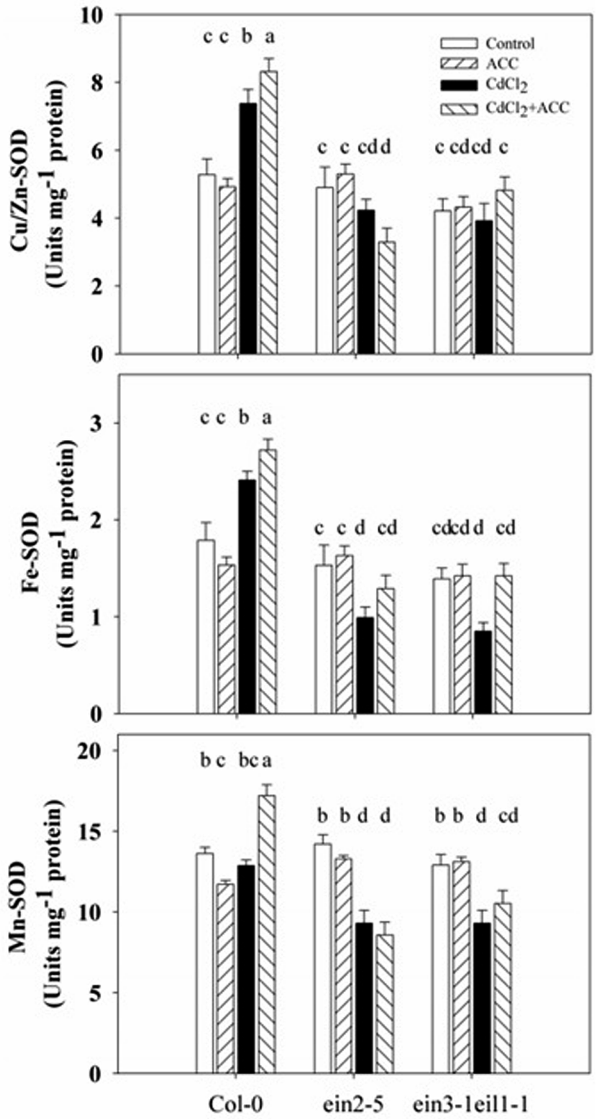

FIGURE 8 | Activities of SOD and its Cu/Zn-SOD, Fe-SOD, and Mn-SOD isoenzymes in the roots of the Col-0, *ein2-5,* and *ein3-1eil1-1* plants under Cd stress. Four-day-old seedlings were transferred for 4 days to agar plates, or agar plates with $CdCl_2$ (75 μM), or with ACC (0.01 μM, a precursor of ethylene biosynthesis), or with $CdCl_2$ (75 μM) plus ACC (0.01 μM), as indicated. Values represent the mean ± SE, and the bars indicate the standard error. The letters indicate significant differences ($P < 0.05$).

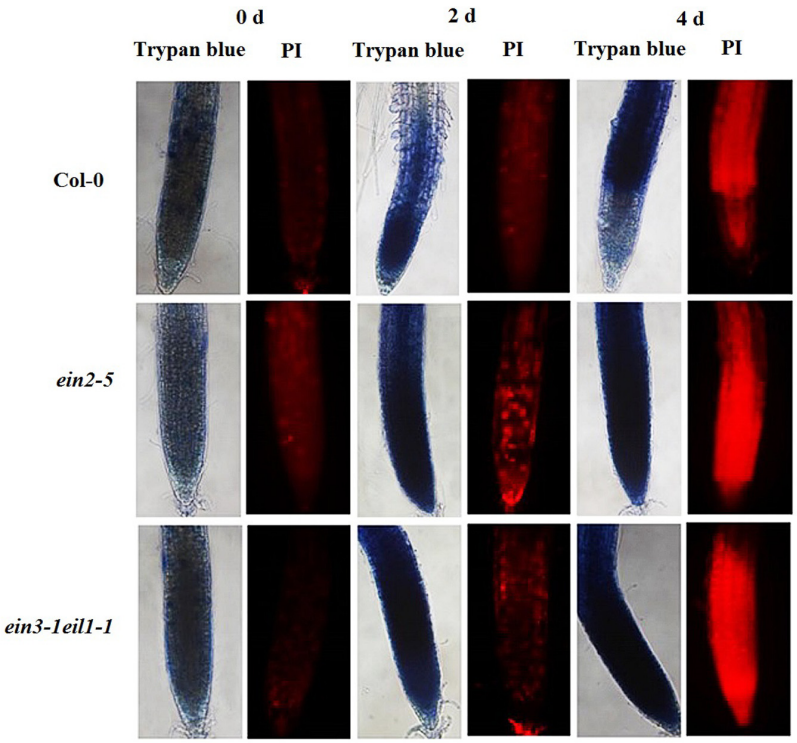

FIGURE 9 | Progression of cell death/necrosis in the root tips of the Col-0, *ein2-5,* and *ein3-1eil1-1* plants during Cd stress. Four-day-old seedlings were transferred to $CdCl_2$ (75 μM)-treated agar plates for different periods, as indicated. The seedlings were then collected and incubated in propidium iodide (PI) or Trypan blue. At least 20 individual roots were analyzed for each genotype and treatment, and one representative image was selected for the figure.

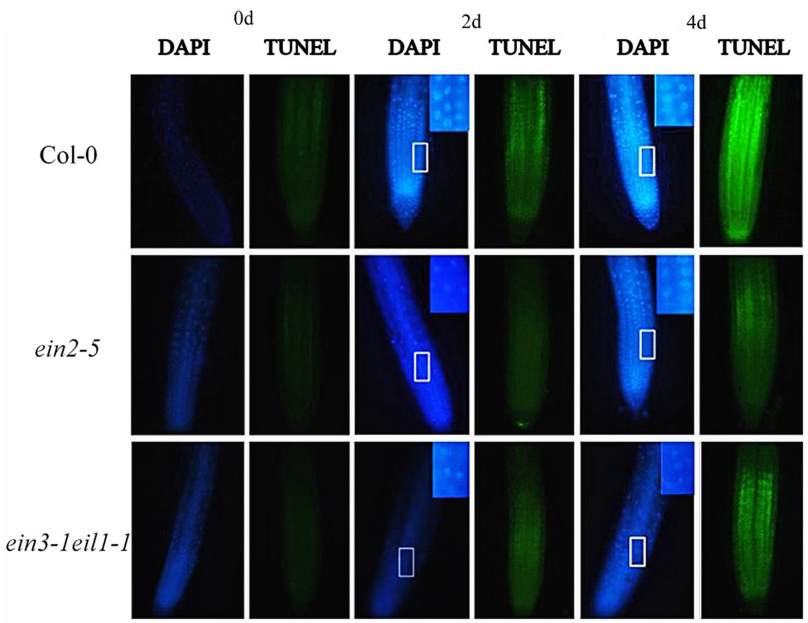

FIGURE 10 | Progression of programmed cell death, indicated by DAPI and TUNEL staining in the root tips of the Col-0, *ein2-5,* and *ein3-1eil1-1* plants during Cd stress. Four-day-old seedlings were transferred to $CdCl_2$ (75 μM)-treated agar plates for different time points, as indicated. Insets: close up observations enlargement of chromatin condensation. At least 20 individual roots were analyzed for each genotype and treatment, and one representative image was selected for the figure.

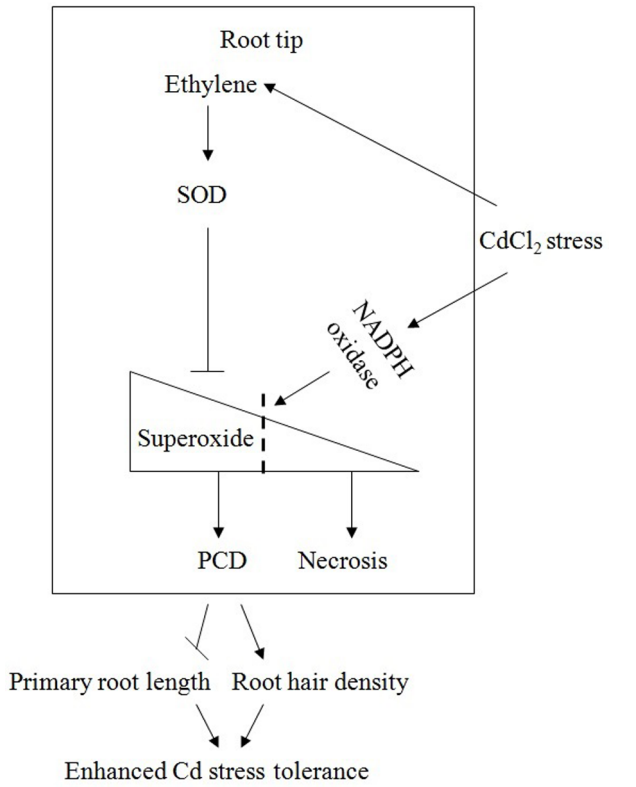

FIGURE 11 | A schematic model elucidating the interaction of ethylene, SOD, superoxide and PCD in the root meristematic and elongation zones under Cd stress.

initiation and emergence in a number of plants including *Arabidopsis* (Aloni et al., 2006; Zolla et al., 2010; Sofo et al., 2013). Thus, the crosstalk between ethylene and axuin in regulating lateral root initiation and emergence may also contribute to root SIMR under Cd stress.

Figure 4 in consistent with a previous study; showed a significant accumulation of Cd content in root treated with Cd (Khan et al., 2016). The Cd contents of *ein2-5* and *ein3-1eil1-1* were even higher than the Cd content of the wild-type. Moreover, the bioaccumulation factors (Bfs) were even bigger in ein2-5 and *ein3-1eil1-1* than Col-0. Application of ACC with different concentrations of Cd (50, 60, and 75 μM) decreased the Cd content in roots compared with roots treated with Cd alone (Supplementary Figure S3). These results suggested that ethylene could play a role in plant response to Cd stress.

The tip of roots is a zone of active ROS production (Liszkay et al., 2004). ROS such as O_2^-, H_2O_2 and $HO^\bullet$ are considered as key factors in the oxidative burst, and play important physiological roles in plants (Mittler et al., 2004). Cd stress is related to the increase of ethylene and ROS (Xu et al., 2010a). The oxidative damage of ROS requires the action of antioxidative enzymes, including SOD, which can convert superoxide radicals into hydrogen peroxide, water and oxygen. As the results indicate, Cd stimulated superoxide production in the root tips (**Figure 5**), consistent with the results of Liptáková et al. (2012). However, the accumulation of superoxide in both the *ein2-5* and *ein3-1eil1-1* mutants was significantly greater than in the wild-type plants. The altered response pattern of superoxide accumulation in *ein2-5* and *ein3-1eil1-1* suggested that ethylene signaling regulates superoxide accumulation in the Cd-stressed root tips.

Application of exogenous ACC suppressed Cd stress-induced production of superoxide in the root tips of wild type plants (**Figure 6**), consistent with the salinity stress results (Lin et al., 2013a). On the other side, application of AIB, the inhibitor of ethylene biosynthesis, together with ACC and Cd reversed the ACC-induced suppression of superoxide production, consistent with the reverse effect of AIB to ACC effect on seed germination under stress (Lin et al., 2013b) and depending on the fact that AIB inhibits the endogenous as well as the ACC-dependent ethylene production (Satoh and Esashi, 1982), these results supports the involvement of ethylene in regulation of superoxide accumulation in the Cd-stressed root tips.

In agreement with former results, $CdCl_2$ treatment increased NADPH oxidase activity while application of exogenous ACC decreased $CdCl_2$ induced NADPH oxidase activity. Moreover, application of AIB with ACC and Cd reversed the ACC effect and increased NADPH oxidase activity (**Figure 7**), indicating ethylene regulation of $O_2^{\bullet-}$ production under Cd stress, consistent with pervious result that an oxidative burst induction by NADPH oxidases under stress is connected to ethylene (Montero-Palmero et al., 2014).

In accompanied to the suppressed Cd stress-induced production of superoxide and the decreased $CdCl_2$ induced NADPH oxidase activity, roots hairs density and root hairs length increased under $CdCl_2$ stress by application of exogenous ACC (Supplementary Figure S4). The effect of ACC (a precursor of ethylene biosynthesis) was reversed by AIB (an inhibitor of ethylene biosynthesis). Taken these results together, we suggested that ethylene modulates root system development under Cd stress by regulating superoxide concentration.

Interestingly, under Cd stress, the activities of all three SOD isoenzymes increased in the wild-type plants compared with *ein2-5* and *ein2-5eil1-1*. Moreover, application of exogenous ACC to the Cd-treated seedlings increased all three SOD isoenzymes activities in the wild-type plants (**Figure 8**), consistent with the increased SOD activity in Col-0 plants that was accompanied by a significant up-regulation of the genes *FeSOD* compared with *ein2-5* mutant under salt stress (Lin et al., 2013a). Results in Supplementary Figure S5 show up-regulation of the three SOD genes in Col-0 plants compared with *ein2-5* mutant under oxidative stress induced by salinity. This observation that suggests that ethylene may directly increase SOD activity under Cd stress, may be the underlying mechanism through which ethylene controls the amount of superoxide, which then initiates distinct forms of responses and acclimations depending upon the levels of superoxide in *Arabidopsis* root tips under Cd stress.

High concentrations of superoxide lead to oxidative stress, which directly inhibits or modifies some proteins and ultimately induces cell death (Miller et al., 2010). There are two types of cell death, necrosis and apoptosis, which is a subset of PCD. PI,

a nucleic acid dye that intercalates into double-stranded nucleic acids, is excluded from viable cells but can penetrate the cell membranes of dead cells (Ning et al., 2002; Duan et al., 2010). Generally, Cd treatment induced the onset of necrosis at the meristematic and elongation zones of all plants compared with the control (**Figure 9**). However, greater PI-positive staining was observed after (4 days) Cd treatment in both the *ein2-5* and *ein3-1eil1-1* mutant root tips compared with the Col-0 plants. In addition, these results were confirmed by Trypan blue staining, another molecular prove for cell necrosis. These results suggest that ethylene may play crucial roles in preventing cells of the meristematic and elongation zones from undergoing necrosis during stress and recovery periods when plants are facing stresses.

Programmed cell death is an activate process of cellular suicide that is essential for development and stress responses in plants. To examine whether PCD is involved in cell death at root tips, DAPI staining and the TUNEL assay, were used, respectively, which are typically used as diagnostic markers for PCD (Duan et al., 2010; Xu et al., 2010b). In contrast to the progression of necrosis, the initiation of PCD was more rapid and intensive in the wild-type plant root tips compared with the *ein2-5* and *ein3-1eil1-1* plants, confirming the critical role of ethylene in the progression of PCD under Cd stress (**Figure 10**).

Based on our combined results, a schematic model (**Figure 11**) elucidating the interaction of ethylene, SOD, superoxide and PCD in the root meristematic and elongation zones under Cd stress, is presented. In this model, Cd treatment induces the rapid production of ethylene and superoxide by the gene up-regulation of ethylene synthesis and the Cd-caused oxidative damage, respectively. Under Cd stress, the presence of ethylene maintains or increases the activity of SOD, which maintains the level of superoxide lower than what expected without ethylene and consequently prevent cells of the meristematic and elongation zones from undergoing necrosis. Superoxide could function as a signaling molecule that initiates the occurrence of PCD in root tips at the early stage of Cd. PCD occurs in the region of root apical meristem in undifferentiated cells, where it alters root apical dominance and remodels the root system architecture, inhibiting primary root elongation and increasing lateral roots number and root hairs density, perhaps to minimize the damage caused by stress conditions. This response is an adaptive and acclimation strategy of plants to adverse environments.

CONCLUSION

The presence of ethylene enables plants to perceive adverse stimuli and to respond effectively, thus enhancing their acclimation and adaptation to stress. In *ein2-5* and *ein3-1eil1-1* seedlings, the increased superoxide concentration induced by Cd stress resulted in cell death and defects in root growth and development in the root meristem zone, by which root elongation was inhibited. In contrast, ethylene reduced the concentration of superoxide maintained in wild type plants. Moreover, superoxide concentration was reduced by ACC application and reversely increased by application of AIB that inhibits the endogenous as well as the ACC-dependent ethylene production. The ethylene-induced suppression of superoxide decreased the occurrence of cells death and initiated PCD to minimize the damage caused by Cd stress. Hence, this is a general adaptive mechanism in *A. thaliana* through ethylene induction to improve root system development by modulating superoxide anion concentration under Cd stress.

AUTHOR CONTRIBUTIONS

ZT conceived and designed the experiments. AA, ZY, and YL performed the experiments and wrote the manuscript. JL and ZZ revised the manuscript. All authors reviewed the manuscript.

ACKNOWLEDGMENTS

The authors thank Prof. Hongwei Guo (Peking University) for providing *Arabidopsis thaliana* seeds. We express our appreciation to Prof. David Lawlor for critical reading of the manuscript. This study was supported by the National Natural Science foundation of China (Grant No. 31370007).

SUPPLEMENTARY MATERIAL

The Supplementary Material for this article can be found online at: http://journal.frontiersin.org/article/10.3389/fpls.2017.00253/full#supplementary-material

REFERENCES

Aloni, R., Aloni, E., Langhans, M., and Ullrich, C. I. (2006). Role of cytokinin and auxin in shaping root architecture: regulating vascular differentiation, lateral root initiation, root apical dominance and root gravitropism. *Ann. Bot.* 97, 883–893. doi: 10.1093/aob/mcl027

Alonso, J. M., Hirayama, T., Roman, G., Nourizadeh, S., and Ecker, J. R. (1999). EIN2, a bifunctional transducer of ethylene and stress responses in *Arabidopsis*. *Science* 284, 2148–2152. doi: 10.1126/science.284.5423.2148

Alonso, J. M., Stepanova, A. N., Solano, R., Wisman, E., Ferrari, S., Ausubel, F. M., et al. (2003). Five components of the ethylene-response pathway identified in a screen for *weak ethylene-insensitive* mutants in *Arabidopsis*. *Proc. Natl. Acad. Sci. U.S.A.* 100, 2992–2997. doi: 10.1073/pnas.0438070100

An, F., Zhao, Q., Ji, Y., Li, W., Jiang, Z., Yu, X., et al. (2010). Ethylene-induced stabilization of ETHYLENE INSENSITIVE3 and EIN3-LIKE1 is mediated by proteasomal degradation of EIN3 binding F-box 1 and 2 that requires EIN2 in *Arabidopsis*. *Plant Cell* 22, 2384–2401. doi: 10.1105/tpc.110.076588

Andresen, E., Kappel, S., Stärk, H. J., Riegger, U., Borovec, J., Mattusch, J., et al. (2016). Cadmium toxicity investigated at the physiological and biophysical levels under environmentally relevant conditions using the aquatic model plant *Ceratophyllum demersum*. *New Phytol.* 210, 1244–1258. doi: 10.1111/nph.13840

Arteca, R. N., and Arteca, J. M. (2007). Heavy-metal-induced ethylene production in *Arabidopsis thaliana*. *J. Plant Physiol.* 164, 1480–1488. doi: 10.1016/j.jplph.2006.09.006

Asgher, M., Khan, M. I. R., Anjum, N. A., and Khan, N. A. (2015). Minimising toxicity of cadmium in plants—role of plant growth regulators. *Protoplasma* 252, 399–413. doi: 10.1007/s00709-014-0710-4

Azevedo, H., Pinto, G., Fernandes, J., Loureiro, S., and Santos, C. (2005). Cadmium effects on sunflower: growth and photosynthesis. *J. Plant Nutr.* 28, 2211–2220. doi: 10.1080/01904160500324782

Binder, B. M., Walker, J. M., Gagne, J. M., Emborg, T. J., Hemmann, G., Bleecker, A. B., et al. (2007). The *Arabidopsis* EIN3 binding F-Box proteins EBF1 and EBF2 have distinct but overlapping roles in ethylene signaling. *Plant Cell* 19, 509–523. doi: 10.1105/tpc.106.048140

Bochicchio, R., Sofo, A., Terzano, R., Gattullo, C. E., Amato, M., and Scopa, A. (2015). Root architecture and morphometric analysis of *Arabidopsis thaliana* grown in Cd/Cu/Zn-gradient agar dishes: a new screening technique for studying plant response to metals. *Plant Physiol. Biochem.* 91, 20–27. doi: 10.1016/j.plaphy.2015.03.010

Burzynski, M., and Klobus, G. (2004). Changes of photosynthetic parameters in cucumber leaves under Cu, Cd, and Pb stress. *Photosynth* 42, 505–510. doi: 10.1007/S11099-005-0005-2

Cao, S. Q., Ren, G., Jiang, L., Yuan, H. B., and Ma, G. H. (2009). The role of β-aminobutyric acid in enhancing cadmium tolerance in *Arabidopsis thaliana*. *Russ. J. Plant Physiol.* 56, 575–579. doi: 10.1134/S1021443709040190

Chae, H., and Lee, W. (2001). Ethylene-and enzyme-mediated superoxide production and cell death in carrot cells grown under carbon starvation. *Plant Cell Rep.* 20, 256–261. doi: 10.1007/s002990000307

Chao, Q., Rothenberg, M., Solano, R., Roman, G., Terzaghi, W., and Ecker, J. R. (1997). Activation of the ethylene gas response pathway in *Arabidopsis* by the nuclear protein ETHYLENE-INSENSITIVE3 and related proteins. *Cell* 89, 1133–1144. doi: 10.1016/S0092-8674(00)80300-1

Chen, G. X., and Asada, K. (1989). Ascorbate peroxidase in tea leaves: occurrence of two isozymes and the differences in their enzymatic and molecular properties. *Plant Cell Physiol.* 30, 987–998. doi: 10.1093/oxfordjournals.pcp.a077844

Choppala, G., Saifullah Bolan, N., Bibi, S., Iqbal, M., Rengel, Z., Kunhikrishinan, A., et al. (2014). Cellular mechanisms in higher plants governing tolerance to cadmium toxicity. *Crit. Rev. Plant Sci.* 33, 374–391. doi: 10.1080/07352689.2014.903747

Demidchik, V., Straltsova, D., Medvedev, S. S., Pozhvanov, G. A., Sokolik, A., and Yurin, V. (2014). Stress-induced electrolyte leakage: the role of K+-permeable channels and involvement in programmed cell death and metabolic adjustment. *J. Exp. Bot.* 65, 1259–1270. doi: 10.1093/jxb/eru004

Dong, C. H., Jang, M., Scharein, B., Malach, A., Rivarola, M., Liesch, J., et al. (2010). Molecular association of the *Arabidopsis* ETR1 ethylene receptor and a regulator of ethylene signaling, RTE1. *J. Biol. Chem.* 285, 40706–40713. doi: 10.1074/jbc.M110.146605

Duan, X., Li, X., Ding, F., Zhao, J., Guo, A., Zhang, L., et al. (2015). Interaction of nitric oxide and reactive oxygen species and associated regulation of root growth in wheat seedlings under zinc stress. *Ecotoxicol. Environ. Saf.* 113, 95–102. doi: 10.1016/j.ecoenv.2014.11.030

Duan, Y., Zhang, W., Li, B., Wang, Y., Li, K., Han, C., et al. (2010). An endoplasmic reticulum response pathway mediates programmed cell death of root tip induced by water stress in *Arabidopsis*. *New Phytol.* 186, 681–695. doi: 10.1111/j.1469-8137.2010.03207.x

Dunand, C., Crèvecoreur, M., and Penel, C. (2007). Distribution of superoxide and hydrogen peroxide in *Arabidopsis* root and their influence on root development: possible interaction with peroxidases. *New Phytol.* 174, 332–341. doi: 10.1111/j.1469-8137.2007.01995.x

Giannopolitis, C. N., and Ries, S. K. (1977). Superoxide dismutases I. Occurrence in higher plants. *Plant physiol.* 59, 309–314. doi: 10.1104/pp.59.2.309

Guo, H., and Ecker, J. R. (2003). Plant responses to ethylene gas are mediated by SCF EBF1/EBF2-dependent proteolysis of EIN3 transcription factor. *Cell* 115, 667–677. doi: 10.1016/S0092-8674(03)00969-3

Guo, H., and Ecker, J. R. (2004). The ethylene signaling pathway: new insights. *Curr. Opin. Plant Biol.* 7, 40–49. doi: 10.1016/j.pbi.2003.11.011

Han, L., Li, G. J., Yang, K. Y., Mao, G., Wang, R., Liu, Y., et al. (2010). Mitogen-activated protein kinase 3 and 6 regulate *Botrytis cinerea*-induced ethylene production in *Arabidopsis*. *Plant J.* 64, 114–127. doi: 10.1111/j.1365-313X.2010.04318.x

Harding, S. A., and Roberts, D. M. (1998). Incompatible pathogen infection results in enhanced reactive oxygen and cell death responses in transgenic tobacco expressing a hyperactive mutant calmodulin. *Planta* 206, 253–258. doi: 10.1007/s004250050397

He, W., Brumos, J., Li, H., Ji, Y., Ke, M., Gong, X., et al. (2011). A small-molecule screen identifies L-kynurenine as a competitive inhibitor of TAA1/TAR activity in ethylene-directed auxin biosynthesis and root growth in Arabidopsis. *Plant Cell* 23, 3944–3960. doi: 10.1105/tpc.111.089029

Hernández, J. A., Ferrer, M. A., Jiménez, A., Barceló, A. R., and Sevilla, F. (2001). Antioxidant systems and O2.-/H2O2 production in the apoplast of pea leaves. its relation with salt-induced necrotic lesions in minor veins. *Plant Physiol.* 127, 817–831. doi: 10.1104/pp.010188

Johnson, P. R., and Ecker, J. R. (1998). The ethylene gas signal transduction pathway: a molecular perspective. *Annu. Rev. Genet.* 32, 227–254. doi: 10.1146/annurev.genet.32.1.227

Kendrick, M. D., and Chang, C. (2008). Ethylene signaling: new levels of complexity and regulation. *Curr. Opin. Plant Biol.* 11, 479–485. doi: 10.1016/j.pbi.2008.06.011

Khan, N. A., Asgher, M., Per, T. S., Masood, A., Fatma, M., and Khan, M. I. R. (2016). Ethylene potentiates sulfur-mediated reversal of cadmium inhibited photosynthetic responses in mustard. *Front. Plant Sci.* 7:1628. doi: 10.3389/fpls.2016.01628

Li, J., Jia, H., and Wang, J. (2014). cGMP and ethylene are involved in maintaining ion homeostasis under salt stress in *Arabidopsis* roots. *Plant Cell Rep.* 33, 447–459. doi: 10.1007/s00299-013-1545-8

Li, X., Yang, Y., Zhang, J., Jia, L., Li, Q., Zhang, T., et al. (2012). Zinc induced phytotoxicity mechanism involved in root growth of *Triticum aestivum* L. *Ecotoxicol. Environ. Saf.* 86, 198–203. doi: 10.1016/j.ecoenv.2012.09.021

Lin, Y., Chen, D., Paul, M., Zu, Y., and Tang, Z. (2013a). Loss-of-function mutation of EIN2 in *Arabidopsis* exaggerates oxidative stress induced by salinity. *Acta Physiol Plant.* 35, 1319–1328. doi: 10.1007/s11738-012-1172-y

Lin, Y., Yang, L., Paul, M., Zu, Y., and Tang, Z. (2013b). Ethylene promotes germination of *Arabidopsis* seed under salinity by decreasing reactive oxygen species: evidence for the involvement of nitric oxide simulated by sodium nitroprusside. *Plant Physiol. Biochem.* 73, 211–218. doi: 10.1016/j.plaphy.2013.10.003

Lin, Y. C., Wang, J. J., Zu, Y. G., and Tang, Z. H. (2012). Ethylene antagonizes the inhibition of germination in *Arabidopsis* induced by salinity by modulating the concentration of hydrogen peroxide. *Acta Physiol. Plant.* 34, 1895–1904. doi: 10.1007/s11738-012-0989-8

Lingam, S., Mohrbacher, J., Brumbarova, T., Potuschak, T., Fink-Straube, C., Blondet, E., et al. (2011). Interaction between the bHLH transcription factor FIT and ETHYLENE INSENSITIVE3/ETHYLENE INSENSITIVE3-LIKE1 reveals molecular linkage between the regulation of iron acquisition and ethylene signaling in *Arabidopsis*. *Plant Cell* 23, 1815–1829. doi: 10.1105/tpc.111.084715

Liptáková, L. U., Boèová, B., Huttová, J., Mistrík, I., and Tamás, L. (2012). Superoxide production induced by short-term exposure of barley roots to cadmium, auxin, alloxan and sodium dodecyl sulfate. *Plant Cell Rep.* 31, 2189–2197. doi: 10.1007/s00299-012-1329-6

Liszkay, A., van der Zalm, E., and Schopfer, P. (2004). Production of reactive oxygen intermediates (O2-, H2O2, and OH) by maize roots and their role in wall loosening and elongation growth. *Plant Physiol.* 136, 3114–3123. doi: 10.1104/pp.104.044784

Liu, Y., Xiong, Y., and Bassham, D. C. (2009). Autophagy is required for tolerance of drought and salt stress in plants. *Autophagy* 5, 954–963. doi: 10.4161/auto.5.7.9290

Liu, Y., Ye, N., Liu, R., Chen, M., and Zhang, J. (2010). H2O2 mediates the regulation of ABA catabolism and GA biosynthesis in *Arabidopsis* seed dormancy and germination. *J. Exp. Bot.* 61, 1–12. doi: 10.1093/jxb/erq125

Livak, K. J., and Schmittgen, T. D. (2001). Analysis of relative gene expression data using real-time quantitative PCR and the 2-ΔΔCT method. *Methods* 25, 402–408. doi: 10.1006/meth.2001.1262

Lorenzo, O., Piqueras, R., Sánchez-Serrano, J. J., and Solano, R. (2003). ETHYLENE RESPONSE FACTOR1 integrates signals from ethylene and jasmonate pathways in plant defense. *Plant Cell* 15, 165–178. doi: 10.1105/tpc.007468

Miller, G. A. D., Suzuki, N., Ciftci-Yilmaz, S., and Mittler, R. O. N. (2010). Reactive oxygen species homeostasis and signalling during drought and

salinity stresses. *Plant Cell Environ.* 33, 453–467. doi: 10.1111/j.1365-3040.2009.02041.x

Mittler, R., Vanderauwera, S., Gollery, M., and Van Breusegem, F. (2004). Reactive oxygen gene network of plants. *Trends Plant Sci.* 9, 490–498. doi: 10.1016/j.tplants.2004.08.009

Montero-Palmero, M. B., Martín-Barranco, A., Escobar, C., and Hernández, L. E. (2014). Early transcriptional responses to mercury: a role for ethylene in mercury-induced stress. *New Phytol.* 201, 116–130. doi: 10.1111/nph.12486

Nagarajan, V. K., and Smith, A. P. (2012). Ethylene's role in phosphate starvation signaling: more than just a root growth regulator. *Plant Cell Physiol.* 53, 277–286. doi: 10.1093/pcp/pcr186

Ning, S. B., Wang, L., and Song, Y. C. (2002). Identification of programmed cell death in situ in individual plant cells in vivo using a chromosome preparation technique. *J. Exp. Bot.* 53, 651–658. doi: 10.1093/jexbot/53.369.651

Olowu, R. A., Adewuyi, G. O., Onipede, O. J., Lawal, O. A., and Sunday, O. M. (2015). Concentration of heavy metals in root, stem and leaves of *Acalypha indica* and *Panicum maximum* jacq from three major dumpsites in ibadan metropolis, South West Nigeria. *Am. J. Chem.* 5, 40–48. doi: 10.5923/j.chemistry.20150501.06

Pan, Y. J., Liu, L., Lin, Y. C., Zu, Y. G., Li, L. P., and Tang, Z. H. (2016). Ethylene antagonizes salt-induced growth retardation and cell death process via transcriptional controlling of ethylene-, BAG-and senescence-associated genes in *Arabidopsis*. *Front. Plant Sci.* 7:696. doi: 10.3389/fpls.2016.00696

Parlanti, S., Kudahettige, N. P., Lombardi, L., Mensuali-Sodi, A., Alpi, A., Perata, P., et al. (2011). Distinct mechanisms for aerenchyma formation in leaf sheaths of rice genotypes displaying a quiescence or escape strategy for flooding tolerance. *Ann. Bot.* 107, 1335–1343. doi: 10.1093/aob/mcr086

Poschenrieder, C. H., and Barceló, J. (1999). "Water relations in heavy metal stressed plants," in *Heavy Metal Stress in Plants*, ed. M. N. V. Prasad (Berlin: Springer), 207–229. doi: 10.1007/978-3-662-07745-0_10

Quartacci, M. F., Cosi, E., and Navari-Izzo, F. (2001). Lipids and NADPH-dependent superoxide production in plasma membrane vesicles from roots of wheat grown under copper deficiency or excess. *J. Exp. Bot*. 52, 77–84. doi: 10.1093/jxb/52.354.77

Radeva, V., Petrov, V., Minkov, I., Toneva, V., and Gechev, T. (2010). Effect of cadmium on *Arabidopsis thaliana* mutants tolerant to oxidative stress. *Biotechnol. Biotechnol. Equip.* 24, 113–118. doi: 10.1080/13102818.2010.10817823

Sandalio, L., Dalurzo, H., Gomez, M., Romero-Puertas, M., and Del Rio, L. (2001). Cadmium-induced changes in the growth and oxidative metabolism of pea plants. *J. Exp. Bot.* 52, 2115–2126. doi: 10.1093/jexbot/52.364.2115

Santos, C., Monteiro, M., and Dias, M. (2010). *Cadmium Toxicity in Crops: A Review. Environmental Science, Engineering and Technology*. Novinka: Nova Publishers.

Satoh, S., and Esashi, Y. (1982). Effects of α-aminoisobutyric acid and D-and L-amino acids on ethylene production and content of 1-aminocyclopropane-1-carboxylic acid in cotyledonary segments of cocklebur seeds. *Physiol. Plant.* 54, 147–152. doi: 10.1111/j.1399-3054.1982.tb06318.x

Schellingen, K., Van Der Straeten, D., Remans, T., Loix, C., Vangronsveld, J., and Cuypers, A. (2015). Ethylene biosynthesis is involved in the early oxidative challenge induced by moderate Cd exposure in *Arabidopsis thaliana*. *Environ. Exp. Bot*. 117, 1–11. doi: 10.1016/j.envexpbot.2015.04.005

Schellingen, K., Van Der Straeten, D., Vandenbussche, F., Prinsen, E., Remans, T., Vangronsveld, J., et al. (2014). Cadmium-induced ethylene production and responses in *Arabidopsis thaliana* rely on ACS2 and ACS6 gene expression. *BMC Plant Biol.* 14:1. doi: 10.1186/s12870-014-0214-6

Shah, M. T., Ara, J., Muhammad, S., Khan, S., Asad, S. A., and Ali, L. (2014). Potential heavy metals accumulation of indigenous plant species along the mafic and ultramafic terrain in the Mohmand Agency, Pakistan. *Clean* 42, 339–346. doi: 10.1002/clen.201200632

Shibuya, K., Barry, K. G., Ciardi, J. A., Loucas, H. M., Underwood, B. A., Nourizadeh, S., et al. (2004). The central role of PhEIN2 in ethylene responses throughout plant development in petunia. *Plant Physiol.* 136, 2900–2912. doi: 10.1104/pp.104.046979

Singh, R., and Agrawal, M. (2007). Effects of sewage sludge amendment on heavy metal accumulation and consequent responses of *Beta vulgaris* plants. *Chemosphere* 67, 2229–2240. doi: 10.1016/j.chemosphere.2006.12.019

Skottke, K. R., Yoon, G. M., Kieber, J. J., and DeLong, A. (2011). Correction: protein phosphatase 2A controls ethylene biosynthesis by differentially regulating the turnover of ACC synthase isoforms. *PLoS Genet.* 7:e1001370. doi: 10.1371/annotation/b4fc15d6-b3ae-4fbb-8d88-b7d674a79697

Smith, J. M., and Arteca, R. N. (2000). Molecular control of ethylene production by cyanide in *Arabidopsis thaliana*. *Physiol. Plant.* 109, 180–187. doi: 10.1034/j.1399-3054.2000.100210.x

Sofo, A., Vitti, A., Nuzzaci, M., Tataranni, G., Scopa, A., Vangronsveld, J., et al. (2013). Correlation between hormonal homeostasis and morphogenic responses in *Arabidopsis thaliana* seedlings growing in a Cd/Cu/Zn multi-pollution context. *Physiol. Plant.* 149, 487–498. doi: 10.1111/ppl.12050

Solano, R., Stepanova, A., Chao, Q., and Ecker, J. R. (1998). Nuclear events in ethylene signaling: a transcriptional cascade mediated by ETHYLENE-INSENSITIVE3 and ETHYLENE-RESPONSE-FACTOR1. *Genes Dev.* 12, 3703–3714. doi: 10.1101/gad.12.23.3703

Swarup, R., Perry, P., Hagenbeek, D., Van Der Straeten, D., Beemster, G. T., Sandberg, G., et al. (2007). Ethylene upregulates auxin biosynthesis in *Arabidopsis* seedlings to enhance inhibition of root cell elongation. *Plant Cell* 19, 2186–2196. doi: 10.1105/tpc.107.052100

Van Gestelen, P., Asard, H., and Caubergs, R. J. (1997). Solubilization and separation of a plant plasma membrane NADPH-O2-synthase from other NAD (P) H oxidoreductases. *Plant Physiol.* 115, 543–550. doi: 10.1104/pp.115.2.543

Vitti, A., Nuzzaci, M., Scopa, A., Tataranni, G., Remans, T., Vangronsveld, J., et al. (2013). Auxin and cytokinin metabolism and root morphological modifications in *Arabidopsis thaliana* seedlings infected with Cucumber mosaic virus (CMV) or exposed to cadmium. *Int. J. Mol. Sci.* 14, 6889–6902. doi: 10.3390/ijms14046889

Wahid, A., and Khaliq, S. (2015). Architectural and biochemical changes in embryonic tissues of maize under cadmium toxicity. *Plant Biol.* 17, 1005–1012. doi: 10.1111/plb.12326

Wang, K. L.-C., Li, H., and Ecker, J. R. (2002). Ethylene biosynthesis and signaling networks. *Plant Cell* 14(Suppl.), S131–S151. doi: 10.1105/tpc.001768

Xu, J., Wang, W. Y., Yin, H. X., Sun, H., and Mi, Q. (2010a). Exogenous nitricoxide improves antioxidative capacity and reduces auxin degradation in roots of *Medicago truncatula* seedlings under cadmium stress. *Plant Soil* 326, 321. doi: 10.1007/s11104-009-0011-4

Xu, J., Yin, H., Li, Y., and Liu, X. (2010b). Nitric oxide is associated with long-term zinc tolerance in *Solanum nigrum*. *Plant Physiol.* 154, 1319–1334. doi: 10.1104/pp.110.162982

Yoo, S. D., Cho, Y., and Sheen, J. (2009). Emerging connections in the ethylene signaling network. *Trends Plant Sci.* 14, 270–279. doi: 10.1016/j.tplants.2009.02.007

Yu, Q., Osborne, L., and Rengel, Z. (1998). Micronutrient deficiency changes activities of superoxide dismutase and ascorbate peroxidase in tobacco plants. *J. Plant Nutr.* 21, 1427–1437. doi: 10.1080/01904169809365493

Yu, Q., and Rengel, Z. (1999). Micronutrient deficiency influences plant growth and activities of superoxide dismutases in narrow-leafed lupins. *Ann. Bot.* 83, 175–182. doi: 10.1006/anbo.1998.0811

Zhu, Z., An, F., Feng, Y., Li, P., Xue, L., Mu, A., et al. (2011). Derepression of ethylene-stabilized transcription factors (EIN3/EIL1) mediates jasmonate and ethylene signaling synergy in *Arabidopsis*. *Proc. Natl. Acad. Sci. U.S.A.* 108, 12539–12544. doi: 10.1073/pnas.1103959108

Zolla, G., Heimer, Y. M., and Barak, S. (2010). Mild salinity stimulates a stress-induced morphogenic response in *Arabidopsis thaliana* roots. *J. Exp. Bot.* 61, 211–224. doi: 10.1093/jxb/erp290

Conflict of Interest Statement: The authors declare that the research was conducted in the absence of any commercial or financial relationships that could be construed as a potential conflict of interest.

The reviewer MA and handling Editor declared their shared affiliation, and the handling Editor states that the process nevertheless met the standards of a fair and objective review.

frontiers in Plant Science

ORIGINAL RESEARCH
published: 02 November 2016
doi: 10.3389/fpls.2016.01628

Ethylene Potentiates Sulfur-Mediated Reversal of Cadmium Inhibited Photosynthetic Responses in Mustard

Nafees A. Khan, Mohd Asgher*, Tasir S. Per, Asim Masood, Mehar Fatma and M. I. R. Khan*

Plant Physiology and Biochemistry Laboratory, Department of Botany, Aligarh Muslim University, Aligarh, India

The potential of exogenous ethylene and sulfur (S) in reversal of cadmium (Cd)-inhibited photosynthetic and growth responses in mustard (*Brassica juncea* L. cv. Pusa Jai Kisan) were studied. Plants grown with 50 μM Cd showed increased superoxide and H_2O_2 accumulation and lipid peroxidation together with increased activity of 1-aminocyclopropane carboxylic acid synthase (ACS) and ethylene production and inhibition of photosynthesis and growth. Application of 1 mM SO_4^{2-} or 200 μL L^{-1} ethephon (ethylene source) influenced photosynthetic and growth performance equally in presence or absence of Cd. However, their combined application synergistically improved photosynthetic performance more in presence of Cd and reduced oxidative stress (lower superoxide and H_2O_2 accumulation) by decreasing ethylene and glucose sensitivity with the increase in cysteine and methionineand a non-proteinogenic thiol (reduced glutathione; GSH) contents. The central role of ethylene in potentiating S-mediated reversal of Cd-induced oxidative stress was evident with the use of ethylene action inhibitor, norbornadiene (NBD). The application of NBD resulted in decreased thiol production and photosynthetic responses. This suggests that ethylene promotes the effects of S in reversal of adverse effects of Cd, and thus, ethylene modulation may be considered as potential tool to substantiate the S effects in reversal of Cd inhibited photosynthesis and growth in mustard.

Keywords: cadmium, ethylene, norbornadiene, photosynthesis, sulfur

OPEN ACCESS

Edited by:
Stanislav Kopriva,
University of Cologne, Germany

Reviewed by:
Fabio Francesco Nocito,
University of Milan, Italy
Ilaria Forieri,
University of Heidelberg, Germany
Lv Jin Yin,
Northwest A&F University, China

****Correspondence:***
Nafees A. Khan
naf9@lycos.com
Mohd Asgher
asghermohd@gmail.com

Specialty section:
This article was submitted to Plant Physiology, a section of the journal Frontiers in Plant Science

Received: *21 July 2016*
Accepted: *14 October 2016*
Published: *02 November 2016*

Citation:
Khan NA, Asgher M, Per TS, Masood A, Fatma M and Khan MIR (2016) Ethylene Potentiates Sulfur-Mediated Reversal of Cadmium Inhibited Photosynthetic Responses in Mustard. Front. Plant Sci. 7:1628. doi: 10.3389/fpls.2016.01628

INTRODUCTION

Cadmium (Cd) with long biological half-life and potentially toxic even at low concentration has become one of the most challenging threats due to its increasing concentration in agricultural system (Choppala et al., 2014; Asgher et al., 2015; Khan et al., 2015a; Wahid and Khaliq, 2015). Cadmium alters chloroplast structure, inhibits nutrients uptake, inactivates enzymes of CO_2 fixation and negatively affects various cellular functions through displacement of essential elements from proteins (Mobin and Khan, 2007; DalCorso et al., 2008; Masood et al., 2012b; Choppala et al., 2014). It accumulates to high levels in leaves and adversely impacts chlorophyll (Chl) biosynthesis and photosynthetic process by disrupting the electron transport chain, and aggregation of pigment protein complexes of the photosystems (Baryla et al., 2001; Liu et al., 2011; Shukla et al., 2014). Excess of Cd reduces plant performance due to increased formation of reactive

oxygen species (ROS) in plants. Plants develop an array of mechanisms including production of thiol compounds that are regarded as essential components for ROS homeostasis (Anjum et al., 2012; Asgher et al., 2014; Kovácik et al., 2014). The decrease in growth under Cd stress results from the inhibition of photosynthesis (Masood et al., 2012b; Asgher et al., 2014; Khan et al., 2015b). Recently, Liu et al. (2014) have reported that the decrease in photosynthesis with Cd stress was related to the inhibition of maximal photochemical efficiency, quantum yield of electron transport, photochemical quenching and electronic transport rate in *Gossypium hirsutum*. Several efforts have been made to counteract the Cd-induced toxicity and restore the photosynthetic capacity of plants. Supplementation of plants with mineral elements is one of the better strategies adopted. Sulfur (S) limitations resulted in the chlorosis of young leaves and inhibition of photosynthetic activity (Hawkesford, 2000), whereas S supply increases photosynthetic capacity of leaves through an increase in stromal and thylakoid protein and regulating stomatal movement under Cd stress (Masood et al., 2012b; Asgher et al., 2014; Khan et al., 2015b).

Sulfur is component of various metabolic compounds such as cysteine (Cys), methionine (Met), reduced glutathione (GSH), sulfolipids, iron−sulfur clusters, allyl Cys, and glucosinolates (Khan N.A. et al., 2014) that may be necessary for Cd tolerance (Anjum et al., 2008). It has been reported that Cys alleviates salt-induced growth inhibition and reduces oxidative stress by modulating cellular redox status due to its own antioxidant property in *Hordeum vulgare* plants (Genisel et al., 2014). Astolfi and Zuchi (2013) showed that adequate S allowed sufficient GSH synthesis that helped in avoiding the effects of ROS on photosynthetic efficiency and growth to cope with salt stress. The increased accumulation of proteinogenic and non-proteinogenic thiols with increasing Cd concentrations in plants suggested that efficient sulfate uptake and assimilation may help in Cd tolerance (Nocito et al., 2002; Sun et al., 2007; Lancilli et al., 2014). The S deficiency leads to reduced Chl content, pigment system (PS) II efficiency, and ribulose 1,5-bisphosphate carboxylase oxygenase (Rubisco) content (Lunde et al., 2008). Sulfur may also regulate photosynthesis through ethylene production as ethylene synthesis is linked to S-assimilation via the formation of Cys and Met. Thus, the S-mediated changes in growth and development of plants also involve ethylene. Further, photosynthetic protection under Cd stress through S-mediated ethylene may also involve glucose (Glc) as antagonistic interaction between Glc and ethylene exists (Yanagisawa et al., 2003). Iqbal et al. (2011) reported that ethephon and N together increased ethylene and decreased Glc sensitivity, which increased photosynthesis and growth.

Phytohormones play key role in the regulation of photosynthetic characteristics (Khan et al., 1998, 2002, 2005; Masood and Khan, 2013; Asgher et al., 2014; Iqbal et al., 2014). Ethylene is a gaseous plant hormone with versatile role in regulating photosynthesis and growth responses under abiotic stress (Wang et al., 2013; Khan and Khan, 2014; Schellingen et al., 2014; Asgher et al., 2015; Thao et al., 2015; Khan et al., 2015c). Fu et al. (2014) studied the regulatory interaction between S-assimilation and ethylene for tolerance to arsenic in *Arabidopsis* Col-0. Exogenously applied GSH positively modulates ethylene biosynthetic pathways enzyme and improves stress tolerance in *Arabidopsis* Col-0 showing that GSH mediated resistance to stresses occurs via an ethylene signaling pathway (Datta et al., 2015). Recent studies showed that ethylene signaling pathways might be involved in the accumulation of GSH under Cd stress (Guan et al., 2015). Recently, Iqbal et al. (2015) have shown that ethylene and N interact to regulate photosynthesis of salt stressed *Brassica juncea*. Nazar et al. (2014) have shown the involvement of ethylene in reversal of salt inhibited photosynthesis by S in *B. juncea*. Study of Masood et al. (2012b) has shown that ethylene alleviated Cd-induced photosynthetic inhibition by S in *B. juncea*. However, the interaction of ethylene with S and antioxidant metabolites to regulate efficiency of PSII and photosynthesis in *B. juncea* under Cd stress has not been worked out. The aim of the research was to elucidate the role of ethylene in modulating antioxidants in presence of S and alleviation of Cd stress in *B. juncea* plants.

MATERIALS AND METHODS

Plants Material and Growth Conditions

Seeds of mustard (*Brassica juncea* L. Czern and Coss. cv. Pusa Jai Kisan) were selected for the study based on our earlier findings of Iqbal et al. (2012b), which showed that Pusa Jai Kisan was sensitive to ethylene. In order to assess the role of ethylene in S-mediated alleviation of Cd stress, seeds were grown individually with 0 or 50 μM Cd. In addition, plants were grown with 1.0 mM SO_4^{2-}, 200 μL L^{-1} ethephon, 1 mM SO_4^{2-} plus 200 μL L^{-1} ethephon in presence or absence of Cd.

Healthy seeds were surface sterilized with 0.01% $HgCl_2$ followed by repeated washings with distilled water. The seeds were sown in 23-cm diameter pots filled with acid-washed sand. Two healthy plants of nearly equal size in each pot were maintained and were fed with 250 mL of modified full strength Hoagland nutrient solution containing 3 mM KNO_3, 2 mM $Ca(NO_3)_2$, 1 mM $NH_4H_3PO_4$, 50 μM KCl, 25 μM H_3BO_4, 2 μM $MnCl_2$, 20 μM $ZnSO_4$, 0.5 μM $CuSO_4$, 0.5 μM $(NH_4)_6Mo_7O_{24}$, and 20 μM Na_2Fe-EDTA on alternate days. $MgSO_4$ was used for obtaining 1.0 mM SO_4^{2-} concentration and a uniform Mg^{2+} concentration in the treatments was maintained by the addition of $MgCl_2$. Plants grown in nutrient solution served as control. Sulfur was given along with the nutrient solution at 15 days after sowing (DAS), and ethephon at 200 μL L^{-1} concentrations was sprayed on foliage as an average of 10−12 mL per plant at 15 DAS. Cadmium was applied as $CdCl_2$ in the nutrient solution.

In another experiment, to substantiate the finding that ethylene has a role in eliciting S-mediated alleviation of Cd stress, plants were grown either with 0 or 50 μM Cd or in combined treatment of 50 μM Cd + 1.0 mM SO_4^{2-} + 200 μL L^{-1} ethephon and 50 μM Cd + 1.0 mM SO_4^{2-} + 200 μL L^{-1} ethephon + 100 μM NBD. Treatment of ethephon or NBD was given at 15 DAS.

The pots were kept in a greenhouse of the Botany Department, Aligarh Muslim University, Aligarh, India under natural day/night conditions of 22/14 ± 3°C, photosynthetically active radiation (PAR; 680 μmol m^{-2} s^{-1}) and relative humidity of 62 ± 5%. Treatments in both the experiments were arranged in a factorial randomized block design. The number of replicates for each treatment was four ($n = 4$). At 30 DAS, determinations were made for oxidative stress, glucose content, ethylene production, and S-assimilation, photosynthesis and growth characteristics in both the experiments.

Determination of Cd Content

Cadmium content was determined in root and leaf samples. Leaves were washed with distilled water, and the roots were washed with an ice-cold 5 mM $CaCl_2$ solution for 10 min to displace extracellular Cd (Rauser, 1987). Leaf and root samples were dried for 48 h at 80°C, ground to fine powder and digested with concentrated HNO_3/$HClO_4$ (3:1, v:v). Cadmium concentration was determined by atomic absorption spectrophotometer (GBC, 932 plus; GBC Scientific Instruments, Braeside, Australia).

Determination of H_2O_2 Content and Lipid Peroxidation

The content of H_2O_2 was determined following the method of Okuda et al. (1991). Fresh leaf tissues (500 mg) were ground in ice-cold 200 mM perchloric acid. After centrifugation at 1,200 *g* for 10 min, perchloric acid of the supernatant was neutralized with 4 M KOH. The insoluble potassium perchlorate was eliminated by centrifugation at 500 *g* for 3 min. In a final volume of 1.5 mL, 1 mL of the eluate, 400 μL of 12.5 mM 3-(dimethylamino) benzoic acid (DMAB) in 0.375 M phosphate buffer (pH 6.5), 80 μL of 3-methyl-2-benzothiazoline hydrazone (MBTH) and 20 μL of peroxidase (0.25 unit) were added. The reaction was started by the addition of peroxidase at 25°C and the increase in absorbance was recorded at 590 nm.

Lipid peroxidation in leaves was determined by estimating the content of TBARS as described by Dhindsa et al. (1981). Fresh leaf tissues (500 mg) were ground in 0.25% 2-thiobarbituric acid (TBA) in 10% trichloroacetic acid (TCA) using mortar and pestle. After heating at 95°C for 30 min, the mixture was rapidly cooled on ice bath and centrifuged at 10,000 *g* for 10 min. To 1 mL aliquot of the supernatant 4 mL 20% TCA containing 0.5% TBA was added. The absorbance of the supernatant was read at 532 nm and corrected for non-specific turbidity by subtracting the absorbance of the same at 600 nm. The content of TBARS was calculated using the extinction coefficient (155 mM^{-1} cm^{-1}).

Histochemical Detection of ROS

For assay of the accumulation of $O_2^{\cdot-}$ by histochemical staining method, nitro blue tetrazolium (NBT) was used to stain the leaves by adopting the method of Wang et al. (2011) with slight modification. The samples from each treatment were immersed into 1 mg/mL NBT solution prepared in 10 mM phosphate buffer (pH 7.8) at ambient temperature under light for 6 h. Blue (NBT staining) spots appeared; the stained samples were boiled in ethanol.

Activities of ATP-Sulfurylase, SAT, and S Content

Activity of ATP-sulfurylase (ATP-S; EC, 2.7.7.4) was measured using molybdate-dependent formation of pyrophosphate as described by Lappartient and Touraine (1996). Fresh leaf tissue (1.0 g) was ground at 4°C in a buffer consisting of 10 mM Na_2EDTA, 20 mM Tris-HCl pH 8.0, 2 mM dithiothreitol (DTT), and 0.01 g mL^{-1} polyvinyl pyrrolidone (PVP), using 1:4 (w/v) tissue to buffer ratio. The homogenate was centrifuged at 20,000 *g* for 10 min at 4°C. The supernatant was used for *in vitro* ATP-sulfurylase assay. The reaction was initiated by adding 0.1 mL of extract to 0.5 mL of the reaction mixture, which contained 7 mM $MgCl_2$, 5 mM Na_2MoO_4, 2 mM Na_2ATP, and 0.032 units mL^{-1} of sulfate-free inorganic pyrophosphate in 80 mM Tris–HCl buffer, pH 8.0. Another aliquot from the same extract was added to the same reaction mixture but without Na_2MoO_4. Incubations were carried out at 37°C for 15 min, after which phosphate was determined.

Activity of serine acetyltransferase (SAT; EC, 2.3.1.30) in the leaf extract was determined by the method of Kredich and Tomkins (1966). Fresh leaf tissue (0.5 g) was ground with a chilled mortar and pestle in 2 mL of ice cold extraction buffer 100 mM Tris–HCl pH 8.0, 100 mM KCl, 20 mM $MgCl_2$, 1% Tween 80, and 10 mM DTT. The samples were centrifuged at 11,600 *g* for 10 min at 4°C. The supernatant obtained was used for SAT assay. The enzyme reaction mixture contained 0.1 mM acetyl CoA, 50 mM Tris–HCl pH 7.6, 1 mM DTNB, 1 mM EDTA, and 1 mM L-serine in 1 mL. Subsequent to reaction initiation by addition of enzyme at 25°C, the initial velocity was estimated by monitoring the increase in absorbance at 412 nm and the rates were calculated using an extinction coefficient of 13,600 for thionitrobenzoic acid. A blank containing all materials except L-serine was run simultaneously and subtracted from the reaction rate obtained with L-serine.

Sulfur content was determined in leaf samples digested in a mixture of concentrated HNO_3 and 60% $HClO_4$ (85:1 v/v) using the turbidimetric method (Chesnin and Yien, 1950).

Determination of Cysteine, Methionine, Reduced Glutathione, and Redox State

Cysteine content in leaves was determined spectrophotometrically adopting the method of Giatonde (1967). Fresh leaf (500 mg) was homogenized in 5% (w:v) ice-cold perchloric acid. The suspension was centrifuged at 2,800 *g* for 1 h at 5°C and supernatant was filtered. After that, 1 mL of filtrate was treated with acid ninhydrin reagent and the absorption was read at 580 nm. The amount of Cys was calculated using the calibration curve obtained for standard Cys.

Methionine content was determined by the method of Horn et al. (1946). Fresh leaf sample (500 mg) was reflexed with 20.0 mL 6.0 N HCl for 20−24 h followed by evaporation on water bath with the addition of 1.0 g activated charcoal. The filtrate was collected to which 4.0 mL de-ionized water and 2.0 mL

of 5 N-NaOH were added followed by the addition of 0.1 mL sodium nitropruside and 2.0 mL glycine solution (3%). Finally, 4.0 ml phosphoric acid was added and color intensity was read at 450 nm.

Reduced glutathione content was determined following the method of Anderson (1985). Reduced glutathione was assayed by an enzymic recycling procedure in which it was sequentially oxidized by 5′5′-dithiobis-2-nitrobenzoic acid (DTNB) and reduced by NADPH in the presence of GR. For specific assay of GSSG, the GSH was masked by derivatization with 2-vinylpyridine. Fresh leaves (500 mg) were homogenized in 2.0 mL of 5% sulfosalicylic acid under cold conditions. The homogenate was centrifuged at 10,000 *g* for 10 min. To 0.5 mL of supernatant, 0.6 mL of phosphate buffer (100 mM, pH 7.0) and 40 μL of DTNB were added. After 2 min the absorbance was read at 412 nm.

Redox state was presented as the ratio of GSH to oxidized glutathione (GSSG).

Determination of Glucose Content

Leaf glucose content was determined with the method of Krishnaveni et al. (1984) by using glucose as the standard. Leaf extract was prepared by extracting dried leaf in 80% ethanol. The extract was heated in a water bath at 60°C for 10 min and then cooled. The samples were then centrifuged at 1500 *g* for 1 min. The supernatant was used for Glc determination. The reaction mixture consisted of 25 mg O-dianisidine, 1 mL methanol, 49 mL of 0.1 M phosphate buffer pH 6.5, 5 mg of peroxidase, and 5 mg of glucose oxidase. The reaction was started by adding 0.5 mL of the extract to 1 mL of the reaction mixture in a test tube. The tubes were incubated at 35°C for 40 min and the reaction was terminated by addition of 2 mL of 6 N HCl. The color intensity was read at 540 nm.

Measurement of ACS Activity and Ethylene Evolution

Activity of 1-aminocyclopropane carboxylic acid synthase (ACS; EC, 4.4.1.14) was measured by adopting the methods of Avni et al. (1994) and Woeste et al. (1999). Leaf tissue (5.0 g) was ground in 100 mM HEPES buffer (pH 8.0) containing 4 mM DTT, 2.5 mM pyridoxal phosphate, and 25% PVP. The homogenized preparation was centrifuged at 12,000 *g* for 15 min. One ml of the supernatant was placed in a 30 mL tube and 0.1 mL of 5 mM *S*-adenosyl methionine (AdoMet) was added and incubated for 2 h at 22°C. The ACC formed was determined by its conversion to ethylene by the addition of 0.1 mL of 20 mM $HgCl_2$ followed by the addition of 0.1 mL of a 1:1 mixture of saturated NaOH/NaCl and placed on ice for 10 min. In the control set, AdoMet was not added.

Ethylene was measured by cutting 0.5 g of leaf material into small pieces that were placed into 30 mL tubes containing moist paper to minimize evaporation from the tissue and were stoppered with secure rubber caps and placed in light for 2 h under the same condition used for plant growth. An earlier experiment showed that 2 h incubation time was adequate for ethylene detection without the interference of wound-induced ethylene, which began after 2 h of leaf incubation. A 1 mL gas sample from the tubes was withdrawn with a hypodermic syringe and assayed on a gas chromatograph (Nucon 5700, New Delhi, India) equipped with a 1.8 m Porapack N (80–100 mesh) column, a flame ionization detector and data station. Nitrogen was used as the carrier gas. The flow rates of nitrogen, hydrogen and oxygen were 30, 30, and 300 mL min^{-1}, respectively. The detector was set at 150°C. Ethylene was identified based on the retention time and quantified by comparison with peaks from standard ethylene concentration.

Determination of Gas Exchange Parameters, Rubisco Activity, and Growth Characteristics

Net photosynthetic rate, stomatal conductance, and intercellular CO_2 concentration were measured in fully expanded uppermost intact leaves of plants in each treatment using infrared gas analyzer (CID-340, Photosynthesis System, Bio-Science, USA). The measurements were done between 11.00 and 12.00 h at light saturating intensity (PAR; 720 μmol m^{-2} s^{-1}) and at 370 ± 75 μmol mol^{-1} atmospheric CO_2 concentrations.

The activity of Rubisco (EC; 4.1.1.39) was determined spectrophotometrically by adopting the method of Usuda (1985) by monitoring NADH oxidation at 30°C at 340 nm. For enzyme extraction, leaf tissue (1.0 g) was homogenized using a chilled mortar and pestle with ice-cold extraction buffer containing 0.25 M Tris–HCl (pH 7.8), 0.05 M $MgCl_2$, 0.0025 M EDTA, and 37.5 mg DTT. The homogenate was centrifuged at 4°C at 10,000 *g* for 10 min. The resulting supernatant was used to assay the enzyme. The reaction mixture (3 mL) contained 100 mM Tris-HCl pH 8.0, 40 mM $NaHCO_3$, 10 mM $MgCl_2$, 0.2 mM NADH, 4 mM ATP, 5 mM DTT, 1U of glyceraldehyde 3-phosphodehydrogenase, and 1U of 3-phosphoglycerate kinase and 0.2 mM ribulose 1,5-bisphosphate (RuBP). Protein was estimated according to Bradford (1976) using bovine serum albumin as standard.

Plants were uprooted carefully from the pots, washed to remove dust. Leaf area was measured with a leaf area meter (LA 211, Systronics, New Delhi, India). Dry mass of plants was recorded after drying the sample in a hot air oven at 80°C till constant weight.

Measurement of Chlorophyll Fluorescence Parameters

Fully expanded leaves were allowed to adapt under dark condition for 30 min before chlorophyll fluorescence measurements using Junior-PAM chlorophyll fluorometer (Heinz Walz, Germany). Minimal fluorescence (F_o) and maximum fluorescence (F_m) were measured in dark-adapted leaves with a low measuring beam at a light intensity of 125 μmol m^{-2} s^{-1}, whereas under light-adapted condition, minimal fluorescence (F_o') and maximum fluorescence (F_m') were measured in the same leaves with a saturating light intensity (720 μmol $m^{-2}s^{-1}$) together with steady-state fluorescence (F_s). The variable fluorescence (F_v and F_v') was calculated using the values of F_m–F_o and F_m'–F_o', and Φ PS II was

determined as $F_m'\_F_s/F_m'$, maximal efficiency of PS II by using F_v/F_m and intrinsic efficiency of PS II by using F_v'/F_m'. Using fluorescence parameters determined in both light- and dark-adapted states, the photochemical quenching (qP) and non-photochemical quenching (NPQ) were calculated. qP was calculated as $(F_m'–F_s)/F_v'$ and NPQ as $(F_m–F_m')/F_m'$ (Maxwell and Johnson, 2000). Electron transport rate (ETR) was calculated by following formula: Φ PS II × photosynthetic photon flux density × 0.5 × 0.84 as suggested by Krall and Edwards (1992).

Statistical Analysis

Data were analyzed statistically and standard errors were calculated. Analysis of variance was performed on the data using SPSS (ver. 17.0 Inc., USA) to determine the significance at $P < 0.05$. Least significant difference (LSD) was calculated for the significant data to identify difference in the mean of the treatment. Data are presented as mean ± SE ($n = 4$).

RESULTS

Influence of Ethylene or/and S on Cd Accumulation

Cadmium treatment resulted in higher root and leaf Cd content than control. Application of either S or ethephon reduced root Cd content equally by about 50% compared to Cd treated plants. The combination of S + ethephon maximally reduced Cd content by about 66% in root. In leaf, the S or ethephon applied individually reduced Cd content equally by about 58%, and the combined S plus ethephon reduced Cd content by about 68% compared to the Cd treated plants (**Figures 1A,B**).

Influence of Ethylene or/and S under Cd Stress

Oxidative Stress

The samples originated from Cd-treated plants showed higher values for content of TBARS and H_2O_2 by 2.7-times and 2.3-times, respectively, compared to control. The observed values for these characteristics in plants receiving S or ethephon without Cd showed that S or ethephon reduced TBARS and H_2O_2 content equally compared to control. However, the combined treatment of S and ethephon more prominently reduced oxidative stress. The application of S plus ethephon reduced TBARS content by 3.7-times and H_2O_2 content by 2.7-times compared to control (**Table 1**).

ROS Accumulation

In Cd treated plants increase in $O_2^{\cdot-}$ was observed as scattered dark blue spots in the leaf compared with the control (**Figure 2**). However, plants grown with combined treatment of S and ethephon more prominently diminished $O_2^{\cdot-}$ accumulation than the individual treatment of S and ethephon compared to control in absence of Cd. On the other hand, applying combined dose of S plus ethephon more prominently reduced the accumulation of $O_2^{\cdot-}$ than individual application of S and ethephon in the presence of Cd compared to Cd-treated plants (**Figure 2**).

Activity of ATP-S, SAT, and Content of S

Activity of ATP-S and SAT increased with Cd treatment by 42.3 and 33.5%, respectively, whereas S content decreased by 27.0% in comparison to control. Application of S or ethephon equally increased ATP-S activity by about 72.3%, SAT activity by 63.6% and S content by 41.6% over the control under non-stress condition. The combined treatment of S and ethephon enhanced ATP-S activity by 2.3-times, SAT activity by 2-times and S content by 56.2% compared to control. In the presence of Cd, application of S and ethephon together increased ATP-S activity by 2.7-times and SAT activity by 2.6-times and S content by 31.2% compared to control (**Table 1**).

Content of Cys, Met, GSH, and Redox State

Sulfur assimilation and ethylene formation are linked through Cys formation. Cysteine is a common metabolite for the

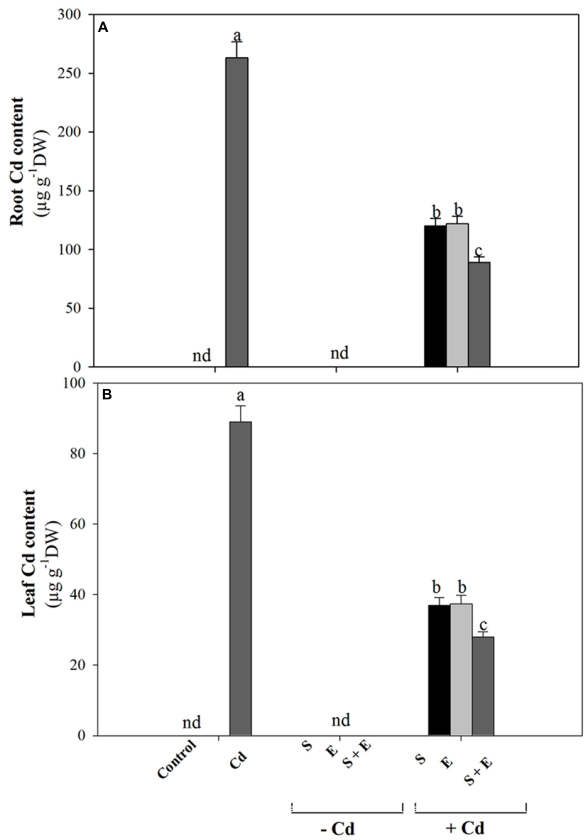

FIGURE 1 | Accmulation of Cd in root (A) and leaf (B) of mustard (*Brassica juncea* L.) at 30 DAS. Plants were grown individually with 0 or 50 μM Cd or with 1 mM SO_4^{2-}(S), 200 μL L^{-1} ethephon (E), 1 mM SO_4^{2-} plus 200 μL L^{-1} ethephon in presence or absence of Cd. Data are presented as treatments mean ± SE ($n = 4$). Data followed by same letter are not significantly different by LSD test at $P < 0.05$. nd, not determined.

TABLE 1 | Content of TBARS (nmol g^{-1} FW) and H_2O_2 (nmol g^{-1} FW), activity of ATP-S (U mg^{-1}protein min^{-1}), SAT (U mg^{-1}protein min^{-1}), and S content (mg g^{-1} DW) in mustard (*Brassica juncea* L.) at 30 DAS.

Parameters	Control	Cd	*S*	*E*	S + E	*Cd + S*	*Cd + E*	*Cd + S + E*
TBARS content	7.4 ± 0.48d	19.8 ± 1.30a	3.2 ± 0.21e	3.0 ± 0.19e	2.0 ± 0.13f	13.0 ± 0.85b	13.2 ± 0.86b	10.1 ± 0.66c
H_2O_2 content	49.3 ± 2.72d	114.4 ± 6.32a	30.1 ± 1.66e	29.8 ± 1. 64e	18.2 ± 1.00f	65.8 ± 3.63b	65.6 ± 3.62b	54.4 ± 3.00c
ATP-S activity	1.70 ± 0.07f	2.42 ± 0.10e	2.93 ± 0.12d	2.97 ± 0.12d	3.94 ± 0.17b	3.58 ± 0.15c	3.62 ± 0.15c	4.60 ± 0.20a
SAT activity	1.82 ± 0.24f	2.43 ± 0.13e	2.98 ± 0.16d	3.0 ± 0.15d	4.0 ± 0.21b	3.51 ± 0.18c	3.62 ± 0.19c	4.71 ± 0.25a
Sulfur content	4.8 ± 0.15e	3.5 ± 0.12f	6.8 ± 0.29b	6.8 ± 0.30b	7.5 ± 0.31a	5.7 ± 0.23d	5.7 ± 0.25d	6.3 ± 0.26c

Plants were grown individually with 0 or 50 μM Cd or with 1 mM SO_4^{2-} (S), 200 μL L^{-1} ethephon (E), 1 mM SO_4^{2-} plus 200 μL L^{-1} ethephon in presence, or absence of Cd. Data are presented as treatments mean ± SE (n = 4). Data followed by same letter are not significantly different by LSD test at $P < 0.05$.

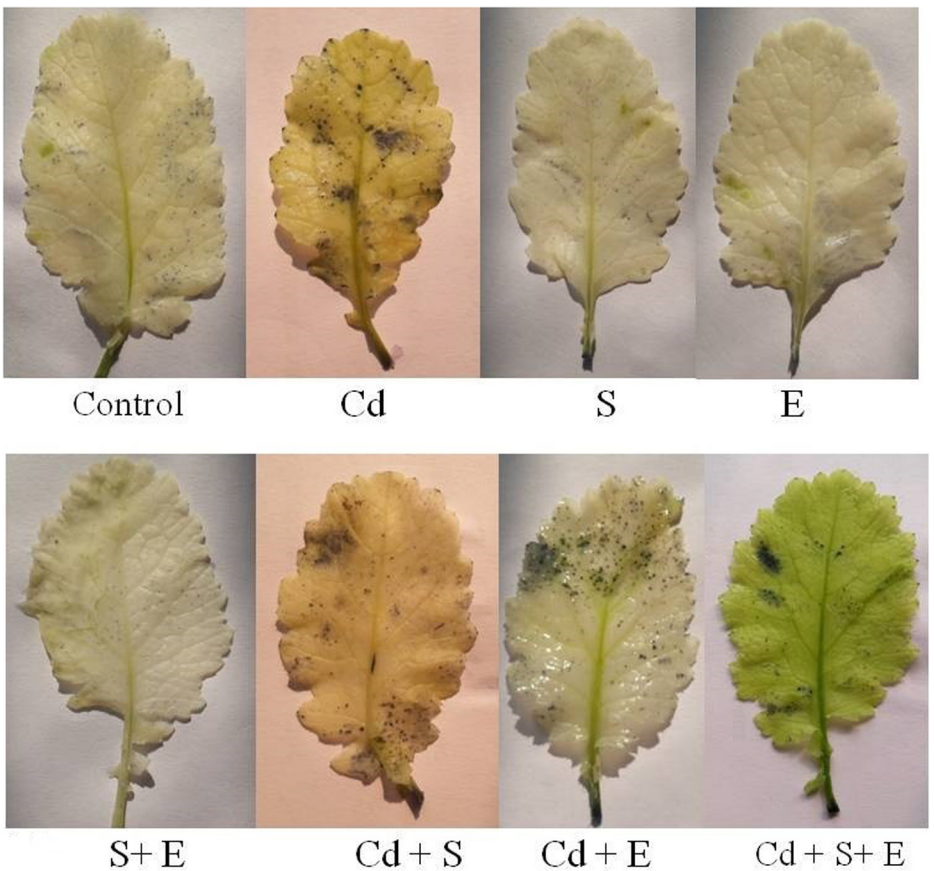

FIGURE 2 | Accmulation of superoxide ion by NBT staining in mustard (*Brassica juncea* L.) at 30 DAS. Plants were grown individually with 0 or 50 μM Cd or with 1 mM SO_4^{2-} (S), 200 μL L^{-1} ethephon (E), 1 mM SO_4^{2-} plus 200 μL L^{-1} ethephon in presence or absence of Cd.

formation of thiols and ethylene. Sulfur availability and its assimilation control thiols synthesis which potentially protects plants against stress.

Cadmium stress significantly increased content of Cys and Met compared to control. Sulfur or ethephon equally increased Cys content by 2-times and Met content by 2.5-times, whereas combination of S and ethephon proved effective in increasing Cys content by 2.9-times and Met content by 3.2-times compared to control. The combination of S and ethephon in the presence of Cd maximally increased Cys content by 3.2-times and Met content by 3.6-times compared to control (**Figures 3A,B**).

Cadmium stress significantly increased GSH content by 23.3% compared to control. Sulfur or ethephon increased GSH content equally by 1.5-times whereas combination of S and ethephon proved effective in increasing GSH content by about 2-times in the absence of Cd compared to control. In the presence of Cd, S plus ethephon reversed the effect of Cd and increased GSH content by 2.3-times compared to control (**Figure 3C**).

The ratio of GSH to GSSG was used to indicate the redox state of plants under different treatments. Redox state decreased under Cd stress by 6-times compared to control. The application of individual S or ethephon proved equally effective in increasing

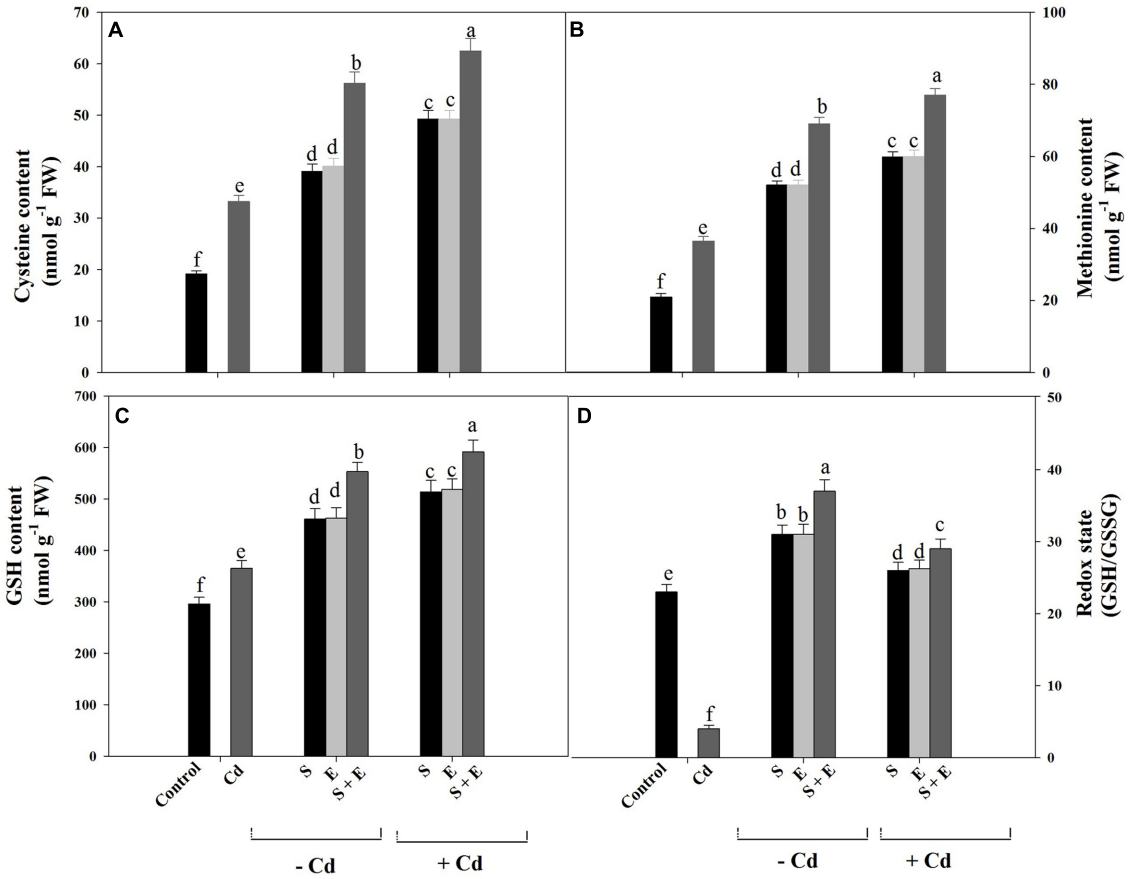

FIGURE 3 | Content of Cys (A), Met (B), GSH (C), and redox state (D) in mustard (*Brassica juncea* L.) at 30 DAS. Plants were grown individually with 0 or 50 μM Cd or with 1 mM SO_4^{2-} (S), 200 μL L^{-1} ethephon (E), 1 mM SO_4^{2-} plus 200 μL L^{-1} ethephon in presence or absence of Cd. Data are presented as treatments mean ± SE ($n = 4$). Data followed by same letter are not significantly different by LSD test at $P < 0.05$.

redox state by 30.4% compared to control. The combination of S and ethephon significantly and maximally increased redox state by 54.1% in plants grown without Cd compared to control. The combination of S and ethephon in the presence of Cd maximally increased redox state by 26.0% compared to control (**Figure 3D**).

Glucose Content

Cadmium stress increased glucose content by 50.0% compared to control. Application of S or ethephon increased glucose content equally by 16.2%. Plant receiving S or ethephon in the presence of Cd showed a reduction of glucose content by 11.3% compared to Cd-treated plants. Application of S plus ethephon in the presence of Cd showed a maximum reduction in glucose content by 16.1% compared to Cd-treated plants (**Figure 4**).

ACS Activity and Ethylene Production

Plants grown with Cd showed increased ACS activity and ethylene production compared to control plants. Cadmium stress increased ACS activity by 5.2-times and ethylene production by 8-times compared to control. Although individual or combined treatment of S and ethephon also increased ACS activity and ethylene production, however, the increase was lesser than Cd treatment. Plants receiving S or ethephon in the presence of Cd equally reduced ACS activity and ethylene production by 3-times compared to Cd-treated plants. The combination of S and ethephon in the presence of Cd maximally reduced ACS activity and ethylene production by 3.5-times compared to Cd-treated plants (**Figures 5A,B**).

Photosynthetic Characteristics

Cadmium stress reduced gas exchange parameters, chlorophyll content and Rubisco activity compared to control. Plants grown in the absence of Cd showed higher photosynthesis with S or ethephon compared to control. In the presence of Cd, plants receiving S and ethephon completely alleviated Cd stress and promoted photosynthesis compared to control. Plants receiving S or ethephon equally increased net photosynthesis by 49.2%, stomatal conductance by 21.9%, intercellular CO_2 concentration by 21.4%, chlorophyll content by 36.9% and Rubisco activity by 50.6% in comparison to control in the absence of Cd. Adding S and ethephon together increased net photosynthesis by 73.0%, stomatal conductance by 33.2%, intercellular CO_2 concentration by 33.7%, Chl content by 53.1% and Rubisco activity by 74.6%, compared to control in plants not receiving

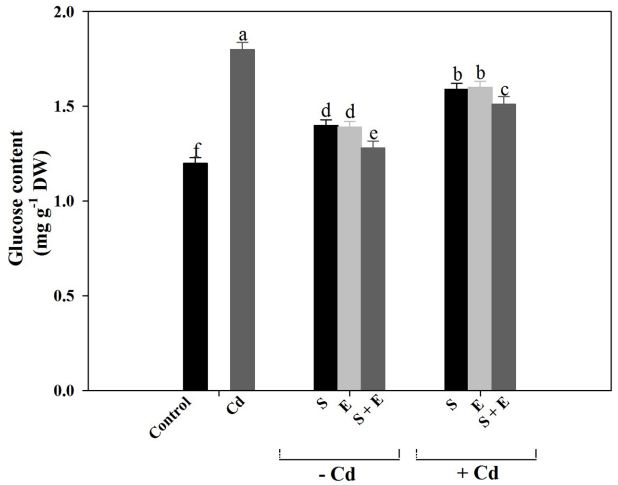

FIGURE 4 | Glucose content in mustard (*Brassica juncea* L.) at 30 DAS. Plants were grown individually with 0 or 50 μM Cd or with 1 mM SO_4^{2-} (S), 200 μL L^{-1} ethephon (E), 1 mM SO_4^{2-} plus 200 μL L^{-1} ethephon in presence or absence of Cd. Data are presented as treatments mean ± SE ($n = 4$). Data followed by same letter are not significantly different by LSD test at $P < 0.05$.

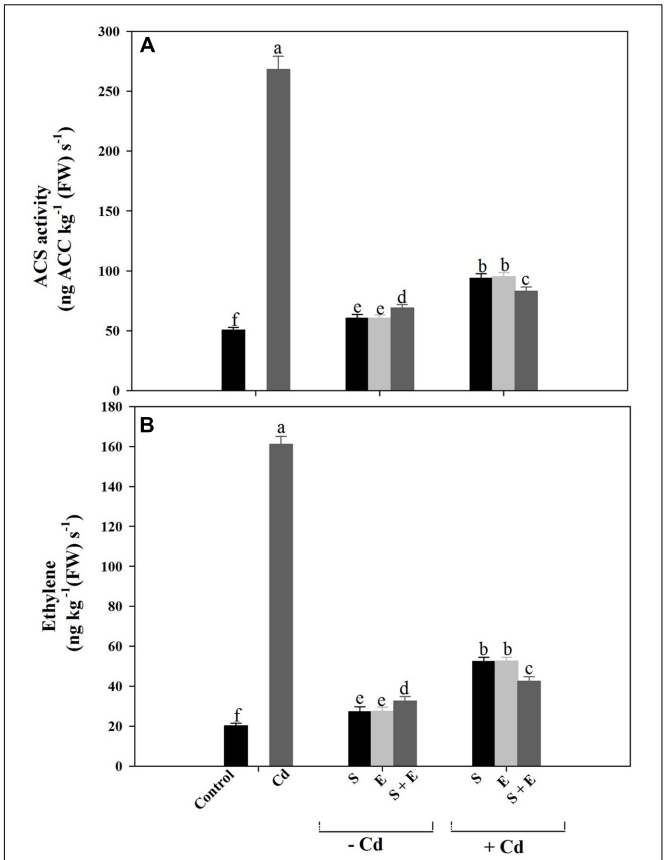

FIGURE 5 | 1-aminocyclopropane carboxylic acid synthase (ACS) activity (A) and ethylene production (B) in mustard (*Brassica juncea* L.) at 30 DAS. Plants were grown individually with 0 or 50 μM Cd or with 1 mM SO_4^{2-} (S), 200 μL L^{-1} ethephon (E), 1 mM SO_4^{2-} plus 200 μL L^{-1} ethephon in presence or absence of Cd. Data are presented as treatments mean ± SE ($n = 4$). Data followed by same letter are not significantly different by LSD test at $P < 0.05$.

Cd. Plants treated with Cd and received S or ethephon proved equally effective in alleviating the Cd-induced oxidative stress and enhanced net photosynthesis by 28.6%, stomatal conductance by 6.3%, intercellular CO_2 concentration by 7.1%, Chl content by 12.9%, and Rubisco activity by 20.4%, compared to control. The combined treatment of S and ethephon maximally alleviated Cd stress and improved net photosynthesis by 42.3%, stomatal conductance by 19.3%, intercellular CO_2 concentration by 19.4%, Chl content by 22.3%, and Rubisco activity by 37.4%, compared to control (**Table 2**).

PS II Activity

Cadmium stress reduced PS II activity [actual PS II efficiency, maximum PS II efficiency, intrinsic PS II efficiency, and qP and electron transport rate], however NPQ increased. Cadmium stress decreased PS II efficiency (actual PS II efficiency by 16.9%, maximum PS II efficiency by 13.9% and intrinsic PS II efficiency by 10.0%, qP by 16.8% and electron transport rate by 16.9%) compared to control. However, NPQ increased with Cd stress by 25.3% compared to control. Sulfur or ethephon application to plants alone improved the above characteristics equally compared to control. Follow up treatment of S plus ethephon to Cd-treated plants proved more effective in improving actual PS II efficiency along with maximum PS II efficiency, intrinsic PS II efficiency, qP, and electron transport rate than Cd plus S and Cd plus ethephon plants compared to Cd stress. Sulfur or ethephon decreased NPQ by 9.0%, however S and ethephon together decreased NPQ by 18.1% compared to control. Plants receiving S or ethephon in presence of Cd equally increased NPQ more prominently than combined treatment of S and ethephon in the presence of Cd compared to control (**Table 2**).

Growth Characteristics

Leaf area, and plant dry mass were inhibited by Cd stress, while S and ethephon increased leaf area by 26.8 and 27.6% and plant dry mass by 35.8 and 35.9% in the absence of Cd compared to control. Application of S + ethephon exhibited maximum leaf area with an increase of 41.3% and plant dry mass by 48.3% compared to control in the absence of Cd. Leaf area and plant dry mass increased with S or ethephon of Cd-treated plants, but the maximum increase was noted with combined treatments of S + ethephon (**Table 2**).

Ethylene is Involved in S-mediated Alleviation of Cd Stress: Effects of Ethylene Action Inhibitor

From the results explained above it is evident that S and ethylene coordinately improved photosynthetic performance of plants under Cd stress by regulating S-assimilation and thiols production. To substantiate the findings that ethylene has a role in S-mediated alleviation of Cd stress, the ethylene

TABLE 2 | Net photosynthesis (μmol CO_2 $m^{-2}s^{-1}$), stomatal conductance (mmol CO_2 m^{-2} s^{-1}), intercellular CO_2 concentration (μmol CO_2 mol^{-1}), Rubisco activity (μmol CO_2 mg^{-1} protein min^{-1}), chlorophyll content (SPAD value), Actual PS II efficiency, Maximum PS II efficiency, Intrinsic PS II efficiency, Photochemical quenching (qP), Non-Photochemical quenching (NPQ), Electron transport rate, leaf area (cm^2 $plant^{-1}$), and plant dry mass (g $plant^{-1}$) in mustard (*Brassica juncea* L.) at 30 DAS.

Parameters	Control	Cd	S	E	S + E	Cd + S	Cd + E	Cd + S + E
Net photosynthesis	16.7 ± 0.83e	10.3 ± 0.50f	24.9 ± 1.20b	24.8 ± 1.20b	28.9 ± 1.4a	21.9 ± 1.06d	21.8 ± 1.05d	23.7 ± 1.15c
Stomatal conductance	324.4 ± 14.8e	294.3 ± 13.4f	411.6 ± 21.6b	412.2 ± 21.6b	432.2 ± 22.7a	352.1 ± 15.4d	353.4 ± 15.4d	386.8 ± 16.2c
Intercellular CO_2 concentration	224.1 ± 10.4e	160.5 ± 7.3f	280.2 ± 13.0b	281.5 ± 13.0b	300.2 ± 13.9a	247.2 ± 11.4d	247.5 ± 11.5d	267.6 ± 12.4c
Rubisco activity	0.83 ± 0.03e	0.50 ± 0.02f	1.25 ± 0.061b	1.26 ± 0.062b	1.45 ± 0.070a	0.98 ± 0.042d	0.99 ± 0.046d	1.14 ± 0.051c
Chlorophyll content	32.2 ± 1.61e	21.3 ± 1.06f	44.1 ± 2.22b	44.4 ± 2.22b	49.3 ± 2.47a	36.4 ± 1.82d	36.4 ± 1.82d	39.4 ± 1.97c
Actual PS II efficiency	0.59 ± 0.026e	0.49 ± 0.022f	0.71 ± 0.032b	0.72 ± 0.032b	0.84 ± 0.035a	0.64 ± 0.028d	0.65 ± 0.028d	0.68 ± 0.029c
Maximum PS II efficiency	0.79 ± 0.017c	0.68 ± 0.016f	0.88 ± 0.020b	0.89 ± 0.020b	0.94 ± 0.023a	0.82 ± 0.019d	0.83 ± 0.019e	0.86 ± 0.022c
Intrinsic PS II efficiency	0.70 ± 0.020e	0.63 ± 0.019f	0.81 ± 0.025b	0.82 ± 0.026b	0.86 ± 0.029a	0.74 ± 0.021d	0.75 ± 0.022d	0.78 ± 0.023c
qP	0.83 ± 0.027c	0.69 ± 0.024f	0.92 ± 0.030b	0.93 ± 0.030b	0.97 ± 0.032a	0.86 ± 0.029d	0.86 ± 0.028d	0.89 ± 0.029e
NPQ	0.67 ± 0.031d	0.84 ± 0.044a	0.62 ± 0.030e	0.61 ± 0.030e	0.54 ± 0.028e	0.74 ± 0.035b	0.73 ± 0.035b	0.70 ± 0.033c
Electron transport rate	178.4 ± 8.7e	148.1 ± 7.2f	214.7 ± 10.5b	217.7 ± 10.7b	254.1 ± 12.5a	193.5 ± 9.5d	196.5 ± 9.6d	205.6 ± 10.1c
Leaf area	142.3 ± 5.95e	86.5 ± 3.61f	180.5 ± 7.55b	181.7 ± 7.60b	201.1 ± 8.40a	165.6 ± 6.92d	166.6 ± 6.97d	176.2 ± 7.37c
Plant dry mass	8.1 ± 0.54e	4.6 ± 0.30f	10.3 ± 0.68b	10.4 ± 0.69b	12.0 ± 0.80a	9.6 ± 0.64d	9.7 ± 0.64d	10.9 ± 0.72c

Plants were grown individually with 0 or 50 μM Cd or with 1 mM SO_4^{2-} (S), 200 μL L^{-1} ethephon (E), 1 mM SO_4^{2-} plus 200 μL L^{-1} ethephon in presence or absence of Cd. Data are presented as treatments mean ± SE (n = 4). Data followed by same letter are not significantly different by LSD test at $P < 0.05$.

action inhibitor, NBD was used and S-assimilation, ethylene production, glucose, photosynthetic and growth characteristics were studied.

Application of Cd increased content of Cys, Met, and GSH compared to control. Plants receiving S and ethephon in the presence of Cd increased content of Cys, Met, and GSH compared to Cd-stressed plant. Application of NBD with S and ethephon in the presence of Cd reduced Cys, Met, and GSH compared to Cd + S + ethephon treated plants. Plants receiving S and ethephon optimized ethylene in the presence of Cd and resulted in ethylene production higher than control but lesser than Cd-treated plants. This action of S and ethephon in Cd-treated plants on ethylene production was reversed with the application of NBD (**Figures 6A−D**).

Cadmium grown plants showed inhibition of Rubisco activity, however glucose content increased. Plants receiving S plus ethephon in the presence of Cd increased Rubisco activity compared to control and Cd-treated plants. Supplementation of NBD to S plus ethephon treatment in Cd-stressed plants reversed the effects and decreased Rubisco activity compared to control, but the Rubisco activity was higher than Cd-treated plants. In contrast, plants receiving S and ethephon in the presence of Cd increased glucose content compared to control but the content was lesser than Cd-treated plants. Application of NBD with combined application of S and ethephon to Cd-treated plants increased glucose content compared to control (**Figures 7A,B**).

Plants grown with Cd showed decreased net photosynthesis and plant dry mass compared to control. Application of S and ethephon together in the presence of Cd increased photosynthesis and dry mass compared to control and Cd-treated plants. However, NBD treatment reversed the effects of S plus ethephon. Photosynthesis and dry mass in this treatment (S + ethephon + NBD) were found higher than Cd-treated plants but lesser than control plants. Plant receiving combined application of S and ethephon in the presence of Cd increased photosynthesis and dry mass compared to control. However, NBD application in plants grown with S and ethephon in the presence of Cd decreased leaf area and plant dry mass (**Figures 8A,B**).

DISCUSSION

Ethylene Application with S Decreases Cd Accumulation

Application of ethephon plus S maximally reduced Cd content in root and leaf. It has been shown earlier that S reduced Cd-induced oxidative stress in *Oryza sativa* (Hassan et al., 2005) and *B. campestris* (Anjum et al., 2008). Ethylene and S interacted to reduce oxidative stress induced by Cd in *B. juncea* and *T. aestivum* (Masood et al., 2012b; Khan et al., 2015b).

Ethylene or/and S Reduces Cd-induced Oxidative Stress

Sulfur application and its assimilation potentially protect plants against stress. In this study, S and ethephon have similar effects on the alleviation of Cd stress by restricting oxidative stress.

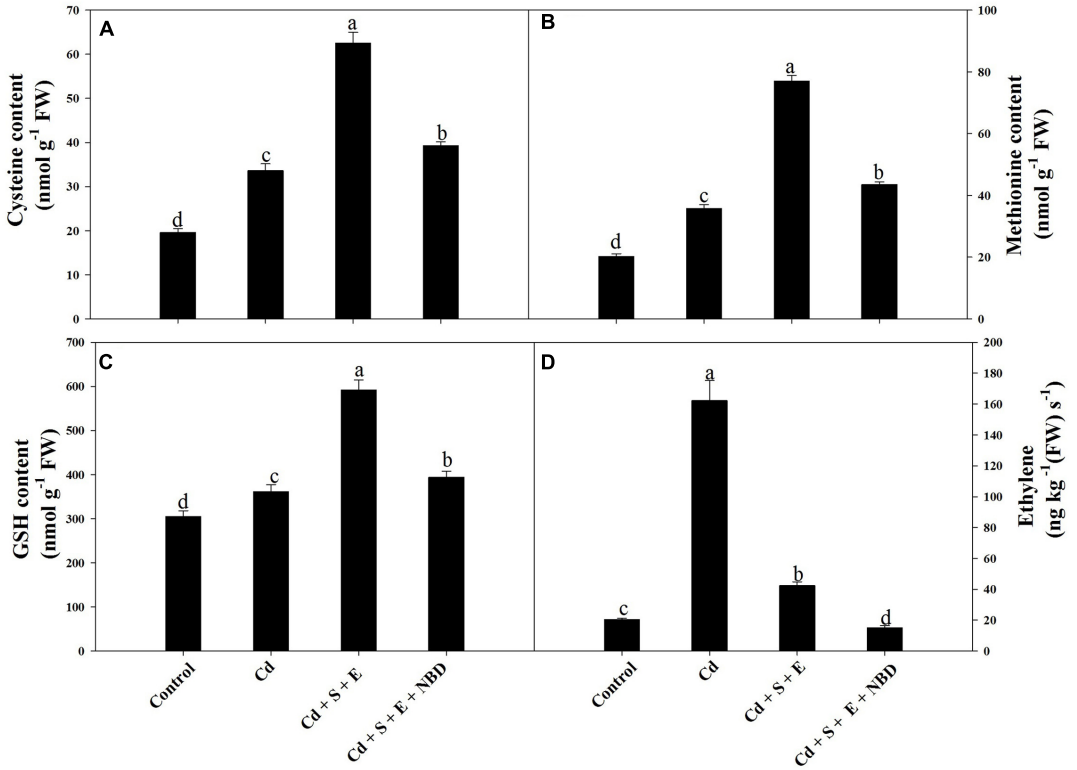

FIGURE 6 | Content of Cys (A), Met (B), GSH (C), and ethylene (D) in mustard (*Brassica juncea* L.) at 30 DAS. Plants were grown individually with 0 or 50 μM Cd (Cd), or with combined treatment of Cd + 1 mM SO_4^{2-} (S) + 200 μL L^{-1} ethephon (E) in absence or presence of NBD. Data are presented as treatments mean ± SE ($n = 4$). Data followed by same letter are not significantly different by LSD test at $P < 0.05$.

Application of ethephon and S in the presence of Cd disrupted Cd uptake and accumulation. The demand for increased thiols for removal of excess ROS under Cd stress was met with higher S-assimilation through increased activity of ATP-S and SAT consequently resulting in efficient detoxification of ROS. Application of S or ethylene minimized H_2O_2 and TBARS content, but the decrease was more prominent when ethylene and S were applied together to Cd grown plants (**Table 1**) apparently because of enhanced S-assimilation capacity of plants. This finding is in agreement with the earlier studies in which S reduced oxidative stress in *B. campestris* (Anjum et al., 2008), *Triticum aestivum* (Gaafar et al., 2012), *H. vulgare* (Astolfi et al., 2012), and *A. thaliana* (Bashir et al., 2013) under Cd stress. Role of ethylene has been found to reduce oxidative stress in *B. juncea* (Masood et al., 2012b; Asgher et al., 2014; Khan and Khan, 2014).

Ethylene or/and S Reduces ROS Accumulation under Cd Stress

The combined treatment of ethephon and S resulted in the least staining due to the increased S-assimilation and GSH synthesis (**Figure 2**). The study provides evidence that ethephon and S influenced the accumulation of ROS in the plants. These findings demonstrated that the GSH synthesis was up-regulated when ethephon and S were applied to Cd treated plants, which in turn induced a strong ROS scavenging capacity and decreased production rate of $O_2^{\cdot-}$. This is the first report regarding the response obtained from the ethephon with S in the inhibition of ROS accumulation using histochemical staining method.

Involvement of Ethylene in S-induced Increase in Redox State (GSH/GSSG) under Cd Stress

Ethephon or/and S increased activity of ATP-S, SAT, and S content which resulted in increased content of Cys, Met, GSH, and redox state (**Table 1**; **Figures 3A,D**). Reports on the effect of ethephon and S on thiol (Cys and GSH) compounds under Cd stress are scanty. In this study, the increase in photosynthesis of Cd treated plants following ethephon and S application was coupled with increased thiol compounds. This suggests that ethephon and S induce tolerance to Cd stress and alleviate photosynthetic inhibition through ethylene by retaining high thiols. Increased activity of GSH potentially keeps redox environment for cell and protects plants against Cd toxicity by maintaining a high level of GSH content which is required for the regeneration of AsA (ascorbate) for the proper functioning of AsA-GSH cycle (Anjum et al., 2008; Asgher et al., 2014). However, reports on how ethylene and S influence Cys and Met synthesis under Cd stress are not available. Lancilli et al. (2014) have

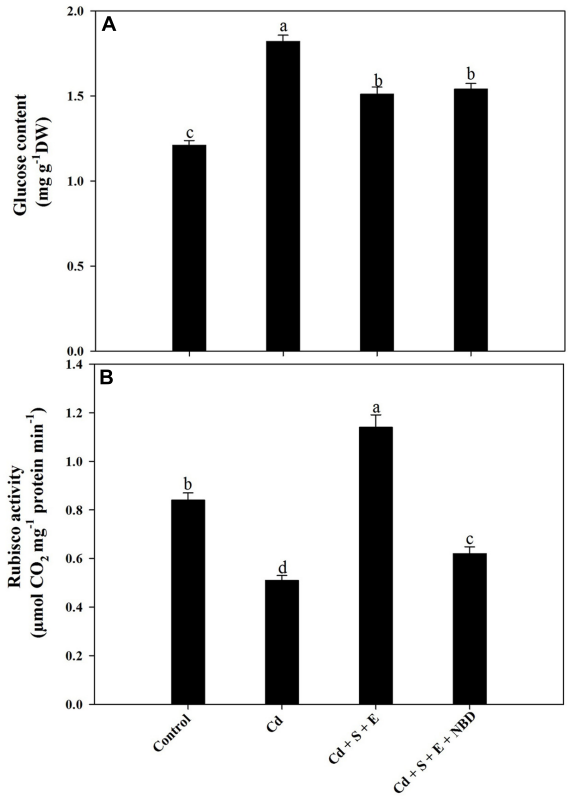

FIGURE 7 | Glucose content (A) and Rubisco activity (B) in mustard (*Brassica juncea* L.) at 30 DAS. Plants were grown individually with 0 or 50 μM Cd (Cd), or with combined treatment of Cd + 1 mM SO_4^{2-} (S) + 200 μL L^{-1} ethephon (E) in absence or presence of NBD. Data are presented as treatments mean ± SE ($n = 4$). Data followed by same letter are not significantly different by LSD test at $P < 0.05$.

reported that S requirement to sustain thiol biosynthesis activated sulfate uptake in *B. juncea*. It is remarkable that high ethylene level in ethylene-sensitive cultivar signifies greater responsiveness to S-metabolism and ethylene synthesis and greater ethylene-induced physiological responses. It has been suggested that thiol metabolism increased in *H. vulgare* plants under Cd stress (Astolfi et al., 2012). It has been reported that GSH strongly reduced the Cd bioavailability by inhibiting its transports from root to shoot in *B. napus* and GSSG was not efficient in reducing Cd availability due to the lack of free thiol groups (Nakamura et al., 2013). Regulation of GSH by ethylene has been suggested under ozone stress in *A. thaliana* (Yoshida et al., 2009), under Cd, Ni, and Zn stress in *B. juncea, T. aestivum* (Masood et al., 2012b; Khan and Khan, 2014; Khan et al., 2015b), salt stress in *Vigna radiata*, *B. juncea* (Khan M.I. et al., 2014; Nazar et al., 2014).

Application of Ethylene or/and S Reduces Glucose Content under Cd Stress

Ethephon and S reduced glucose-mediated photosynthetic repression of Cd grown plants. It has been reported that Rubisco expression was strongly inhibited by high endogenous glucose level in the ethylene-insensitive genotypes (Tholen et al., 2007). Masood et al. (2012a) have shown that glucose sensitivity increased under Cd stress that resulted in the inhibition of Rubisco activity and photosynthesis in *B. juncea*. The present work reports that in addition to the involvement of S-mediated ethylene production in alleviation of Cd stress through thiols synthesis, there also exists a relationship between ethylene and glucose and Cd tolerance. Iqbal et al. (2011) reported that ethephon application at each level of N increased ethylene and decreased glucose sensitivity, which increased photosynthesis and growth. Ethylene-sensitive cultivar has ability to overcome the inhibitory effect of glucose on photosynthesis and growth and was not sensitive to glucose developmental arrest. Reduction in Rubisco content and photosynthetic capacity in ethylene-insensitive *Nicotiana tabacum* genotypes was due to the absence of functional ethylene receptors (Tholen et al., 2008).

Reversal of Stress Ethylene Production by Ethylene and S under Cd Stress

Ethephon or S treatment decreased ethylene production as compared to Cd stressed plants (**Figure 5B**) and resulted in

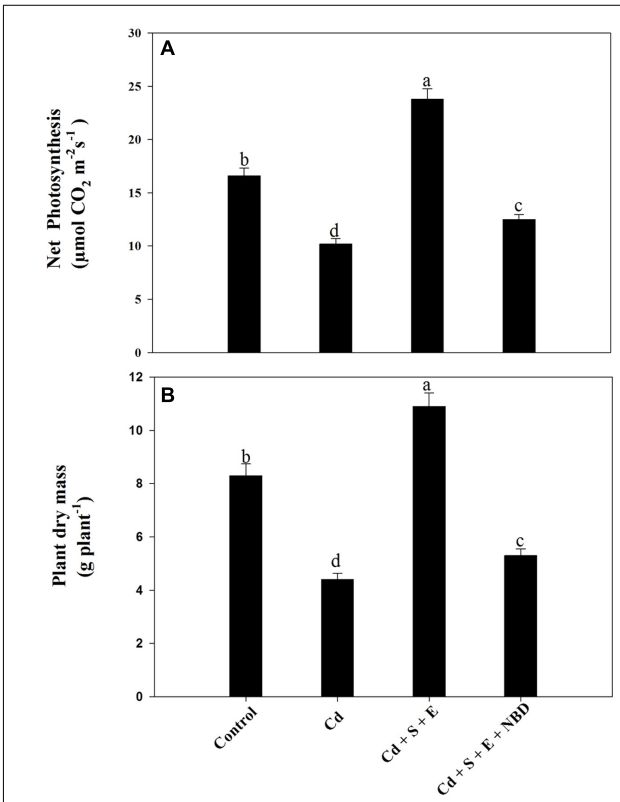

FIGURE 8 | Net photosynthesis (A) and plant dry mass (B) in mustard (*Brassica juncea* L.) at 30 DAS. Plants were grown individually with 0 or 50 μM Cd (Cd), or with combined treatment of Cd + 1 mM SO_4^{2-} (S) + 200 μL L^{-1} ethephon (E) in absence or presence of NBD. Data are presented as treatments mean ± SE ($n = 4$). Data followed by same letter are not significantly different by LSD test at $P < 0.05$.

favorable response with improvement in photosynthesis and growth. Plants grown with Cd were less sensitive to ethylene and exhibited adverse effects on photosynthesis and growth, but S or ethephon treatment increased the sensitivity of plants to ethylene. It has been reported by Iqbal et al. (2012a) that ACS activity and ethylene production increased with the application of 200 $\mu L\ L^{-1}$ ethephon compared to control. Application of ethylene and S optimizes ethylene production under Cd stress resulting in improved photosynthesis and growth. However, in the presence of Cd the requirement of S by plants increased for GSH synthesis, and resulted in reduced ethylene synthesis, which was adequate for favorable effect on photosynthesis and growth. The inhibition of Cd-induced stress ethylene by S or ethephon may result increase in sensitivity of plants to ethylene and promote thiol metabolism.

Involvement of Ethylene in S-mediated Alleviation of Cd stress on Photosynthetic Characteristics

As S-assimilation leads to ethylene formation via Cys, it is likely that S influences ethylene sensitivity, and ethylene is involved in the control of thiols synthesis and alleviation of Cd stress. Cadmium stress produces stress ethylene which was minimized to optimal range with S and ethephon favoring thiols synthesis via S-assimilation pathway and protected photosynthetic apparatus from Cd-induced oxidative stress resulting in increased photosynthesis. The increase in photosynthesis with ethephon and S involved stomatal and non-stomatal limitations as the treatments increased stomatal conductance allowing more exchange of intercellular CO_2 concentration on one hand and increased Rubisco activity and expression on the other. The combined effect of ethephon plus S was found more promising in increasing gas exchange parameters, chlorophyll content and Rubisco activity (**Table 2**). Earlier, it has been shown that ethylene increases photosynthesis by increasing stomatal conductance and Rubisco protein of *B. juncea* (Iqbal et al., 2011). The modulation of photosynthesis by ethylene may result from increased diffusion rate of CO_2 from the atmosphere to the intercellular spaces through increased stomatal aperture (Acharya and Assmann, 2009). Tholen et al. (2007) found that ethylene insensitivity in *N. tabacum* resulted in decreased photosynthetic rate associated with a strong reduction of Rubisco protein content. The interactive effect of ethephon and S on the photosynthetic response in plants under Cd stress has not been worked out in detail. The reason for the increase in photosynthesis with ethephon and S was due to S-induced ethylene and ethylene-mediated changes in allocation of S to Rubisco protein and also through increase in stomatal conductance under Cd stress.

Reversal of photo-inhibition and damage to photosynthetic attributes caused by Cd was modulated by the application of S and ethephon equally (**Table 2**). The increase in efficiency of PS II by ethephon and S treatment under Cd stress involved increased electron transport that helped plants to limit singlet oxygen production resulting in increased PS II activity under stress. Recently, it has been shown that exogenously sourced ethephon significantly reversed metals-induced photosynthetic inhibition by modulating PS II in *B. juncea* by lowering metal-induced stress ethylene to optimal range ethylene (Khan and Khan, 2014). However, no report is available on the role of ethylene in S-mediated protection of photosynthesis involving PS II activity and thiols metabolism under Cd stress.

Ethylene or/and S promote Growth Characteristics under Cd Stress

The increase in growth with ethephon and S is attributed to S-induced ethylene-mediated changes in photosynthesis. The maximum alleviation of Cd-induced inhibition in growth was observed with the combined treatment of ethylene plus S apparently because of more efficient production of thiols that resulted in maximum protection of photosynthetic apparatus and thus leaf area and plant dry mass in Cd-treated plants. It has been reported by Zhang et al. (2014) that ethylene was involved in alleviating Cd-toxicity in *N. tabacum*.

Inhibiting Ethylene Action Reversed S-mediated Alleviation of Cd Stress

In the presence of NBD, ethylene formation was reduced due to inhibition of ethylene action as it is a competitive inhibitor of ethylene, and by binding to ethylene receptors it reduced ethylene formation through autocatalytic regulation. Thus, ethylene concentration determines sensitivity and photosynthetic and growth responses. The action of both endogenous and exogenous ethylene can be modulated by the use of NBD and ethephon together. A critical threshold of ethylene concentration with sensitivity determines the overall response of plants. It may be said that ethylene-sensitive cultivar used in the present study had a lower threshold value for the response, and ethylene synthesis after ethephon application in Cd-stressed plants lowered stress ethylene to optimal level for maximum response.

Further, the content of glucose increased with Cd alone but the glucose content was reduced with S under Cd stress where the ethylene evolved was perceived by the plants and thus promoted photosynthesis by reducing the negative effect of glucose on Rubisco. Earlier, it has been reported that Rubisco expression was strongly inhibited by high endogenous glucose level in ethylene-insensitive plants (Tholen et al., 2007). In the present study, increased ethylene sensitivity in mustard plants metabolized increased glucose content that had negative consequences for Rubisco and photosynthetic capacity in Cd-treated plants. Ethylene induced in plants treated with Cd was responsible for photosynthetic inhibition, but NBD given with ethephon and S to Cd-treated plants showed lesser reduction in net photosynthesis and dry mass compared to Cd treatment alone (**Figure 8**). It appears that receptors were not available for stress ethylene induced by Cd as all the receptors were occupied by NBD resulting in lesser adverse effects of Cd-induced ethylene. Study on *B. juncea* grown with Ni and Zn stress by Khan and Khan (2014) showed that ethylene induced in plants treated with Ni and Zn stress was responsible for photosynthetic inhibition, but NBD treatment resulted in lesser reduction in photosynthetic attributes compared with Ni and Zn treatment alone.

CONCLUSION

It may be concluded that the adverse effect of Cd on photosynthesis and growth was reversed more conspicuously when ethephon and S were applied together by reduced Cd-induced ROS production through optimization of ethylene level, increased S-assimilation and thiol (Cys, GSH) production. Moreover, this combined treatment reduced glucose mediated photosynthetic inhibition under Cd stress. The use of ethylene action inhibitor, NBD also confirmed that ethylene was responsible for S-induced alleviation of Cd stress. The present work suggests that S supplementation in agricultural system and ethylene optimization may be adopted for augmenting photosynthesis and growth under Cd stress.

AUTHOR CONTRIBUTIONS

NK conceived the concept and MA performed the experiments. TP, AM, MF, and MK helped in plant sampling and data analyses. NK and MA wrote the manuscript. All authors read and approved the manuscript.

ACKNOWLEDGMENTS

Financial assistance to NK laboratory by the Department of Biotechnology (DBT), Government of India, New Delhi under the scheme of DBT-BUILDER programme (No. BT/PR4872/INF/22/150/2012) is gratefully acknowledged.

REFERENCES

Acharya, B. R., and Assmann, S. M. (2009). Hormone interactions in stomatal function. *Plant. Mol. Biol.* 69, 451–462. doi: 10.1007/s11103-008-9427-0

Anderson, M. E. (1985). Determination of glutathione and glutathione disulfide in biological samples. *Methods Enzymol.* 113, 548–555. doi: 10.1016/S0076-6879(85)13073-9

Anjum, N. A., Ahmad, I., Mohmood, I., Pacheco, M., Duarte, A. C., Pereira, E., et al. (2012). Modulation of glutathione and its related enzymes in plants' responses to toxic metals and metalloids—a review. *Environ. Exp. Bot.* 75, 307–324.

Anjum, N. A., Umar, S., Gill, S. S., Nazar, R., and Khan, N. A. (2008). "Sulfur assimilation and cadmium tolerance in plants," in *Sulfur Assimilation and Abiotic Stress in Plants*, eds N. A. Khan, S. Singh, and S. Umar (Berlin: Springer-Verlag), 271–302.

Asgher, M., Khan, M. I. R., Anjum, N. A., and Khan, N. A. (2015). Minimising toxicity of cadmium in plants—role of plant growth regulators. *Protoplasma* 252, 399–413. doi: 10.1007/s00709-014-0710-4

Asgher, M., Khan, N. A., Khan, M. I. R., Fatma, M., and Masood, A. (2014). Ethylene production is associated with alleviation of cadmium-induced oxidative stress by sulfur in mustard types differing in ethylene sensitivity. *Ecotoxicol. Environ. Saf.* 106, 54–61. doi: 10.1016/j.ecoenv.2014.04.017

Astolfi, S., and Zuchi, S. (2013). Adequate S supply protects barley plants from adverse effects of salinity stress by increasing thiol contents. *Acta Physiol. Plant.* 35, 175–181. doi: 10.1007/s11738-012-1060-5

Astolfi, S., Zuchi, S., Neumann, G., Cesco, S., Sanita' di Toppi, L., and Pinton, R. (2012). Response of barley plants to Fe deficiency and Cd contamination as affected by S starvation. *J. Exp. Bot.* 63, 1241–1250. doi: 10.1093/jxb/err344

Avni, A., Bailey, B. A., Mattoo, A. K., and Anderson, J. D. (1994). Induction of ethylene biosynthesis in *Nicotiana tabacum* by a *Trichoderma viride* xylanase is correlated to the accumulation of 1-aminocyclopropane carboxylic acid (ACC) synthase and ACC oxidase transcripts. *Plant Physiol.* 106, 1049–1055. doi: 10.1104/pp.106.3.1049

Baryla, A., Carrier, P., Franck, F., Coulomb, C., Sahut, C., and Havaux, M. (2001). Leaf chlorosis in oilseed rape plants (*Brassica napus*) grown on cadmium-polluted soil: causes and consequences for photosynthesis and growth. *Planta* 212, 696–709. doi: 10.1007/s004250000439

Bashir, H., Ahmad, J., Bagheri, R., Nauman, M., and Qureshi, M. I. (2013). Limited sulfur resource forces *Arabidopsis thaliana* to shift towards non-sulfur tolerance under cadmium stress. *Environ. Exp. Bot.* 94, 19–32. doi: 10.1016/j.envexpbot.2012.05.004

Bradford, M. M. (1976). A rapid and sensitive method for the quantitation of micro-gram quantities of proteins utilising the principle of protein–dye binding. *Anal. Biochem.* 72, 248–254. doi: 10.1016/0003-2697(76)90527-3

Chesnin, L., and Yien, C. H. (1950). Turbidimetric determination of available sulphates. *Soil Sci. Soc. Am. Proc.* 15, 149–151. doi: 10.2136/sssaj1951.036159950015000C0032x

Choppala, G., Saifullah Bolan, N., Bibi, S., Iqbal, M., Rengel, Z., Kunhikrishinan, A., et al. (2014). Cellular mechanisms in higher plants governing tolerance to cadmium toxicity. *Crit. Rev. Plant Sci.* 33, 374–391. doi: 10.1080/07352689.2014.903747

DalCorso, G., Farinati, S., Maistri, S., and Furini, A. (2008). How plants cope with cadmium:staking all on metabolism and gene expression. *J. Integr. Plant Biol.* 50, 1268–1280. doi: 10.1111/j.1744-7909.2008.00737.x

Datta, R., Kumar, D., Sultana, A., Bhattacharyya, D., and Chattopadhyay, S. (2015). Glutathione regulates ACC synthase transcription via WRKY33 and ACC oxidase by modulating mRNA stability to induce ethylene synthesis during stress. *Plant Physiol.* 169, 2963–2981.

Dhindsa, R. H., Plumb-Dhindsa, P., and Thorpe, T. A. (1981). Leaf senescence correlated with increased level of membrane permeability, lipid peroxidation and decreased level of SOD and CAT. *J. Exp. Bot.* 32, 93–101. doi: 10.1093/jxb/32.1.93

Fu, S. F., Chen, P. Y., Nguyen, T., Huang, L. Y., Zeng, G. R., and Huang, T. L. (2014). Transcriptome profiling of genes and pathways associated with arsenic toxicity and tolerance in *Arabidopsis*. *BMC Plant Biol.* 14:94. doi: 10.1186/1471-2229-14-94

Gaafar, A. R. Z., Ghdan, A. A., Siddiqui, M. H., Al-Whaibi, M. H., Basalah, M. O., Ali, H. M., et al. (2012). Influence of sulfur on cadmium (Cd) stress tolerance in *Triticum aestivum* L. *Afr. J. Biotechnol.* 11, 10108–10114.

Genisel, M., Erdal, S., and Kizilkaya, M. (2014). The mitigating effect of cysteine on growth inhibition in salt-stressed barley seeds is related to its own reducing capacity rather than its effects on antioxidant system. *Plant Growth Regul.* 75, 187–197. doi: 10.1007/s10725-014-9943-7

Giatonde, M. K. (1967). A spectrophotometric method for the direct determination of cysteine in the presence of other naturally occurring amino acids. *Biochem. J.* 104, 627–633. doi: 10.1042/bj1040627

Guan, C., Ji, J., Wu, D., Li, X., Jin, C., Wenzhu, G., et al. (2015). The glutathione synthesis may be regulated by cadmium-induced endogenous ethylene in *Lycium chinense*, and overexpression of an ethylene responsive transcription factor gene enhances tolerance to cadmium stress in tobacco. *Mol. Breed.* 35, 1–13. doi: 10.1007/s11032-015-0313-6

Hassan, M. J., Wang, Z., and Zhang, G. (2005). Sulfur alleviates growth inhibition and oxidative stress caused by cadmium toxicity in rice. *J Plant Nutr.* 28, 1785–1800. doi: 10.1080/01904160500251092

Hawkesford, M. J. (2000). Plant responses to sulphur deficiency and the genetic manipulation of sulphate transporters to improve S-utilization efficiency. *J. Exp. Bot.* 51, 131–138. doi: 10.1093/jexbot/51.342.131

Horn, J. M., Jones, D. B., and Blum, A. E. (1946). Colorimetric determination of methionine in protein and foods. *J. Biol. Chem.* 166, 313–320.

Iqbal, N., Khan, N. A., Nazar, R., and Silva, J. A. (2012a). Ethylene-stimulated photosynthesis results from increased nitrogen and sulfur assimilation in mustard types that differ in photosynthetic capacity. *Environ. Exp. Bot.* 78, 84–90. doi: 10.1016/j.envexpbot.2011.12.025

Iqbal, N., Nazar, R., Khan, M. I. R., and Khan, N. A. (2012b). Variation in photosynthesis and growth of mustard cultivars: role of ethylene sensitivity. *Sci. Hortc.* 135, 1–6. doi: 10.1016/j.scienta.2011.12.005

Iqbal, N., Nazar, R., Syeed, S., Masood, A., and Khan, N. A. (2011). Exogenously-sourced ethylene increases stomatal conductance, photosynthesis, and growth

under optimal and deficient nitrogen fertilization in mustard. *J. Exp. Bot.* 62, 4955–4963. doi: 10.1093/jxb/err204

Iqbal, N., Umar, S., and Khan, N. A. (2015). Nitrogen availability regulates proline and ethylene production and alleviates salinity stress in mustard (*Brassica juncea*). *J. Plant Physiol.* 178, 84–91. doi: 10.1016/j.jplph.2015.02.006

Iqbal, N., Umar, S., Khan, N. A., and Khan, M. I. R. (2014). A new perspective of phytohormones in salinity tolerance: regulation of proline metabolism. *Environ. Exp. Bot.* 100, 34–42. doi: 10.1016/j.envexpbot.2013.12.006

Khan, M. I., Asgher, M., and Khan, N. A. (2014). Alleviation of salt-induced photosynthesis and growth inhibition by salicylic acid involves glycinebetaine and ethylene in mungbean (*Vigna radiata* L.). *Plant Physiol. Biochem.* 80, 67–74. doi: 10.1016/j.plaphy.2014.03.026

Khan, M. I. R., Iqbal, N., Masood, A., Mobin, M., Anjum, N. A., and Khan, N. A. (2015a). Modulation and significance of nitrogen and sulfur metabolism in cadmium challenged plants. *Plant Growth Regul.* 78, 1–11. doi: 10.1007/s10725-015-0071-9

Khan, M. I. R., and Khan, N. A. (2014). Ethylene reverses photosynthetic inhibition by nickel and zinc in mustard through changes in PS II activity, photosynthetic nitrogen use efficiency, and antioxidant metabolism. *Protoplasma* 251, 1007–1019. doi: 10.1007/s00709-014-0610-7

Khan, M. I. R., Nazir, F., Asgher, M., Per, T. S., and Khan, N. A. (2015b). Selenium and sulfur influence ethylene formation and alleviate cadmium-induced oxidative stress by improving proline and glutathione production in wheat. *J. Plant Physiol.* 173, 9–18. doi: 10.1016/j.jplph.2014.09.011

Khan, M. I. R., Trivellini, A., Fatma, M., Masood, A., Francini, A., Iqbal, N., et al. (2015c). Role of ethylene in responses of plants to nitrogen availability. *Front. Plant Sci.* 6:927. doi: 10.3389/fpls.2015.00927

Khan, N. A., Ansari, H. R., and Samiullah. (1998). Effect of gibberellic acid spray during ontogeny of mustard on growth, nutrient uptake and yield characteristics. *J. Agr. Crop Sci.* 181, 61–63. doi: 10.1111/j.1439-037X.1998.tb00399.x

Khan, N. A., Khan, M., and Samiullah. (2002). Changes in ethylene level associated with defoliation and its relationship with seed yield in rapeseed-mustard. *Brassica* 4, 12–17.

Khan, N. A., Khan, M. I. R., Asgher, M., Fatma, M., Masood, A., and Syeed, S. (2014). Salinity tolerance in plants: revisiting the role of sulfur metabolites. *J. Plant. Biochem. Physiol.* 2:120.

Khan, N. A., Mobin, M., and Samiullah. (2005). The influence of gibberellic acid and sulphur fertilization rate on growth and S-use efficiency of mustard (*Brassica juncea*). *Plant Soil* 270, 269–274. doi: 10.1007/s11104-004-1606-4

Kovácik, J., Babula, P., Klejdus, B., and Hedbavny, J. (2014). Comparison of oxidative stress in four *Tillandsia* species exposed to cadmium. *Plant Physiol. Biochem.* 80, 33–40. doi: 10.1016/j.plaphy.2014.03.015

Krall, J. P., and Edwards, G. E. (1992). Relationship between photosystem II activity and CO2 fixation in leaves. *Physiol. Plant.* 86, 180–187. doi: 10.1111/j.1399-3054.1992.tb01328.x

Kredich, N. M., and Tomkins, G. M. (1966). The enzymic synthesis of l-cysteine in *Escherichia coli* and *Salmonella typhimurium*. *J. Biol. Chem.* 21, 4955–4965.

Krishnaveni, S., Balasubramanian, T., and Sadasivam, S. (1984). Sugar distribution in sweet stalk sorghum. *Food Chem.* 15, 229–232. doi: 10.1016/0308-8146(84)90007-4

Lancilli, C., Giacomini, B., Lucchini, G., Davidian, J. C., Cocucci, M., Sacchi, G. A., et al. (2014). Cadmium exposure and sulfate limitation reveal differences in the transcriptional control of three sulfate transporter (Sultr1;2) genes in *Brassica juncea*. *BMC Plant Biol.* 14:132. doi: 10.1186/1471-2229-14-132

Lappartient, A. G., and Touraine, B. (1996). Demand-driven control of root ATP-sulfurylase activity and S uptake in intact canola. *Plant Physiol.* 111, 147–157. doi: 10.1104/pp.111.1.147

Liu, C., Guo, J., Cui, Y., Lu, T., Zhang, X., and Shi, G. (2011). Effects of cadmium and salicylic acid on growth, spectral reflectance and photosynthesis of castor bean seedlings. *Plant Soil* 344, 131–141. doi: 10.1007/s11104-011-0733-y

Liu, L., Sun, H., Chen, J., Zhang, Y., Li, D., and Li, C. (2014). Effects of cadmium (Cd) on seedling growth traits and photosynthesis parameters in cotton (*Gossypium hirsutum* L.). *Plant Omics J* 7, 284–290. doi: 10.1111/tpj.12387

Lunde, C., Zygadlo, A., Simonsen, H. T., Nielsen, P. L., Blennow, A., and Haldrup, A. (2008). Sulfur starvation in rice: the effect on photosynthesis, carbohydrate metabolism, and oxidative stress protective pathways. *Physiol. Plant.* 134, 508–521. doi: 10.1111/j.1399-3054.2008.01159.x

Masood, A., Iqbal, N., Khan, M. I. R., and Khan, N. A. (2012a). The coordinated role of ethylene and glucose in sulfur-mediated protection of photosynthetic inhibition by cadmium. *Plant Signal. Behav.* 7, 1420–1422. doi: 10.4161/psb.22079

Masood, A., Iqbal, N., and Khan, N. A. (2012b). Role of ethylene in alleviation of cadmium-induced photosynthetic capacity inhibition by sulphur in mustard. *Plant Cell Environ.* 35, 524–533. doi: 10.1111/j.1365-3040.2011.02432.x

Masood, A., and Khan, N. A. (2013). Ethylene and gibberellic acid interplay in the regulation of photosynthetic capacity inhibition by cadmium. *J. Plant Biochem. Physiol.* 1:3.

Maxwell, K., and Johnson, G. (2000). Chlorophyll fluorescence–a practical guide. *J. Exp. Bot.* 51, 659–668. doi: 10.1093/jexbot/51.345.659

Mobin, M., and Khan, N. A. (2007). Photosynthetic activity, pigment composition and antioxidative response of two mustard (*Brassica juncea*) cultivars differing in photosynthetic capacity subjected to cadmium stress. *J. Plant Physiol.* 164, 601–610. doi: 10.1016/j.jplph.2006.03.003

Nakamura, S., Suzui, N., Nagasaka, T., Komatsu, F., Ishioka, N. S., Ito-Tanabata, S., et al. (2013). Application of glutathione to roots selectively inhibits cadmium transport from roots to shoots in oilseed rape. *J. Exp. Bot.* 64, 1073–1081. doi: 10.1093/jxb/ers388

Nazar, R., Khan, M. I. R., Iqbal, N., Masood, A., and Khan, N. A. (2014). Involvement of ethylene in reversal of salt-inhibited photosynthesis by sulfur in mustard. *Physiol. Plant.* 152, 331–344. doi: 10.1111/ppl.12173

Nocito, F. F., Pirovano, L., Cocucci, M., and Sacchi, G. A. (2002). Cadmium-induced sulfate uptake in maize roots. *Plant Physiol.* 129, 1872–1879. doi: 10.1104/pp.002659

Okuda, T., Masuda, Y., Yamanaka, A., and Sagisaka, S. (1991). Abrupt increase in the level of hydrogen peroxide in leaves of winter wheat is caused by cold treatment. *Plant Physiol.* 97, 1265–1267. doi: 10.1104/pp.97.3.1265

Rauser, W. E. (1987). Compartmental efflux analysis and removal of extracellular cadmium from roots. *Plant Physiol.* 85, 62–65. doi: 10.1104/pp.85.1.62

Schellingen, K., Van Der Straeten, D., Vandenbussche, F., Prinsen, E., Remans, T., Vangronsveld, J., et al. (2014). Cadmium-induced ethylene production and responses in *Arabidopsis thaliana* rely on ACS2 and ACS6 gene expression. *BMC Plant Biol.* 14:214. doi: 10.1186/s12870-014-0214-6

Shukla, D., Huda, K. M. K., Banu, M. S. A., Gill, S. S., Tuteja, R., and Tuteja, N. (2014). OsACA6, a P-type 2B Ca^{2+}ATPase functions in cadmium stress tolerance in tobacco by reducing the oxidative stress load. *Planta* 240, 809–824. doi: 10.1007/s00425-014-2145-8

Sun, X. M., Lu, B., Huang, S. Q., Mehta, S. K., Xu, L. L., and Yang, Z. M. (2007). Coordinated expression of sulfate transporters and its relation with sulfur metabolites in *Brassica napus* exposed to cadmium. *Bot. Stud.* 48, 43–54.

Thao, N. P., Khan, M. I. R., Thu, N. B. A., Hoang, X. L. T., Asgher, M., Khan, N. A., et al. (2015). Role of ethylene and its cross talk with other signaling molecules in plant responses to heavy metal stress. *Plant Physiol.* 169, 73–84. doi: 10.1104/pp.15.00663

Tholen, D., Pons, T. L., Voesenek, L. A. C. J., and Poorter, H. (2007). Ethylene insensitivity results in down-regulation of rubisco expression and photosynthetic capacity in tobacco. *Plant Physiol.* 144, 1305–1315. doi: 10.1104/pp.107.099762

Tholen, D., Pons, T. L., Voesenek, L. A. C. J., and Poorter, H. (2008). The role of ethylene perception in the control of photosynthesis. *Plant Signal. Behav.* 3, 108–109. doi: 10.4161/psb.3.2.4968

Usuda, H. (1985). The activation state of ribulose 1,5-bisphosphate carboxylase in maize leaves in dark and light. *Plant Cell Physiol.* 26, 1455–1463.

Wahid, A., and Khaliq, S. (2015). Architectural and biochemical changes in embryonic tissues of maize under cadmium toxicity. *Plant Biol. (Stuttg)* 17, 1005–1012. doi: 10.1111/plb.12326

Wang, F., Cui, X., Sun, Y., and Chun-Hai, D. (2013). Ethylene signaling and regulation in plant growth and stress responses. *Plant Cell Rep.* 32, 1099–1109. doi: 10.1007/s00299-013-1421-6

Wang, J., Sun, P. P., Chen, C. L., Wang, Y., Fu, X. Z., and Liu, J. H. (2011). An arginine decarboxylase gene PtADC from *Poncirus trifoliata* confers abiotic stress tolerance and promotes primary root growth in *Arabidopsis*. *J. Exp. Bot.* 62, 2899–2914. doi: 10.1093/jxb/erq463

Woeste, K. E., Ye, C., and Kieber, J. J. (1999). Two *Arabidopsis* mutants that over-produce ethylene are affected in the post-transcriptional regulation of 1-aminocyclopropane 1-carboxylic acid synthase. *Plant Physiol.* 119, 521–529. doi: 10.1104/pp.119.2.521

Yanagisawa, S., Yoo, S. D., and Sheen, J. (2003). Differential regulation of EIN3 stability by glucose and ethylene signalling in plants. *Nature* 425, 521–525. doi: 10.1038/nature01984

Yoshida, S., Tamaoki, M., Ioki, M., Ogawa, D., Sato, Y., Aono, M., et al. (2009). Ethylene and salicylic acid control glutathione biosynthesis in ozone-exposed *Arabidopsis thaliana*. *Physiol. Plant* 136, 284–298. doi: 10.1111/j.1399-3054.2009.01220.x

Zhang, B., Shang, S., Jabeen, Z., and Zhang, G. (2014). Involvement of ethylene in alleviation of Cd toxicity by NaCl in tobacco plants. *Ecotoxicol. Environ. Saf.* 101, 64–69. doi: 10.1016/j.ecoenv.2013.12.013

Conflict of Interest Statement: The authors declare that the research was conducted in the absence of any commercial or financial relationships that could be construed as a potential conflict of interest.

frontiers in Plant Science

ORIGINAL RESEARCH
published: 18 April 2016
doi: 10.3389/fpls.2016.00461

Foliar Abscisic Acid-To-Ethylene Accumulation and Response Regulate Shoot Growth Sensitivity to Mild Drought in Wheat

Ravi Valluru[1,2]*, *William J. Davies*[2], *Matthew P. Reynolds*[1] *and Ian C. Dodd*[2]

[1] Global Wheat Program, International Maize and Wheat Improvement Center (CIMMYT), El Batan, Mexico, [2] Plant Biology Department, Lancaster Environmental Center, Lancaster University, Lancaster, UK

Although, plant hormones play an important role in adjusting growth in response to environmental perturbation, the relative contributions of abscisic acid (ABA) and ethylene remain elusive. Using six spring wheat genotypes differing for stress tolerance, we show that young seedlings of the drought-tolerant (DT) group maintained or increased shoot dry weight (SDW) while the drought-susceptible (DS) group decreased SDW in response to mild drought. Both the DT and DS groups increased endogenous ABA and ethylene concentrations under mild drought compared to control. The DT and DS groups exhibited different SDW response trends, whereby the DS group decreased while the DT group increased SDW, to increased concentrations of ABA and ethylene under mild drought, although both groups decreased ABA/ethylene ratio under mild drought albeit at different levels. We concluded that SDW of the DT and DS groups might be distinctly regulated by specific ABA:ethylene ratio. Further, a foliar-spray of low concentrations (0.1 μM) of ABA increased shoot relative growth rate (RGR) in the DS group while ACC (1-aminocyclopropane-1-carboxylic acid, ethylene precursor) spray increased RGR in both groups compared to control. Furthermore, the DT group accumulated a significantly higher galactose while a significantly lower maltose in the shoot compared to the DS group. Taken all together, these results suggest an impact of ABA, ethylene, and ABA:ethylene ratio on SDW of wheat seedlings that may partly underlie a genotypic variability of different shoot growth sensitivities to drought among crop species under field conditions. We propose that phenotyping based on hormone accumulation, response and hormonal ratio would be a viable, rapid, and an early–stage selection tool aiding genotype selection for stress tolerance.

Keywords: abscisic acid, drought, ethylene, growth sensitivity, hormonal ratio, mild drought

OPEN ACCESS

Edited by:
M. Iqbal R. Khan, International Rice Research Institute, Philippines

Reviewed by:
Maren Müller, University of Barcelona, Spain
Alice Trivellini, Scuola Superiore Sant'Anna, Italy

***Correspondence:**
Ravi Valluru
r.valluru@cgiar.org

Specialty section:
This article was submitted to Plant Physiology, a section of the journal Frontiers in Plant Science

Received: *21 December 2015*
Accepted: *24 March 2016*
Published: *18 April 2016*

Citation:
Valluru R, Davies WJ, Reynolds MP and Dodd IC (2016) Foliar Abscisic Acid-To-Ethylene Accumulation and Response Regulate Shoot Growth Sensitivity to Mild Drought in Wheat. Front. Plant Sci. 7:461. doi: 10.3389/fpls.2016.00461

INTRODUCTION

Drought is a major abiotic stress limiting plant growth and yield. While plant responses differ with drought intensity, timing, and duration (Claeys and Inzé, 2013), we now understand that traits that confer survival of severe stress episodes will not deliver sustained growth and yield under mild stress (Skirycz et al., 2011). From an agricultural viewpoint, severe growth reduction may result in

significant yield loss even under mildly stressed field conditions. Most crop species exhibit a large genetic variability of expansion growth (Pereyra-Irujo et al., 2008; Parent et al., 2010; Welcker et al., 2011; Tardieu et al., 2014) and biomass growth (Wang et al., 2008; Boutraa et al., 2010; González, 2011) in response to drought. Therefore, identifying genotypes that maintain, or at least limit the reduction of, growth under stress might be a useful strategy to boost plant biomass (Skirycz et al., 2011; Hatier et al., 2014). Efficient translation of biomass into grains would also enhance yield productivity under stress conditions.

Plants have evolved some adaptive strategies to cope with mild and severe restriction in water availability (Davies and Zhang, 1991). In showing selectivity over the maintenance of either water balance and/or gas exchange, plant species favor either "survival" or "growth" behavior, respectively, when they encounter stress conditions (Tardieu et al., 2014). The latter strategy, which is an opportunistic risk-taking, is generally regarded as a stress-resistance trait (Sade et al., 2012) and plants with this behavior tend to occupy more mild to moderate drought-prone natural habitats (McDowell et al., 2008). This behavior may allow vegetative and reproductive growth under mild to moderate stress conditions but will confer no benefit under conditions of prolonged and severe stress in which plants with the former strategy may survive (Tardieu et al., 2014) but yield can be minimal. Hence, a survival vs. growth strategy of plants differs according to soil moisture. A homeostatic hydraulic regulation is known to partly drive this species specificity (Meinzer et al., 2014); however, some species, grapevine (Chaves et al., 2010), and poplar (Almeida-Rodriguez et al., 2010), can switch between "survival-growth" strategies in response to fluctuating soil moisture. The mechanistic basis of such a dual growth habit is yet to be fully understood, however, it could be regulated by an interaction of hydraulic and chemical signaling.

When drought stress develops, not all leaves respond similarly in stomatal closure (Blum, 2011). It was recently argued that drought insensitive stomata may favor carbon gain at the expense of expansive growth (Caldeira et al., 2014; Tardieu et al., 2014). Biomass accumulation and expansive growth may be controlled by independent environmental and genetic factors (Fatichi et al., 2014) and may govern yield under stress. The positive effect could be through enhancing carbon acquisition, in addition to specific adaptations that allow continued growth under drought (e.g., reprogrammed energy metabolism, osmotic adjustment and high cell wall extensibility; Claeys and Inzé, 2013). The negative effect of wide stomatal aperture on expansion growth could be a consequence of lower hydraulic conductivity (Caldeira et al., 2014). Though the role of abscisic acid (ABA) in plant hydraulics has been debated (Dodd, 2013), ABA can regulate hydraulic conductance (Jia and Davies, 2007; Pantin et al., 2012) via regulation of aquaporins (Sade et al., 2009; Prado et al., 2013). In addition, ethylene, under flooding, can promote (Kamaluddin and Zwiazek, 2002) or inhibit (Li et al., 2009) hydraulic conductivity under phosphorus deficiency depending on the environmental conditions. In addition, auxins and cytokinins closely regulate hydraulic conductivity, and thereby shoot growth, under stress conditions. The interaction between hydraulic and hormonal traits may therefore deliver differences in growth and yielding of crops under drought. We hypothesize that the subtle sensitivity of stomatal and growth traits to chemical regulators can be viewed as a model for species survival–growth behavioral plasticity (Soar et al., 2006; Rogiers et al., 2012) especially under drought.

Plant hormones are well-known to act as growth regulators and their concentrations change in response to numerous stresses (Hays et al., 2007; Ji et al., 2011). Both ABA and ethylene have been shown to exert dual effect on growth: stimulatory at low concentration (Ku et al., 1970; Suge, 1971; Nishizawa and Suge, 1995a,b; Lehman et al., 1996; Smalle et al., 1997) while inhibitory at high (Pratt and Goeschl, 1969; Guzmán and Ecker, 1990; Kieber et al., 1993; Tanaka et al., 2013), a "dose-growth" response phenomenon known as "hormesis" (Pierik et al., 2006; Gressel and Dodds, 2013). Relatively few studies have examined the stimulatory properties of low concentrations of ABA and ethylene (Suge, 1971; Takahashi, 1972; Neskovic et al., 1977; Pierik et al., 2006), suggesting that low concentrations ($\leq 0.1\,\mu l\ L^{-1}$ or $\leq 0.1\,\mu M$) of ethylene and ABA stimulate organ growth to the extent that, across planta, varies widely (0% to >100%) depending on the timing of application, level of organization (e.g., cell, organ), plant species, seedling age, and the physiological and growth conditions. The mechanisms controlling hormone dose-dependent growth response are largely unexplored. Nevertheless, hormetic growth response in general has been vigorously debated in ecotoxicology and medicine and its potential for increasing plant productivity has recently been discussed (Pierik et al., 2006; Gressel and Dodds, 2013).

In this study, we hypothesize that different genotypes may exhibit differential growth sensitivity to drought stress particularly via hormone responses that are normally induced by numerous stresses (Hays et al., 2007; Ji et al., 2011). We show that six spring wheat genotypes differing for stress-susceptibility (see below) exhibit a large genetic variability for early-stage growth sensitivity to very low concentrations of exogenous ABA and ethylene which reflects the yield performance of the genotype under mild stress and/or may indicate more general genotype-specific hormone responses that can benefit growth and yield later in plant development. Further, we show that drought-tolerant and drought-susceptible genotypes differ in their ABA and ethylene accumulation, which might be most likely to occur under mild drought-stressed natural habitats.

MATERIALS AND METHODS

Plant Material and Growth Conditions

Six spring wheat (*Triticum aestivum* L.) genotypes were selected and designated as drought-tolerant (DT: Kea, Attila, Florkwa) or drought-sensitive (DS: SeriM32, Simorge, Barbet1) groups based on their stress susceptibility, biomass accumulation and yield potential in the field (Lopes et al., 2012). These groups were selected in such a way that both the DT and DS groups show contrasting yield susceptibility to stress and non-stress

conditions (**Figure 1**). The DS group had higher yield under non-stress (1094 g/m^2) while they maintain only 43% of non-stress yields (474 g/m^2) under stress conditions. In contrast, DT group had lower grain yield under non-stress (829 g/m^2) as compared to DS group but they maintain 73% (606 g/m^2) of non-stress yields under stress conditions. Therefore, both groups have differential yield susceptibilities to stress and non-stress conditions. This atypical selection is at marked contrast to a widely accepted breeders conception that selection for high yield potential under non-stress conditions has also improved yield under stress especially for mild to moderate drought stress (Araus et al., 2002, 2008; Trethowan et al., 2002; Cattivelli et al., 2008). However, such genotype selection may be useful to understand the underlying mechanisms of growth and yield responses to the environment.

For all experiments, seeds were initially germinated on a wet-filter paper placed in the Petri dish at room temperature, and a 7-day-old seedlings were transplanted into 0.5 L plastic pots containing a well-prepared mixture of a soil-based compost (John Innes No. 2, UK). Plants were initially grown in a naturally lit glasshouse with supplementary artificial lighting of 200 μmol m^{-2} s^{-1} photosynthetically active radiation (PAR), and a photoperiod of 12 h with day/night temperatures of 25/18°C, respectively. When seedlings reached two-leaf stage, plants were shifted to growth cabinets with an average day/night temperature of 25/22°C, 12 h photoperiod with a relative humidity (RH) of 90%. All plants were well-watered daily and half-strength Hoagland nutrient solution was provided on alternative days. In chemical spray experiments, seedlings (two-leaf stage) were shifted to a modified hydroponic system (50 ml tube-system), in which nutrient solution was changed every 2-days and aeration was continuously provided with aquarium air-pump (BOYU, S-4000B, 3.2 L min^{-1}).

Mild Drought Stress under Controlled Conditions

Mild water deficit (MWD) was imposed as described previously (Deokar et al., 2011). When seedlings reached three-leaf stage, water was withheld from all pots to initiate a dry-down procedure. Weight of all individual pots was recorded daily in the morning at ∼10.30 h to monitor soil moisture content in both treatments. Daily loss of water through evapotranspiration (ET) was calculated as the difference in pot weight on the current day from that of the previous day. After 7–8 days, when the soil moisture content reached target values of approximately 0.44 and 0.33 g per g^{-1} dry soil in WW and MWD treatments, respectively, (**Supplementary Figures S1A–C**) all plants were watered daily with the amount of water lost through ET of each pot daily. Thus, WW and MWD plants were maintained at ∼94 and 70% of field capacity, reflecting a soil matric potential of ∼ −0.0048 and −0.08 MPa respectively, as determined from a moisture release curve of the same soil type (Dodd et al., 2006). Both treatments were maintained at the targeted soil moisture for 7 days and leaf samples were then collected before watering to determine endogenous ABA and ethylene accumulation. The remainder of the shoot was harvested separately. Shoot dry weight was determined after samples were oven-dried at 80°C for 72 h. Root growth was not measured in the study. Two experiments with four completely randomized replications for each genotype were conducted.

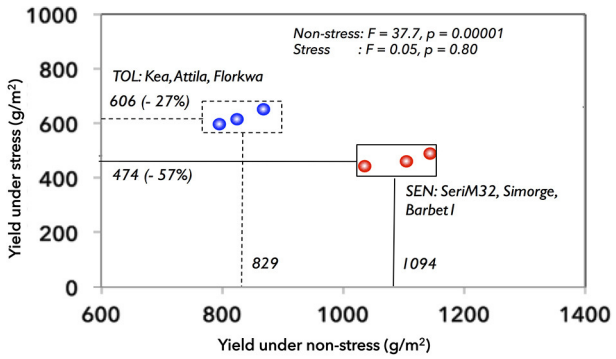

FIGURE 1 | Grain yields of six different wheat genotypes grown under non-stress and stress conditions in the field. The selected wheat genotypes were: Tolerant: Kea, Attila, Florkwa; Sensitive: Simorge; Barbeti; SeriM82. SEN, sensitive group; TOL, tolerant group.

Determination of Endogenous ABA and Ethylene

Endogenous ABA concentrations and ethylene evolution were measured in MWD experiment. For ABA determination, leaf tissues (0.2–0.4 g fresh weight) were collected and immediately frozen in liquid nitrogen. Frozen leaf tissue was freeze-dried for 48 h, finely ground and then extracted in distilled deionized water with an extraction ratio of 1:40 (gram dry weight:mL water) at 4°C overnight. ABA concentrations of the extract were determined using a radioimmunoassay as described (Chen et al., 2013).

Endogenous ethylene emission from leaves was measured using a commercial laser-based ethylene detector (ETD-300, Sensor Sense B.V., Nijmegen, The Netherlands) in combination with a gas handling system (VC-6, Sensor Sense B.V.) as described previously (Wang et al., 2013). Leaf tissues (0.25–0.45 g fresh weight) of WW and MWD plants were sampled, weighed immediately, and placed in 50 mL glass tubes containing moistened filter paper and were allowed wound-induced ethylene to subside (Yang et al., 2006). Later, glass tubes were tightly capped with a double-bent rubber stopper and were further incubated for 5 h in the light at the room temperature. Using a 5-mL syringe, 4 mL gas was extracted through rubber stopper, and stored in 4 mL sealed glass vials. These vials were connected to inlet and outlet cuvettes of VC-6 system, which allow six cuvettes at once, and continuously flushed with air at a constant flow of 4 L h^{-1}. Ethylene emission from each vial was monitored alternatively by ethylene detector in sample-mode for 10 min. To remove any traces of external ethylene or other hydrocarbons, the airflow was passed through a platinum-based catalyser before entering the cuvettes. A scrubber with KOH and $CaCl_2$ was placed before ethylene detector to reduce the CO_2 and water content in the gas flow, respectively. The ethylene emission was

corrected for tissue fresh weight and the duration of incubation to determine ethylene emission rate.

Drought Trials under Field Conditions

Four field trials were conducted during 2009–10 and 2010–11 under two different growth environments: two under well-irrigated conditions (controls, total crop water supply >700 mm), and two under drought (total crop water supply ≤300 mm). All trials were sown in alpha-lattice design with two replicates in the Yaqui Valley at CIMMYT's Obregon Experimental Station in North-Western Mexico (27°25′N 109°54′W, 38 m above sea level). Detailed trial procedures and meteorological data were described elsewhere (Lopes et al., 2012, 2015; Sukumaran et al., 2015). Briefly, the sowings were made in late November each year with either irrigation or drought. In drought trials, irrigation was at sowing with no further irrigation, making ∼180 mm of water available to the crop. The experimental design was a randomized lattice with two replications in 2 m long and 0.8 m wide plots consisting of one raised bed with two rows per bed at seed rate of 120 kg/ha. Appropriate weed, fertilization, disease, and pest control were followed to avoid any yield limitations. When seedlings were at three-leaf stage (∼23 days after sowing), normalized difference vegetation index (NDVI, a proxy for biomass) was measured along the length of the plot but avoided the boarders (0.25 m each side), averaged across trials and years and mean values were presented.

ABA and ACC Spray Experiment

When the seedlings reached three-fully emerged leaves, plants were foliar-sprayed with ABA and ACC (1-aminocyclopropane-1-carboxylic acid, ethylene precursor) as described previously (Chen et al., 2013). The optimal concentrations (at which shoot growth response is maximal) of ABA and ACC concentrations were determined in preliminary experiments (**Supplementary Figure S1D**). ACC, the endogenous ethylene precursor, was preferred as a source of ethylene to ethephon (a phosphonic acid), since non-ethylene generating phosphonic acids can have physiological effects on plants (Ernst et al., 1992; Chen et al., 2013). ACC was dissolved in water while ABA was dissolved in ethanol for stock solution preparation and a wetting agent Silwet (L-77, De Sangosse Ltd, Cambridge, UK) at 0.025% (v/v) was included in all solutions. Two-hours into the photoperiod, plants were foliar-sprayed (4-5 mL plant^{-1}) either with water that contain ethanol and Silwet (controls), ABA (0.1 μM), or ACC (0.1 μM) assuming that a proportion of each chemical sprayed onto leaf surface will penetrate the leaf interior (Wilkinson and Davies, 2008). After spraying, plants were grown further for 7 days in the same hydroponic system and then harvested to determine shoot fresh weight. Shoot dry weight was determined after oven-drying at 80°C for 72 h. Shoot dry weight at the beginning (just before spray) and end of (7-days) treatment were used to calculate relative shoot growth rate (RGR) according to (Hoffmann and Poorter, 2002). The experiment was repeated twice, with four completely randomized replications for each genotype. We also measured RGR at six-leaf stage whereby plants were foliar-sprayed with ABA and ACC at the same concentration (0.1 μM) at the three-leaf stage.

Determination of Carbohydrates

In the chemical spray experiment, sugars, and sugar alcohols (sucrose, glucose, fructose, raffinose, erlose, maltose, galactose, rhamnose, sorbitol) of the leaf tissue were quantified using high performance liquid chromatography (HPLC) method as described previously (O'Rourke et al., 2015). Grounded dry tissue samples (20–50 mg) were extracted two-times with 2.5 ml of 80% ethanol by boiling the samples in glass tubes in a 60°C water bath for 30 min each. After each extraction, the tubes were centrifuged at 4500 rpm for 10 min, and the extracts were then pooled and dried in a speedvac for ∼3–4 h. From this, final extract 200 μL was further dried down to remove the ethanol and rediluted with 200 μL deionized water. HPLC with a Dionex IC-3000 system including electrochemical detection cell with gold electrode and temperature controlled column compartment at 30°C (Thermo Scientific, Hemel Hempsted, UK) was used. The column used was a Dionex CarboPac PA20 3 × 150 mm analytical column (Thermo Scientific, Hemel Hempsted, UK). Ten microliters of sample was injected into the sample loop connected to the ion exchange column. The peaks were identified by comparing retention times with those of standard sugar markers with Dionex Chromeleon software.

Data Analyses

Statistical analyses were performed with R 3.0.1 (R Development Core Team, 2013). Data were averaged across genotypes, groups and treatments and mean values were reported. Two-way ANOVA considered treatments (WW and MWD) and groups (DT and DS) as explanatory variables while shoot dry weight was a response variable. An ANCOVA model was used considering SDW as the dependent variable with groups as the factor and hormones as the covariates. Principal component analysis (PCA) was performed on carbohydrate data to identify the carbohydrate response patterns between DT and DS groups as well as between the treatments. One-way ANOVA was used for the effects of exogenous hormones on the shoot growth rate, carbohydrates, and a Student's *t*-test was used to compute the pair-wise comparisons between group means with Bonferroni correction.

RESULTS

Drought-Tolerant and Drought-Sensitive Genotypes Show Different Shoot Growth Responses to Mild Drought

We studied the effect of mild drought on shoot growth response at the three-leaf stage of six wheat genotypes differing for drought sensitivity. Across all genotypes, average NDVI values measured at the three-leaf stage (23 DAS) in the field were comparable between WW and WD conditions (data not shown). When all genotypes were separated into drought-tolerant (DT, 3) and drought-sensitive (DS, 3) groups, the DS group showed a higher NDVI (13%) compared to DT group in WW conditions (**Figure 2A**). However, under mild drought,

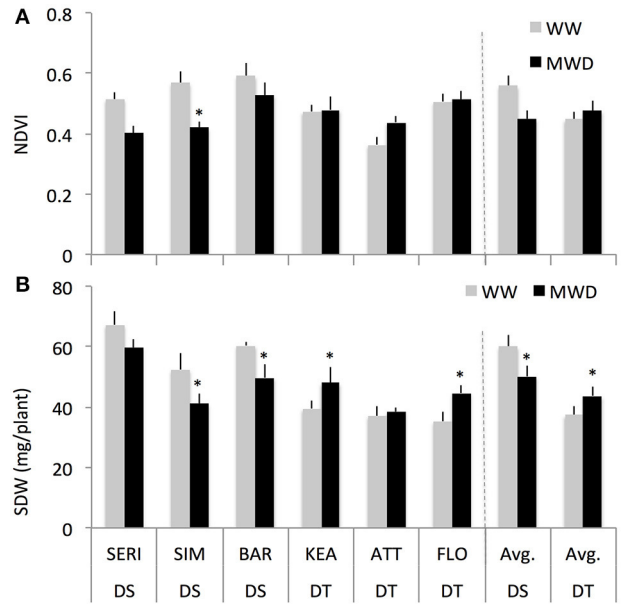

FIGURE 2 | The normalized difference vegetation index (NDVI) values (A) and shoot dry weight [SDW, (B)] of drought-tolerant (DT) and drought-susceptible (DS) genotypes at 3rd leaf stage grown under field-drought (with two replications) and controlled drought conditions with four replications for each genotype, respectively. * indicates $p <$ 0.05.

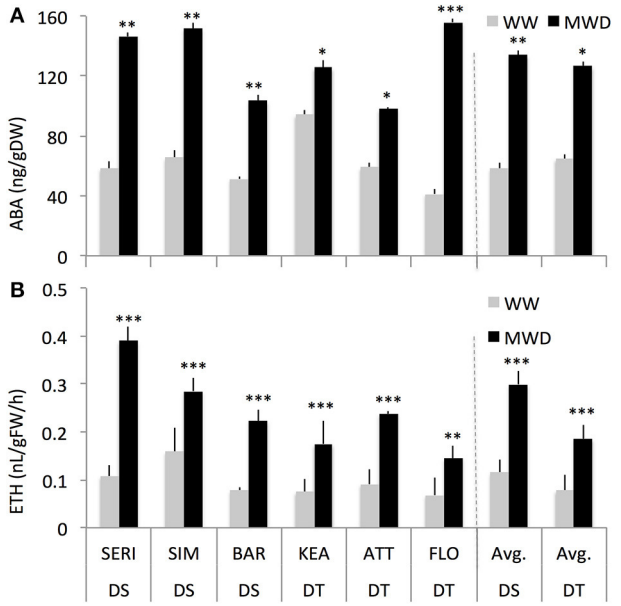

FIGURE 3 | Shoot ABA concentration (A) and ethylene production (B) of drought-tolerant (DT) and drought-susceptible (DS) genotypes grown under well-watered (WW) or mild water-deficit (MWD) conditions with four replications for each genotype. *, **, *** Indicate $p <$ 0.001, $<$ 0.01, and $<$ 0.05, respectively.

the DS group showed a reduction in NDVI (−7%) while the DT group had a slightly increased NDVI (+0.6%). Such NDVI responses were not significantly different between the DT and DS groups.

Consistent with the NDVI results (**Figure 2A**), both the DT and DS groups showed similar shoot dry weight (SDW) responses under controlled mild drought conditions albeit with a greater relative response (**Figure 2B**). The DS group had higher SDW (60%) than DT group under WW conditions. Under MWD, the DS group however showed a reduction in SDW (–16%) while the DT group had an increased SDW (+17%) relative to WW plants of the same group. A two-way ANOVA indicates that there was a significant interaction effect of groups and treatments on SDW ($P = 0.008$; for groups: $P < 0.001$; for treatments: $P = 0.05$). Further, treatments have significant effect on SDW within DS ($P = 0.03$) and DT ($P = 0.03$) groups. Similar shoot fresh weight responses of DT and DS groups in WW and MWD conditions were observed (**Supplementary Figure S2A**).

We examined whether differences in SDW of DT and DS groups could be related to plant water content. This seems unlikely, as both groups showed a tight association between FW and DW in both the conditions (**Supplementary Figure S2B**). DS plants have slightly more water content (<1%) but both groups responded similarly to MWD (**Supplementary Figure S2C**). Overall, these results suggest that the two groups of wheat cultivars responded differently to mild drought.

Shoot Growth Sensitivity of Drought-Tolerant and Drought-Sensitive Groups was Closely Associated with Endogenous ABA and Ethylene Accumulation and Responses

Previous studies have reported that wheat genotypes differ in the accumulation of, and their sensitivity to, ABA (Ji et al., 2011). We, therefore, measured endogenous ABA and ethylene in DT and DS genotypes grown under WW and MWD conditions. The DS and DT groups showed similar pattern of ABA and ethylene accumulation with both groups showing significantly higher ABA concentration (129% and 95%, respectively; $P < 0.001$) and ethylene production (160 and 138%, respectively; $P = 0.001$) in response to MWD (**Figure 3**, **Supplementary Figures S3A,B**). The main group effect on ABA was not significant ($P > 0.05$) but was significant for ethylene production ($P = 0.01$), indicating that both groups (DT and DS) significantly differed for ethylene production.

Across two treatments, SDW responses of the DT and DS groups to endogenous ABA and ethylene showed a tendency toward two response trends (**Figures 4A,B**, group effects for ABA: $P < 0.0001$; group effects for ethylene: $P < 0.0001$). The DT group showed an increased SDW with increasing concentrations of ABA (round circles, **Figure 4A**). In contrast, the DS group showed a decreased SDW with increasing concentrations of ABA (squares, **Figure 4A**). Such SDW responses of the DT and DS groups were consistent with ethylene whereby both the DT and DS groups showed an increased and a decreased SDW response

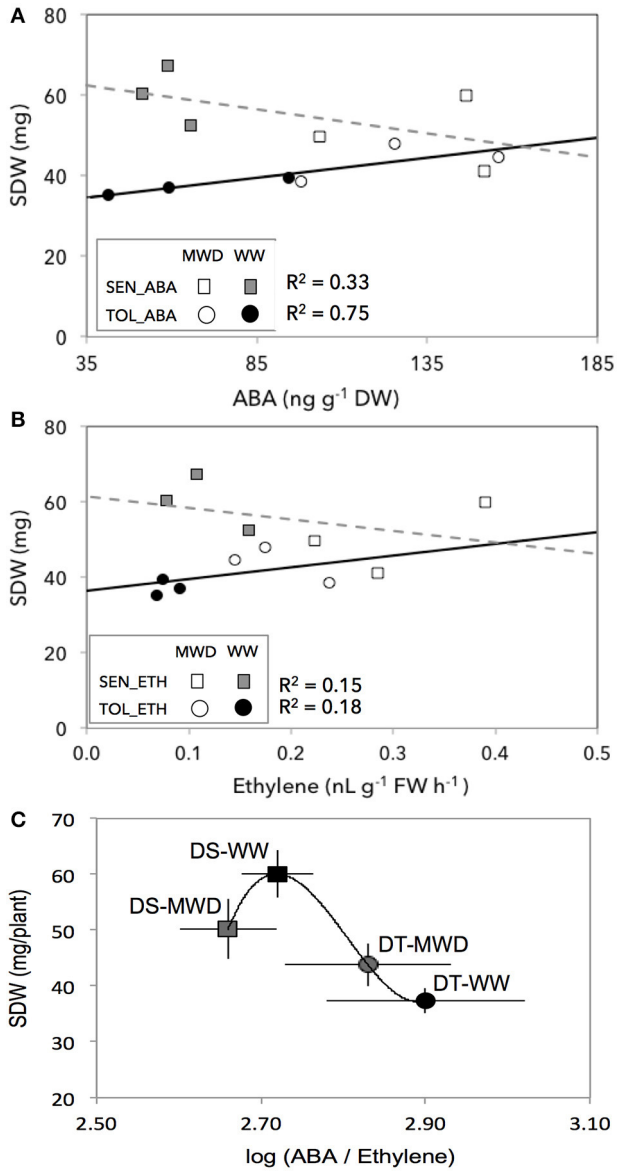

FIGURE 4 | The association between shoot dry weight (SDW) and endogenous ABA (A), ethylene (B), and ABA:ethylene ratio (C) in drought-tolerant (circles, DT) and drought-susceptible (squares, DS) genotypes grown under well-watered (filled symbols) and mild drought (open symbols) with four replications for each genotype. SEN, drought-susceptible; TOL, drought-tolerant. ETH, ethylene; ABA, abscisic acid.

to increasing levels of ethylene, respectively (**Figure 4B**). Such differential SDW response trends between DT and DS groups were largely driven by WW conditions, suggesting that hormone concentrations may regulate shoot growth even under optimal growing conditions.

Across treatments (WW and MWD) and groups (DT and DS), SDW did not correlate with ABA ($r^2 = 0.003$, $P = 0.81$; **Supplementary Figure S3C**) and ethylene ($r^2 = 0.15$, $P = 0.12$; **Supplementary Figure S3D**). However, SDW responses of both groups followed ABA:ethylene ratio (**Figure 4C**) that fits well with their SDW responses to mild drought (**Figure 2B**). Among the four-subgroups (DS-WW, DS-MWD, DT-WW, and DT-MWD), DS-WW subgroup had a higher SDW with an ABA/ethylene ratio of 2.72 while DT-WW subgroup had a lower SDW with an ABA/ethylene ratio of 2.90. However, both groups reduced ABA:ethylene ratio in response to MWD albeit at different level (2.66 and 2.83, respectively) but were not significantly different between two groups. These results suggest that an appropriate ABA:ethylene ratio might be critical and the DT and DS groups exhibited a differential growth sensitivity to MWD by differential accumulation of ABA and ethylene.

Foliar-Spray of Exogenous ABA and ACC Increase Shoot Relative Growth Rate of Drought-Tolerant and Drought-Sensitive Groups under Well-Watered Condition

Previous studies have often shown that very mild concentrations of exogenous ABA (Takahashi, 1972; Watanabe and Takahashi, 1997) and ethylene (Burg and Burg, 1966, 1968) stimulated growth of various organs of a range of plant species. We, therefore, examined whether low concentrations of exogenous ABA and ethylene could stimulate growth of DT and DS genotypes under WW condition. Both the DT and DS groups showed a significantly different shoot relative growth rate (RGR) response to exogenous ABA and ACC spray (**Figure 5**). ABA and ACC strongly promoted RGR of DS genotypes (131 and 130% respectively; $P = 0.01$) but had modest effect on RGR of DT genotypes (5 and 32% respectively; $P = 0.03$). Across all groups, ABA had an increased RGR by 50% ($P = 0.04$), while ACC was slightly more effective in stimulating shoot RGR (78%, $P = 0.002$). Such growth stimulation responses to exogenous ABA and ACC sprayed at the three-leaf stage were not significantly different from control at the 6th leaf-stage (**Supplementary Figure S4**), suggesting that low concentrations of ABA and ACC stimulated growth response may be dependent on the developmental stages.

Foliar-Spray of Exogenous ABA and ACC Had Differential Effects on Carbohydrates Status of Drought-Tolerant and Drought-Sensitive Groups under Well-Watered Condition

We hypothesized that an increased RGR response to low concentrations of ABA and ACC could be related to an altered carbohydrate status in DT and DS groups. A two-way ANOVA indicates that there was a significant interaction effect of groups and treatments for carbohydrates such as rhamnose ($P = 0.025$), raffinose ($P = 0.003$), and maltose ($P = 0.000$) (**Supplementary Table S1**). Further, treatments and groups have significant effect on galactose ($P = 0.000$ and 0.000, respectively), glucose ($P = 0.000$ and 0.000, respectively), fructose ($P = 0.004$ and 0.054, respectively; group has marginal effect on fructose), and maltose ($P = 0.004$ and 0.000, respectively). However,

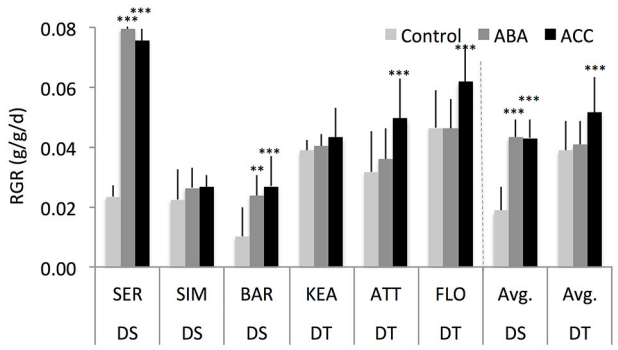

FIGURE 5 | Shoot relative growth rate (RGR) of six wheat genotypes at 3rd leaf stage that were either sprayed with water (controls), abscisic acid (ABA, 0.1 μM), or the ethylene-precursor, 1-aminocyclopropane -1-carboxylic acid (ACC, 0.1 μM) with four replications for each genotype. **, *** indicate $p < 0.01$, and < 0.05, respectively.

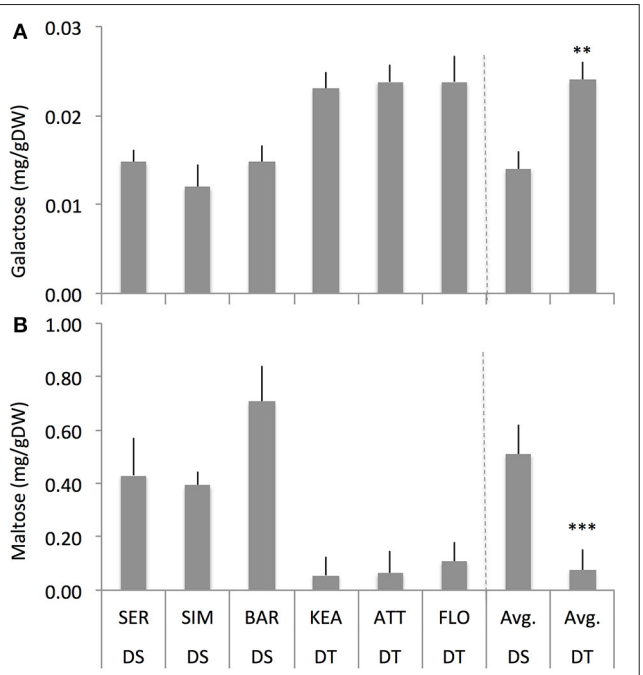

FIGURE 6 | The concentrations of galactose (A) and maltose (B) of drought-susceptible (DS) and drought-tolerant (DT) genotypes across the treatments (control, ABA and ACC (1-aminocyclopropane-1-carboxylic acid) spray) with four replications for each genotype. **, *** indicate $p < 0.01$, and < 0.05, respectively.

there was no interaction effect of treatment and group on these carbohydrates (**Supplementary Table S1**).

Across two treatments, DS group had significantly lower galactose (–45%, $P = 0.008$) but had significantly higher maltose (+575%, $P = 0.000$) compared to the DT group (**Figure 6**) while both DS and DT groups do not show significant difference for sucrose, fructose, rhamnose, raffinose, erlose, and sorbitol (**Supplementary Figure S5**). Among the treatments, ACC had consistently significant effect on galactose ($P = 0.000$ and 0.001), and maltose ($P = 0.000$ and 0.025) in both the DS and DT groups, respectively (**Figure 7**). Although ABA increased these carbohydrates as well, it had significant effect only for maltose ($P = 0.023$) in DS group but not in DT group. Overall, these results indicate that both the DT and DS groups had altered carbohydrates status in response to foliar ABA and ACC spray (**Figures 6**, **7**).

DISCUSSION

Previous studies on shoot growth plasticity to varying soil moisture have provided valuable information leading to current understanding of growth control by multiple processes. We have further extended our understanding to assess the importance of individual physiological traits in the context of crop growth under stress conditions. First, we propose that a simple shoot biomass growth assay (**Figure 2**) can be used as a sensitive indicator of stress tolerance (Claeys et al., 2014). Second, an early seedling stage represents a suitable growing tissue for deducing precise drought adaptive mechanisms controlling growth since drought adaptive mechanisms differ between young growing- and mature-tissues (Harb et al., 2010; Skirycz et al., 2010). Third, many QTLs for several seedling-stage traits, including early shoot biomass, co-locate with QTLs linked with grain yields (Sandhu et al., 2015); hence, seedling responses can be relevant for crop yields under field conditions. This study encompasses the first two propositions and further suggests that an early seedling-stage can predict stress-adapted traits and reduces the time needed for genotype selections prior to time-consuming phenotypic evaluations under field conditions.

Mild Drought Stress Enhanced Shoot Dry Biomass in Drought-Tolerant Genotypes but not in Drought-Susceptible Genotypes

Our study showed that the DT group could enhance, or maintain, shoot biomass growth under mild drought conditions as compared to the DS group (**Figures 2A,B**). Such differential growth responses between DT and DS groups may be controlled by genotype-specific mechanisms (Hall et al., 1982; Chaves et al., 2002; Campos et al., 2004; An et al., 2014). Supporting, both DT and DS groups exhibited differential hormone responses (**Figure 3**) and ABA:ethylene ratios (**Figure 4**) when exposed to mild drought. Though marginally significant ($P = 0.056$), the DT group had a higher g_s under MWD compared to WW conditions (**Supplementary Figure S2D**), suggesting a sustained g_s may enhance carbon gain (Caldeira et al., 2014; Tardieu et al., 2014), and subsequently crop yield (Fischer et al., 1998; Lu et al., 1998), under mild stress conditions. Such differential stomatal responses between DT (small stomatal responses) and DS (large stomatal responses) genotypes have previously been reported and have also been shown to correlate with yield under stress conditions (Tardieu and Simonneau, 1998; Munns et al., 2010; Sade et al., 2012; Tardieu et al., 2014).

The enhanced shoot growth of DT group under MWD in our study might be related to the fact that we imposed a steady-state MWD on growing tissues of young seedlings, which

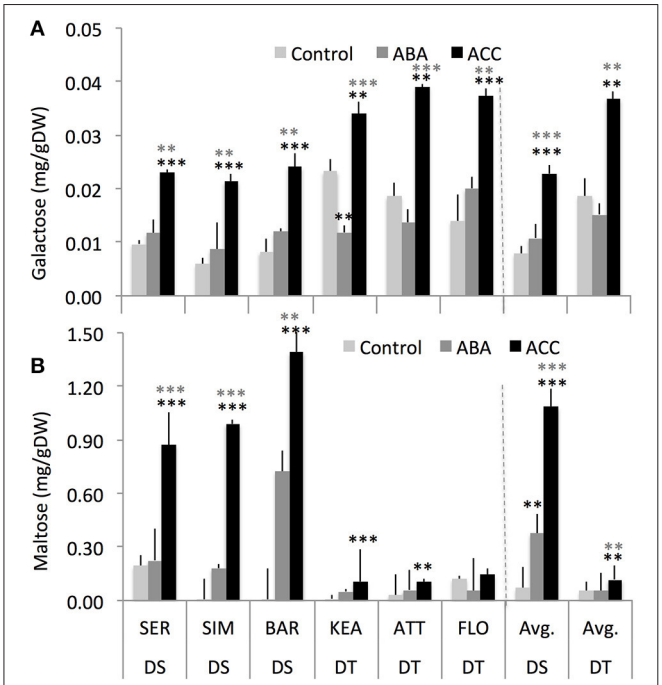

FIGURE 7 | The effect of chemical spay on the concentrations of galactose (A), and maltose (B) between drought-susceptible (DS) and drought-tolerant (DT) genotypes at 3rd leaf stage that were either sprayed with water (controls), abscisic acid (ABA, 0.1 μM), or the ethylene-precursor, 1-aminocyclopropane-1-carboxylic acid (ACC, 0.1 μM) with four replications for each genotype. **, *** indicate $p < 0.01$, and < 0.05, respectively.

greatly differ with mature tissues, for stress adaptive mechanisms (Lechner et al., 2008). We further propose that the positive growth response of young growing seedlings, such as in this study, might be easier to detect when not dominated by a negative or no growth response of mature tissues particularly at later developmental stages. While such differential growth responses between young and mature tissues at different developmental stages under MWD is worth for follow-up studied, it may partly explain a widely reported negative growth response of plants under drought that contain proportionately more mature tissue than young growing tissue. Such mechanisms may differ between the DT and DS genotypes (Ji et al., 2011).

Our results agree with previous studies that have reported enhanced shoot dry biomass under mild drought (Liu and Li, 2005; Boutraa et al., 2010). Additional evidence that mild-stresses can enhance shoot biomass growth comes from studies with two indica rice cultivars, where mild-salt stress (NaCl at 0.5% w/v) increased shoot dry weight in 4-weeks after treatment (Sripinyowanich et al., 2013; Tada et al., 2014). Taken all together, we postulate that mild stresses may enhance biomass growth at least in stress-tolerant genotypes although the precise underlying mechanisms can be debatable. Higher g_s can be an obvious important stress-associated trait that can contribute to an increased carbon (C) gain in the DT genotypes during an initial stages of drought stress (Caldeira et al., 2014; Tardieu et al., 2014). In addition, mechanisms that involve lower energy costs, for example, lower root respiration could be important for growth regulation under MWD, as reported in drought-tolerant wheat genotype (Liu and Li, 2005).

ABA:Ethylene Ratio is an Important Trait in Shoot Growth Regulation under Mild Drought that Differs between Drought-Tolerant and Drought-Susceptible Genotypes

It has long been known that plant hormones form a complex network to coordinate the regulation of numerous development processes. ABA and ethylene interactions in regulating numerous biological processes have been well-reported at the cell level (Tanaka et al., 2005; Beguerisse-Dıaz et al., 2012; Chen et al., 2013; Watkins et al., 2014). However, although the chemical control of growth by these hormones has been demonstrated in specific tissues (Sharp and LeNoble, 2002), our eco-physiological understanding of the regulation of these hormones in field crops at the whole plant/crop level is rather limited (Parent et al., 2009; Caldeira et al., 2014; Planes et al., 2015) as these hormones affect a very large number of processes and their interactions are complex. This study suggests a key role for an optimum threshold of ABA:ethylene ratio in regulating shoot biomass growth (**Figure 4**) whereby both the DT and DS groups had different ABA:ethylene ratios in response to mild drought. Such an ABA:ethylene ratio might be different for other crop species and physiological processes studied and may be specific to developmental stages, an issue worthy to be studied. We propose that genotypes and/or environmental conditions that lead to an optimum hormonal ratio under mild stress conditions—as was shown in this study—may allow greater shoot biomass gain as long as the hormonal ratio in other tissues is not detrimental, which may be different under more severe stress.

Our results complement several studies that have previously demonstrated the key roles of hormonal ratio sensing, for example, auxin:cytokinin ratio in shoot, root induction (Skoog and Miller, 1957; Mercier et al., 2003), and shoot vigor (Albacete et al., 2008), cytokinin:auxin ratio in shoot and inflorescence regeneration (Cheng et al., 2010), gibberellin:abscisic acid ratio in barley grains (Weier et al., 2014), and arabidopsis seed development (Yamaguchi, 2008), most likely through differential gene expressions (Weier et al., 2014). Knowing that ethylene is neither actively transported nor degraded, although ACC oxidase activity is constitutively present in most vegetative plant tissues, and that both DT and DS groups significantly differed for ethylene accumulation but not for ABA, strongly suggest that genetic variability in ethylene biosynthesis may play a crucial role in the changes of ABA:ethylene ratio and its effect on shoot dry biomass of plants. This is further supported by the fact that, across two groups, ethylene was increased by 149% while ABA was increased by 112% under mild drought, not inconsistent with previous studies reporting a higher (five-fold) and lower (two-five-fold) increases for ethylene and ABA, respectively, in a salt-stressed tomato (Albacete et al., 2008). Indeed, ethylene response transcription factors (ERF5/ERF6) have been proposed to act as molecular nodes in the stress-related network where

growth control and stress tolerance diverge (Claeys and Inzé, 2013; Dubois et al., 2013). Because, wheat genotypes exhibit a large genetic variability in biosynthesis of, and sensitivity to, ABA and ethylene (Quarrie and Lister, 1983; Sridhar, 2003; Iehisa and Takumi, 2012; Valluru et al., 2014), a natural variation in ABA and ethylene biosynthesis, and consequently ABA:ethylene ratio, might reflect a genetic determinism that partly drive biomass accumulation among crop species under mild stress conditions. Therefore, hormonal ratio can be an invaluable candidate trait for the selection of genotypes for achieving higher biomass and yield under mild stress conditions (Wilkinson et al., 2012).

While our study emphasizes hormonal ratio influences on both plant growth and functioning, it does not throw light upon the mechanistic basis of the maintenance of an appropriate ABA:ethylene ratio in plants. We, however, propose that such an optimal ABA:ethylene ratio, rather than single hormone level, could be a sensitive regulator (or sensor) of, for instance, appropriate morphological development and physiological functioning (Weier et al., 2014; Zhang et al., 2014) providing a fitness advantage in complex natural environments. Plants may respond to environmental perturbations by synthesizing different hormone levels, thereby different hormonal ratio, enabling the communication and transduction of environmental cues into plastic responses (Pozo et al., 2015). It is now widely accepted that ethylene and ABA interact at multiple levels (Cheng et al., 2009; Krouk et al., 2011) and ABA induced stomatal closure has been widely shown to be antagonized by ethylene. An optimal ABA:ethylene ratio therefore keeps stomata partly open (higher g_s) allowing enhanced gas exchange that indeed allow continued C gain in DT genotypes under mild drought. While expansive growth may be directly limited by hydraulic signals (Caldeira et al., 2014), continued C gain is important for attaining dry biomass gain when water status is re-established. However, modifying the hormonal ratio by attaining moderate levels of hormones through breeding remains a major challenge. Exploring phenotypic screens of large numbers of genotypes including landraces, wild relatives (Sridhar, 2003; Iehisa and Takumi, 2012; Valluru et al., 2014) and the use of molecular approaches targeted at specific tissues and growth stages (Habben et al., 2014) would facilitate the development of crop cultivars that are able to grow under numerous abiotic stress conditions with minimal yield losses (Peleg and Blumwald, 2011).

Low Concentrations of ABA and ACC Increase Shoot Relative Growth and Alter Carbohydrate Status that Differ between Drought-Tolerant and Drought-Susceptible Genotypes

Generally, the action of ABA and ethylene at the higher concentration has been related with the process of growth inhibition. However, there is recent evidence of their presence in developing tissues and also of being organ/tissue and development stage-specific where they may have a promoting action (Finkelstein and Rock, 2002; Sansberro et al., 2004; Peng et al., 2006; Skirycz et al., 2010; Duan et al., 2013). Our results demonstrate that low concentrations of ABA and ACC sprayed onto the seedlings favored vegetative growth, benefitting dry matter accumulation of wheat seedlings under optimal growing conditions particularly for DS genotypes (**Figure 5**). These results agree with previous studies that have reported that field-grown wheat plants treated with ABA (300 mg L^{-1}) under water stress showed higher shoot biomass accumulation (Travaglia et al., 2007, 2010). Further, exogenous ABA (10 mg L^{-1}) application at anthesis stage increased dry matter accumulation 7 days after anthesis in a field-grown stay-green wheat line (Yang et al., 2014). In addition, ABA (300 mg L^{-1}) sprayed onto the leaves of soybean plants showed an enhanced dry matter accumulation under field conditions (Travaglia et al., 2009). Moreover, ABA and ACC spray lead to the accumulation of specific carbohydrates in leaves (**Figure 7**). Overall, these results suggest that both ABA and ethylene at low concentration may be important regulators of shoot biomass likely due to improved physiological parameters such as chlorophyll, green leaf area and duration, photosynthesis, and carbohydrate status (source effects), as reported previously (Khan, 2004; Travaglia et al., 2007, 2010; Khan et al., 2008; Iqbal et al., 2011, 2012).

Again, both DT and DS groups showed differences in the accumulation of specific carbohydrates (**Figure 6**). The DS group had significantly lower galactose but had significantly higher maltose contents compared to the DT group. This suggest that the DS group had more utilization of sugars such as galactose (galactose is directly converted to glucose, for example, in wheat seedlings; Hassid et al., 1956), and maltose levels (**Figure 6**) compared to the DT group. Higher maltose levels indicate high turnover of starch. Although galactose at higher concentration has often been shown to be detrimental to organ growth, lower concentrations of galactose can transiently increase the sink demand for carbon, and therefore, enhances carbon unloading from the phloem (Thorpe et al., 1999). Because galactose is known as a unique sugar that increase carbon import and phloem unloading, it may offer avenues to examine possible sugar signals resulting in phloem unloading in sink tissues and consequent biomass development (Seifert et al., 2002) especially when compared the DT and DS genotypes.

In addition to growth stimulation, low-concentrations of ABA and ethylene may condition the crop plants that, in essence, would provide competence for adaptation to stresses of similar or others (Bartels et al., 1990). Since these hormones have knock-on effects on several growth processes that can also be measured, this study therefore suggests that phenotyping for low-concentrations of ABA- and ethylene-induced growth *per se* would potentially represent a positive contribution to crop biomass and yield under field conditions (**Figure 5**, Cai et al., 2014), and may also lead to novel germplasm being made available to breeders for the development of high yielding and stress adapted crop cultivars.

In conclusion, the hormone interaction presented here may deliver benefits in terms of dry biomass gain under mild stress conditions. In environments with optimal to sub-optimal growing conditions, which induce slightly elevated concentrations of both hormones, the ABA and ethylene ratio presented here may underlie a part of genetic determinism that

control shoot dry biomass gain in wheat. This is supported by our results that (1) both the DT and DS groups exhibited different SDW responses to mild drought (**Figure 2**; Liu and Li, 2005; Boutraa et al., 2010), (2) mild drought induced low concentrations of ABA and ethylene (**Figure 3** Wright, 1977; Ali et al., 1999; Dodd et al., 2010), and (3) low concentrations of ABA and ACC stimulated SDW of wheat seedlings (**Figure 5**; Takahashi, 1972; Watanabe and Takahashi, 1997) likely through altered carbohydrates status of the plants (**Figures 6**, **7**).

AUTHOR CONTRIBUTIONS

RV, WD: Designed, conducted and oversee the glasshouse experiments; MR: designed and oversee the field experiments; RV, WD, MR and ID: wrote the paper. All authors read and approved the final manuscript.

ACKNOWLEDGMENTS

This work is supported by the Consultative Group on International Agricultural Research (CGIAR) Research Program (CRP-WHEAT, SI-6) through the CIMMYT. Authors thank Xiaoqing Li and Guofeng Hu for their assistance in the glasshouse experiments and Timothy Gregson for the sugars analysis.

SUPPLEMENTARY MATERIAL

The Supplementary Material for this article can be found online at: http://journal.frontiersin.org/article/10.3389/fpls.2016.00461

Supplementary Figure S1 | (A), Soil moisture content (g H_2O g^{-1} dry soil) in both well-watered and mild drought stress treatments; **(B)**, Soil water potential (MPa) of both well-watered and mild-drought stressed plants; **(C)**, Temperature and humidity levels during the experiment, and **(D)**, Primary leaf growth response to different concentrations of ABA and ACC.

Supplementary Figure S2 | (A) Shoot fresh weight of six wheat genotypes that were either grown under well-watered (WW) or mild water-deficit (MWD) conditions. **(B)**, the relationship between log values of fresh weight (FW) and dry weight (DW) in WW and MWD treatments; **(C)**, plant water content (%) of drought-susceptible and drought-tolerant wheat genotypes in WW and MWD treatments; **(D)**, stomatal conductance of drought-susceptible and drought-tolerant wheat genotypes in WW and MWD treatments.

Supplementary Figure S3 | ABA concentration (A) and ethylene evolution (B) in well-watered (WW) and mild-drought stress (MWD) treatments across all genotypes. Linear correlations between shoot dry weight (SDW) and endogenous ABA **(C)** and ethylene **(D)** across all groups and treatments. ** indicates $p < 0.01$.

Supplementary Figure S4 | Shoot relative growth rate in drought-susceptible (A) and drought-tolerant (B) wheat genotypes that were either sprayed with water (controls), abscisic acid (ABA, 0.1 μM) or the ethylene-precursor, 1-aminocyclopropane-1-carboxylic acid (ACC, 0.1 μM) at the 6th leaf stage.

Supplementary Figure S5 | Sucrose (A), fructose (B), rhamnose (C), raffinose (D), erlose (E), and sorbitol (F) concentrations of drought-susceptible (DS) and drought-tolerant (DT) wheat genotypes across the treatments [control, ABA and ACC (1-aminocyclopropane-1-carboxylic acid) spray].

Supplementary Table 1 | Two-way ANOVA for the effects of treatments (well-watered and mild drought) and stress group (drought-tolerant and drought-susceptible) and their interaction on several carbohydrate concentrations of six wheat genotypes that were either sprayed with water (controls), abscisic acid (ABA, 0.1 μM) or the ethylene-precursor, 1-aminocyclopropane-1-carboxylic acid (ACC, 0.1 μM) at the 3rd leaf stage. *, **, *** indicate $p < 0.001$, < 0.01, and < 0.05, respectively.

REFERENCES

Albacete, A., Ghanem, M. E., Martínez-Andújar, C., Acosta, M., Sánchez-Bravo, J., Martínez, V., et al. (2008). Hormonal changes in relation to biomass partitioning and shoot growth impairment in salinized tomato (*Solanum lycopersicum* L.) plants. *J. Exp. Bot.* 59, 4119–4131. doi: 10.1093/jxb/ern251

Ali, M., Jensen, C. R., Mogensen, V. O., Andersen, M. N., and Henson, I. E. (1999). Root signalling and osmotic adjustment during intermittent soil drying sustain grain yield of field grown wheat. *Field Crops Res.* 62, 35–52. doi: 10.1016/S0378-4290(99)00003-9

Almeida-Rodriguez, A. M., Cooke, J. E. K., Yeh, F., and Zwiazek, J. J. (2010). Functional characterization of drought-responsive aquaporins in Populus balsamifera and Populus simonii×balsamifera clones with different drought resistance strategies. *Physiol. Plant.* 140, 321–333. doi: 10.1111/j.1399-3054.2010.01405.x

An, Y., Zhou, P., and Liang, J. (2014). Effects of exogenous application of abscisic acid on membrane stability, osmotic adjustment, photosynthesis and hormonal status of two lucerne (*Medicago sativa* L.) genotypes under high temperature stress and drought stress. *Crop Pasture Sci.* 65, 274–286. doi: 10.1071/CP13162

Araus, J. L., Slafer, G. A., Reynolds, M. P., and Royo, C. (2002). Plant Breeding and drought in C3 cereals: what should we breed for? *Ann. Bot.* 89, 925–940. doi: 10.1093/aob/mcf049

Araus, J. L., Slafer, G. A., Royo, C., and Serret, M. D. (2008). Breeding for yield potential and stress adaptation in cereals. *Crit. Rev. Plant Sci.* 27, 377–412. doi: 10.1080/07352680802467736

Bartels, D., Schneider, K., Terstappen, G., Piatkowski, D., and Salamini, F. (1990). Molecular cloning of abscisic acid-modulated genes which are induced during desiccation of the resurrection plant *Craterostigma plantagineum*. *Planta* 181, 27–34. doi: 10.1007/BF00202321

Beguerisse-Diaz, M., Hernández-Gómez, M. C., Lizzul, A. M., Barahona, M., and Desikan, R. (2012). Compound stress response in stomatal closure: a mathematical model of ABA and ethylene interaction in guard cells. *BMC Syst. Biol.* 6:146. doi: 10.1186/1752-0509-6-146

Blum, A. (2011). "Plant water relations, plant stress and plant production," in *Plant Breeding for Water-Limited Environments*, (New York, NY: Springer), 11–52. Available online at: http://link.springer.com/chapter/10.1007/978-1-4419-7491-4_2 (Accessed on October 8, 2014).

Boutraa, T., Akhkha, A., Al-Shoaibi, A. A., and Alhejeli, A. M. (2010). Effect of water stress on growth and water use efficiency (WUE) of some wheat cultivars (Triticum durum) grown in Saudi Arabia. *J. Taibah Univ. Sci.* 3, 39–48. doi: 10.1016/S1658-3655(12)60019-3

Burg, S. P., and Burg, E. A. (1966). The interaction between auxin and ethylene and its role in plant growth. *Proc. Natl. Acad. Sci. U.S.A.* 55, 262–269. doi: 10.1073/pnas.55.2.262

Burg, S. P., and Burg, E. A. (1968). Ethylene formation in pea seedlings; its relation to the inhibition of bud growth caused by Indole-3-Acetic acid. *Plant Physiol.* 43, 1069–1074. doi: 10.1104/pp.43.7.1069

Cai, T., Xu, H., Peng, D., Yin, Y., Yang, W., Ni, Y., et al. (2014). Exogenous hormonal application improves grain yield of wheat by optimizing tiller productivity. *Field Crops Res.* 155, 172–183. doi: 10.1016/j.fcr.2013.09.008

Caldeira, C. F., Bosio, M., Parent, B., Jeanguenin, L., Chaumont, F., and Tardieu, F. (2014). A hydraulic model is compatible with rapid changes in leaf elongation under fluctuating evaporative demand and soil water status. *Plant Physiol.* 164, 1718–1730. doi: 10.1104/pp.113.228379

Campos, H., Cooper, M., Habben, J. E., Edmeades, G. O., and Schussler, J. R. (2004). Improving drought tolerance in maize: a view from industry. *Field Crops Res.* 90, 19–34. doi: 10.1016/j.fcr.2004.07.003

Cattivelli, L., Rizza, F., Badeck, F.-W., Mazzucotelli, E., Mastrangelo, A. M., Francia, E., et al. (2008). Drought tolerance improvement in crop plants: an integrated view from breeding to genomics. *Field Crops Res.* 105, 1–14. doi: 10.1016/j.fcr.2007.07.004

Chaves, M. M., Pereira, J. S., Maroco, J., Rodrigues, M. L., Ricardo, C. P., Osório, M. L., et al. (2002). How plants cope with water stress in the field? *Photosynthesis and growth. Ann. Bot.* 89, 907–916. doi: 10.1093/aob/mcf105

Chaves, M. M., Zarrouk, O., Francisco, R., Costa, J. M., Santos, T., Regalado, A. P., et al. (2010). Grapevine under deficit irrigation: hints from physiological and molecular data. *Ann. Bot.* 105, 661–676. doi: 10.1093/aob/mcq030

Chen, L., Dodd, I. C., Davies, W. J., and Wilkinson, S. (2013). Ethylene limits abscisic acid- or soil drying-induced stomatal closure in aged wheat leaves. *Plant Cell Environ.* 36, 1850–1859. doi: 10.1111/pce.12094

Cheng, W.-H., Chiang, M.-H., Hwang, S.-G., and Lin, P.-C. (2009). Antagonism between abscisic acid and ethylene in *Arabidopsis* acts in parallel with the reciprocal regulation of their metabolism and signaling pathways. *Plant Mol. Biol.* 71, 61–80. doi: 10.1007/s11103-009-9509-7

Cheng, Z. J., Zhu, S. S., Gao, X. Q., and Zhang, X. S. (2010). Cytokinin and auxin regulates WUS induction and inflorescence regeneration *in vitro* in *Arabidopsis*. *Plant Cell Rep.* 29, 927–933. doi: 10.1007/s00299-010-0879-8

Claeys, H., and Inzé, D. (2013). The agony of choice: how plants balance growth and survival under water-limiting conditions. *Plant Physiol.* 162, 1768–1779. doi: 10.1104/pp.113.220921

Claeys, H., Landeghem, S. V., Dubois, M., Maleux, K., and Inzé, D. (2014). What is stress? dose-response effects in commonly used in *vitro* stress assays. *Plant Physiol.* 165, 519–527. doi: 10.1104/pp.113.234641

Davies, W. J., and Zhang, J. (1991). Root signals and the regulation of growth and development of plants in drying soil. *Annu. Rev. Plant Physiol. Plant Mol. Biol.* 42, 55–76. doi: 10.1146/annurev.pp.42.060191.000415

Deokar, A. A., Kondawar, V., Jain, P. K., Karuppayil, S. M., Raju, N. L., Vadez, V., et al. (2011). Comparative analysis of expressed sequence tags (ESTs) between drought-tolerant and -susceptible genotypes of chickpea under terminal drought stress. *BMC Plant Biol.* 11:70. doi: 10.1186/1471-2229-11-70

Dodd, I. C., Egea, G., Watts, C. W., and Whalley, W. R. (2010). Root water potential integrates discrete soil physical properties to influence ABA signalling during partial rootzone drying. *J. Exp. Bot.* 61, 3543–3551. doi: 10.1093/jxb/erq195

Dodd, I. C., Theobald, J. C., Bacon, M. A., and Davies, W. J. (2006). Alternation of wet and dry sides during partial rootzone drying irrigation alters root-to-shoot signalling of abscisic acid. *Funct. Plant Biol.* 33, 1081–1089. doi: 10.1071/FP06203

Dodd, I. C. (2013). Abscisic acid and stomatal closure: a hydraulic conductance conundrum. *New Phytol* 197, 6–8. doi: 10.1111/nph.12052

Duan, L., Dietrich, D., Ng, C. H., Chan, P. M. Y., Bhalerao, R., Bennett, M. J., et al. (2013). Endodermal ABA signaling promotes lateral root quiescence during salt stress in *Arabidopsis* seedlings. *Plant Cell Online* 25, 324–341. doi: 10.1105/tpc.112.107227

Dubois, M., Skirycz, A., Claeys, H., Maleux, K., Dhondt, S., De Bodt, S., et al. (2013). ETHYLENE RESPONSE FACTOR6 acts as a central regulator of leaf growth under water-limiting conditions in *Arabidopsis*. *Plant Physiol.* 162, 319–332. doi: 10.1104/pp.113.216341

Ernst, R., Bjornsen, J. E., and Arditti, J. (1992). Effects of ethephon, its nonethylene-generating analog ethylphosphonic acid, and phosphorous acid in aseptic culture of orchid seedlings. *Am. J. Bot.* 79, 275–278. doi: 10.2307/2445015

Fatichi, S., Leuzinger, S., and Körner, C. (2014). Moving beyond photosynthesis: from carbon source to sink-driven vegetation modeling. *New Phytol.* 201, 1086–1095. doi: 10.1111/nph.12614

Finkelstein, R. R., and Rock, C. D. (2002). Abscisic acid biosynthesis and response. *Arabidopsis Book* 1:e0058. doi: 10.1199/tab.0058

Fischer, R. A., Rees, D., Sayre, K. D., Lu, Z.-M., Condon, A. G., and Saavedra, A. L. (1998). Wheat yield progress associated with higher stomatal conductance and photosynthetic rate, and cooler canopies. *Crop Sci.* 38, 1467. doi: 10.2135/cropsci1998.0011183X003800060011x

González, Á. (2011). Response of coleoptiles to water deficit: growth, turgor maintenance and osmotic adjustment in barley plants (*Hordeum vulgare* L.). *Agric. Sci.* 2, 159–166. doi: 10.4236/as.2011.23022

Gressel, J., and Dodds, J. (2013). Commentary: hormesis can be used in enhancing plant productivity and health; but not as previously envisaged. *Plant Sci.* 213, 123–127. doi: 10.1016/j.plantsci.2013.09.007

Guzmán, P., and Ecker, J. R. (1990). Exploiting the triple response of *Arabidopsis* to identify ethylene-related mutants. *Plant Cell Online* 2, 513–523. doi: 10.1105/tpc.2.6.513

Habben, J. E., Bao, X., Bate, N. J., DeBruin, J. L., Dolan, D., Hasegawa, D., et al. (2014). Transgenic alteration of ethylene biosynthesis increases grain yield in maize under field drought-stress conditions. *Plant Biotechnol. J.* 12, 685–693. doi: 10.1111/pbi.12172

Hall, A. J., Vilella, F., Trapani, N., and Chimenti, C. (1982). The effects of water stress and genotype on the dynamics of pollen-shedding and silking in maize. *Field Crops Res.* 5, 349–363. doi: 10.1016/0378-4290(82)90036-3

Harb, A., Krishnan, A., Ambavaram, M. M. R., and Pereira, A. (2010). Molecular and physiological analysis of drought stress in *Arabidopsis* reveals early responses leading to acclimation in plant growth. *Plant Physiol.* 154, 1254–1271. doi: 10.1104/pp.110.161752

Hassid, W. Z., Putman, E. W., and Ginsburg, V. (1956). Metabolism of galactose in canna leaves and wheat seedlings. *Biochim. Biophys. Acta* 20, 17–22. doi: 10.1016/0006-3002(56)90256-6

Hatier, J.-H. B., Faville, M. J., Hickey, M. J., Koolaard, J. P., Schmidt, J., Carey, B.-L., et al. (2014). Plant vigour at establishment and following defoliation are both associated with responses to drought in perennial ryegrass (*Lolium perenne* L.). *J. Exp. Bot.* 65, 5823–5834. doi: 10.1093/jxb/eru318

Hays, D. B., Do, J. H., Mason, R. E., Morgan, G., and Finlayson, S. A. (2007). Heat stress induced ethylene production in developing wheat grains induces kernel abortion and increased maturation in a susceptible cultivar. *Plant Sci.* 172, 1113–1123. doi: 10.1016/j.plantsci.2007.03.004

Hoffmann, W. A., and Poorter, H. (2002). Avoiding bias in calculations of relative growth rate. *Ann. Bot.* 90, 37–42. doi: 10.1093/aob/mcf140

Iehisa, J. C. M., and Takumi, S. (2012). Variation in abscisic acid responsiveness of *Aegilops tauschii* and hexaploid wheat synthetics due to the D-genome diversity. *Genes Genet. Syst.* 87, 9–18. doi: 10.1266/ggs.87.9

Iqbal, N., Khan, N. A., Nazar, R., and Silva, J. A. T., da (2012). Ethylene-stimulated photosynthesis results from increased nitrogen and sulfur assimilation in mustard types that differ in photosynthetic capacity. *Environ. Exp. Bot.* 78, 84–90. doi: 10.1016/j.envexpbot.2011.12.025

Iqbal, N., Nazar, R., Syeed, S., Masood, A., and Khan, N. A. (2011). Exogenously-sourced ethylene increases stomatal conductance, photosynthesis, and growth under optimal and deficient nitrogen fertilization in mustard. *J. Exp. Bot.* 62, 4955 –4963. doi: 10.1093/jxb/err204

Ji, X., Dong, B., Shiran, B., Talbot, M. J., Edlington, J. E., Hughes, T., et al. (2011). Control of abscisic acid catabolism and abscisic acid homeostasis is important for reproductive stage stress tolerance in cereals. *Plant Physiol.* 156, 647–662. doi: 10.1104/pp.111.176164

Jia, W., and Davies, W. J. (2007). Modification of leaf apoplastic pH in relation to stomatal sensitivity to root-sourced abscisic acid signals. *Plant Physiol.* 143, 68–77. doi: 10.1104/pp.106.089110

Kamaluddin, M., and Zwiazek, J. J. (2002). Ethylene enhances water transport in hypoxic aspen. *Plant Physiol.* 128, 962 –969. doi: 10.1104/pp.010791

Khan, N. A., Mir, M. R., Nazar, R., and Singh, S. (2008). The application of ethephon (an ethylene releaser) increases growth, photosynthesis and nitrogen accumulation in mustard (*Brassica juncea* L.) under high nitrogen levels. *Plant Biol.* 10, 534–538. doi: 10.1111/j.1438-8677.2008.00054.x

Khan, N. A. (2004). An evaluation of the effects of exogenous ethephon, an ethylene releasing compound, on photosynthesis of mustard (Brassica juncea) cultivars that differ in photosynthetic capacity. *BMC Plant Biol.* 4:21. doi: 10.1186/1471-2229-4-21

Kieber, J. J., Rothenberg, M., Roman, G., Feldmann, K. A., and Ecker, J. R. (1993). *CTR1*, a negative regulator of the ethylene response pathway in *Arabidopsis*, encodes a member of the Raf family of protein kinases. *Cell* 72, 427–441. doi: 10.1016/0092-8674(93)90119-B

Krouk, G., Ruffel, S., Gutiérrez, R. A., Gojon, A., Crawford, N. M., Coruzzi, G. M., et al. (2011). A framework integrating plant growth with hormones and nutrients. *Trends Plant Sci.* 16, 178–182. doi: 10.1016/j.tplants.2011.02.004

Ku, H. S., Suge, H., Rappaport, L., and Pratt, H. K. (1970). Stimulation of rice coleoptile growth by ethylene. *Planta* 90, 333–339. doi: 10.1007/BF00386385

Lechner, L., Pereyra-Irujo, G. A., Granier, C., and Aguirrezábal, L. A. N. (2008). Rewatering plants after a long water-deficit treatment reveals that leaf epidermal cells retain their ability to expand after the leaf has apparently reached its final size. *Ann. Bot. (Lond.)* 101, 1007–1015. doi: 10.1093/aob/mcn029

Lehman, A., Black, R., and Ecker, J. R. (1996). HOOKLESS1, an ethylene response gene, is required for differential cell elongation in the *Arabidopsis* hypocotyl. *Cell* 85, 183–194. doi: 10.1016/S0092-8674(00)81095-8

Li, Y.-S., Mao, X.-T., Tian, Q.-Y., Li, L.-H., and Zhang, W.-H. (2009). Phosphorus deficiency-induced reduction in root hydraulic conductivity in Medicago falcata is associated with ethylene production. *Environ. Exp. Bot.* 67, 172–177. doi: 10.1016/j.envexpbot.2009.05.013

Liu, H. S., and Li, F. M. (2005). Root Respiration, Photosynthesis and grain yield of two spring wheat in response to soil drying. *Plant Growth Regul.* 46, 233–240. doi: 10.1007/s10725-005-8806-7

Lopes, M. S., Dreisigacker, S., Peña, R. J., Sukumaran, S., and Reynolds, M. P. (2015). Genetic characterization of the wheat association mapping initiative (WAMI) panel for dissection of complex traits in spring wheat. *Theor. Appl. Genet.* 128, 453–464. doi: 10.1007/s00122-014-2444-2

Lopes, M. S., Reynolds, M. P., Jalal-Kamali, M. R., Moussa, M., Feltaous, Y., Tahir, I. S. A., et al. (2012). The yield correlations of selectable physiological traits in a population of advanced spring wheat lines grown in warm and drought environments. *Field Crops Res.* 128, 129–136. doi: 10.1016/j.fcr.2011.12.017

Lu, Z., Percy, R. G., Qualset, C. O., and Zeiger, E. (1998). Stomatal conductance predicts yields in irrigated Pima cotton and bread wheat grown at high temperatures. *J. Exp. Bot.* 49, 453–460. doi: 10.1093/jxb/49.Special_Issue.453

McDowell, N., Pockman, W. T., Allen, C. D., Breshears, D. D., Cobb, N., Kolb, T., et al. (2008). Mechanisms of plant survival and mortality during drought: why do some plants survive while others succumb to drought? *New Phytol.* 178, 719–739. doi: 10.1111/j.1469-8137.2008.02436.x

Meinzer, F. C., Woodruff, D. R., Marias, D. E., Mcculloh, K. A., and Sevanto, S. (2014). Dynamics of leaf water relations components in co-occurring iso- and anisohydric conifer species. *Plant Cell Environ.* 37, 2577–2586. doi: 10.1111/pce.12327

Mercier, H., Souza, B. M., Kraus, J. E., Hamasaki, R. M., and Sotta, B. (2003). Endogenous auxin and cytokinin contents associated with shoot formation in leaves of pineapple cultured *in vitro*. *Braz. J. Plant Physiol.* 15, 107–112. doi: 10.1590/S1677-04202003000200006

Munns, R., James, R. A., Sirault, X. R. R., Furbank, R. T., and Jones, H. G. (2010). New phenotyping methods for screening wheat and barley for beneficial responses to water deficit. *J. Exp. Bot.* 61, 3499–3507. doi: 10.1093/jxb/erq199

Neskovic, M., Petrović, J., Radojević, L., and Vujičić, R. (1977). Stimulation of growth and nucleic acid biosynthesis at low concentration of abscisic acid in tissue culture of spinacia oleracea. *Physiol. Plant.* 39, 148–154. doi: 10.1111/j.1399-3054.1977.tb04027.x

Nishizawa, T., and Suge, H. (1995a). Ethylene and carbon dioxide: regulation of oat mesocotyl growth. *Plant Cell Environ.* 18, 197–203.

Nishizawa, T., and Suge, H. (1995b). The regulation of maize mesocotyl growth by ethylene and carbon dioxide. *Jpn. J. Crop Sci.* 64, 794–800.

O'Rourke, C., Gregson, T., Murray, L., Sadler I. H., and Fry, S. C. (2015). Sugar composition of the pectic polysaccharides of charophytes, the closest algal relatives of land-plants: presence of 3-*O*-methyl-D-galactose residues. *Ann. Bot.* 116, 225–236. doi: 10.1093/aob/mcv089

Pantin, F., Monnet, F., Jannaud, D., Costa, J. M., Renaud, J., Muller, B., et al. (2012). The dual effect of abscisic acid on stomata. *New Phytol.* 197, 65–72. doi: 10.1111/nph.12013

Parent, B., Hachez, C., Redondo, E., Simonneau, T., Chaumont, F., and Tardieu, F. (2009). Drought and abscisic acid effects on aquaporin content translate into changes in hydraulic conductivity and leaf growth rate: a trans-scale approach. *Plant Physiol.* 149, 2000–2012. doi: 10.1104/pp.108.130682

Parent, B., Suard, B., Serraj, R., and Tardieu, F. (2010). Rice leaf growth and water potential are resilient to evaporative demand and soil water deficit once the effects of root system are neutralized. *Plant Cell Environ.* 33, 1256–1267. doi: 10.1111/j.1365-3040.2010.02145.x

Peleg, Z., and Blumwald, E. (2011). Hormone balance and abiotic stress tolerance in crop plants. *Curr. Opin. Plant Biol.* 14, 290–295. doi: 10.1016/j.pbi.2011.02.001

Peng, Y.-B., Zou, C., Wang, D.-H., Gong, H.-Q., Xu, Z.-H., and Bai, S.-N. (2006). Preferential localization of abscisic acid in primordial and nursing cells of reproductive organs of *Arabidopsis* and cucumber. *New Phytol.* 170, 459–466. doi: 10.1111/j.1469-8137.2006.01683.x

Pereyra-Irujo, G. A., Velázquez, L., Lechner, L., and Aguirrezábal, L. A. N. (2008). Genetic variability for leaf growth rate and duration under water deficit in sunflower: analysis of responses at cell, organ, and plant level. *J. Exp. Bot.* 59, 2221–2232. doi: 10.1093/jxb/ern087

Pierik, R., Tholen, D., Poorter, H., Visser, E. J. W., and Voesenek, L. A. C. J. (2006). The Janus face of ethylene: growth inhibition and stimulation. *Trends Plant Sci.* 11, 176–183. doi: 10.1016/j.tplants.2006.02.006

Planes, M. D., Niñoles, R., Rubio, L., Bissoli, G., Bueso, E., García-Sánchez, M. J., et al. (2015). A mechanism of growth inhibition by abscisic acid in germinating seeds of *Arabidopsis thaliana* based on inhibition of plasma membrane H^+-ATPase and decreased cytosolic pH, K^+, and anions. *J. Exp. Bot.* 66, 813–825. doi: 10.1093/jxb/eru442

Pozo, M. J., López-Ráez, J. A., Azcón-Aguilar, C., and García-Garrido, J. M. (2015). Phytohormones as integrators of environmental signals in the regulation of mycorrhizal symbioses. *New Phytol.* 205, 1431–1436. doi: 10.1111/nph.13252

Prado, K., Boursiac, Y., Tournaire-Roux, C., Monneuse, J.-M., Postaire, O., Ines, O. D., et al. (2013). Regulation of *Arabidopsis* leaf hydraulics involves light-dependent phosphorylation of aquaporins in veins. *Plant Cell Online* 25, 1029–1039. doi: 10.1105/tpc.112.108456

Pratt, H. K., and Goeschl, J. D. (1969). Physiological roles of ethylene in plants. *Annu. Rev. Plant Physiol.* 20, 541–584. doi: 10.1146/annurev.pp.20.060169.002545

Quarrie, S. A., and Lister, P. G. (1983). Characterization pf Spring wheat genotypes differing in drought-induced abscisic acid accumulation I. Drought-stressed abscisic acid production. *J. Exp. Bot.* 34, 1260–1270. doi: 10.1093/jxb/34.10.1260

R Development Core Team (2013). *R: A Language and Environment for Statistical Computing*. Vienna: R Foundation for Statistical Computing. Available online at: http://www.R-project.org/

Rogiers, S. Y., Greer, D. H., Hatfield, J. M., Hutton, R. J., Clarke, S. J., Hutchinson, P. A., et al. (2012). Stomatal response of an anisohydric grapevine cultivar to evaporative demand, available soil moisture and abscisic acid. *Tree Physiol.* 32, 249–261. doi: 10.1093/treephys/tpr131

Sade, N., Gebremedhin, A., and Moshelion, M. (2012). Risk-taking plants: anisohydric behavior as a stress-resistance trait. *Plant Signal. Behav.* 7, 767–770. doi: 10.4161/psb.20505

Sade, N., Vinocur, B. J., Diber, A., Shatil, A., Ronen, G., Nissan, H., et al. (2009). Improving plant stress tolerance and yield production: is the tonoplast aquaporin SlTIP2;2 a key to isohydric to anisohydric conversion? *New Phytol.* 181, 651–661. doi: 10.1111/j.1469-8137.2008.02689.x

Sandhu, N., Torres, R. O., Sta Cruz, M. T., Maturan, P. C., Jain, R., Kumar, A., et al. (2015). Traits and QTLs for development of dry direct-seeded rainfed rice varieties. *J. Exp. Bot.* 66, 225–244. doi: 10.1093/jxb/eru413

Sansberro, P. A., Mroginski, L. A., and Bottini, R. (2004). Foliar sprays with ABA promote growth of Ilex paraguariensis by alleviating diurnal water stress. *Plant Growth Regul.* 42, 105–111. doi: 10.1023/B:GROW.0000017476.12491.02

Seifert, G. J., Barber, C., Wells, B., Dolan, L., and Roberts, K. (2002). Galactose biosynthesis in *Arabidopsis*: genetic evidence for substrate channeling from UDP-D-Galactose into cell wall polymers. *Curr. Biol.* 12, 1840–1845. doi: 10.1016/S0960-9822(02)01260-5

Sharp, R. E., and LeNoble, M. E. (2002). ABA, ethylene and the control of shoot and root growth under water stress. *J. Exp. Bot.* 53, 33–37. doi: 10.1093/jexbot/53.366.33

Skirycz, A., Bodt, S. D., Obata, T., Clercq, I. D., Claeys, H., Rycke, R. D., et al. (2010). Developmental stage specificity and the role of mitochondrial metabolism in the response of *Arabidopsis* leaves to prolonged mild osmotic stress. *Plant Physiol.* 152, 226–244. doi: 10.1104/pp.109.148965

Skirycz, A., Vandenbroucke, K., Clauw, P., Maleux, K., De Meyer, B., Dhondt, S., et al. (2011). Survival and growth of *Arabidopsis* plants given limited water are not equal. *Nat. Biotechnol.* 29, 212–214. doi: 10.1038/nbt.1800

Skoog, F., and Miller, C. O. (1957). Chemical regulation of growth and organ formation in plant tissues cultured *in vitro*. *Symp. Soc. Exp. Biol.* 11, 118–130.

Smalle, J., Haegman, M., Kurepa, J., Montagu, M. V., and Straeten, D. V. D. (1997). Ethylene can stimulate *Arabidopsis* hypocotyl elongation in the light. *Proc. Natl. Acad. Sci. U.SA.* 94, 2756–2761. doi: 10.1073/pnas.94.6.2756

Soar, C. J., Speirs, J., Maffei, S. M., Penrose, A. B., Mccarthy, M. G., and Loveys, B. R. (2006). Grape vine varieties Shiraz and Grenache differ in their stomatal response to VPD: apparent links with ABA physiology and gene expression in leaf tissue. *Aust. J. Grape Wine Res.* 12, 2–12. doi: 10.1111/j.1755-0238.2006.tb00038.x

Sridhar, G. (2003). *Studies on Endogenous Hormonal Changes during Grain Development in Wheat Genotypes.* Available online at: https://www.researchgate.net/publication/46093009_Studies_on_Endogenous_Hormonal_Changes_during_Grain_Development_in_Wheat_Genotypes_(PhD_Thesis) (Accessed on June 10, 2014).

Sripinyowanich, S., Klomsakul, P., Boonburapong, B., Bangyeekhun, T., Asami, T., Gu, H., et al. (2013). Exogenous ABA induces salt tolerance in indica rice (*Oryza sativa* L.): the role of OsP5CS1 and OsP5CR gene expression during salt stress. *Environ. Exp. Bot.* 86, 94–105. doi: 10.1016/j.envexpbot.2010.01.009

Suge, H. (1971). Stimulation of oat and rice mesocotyl growth by ethylene. *Plant Cell Physiol.* 12, 831–837.

Sukumaran, S., Dreisigacker, S., Lopes, M., Chavez, P., and Reynolds, M. P. (2015). Genome-wide association study for grain yield and related traits in an elite spring wheat population grown in temperate irrigated environments. *Theor. Appl. Genet.* 128, 353–363. doi: 10.1007/s00122-014-2435-3

Tada, Y., Komatsubara, S., and Kurusu, T. (2014). Growth and physiological adaptation of whole plants and cultured cells from a halophyte turf grass under salt stress. *AoB Plants* doi: 10.1093/aobpla/plu041

Takahashi, K. (1972). Abscisic acid as a stimulator for rice mesocotyl growth. *Nature* 238, 92–93. doi: 10.1038/newbio238092a0

Tanaka, Y., Nose, T., Jikumaru, Y., and Kamiya, Y. (2013). ABA inhibits entry into stomatal-lineage development in *Arabidopsis* leaves. *Plant J.* 74, 448–457. doi: 10.1111/tpj.12136

Tanaka, Y., Sano, T., Tamaoki, M., Nakajima, N., Kondo, N., and Hasezawa, S. (2005). Ethylene inhibits abscisic acid-induced stomatal closure in *Arabidopsis*. *Plant Physiol.* 138, 2337–2343. doi: 10.1104/pp.105.063503

Tardieu, F., Parent, B., Caldeira, C. F., and Welcker, C. (2014). Genetic and physiological controls of growth under water deficit. *Plant Physiol.* 164, 1628–1635. doi: 10.1104/pp.113.233353

Tardieu, F., and Simonneau, T. (1998). Variability among species of stomatal control under fluctuating soil water status and evaporative demand: modelling isohydric and anisohydric behaviours. *J. Exp. Bot.* 49, 419–432. doi: 10.1093/jxb/49.Special_Issue.419

Thorpe, M. R., MacRae, E. A., Minchin, P. E. H., and Edwards, C. M. (1999). Galactose stimulation of carbon import into roots is confined to the Poaceae. *J. Exp. Bot.* 50, 1613–1618. doi: 10.1093/jxb/50.339.1613

Travaglia, C., Cohen, A. C., Reinoso, H., Castillo, C., and Bottini, R. (2007). Exogenous abscisic acid increases carbohydrate accumulation and redistribution to the grains in wheat grown under field conditions of soil water restriction. *J. Plant Growth Regul.* 26, 285–289. doi: 10.1007/s00344-007-9018-3

Travaglia, C., Reinoso, H., and Bottini, R. (2009). Application of abscisic acid promotes yield in field-cultured soybean by enhancing production of carbohydrates and their allocation in seed. *Crop Pasture Sci.* 60, 1131–1136. doi: 10.1071/CP08396

Travaglia, C., Reinoso, H., Cohen, A., Luna, C., Tommasino, E., Castillo, C., et al. (2010). Exogenous ABA increases yield in field-grown wheat with moderate water restriction. *J. Plant Growth Regul.* 29, 366–374. doi: 10.1007/s00344-010-9147-y

Trethowan, R. M., van Ginkel, M., and Rajaram, S. (2002). Progress in breeding wheat for yield and adaptation in global drought affected environments. *Crop Sci.* 42, 1441. doi: 10.2135/cropsci2002.1441

Valluru, R., Thiry, A., Wilkinson, S., Davies, W., and Reynolds, M. (2014). "Phenotypic selection for wheat spike-ethylene," in *Proceedings of the 4th International Workshop of the Wheat Yield Consortium* (Ciudad Obregon), 109–113.

Wang, H., Stier, G., Lin, J., Liu, G., Zhang, Z., Chang, Y., et al. (2013). Transcriptome changes associated with delayed flower senescence on transgenic petunia by inducing expression of etr1-1, a mutant ethylene receptor. *PLoS ONE* 8:e65800. doi: 10.1371/journal.pone.0065800

Wang, Z.-Y., Li, F.-M., Xiong, Y.-C., and Xu, B.-C. (2008). Soil-water threshold range of chemical signals and drought tolerance was mediated by ROS homeostasis in winter wheat during progressive soil drying. *J. Plant Growth Regul.* 27, 309–319. doi: 10.1007/s00344-008-9057-4

Watanabe, H., and Takahashi, K. (1997). Effects of abscisic acid, fusicoccin, and potassium on growth and morphogenesis of leaves and internodes in dark-grown rice seedlings. *Plant Growth Regul.* 21, 109–114. doi: 10.1023/A:1005783425363

Watkins, J. M., Hechler, P. J., and Muday, G. K. (2014). Ethylene-induced flavonol accumulation in guard cells suppresses reactive oxygen species and moderates stomatal aperture. *Plant Physiol.* 164, 1707–1717. doi: 10.1104/pp.113.233528

Weier, D., Thiel, J., Kohl, S., Tarkowská, D., Strnad, M., Schaarschmidt, S., et al. (2014). Gibberellin-to-abscisic acid balances govern development and differentiation of the nucellar projection of barley grains. *J. Exp. Bot.* 65, 5291–5304. doi: 10.1093/jxb/eru289

Welcker, C., Sadok, W., Dignat, G., Renault, M., Salvi, S., Charcosset, A., et al. (2011). A common genetic determinism for sensitivities to soil water deficit and evaporative demand: meta-analysis of quantitative trait loci and introgression lines of maize. *Plant Physiol.* 157, 718–729. doi: 10.1104/pp.111.176479

Wilkinson, S., and Davies, W. J. (2008). Manipulation of the apoplastic pH of intact plants mimics stomatal and growth responses to water availability and microclimatic variation. *J. Exp. Bot.* 59, 619–631. doi: 10.1093/jxb/erm338

Wilkinson, S., Kudoyarova, G. R., Veselov, D. S., Arkhipova, T. N., and Davies, W. J. (2012). Plant hormone interactions: innovative targets for crop breeding and management. *J. Exp. Bot.* 63, 3499–3509. doi: 10.1093/jxb/ers148

Wright, S. T. C. (1977). The relationship between leaf water potential ψ leaf and the levels of abscisic acid and ethylene in excised wheat leaves. *Planta* 134, 183–189. doi: 10.1007/BF00384969

Yamaguchi, S. (2008). Gibberellin metabolism and its regulation. *Annu. Rev. Plant Biol.* 59, 225–251. doi: 10.1146/annurev.arplant.59.032607.092804

Yang, D., Luo, Y., Ni, Y., Yin, Y., Yang, W., Peng, D., et al. (2014). Effects of exogenous ABA application on post-anthesis dry matter redistribution and grain starch accumulation of winter wheat with different staygreen characteristics. *Crop J.* 2, 144–153. doi: 10.1016/j.cj.2014.02.004

Yang, J., Zhang, J., Wang, Z., Liu, K., and Wang, P. (2006). Post-anthesis development of inferior and superior spikelets in rice in relation to abscisic acid and ethylene. *J. Exp. Bot.* 57, 149–160. doi: 10.1093/jxb/erj018

Zhang, G.-B., Yi, H.-Y., and Gong, J.-M. (2014). The *Arabidopsis* ethylene/jasmonic Acid-NRT signaling module coordinates nitrate reallocation and the trade-off between growth and environmental adaptation. *Plant Cell* 26, 3984–3998. doi: 10.1105/tpc.114.129296

Conflict of Interest Statement: The authors declare that the research was conducted in the absence of any commercial or financial relationships that could be construed as a potential conflict of interest.

frontiers in Plant Science

REVIEW
published: 24 January 2017
doi: 10.3389/fpls.2017.00040

The Understanding of the Plant Iron Deficiency Responses in Strategy I Plants and the Role of Ethylene in This Process by Omic Approaches

Wenfeng Li[1,2] *and Ping Lan*[2]*

[1] Collaborative Innovation Center of Sustainable Forestry in Southern China of Jiangsu Province, College of Biology and the Environment, Nanjing Forestry University, Nanjing, China, [2] State Key Laboratory of Soil and Sustainable Agriculture, Institute of Soil Science, Chinese Academy of Sciences, Nanjing, China

Iron (Fe) is an essential plant micronutrient but is toxic in excess. Fe deficiency chlorosis is a major constraint for plant growth and causes severe losses of crop yields and quality. Under Fe deficiency conditions, plants have developed sophisticated mechanisms to keep cellular Fe homeostasis via various physiological, morphological, metabolic, and gene expression changes to facilitate the availability of Fe. Ethylene has been found to be involved in the Fe deficiency responses of plants through pharmacological studies or by the use of ethylene mutants. However, how ethylene is involved in the regulations of Fe starvation responses remains not fully understood. Over the past decade, omics approaches, mainly focusing on the RNA and protein levels, have been used extensively to investigate global gene expression changes under Fe-limiting conditions, and thousands of genes have been found to be regulated by Fe status. Similarly, proteome profiles have uncovered several hallmark processes that help plants adapt to Fe shortage. To find out how ethylene participates in the Fe deficiency response and explore putatively novel regulators for further investigation, this review emphasizes the integration of those genes and proteins, derived from omics approaches, regulated both by Fe deficiency, and ethylene into a systemic network by gene co-expression analysis.

Keywords: iron deficiency, transcriptomics, proteomics, co-expression, ethylene

OPEN ACCESS

Edited by:
M. Iqbal R. Khan, International Rice Research Institute, Philippines

Reviewed by:
Shabir Hussain Wani, Michigan State University, USA
Francisco Javier Romera, University of Córdoba, Spain

***Correspondence:**
Ping Lan
plan@issas.ac.cn

Specialty section:
This article was submitted to Plant Physiology, a section of the journal Frontiers in Plant Science

Received: *29 November 2016*
Accepted: *09 January 2017*
Published: *24 January 2017*

Citation:
Li W and Lan P (2017) The Understanding of the Plant Iron Deficiency Responses in Strategy I Plants and the Role of Ethylene in This Process by Omic Approaches. Front. Plant Sci. 8:40. doi: 10.3389/fpls.2017.00040

INTRODUCTION

Iron (Fe) is an essential element for living organisms including plants. Fe-containing proteins play a variety of vital roles in cellular respiration, intermediary metabolism, oxygen transport, and DNA stability and repair, as well as photosynthesis in plants. In human beings, Fe deficiency causes severe healthy problems, including anemia, which affects billions of people worldwide (McLean et al., 2009). Although Fe is an abundant element in the earth's crust, it is one of the least available elements for plants grown on aerobic soils with neutral to basic pH. Approximately 30% of the land worldwide consists of alkaline soils, leading to a demand in bioavailable Fe for plant fitness. As a consequence, Fe deficiency is a major constraint for crop yield and quality, which eventually affects human health via food-chain, particularly to those people whose diets mainly relying on plant resources (Abadia et al., 2011). To cope with Fe deficiency, plants have developed sophisticated mechanisms to keep cellular Fe homeostasis via various physiological, morphological, metabolic,

and gene expression changes to facilitate the availability of Fe (Jeong and Guerinot, 2009; Ivanov et al., 2012; Kobayashi and Nishizawa, 2012).

Two distinct strategies of plant Fe uptake mechanisms have been proposed, i.e., Strategy I and Strategy II (Romheld and Marschner, 1986), although a combined strategy has been mentioned mainly because the Strategy II plant rice can also absorb Fe^{2+} (Ricachenevsky and Sperotto, 2014). Grasses use a chelation strategy (Strategy II) to obtain Fe from soil. This process is largely dependent on the release of PhytoSiderophores (PS) by root, which would form stable Fe-PS chelates. These chelates are taken up by a plasma membrane-localized oligopeptide transporter, YELLOW-STRIP1 (Curie et al., 2001). Dicotyledonous plants including model plant *Arabidopsis thaliana* and non-graminaceous monocots mobilize Fe via reduction strategy (Strategy I). The first step in this strategy is the acidification of the rhizosphere mediated by the H^+-translocating P-type ATPase AHA2 (Santi and Schmidt, 2009; Ivanov et al., 2012), which leads to an increase of the chelated Fe (III) concentration. Subsequently, the root surface-localized ferric chelate reductase FERRIC-REDUCTION OXIDASE2 (FRO2) (Robinson et al., 1999) reduces Fe (III) to soluble Fe (II), which is then taken up into epidermal cells by the Fe-REGULATED TRANSPORTER1 (IRT1) (Eide et al., 1996).

Expression of both FRO2 and IRT1 genes is regulated by the basic helix-loop-helix (bHLH) transcription factor FER-LIKE Fe DEFICIENCY-INDUCED TRANSCRIPTION FACTOR (FIT) (Colangelo and Guerinot, 2004; Bauer et al., 2007). FIT exerts its regulation by forming heterodimers with bHLH38 and bHLH39 (Yuan et al., 2008). Studies have shown that the Ib sub-group of bHLH proteins bHLH100 and bHLH101 are also involved in Arabidopsis Fe deficiency responses by interacting with FIT (Wang et al., 2013) or via a FIT-independent manner (Sivitz et al., 2012). Moreover, the mediator16 (MED16) is reported to regulate the expression of *FRO2* and *IRT1* by interacting with FIT (Yang et al., 2014; Zhang et al., 2014).

There is increasing evidence showing that phytohormones play vital roles in the Fe deficiency response of plants. For example, it has been reported that the expression of *FRO2* and *IRT1* is positively or negatively affected by several hormones, such as auxin, ethylene, cytokinins, jasmonic acid, and brassinosteroids, and other signaling molecules, including nitric oxide (Hindt and Guerinot, 2012; Kobayashi and Nishizawa, 2012). Among them, ethylene has been extensively explored in the involvement of Fe deficiency response by application of ethylene precursors or inhibitors or ethylene related mutants (Romera and Alcantara, 1994; Schmidt et al., 2000; Schikora and Schmidt, 2001, 2002; Schmidt and Schikora, 2001; Zaid et al., 2003; Lucena et al., 2006; Waters et al., 2007; Garcia et al., 2010, 2011; Wu et al., 2011; Kabir et al., 2012; Garcia et al., 2015; Ye et al., 2015). It has been uncovered (Lingam et al., 2011) that ethylene regulates the expression of Fe acquisition genes via modulation of FIT protein stability through the interaction between FIT and ETHYLENE INSENSITIVE3 (EIN3)/ETHYLENE INSENSITIVE3-LIKE1 (EIL1). Transcription factors EIN3 and EIL1, two major downstream players (Chao et al., 1997), once activated by EIN2 (Alonso et al., 1999), could trigger extensive ethylene responses, including the expression changes of ethylene-responsive genes (Zhang F. et al., 2016). Under Fe deficiency, however, only a small portion of differentially expressed genes is ethylene-responsive, the number being much less than that of ethylene-regulated genes (Garcia et al., 2010). Thus, it remains unclear whether EIN2, a key positive regulator mediating ethylene signaling, is required or not to fascinate the interaction between FIT and EIN3/EIL1 under Fe starvation. On the other hand, whether the interaction of FIT and EIN3/EIL1 could stabilize EIN3/EIL1 is unknown, although this interaction could modulate the FIT stability (Lingam et al., 2011). All these studies suggest that the regulatory mechanism of FIT and the interaction of Fe deficiency and ethylene are far from complete.

Over the past 10 years, omic approaches have been widely used to investigate the genome-wide gene expression changes under Fe deficiency. Hundreds of genes, some of which also being annotated as ethylene-responsive genes, are reported to be regulated by Fe status, and these studies have led to the identification of some novel regulators, such as FIT (Colangelo and Guerinot, 2004), POPEYE (Long et al., 2010), MYB72 and MYB10 (Palmer et al., 2013), and others involved in the Fe response. Although the number of detected proteins regulated by Fe deficiency is much less than that the number of transcripts, some robust biological processes have been uncovered by proteomics and some Fe-responsive proteins are not regulated at transcript level, suggesting that the integration of both proteomics and transcriptomics is better to acquire a comprehensive understanding of how plants respond to Fe stress. A comprehensive understanding of the interaction between ethylene and Fe deficiency can be referenced in a recent review (Lucena et al., 2015). To avoid redundancy, ethylene synthesis and signaling under Fe deficiency will not be repeatedly presented in this review, which are available in the recent research topics. By contrast, in this review we would mainly focus on the genes and proteins, which are regulated by both Fe and ethylene, revealed by omic approaches. Given that studies on the regulatory roles of ethylene in the Fe deficiency response in Strategy II species is less and most of the comprehensive results are based on the Arabidopsis research, in this review most results are based on this model plant.

MORPHOLOGICAL AND PHYSIOLOGICAL CHANGES UNDER FE DEFICIENCY WITH OR WITHOUT ETHYLENE

Over last three decades, scientists have already observed that plants suffered from Fe deficiency could form transfer cells and subapical root hairs from root epidermal cells and even develop cluster roots, as well as swollen apical root tips (Schmidt et al., 2000; Schikora and Schmidt, 2001, 2002). These morphological changes have been believed to increase the absorption surface area, evolutionally facilitate the growth of plants under Fe starvation. Along with these findings, ethylene has always been reported to be involved in these morphological alterations under Fe deficiency, which is revealed by the use of ethylene inhibitors

and precursors, as well as the use of ethylene mutants (Schmidt et al., 2000; Curie et al., 2001; Garcia et al., 2015). Subapical root hairs, transfer cells, and cluster roots have been found to be inhibited by the addition of ethylene inhibitors to the Fe-deficient roots, while an increase of the ethylene level will promote their formation even under Fe-sufficient conditions (Schmidt et al., 2000; Garcia et al., 2015). Similarly, the formation of subapical root hairs was blocked in the ethylene insensitive mutants *etr1* and *ein2* in *Arabidopsis*, *etr1* in the soybean and *sickle* in the *Medicago truncatula* both under Fe limiting and the addition of ethylene precursors (Garcia et al., 2015). However, the boosted ferric reductase activity and the expression of Fe acquisition genes are not affected in these mutants under Fe starvation, implying that morphological and physiological responses are carried out by different regulatory mechanism (O'rourke et al., 2007a,b, 2009). How ethylene exerts its distinct roles under Fe deficiency remains to be further explored.

TRANSCRIPTOMICS OF FE DIFICIENCY AND THE INVOVLEMENT OF ETHYLENE IN STRATEGY I PLANTS

Since 2001, toward the genome-wide understanding of plant response to Fe deficiency, transcriptome profiling studies, using custom-made or commercial-based microarrays and next-generation sequencing-based techniques (RNA-seq), have been carried out in a broad range of plant species, including model strategy I plant Arabidopsis, Medicago, soybean, as well as Strategy II plant rice and others (Thimm et al., 2001; Wang et al., 2003; Colangelo and Guerinot, 2004; Besson-Bard et al., 2009; Buckhout et al., 2009; Garcia et al., 2010; Sivitz et al., 2012; Zamboni et al., 2012; Li et al., 2013; Lan et al., 2013b; Rodriguez-Celma et al., 2013b; Bashir et al., 2014; Pan et al., 2015; Mai et al., 2016). Most of these omic studies have been carried out in the wild type plants either in Fe-deficient roots or shoots, also in the whole seedlings, while few of them are performed either in the ethylene mutants under Fe deficiency (Bauer and Blondet, 2011) or under Fe deficiency with ethylene inhibitors (Garcia et al., 2010). Nevertheless, a suit of Fe deficiency-regulated genes was revealed to be ethylene responsive by omic studies (Garcia et al., 2010; Bauer and Blondet, 2011; Lingam et al., 2011), and their expression depending on ethylene was further confirmed by reverse transcription-PCR (RT-PCR) as well as enzyme activity determination (Lucena et al., 2006; Garcia et al., 2010).

Although transcriptomic studies have identified hundreds and thousands of Fe-responsive genes, the overlapping genes among different studies are not high, probably due to the variations in growth conditions, sampling time and handling, differences in the experimental design, or combinations of these factors. Nevertheless, some novel regulators, such as FIT, MYB72, MYB10, and POPEYE, controlling plant response to Fe deficiency have been identified by omic approaches and further confirmed by genetic studies (Colangelo and Guerinot, 2004; Long et al., 2010; Palmer et al., 2013). Moreover, each of these studies has uncovered, more or less, a subset of Fe-responsive genes, which are also regulated by ethylene. To identify such group of genes that are robustly regulated by both Fe deficiency and ethylene across a wide range of conditions, publicly accessible transcriptomic data were first surveyed to define Fe-responsive core genes, followed by mining those genes that are also regulated by ethylene from these Fe-responsive core genes. Since most of extensive transcriptomic studies focused on the model plant Arabidopsis, the core Fe-responsive genes are depicted here for Arabidopsis. Three microarray studies relying on commercially available Affymetrix ATH1 GeneChips (Dinneny et al., 2008; Yang et al., 2010; Mai et al., 2016) and one RNA-seq data set (Lan et al., 2013b) have been chosen for this attempt. The reason for choosing these studies is below: (1) the plants used in all these studies were similar age; (2) all these studies provided both up- and down-regulated genes upon Fe deficiency; (3) all these studies provided differentially expressed genes in wild type plants.

Such analysis results in an overlap of 71 differentially expressed genes (fold-change $\geq$ 1.5 and $P < 0.05$) from the four data sets, herein named Fe deficiency-response core genes, with 61 being up-regulated and 10 down-regulated (**Figure 1**; **Table 1**). Although no ethylene-responsive gene is found in the down-regulated core genes, a subset of seven ethylene-responsive genes, including the transcription factor genes *bHLH39* (Yuan et al., 2008; Garcia et al., 2010) and *MYB72* (Zamioudis et al., 2014), Fe transporter gene *IRT1* (Garcia et al., 2013), and Fe homeostasis gene *NAS1* (Garcia et al., 2010), methylthioribose kinase gene *MTK* (Burstenbinder et al., 2007; Garcia et al., 2011), as well as other two genes AT3G12900 (Garcia et al., 2010) and AT5G38820 (Garcia et al., 2010) encoding proteins with unidentified functions, is identified within the up-regulated core genes (**Table 1**). Although the number of identified genes, whose expression is affected by ethylene, is small in the Fe responsive core genes, most of them have very significant roles in Fe acquisition and homeostasis. By forming heterodimers with FIT, bHLH39 controls the expression of subsets of Fe responsive genes (Yuan et al., 2008), while MYB72 directly regulates the expression of beta-Glucosidase BGLU42, a key player of rhizobacteria-induced systemic resistance (Zamioudis et al., 2014), and is required for plant growth under Fe deficiency (Palmer et al., 2013). Iron transporter IRT1 is the major transporter absorbing Fe^{2+} from soil, required for plant survival (Vert et al., 2002). It has been recognized that the nicotianamine (NA) is a key chelator of Fe^{2+}, involved in the phloem-based transport of Fe to sink organs such as young leaves and seeds, thus mediating Fe homeostasis; while NA is synthesized by NA synthase (NAS) from S-adenosylmethionine (SAM), underlying the importance of controlling the expression of NAS genes including NAS1 gene (Schuler et al., 2012). *MTK*, an enzyme of the "Yang cycle" maintaining methionine (Met) recycling for ethylene synthesis, is encoded by single gene in Arabidopsis genome, indicating the importance to tightly control its expression (Burstenbinder et al., 2007). Expression of *MTK* was induced by both ethylene and Fe deficiency, suggesting proper ethylene production might be crucial for plant fitness under Fe shortage conditions. Gene AT3G12900 encodes a protein belonging to the 2OG-Fe(II) oxygenase family; proteins in this family is generally considered to possess oxidoreductase activity catalysing the 2-oxoglutarate-

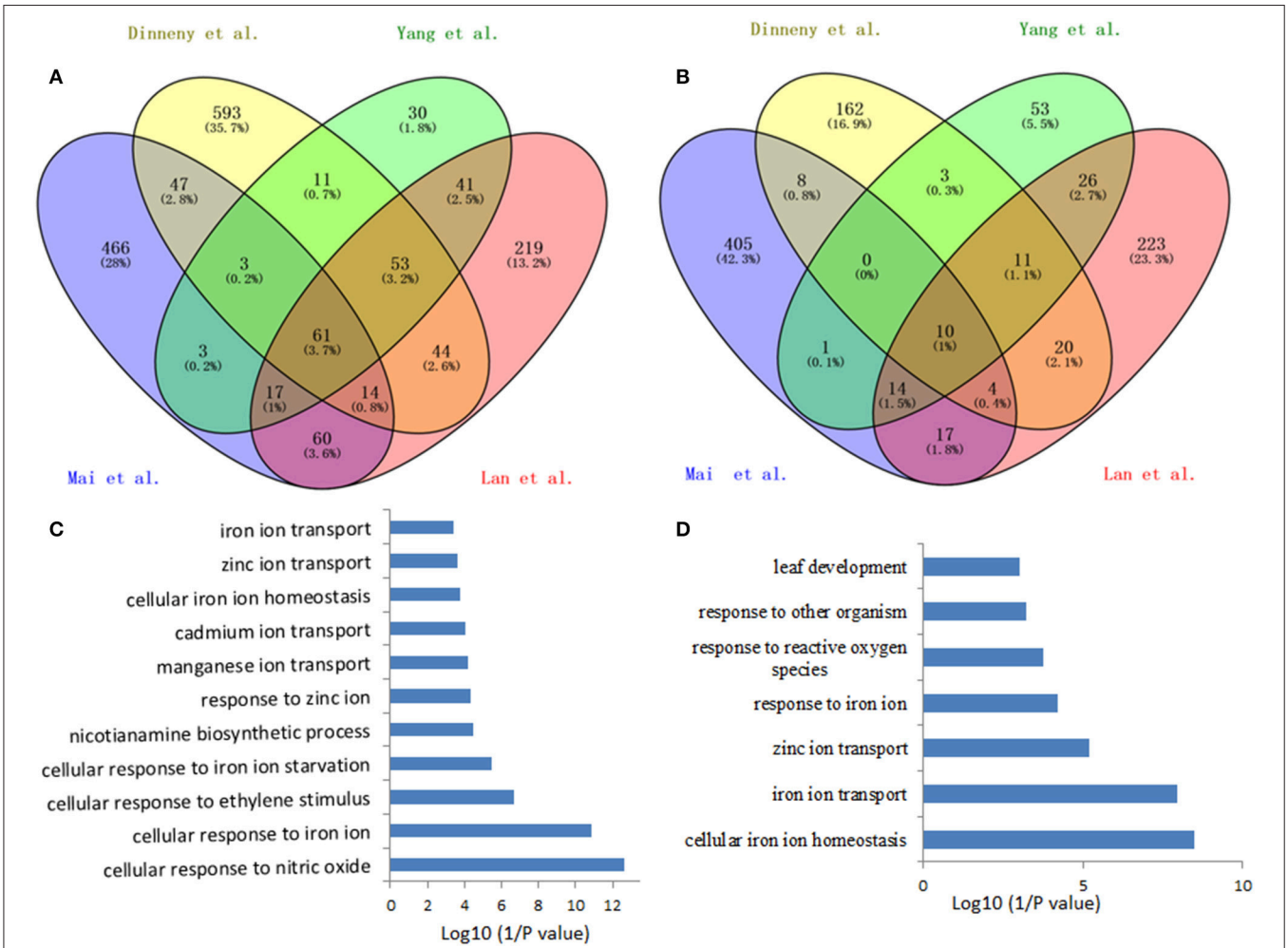

FIGURE 1 | Venn diagram of the overlap of the iron deficiency response genes among the data sets for defining the conserved iron starvation response genes. (A) upregulated genes; **(B)** downregulated genes; **(C,D)** Gene ontology enrichment analysis (biological process, $P < 0.001$) of the overlap genes, 61 and 10, from the up- and down-regulated genes under iron starvation among the four data sets, respectively.

and Fe(II)-dependent oxidation of an organic substrate using a dioxygen molecule. Previous study showed that the ethylene synthesis protein ACC oxidase also belongs to 2OG-Fe(II) oxygenase superfamily (Aravind and Koonin, 2001). Therefore, it is reasonable to assume that this gene might be involved in the ethylene production under Fe deficiency, although its exact biological functions remain to be verified. Omic studies thus revealed the involvement of ethylene in the Fe deficiency response.

Among the up-regulated core genes, those genes encoding proteins with unknown functions represent the largest group, indicating that molecular mechanisms of Fe deficiency responses remain incomplete and potentially novel players could be discovered in the future study. In this group, none of them is ethylene responsive. Of particular interest are three highly induced genes AT1G12030, AT1G47400, and AT5G05250, which are tightly co-expressed with several well-studied Fe-related genes such as POPEYE (Long et al., 2010), NAS4 (Koen et al., 2013), OPT3 (Zhai et al., 2014), bHLH101 (Sivitz et al., 2012), etc. POPEYE has been reported to be required for plant growth and development under Fe-deficient conditions, probably through affecting cellular Fe homeostasis by directly regulating the expression of known Fe homeostasis genes such as *NSA4* and *FRO3* (Long et al., 2010), while OPT3 has been verified to be a phloem-specific Fe transporter, essential for systemic Fe signaling and redistribution of Fe in Arabidopsis (Mendoza-Cozatl et al., 2014; Zhai et al., 2014). Thus, it is reasonable to assume that these co-expressed presently functional unknown genes could play important roles in Fe homeostasis or in Fe distribution intracellularly and/or intercellularly. Other three genes AT3G07720, AT3G61930, and AT5G67370 are also highly induced by Fe deficiency and this induction occurs in the early treatment and lasts for 3 days, suggesting that these genes might be involved in the early Fe deficiency response and their biological functions are worthy of further study. To meet the cellular demand of Fe under Fe deficiency, plants have

TABLE 1 | Iron deficiency regulated conserved genes in *Arabidopsis.*

AGI[a]	Name and annotation	Dinneny et al., 2008 −Fe				Yang et al., 2010 −Fe 3d	Lan et al., 2013b −Fe 3d	Mai et al., 2016 −Fe 6 d
		12h	24 h	48 h	72 h			
		Roots				Roots	Roots	Seedlings
Fold-changes (−Fe/+Fe)								
UP-REGULATED CORE GENES UNDER Fe DEFICIENCY								
Glycolysis								
AT1G53310	PPC1, phosphoenolpyruvate carboxylase	1.0	2.2	2.6	2.1	2.2	2.4	1.6
Cell wall								
AT1G09790	Phytochelatin synthetase-related	1.2	3.3	5.9	5.3	8.4	53.4	1.9
AT4G02330	Pectinesterase family protein	1.9	11.0	21.3	21.3	10.3	4.8	1.9
Amino acid metabolism								
AT1G49820	MTK, 5-methylthioribose kinase, involved in methionine cycle	1.1	2.8	3.6	3.3	2.5	2.7	1.7
Metal handling								
AT1G23020	FRO3, ferric chelate reductase 3	1.5	5.6	6.4	5.1	8.4	8.0	3.9
AT1G56430	NAS4, nicotianamine synthase 4	1.8	6.8	14.6	16.3	5.0	5.0	2.9
AT5G04950	NAS1, nicotianamine synthase 1	1.2	3.7	4.9	5.0	3.1	4.4	2.0
Secondary metabolism								
AT3G21240	4CL2, 4-coumarate:CoA ligase 2	1.2	3.5	5.6	5.7	3.9	3.6	1.6
AT3G50740	UGT72E1, UDPG:coniferyl alcohol glucosyltransferase	1.1	3.8	6.0	5.9	4.2	8.5	2.2
Hormone metabolism								
AT3G12900	Oxidoreductase, 2OG-Fe(II) oxygenase family protein	1.7	11.4	33.0	36.6	97.2	546.9	14.7
Stress								
AT1G09560	GLP5, GERMIN-LIKE PROTEIN 5	1.1	2.4	2.3	2.1	3.0	7.7	3.7
AT2G42750	DNAJ heat shock N-terminal domain-containing protein	1.3	3.0	4.8	4.1	2.0	1.9	2.2
AT3G48450	Nitrate-responsive NOI protein, putative	1.4	3.9	9.5	8.6	8.1	5.1	2.0
AT5G45070	PP2-A8, PHLOEM PROTEIN 2-A8	0.8	2.6	6.3	5.8	6.0	8.4	3.7
Misc								
AT4G31940	CYP82C4, cytochrome P450 enzyme	2.1	6.6	9.3	10.8	71.8	188.0	48.6
AT5G02780	In2-1 protein, the lambda family of glutathione transferases	2.6	9.7	12.9	11.4	30.7	54.7	19.6
RNA								
AT1G56160	MYB72, R2R3 transcription factor	1.3	4.2	6.5	6.8	86.1	∞	7.5
AT3G12820	MYB10, R2R3 transcription factor	1.3	3.5	6.2	6.6	24.3	24.6	4.1
AT3G18290	EMB2454, BRUTUS (BTS), a putative E3 ligase protein	1.5	4.8	7.7	8.4	2.7	2.5	2.5
AT3G47640	POPEYE (PYE), a bHLH transcription factor	1.2	2.5	3.6	3.7	2.6	2.2	3.2
AT3G56980	ORG3, bHLH39	1.6	4.6	6.0	5.6	26.4	31.8	10.6
AT5G04150	BHLH101	1.6	5.8	7.0	6.7	13.9	18.0	9.0
DNA								
AT3G13610	F6′H1, Fe(II)-, and 2-oxoglutarate-dependent dioxygenase	1.5	4.6	6.4	6.2	5.4	10.3	2.8
Protein								
AT1G18910	Zinc finger (C3HC4-type RING finger) family protein	1.1	3.0	5.2	5.0	3.3	3.3	1.6
AT1G60610	Protein binding / zinc ion binding	1.3	2.2	3.4	2.8	2.3	2.0	1.8
AT1G77280	Protein kinase family protein	1.1	2.6	4.2	4.1	3.8	4.1	1.6
AT4G09110	Zinc finger (C3HC4-type RING finger) family protein	1.0	1.5	2.5	2.3	3.6	19.6	6.0
AT4G10510	Subtilase family protein	1.1	1.5	4.3	3.7	5.8	7.1	3.6

(Continued)

TABLE 1 | Continued

AGI[a]	Name and annotation	Dinneny et al., 2008 −Fe				Yang et al., 2010 −Fe 3d	Lan et al., 2013b −Fe 3d	Mai et al., 2016 −Fe 6 d
		12h	24 h	48 h	72 h			
		Roots				Roots	Roots	Seedlings
AT4G26470	Calcium ion binding	1.1	2.0	3.3	2.8	1.8	1.6	2.1
AT5G53450	ORG1, OBP3-RESPONSIVE GENE 1	1.4	5.8	7.4	6.8	5.4	5.2	5.9
Signaling								
AT1G16150	WAKL4, WAK-like receptor-like kinase	1.2	2.1	3.6	3.0	2.4	2.7	1.6
AT1G34760	GRF11, GENERAL REGULATORY FACTOR 11	1.2	3.7	5.1	4.1	9.4	14.7	2.7
AT4G29900	ACA10, AUTOINHIBITED CA(2+)-ATPASE 10	1.5	3.2	4.4	3.8	2.3	1.9	1.6
Transport								
AT3G46900	COPT2, COPPER TRANSPORTER 2	1.6	5.5	6.5	6.8	15.7	42.9	8.7
AT3G53480	ABCG37/PDR9, ATP-BINDING CASSETTE G37/ PLEIOTROPIC DRUG RESISTANCE 9	0.9	2.5	3.2	2.8	3.5	5.3	2.1
AT3G58060	MTP8, Mn transporter	1.2	3.3	6.5	6.2	22.4	54.9	1.7
AT3G58810	MTPA2, METAL TOLERANCE PROTEIN 3	1.3	3.8	4.8	4.3	9.7	17.1	3.4
AT4G16370	OPT3, OLIGOPEPTIDE TRANSPORTER	1.9	6.5	9.4	10.3	7.6	7.0	2.6
AT4G19690	IRT1, IRON-REGULATED TRANSPORTER 1	1.4	2.4	2.3	2.3	21.8	57.1	38.6
AT5G01490	CAX4, CATION EXCHANGER 4	1.1	2.2	3.6	3.4	2.0	2.6	1.7
AT5G03570	IREG2, IRON REGULATED 2	1.2	4.5	7.4	6.8	6.7	7.7	3.5
AT5G13740	ZIF1, ZINC INDUCED FACILITATOR 1	1.5	5.6	8.7	8.2	2.6	2.8	2.8
AT5G38820	Amino acid transporter family protein	1.4	3.8	5.6	6.0	17.0	49.6	3.5
AT5G67330	NRAMP4, ARABIDOPSIS THALIANA NATURAL RESISTANCE ASSOCIATED MACROPHAGE PROTEIN 4	1.5	4.3	6.3	6.6	2.2	2.4	1.7
Not assigned								
AT1G12030	Unknown protein	1.0	1.4	5.3	6.4	2.4	21.5	8.9
AT1G22930	T-complex protein 11	1.0	2.6	3.6	3.3	1.9	2.2	1.6
AT1G47400	Unknown protein	1.8	5.8	11.6	11.5	15.7	18.5	16.3
AT1G49000	Unknown protein	1.2	2.7	5.4	4.8	6.1	6.7	2.1
AT1G73120	Unknown protein	1.4	3.3	3.1	2.4	8.4	7.3	8.8
AT1G74770	Unknown protein	1.1	2.8	4.7	3.9	5.3	6.3	3.6
AT2G46750	FAD-binding domain-containing protein	1.6	3.4	4.6	3.4	2.8	2.7	3.4
AT3G06890	Unknown protein	1.3	2.8	4.2	3.8	3.6	3.3	2.0
AT3G07720	Kelch repeat-containing protein	1.9	5.5	6.2	5.2	11.9	23.0	7.9
AT3G18560	Unknown protein	1.0	2.7	3.9	4.4	4.0	3.6	1.9
AT3G56360	Unknown protein	1.2	2.4	2.6	2.7	2.3	2.3	2.7
AT3G61410	Unknown protein	1.1	2.2	3.0	2.6	4.3	6.0	2.4
AT3G61930	Unknown protein	2.4	7.3	14.0	13.2	24.7	24.3	4.9
AT5G02580	Unknown protein	1.1	3.1	5.2	5.8	2.6	1.8	2.1
AT5G05250	Unknown protein	1.4	3.2	4.5	4.7	6.1	6.5	4.7
AT5G61250	Glycosyl hydrolase family 79 N-terminal domain-containing protein	1.5	3.3	4.0	3.3	2.6	2.6	1.7
AT5G67370	Unknown protein	1.5	5.7	11.2	12.1	7.4	9.8	2.8
DOWN-REGULATED CORE GENES UNDER Fe DEFICIENCY								
Metal handling								
AT3G56090	FER3, FERRITIN 3	1.0	0.9	0.6	0.5	0.5	0.5	0.5
AT5G01600	FER1, FERRITIN 1	0.7	0.5	0.4	0.4	0.2	0.2	0.4
Secondary metabolism								
AT2G37130	Peroxidase 21	1.1	0.9	0.2	0.1	0.4	0.5	0.6

(Continued)

TABLE 1 | Continued

AGI[a]	Name and annotation	Dinneny et al., 2008 −Fe				Yang et al., 2010 −Fe 3d	Lan et al., 2013b −Fe 3d	Mai et al., 2016 −Fe 6 d
		12h	24 h	48 h	72 h			
		Roots				Roots	Roots	Seedlings
Redox								
AT4G08390	SAPX, STROMAL ASCORBATE PEROXIDASE	0.9	0.7	0.4	0.3	0.5	0.5	0.6
Misc								
AT3G09220	LAC7, LACCASE 7	1.2	1.3	0.3	0.2	0.3	0.3	0.3
Protein								
AT4G04770	ABC1, ARABIDOPSIS THALIANA NUCLEOSOME ASSEMBLY PROTEIN 1	0.9	0.7	0.4	0.4	0.4	0.4	0.6
Transport								
AT1G60960	IRT3, IRON REGULATED TRANSPORTER 3	0.8	0.6	0.3	0.3	0.4	0.5	0.3
AT2G32270	ZIP3, ZINC TRANSPORTER 3 PRECURSOR	0.5	0.4	0.2	0.2	0.4	0.5	0.3
Not assigned								
AT1G68650	Unknown protein	0.9	0.7	0.5	0.5	0.4	0.4	0.4
AT2G36885	Unknown protein	0.9	0.6	0.4	0.4	0.4	0.3	0.4

[a] *Underlined genes were also regulated by ethylene.*

evolutionally developed a complex mechanism to cope with Fe starvation, including the release of vacuolar Fe via transporter (Lanquar et al., 2005), increasing the rhizosphere available Fe via ABCG37/PDR9 (Rodriguez-Celma et al., 2013b; Fourcroy et al., 2014), as well as an enhanced uptake of Fe into the cell through the induction of IRT1 (Vert et al., 2002). Genes encode these transporters were observed to be induced by Fe deficiency in all studies, with IRT1 being ethylene responsive (Garcia et al., 2013). However, the non-specific transport character of IRT1 allows the transport of other essential and non-essential metals besides Fe, which results in an enhanced concentration of these metals. To avoid toxicity of these byproducts, an array of genes encoding transporters were observed to be induced under Fe deficiency, including copper transporter (Perea-Garcia et al., 2013), Zinc transporter (Haydon et al., 2012), manganese transporter (Arrivault et al., 2006), and other cation transporters, which could sequester these ions into vacuoles. These results indicate that plants have evolved an excellent system to monitor the cellular ions, maintaining the homeostasis of required ions, and avoiding the toxicity of "unwanted" ions, under Fe deficiency and maybe upon other nutritional disorder. In addition, genes encode transporters OPT3 (Zhai et al., 2014) and AtIREG2 (Schaaf et al., 2006), which are involved in the intercellular Fe distribution, are robustly induced by Fe shortage, underlying the importance of Fe distribution upon Fe deficiency. High induction was also observed for the gene AT5G38820 whose expression is also controlled by ethylene, which encodes putatively an amino acid transporter. By now, it remains unclear what is the biological function of this transporter. Is it possible to transport Met under Fe deficiency? Indeed, as mentioned above, the gene encoding MTK was robustly up-regulated by Fe deficiency (Dinneny et al., 2008; Garcia et al., 2010; Yang et al., 2010; Lan et al., 2013b; Mai et al., 2016). MTK is a key kinase of Yang-cycle involved in the Met salvage by phosphorylating methylthioribose (MTR). Phosphorylated MTR will finally be converted to Met by serials of biochemical reactions. Met is then converted to SAM which is used to synthesize ethylene, polyamines, NA, as well as phytosiderophores in Strategy II species. Although neither ACC synthase (ACS) gene nor ACC oxidase (ACO) gene was found within the Fe deficiency response core genes by transcriptomics, transcriptional expression changes of these genes do have been monitored by RT-PCR and their encoded proteins were differentially accumulated upon Fe deficiency (Garcia et al., 2010; Ye et al., 2015), which is consistent with the increase of ethylene production under Fe deficiency (Lucena et al., 2015). By contrast, two of three genes associated with metal handling encode NAS were up-regulated by Fe deficiency with *NAS1* and *NAS2* being ethylene responsive (Garcia et al., 2010); while NA, which is synthesized by NAS, is a key chelator of Fe^{2+}, involved in the phloem-based transport of Fe to sink organs (Schuler et al., 2012). These results suggest that ethylene and NA are both important for the regulation of Fe deficiency responses. A group of genes encode transcription factors were strongly induced among the core genes, with MYB72 and MYB10 being shown to be functional redundancy but crucial for plant growth under iron-limiting conditions (Palmer et al., 2013). In addition, several genes encoding regulatory proteins, such as protein kinases, involved in posttranslational protein modification, RING domain-containing Zinc finger family proteins, associated with protein degradation and other zinc/calcium binding proteins, have been shown upregulated among the core genes, although most of them remain functionally unclear. Besides, three genes encoding proteins involved in the signaling were identified in the core, with the general regulatory factor 11 (GRF11) being confirmed to be a key downstream player of nitric oxide to regulate Fe acquisition (Yang et al., 2013). Surprisingly,

only two genes encoding proteins involved in cell wall process are presented in the core, despite the pronounced alternations in the root morphology. Similarly, one gene encoding an isoform of 4-coumarate: CoA ligase (4CL2) involved in the last step of the general phenylpropanoid pathway was significantly induced by Fe starvation. In addition, several stress-response genes are also represented in the upregulated core genes.

In total, 10 genes were observed down-regulated in the core genes, but none of them is ethylene responsive. In Arabidopsis genome, four genes encoding FERRITINs (FER), functioning as ferric iron binding and participating in the cellular iron ion homeostasis, are essential to protect cells against oxidative damage and flowering (Sudre et al., 2013). Two genes encoding FER3 and FER1 were identified to be robustly down-regulated in the core genes. In addition, two genes encoding a plasma membrane localized zinc/iron transporter IRT3 (Lin et al., 2009) and a Zn^{2+} transporter ZIP3 (Yang et al., 2010) were down-regulated under Fe deficiency in order to decrease the uptake of zinc ion under Fe starvation, avoiding toxicity of excess zinc. Gene AT2G37130, which encodes a peroxidase and is associated with defense response to fungus, hydrogen peroxide catabolic process, oxidation-reduction process, and oxidative stress response, was identified in the core with less-explored. Similarly, three genes encoding a chloroplastic stromal ascorbate peroxidase SAPX (Maruta et al., 2010), a laccase LAC7 (Turlapati et al., 2011), and an iron-stimulated ATPase ABC1 (Moller et al., 2001), respectively, have been identified in the down-regulated core genes. Ascorbate peroxidases are enzymes possessing hydroquinone:oxygen oxidoreductase activity that can scavenge hydrogen peroxide in plant cells, and laccase has oxidoreductase activity capable of oxidizing metal ions, involving lignin catabolic process and oxidation-reduction process, while ABC1 belongs to the member of the NAP subfamily of ABC transporters involved in Fe-S cluster assembly (Xu and Moller, 2004; Xu et al., 2005). Thus, similar to SufB, AtABC1 is associated with the regulation of iron homeostasis (Xu and Moller, 2004; Xu et al., 2005). Notably, two genes AT1G68650 and AT2G36885 encoding proteins with unknown functions were observed to be down-regulated more than two-fold and await further study.

CO-EXPRESSION NETWORK OF FE/ETHYLEN RESPONSE CORE GENES

It is assumed that genes showing similar expression patterns under various conditions have a high possibility to exert similar functions. Co-expression network can help to predicate the functions of those genes, which remain unclear, from those well-studied genes in the network via the "guilt-by-association" paradigm. In addition, co-expression network might also work in identifying novel functions of the well-known "old" genes under certain conditions. Co-expression network of the 71 Fe deficiency response core genes was generated using MACCU program from 300 public microarrays restricted to roots with a Pearson correlation coefficient greater or equal to 0.7, a threshold frequently used to create compression networks of relatively high stringency (Lin et al., 2011). This procedure yielded a co-expression network containing 20 core genes, subdivided into four subclusters (**Figure 2A**). Unexpectedly, none of the down-regulated core genes was co-expressed in the network, suggesting that these down-regulated core genes might be associated with diverse biological processes. Four out of 20 genes (nodes) in the co-expression network were also ethylene responsive (nodes in diamond shape) and were distributed in the three subclusters (**Figure 2B**). In the largest subcluster, several genes encoding transporters, such as IRT1(Vert et al., 2002), ABCG37/PDR9(Rodriguez-Celma et al., 2013b), IREG2 (Schaaf et al., 2006), and MTPA2 (Arrivault et al., 2006) associated with Fe acquisition and distribution, as well as the sequestration of Zn^{2+} into vacuoles, have been identified as strongly co-expressed, particularly the direct connectivity of IRT1 and MTPA2, indicating that avoiding toxicity of excess Zn might be equally important to Fe absorption and distribution under Fe deficiency. Among the genes with the highest connectivity (largest amount of edges) was the gene AT3G13610 encoding a Fe (II)- and 2-oxoglutarate-dependent dioxygenase family gene F6'H1 (Rodriguez-Celma et al., 2013b). Mutations in this gene compromise iron uptake and the production of fluorescent phenolics involved in Fe uptake. The second largest subcluster comprises three genes. AT3G58060 encodes a tonoplast localized member of CDF family of cation transporters MTP8 (Eroglu et al., 2016), which functions as a manganese (Mn) transporter. MTP8 transports Mn ion into root vacuoles of iron-deficient plants and thereby avoids toxicity of excess Mn ion in Fe deficiency-roots. AT3G12900, an ethylene response gene (Garcia et al., 2010), directly connected with *MTP8*, is strongly induced by Fe deficiency, which encodes a 2-oxoglutarate (2OG) and Fe (II)-dependent oxygenase superfamily protein putatively assumed to be involved in hormone metabolism by MapMan analysis. The gene co-expressed with AT3G12900 is AT5G38820, whose expression is also regulated by ethylene (Garcia et al., 2010), encoding a putative amino acid transporter with no known function yet. Each of the other two subclusters contains only two genes, with one cluster comprising MYB72 and MYB10 (Palmer et al., 2013), and the other one being composed of two functional unknown genes. *MYB72*, an ethylene responsive gene (Garcia et al., 2010), and *MYB10* have been confirmed to be crucial for plant growth under Fe shortages (Palmer et al., 2013; Zamioudis et al., 2014). AT5G67370 and AT2G42750 were directly connected, comprising a small network. AT5G67370 encodes a protein of unknown function, while mutations in this gene shows a stronger growth defect compared to wild type in low Fe (1 μM Fe) conditions (Urzica et al., 2012). AT2G42750 encodes a DNAJ heat shock N-terminal domain-containing protein; gene ontology (GO) analysis shows the protein encoded by this gene can function in unfolded protein and heat shock protein binding, involving electron carrier activity and iron ion binding. In summary, several genes encoding proteins with unknown functions were observed to be directly connected to these well-studied genes, indicating that these functional unknown genes might be crucial for Fe homeostasis under Fe deficiency. Co-expression network thus filter out prioritized genes for follow-up research from large data sets derived from high-throughput omic approaches.

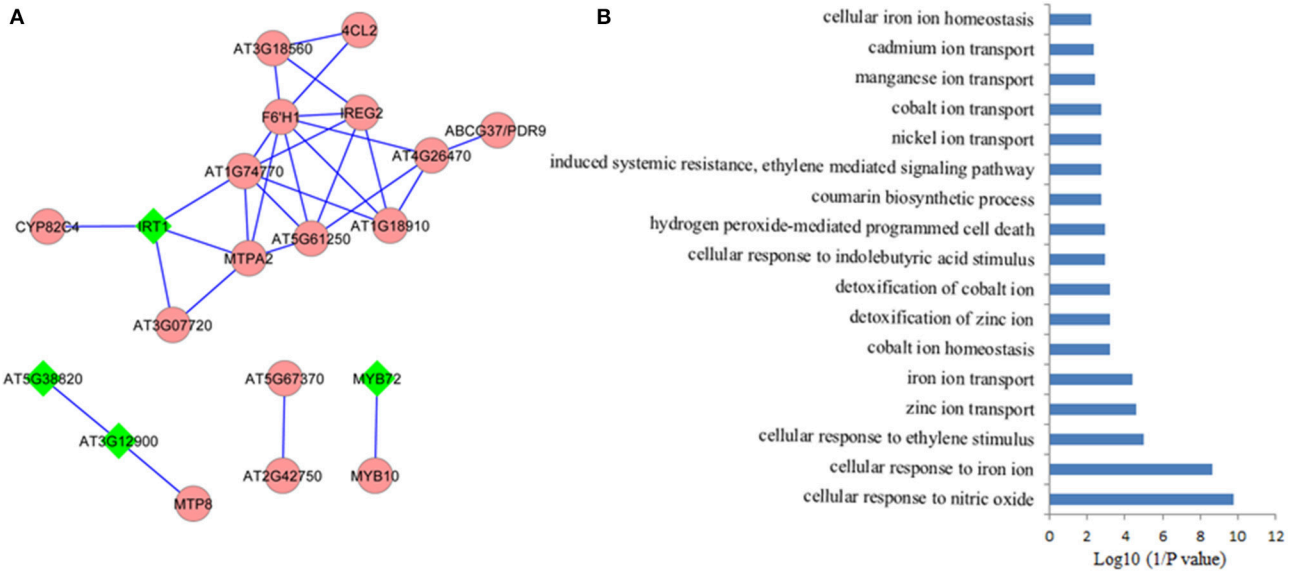

FIGURE 2 | Coexpression network of the conserved iron deficiency induced genes. (A) Pair-wise coexpression relationships were calculated with the MACCU toolbox as described by Lin et al. (2011) using a Pearson coefficient cut-off of $P \geqq 0.7$. Nodes in diamond filled in green color indicate ethylene regulated genes; **(B)** Gene ontology (GO) enrichment analysis (biological process, $P < 0.01$) of the genes from the network in **(A)**.

PROTEOMES OF FE DEFICIECNY IN PLANTS

Although high-throughput transcriptomic studies have provided a global view of gene expression changes, surveys at the transcript level often could not directly estimate the abundance and functions of the encoded proteins, the ultimate players of biological function, due to alternative RNA splicing and complex posttranslational modifications such as phosphorylation, glycosylation, methylation, ubiquitination, and so on (Lan et al., 2012a, 2013a; Marmiroli et al., 2015; Dong et al., 2016). These various modifications thus change protein localization, stability, interactions, and functions, leading to much more complex of proteomics than that of transcriptomics. Therefore, a global view of protein changes both in abundance and isoforms can only be relatively precisely estimated and identified by proteomics methods.

With the advances in Mass spectrometry techniques coupled with powerful computational algorithms, a wealth of knowledge has arisen on the protein changes upon various stresses including Fe deficiency (Lopez-Millan et al., 2013). Overall, compared to the extensive transcriptomic investigation upon Fe deficiency, knowledge on the changes in the proteome in response to Fe deficiency has been still largely limited, particularly in Strategy II species (Lopez-Millan et al., 2013). So far, only one study on proteome profiling in Fe-deficient rice roots and shoots (Chen et al., 2015) and two in maize, with one in Fe-deficient root hairs (Li et al., 2015) and the other in roots (Hopff et al., 2013), have been carried out to investigate the global protein changes or the alterations in the plasma membrane proteome, by means of two-dimensional electrophoresis (2-DE), or 1-DE coupled with matrix-assisted laser desorption/ionization time of flight mass spectrometry (MALDI-TOF/MS) or LC-MS/MS. By contrast, most of the proteomic studies upon Fe deficiency have been performed in Strategy I species, including *Beta vulgaris* (Andaluz et al., 2006; Rellan-Alvarez et al., 2010; Gutierrez-Carbonell et al., 2016), Tomato (*Solanum lycopersicum* L.) (Brumbarova et al., 2008; Genannt Bonsmann et al., 2008; Muneer and Jeong, 2015), cucumber (*Cucumis sativus*) (Donnini et al., 2010; Li and Schmidt, 2010; Vigani et al., 2017), pea (*Pisum sativum* L.) (Meisrimler et al., 2011, 2016), Prunus hybrid GF 677 rootstock (*P. dulcis* × *P. persica*) (Rodriguez-Celma et al., 2013a), *Lupinus texensis* (Lattanzio et al., 2013), *Hyoscyamus albus* (Khandakar et al., 2013), *Medicago truncatula* (Rodriguez-Celma et al., 2011, 2016), citrus rootstocks (Muccilli et al., 2013), *Brassica napu* (Gutierrez-Carbonell et al., 2015), *Populus cathayana* (Zhang S. et al., 2016), and Arabidopsis (Laganowsky et al., 2009; Lan et al., 2011, 2012b; Mai et al., 2015; Pan et al., 2015; Zargar et al., 2015a,b). Most of the protein profiling studies were focused on the global protein changes in the whole roots/shoots, and few of them investigated proteome of the specific plant parts such as root hairs (Li et al., 2015), cellular compartments including root plasma membrane (Hopff et al., 2013), thylakoid membranes (Andaluz et al., 2006), and shoot microsomal fragments (Zargar et al., 2015b), as well as phloem saps (Lattanzio et al., 2013; Gutierrez-Carbonell et al., 2015).

Several features of Fe-related proteomics should be noticed. First, the focuses of the proteomic studies under Fe limiting conditions by now are still the determination and quantification of changed proteins. So far, only one proteomic study has explored the alterations of protein posttranslational modification (PTM), and this study does have uncovered new layer of

regulation in gene activity in response to Fe deficiency (Lan et al., 2012b), suggesting that PTM proteomic studies should be emphasized in the future. Second, until 2011, a gel-based approach (particularly 2DE) is the most commonly employed approach to explore the changes in protein abundance upon Fe deficiency. Overall, the number of proteins that are identified to be changed in abundance by 2DE-based proteomics is generally not high, often ~50 by mean, which is irrelevant to the gel size (Lopez-Millan et al., 2013). Moreover, most of the identified proteins are highly abundant soluble proteins which associated with various metabolisms, with few proteins involved in transporting, signaling and regulation being uncovered. Furthermore, exact quantification of differentially expressed proteins has proven difficult with this approach. Since 2011, high-throughput proteomic analyses have been carried out by means of iTRAQ (Isobaric Tag for Relative and Absolute Quantification) based LC-MS (Lan et al., 2011; Zargar et al., 2013, 2015a,b; Pan et al., 2015; Zhang S. et al., 2016) and label-free LC-MS (Li et al., 2015; Meisrimler et al., 2016), although 2DE is still in use. These approaches have proven powerful to increase not only the numbers of differentially accumulated proteins but also the types of proteins, which provide much more knowledge of plant response to Fe deficiency. Third, although each of the proteomic studies can yield more or less differentially accumulated proteins, and those proteins, with the help of bioinformatics, can be further assigned to one or more metabolic pathways to a certain extent, the direct comparison of proteomes both among plant species, and within the same species has proven not straightforward, due to various differences in each proteomics study, from growth conditions, sampling time and handling, experimental design, types of spectrometry and computational software, stringency of searching parameters, to richness of genomic information.

PROTEOMICS REVEAL THAT S-ADENOSYL-METHIONINE SYNTHESIS IS ONE OF THE CENTRAL METABOLIC PROCESSES UPON FE DEFICIENCY

Although nearly no protein with changes in abundance upon Fe deficiency has been uncovered across a wide range of plant species, a comprehensive comparison of these studies indeed has revealed some common elements in proteome under Fe limitation. In brief, proteins associated with "oxidative stress and defense," "C metabolism," "N metabolism," "cell wall," "secondary metabolism, particularly the phenylpropanoid metabolism," "energy and ATP-coupled transport processes," and "protein metabolism" have been identified as differentially accumulated proteins among plant species, which is well-summarized in an excellent review published in 2013 (Lopez-Millan et al., 2013). Update of that review is out of the scope of present one. By contrast, this review will focus on the changed proteins associated with methionine (Met) salvage cycle and ethylene synthesis under Fe shortage (**Figure 3**). Indeed, as shown in Table S1, many of the proteomic studies have uncovered that S-adenosyl-methionine (SAM), a precursor for ethylene production, is a central metabolite under Fe deficiency in multiple plant species

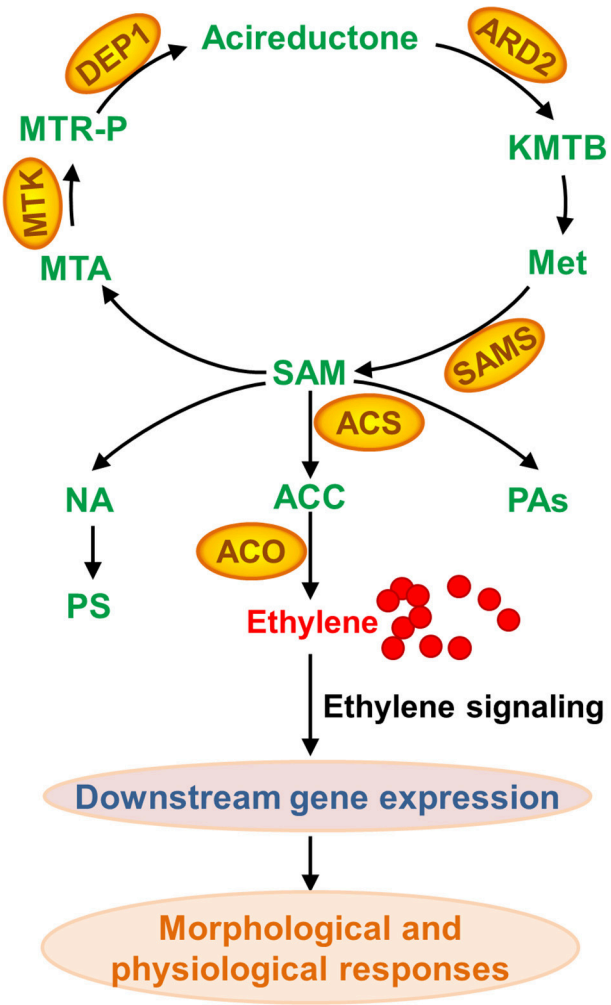

FIGURE 3 | Methionine (Met) salvage cycle and ethylene, nicotianamine (NA), phtosiderophore (PS), and polyamine (PA) synthesis associated with proteins that are differentially accumulated upon Fe deficiency. As a central metabolite, SAM (S-adenosyl-methionine) is synthesized by SAMS (S-adenosylmethionine synthetase) from Met. Followed, SAM can be converted to MTA (methylthioadenosine) and ACC (aminocyclopropane-1-carboxylate) that is further converted to ethylene. SAM is also a precursor of PA and NA, which is converted to PS in Strategy II plant species. KMTB, 2-keto-4-methylthiobutyrate; MTR-P, methylthioribose phosphate; ARD, acireductone dioxygenase; ACS, ACC synthase; MTK, 5-methylthioribose kinase; DEP1, EHYDRATASE-ENOLASE-PHOSPHATASE-COMPLEX 1; ACO, ACC oxidase.

(Li et al., 2008; Donnini et al., 2010; Li and Schmidt, 2010; Lan et al., 2011; Rodriguez-Celma et al., 2011; Gutierrez-Carbonell et al., 2015; Pan et al., 2015). SAM is synthesized by S-adenosylmethionine synthetase (SAMS) from Met. Under Fe deficiency, proteomic studies have shown that SAMSs are remarkably increased in abundance at the protein level among plant species. By 2DE-based proteomic study, Li et al., for the first time, reported the increase of a SAMS in abundance in tomato roots upon Fe deficiency (Li et al., 2008). Meanwhile, they found three Met synthases, which are associated with Met metabolism, were induced upon Fe starvation (Li et al., 2008).

Subsequently, the abundance of SAMS was shown to increase in cucumber roots upon Fe starvation by means of 2DE approach (Li and Schmidt, 2010). Similarly, another proteomic study in cucumber roots showed two SAMSs, the *Populus trichocarpa* ortholog MAT1-a and the *Medicago sativa* ortholog, are up-regulated under Fe shortage (Donnini et al., 2010). While this study also reported another SAMS, the *Populus trichocarpa* ortholog MAT1-b, which was deceased in protein abundance upon Fe deficiency, and it could be the first case that SAMS was down-regulated upon Fe deficiency (Donnini et al., 2010). The down-regulation of SAMS might be due to the treatment and sampling time since Fe deficiency responses are rhythmic (Chen et al., 2013; Hong et al., 2013; Salome et al., 2013). Recently, for the second time, an ortholog of Arabidopsis SAMS2 was identified to be down-regulated from *Brassica napus* phloem sap upon Fe deficiency by using of 2DE technique; by means of Fe-affinity chromatography coupled with 1DE, the authors revealed two ACC oxidases (ACOs) that were induced in *Brassica napus* phloem sap upon Fe deficiency, which is consistent with the decrease of ACC content (Gutierrez-Carbonell et al., 2015). A putative SAMS, ortholog of AT1G78240, was reported to be up-regulated in *Medicago truncatula* under Fe limitation (Rodriguez-Celma et al., 2011). By combining HPLC-MS and iTRAQ, Lan et al. identified 4454 proteins in Arabidopsis roots and 2882 proteins were reliably quantified; of which, a suit of 101 proteins were identified as differentially accumulated in abundance upon Fe deficiency (Lan et al., 2011). Remarkably, this study revealed that six proteins associated with Met cycle, such as SAMS1, SAMS2, SAMS3, and SAMS4, the cobalmine-independent Met synthase ATMS1, and the S-adenosyl-L-homo-Cys hydrolase SAHH1, were found among the most abundant proteins, indicating the importance of this pathway in roots. Particularly, three out of four SAMSs showed an increase in protein abundance upon Fe deficiency, and two enzymes ARD2 (acireductone dioxygenase 2) and DEP1 (DEHYDRATASE-ENOLASE-PHOSPHATASE-COMPLEX 1), with a proposed function in the salvage of L-Met from methylthioadenosine (**Figure 3**), were also up-regulated by Fe shortage, underlying the importance of SAM synthesis and the sustainable Met cycle under Fe limiting conditions. Enhanced synthesis of SAM, combined with the up-regulation of NAS4, can lead to an increase of NA content, which is crucial for Fe homeostasis. Alternatively, increased SAM content would result in more ethylene production, which plays multiple roles in various biological processes by controlling the expression of downstream genes.

CONCLUSIONS

Omic approaches have been widely employed to explore the responses of plant to Fe deficiency, and have uncovered diverse metabolic adaptations upon Fe starvation. A subset of conserved Fe-responsive genes and some common metabolic pathways have been revealed by transcriptome and proteome across a range of plant species. It has been clear that the concordance between the abundance of mRNA and their related proteins is not strong correlated (Lan et al., 2012a, 2013a; Li et al., 2013; Marmiroli et al., 2015; Dong et al., 2016). The integration of transcriptome and proteome is mandatory for generating a complete inventory of the components that are crucial for Fe homeostasis. Several core genes encoding proteins with unknown functions, which are robustly induced by Fe starvation and tightly co-expressed, require further validation. The involvement of ethylene in the morphological and physiological Fe deficiency responses in multiple plant species has been observed, and omic studies provide further molecular evidence that ethylene plays a role in the Fe deficiency responses of plants.

AUTHOR CONTRIBUTIONS

All authors listed, have made substantial, direct and intellectual contribution to the work, and approved it for publication.

ACKNOWLEDGMENTS

This work was supported by the Natural Science Foundation of China (31470346, 31370280), the Strategic Priority Research Program of the Chinese Academy of Sciences (Grant No. XDB15030103), the National Science Foundation in Jiangsu Provinces (BK20141511, BK20141470), the Project of Priority and Key Areas, ISSCAS (ISSASIP1605), and the Priority Academic Program Development of Jiangsu Higher Education Institutions (PAPD). We thank Mr. Mingke Yan and Miss Caiwen Xue for the critical read of this manuscript. We are grateful to two reviewers for their invaluable comments and suggestions to substantially improve the manuscript. We apologize to all the people whose excellent work is not cited due to limiting space.

SUPPLEMENTARY MATERIAL

The Supplementary Material for this article can be found online at: http://journal.frontiersin.org/article/10.3389/fpls.2017.00040/full#supplementary-material

REFERENCES

Abadia, J., Vazquez, S., Rellan-Alvarez, R., El-Jendoubi, H., Abadia, A., Alvarez-Fernandez, A., et al. (2011). Towards a knowledge-based correction of iron chlorosis. *Plant Physiol. Biochem.* 49, 471–482. doi: 10.1016/j.plaphy.2011.01.026

Alonso, J. M., Hirayama, T., Roman, G., Nourizadeh, S., and Ecker, J. R. (1999). EIN2, a bifunctional transducer of ethylene and stress responses in Arabidopsis. *Science* 284, 2148–2152. doi: 10.1126/science.284.5423.2148

Andaluz, S., Lopez-Millan, A. F., De Las Rivas, J., Aro, E. M., Abadia, J., and Abadia, A. (2006). Proteomic profiles of thylakoid membranes and changes in response to iron deficiency. *Photosyn. Res.* 89, 141–155. doi: 10.1007/s11120-006-9092-6

Aravind, L., and Koonin, E. V. (2001). The DNA-repair protein AlkB, EGL-9, and leprecan define new families of 2-oxoglutarate- and iron-dependent dioxygenases. *Genome Biol.* 2:research0007. doi: 10.1186/gb-2001-2-3-research0007

Arrivault, S., Senger, T., and Kramer, U. (2006). The Arabidopsis metal tolerance protein AtMTP3 maintains metal homeostasis by mediating Zn exclusion

from the shoot under Fe deficiency and Zn oversupply. *Plant J.* 46, 861–879. doi: 10.1111/j.1365-313X.2006.02746.x

Bashir, K., Hanada, K., Shimizu, M., Seki, M., Nakanishi, H., and Nishizawa, N. K. (2014). Transcriptomic analysis of rice in response to iron deficiency and excess. *Rice* 7, 18. doi: 10.1186/s12284-014-0018-1

Bauer, P., and Blondet, E. (2011). Transcriptome analysis of ein3 eil1 mutants in response to iron deficiency. *Plant Signal. Behav.* 6, 1669–1671. doi: 10.4161/psb.6.11.17847

Bauer, P., Ling, H. Q., and Guerinot, M. L. (2007). FIT, the FER-LIKE IRON DEFICIENCY INDUCED TRANSCRIPTION FACTOR in Arabidopsis. *Plant Physiol. Biochem.* 45, 260–261. doi: 10.1016/j.plaphy.2007.03.006

Besson-Bard, A., Gravot, A., Richaud, P., Auroy, P., Duc, C., Gaymard, F., et al. (2009). Nitric oxide contributes to cadmium toxicity in Arabidopsis by promoting cadmium accumulation in roots and by up-regulating genes related to iron uptake. *Plant Physiol.* 149, 1302–1315. doi: 10.1104/pp.108.133348

Brumbarova, T., Matros, A., Mock, H. P., and Bauer, P. (2008). A proteomic study showing differential regulation of stress, redox regulation and peroxidase proteins by iron supply and the transcription factor FER. *Plant J.* 54, 321–334. doi: 10.1111/j.1365-313X.2008.03421.x

Buckhout, T. J., Yang, T. J., and Schmidt, W. (2009). Early iron-deficiency-induced transcriptional changes in Arabidopsis roots as revealed by microarray analyses. *BMC Genomics* 10:147. doi: 10.1186/1471-2164-10-147

Burstenbinder, K., Rzewuski, G., Wirtz, M., Hell, R., and Sauter, M. (2007). The role of methionine recycling for ethylene synthesis in Arabidopsis. *Plant J.* 49, 238–249. doi: 10.1111/j.1365-313X.2006.02942.x

Chao, Q., Rothenberg, M., Solano, R., Roman, G., Terzaghi, W., and Ecker, J. R. (1997). Activation of the ethylene gas response pathway in Arabidopsis by the nuclear protein ETHYLENE-INSENSITIVE3 and related proteins. *Cell* 89, 1133–1144. doi: 10.1016/S0092-8674(00)80300-1

Chen, L., Ding, C., Zhao, X., Xu, J., Mohammad, A. A., Wang, S., et al. (2015). Differential regulation of proteins in rice (*Oryza sativa* L.) under iron deficiency. *Plant Cell Rep.* 34, 83–96. doi: 10.1007/s00299-014-1689-1

Chen, Y. Y., Wang, Y., Shin, L. J., Wu, J. F., Shanmugam, V., Tsednee, M., et al. (2013). Iron is involved in the maintenance of circadian period length in Arabidopsis. *Plant Physiol.* 161, 1409–1420. doi: 10.1104/pp.112.212068

Colangelo, E. P., and Guerinot, M. L. (2004). The essential basic helix-loop-helix protein FIT1 is required for the iron deficiency response. *Plant Cell* 16, 3400–3412. doi: 10.1105/tpc.104.024315

Curie, C., Panaviene, Z., Loulergue, C., Dellaporta, S. L., Briat, J. F., and Walker, E. L. (2001). Maize yellow stripe1 encodes a membrane protein directly involved in Fe(III) uptake. *Nature* 409, 346–349. doi: 10.1038/35053080

Dinneny, J. R., Long, T. A., Wang, J. Y., Jung, J. W., Mace, D., Pointer, S., et al. (2008). Cell identity mediates the response of Arabidopsis roots to abiotic stress. *Science* 320, 942–945. doi: 10.1126/science.1153795

Dong, Y., Deng, M., Zhao, Z., and Fan, G. (2016). Quantitative proteomic and transcriptomic study on autotetraploid paulownia and its diploid parent reveal key metabolic processes associated with paulownia autotetraploidization. *Front. Plant Sci.* 7:892. doi: 10.3389/fpls.2016.00892

Donnini, S., Prinsi, B., Negri, A. S., Vigani, G., Espen, L., and Zocchi, G. (2010). Proteomic characterization of iron deficiency responses in *Cucumis sativus* L. *roots. BMC Plant Biol.* 10:268. doi: 10.1186/1471-2229-10-268

Eide, D., Broderius, M., Fett, J., and Guerinot, M. L. (1996). A novel iron-regulated metal transporter from plants identified by functional expression in yeast. *Proc. Natl. Acad. Sci. U.S.A.* 93, 5624–5628. doi: 10.1073/pnas.93.11.5624

Eroglu, S., Meier, B., Von Wiren, N., and Peiter, E. (2016). The vacuolar manganese transporter MTP8 determines tolerance to iron deficiency-induced chlorosis in Arabidopsis. *Plant Physiol.* 170, 1030–1045. doi: 10.1104/pp.15.01194

Fourcroy, P., Siso-Terraza, P., Sudre, D., Saviron, M., Reyt, G., Gaymard, F., et al. (2014). Involvement of the ABCG37 transporter in secretion of scopoletin and derivatives by Arabidopsis roots in response to iron deficiency. *New Phytol.* 201, 155–167. doi: 10.1111/nph.12471

Garcia, M. J., Lucena, C., Romera, F. J., Alcantara, E., and Perez-Vicente, R. (2010). Ethylene and nitric oxide involvement in the up-regulation of key genes related to iron acquisition and homeostasis in Arabidopsis. *J. Exp. Bot.* 61, 3885–3899. doi: 10.1093/jxb/erq203

Garcia, M. J., Romera, F. J., Lucena, C., Alcantara, E., and Perez-Vicente, R. (2015). Ethylene and the regulation of physiological and morphological responses to nutrient deficiencies. *Plant Physiol.* 169, 51–60. doi: 10.1104/pp.15.00708

Garcia, M. J., Romera, F. J., Stacey, M. G., Stacey, G., Villar, E., Alcantara, E., et al. (2013). Shoot to root communication is necessary to control the expression of iron-acquisition genes in Strategy I plants. *Planta* 237, 65–75. doi: 10.1007/s00425-012-1757-0

Garcia, M. J., Suarez, V., Romera, F. J., Alcantara, E., and Perez-Vicente, R. (2011). A new model involving ethylene, nitric oxide and Fe to explain the regulation of Fe-acquisition genes in Strategy I plants. *Plant Physiol. Biochem.* 49, 537–544. doi: 10.1016/j.plaphy.2011.01.019

Genannt Bonsmann, S. S., Walczyk, T., Renggli, S., and Hurrell, R. F. (2008). Oxalic acid does not influence nonhaem iron absorption in humans: a comparison of kale and spinach meals. *Eur. J. Clin. Nutr.* 62, 336–341. doi: 10.1038/sj.ejcn.1602721

Gutierrez-Carbonell, E., Lattanzio, G., Albacete, A., Rios, J. J., Kehr, J., Abadia, A., et al. (2015). Effects of Fe deficiency on the protein profile of Brassica napus phloem sap. *Proteomics* 15, 3835–3853. doi: 10.1002/pmic.201400464

Gutierrez-Carbonell, E., Takahashi, D., Luthje, S., Gonzalez-Reyes, J. A., Mongrand, S., Contreras-Moreira, B., et al. (2016). A shotgun proteomic approach reveals that Fe deficiency causes marked changes in the protein profiles of plasma membrane and detergent-resistant microdomain preparations from Beta vulgaris Roots. *J. Proteome Res.* 15, 2510–2524. doi: 10.1021/acs.jproteome.6b00026

Haydon, M. J., Kawachi, M., Wirtz, M., Hillmer, S., Hell, R., and Kramer, U. (2012). Vacuolar nicotianamine has critical and distinct roles under iron deficiency and for zinc sequestration in Arabidopsis. *Plant Cell* 24, 724–737. doi: 10.1105/tpc.111.095042

Hindt, M. N., and Guerinot, M. L. (2012). Getting a sense for signals: regulation of the plant iron deficiency response. *Biochim. Biophys. Acta* 1823, 1521–1530. doi: 10.1016/j.bbamcr.2012.03.010

Hong, S., Kim, S. A., Guerinot, M. L., and Mcclung, C. R. (2013). Reciprocal interaction of the circadian clock with the iron homeostasis network in Arabidopsis. *Plant Physiol.* 161, 893–903. doi: 10.1104/pp.112.208603

Hopff, D., Wienkoop, S., and Luthje, S. (2013). The plasma membrane proteome of maize roots grown under low and high iron conditions. *J. Proteomics* 91, 605–618. doi: 10.1016/j.jprot.2013.01.006

Ivanov, R., Brumbarova, T., and Bauer, P. (2012). Fitting into the harsh reality: regulation of iron-deficiency responses in dicotyledonous plants. *Mol. Plant* 5, 27–42. doi: 10.1093/mp/ssr065

Jeong, J., and Guerinot, M. L. (2009). Homing in on iron homeostasis in plants. *Trends Plant Sci.* 14, 280–285. doi: 10.1016/j.tplants.2009.02.006

Kabir, A. H., Paltridge, N. G., Able, A. J., Paull, J. G., and Stangoulis, J. C. (2012). Natural variation for Fe-efficiency is associated with upregulation of Strategy I mechanisms and enhanced citrate and ethylene synthesis in Pisum sativum L. *Planta* 235, 1409–1419. doi: 10.1007/s00425-011-1583-9

Khandakar, J., Haraguchi, I., Yamaguchi, K., and Kitamura, Y. (2013). A small-scale proteomic approach reveals a survival strategy, including a reduction in alkaloid biosynthesis, in *Hyoscyamus albus* roots subjected to iron deficiency. *Front. Plant Sci.* 4:331. doi: 10.3389/fpls.2013.00331

Kobayashi, T., and Nishizawa, N. K. (2012). Iron uptake, translocation, and regulation in higher plants. *Annu. Rev. Plant Biol.* 63, 131–152. doi: 10.1146/annurev-arplant-042811-105522

Koen, E., Besson-Bard, A., Duc, C., Astier, J., Gravot, A., Richaud, P., et al. (2013). *Arabidopsis thaliana* nicotianamine synthase 4 is required for proper response to iron deficiency and to cadmium exposure. *Plant Sci.* 209, 1–11. doi: 10.1016/j.plantsci.2013.04.006

Laganowsky, A., Gomez, S. M., Whitelegge, J. P., and Nishio, J. N. (2009). Hydroponics on a chip: analysis of the Fe deficient Arabidopsis thylakoid membrane proteome. *J. Proteomics* 72, 397–415. doi: 10.1016/j.jprot.2009.01.024

Lan, P., Li, W., Lin, W. D., Santi, S., and Schmidt, W. (2013a). Mapping gene activity of Arabidopsis root hairs. *Genome Biol.* 14:R67. doi: 10.1186/gb-2013-14-6-r67

Lan, P., Li, W., and Schmidt, W. (2012a). Complementary proteome and transcriptome profiling in phosphate-deficient Arabidopsis roots reveals multiple levels of gene regulation. *Mol. Cell. Proteomics* 11, 1156–1166. doi: 10.1074/mcp.M112.020461

Lan, P., Li, W., and Schmidt, W. (2013b). A digital compendium of genes mediating the reversible phosphorylation of proteins in Fe-deficient Arabidopsis roots. *Front. Plant Sci.* 4:173. doi: 10.3389/fpls.2013.00173

Lan, P., Li, W., Wen, T. N., and Schmidt, W. (2012b). Quantitative phosphoproteome profiling of iron-deficient Arabidopsis roots. *Plant Physiol.* 159, 403–417. doi: 10.1104/pp.112.193987

Lan, P., Li, W., Wen, T. N., Shiau, J. Y., Wu, Y. C., Lin, W., et al. (2011). iTRAQ protein profile analysis of Arabidopsis roots reveals new aspects critical for iron homeostasis. *Plant Physiol.* 155, 821–834. doi: 10.1104/pp.110.169508

Lanquar, V., Lelievre, F., Bolte, S., Hames, C., Alcon, C., Neumann, D., et al. (2005). Mobilization of vacuolar iron by AtNRAMP3 and AtNRAMP4 is essential for seed germination on low iron. *EMBO J.* 24, 4041–4051. doi: 10.1038/sj.emboj.7600864

Lattanzio, G., Andaluz, S., Matros, A., Calvete, J. J., Kehr, J., Abadia, A., et al. (2013). Protein profile of *Lupinus texensis* phloem sap exudates: searching for Fe- and Zn-containing proteins. *Proteomics* 13, 2283–2296. doi: 10.1002/pmic.201200515

Li, J., Wu, X. D., Hao, S. T., Wang, X. J., and Ling, H. Q. (2008). Proteomic response to iron deficiency in tomato root. *Proteomics* 8, 2299–2311. doi: 10.1002/pmic.200700942

Li, W., Lin, W. D., Ray, P., Lan, P., and Schmidt, W. (2013). Genome-wide detection of condition-sensitive alternative splicing in Arabidopsis roots. *Plant Physiol.* 162, 1750–1763. doi: 10.1104/pp.113.217778

Li, W., and Schmidt, W. (2010). A lysine-63-linked ubiquitin chain-forming conjugase, UBC13, promotes the developmental responses to iron deficiency in Arabidopsis roots. *Plant J.* 62, 330–343. doi: 10.1111/j.1365-313X.2010.04150.x

Li, Z., Phillip, D., Neuhauser, B., Schulze, W. X., and Ludewig, U. (2015). Protein dynamics in young maize root hairs in response to macro- and micronutrient deprivation. *J. Proteome Res.* 14, 3362–3371. doi: 10.1021/acs.jproteome.5b00399

Lin, W. D., Liao, Y. Y., Yang, T. J., Pan, C. Y., Buckhout, T. J., and Schmidt, W. (2011). Coexpression-based clustering of Arabidopsis root genes predicts functional modules in early phosphate deficiency signaling. *Plant Physiol.* 155, 1383–1402. doi: 10.1104/pp.110.166520

Lin, Y. F., Liang, H. M., Yang, S. Y., Boch, A., Clemens, S., Chen, C. C., et al. (2009). Arabidopsis IRT3 is a zinc-regulated and plasma membrane localized zinc/iron transporter. *New Phytol.* 182, 392–404. doi: 10.1111/j.1469-8137.2009.02766.x

Lingam, S., Mohrbacher, J., Brumbarova, T., Potuschak, T., Fink-Straube, C., Blondet, E., et al. (2011). Interaction between the bHLH transcription factor FIT and ETHYLENE INSENSITIVE3/ETHYLENE INSENSITIVE3-LIKE1 reveals molecular linkage between the regulation of iron acquisition and ethylene signaling in Arabidopsis. *Plant Cell* 23, 1815–1829. doi: 10.1105/tpc.111.084715

Long, T. A., Tsukagoshi, H., Busch, W., Lahner, B., Salt, D. E., and Benfey, P. N. (2010). The bHLH transcription factor POPEYE regulates response to iron deficiency in Arabidopsis roots. *Plant Cell* 22, 2219–2236. doi: 10.1105/tpc.110.074096

Lopez-Millan, A. F., Grusak, M. A., Abadia, A., and Abadia, J. (2013). Iron deficiency in plants: an insight from proteomic approaches. *Front. Plant Sci.* 4:254. doi: 10.3389/fpls.2013.00254

Lucena, C., Romera, F. J., Garcia, M. J., Alcantara, E., and Perez-Vicente, R. (2015). Ethylene participates in the regulation of Fe deficiency responses in Strategy I plants and in rice. *Front. Plant Sci.* 6:1056. doi: 10.3389/fpls.2015.01056

Lucena, C., Waters, B. M., Romera, F. J., Garcia, M. J., Morales, M., Alcantara, E., et al. (2006). Ethylene could influence ferric reductase, iron transporter, and H+-ATPase gene expression by affecting FER (or FER-like) gene activity. *J. Exp. Bot.* 57, 4145–4154. doi: 10.1093/jxb/erl189

Mai, H. J., Lindermayr, C., Von Toerne, C., Fink-Straube, C., Durner, J., and Bauer, P. (2015). Iron and FER-LIKE IRON DEFICIENCY-INDUCED TRANSCRIPTION FACTOR-dependent regulation of proteins and genes in Arabidopsis thaliana roots. *Proteomics* 15, 3030–3047. doi: 10.1002/pmic.201400351

Mai, H. J., Pateyron, S., and Bauer, P. (2016). Iron homeostasis in Arabidopsis thaliana: transcriptomic analyses reveal novel FIT-regulated genes, iron deficiency marker genes and functional gene networks. *BMC Plant Biol.* 16:211. doi: 10.1186/s12870-016-0899-9

Marmiroli, M., Imperiale, D., Pagano, L., Villani, M., Zappettini, A., and Marmiroli, N. (2015). The proteomic response of *Arabidopsis thaliana* to cadmium sulfide quantum dots, and its correlation with the transcriptomic response. *Front. Plant Sci.* 6:1104. doi: 10.3389/fpls.2015.01104

Maruta, T., Tanouchi, A., Tamoi, M., Yabuta, Y., Yoshimura, K., Ishikawa, T., et al. (2010). Arabidopsis chloroplastic ascorbate peroxidase isoenzymes play a dual role in photoprotection and gene regulation under photooxidative stress. *Plant Cell Physiol.* 51, 190–200. doi: 10.1093/pcp/pcp177

McLean, E., Cogswell, M., Egli, I., Wojdyla, D., and De Benoist, B. (2009). Worldwide prevalence of anaemia, WHO vitamin and mineral nutrition information system, 1993-2005. *Public Health Nutr.* 12, 444–454. doi: 10.1017/S1368980008002401

Meisrimler, C. N., Planchon, S., Renaut, J., Sergeant, K., and Luthje, S. (2011). Alteration of plasma membrane-bound redox systems of iron deficient pea roots by chitosan. *J. Proteomics* 74, 1437–1449. doi: 10.1016/j.jprot.2011.01.012

Meisrimler, C. N., Wienkoop, S., Lyon, D., Geilfus, C. M., and Luthje, S. (2016). Long-term iron deficiency: tracing changes in the proteome of different pea (Pisum sativum L.) cultivars. *J. Proteomics* 140, 13–23. doi: 10.1016/j.jprot.2016.03.024

Mendoza-Cozatl, D. G., Xie, Q., Akmakjian, G. Z., Jobe, T. O., Patel, A., Stacey, M. G., et al. (2014). OPT3 is a component of the iron-signaling network between leaves and roots and misregulation of OPT3 leads to an over-accumulation of cadmium in seeds. *Mol. Plant* 7, 1455–1469. doi: 10.1093/mp/ssu067

Moller, S. G., Kunkel, T., and Chua, N. H. (2001). A plastidic ABC protein involved in intercompartmental communication of light signaling. *Genes Dev.* 15, 90–103. doi: 10.1101/gad.850101

Muccilli, V., Licciardello, C., Fontanini, D., Cunsolo, V., Capocchi, A., Saletti, R., et al. (2013). Root protein profiles of two citrus rootstocks grown under iron sufficiency/deficiency conditions. *Eur. J. Mass Spectrom.* 19, 305–324. doi: 10.1255/ejms.1230

Muneer, S., and Jeong, B. R. (2015). Genotypic variation under Fe deficiency results in rapid changes in protein expressions and genes involved in Fe metabolism and antioxidant mechanisms in tomato seedlings (*Solanum lycopersicum* L.). *Int. J. Mol. Sci.* 16, 28022–28037. doi: 10.3390/ijms161226086

O'rourke, J. A., Charlson, D. V., Gonzalez, D. O., Vodkin, L. O., Graham, M. A., Cianzio, S. R., et al. (2007a). Microarray analysis of iron deficiency chlorosis in near-isogenic soybean lines. *BMC Genomics* 8:476. doi: 10.1186/1471-2164-8-476

O'rourke, J. A., Graham, M. A., Vodkin, L., Gonzalez, D. O., Cianzio, S. R., and Shoemaker, R. C. (2007b). Recovering from iron deficiency chlorosis in near-isogenic soybeans: a microarray study. *Plant Physiol. Biochem.* 45, 287–292. doi: 10.1016/j.plaphy.2007.03.008

O'rourke, J. A., Nelson, R. T., Grant, D., Schmutz, J., Grimwood, J., Cannon, S., et al. (2009). Integrating microarray analysis and the soybean genome to understand the soybeans iron deficiency response. *BMC Genomics* 10:376. doi: 10.1186/1471-2164-10-376

Palmer, C. M., Hindt, M. N., Schmidt, H., Clemens, S., and Guerinot, M. L. (2013). MYB10 and MYB72 are required for growth under iron-limiting conditions. *PLoS Genet.* 9:e1003953. doi: 10.1371/journal.pgen.1003953

Pan, I. C., Tsai, H. H., Cheng, Y. T., Wen, T. N., Buckhout, T. J., and Schmidt, W. (2015). Post-transcriptional coordination of the Arabidopsis iron deficiency response is partially dependent on the E3 Ligases RING DOMAIN LIGASE1 (RGLG1) and RING DOMAIN LIGASE2 (RGLG2). *Mol. Cell. Proteomics* 14, 2733–2752. doi: 10.1074/mcp.M115.048520

Perea-Garcia, A., Garcia-Molina, A., Andres-Colas, N., Vera-Sirera, F., Perez-Amador, M. A., Puig, S., et al. (2013). Arabidopsis copper transport protein COPT2 participates in the cross talk between iron deficiency responses and low-phosphate signaling. *Plant Physiol.* 162, 180–194. doi: 10.1104/pp.112.212407

Rellan-Alvarez, R., Andaluz, S., Rodriguez-Celma, J., Wohlgemuth, G., Zocchi, G., Alvarez-Fernandez, A., et al. (2010). Changes in the proteomic and metabolic profiles of Beta vulgaris root tips in response to iron deficiency and resupply. *BMC Plant Biol.* 10:120. doi: 10.1186/1471-2229-10-120

Ricachenevsky, F. K., and Sperotto, R. A. (2014). There and back again, or always there? The evolution of rice combined strategy for Fe uptake. *Front. Plant Sci.* 5:189. doi: 10.3389/fpls.2014.00189

Robinson, N. J., Procter, C. M., Connolly, E. L., and Guerinot, M. L. (1999). A ferric-chelate reductase for iron uptake from soils. *Nature* 397, 694–697. doi: 10.1038/17800

Rodriguez-Celma, J., Lattanzio, G., Grusak, M. A., Abadia, A., Abadia, J., and Lopez-Millan, A. F. (2011). Root responses of *Medicago truncatula* plants grown in two different iron deficiency conditions: changes in root

protein profile and riboflavin biosynthesis. *J. Proteome Res.* 10, 2590–2601. doi: 10.1021/pr2000623

Rodriguez-Celma, J., Lattanzio, G., Jimenez, S., Briat, J. F., Abadia, J., Abadia, A., et al. (2013a). Changes induced by Fe deficiency and Fe resupply in the root protein profile of a peach-almond hybrid rootstock. *J. Proteome Res.* 12, 1162–1172. doi: 10.1021/pr300763c

Rodriguez-Celma, J., Lattanzio, G., Villarroya, D., Gutierrez-Carbonell, E., Ceballos-Laita, L., Rencoret, J., et al. (2016). Effects of Fe deficiency on the protein profiles and lignin composition of stem tissues from *Medicago truncatula* in absence or presence of calcium carbonate. *J. Proteomics* 140, 1–12. doi: 10.1016/j.jprot.2016.03.017

Rodriguez-Celma, J., Lin, W. D., Fu, G. M., Abadia, J., Lopez-Millan, A. F., and Schmidt, W. (2013b). Mutually exclusive alterations in secondary metabolism are critical for the uptake of insoluble iron compounds by Arabidopsis and *Medicago truncatula*. *Plant Physiol.* 162, 1473–1485. doi: 10.1104/pp.113.220426

Romera, F. J., and Alcantara, E. (1994). Iron-deficiency stress responses in cucumber (*Cucumis sativus* L.) roots (A possible role for ethylene?). *Plant Physiol.* 105, 1133–1138. doi: 10.1104/pp.105.4.1133

Romheld, V., and Marschner, H. (1986). Evidence for a specific uptake system for iron phytosiderophores in roots of grasses. *Plant Physiol.* 80, 175–180. doi: 10.1104/pp.80.1.175

Salome, P. A., Oliva, M., Weigel, D., and Kramer, U. (2013). Circadian clock adjustment to plant iron status depends on chloroplast and phytochrome function. *EMBO J.* 32, 511–523. doi: 10.1038/emboj.2012.330

Santi, S., and Schmidt, W. (2009). Dissecting iron deficiency-induced proton extrusion in Arabidopsis roots. *New Phytol.* 183, 1072–1084. doi: 10.1111/j.1469-8137.2009.02908.x

Schaaf, G., Honsbein, A., Meda, A. R., Kirchner, S., Wipf, D., and Von Wiren, N. (2006). AtIREG2 encodes a tonoplast transport protein involved in iron-dependent nickel detoxification in *Arabidopsis thaliana* roots. *J. Biol. Chem.* 281, 25532–25540. doi: 10.1074/jbc.M601062200

Schikora, A., and Schmidt, W. (2001). Acclimative changes in root epidermal cell fate in response to Fe and P deficiency: a specific role for auxin? *Protoplasma* 218, 67–75. doi: 10.1007/BF01288362

Schikora, A., and Schmidt, W. (2002). Formation of transfer cells and H(+)-ATPase expression in tomato roots under P and Fe deficiency. *Planta* 215, 304–311. doi: 10.1007/s00425-002-0738-0

Schmidt, W., and Schikora, A. (2001). Different pathways are involved in phosphate and iron stress-induced alterations of root epidermal cell development. *Plant Physiol.* 125, 2078–2084. doi: 10.1104/pp.125.4.2078

Schmidt, W., Tittel, J., and Schikora, A. (2000). Role of hormones in the induction of iron deficiency responses in Arabidopsis roots. *Plant Physiol.* 122, 1109–1118. doi: 10.1104/pp.122.4.1109

Schuler, M., Rellan-Alvarez, R., Fink-Straube, C., Abadia, J., and Bauer, P. (2012). Nicotianamine functions in the Phloem-based transport of iron to sink organs, in pollen development and pollen tube growth in Arabidopsis. *Plant Cell* 24, 2380–2400. doi: 10.1105/tpc.112.099077

Sivitz, A. B., Hermand, V., Curie, C., and Vert, G. (2012). Arabidopsis bHLH100 and bHLH101 control iron homeostasis via a FIT-independent pathway. *PLoS ONE* 7:e44843. doi: 10.1371/journal.pone.0044843

Sudre, D., Gutierrez-Carbonell, E., Lattanzio, G., Rellan-Alvarez, R., Gaymard, F., Wohlgemuth, G., et al. (2013). Iron-dependent modifications of the flower transcriptome, proteome, metabolome, and hormonal content in an Arabidopsis ferritin mutant. *J. Exp. Bot.* 64, 2665–2688. doi: 10.1093/jxb/ert112

Thimm, O., Essigmann, B., Kloska, S., Altmann, T., and Buckhout, T. J. (2001). Response of Arabidopsis to iron deficiency stress as revealed by microarray analysis. *Plant Physiol.* 127, 1030–1043. doi: 10.1104/pp.010191

Turlapati, P. V., Kim, K. W., Davin, L. B., and Lewis, N. G. (2011). The laccase multigene family in *Arabidopsis thaliana*: towards addressing the mystery of their gene function(s). *Planta* 233, 439–470. doi: 10.1007/s00425-010-1298-3

Urzica, E. I., Casero, D., Yamasaki, H., Hsieh, S. I., Adler, L. N., Karpowicz, S. J., et al. (2012). Systems and trans-system level analysis identifies conserved iron deficiency responses in the plant lineage. *Plant Cell* 24, 3921–3948. doi: 10.1105/tpc.112.102491

Vert, G., Grotz, N., Dedaldechamp, F., Gaymard, F., Guerinot, M. L., Briat, J. F., et al. (2002). IRT1, an Arabidopsis transporter essential for iron uptake from the soil and for plant growth. *Plant Cell* 14, 1223–1233. doi: 10.1105/tpc.001388

Vigani, G., Di Silvestre, D., Agresta, A. M., Donnini, S., Mauri, P., Gehl, C., et al. (2017). Molybdenum and iron mutually impact their homeostasis in cucumber (*Cucumis sativus*) plants. *New Phytol.* 213, 1222–1241. doi: 10.1111/nph.14214

Wang, N., Cui, Y., Liu, Y., Fan, H., Du, J., Huang, Z., et al. (2013). Requirement and functional redundancy of Ib subgroup bHLH proteins for iron deficiency responses and uptake in *Arabidopsis thaliana*. *Mol. Plant* 6, 503–513. doi: 10.1093/mp/sss089

Wang, R., Okamoto, M., Xing, X., and Crawford, N. M. (2003). Microarray analysis of the nitrate response in Arabidopsis roots and shoots reveals over 1,000 rapidly responding genes and new linkages to glucose, trehalose-6-phosphate, iron, and sulfate metabolism. *Plant Physiol.* 132, 556–567. doi: 10.1104/pp.103.021253

Waters, B. M., Lucena, C., Romera, F. J., Jester, G. G., Wynn, A. N., Rojas, C. L., et al. (2007). Ethylene involvement in the regulation of the H(+)-ATPase CsHA1 gene and of the new isolated ferric reductase CsFRO1 and iron transporter CsIRT1 genes in cucumber plants. *Plant Physiol. Biochem.* 45, 293–301. doi: 10.1016/j.plaphy.2007.03.011

Wu, J., Wang, C., Zheng, L., Wang, L., Chen, Y., Whelan, J., et al. (2011). Ethylene is involved in the regulation of iron homeostasis by regulating the expression of iron-acquisition-related genes in *Oryza sativa*. *J. Exp. Bot.* 62, 667–674. doi: 10.1093/jxb/erq301

Xu, X. M., Adams, S., Chua, N. H., and Moller, S. G. (2005). AtNAP1 represents an atypical SufB protein in Arabidopsis plastids. *J. Biol. Chem.* 280, 6648–6654. doi: 10.1074/jbc.M413082200

Xu, X. M., and Moller, S. G. (2004). AtNAP7 is a plastidic SufC-like ATP-binding cassette/ATPase essential for Arabidopsis embryogenesis. *Proc. Natl. Acad. Sci. U.S.A.* 101, 9143–9148. doi: 10.1073/pnas.0400799101

Yang, J. L., Chen, W. W., Chen, L. Q., Qin, C., Jin, C. W., Shi, Y. Z., et al. (2013). The 14-3-3 protein GENERAL REGULATORY FACTOR11 (GRF11) acts downstream of nitric oxide to regulate iron acquisition in *Arabidopsis thaliana*. *New Phytol.* 197, 815–824. doi: 10.1111/nph.12057

Yang, T. J., Lin, W. D., and Schmidt, W. (2010). Transcriptional profiling of the Arabidopsis iron deficiency response reveals conserved transition metal homeostasis networks. *Plant Physiol.* 152, 2130–2141. doi: 10.1104/pp.109.152728

Yang, Y., Ou, B., Zhang, J., Si, W., Gu, H., Qin, G., et al. (2014). The Arabidopsis mediator subunit MED16 regulates iron homeostasis by associating with EIN3/EIL1 through subunit MED25. *Plant J.* 77, 838–851. doi: 10.1111/tpj.12440

Ye, L., Li, L., Wang, L., Wang, S., Li, S., Du, J., et al. (2015). MPK3/MPK6 are involved in iron deficiency-induced ethylene production in Arabidopsis. *Front. Plant Sci.* 6:953. doi: 10.3389/fpls.2015.00953

Yuan, Y., Wu, H., Wang, N., Li, J., Zhao, W., Du, J., et al. (2008). FIT interacts with AtbHLH38 and AtbHLH39 in regulating iron uptake gene expression for iron homeostasis in Arabidopsis. *Cell Res.* 18, 385–397. doi: 10.1038/cr.2008.26

Zaid, H., El Morabet, R., Diem, H. G., and Arahou, M. (2003). Does ethylene mediate cluster root formation under iron deficiency? *Ann. Bot.* 92, 673–677. doi: 10.1093/aob/mcg186

Zamboni, A., Zanin, L., Tomasi, N., Pezzotti, M., Pinton, R., Varanini, Z., et al. (2012). Genome-wide microarray analysis of tomato roots showed defined responses to iron deficiency. *BMC Genomics* 13:101. doi: 10.1186/1471-2164-13-101

Zamioudis, C., Hanson, J., and Pieterse, C. M. (2014). beta-Glucosidase BGLU42 is a MYB72-dependent key regulator of rhizobacteria-induced systemic resistance and modulates iron deficiency responses in Arabidopsis roots. *New Phytol.* 204, 368–379. doi: 10.1111/nph.12980

Zargar, S. M., Fujiwara, M., Inaba, S., Kobayashi, M., Kurata, R., Ogata, Y., et al. (2015a). Correlation analysis of proteins responsive to Zn, Mn, or Fe deficiency in Arabidopsis roots based on iTRAQ analysis. *Plant Cell Rep.* 34, 157–166. doi: 10.1007/s00299-014-1696-2

Zargar, S. M., Kurata, R., Inaba, S., and Fukao, Y. (2013). Unraveling the iron deficiency responsive proteome in Arabidopsis shoot by iTRAQ-OFFGEL approach. *Plant Signal Behav.* 8:e26892. doi: 10.4161/psb26892

Zargar, S. M., Kurata, R., Inaba, S., Oikawa, A., Fukui, R., Ogata, Y., et al. (2015b). Quantitative proteomics of Arabidopsis shoot microsomal proteins reveals a cross-talk between excess zinc and iron deficiency. *Proteomics* 15, 1196–1201. doi: 10.1002/pmic.201400467

Zhai, Z., Gayomba, S. R., Jung, H. I., Vimalakumari, N. K., Pineros, M., Craft, E., et al. (2014). OPT3 is a phloem-specific iron transporter that is essential for systemic iron signaling and redistribution of iron and cadmium in Arabidopsis. *Plant Cell* 26, 2249–2264. doi: 10.1105/tpc.114.123737

Zhang, F., Qi, B., Wang, L., Zhao, B., Rode, S., Riggan, N. D., et al. (2016). EIN2-dependent regulation of acetylation of histone H3K14 and non-canonical histone H3K23 in ethylene signalling. *Nat. Commun.* 7:13018. doi: 10.1038/ncomms13018

Zhang, S., Zhang, Y., Cao, Y., Lei, Y., and Jiang, H. (2016). Quantitative proteomic analysis reveals populus cathayana females are more sensitive and respond more sophisticatedly to iron deficiency than males. *J. Proteome Res.* 15, 840–850. doi: 10.1021/acs.jproteome.5b00750

Zhang, Y., Wu, H., Wang, N., Fan, H., Chen, C., Cui, Y., et al. (2014). Mediator subunit 16 functions in the regulation of iron uptake gene expression in Arabidopsis. *New Phytol.* 203, 770–783. doi: 10.1111/nph.12860

Conflict of Interest Statement: The authors declare that the research was conducted in the absence of any commercial or financial relationships that could be construed as a potential conflict of interest.

frontiers in Plant Science

ORIGINAL RESEARCH
published: 18 January 2017
doi: 10.3389/fpls.2016.02029

Application of Exogenous Ethylene Inhibits Postharvest Peel Browning of 'Huangguan' Pear

Yurong Ma[1†], Mengnan Yang[1†], Jingjing Wang[1], Cai-Zhong Jiang[2,3] and Qingguo Wang[1]**

[1] Postharvest Laboratory, College of Food Science and Engineering, Shandong Agricultural University, Tai'an, China, [2] Crops Pathology and Genetics Research Unit, United States Department of Agriculture-Agricultural Research Service, Davis, CA, USA, [3] Department of Plant Sciences, University of California, Davis, Davis, CA, USA

Peel browning disorder has an enormous impact on the exterior quality of 'Huangguan' pear whereas the underlying mechanism is still unclear. Although different methods have been applied for inhibiting the peel browning of 'Huangguan' pear, there are numerous issues associated with these approaches, such as time cost, efficacy, safety and stability. In this study, to develop a rapid, efficient and safe way to protect 'Huangguan' pear from skin browning, the effect of exogenous ethylene on peel browning of pear fruits stored at 0°C was evaluated. Results showed that ethylene treatments at 0.70–1.28 μL/L significantly decreased the browning rate and browning index from 73.80% and 0.30 to 6.80% and 0.02 after 20 days storage at 0°C, respectively, whereas ethylene treatments at 5 μL/L completely inhibited the occurrence of browning. In addition, ethylene treatments at 5 μL/L decreased the electrolyte leakage and respiration rate, delayed the loss of total phenolic compounds. Furthermore, ethylene (5 μL/L) treatment significantly enhanced the activity of catalase (CAT), ascorbate peroxidase (APX) and superoxide dismutase (SOD) and increased the 1, 1-diphenyl-2-picrylhydrazyl inhibition rate, but inhibited the activity of polyphenol oxidase (PPO) and peroxidase (POD). Our data revealed that ethylene prevented the peel browning through improving antioxidant enzymes (CAT, APX and SOD) activities and reducing PPO activity, electrolyte leakage rate and respiration rate. This study demonstrates that exogenous ethylene application may provide a safe and effective alternative method for controlling browning, and contributes to the understanding of peel browning of 'Huangguan' pear.

Keywords: 'Huangguan' pear, browning disorder, exogenous ethylene, antioxidant enzymes, total phenolics

OPEN ACCESS

Edited by:
Nafees A. Khan, Aligarh Muslim University, India

Reviewed by:
Alessandra Francini, Sant'Anna School of Advanced Studies, Italy
Giacomo Cocetta, Università degli Studi di Milano, Italy

***Correspondence:**
Cai-Zhong Jiang
cjiang@ucdavis.edu
Qingguo Wang
wqgyyy@126.com

[†]These authors have contributed equally to this work.

Specialty section:
This article was submitted to Crop Science and Horticulture, a section of the journal Frontiers in Plant Science

Received: *16 November 2016*
Accepted: *19 December 2016*
Published: *18 January 2017*

Citation:
Ma Y, Yang M, Wang J, Jiang C-Z and Wang Q (2017) Application of Exogenous Ethylene Inhibits Postharvest Peel Browning of 'Huangguan' Pear. Front. Plant Sci. 7:2029. doi: 10.3389/fpls.2016.02029

INTRODUCTION

Huangguan pear (*Pyrus bretschneideri* Rehd cv. Huangguan) is a new cultivar with comprehensive qualities and widely planted in northern China (Wang, 1998). However, a surface brown disorder in the peel (also known as chicken-claw disease by farmers in China) often occurs before harvest or during early stage of storage. Symptom in the affected area of the peel is lightly brown at first, and then becomes darker as the disorder progresses. The disorder usually only affects the peel of fruits but not the flesh. However, the surface brown disorder often seriously impacts on the exterior quality of 'Huangguan' pear and causes enormous economic loss.

Browning disorder of pears is affected by both preharvest factors (such as picking date, maturity, fruit size and kind of fruit-bags) and postharvest factors (such as the duration of cooling period, the storage temperature and the CO_2 and O_2 concentrations; Lammertyn et al., 2000; Guan et al., 2005, 2008; Galvis-Sánchez et al., 2006; Wang and Wang, 2011). For example, pears with higher content of chlorogenic acid, a dominant phenolic acid in 'Huangguan' pears, are prone to browning (Franck et al., 2007; Kou et al., 2015). Moreover, the occurrence of surface browning in 'Huangguan' pear was also reported to be related to the Ca^{2+} deficiency and the cellular Ca^{2+} distribution in skin tissues (Dong et al., 2015). In addition, heart browning and flesh browning of 'Rocha' pears are increased by the combination of 2 kPa O_2 + 5 kPa CO_2 (Galvis-Sánchez et al., 2006).

A number of different approaches such as slow cooling, methyl jasmonate, cold conditioning, 1-MCP and $CaCl_2$ are being tried to reduce the incidence of peel browning of pears (Wang and Wang, 2011; Xing et al., 2013). Methyl jasmonate can effectively inhibit the peel browning of 'Huangguan' pear when cooled rapidly (Xing et al., 2013). A cold-conditioning at appropriate temperature (8–9°C) before cold storage (0°C) significantly inhibits the peel and core browning as well as reduces the accumulation of ethanol during storage and shelf life, maintaining the high edible quality of 'Huangguan' pear (Wang and Wang, 2011). Compared with control, treatments with 1-MCP, $CaCl_2$ and 1-MCP + $CaCl_2$ dramatically reduces the skin browning of 'Huanguan' pear (Gong et al., 2010).

Peel browning of fruits appears to be related to the damage of membrane integrity (Kou et al., 2015). The antioxidant enzymes such as superoxide dismutase (SOD), ascorbate peroxidase (APX), catalase (CAT) and peroxidase (POD) are believed participating in the browning of fruits and vegetables (Duan et al., 2011; Kou et al., 2015). These enzymes could protect the integrity of membrane from damage by scavenging H_2O_2, superoxide and other free radicals. Dipping with $CaCl_2$ and pullulan reduces the incidence of brown spots of 'Huangguan' pear by decreasing the activity of polyphenol oxidase (PPO) and POD and increasing the activity of CAT and SOD (Kou et al., 2015). Application of pure oxygen induces the antioxidant enzymes (SOD, APX and CAT) activity in lichi fruit, thereby maintaining the membrane integrity and inhibiting the pericarp browning (Duan et al., 2011).

Though different methods have been applied for inhibiting the peel browning of 'Huangguan' pear, there are numerous issues associating with the approaches, such as time-consuming, higher cost, efficacy, safety and the stability of the efficiency. For example, slow cooling is commercially applied for the inhibition of peel browning. However, this cooling process is time-consuming. Moreover, after slow cooling, fruits show a higher rot rate and withered stalk rate (Wang and Wang, 2011). Thereby, developing a rapid, efficient and safe way to protect 'Huangguan' pear from skin browning is urgent and essential.

As a plant hormone, ethylene is believed to be responsible for the ripening and senescence of fruits and vegetables after harvest. However, some positive effects of ethylene on maintaining the quality of fruits are also reported (Zhou et al., 2001; Candan et al., 2008; Malerba et al., 2010; Lafuente et al., 2014). Ethylene plays important roles in protecting plants from various stresses. Zhou et al. (2001) found that the presence of ethylene during cold storage alleviated the woolliness of nectarines, a chilling injury phenomenon. Furthermore, ethylene conditioning at 12°C extended the shelf life of chilling injury sensitive and non-chilling peel pitting (NCPP) sensitive oranges. Moreover, ethylene conditioning prevented the initial decrease in flavonoid content and reduced the calyx abscission and NCPP (Lafuente et al., 2014).

Although application of ethylene has been well documented in various fruits, the effect of ethylene on the browning and antioxidant capacity in 'Huangguan' pear has not been reported. Thereby, the effect of ethylene on peel browning of 'Huangguan' pear was investigated. In order to understand the possible mechanism of browning, changes of total phenolics, the activity of PPO and antioxidant enzymes (POD, SOD, CAT and APX) during storage were also examined. Results of this study could benefit to the understanding of peel browning disorder of 'Huangguan' pear, and could also provide a safe and effective way for controlling pear peel browning for the industry.

MATERIALS AND METHODS

Materials

Pears with optimum commercial maturity (based on soluble solid and firmness) were harvested in the harvest season from commercial orchards located in Jinzhou city and Gaocheng city, Hebei Province, China. After harvest, pears were immediately transported to the laboratory at Shandong Agricultural University (Tai'an, China). Fruits with similar size, maturity and without physical injury or infection were selected and randomly divided into groups for further use.

Slow-released ethephon (5% solid ethephon powder/sachet, 0.3 g/sachet) and 1-MCP (0.045% 1-MCP cyclodextrin powder, 0.4 g/sachet) were supplied by Shandong Yingyangyuan Food Technology Co., Ltd (Shandong, China).

Ethylene Treatment

To investigate the effect of ethylene and 1-MCP on peel browning rate, pears harvested from Gaocheng city (Hebei Province, China) in 2012 were used. The fruits were packed in boxes with plastic liner, and 15 boxes of pears were randomly divided into five groups (three boxes of fruits for each group) with a total of 144 fruits (48 fruits per box as one repeat with three repeats, 48*3 = 144 fruits). The fruits immediately stored at 0°C served as control. For air, 1-MCP, ethylene, and 1-MCP + ethylene treatments, fruits were treated by air (served as air control), slow-released 1-MCP (a sachet/box), slow-released ethylene (a sachet/box), and slow-released 1-MCP (a sachet/box) and ethylene (a sachet/box) at 20°C for 8 h, then stored at 0°C for 30 days. During the 8 h treatment, the concentrations of ethylene and 1-MCP were detected at 0.70–1.28 and 1 μL/L, respectively. On sampling day, fruits were taken from each treatment (48 fruits per repeat with three biological repeats, total of 144 fruits).

Effect of ethylene on physiological functions of 'Huangguan' pear was investigated with fresh pears harvested from Jinzhou

city (Hebei Province, China) in 2014. Pears were randomly divided into three groups with 168 fruits per group (eight fruits per repeat for each sampling day, 7 sampling days, three repeats) and placed in the containers as mentioned above. For control, pears were packed with plastic foam sleaves, placed into trays overwrapped with plastic film, and immediately stored at 0°C (rapid cooling). For ethylene treatment, ethylene (10000 μL/L, ethylene/nitrogen) was injected into the sealed containers, maintaining the final concentration of ethylene (5 μL/L) at 20°C for 8 h. For air treatment, air with equal volume to ethylene was injected into the sealed container. Treatments were carried out at 20°C. After treatment, the pears were repacked with plastic foam sleeves, placed into trays wrapped with plastic film and stored at 0°C for 30 days. In addition, during cold storage, 24 fruits from each group (eight fruits per repeat with three biological repeats) were sampled on 0, 5, 10, 15, 20, 25, and 30 days, hand-peeled and manually cut into slices, and immediately frozen in liquid nitrogen. Samples (peel and pulp) were ground to fine powder in a mill and stored at -80°C for further analysis.

Prior to above experiments, a preliminary test was conducted to investigate the influence of ethylene concentration on peel browning. In this test, fruits harvested from Gaocheng city, Hebei Province, China, in 2012, were treated by 0, 5, and 50 μL/L ethylene at 20°C for 8 h as mentioned above (40 fruits per repeat with 3 replicates per treatment, 40*3 = 120 fruits/treatment). Fruits immediately stored at 0°C were served as control (rapid cooling). Peel browning index and browning rate were determined 20 and 30 days post storage.

To examine long-term effects of ethylene treatments on the fruit quality, the firmness, titratable acidity (TA) and total soluble solids (TSS) were measured using the pears harvested in 2013. For detailed information, see Supplementary Table S1.

Evaluation of Brown Spot Disorder

The degree of brown spot disorder was evaluated by the method previously described by Xing et al. (2013). This method was scored visually by the percentage of pear fruit surface covered by spots, with a scale from 0 to 4: 0 for no browning, 1 for 1–10%, 2 for 11–20%, 3 for 21–40% and 4 for 41–100%. Disorder index was calculated based on the formula of (fruit number × scale)/[total fruit number × 4 (the severest scale)].

Electrolyte Leakage Assessment

Electrolyte leakage rate was determined using the method described by Liu et al. (2013) with a slight modification. Twelve disks were collected from eight fruits with a cork-borer (diameter 8 mm) and washed in distilled water three times. The disks were soaked in a glass tube containing 20 mL distilled water and incubated in a water bath shaker at 25°C for 2 h. The initial electric conductivity (C_0) was measured using a conductivity meter. Then the glass tube was boiled for 30 min, cooled in room temperature and total electric conductivity (C_1) was taken. Three biological replications were used for each treatment. Electrolyte leakage rate was calculated using the following equation: $\text{electrolyte leakage}\ (\%) = \left(C_0/C_1\right) \times 100\%$.

Respiration Rate Assessment

For each treatment, fruits were sealed in 4.5 L gas-tight jars at 0°C for 24 h. Gas samples were taken and then CO_2 concentration was measured using a gas analyser (PBI-940437B). Three biological replications were used with six fruits in each treatment (six fruits per repeat). The respiration rate was expressed as L/(kg·h).

Determination of Total Phenolics

The amount of total phenolics in pear peel was determined according to the Folin–Ciocalteu method described by Singleton and Rossi (1965). Two grams frozen pear peel tissues were extracted with 20 mL of 70% acetone and kept for 3 h in the dark. The extracts were centrifuged at 10000 × *g* for 20 min at 4°C. A 0.5 mL aliquot of supernatant was added to the reaction mixture (0.5 mL Folin–Ciocalteu and 0.5 mL of 10% Na_2CO_3). Then the mixture was diluted with distilled water to 10 mL and incubated in a water bath shaker at 25°C for 2 h. The absorbance was measured at 765 nm. The content of total phenolics was calculated from a standard curve developed with gallic acid and expressed as milligram gallic acid per gram fresh tissue (mg/g FW).

Enzyme Assays

Polyphenol oxidase activity was assayed as previously described by Huang et al. (2009) with a slight modification. Peel (4 g) was extracted with 20 mL of 0.1 mol/L sodium phosphate buffer (pH 6.8) containing 5% polyvinylpolypyrrolidone (PVPP). Then the sample was homogenized and centrifuged at 10000 × *g* for 20 min at 4°C. The supernatant was used for analysis of PPO activity as well as POD activity (see below). Supernatants (0.4 mL) were mixed with 1 mL catechol (0.1 mol/L) and 2 mL of sodium phosphate buffer (0.1 mol/L, pH 6.8). The change in absorbance at 420 nm was measured every 30 s for 5 min. One unit of PPO activity was defined as the increase of 0.01 in absorbance per min under assay conditions. PPO activity was expressed as U/g FW.

The POD activity was determined according to Jiang et al. (2002) with some modifications. The reaction mixture contained 500 μL supernatant (see above), 2 mL 0.06% guaiacol in 0.1 mol/L sodium phosphate buffer (pH 6.0) and 1 mL 0.04% H_2O_2. One unit of POD activity was expressed as the change of 0.01 in absorbance at 470 nm per min. The result of POD was expressed as U/g FW.

To determine CAT activity, three grams of frozen tissue were ground with 10 mL sodium phosphate buffer (0.1 mol/L, pH 7.0) containing 5% PVPP. Then the sample was homogenized and centrifuged at 10000 × *g* for 20 min at 4°C. CAT activity was measured using the method of Beers and Sizer (1952) with some modification. 500 μL of supernatant was mixed with 2 mL sodium phosphate buffer (pH 7.0) and 500 μL H_2O_2 (0.1 mol/L). The absorbance was recorded every 30 s for 3 min. One unit of CAT activity was defined as the change of 0.01 in absorbance at 240 nm per min. The CAT activity was expressed as U/g FW.

Ascorbate peroxidase was determined according to Chen and Asada (1989) with modifications. APX was extracted from 3 g of the frozen pear peel tissue with 10 mL sodium phosphate buffer (50 mmol/L, pH 7.0, containing 0.1 mmol/L EDTA-Na2

and 5% PVPP) at 4°C. The homogenate was centrifuged at 10000 × *g* for 20 min at 4°C and the supernatant was used for the APX assay. Then, 500 μL supernatant was added to 3 mL reaction mixture containing 50 mmol/L sodium phosphate buffer (pH 7.0), 0.5 mmol/L ascorbate (extinction coefficient, 2.8 mM^{-1} cm^{-1}) and 0.1 mmol/L H_2O_2. The absorbance of mixture was measured at 290 nm every 10 s for 1 min. One unit of APX was defined as the decrease of 0.01 in absorbance per min at assay conditions. The APX activity was expressed as U/g FW.

Superoxide dismutase was extracted from 3 g of the frozen pear peel tissue with 10 mL sodium phosphate buffer (50 mmol/L, containing 5% PVPP, pH 7.8) at 4°C. The homogenate was centrifuged at 10000 × *g* for 20 min at 4°C and the supernatant was used for the SOD assay. Then 500 μL enzyme extract was mixed with 1 mL sodium phosphate buffer (50 mmol/L, pH 7.8), 0.5 mL methionine (13 mmol/L), 0.5 mL nitroblue tetrazolium (NBT, 75 μmol/L), 10 μmol/L EDTA-Na_2 and 2 μmol/L riboflavin. The mixtures were illuminated under 4000 Lux light for 15 min at 25°C (Li et al., 2013). The absorbance was determined spectrophotometrically at 560 nm. Non-illuminated solutions held in the dark served as a control. One unit of SOD activity was defined as the amount of enzyme that gave half-maximal inhibition of NBT reduction. The SOD activity was expressed as U/g FW.

1, 1-diphenyl-2-picrylhydrazyl (DPPH) Radical Scavenging Activity

The extraction method for 1, 1-diphenyl-2-picrylhydrazyl (DPPH) assay was used according to Gou et al. (2010). Three grams of the frozen pear peel was mixed with 12 mL of 95% ethanol and ultrasonically shaken at 50°C for 30 min. Then, the homogenate was centrifuged at 10000 × *g* for 10 min, and 2 mL supernate was added to 2 mL DPPH methanolic solution (0.2 mmol/L). After incubation for 30 min at room temperature in the dark, the bleaching of DPPH was measured at 517 nm. The DPPH radical scavenging activity was calculated by the formula described by Salta et al. (2010).

Statistical Analysis

All measurements were carried out in three biological replicates. Data were expressed as the mean ± standard deviation. A two-way ANOVA analysis for treatment and time of storage was performed. When the effect of treatment was compared with control, a one-way ANOVA analysis for the treatment effect as run at each time of storage. The mean values were separated using the Tukey HSD test ($p < 0.05$). The data were analyzed with the SPSS 17.0 software (SPSS Inc., Chicago, IL, USA).

RESULTS

Influences of Ethylene Treatment on Peel Browning of 'Huangguan' Pear

Though ethylene was widely used for the ripening of fruits, the present research studied the effects of ethylene treatments on peel browning inhibition of 'Huangguan' pear. We first examined whether ethylene treatments affect fruit quality. Compared with control, ethylene treatments at 50 μL/L exhibited no significant influence on TA, TSS and firmness of fruits stored at 0°C for 100 and 200 days (Supplementary Table S1). Ethylene treatments at different concentrations (0, 5, and 50 μL/L) were performed for investigating its effect on skin browning of 'Huangguan' pear (**Figure 1**). We found that the peel browning mainly occurred at the early storage stage (data not shown), which is consistent with the investigations of many postharvest industries in the production area. Thereby, the browning rate and browning index were examined only on day 20 and 30 post storage. Peel browning index and rate were significantly affected by treatment, storage time and their interaction. Therefore the single effects were reported in **Figure 1**. The results showed that ethylene at various concentrations significantly reduced the browning compared with control when pears were stored at 0°C for 20 and 30 days. Ethylene treatments at 5 and 50 μL/L prevented the browning disorder during 200 days storage (data not shown). Interestingly, compared with control (rapid cooling

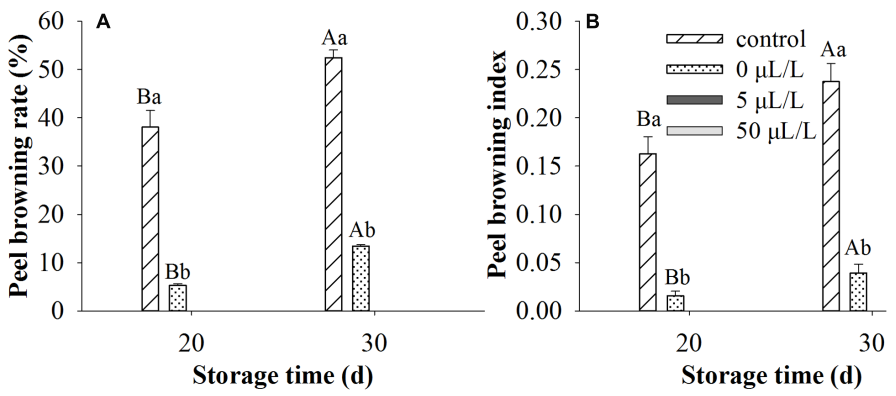

FIGURE 1 | The incidence of brown spot disorder in 'Huangguan' pears treated with ethylene. (A) Peel browning rate (%); **(B)** Peel browning index. Fruits with rapid cooling at 0°C after harvest served as control. Fruits were first treated with various concentrations of ethylene at 20°C for 8 h and then stored at 0°C for evaluations. Bars marked by the same capital letter or lowercase letter indicate that values were not statistically different among sampling days for the same treatment or among treatments for the same sampling day, respectively ($p > 0.05$).

TABLE 1 | Effect of ethylene and 1-MCP on peel browning rate and index of 'Huangguan' pear.

	Peel browning rate		Peel browning index	
	20 days	30 days	20 days	30 days
Control	73.80 ± 9.28^{a}	86.92 ± 7.78^{a}	0.30 ± 0.02^{a}	0.48 ± 0.05^{a}
Air	49.48 ± 13.51^{a}	82.08 ± 15.8^{a}	0.17 ± 0.07^{b}	0.37 ± 0.12^{a}
1-MCP	54.77 ± 2.83^{a}	73.91 ± 6.52^{a}	0.18 ± 0.02^{ab}	0.32 ± 0.08^{a}
Ethylene	6.80 ± 2.18^{b}	16.59 ± 5.33^{b}	0.02 ± 0.01^{c}	0.04 ± 0.01^{b}
1-MCP + Ethylene	64.52 ± 11.8^{a}	83.70 ± 15.13^{a}	0.24 ± 0.09^{ab}	0.45 ± 0.06^{a}

Control: fruits were rapidly cooled at 0°C; Air: fruits were first placed at 20°C for 8 h, then held at 0°C; 1-MCP: fruits were first treated with 1-MCP at 20°C for 8 h, then held at 0°C; Ethylene: fruits were first treated with ethylene (ethephon sachet) at 20°C for 8 h, then held at 0°C; 1-MCP + ethylene: fruits were first treated with 1-MCP and ethylene at 20°C for 8 h, then held at 0°C. During the 8 h treatment, the concentrations of ethylene and 1-MCP were detected at 0.70–1.28 and 1 μL/L, respectively. Data are expressed as mean ± SD (n = 3). Values in a column marked by the same letter were not statistically different (p > 0.05).

at 0°C after harvest), 0 μL/L treatment (fruits were first placed at 20°C for 8 h and then stored at 0°C) also reduced the disorder.

As shown in **Table 1**, the browning index of pears stored at 0°C (rapid cooling) for 20 days reached 0.30. However, stored at 20°C for 8 h prior to cold storage (slow cooling) significantly decreased the browning index to 0.17. Nevertheless, this browning inhibition effect was no longer significant 30 days post storage at 0°C, compared to control. Though slow cooling significantly decreased the browning index, no differences were found in browning rate, indicating that slow cooling delayed the onset of browning, not the occurrence. 1-MCP slightly reduced the browning rate and index, however, no significant difference was existed when compared with control. Ethylene dramatically decreased the incidence of browning. The browning rates were only 6.80 and 16.59% after storage for 20 and 30 days, respectively. When ethylene was applied with 1-MCP, its inhibition efficiency was no longer remarkable (**Table 1** and Supplementary Figure S1).

The effect of ethylene treatment on peel browning was verified (**Figure 2**). The results showed that ethylene treatment at 5 μL/L significantly inhibited the browning. Thereby, ethylene concentration at 5 μL/L was used in the following experiment to investigate the physiological functions of ethylene on 'Huangguan' pear.

Membrane Permeability

To understand the physiological bases for the ethylene inhibition effects on the peel browning, we first measured electrolyte leakage, an indicator of the change of pear peel fruit in membrane permeability. Given that the effect of treatment, storage time as well as their interaction were significant for membrane permeability, therefore the single effects were reported in **Figure 3**. Electrolyte leakage in the control and treatments was sharply increased during the first 5 days of storage and then slightly decreased, which was still higher than 0 day (**Figure 3**). After 10 days storage, no significant difference was found between the control and air treatment in the electrolyte leakage. However, the electrolyte leakage in the pear fruit treated with ethylene changed slowly during the whole storage period. The difference in electronic conductivity among

FIGURE 2 | Effect of ethylene on the incidence of spots brown in 'Huangguan' pear after 30 days storage at 0°C. Fruits with rapid cooling at 0°C after harvest served as control. Fruits were treated with air or ethylene (5 μL/L) at 20°C for 8 h and then stored at 0°C for analysis.

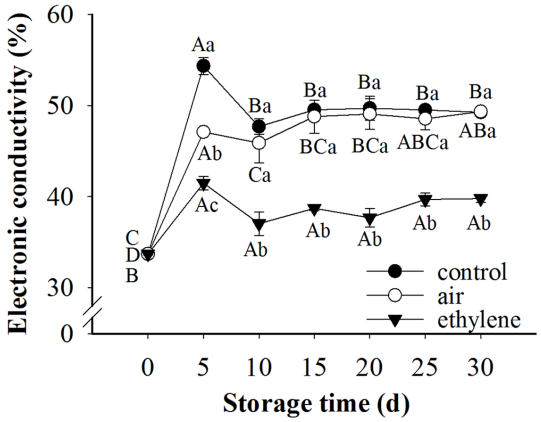

FIGURE 3 | Effect of ethylene on the electrolyte leakage rate of 'Huangguan' pear peel. Fruits with rapid cooling at 0°C after harvest were served as control. Fruits were first treated with air and ethylene (5 μL/L) at 20°C for 8 h and then stored at 0°C for evaluations. Values marked by the same capital letter or lowercase letter indicate that values were not statistically different among sampling days for the same treatment or among treatments for the same sampling day, respectively ($p > 0.05$).

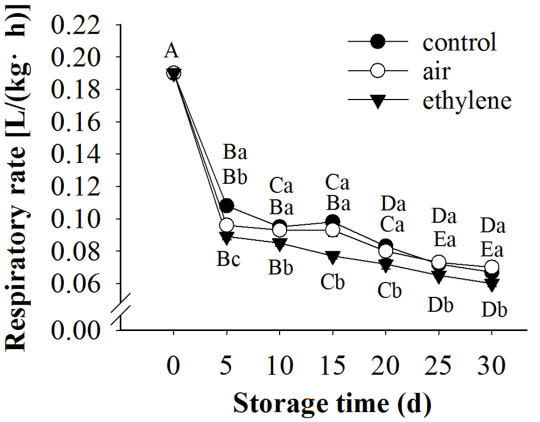

FIGURE 4 | Effect of ethylene on the respiration rate of 'Huangguan' pear. Fruits with rapid cooling at 0°C after harvest were served as control. Fruits were first treated with air and ethylene (5 μL/L) at 20°C for 8 h and then stored at 0°C for analysis. Values marked by the same capital letter or lowercase letter indicate that values were not statistically different among sampling days for the same treatment or among treatments for the same sampling day, respectively ($p > 0.05$).

treatments after 5 days storage was attributed to the difference in treatment since the effect of storage time on electronic conductivity was slight. Compared with control and air treated fruits, ethylene-treated fruits exhibited much lower electronic conductivity, indicating that the electrolyte leakage caused by the disruption of membrane permeability was dramatically prevented by ethylene.

Respiration Rate of Pear Fruit

The respiration rate of fruits was sharply decreased during the first 5 days of storage, and the decreasing trend slowed afterward (**Figure 4**). The respiration rate was significantly affected by treatment and storage time as well as their interaction. Ethylene application significantly inhibited the respiration rate, compared to the control and air treatment.

Total Phenolics Content and PPO Activity

Total phenolics content and PPO activity in pears during cold storage were significantly affected by treatment, storage time and their interaction (**Figure 5**). Significant differences were found between ethylene-treated and non-ethylene-treated pears in total phenolics content and PPO activity, except for total phenolics content in air-treated pears at day 5. Compared with control, ethylene at 0 μL/L showed no effect on preventing the loss of phenolics, except for day 10. Ethylene maintained higher content of phenolics during the 30 days storage, whereas the rapid cooling control and 0 μL/L ethylene (air) decreased the contents. Fruits in all three groups exhibited similar patterns in PPO activity, which was increased during the whole storage time. However, ethylene treatments significantly prevented the increase of PPO activity (**Figure 5**).

POD, CAT, APX and SOD Activities

Peroxidase, CAT, APX and SOD are considered as antioxidant enzymes, participate in the defense of fruit against stresses through scavenging free radicals. The ANOVA result showed that treatment, storage time and their interaction were significant for POD, CAT and APX as well as SOD. The changes in the activity of these enzymes in fruits treated with ethylene and air were demonstrated in **Figure 6**. Peroxidase activity in all samples was increased during cold storage. However, ethylene treatment showed strong inhibition on the increase of POD activity (**Figure 6A**). Catalase activity was increased at the early stage of storage and then decreased thereafter. Fruits without ethylene treatment (rapid cooling) and treated with air (slow cooling) only showed distinctively lower levels of CAT activity than fruits treated with 5 μL/L ethylene (**Figure 6B**). Ascorbate peroxidase activity in the fruits treated with ethylene was increased at the early stage of storage and then slightly decrease (**Figure 6C**), and was remarkably higher than that in control and air-treated fruits. APX activity in untreated fruits was stable during the first 15 days storage and dramatically decreased thereafter. Ethylene treatments resulted in the induction of SOD activity (**Figure 6D**). In general, SOD activity in ethylene-treated fruit peel was remarkably higher than that in the control and air-treated fruit. Interestingly, SOD activity in air-treated fruits was also significantly higher than the control ($p < 0.05$).

DPPH Radical Scavenging Activity

The radical scavenging activity in the pear samples was decreased with the extension of storage (**Figure 7**). During the whole storage, the radical scavenging activity in the ethylene-treated fruits was over 90%, and remarkably higher than the control and air treatment. After 5 days storage, no significant difference in

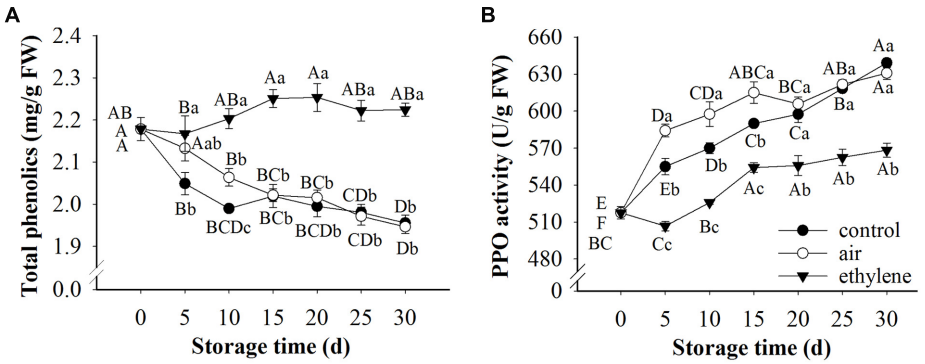

FIGURE 5 | Effects of ethylene on pear phenolic metabolism during the storage at 0°C. (A) Total phenolic content; **(B)** PPO activity. Fruits with rapid cooling at 0°C after harvest were served as control. Fruits were first treated with air and ethylene (5 μL/L) at 20°C for 8 h and then stored at 0°C for analysis. Values marked by the same capital letter or lowercase letter indicate that values were not statistically different among sampling days for the same treatment or among treatments for the same sampling day, respectively ($p > 0.05$).

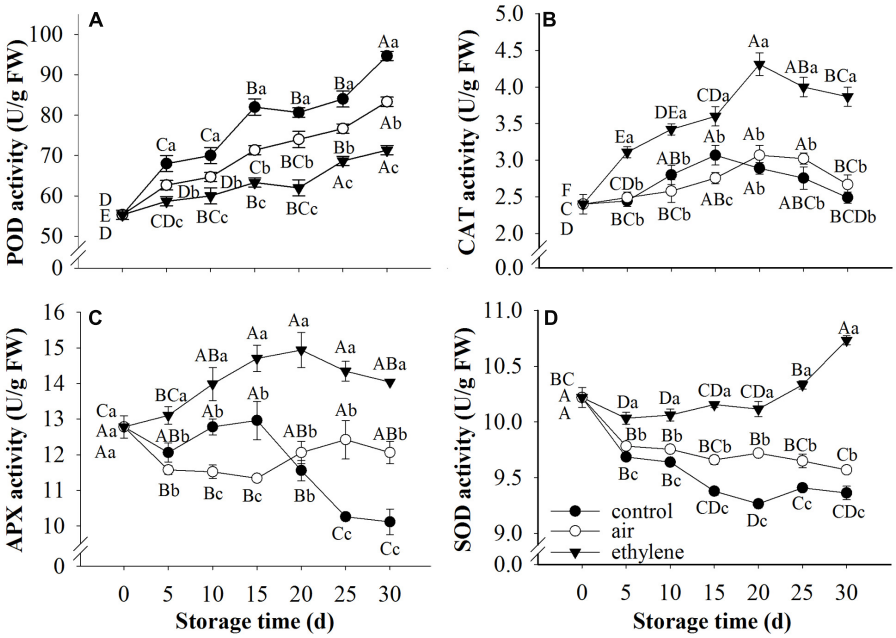

FIGURE 6 | Effects of ethylene on the activities of antioxidant enzymes. (A) POD activity; **(B)** CAT activity; **(C)** APX activity; **(D)** SOD activity. Fruits with rapid cooling at 0°C after harvest were served as control. Fruits were first treated with air and ethylene (5 μL/L) at 20°C for 8 h and then stored at 0°C for analysis. Values marked by the same capital letter or lowercase letter indicate that values were not statistically different among sampling days for the same treatment or among treatments for the same sampling day, respectively ($p > 0.05$).

radical scavenging activity was observed between the control and air treatment ($p > 0.05$).

DISCUSSION

As a commonly occurred physiological disorder in fruits and vegetables, browning disorder has been heavily studied (Cantos et al., 2002; Franck et al., 2007; Chung and Moon, 2009; Gong et al., 2010). The present study demonstrated that postharvest "Huangguan" pear fruits were susceptible to brown spot disorder a few days after storage at 0°C (**Table 1** and **Figure 1**). Though ethylene was believed to be responsible for the ripening and senescence of fruits, the present study revealed that application of exogenous ethylene inhibited the peel browning of 'Huangguan' pear. Most of all, compared with control, no change in edible quality (TA, TSS and firmness) in the fruits treated with ethylene were observed. Overall, ethylene showed no negative influence on the edible quality (Supplementary Table S1). Similarly, Bower et al. (2003) reported that after 3-month cold

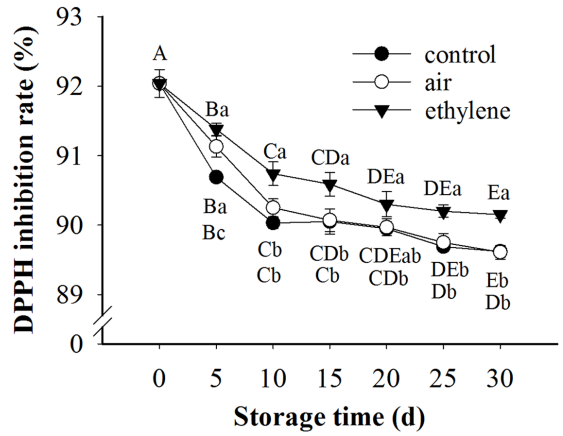

FIGURE 7 | Effect of ethylene on DPPH scavenging activity in 'Huangguan' pear. Fruits with rapid cooling at 0°C after harvest were served as control. Fruits were first treated with air and ethylene (5 μL/L) at 20°C for 8 h and then stored at 0°C for analysis. Values marked by the same capital letter or lowercase letter indicate that values were not statistically different among sampling days for the same treatment or among treatments for the same sampling day, respectively ($p > 0.05$).

storage and 4 days ripening at 20°C, pears treated with various concentrations of ethylene exhibited almost the same firmness to control.

Ethylene at the concentrations of 5 and 50 μL/L effectively prevented the browning disorder of fruits during 200 days storage (data not shown). Compared with control (rapid cooling at 0°C after harvest), 0 μL/L treatment also decreased the disorder. The inhibiting effect of 0 μL/L treatment may be due to delay cooling, since fruits treated with ethylene were placed at 20°C for 8 h before being stored at 0°C. Our previous research showed that delayed cooling can reduce the browning disorder of 'Huangguan' pear, though the effects are limited (Wang and Wang, 2011).

The inhibition of 1-MCP on the browning of fruits is widely reported (Argenta et al., 2003; Fu et al., 2007). The core browning of 1-MCP treated 'Yali' pear was reduced by 91% after 100 days storage (Fu et al., 2007). They assumed that the beneficial effect of 1-MCP on reducing physiological disorder may be attributed to the increase in antioxidant potential as well as the inhibition of ethylene production and respiration rate. However, this study showed that the browning inhibition of 1-MCP on 'Huangguan' pear was not significant (**Table 1** and Supplementary Figure S1). The differences between studies may be due to the differences in pear varieties and the concentration of 1-MCP applied, since it was reported that the 1-MCP-induced response was dose-dependent (Argenta et al., 2003).

Interestingly, our data demonstrated that the presence of ethylene inhibited the occurrence of peel browning of 'Huangguan' pear up to 200 days of storage (Supplementary Figure S1). However, it was reported that low levels of ethylene (0.01 and 1 μL/L) aggravated the flesh and core browning of Japanese pears (Szczerbanik et al., 2007). The contradiction between studies may result from the amounts and duration of ethylene as well as the pear cultivars used. In the present study, 'Huangguan' pears were treated by 5 or 50 μL/L ethylene for 8 h before cold storage, whereas Szczerbanik et al. (2007) treated 'Nijisseiki' pear with <0.005, 0.01, 0.1 and 1 μL/L ethylene for 26 weeks. Moreover, the incidence of physiological disorder (such as browning) of 'Bartlett' pear was increased after treated by ethylene (0, 1, 5 and 10 μL/L) for 3 months (Bower et al., 2003). These results indicated that when ethylene was used for browning inhibition, the treatment time should be well controlled, otherwise adverse results may be observed.

Due to its competitive binding to ethylene receptors with ethylene, 1-MCP was widely used to alleviate the ripening and senescence of fruits caused by ethylene (Argenta et al., 2003; Liu et al., 2013). It is worth noting that the browning inhibition effect of ethylene was eliminated when ethylene was applied with 1-MCP at the same time (**Table 1** and Supplementary Figure S1). This may be attributed to the competitive binding of 1-MCP to ethylene receptor, which affected the transduction of ethylene signal and thereby influenced the response of ethylene (Morgan and Drew, 1997).

Membrane integrity plays an important role in prevention of the occurrence of browning, since it separates the substrates from enzymes (Kou et al., 2015). Moreover, Duan et al. (2011) demonstrated that the electrolyte leakage was alleviated while the compartmentation of enzymes and substrate was maintained by pure oxygen treatment. Electrolyte leakage rate is considered as an indirect measure of membrane damage (Liu and Wang, 2012). The higher the electrolyte leakage rate is, the more the membrane damage. The disruption of membrane integrity was associated with the browning of mushroom (Liu and Wang, 2012). Also, Cantos et al. (2002) found that maintaining membrane integrity was potentially an important approach to control browning. In the present research, the electronic conductivity of fruits was significantly increased after 5 days storage at 0°C. This may be attributed to the stress response of fruits to cold storage, since 'Huangguan' pear is very sensitive to cold. Ethylene treatment obviously restrained the increase of the electrolyte leakage rate and maintained the integrity of the cell membrane, (**Figures 1–3**). The lower electronic conductivity of ethylene treated fruits indicated the improved defense capacity of fruits to stresses. These results revealed that ethylene increased the defense capacity of fruits and thereby inhibited the peel browning which may be caused by chilling injury. This was consistent with previous reports that ethylene was involved in chilling injury and recovery of fruits (Yang and Hoffman, 1984; Morgan and Drew, 1997).

Higher respiration rate triggers a faster overall deterioration and metabolic activity (Chung and Moon, 2009). Endogenous or exogenous ethylene is usually considered to be associated with high respiration rate. However, in the present study, the respiration rate of fruits treated with ethylene was significantly lower than that in the control and air-treated fruits (**Figure 4**). This may be attributed to the effect of ethylene to the internal gas partial pressure, which could influence the respiration rate and the antioxidant system (Franck et al., 2007). Moreover, it was reported that application of ethylene to pears increased the

internal level of ethylene and CO_2, but decreased the level of O_2 (Szczerbanik et al., 2007).

Phenolics and PPO are believed to be associated with enzymatic browning. Ethylene treatment maintained the high content of phenolics and inhibited the activity of PPO, thereby preventing the incurrence of browning. Similarly, Kou et al. (2015) reported that pear browning was inhibited by 2% $CaCl_2$ or 1% pullulan, which delayed the degradation of phenolics and inhibited PPO activity. The higher content of phenolics in ethylene treated fruits may be due to the induction of ethylene to PAL, which is the initial rate controlling enzyme in phenolic synthesis (Ke and Saltveit, 1989). To some extent, ethylene induced the defense response of fruits to stress, leading to the synthesis of phenolics. Previous research also found that exposure lettuce to 10 μL/L ethylene induced the production of individual phenolic compounds (Tomás-Barberán et al., 1997). The inhibition of ethylene on PPO activity may be due to its influence on Cu^{2+}, which is contained in the active center of PPO (Kou et al., 2015). However, further study needs to be done to reveal the mechanism of ethylene inhibiting PPO activity. Pear fruits treated with ethylene exhibited higher DPPH radical scavenging activity than the control and air treatment. The higher antioxidant activity may be due to the higher content of phenolics in ethylene-treated fruits, since the phenolics content was strongly correlated with antioxidant activity (Malenèič et al., 2007; Ma and Huang, 2014). Moreover, the antioxidant capacity of banana fruit was promoted by the accumulation of phenolic compounds (Wang et al., 2014).

Under normal circumstances, reactive oxygen species (ROS) are produced during cellular functional activity and participate in cellular metabolism (Lü et al., 2010). Usually, the organisms scavenge excessive radicals and keep the balance of ROS in cells through the enzymatic and non-enzymatic antioxidant systems. However, under various stresses, ROS may accumulate, resulting in the breaking of the balance and inducing the occurrence of physiological disorders (Valko et al., 2006; Ma et al., 2014). The accumulation of ROS may lead to the peroxidation of membrane lipid, thereby disrupting the membrane integrity and, resulting in the occurrence of browning. Antioxidant enzymes such as POD, SOD, CAT and APX play important roles in scavenging ROS. SOD catalyzes the superoxide radical to H_2O_2 while POD, CAT and APX responsible for the elimination of H_2O_2 (Duan et al., 2011; Liu et al., 2013). In this study, severe browning was observed in pear fruits without treatment. Due to the sensitivity of 'Huangguan' pear to cold, the peel browning of fruits may be caused by chilling, which is a severe stress for fruits. Accompanied with browning, the activity of SOD and APX were decreased with storage, while CAT was first increased and followed by a slight decrease (**Figure 6**). Results from the electronic conductivity showed that the membrane integrity was disrupted since the electronic conductivity significantly increased after 5 days storage (**Figure 3**). All together, these results indicated that browning of 'Huangguan' pear resulted from the accumulation of ROS and the decreasing activity of antioxidant enzymes. This is in agreement with previous studies that the membrane lipid peroxidation induced by the decreased scavenging activity and accumulation of free radicals contributes to the skin browning of 'Huangguan' pear (Kou et al., 2015). Results from this study demonstrated that ethylene treatment maintained the high activity of SOD, CAT and APX, stabilized the membrane integrity and eventually prevented the peel browning of 'Huangguan' pear fruits. We concluded that the browning inhibition of ethylene on 'Huangguan' pear was achieved by improving the antioxidant defense systems of fruits. Similarly, studies reported that exposure to pure oxygen induced the activities of SOD, CAT and APX, alleviated the lipid peroxidation and kept membrane integrity, thereby inhibited the browning of litchi fruit (Duan et al., 2011; Liu et al., 2013). Moreover, the inhibition of browning is concomitant with higher phenolic compounds content, lower PPO activity, and higher CAT and SOD activities (Kou et al., 2015). Interestingly, the similarity between ethylene and pure oxygen treatments was that they both improved the enzymatic antioxidant defense system of fruits by affecting the activity of antioxidant enzymes (SOD, APX and CAT). Pure oxygen treatment may promote ethylene production through enhancing of ACC oxidase activity, implying that they may share a common mode of action via ethylene pathway.

CONCLUSION

Ethylene treatment enhanced the antioxidant defense capacity of fruits to stress. Fruits treated by ethylene exhibited higher phenolic content and DPPH radical scavenging activity, higher activity of antioxidant enzymes (SOD, CAT and APX) and lower PPO activity and electrolyte leakage rate. These factors were evidently responsible for the lower browning incidence of ethylene-treated 'Huangguan' pears.

AUTHOR CONTRIBUTIONS

QW and C-ZJ conceived the concept. MY, JW, and YM performed the experiments and data analyses. YM, QW, and C-ZJ wrote the manuscript. C-ZJ extensively revised the manuscript. All authors read and approved the manuscript.

ACKNOWLEDGMENTS

This work was supported by grants from National Science and Technology Plan for Rural Areas in 12th Five-Year, the People's Republic of China (2015BAD16B03) and from the development of safe postharvest products for quality maintenance of fresh fruits and vegetables, Major Innovation of Applied Agricultural Technology, Shandong Province.

SUPPLEMENTARY MATERIAL

The Supplementary Material for this article can be found online at: http://journal.frontiersin.org/article/10.3389/fpls.2016.02029/full#supplementary-material

REFERENCES

Argenta, L. C., Fan, X. T., and Mattheis, J. P. (2003). Influence of 1-methylcyclopropene on ripening, storage life, and volatile production by d'Anjou cv. pear fruit. *J. Agric. Food Chem.* 51, 3858–3864. doi: 10.1021/jf034028g

Beers, R. F., and Sizer, I. W. (1952). A spectrophotometric method for measuring the breakdown of hydrogen peroxide by catalase. *J. Biol. Chem.* 195, 133–140.

Bower, J. H., Blasi, W. V., and Mitcham, E. J. (2003). Effect of ethylene in the storage environment on quality of 'Bartlett pears.' *Postharvest Biol. Technol.* 28, 371–379. doi: 10.1016/S0925-5214(02)00210-7

Candan, A. P., Graell, J., and Larrigaudiere, C. (2008). Roles of climacteric ethylene in the development of chilling injury in plums. *Postharvest Biol. Technol.* 47, 107–112. doi: 10.1016/j.postharvbio.2007.06.009

Cantos, E., Tudela, J. A., Gil, M. I., and Espín, J. C. (2002). Phenolic compounds and related enzymes are not rate-limiting in browning development of fresh-cut potatoes. *J. Agric. Food Chem.* 50, 3015–3023. doi: 10.1021/jf011 6350

Chen, G. X., and Asada, K. (1989). Ascorbate peroxidase in tea leaves: occurrence of two isozymes and the differences in their enzymatic and molecular properties. *Plant Cell Physiol.* 30, 987–998.

Chung, H.-S., and Moon, K.-D. (2009). Browning characteristics of fresh-cut 'Tsugaru' apples as affected by pre-slicing storage atmospheres. *Food Chem.* 114, 1433–1437. doi: 10.1016/j.foodchem.2008.11.027

Dong, Y., Guan, J.-F., Ma, S.-J., Liu, L.-L., Feng, Y.-X., and Cheng, Y.-D. (2015). Calcium content and its correlated distribution with skin browning spot in bagged Huangguan pear. *Protoplasma* 252, 165–171. doi: 10.1007/s00709-014-0665-5

Duan, X., Liu, T., Zhang, D., Su, X., Lin, H., and Jiang, Y. (2011). Effect of pure oxygen atmosphere on antioxidant enzyme and antioxidant activity of harvested litchi fruit during storage. *Food Res. Int.* 44, 1905–1911. doi: 10.1016/j.foodres.2010.10.027

Franck, C., Lammertyn, J., Ho, Q. T., Verboven, P., Verlinden, B., and Nicolai, B. A. (2007). Browning disorders in pear fruit. *Postharvest Biol. Technol.* 43, 1–13. doi: 10.1016/j.postharvbio.2006.08.008

Fu, L., Cao, J., Li, Q., Lin, L., and Jiang, W. (2007). Effect of 1-methylcyclopropene on fruit quality and physiological disorders in Yali pear (*Pyrus bretschneideri* Rehd.) during storage. *Food Sci. Technol. Int.* 13, 49–54. doi: 10.1177/1082013207075600

Galvis-Sánchez, A. C., Fonseca, S. C., Gil-Izquierdo, A., Gil, M. I., and Malcata, F. X. (2006). Effect of different levels of CO2 on the antioxidant content and the polyphenol oxidase activity of 'Rocha' pears during cold storage. *J. Sci. Food Agric.* 86, 509–517. doi: 10.1002/jsfa.2359

Gong, X., Guan, J., and Zhang, J. (2010). Effects of postharvest 1-MCP and calcium treatments on the quality and skin browning spot incidence of Huangguan pear fruit. *Acta Hortic. Sin.* 37, 375–382.

Gou, M., Liu, L., and Zhang, C. (2010). Determination of antioxidant activity in 26 plants by DPPH method. *Food Ferment. Ind.* 36, 148–150.

Guan, J., Ji, H., Feng, Y., Li, L., Sun, Y., and Si, J. (2005). The correlation of peel browning spot with phenolics metabolism in huangguan pears. *Acta Agric. Boreali Sin.* 20, 80–83.

Guan, J., Ji, H., Feng, Y., Sun, Y., Liu, L., Zhang, Z., et al. (2008). Effects of fruit-bag kinds on browning spot and nutrition of Ca,Mg and K in Huangguan pear. *J. Anhui Agric. Sci.* 36, 1758–1759. ,1762,

Huang, C., Yu, B., Teng, Y., Su, J., Shu, Q., Cheng, Z., et al. (2009). Effects of fruit bagging on coloring and related physiology, and qualities of red Chinese sand pears during fruit maturation. *Sci. Hortic.* 121, 149–158. doi: 10.1016/j.scienta.2009.01.031

Jiang, A. L., Tian, S. P., and Xu, Y. (2002). Effects of controlled atmospheres with high-O2 or high-CO2 concentrations on postharvest physiology and storability of "Napoleon" sweet cherry. *Acta Bot. Sin.* 44, 925–930.

Ke, D., and Saltveit, M. E. (1989). Wound-induced ethylene production, phenolic metabolism and susceptibility to russet spotting in iceberg lettuce. *Physiol. Plant.* 76, 412–418. doi: 10.1111/j.1399-3054.1989.tb06212.x

Kou, X., Wu, M., Li, L., Wang, S., Xue, Z., Liu, B., et al. (2015). Effects of CaCl2 dipping and pullulan coating on the development of brown spot on 'Huangguan' pears during cold storage. *Postharvest Biol. Technol.* 99, 63–72. doi: 10.1016/j.postharvbio.2014.08.001

Lafuente, M. T., Alferez, F., and Romero, P. (2014). Postharvest ethylene conditioning as a tool to reduce quality loss of stored mature sweet oranges. *Postharvest Biol. Technol.* 94, 104–111. doi: 10.1016/j.postharvbio.2014.03.011

Lammertyn, J., Aerts, M., Verlinden, B. E., Schotsmans, W., and Nicolai, B. M. (2000). Logistic regression analysis of factors influencing core breakdown in 'Conference' pears. *Postharvest Biol. Technol.* 20, 25–37. doi: 10.1016/S0925-5214(00)00114-9

Li, F., Zhang, X., Song, B., Li, J., Shang, Z., and Guan, J. (2013). Combined effects of 1-MCP and MAP on the fruit quality of pear (*Pyrus bretschneideri* Reld cv. Laiyang) during cold storage. *Sci. Hortic.* 164, 544–551.

Liu, R., Lai, T., Xu, Y., and Tian, S. (2013). Changes in physiology and quality of Laiyang pear in long time storage. *Sci. Hortic.* 150, 31–36. doi: 10.1016/j.scienta.2012.10.017

Liu, Z., and Wang, X. (2012). Changes in color, antioxidant, and free radical scavenging enzyme activity of mushrooms under high oxygen modified atmospheres. *Postharvest Biol. Technol.* 69, 1–6. doi: 10.1016/j.postharvbio.2012.02.008

Lü, J. M., Lin, P. H., Yao, Q. Z., and Chen, C. Y. (2010). Chemical and molecular mechanisms of antioxidants: experimental approaches and model systems. *J. Cell. Mol. Med.* 14, 840–860. doi: 10.1111/j.1582-4934.2009.00897.x

Ma, Y., and Huang, H. (2014). Characterisation and comparison of phenols, flavonoids and isoflavones of soymilk and their correlations with antioxidant activity. *Int. J. Food Sci. Technol.* 49, 2290–2298. doi: 10.1111/ijfs.12545

Ma, Y., Liu, S., and Huang, H. (2014). Alleviation effect of heat-treated and in vitro gastrointestinal digested soymilks on AAPH-induced oxidative stress in human erythrocytes. *Food Res. Int.* 66, 228–234. doi: 10.1016/j.foodres.2014.09.022

Malenèič, D., Popovič, M., and Miladinovič, J. (2007). Phenolic content and antioxidant properties of soybean (*Glycine max* (L.) Merr.) seeds. *Molecules* 12, 576–581. doi: 10.3390/12030576

Malerba, M., Crosti, P., and Cerana, R. (2010). Ethylene is involved in stress responses induced by fusicoccin in sycamore cultured cells. *J. Plant Physiol.* 167, 1442–1447. doi: 10.1016/j.jplph.2010.05.014

Morgan, P. W., and Drew, M. C. (1997). Ethylene and plant responses to stress. *Physiol. Plant.* 100, 620–630. doi: 10.1034/j.1399-3054.1997.1000325.x

Salta, J., Martins, A., Santos, R. G., Neng, N. R., Nogueira, J. M. P., Justino, J., et al. (2010). Phenolic composition and antioxidant activity of Rocha pear and other pear cultivars – A comparative study. *J. Funct. Foods* 2, 153–157. doi: 10.1016/j.jff.2010.02.002

Singleton, V. L., and Rossi, J. A. (1965). Colorimetry of total phenolics with phosphomolybdic-phosphotungstic acid reagents. *Am. J. Enol. Vitic.* 16, 144–158.

Szczerbanik, M. J., Scott, K. J., Paton, J. E., and Best, D. J. (2007). Susceptibility of Japanese pears to low concentrations of ethylene during storage. *Aust. J. Exp. Agric.* 47, 1480–1483. doi: 10.1071/EA06186

Tomás-Barberán, F. A., Loaiza-Velarde, J., Bonfanti, A., and Saltveit, M. E. (1997). Early wound- and ethylene-induced changes in phenylpropanoid metabolism in harvested lettuce. *J. Am. Soc. Hort. Sci.* 122, 399–404.

Valko, M., Rhodes, C. J., Moncol, J., Izakovic, M., and Mazur, M. (2006). Free radicals, metals and antioxidants in oxidative stress-induced cancer. *Chem. Biol. Interact.* 160, 1–40. doi: 10.1016/j.cbi.2005.12.009

Wang, J., and Wang, Q. (2011). Effect of cold conditioning on postharvest fruit quality of Huangguan pear. *Food Ferment. Ind.* 37, 235–239.

Wang, Y. (1998). The breeding and application of the middle season ripening, scab resistant new pear variety-Huangguan pear. *J. Hebei Agric. Sci.* 2, 40–42.

Wang, Y., Luo, Z., Huang, X., Yang, K., Gao, S., and Du, R. (2014). Effect of exogenous gamma-aminobutyric acid (GABA) treatment on chilling injury and antioxidant capacity in banana peel. *Sci. Hortic.* 168, 132–137. doi: 10.1016/j.scienta.2014.01.022

Xing, D. D., Mu, W. L., and Wang, Q. G. (2013). Effect of methyl jasmonate on peel browning of postharvest Huangguan pear. *Food Ferment. Technol.* 49:29.

Yang, S. F., and Hoffman, N. E. (1984). Ethylene biosynthesis and its regulation in higher plants. *Annu. Rev. Plant Physiol.* 35, 155–189. doi: 10.1146/annurev.pp.35.060184.001103

Zhou, H. W., Dong, L., Ben-Arie, R., and Lurie, S. (2001). The role of ethylene in the prevention of chilling injury in nectarines. *J. Plant Physiol.* 158, 55–61. doi: 10.1078/0176-1617-00126

Conflict of Interest Statement: The authors declare that the research was conducted in the absence of any commercial or financial relationships that could be construed as a potential conflict of interest.

frontiers in Plant Science

ORIGINAL RESEARCH
published: 15 February 2017
doi: 10.3389/fpls.2017.00195

Comparative Transcriptomic Analysis Reveals That Ethylene/H_2O_2-Mediated Hypersensitive Response and Programmed Cell Death Determine the Compatible Interaction of Sand Pear and *Alternaria alternata*

Hong Wang[1], *Jing Lin*[1]*, *Youhong Chang*[1] and *Cai-Zhong Jiang*[2,3]*

[1] Institute of Horticulture, Jiangsu Academy of Agricultural Sciences/Jiangsu Key Laboratory for Horticultural Crop Genetic Improvement, Nanjing, China, [2] Department of Plant Sciences, University of California at Davis, Davis, CA, USA, [3] Crops Pathology and Genetics Research Unit, United States Department of Agriculture, Agricultural Research Service, Davis, CA, USA

A major restriction on sand pear (*Pyrus pyrifolia*) production is black spot disease caused by the necrotrophic fungus *Alternaria alternata*. However, the pear response mechanism to *A. alternata* is unknown at the molecular level. Here, host responses of a resistant cultivar Cuiguan (CG) and a susceptible cultivar Sucui1 (SC1) to *A. alternata* infection were investigated. We found that the primary necrotic lesion formed at 1 dpi and the expansion of lesions was aggressive in SC1. Data from transcriptomic profiles using RNA-Seq technology identified a large number of differentially expressed genes (DEGs) between CG and SC1 in the early phase of *A. alternata* infection. K-mean cluster and Mapman analysis revealed that genes involved in ethylene (ET) biosynthesis and ET signaling pathway, such as ACS, ACOs, and ERFs, and in hypersensitive response (HR) and programmed cell death (PCD) were significantly enriched and up-regulated in the susceptible cultivar SC1. Conversely, genes involved in response to hydrogen peroxide and superoxide were differentially up-regulated in the resistant cultivar CG after inoculation with the fungus. Furthermore, ET levels were highly accumulated in SC1, but not in CG. Higher activities of detoxifying enzymes such as catalases were detected in CG. Our results demonstrate that the ET-/H_2O_2-mediated PCD and detoxifying processes play a vital role in the interaction of pear and *A. alternata.*

Keywords: sand pear, *Alternaria alternata* (Fr.) Keissler, hypersensitive response, programmed cell death, ethylene, hydrogen peroxide, antioxidant enzyme

OPEN ACCESS

Edited by:
Antonio Ferrante, University of Milan, Italy

Reviewed by:
Lorella Navazio, University of Padua, Italy
Andrew Macnish, Department of Agriculture and Fisheries, Australia

***Correspondence:**
Jing Lin
lj84390224@126.com
Cai-Zhong Jiang
cjiang@ucdavis.edu

Specialty section:
This article was submitted to Plant Physiology, a section of the journal Frontiers in Plant Science

Received: *21 October 2016*
Accepted: *31 January 2017*
Published: *15 February 2017*

Citation:
Wang H, Lin J, Chang Y and Jiang C-Z (2017) Comparative Transcriptomic Analysis Reveals That Ethylene/H_2O_2-Mediated Hypersensitive Response and Programmed Cell Death Determine the Compatible Interaction of Sand Pear and Alternaria alternata. Front. Plant Sci. 8:195. doi: 10.3389/fpls.2017.00195

INTRODUCTION

In plant-pathogen interactions, plant response to pathogens is based on two main mechanisms including microbe-associated molecular patterns (MAMPs) and the adaptive immune system (Bonardi et al., 2011). The action of plant resistance (R) genes belongs to the adaptive immune system (Bonardi et al., 2011). After recognition of the pathogen, the plant initiates defense strategies against pathogen attack. These include the hypersensitive response (HR) and the programmed cell death (PCD) at the infection site (Greenberg and Yao, 2004), followed by the complicated defense response and metabolic changes in the surrounding tissues and distal un-infected parts (La Camera et al., 2004). One of the earliest events in the HR is a burst of reactive oxygen species (ROS) including superoxide (O_2^-), hydroxyl radical (OH^-) and subsequent accumulation of H_2O_2 (Lamb and Dixon, 1997). The infection of an avirulent *Pseudomonas syringae* strain stimulated the production of O_2^- and H_2O_2, and induced defense-related gene expression and cell death in Arabidopsis (Alvarez et al., 1998). H_2O_2 accumulation associated with the HR was detected when lettuce cells were inoculated with *P. syringae* pv *phaseolicola* (Bestwick et al., 1997). Whether ROS plays positive or negative roles during the HR is dependent on the type of pathogen. For example, in the Arabidopsis-*P. syringae* system, the accumulation of H_2O_2 induces cell death and restricts lesion development (Alvarez et al., 1998). However, in necrotrophic pathogen systems, such as *Botrytis cinerea* and *Sclerotinia sclerotiorum*, pathogens proliferate on dead tissues caused by the generation of oxidative burst (Govrin and Levine, 2000).

Plant hormones such as salicylic acid (SA), jasmonic acid (JA), ethylene (ET), and ROS, play key roles in PCD, as well as in the activation of plant defense responses. SA is required in plant resistance associated with the hypersensitive cell death during plant–pathogen interactions (Greenberg, 1997; Alvarez, 2000). At infection sites, SA binds to NON-EXPRESSOR OF PATHOGENESIS-RELATED GENES 3 (NPR3; Fu et al., 2012) and mediates the degradation of the cell-death suppressor (NPR1), therefore facilitating the occurrence of PCD and local effector-triggered immunity (ETI; Gust and Nurnberger, 2012). NPR1 interacting with TGAs, bZIP transcription factors, directly promotes the expression of pathogenesis-related (PR) proteins such as PR1, BGL2, and PR5 (Glazebrook, 2001), and therefore limits growth of pathogens and contributes to resistance. Several studies suggest that SA-mediated signaling pathways are involved in resistance to biotrophic or hemibiotrophic pathogens (McDowell and Dangl, 2000). For example, Pto-mediated resistance against the hemibiotrophic pathogen *P. syringae* is SA-dependent in tomato (Ekengren et al., 2003).

Pathogens also elicit JA and ET pathways. Unlike the SA pathway, a JA/ET-dependent defense provides strong resistance against necrotrophic pathogens that benefit from host cell death (Grant and Lamb, 2006). JA and ET are considered to act synergistically in response to pathogens and activate defense-related gene expression in Arabidopsis (Thomma et al., 1999). ETHYLENE RESPONSE FACTOR 1 (ERF1) integrates ET and JA signaling pathways to regulate the expression of downstream defense-related genes (Lorenzo et al., 2003). Plant defense-related genes such as *Defensin* (*PDF1*) or *proteinase inhibitors I* and *II* (*PI I* and *PI II*) are known as indicators of the ET and JA responses (Penninckx et al., 1996). ET is also involved in the regulation of both the timing and degree of PCD during plant-pathogen interactions (Greenberg, 1997; Wang H. et al., 2013). The initiation of HR results in a large burst of ET (Boller, 1991). In addition, ET acts in concert with SA as a positive regulator of cell death progression in an Arabidopsis *vad1* (*vascular associated death 1*) mutant (Bouchez et al., 2007). Transgenic petunia plants over-expressing the *A. thaliana* ET receptor mutant *ethylene-insensitive1-1* (*etr1-1*) have inhibited expression of senescence-associated genes *PhCP8* and *PhCP10*, thereby retarding the senescence caused by *B. cinerea* infection (Wang H. et al., 2013). The role of an ET-dependent pathway has been elucidated in AAL-toxin induced cell death (Moore et al., 1999). However, whether ET is involved in plant-*Alternaria alternata* (Fr.) Keissler (AK-toxin) interactions is still largely unknown.

Pears (*Pyrus* spp.) are one of the most important fruit trees in Europe, East Asia, and North America (Terakami et al., 2007). Black spot disease, caused by the Japanese pear pathotype of *A. alternata* (Fr.) Keisser, is one of the most serious diseases in Asian pear cultivation (Terakami et al., 2007). *A. alternata* (Fr.) Keisser produces host-selective toxins, AK-toxin, resulting in necrosis and leaf fall, which seriously restrict fruits yield in Asian pears (Terakami et al., 2007). A sand pear cultivar, Sucui1 (SC1), is widely cultivated in the Yangtze River basin, mainly because its fruits have excellent flavor and a less rusty exocarp than its male parent Cuiguan (CG). However, SC1 displays much stronger susceptibility to *A. alternata* (Fr.) Keisser than its parent CG in the field. To better understand molecular mechanisms governing the susceptibility and compatible interaction of pear-*A. alternata*, the transcriptome dynamics of the diverse responses between the resistant (CG) and susceptible (SC1) pear cultivars to the pathogen *A. alternata* were investigated using the RNA-seq technology. Our results illustrated that the ET-/H_2O_2-mediated PCD and detoxification play a vital role in the interaction of pear and *A. alternata.*

MATERIALS AND METHODS

Plant Materials

Seven-year-old "Cuiguan" (CG) and "Sucui 1" (SC1) sand pear trees [*Pyrus pyrifolia* (Burm.f.) Nakai; rootstock: *Pyrus betulaefolia* Burge] were grown at the Pear Germplasm Resource Preservation Center, Jiangsu Academy of Agricultural Sciences, Nanjing, China. Leaves were collected from the orchard for inoculation assays.

Inoculation Assays

A. alternata was grown on potato dextrose agar plates (Sigma-Aldrich, USA) at 25°C for 7 days (Suzuki et al., 2003). The conidial suspension was obtained through rinsing mycelia mats with distilled water. The spore concentration was 1.0×10^6 sprores mL^{-1} for inoculation.

Adaxial epidermis of detached leaves was punctured by a 0.30 mm needle to form four infection sites along both sides of

the center vein. Ten microliters of the inoculants were applied to each punctured site. Sterilized distilled water was used as a mock control (Wang H. et al., 2013). The inoculated and mock treated leaves were incubated at the same boxes at 25°C under dark conditions with 100% relative humidity. The fungal growth process was evaluated for disease severity and disease incidence every day after inoculation. At least 20 detached leaves were used for each treatment. The experiments were repeated five times. Leaves were pooled at 0, 1, 2, 3, and 5 days post inoculation (dpi) for RNA-seq analysis.

RNA Extraction, Library Construction, and Sequencing

Ten leaves were pooled at a given time point and three independent biological replicates of every pool were used for RNA preparation, library construction and sequencing. Total RNA was extracted using the Trizol method (Invitrogen, USA), combined with Ambion RiboPure™ Kit (Ambion, USA) (Wang H. et al., 2013). Quality and quantity of RNA were determined using a NanoDrop 3100 spectrophotometer (Thermo Scientific, USA). mRNA was obtained using Sera-mag (Thermo Scientific, USA). The cDNA libraries were prepared according to the Illumina protocols. Fragments of about 300 bp were excised from agarose and enriched by PCR for 16 cycles. Finally, the cDNA libraries were sequenced using an Illumina HiSeq 2500 machine to perform 100 paired-end sequencing according to HiSeq 2500 User Guide.

Sequence Data Processing and Differential Gene Expression Analysis

Clean data were obtained from raw data by removing adapter sequences, trimming reads with poly-N and low quality reads. Clean reads from all 30 samples (five time points, three biological replicates, and two cultivars) were pooled and the read counts were normalized for quantifying the gene expression level. Sequences were mapped to a pear reference genome (http://peargenome.njau.edu.cn) for further analysis.

Gene expression values of RNA-Seq data were obtained by FKPM (Trapnell et al., 2010). For each pear genotype, DEGs were generated by comparing multiple treatments or two treatments (pairwise analysis) with the cut off FDR $\leq$ 0.05 and Fold change [FC] $\geq$ 2.0 (Trapnell et al., 2010). K-means clustering was exploited to obtain knowledge about expression profiles throughout the five time points with two genotypes (Nham et al., 2015). Gene Ontology (GO; FDR $<$ 0.01) was used to describe gene function. KEGG Ortholog database (KO; FDR $<$ 0.01) was used to elucidate the pathways of DEGs (Shin et al., 2014). Diverse GO terms with similar expression patterns of CG and SC1 were compared and analyzed.

Mapman visualization was performed as described previously (Thimm et al., 2004) to identify specific and common genes involved in response of two genotypes to *A. alternata*. Contigs were uploaded into Mapman as described previously (Nham et al., 2015). Mapping files produced by Mecrator and gene expression changes were viewed in Mapman v.3.5.1R2 (Thimm et al., 2004).

Hormone Measurements

ET emission was monitored using a gas chromatograph with a flame ionization detector as previously described (Bashan, 1994). Infected leaves of CG and SC1 were placed into 50 ml volume closed glass vials and incubated at 28 $\pm$ 1°C for 24 h. ET production was measured. As a control, leaves inoculated with sterile distilled water were subjected to the same sampling procedures. The rate of ET was calculated according to previous report (Bashan, 1994). Each experiment was repeated three times with at least three biological replicates.

H_2O_2, O_2^- and Antioxidant Enzyme Activity Measurements

The level of H_2O_2 was measured according to Sagisaka (1976). Briefly, 0.5 g FW of detached leaves were homogenized in a pre-chilled mortar and pestle in liquid nitrogen with 5% cold trichloroacetic acid (TCA) and then centrifuged (Eppendorf, Hamburg, Germany) at 17,000 g for 10 min at 0°C. The supernatants (1.6 mL) were mixed with 0.4 mL of 5% TCA, 0.4 mL of 10 mM ferrous ammonium sulfate and 0.2 mL of 2.5 mM potassium thiocyanate and used to measure H_2O_2 levels. Activities of superoxide dismutase (SOD) and catalase (CAT) were assayed according to previous descriptions (Wang H. et al., 2013). Briefly, the ground tissues were incubated in the enzyme extraction buffer containing potassium phosphate (pH 7.5) for 0.5 h at 4°C. The extracted solutions were then centrifuged at 13,000 g for 20 min at 4°C. The supernatants were divided into two identical aliquots and supplemented with the reaction buffer either for SOD or CAT analysis. The level of O_2^- was measured using the commercial kits (Catalog #: A052-1, Nanjing Jiancheng Bioengineering Institute, China) according to the manufacturer's instruction. Quantification of enzyme activities, levels of O_2^- and H_2O_2 were carried out spectrophotometrically at 25°C with UV-VISO 2450 (Shimadzu, Kyoto, Japan). Five biological samples were used from each experiment.

qRT-PCR Analysis

Leaves were pooled at 0, 9, 24, and 48 h post inoculation (hpi) for quantitative real-time PCR (qRT-PCR) (ABI 7300; Applied Biosystem, Foster City, CA, USA) as previously described (Ma et al., 2015). Gene sequences were retrieved from the pear genome database. Specific primers were designed by the PRIMER 3 program and listed in Supplementary Table S1. The $2^{-\Delta\Delta CT}$ method was used for evaluation of the relative levels of gene expression (Ma et al., 2015). A house-keeping gene, *GAPDH* (Glyceraldehyde 3-phosphate dehydrogenase), was used as an internal standard for normalization (Yang et al., 2015).

Statistical Analyses

All statistical analyses were performed using the SPSS package (Version 16.0; SPSS Inc., Chicago, IL, USA). One-way analysis of variance (ANOVA) was performed for experiments with one independent variable. Duncan's test was used if significant differences were found.

RESULTS

Assessment of *A. alternata* Growth in Two Different Genotypes

We found that two genotypes of SC1 and CG infected with *A. alternata* exhibited different progressions of leaf symptom development. The pear cultivar SC1 showed more severe disease symptoms of black spots (**Figure 1A**). The first symptom, necrotic spots, was observed at 1 dpi, followed by rapidly expanding lesions at 3 dpi and leaf soaking at 5 dpi. However, primary necrotic lesions in leaf tissue of its male parent CG formed at 1 dpi and spread very slowly at 5 dpi. The disease incidence in leaf tissue of CG was <70%, whereas it was ∼100% in SC1 leaves (**Figure 1B**). The disease severity was significantly greater in SC1 leaves (3.47 cm at 5 dpi) than CG leaves (1.67 cm at 5 dpi; **Figure 1C**).

Sequence Identity and Expression Analysis of RNA-Seq Transcriptome Data

The raw reads were trimmed by removing adaptor sequences, empty reads and low-quality sequences to produce the clean reads. As a result, more than 97% clean ratio for each sample was obtained (**Table 1**). The majority of clean reads (more than 65%) were successfully mapped to the pear reference genome (Wu et al., 2013). As evidence of disease development in pear cultivars of SC1 and CG, the clean reads were also mapped to *A. alternata* genome (Dang et al., 2015). An insignificant proportion of reads were mapped to *A. alternata* reference genomes, for example, 0.2263% for SC1 and 0.2596% for CG in the symptomatic samples (5 dpi), compared with 0.0063% for SC1 and 0.0053% for CG in non-symptomatic leaves (0 dpi; **Table 1**).

The significantly increased numbers of DEGs between the two genotypes before and after 3 dpi were determined (Supplementary Table S2), ranging from 1188 (C0–S0), 1154 (C1–S1), and 1414 (C2–S2) to 3114 (C3–S3) and 2623 (C5–S5). The number of DEGs between the early stage (0–2 dpi) and later stage (3–5 dpi) in the same genotype, was significantly increased (Supplementary Table S2), ranging from 951 (C1–C0) and 1134 (C2–C0) to 5834 (C3–C0) and 6000 (C5–C0) in the CG leaves, and from 1040 (S1–S0) and 1319 (S2–S0) to 7222 (S3–S0) and 7526 (S5–S0) in the SC1 leaves, respectively. Further analysis identified unique and shared DEGs between these two genotypes (**Figure 2**). The general biological functions of these DEGs were analyzed using Mapman. The

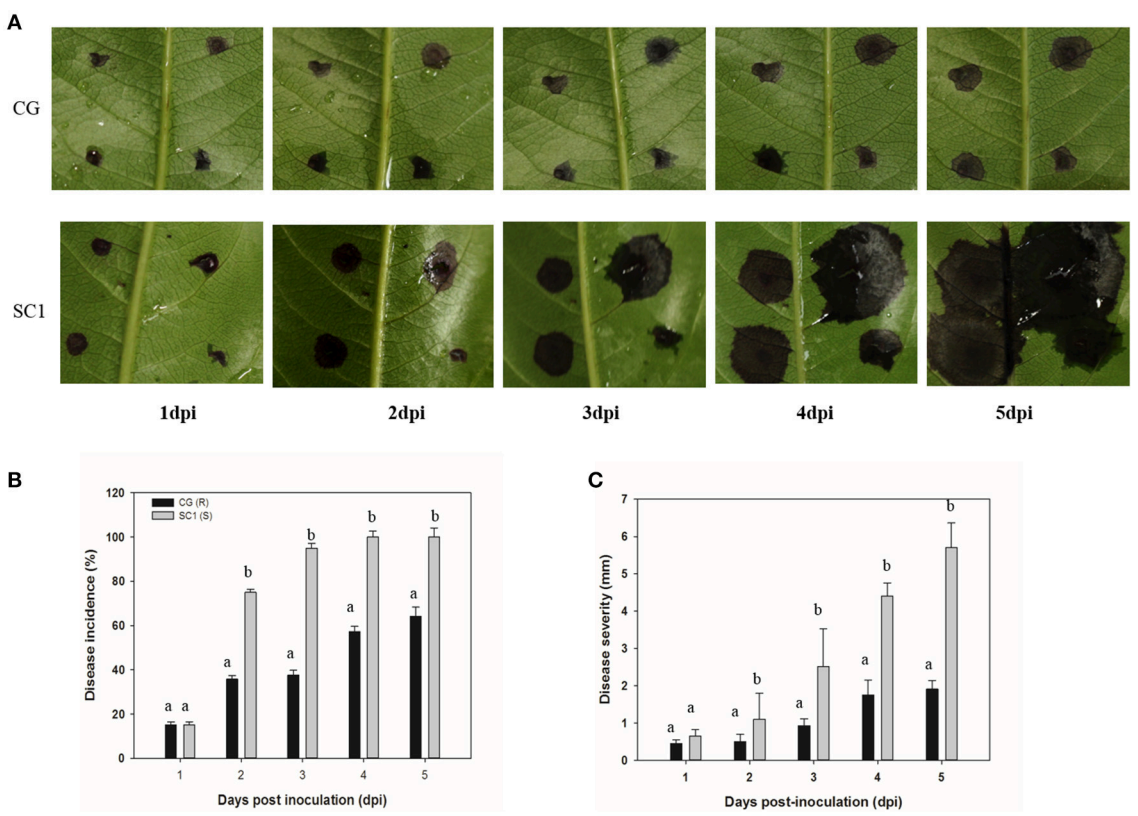

FIGURE 1 | Development of *A. alternata* on CG and SC1. (A) Representative phenotypes of CG and SC1 inoculated with *A. alternata*. **(B)** Disease incidence (percentage of inoculation sites with expanding lesions) of the fourth leaves from the top on CG and SC1 branches *in vitro*. **(C)** Disease severity (diameter of expanding lesions) of the fourth leaves from the top on CG and SC1 branches *in vitro*. Mean values are shown from three independent biological replicates [error bars, ±standard error (SE)] containing at least 20 leaves (80 droplets) for every experiment. Different letters indicate significant differences between two genotypes at a given time point ($P \leq 0.05$).

results showed that the highest numbers of DEGs were assigned to biological processes of protein (11.65%), RNA (9.61%), signaling (5.96%), and misc (5.11%). Other over-represented categories of biological processes included biotic stress (4.62%), transport (3.98%), cell (2.86%), hormone metabolism (2.64%), development (2.59%), and secondary metabolism (2.34%; Figure S1).

Time-Course Expression Profiles Analysis

To understand the molecular mechanisms governing the susceptibility of two genotypes, dynamic expression trends of DEGs were analyzed using K-mean clustering. Ten profiles were obtained for dissecting the expression patterns (Figures S1, S2). Dynamic processes of plant response to pathogen were illuminated by significantly enriched GO terms. For example, the terms of "phytosphingosine metabolic process," "response to hydrogen peroxide," and "response to superoxide/carbohydrate" were enriched in an up-regulated pattern in the resistant genotype CG leaves (**Figure 3A**). Biological processes such as "polysaccharide biosynthetic processes," "response of hormone levels," and "very long-chain fatty acid metabolic" were enriched in a down-regulated pattern in CG (**Figure 3B**). However, the terms of "jasmonic acid mediated signaling pathway," "response to ethylene/wound," "ABA-activated signaling pathway," "regulation of plant-type hypersensitive response," and "respiratory burst involved in defense response" were enriched in an up-regulated pattern in the susceptible genotype SC1 leaves (**Figure 3C**). Biological processes including "photosynthesis," "polysaccharide biogenesis," "plant-type cell wall biogenesis," and "cell wall organization" were enriched in a down-regulated pattern in SC1 (**Figure 3D**). In addition, down-regulated expression patterns of cellular components were observed, such as "Golgi apparatus," "nucleus," "endosome" and "trans-Golgi network" in infected leaves of CG and "chloroplast thylakoid membrane," and "chloroplast thylakoid" in infected leaves of SC1 (**Figures 3B,D**).

TABLE 1 | Mapping characteristics of CG, SC1, and *A. alternata* reads to the reference genomes in the thirty samples at different time points after inoculation.

Sample	Raw reads	Clean reads	Reads mapped Pear genome	Reads mapped *Alternaria* genome
C0	42,426,142	41,508,319	27,268,734 (68.22%)	2,019 (0.0053%)
C1	47,619,512	46,601,111	30,788,480 (68.21%)	14,328 (0.0320%)
C2	45,182,075	44,201,272	28,825,665 (68.00%)	9,849 (0.0240%)
C3	42,782,298	40,718,867	27,383,506 (68.14%)	35879 (0.1210%)
C5	41,217,044	39,267,755	27,138,755 (67.35%)	82489 (0.2596%)
S0	48,690,054	47,668,210	30,059,693 (65.75%)	2605 (0.0063%)
S1	46,843,642	45,854,345	27,930,754 (65.74%)	8409 (0.0196%)
S2	45,106,658	44,132,629	28,423,723 (66.22%)	20278 (0.0766%)
S3	39,591,996	38,006,025	28,025,023 (66.23%)	85039 (0.2001%)
S5	40,196,180	38,494,785	28,629,681 (65.45%)	69859 (0.2263%)

Genes Involved in Regulation of Hypersensitive Response and Programmed Cell Death

K-mean analysis suggested that genes related to HR, PCD, hormone biosynthesis, and signaling pathways, and transcription factors were significantly enriched after inoculation (**Figure 3**). In addition, genes related to defense responses displayed either induced or repressed expression patterns in two different genotypes (**Figure 3** and Figure S1). Therefore, genes classified in "regulation of plant-type hypersensitive response" and "programmed cell death" were further analyzed. Of 32 DEGs

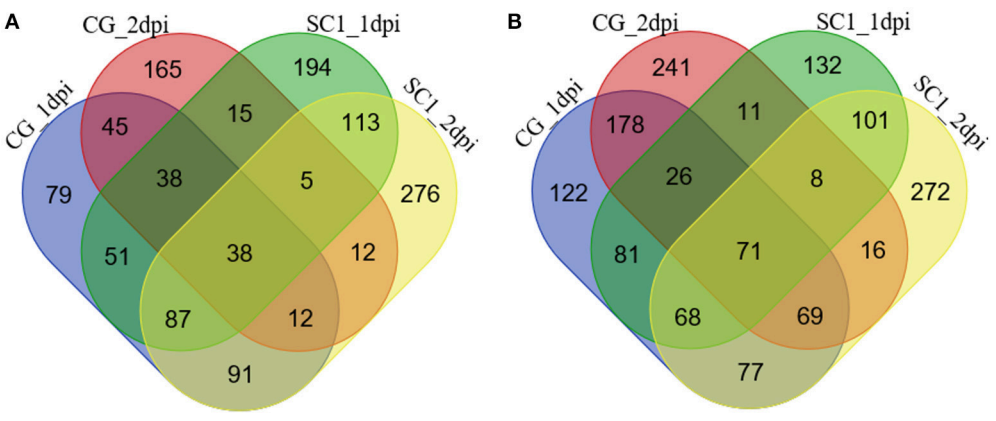

FIGURE 2 | Unique and shared differentially up-regulated (A) and down-regulated **(B)** unigenes in CG and SC1 at given time points. Blue, CG 1 dpi; purple, CG 2 dpi; green, SC1 1 dpi; yellow, SC1 2 dpi.

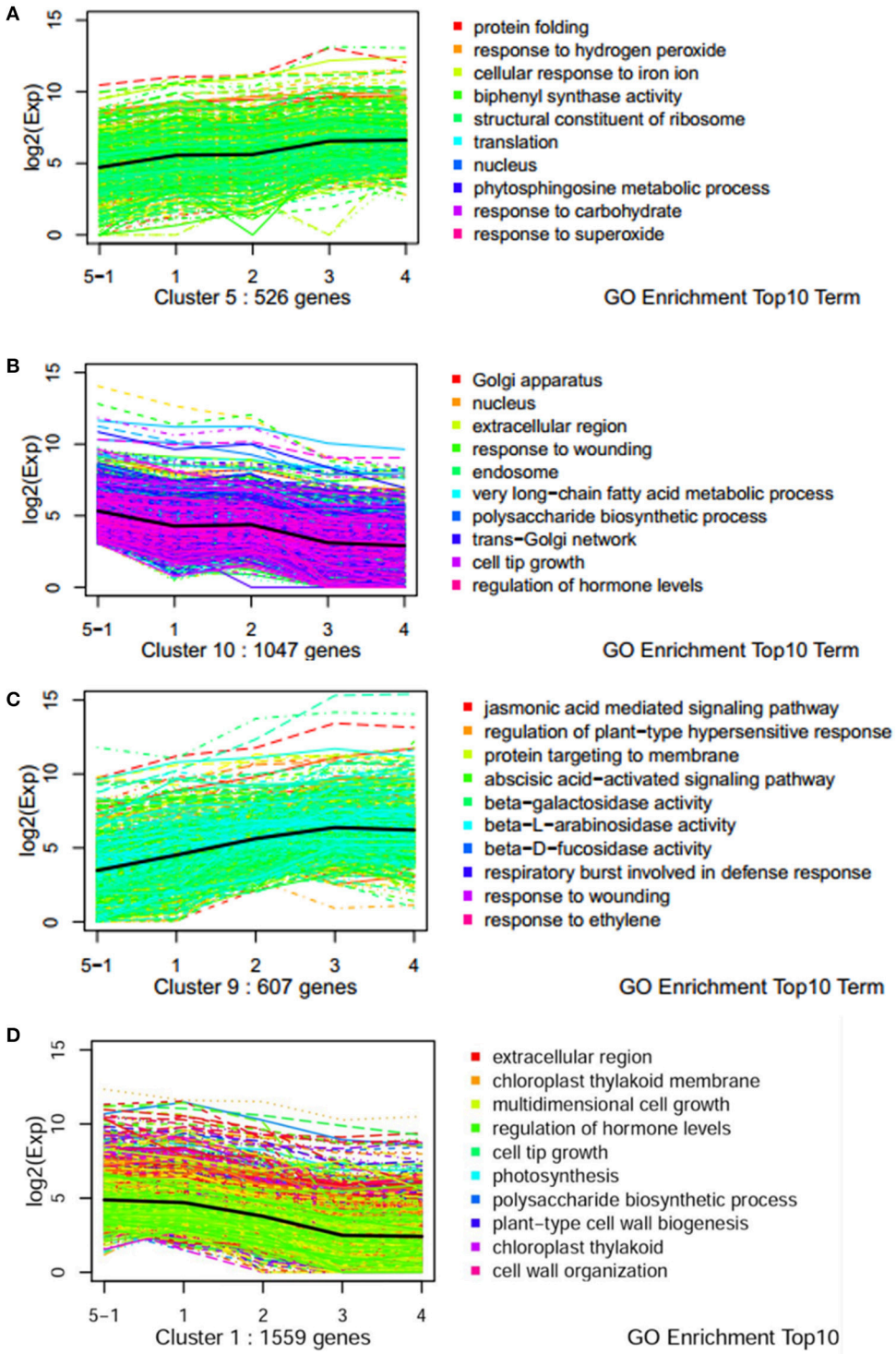

FIGURE 3 | Expression profiles of genes with top 10 GO term across five stages of two genotypes by k-mean analysis. (A) Up pattern in CG; **(B)** Down pattern in CG; **(C)** Up pattern in SC1; **(D)** Down pattern in SC1.

related to these two biological processes, a gene encoding patatin-like protein 2 (PLP2) (Pbr004131.1) was continuously and differentially induced in the susceptible genotype SC1 but not in the resistant genotype CG (**Table 2**). Kunitz trypsin inhibitor (KTI) (Pbr037895.1), WRKY 40 (Pbr022408.1), PGIP (Pbr030600.1 and Pbr030601.1), HSL1 (Pbr006072.1), UGT85A

TABLE 2 | Unigenes associated with related biological function exhibiting a Log2 FC ≥ 1 and $p \leq 0.05$ in at least one transition.

Gene ID	CG (Resistant)			SC1 (Susceptible)			Description
	FCC1/C0	FCC2/C0	FCC3/C0	FCS1/S0	FCS2/S0	FCS3/S0	
HYPERSENSITIVE RESPONSE AND PROGRAMMED CELL DEATH							
pbr010964.1	0.84	0.20	−1.36*	2.35*	0.70	−0.06	SAG20
pbr006728.1	–	–	–	−0.04	0	2.60*	SAG12
Pbr012334.1	1.37	−0.68	−3.37	6.98	9.76*	10.96*	PLP2
Pbr004131.1	2.59*	1.78*	−1.92*	5.60*	8.25*	8.97*	PLP2
Pbr012337.1	2.10*	0.33	−2.09	7.59	10.45*	12.67*	PLP2
Pbr035719.1	1.44	0.37	0.44	3.15	3.15	5.27*	SYP21
Pbr037895.1	1.74*	0.50	−1.14*	1.47*	3.59*	6.56*	KTI
Pbr030600.1	−1.10*	−4.66*	−4.87*	3.13*	3.98*	3.96*	PGIP
Pbr030601.1	−1.24*	−5.03*	−6.96*	4.08*	4.74*	5.88*	PGIP
Pbr010566.1	0.51	−1.18	−1.62	2.81	3.17	6.50*	PDR1
Pbr006072.1	0.64	−1.12*	0.09	1.12*	1.30*	1.54*	HSL1
Pbr008587.1	1.51*	0.21	−1.68*	0.35	1.32	2.63*	HSL1
Pbr015532.1	−0.30	−1.55	−0.06	0.75	1.57	3.13*	HSL1
Pbr008766.1	1.24	−1.13	0.16	1.29	2.22*	2.65*	HSL1
Pbr007513.1	0.71	−0.19	−1.46*	1.56	2.67	2.49*	UGT85A24A5-like
Pbr007515.1	0.96	−0.59	1.59	2.57*	4.18*	7.09*	UGT85A24A5-like
Pbr007514.1	0.77	−0.54	−0.32	1.66*	2.98*	5.56*	UGT85A23
Pbr021700.1	0.72	0.32	−1.34*	0.26	1.56*	2.33*	UGT85A24
Pbr040910.1	0.26	−1.26*	−0.51	1.81*	1.20*	1.98*	HAIKU2
Pbr037476.1	1.08*	−0.27	0.11	2.17*	2.09*	2.63*	CAT1
Pbr003247.1	0.06	−0.27	−1.24	1.04*	0.79	1.30*	ARG2-like
Pbr019124.1	2.11	0.86	4.04*	1.56	2.90	5.60*	ABCG36
Pbr026949.2	0.10	−0.63	0.50	0.60	2.28*	4.49*	NAC25-like
Pbr004500.1	0.85	0.64	0.26	1.20*	1.03*	1.46*	NAC25-like
Pbr004703.1	2.97	1.11	−0.20	1.71	3.11	4.95*	RIP3
RESPONSE TO HYDROGEN PEROXIDE AND SUPEROXIDE							
Pbr027587.1	1.13*	1.69*	2.29*	0.91	0.15	2.17*	MBF1C
Pbr016628.1	1.68*	2.78*	2.88*	1.36*	1.08	1.00	HSP20
Pbr032362.1	0.26	0.96	0.32	0.95	0.51	2.23*	HSP70
Pbr040066.1	1.79	1.63	1.98	2.14*	1.16	2.65*	HSP22
Pbr003834.1	0.53	0.57	1.11*	0.60	0.39	1.45*	RAB11C
Pbr028049.1	0.26	0.44	1.09	0.43	0.76	2.38*	CINV2
Pbr028718.1	1.21	1.48	2.75	3.04*	−0.16	2.66*	dnaJ6-like
Pbr031275.1	0.62	0.83	1.36*	0.40	−0.14	0.84	SRO3
Pbr013783.1	0.68	1.24*	0.83	0.63	0.36	0.91	RCD1
Pbr025956.1	0.52	0.61	1.27*	0.93	0.24	1.17*	RCD1
Pbr016212.1	0.31	0.77	1.20	0.72	0.40	1.91*	dnaJB13
Pbr027173.1	0.48	0.36	1.37*	1.74*	0.95	2.65*	GIGANTEA-like
Pbr035808.1	0.45	0.48	1.16*	0.04	0.26	1.33*	AHSA1
Pbr036899.1	0.49	0.33	1.55*	0.49	0.09	2.01*	EXO70B1
Pbr033477.1	2.00	0.34	2.40*	1.61	1.96	5.15*	ABCB5
Pbr019106.1	1.12	2.07	3.75*	−0.51	−1.09	2.55	PTP1
Pbr014824.1	2.88*	3.07*	2.79*	0.26	1.07*	−1.10	GRXS10
Pbr016271.1	0.41	1.01*	0.50	0.42	0.38	−0.63	GRXS17
Pbr016203.1	−0.26	−0.68	−1.12*	1.28	1.78	3.21*	GRXS9

*HAIKU2, receptor-like protein kinase; CAT1, cationic amino acid transporter 1-like; RIP3, ras-interacting protein; indole-3-acetic acid-induced protein ARG2-like; PTP1-like, protein-tyrosine-phosphatase. *The gene was differentially expressed in the correspondent pairwise analysis ($p \leq 0.05$).*

(Pbr007515.1 and Pbr007514.1), receptor-like protein kinase HAIKU2 (Pbr040910.1), cationic amino acid transporter 1-like (CAT1) (Pbr037476.1), NAC25 (Pbr004500.1) were significantly and continuously induced in infected leaves of SC1 but not CG (**Table 2**). SAG20 (senescence associated gene, Pbr010964.1) was induced in SC1 but not CG. Similarly, a gene encoding senescence-associated protein SAG12 (pbr006728.1) was significantly up-regulated at 3 dpi of SC1 but not CG (**Table 2**).

Genes Involved in Response to Hydrogen Peroxide, Superoxide, and Carbohydrate

K-mean analysis suggested that genes related to the responses to hydrogen peroxide, superoxide and carbohydrate were significantly up-regulated in the resistant genotype CG but not in the susceptible genotype SC1 (**Figure 3A**). The expression patterns of genes enriched in these GO terms were further analyzed (**Table 2**). The expression of majority of the genes (20/21) enriched in these GO terms was induced in the resistant genotype CG (**Table 2**). Of those genes, MULTIPROTEIN BRIDGING FACTOR 1c (MBF1c) (Pbr027587.1), Heat shock proteins (HSP20) (Pbr016628.1), and Glutaredoxins10 (GRXS10) (Pbr014824.1) were significantly and continuously up-regulated in the resistant genotype CG but not in the susceptible genotype SC1 (**Table 2**).

Genes Involved in Hormone Biosynthesis and Signaling

GO terms such as "JA, ABA-mediated signaling pathway" and "response wounding and ET" were clustered in significantly up-regulated expression patterns in SC1 (**Figure 3C**) and down-regulated expression patterns in CG (**Figure 3B**). We further dissected the expression patterns of the genes involved in the biosynthesis and signaling pathways for plant hormones ET, SA, JA, and ABA during plant–pathogen interactions.

A predominance of up-regulated genes related to the ET biosynthesis and signaling pathways was found in the susceptible genotype SC1 (**Figure 4** and **Table 3**). Transcript abundances were highly accumulated in the infected leaves of SC1 for most ET biosynthesis-related genes i.e., ACS (Pbr032688.1), ACO1-like (Pbr023057.1, Pbr023059.1, Pbr0326881, Pbr031954.1, Pbro15589.1), ACO4-like (Pbr012109.1, Pbr015355.1, and Pbr021636.1), ACO5-like (Pbr040048.1, Pbr040049.1, and Pbr013513.1) as well as for ET signaling components such as ETR2 (Pbr002199.1) and ERS1 (Pbr022706.1). Notably, ACS (Pbr032688.1), ACO1-like (Pbr023057.1 and Pbr023059.1), and ACO5-like (Pbr013513.1) were sustained and differentially induced in the leaves of the susceptible genotype SC1 but not in the resistant genotype CG (**Table 3**).

A predominance of down-regulated genes was found in the JA pathway in CG and SC1 (**Figure 4** and **Table 3**). For example, genes encoding LOX2 (Pbr004541.1, Pbr004568.1 and Pbr023784.2), LOX3 (Pbr005350.1), AOS (Pbr006204.1 and Pbr006205.1), AOC (Pbr013257.1, Pbr027476.1 and Pbr030638.1), an OPR3 (Pbr041531.1), S-adenosyl-L-methionine (JMT, Pbr005926.1), three JAZ (Pbr027730.1, Pbr037418.1 and Pbr012103.1) were down-regulated in both CG and SC1 (**Table 3**).

PAD4 (Phytoalexin Deficient 4, Pbr027953.1) was differentially up-regulated after 2 dpi in the susceptible genotype SC1 but down-regulated in the resistant genotype CG (**Table 3**). The differential expression of *ICS1* (isochorismate synthase 1, Pbr011477.1) and *EDS1* (Enhanced Disease Susceptibility 1) was not observed in either SC1 or CG (Supplementary Table S3).

Based on K-means analysis, the ABA-activated signaling pathway was up-regulated in SC1 but down-regulated in CG (**Figure 3** and Figures S1, S2). Genes enriched in this GO term were further analyzed. Of seven DEGs, only genes encoding PYL4-like (Pbr019415.1 and Pbr028222.1) were differentially induced in the susceptible genotype SC1 (**Table 3**). These results suggested that ABA, JA, and SA pathways were triggered in the early stage of inoculation neither in SC1 nor CG.

Transcription Factors Analysis

In the category of "response to biotic stresses," transcripts of the AP2/EREBP and WRKY family members were the most abundant (**Figure 4**). To identify key genes that regulate pear response to *A. alternata*, we carried out a detailed analysis on these two TFs using Heat Map (Figures S3, S4) and Mapman (**Figure 4** and **Table 4**). Of those, 21 DEGs were identified as ERFs in the transcriptome data (Figure S3). Genes encoding ERF2-like (Pbr035775.1), ERF1-like (Pbr001363.1), ERF113-like (Pbr029841.1), PTI (Pbr016185.1), and RAP2.3 (Pbr012024.1) were differentially up-regulated in the susceptible genotype SC1 leaves (**Table 4**). Approximately 25 WRKY genes were differentially expressed (Figure S4). A gene encoding WRKY40 (Pbr022408.1) was differentially up-regulated in the susceptible genotype SC1 leaves (**Table 4**).

Genes Involved in Disease Resistant Proteins and Defense Response

We found that nine R genes encoding nucleotide-binding site-leucine-rich repeat (NBS-LRR) proteins were differentially expressed. Of these, ADR1-L1 (Pbr036409.1), and CC-NBS-LRR (Pbr016325.1) were differentially up-regulated at the early stage of infection in the susceptible genotype SC1 (Supplementary Table S3).

Based on K-mean results, defense responses were significantly up-regulated in SC1 (**Figure 3C**). DEGs related to defense responses were further analyzed. Genes encoding PR proteins exhibited similar expression patterns. For example, most genes were differentially up-regulated at the early stage of infection in the resistant genotype CG but the later stage of infection in the susceptible genotype SC1, i.e., PR1 (Pbr022550.1), PR5 (Pbr036399.1), EP3 (Pbr009767.1), and Chitinase A (Pbr018708.1), endo-1,3-beta-glucosidase 14 (Pbr001155.2) (**Table 5**).

We further analyzed DEGs involved in secondary metabolism. All DEGs related to the secondary metabolism were classified into the Shikimate, phenylpropanoid, and flavonoid pathways. Most genes related to the Shikimate acid pathway were

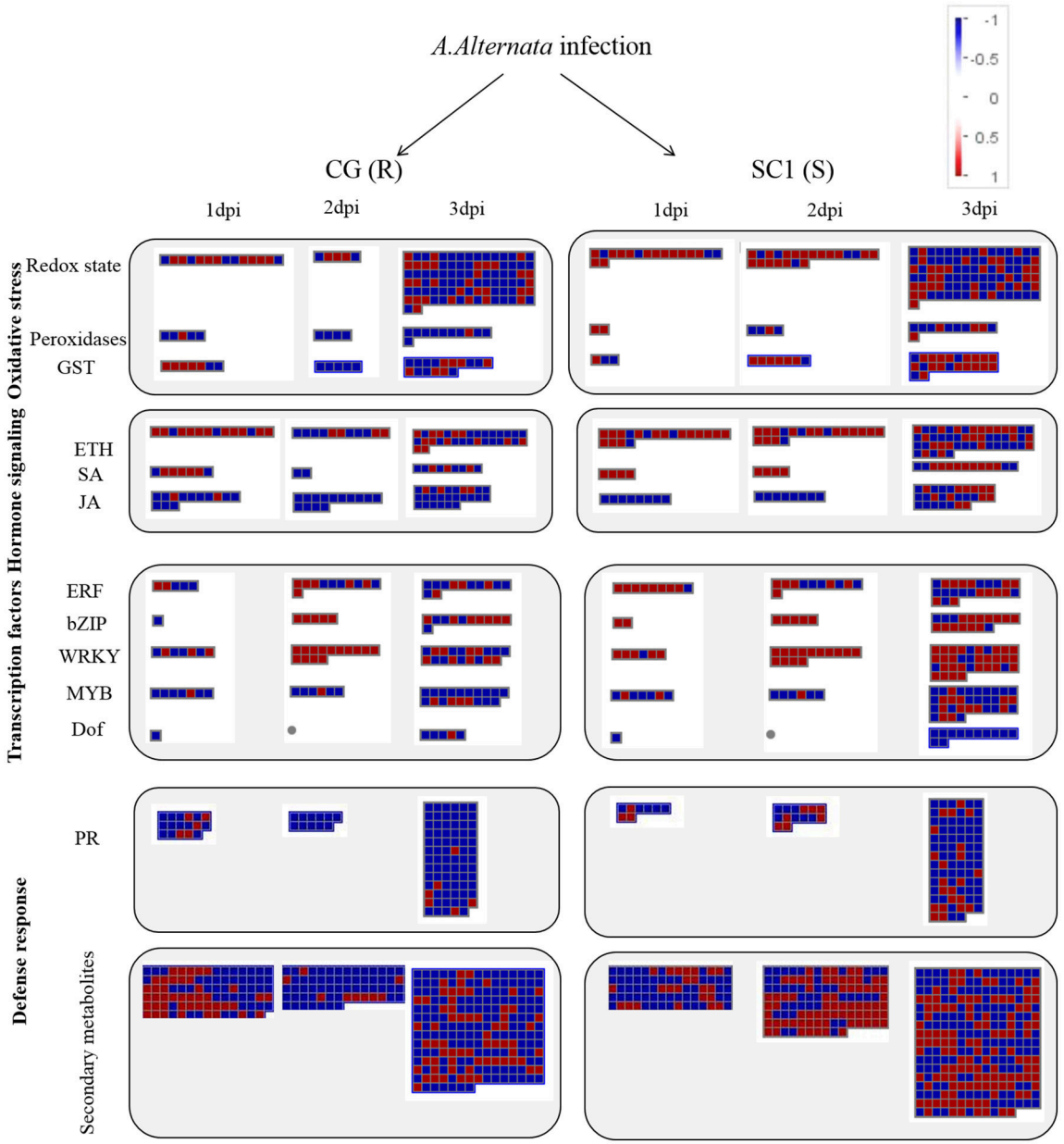

FIGURE 4 | Display of transcriptional response of CG and SC1 to biotic stress. Significantly differentially expressed genes (Log_2 fold changes [FC] $\geq$ 1, FDR $\leq$ 0.05) were visualized using Mapman software and organized into functional categories (BINs). Blue indicates a decrease and red an increase gene expression (see color set scale on top right corner). Detailed information on each gene and its expression level were listed in **Tables 2**–**5** and Supplementary Table S3.

only differentially induced at 3 dpi either in CG or SC1, such as chorismate synthase (Pbr042387.1), EPSP synthase 2 (Pbr040661.1) and prephenate dehydrogenase (Pbr029378.1) (**Table 5**). Nineteen DEGs were related to the phenylpropanoid pathway. Seven DEGs were related to the flavonoid pathway. Of these, genes encoding chalcone synthase (CHS) (Pbr027907.1) and leucoanthocyanidin dioxygenase (Pbr007997.1) were differentially induced in the susceptible genotype SC1 leaves (**Table 5**).

ET Level and Gene Expression of Hormone Biosynthesis Pathway

To further confirm the link between ET level and susceptibility response of pear to the pathogen, we determined ET levels in CG and SC1 leaves after inoculation (**Figure 5**). In infected leaves, ET levels were much higher in the susceptible genotype SC1 than in the resistant genotype CG. Levels of ET continuously increased after 1 dpi and peaked at 5 dpi in the SC1 leaves. In comparison, ET evolution was much slower in the resistant

TABLE 3 | Unigenes associated with hormone biosynthesis and signaling pathway exhibiting a Log2 FC ≥ 1 and $p \leq 0.05$ in at least one transition.

Gene ID	CG (Resistant)			SC1 (Susceptible)			Description
	FCC1/C0	FCC2/C0	FCC3/C0	FCS1/S0	FCS2/S0	FCS3/S0	
HORMONE BIOSYNTHESIS AND SIGNALING PATHWAY–ETHYLENE PATHWAY							
Pbr032688.1	1.99	1.65	0.41	2.91	6.58*	656.2*	ACS
Pbr023057.1	1.18*	0.38	−0.11	1.06*	1.50*	2.42*	ACO1-like
Pbr023059.1	1.26*	0.45	0.77	1.10*	1.71*	3.74*	ACO1-like
Pbr032688.1	2.00	1.65	−1.27	2.91	6.58*	9.36*	ACO1-like
Pbr031954.1	1.49*	−3.94*	−5.57	1.96	4.26*	1.42	ACO1-like
Pbr015589.1	0.55	−1.27	−4.40*	5.69*	3.97	1.14	ACO1-like
Pbr005179.1	−1.22*	−1.89*	−1.85*	−1.08*	−1.55*	−1.83*	ACO3-like
Pbr012109.1	0.33	−0.59	−0.52	−0.13	0.81	0.79	ACO4-like
Pbr015355.1	1.73	−0.46	0.97	2.81*	4.38*	4.67*	ACO4-like
Pbr021636.1	1.80*	−2.46*	−4.29*	1.08	3.78*	2.65*	ACO4-like
Pbr040048.1	1.17	2.09*	0.77	0.42	2.43*	2.43*	ACO5-like
Pbr040049.1	1.95*	2.61*	1.25	0.53	2.76*	2.47*	ACO5-like
Pbr013513.1	0.97	0.93	−0.36	1.80*	2.35*	1.81*	ACO5-like
Pbr023072.1	1.92*	0.83	−1.10	1.37*	0.42	−3.12*	ETR2
Pbr022706.1	1.99*	0.01	−1.39*	1.24*	1.23*	0.51	ERS1
Pbr026603.1	0.65	0.82	1.22*	0.72	0.33	0.88	EIN3-like
Pbr033210.1	0.89	0.93	1.47*	0.61	0.35	0.63	EIN3-like
HORMONE BIOSYNTHESIS AND SIGNALING PATHWAY–SA PATHWAY							
Pbr027953.1	−0.49	−1.20*	−1.36*	0.19	1.13*	1.87*	PAD4
Pbr025644.1	1.78*	−0.29	2.40*	1.62*	2.60*	5.04*	UGT72E2
Pbr025645.1	1.89	−0.36	1.54	1.32	2.91*	6.15*	UGT72E2
Pbr025643.1	–	−0.38*	1.68	0.17	0.43	2.09*	UGT74E1
Pbr002691.1	–	0.07	−0.04	0.40	1.95*	2.08*	UGT73B4
Pbr007397.1	1.06*	−1.35	−2.10	1.48	4.06*	6.25*	UGT74E2
Pbr020349.1	0.84	−0.91	−2.39*	1.93*	2.55*	5.04*	SAM
Pbr025059.1	1.67	−1.04	3.32	2.23*	0.30	10.02*	SABP2
Pbr031493.1	−0.07	0.33	0.83	1.69	−0.41	1.70	NPR3-like
HORMONE BIOSYNTHESIS AND SIGNALING PATHWAY—JA PATHWAY							
Pbr020412.1	3.07*	0.07	−1.93	3.85	8.25*	9.25*	LOX1-like
Pbr020414.1	0.01	−1.76*	−1.40*	0.83	1.07	0.64	LOX1-like
Pbr020415.1	0.71	0.32	−0.96	1.37	3.16*	4.30*	LOX1-like
Pbr004969.1	−2.33*	−1.11*	−4.67*	−1.28*	−1.44*	−7.30*	LOX2
Pbr005350.1	−1.84*	−1.83*	−0.95	−1.00	−1.25*	−1.16*	LOX3
Pbr006204.1	−2.48*	−2.24*	−4.20*	−1.60	−0.96	−3.46*	AOS-like
Pbr006205.1	−2.37*	−2.00*	−1.90*	−1.69	−1.22	−0.41	AOS-like
Pbr004466.1	4.73	0.09	−0.26	−1.57	2.72*	0.18	AOS-like
Pbr008503.1	3.85	−0.37	1.18	−2.14	2.38*	4.76*	AOS-like
Pbr013257.1	−1.80*	−2.21*	−3.25*	−0.66	0.21	0.29	AOC4-like
Pbr027476.1	−0.98	−1.17*	−2.22*	−1.14*	−0.92	−3.19*	AOC4-like
Pbr030638.1	−6.82*	−5.18*	−5.78*	−3.10*	−1.95*	0.59	AOC4-like
Pbr005926.1	−5.84*	−2.95*	–	−2.08	−3.40	−3.79	JMT
Pbr027730.1	−2.30	−2.09*	−2.02*	−1.57*	−0.99	−0.12	TIFY 10A
Pbr039229.1	−0.41	−1.52*	−4.04*	1.81	3.38*	4.59*	TIFY10B-like
Pbr012103.1	−2.19*	−1.55	−3.56*	−1.61	−1.39	−3.63*	TIFY6A-like
Pbr037418.1	−4.51*	−3.71*	−6.56*	−3.08*	−2.79*	−4.42*	TIFY10A-like
HORMONE BIOSYNTHESIS AND SIGNALING PATHWAY—ABA PATHWAY							
Pbr010367.1	2.21*	0.95	−2.02	1.30	1.61*	1.79*	HVA22like
Pbr005978.1	1.12*	−0.18	−0.39	0.94	1.73*	2.51*	AAO1-like

(Continued)

TABLE 3 | Continued

Gene ID	CG (Resistant)			SC1 (Susceptible)			Description
	FCC1/C0	FCC2/C0	FCC3/C0	FCS1/S0	FCS2/S0	FCS3/S0	
Pbr008947.1	1.08*	−0.09	0.32	0.41	0.90	−0.31	AAO1-like
Pbr029414.1	1.06	−0.66	−3.60	2.43*	0.11	−4.40	ABA 8′-hydroxylase
Pbr019415.1	0.48	−0.04	0.16	2.96*	2.44*	3.62*	PYL4-like
Pbr028222.1	0.47	0.33	0.99	4.22*	3.47*	4.46*	PYL4-like
Pbr027457.1	0.93	0.34	0.42	0.98	0.92	1.25*	PYL9

**The gene was differentially expressed in the correspondent pairwise analysis ($p \leq 0.05$).*

genotype CG. To further confirm the involvement of ET in the susceptibility response of pear to the pathogen, we monitored the expression of an *ACO1*-like gene at earlier time points post inoculation using qRT-PCR. The results showed that the expression of an *ACO1*-like gene was continuously higher in the susceptible genotype SC1 than in the resistant genotype CG (**Figure 6A**). Approximately 6-fold increases in the *ACO1*-like gene expression were detected in SC1 as early as 9 hpi, compared to 0 hpi. Approximately 11.94- and 14.69-fold increases were observed at 24 and 48 hpi in the susceptible genotype SC1. On the other hand, 0.52-fold decreases were found at 9 hpi, with 1.1-fold increases at 24 and 48 hpi in the resistant genotype CG (**Figure 6A**). In addition, to determine whether JA biosynthesis was involved in early response of pear to the pathogen, we performed gene expression analysis for a JA biosynthesis gene *AOC*. Expression of the *AOC* gene displayed 0.43-fold increases only at 2 dpi in the susceptible genotype SC1, while the gene expression was repressed in the resistant genotype CG (**Figure 6B**).

H_2O_2 and Antioxidant Enzyme Analysis

To acquire more information about whether H_2O_2 and antioxidant enzymes were involved in response of the susceptible and resistant genotypes pear to the pathogen, we determined the levels of O_2^-, SOD, H_2O_2, and CAT in the CG and SC1 leaves (**Figure 7**). The results showed that the activities of O_2^- and SOD were induced in the susceptible genotype SC1 but repressed in the resistant genotype CG after inoculation (**Figures 7A,B**). The levels of H_2O_2 were increased by the pathogen infection in both genotypes of CG and SC1 (**Figure 7C**). CAT activity was increased significantly in the resistant genotype CG, but reduced significantly in the susceptible genotype SC1 (**Figure 7D**).

Validation of Transcriptome Data Using qRT-PCR

To validate RNA-seq data, we selected six genes to confirm the expression patterns by qRT-PCR using a house-keeping *GAPDH* gene as an internal control. As shown in **Figure 8**, results of qRT-PCR were consistent with the RNA-seq data either in CG or SC1, thereby validating the RNA-seq data.

DISCUSSION

Hypersensitive Response and Programmed Cell Death during Successful Pathogen Infections

Host cell death is a programmed event during interactions between plants and pathogens (Greenberg and Yao, 2004). Whether disease resistance or susceptibility is associated with PCD is dependent on the lifestyle of the pathogen (Greenberg and Yao, 2004). PCD plays a critical role in enhancing the growth of *A. alternata* f. sp. *lycopersici* (Greenberg and Yao, 2004). Herein, during the entire infection period, stronger symptoms of PCD in the susceptible cultivar SC1 than its male parental, resistant cultivar CG was illustrated by continuously and differentially up-regulated expression of PCD-related genes (**Table 2**), for example, PLP2. A positive relationship between *PLP2* expression and cell death was found in Arabidopsis (La Camera et al., 2009). *PLP2*-silenced plants are more resistant to *B. cinerea* and *P. syringae*. On the other hand, transgenic plants overexpressing *PLP2* exhibit enhanced susceptibility to these pathogens (La Camera et al., 2005). Significantly higher expression levels of the gene encoding PLP2 in SC1 than in CG suggested that PLP2 might facilitate necrotic symptoms in SC1, supporting by more lesion developments in the susceptible genotype SC1 than in the resistant genotype CG (**Figure 1A**).

A Predominant Role of ET Biosynthesis in PCD during Successful Pathogen Infections

ET is produced by converting methionine to S-adenosylmethionine to 1-aminocyclopropane-1-carboxylic acid (ACC) via ACC synthase (ACS) and ACC oxidase (ACO), respectively (Kende, 1993). ET causes necrosis in plant tissues in response to unfavorable environmental and biotic stresses. Host-derived ET is considered to be an important signal for disease development (Bouchez et al., 2007). ET production is induced by several pathogen systems (Broekaert et al., 2006). The pathogen *A. alternata* cannot produce ET in culture but can induce higher accumulation of ET in infected plant tissues in cotton (Bashan, 1994). A positive correlation between the susceptibility of plants to *A. alternata* and ET levels suggests that ET could serve as a possible marker of susceptibility to *A. alternata* pv. *citri* (Ortuno et al., 2008). AAL toxin extracted

TABLE 4 | Unigenes associated with TFs exhibiting a Log2 FC ≥ 1 and $p \leq 0.05$ in at least one transition.

Gene ID	CG (Resistant)			SC1 (Susceptible)			Description
	FCC1/C0	FCC2/C0	FCC3/C0	FCS1/S0	FCS2/S0	FCS3/S0	
TRANSCRIPTION FACTORS-AP2/EREBP							
Pbr017391.1	0.58	0.20	0.78	−0.53	−1.49*	−1.51*	ERF4-like
Pbr000396.1	−1.15	−1.79*	−4.60*	−2.04*	−2.08*	−4.39*	ERF12-like
Pbr001362.1	1.09*	0.53	−0.56	0.81	−0.41	−1.54*	ERF105-like
Pbr037414.1	−0.45	0.68	0.04	−1.64*	−4.28*	−1.59*	ERF017-like
Pbr019669.1	0.49	1.71*	2.29*	1.59	0.98	2.82*	ERF011
Pbr013255.1	0.67	0.03	0.68	1.73*	0.82	1.99*	RAV1-like
Pbr027478.1	−0.12	−1.05*	−0.99	1.10*	−0.23	−0.18	RAV1-like
Pbr016185.1	0.44	−0.88	−0.07	1.00*	1.09*	3.37*	PTI
Pbr004315.1	−2.94*	−2.28*	–	2.21	2.93	4.05	ERF1B-like
Pbr035775.1	0.43	−0.71	−0.93	2.17*	1.97*	1.97*	ERF2-like
Pbr037846.1	0.14	−1.15	−0.33	1.46	3.65*	4.05*	ERF113-like
Pbr030542.1	0.04	−1.79*	−0.68	1.38*	1.83*	1.17	ERF1B-like
Pbr001363.1	1.22	−0.56	0.52	2.95*	1.86*	2.31*	ERF1-like
Pbr030542.1	0.04	−1.79*	−0.68	1.38*	1.83*	1.17	ERF1B-like
Pbr023899.1	−0.10	−0.60	−0.71	1.10	0.72	1.60	ERF2-like
Pbr029841.1	−0.37	−1.87*	−0.70	2.41*	3.15*	3.67*	ERF113-like
Pbr012024.1	2.15*	1.14	−0.05	1.35*	2.24*	2.69*	RAP2-3
Pbr001361.1	1.16*	0.32	−2.47*	2.46*	1.60*	−0.58	ERF107-like
Pbr013149.1	1.05*	0.07	−0.66	1.05*	1.32*	0.44	PTI
Pbr007473.1	0.86	0.38	−0.70	1.33*	1.46*	0.34	ERF060
TRANSCRIPTION FACTORS–WRKY							
Pbr018160.1	0.64	0.27	1.57*	1.11*	0.46	1.49*	WRKY11
Pbr037640.1	−1.28*	−1.48*	−1.04*	−0.71	−0.35	−0.64	WRKY11
Pbr018132.1	0.68	0.27	−1.26*	1.14*	0.49	−0.09	WRKY17
Pbr018160.1	0.64	0.27	1.57*	1.11*	0.46	1.49*	WRKY17
Pbr020000.1	0.17	1.63*	−1.46*	1.99	4.47*	5.75*	WRKY18
Pbr011544.2	0.54	−0.4	−1.63	0.71	1.04*	1.18*	WRKY33
Pbr004885.1	0.39	−1.08	−0.18	0.35	0.43	0.4	WRKY40
Pbr019026.1	1.8*	3.01*	0.94	1.41	3.32*	3.61*	WRKY40
Pbr019030.1	−1.22*	−1.87*	0.8	−0.21	−0.59	1.73*	WRKY40
Pbr020001.1	−2.03*	−1.86*	−0.7	0.43	0.27	3.56*	WRKY40
Pbr022408.1	−0.49	−2.43	−1.36	1.39*	1.33*	2.19*	WRKY40
Pbr019883.1	−0.66	−0.7	0.26	−1.67*	−1.26	0.54	WRKY50
Pbr026903.1	0.67	1.24	−0.42	1.23	2.04*	4.69*	WRKY51
Pbr031922.1	0.73	−0.98	−0.31	0.9	1.52*	2.41*	WRKY6
Pbr022698.1	1.69*	1.75*	2.74*	1.06*	0.03	0.85	WRKY65
Pbr001424.1	0.77	0.6	0.59	0.93	1.32*	2.30*	WRKY70
Pbr002398.1	1.34	0.78	0.81	0.8	3.21*	4.48*	WRKY28
Pbr015149.1	1.48	−0.17	2.80*	2.53	4.09*	7.34*	WRKY75
Pbr042883.1	1.45*	0.34	0.65	0.98	2.40*	3.97*	WRKY75
TRANSCRIPTION FACTORS–bZIP							
Pbr002622.1	0.28	0.13	2.29	0.07	1.36*	1.27	bZIP
Pbr004364.1	−1.12	−0.35	−2.65	0.37	1.04*	1.08	BZO2H3
Pbr009262.1	0.26	−0.44	0.72	3.01	4.18*	7.23*	bZIP9
Pbr018534.1	0.90	0.60	−0.17	0.98	2.22*	2.20*	bZIP11-like
Pbr040479.1	0.85	0.08	−0.21	1.24*	1.56*	0.23	bZIP11-like

**The gene was differentially expressed in the correspondent pairwise analysis ($p \leq 0.05$).*

TABLE 5 | Unigenes associated with defense response exhibiting a Log2 FC ≥ 1 and $p \leq 0.05$ in at least one transition.

Gene ID	CG (Resistant)			SC1 (Susceptible)			Description
	FCC1/C0	FCC2/C0	FCC3/C0	FCS1/S0	FCS2/S0	FCS3/S0	
DEFENSE RESPONSE/PATHOGENESIS-RELATED PROTEINS							
Pbr022550.1	1.63*	0.29	−0.19	−0.25	1.52*	1.77*	PR1
Pbr036399.1	3.22*	0.96	1.85*	0.01	5.05*	7.61*	PR5
Pbr009767.1	1.55*	0.08	−2.97	−1.05	1.07*	−0.06	EP3
Pbr009783.1	1.16	−0.41	1.88	−1.13	1.24*	3.16*	EP3
Pbr009781.1	1.50	0.20	4.23*	−0.98	1.37*	5.22*	EP3
Pbr027703.1	1.18	0.31	−3.56	1.64	3.16*	3.01*	PR3
Pbr007327.1	4.67	1.40	–	4.21	7.46*	7.72*	Chitinase II
Pbr001155.2	1.00*	−1.61	−2.02	−0.65	2.99*	4.19*	ß-1,3-BGL14
Pbr007327.1	4.67	1.40	–	4.21	7.46	7.72	CHI II
Pbr041409.1	1.05*	−0.02	1.90*	0.43	0.35	2.78*	BSP
Pbr039396.1	0.70	1.81*	2.67*	−1.39*	−0.13	1.50*	PRX2
SECONDARY METABOLITES—SHIKIMATE ACID PATHWAY							
Pbr006578.1	1.15*	−0.79	−2.65	0.24	2.56*	2.43*	Shikimate 5-dehydrogenase
Pbr042387.1	−0.59	−0.98	2.09*	−0.33	0.01	2.55*	Chorismate synthase
Pbr040661.1	−1.19	−1.06	2.27*	−0.64	−0.36	3.01*	EPSP synthase 2
Pbr029378.1	0.00	−0.12	3.55*	−0.09	0.18	3.16*	Prephenate dehydrogenase
Pbr003095.1	0.71	0.45	1.33	1.36	1.70	3.84*	Arogenate dehydrogenase
SECONDARY METABOLISM-PHENYLPROPANOIDS							
Pbr041924.1	4.20*	1.65	0.65	1.56	5.10*	6.45*	LAC7
Pbr012356.2	2.13*	−0.82	−1.19	2.42*	1.92*	0.65	BAHD acyltransferase
Pbr035966.1	1.08*	0.44	−0.90	0.91	2.55*	−0.14	BAHD acyltransferase
Pbr037017.1	1.39*	0.73	0.73	0.35	1.06*	2.12*	Kynurenine–oxoglutarae transaminase 1
Pbr040249.1	0.72	0.05	4.36*	1.61*	1.00	5.05*	Cinnamyl alcohol dehydrogenase 1
Pbr040236.1	0.57	0.01	−0.54	1.51*	0.77	0.62	Cinnamyl alcohol dehydrogenase 1
Pbr040244.1	0.75	0.25	1.62*	1.28*	0.77	2.82*	Cinnamyl alcohol dehydrogenase 1
Pbr011592.1	0.93	1.79*	1.35*	1.01*	0.12	0.21	Cinnamoyl-CoA reductase 1
Pbr008363.1	−0.17	−2.04	−4.19	0.73	2.24*	1.76*	PAL1
Pbr030350.1	0.75	−0.16	0.96	0.12	1.37*	2.66*	4-coumarate–CoA ligase-like 7
Pbr039972.1	−0.34	−1.83	−1.90	0.52	1.23*	2.37*	4-coumarate–CoA ligase-like 2
Pbr020454.1	1.40*	0.72	−1.09	−0.02	0.98	−0.55	SRG1
Pbr020456.1	1.38*	0.64	3.06*	0.40	1.18*	3.94*	SRG1
Pbr020457.1	1.16*	0.57	1.87*	0.38	1.15*	3.49*	SRG1
Pbr002584.2	1.09*	−0.74	−2.92	2.35	2.54*	1.03	SRG1
Pbr038607.1	2.44	3.99*	3.65*	2.67	5.66*	5.07*	Feruloyl CoA ortho-hydroxylase 2
Pbr004156.1	1.05*	−0.02	0.54	0.24	1.30*	1.72*	CYP736A12
Pbr007791.1	3.45*	0.52	0.45	0.85	1.54*	1.13	Caffeic acid 3-O-methyltransferase
Pbr037476.1	1.08*	−0.27	2.17	0.11	0.58	2.63*	Cationic amino acid transporter 1
SECONDARY METABOLISM-FLAVONOIDS							
Pbr021494.1	5.73*	2.70	−0.94	6.56	9.26*	5.24	CHS
Pbr021495.1	5.24*	2.65	−0.68	3.14	5.46*	1.31	CHS
Pbr027910.1	4.53*	2.27	4.03*	4.92	7.74*	8.85*	CHS
Pbr027907.1	3.54*	1.78	3.32*	3.32*	7.11*	6.20*	CHS
Pbr027916.1	4.38*	1.72	5.87*	2.23	4.86*	6.91*	CHS
Pbr029502.1	2.86*	−0.37	−1.92	2.82	6.08*	2.43	Flavonol synthase 3
Pbr007997.1	0.16	−1.64	−5.97	1.31*	1.96*	1.65*	Leucoanthocyanidin dioxygenase

**The gene was differentially expressed in the correspondent pairwise analysis ($p \leq 0.05$).*

from *A. alternata* f. sp. *lycopersici* induces ET production in tomato (Moussatos et al., 1994) and Arabidopsis (Gechev et al., 2004). Exogenous ET treatment results in enhanced disease development with necrotrophic pathogens (Abeles et al., 2012). In *B. cinerea*, application of ET synthesis inhibitors decreases susceptibility of plants to the pathogen (Abeles et al., 2012).

In this study, we also observed the continuously up-regulated expression of ET biosynthesis genes ACS, ACO1, and ACO4, accompanied by a dramatic increase in ET production after inoculation in the susceptible genotype SC1 but not in the resistant genotype CG (**Figures 5**, **6** and **Table 3**).

ET is perceived by receptors such as ETR2 and ERS1 (Alexander and Grierson, 2002). ET signaling components such as *EIN2, EIN3, EIN4,* and *ERF1* are involved in the regulation of cell death and defense responses (Bouchez et al., 2007). In addition, previous studies demonstrated that MACD1, an APETALA2/ERF transcription factor, participates in AAL-triggered cell death (ACD) and acts in the downstream of ET signaling during ACD (Mase et al., 2013). The activation of ERF1 requires both ET and JA signaling pathways (Lorenzo et al., 2003). Similarly, ERF2 is induced by the pathogen *A. brassicicola*, MeJA, and ET (McGrath et al., 2005). Interestingly, ERF2 regulates the transcription of the genes related to the JA/ET-mediated defense response pathways such as Plant Defensin1.2 (*PDF1.2*) and pathogenesis-related protein 4 (*PR4*) (Ohme-Takagi and Shinshi, 1995; Brown et al., 2003). In this study, we found that the expression of ERF1 (Pbr001363.1) and ERF2 (Pbr035775.1) was differentially induced by the infection of the pathogen in the susceptible genotype SC1 leaves. However, genes encoding PDF1.2 (Pbr012199.1 and Pbr020807.1) and PR4 (Pbr009764.1, Pbr009765.1, Pbr009785.1, and Pbr009786.1) did not display sustained and differentially up-regulated expression in either CG or SC1 (Supplementary Table S3). Furthermore, our data revealed that other ERF genes such as PTI (Pbr016185.1), ERF113-like (Pbr029841.1), and RAP2-3 (Pbr012024.1) were highly activated by the pathogen in the susceptible genotype SC1 but not in the resistant genotype CG (**Table 4**). Taken together, our data suggest that ET biosynthesis and ET signaling pathway play a predominant positive role in PCD, attributing to the successful pathogen infection in the susceptible genotype SC1 (**Figure 9**).

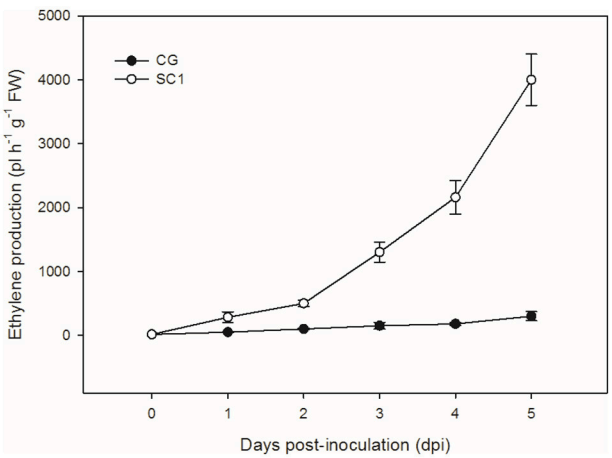

FIGURE 5 | Ethylene production. Levels of ET were measured in inoculated leaves of CG and SC1 at given time points. Mean values are shown from five independent biological replicates [error bars, ±standard error (SE)] containing at least 20 leaves for every experiment.

The Role of Antioxidant Enzymes during Pear-Pathogen Incompatible Interactions

Studies suggest that ROS in the form of H_2O_2 and $O_2\cdot^-$ are key mediators of PCD during HR (Bozhkov and Lam, 2011). The production of $O2\cdot^-$ is catalyzed by SOD (superoxide dismutase) into H_2O_2 (Bestwick et al., 1997). H_2O_2 is formed extra-cellularly and then diffuses into cells, resulting in the occurrence of PCD (Bestwick et al., 1997). CAT (catalase), as a key H_2O_2-detoxifying enzyme, decomposes H_2O_2 into molecular oxygen (O_2) and water (H_2O), maintaining leaf redox homeostasis (Wang Y. et al., 2013). The CAT mutants with reduced CAT activity display H_2O_2-induced leaf cell death phenotype in plants (Wang Y. et al., 2013). In this study, higher activities of $O2^{\cdot-}$, SOD and H_2O_2 suggested that ROS occurred at the early stage in the susceptible genotype SC1. H_2O_2 production was also triggered by the pathogen infection in the resistant genotype CG.

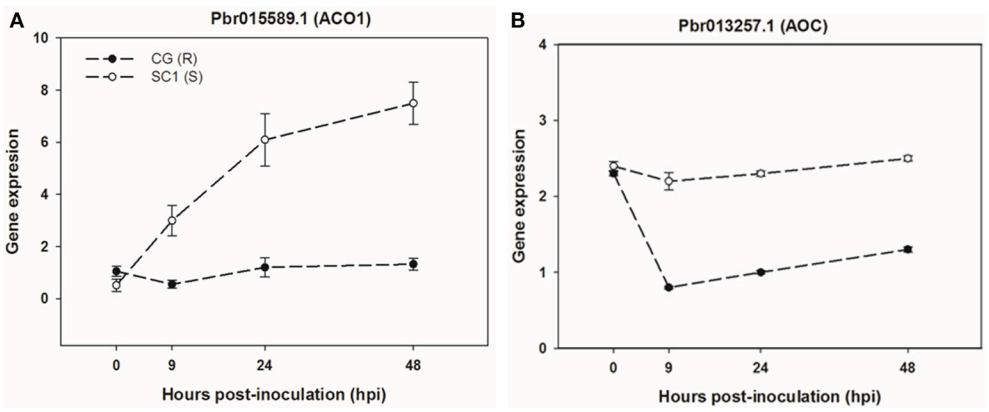

FIGURE 6 | Gene expression of ET biosynthesis gene *ACO1* (A) and JA biosynthesis gene *AOC* **(B)** in sand pear cultivars CG and SC1 in response to *A. alternata* infections. Relative expression was obtained using qRT-PCR. *GAPDH* was used as an internal control. Mean values are shown from three independent biological replicates [error bars, ±standard error (SE)].

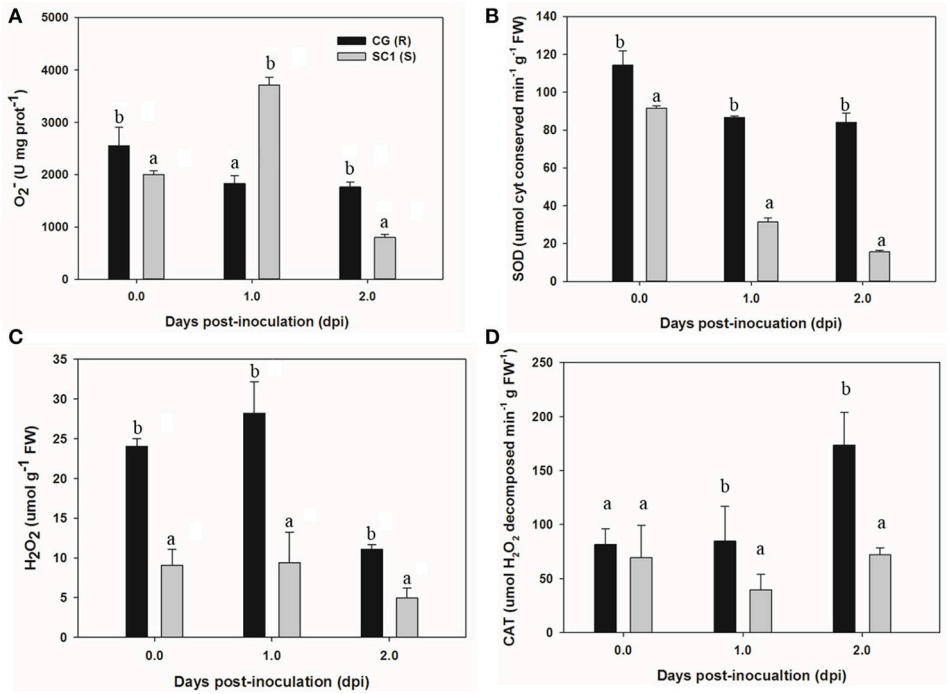

FIGURE 7 | Activities of H_2O_2 and antioxidant enzymes in sand pear cultivars CG and SC1 in response to *A. alternata* infections. Levels of O_2^- **(A)**, SOD **(B)**, H_2O_2 **(C)**, and CAT **(D)** were measured in inoculated leaves of CG and SC1 at given time points. Mean values are shown from five independent biological replicates [error bars, ±standard error (SE)] containing at least five leaves for every experiment. Different letters indicate significant differences between two genotypes at a given time point ($P \leq 0.05$).

However, increased CAT activity was detected in the resistant genotype CG but not in the susceptible genotype SC1. Our results demonstrate that the higher levels of CAT are likely to enhance the capability of cells to detoxify H_2O_2 and therefore repress H_2O_2-derived PCD during pear-pathogen interactions in the resistant genotype CG (**Figure 9**).

Notably, the expression of *CAT4* (Pbr001170.1) was not induced by the pathogen in either CG or SC1. Nevertheless, our results showed that genes encoding MBF1c (Pbr027587.1), HSP20 (Pbr016628.1), and Glutaredoxins10 (GRXS10) (Pbr014824.1) were significantly and continuously up-regulated in the resistant genotype CG but not in the susceptible genotype SC1 (**Table 2**). Previous researches demonstrate that MBF1c is a member of highly conserved transcriptional co-activator gene family which responds to oxidative stress (Arce et al., 2010). HSPs are induced by pathogen attack (Piterková et al., 2013). A positive relationship has been established between increased ROS production and HSPs expression. For example, *Oidium neolycopersici* infection stimulates HSP70 accumulation associated with increasing endogenous ROS levels in *S. chmielewskii* (Piterková et al., 2013). Glutaredoxins (GRX) are involved in the ROS-scavenging/antioxidant network. For example, the expression of GRXS13 restricts basal and high light stress-induced ROS production (Laporte et al., 2011). These results suggested that H_2O_2-derived PCD might be repressed by differentially up-regulated expression of MBF1c, HSP20, and GRXS10, and that higher H_2O_2 levels might be accumulated and redox homeostasis could be reached in the resistant genotype CG.

In addition, it is worth mentioning that several GO terms related to chloroplast and photosynthesis were significantly enriched. Analysis in detail showed that expression of those genes was increased after 2 dpi in the resistant genotype CG but decreased during the entire infection time in the susceptible genotype SC1 (Supplementary Table S3). The data suggested that the increases in photosynthetic processes may protect the photosynthetic apparatus against oxidative damage in the resistant genotype CG.

Resistance Responses of Pear to *A. alternata* Infection

The action of plant Resistance (R) genes belongs to the adaptive immune system in plant-pathogen interactions (Bonardi et al., 2011). When R genes recognize corresponding AVR genes, plant resistance to the pathogen is activated (Bonardi et al., 2011). In our transcriptome data, only two NBS-LRR genes (*RPM1* and *ADR1-L1*) were differentially up-regulated at 1 dpi in the susceptible genotype SC1. However, none were found in the infected resistant genotype CG leaf tissues (Supplementary Table S3). Yang et al. (2015) proposed that 28 candidate resistance genes with conserved leucine-rich repeats (LRR) domain might contribute to sand pear resistance to *A. alternata*. We found 23 of these genes in our transcriptome data. None of these genes were differentially expressed (Supplementary Table S3).

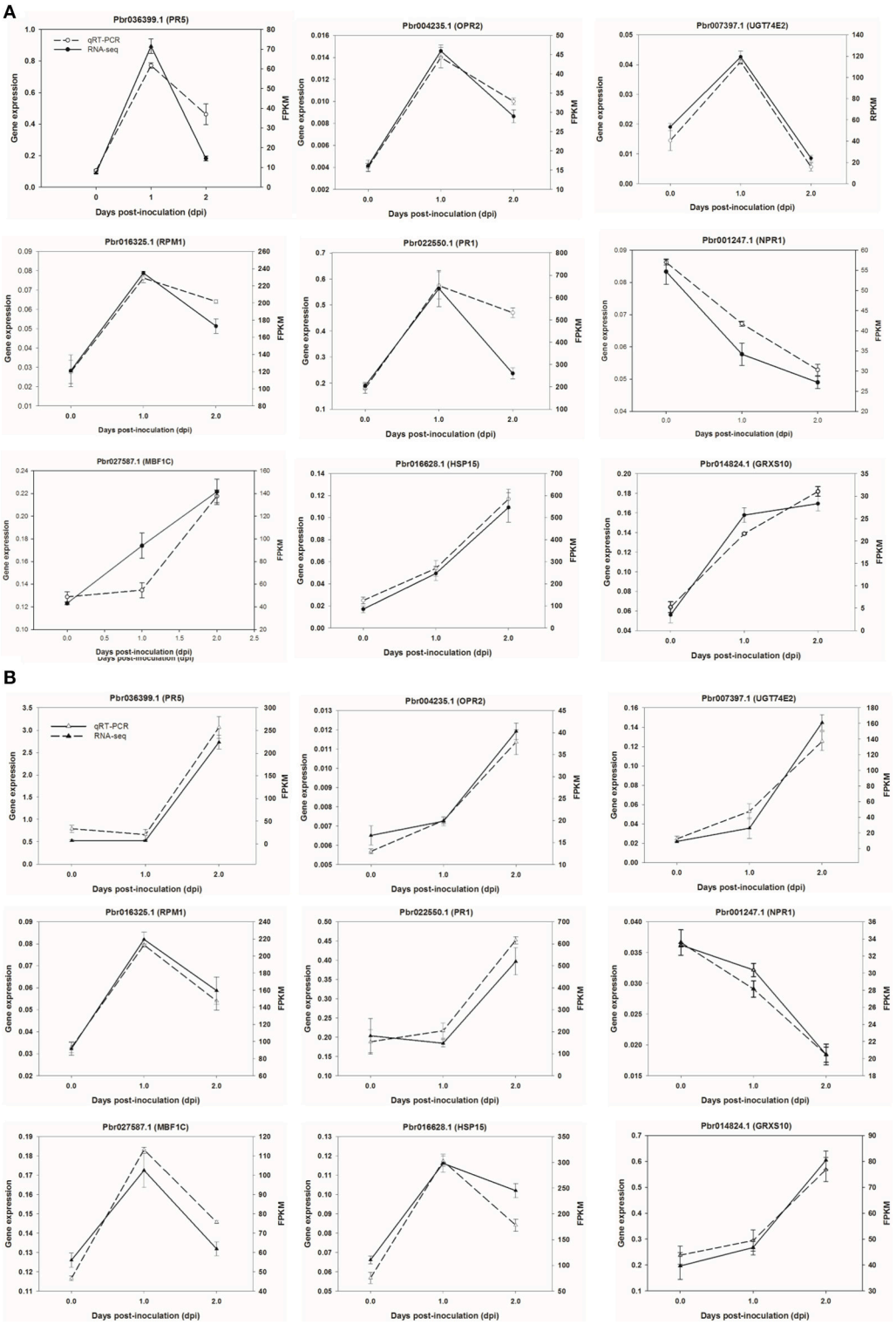

FIGURE 8 | Validation of RNA-seq data by quantitative real-time PCR. Six genes were selected and their time course expression profiles were evaluated by quantitative real-time PCR in CG **(A)** and SC1 **(B)** at given time points. Relative expression was obtained using *GAPDH* as an internal control. cDNAs were synthesized from three biological replicates.

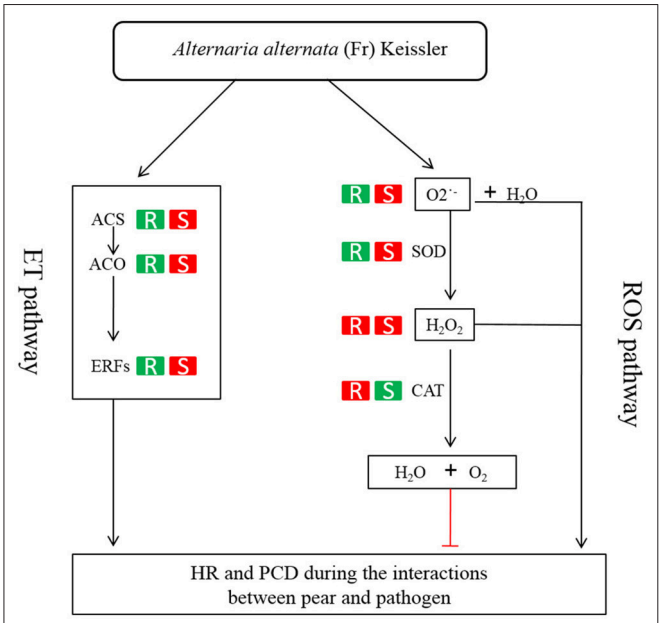

FIGURE 9 | Model of ET and H_2O_2 mediated pathways determining the compatible interaction of pear and *A. alternata*. When pear encounters the pathogen, ET biosynthesis (ACS, ACO) and ET signaling pathway (ERFs) are triggered and H_2O_2 and O_2^- productions are induced. Consequently, HR and PCD occur and the successful infection is established in the susceptible genotype SC1. On the other hand, the ET biosynthesis and ET signaling pathway is repressed. The CAT activity is induced to decompose H_2O_2 into water and oxygen. Subsequently, the resistant response of pear to the pathogen is established in the resistant genotype CG. R, the resistant genotype CG; S, the susceptible genotype SC1; Red boxes, up-regulated expression or increased level of enzyme; green boxes, down-regulated expression or reduced level of enzyme.

The inconsistent results might be due to different cultivars or the biological samples collected from different time points. Our study aims to obtain a glimpse of early responses of sand pear to *A. alternata* attack. Interestingly, those candidate resistance genes referred by Yang et al. (2015) were not detected in the early response of sand pear to *A. alternata* in the study here. Further study is required to clarify the discrepancy.

The data presented here demonstrate that a compatible reaction in the susceptible genotype SC1 to *A. alternata* infection is established early during the interaction. Higher ET production and ROS levels culminate the occurrence of PCD and necrotic cells, promoting pathogen development in the susceptible genotype SC1. However, the differential expression of genes related to HR and the induced higher levels of CAT in the resistant genotype CG lead to reduced ROS accumulation and limited the growth of necrotic cells, therefore resulting in an incompatible process with resistance. Our study demonstrates that ET biosynthesis and ET signaling pathways and detoxifying of H_2O_2 determine whether the interaction of sand pear and *A. alternata* is incompatible or compatible (**Figure 9**).

AUTHOR CONTRIBUTIONS

HW, JL and CJ conceived and designed the experiments. HW performed the experiments. HW and CJ analyzed the data. JL and YC contributed reagents/materials/analysis tools. HW and CJ wrote the manuscript.

FUNDING

This work was supported by the National Natural Science Foundation of China (Grant No. 31540052), the Jiangsu Natural Science Foundation of China (Grant No. BK 20141383) and the Jiangsu Agricultural Science and Technology Independent Innovation Fund of China [Grant No. CX (14)5016]. The funders had no role in study design, data collection and analysis, decision to publish, or preparation of the manuscript.

ACKNOWLEDGMENTS

We thank Chuan-Bei Jiang (Genepioneer Biotechnologies, Nanjing 210014, China) and Xiao-Tao Cheng (Shanghai Biotechnology Corporation, Shanghai 201203, China) for providing bioinformatics analysis.

SUPPLEMENTARY MATERIAL

The Supplementary Material for this article can be found online at: http://journal.frontiersin.org/article/10.3389/fpls.2017.00195/full#supplementary-material

REFERENCES

Abeles, F. B., Morgan, P. W., and Saltveit, M. E. Jr. (2012). *Ethylene in Plant Biology*. (San Diego, CA: Academic Press).

Alexander, L., and Grierson, D. (2002). Ethylene biosynthesis and action in tomato: a model for climacteric fruit ripening. *J. Exp. Bot.* 53, 2039–2055. doi: 10.1093/jxb/erf072

Alvarez, M. E., Pennell, R. I., Meijer, P. J., Ishikawa, A., Dixon, R. A., and Lamb, C. (1998). Reactive oxygen intermediates mediate a systemic signal network in the establishment of plant immunity. *Cell* 92, 773–784. doi: 10.1016/S0092-8674(00)81405-1

Alvarez, M. E. (2000). "Salicylic acid in the machinery of hypersensitive cell death and disease resistance," in *Programmed Cell Death in Higher Plants*, eds E. Lam, H. Fukuda and J. Greenberg (Dordrecht: Springer), 185–198.

Arce, D. P., Godoy, A. V., Tsuda, K., Yamazaki, K. I., Valle, E. M., Iglesias, M. J., et al. (2010). The analysis of an Arabidopsis triple knock-down mutant reveals functions for MBF1 genes under oxidative stress conditions. *J. Plant Physiol.* 167, 194–200. doi: 10.1016/j.jplph.2009.09.003

Bashan, Y. (1994). Symptom expression and ethylene production in leaf blight of cotton caused by *Alternaria macrospora* and *Alternaria alternata* alone and in combination. *Can. J. Bot.* 72, 1574–1579. doi: 10.1139/b94-194

Bestwick, C. S., Brown, I. R., Bennett, M., and Mansfield, J. W. (1997). Localization of hydrogen peroxide accumulation during the hypersensitive reaction of lettuce cells to *Pseudomonas syringae* pv phaseolicola. *Plant Cell* 9, 209–221. doi: 10.1105/tpc.9.2.209

Boller, T. (1991). "Ethylene in pathogenesis and disease resistance," *Plant Hormone Ethylene*, eds A. K. Mattoo and J. C. Suttle (Boca Raton, FL: CRC Press), 293–314.

Bonardi, V., Tang, S., Stallmann, A., Roberts, M., Cherkis, K., and Dangl, J. L. (2011). Expanded functions for a family of plant intracellular immune receptors beyond specific recognition of pathogen effectors. *Proc. Natl. Acad. Sci. U.S.A.* 108, 16463–16468. doi: 10.1073/pnas.1113726108

Bouchez, O., Huard, C., Lorrain, S., Roby, D., and Balagué, C. (2007). Ethylene is one of the key elements for cell death and defense response control in the Arabidopsis lesion mimic mutant vad1. *Plant. Physiol.* 145, 465–477. doi: 10.1104/pp.107.106302

Bozhkov, P. V., and Lam, E. (2011). Green death: revealing programmed cell death in plants. *Cell Death Differ.* 18, 1239–1240. doi: 10.1038/cdd.2011.86

Broekaert, W. F., Delauré, S. L., De Bolle, M. F., and Cammue, B. P. (2006). The role of ethylene in host-pathogen interactions. *Annu. Rev. Phytopathol.* 44, 393–416. doi: 10.1146/annurev.phyto.44.070505.143440

Brown, R. L., Kazan, K., McGrath, K. C., MacLean, D. J., and Manners, J. M. (2003). A role for the GCC-box in jasmonate-mediated activation of the *PDF1*. 2 gene of Arabidopsis. *Plant Physiol.* 132, 1020–1032. doi: 10.1104/pp.102.017814

Dang, H. X., Pryor, B., Peever, T., and Lawrence, C. B. (2015). The Alternaria genomes database: a comprehensive resource for a fungal genus comprised of saprophytes, plant pathogens, and allergenic species. *BMC Genomics* 16:1. doi: 10.1186/s12864-015-1430-7

Ekengren, S. K., Liu, Y., Schiff, M., Dinesh-Kumar, S., and Martin, G. B. (2003). Two MAPK cascades, NPR1, and TGA transcription factors play a role in Pto-mediated disease resistance in tomato. *Plant J.* 36, 905–917. doi: 10.1046/j.1365-313X.2003.01944.x

Fu, Z. Q., Yan, S., Saleh, A., Wang, W., Ruble, J., Oka, N., et al. (2012). NPR3 and NPR4 are receptors for the immune signal salicylic acid in plants. *Nature* 486, 228–232. doi: 10.1038/nature11162

Gechev, T., Gadjev, I., and Hille, J. (2004). An extensive microarray analysis of AAL-toxin-induced cell death in *Arabidopsis thaliana* brings new insights into the complexity of programmed cell death in plants. *Cell. Mol. Life Sci.* 61, 1185–1197. doi: 10.1007/s00018-004-4067-2

Glazebrook, J. (2001). Genes controlling expression of defense responses in Arabidopsis–2001 status. *Curr. Opin. Plant Biol.* 4, 301–308. doi: 10.1016/S1369-5266(00)00177-1

Govrin, E. M., and Levine, A. (2000). The hypersensitive response facilitates plant infection by the necrotrophic pathogen *Botrytis cinerea*. *Curr. Biol.* 10, 751–757. doi: 10.1016/S0960-9822(00)00560-1

Grant, M., and Lamb, C. (2006). Systemic immunity. *Curr. Opin. Plant Biol.* 9, 414–420. doi: 10.1016/j.pbi.2006.05.013

Greenberg, J. T. (1997). Programmed cell death in plant-pathogen interactions. *Annu. Rev. Plant Physiol. Plant Mol. Biol.* 48, 525–545. doi: 10.1146/annurev.arplant.48.1.525

Greenberg, J. T., and Yao, N. (2004). The role and regulation of programmed cell death in plant–pathogen interactions. *Cell. Microbiol.* 6, 201–211. doi: 10.1111/j.1462-5822.2004.00361.x

Gust, A. A., and Nurnberger, T. (2012). Plant immunology: a life or death switch. *Nature* 486, 198–199. doi: 10.1038/486198a

Kende, H. (1993). Ethylene Biosynthesis. *Annu. Rev. Plant Physiol. Plant Mol. Biol.* 44, 283–307. doi: 10.1146/annurev.pp.44.060193.001435

La Camera, S., Balagué, C., Göbel, C., Geoffroy, P., Legrand, M., Feussner, I., et al. (2009). The Arabidopsis patatin-like protein 2 (PLP2) plays an essential role in cell death execution and differentially affects biosynthesis of oxylipins and resistance to pathogens. *Mol. Plant Microbe Interact.* 22, 469–481. doi: 10.1094/MPMI-22-4-0469

La Camera, S., Geoffroy, P., Samaha, H., Ndiaye, A., Rahim, G., Legrand, M., et al. (2005). A pathogen-inducible patatin-like lipid acyl hydrolase facilitates fungal and bacterial host colonization in Arabidopsis. *Plant J.* 44, 810–825. doi: 10.1111/j.1365-313X.2005.02578.x

La Camera, S., Gouzerh, G., Dhondt, S., Hoffmann, L., Fritig, B., Legrand, M., et al. (2004). Metabolic reprogramming in plant innate immunity: the contributions of phenylpropanoid and oxylipin pathways. *Immunol. Rev.* 198, 267–284. doi: 10.1111/j.0105-2896.2004.0129.x

Lamb, C., and Dixon, R. A. (1997). The oxidative burst in plant disease resistance. *Annu. Rev. Plant Physiol. Plant Mol. Biol.* 48, 251–275. doi: 10.1146/annurev.arplant.48.1.251

Laporte, D., Olate, E., Salinas, P., Salazar, M., Jordana, X., and Holuigue, L. (2011). Glutaredoxin GRXS13 plays a key role in protection against photooxidative stress in Arabidopsis. *J. Exp. Bot.* 63, 503–515. doi: 10.1093/jxb/err301

Lorenzo, O., Piqueras, R., Sánchez-Serrano, J. J., and Solano, R. (2003). ETHYLENE RESPONSE FACTOR1 integrates signals from ethylene and jasmonate pathways in plant defense. *Plant Cell* 15, 165–178. doi: 10.1105/tpc.007468

Ma, C., Wang, H., Macnish, A. J., Estrad-Melo, A. C., Lin, J., Chang, Y., et al. (2015). Transcriptomic analysis reveals numerous diverse protein kinases and transcription factors involved in desiccation tolerance in the resurrection plant Myrothamnus flabellifolia. *Hortic. Res.* 2:15034. doi: 10.1038/hortres.2015.34

Mase, K., Ishihama, N., Mori, H., Takahashi, H., Kaminaka, H., Kodama, M., et al. (2013). Ethylene-responsive AP2/ERF transcription factor MACD1 participates in phytotoxin-triggered programmed cell death. *Mol. Plant Microbe Interact.* 26, 868–879. doi: 10.1094/MPMI-10-12-0253-R

McDowell, J. M., and Dangl, J. L. (2000). Signal transduction in the plant immune response. *Trends Biochem. Sci.* 25, 79–82. doi: 10.1016/S0968-0004(99)01532-7

McGrath, K. C., Dombrecht, B., Manners, J. M., Schenk, P. M., Edgar, C. I., MacLean, D. J., et al. (2005). Repressor- and activator-type ethylene response factors functioning in jasmonate signaling and disease resistance identified via a genome-wide screen of Arabidopsis transcription factor gene expression. *Plant Physiol.* 139, 949–959. doi: 10.1104/pp.105.068544

Moore, T., Martineau, B., Bostock, R., Lincoln, J., and Gilchrist, D. (1999). Molecular and genetic characterization of ethylene involvement in mycotoxin-induced plant cell death. *Physiol. Mol. Plant Pathol.* 54, 73–85. doi: 10.1006/pmpp.1998.0190

Moussatos, V., Yang, S., Ward, B., and Gilchrist, D. (1994). AAL-toxin induced physiological changes in *Lycopersicon esculentum* Mill: roles for ethylene and pyrimidine intermediates in necrosis. *Physiol. Mol. Plant Pathol.* 44, 455–468. doi: 10.1016/S0885-5765(05)80101-8

Nham, N. T., de Freitas, S. T., Macnish, A. J., Carr, K. M., Kietikul, T., Guilatco, A. J., et al. (2015). A transcriptome approach towards understanding the development of ripening capacity in 'Bartlett' pears (*Pyrus communis* L.). *BMC Genomics* 16:1. doi: 10.1186/s12864-015-1939-9

Ohme-Takagi, M., and Shinshi, H. (1995). Ethylene-inducible DNA binding proteins that interact with an ethylene-responsive element. *Plant Cell* 7, 173–182. doi: 10.1105/tpc.7.2.173

Ortuno, A., Nemsa, I., Alvarez, N., Lacasa, A., Porras, I., Lidón, A. G., et al. (2008). Correlation of ethylene synthesis in Citrus fruits and their susceptibility to *Alternaria alternata* pv. citri. *Physiol. Mol. Plant Pathol.* 72, 162–166. doi: 10.1016/j.pmpp.2008.08.003

Penninckx, I. A., Eggermont, K., Terras, F. R., Thomma, B. P., De Samblanx, G. W., Buchala, A., et al. (1996). Pathogen-induced systemic activation of a plant defensin gene in Arabidopsis follows a salicylic acid-independent pathway. *Plant Cell* 8, 2309–2323. doi: 10.1105/tpc.8.12.2309

Piterková, J., Luhová, L., Mieslerová, B., Lebeda, A., and Petrivalský, M. (2013). Nitric oxide and reactive oxygen species regulate the accumulation of heat shock proteins in tomato leaves in response to heat shock and pathogen infection. *Plant Sci.* 207, 57–65. doi: 10.1016/j.plantsci.2013.02.010

Sagisaka, S. (1976). The occurrence of peroxide in perennial plant, *Populus gelrica*. *Plant Physiol.* 57, 308–309. doi: 10.1104/pp.57.2.308

Shin, S., Lv, J., Fazio, G., Mazzola, M., and Zhu, Y. (2014). Transcriptional regulation of ethylene and jasmonate mediated defense response in apple (*Malus domestica*) root during *Pythium ultimum* infection. *Hort. Res.* 1:14053. doi: 10.1038/hortres.2014.53

Suzuki, T., Shinogi, T., Narusaka, Y., and Park, P. (2003). Infection behavior of *Alternaria alternata* Japanese pear pathotype and localization of 1,3-β-D-glucan in compatible and incompatible interactions between the pathogen and host plants. *J. Gen. Plant Pathol.* 69, 91–100. doi: 10.1007/s10327-002-0001-3

Terakami, S., Adachi, Y., Iketani, H., Sato, Y., Sawamura, Y., Takada, N., et al. (2007). Genetic mapping of genes for susceptibility to black spot disease in Japanese pears. *Genome* 50, 735–741. doi: 10.1139/G07-053

Thimm, O., Bläsing, O., Gibon, Y., Nagel, A., Meyer, S., Krüger, P., et al. (2004). mapman: a user-driven tool to display genomics data sets onto diagrams

of metabolic pathways and other biological processes. *Plant J.* 37, 914–939. doi: 10.1111/j.1365-313X.2004.02016.x

Thomma, B. P., Eggermont, K., Tierens, K. F., and Broekaert, W. F. (1999). Requirement of functional ethylene-insensitive 2 gene for efficient resistance of Arabidopsis to infection by *Botrytis cinerea*. *Plant Physiol.* 121, 1093–1101. doi: 10.1104/pp.121.4.1093

Trapnell, C., Williams, B. A., Pertea, G., Mortazavi, A., Kwan, G., Van Baren, M. J., et al. (2010). Transcript assembly and quantification by RNA-Seq reveals unannotated transcripts and isoform switching during cell differentiation. *Nat. Biotechnol.* 28, 511–515. doi: 10.1038/nbt.1621

Wang, H., Liu, G., Li, C., Powell, A. L., Reid, M. S., Zhang, Z., et al. (2013). Defence responses regulated by jasmonate and delayed senescence caused by ethylene receptor mutation contribute to the tolerance of petunia to *Botrytis cinerea*. *Mol. Plant Pathol.* 14, 453–469. doi: 10.1111/mpp.12017

Wang, Y., Lin, A., Loake, G. J., and Chu, C. (2013). H_2O_2-induced leaf cell death and the crosstalk of reactive nitric/oxygen species. *J. Integr. Plant Biol.* 55, 202–208. doi: 10.1111/jipb.12032

Wu, J., Wang, Z., Shi, Z., Zhang, S., Ming, R., Zhu, S., et al. (2013). The genome of the pear (*Pyrus bretschneideri* Rehd.). *Genome Res.* 23, 396–408. doi: 10.1101/gr.144311.112

Yang, X., Hu, H., Yu, D., Sun, Z., He, X., Zhang, J., et al. (2015). Candidate resistant genes of sand pear (*Pyrus pyrifolia* nakai) to *Alternaria alternata* revealed by transcriptome sequencing. *PLoS ONE* 10:e0135046. doi: 10.1371/journal.pone.0135046

Conflict of Interest Statement: The authors declare that the research was conducted in the absence of any commercial or financial relationships that could be construed as a potential conflict of interest.

frontiers in Plant Science

ORIGINAL RESEARCH
published: 23 March 2016
doi: 10.3389/fpls.2016.00361

The Mechanism of Ethylene Signaling Induced by Endophytic Fungus *Gilmaniella* sp. AL12 Mediating Sesquiterpenoids Biosynthesis in *Atractylodes lancea*

*Jie Yuan, Kai Sun, Meng-Yao Deng-Wang and Chuan-Chao Dai **

Jiangsu Key Laboratory for Microbes and Functional Genomics, Jiangsu Engineering and Technology Research Center for Industrialization of Microbial Resources, College of Life Sciences, Nanjing Normal University, Jiangsu, China

Ethylene, the first known gaseous phytohormone, is involved in plant growth, development as well as responses to environmental signals. However, limited information is available on the role of ethylene in endophytic fungi induced secondary metabolites biosynthesis. *Atractylodes lancea* is a traditional Chinese herb, and its quality depends on the main active compounds sesquiterpenoids. This work showed that the endophytic fungus *Gilmaniella* sp. AL12 induced ethylene production in *Atractylodes lancea*. Pre-treatment of plantlets with ethylene inhibiter aminooxyacetic acid (AOA) suppressed endophytic fungi induced accumulation of ethylene and sesquiterpenoids. Plantlets were further treated with AOA, salicylic acid (SA) biosynthesis inhibitor paclobutrazol (PAC), jasmonic acid inhibitor ibuprofen (IBU), hydrogen peroxide (H_2O_2) scavenger catalase (CAT), nitric oxide (NO)-specific scavenger 2-(4-Carboxyphenyl)-4,4,5,5-tetramethylimidazoline-1-oxyl-3-oxide potassium salt (cPTIO). With endophytic fungi inoculation, IBU or PAC did not inhibit ethylene production, and JA and SA generation were suppressed by AOA, showing that ethylene may act as an upstream signal of JA and SA pathway. With endophytic fungi inoculation, CAT or cPTIO suppressed ethylene production, and H_2O_2 or NO generation was not affected by 1-aminocyclopropane-1-carboxylic acid (ACC), showing that ethylene may act as a downstream signal of H_2O_2 and NO pathway. Then, plantlets were treated with ethylene donor ACC, JA, SA, H_2O_2, NO donor sodium nitroprusside (SNP). Exogenous ACC could trigger JA and SA generation, whereas exogenous JA or SA did not affect ethylene production, and the induced sesquiterpenoids accumulation triggered by ACC was partly suppressed by IBU and PAC, showing that ethylene acted as an upstream signal of JA and SA pathway. Exogenous ACC did not affect H_2O_2 or NO generation, whereas exogenous H_2O_2 and SNP induced ethylene production, and the induced sesquiterpenoids accumulation triggered by SNP or H_2O_2 was partly suppressed by ACC, showing that ethylene acted as a downstream signal of NO and H_2O_2 pathway.

OPEN ACCESS

Edited by:
Antonio Ferrante,
Università degli Studi di Milano, Italy

Reviewed by:
Nabil I. Elsheery,
Tanta Univeristy, Egypt
Rita Maggini,
University of Pisa, Italy

***Correspondence:**
Chuan-Chao Dai
daichuanchao@njnu.edu.cn

Specialty section:
This article was submitted to Plant Physiology, a section of the journal Frontiers in Plant Science

Received: *16 January 2016*
Accepted: *08 March 2016*
Published: *23 March 2016*

Citation:
Yuan J, Sun K, Deng-Wang M-Y and Dai C-C (2016) The Mechanism of Ethylene Signaling Induced by Endophytic Fungus Gilmaniella sp. AL12 Mediating Sesquiterpenoids Biosynthesis in Atractylodes lancea. Front. Plant Sci. 7:361. doi: 10.3389/fpls.2016.00361

Taken together, this study demonstrated that ethylene is an upstream signal of JA and SA, and a downstream signal of NO and H_2O_2 signaling pathways, and acts as an important signal mediating sesquiterpenoids biosynthesis of *Atractylodes lancea* induced by the endophytic fungus.

Keywords: *Atractylodes lancea*, endophytic fungi, sesquiterpenoids, ethylene, medicinal plants, tissue culture

INTRODUCTION

Atractylodes lancea, belonging to the Compositae family, is a traditional Chinese medicinal plant and is used as a main ingredient in many famous Chinese medicines. Sesquiterpenoids are the main active compounds in *A. lancea* and have medicinal efficacy against influenza, digestive disorders, rheumatic diseases, and night blindness (Wang et al., 2008). The quality of this herb depends on where it is cultivated. The plantlet grown in the Maoshan area of the Jiangsu Province is the geo-authetic medicinal plant (Ouyang et al., 2012), and is characterized by higher content of sesquiterpenoids (Ji et al., 2001). In recent years, the natural sources of *A. lancea* have been in sharp decline as they grow slowly and have been over exploited (Zhou et al., 2015). Although artificially cultivated sources of *A. lancea* ensure the production of this herb, the content of sesquiterpenoids is relatively low (Zhou et al., 2015). Currently, guaranteeing sesquiterpenoids content in *A. lancea* has become a hot topic. Endophytes play active roles in promoting plant growth and secondary metabolites accumulation (Wang et al., 2011; Ludwig-Müller, 2015). Our previous studies have shown that several endophytes, such as *Gilmaniella* sp. AL12, *Acinetobacter* sp. ALEB16, and *Pseudomonas fluorescens* ALEB7B, can establish symbiotic relationships with *A. lancea*, and also greatly promote sesquiterpenoids accumulation in the herb (Wang et al., 2012, 2015a; Zhou et al., 2015). How endophytes promote the accumulation of sesquiterpenoids in *A. lancea* is an intriguing issue.

Some works have been done to explain the phenomenon of the improving sesquiterpenoids accumulation in *A. lancea* caused by the endophytes (Wang et al., 2011, 2012, 2015a; Ren and Dai, 2012, 2013; Ren et al., 2013). Our previous studies demonstrated that AL12 can activate signals, such as nitric oxide (NO), hydrogen peroxide (H_2O_2), salicylic acid (SA) (Wang et al., 2011), jasmonic acid (JA) (Ren and Dai, 2012), brassinosteroid (Br) (Ren and Dai, 2013), and Calcium (Ca^{2+}) (Ren et al., 2013), increasing the biosynthesis of sesquiterpenoids in *A. lancea*. Whether there are other signals involved in the signaling pathway for AL12-induced sesquiterpenoids accumulation of *A. lancea* is worthy of attention.

Ethylene (ET) is the first known gaseous phytohormone, and affects plant growth, development, and responses to environmental signals (Arc et al., 2013; Steffens, 2014; Bakshi et al., 2015; Wei et al., 2015). ET acted as an important signal and was involved in the production of β-thujaplicin (Zhao et al., 2004), lycopene (Liu et al., 2012), ginsenoside (Rahimi et al., 2015), and terpenoid (Arimura et al., 2007). We have mainly focused on the signals of JA, SA, NO, H_2O_2 in AL12-induced sesquiterpenoids accumulation of *A. lancea*, and did not pay attention to the ET signaling. The aims of this study are to investigate whether the endophytic fungus AL12 can induce ET generation, and to discuss the possible role of ET in sesquiterpenoids accumulation, and also to expound the possible relationship between ET and other signals. Furthermore, we compared the signaling pathways mediating sesquiterpenoids accumulation induced by endophytic fungi and endophytic bacterium. This work comprehensively demonstrated the signaling pathways of sesquiterpenoids biosynthesis and provided a theoretical basis for the industrialization of active compounds in *A. lancea*. And this work will provide a theoretical reference for the biosynthesis of other active compounds such as artemisinin, paclitaxel, menthol, glycyrrhizic acid, and ginseng saponin, and will help to further clarify plant-endophyte interactions.

Abbreviations: A. lancea, Atractylodes lancea; AL12, Endophytic fungus *Gilmaniella* sp. AL12;NO, Nitric oxide; H_2O_2, Hydrogen peroxide; SA, Salicylic acid; JA, Jasmonic acid; ET, Ethylene; AOA, Aminooxyacetic acid; IBU, Ibuprofen; PAC, Paclobutrazol; CAT, Catalase; cPTIO, 2-(4-Carboxyphenyl)-4,4,5,5-tetramethylimidazoline-1-oxyl-3-oxide potassium salt; ACC, 1-aminocyclopropane-1-carboxylic acid; SNP, Sodium nitroprusside; GC, Gas chromatography; HPLC, High-performance liquid chromatography.

MATERIALS AND METHODS

Plant Material and Growth Conditions

Meristem cultures of *A. lancea* were established using tissue culture as previously described (Wang et al., 2012). Briefly, sterilized plantlets were grown in 50 mL Murashige and Skoog medium containing 30 g L^{-1} sucrose, 10% agar (w/v), 0.3 mg L^{-1} naphthaleneacetic acid, and 2.0 mg L^{-1} 6-benzyladenine in 150-mL Erlenmeyer flasks. When newborn axillary buds produced by the meristem cultures were sufficient, they were separated and transplanted into 50 mL Murashige and Skoog medium containing 30 g L^{-1} sucrose, 10% agar (w/v), and 0.25 mg L^{-1} naphthaleneacetic acid in 150-mL Erlenmeyer flasks. All media pH was adjusted to 6.0 before autoclaving at 121°C for 20 min. Plants were maintained in a growth chamber at 25/18°C day/night cycle, with a light intensity of 3400 lm/m^2 and a photoperiod of 12 h, and were sub-cultured every 30 days.

Endophytic Fungi and Inoculation

The fungal endophyte AL12 (*Gilmaniella* sp.) was isolated from *A. lancea*, cultured on potato dextrose agar, and incubated at 28°C for 5 days prior to starting any experiments (Wang et al., 2012). Thirty-day-old rooting plantlets were inoculated with 5-mm AL12 mycelial disks, which were placed near the plant caudexes on the medium. Meantime, controls were established

using equal sized potato dextrose agar disks. All treatments were performed under sterile conditions and performed in triplicate.

Chemicals and Treatments

Aminooxyacetic acid (AOA), ibuprofen (IBU), paclobutrazol (PAC), catalase (CAT), 2-(4-Carboxyphenyl)-4,4,5,5-tetramethylimidazoline-1-oxyl-3-oxide potassium salt (cPTIO) were used as specific inhibitors or scavengers of ethylene, JA, SA, H_2O_2, NO synthesis, and they were obtained from Sigma-Aldrich (St. Louis, MO, USA). 1-aminocyclopropane-1-carboxylic acid (ACC), Sodium nitroprusside (SNP) were used as donors of ethylene and NO, respectively. JA, SA, hydrogen peroxide solution were obtained from Sigma-Aldrich (St. Louis, MO, USA). All inhibitors or scavengers and exogenous donors were dissolved in double distilled water and filtered through 0.22-μm diameter microporous membranes before use. The concentration of the above chemicals was according to our previous studies (Wang et al., 2011; Ren and Dai, 2012, 2013; Ren et al., 2013). Inhibitors or scavengers were sprayed on plant leaves and roots 1-day before the application of exogenous donors or AL12 inoculation. An equal volume of double distilled water was used as the control. The chemicals used in this study were chosen according to our previous studies. Unless stated otherwise, plants were harvested 15 days after the application of exogenous donors or AL12 inoculation. Each treatment was performed in triplicate.

Ethylene Extraction and Measurement

Thirty-day-old plantlets treated with 5-mm AL12 mycelial disks or potato dextrose agar disks were harvested to determine the ethylene content at 0, 5, 10, 15, and 20 days. Fresh samples (1 g) were ground with 10 ml 0.1 M phosphate buffer solution (pH 7.4), and then centrifuged (3000 g, 20 min, 4°C). The supernatant was used for ethylene measurement. The production of ethylene was measured using the Plant ETH ELISA Kit (Shanghai Fankel Biological Technology Co., Ltd., China) following the manufacturer's instructions. At each time point, at least 15 plantlets were employed. Each treatment was performed in triplicate.

Sesquiterpenoids Extraction and Gas Chromatograph Analysis

Harvested plants were dried at 30°C to a constant weight. After dry weights were measured, total sesquiterpenoids were extracted from whole plantlets according to Wang et al. (2015a). Briefly, dried plants were ground to a fine powder and one gram of plant powder was extracted with 4 mL cyclohexane for 10 h. After sonication (15 min, 60 Hz) and centrifugation (5000 g, 5 min, 4°C), total sesquiterpenoids extracts were dried over anhydrous sodium sulfate and filtered through 0.22-μm diameter microporous membranes, and then stored in dark glass bottles at 4°C before gas chromatography (GC) analysis.

GC analysis was conducted using an Agilent 7890A GC equipped with a fame ionization detector (Agilent, Santa Clara, CA, USA). GC operating conditions were as follows. An Agilent DB-1ms column (30 m × 0.32 mm × 0.10 μm) was used with the temperature program according to the method established in our laboratory (Zhou et al., 2015). The column temperature was held at 100°C for 4 min after injection, increased by 10°C min^{-1} to 140°C, held for 10 min, increased by 10°C min^{-1} to 220°C, held for 10 min, increased by 10°C min^{-1} to 260°C, and held for 2 min. High-purity nitrogen was used as a carrier at a flow rate of 0.8 mL min^{-1}, and 1 μL was injected onto the column at injection temperature of 240°C. The detector temperature was set at 350°C and the pre-column pressure was 70 KPa. Seven sesquiterpenoids (including β-caryophyllene, zingiberene, β-sesquiphellandrene, caryophyllene oxide, hinesol, β-eudesmol, and atractylone) were identified according to the retention times of authentic standards (Ren and Dai, 2012; Wang et al., 2015a; Zhou et al., 2015), and their retention time (min) were 11.136, 12.999, 13.827, 15.549, 17.702, 17.946, and 18.535 respectively (**Supplemental Figure S1**). Standard curves were constructed for quantitative measurement of sesquiterpenoids. At each time point, at least 15 plantlets were employed. Each treatment was performed in triplicate.

JA Extraction and Measurement

JA was extracted according to the established method (Engelberth et al., 2003; Ren and Dai, 2012). Five grams of plant materials were ground in liquid nitrogen and extracted with 20 mL H_2O: acetone (30:70, v:v). Samples were stored in dark glass bottles at 4°C for analysis. JA content was measured using the Plant JA ELISA Kit (Shanghai Fankel Biological Technology Co., Ltd., China) following the manufacturer's instructions.

SA Extraction and HPLC Analysis

SA was extracted according to our previous method with some modification (Wang et al., 2015a). Briefly, five grams of plant materials were ground in liquid nitrogen and extracted with 5 mL methanol for 10 min by sonication (60 Hz). After centrifugation (12,000 g, 5 min, 4°C), the supernatant was collected. The residue was extracted with 5 mL methanol for 10 min by sonication (60 Hz) and centrifuged (12,000 g, 5 min, 4°C) three times. The combined supernatant was mixed with 10 μL 0.2 M NaOH, evaporated under vacuum to dryness, dissolved in 250 μL of 5% trichloroacetic acid. The mixture was subjected to three consecutive liquid-liquid extractions with 800 μL ethyl acetate: cyclohexane (1:1, v/v). The combined organic phase was mixed with 60 μL 0.2 M acetate buffer (NaOAc) (pH 5.5), and evaporated under vacuum to dryness, dissolved in 600 μL mobile phase (methanol:2% acetic acid:H_2O, 50:40:10, v:v:v), and filtered using a 0.22-μm diameter microporous membrane for analysis.

SA was quantified via high-performance liquid chromatography (HPLC) using an Agilent C18 column (250 × 4.6 mm, 5 μm) according to our previous method (Wang et al., 2011, 2015a; Ren and Dai, 2012). An Agilent 1290 Infinity (Agilent Technology, Germany) with UV detector and Agilent Chem-Station Software were used for quantification of SA. The injection volume was 20 μL and the column temperature was 25°C. The detection wavelength was set at 290 nm and isocratic elution was used at a flow rate of 0.5 mL min^{-1}. Qualification and quantification analyses were based on comparison with SA standard. The SA peak in the fresh samples was identified by

comparing retention time and area with that of the matching standard.

Extraction and Measurement of NO and H_2O_2

The production of NO and H_2O_2 was measured using the NO or H_2O_2 assay kit (Nanjing Jiancheng Bio-engineering Institute, China) following the manufacturer's instructions (Wang et al., 2011). Fresh sample of plant materials (1 g) were ground with 5 mL of 40 mM 4-(2-hydroxyethyl)-1-piperazineethanesulfonic acid (pH 7.2) for NO, or 5 mL of double distilled water for H_2O_2. After centrifugation (14,000 g, 10 min, 4°C), the supernatant was used for the measurement of NO and H_2O_2, respectively.

Statistical Analysis

Each experiment was performed in triplicate, and the whole experimental setup was repeated in triplicate with other batches of plant material to examine the reproducibility. The means and standard deviations (SD) were calculated using SPSS Statistics 17.0 software (SPSS Inc., Chicago, USA). The independent-Samples *T*-Test was used for statistical evaluation between two treatments. The one-way analysis of variance (ANOVA) followed by Tukey's multiple-comparison test ($P < 0.05$) was used for statistical evaluation between more than two treatments. The ANOVA was performed separately on sesquiterpenoids, ET, JA, SA, H_2O_2, and NO. Bars represent standard deviations. Asterisks denote significant differences from the control (*t*-test; $^{*}p < 0.05$; $^{**}p < 0.01$). Values followed by different types of lowercase letters (e.g., a, b, c; a′, b′, c′; a″, b″, c″) differ significantly at $P = 0.05$.

RESULTS

Involvement of Ethylene in AL12-Induced Sesquiterpenoids Accumulation

The ET contents of *A. lancea* increased significantly after endophytic fungus AL12 inoculation (**Figure 1A**), indicating that AL12 may trigger the biosynthesis of ET in *A. lancea*. AOA, an inhibitor of ACC biosynthesis, is usually applied as an inhibiter of ethylene production. To investigate whether ET was involved in AL12-induced sesquiterpenoids accumulation, the effects of AOA on the production of AL12-induced sesquiterpenoids in *A. lancea* were determined.

As shown in **Figure 1B**, AOA suppressed not only AL12-triggered ET production, but also AL12-induced sesquiterpenoids accumulation. The sesquiterpenoids concentrations of plantlets treated with 0.5, 1, and 2 mM AOA were 12.69, 28.7%, and 28.77% lower than that of AL12-innoculated plantlets, respectively. The results suggested that the production of ET is involved in AL12-induced sesquiterpenoids accumulation of *A. lancea*. And, 1 mM AOA was chosen for the following experiments.

Dependence of Ethylene-Induced Sesquiterpenoids Accumulation on JA

IBU is an inhibitor of the octadecanoid pathway that synthesizes JA, and is applied as a specific inhibitor of JA (Ren and Dai, 2012). **Figure 2A** showed that both AOA and IBU could significantly suppress AL12-induced sesquiterpenoids accumulation in *A. lancea*. AOA can strongly suppress AL12-induced JA generation; whereas IBU did not affect AL12-triggered ET generation (**Figure 2A**). This result suggested that the ET and JA signaling pathway were connected, and that ET might act as an upstream signal of AL12-induced JA generation and sesquiterpenoids production in the *A. lancea* plantlets. The data showing that the application of exogenous ACC and JA could reverse the suppression of AL12-induced sesquiterpenoids production by AOA and IBU further confirmed our results (**Figure 2A**).

To investigate if exogenous ET-induced sesquiterpenoids accumulation also depended on JA signaling, the effects of exogenous ACC, JA, AOA, and IBU on the accumulation of sesquiterpenoids, ET and JA were determined. **Figure 2B** showed that both exogenous ACC and JA could significantly induce

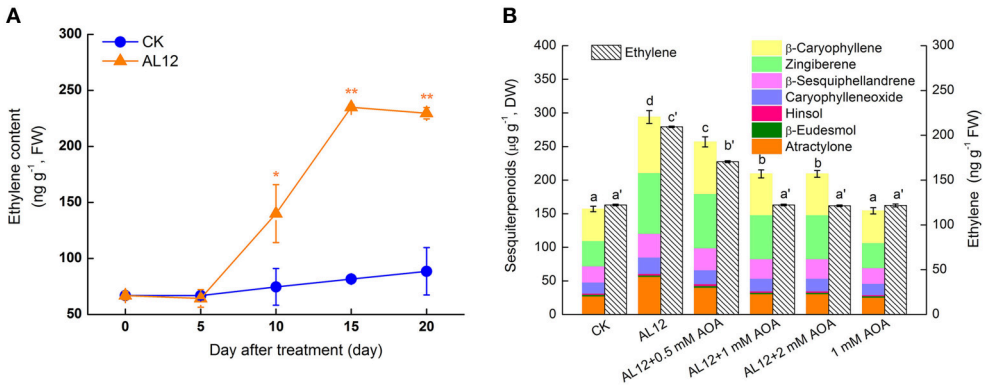

FIGURE 1 | Involvement of ethylene in endophytic fungus AL12-induced sesquiterpenoids accumulation in *Atractylodes lancea* plantlets. (A) AL12-induced ethylene generation in plantlets. Thirty-day-old plantlets treated with 5-mm AL12 mycelial disks were harvested for ethylene measurement at 0, 5, 10, 15, and 20 day. Controls were established using equal sized potato dextrose agar disks. Values are the means of three independent experiments. Bars represent standard deviations. Asterisks denote significant differences from the control (*t*-test; $^{*}P < 0.05$; $^{**}P < 0.01$). **(B)** Effects of AOA (ethylene inhibitor) on AL12-induced sesquiterpenoids accumulation after 15 days. Inhibitors (0.5, 1, or 2 mM AOA) were added 1 day prior to AL12 inoculation. Controls were established using equal sized potato dextrose agar disks. Values are the means of three independent experiments ± SD. Bars with different lowercase letters (e.g., a, b, c; a′, b′, c′) are significantly different ($P < 0.05$).

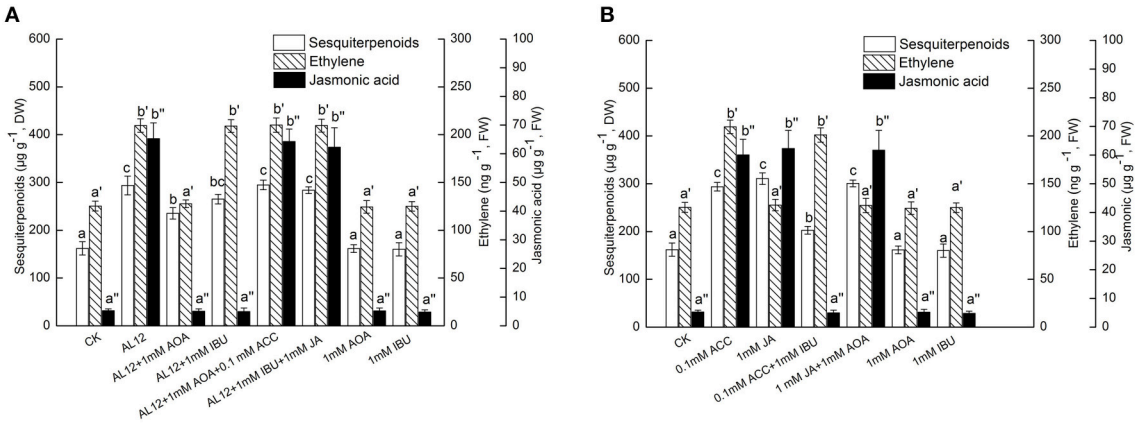

FIGURE 2 | (A) Interaction between ethylene and JA signaling pathways for endophytic fungus AL12-induced sesquiterpenoids accumulation in *Atractylodes lancea* plantlets. Thirty-day-old plantlets treated with 5-mm AL12 mycelial disks, 1 mM AOA, 1 mM IBU, 0.1 mM ACC, and 1 mM JA were harvested after 15 days to determine the sesquiterpenoids, ethylene and JA contents. Inhibitors were added 1 day prior to endophytic fungus AL12 inoculation or exogenous signal donor application. Controls were established using equal sized potato dextrose agar disks. Values are the means of three independent experiments ± SD. Bars with different lowercase letters (e.g., a, b, c; a′, b′, c′; a″, b″, c″) are significantly different ($P < 0.05$). **(B)** Dependence of ethylene-induced sesquiterpenoids accumulation on JA in *Atractylodes lancea* plantlets. Thirty-day-old plantlets treated with 0.1 mM ACC, 1 mM JA, 1 mM AOA, and 1 mM IBU were harvested 15 days later to determine the sesquiterpenoids, ethylene and JA contents. Inhibitors were added 1 day prior to exogenous signal donor application. Controls were established using equal volume of double distilled water. Values are the means of three independent experiments ± SD. Bars with different lowercase letters (e.g., a, b, c; a′, b′, c′; a″, b″, c″) are significantly different ($P < 0.05$).

sesquiterpenoids accumulation in *A. lancea*. The increased sesquiterpenoids accumulation triggered by ACC was partly suppressed by IBU; whereas the increased sesquiterpenoids accumulation triggered by JA was not affected by AOA (**Figure 2B**). In addition, exogenous ACC could trigger JA generation; whereas exogenous JA did not affect ET production (**Figure 2B**). And, exogenous AOA or IBU itself had no adverse effect on the accumulation of sesquiterpenoids, ET and JA in the *A. lancea* plantlets compared to the control (**Figure 2B**). These results further demonstrated that ET acted as an upstream signal of JA in AL12-induced sesquiterpenoids accumulation of *A. lancea*. Additionally, IBU could not completely abolish ACC-induced sesquiterpenoids accumulation (**Figure 2B**), suggesting that ET-induced sesquiterpenoids accumulation is not solely dependent on the JA signaling pathway.

Dependence of Ethylene-Induced Sesquiterpenoids Accumulation on SA

PAC is an inhibitor of benzoic acid hydroxylase that related to SA biosynthesis (Wang et al., 2011; Ren and Dai, 2012), and is applied as SA-inhibitor in many plants. **Figure 3A** showed that both AOA and PAC could significantly suppress AL12-induced sesquiterpenoids accumulation in *A. lancea*. AOA can strongly suppress AL12-induced SA generation; whereas PAC did not affect AL12-triggered ET generation (**Figure 3A**). This result suggested that the ET and SA signaling pathway were connected, and that ET might act as an upstream signal of AL12-induced SA generation and sesquiterpenoids production in the *A. lancea* plantlets. The data showing that the application of exogenous ACC and SA could reverse the suppression of AL12-induced sesquiterpenoids production by AOA and PAC further confirmed our results (**Figure 3A**).

To investigate if exogenous ET-induced sesquiterpenoids accumulation also depended on SA signaling, the effects of exogenous ACC, SA, AOA, and PAC on the accumulation of sesquiterpenoids, ET and SA were determined. **Figure 3B** showed that both exogenous ACC and SA could significantly induce sesquiterpenoids accumulation in *A. lancea*. The increased sesquiterpenoids accumulation triggered by ACC was partly suppressed by PAC; whereas the increased sesquiterpenoids accumulation triggered by SA was not affected by AOA (**Figure 3B**). In addition, exogenous ACC could trigger SA generation; whereas exogenous SA did not affect ET production (**Figure 3B**). And, exogenous AOA or PAC itself had no adverse effect on the accumulation of sesquiterpenoids, ET and SA in the *A. lancea* plantlets compared to the control (**Figure 3B**). These results further demonstrated that ET acted as an upstream signal of SA in AL12-induced sesquiterpenoids accumulation of *A. lancea*. Additionally, PAC could not completely abolish ACC-induced sesquiterpenoids accumulation (**Figure 3B**), suggesting that ET-induced sesquiterpenoids accumulation is not solely dependent on the SA signaling pathway.

Ethylene Acts as a Downstream Signal of H_2O_2

CAT is an inhibitor of NADPH oxidase, and is applied as H_2O_2 scavenger (Wang et al., 2011; Ren and Dai, 2012). **Figure 4A** showed that both AOA and CAT could significantly suppress AL12-induced sesquiterpenoids accumulation in *A. lancea*. CAT can strongly suppress AL12-induced ET generation;

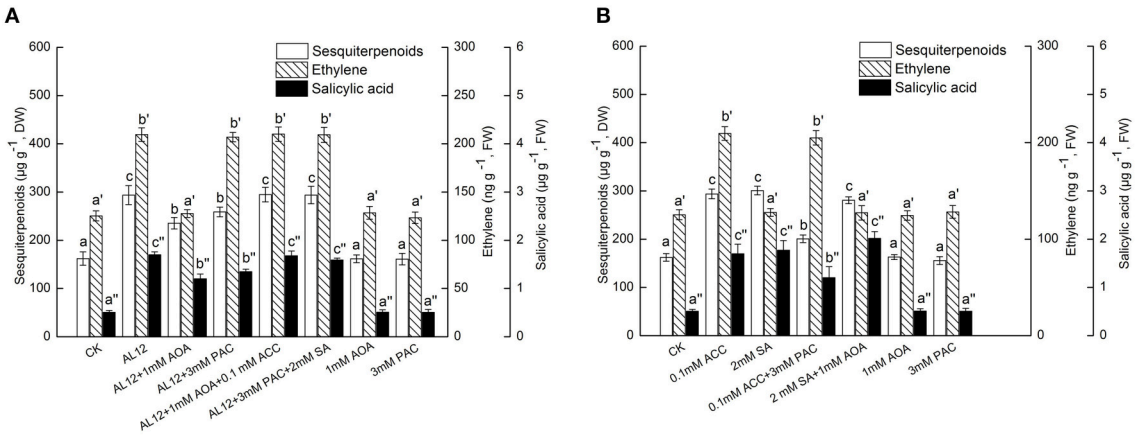

FIGURE 3 | (A) Interaction between ethylene and SA signaling pathways for endophytic fungus AL12-induced sesquiterpenoids accumulation in *Atractylodes lancea* plantlets. Thirty-day-old plantlets treated with 5-mm AL12 mycelial disks, 1 mM AOA, 3 mM PAC, 0.1 mM ACC, and 2 mM SA were harvested after 15 days to determine the sesquiterpenoids, ethylene and SA contents. Inhibitors were added 1 day prior to endophytic fungus AL12 inoculation or exogenous signal donor application. Controls were established using equal sized potato dextrose agar disks. Values are the means of three independent experiments ± SD. Bars with different lowercase letters (e.g., a, b, c; a′, b′, c′; a″, b″, c″) are significantly different ($P < 0.05$). **(B)** Dependence of ethylene-induced sesquiterpenoids accumulation on SA in *Atractylodes lancea* plantlets. Thirty-day-old plantlets treated with 0.1 mM ACC, 2 mM SA, 1 mM AOA, and 3 mM PAC were harvested 15 days later to determine the sesquiterpenoids, ethylene and SA contents. Inhibitors were added 1 day prior to exogenous signal donor application. Controls were established using equal volume of double distilled water. Values are the means of three independent experiments ± SD. Bars with different lowercase letters (e.g., a, b, c; a′, b′, c′; a″, b″, c″) are significantly different ($P < 0.05$).

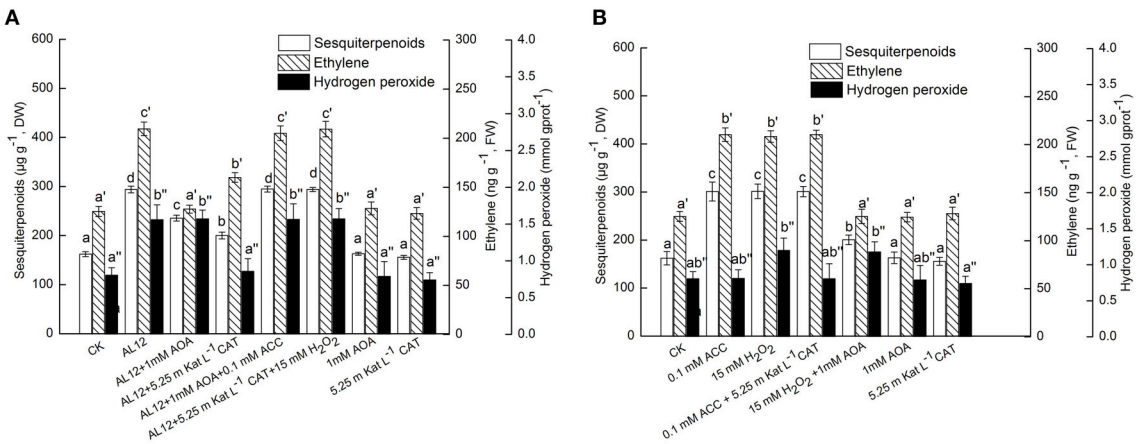

FIGURE 4 | (A) Interaction between ethylene and H_2O_2 signaling pathways for endophytic fungus AL12-induced sesquiterpenoids accumulation in *Atractylodes lancea* plantlets. Thirty-day-old plantlets treated with 5-mm AL12 mycelial disks, 1 mM AOA, 5.25 m Kat L^{-1} CAT, 0.1 mM ACC and 15 mM H_2O_2 were harvested after 15 days to determine the sesquiterpenoids, ethylene and H_2O_2 contents. Inhibitors were added 1 day prior to endophytic fungus AL12 inoculation or exogenous signal donor application. Controls were established using equal sized potato dextrose agar disks. Values are the means of three independent experiments ± SD. Bars with different lowercase letters (e.g., a, b, c; a′, b′, c′; a″, b″, c″) are significantly different ($P < 0.05$). **(B)** Dependence of H_2O_2-induced sesquiterpenoids accumulation on ethylene in *Atractylodes lancea* plantlets. Thirty-day-old plantlets treated with 0.1 mM ACC, 15 mM H_2O_2, 1 mM AOA, and 5.25 m Kat L^{-1} CAT were harvested 15 days later to determine the sesquiterpenoids, ethylene and H_2O_2 contents. Inhibitors were added 1 day prior to exogenous signal donor application. Controls were established using equal volume of double distilled water. Values are the means of three independent experiments ± SD. Bars with different lowercase letters (e.g., a, b, c; a′, b′, c′; a″, b″, c″) are significantly different ($P < 0.05$).

whereas AOA did not affect AL12-triggered H_2O_2 generation (**Figure 4A**). This result suggested that the ET and H_2O_2 signaling pathway were connected, and that ET might act as a downstream signal in H_2O_2-mediated sesquiterpenoids accumulation induced by AL12. The data showing that the application of exogenous ACC and H_2O_2 could reverse the suppression of AL12-induced sesquiterpenoids production by AOA and CAT further confirmed our results (**Figure 4A**).

To investigate if exogenous ET also acted as a downstream signal in H_2O_2-mediated sesquiterpenoids accumulation, the effects of exogenous ACC, H_2O_2, AOA, and CAT on the accumulation of sesquiterpenoids, ET and H_2O_2 were

determined. **Figure 4B** showed that both exogenous ACC and H_2O_2 could significantly induce sesquiterpenoids accumulation in *A. lancea*. The increased sesquiterpenoids accumulation triggered by H_2O_2 was partly suppressed by AOA; whereas the increased sesquiterpenoids accumulation triggered by ACC was not affected by CAT (**Figure 4B**). In addition, exogenous H_2O_2 could trigger ET generation; whereas exogenous ACC did not affect H_2O_2 production (**Figure 4B**). And, exogenous AOA or CAT itself had no adverse effect on the accumulation of sesquiterpenoids, ET and H_2O_2 in the *A. lancea* plantlets compared to the control (**Figure 4B**). These results further demonstrated that ET acted as a downstream signal in H_2O_2-mediated sesquiterpenoids accumulation induced by AL12. And, AOA could not completely abolish H_2O_2-induced sesquiterpenoids accumulation (**Figure 4B**), suggesting that H_2O_2 was not the sole upstream signal of ET.

Ethylene Acts as a Downstream Signal of NO

NO specific scavenge cPTIO and exogenous NO donor SNP were applied in this work. **Figure 5A** showed that both AOA and cPTIO could significantly suppress AL12-induced sesquiterpenoids accumulation in *A. lancea*. NO specific scavenge cPTIO can strongly suppress AL12-induced ET generation; whereas AOA did not affect AL12-triggered NO generation (**Figure 5A**). This result suggested that the ET and NO signaling pathway were connected, and that ET might act as a downstream signal in NO-mediated sesquiterpenoids accumulation induced by AL12. The data showing that the application of exogenous ACC and SNP could reverse the suppression of AL12-induced sesquiterpenoids production by AOA and cPTIO further confirmed our results (**Figure 5A**).

To investigate if exogenous ET also acted as a downstream signal in NO-mediated sesquiterpenoids accumulation, the effects of exogenous ACC, SNP, AOA, and cPTIO on the accumulation of sesquiterpenoids, ET and NO were determined. **Figure 5B** showed that both exogenous ACC and SNP could significantly induce sesquiterpenoids accumulation in *A. lancea*. The increased sesquiterpenoids accumulation triggered by SNP was partly suppressed by AOA; whereas the increased sesquiterpenoids accumulation triggered by ACC was not affected by cPTIO (**Figure 5B**). In addition, exogenous SNP could trigger ET generation; whereas exogenous ACC did not affect NO production (**Figure 5B**). And, exogenous AOA or cPTIO itself had no adverse effect on the accumulation of sesquiterpenoids, ET and NO in the *A. lancea* plantlets compared to the control (**Figure 5B**). These results further demonstrated that ET acted as a downstream signal in NO-mediated sesquiterpenoids accumulation induced by AL12. And, AOA could not completely abolish SNP-induced sesquiterpenoids accumulation (**Figure 5B**), suggesting that NO was not the sole upstream signal of ET.

Contributions of Five Signals in AL12-Induced Sesquiterpenoids Accumulation

The endophytic fungus AL12 induced sesquiterpenoids accumulation of the *A. lancea* plantlets through multiple signals. Here, we compared the contributions of ET, JA, SA, H_2O_2, and NO signals in AL12-induced sesquiterpenoids in *A. lancea*. As shown by **Figure 6A**, AOA, IBU, PAC, CAT, and cPTIO

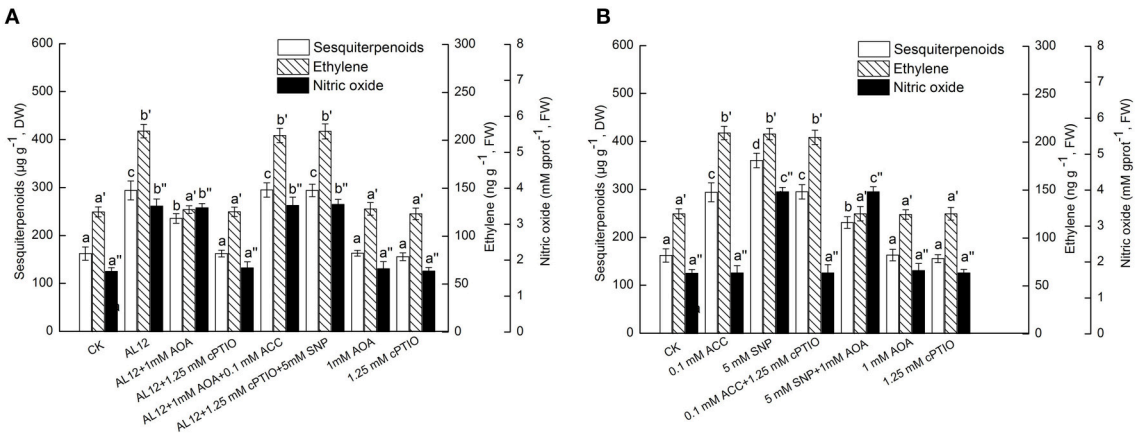

FIGURE 5 | (A) Interaction between ethylene and NO signaling pathways for endophytic fungus AL12-induced sesquiterpenoids accumulation in *Atractylodes lancea* plantlets. Thirty-day-old plantlets treated with 5-mm AL12 mycelial disks, 1 mM AOA, 1.25 mM cPTIO, 0.1 mM ACC, and 5 mM SNP were harvested after 15 days to determine the sesquiterpenoids, ethylene and NO contents. Inhibitors were added 1 day prior to endophytic fungus AL12 inoculation or exogenous signal donor application. Controls were established using equal sized potato dextrose agar disks. Values are the means of three independent experiments ± SD. Bars with different lowercase letters (e.g., a, b, c; a′, b′, c′; a″, b″, c″) are significantly different ($P < 0.05$). **(B)** Dependence of NO-induced sesquiterpenoids accumulation on ethylene in *Atractylodes lancea* plantlets. Thirty-day-old plantlets treated with 0.1 mM ACC, 5 mM SNP, 1 mM AOA, and 1.25 mM cPTIO were harvested 15 days later to determine the sesquiterpenoids, ethylene and NO contents. Inhibitors were added 1 day prior to exogenous signal donor application. Controls were established using equal volume of double distilled water. Values are the means of three independent experiments ± SD. Bars with different lowercase letters (e.g., a, b, c; a′, b′, c′; a″, b″, c″) are significantly different ($P < 0.05$).

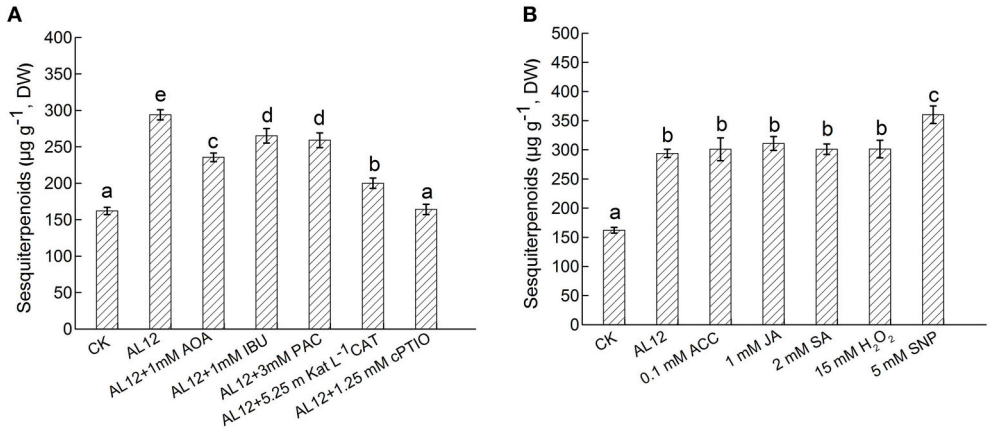

FIGURE 6 | (A) Contributions of five signals in endophytic fungus AL12-induced sesquiterpenoids accumulation in *Atractylodes lancea* plantlets. Thirty-day-old plantlets treated with 5-mm AL12 mycelial disks, 1 mM AOA, 1 mM IBU, 3 mM PAC, 5.25 m Kat L^{-1} CAT and 1.25 mM cPTIO were harvested after 15 days to determine the sesquiterpenoids content. Inhibitors were added 1 day prior to endophytic fungus AL12 inoculation. Controls were established using equal sized potato dextrose agar disks. Values are the means of three independent experiments ± SD. Bars with different lowercase letters (e.g., a, b, c) are significantly different ($P < 0.05$). **(B)** Comparison of five exogenous signal donor. Thirty-day-old plantlets treated with 5-mm AL12 mycelial disks, 0.1 mM ACC, 1 mM JA, 2 mM SA, 15 mM H_2O_2, and 5 mM SNP were harvested after 15 days to determine the sesquiterpenoids content. Controls were established using equal volume of double distilled water. Values are the means of three independent experiments ± SD. Bars with different lowercase letters (e.g., a, b, c) are significantly different ($P < 0.05$).

all significantly suppressed AL12-induced sesquiterpenoids accumulation. And the inhibition effect of cPTIO, CAT, and AOA on sesquiterpenoids accumulation were stronger than other inhibitors (**Figure 6A**), indicating that ET, H_2O_2, and NO signaling acted as three main pathways in AL12-induced sesquiterpenoids accumulation. Further, we compared the contributions of exogenous ACC, JA, SA, H_2O_2, and SNP on sesquiterpenoids accumulation. As shown by **Figure 6B**, exogenous ACC, JA, SA, H_2O_2, and SNP significantly induced sesquiterpenoids accumulation, and the induction effect of SNP was strongest.

Comparison of Signaling Pathways Involved in Sesquiterpenoids Biosynthesis Induced by Different Endophytes

Based on our previous results, we summarized the signaling pathways induced by the endophytic fungi and the endophytic bacteria (Wang et al., 2011, 2015a; Ren and Dai, 2012, 2013; Ren et al., 2013). As shown by **Figure 7**, the endophytic fungus AL12 induced sesquiterpenoids biosynthesis through NO, H_2O_2, ET, SA, JA, brassinosteroid (BR), and calcium (Ca^{2+}) signals; whereas the endophytic bacteria ALEB16 induced sesquiterpenoids biosynthesis through abscisic acid (ABA) and SA signals. Therefore, sesquiterpenoids biosynthesis of *A. lancea* triggered by different endophytes may not be the same.

DISCUSSION

Plant secondary metabolites plays an important role in plant defense system, and the accumulation of active compounds is regulated by cross-talking signaling cascades (Jacobo-Velázquez et al., 2015). This study showed that ET was involved in the signaling pathway for AL12-induced sesquiterpenoids accumulation of the *A. lancea* plantlets (**Figure 1**). Some reports indicated that ET may be a common signal that can be used to induce the biosynthesis of diverse secondary metabolites (Zhao et al., 2004; Arimura et al., 2007; Liu et al., 2012; Rahimi et al., 2015). As shown by **Figures 6A,B**, ET and NO signaling acted as two main pathways in AL12-induced sesquiterpenoids accumulation. Ethephon, an agricultural plant ripening agent, can produce ethylene when dissolves in water, and is very cheap and easy to purchase (Navet et al., 2003; Ban et al., 2007). Ethephon may be used as a signal in inducing the biosynthesis of secondary metabolites in medicinal plants. The application of ethephon will promote the development of medicinal plants industry, and will help to solve the problems of medicinal plants quality.

Different signaling pathways act synergistically or antagonistically, providing a powerful regulatory system for plants adapting to various environmental signals (Verhage et al., 2010). Intriguingly, ET interacts with more than one signal in plants. Typically, JA/ET signaling mediates plants resistance against necrotrophic pathogens, and JA and ET signaling interacts synergistically or antagonistically (Verhage et al., 2010). It has been reported that ET and JA signaling interacted in yeast elicitor induction of β-thujaplicin, with JA signaling acting as a main control and ET as a fine modulator (Zhao et al., 2004). Another study shows that ET and JA played a positive role in the biosynthesis of a tetraterpenoid, lycopene, in tomato fruits, with JA functioning independently of ET (Liu et al., 2012). In this study, we investigate the possible relationship between ET and JA signaling. As suggested by **Figure 2**, ET acted as the sole upstream signal of AL12-induced JA generation and sesquiterpenoids production in the *A. lancea* plantlets. Our previous study has shown that JA has a complementary

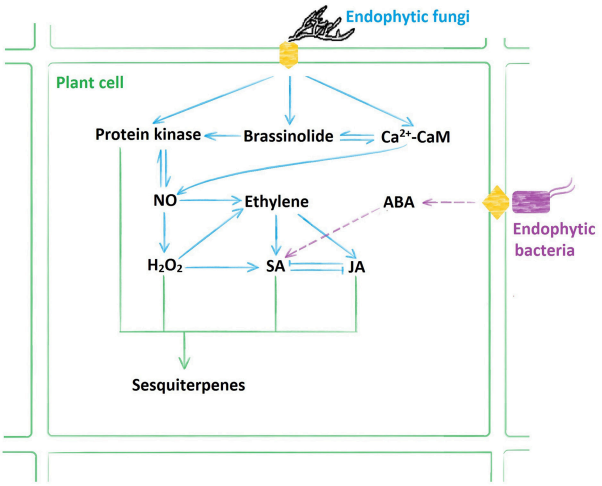

FIGURE 7 | Model illustrating multiple signaling pathways involved in sesquiterpenoids biosynthesis induced by the endophytes. The endophytic fungus AL12 induced sesquiterpenoids biosynthesis through NO, H_2O_2, ET, SA, JA, brassinosteroid (BR), and calcium (Ca^{2+}) signaling pathways; whereas the endophytic bacteria ALEB16 induced sesquiterpenoids biosynthesis through abscisic acid (ABA) and SA signaling pathways.

interaction with the SA signaling pathway in AL12 induction of sesquiterpenoids (Ren and Dai, 2012). Therefore, we investigate the possible relationship between ET and SA signaling in this study. As indicated by **Figure 3**, ET acted as an upstream signal of AL12-induced SA generation and sesquiterpenoids production in the *A. lancea* plantlets. Therefore, ET, JA, and SA signaling interacted in AL12 induction of sesquiterpenoids accumulation, with ET is the upstream signal of JA and SA (**Figures 2**, **3**), and JA has a complementary interaction with the SA signaling (Ren and Dai, 2012). It has been reviewed that ET, JA, and, SA are three endogenous plant signaling molecules involved in plant immunity (Verhage et al., 2010). It has been reported that volatiles compounds from the rhizobacterium *Bacillus subtilis* GB03 up-regulate several genes related to ET biosynthesis and response, JA response, and SA response in *Arabidopsis* (Kwon et al., 2010). Here, we speculate that the SA, JA, and ET signaling pathways maybe utilized and/or modulated in different ways in different plant species.

ET interacts with other signals such as NO and H_2O_2. It has been reported that wound-induced accumulation of plant secondary metabolites is mediated by reactive oxygen species (ROS), ET and JA, whereas ET and JA are essential to modulate reactive oxygen species ROS levels (Jacobo-Velázquez et al., 2015). Our previous studies have revealed that NO acted as an upstream signal of H_2O_2 and SA, H_2O_2 regulated SA production (Wang et al., 2011), and JA acted as a downstream signal of NO and H_2O_2 (Ren and Dai, 2012). As shown by **Figures 2**, **3**, ET is the upstream signal of JA and SA. In this study, we investigate the possible relationship between ET and H_2O_2 or NO signaling. As indicated by **Figures 4**, **5**, ET acted as a downstream signal in NO- and H_2O_2-mediated sesquiterpenoids accumulation induced by AL12. To summarize, ET is the upstream signal of JA and SA (**Figures 2**, **3**), and the downstream signal of NO and H_2O_2 (**Figures 4**, **5**), showing that ET acted as an important signal mediating AL12-induced sesquiterpenoids accumulation.

Multiple signaling pathways connected and mediated plant defense-related genes expression, and also induced secondary metabolites biosynthesis. As shown by **Figure 7**, signaling pathways induced by the endophytic fungi and the endophytic bacteria mediating sesquiterpenoids biosynthesis of *A. lancea* are of some differences. It has reported that *Arabidopsis thaliana* MYC2, a basic helix-loop-helix transcription factor, could directly bind to promoters of the sesquiterpene synthase genes *TPS21* and *TPS11*, thus activating their expression (Hong et al., 2012). Exogenous gibberellin and JA could induce MYC2, thus activating the expression of *TPS21* and *TPS11* (Hong et al., 2012). The activation of *TPS21* and *TPS11* induced the emission of sesquiterpene, especially (E)-β-caryophyllene (Hong et al., 2012). Since multiple signaling pathways were induced by the endophytic fungus, is there one or one class of common targets? And, proteomics, transcriptomics, and other advanced technologies are required to be employed to study the cross-talk between multiple signaling pathways, which will help to understand their roles in promoting the biosynthesis of the secondary metabolites.

Cultivated plantlets of *A. lancea* are of relatively low survival ratio and sesquiterpenoids content (Zhou et al., 2014, 2015). Our previous studies showed that AL12 can promote plant growth, induce secondary metabolites accumulation, and enhance plant defense responses in the plantlets of *A. lancea* (Wang et al., 2012). Several studies have reported that ethylene could increase cell expansion, stimulate internode expansion, improve seed germination, stimulate fruit ripening, and help plants resisting against various stresses such as *Pseudomonas syringae*, high salt, heavy metal, flooding, and drought (Arc et al., 2013; Steffens, 2014; Arraes et al., 2015; Bakshi et al., 2015; Guan et al., 2015; Wei et al., 2015). It has been reviewed that, ethylene, JA, and SA are three key signals mediating plant defense against microbial attack (Kunkel and Brooks, 2002). Therefore, we speculate that ethylene, JA, SA and other signals induced by the endophytic fungus AL12 help *A. lancea* resisting adverse environmental factors, promote plant growth, and also induce secondary metabolites biosynthesis. It also indicated that endophytes are of potential application value in cultivating of medicinal plants.

Many medicinal plants contain active secondary metabolites (such as terpenes, flavones, and alkaloids), and are an important source of modern drugs (Wangchuk and Tobgay, 2015). You-You Tu, the mother of artemisinin, was awarded Nobel Prize in medicine in 2015. The development of traditional medicinal plants gradually becomes a hot issue, and endophytes-medicinal plants interactions will receive much attention. Sesquiterpenoids are the main medicinal compounds in *A. lancea* (Wang et al., 2008). Several endophytes, such as *Gilmaniella* sp. AL12, *Acinetobacter* sp. ALEB16, and ALEB7B, can establish symbiotic relationships with *A. lancea*, and also greatly promote sesquiterpenoids accumulation in the herb (Wang et al., 2012, 2015a; Zhou et al., 2015), indicating that these endophytes are of potential application value in guaranteeing the quality of medicinal materials. In recent

years, *A. lancea*-endophytes interactions gradually become one model of medicinal plants-endophytes interactions (Wang et al., 2011, 2012, 2015a,b; Ren and Dai, 2012, 2013; Ren et al., 2013; Yang et al., 2013, 2014; Zhou et al., 2014, 2015), and provides a theoretical reference for the biosynthesis of other medicinal compounds. In this work, plant materials of *A. lancea* obtained from plant tissue culture were sterile, and were appropriate for investigating the effect of one specific factor on plant materials without the distraction of other factors. Plant tissue culture will help to study the effects of endophytes on plants, thus helping to understand plant-endophyte interactions.

CONCLUSIONS

In summary, this study showed that ethylene is an upstream signal of JA and SA, and a downstream signal of NO and H_2O_2, and acts as an important signal mediating AL12-induced sesquiterpenoids accumulation. And, signaling pathways induced by the endophytic fungi and the endophytic bacteria mediating sesquiterpenoids biosynthesis of *A. lancea* are of some differences. This study comprehensively demonstrates the signaling pathways of sesquiterpenoids biosynthesis, and provides a theoretical basis for the industrialization of active compounds in *A. lancea*.

AUTHOR CONTRIBUTIONS

JY designed the experiments, carried out most of the experimental work, analyzed data, and wrote the manuscript. KS and MY helped for the measurement of ET, NO, and H_2O_2. CC supervised the work. All authors read and approved the final manuscript.

ACKNOWLEDGMENTS

Financial support was provided by the National Natural Science Foundation of China (grant nos. 31070443), a project funded by the Priority Academic Program Development of Jiangsu Higher Education Institutions, Promoting Project for Industrialization of Jiangsu Higher Education Institutions (grant no. JHB2012-16), and Nanjing Produce-Learn-Research Project (grant no. 201306019).

SUPPLEMENTARY MATERIAL

The Supplementary Material for this article can be found online at: http://journal.frontiersin.org/article/10.3389/fpls.2016.00361

Supplemental Figure S1 | Gas chromatograph analysis of sesquiterpenoids in *Atractylodes lancea*.

REFERENCES

Arc, E., Sechet, J., Corbineau, F., Rajjou, L., and Marion-Poll, A. (2013). ABA crosstalk with ethylene and nitric oxide in seed dormancy and germination. *Front. Plant Sci.* 4:63. doi: 10.3389/fpls.2013.00063

Arimura, G.-I., Garms, S., Maffei, M., Bossi, S., Schulze, B., Leitner, M., et al. (2007). Herbivore-induced terpenoid emission in *Medicago truncatula*: concerted action of jasmonate, ethylene and calcium signaling. *Planta* 227, 453–464. doi: 10.1007/s00425-007-0631-y

Arraes, F. B., Beneventi, M. A., Lisei de Sa, M. E., Paixao, J. F., Albuquerque, E. V., Marin, S. R., et al. (2015). Implications of ethylene biosynthesis and signaling in soybean drought stress tolerance. *BMC Plant Biol.* 15:213. doi: 10.1186/s12870-015-0597-z

Bakshi, A., Shemansky, J. M., Chang, C., and Binder, B. M. (2015). History of research on the plant hormone ethylene. *J. Plant Growth Regul.* 34, 809–827. doi: 10.1007/s00344-015-9522-9

Ban, T., Kugishima, M., Ogata, T., Shiozaki, S., Horiuchi, S., and Ueda, H. (2007). Effect of ethephon (2-chloroethylphosphonic acid) on the fruit ripening characters of rabbiteye blueberry. *Sci. Hortic.* 112, 278–281. doi: 10.1016/j.scienta.2006.12.027

Engelberth, J., Schmelz, E. A., Alborn, H. T., Cardoza, Y. J., Huang, J., and Tumlinson, J. H. (2003). Simultaneous quantification of jasmonic acid and salicylic acid in plants by vapor-phase extraction and gas chromatography-chemical ionization-mass spectrometry. *Anal. Biochem.* 312, 242–250. doi: 10.1016/S0003-2697(02)00466-9

Guan, R., Su, J., Meng, X., Li, S., Liu, Y., Xu, J., et al. (2015). Multilayered regulation of ethylene induction plays a positive role in arabidopsis resistance against *Pseudomonas syringae*. *Plant Physiol.* 169, 299–312. doi: 10.1104/pp.15.00659

Hong, G. J., Xue, X. Y., Mao, Y. B., Wang, L. J., and Chen, X. Y. (2012). Arabidopsis MYC2 interacts with DELLA proteins in regulating sesquiterpene synthase gene expression. *Plant Cell* 24, 2635–2648. doi: 10.1105/tpc.112.098749

Jacobo-Velázquez, D. A., González-Agüero, M., and Cisneros-Zevallos, L. (2015). Cross-talk between signaling pathways: the link between plant secondary metabolite production and wounding stress response. *Sci. Rep.* 5:8608. doi: 10.1038/srep08608

Ji, L., Ao, P., Pan, J. G., Yang, J. Y., Yang, J., and Hu, S. L. (2001). [GC-MS analysis of essential oils from rhizomes of *Atractylodes lancea* (Thunb.) DC. and A. chinensis (DC.) Koidz]. *Zhongguo Zhong Yao Za Zhi* 26, 182–185.

Kunkel, B. N., and Brooks, D. M. (2002). Cross talk between signaling pathways in pathogen defense. *Curr. Opin. Plant Biol.* 5, 325–331. doi: 10.1016/S1369-5266(02)00275-3

Kwon, Y. S., Ryu, C. M., Lee, S., Park, H. B., Han, K. S., Lee, J. H., et al. (2010). Proteome analysis of Arabidopsis seedlings exposed to bacterial volatiles. *Planta* 232, 1355–1370. doi: 10.1007/s00425-010-1259-x

Liu, L., Wei, J., Zhang, M., Zhang, L., Li, C., and Wang, Q. (2012). Ethylene independent induction of lycopene biosynthesis in tomato fruits by jasmonates. *J. Exp. Bot.* 63, 5751–5761. doi: 10.1093/jxb/ers224

Ludwig-Müller, J. (2015). Plants and endophytes: equal partners in secondary metabolite production? *Biotechnol. Lett.* 37, 1325–1334. doi: 10.1007/s10529-015-1814-4

Navet, R., Jarmuszkiewicz, W., Almeida, A. M., Sluse-Goffart, C., and Sluse, F. E. (2003). Energy conservation and dissipation in mitochondria isolated from developing tomato fruit of ethylene-defective mutants failing normal ripening: the effect of ethephon, a chemical precursor of ethylene. *J. Bioenerg. Biomembr.* 35, 157–168. doi: 10.1023/A:1023750204310

Ouyang, Z., Zhang, L., Zhao, M., Wang, P. X., Wei, Y., and Fang, J. (2012). Identification and quantification of sesquiterpenes and polyacetylenes in *Atractylodes lancea* from various geographical origins using GC-MS analysis. *J. Pharmacogn.* 22, 957–963. doi: 10.1590/S0102-695X2012005000051

Rahimi, S., Kim, Y. J., and Yang, D. C. (2015). Production of ginseng saponins: elicitation strategy and signal transductions. *Appl. Microbiol. Biotechnol.* 99, 6987–6996. doi: 10.1007/s00253-015-6806-8

Ren, C.-G., Chen, Y., and Dai, C.-C. (2013). Cross-talk between calcium–calmodulin and brassinolide for fungal endophyte-induced volatile oil accumulation of *Atractylodes lancea* plantlets. *J. Plant Growth Regul.* 33, 285–294. doi: 10.1007/s00344-013-9370-4

Ren, C. G., and Dai, C. C. (2012). Jasmonic acid is involved in the signaling pathway for fungal endophyte-induced volatile oil accumulation of *Atractylodes lancea* plantlets. *BMC Plant Biol.* 12:128. doi: 10.1186/1471-2229-12-128

Ren, C. G., and Dai, C. C. (2013). Nitric oxide and brassinosteroids mediated fungal endophyte-induced volatile oil production through protein phosphorylation pathways in *Atractylodes lancea* plantlets. *J. Integr. Plant Biol.* 55, 1136–1146. doi: 10.1111/jipb.12087

Steffens, B. (2014). The role of ethylene and ROS in salinity, heavy metal, and flooding responses in rice. *Front. Plant Sci.* 5:685. doi: 10.3389/fpls.2014.00685

Verhage, A., van Wees, S. C., and Pieterse, C. M. (2010). Plant immunity: it's the hormones talking, but what do they say? *Plant Physiol.* 154, 536–540. doi: 10.1104/pp.110.161570

Wang, H. X., Liu, C. M., Liu, Q., and Gao, K. (2008). Three types of sesquiterpenes from rhizomes of *Atractylodes lancea*. *Phytochemistry* 69, 2088–2094. doi: 10.1016/j.phytochem.2008.04.008

Wang, X. M., Yang, B., Ren, C. G., Wang, H. W., Wang, J. Y., and Dai, C. C. (2015a). Involvement of abscisic acid and salicylic acid in signal cascade regulating bacterial endophyte-induced volatile oil biosynthesis in plantlets of *Atractylodes lancea*. *Physiol. Plant.* 153, 30–42. doi: 10.1111/ppl.12236

Wang, X. M., Yang, B., Wang, H. W., Yang, T., Ren, C. G., Zheng, H. L., et al. (2015b). Consequences of antagonistic interactions between endophytic fungus and bacterium on plant growth and defense responses in *Atractylodes lancea*. *J. Basic Microbiol.* 55, 659–670. doi: 10.1002/jobm.201300601

Wang, Y., Dai, C. C., Cao, J. L., and Xu, D. S. (2012). Comparison of the effects of fungal endophyte *Gilmaniella* sp. *and its elicitor on Atractylodes lancea plantlets. World J. Microbiol. Biotechnol.* 28, 575–584. doi: 10.1007/s11274-011-0850-z

Wang, Y., Dai, C.-C., Zhao, Y.-W., and Peng, Y. (2011). Fungal endophyte-induced volatile oil accumulation in *Atractylodes lancea* plantlets is mediated by nitric oxide, salicylic acid and hydrogen peroxide. *Process Biochem.* 46, 730–735. doi: 10.1016/j.procbio.2010.11.020

Wangchuk, P., and Tobgay, T. (2015). Contributions of medicinal plants to the Gross National Happiness and Biodiscovery in Bhutan. *J. Ethnobiol. Ethnomed.* 11, 48. doi: 10.1186/s13002-015-0035-1

Wei, L. J., Deng, X. G., Zhu, T., Zheng, T., Li, P. X., Wu, J. Q., et al. (2015). Ethylene is involved in brassinosteroids induced alternative respiratory pathway in cucumber (*Cucumis sativus* L.) seedlings response to abiotic stress. *Front. Plant Sci.* 6:982. doi: 10.3389/fpls.2015.00982

Yang, T., Du, W., Zhou, J., Wang, X.-X., and Dai, C.-C. (2013). Effects of the symbiosis between fungal endophytes and *Atractylodes lancea* on rhizosphere and phyllosphere microbial communities. *Symbiosis* 61, 23–36. doi: 10.1007/s13199-013-0254-y

Yang, T., Ma, S., and Dai, C. C. (2014). Drought degree constrains the beneficial effects of a fungal endophyte on *Atractylodes lancea*. *J. Appl. Microbiol.* 117, 1435–1449. doi: 10.1111/jam.12615

Zhao, J., Zheng, S. H., Fujita, K., and Sakai, K. (2004). Jasmonate and ethylene signalling and their interaction are integral parts of the elicitor signalling pathway leading to beta-thujaplicin biosynthesis in *Cupressus lusitanica* cell cultures. *J. Exp. Bot.* 55, 1003–1012. doi: 10.1093/jxb/erh127

Zhou, J. Y., Yuan, J., Li, X., Ning, Y. F., and Dai, C. C. (2015). Endophytic bacterium-triggered reactive oxygen species directly increase oxygenous sesquiterpenoid content and diversity in *Atractylodes lancea*. *Appl. Environ. Microbiol.* 82, 1577–1585. doi: 10.1128/AEM.03434-15

Zhou, J. Y., Zhao, X. Y., and Dai, C. C. (2014). Antagonistic mechanisms of endophytic *Pseudomonas fluorescens* against *Athelia rolfsii*. *J. Appl. Microbiol.* 117, 1144–1158. doi: 10.1111/jam.12586

Conflict of Interest Statement: The authors declare that the research was conducted in the absence of any commercial or financial relationships that could be construed as a potential conflict of interest.

frontiers in Plant Science

ORIGINAL RESEARCH
published: 28 March 2017
doi: 10.3389/fpls.2017.00415

Seed-Derived Ethylene Facilitates Colonization but Not Aflatoxin Production by *Aspergillus flavus* in Maize

Shi Wang[1,2†], Yong-Soon Park[3,4†], Yang Yang[1,2], Eli J. Borrego[3], Tom Isakeit[2,3], Xiquan Gao[1,2] and Michael V. Kolomiets[3*]*

[1] State Key Laboratory of Crop Genetics and Germplasm Enhancement, College of Agriculture, Nanjing Agricultural University, Nanjing, China, [2] Jiangsu Collaborative Innovation Center for Modern Crop Production, Nanjing Agricultural University, Nanjing, China, [3] Department of Plant Pathology and Microbiology, Texas A&M University, College Station, TX, USA, [4] Division of Biotechnology, Chonbuk National University, Iksan, South Korea

OPEN ACCESS

Edited by:
Péter Poór,
University of Szeged, Hungary

Reviewed by:
Jinpeng Gao,
Washington State University, USA
Zhitong Yin,
Yangzhou University, China

***Correspondence:**
Xiquan Gao
xgao@njau.edu.cn
Michael V. Kolomiets
kolomiets@tamu.edu

† These authors have contributed equally to this work.

Specialty section:
This article was submitted to Plant Physiology, a section of the journal Frontiers in Plant Science

Received: *16 November 2016*
Accepted: *10 March 2017*
Published: *28 March 2017*

Citation:
Wang S, Park Y-S, Yang Y, Borrego EJ, Isakeit T, Gao X and Kolomiets MV (2017) Seed-Derived Ethylene Facilitates Colonization but Not Aflatoxin Production by Aspergillus flavus in Maize. Front. Plant Sci. 8:415. doi: 10.3389/fpls.2017.00415

Ethylene (ET) emitted by plant tissues has been broadly reported to play important roles in plant development, response to environmental stresses and defense against certain pathogens. Recent evidence obtained from using *in vitro* fungal cultures exposed to ET suggested that exogenous ET may regulate the production of aflatoxin by *Aspergilli*. However, the function of endogenous, seed-derived ET has not been explored. In this study, we found that the maize lipoxygenase *lox3* mutant, previously reported to be susceptible to *Aspergillus* spp., emitted greater levels of ET upon *A. flavus* infection, suggesting the potential involvement of endogenous ET in the susceptibility of maize to *A. flavus*. Supporting this idea, both colonization and conidiation of *A. flavus* were reduced in wild-type (WT) kernels treated with $AgNO_3$, an ET synthesis inhibitor. There was no ET emission from non-viable kernels colonized by *A. flavus*, suggesting that living seed but not the fungus itself was the primary source of ET released upon infection with *A. flavus*. The kernels of *acs2* and *acs6*, two ET biosynthetic mutants carrying *Mutator* transposons in the ACC synthase genes, *ACS2* and *ACS6,* respectively, displayed enhanced seed colonization and conidiation, but not the levels of aflatoxin, upon infection with *A. flavus*. Surprisingly, both *acs2* and *acs6* mutant kernels emitted greater levels of ET in response to infection by *A. flavus* as compared with WT seed. The increased ET in single mutants was found to be due to overexpression of functional ACS genes in response to *A. flavus* infection. Collectively, these findings suggested that ET emitted by infected seed facilitates colonization by *A. flavus* but not aflatoxin production.

Keywords: *Aspergillus flavus*, ethylene, maize, colonization, aflatoxin

INTRODUCTION

Aspergillus is one of the most common mycotoxin producing fungi that contaminate a large number of crops, both pre- and post-harvest. Some of the major economic losses are caused by aflatoxin (produced by *A. flavus*) contamination of maize and other oil rich seed crops worldwide. Aflatoxin is one of the most potent natural carcinogens hazardous to health of humans and animals

when consumed as food or feed, respectively. Unfortunately, conventional agronomic approaches have limited effectiveness for reducing mycotoxin contamination. The ideal solution would be to decrease contamination by improving genetic resistance of these crop plants. Sources of resistance that limit the ability of *Aspergillus* spp. to grow, reproduce and synthesize mycotoxins have been identified. However, despite significant efforts by public and private breeding programs, adequate levels of resistance have not been achieved primarily due to lacking major single resistance genes against those fungi Munkvold (2003). One strategy to accelerate resistance breeding efforts is to combine the approaches of genome-wide association analysis (GWAS) and traditional linkage mapping analysis to identify the *A. flavus* resistance quantitative trait loci (QTL) or genes, and closely linked markers. Recently, a linkage mapping was performed using 228 recombinant inbred lines (RILs) of maize, and a highly significant QTL that affected aflatoxin accumulation, qAA8, was mapped to chromosome 8, which can explain 6.7 to 26.8% of the phenotypic variation (Zhang et al., 2016). Several other large QTLs have also reported to be located on chromosomes one, three, four, five, and nine (Xiang et al., 2010; Warburton et al., 2011; Willcox et al., 2013). Another promising approach to aid conventional breeding efforts is to identify genes and signaling pathways regulated by these genes that underlie host resistance (or susceptibility) mechanisms. This information can be used to develop and breed beneficial alleles of these genes or genetic engineering approaches to control infection and mycotoxin production.

One of the plant-derived molecular signals that have been implicated in the regulation of aflatoxin biosynthesis is a gaseous plant hormone ethylene (ET). In higher plants, ET is initially synthesized from methionine (Met) via S-adenosyl-L-methionine (S-AdoMet) by SAM synthetase. S-AdoMet is subsequently converted to 1-aminocyclopropane-1-carboxylate (ACC) by ACC synthase (ACS, S-adenosyl-L-methionine methylthioadenosine-lyase) and finally to ET by ACC oxidase (ACO) (Yang, 1985; Kende, 1993). As a by-product of this reaction, ACS also produces 5′-methylthioadenosine (5′-MTA), which is recycled in the Yang Cycle to synthesize methionine (Met), to maintain the constant level of the cellular Met for continuous protein and ET biosynthesis (Yang, 1985; Bleecker and Kende, 2000).

Besides higher plants, ET is also synthesized by micro-organisms, including phytopathogenic fungi and bacteria (Fukuda et al., 1993), through either 2-keto-4-methylbutyric acid (KMBA) as reported for *Escherichia coli* (Ince and Knowles, 1986) and *Cryptococcus albidus* (Fukuda et al., 1989b), or via 2-oxoglutarate by *Penicillium digitatum* (Fukuda et al., 1989a) and *Pseudomonas syringae* (Nagahama et al., 1991). The fungus *Penicillium citrinum* can also synthesize ACC from SAM (Jia et al., 1999), while *Botrytis cinerea* appears to utilize the KMBA pathway to produce ET (Cristescu et al., 2002; Chague et al., 2006). However, the physiological significance of ET production by these microorganisms has not been well studied, but is hypothesized to facilitate pathogen virulence.

In plants, ET has been broadly reported to play important roles in regulating diverse physiological and defense processes, including seed germination, organ senescence, abscission and fruit ripening (Kende, 1993; Johnson and Ecker, 1998), and responses to abiotic and biotic stresses, such as wounding, chilling, drought, flooding, hypoxia, ozone damage and pathogen attack (Paul et al., 2003; Lin et al., 2009; Musungu et al., 2016). ET modulates various defense responses against pathogens either individually or in combination with other phytohormones (Guo and Ecker, 2004; Broekaert et al., 2006; Adie et al., 2007; Kendrick and Chang, 2008). For instance, the resistance of plants to the necrotrophic fungal pathogen *B. cinerea* was moderately enhanced by exogenous treatment of plants with ET (Diaz et al., 2002). Also, ET biosynthesis is activated when plants are challenged by pathogens; on the other hand, increased ET production is associated with enhanced defense-related gene expression (Penninckx et al., 1998; Cohn and Martin, 2005). ET acts synergistically with jasmonates (JAs) in defense responses (Penninckx et al., 1998; Ellis and Turner, 2001; Catinot et al., 2015), often accompanied by induction of clusters of genes regulated by ET or jasmonic acid (JA) (Glazebrook et al., 2003; Broekaert et al., 2006).

In addition to acting as a signaling molecule in plant defense against pathogens, ET has also been implicated in the regulation of mycotoxin production by *Aspergillus* spp. When ET was exogenously applied to peanuts inoculated with *A. parasiticus*, aflatoxin accumulation was significantly reduced (Roze et al., 2004; Gunterus et al., 2007; Huang et al., 2009). An ET generator, 2-chloroethyl phosphoric acid (CEPA, ethephon), also suppressed aflatoxin biosynthesis in *A. flavus*, and this suppression was probably due to the reduction of reactive oxygen species (ROS) (Huang et al., 2009). These data suggest a role for exogenous ET in modulating secondary metabolism of *Aspergillus* spp. However, it remains to be explored whether and how the endogenous ET derived from host plants impacts the fungal colonization and mycotoxin production. In this study, the role of seed-derived ET in maize interactions with *A. flavus* was elucidated by kernel bioassay using maize mutants disrupted by transposon insertions in the *ACS2* and *ACS6* genes.

MATERIALS AND METHODS

Plant Materials and Fungal Strains

Maize *acs* mutants (*acs2* and *acs6*) and lipoxygenase *lox3-4* mutants were generated by *Mutator*-transposable element-insertional mutagenesis as described previously (Young et al., 2004; Gao et al., 2007). These *acs* mutants were backcrossed seven times into B73 background resulting in generation of mutants that are near-isogenic to the recurrent parent line B73. The *lox3-4* mutants are at the BC_5F_3 genetic stage. In all experiments, *lox3-4* mutants were compared to near-isogenic WTs obtained by self-pollinating WT siblings identified in the BC_5F_2 segregating population.

To measure the expression levels of *ACS2*, *6* and *7* in different organs, the samples were collected from different organs at different stages. For geminating stage, the embryos and roots were excised from the 2-day-old or 4-day-old germinated seeds, respectively. For seedling stage, roots, stems and leaves were harvested from V1 and V3 stages grown in a light shelf,

respectively. For adult stage, roots, stems, leaves, pollens, tassels and ears were harvested from the matured plants. The seeds after completely matured were also harvested for gene expression study at matured stage.

Aspergillus flavus NRRL 3357 was cultured at room temperature on potato dextrose agar (PDA: Difco) as described previously (Gao et al., 2009).

Fungal Inoculation and Spore Counting on Kernels

Maize kernels in similar size were selected and weighed to ensure equivalent average seed weights across all samples. Seeds were then surface-sterilized with 100% Clorox bleach (containing 6% sodium hypochlorite) for 10–15 min and rinsed with sterilized, distilled H_2O at least five times. The embryos of kernels were cut longitudinally using a razor blade to a depth of about 0.5 cm to provide an infection court for fungal inoculation. Seeds were then blotted dry with paper towel and placed in a 20-ml glass-scintillation vial (Wheaton Science, Millville, NJ, USA) and inoculated with 200 μl of conidia suspension (1×10^6/ml) of *A. flavus* NRRL 3357. Conidia were harvested with 0.001% Tween 20 from fungal strains grown in PDA plate. Control seeds (mock) received equal amount of 0.001% Tween 20. Four or six inoculated or mock-treated kernels were used per replicate with at least four replicates per experiment. The inoculated kernels were kept in a plastic transparent container with a wet filter paper to provide humidity and incubated with 12 h light/day at 26–29°C. Sterile, distilled H_2O was added to containers as needed to maintain high humidity. Kernels were harvested at designated intervals after inoculation, either to enumerate conidia or to quantify mycotoxins.

To measure levels of conidia production, infected kernels were placed in a 20 mL glass vial with 2 mL of 0.001% Tween 20, and vortexed for 20 s to dislodge spores. The spore suspension was decanted and spores were enumerated using a hemacytometer.

Semi Quantitative RT-PCR and qRT-PCR for Gene Expression

B73 genetic background kernels were sterilized and inoculated with mock control, *A. flavus*. All seeds were applied with either control or fungi as described above. Control or fungi-challenged seeds were harvested at 0, 12, 24, 48, and 96 h after inoculation. Total RNA was extracted by using TRI reagent (Molecular research Center Inc., Cincinnati, OH, USA) following the manufacturer's protocol. After extracting total RNA, these RNA samples were treated with RNase-free rDNase at 37°C for 30 min using a DNA-free kit (Ambion Inc., Austin, TX, USA). First strand cDNA synthesis (5 μg of RNA as a template for each sample) was carried out by using a First-Strand Synthesis Kit (GE Healthcare Bio-Sciences Corp., Piscataway, NJ, USA) following the manufacturer's protocol. The synthesized cDNA was diluted and equalized for all samples. The cDNA as a template was amplified with two gene-specific primers for each gene, and for the house-keeping gene *ZmGAPc*. The cDNA was denatured at 94°C for 5 min and amplified by following 27–32 cycles (each cycle: 45 s at 94°C, 1 min at 56°C, and 2 min at 72°C). Amplified PCR products were loaded and separated on 1.2–1.5% agarose gels.

Quantitative reverse transcription-polymerase chain reaction (qPCR) assay was performed using qRT-PCR kit purchased from Takara (Takara, Japan). Reactions were optimized for RNA and primer concentrations with each 10 μl reaction consisting of 40 ng of DNase-free RNA and 200 nM primers. qPCR analysis was performed in the ABI Prism 7000 system (Applied Biosystems, USA). The program used was as follows: 94°C for 1 min; followed by 40 cycles of 94°C for 5 s, 65°C for 15 s and 72°C for 30 s. Primers used in this study are described in Supplementary Table 1, and Tublin gene was used as internal control. The quantification of gene expression was repeated at least three times.

Quantification of Aflatoxin and Ergosterol

Infected or mock-treated kernels from each treatment were ground using a Waring blender (Waring laboratory, Torrington, CT, USA), and aflatoxin was subsequently quantified with a fluorometer using the VICAM AflaTest® USDA-FGIS procedure (VICAM, Watertown, MA, USA) with six infected kernels per replicate were frozen in liquid nitrogen until assayed. Ergosterol was extracted from infected kernels overnight with 5 ml chloroform:methanol (2:1 v/v) at room temperature as described by previous study (Woloshuk et al., 1989) with some modifications. Ergosterol was analyzed on a Shimatzu LC-20AT HPLC system (Shimatzu Scientific Instruments, Inc., Kyoto, Japan) equipped with a 4.6 U ODS column (250 mm × 4.6 mm) and a UV detector (282 nm). Quantities were calculated by comparing HPLC peak areas with ergosterol standards (Sigma). The experiment was repeated at least four times, with consistent results.

Measurement of Ethylene Produced by Kernels, Leaves and Pathogens

ET produced by infected and by control kernels was quantified as described by Gao et al. (2008) with some modifications. Briefly, the vials containing infected kernels were kept at 12 h light/day at 26–29°C and ET was measured at 1, 2, 4, and 7 days post-inoculation (dpi). Vials were sealed with screw caps with septa. The headspace gas (1 ml) was withdrawn from vials by a syringe and analyzed using gas chromatography.

To measure the ET levels produced in the leaves of B73 and *acs6* mutant, the plants were grown at 25 to 28°C in commercial soil (Metro-Mix 366; Scotts-Sierra Horticultural Products, Marysville, OH, USA) under 14 h of daylight with 120 $\mu M\ m^{-2}\ s^{-1}$ (Quantum Meter; Apogee Instruments, Logan, UT, USA). The seedlings were grown in long conical tubes (20.5 by 4 cm) for 2 to 3 weeks until they had three fully expanded leaves (V3 developmental stage). The leaves of B73 and *acs6* were excised from the plants and immediately transferred into a 20 ml of glass scintillation vial (Wheaton Science). The vials were then tightly sealed with a plastic lid for 1 to 2 h prior to analysis to allow enough ethylene was accumulated. ET was measured as described by Gao et al. (2008).

Treatment with Ethylene Inhibitor and Precursor ACC

The pretreatment of kernels with ET inhibitor $AgNO_3$ was performed by adding 1 ml of $AgNO_3$ (Sigma-Aldrich, St. Louis, MO, USA) at 20 mM in 0.001% Tween-20, to the freshly wounded kernels as described above (four kernels per vial per replicate) and mixed thoroughly to ensure the complete soaking of kernels with the chemical. At least four replicates were used per treatment/genotype combination. Control kernels received the same volume of 0.001% Tween-20. The kernels were incubated for 30 min and blotted dry to remove excessive solution and were subsequently inoculated with *A. flavus* suspensions as described.

For the treatment with ET precursor, ACC, the kernels were pretreated with ACC (20 nM) in 0.001% Tween-20 for 30 min, followed by inoculation with 1×10^6 spores, then cultured and analyzed as described above. Pretreatment with same amount of 0.001% Tween-20 was used as control.

RESULTS

ET Production Is Enhanced in *A. flavus*-Inoculated *lox3-4* Mutant Kernels

We have previously reported that mutation of a maize 9-lipoxygenase gene, *ZmLOX3*, resulted in the increased susceptibility of kernels to the infection with *A. flavus* and *A. nidulans* (Gao et al., 2009). In an earlier study, we found that the *lox3-4* mutants produced greater levels of ethylene in the roots compared to the WT (Gao et al., 2008), which prompted us to investigate whether ET production was also altered in the *lox3-4* mutant kernels in response to *A. flavus* infection.

As shown in **Figure 1**, infection with *A. flavus* substantially increased ET emission in both near-isogenic WT and *lox3-4* mutant, with the latter significantly more than the former at 7 dpi. Because *lox3-4* mutant is substantially more susceptible to *A. flavus* colonization (Gao et al., 2009), we reasoned that one potential mechanism underlying increased susceptibility of the mutant is increased ET. To test whether volatiles including ET emitted by infected kernels impact fungal growth, sporogenesis and toxin production, we performed an *in vitro* plate assay by co-incubating *A. flavus* grown on PDA media in close proximity with maize kernels infected with *A. flavus* simultaneously (**Figure 2A**). The plates were cultured under constant dark condition for 4 days to allow for vegetative growth but prevent sporulation, then transferred to light/dark cycle (8 h dark/16 h light conditions) for another 2 days, This will allow us to investigate whether synchronizing the switch from vegetative growth to asexual reproduction is regulated by exposure to volatiles produced from infected kernels. Exposure to light/dark regimes is required for conidia production as evidenced by rapid green pigmentation of fungal hyphal mass in *Aspergilli* spp. (Rodriguez-Romero et al., 2010; Ruger-Herreros et al., 2011). Conidia and aflatoxin produced by the fungal cultures in response to volatiles emitted by the infected WT or *lox3-4* mutant kernels were measured. As shown in **Figures 2B,C**, after expose to light for 2 days, in contrast to the colonies co-incubated with infected WT kernels, fungal colonies exposed to volatiles emitted by infected *lox3-4* kernels produced greater levels of conidia as evidenced by green pigmentation of fungal colonies and conidia enumeration. However, aflatoxin content produced by *A. flavus* was not different among the plates supplemented with *lox3-4* or WT.

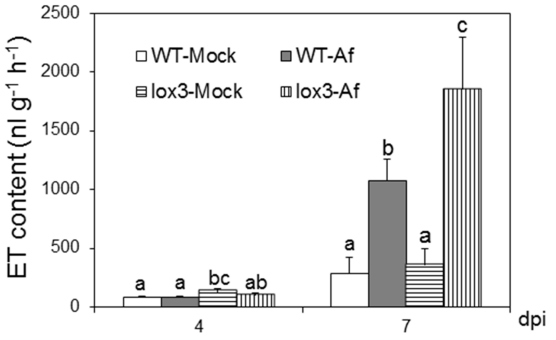

FIGURE 1 | Ethylene production on *lox3-4* mutants upon inoculation with *A. flavus* NRRL 3357. The kernels were inoculated with 1×10^6 spores and cultured in a 20 ml of glass scintillation vial (Wheaton Science) at 29°C under 12L/12D for 4 and 7 days. ET was measured by withdrawing 1 mL volume of headspace gas with a syringe and injecting into a digital gas chromatograph (Photovac 10 plus, PerkinElmer, Inc., Norwalk, CT, USA) The values are the mean ± SD of three replicates (four vials each treatment each genotype), with six kernels in each vial. Different letters above bars denote significant differences ($P < 0.05$, ANOVA) between genotypes and treatments within same time point.

Ethylene Biosynthetic Genes Are Differentially Induced in Seed in Response to Infection with *A. flavus*

To investigate the role of ET and ET-biosynthesis genes in the regulation of seed colonization of maize by *A. flavus*, we inoculated the WT kernels (B73 inbred line) with fungal spore suspension of *A. flavus* at 1×10^6 spores/ml or H_2O as a mock control, and the transcript levels of three ET biosynthesis genes, *ZmACS2*, *ZmACS6,* and *ZmACO31* (ACC oxidase 31), were quantified in either mock-treated or *A. flavus* inoculated kernels at different time points post treatments. While the expression of *ZmACO31* was found to be induced in the kernels infected with *A. flavus* at 24 and 48 hpi, the transcriptional level of *ZmACS2* and *ZmACS6* was induced at 96 and 24 hpi, respectively (**Figure 3**). These results suggest that seed respond to pathogen infection by increased synthesis of ET.

To test whether ET biosynthesis genes are differentially regulated in seeds compared to other tissues, we examined the expression levels of *ACS2*, *6* and *7* in different tissues at different developmental stages. While all three genes are found to be differentially expressed in different tissues, the expression levels are relatively higher in the tissues from mature plants compared to young seedling tissues. Expression levels of *ACS2*, *6* and *7* in the mature dry seeds are much lower than other tissues at mature stages (**Supplementary Figures S1A–C**). This data corresponds

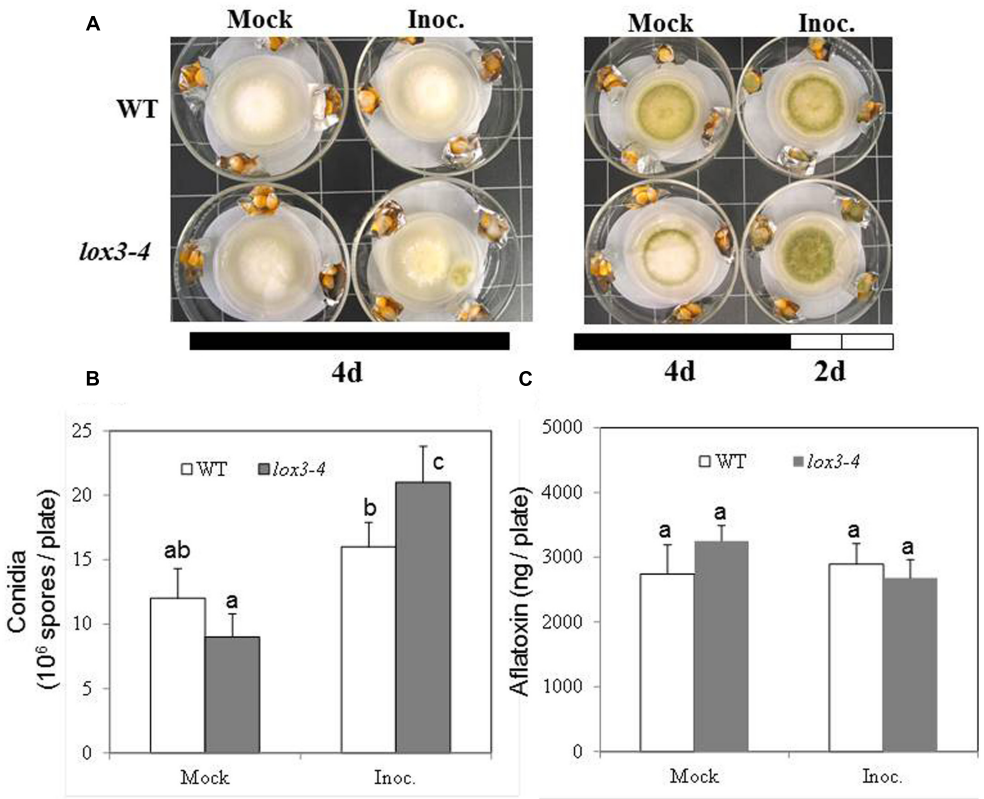

FIGURE 2 | Kernel plate assay for testing the effect of potent gas produced by *lox3-4* kernels inoculated with *A. flavus* on the fungal growth, sporulation, and aflatoxin production by *A. flavus* grown on a plate. WT and *lox3-4* kernels were inoculated with 1×10^6 spores and placed in a large petri dish, containing a smaller petri dish where the *A. flavus* was growing on the PDA media **(A)**. **(A)** The infected kernels were co-incubated with the fungal plate for either 4 days under continuous darkness or 4 days continuous darkness then moving to the continuous light for an additional 2 days. **(B)** The conidia, and **(C)** aflatoxin produced from the fungi grown on the PDA plates inside the small petri dishes was determined, respectively, at 6 days post culture (4 days dark+2 days light). The values are the mean ± SD of three replicates, and different letters above bars denote significant differences ($P < 0.05$, ANOVA) between genotypes and treatments.

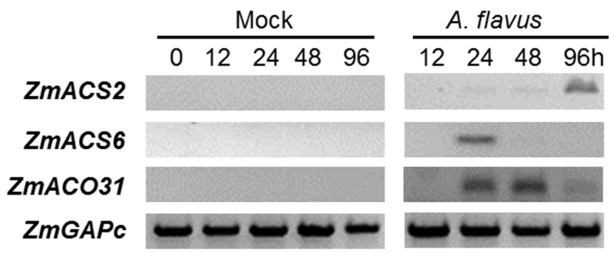

FIGURE 3 | Genes encoding ethylene biosynthesis enzymes, ACC synthase (*ZmACS*) and ACC oxidase (*ZmACO*) are induced in maize seed in response to *A. flavus* infection. The WT kernels (B73 inbred line) were inoculated with *A. flavus* or mock-inoculated, incubated and harvested at 0, 12, 24, 48, and 96 h post-inoculation. The expression of two *ACS* genes, *ZmACS2* and *ZmACS6*, and *ZmACO31* were tested. Expression of a house-keeping gene *ZmGAPc* was used as an internal standard in this experiment.

to our finding that ACSs are not expressed in the uninfected seeds at detectable levels, but induced to higher levels upon pathogen attack (**Figure 3**). Unlike seeds, ethylene is normally produced in the vegetative tissues, particularly at mature stages. This could explain that plants likely deploy different ACS genes to produce ET in diverse tissues and under pathogen attack.

Colonization, Sporulation and Mycotoxin Production by *A. flavus* Grown on the *acs* Mutant Kernels

To examine the role of seed-derived ET in colonization and conidiation of *A. flavus*, we performed kernel assays using previously reported ET biosynthesis mutants that carry the *Mutator* transposons in the ACC synthase genes *ZmACS2* and *ZmACS6*, respectively (Young et al., 2004). The knockout mutants for the remaining maize ACS gene family member, *ZmACS7*, was not available for this study. The loss of *ZmACS6* expression in the *acs6* mutant resulted in a reduction of 90% of foliar ethylene, while ethylene evolution from the *acs2* mutants was only 55% of the levels produced in WT leaves (Young et al., 2004). We reasoned that these two mutants are excellent tools to investigate the role of ET in resistance to *A. flavus*. As shown in **Figure 4A**, we found that infection of both *acs2* and *acs6* mutants with *A. flavus* resulted in greater levels of

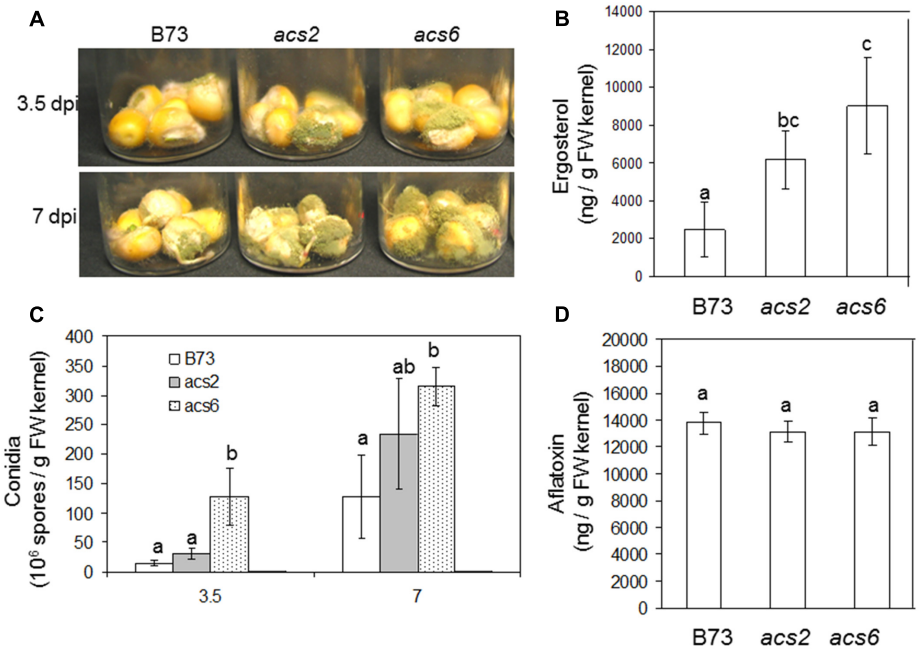

FIGURE 4 | Kernel infection bioassay of the *acs* mutants by *A. flavus*. **(A)** Infected kernels of WT and *acs* mutants were cultured in glass vials and incubated for 3.5 and 7 days. **(C)** Enumeration of conidia in the *acs* mutants and WT (B73) following inoculation with *A. flavus*. **(D)** Aflatoxin and **(B)** ergosterol was measured at 7 days post-inoculation (dpi), respectively. The *acs2*, *acs6* single mutants were generated by back crossing to B73 seven times (BC_7 stage). The values are the mean ± SD of four replicates. Different letters above bars denote significant differences ($P < 0.05$, ANOVA) analyzed by the SPSS program (SPSS Inc., Chicago, IL, USA) between the host genotypes within same time point. Similar results were obtained in three independent experiments. dpi, days post infection.

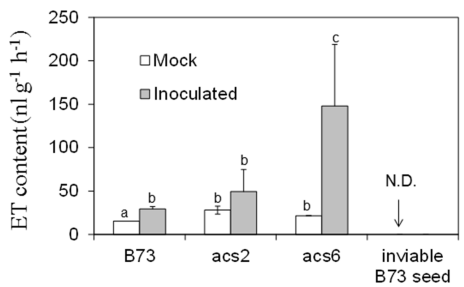

FIGURE 5 | Ethylene production on *acs* mutants upon inoculation with *A. flavus NRRL* 3357. The kernels were inoculated with 1×10^6 spores and cultured in a 20 ml of glass scintillation vial (Wheaton Science) at 29°C under 12L/12D for 7 days. The vial was then tightly sealed with a plastic lid for 1 to 2 h prior to analysis to allow enough ethylene was accumulated. ET was measured by withdrawing 1 mL volume of headspace gas with a syringe and injecting into a digital gas chromatograph (Photovac 10 plus, PerkinElmer, Inc., Norwalk, CT, USA) The values are the mean ± SD of four replicates (four vials each treatment each genotype), with six kernels in each vial. Different letters above bars denote significant differences ($P < 0.05$, ANOVA) analyzed by SPSS program (SPSS Inc., Chicago, IL, USA) between the host genotypes within same time point. Similar results were obtained in three independent experiments. dpi, days post infection. N.D., not detectable.

seed colonization compared to WT kernels at both 3.5 and 7 dpi. Increased biomass of the fungus grown in the mutant seed was also demonstrated by increased amount of the fungus-specific lipid, ergosterol (**Figure 4B**). The enhanced colonization of the *acs* mutants was supported by increased number of conidia produced by the fungus on both mutants (**Figure 4C**). Unexpectedly, while fungal vegetative growth on *acs2* and *acs6* mutants was increased, aflatoxin B1 levels remained similar in all maize genotypes (**Figure 4D**). These results suggest that the *ACS2* and *ACS6* genes function in maize responses to *A. flavus* colonization and spore production but are irrelevant to the fungal ability to produce aflatoxin.

ET Production Is Induced in the *acs* Mutants Infected with *A. flavus*

Expression pattern of ET biosynthesis genes after inoculation with *A. flavus* (**Figure 3**) and greater colonization of *acs* mutant kernels by *A. flavus* (**Figure 4**) suggested that ET could be a key factor in the regulation of seed colonization by *A. flavus*.

To confirm that *acs* mutants are true knock-out alleles, we measured ET levels in B73 and *acs6* mutant leaves. As shown in **Supplementary Figure S1D**, almost no ET was detected in the leaves of the *acs6* mutant, confirming the mutant is indeed a true knock-out mutant. To further test whether ET production is altered in kernels of the *acs* mutants in response to *A. flavus* infection, we measured ET emission in WT and the *acs* mutants kernels in response to infection by *A. flavus*. ET was quantified from the headspace of the vials containing WT or the *acs* mutant kernels at 7 dpi. While infected WT kernels emitted only slightly greater levels of ET, unexpectedly, ET levels were strongly enhanced in the kernels of both *acs2* and *acs6* mutants, with the

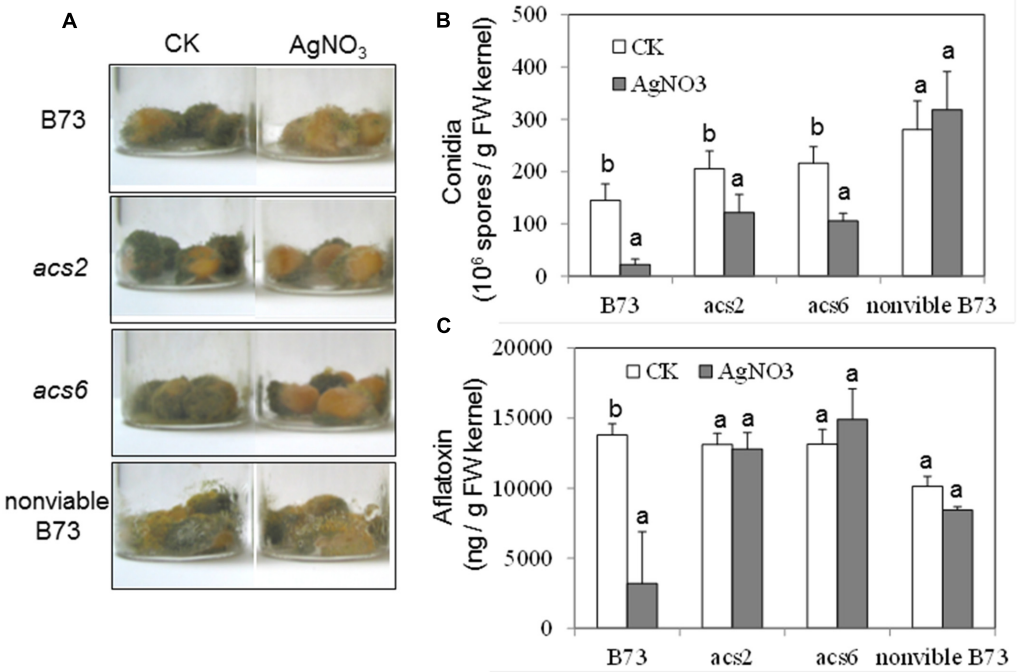

FIGURE 6 | Effect of ethylene inhibitor $AgNO_3$ on the colonization, conidiation and aflatoxin production of *A. flavus NRRL* 3357 on *acs* mutants. **(A)** The kernels were pretreated with $AgNO_3$ (20 mM) 30 min, followed by inoculation with 1×10^6 spores, then cultured in a 20 ml of glass scintillation vial (Wheaton Science) at 29°C under 12L/12D for 7 days. **(B)** Conidiation of *acs* mutants upon infection of *A. flavus NRRL* 3357. The values are the mean ± SD of four replicates (four vials each treatment each genotype), with six kernels in each vial. **(C)** Aflatoxin B1 was quantified using Vicam Aflatest (Vicam, Watertown, MA, USA), according to the USDA-FGIS protocol. The values are the mean ± SD of four replicates (four vials each treatment each genotype), with six kernels in each vial. Different letters above bars denote significant differences ($P < 0.05$, ANOVA) analyzed by SPSS program within same host genotypes. Similar results were obtained in at least three independent experiments. dpi, days post infection.

significantly higher levels in *acs6* mutants (**Figure 5**). This is in sharp contrast to the reported reduced ET production levels in the leaves of the two mutants (Young et al., 2004). Non-infected desiccated seed of the mutants or WT did not emit any detectable ET (data not shown).

Seed but not the Fungus Is Responsible for Induced ET Emission

Because the *acs2* and *acs6* infected seed emitted greater than WT levels of ET, we tested whether ET was produced by *A. flavus* rather than by the host (or in addition to the host). We reasoned that autoclaved, and thus non-viable, seed will not be able to synthesize ET, while the fungus that colonizes such seed may produce ET. In contrast to viable seed, no ET emission could be detected when non-viable kernels were infected by *A. flavus* (**Figure 5**). These data suggest that ET is originated from maize host but not the fungus.

Effects of an ET Inhibitor on the Colonization and Sporulation of *A. flavus*

To confirm the role of ET in the kernel-*A. flavus* interaction by a pharmacological approach, the potent ET inhibitor, $AgNO_3$, was applied to the kernels prior to inoculation. The pretreatment with the inhibitor reduced fungal colonization of both WT and the single *acs* mutants, as evidenced by the reduced number of conidia (**Figures 6A,B**). In the WT kernels, the inhibitor pretreatment resulted in reduced production of aflatoxin, which correlated with the lower fungal growth (**Figure 6C**). However, pretreatment with the inhibitor did not appear to have an effect on the levels of aflatoxin in both *acs* mutants (**Figure 6C**).

We also tested whether the inhibitor treatment had any unintended effect on the ability of *A. flavus* to colonize seed, and produce conidia and aflatoxin in the infected, non-viable seeds. As shown in **Figure 6A**, the ability of *A. flavus* to colonize kernels and to produce conidia was not affected by $AgNO_3$ in the non-viable seeds, compared to control non-treated seeds (**Figures 6A,B**). These data suggested that $AgNO_3$ treatment itself unlikely affected fungal development and secondary metabolism (e.g., toxin production) directly, and that the inhibitor effects observed on the living seed were due to the suppression of ET effect in the host seed.

To test whether ET precursor, ACC, could itself promote pathogenicity of *A. flavus* in maize kernels, we pretreated kernels of B73, *acs2* and *acs6* mutant seeds with ACC, followed by inoculation with *A. flavus*. While we found that both *acs2* and *acs6* displayed enhanced conidiation of *A. flavus* on mutant kernels compared to B73, ACC treatment showed increased but not statistically significantly higher number of conidia produced by *A. flavus*, compared to the mock treatment (**Supplementary Figures S2A,B**). However, pretreatment with ACC treatment

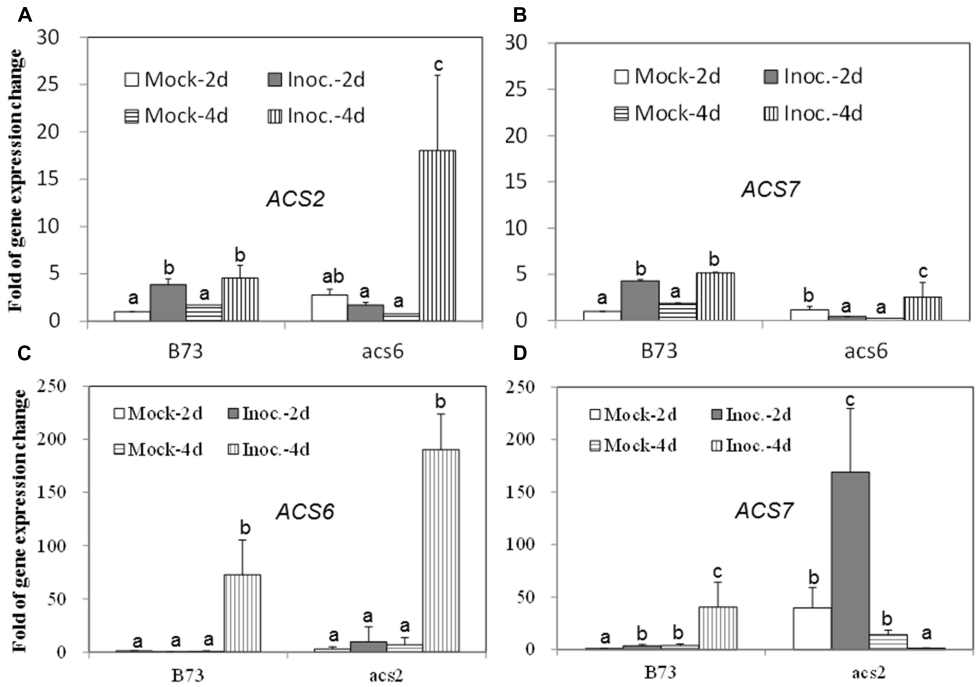

FIGURE 7 | The expression of ET biosynthetic genes, *ACS2, ACS6* and *ACS7*, in the WT and *acs* mutant kernels infected with *A. flavus*. The kernels were inoculated with 1×10^6 spores and cultured in a 20 ml of glass scintillation vial (Wheaton Science) at 29°C under 12L/12D for 2 and 4 days, and gene expression levels of *ACS2* **(A)** and *ACS7* **(B)** in B73 vs. *acs6* mutants, and *ACS6* **(C)** and *ACS7* **(D)** in B73 vs. *acs2* mutants, respectively, were quantified using qRT-PCR. Different letters above bars denote significant differences ($P < 0.05$, ANOVA) analyzed by the SPSS program between different treatments within the host genotypes. Similar results were obtained in three independent experiments.

could significantly increase the ergosterol content in B73 seeds, compated to the control (**Supplementary Figure S2C**), supporting our findings that ET might serve as a susceptibility factor for fungal growth. The effect of ACC on ergosterol was not observed in either *acs* mutant. This could be due to possible saturation of the seed capability of converting ACC to yet additional ET in the acs mutant kernels in response to *A. flavus*.

Expression of ET Biosynthetic Genes in WT and *acs6* Mutants upon Infection with *A. flavus*

Since the *acs* mutants, produced more ET compared to WT, in response to the infection with *A. flavus*, we hypothesized that the increased ET levels observed in the single mutants might be due to the overexpression of other *ACS* genes. As shown in **Figures 7A,B**, the expression of both *ACS2* and *ACS6* was moderately increased in WT seed upon *A. flavus* infection, while *ACS2* expression, but not *ACS7*, was strongly induced to a much higher levels in the *acs6* mutant compared to that in WT seeds, at 4 dpi. In the *acs2* mutant seed, *ACS6* expression was induced to a higher level upon infection, compared to that in WT seed (**Figure 7C**), at 4 dpi. However, the expression of *ACS7* was enhanced earlier, at 2 dpi, in the *acs2* mutant seed, compared to that in WT, where it was induced to a higher level at 4 dpi (**Figure 7D**). In support of this finding, the expression of both *ACS2* and *ACS7* was significantly higher in the *lox3-4* mutants after infection with *A. flavus* at 4 dpi, compared to that in WT (**Figures 8A,B**). Although the expression of *ACS6* was also strongly increased in *lox3-4* mutant, however, that numerical increase was not statistically different (**Figure 8C**).

DISCUSSION

Aspergillus flavus colonizes the same niche, i.e., maize kernels, but is evolutionarily and ecologically distinct from *Fusarium* spp. Kernel assays showed consistently that *acs* mutants were more susceptible to *A. flavus*. The increased colonization and sporulation of *A. flavus* on *acs* mutant kernels was associated with the enhanced ET production, especially in *acs6* (**Figure 5**). Here we also demonstrated that susceptible to *Aspergilli* spp. *lox3-4* mutant (Gao et al., 2009), also produced greater levels of ET upon infection with *A. flavus* compared to WT and provides a support for presumptive role of ET in facilitating *A. flavus* pathogenesis (**Figure 1**). Coincidently, *lox3-4* mutant was also reported to produce greater levels of ET in the roots, suggesting that 9-oxylipins produced by the LOX3 isoform are potent inhibitors of ET synthesis in both seeds and roots.

Taken together, the findings from this study suggest that seed derived ET facilitate seed colonization and conidiation by *A. flavus*. Our results did not provide conclusive evidence as to whether host-derived ET has a role in the regulation of aflatoxin biosynthesis. While fungal colonization and spore

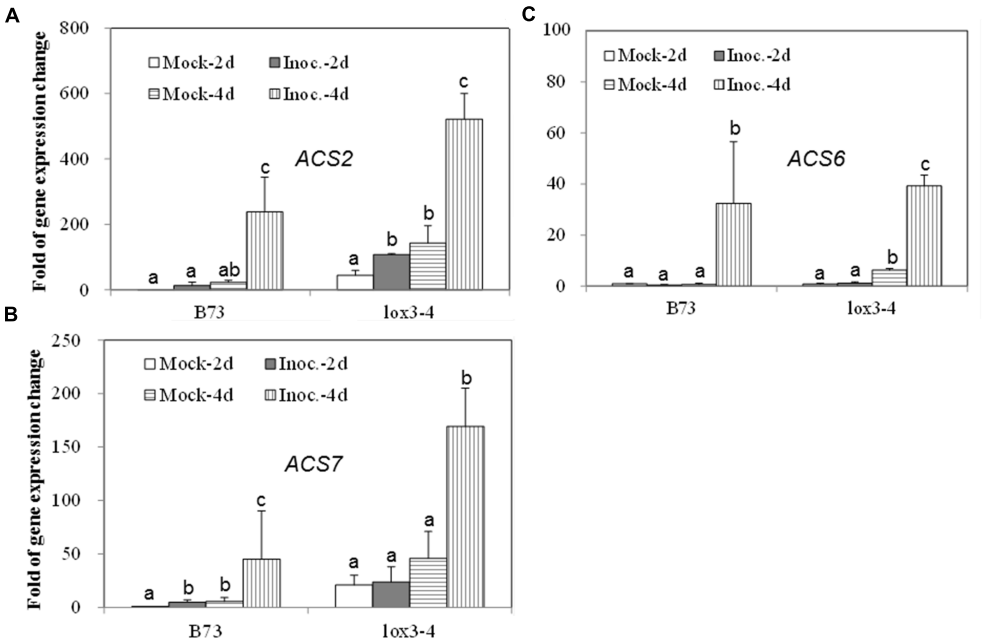

FIGURE 8 | The expression of ET biosynthetic genes, *ACS2, ACS6* and *ACS7*, in the WT and *lox3-4* mutant kernels infected with *A. flavus*. The kernels were inoculated with 1×10^6 spores and cultured in a 20 ml of glass scintillation vial (Wheaton Science) at 29°C under 12L/12D for 2 and 4 days, and gene expression levels of *ACS2* **(A)**, *ACS6* **(B)** and *ACS7* **(C)** in B73 vs. *lox3-4* mutants, respectively, were quantified using qRT-PCR. Different letters above bars denote significant differences ($P < 0.05$, ANOVA) analyzed by the SPSS program between different treatments within the host genotypes. Similar results were obtained in three independent experiments.

production by *A. flavus* were increased in the *acs* mutant kernels, aflatoxin production was not impacted in *acs2* or *acs6* (**Figure 4**), suggesting that ET function differentially in the regulation of fungal growth and secondary metabolite production. It appears, however, that the increased colonization of *acs* mutants may be responsible for the same level of aflatoxin produced by relatively lower fungal biomass in WT seed.

It was intriguing to find that seed-derived ET upon the infection stimulates the growth of *A. flavus*, whereas did not show any impact on aflatoxin production in corn seeds. This contrasts with the studies showing that exogenously applied ET could inhibit aflatoxin production by *A. parasiticus* in peanuts (Roze et al., 2004; Gunterus et al., 2007; Huang et al., 2009). ET and its generator, ethephon, also suppressed aflatoxin biosynthesis in *A. flavus in vitro*, which might be due to ROS reduction (Huang et al., 2009). There are three possible reasons for this discrepancy. First, the amount of seed-derived endogenous ET that we detected is within the range of nl/L, which was far below the amount of ET that previous studies used (1∼100ppm, within a range of ul/L) (Roze et al., 2004; Gunterus et al., 2007; Huang et al., 2009). Another possible reason is that endogenous ET at low threshold produced by host upon infection could serve as signaling molecule facilitating *A. flavus* vegetative growth, but not aflatoxin synthesis. There is also a possibility that ET role in the pathogenicity is host-dependent (peanut vs. maize). Further studies are required to investigate the precise function and mechanisms of ET in different pathosystems.

One of the intriguing findings of this study is that ET production in response to *A. flavus* infection was not reduced, as expected, in both *acs2* and *acs6* mutant kernels (**Figure 5**). On the contrary, ET was increased in *acs2* and even higher in *acs6* mutants. Further analyses of why the single mutants produce greater levels of ET revealed that they overexpress other members of the ACS gene family. Maize *ACS* gene family consists of at least three members, *ZmACS2*, its closely related paralog *ZmACS7*, and a distantly related *ZmACS6* (Gallie and Young, 2004; Young et al., 2004). *ACS2* and to a lesser extent *ACS7* transcript abundance was enhanced in the *acs6* mutant seed upon the infection with the fungus, and *acs2* mutant overexpressed the *ACS6* gene. Interestingly, it has been shown in an unrelated study that maize *acs6* mutants overexpress *ZmACS2* gene while expression of the *ZmACS7* gene was reduced (Young et al., 2004). Similar to our finding that single *acs* mutants overproduce ET, previous study showing that the Arabidopsis *eto2* mutant, which produces 20-fold greater levels of ET, is deficient in the *ACS5* gene expression supports the idea of antagonistic interaction between ET-producing enzyme isoforms or the ability of the functional genes to compensate for the lack of a missing gene family member (Vogel et al., 1998).

Previous reports showed that *A. parasiticus* produces ET on solid culture medium (Roze et al., 2004). In this study, however, no fungus-derived ET was detected in either fungal culture plates (data not shown) or from the fungus grown on non-viable seeds (**Figure 5**), suggesting that *A. flavus* is not the source of increased ET in the assays with living seeds. This discrepancy may be

explained by different timing of ET sampling. For example, it has been reported that *A. flavus* produced much less ET compared to *A. parasiticus,* and the emission of ET by the former occurred at the early period of their growth, after which the ET level declined to the level that was not detectable in the system (Sharma et al., 1985). Alternatively, even if *A. flavus* produces ET when grown on a medium, this production may be inhibited on a plant tissue. This scenario was reported in *B. cinerea*-tobacco pathosystem, where *B. cinerea* produced easily detectable levels of ET *in vitro* but did not produce any ET *in planta* (Chague et al., 2006).

Our findings in this study provide strong evidence that ET biosynthetic enzymes *ZmACS2* and *ZmACS6* and their final product ET directly or indirectly play a major role in governing the outcomes of seed interactions with the mycotoxin-producing fungi. The phenotypes of the two mutants resemble closely the disease phenotypes previously reported for the 9-lipoxygenase mutant, *lox3-4*, except that *F. verticillioides* grew equally well on both the *lox3-4* mutant and B73, but produced up to 200-fold lower fumonisin and threefold lower conidia levels (Gao et al., 2007). Supporting the hypothesis that ET may facilitate fungal growth and conidia production is our finding that *A. flavus*-infected *lox3-4* mutants emitted greater levels of ET compared to WT (**Figure 1**). Similar to ET positive correlation with fungal growth and conidiation shown in this study, in the *lox3-4* studies increased colonization by *A. flavus* of *lox3-4 mutant* and greater spore and mycotoxin production by *F. verticillioides* grown on WT kernels correlated with the increased accumulation of fatty acids (Gao et al., 2009). Therefore, we propose that both fungi exploit not only ET but also lipids to facilitate their virulence. It is possible that the two groups of signals, *ZmLOX3*-dependent lipid-derived molecules and *ZmACS2/6*-dependent ET, may act synergistically or are interdependent. The precise mechanism of their interactions, if any, is not clear and needs to be further examined by using the *lox3* and the *acs* double and triple mutants being constructed in our laboratories.

DISTRIBUTION OF MATERIALS

Novel materials described in this publication may be available for non-commercial research purposes upon acceptance and signing of a material transfer agreement. In some cases such materials may contain or be derived from materials obtained from a third party. In such cases, distribution of material will be subject to the requisite permission from any third-party owners, licensors, or controllers of all or parts of the material. Obtaining any permission will be the sole responsibility of the requestor. Plant germplasm will not be made available except at the discretion of the owner and then only in accordance with all applicable governmental regulations.

AUTHOR CONTRIBUTIONS

XG and MK designed the research. SW, Y-SP, YY, TI, and XG performed research. SW, Y-SP, EB, XG, and MK performed data analysis. Y-SP, XG, and MK drafted the article. XG and MK performed critical revision of the article. XG and MK carried out final approval of the final version.

FUNDING

This research was supported by National Science Foundation grants NSF IOB-0544428 and NSF IOS-0951272 to MK, and grants from NSFC (No. 31471508, No. 31671702), The National Key Research and Development Program of China (No. 2016YFD0101002), Natural Science Foundation of Jiangsu Province (No. BK20141370) and Jiangsu Collaborative Innovation Center for Modern Crop Production (JCIC-MCP) to XG.

ACKNOWLEDGMENT

We thank Dr. Daniel R. Gallie (University of California at Riverside) for his kind gift of the seeds of *acs2* and *acs6* mutants used in this study.

SUPPLEMENTARY MATERIAL

The Supplementary Material for this article can be found online at: http://journal.frontiersin.org/article/10.3389/fpls.2017.00415/full#supplementary-material

FIGURE S1 | Expression levels of *ACS2*, *ACS6* and *ACS7* in different maize organs from different growth stages (A–C), and ET levels in the leaves of *acs6* mutant **(D)**. Expression levels of *ACS2* **(A)**, *ACS6* **(B)** and *ACS7* **(C)** was examined by qRT-PCR in different maize organs from different growth stages. Eg, embryo from geminating seeds (2-day-old); Rg, root from geminating seeds (4-day-old); R1, root at V1 stage; S1, stem at V1 stage; L1, leaf at V1 stage; R3, root at V3 stage; S3, stem at V3 stage; L3, leaf at V3 stage; Rf, root at flowering time; Sf, stem at flowering time; Lf, leaf at flowering time; T, tassel; E, ear; P, pollen; K, kernel. **(D)** ET levels in the leaves of B73 and *acs6* mutant. The plants were grown as described in Section "Materials and Methods." The leaves of B73 and acs6 were excised from the plants and immediately transferred into a 20 ml of glass scintillation vial (Wheaton Science). The vial was then tightly sealed with a plastic lid for 1 to 2 h prior to analysis to allow sufficient levels of ethylene to accumulate. ET was measured by gas chromatograph as described. The values are the mean ± SD of four replicates (four vials each treatment each genotype), with three leaf segments in each vial.

FIGURE S2 | Effect of ethylene precursor ACC on the colonization, conidiation, and ergosterol production by *A. flavus* NRRL 3357 on *acs* mutants. (A) The kernels were pretreated with ACC (20 nM) for 30 min, followed by inoculation with 1×10^6 spores, then cultured in a 20 ml of glass scintillation vial (Wheaton Science) at 29°C under 12L/12D for 7 days. CK is the control by pretreatment with same amount of 0.001% Tween-20 as that used for inoculum of *A. flavus*. **(B)** Conidiation observed on the *acs* mutants upon infection of *A. flavus NRRL* 3357. The values are the mean ± SD of at least four replicates (four vials each treatment each genotype), with four kernels in each vial. Different letters above bars denote significant differences ($P < 0.05$, ANOVA) analyzed by SPSS program over B73-CK. Similar results were obtained in two independent experiments. **(C)** Ergosterol content was measured at 7 days post-inoculation (dpi).

REFERENCES

Adie, B., Chico, J. M., Rubio-Somoza, I., and Solano, R. (2007). Modulation of plant defenses by ethylene. *J. Plant Growth Regul.* 26, 160–177. doi: 10.1016/j.jplph.2014.12.013

Bleecker, A. B., and Kende, H. (2000). Ethylene: a gaseous signal molecule in plants. *Annu. Rev. Cell Dev. Biol.* 16, 1–18. doi: 10.1146/annurev.cellbio.16.1.1

Broekaert, W. F., Delaure, S. L., De Bolle, M. F. C., and Cammue, B. P. A. (2006). The role of ethylene in host-pathoven interactions. *Annu. Rev. Phytopathol.* 44, 393–416. doi: 10.1146/annurev.phyto.44.070505.143440

Catinot, J., Huang, J. B., Huang, P. Y., Tseng, M. Y., Chen, Y. L., Gu, S. Y., et al. (2015). ETHYLENE RESPONSE FACTOR 96 positively regulates *Arabidopsis* resistance to necrotrophic pathogens by direct binding to GCC elements of jasmonate - and ethylene-responsive defence genes. *Plant Cell Environ.* 38, 2721–2734. doi: 10.1111/pce.12583

Chague, V., Danit, L. V., Siewers, V., Gronover, C. S., Tudzynski, P., Tudzynski, B., et al. (2006). Ethylene sensing and gene activation in *Botrytis cinerea*: a missing link in ethylene regulation of fungus-plant interactions? *Mol. Plant Microbe Interact.* 19, 33–42. doi: 10.1094/MPMI-19-0033

Cohn, J. R., and Martin, G. B. (2005). *Pseudomonas syringae* pv. tomato type III effectors AvrPto and AvrPtoB promote ethylene-dependent cell death in tomato. *Plant J.* 44, 139–154. doi: 10.1111/j.1365-313X.2005.02516.x

Cristescu, S. M., De Martinis, D., Hekkert, S. T., Parker, D. H., and Harren, F. J. M. (2002). Ethylene production by *Botrytis cinerea* in vitro and in tomatoes. *Appl. Environ. Microbiol.* 68, 5342–5350. doi: 10.1128/AEM.68.11.5342-5350.2002

Diaz, J., ten Have, A., and van Kan, J. A. L. (2002). The role of ethylene and wound signaling in resistance of tomato to *Botrytis cinerea*. *Plant Physiol.* 129, 1341–1351. doi: 10.1104/pp.001453

Ellis, C., and Turner, J. G. (2001). The Arabidopsis mutant cev1 has constitutively active jasmonate and ethylene signal pathways and enhanced resistance to pathogens. *Plant Cell* 13, 1025–1033. doi: 10.1105/tpc.13.5.1025

Fukuda, H., Kitajima, H., Fujii, T., Tazaki, M., and Ogawa, T. (1989a). Purification and some properties of a novel ethylene-forming enzyme produced by *Penicillium digitatum*. *FEMS Microbiol. Lett.* 59, 1–5. doi: 10.1111/j.1574-6968.1989.tb03072.x

Fukuda, H., Takahashi, M., Fujii, T., Tazaki, M., and Ogawa, T. (1989b). An Nadh-Fe(III)Edta Oxidoreductase from *Cryptococcus albidus* - an enzyme involved in ethylene production In vivo. *FEMS Microbiol. Lett.* 60, 107–111.

Fukuda, H., Ogawa, T., and Tanase, S. (1993). Ethylene production by microorganisms. *Adv. Microb. Physiol.* 35, 275–306. doi: 10.1016/S0065-2911(08)60101-0

Gallie, D. R., and Young, T. E. (2004). The ethylene biosynthetic and perception machinery is differentially expressed during endosperm and embryo development in maize. *Mol. Genet. Genomics* 271, 267–281. doi: 10.1007/s00438-004-0977-9

Gao, X. Q., Brodhagen, M., Isakeit, T., Brown, S. H., Gobel, C., Betran, J., et al. (2009). Inactivation of the lipoxygenase ZmLOX3 increases susceptibility of maize to *Aspergillus* spp. *Mol. Plant Microbe Interact.* 22, 222–231. doi: 10.1094/MPMI-22-2-0222

Gao, X. Q., Shim, W. B., Gobel, C., Kunze, S., Feussner, I., Meeley, R., et al. (2007). Disruption of a maize 9-lipoxygenase results in increased resistance to fungal pathogens and reduced levels of contamination with mycotoxin fumonisin. *Mol. Plant Microbe Interact.* 20, 922–933. doi: 10.1094/MPMI-20-8-0922

Gao, X. Q., Starr, J., Gobel, C., Engelberth, J., Feussner, I., Tumlinson, J., et al. (2008). Maize 9-lipoxygenase ZmLOX3 controls development, root-specific expression of defense genes, and resistance to root-knot nematodes. *Mol. Plant Microbe Interact.* 21, 98–109. doi: 10.1094/MPMI-21-1-0098

Glazebrook, J., Chen, W. J., Estes, B., Chang, H. S., Nawrath, C., Metraux, J. P., et al. (2003). Topology of the network integrating salicylate and jasmonate signal transduction derived from global expression phenotyping. *Plant J.* 34, 217–228. doi: 10.1046/j.1365-313X.2003.01717.x

Gunterus, A., Roze, L. V., Beaudry, R., and Linz, J. E. (2007). Ethylene inhibits aflatoxin biosynthesis in *Aspergillus parasiticus* grown on peanuts. *Food Microbiol.* 24, 658–663. doi: 10.1016/j.fm.2006.12.006

Guo, H. W., and Ecker, J. R. (2004). The ethylene signaling pathway: new insights. *Curr. Opin. Plant Biol.* 7, 40–49. doi: 10.1016/j.pbi.2003.11.011

Huang, J. Q., Jiang, H. F., Zhou, Y. Q., Lei, Y., Wang, S. Y., and Liao, B. S. (2009). Ethylene inhibited aflatoxin biosynthesis is due to oxidative stress alleviation and related to glutathione redox state changes in *Aspergillus flavus*. *Int. J. Food Microbiol.* 130, 17–21. doi: 10.1016/j.ijfoodmicro.2008.12.027

Ince, J. E., and Knowles, C. J. (1986). Ethylene formation by cell-free-extracts of *Escherichia coli*. *Arch. Microbiol.* 146, 151–158. doi: 10.1007/BF00402343

Jia, Y. J., Kakuta, Y., Sugawara, M., Igarashi, T., Oki, N., Kisaki, M., et al. (1999). Synthesis and degradation of 1-aminocyclopropane-1-carboxylic acid by *Penicillium citrinum*. *Biosci. Biotechnol. Biochem.* 63, 542–549. doi: 10.1271/bbb.63.542

Johnson, P. R., and Ecker, J. R. (1998). The ethylene gas signal transduction pathway: a molecular perspective. *Annu. Rev. Genet.* 32, 227–254. doi: 10.1146/annurev.genet.32.1.227

Kende, H. (1993). Ethylene biosynthesis. *Annu. Rev. Plant Phys.* 44, 283–307. doi: 10.1146/annurev.pp.44.060193.001435

Kendrick, M. D., and Chang, C. (2008). Ethylene signaling: new levels of complexity and regulation. *Curr. Opin. Plant Biol.* 11, 479–485. doi: 10.1016/j.pbi.2008.06.011

Lin, Z. F., Zhong, S. L., and Grierson, D. (2009). Recent advances in ethylene research. *J. Exp. Bot.* 60, 3311–3336. doi: 10.1093/jxb/erp204

Munkvold, G. P. (2003). Cultural and genetic approaches to managing mycotoxins in maize. *Annu. Rev. Phytopathol.* 41, 99–116. doi: 10.1146/annurev.phyto.41.052002.095510

Musungu, B. M., Bhatnagar, D., Brown, R. L., Payne, G. A., OBrian, G., Fakhoury, A. M., et al. (2016). A network approach of gene co-expression in the *Zea mays*/*Aspergillus flavus* pathosystem to map host/pathogen interaction pathways. *Front. Genet.* 7:206. doi: 10.3389/fgene.2016.00206

Nagahama, K., Ogawa, T., Fujii, T., Tazaki, M., Tanase, S., Morino, Y., et al. (1991). Purification and properties of an ethylene-forming enzyme from *Pseudomonas* syringae Pv Phaseolicola-Pk2. *J. Gen. Microbiol.* 137, 2281–2286. doi: 10.1099/00221287-137-10-2281

Paul, C., Naidoo, G., Forbes, A., Mikkilineni, V., White, D., and Rocheford, T. (2003). Quantitative trait loci for low aflatoxin production in two related maize populations. *TAG Theor. Appl. Genet.* 107, 263–270. doi: 10.1007/s00122-003-1241-0

Penninckx, I. A. M. A., Thomma, B. P. H. J., Buchala, A., Metraux, J. P., and Broekaert, W. F. (1998). Concomitant activation of jasmonate and ethylene response pathways is required for induction of a plant defensin gene in Arabidopsis. *Plant Cell* 10, 2103–2113. doi: 10.1105/tpc.10.12.2103

Rodriguez-Romero, J., Hedtke, M., Kastner, C., Muller, S., and Fischer, R. (2010). Fungi, hidden in soil or up in the air: light makes a difference. *Annu. Rev. Microbiol.* 64, 585–610. doi: 10.1146/annurev.micro.112408.134000

Roze, L. V., Calvo, A. M., Gunterus, A., Beaudry, R., Kall, M., and Linz, J. E. (2004). Ethylene modulates development and toxin biosynthesis in *Aspergillus* possibly via an ethylene sensor-mediated signaling pathway. *J. Food Prot.* 67, 438–447. doi: 10.4315/0362-028X-67.3.438

Ruger-Herreros, C., Rodriguez-Romero, J., Fernandez-Barranco, R., Olmedo, M., Fischer, R., Corrochano, L. M., et al. (2011). Regulation of conidiation by light in *Aspergillus nidulans*. *Genetics* 188, 809–822. doi: 10.1534/genetics.111.130096

Sharma, A., Padwaldesai, S. R., and Nadkarni, G. B. (1985). Possible implications of reciprocity between ethylene and aflatoxin biogenesis in *Aspergillus flavus* and *Aspergillus parasiticus*. *Appl. Environ. Microbiol.* 49, 79–82.

Vogel, J. P., Woeste, K. E., Theologis, A., and Kieber, J. J. (1998). Recessive and dominant mutations in the ethylene biosynthetic gene ACS5 of Arabidopsis confer cytokinin insensitivity and ethylene overproduction, respectively. *Proc. Natl. Acad. Sci. U.S.A.* 95, 4766–4771. doi: 10.1073/pnas.95.8.4766

Warburton, M. L., Brooks, T. D., Windham, G. L., and Williams, W. P. (2011). Identification of novel QTL contributing resistance to aflatoxin accumulation in maize. *Mol. Breed.* 27, 491–499. doi: 10.1007/s11032-010-9446-9

Willcox, M. C., Davis, G. L., Warburton, M. L., Windham, G. L., Abbas, H. K., Betran, J., et al. (2013). Confirming quantitative trait loci for aflatoxin resistance from Mp313E in different genetic backgrounds. *Mol. Breed.* 32, 15–26. doi: 10.1007/s11032-012-9821-9

Woloshuk, C. P., Seip, E. R., Payne, G. A., and Adkins, C. R. (1989). Genetic transformation system for the aflatoxin-producing fungus *Aspergillus flavus*. *Appl. Environ. Microbiol.* 55, 86–90.

Xiang, K., Zhang, Z. M., Reid, L. M., Zhu, X. Y., Yuan G.-S., and Pan, G. T. (2010). A meta-analysis of QTL associated with ear rot resistance in maize. *Maydica* 55, 281–290.

Yang, S. F. (1985). Biosynthesis and action of ethylene. *HortScience* 20, 41–45.

Young, T. E., Meeley, R. B., and Gallie, D. R. (2004). ACC synthase expression regulates leaf performance and drought tolerance in maize. *Plant J.* 40, 813–825. doi: 10.1111/j.1365-313X.2004.02255.x

Zhang, Y., Cui, M., Zhang, J., Zhang, L., Li, C., Kan, X., et al. (2016). Confirmation and fine mapping of a major QTL for aflatoxin resistance in maize using a combination of linkage and association mapping. *Toxins* 8:E258. doi: 10.3390/toxins8090258

Conflict of Interest Statement: The authors declare that the research was conducted in the absence of any commercial or financial relationships that could be construed as a potential conflict of interest.

frontiers in Plant Science

ORIGINAL RESEARCH
published: 30 August 2016
doi: 10.3389/fpls.2016.01246

An Ethylene-Protected Achilles' Heel of Etiolated Seedlings for Arthropod Deterrence

Edouard Boex-Fontvieille[1†], Sachin Rustgi[2,3], Diter von Wettstein[3], Stephan Pollmann[4], Steffen Reinbothe[1*] and Christiane Reinbothe[1]*

[1] Laboratoire de Génétique Moléculaire des Plantes and Biologie Environnementale et Systémique, Université Grenoble-Alpes – Laboratoire de Bioénergétique Fondamentale et Appliquée, Grenoble, France, [2] Department of Agricultural and Environmental Sciences–Pee Dee Research and Education Center, Clemson University, Florence, SC, USA, [3] Department of Crop and Soil Sciences – Center for Reproductive Biology, School of Molecular Biosciences, Washington State University, Pullman, WA, USA, [4] Centro de Biotecnología y Genómica de Plantas, Univerdidad Politécnica de Madrid – Instituto Nacional de Investigación y Tecnología Agraria y Alimentación, Madrid, Spain

OPEN ACCESS

Edited by:
Péter Poór, University of Szeged, Hungary

Reviewed by:
Clay Carter, University of Minnesota, USA
Jorge Alberto Zavala, National Scientific and Technical Research Council, Argentina

***Correspondence:**
Steffen Reinbothe
sreinbot@ujf-grenoble.fr
Sachin Rustgi
rustgi@wsu.edu
srustgi@clemson.edu

†Present address:
Edouard Boex-Fontvieille, Laboratoire de Biotechnologies Végétales Appliquées aux Plantes Aromatiques et Médicinales, FRE CNRS3727, Université Jean Monnet, 10 Rue Tréfilerie, Saint-Étienne, France

Specialty section:
This article was submitted to Plant Physiology, a section of the journal Frontiers in Plant Science

Received: *14 April 2016*
Accepted: *05 August 2016*
Published: *30 August 2016*

Citation:
Boex-Fontvieille E, Rustgi S, von Wettstein D, Pollmann S, Reinbothe S and Reinbothe C (2016) An Ethylene-Protected Achilles' Heel of Etiolated Seedlings for Arthropod Deterrence. Front. Plant Sci. 7:1246. doi: 10.3389/fpls.2016.01246

A small family of Kunitz protease inhibitors exists in *Arabidopsis thaliana*, a member of which (encoded by At1g72290) accomplishes highly specific roles during plant development. *Arabidopsis* Kunitz-protease inhibitor 1 (Kunitz-PI;1), as we dubbed this protein here, is operative as cysteine PI. Activity measurements revealed that despite the presence of the conserved Kunitz-motif the bacterially expressed Kunitz-PI;1 was unable to inhibit serine proteases such as trypsin and chymotrypsin, but very efficiently inhibited the cysteine protease RESPONSIVE TO DESICCATION 21. Western blotting and cytolocalization studies using mono-specific antibodies recalled Kunitz-PI;1 protein expression in flowers, young siliques and etiolated seedlings. In dark-grown seedlings, maximum *Kunitz-PI;1* promoter activity was detected in the apical hook region and apical parts of the hypocotyls. Immunolocalization confirmed Kunitz-PI;1 expression in these organs and tissues. No transmitting tract (NTT) and HECATE 1 (HEC1), two transcription factors previously implicated in the formation of the female reproductive tract in flowers of *Arabidopsis*, were identified to regulate Kunitz-PI;1 expression in the dark and during greening, with NTT acting negatively and HEC1 acting positively. Laboratory feeding experiments with isopod crustaceans such as *Porcellio scaber* (woodlouse) and *Armadillidium vulgare* (pillbug) pinpointed the apical hook as ethylene-protected Achilles' heel of etiolated seedlings. Because exogenous application of the ethylene precursor 1-aminocyclopropane-1-carboxylic acid (ACC) and mechanical stress (wounding) strongly up-regulated HEC1-dependent *Kunitz-PI;1* gene expression, our results identify a new circuit controlling herbivore deterrence of etiolated plants in which Kunitz-PI;1 is involved.

Keywords: skotomorphogenesis, apical hook, *Arabidopsis thaliana*, protease inhibitor action, herbivore deterrence

Abbreviations: ACC, 1-aminocyclopropane-1-carboxylic acid; HEC1, HECATE 1; HR, hypersensitive response; IAA, indole acetic acid; NTT, no transmitting tract; PCD, programmed cell death; PI, protease inhibitor.

INTRODUCTION

When seeds germinate underneath the soil or fallen leaves, they pass through a developmental program known as skotomorphogenesis (von Wettstein et al., 1995). Dark-grown (etiolated) seedlings establish an elongated hypocotyl (epicotyl) terminating in an apical hook with closely apposed, unexpanded cotyledons. This specific morphology and especially the presence of the apical hook enables etiolated seedlings to grow through the soil without mechanical damage (Darwin, 1896). When dark-grown seedlings break through the soil, they switch to another developmental program, that is, photomorphogenesis, during which hypocotyl growth is arrested and unfolding of the cotyledons and greening proceed. Mechanisms have been identified that maintain the skotomorphogenetic program in the dark and trigger photomorphogenesis in the light.

Several phytohormones comprising brassinosteroids, auxins, gibberellins, jasmonic acid, and ethylene regulate skotomorphogenetic growth (Alabadí et al., 2004; Alabadí and Blázquez, 2009; Zhong et al., 2009; Li et al., 2012; Li and He, 2013; Hsieh and Okamoto, 2014). For example, pioneering work performed on pea epicotyls revealed that increased mechanical impedance caused enhanced rates of ethylene biosynthesis (Harpham et al., 1991). As a consequence, an increased radial expansion and decreased elongation of the epicotyl were observed (Goeschl et al., 1966). Ethylene production was confined to the epicotyl hook and plumule and shown to decrease upon illumination with red light (Goeschl et al., 1967). Ethylene was also demonstrated to be necessary for the formation and maintenance of the apical hook in etiolated seedlings of *Arabidopsis thaliana* (Raz and Ecker, 1999).

Analysis of the cell wall proteome corresponding to different stages of hypocotyl elongation of etiolated seedlings revealed a great dynamics in cell wall protein composition in *Arabidopsis* (Irshad et al., 2008). Among the identified proteins were aspartate, cysteine, and serine proteases as well PIs of the Kunitz family (Irshad et al., 2008). Both ethylene and proteases are normally implicated in controlling PCD in a vast range of physiological contexts, including the HR to pathogen attack, tracheary-element differentiation, and senescence. For example, some fungal elicitors were shown to induce ethylene biosynthesis and PCD in tobacco leaves (Anderson et al., 1982). It was observed that treatment with phenylmethanesulfonyl fluoride (PMSF) and soybean trypsin inhibitor (two serine PIs), but not pepstatin A (a carboxyl PI) abrogated this response (Anderson et al., 1982). Other studies have implemented ethylene and protease action in PCD during the HR to pathogen attack (Beers et al., 2000), oxidative stress (Solomon et al., 1999), leaf senescence (Chen et al., 2002), and flower petal senescence (Jones et al., 1995). The fungal elicitor ethylene-inducing xylanase (EIX) was shown to elicit ethylene biosynthesis in tomato and tobacco leaves through induction of ACC synthase gene expression. Evidence was obtained for a role of a cysteine protease in controlling ACC synthase expression (Matarasso et al., 2005). The protease specifically binds to a *cis*-element of the ACC synthase gene and acts as a transcription factor. Last but not least, plant responses to ethylene are mediated by SCF(EBF1/EBF2)-dependent proteolysis of EIN3 transcription factor (Guo and Ecker, 2003; Christians et al., 2008; An et al., 2010), highlighting the role of proteolysis in ethylene signal transduction.

With regard to skotomorphogenesis, it is somewhat unexpected to see aspartate, cysteine and serine proteases accumulating. However, their location in cell walls is rather suggestive of a direct defense function against biotic foes. On the other hand, endogenous PIs such as Kunitz-protease inhibitors could regulate their activity. Because Kunitz-protease inhibitors were also identified in the cell wall proteome of the elongating parts of dark-grown chickpea (*Cicer arietinum*), a role in growth regulation was proposed (Jiménez et al., 2007; Hernández-Nistal et al., 2009). Here, we report on a Kunitz-protease inhibitor that accumulates in the apical hook of etiolated *Arabidopsis* seedlings and is part of a mechanism of arthropod deterrence through which young-born seedlings are protected against herbivory during greening (Boex-Fontvieille et al., 2015a). Expression studies of this novel Kunitz-PI, termed Kunitz-PI;1, identified a new regulatory circuit that comprises ethylene, auxin, and the transcription factors NTT and HEC1, previously implicated in female reproductive tract development in flowers of *A. thaliana* (Crawford et al., 2007; Gremski et al., 2007). Together, our results provide new insights into the mechanisms that govern skotomorphogenesis in the model plant *Arabidopsis*.

MATERIALS AND METHODS

Plant Material

The following *A. thaliana* genotypes were used in this study: Columbia (Col-0; referred to as wild-type, WT), SALK_009681 (renamed to *Kunitz-PI;1*) that carries a T-DNA insertion in the At1g72290 gene encoding the Kunitz-PI;1 (Boex-Fontvieille et al., 2015a), Kunitz-PI;1 overexpressor (WT transformed with the plasmid pB7WG2 containing the coding frame for Kunitz-PI;1, referred to as *35S::Kunitz-PI;1*; Boex-Fontvieille et al., 2015a), Kunitz-PI;1 promoter-ß-glucuronidase (*pKunitz-PI;1::GUS*) consisting of the promoter region of Kunitz-PI;1 in front of the ß-glucuronidase coding sequence (Boex-Fontvieille et al., 2015a), *ntt-2* (SALK_007406; Alonso et al., 2003; Crawford et al., 2007), *hec1* (GABI-KAT 297B10), *hec3* (SALK_005294, Alonso et al., 2003), and *hec1::hec3* (Alonso et al., 2003; Gremski et al., 2007).

Growth Conditions

Dark- and light-grown seedlings were obtained from seeds that had been surface-sterilized by imbibition in hypochlorite solution and ethanol. Seeds were plated on petri dishes containing Murashige–Skoog mineral salts (Sigma–Aldrich; 4.3 g/L), MES (0.5 g/L), and agar (10 g/L), pH 5.7, and kept in the dark at 4°C for 48 h. Germination was induced by illumination with white light of 70 μE $m^{-2}s^{-1}$ for 3 h. The plates were then either returned to darkness or kept in white light for appropriate periods. Plates to be used for phytohormone tests contained 10 μM IAA, 10 μM ACC, or 100 μM silver nitrate ($AgNO_3$). For seed production, seedlings were grown to maturity

on soil in a culture room in 16 h light/8 h dark cycles at 70 $\mu M \times s^{-1} \times cm^{-2}$.

Protein Expression and Purification

cDNA encoding the precursor Kunitz-PI;1 protein including the predicted NH_2-terminal, 23 amino acids signal sequence[1] was amplified by PCR (Innis et al., 1990) with primers 5′-GGGGACAAGTTTGTACAAAAAAGCAGGCTTCAAGAATCCTTCAGTGATCTCTTTT-3′ and 5′-GGGGACCACTTTGTACAAGAAAGCTGGGTCTCAACCCGGGAAGTATAAGTTGCT-3′. Similarly, cDNA encoding the predicted mature Kunitz-PI;1 protein was amplified with the primers 5′-GGGGACAAGTTTGTACAAAAAAGCAGGCTTCCACGGAAATGAACCGGTG-3′ and 5′-GGGGACCACTTTGTACAAGAAAGCTGGGTCTCAACCCGGGAAGTATAAGTTGCT-3′. The PCR products were cloned into pDONR221 (Plant System Biology, VIB-Ghent University) using Gateway technology (Invitrogen). For allowing protein expression, the cDNA were introduced into pDEST17 (Plant System Biology, VIB-Ghent University) and then used to transform *Escherichia coli*, strain BL21. The NH_2-terminal $(His)_6$-tagged Kunitz-PI;1 precursor or Kunitz-PI;1 mature protein was expressed after induction with arabinose (0.2% [w/v] final concentration) and growth at 37°C for 3 h. Pellets obtained from 0.5 L-batches of the bacterial cultures were lysed in a buffer containing 20 mM NaH_2PO_4, pH 7.5, 6 M urea, 20 mM imidazole, 500 mM NaCl and 0.5 mM PMSF and passed through a French Press (Thermo Electron, FA-078A). After centrifugation, the clear lysate was subjected to Ni-NTA agarose chromatography according to the manufactures instructions (Qiagen). Approximately 90–95% pure protein was obtained.

Determination of Protease Inhibitor Activity

Pilot experiments were carried out as described (Halls et al., 2006; Homaei et al., 2010; Boex-Fontvieille et al., 2015b), using 10^{-3} to 10^{-6} moles of bacterially expressed and purified Kunitz-PI;1 or soybean trypsin inhibitor and a fixed, 10^{-6} molar concentration of papain or trypsin (all chemicals from Sigma–Aldrich). The results shown in Supplementary Figure S1 refer to a 10-fold molar excess of PI to protease and refer to three independent experiments. In more refined studies, purified Kunitz-PI;1 was mixed with 6×10^{-6} moles of trypsin from swine pancreas (Sigma–Aldrich) at molar ratios of either 1:1 or 1:10 in 2.5 mL of reaction buffer containing 50 mM Tris-HCl, pH 7.5, and incubated for 5 min at 25°C. Then, a 2 mL-aliquot was withdrawn and mixed with 100 µL benzoyl-L-arginine ethyl ester (BAEE, 10 mM stock solution). Substrate conversion was followed over a period of 4 min by absorbance measurements at 253 nm in a Cari 100 spectrophotometer. Control incubations contained soybean trypsin inhibitor (3.10^{-9} moles per assay; Sigma–Aldrich).

Reverse zymography was carried out on SDS-polyacrylamide (PAA) gels containing 0.1% (w/v) porcine skin gelatine (Sigma–Aldrich). After electrophoresis, the gels were incubated twice for 30 min in a buffer containing 0.1 M Tris-HCl, pH 7.5, and 2.5% (v/v) Triton X100. The gels were rinsed several times with distilled water and successively incubated in 50 mM Tris-HCl, pH 8.2, supplemented with either trypsin or chymotrypsin at a concentration of 0.1% (v/v), at 4°C for 30 min and at 37°C for 90 min. Thereafter, the gels were briefly rinsed with distilled water and stained with Coomassie brilliant blue.

Protein Analyses

Either etiolated seedlings or their upper parts comprising the apical hook and the cotyledons were frozen in liquid nitrogen and ground in a mortar. Three-hundred mg of the resulting powder was mixed with 600 µL extraction buffer containing 0.5 M Tris-HCl, pH 8, 5 mM EDTA, 0.1 M NaCl, 10 % (v/v) ß-mercaptoethanol, 2 mM PMSF, and 0.7 M sucrose. After addition of one volume of phenol (equilibrated with 10 mM Tris-HCl, pH 8) the tubes were shaken at room temperature for 20 min. The upper phase obtained after centrifugation at 12,000 rpm in an Eppendorf microcentrifuge, model 5414, was aspirated with a pipette, transferred into a new test tube and mixed with five volumes of ammonium acetate (0.1 M in methanol). Protein was precipitated at −20°C for 2 h and pelleted by centrifugation at 12,000 rpm at 4°C for 5 min. The pellets were washed twice with ammonium acetate and once with 500 µL 80% (v/v) acetone, dried at room temperature, dissolved in 100 µL twofold concentrated SDS sample buffer containing 125 mM Tris-HCl, pH 6.8, 20% (v/v) glycerol, 4% (w/v) SDS, 10% (v/v) ß-mercaptoethanol, and boiled at 96°C for 5 min. Protein from all other types of plant samples was obtained by a quick-step method of boiling plant tissue powders in SDS-sample buffer at 100°C for 1 min. The homogenates were cleared by centrifugation at 8,000 rpm for 1 min and the supernatant transferred to a new test tube. Protein concentration was determined according to Esen (1978). SDS-PAGE was carried out on 12% (w/v) PAA gels containing SDS. After electrophoresis, protein was blotted onto nitrocellulose membranes (0.45 µm, Whatman) according to Towbin et al. (1979). Immunodetection of protein was made using Kunitz-PI;1 antibodies (Boex-Fontvieille et al., 2015a) and alkaline phosphatase-conjugated goat anti-rabbit antibodies (diluted 1:3000) or horseradish peroxidase-conjugated goat anti-rabbit antibodies (diluted 1:5000). Crossreactive bands were detected with 5-bromo-4-chloro-3-indolyl phosphate (BCIP) and nitro blue tetrazolium (NBT) or via enhanced chemiluminescence (ECL Western Blotting Analysis system, Amersham), respectively.

Immunolocalization

Etiolated seedlings were infiltrated for 10 min in a solution containing 5% (v/v) glacial acetic acid, 3.7% (v/v) formaldehyde and 50% (v/v) ethanol and incubated for 24 h at 4°C. Thereafter, the samples were dehydrated by successive incubations in solutions of increasing ethanol concentrations (70% [v/v], 90% [v/v], and 100% [v/v], 1 h each) and Histoclear (25% [v/v], 50% [v/v], 75% [v/v], and 100% [v/v], 1 h each). Embedding was done in paraffin (Paraplast X-TRA, Tyco Healthcare). Ten-µm tissue-sections were prepared with a microtome (Microtom HM

[1] www.cbs.dtu.dk/services/TargetP

355S, Zeiss), mounted on glass slides and incubated for 3 h at 45°C. Paraffin was removed by two incubations with Histoclear, for 2 × 10 min each. Rehydration of samples was achieved by successive incubations in solutions of decreasing ethanol concentrations.

For immunolocalization, the samples were first depleted of endogenous alkaline phosphatase activity[2]. Tissue sections were incubated at 95°C for 40 min in buffer consisting of 10 mM citric acid, pH 6, and 0.05% (v/v) Tween 20, then cooled to room temperature, and finally incubated in a solution containing 0.05% (v/v) Tween 20 and 5% (w/v) low-fat milk powder dissolved in Tris-buffered saline (TBS). Kunitz-PI;1 antiserum (Boex-Fontvieille et al., 2015a) was diluted 1:300 and the samples incubated at room temperature for 2 h. Excess antibodies were removed by consecutive washes in 0.05% (v/v) Tween 20 dissolved in TBS. In turn, incubation was carried out with secondary antibodies (goat anti-rabbit IgG conjugated with alkaline phosphatase, Sigma). After numerous washes, the antigen-antibody complexes were visualized with a solution containing 100 mM NaCl, 100 mM Tris-HCl, pH 9, 50 mM $MgCl_2$, 0.5 mM NBT, and 0.5 mM BCIP. Slides were rinsed, mounted in water and viewed under a light microscope (Eclipse E-600, Nikon).

cDNA Synthesis and Semi-quantitative PCR

Total RNA was isolated from etiolated seedlings and 2 μg were incubated in the presence of 300 pmols of oligo-dT primers at 65°C for 5 min. Subsequent synthesis of the first cDNA strand was carried out with reverse transcriptase at 42°C for 2 h as recommended by the supplier (SUPERSCRIPT II, Invitrogen). Reactions were stopped by incubation at 72°C for 10 min and a 1 μL aliquot (1/30 of the final reaction volume) was subjected to semi-quantitative PCR (Innis et al., 1990), using the following primer pairs: HEC1fow 5′-TAATGTGTTTGAAGGGTTCTG-3′; HEC1rev 5′-CCATATCGATCCCGAGGC-3′; NTTfow 5′-TTCTCATTGGCCCTACTCAG-3′; NTTrev 5′-TTGTTCTACCTCAGAGGCAGG-3′; ACTfow 5′-CAGAATCAGATATCTAAAAATCCCGGAAA-3′; ACTrev 5′-TGGGATGACATGGAGAAGAT-3′; Kunitz-PIfow 5′-TGGCATGAGGAAAAAGCCAAG-3′; Kunitz-PIrev 5′-TCAATGTTTTCTCAAGCTCAA-3′. PCR cycle numbers were 28 for *ACTIN*, 30 for *Kunitz-PI;1* and 32 each for *NTT* and *HECATE1*. Data are representative and refer to three independent biological experiments.

Kunitz-PI;1 Promoter Activity Test

Plant tissues to be used to detect Kunitz-PI;1 promoter activity were first infiltrated in a solution containing 100 mM phosphate buffer, pH7, 10 mM EDTA, and 1 mM 5-bromo-4-chloro-3-indolyl-beta-D-glucuronic acid (X-Gluc, Sigma–Aldrich) for 10 min and then kept overnight at 37°C. Destaining was achieved by successively incubating plant tissue in solutions containing 50% (v/v), 75% (v/v), and 96% (v/v) ethanol. Finally, the tissues were transferred into a solution containing 50% (v/v) ethanol/30% (v/v) glycerol and viewed under a microscope (Eclipse E-600, Nikon) or binocular (SZX12, Olympus). Photos were taken with an Olympus DP70 camera.

Whole-Plant Predation Assay

Whole-plant predation assays were carried out according to Farmer and Dubugnon (2009). Accordingly, *P. scaber* and *A. vulgare* were fed pesticide-free adult *Arabidopsis* WT plants, then starved for 3 days and transferred into a growth chambers filled with soil. Feeding activity was monitored with 1–3 arthrpods per liter soil for 4-days old WT, Kunitz-PI;1 knock-out mutant and Kunitz-PI;1 overexpressor seedlings as described (Boex-Fontvieille et al., 2015a). Populations of 120 seedlings were analyzed in three independent experiments and feeding scored by counting the number of plants with damaged apical hooks and/or dropped cotyledons. For diet feeding experiments, starved pillbugs and woodlice were transferred at high density (24 individuals) onto agar plates containing different concentrations of bacterially expressed, chemically purified Kunitz-PI;1 or commercial soybean trypsin inhibitor. Arthropod viability was assessed after 4–5 days and expressed as percentage of living to dead individuals.

RESULTS

Activity of Bacterially Expressed *Arabidopsis* Kunitz-PI;1

In *Arabidopsis thaliana,* a small family of Kunitz-type protease inhibitors exists. The protein encoded by At1g72290 contains the Kunitz-motif [LIVM]-X-D-X-[EDNTY]-[DG]-[RKHDENQ] and a chlorophyll(ide)-binding motif related to one of the chlorophyll-binding motifs in LHCII, the major light-harvesting chlorophyll-binding proteins of photosystem II (Green and Kühlbrandt, 1995). Based on the presence of these motifs, this protein is related to the family of water-soluble chlorophyll proteins (WSCPs) of *Brassicaceae* (Satoh et al., 2001; Bektas et al., 2012; Boex-Fontvieille et al., 2015a,b). We renamed this protein to *A. thaliana* Kunitz-PI;1.

Gateway cloning was used to create constructs permitting *Kunitz-PI;1* expression in *E. coli* and subsequent protein purification and activity measurements (Boex-Fontvieille et al., 2015a,b; see also Materials and Methods). Two types of constructs were prepared, encoding the full-length protein and a variant lacking the predicted NH_2-terminal, 23 amino acids comprising signal peptide for intracellular targeting[3].

Protease inhibitor tests were carried out with pancreas trypsin, a protease predicted to be a Kunitz-PI target, and papain. Pilot experiments revealed that Kunitz-PI;1 displayed an unusual target protease specificity. Instead of acting on trypsin, Kunitz-PI;1 inhibited papain (Supplementary Figure S1), a cysteine protease that had previously been identified as potential Kunitz-PI;1 target (Halls et al.,

[2]http://www.ihcworld.com/_protocols/epitope_retrieval/citrate_buffer.htm

[3]http://www.cbs.dtu.dk/services/TargetP/

2006). This result was confirmed by additional activity measurements. Swine pancreas trypsin was incubated with benzoyl-L-arginine ethyl ester (BAEE) and cleavage of the substrate followed by absorbance measurements at 253 nm in assays containing or lacking *Arabidopsis* Kunitz-PI;1 added at a 1:1 or 1:10 molar ratio (**Figures 1C,D**). For comparison, parallel assays contained soybean trypsin inhibitor (**Figures 1A,B**).

Whereas trypsin activity was inhibited by added soybean trypsin inhibitor, *Arabidopsis* Kunitz-PI;1 was ineffective. This result is consistent with previous results (Boex-Fontvieille et al., 2015a,b) and was confirmed by reverse zymography. Soybean trypsin inhibitor and Kunitz-PI;1 were separated by SDS-PAGE on gels containing gelatine. After separation, the proteins were renatured and incubated in protease-containing solution which led to the digestion of gelatine and all of the other protein bands, except for the PI bands corresponding to soybean trypsin inhibitor (**Figures 1F,G**, respectively, left panels). By contrast, the Kunitz-PI;1 band was rapidly degraded, as demonstrated by Coomassie staining (**Figures 1F,G**, respectively, right panels). We concluded that *Arabidopsis* Kunitz-PI;1 is not active on serine proteases. In line with this view, Halls et al. (2006) showed that Kunitz-PI;1 inhibits cysteine proteases containing a granulin domain, such as papain, but has only weak or no activity toward serine and aspartate proteases. Another cysteine protease targeted by Kunitz-PI;1 is RESPONSIVE TO DESICCATION 21 (RD21; Boex-Fontvieille et al., 2015a,b).

Expression Pattern of *A. thaliana* Kunitz-PI;1 *In planta*

Previously raised Kunitz-PI;1-specific antibodies (Boex-Fontvieille et al., 2015b) were used for carrying out expression and cytolocalization studies. These were combined with promoter activity measurements, using the *Kunitz-PI;1* regulatory region fused to the coding region of bacterial β-glucuronidase (GUS), and semi-quantitative reverse transcription (RT)-PCR analyses.

According to information obtained from the Bio-Array Resource for Plant Functional Genomics[4], Kunitz-PI;1 expression is high in dark-grown seedlings but low in light-grown seedlings (Winter et al., 2007). In mature plants, highest transcript levels were found in flowers (Winter et al., 2007). Confirming these results, *Kunitz-PI;1* RNA was detectable in etiolated seedlings and flowers. Semi-quantitative RT-PCR revealed that, compared to flower extracts, only small quantities of *Kunitz-PI;1* transcript accumulated in etiolated seedlings. No *Kunitz-PI;1* transcript was present in leaves of 3 weeks-old green plants (**Figure 2A**). Western blot analyses performed with the Kunitz-PI;1-specific antibody confirmed Kunitz-PI;1 protein accumulation in etiolated seedlings, although at much lower quantities than in flower extracts. Reflecting the absence of respective transcript, Kunitz-PI;1 protein was undetectable in leaves of 3 weeks-old, green plants and the cotyledons of 4-days old light-grown seedlings (**Figure 2B**).

[4]www.bar.utoronto.ca

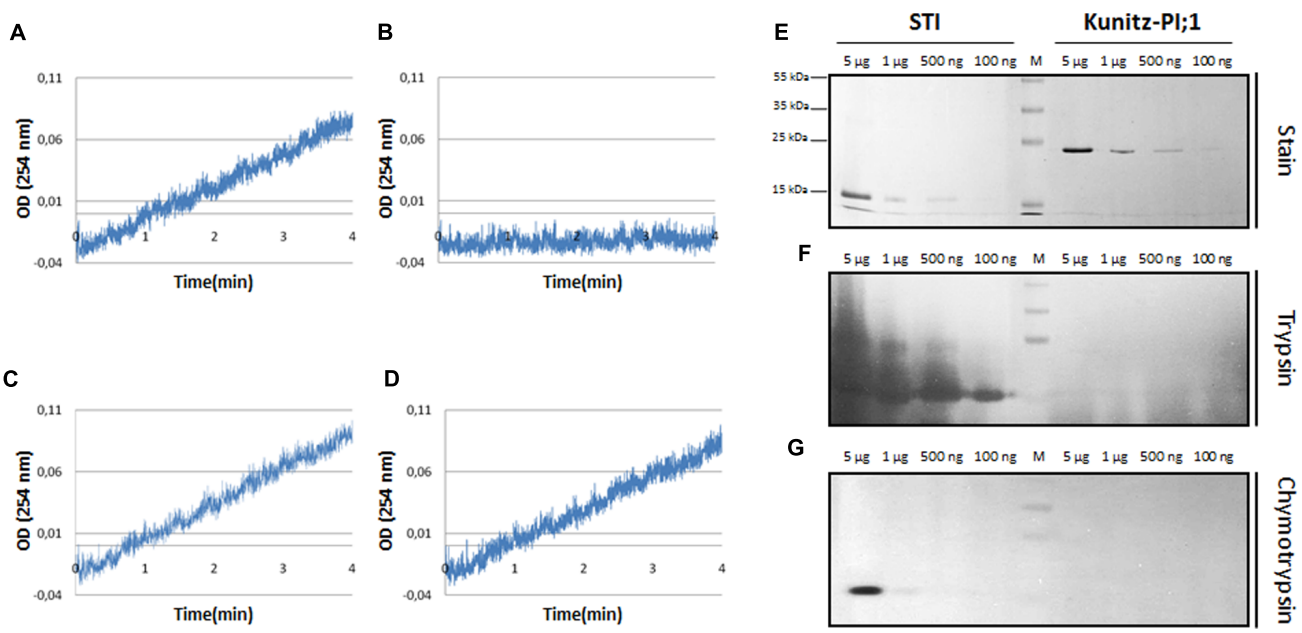

FIGURE 1 | Analysis of protease-inhibitor activity of bacterially expressed and purified *Arabidopsis* Kunitz-PI;1. (A–D) Trypsin activity measured in the absence of protease inhibitors **(A)** or presence of either soybean trypsin inhibitor **(B)** or *Arabidopsis* Kunitz-PI;1 added at molar ratios of 1:1 **(C)** or 1:10 **(D)**. Trypsin activity was determined by cleavage of BAEE and measuring the absorption of the product at 253 nm. **(E–G)** Reverse zymography to reveal protease inhibitor activity of soybean trypsin inhibitor (STI, left part) and *Arabidopsis* Kunitz-PI;1 (right part). **(E)** Pls were separated on a SDS-PAA gel and stained with Coomassie brilliant blue. (**F** as **E**) But showing soybean trypsin inhibitor (STI) (left part) and *Arabidopsis* Kunitz-PI;1 (right part) on a SDS-PAA gel containing gelatine after renaturation and incubation with trypsin. (**G** as **F**) But depicting the results obtained with chymotrypsin.

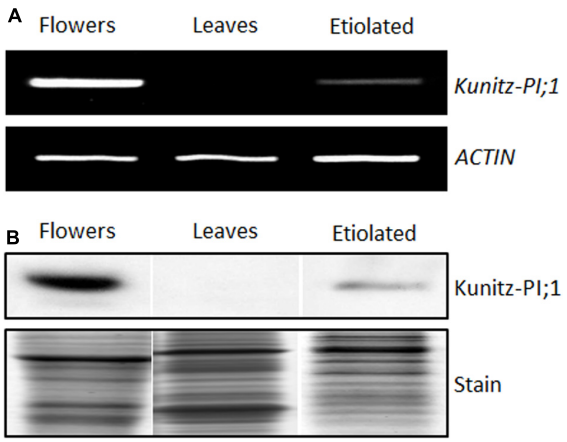

FIGURE 2 | Organ-specific expression of *Arabidopsis* Kunitz-PI;1. **(A,B)** *Kunitz-PI;1* transcript **(A)** and Kunitz-PI;1 protein **(B)** abundance in flowers, in leaves of 3-week-old plants, and in 3-days old etiolated seedlings. The gel in **(A)** shows RT-PCR products visualized by ethidium bromide staining. Actin transcript levels were analyzed as internal constitutive marker. For SDS-PAGE **(B)**, 50 μg of total protein was loaded per lane. Replicate gels were used for immunodetection using Kunitz-PI;1-specific antibodies (upper panel) and Coomassie staining (lower panel). Note that **(B)** is a composite diagram.

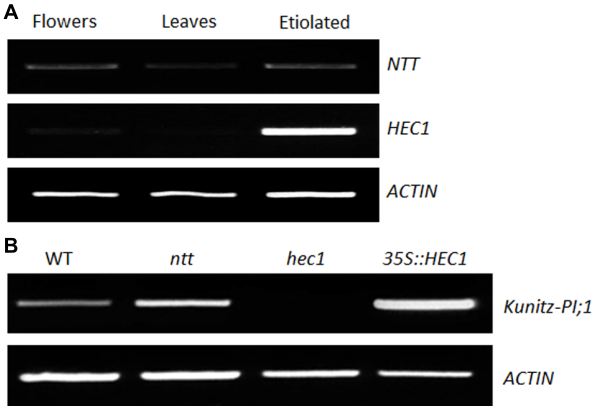

FIGURE 3 | Expression of *NTT* and *HEC1* genes in *Arabidopsis*. **(A)** Semi-quantitative RT-PCR to analyze the expression of the *NTT* and *HEC1* genes in flowers, the leaves of 3-week-old plants, and in 3-days old etiolated seedlings. (**B** as **A**) But showing RT-PCR data for *Kunitz-PI;1* transcripts in *ntt* and *hec1* mutants as well as *35S::hec1* overexpressing lines after growth in darkness for 3 days. Actin transcript levels were assessed as internal standard.

Transcription Factors NTT and HEC1 Regulate the Expression of Kunitz-PI;1 in Etiolated Seedlings

No transmitting tract and HEC1 are transcription factors involved in female reproductive tract development in flowers of *Arabidopsis* (Crawford et al., 2007; Gremski et al., 2007). We asked whether NTT and HEC1 could regulate *Kunitz-PI;1* transcription also in etiolated seedlings. As a first step to answer this question, the presence of *NTT* and *HEC1* transcripts in etiolated seedlings was assessed by semi-quantitative RT-PCR. For comparison, RNA extracts from flowers and leaves were used as positive and negative controls, respectively. Indeed, *NTT* and *HEC1* transcripts were detectable in total RNA preparations of etiolated seedlings. Remarkably, *NTT* transcript abundance was comparable for flowers and etiolated seedlings (**Figure 3A**). *HEC1* transcripts, however, appeared at much higher abundance in etiolated seedlings than in flowers (**Figure 3A**). Only small amounts of *NTT* and *HEC1* transcript were present in leaves of adult plants (**Figure 3A**).

ntt and *hec1* knock-out mutants as well as a line overexpressing *HEC1* under control of the *35S*-cauliflower mosaic virus promoter (*35S::HEC1*) were obtained (Crawford et al., 2007; Gremski et al., 2007) and the presence of Kunitz-PI;1 transcript investigated by semi-quantitative RT-PCR. Accordingly, no *Kunitz-PI;1* transcript was detectable in the *hec1* mutant (**Figure 3B**), suggesting that HEC1 positively controls Kunitz-PI;1 accumulation. On the other hand, slightly higher levels of Kunitz-PI;1 transcript accumulated in the *ntt* mutant than in the WT (**Figure 3B**), indicating that NTT negatively regulates Kunitz-PI;1 expression in etiolated seedlings. Consistent with this view, higher levels of Kunitz-PI;1 transcript were detectable in *35S::HEC1* plants, as compared to WT plants (**Figure 3B**).

Phytohormone Influence on the Accumulation of *Kunitz-PI;1* mRNA

Ethylene, brassinosteroids, gibberellins, jasmonic acid, and auxins regulate skotomorphogenesis and the switch to photomorphogenetic growth (see Introduction). We asked whether auxin (IAA) and ethylene could influence the expression of Kunitz-PI;1 in dark-grown *Arabidopsis* seedlings. Seeds of the *pKunitz-PI;1::GUS* line were germinated in the dark in the absence or presence of the ethylene precursor ACC or ethylene biosynthesis inhibitor silver nitrate. Parallel plates contained the auxin IAA, while mock plates lacked any additives. After 3 days in darkness, GUS activity was monitored.

Confirming previous results (Boex-Fontvieille et al., 2015a), maximum *Kunitz-PI;1* promoter activity was detected in the apical hook of etiolated seedlings and especially in the vascular tissues (**Figure 4**). Etiolated seedlings that had been germinated in the presence of ACC exhibited the well-known 'triple response,' which comprises (i) inhibition of elongation and swelling of the hypocotyls, (ii) inhibition of root elongation, and (iii) exaggeration of apical hook curvature (Knight and Crocker, 1913). *Kunitz-PI;1* promoter activity seemed higher in the presence of ACC than in the hormone-free control and was located to the apical hook (**Figure 4**). When the ethylene biosynthesis inhibitor silver nitrate was present in the growth medium, *Kunitz-PI;1* promoter activity was abrogated (**Figure 4**). Similarly, IAA dropped *Kunitz-PI;1* promoter activity to negligible levels (**Figure 4**).

Etiolated seedlings that had been stably transformed with a fusion construct of the *HEC1* promoter and GUS (*pHEC1::GUS*) were next analyzed. In the absence of additives, *HEC1* promoter

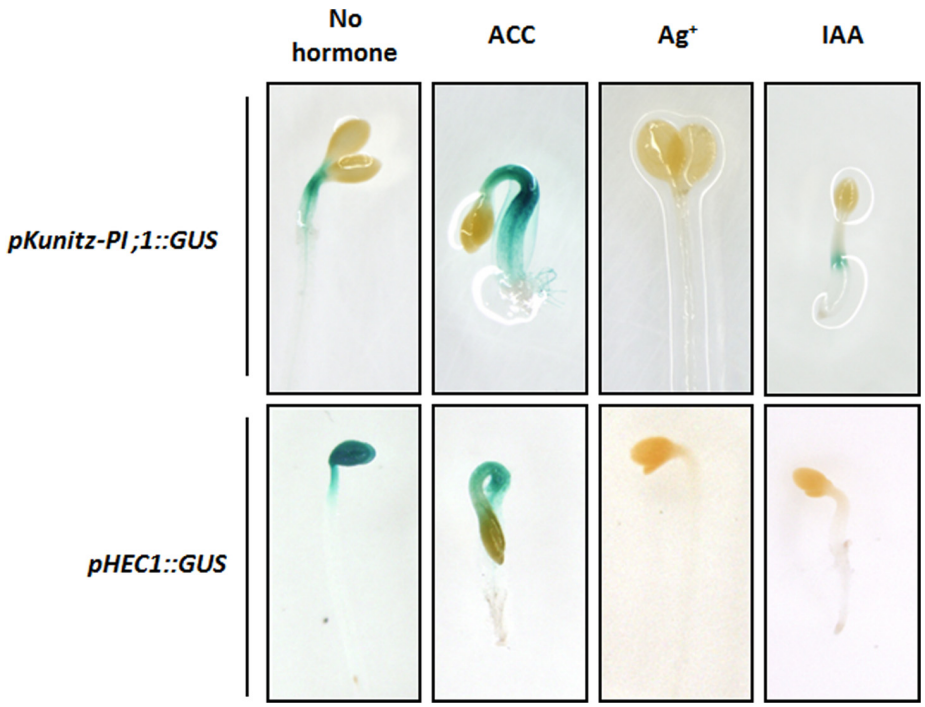

FIGURE 4 | Influence of phytohormones on *Kunitz-PI;1* promoter activity (Upper row) and *HEC1*-promoter activity (Lower row). Etiolated seedlings of the *pKunitz-PI;1::GUS* and *pHEC1::GUS* lines, respectively, were grown on Murashige–Skoog medium containing ACC as ethylene precursor, silver nitrate as ethylene biosynthesis inhibitor, or IAA as auxin, for 3 days. Then, GUS activity was monitored to visualize promoter activity.

activity was easily detectable in the cotyledons and the apical hook. Exogenous application of ACC led to a change in the pattern of *HEC1* promoter activity that was reduced in the cotyledons but maintained in the hypocotyls (**Figure 4**). In the presence of either silver nitrate or IAA, *HEC1* promoter activity was completely abolished (**Figure 4**).

Semi-quantitative RT-PCR was performed to correlate *Kunitz-PI;1* promoter activity with respective changes in transcript abundance. In addition to the *Kunitz-PI;1* transcript, *NTT*, *HEC1* and *ACTIN* transcripts were quantified by RT-PCR. **Figure 5A** shows that increased *Kunitz-PI;1* transcript levels were found in the presence of ACC, whereas no *Kunitz-PI;1* transcript was detectable in seedlings that had been grown on silver nitrate or IAA. Interestingly, similar effects were seen at the protein level (**Figure 5B**). Seedlings grown on ACC-containing medium expressed higher amounts of Kunitz-PI;1 protein than those grown on hormone-free medium. After growth in the presence of silver nitrate, Kunitz-PI;1 protein levels were negligibly low, in most cases undetectable (**Figure 5B**).

NTT transcript levels quantified in parallel were augmented in seedlings that had been treated with silver nitrate or IAA, as compared to seedlings grown on hormone-free medium (**Figure 5A**). By contrast, *HEC1* transcript levels were reduced on silver nitrate- and IAA-containing medium but increased in the presence of ACC (**Figure 5A**). In etiolated *ntt* mutant seedlings, more Kunitz-PI;1 protein was detected than in WT seedlings treated with ACC (**Figure 5C**). *hec1* mutant seedlings showed drastically reduced Kunitz-PI;1 protein levels in the presence of ACC. In line with this observation, the *HEC1* overexpressing line accumulated 10- to 20-fold more Kunitz-PI;1 protein in response to ACC than WT seedlings (**Figure 5C**).

Immunolocalization of Kunitz-PI;1 Protein in Etiolated Seedlings after Ethylene Treatment

The promoter-GUS studies had revealed strong Kunitz-PI;1 expression in the vascular tissues of the apical hook. To back-up this observation, the localization of Kunitz-PI;1 protein was assessed by carrying out *in situ*-localization studies. Whereas no Kunitz-PI;1 protein could be detected in the cotyledons (**Figure 6D**) and the basal part of the hypocotyls (**Figure 6A**), clear signals were obtained for the apical part of the hypocotyls (**Figure 6B**) and especially the apical hook region (**Figure 6C**). At the latter place, the protein was localized in the cortex and endodermis of the convex part (**Figures 6B,C,I**). No signal was obtained with a respective preimmune serum (**Figures 6E–H**).

Induction of Kunitz-PI;1 Promoter Activity by Wounding

Ethylene functions as plant growth regulator at many stages of development and is also known to be a stress hormone mediating responses to mechanical constraints (Lin et al., 2009). Etiolated seedling need to protect their apical hooks and embedded meristem against mechanical damage when growing through the soil. We hypothesized that Kunitz-PI;1 could contribute to this

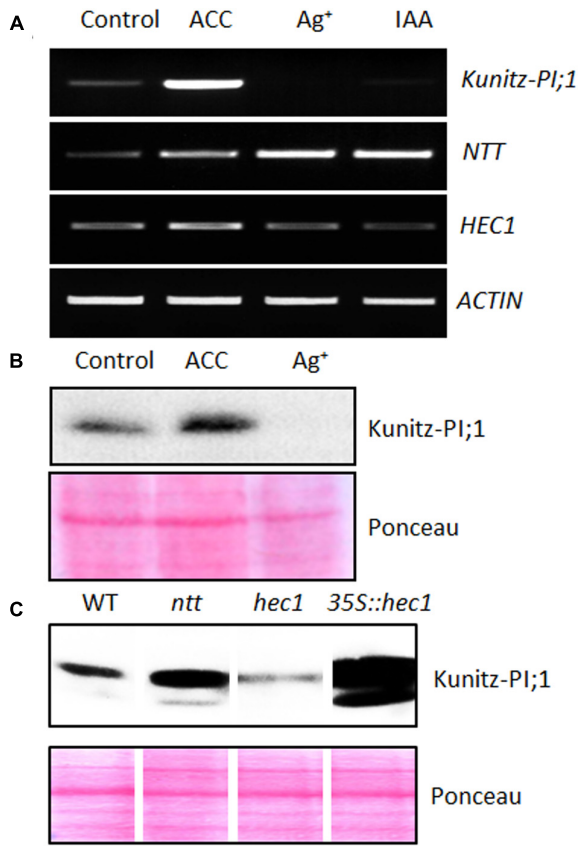

FIGURE 5 | Expression of *NTT* and *HEC1* versus *Kunity-PI;1* transcripts in response to phytohormones. (A) Semi-quantitative RT-PCR analysis of *NTT*, *HEC1*, and *Kunitz-PI;1* expression in 3-days old etiolated seedlings grown on ACC-containing, silver nitrate-containing or IAA-containing Murashige–Skoog medium. For comparison, actin transcript levels were assessed as internal standard. **(B)** Kunitz-PI;1 protein levels in 3-days old etiolated seedlings after growth on ACC-containing or Ag^+-containing medium analyzed by Western blotting. **(C)** Kunitz-PI;1 protein accumulation in etiolated seedlings of WT, *ntt* and *hec1* mutant, as well as *35S::hec1* overexpressor. For SDS-PAGE **(B,C)**, 40 μg protein was loaded per lane and subjected to Western blotting using Kunitz-PI;1-specific antibodies (upper panels); loading was confirmed by Ponceau-staining of the nitrocellulose-blotted proteins (lower panels). Note that the lower panels in **(C)** are composite diagrams.

protection mechanism and therefore tested *Kunitz-PI;1* promoter activity in response to wounding. 3-days old etiolated seedlings of the *pKunitz-PI;1::GUS* line were subjected to wounding, exerted by cutting the seedlings equidistantly from the apical hook and root tip or crushing the apical hook with tweezers. Afterward, the seedlings were kept in the dark for another 24 h-period before measuring *Kunitz-PI;1* promoter activity.

Figure 7 shows that cutting the seedlings into an upper, aerial part and lower, mostly root part, triggered local and systemic *Kunitz-PI;1* promoter activation in the cut hypocotyls but neither in the apical hooks nor cotyledons (**Figures 7A,B**, red versus black arrows). Crushing the apical hook led to a local up-regulation of *Kunitz-PI;1* promoter activity that now was no longer confined to the apical hook but was also detectable in the vascular bundles of the cotyledons (**Figures 7D,E**), as compared to the untreated controls (**Figure 7C**). Together, these results revealed that the *Kunitz-PI;1* promoter is wound-responsive.

Ethylene Protects the Apical Hook against Arthropod Feeding

Ethylene-induced stem thickening and hook curvature are supposed to be measures against mechanical impedance (Harpham et al., 1991). Other reasons for the obvious phenotypic effects triggered by ethylene could be biotic foes such as arthropod isopods including pillbugs and woodlice that live underneath stones and fallen leaves and act as seed predators and facultative herbivores. We asked whether ethylene-triggered *Kunitz-PI;1* gene expression could contribute to the protection of etiolated seedlings against herbivorous arthropods such as *Porcellio scaber* (woodlouse) and *Armadillidium vulgare* (pillbug). Laboratory feeding experiments were carried out as described by Farmer and Dubugnon (2009). In addition to WT seedlings, a homozygous knock-out mutant line that contains a T-DNA insertion in the single exon of the *Kunitz-PI;1* gene was included (Boex-Fontvieille et al., 2015a). Furthermore, *Arabidopsis* WT plants that had been transformed with a construct containing the *Kunitz-PI;1* coding region under control of the *35S*-promoter (*35S::Kunitz-PI;1*; Boex-Fontvieille et al., 2015a) were used for comparison. These tools were employed to assess the role of Kunitz-PI;1 protein irrespective of the NTT and HEC1 transcription factors.

Etiolated seedlings of the *Kunitz-PI;1* knock-out mutant as well as Kunitz-PI;1 overexpressing line showed no obvious phenotypic differences when grown on hormone-free medium, neither with regard to hypocotyl length nor apical hook structure (Boex-Fontvieille et al., 2015a) and all displayed the typical triple response when treated with ACC (Supplementary Figure S2). In laboratory feeding experiments with *Porcellio scaber* (woodlouse) and *Armadillidium vulgare* (pillbug), however, marked differences were observed. Ethylene caused a higher proportion of seedlings that were protected against pillbugs and woodlice feeding as compared to respective mock controls (**Figure 8**; see also Supplementary Table S1 for a statistical analysis). This effect seemed to be, at least in part, due to the enhanced expression of Kunitz-PI;1. Supporting this view, seedlings of the *Kunitz-PI;1* knock-out mutant treated with ACC were much less protected against pillbug and woodlice attack than WT seedlings (**Figure 8**). The ethylene effect on WT seedlings was abrogated in the presence of silver nitrate as ethylene biosynthesis inhibitor or IAA. Overexpression of Kunitz-PI;1 gave rise to a seemingly phytohormone-insensitive, constitutive mechanism of arthropod deterrence of etiolated seedlings (**Figure 8**).

Kunitz-PI;1 Efficiently Inhibits Cysteine Proteases of the Arthropod Gut

The results presented thus far suggested that Kunitz-PI:1 may function in herbivore deterrence by inhibiting digestive proteases in the arthropod gut. To examine this point, laboratory feeding experiments were carried out with bacterially expressed and

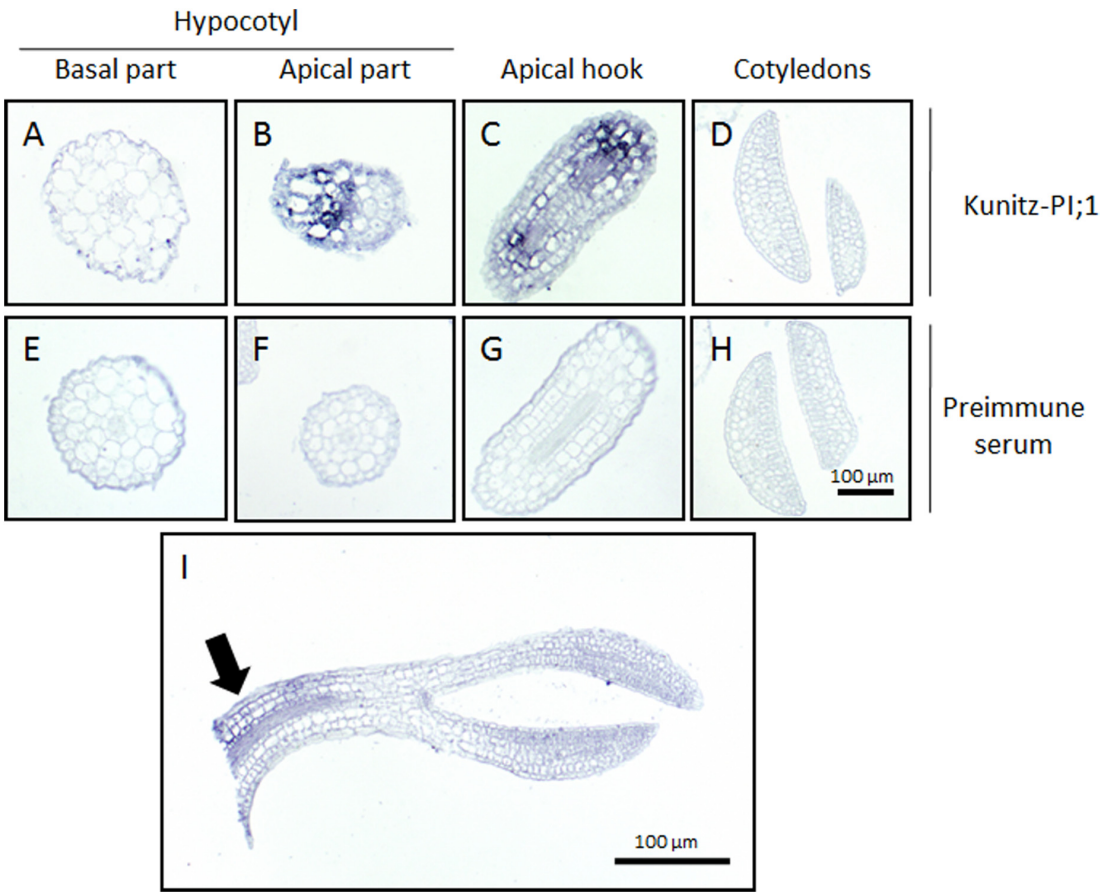

FIGURE 6 | Immunolocalization of *Arabidopsis* Kunitz-PI;1 protein. Seedlings were grown for 3 days on ACC-containing medium. Tissue sections from the basal part of the hypocotyls **(A,E)** and apical part of the hypocotyls **(B,F)**, the apical hook **(C,G)**, the cotyledons **(D,H)**, and a longitudinal section of the upper half of a seedling **(I)** were incubated with Kunitz-PI;1-specific antibodies **(A–D,I)** or preimmune serum **(E–H)**. Detection of the antigen-antibody complexes was made using an alkaline phosphatase-based assay with NBT and BCIP.

purified Kunitz-PI;1. As control, chemically pure soybean trypsin inhibitor was used. Both PIs were offered to pillbugs and woodlice that had been starved for nutrients for three days. **Figure 9** shows that Kunitz-PI;1 was a very poor diet for both arthropod species (see also Supplementary Table S2 for a statistical analysis). By contrast, both arthropods rapidly consumed the soybean trypsin inhibitor diet. While pillbugs and woodlice easily survived if fed the soybean trypsin inhibitor, they passed away on Kunitz-PI;1 diet presumably as a result of nutrient deprivation and indigestibility of Kunitz-PI;1. Taking into account the known specificity of both PIs, we concluded that the arthropod gut of both crustacean is mostly containing cysteine proteases.

DISCUSSION

A member of the family of Kunitz-PIs in *A. thaliana* (encoded by At1g72290) was subject of this analysis. *Arabidopsis* Kunitz-PI;1, as we dubbed the protein here, has a molecular mass of ≈21 kDa which is similar to that of other Kunitz-PIs (Oliva and Sampaio, 2008, 2009). However, despite the presence of the family-defining Kunitz motif, *Arabidopsis* Kunitz-PI;1 was unable to inhibit trypsin and chymotrypsin (**Figure 1**). Although Kunitz-PIs mainly inhibit serine proteases, such as trypsin and chymotrypsin, some of them were shown to inhibit cysteine (thiol) or aspartate proteases (Rawlings et al., 2004). Even bifunctional activity, e.g., against both serine and cysteine proteases, has been reported (Franco et al., 2002). *Arabidopsis* Kunitz-PI;1 does not seem to exhibit bifunctional activity but was active on cysteine proteases possessing a granuline domain such as papain and RD21 (Halls et al., 2006; Boex-Fontvieille et al., 2015a,b).

Expression of *Arabidopsis* Kunitz-PI;1 was analyzed over plant development and in different plant organs. Kunitz-PI;1 transcript and protein accumulated in flowers and young siliques but not in leaves and roots of adult plants (**Figure 2**; cf. Boex-Fontvieille et al., 2015b). This result is in agreement with microarray data showing *Arabidopsis* Kunitz-PI;1 expression during flower development and especially in the female reproductive tract (Scutt et al., 2003; Tung et al., 2005; Bektas et al., 2012; Boex-Fontvieille et al., 2015b). Kunitz-PI;1 protein was not

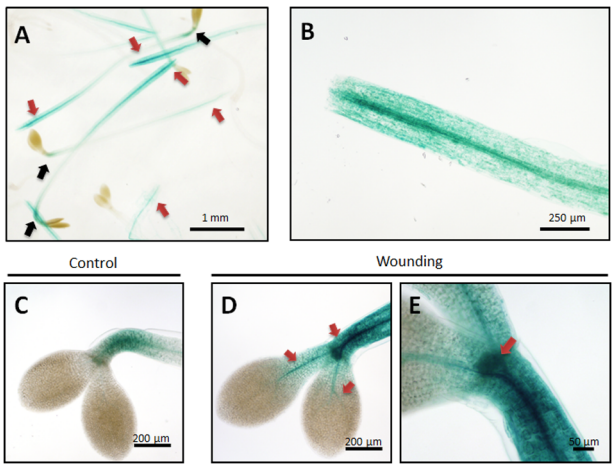

FIGURE 7 | *Kunitz-PI;1* promoter activity in response to wounding. **(A,B)** The hypocotyls of 3-days old etiolated seedlings were cut into two halves of which the aerial part comprising the apical hook and cotyledons **(A)** and the basal part comprising the root **(B)** were analyzed further by GUS staining. Red and black arrows mark regions of high and low *Kunitz-PI;1* promoter activity, respectively. **(C–E)** Etiolated seedlings were wounded by crushing the hypocotyls with tweezers near the apical hook region (red arrows) and GUS staining made 24 h thereafter **(D,E)**. **(C)** Unwounded control. Size markers are indicated.

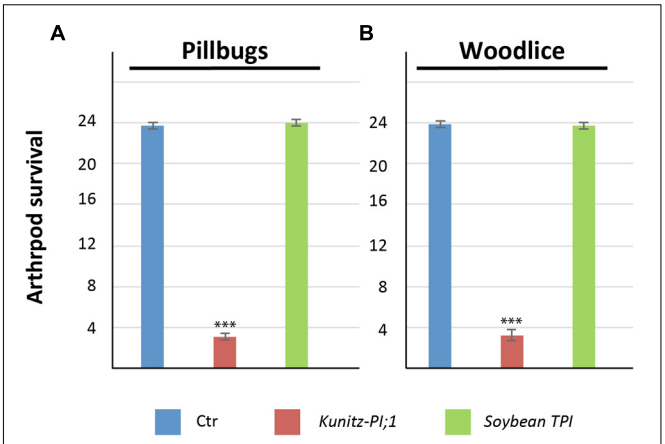

FIGURE 9 | Diet test conducted with bacterially expressed and purified *Arabidopsis* Kunitz-PI;1 and commercially available soybean trypsin inhibitor. (A) Survival rates of nutrient-starved pillbugs on Kunitz-PI;1 and soybean trypsin inhibitor diets. For control (Ctr), a senescent *Arabidopsis* leave was used as diet. **(B)** as **(A)**, but depicting the results for nutrient-starved woodlice on Kunitz-PI;1 and soybean trypsin inhibitor versus control diets. Asterisks indicate statistically significant changes compared with the corresponding WT sample for each condition calculated by a two-tailed Student's *t*-test; ***$P < 0.001$ (cf. Supplementary Table S2).

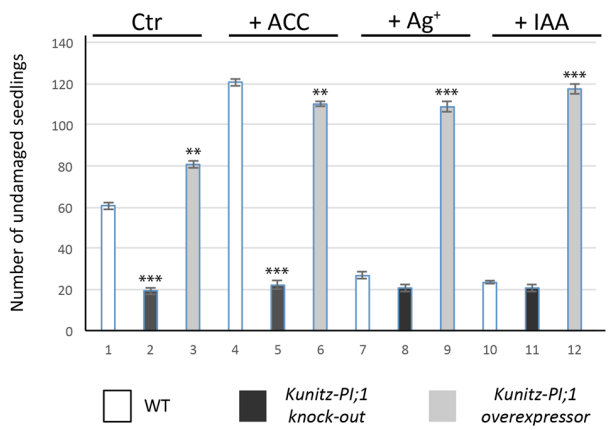

FIGURE 8 | Feeding of *P. scaber* on etiolated WT (white columns), *AtKunitz-PI;1* mutant (black bars) and *35S::Kunitz-PI;1* overexpressor (gray columns) seedlings. In parallel assays, feeding was tested for seedlings that had been grown on agar plates containing the ethylene precursor ACC, ethylene biosynthesis inhibitor silver nitrate, or the auxin IAA. Mock plates (control, Ctr) lacked any additives. Isopod feeding activity was scored by counting the number of damaged versus undamaged seedlings and is expressed as number of undamaged seedlings in the population of 120 seedlings analyzed. Error bars refer to three independent experiments. Asterisks indicate statistically significant changes compared with the corresponding WT sample for each condition calculated by a two-tailed Student's *t*-test; **$P < 0.01$, ***$P < 0.001$ (cf. Supplementary Table S1).

detected in dry seeds and thus is not a seed storage protein. Substantial *Kunitz-PI;1* transcript (**Figure 2A**) and Kunitz-PI;1 protein (**Figure 2B**) were detected in etiolated seedlings. Interestingly, the highest *Kunitz-PI;1* promoter activity was found in the region around the vascular bundles of the apical hook (**Figure 2C**). In chickpea, two Kunitz trypsin inhibitors were characterised, designated TPI-1 and TPI-2, of which TPI-1 accumulated in epicotyls and roots of etiolated seedlings (Jiménez et al., 2007, 2008; Hernández-Nistal et al., 2009). In either organ, TPI-1 was found in cell walls of vascular tissue and it was therefore proposed that TPI-1 could play a role in vascular tissue formation during growth. This function would be restricted to etiolated seedlings since TPI-1 expression was shown to be negatively light-regulated (Jiménez et al., 2007). We observed a similar, dark-specific expression for *Arabidopsis* Kunitz-PI;1 that was not detectable in greening seedlings and light-grown plants (**Figures 2A,B**). Moreover, *Arabidopsis* Kunitz-PI;1 protein was found in cell walls/apoplastic spaces by *in situ*-localization studies (Boex-Fontvieille et al., 2015a).

Considerable progress has been made during the last few years in the elucidation of the signal transduction cascades regulating skotomorphogenesis and photomorphogenesis. Generally, transcription factors that act as positive regulators of photomorphogenesis are degraded in the dark (Bae and Choi, 2008). On the other hand, transcription factors that negatively regulate photomorphogenesis, are degraded during greening (Kim et al., 2002). Here, we show that transcription factors such as NTT and HEC1 that regulate female reproductive tract development in *Arabidopsis* flowers (Crawford et al., 2007; Gremski et al., 2007) also are operative during skotomorphogenesis (**Figures 2A** and **3A**). While HEC1 functioned as positive regulator of *Kunitz-PI;1* gene expression, NTT acted negatively (**Figures 2B** and **3B**). How HEC1 and NTT may accomplish their roles in dark-grown seedlings and

how they interact with other known components of the PHY-mediated signal transduction chain needs to be resolved in future work. Zhu et al. (2016) provided evidence for a negative feedback loop between key players of phytochrome signal transduction, such as the phytochrome-interacting factors, and HECATE proteins.

HECATE1 and NTT appear to be part of a phytohormone response pathway that controls *Kunitz-PI;1* gene expression during skotomorphogenesis and greening (**Figure 5A**). In the presence of IAA, expression of the *Kunitz-PI;1* gene was abrogated through a mechanism involving NTT and HEC1 that were up and down-regulated, respectively. The proposed positive role of HEC1 on transcription of the *Kunitz-PI;1* gene was strengthened by co-localization of *HEC1* and *Kunitz-PI;1* promoter activities in the apical hook (**Figure 4**).

Ethylene (produced from its precursor ACC in the medium) caused an increase of *Kunitz-PI;1* promoter activity around the vascular bundles of the apical hook (**Figure 4**), which resulted in higher transcript (**Figure 5A**) and protein levels (**Figure 5B**) in etiolated seedlings. Furthermore, Kunitz-PI;1 protein accumulation in the cortex and endodermis of the convex part of the apical hook (**Figure 6**) was dependent on HEC1 and NTT (**Figure 5C**). When ethylene biosynthesis was blocked by the application of silver nitrate, Kunitz-PI;1 promoter activity was undetectable (**Figure 4**). Based on these results we conclude that the expression of *Arabidopsis* Kunitz-PI;1 is normally induced by endogenous ethylene produced in the apical hook region. As shown previously, ethylene production is high in the apical hook of dark-grown seedlings of different plant species such as pea (Goeschl et al., 1967) and bean (Kang et al., 1967). Both, ethylene production and hook formation were negatively regulated by red light in dark-grown bean seedlings (Kang et al., 1967).

In *Arabidopsis*, a change in the sensitivity to ethylene in response to red, far red or blue light was reported to be responsible for hook opening (Knee et al., 2000). The fact that Kunitz-PI;1 expression was highest in the apical hook and further up-regulated by exogenous ethylene suggests a direct involvement of this PI in hook formation and/or maintenance. However, when etiolated seedlings of WT, Kunitz-PI;1 knock-out mutant and Kunitz-PI;1 overexpressing lines were compared, no difference in either apical hook formation and structure or hypocotyl growth was observed (Supplementary Figure S2), disproving the idea of Kunitz-PI;1 operating as structural component. On the other hand, no difference in their physiological responses to the exogenous addition of phytohormones became apparent such as the well-known triple response to ethylene (Supplementary Figure S2). Illumination of etiolated seedlings showed that all three genotypes were unimpaired in hook opening, cotyledon expansion and greening (Boex-Fontvieille et al., 2015a).

A clue toward the understanding of Kunitz-PI;1's physiological function was provided by the pioneering work of Harpham et al. (1991) who suggested a role of ethylene under conditions of mechanical impedance. Through its effect on stem thickening and hook curvature, ethylene was proposed to permit unhindered seedling growth through the soil during skotomorphogenesis. We were able to demonstrate that *Arabidopsis Kunitz-PI;1* promoter activity was induced after wounding (**Figure 7**) and that this response may be part of a defense mechanism against herbivorous arthropods, living underneath stones and fallen leaves, such as pillbugs and woodlice. These nocturnal isopods are detritivores but can also live as facultative herbivores that feed on etiolated seedlings. Pillbugs and woodlice are seed predators but also ingest the apical hook and drop the cotyledons that are later consumed as main nutrient source (Boex-Fontvieille et al., 2015a). The apical hook provides the Achilles' heel of etiolated seedlings that is protected, as we show here (**Figure 8**), by an ethylene-mediated mechanism involving Kunitz-PI;1 and maybe other PIs. It is attractive to suppose that Kunitz-PI;1 operates as inhibitor of digestive proteases of the arthropod gut when these begin their feeding on etiolated seedlings. Laboratory feeding experiments revealed that Kunitz-PI;1 is a poor diet for nutrient-deprived pillbugs and woodlice, indicating the presence of cysteine proteases that were rendered inactive. In other systems, both serine and cysteine PIs have been identified as main digestive proteases. For example, *Nicotiana attenuata* plants attacked by herbivore such as *Manduca sexta* accumulate trypsin PIs (Zavala et al., 2004), the neurotoxin nicotine (Baldwin, 1999), and various secondary metabolites comprising oxylipins (Wu et al., 2008; see Howe and Jander, 2008; Wu and Baldwin, 2010, for reviews). Serine proteases have been detected in many insect orders, including *Lepidoptera*, *Diptera*, *Orthoptera*, *Hymenoptera*, and *Coleoptera* (Christeller et al., 1992). Analysis of larval midgut extracts of 12 lepidopteran species revealed that most of them use a trypsin- and elastase-based digestive system, whereas others depend on chymotrypsins (Christeller et al., 1992). Both trypsin and chymotrypsin-like enzymes have been identified in the tobacco budworm (*Heliothis virescens*; Johnston et al., 1995). Cysteine protease activity has been detected in many coleopterans, such as corn rootworm (*Diabrotica virgifera*; Koiwa et al., 2000), Colorado potato beetle (*Leptinotarsa decemlineata*; Gruden et al., 2003), and sugarcane weevil (*Sphenophorus levis*; Soares-Costa et al., 2011). In summary, the complement of digestive proteases in phytophagous insects is quite complex and comprises all catalytic types, i.e., serine, threonine, cysteine, aspartic, and metallo enzymes (Terra and Ferreira, 1994). Their activity is counteracted by plant PIs as part of their natural plant defense against herbivores (e.g., Bode et al., 2013; see Hartl et al., 2011; Zhu-Salzman and Zeng, 2015, for reviews).

The wound set by arthropod feeding in the model system studied here, obviously elicits accumulation of ethylene, leading to a boost in Kunitz-PI:1 expression and maybe the induction of other direct and indirect defenses aimed to prevent mass ingestion of larger seedling populations. Such direct and indirect defenses would comprise hypocotyl thickening and exaggerating apical hook curvature (Knight and Crocker, 1913). A subsequent, second line of defense could be the release of the defense protein RD21 to degrade via its intrinsic activity as cysteine protease digestive proteases of the arthropod gut during the subtle period when etiolated seedlings break through the soil and need to open the apical hook for

cotyledon expansion and greening, permitting the switch to photomorphogenetic growth (Boex-Fontvieille et al., 2015a). This hypothetical model would not exclude the operation of additional mechanisms. For example, an unusual serine protease was described for *Arabidopsis* and to function in resistance to both necrotrophic fungi and insect herbivory (Laluk and Mengiste, 2011). Work is needed to identify the network of ethylene-response genes operating in the apical hook of etiolated seedlings and define their functions in induced arthropod deterrence.

AUTHOR CONTRIBUTIONS

EB-F: Carried out research and analyzed data. SRu: Carried out research and analyzed data. DvW: Analyzed data. SP: Carried out research, analyzed data. CR: Designed research, analyzed data, and wrote the paper. SRe: Designed research, carried out research, analyzed data, and wrote the paper.

FUNDING

This work was supported by a research project grant of the Chaire d'Excellence Program of the French Ministry of Research and Education to CR and a research project grant 3143956-01 of the Life Sciences Discovery Fund to SRu.

ACKNOWLEDGMENTS

We thank Brian Crawford, Gary Ditta and Martin Yanofsky (University of California San Diego, La Jolla, CA) for generous gifts of the *Arabidopsis ntt* and *hec1* and *hec3* mutant seeds.

SUPPLEMENTARY MATERIAL

The Supplementary Material for this article can be found online at: http://journal.frontiersin.org/article/10.3389/fpls.2016.01246

REFERENCES

Alabadí, D., and Blázquez, M. A. (2009). Molecular interactions between light and hormone signaling to control plant growth. *Plant Mol. Biol.* 69, 409–417. doi: 10.1007/s11103-008-9400-y

Alabadí, D., Gil, J., Blázquez, M. A., and García-Martínez, J. L. (2004). Gibberellins repress photomorphogenesis in darkness. *Plant Physiol.* 134, 1050–1057. doi: 10.1104/pp.103.035451

Alonso, J. M., Stepanova, A. N., Leisse, T. J., Kim, C. J., Chen, H., Shinn, P., et al. (2003). Genome-wide insertional mutagenesis of *Arabidopsis thaliana*. *Science* 301, 653–657. doi: 10.1126/science.1086391

An, F., Zhao, Q., Ji, Y., Li, W., Jiang, Z., Yu, X., et al. (2010). Ethylene-induced stabilization of ETHYLENE INSENSITIVE3 and EIN3-LIKE1 is mediated by proteasomal degradation of EIN3 binding F-box 1 and 2 that requires EIN2 in *Arabidopsis*. *Plant Cell* 22, 2384–2401. doi: 10.1105/tpc.110.076588

Anderson, J. D., Mattoo, A. K., and Lieberman, M. (1982). Induction of ethylene biosynthesis in tobacco leaf discs by cell wall disesting enzymes. *Biochem. Biophys. Res. Commun.* 107, 588–596.

Bae, G., and Choi, G. (2008). Decoding of light signals by plant phytochromes and their interacting proteins. *Annu. Rev. Plant Biol.* 59, 281–311. doi: 10.1146/annurev.arplant.59.032607.092859

Baldwin, I. T. (1999). Functional interactions in the use of direct and indirect defences in native *Nicotiana* plants. *Novartis Found. Symp.* 223, 74–87; discussion 87–94, 160–165.

Beers, E. P., Woffenden, B. J., and Zhao, C. (2000). Plant proteolytic enzymes: possible roles during programmed cell death. *Plant Mol. Biol.* 44, 399–415. doi: 10.1023/A:1026556928624

Bektas, I., Fellenberg, C., and Paulsen, H. (2012). Water-soluble chlorophyll protein (WSCP) of *Arabidopsis* is expressed in the gynoecium and developing silique. *Planta* 236, 251–259. doi: 10.1007/s00425-012-1609-y

Bode, R. F., Halitschke, R., and Kessler, A. (2013). Herbivore damage-induced production and specific anti-digestive function of serine and cysteine protease inhibitors in tall goldenrod, *Solidago altissima* L. (Asteraceae). *Planta* 237, 1287–1296. doi: 10.1007/s00425-013-1845-9

Boex-Fontvieille, E., Rustgi, S., Reinbothe, S., and Reinbothe, C. (2015a). A Kunitz-type protease inhibitor regulates programmed cell death during flower development in *Arabidopsis thaliana*. *J. Exp. Bot.* 66, 6119–6135. doi: 10.1093/jxb/erv327

Boex-Fontvieille, E., Rustgi, S., von Wettstein, D., Reinbothe, S., and Reinbothe, C. (2015b). Water-soluble chlorophyll protein is involved in herbivore resistance activation during greening of *Arabidopsis thaliana*. *Proc. Natl. Acad. Sci. U.S.A.* 112, 7303–7308. doi: 10.1073/pnas.1507714112

Chen, G. H., Huang, L. T., Yap, M. N., Lee, R. H., Huang, Y. J., Cheng, M. C., et al. (2002). Molecular characterization of a senescence-associated gene encoding cysteine proteinase and its gene expression during leaf senescence in sweet potato. *Plant Cell Physiol.* 43, 984–991. doi: 10.1093/pcp/pcf125

Christeller, J. T., Laing, W. A., Markwick, N. P., and Burgess, E. P. J. (1992). Midgut protease activities in 12 phytophagous Lepidopteran larvae: dietary and protease inhibitor interactions. *Insect Biochem. Mol. Biol.* 22, 735–746. doi: 10.1016/0965-1748(92)90052-G

Christians, M. J., Robles, L. M., Zeller, S. M., and Larsen, P. B. (2008). The eer5 mutation, which affects a novel proteasome-related subunit, indicates a prominent role for the COP9 signalosome in resetting the ethylene-signaling pathway in *Arabidopsis*. *Plant J.* 55, 467–477. doi: 10.1111/j.1365-313X.2008.03521.x

Crawford, B. C., Ditta, G., and Yanofsky, M. F. (2007). The *NTT* gene is required for transmitting-tract development in carpels of *Arabidopsis thaliana*. *Curr. Biol.* 17, 1101–1108. doi: 10.1016/j.cub.2007.05.079

Darwin, C. (1896). *The Power of Movement in Plants*. New York, NY: D. Appleton and Company.

Esen, A. (1978). A simple method for quantitative, semiquantitative, and qualitative assay of protein. *Anal. Biochem.* 89, 264–273. doi: 10.1016/0003-2697(78)90749-2

Farmer, E. E., and Dubugnon, L. (2009). Detritivorous crustaceans become herbivores on jasmonate-deficient plants. *Proc. Natl. Acad. Sci. U.S.A.* 106, 935–940. doi: 10.1073/pnas.0812182106

Franco, O. L., Grossi de Sá, M. F., Sales, M. P., Mello, L. V., Oliveira, A. S., and Rigden, D. J. (2002). Overlapping binding sites for trypsin and papain on a Kunitz-type proteinase inhibitor from *Prosopis juliflora*. *Proteins* 49, 335–341. doi: 10.1002/prot.10228

Goeschl, J. D., Pratt, H. K., and Bonner, B. A. (1967). An effect of light on the production of ethylene and the growth of the plumular portion of etiolated pea seedlings. *Plant Physiol.* 42, 1077–1080. doi: 10.1104/pp.42.8.1077

Goeschl, J. D., Rappaport, L., and Pratt, H. K. (1966). Ethylene as a factor regulating the growth of pea epicotyls subjected to physical stress. *Plant Physiol.* 41, 877–884. doi: 10.1104/pp.41.5.877

Green, B., and Kühlbrandt, W. (1995). Sequence conservation of light-harvesting and stress-response proteins in relation to the three-dimensional molecular structure of LHCII. *Phytosynth. Res.* 44, 139–148. doi: 10.1007/BF00018304

Gremski, K., Ditta, G., and Yanofsky, M. F. (2007). The HECATE genes regulate female reproductive tract development in *Arabidopsis thaliana*. *Development* 134, 3593–3601. doi: 10.1242/dev.011510

Gruden, K., Popovic, T., Cimerman, N., Krizaj, I., and Strukelj, B. (2003). Diverse enzymatic specificities of digestive proteases, 'intestains', enable Colorado potato beetle larvae to counteract the potato defence mechanism. *Biol. Chem.* 384, 305–310. doi: 10.1515/BC.2003.034

Guo, H., and Ecker, J. R. (2003). Plant responses to ethylene gas are mediated by SCF(EBF1/EBF2)-dependent proteolysis of EIN3 transcription factor. *Cell* 115, 667–677. doi: 10.1016/S0092-8674(03)00969-3

Halls, C. E., Rogers, S. W., Oufattole, M., Østergard, O., Svensson, B., and Rogers, J. C. (2006). A Kunitz-type cysteine protease inhibitor from cauliflower and *Arabidopsis*. *Plant Sci.* 170, 1102–1110. doi: 10.1016/j.plantsci.2006.01.018

Harpham, N. V. J., Berry, A. W., Knee, E. M., Roveda-Hoyos, G., Raskin, I., Sanders, I. O., et al. (1991). The effect of ethylene on the growth and development of wild-type and mutant *Arabidopsis thaliana* (L.) Heynh. *Ann. Bot.* 68, 55–61.

Hartl, M., Giri, A. P., Kaur, H., and Baldwin, I. T. (2011). The multiple functions of plant serine protease inhibitors: defense against herbivores and beyond. *Plant Signal Behav.* 6, 1009–1011. doi: 10.4161/psb.6.7.15504

Hernández-Nistal, J., Martin, I., Jiménez, T., Dopico, B., and Labrador, E. (2009). Two cell wall Kunitz trypsin inhibitors in chickpea during seed germination and seedling growth. *Plant Physiol. Biochem.* 47, 181–187. doi: 10.1016/j.plaphy.2008.11.009

Homaei, A. A., Sajedi, R. H., Sariri, R., Seyfzadeh, S., and Stevanato, R. (2010). Cysteine enhances activity and stability of immobilized papain. *Amino Acids* 38, 937–942. doi: 10.1007/s00726-009-0302-3

Howe, G. A., and Jander, G. (2008). Plant immunity to insect herbivores. *Annu. Rev. Plant Biol.* 59, 41–66. doi: 10.1146/annurev.arplant.59.032607.092825

Hsieh, H. L., and Okamoto, H. (2014). Molecular interaction of jasmonate and phytochrome A signalling. *J. Exp. Bot.* 65, 2847–2857. doi: 10.1093/jxb/eru230

Innis, M. A., Gelfand, D. H., Sninsky, J. J., and White, T. J. (eds). (1990). *PCR Protocols*. San Diego, CA: Academic Press.

Irshad, M., Canut, H., Borderies, G., Pont-Lezica, R., and Jamet, E. (2008). A new picture of cell wall protein dynamics in elongating cells of *Arabidopsis thaliana*: confirmed actors and newcomers. *BMC Plant Biol.* 8:94. doi: 10.1186/1471-2229-8-94

Jiménez, T., Martin, I., Hernández-Nistal, J., Labrador, E., and Dopico, B. (2008). The accumulation of a Kunitz trypsin inhibitor from chickpea (TPI-2) located in cell walls is increased in wounded leaves and elongating epicotyls. *Physiol. Plant.* 132, 306–317. doi: 10.1111/j.1399-3054.2007.01010.x

Jiménez, T., Martin, I., Labrador, E., and Dopico, B. (2007). A chickpea Kunitz trypsin inhibitor is located in cell wall of elongating seedling organs and vascular tissue. *Planta* 226, 45–55. doi: 10.1007/s00425-006-0465-z

Johnston, K. A., Lee, M. J., Brough, G., Hilder, V. A., Gatehouse, A. M. R., and Gatehouse, J. A. (1995). Protease activities in the larval midgut of *Heliothis virescens*: evidence for trypsin and chymotrypsin-like enzymes. *Insect Biochem. Mol. Biol.* 25, 375–383. doi: 10.1016/0965-1748(94)00077-U

Jones, M. L., Larsen, P. B., and Woodson, W. R. (1995). Ethylene-regulated expression of a carnation cysteine proteinase during flower petal senescence. *Plant Mol. Biol.* 28, 505–512. doi: 10.1007/BF00020397

Kang, B. G., Yocum, C. S., Burg, S. P., and Ray, P. M. (1967). Ethylene and carbon dioxide: mediation of hypocotyl hook-opening response. *Science* 156, 958–959. doi: 10.1126/science.156.3777.958

Kim, H. J., Kim, Y. K., Park, J. Y., and Kim, J. (2002). Light signaling mediated by phytochrome plays an important role in cold-induced gene expression through the C-repeat/dehydration responsive element (C/DRE) in *Arabidopsis thaliana*. *Plant J.* 29, 693–704. doi: 10.1046/j.1365-313X.2002.01249.x

Knee, E. M., Hangarter, R. P., and Knee, M. (2000). Interactions of light and ethylene in hypocotyl hook maintenance in *Arabidopsis thaliana* seedlings. *Physiol. Plant.* 108, 208–215. doi: 10.1034/j.1399-3054.2000.108002208.x

Knight, L. I., and Crocker, W. (1913). Toxicity of smoke. *Bot. Gaz.* 55, 337–371. doi: 10.1086/331066

Koiwa, H., Shade, R. E., Zhu-Salzman, K., D'Urzo, M. P., Murdock, L. L., Bressan, R. A., et al. (2000). A plant defensive cystatin (soyacystatin) targets cathepsin L-like digestive cysteine proteinases (DvCALs) in the larval midgut of western corn rootworm (*Diabrotica virgifera virgifera*). *FEBS Lett.* 471, 67–70. doi: 10.1016/S0014-5793(00)01368-5

Laluk, K., and Mengiste, T. (2011). The *Arabidopsis* extracellular UNUSUAL SERINE PROTEASE INHIBITOR functions in resistance to necrotrophic fungi and insect herbivory. *Plant J.* 68, 480–494. doi: 10.1111/j.1365-313X.2011.04702.x

Li, Q. F., and He, J. X. (2013). Mechanisms of signaling crosstalk between brassinosteroids and gibberellins. *Plant Signal Behav.* 8:e24686. doi: 10.4161/psb.24686

Li, Q. F., Wang, C., Jiang, L., Li, S., Sun, S. S., and He, J. X. (2012). An interaction between BZR1 and DELLAs mediates direct signaling crosstalk between brassinosteroids and gibberellins in *Arabidopsis*. *Sci. Signal.* 5, ra72. doi: 10.1126/scisignal.2002908

Lin, Z., Zhong, S., and Grierson, D. (2009). Recent advances in ethylene research. *J. Exp. Bot.* 60, 3311–3336. doi: 10.1093/jxb/erp204

Matarasso, N., Schuster, S., and Avni, A. (2005). A novel plant cysteine protease has a dual function as a regulator of 1-aminocyclopropane-1-carboxylic acid synthase gene expression. *Plant Cell* 17, 1205–1206. doi: 10.1105/tpc.105.030775

Oliva, M. L., and Sampaio, U. M. (2008). *Bauhinia* Kunitz-type proteinase inhibitors: structural characteristics and biological properties. *Biol. Chem.* 389, 1007–1013. doi: 10.1515/BC.2008.119

Oliva, M. L. V., and Sampaio, M. U. (2009). Action of plant proteinase inhibitors on enzymes of physiopathological importance. *An. Acad. Bras. Ciênc.* 81, 615–621. doi: 10.1590/S0001-37652009000300023

Rawlings, N. D., Tolle, D. P., and Barrett, A. J. (2004). Evolutionary families of peptidase inhibitors. *Biochem. J.* 378, 705–716. doi: 10.1042/bj20031825

Raz, V., and Ecker, J. R. (1999). Regulation of differential growth in the apical hook of *Arabidopsis*. *Development* 126, 3661–3668.

Satoh, H., Uchida, A., Nakayama, K., and Okada, M. (2001). Water-soluble chlorophyll protein in *Brassicaceae* plants is a stress-induced chlorophyll-binding protein. *Plant Cell Physiol.* 42, 906–911. doi: 10.1093/pcp/pce117

Scutt, C. P., Vinauger-Douard, M., Fourquin, C., Ailhas, J., Kuno, N., Uchida, K., et al. (2003). The identification of candidate genes for a reverse genetic analysis of development and function in the *Arabidopsis* gynoecium. *Plant Physiol.* 132, 653–665. doi: 10.1104/pp.102.017798

Soares-Costa, A., Dias, A. B., Dellamano, M., de Paula, F. F., Carmona, A. K., Terra, W. R., et al. (2011). Digestive physiology and characterization of digestive cathepsin L-like proteinase from the sugarcane weevil *Sphenophorus* levis. *J. Insect Physiol.* 57, 462–468. doi: 10.1016/j.jinsphys.2011.01.006

Solomon, M., Belenghi, B., Delledonne, M., Menachem, E., and Levine, A. (1999). The involvement of cysteine proteases and protease inhibitor genes in the regulation of programmed cell death in plants. *Plant Cell* 11, 431–444. doi: 10.2307/3870871

Terra, W. R., and Ferreira, C. (1994). Insect digestive enzymes: properties, compartmentalization and function. *Comp. Biochem. Phys. B* 109, 1–62.

Towbin, H., Staehelin, T., and Gordon, J. (1979). Electrophoretic transfer of proteins from polyacrylamide gels to nitrocellulose sheets: Procedure and some applications. *Proc. Natl. Acad. Sci. U.S.A.* 76, 4350–4354. doi: 10.1073/pnas.76.9.4350

Tung, C. W., Dwyer, K. G., Nasrallah, M. E., and Nasrallah, J. B. (2005). Genome-wide identification of genes expressed in *Arabidopsis* pistils specifically along the path of pollen tube growth. *Plant Physiol.* 138, 977–989. doi: 10.1104/pp.105.060558

von Wettstein, D., Gough, S., and Kannangara, C. G. (1995). Chlorophyll biosynthesis. *Plant Cell* 7, 1039–1057. doi: 10.2307/3870056

Winter, D., Vinegar, B., Nahal, H., Ammar, R., Wilson, G. V., and Provart, N. J. (2007). An "Electronic Fluorescent Pictograph" browser for exploring and analyzing large-scale biological data sets. *PLoS ONE* 2:e718. doi: 10.1371/journal.pone.0000718

Wu, J., and Baldwin, I. T. (2010). New insights into plant responses to the attack from insect herbivores. *Annu. Rev. Genet.* 44, 1–24. doi: 10.1146/annurev-genet-102209-163500

Wu, J., Wang, L., and Baldwin, I. T. (2008). Methyl jasmonate-elicited herbivore resistance: does MeJA function as a signal without being hydrolyzed to JA? *Planta* 227, 1161–1168. doi: 10.1007/s00425-008-0690-8

Zavala, J. A., Patankar, A. G., Gase, K., Hui, D., and Baldwin, I. T. (2004). Manipulation of endogenous trypsin proteinase inhibitor production in *Nicotiana attenuata* demonstrates their function as antiherbivore defenses. *Plant Physiol.* 134, 1181–1190. doi: 10.1104/pp.103.035634

Zhong, S., Zhao, M., Shi, T., Shi, H., An, F., Zhao, Q., et al. (2009). EIN3/EIL1 cooperate with PIF1 to prevent photo-oxidation and to promote greening of *Arabidopsis* seedlings. *Proc. Natl. Acad. Sci. U.S.A.* 106, 21431–21436. doi: 10.1073/pnas.0907670106

Zhu, L., Xin, R., Bu, Q., Shen, H., Dang, J., and Huq, E. (2016). A negative feedback loop between PHYTOCHROME INTERACTING FACTORs and HECATE proteins fine tunes photomorphogenesis in *Arabidopsis*. *Plant Cell* 28, 855–874. doi: 10.1105/tpc.16.00122

Zhu-Salzman, K., and Zeng, R. (2015). Insect response to plant defensive protease inhibitors. *Annu. Rev. Entomol.* 60, 233–252. doi: 10.1146/annurev-ento-010814-020816

Conflict of Interest Statement: The authors declare that the research was conducted in the absence of any commercial or financial relationships that could be construed as a potential conflict of interest.

Advantages of publishing in Frontiers

OPEN ACCESS
Articles are free to read, for greatest visibility

COLLABORATIVE PEER-REVIEW
Designed to be rigorous – yet also collaborative, fair and constructive

FAST PUBLICATION
Average 85 days from submission to publication (across all journals)

COPYRIGHT TO AUTHORS
No limit to article distribution and re-use

TRANSPARENT
Editors and reviewers acknowledged by name on published articles

SUPPORT
By our Swiss-based editorial team

IMPACT METRICS
Advanced metrics track your article's impact

GLOBAL SPREAD
5'100'000+ monthly article views and downloads

LOOP RESEARCH NETWORK
Our network increases readership for your article

Frontiers
EPFL Innovation Park, Building I • 1015 Lausanne • Switzerland
Tel +41 21 510 17 00 • Fax +41 21 510 17 01 • info@frontiersin.org
www.frontiersin.org

Find us on